

Earth Observation: Data, Processing and Applications

Volume 3A: Applications—Terrestrial Vegetation



The report is available in PDF format at <https://www.eoa.org.au/earth-observation-textbooks>. We welcome your comments regarding the readability and usefulness of this report. To provide feedback, please contact us at communications@eo.org.au.

Publisher:

Australia and New Zealand CRC for Spatial Information

ISBN [ONLINE]:

978-0-6482278-5-4

Copyright:

All material in this publication is licensed under a Creative Commons Attribution 4.0 Australia Licence, save for content supplied by third parties, and logos. Creative Commons Attribution 4.0 Australia Licence is a standard form licence agreement that allows you to copy, distribute, transmit, and adapt this publication provided you attribute the work. The full licence terms are available from <https://creativecommons.org/licenses/by/4.0/legalcode>. A summary of the licence terms is available from <https://creativecommons.org/licenses/by/4.0/>.



Disclaimer:

While every effort has been made to ensure its accuracy, the CRCSI does not offer any express or implied warranties or representations as to the accuracy or completeness of the information contained herein. The CRCSI and its employees and agents accept no liability in negligence for the information (or the use of such information) provided in this report.

Recommended Citation for Volume 3A:

CRCSI (2021). *Earth Observation: Data, Processing and Applications. Volume 3A: Applications—Terrestrial Vegetation*. (Eds: Harrison, B.A., Gibson, R., Bastin, G., Thackway, R., Huete, A., Donald, G., Lyons, M., Sparks, T., Byrne, G., Lewis, M.M., and Xie, Q.). CRCSI, Melbourne.

The recommended citation for each contributed chapter is given on the first page of the chapter.

Background image on previous page: Sentinel-2A imagery acquired on 8 June 2020 over the eastern portion of the Wide Bay Burnett region in southeast Queensland. This region includes the cities of Bundaberg in the northeast and Maryborough, west of Fraser Island. In addition to tourism and fishing, this district supports a variety of agricultural production, principally beef, citrus, sugarcane, and forestry.

Source: Norman Mueller, Geoscience Australia

Acknowledgements

Production of this series of texts would not have been possible without the financial support of CSIRO, CRC SI, GA and BNHCRC, input from members of the editorial panels, and direction from members of the various advisory panels. Administrative support from FrontierSI is also gratefully acknowledged.

Volumes 1 and 2 of this series are based on text originally published in Harrison and Jupp (1989, 1990, 1992, and 1993)¹. Many illustrations and some text from these publications have been reproduced with permission from CSIRO.

The following authors are thanked for their contributed chapters:

- **12. Crops:** Barbara Harrison (ex CSIRO) and Graham Donald (ex CSIRO)
- **13. Irrigated Horticulture:** Des Whitfield, Andrew McAllister, Mohammad Abuzar, and Mark O'Connell (Agriculture Victoria)
- **14. Pastures:** Graham Donald (ex CSIRO)
- **15. Rangelands:** Gary Bastin (ex CSIRO)
- **16. Forestry:** Nicholas Coops (University of British Columbia) and Barbara Harrison (ex CSIRO)
- **17. Carbon Cycling:** Alfredo Huete (University of Technology, Sydney)
- **18. Fire:** Rebecca Gibson (Environment NSW), Marta Yebra (Australian National University), Barbara Harrison (ex CSIRO), and Ross Bradstock (University of Wollongong)

Other contributors are gratefully acknowledged:

- **excursus authors:** Nicholas Coops and Glenn Newnham (Excursus 5.1), Qiaoyun Xie (Excursus 9.1), John Carter (Excursus 10.1), Graham Donald (Excursus 14.1), Peter Scarth (Excursus 14.2), Alfredo Huete (Excursus 17.1, Excursus 17.2)
- **reviewers:** Albert van Dijk (full draft), Laurie Chisholm (early draft), Michael Hill (Sections 1 to 4), Richard Lucas (Sections 3.2 and 20.5), David Jupp (Excursus 5.1), Peter Scarth (Excursus 6.1 and Section 14.5), James Cleverly, Jason Beringer, Peter Isaac, and Caitlin Moore (Excursus 7.2), Bob Denholm (Excursus 8.2), Juan Pablo Guerschman (Sections 8, 11, 12, 14, and 15), Franz Waldner (Sections 11 and 12), Jorge L. Peña-Arancibia (Section 13), Terry Beutel (Excursus 15.1), Glenn Newnham and Stuart Davey (Section 16), Norman Mueller (Section 18), Angela Robb (Excursus 19.2), Alison Cowood and Terry Hills (Section 20.5), David Hudson (Section 21), Brian Walker (Excursus 21.1)
- **illustrations:** Norman Mueller, Tony Sparks, Richard Thackway, Gary Bastin, John Ludwig, Laurie Chisholm, Mitchell Lyons, Jenny Lovell, Glenn Newnham, Randall Donohue, Qiaoyun Xie, Mark Grant, Franz Waldner, Fred Hughes, Graham Donald, Mark O'Connell, Des Whitfield, Mohammad Abuzar, Peter Scarth, Barney Foran, John Carter, Terry Beutel, Ivan Kotzur, Robert Norman, Sue Ogilvy, Kirsty Yeates, Matthew Bolton, Carl Davies (CMDphotographics), Peter Harrison.

We thank those owners of copyrighted illustrative material for permission to reproduce their work. Credits for individual illustrations are provided below the relevant graphic.

All volumes in this series are covered by the copyright provisions of CC BY 4.0 AU.

¹ Harrison, B.A., and Jupp, D.L.B. (1989) Introduction to Remotely Sensed Data: Part ONE of the microBRIAN Resource Manual. CSIRO, Melbourne. 156 p.
Harrison, B.A., and Jupp, D.L.B. (1990) Introduction to Image Processing: Part TWO of the microBRIAN Resource Manual. CSIRO, Melbourne. 256 p.
Harrison, B.A., and Jupp, D.L.B. (1992) Image Rectification and Registration: Part FOUR of the microBRIAN Resource Manual. MPA, Melbourne.
Harrison, B.A., and Jupp, D.L.B. (1993) Image Classification and Analysis: Part THREE of the microBRIAN Resource Manual. MPA, Melbourne.

Table of Contents

Volume 3A: Applications—Terrestrial Vegetation

a

Acknowledgements

i

Introduction

1

1 The Vegetated Landscape	3
1.1 Environmental Factors and Gradients	3
1.1.1 Biotic factors	5
1.1.2 Abiotic factors	6
1.1.3 Environmental gradients	9
1.2 Ecological Units	10
1.2.1 Individuals and populations	10
1.2.2 Communities	11
1.2.3 Ecosystems	11
1.3 Terrestrial Ecosystems	13
1.3.1 Biogeography and biodiversity	13
1.3.2 Major habitat zones	13
1.3.3 A dynamic tapestry	15
1.4 Further Information	18
1.5 References	18
2 The Australian Environment	21
2.1 Topography and Hydrology	24
2.2 Climate	27
2.2.1 Weather patterns	27
2.2.2 Climatic drivers	31
2.2.3 Climate classifications	31
2.3 Biota	35
2.3.1 Classifying vegetation	35
2.3.2 Weeds	39
2.3.3 Indigenous and feral animals	39
2.4 Ecoregions and Fire Patterns	40
2.4.1 Deserts and xeric shrublands	42
2.4.2 Mediterranean forests, woodlands and scrub	42
2.4.3 Montane grasslands and shrublands	43
2.4.4 Temperate broadleaf and mixed forest	43
2.4.5 Temperate grasslands, savannas and shrublands	43
2.4.6 Tropical and subtropical grasslands, savannas and shrublands	44
2.4.7 Tropical and subtropical moist broadleaf forests	44
2.5 Land Use	45
2.5.1 Indigenous patterns	46

2.5.2	European settlement patterns	47
2.5.3	Current land use	47
2.6	Further Information	49
2.7	References	50
3	Mapping Vegetated Landscapes	57
3.1	Key Concepts in Landscape Mapping	57
3.1.1	Vegetation type versus vegetation condition	57
3.1.2	Land cover versus land use	58
3.2	How Do We Map Land Cover?	59
3.2.1	Classification schemes	59
3.2.2	Mapping methods and accuracy assessment	63
3.3	Mapping Approaches	66
3.3.1	Land evaluation based on mapping units	66
3.3.2	Actual distribution of current vegetation	68
3.3.3	Probable distribution of natural vegetation	68
3.3.4	Actual distribution of current land use	69
3.4	Monitoring Landscape Change	73
3.4.1	Changes in land condition	74
3.4.2	Changes in land use	78
3.5	Further Information	81
3.6	References	82

Measurable Properties of Terrestrial Vegetation 87

4	Attributes of Foliage	89
4.1	Structure and Shape	89
4.1.1	Anatomy	89
4.1.2	Morphology	90
4.1.3	Texture	92
4.1.4	Strength	92
4.2	Chemical Composition	93
4.2.1	Water	93
4.2.2	Inorganic components	95
4.2.3	Organic components	96
4.3	Spectral Properties	99
4.4	Boundary layer	101
4.5	Further Information	103
4.6	References	103
5	Attributes of Individual Plants	107
5.1	Structure	107
5.1.1	Growth form	107
5.1.2	Biomass	111
5.2	Physiological Processes	111
5.2.1	Photosynthesis	111
5.2.2	Respiration	113

5.2.3	Transpiration	114
5.2.4	Thermal stability	114
5.3	Growth	116
5.3.1	Life cycle	116
5.3.2	Phenology	116
5.3.3	Abscission	117
5.3.4	Photomorphogenesis	118
5.3.5	Nutrient use efficiency	118
5.4	Further Information	119
5.5	References	119
6	Attributes of Plant Communities	125
6.1	Formations	126
6.2	Horizontal Spacing and Pattern	130
6.3	Density and Cover	130
6.3.1	Foliage cover	130
6.3.2	Cover-abundance	131
6.3.3	Leaf area index (LAI)	131
6.3.4	Fraction of absorbed photosynthetically active radiation (fAPAR)	132
6.3.5	Basal area (BA)	133
6.3.6	Fractional cover	133
6.4	Canopy Colour and Texture	133
6.5	Growth Stages	135
6.6	Succession	135
6.7	Further Information	137
6.8	References	137
7	Attributes of Ecosystems	141
7.1	Biodiversity	142
7.2	Stability and Equilibrium	143
7.3	Function and Condition	147
7.4	Productivity	150
7.5	Energy Balance	152
7.6	Water Balance	155
7.7	Further Information	156
7.8	References	156
EO Methods		163
8	Mapping	165
8.1	Spectral Indices	166
8.1.1	Greenness	166
8.1.2	Hyperspectral indices	170
8.1.3	Vegetation cover and condition	171
8.1.4	Plant productivity	172
8.1.5	Water content	173
8.1.6	Landscape 'leakiness'	174

8.2 Spectral Classification	174
8.2.1 Vegetation	175
8.2.2 Geology and soils	176
8.2.3 Water	178
8.2.4 Urban features	178
8.3 Sub-pixel Analyses	179
8.4 Further Information	183
8.5 References	183
9 Monitoring	191
9.1 Vegetation types	193
9.2 Change Indices	194
9.2.1 Fire footprints	194
9.2.2 Ecosystem disturbance	195
9.3 Phenology	195
9.4 Evapotranspiration	200
9.5 Plant Water Stress	203
9.6 Plant Vigour	204
9.7 Further Information	205
9.8 References	206
10 Modelling	213
10.1 Modelling Considerations	214
10.1.1 Underlying EO model	214
10.1.2 Interpolation and extrapolation	215
10.1.3 Scaling	216
10.1.4 Spatial patterns	217
10.2 EO-based Models for Terrestrial Vegetation	218
10.2.1 Leaf models	218
10.2.2 Plant productivity models	219
10.2.3 Global and regional models	220
10.3 Further Information	224
10.4 References	224

Observing Agriculture 229

11 Agriculture Overview	231
11.1 Agriculture in Australia	232
11.2 Essential Agricultural Variables	233
11.3 Monitoring Managed Landscapes	235
11.4 Land Degradation	237
11.5 Food Security	241
11.6 Further Information	243
11.7 References	243
12 Crops	249
<i>Barbara Harrison and Graham Donald</i>	
12.1 Crops in Australia	249

12.2	EO Sensors for Crops	250
12.3	Crop Type and Agricultural Land Use	251
12.4	Crop Extent, Condition and Production Forecasts	252
12.5	Global Crop Monitoring Systems	255
12.6	Precision Agriculture	256
12.7	Further Information	258
12.8	References	258
13	Irrigated Horticulture	263
	<i>Des Whitfield, Andrew McAllister, Mohammad Abuzar, and Mark O'Connell</i>	
13.1	Irrigated Horticulture in Southeast Australia	263
13.2	EO Sensors for Irrigated Horticulture	264
13.3	Fundamentals of Irrigation Management	265
13.4	Irrigation Requirements of Horticultural Crops	266
13.4.1	Weather-based estimates of soil water status in orchards	266
13.4.2	Reference crop evapotranspiration	266
13.4.3	Crop characteristics	267
13.4.4	Why two reference crops?	267
13.5	Satellite-based Estimates of ET	268
13.5.1	K_c -VI relationships	268
13.5.2	T_s -VI relationships	268
13.5.3	Surface energy balance models	269
13.6	METRIC Model: Summer Crops	269
13.7	METRIC Model: Irrigated Horticulture	270
13.7.1	Introduction	270
13.7.2	Model implementation	271
13.7.3	ET _F /NDVI relationships	273
13.8	Application to Irrigated Horticultural Crops in Southeast Australia	278
13.9	Further Information	279
13.10	References	279
14	Pastures	281
	<i>Graham Donald</i>	
14.1	Pastures in Australia	282
14.2	EO Sensors for Pastures	283
14.3	Phenology and Production	284
14.4	Pasture Growth Rate	286
14.5	Biomass Monitoring	290
14.6	Precision Grazing	294
14.7	Wool Production	294
14.8	Further Information	295
14.9	References	295
15	Rangelands	299
	<i>Gary Bastin</i>	
15.1	Rangelands in Australia	300
15.1.1	Vegetation	302
15.1.2	Water	303

15.1.3 Fire	304
15.1.4 Grazing	304
15.1.5 Socio-economic factors	306
15.2 EO Sensors for Rangelands	307
15.3 Rangeland Condition	308
15.3.1 Vegetation resilience	310
15.3.2 Landscape condition and leakiness	311
15.3.3 Persistence of ground cover	312
15.4 Operational Systems for Monitoring Rangelands	313
15.5 Conserving Biodiversity	315
15.6 Further Information	318
15.7 References	318
16 Forestry	323
<i>Nicholas Coops and Barbara Harrison</i>	
16.1 Forestry in Australia	324
16.2 EO Sensors for Forestry	327
16.3 Forest Type	329
16.4 Forest Hydrology	329
16.5 Forest Structure	330
16.5.1 Stand height and cover	330
16.5.2 Individual trees	331
16.5.3 Geometric-optical models	332
16.5.4 Biomass and fuel load	333
16.6 Forest Functionality	334
16.6.1 Plant nutrition	334
16.6.2 Plant stress	334
16.7 Forest Diversity	335
16.7.1 Floral diversity	335
16.7.2 Faunal monitoring	338
16.8 Forest Disturbance	338
16.8.1 Insect damage	338
16.8.2 Fire monitoring	338
16.8.3 Environmental monitoring	339
16.9 Further Information	340
16.10 References	340

Observing Carbon Dynamics 351

17 Carbon Cycling	353
<i>Alfredo Huete</i>	
17.1 Carbon Cycling in Australia	359
17.2 EO Sensors for Carbon Cycling	360
17.3 Biosphere productivity	361
17.3.1 Relationships between EO and flux tower GPP estimates	362
17.3.2 Solar-induced chlorophyll fluorescence (SIF) as proxy for GPP	363
17.4 Net Primary Productivity	363

17.4.1	VIs as proxies for ANPP	363
17.4.2	Ecosystem respiration	364
17.4.3	Net ecosystem productivity and net biome productivity	364
17.4.4	Growing season phenology	364
17.4.5	Photochemical Reflectance Index	365
17.5	Carbon Models	365
17.5.1	EO-based LUE models	366
17.5.2	Greenness and radiation (G-R) models	366
17.5.3	Temperature-Greenness (T-G) model	367
17.5.4	Carbon modelling	368
17.5.5	Vegetation Photosynthesis Model (VPM)	370
17.6	Anthropogenic carbon emissions	371
17.6.1	CO ₂ emissions	372
17.6.2	Examples of satellite studies of CO ₂ emissions and flux inversions	373
17.6.3	Land use and land cover modification	373
17.6.4	Effects of Carbon Cycle Changes	374
17.7	Carbon stocks	376
17.7.1	Biomass carbon stock	376
17.7.2	Soil organic carbon	376
17.7.3	Microwave EO	377
17.7.4	Lidar and above ground biomass	378
17.8	The Future	378
17.9	Further Information	379
17.10	References	379
18	Fire	389
	<i>Rebecca Gibson, Marta Yebra, Barbara Harrison, and Ross Bradstock</i>	
18.1	Fire in Australia	390
18.2	EO Sensors for Fire	392
18.3	Predictive Fire Analyses	395
18.3.1	Fuels	395
18.3.2	Weather conditions and topography	398
18.3.3	Ignitions	399
18.3.4	Risk analysis	399
18.4	Active Fire Analyses	400
18.4.1	Satellite imagery	400
18.4.2	Airborne imagery	401
18.5	Retrospective Fire Analyses	403
18.5.1	Fire extent and severity	404
18.5.2	Fire recovery	407
18.5.3	Fire history and behaviour	408
18.6	Operational Systems for Fire Management	409
18.6.1	Flammability models	409
18.6.2	Hotspot imagery	410
18.6.3	Fire extent and severity	410
18.7	Further Information	412
18.8	References	413

Observing Ecosystems

427

19 Biodiversity	429
19.1 Biodiversity in Australia	432
19.2 EO Sensors for Biodiversity	434
19.3 Global Biodiversity Indicators	435
19.4 Risk Assessment	437
19.5 Australian Biodiversity Monitoring	442
19.6 Further Information	445
19.7 References	446
20 Sustainability	451
20.1 Sustainability in Australia	453
20.2 EO Sensors for Sustainability	454
20.3 Ecosystem Services	455
20.4 Sustainable Development	460
20.5 Environmental-Economic Accounting	464
20.6 Further Information	471
20.7 References	472

Observing Our Future

477

21 The Road Ahead	479
21.1 The Smart Environment	479
21.2 An Objective Worldview	482
21.3 Societal Benefit Areas	483
21.4 Stewards of Tomorrow	486
21.5 Further Information	488
21.6 References	488
Glossary	490

List of Figures

Figure 1.1	Holdridge life zone classification scheme	13
Figure 1.2	Whittaker's biome classification	14
Figure 1.3	Processes and interactions within Earth System Science	16
Figure 1.4	Terrestrial carbon cycle	17
Figure 2.1	Australia	22
Figure 2.2	Major landform categories	25
Figure 2.3	Australian Soil Resource Information System (ASRIS)	25
Figure 2.4	Major drainage basins	26
Figure 2.5	Great Artesian Basin	27
Figure 2.6	Climate zones derived from humidity and temperature	28
Figure 2.7	Average annual rainfall	28
Figure 2.8	Seasonal temperature variations in Australia	29
Figure 2.9	Evaporation and evapotranspiration over Australia	30
Figure 2.10	Modified Köppen climate classification	32
Figure 2.11	Agroclimatic classifications	33
Figure 2.12	Major Vegetation Groups derived from NVIS Version 3	38
Figure 2.13	Interim Biogeographic Regionalisation of Australia (IBRA) Version 7	41
Figure 2.14	Terrestrial Ecoregions in Australia	41
Figure 2.15	Australia's towns by population size groupings, 2016	45
Figure 2.16	Aboriginal grain harvest map	46
Figure 2.17	Land use in Australia for 2010–11	48
Figure 3.1	Multi-level EO	64
Figure 3.2	Idealised spectral signatures	65
Figure 3.3	National VAST-2 dataset	76
Figure 3.4	Landscape change summary	78
Figure 3.5	Likelihood of ALUM land use change	80
Figure 4.1	Typical leaf cell structure	90
Figure 4.2	Absorption spectra of leaf pigments	97
Figure 4.3	Reflectance of green foliage	100
Figure 4.4	Leaf reflectance changes with stress	101
Figure 4.5	Impact of vegetation density on wind flow	102
Figure 5.1	Vegetation cover classes	108

Figure 5.2	Foliage profile	108
Figure 5.3	Lidar operation	109
Figure 5.4	TLS-based three-dimensional complexity of forest	110
Figure 5.5	Reflectance characteristics of typical green leaf structure	112
Figure 6.1	Height strata	126
Figure 6.2	Processing overview	128
Figure 6.3	Vegetation height and structure	129
Figure 6.4	Population distribution patterns	130
Figure 6.5	Fraction of Absorbed Photosynthetically Active Radiation (fAPAR)	132
Figure 6.6	Vegetation cover triangle	134
Figure 6.7	Simulated reflectance for increasing grass cover	134
Figure 6.8	Forest succession	136
Figure 7.1	Biodiversity factors	142
Figure 7.2	The grazing system	144
Figure 7.3	Ecosystem processes and feedback loops	147
Figure 7.4	Landscape function examples	148
Figure 7.5	Landscape function versus landscape condition	149
Figure 7.6	GPP over Australia	150
Figure 7.7	Flux tower distribution and site data	154
Figure 8.1	Normalisation effect in 'Normalised Difference Vegetation Index' (NDVI)	167
Figure 8.2	Within field crop variability	171
Figure 8.3	Leakiness index	174
Figure 8.4	Fractional cover index image	181
Figure 8.5	Fractional cover endmembers	182
Figure 9.1	Seasonal vegetation trends derived from AVHRR NDVI data 1981–2006	194
Figure 9.2	Greenness changes in annual plants	197
Figure 9.3	NDVI time series of pine plantation	198
Figure 9.4	Australian Phenology Product	199
Figure 9.5	Seasonally-integrated EVI from Australian Phenology Product	199
Figure 9.6	Budyko's framework and curve	201
Figure 10.1	Modelling error	213
Figure 10.2	Measurement and analysis of image features	214
Figure 10.3	Basic framework for extrapolation in ecology	215
Figure 10.4	Scaling procedure	216
Figure 10.5	Hypothetical landscape patterns	217

Figure 10.6	Modular structure of Dynamic Global Vegetation Models	221
Figure 11.1	Agricultural land uses in Australia	232
Figure 11.2	Driving force–pressure–state–impact–response (DPSIR) framework	233
Figure 11.3	Essential Variables in the context of UN Sustainable Development Goals	234
Figure 11.4	Seasonal quality matrix	235
Figure 11.5	Dust storm	239
Figure 12.1	Crop response to fertiliser application	257
Figure 13.1	Variation of surface–air temperature differences with vegetation cover	268
Figure 13.2	Crop coefficient variations	270
Figure 13.3	Typical crop coefficient curve	271
Figure 13.4	Irrigation districts	272
Figure 13.5	Quartile representations	274
Figure 13.6	Relationships for selected crops	275
Figure 13.7	Representative ET _r F/NDVI relationships for selected crops	276
Figure 13.8	Endmember regression estimates of ET _r F _{min} and ET _r F _{max}	277
Figure 14.1	Area of agricultural land	282
Figure 14.2	Basic metrics	284
Figure 14.3	Examples of Pasture Growth Rate imagery	288
Figure 14.4	Biomass calibration/validation sites	292
Figure 14.5	Sample national biomass map, September 2020	293
Figure 15.1	Framework for ACRIS reporting	300
Figure 15.2	Land uses in Australian rangelands	301
Figure 15.3	Vegetation Recovery	303
Figure 15.4	Density of waterpoints	304
Figure 15.5	Impact of artificial waterpoints on native species	305
Figure 15.6	Remote populations in Australia	306
Figure 15.7	Monitoring approaches	309
Figure 15.8	Stylised grazing gradient based on remotely sensed ground cover	310
Figure 15.9	Landscape function	311
Figure 15.10	Leakiness index example	312
Figure 15.11	VegMachine comparisons	314
Figure 16.1	Australian forests	326
Figure 16.2	Native forest categories	327
Figure 16.3	Penetration of radar wavelengths into vegetation layer	328
Figure 16.4	TLS-derived tree structure	332

Figure 16.5	Spectranomics Database elements	337
Figure 17.1	The carbon cycle between land, atmosphere, and oceans	354
Figure 17.2	Terrestrial photosynthetic carbon cycle	355
Figure 17.3	Seasonal variations in photosynthesis (GPP) between hemispheres	357
Figure 17.4	EO of terrestrial carbon cycle studies	359
Figure 17.5	Australian territorial carbon budget 1990–2011	360
Figure 17.6	NDVI-APAR relationship	362
Figure 17.7	Combined temperature-greenness model	368
Figure 17.8	MODIS NPP product based on BIOME-BGC model	369
Figure 17.9	Primarily Satellite-based Vegetation Photosynthesis and Respiration Model (VPRM)	370
Figure 17.10	Global Carbon Budget 2009–2018	371
Figure 17.11	Changes in carbon dioxide concentration	372
Figure 17.12	Change in global leaf area across 1982–2015	374
Figure 17.13	Australian interannual variations in carbon-related indicators	375
Figure 18.1	Fire seasonality in Australia	390
Figure 18.2	Fuel Moisture Content estimates	394
Figure 18.3	Aerial imagery of active fire	403
Figure 19.1	Human population growth	430
Figure 19.2	Response-pressure-state-benefit (RPSB) framework	435
Figure 19.3	Biodiversity change in terms of loss and alterations	437
Figure 19.4	EO framework for ecosystem risk assessment	438
Figure 19.5	RLE categories and criteria and categories	440
Figure 19.6	Application of RLE	441
Figure 20.1	Global GDP versus global material extraction 1900 to 2005	452
Figure 20.2	System of Environmental Economic Accounting	454
Figure 20.3	Ecosystem services in extensive agriculture	457
Figure 20.4	EO in ecosystem service assessment	459
Figure 20.5	Three pillars of sustainability	460
Figure 20.6	Ecological Footprint and Biocapacity for Australia	463
Figure 20.7	Overview of SEEA Central Framework	467
Figure 20.8	Environmental accounts versus environmental-economic accounts	468
Figure 21.1	The Internet of Things technology roadmap	480

List of Tables

Table 1.1	The plant kingdom	4
Table 1.2	Interactions between biotic components	5
Table 1.3	Ecosystem processes	12
Table 1.4	Terrestrial biomes	15
Table 2.1	Geography and settlement of Australia	23
Table 2.2	Australian DEM	24
Table 2.3	Australian climate types	31
Table 2.4	Agroclimatic class descriptions for Figure 2.11	34
Table 2.5	Common definitions for Australian vegetation	36
Table 2.6	Structural classification of Australian vegetation	37
Table 2.7	NVIS information hierarchy	37
Table 2.8	Native vegetation classification systems	38
Table 2.9	Land uses in Australia 2010–11	47
Table 3.1	Structure of FAO Land Cover Classification System	60
Table 3.2	Dichotomous phase classifiers and land cover types	61
Table 3.3	LCCS classification of primarily vegetated areas	62
Table 3.4	LCCS classification of primarily non-vegetated areas	63
Table 3.5	Australian landscape mapping approaches	67
Table 3.6	ALUM classification	70
Table 3.7	National Landcare Program	73
Table 3.8	VAST-2 diagnostic components, criteria and indicators	75
Table 3.9	Selected site attributes	77
Table 3.10	Drivers of land use change	79
Table 4.1	Photosynthetic pigments	98
Table 5.1	Photosynthetic pathways	113
Table 5.2	Plant growth factors	116
Table 6.1	Vegetation formations	127
Table 6.2	Height strata	127
Table 6.3	Height classes	127
Table 6.4	Summary of structural classes	128
Table 6.5	Effect of sensor quantisation on radiometric sensitivity	134
Table 7.1	Equilibrium versus nonequilibrium systems	145

Table 7.2	Rangeland management models	145
Table 7.3	State-and-Transition model terms	146
Table 7.4	Grazing land condition classes	146
Table 7.5	Examples of land condition indicators	149
Table 8.1	Sampling dimensions in EO imagery	166
Table 8.2	SVTM workflow	177
Table 9.1	Potential reference site measurements	192
Table 9.2	Ecohydrological characteristics of perennial and annual vegetation	193
Table 9.3	Significant phenological metrics	196
Table 9.4	Phenological stages of rice crop	197
Table 10.1	Leaf models	219
Table 11.1	RaPP spatial datasets	236
Table 11.2	Eight extended droughts in Australia	239
Table 11.3	Total economic value of ecosystem services	240
Table 12.1	EO sensors relevant to crops	250
Table 12.2	Crop-SI model	253
Table 12.3	Scales of crop forecasting	254
Table 12.4	Global and regional agricultural monitoring systems	256
Table 13.1	EO sensors relevant to irrigated horticulture	264
Table 13.2	Definition of major water use terms	266
Table 13.3	Values of C_n and C_d coefficients	266
Table 13.4	Landsat-5 images used in analysis	272
Table 13.5	Automatic weather station sites	273
Table 14.1	EO sensors relevant to pastures	283
Table 14.2	Description of NDVI metrics	285
Table 14.3	Supplementary metrics	285
Table 15.1	Potential responses of vegetation to grazing exclusion	305
Table 15.2	EO sensors relevant to rangelands	307
Table 15.3	Rangelands in Australia	313
Table 15.4	BioCondition indicators	316
Table 16.1	Forest area in Australia	325
Table 16.2	Native forest classes	325
Table 16.3	EO sensors relevant to forestry	328
Table 17.1	EO sensors relevant to carbon cycling	361
Table 18.1	Major bushfires in Australia	391

Table 18.2	EO sensors relevant to fire-related studies	393
Table 18.3	Current and potential uses of the Australian Flammability Monitoring System	410
Table 19.1	Land management practices with ongoing impact on biodiversity in Australia	432
Table 19.2	Biodiversity in Australia's terrestrial vegetation	433
Table 19.3	EO sensors relevant to biodiversity	434
Table 19.4	RPSB indicators	436
Table 19.5	EBV classes and candidates	436
Table 19.6	Policy tools	442
Table 19.7	Australian Biodiversity Conservation Strategy 2010–2030 Targets	443
Table 19.8	NSW Biodiversity Indicator Program	443
Table 19.9	VQA scoring	444
Table 20.1	Comparison of natural resource management models	452
Table 20.2	EO sensors relevant to sustainability	454
Table 20.3	Ecosystem services—challenges and opportunities	457
Table 20.4	EO capabilities relevant to ecosystem services	458
Table 20.5	Definitions of sustainability pillars	461
Table 20.6	Examples of ecosystem accounting measures	465
Table 20.7	Australian environmental economic accounts based on SEEA	469
Table 21.1	GEO projects	485
Table 21.2	Recommended reading	487

List of Excurses

Excursus 1.1 —Classifying Vegetation	4
Excursus 1.2 —Earth System Science	16
Excursus 3.1 —FAO Land Cover Classification System	61
Excursus 3.2 —Vegetation Assets, States and Transitions (VAST)	76
Excursus 4.1 —Plant Pigments	97
Excursus 5.1 —Lidar	109
Excursus 6.1 —Vegetation Height and Structure Map	127
Excursus 7.1 —Modelling Grazed Landscapes	144
Excursus 7.2 —Flux Towers	153
Excursus 8.1 —Composite Image Products	170
Excursus 8.2 —NSW State Vegetation Type Map (SVTM)	177
Excursus 8.3 —Fractional Cover	181
Excursus 9.1 —Australian Phenology Product	198
Excursus 9.2 —Budyko Framework	200
Excursus 10.1 —AussieGRASS	222
Excursus 10.2 —Water Resources Assessment	223
Excursus 11.1 —GEOGLAM RaPP	236
Excursus 11.2 —Learning from History	238
Excursus 12.1 —Graincast	254
Excursus 14.1 —EO-based Pasture Products	287
Excursus 14.2 —Integrated Biomass Estimation	291
Excursus 15.1 —VegMachine	314
Excursus 15.2 —Rangelands Biodiversity Monitoring Framework	317
Excursus 16.1 —Carnegie Spectranomics Project	336
Excursus 17.1 —The Carbon Cycle	354
Excursus 17.2 —Measuring Biosphere Productivity	358
Excursus 18.1 —Fire Detection Products	402
Excursus 19.1 —IUCN Red Lists of Threatened Species and Ecosystems	439
Excursus 19.2 —Vegetation Quality Assessment	444
Excursus 20.1 —Millennium Ecosystem Assessment	456
Excursus 20.2 —Global Sustainable Development Agreements	462
Excursus 20.3 —Global Footprint Network	463
Excursus 20.4 —System of Environmental Economic Accounting	466
Excursus 21.1 —Social-ecological Resilience	484

Introduction



This series of publications, *Earth Observation: Data, Processing and Applications*, comprises three volumes. Volume 1 in this series, *Data*, is presented as three sub-volumes, which together outline the basics of Earth Observation (EO) in terms of energy sources, data acquisition, sampling characteristics, image availability, data interpretation, and usage. Volume 2, *Processing*, (six sub-volumes) describes the various options involved with image representation, analysis, transformation, integration, and modelling, including details of relevant algorithms, with emphasis on their underlying mathematical and statistical principles. These volumes provide valuable background information for understanding specific applications of EO. They also define terminology used in Volume 3, *Applications*, which currently comprises two sub-volumes: 3A, Terrestrial Vegetation, and 3B, Surface Waters.

Volume 3A details how EO methods can be used to understand and monitor vegetation growing on land. The introductory sections in this sub-volume describe background topics that are relevant to maximising the value of EO for studies of terrestrial vegetation. Sections 1 to 3 below introduce the Australian vegetated environment in terms of topography, climate, ecoregions, land use, and vegetation dynamics, and some of the methods that have been developed to map and monitor it. Sections 4 to 7 respectively summarise attributes of foliage, plants, communities, and ecosystems that are relevant to EO-based studies. Sections 8 to 10 review EO-based methods that are relevant to vegetation mapping, monitoring, and modelling, while Sections 11 to 20 introduce specific application areas where EO datasets are being used in Australia. Section 21 concludes this sub-volume by looking ahead.

Contents

1	The Vegetated Landscape	3
2	The Australian Environment	21
3	Mapping Vegetated Landscapes	57

Background image on previous page: This view of the Australian continent (shown as Mercator projection) was created by merging colour-coded topography with relief shading using data acquired by the Shuttle Radar Topography Mission (SRTM; see Volume 1) in February 2002. Northeast slopes appear bright and southeast slopes appear dark, with green indicating low elevations, rising through yellow and tan to white for highest elevations

Source: NASA. (Retrieved from <https://earthobservatory.nasa.gov/images/5100/australia-shaded-relief-and-colored-height>)

1 The Vegetated Landscape

Vegetation plays a crucial role in regulating environmental conditions, including weather and climate. The amount of water and carbon dioxide in the air and the albedo of our planet are all influenced by vegetation, which in turn influences all life on Earth. Soil properties are also strongly influenced by vegetation, through biogeochemical cycles and feedback loops (see Volume 1A—Section 4). Vegetated landscapes on Earth provide habitat and energy for a rich diversity of animal species, including humans. Vegetation is also a major component of the world economy, through the global production of food, fibre, fuel, medicine, and other plant-based resources for human consumption.

In this section, we introduce vegetation in the context of:

- environmental factors and gradients (see Section 1.1);
- ecological units (see Section 1.2); and
- terrestrial ecosystems (see Section 1.3).

*Life did not take over the globe by combat,
but by networking.*
(Margulis and Sagan, from 'Microcosmos')

1.1 Environmental Factors and Gradients

All living organisms interact with the environment in which they live. The environment largely determines where organisms can survive and reproduce and, conversely, organisms modify their environment over time to enhance their survival and prosperity.

Any element of the environment that influences living organisms is termed an environmental factor. While these factors are interrelated, they are generally discussed individually to discern the many and complex relationships that exist within the environment as a whole. These factors are generally subdivided into two categories:

- biotic—plants (see Excursus 1.1), animals (including humans), and microorganisms (see Section 1.1.1); and
- abiotic—climate, substrate, and disturbances (see Section 1.1.2).

Environmental factors can have a wide and diverse range of potential influences on vegetation establishment and development. Different species have varying tolerances to various environmental factors, their impact being most critical at the stages of reproduction and establishment. While a balance is important in any environment, all factors can interact and compensate for changes in other factors. For example, nutrient requirements for certain plants are altered when growing in shade rather than in full sun (see Section 4).

Some environmental factors, such as parent material, can change abruptly, but most change gradually with boundary conditions being defined along a gradient (see Section 1.1.3). Both abrupt and gradual environmental changes are generally evidenced by corresponding changes in the distributions and assemblages of species, although gene flow and genetic drift may explain cases where the range of species ends abruptly along smooth environmental gradients (Polechova and Barton, 2015).

Excursus 1.1—Classifying Vegetation

Classification of life forms was introduced in Volume 1A—Section 3.4. The Plant Kingdom has been further sub-divided on the basis of morphology and reproductive characteristics. Many classifications have been developed for this purpose based on the basis of different distinguishing traits. The terms referenced in this text are summarised in Table 1.1.

Vascular plants are those with vascular tissues (xylem and phloem) to distribute water and nutrients, such as ferns, grasses, shrubs, trees, and other flowering plants. Please note that some photosynthesising forms of algae, such as blue-green algae, are now regarded as bacteria, not plants (see Volume 3B).

Table 1.1 The plant kingdom

Internal transport mechanism	Reproductive mechanism	Group	Sub-group
Non-vascular	Non-flowering and non-seeding plants; reproduce via spores	Algae and fungi	Mostly aquatic algae (see Volume 3B)
		Bryophytes	Liverworts
			Hornworts
			Mosses
Vascular	Non-flowering and non-seeding plants; reproduce via spores	Pteidophytes	Psilophytes (two small genera of fern-like plants)
			Lycophytes (club mosses; five genera with > 1000 species)
			Sphenophytes (horsetails; one genus)
			Pterophytes (ferns; ~9,000 species)
	seeding plants with roots, stems, and leaves	Gymnosperms (non-flowering; seed not enclosed in fruit)	Cycads (one genus: <i>Cycadaceae</i> ; < 200 species)
			Ginkgo (one genus and species: <i>Ginkgo biloba</i>)
			Conifers (two orders: Pinales and Taxale; ~200 species)
			Gnetophytes (three genera; ~ 100 species)
		Angiosperms (flowering plants with enclosed seeds)	Monocotyledons (one seed leaf; ~60,000 species)
			Dicotyledons (two seed leaves; ~200,000 species)

Adapted from: Campbell *et al.* (2006) Table 29.1

A number of categorisation schemes have been proposed to differentiate plants on the basis of defined traits and/or their function within an ecosystem, such as:

- life form—based on perennating bud height (Raunkiaer, 1904):
 - ♦ phanerophytes (> 50 cm above ground);
 - ♦ chamaephytes (< 50 cm above ground);
 - ♦ hemicryptophytes (at soil surface);
 - ♦ cryptophytes (below ground or under water);
 - ♦ therophytes (annuals from seed); or
 - ♦ epiphytes (in the air, on other plants);
- growth form—based on general appearance or habit:
 - ♦ woody (trees and shrubs); or
 - ♦ herbaceous (grasses), see Section 5.1);
- habitat—based on growing conditions:
 - ♦ terrestrial;
 - ♦ aquatic;
 - ♦ aerial; or
 - ♦ lithophytes;
- water content—based on moisture requirements:
 - ♦ hydrophytes (aquatic);
 - ♦ helophytes (marsh);
 - ♦ hygrophytes (moist); or
 - ♦ xerophyte (dry);
- leaf loss—based on foliage longevity:
 - ♦ evergreen;
 - ♦ semi-deciduous; or
 - ♦ deciduous; and
- longevity—based on plant life span:
 - ♦ annual;
 - ♦ biennial; or
 - ♦ perennial.

1.1.1 Biotic factors

Biotic environmental factors include all living and dead organisms. These components can be broadly divided into three categories on the basis of their environmental function:

- producers (autotrophs)—plants that convert solar energy into food via photosynthesis;
- consumers (heterotrophs)—animals and fungi that rely on producers (or other consumers) for food; and
- decomposers (detritivores)—microorganisms that decompose producers and consumers to recycle their components.

For an environment to be stable, it is important that the size of these groups be balanced with respect to the available resources. Producers extract basic nutrients from the abiotic environment and thereby increase their availability to consumers and decomposers. While plant growth assists soil formation, plant decomposition enriches the humic content of soil. Decomposers play an essential role by recycling nutrients within the environment. In excess, however, they may threaten the livelihood of both consumers and producers. Likewise, an excess of consumers would devour all producers and threaten their own existence.

Both within and between these sub-categories, various types of interactions can exist between a given pair of organisms. As summarised in Table 1.2, some interactions benefit one or both organisms, while others are detrimental to one organism. The dynamics of these interactions, however, continuously change with the number of organisms, limitations in resources, and variations in abiotic factors.

By virtue of their consumption, heterotrophs use the productivity of autotrophs to survive. Animals, for example, eat plants (or other animals). These dependencies create a unidirectional flow of energy within the local environment in the form of food. Most environments involve a series of dependent organisms that can be represented as a food chain. These may be interlinked to form a food web in large ecosystems, with simple food webs tending to occur in less stable ecosystems (see Section 1.2.3).

Consumers assist producers by spreading reproductive material (called propagules: seeds, spores or cuttings). Propagules can be either carried by animals or eaten then excreted. These processes allow species to be introduced into new areas, which may offer more appropriate conditions and/or less competition. Plant species can also migrate to new regions when propagules are dispersed by wind or water.

Migration enables organisms to escape an unfavourable environment and, over time, can lead to large scale environmental changes. Dispersion and emigration may occur to avoid a variety of undesirable outcomes, such as competition for mates or resources, inbreeding, or aggression resulting from overcrowding.

Various interactions can also occur between producers, which can help or hinder other species. Canopy vegetation in a tropical rainforest, for example, creates microclimates that allow more delicate species to survive. In other environments, such as pine forests, dominant species expand to use all available resources (space, light, water, and nutrients) to the exclusion of less vigorous plants.

Table 1.2 Interactions between biotic components

Interaction	Impact	Description	Example
Mutualism	Favourable	Mutual interdependence between species for growth and survival	Bees pollinating flowers while collecting nectar; Legumes growing with soil bacteria to fix nitrogen
Commensalism	Neutral	One species depends on another without cost to the host	Epiphytes growing on host plants; Exocarpus deriving nutrients from eucalypt roots
Co-operation	Neutral	Both species can live separately but choose to help each other	Predator alarm systems between species
Exploitation	Unfavourable	Host species is harmed by dependent species	Parasites and predators
Competition	Unfavourable	One species is suppressed by the presence of another	Often related to restricted resources such as light or food
Amensalism	Unfavourable	One species is inhibited by another without benefit to either	Animal traffic on vegetation

Vegetative cover also modifies the impact of specific abiotic factors. For example, vegetation tends to reduce throughfall, that is, the amount of atmospheric water reaching the ground. Different forest types allow different degrees of throughfall: 50–80% in broadleaf evergreen forests compared with 90% in eucalypt forests. A reduction in throughfall reduces the risk of soil erosion and enables vegetation to absorb more moisture. Similarly, vegetative cover insulates the soil from solar radiation and reduces soil temperature and evaporation. It also offers protection from wind and water erosion (see Section 11.5).

Many plants growing in harsh environments have adapted to those conditions and developed mechanisms to withstand climatic extremes and capitalise on favourable conditions. The continued survival of all biotic components depends on adaptation to changes in abiotic factors.

Some plant and animal species are opportunistic—they can exploit the conditions created by disturbance and rapidly colonise the modified environment. Opportunistic plants are often labelled ‘weeds’ and can present significant challenges to land managers (see Sections 2.3.2 and 15).

Indicators serve four basic functions: simplification, quantification, standardisation and communication. They summarise complex and often disparate sets of data and thereby simplify information. They should be based on comparable scientific observations and statistical measures. They also need to provide a clear message that can be communicated to, and used by, decision makers, stakeholders and the general public.

(UNEP, 2003)

1.1.2 Abiotic factors

Abiotic factors will be discussed in terms of three groups:

- climate—precipitation, rainfall, light, and wind (see Section 1.1.2.1);
- edaphic factors—parent material, soil, and topography (see Section 1.1.2.2); and
- disturbances—fire, storms, and tectonic activity (see Section 1.1.2.3).

1.1.2.1 Climatic factors

Climate is the net result of a delicate balance of physical factors, being expressed as the pattern in weather over a period of time (see Volume 1A—Section 4). It is primarily concerned with parameters such as light, temperature, precipitation, humidity, evaporation, and wind. While these factors largely shape global vegetation distribution, their impact on the local environment is moderated by vegetative cover. Conversely, vegetation has been recognised as one of the primary indicators of land condition (see Section 7.3) and can affect regional climate and weather patterns due to the release of water vapour during photosynthesis (Green *et al.*, 2017).

Although the ‘macroclimate’, or major climate forces, is easily discernible, its manifestation can vary considerably within short distances and with changes in edaphic factors (see Section 1.1.2.2) and the blanketing effect of vegetation cover. The principal climatic factors impacting terrestrial vegetation are:

- Precipitation—while the frequency, abundance, and form of precipitation collectively shape biome distribution, vegetation cover also influences the volume of water that can penetrate the soil to recharge the water table (see Volume 3B). Furthermore, precipitation responds to vegetation changes through land-atmosphere feedbacks (Sheil and Murdiyarso, 2009; Li *et al.*, 2018). Precipitation is viewed as the major limiting factor in terrestrial ecosystems and has been correlated with Gross Primary Productivity (GPP; see Section 7.4).
- Humidity—the proportion of atmospheric moisture, directly impacts—and is impacted by—biota. Relative humidity within dense vegetation, for example, is higher than in the air above bare ground due to plant transpiration (see Section 5.2.3). Such variations create microclimates for a range of organisms.

- Temperature—both affects and is affected by vegetation cover. Vegetation distribution is directly related to air and soil temperature. Evapotranspiration, the release of water vapour into the atmosphere from evaporation and transpiration, increases with air temperature (see Sections 5.2.3 and 7.5). Thermal profiles, showing changes in temperature with height above ground, reveal that the greatest variations in the diurnal temperature range occurs near the soil due to absorption of solar energy (see Section 7.5). Shading by vegetation can also modify thermal profiles (Pianka, 2011). For example, forest vegetation can reduce heat loss by 1–3° over the annual cycle. A suitable temperature range for a species generally coincides with a particular geographic range but pockets of atypical temperature can result from topographic variations, or microclimates created by other plants, allowing species to exist outside their usual range.
- Light levels—also help to determine species distribution. Many plant species are light dependent, with seedlings relying on canopy gaps to become established beneath overstorey plants. Those species occupying the upper stratum of vegetation, whose foliage is more exposed to solar radiation, generally contain the largest portion of total biomass. Diurnal and seasonal cycles determine photoperiodism, the length of day or night, which is also important for germination and flowering.
- Wind—aspect and topography determine the degree of exposure, and hence the effect of wind, at a given location. Vegetation growing along ridgelines is generally smaller and less densely spaced as a result of exposure to wind, although ridgelines are also generally more eroded, which results in shallower and drier soils to support growth. Diurnal cycles in wind are also common, with greatest velocities being observed shortly after solar noon. The interaction of wind and vegetation (fuels) is also a key driver in the rate of spread for fire (see Section 18). Forest vegetation can reduce wind run by 50–75%, and thus mollifies the impact of harsh environments on more sensitive plants. A similarly protective microclimate can be observed in aquatic vegetation, where the presence of periphyton (such as algal films) reduces water turbulence (see Volume 3B).

Disturbance by fire, defoliation, or other agents is an intrinsic and necessary part of the function of most terrestrial ecosystems—a mechanism for reversing declining rates of nutrient cycling or relieving stand stagnation.
(Aber and Melillo, 1991)

1.1.2.2 Edaphic factors

Edaphic factors include the physical landform, geological substratum (or parent material) and soil. Although modified by altitude and aspect, the trends in vegetation across elevation gradients are quite marked, with interacting factors including soil depth, temperature, and effective rainfall having the greatest influence.

The effect of soils on vegetation distribution is secondary to that of climate. Within a given climate, however, much of the variation in soil and vegetation is caused by the substratum. Soils characteristics impact water availability, nutrient status, and soil depth. Topographic factors, such as slope and aspect,

can create microclimates that suit particular species. The major edaphic factors influencing the distribution of terrestrial vegetation are:

- Parent material—whereas climatic boundaries are generally gradational, parent material boundaries are often sharp, causing a very marked change in species. The substratum can also have pronounced effects on vegetation in extreme climates, such as the very dry or very cold, where soil development tends to be slow. Similarly, there is a marked effect on vegetation where the parent material contains an excess of particular mineral compounds, such as dolomite. In this way, highly distinctive parent material can underlie similar soils and vegetation even in areas with different climates.

- Soil—results from the interaction of climate and vegetation on the substratum, but it is often very difficult to separate soil from the substratum. Being developed over a period of time, certain characteristics of soil will be indicative of past and present local environments. Nutrient status tends to be reflected in the age of a soil with the older, degraded soils generally only supporting poor quality vegetation. Nonetheless, there are many examples of plant adaptations to relatively poor soils. Soils have a very complex physical/biological system, being the action site for the decomposers in nutrient cycling. Physical properties, such as pore size, will affect the infiltration rate of light rain. Such soil factors can also potentially limit root penetration and thus moisture availability to plants.
- Topography—changes in altitude are accompanied by evident changes in vegetation. Increasing altitude generally parallels decreasing temperature and, often, reduced soil depth. In many ways, the climatic changes involved with increased altitude are similar to those involved with increasing latitude. Aspect can enhance or diminish altitudinal changes in vegetation. For example, in the Southern Hemisphere, the more sheltered eastern and southern facing aspects experience a smaller diurnal temperature range than the more exposed western and northern faces so are generally cooler and moister. Soil depth and moisture tend to increase with decreasing slope. Lower, shallower, and less exposed slopes generally have deeper, alluvial deposits with improved fertility and moisture, and support a greater variety of larger, more productive plants. Topography also determines drainage, the ease with which water in the landscape flows or percolates into the ground.

The richness and diversity of ecosystems are in large measure the result of the pattern of their disturbances: the storms, fires, droughts, frosts and the animals, following occasional major events. Because the disturbances occur unexpectedly, systems need to be able to cope with them when they do occur. Coping capacity is another term for being resilient and it is maintained and enhanced by continuous exposure to all the different kinds of disturbances across all locations at different timescales under which the systems developed. Novel disturbances due to humans often exceed the evolved resilience of ecosystems, frequently reaching tipping points into new, mostly unwanted states.
(Walker, 2019)

1.1.2.3 Disturbances

Disturbances are responsible for the largest environmental changes in the shortest time. They often result in ‘ecological drift’, a major change in the composition and/or structure of an ecosystem (Jackson, 1968; Bowman and Wood, 2009; Bowman and Haberle, 2010). The primary disturbances shaping terrestrial vegetation distribution are:

- Fire is a significant ecological factor in many locations and its effects can be long lasting. The impact of fire on an environment varies with its frequency, intensity, and environmental history. Various indigenous plant species in Australia have developed mechanisms, such as epicormic shoots and lignotubers, that accelerate recovery from fire. Many species also have hard seed coatings

that require fire to germinate. Serotiny describes the adaptation by some plants in which seed release occurs in response to an external trigger factor, such as fire (pyriscence), even when the parent plant is killed by fire. Fire changes the light and moisture environments and acts as a nutrient recycling process, which may promote germination. This is particularly important in dry conditions where decomposition rates are slow. The ash bed bequeathed by fire also provides a fertile environment for establishment of seedlings. Not surprisingly, fire-adapted plant traits tend to dominate in areas that experience high fire incidence. Given its frequency in some landscapes such as Australia, however, Jurkis (2015) questions the classification of fire as a disturbance.

- Storms or wild weather is a form of environmental disturbance that involves excessive rain and wind. Apart from lightning strikes, the primary impacts of storms on vegetation are flooding and windthrow. While most plants benefit from additional moisture, a massive excess of moisture can overwhelm the requirements of many species. Combined with loosened soil and strong winds, saturated substrates often result in uprooted vegetation and consequent damage to other organisms. In sloping ground, saturation also accelerates erosion and invites landslides. The environmental damage resulting from extreme weather is often substantial and widespread. While never welcomed, such changes allow environments to re-establish, often on a more stable underlying landscape.
- Tectonic activity, such as earthquakes and volcanoes, are expressions of movement within or between tectonic plates (see Volume 1A—Section 3). Earthquakes release energy from strained fault planes along tectonic plate boundaries. This energy creates major upheaval on the Earth's crust and generates tsunami when the fault lies beneath the ocean. Volcanoes introduce new mineral matter into the atmosphere and lithosphere from the Earth's interior. When viewed from a sufficiently long timeframe, both types of tectonic activity refresh the environment on the surface of Earth. When measured in terms of human life however, recovery from such massive damage is extremely slow.
- Anthropogenic disturbances that drive vegetation and ecosystem change include land clearing for agriculture and urban development, invasive species, altered disturbance regimes and altered hydrological and biogeochemical cycles. Human-induced changes in ecosystems have reached all corners of the globe and the rates of impact are increasing exponentially as human population density increases (see Sections 19 and 20).

The precise impact of these factors on any environment will depend on the prevailing climatic and edaphic conditions. Human activity causes significant disturbance to ecosystem function and declines in biodiversity, both locally and globally. While some plant species are opportunistic, exploiting the conditions created by disturbance to rapidly colonise the modified environment, others are susceptible to local extinction. EO-based time series analyses are particularly suited to assessing the impact of disturbances on terrestrial landscapes (see Section 9 and Volume 2D).

Resilient systems are learning systems. ...Trying to prevent one disturbance completely, in the name of keeping a system safe, actually reduces its resilience.
(Walker, 2020)

1.1.3 Environmental gradients

Environmental factors, both biotic and abiotic, change with space and time. In many landscapes, the natural distribution of botanical species is closely related to the environmental gradients of elevation, latitude, soils, and fire (Kessell, 1979, Billings, 1970). While it is convenient to draw clear boundaries on maps showing vegetation distribution, welldefined transitions rarely occur in nature. Changes in species composition are often very gradual and can result in a variety of mixtures along the way (see Section 1.3).

A population of organisms with a particular genetic form resulting from genetic sorting is called an ecotype. This can be considered as a subspecies with particular environmental adaptations or preferences for survival. Ecotypes of the same species can interbreed without detrimental consequences.

A gradual change in ecotypes is called an ecocline and is often related to changes in climate (since parent material changes tend to occur more abruptly; see Section 1.1.2.2). Examples of ecoclines include:

- thermocline—a temperature gradient;
- halocline—a salinity gradient; and
- chemocline—a chemistry gradient (see Volume 3B).

Ecoclines and ecotypes allow a given species to increase its geographic range by extending the interactions that can occur with its environment. In time, a greater geographic range is likely to provide a greater chance of survival for that species.

Hybrid zones, where the ranges of species or evolutionarily significant units overlap and result in genetic hybridisation, are considered a sensitive marker of environmental change (Taylor *et al.*, 2015). Changes in hybrid zone extent may shift, expand, or originate in new locations in response to changing environmental conditions.

Despite all of our accomplishments we owe our existence to a six-inch layer of topsoil and the fact that it rains. (Farm equipment association of Minnesota and South Dakota)²

1.2 Ecological Units

Dynamic vegetated landscapes cover around 80% of the terrestrial surfaces of our planet. Vegetation can be considered in terms of three broad spatial scales:

- single plants (or individuals) and groups of similar individuals (or populations; see Section 1.2.1);
- gatherings of populations—communities (see Section 1.2.2); and
- tapestries of communities—ecosystems (see Section 1.2.3).

A key concept in ecology is that of habitat, namely that region where an organism likes to live. Organism habitats are generally defined by both biotic and abiotic factors. Biotic factors are important in the structure and pattern of vegetation communities (see Sections 1.1.1). The term habitat can also be used to refer to the locality of a community, in which case it is defined by abiotic environmental factors (see Sections 1.1.2). A related concept is the ecological niche, which describes the habitat characteristics as well as the role of the organism in its environment, including ecological functions, services, and interactions (see Section 1.2.3). For organisms to coexist they either become tolerant of each other, and sympatric, or they compete until one species is eliminated. Successive generations may also hybridise.

The combined impact of vegetative scale on the landscape is to create a mosaic of colour and texture. This mosaic not only informs about vegetation type and condition but also highlights the underlying landscape characteristics. With an understanding of the dominant environmental factors that shape this mosaic, landscapes can be better managed to improve productivity and sustainability.

1.2.1 Individuals and populations

Populations comprise collective groups of individuals from the same species—that is, genetically related plants that can interbreed. Sexual reproduction results in more genetically diverse offspring than asexual means and generally delivers the benefits of greater capacity for seed dispersal, more offspring, and higher success rates for germination and establishment. While individuals are characterised by those traits that are common to their species, namely germination, growth habit, and reproduction (see Section 5), populations are characterised by the way they group, persist, disperse, and survive (see Section 6). Thus, measures of size, density, age composition, and growth rate are used to compare populations and derive management concepts such as carrying capacity.

Populations change with the survival rates of individuals and the immigration or emigration of species. A stable population of plants achieves a balance between the initial life cycle phases of seed dispersal, germination, and establishment, and the final stages of senescence and death. The success or failure of a plant largely depends on the impact of the environment on the rates of its vital processes.

Disturbance of one kind or another plays a crucial role in all ecosystems. (Walker, 2020)

² Sourced from NSW Soil Knowledge Network: <http://www.nswskn.com/soil-quotes-2/>

1.2.2 Communities

At any locality, the assemblage of plant species into a community results from the cumulative, extended impact of all environmental factors on the ambient flora (Billings, 1970). Vegetation communities can indicate past environmental conditions or events (such as forest fires or past climatic cycles), soil conditions (physical structure, salts, or available nutrients) and the presence of predatory animals. A community is characterised by a sense of order in that it has an identity over and above the individual and population, and functions as a unit via combined metabolic processes (Odum, 1971).

The distribution of organisms in their environment, and their interaction with that environment, creates a structure that ecologists call 'pattern' (Hutchinson, 1953). Within a vegetation community, pattern principally occurs in terms of vertical layering or stratification, horizontal segregation or zonation, and

periodicity of organism life cycles (see Section 6). Stratification is obvious in many natural communities, for example, as different species and individuals adapt to different levels of light and moisture. For example, some species, such as acacias, typically play a transitory role in Australian forests, with both high light requirements and lack of dominance, while others are destined to exert dominance but may require specific conditions for establishment. Certain pathogens can also influence species distribution in favourable locations.

The transition between two communities is called an ecotone, that is, the region where they can integrate and develop hybrid species. Such transitions may be sharp or gradual, as evidenced by changes in vegetation colour or height, or represent a change in species prevalence. Species diversity may increase within ecotones as members of both communities co-exist.

Wherever the reign of nature is not disturbed by human interference, the different plant species join together in communities, each of which has a characteristic form, and constitutes a feature in the landscape of which it is a part. These communities are distributed and grouped together in a great variety of ways, and, like the lines on a man's face, they give a particular impress to the land where they grow. The species of which a community is composed may belong to the most widely different natural groups of plants. The reason for their living together does not lie in their being of common origin, but in the nature of the habitat. They are forced into companionship not by any affinity to one another but by the fact that their vital necessities are the same.

A knowledge of the communities which exist within the realm of plants is of great importance in many ways. It throws a strong light, not only on the mutual relations of the different species which are associated by common or similar needs, but also on the connection of plant-life with local and climatic conditions and with the nature of the soil. It may fairly be said that in the various zones and regions of our earth no kind of phenomenon so thoroughly gives expression to the climate and the constitution of the soil as the presence of particular plant-communities which prevail, and, accordingly, the determination and description of such communities constitutes an important part of geography.

(Anton Kerner Von Marilaun, 1895)

1.2.3 Ecosystems

The total biotic and abiotic factors of an environment present in a particular area is called an ecosystem. It represents the net result of all interactions of biotic and abiotic factors (see Sections 1.1.1 and 1.1.2). Ecosystems are self-regulatory and self-sustaining systems. Other definitions include:

- a symbol of structure and function of nature (Tansley, 1935); and
- the smallest structural and functional unit of nature or environment (Odum, 1969).

The concept of an ecosystem has also been referred to as biocoenosis (Möbius, 1877) or biogeocoenosis (Sukachev, 1944; Puzachenko, 2008), or a biome. More recently the term biome has been used to describe a group of terrestrial ecosystems (Whittaker, 1962; see Section 1.3.2).

Ecosystem boundaries are often indistinct and overlapping. They can be large or small, short term or long term, natural or artificial. A stable ecosystem achieves and maintains balance between living organisms, water, atmosphere, and earth (Patten, 1991). The process of balancing food webs and chains to maintain a stable ecosystem is called homeostasis.

Table 1.3 Ecosystem processes

Ecosystem Process	Function		Balanced Ecosystem	Unbalanced Ecosystem
	Landscape/Community	Organisms		
Water Cycle	Maintain healthy aquifers, surface water flows and soil moisture	Maintain adequate moisture for all metabolic processes	Precipitation replenishes soil moisture to support plant growth and decomposition, recharges stores in aquifers, collects in reservoirs for consumers to drink, and/or flows into rivers and oceans to support aquatic life	Precipitation insufficient for plant growth, and runs off ground surface removing soil and propagules Moisture insufficient for healthy nutrient levels
Energy Flow	Conserve energy levels and maintain stores	Maintain adequate energy for all metabolic processes	Producers capture sufficient solar energy for the needs of consumers and decomposers	Insufficient solar energy captured by producers to feed consumers and decomposers
Mineral Cycle	Maintain nutrient availability and replenish stores; avoid excessive availability	Maintain adequate nutrients for all metabolic processes	Nutrients from plant and animal wastes are recycled by decomposers to enrich the soil	Plant and animal wastes are not decomposed but washed away or burnt Excessive nutrients encourage dominance
Community Dynamics	Balance population growth with available resources	Maintain adequate diversity in communities	High diversity of producers, consumers, and decomposers Size of populations suited to constraints of resources	Low diversity of producers, consumers, and decomposers Excessive competition for resources

Ecosystem services describe ecosystem changes in terms of their impact on human populations, that is the the services they deliver (see Section 20.3). Ecosystems can also be viewed in terms of their structure or function, and how these change over space and time. Some basic biological, physical and chemical processes sustain ecosystems. Four key ecosystem processes include:

- the water cycle—how and why water interacts with the ecosystem (see Section 7.6 and Volume 3B);
- the energy cycle—how energy flows drive ecosystems (see Section 7.5, including food chains/webs: see Section 1.1.1; productivity: see Section 7.4; and the carbon cycle: see Section 17 and Excursus 1.2);
- the mineral cycle—how biogeochemical nutrients are recycled by the ecosystem, including the nitrogen cycle (see Volume 1A—Section 4.2); and
- community dynamics—how communities develop and change within an ecosystem, including diversity patterns, succession, and cybernetics (see Sections 1.3.3, 6 and 19).

Balanced and unbalanced ecosystems are compared in terms of these processes in Table 1.3.

Analysis of energy cycling underlies many modelling applications of EO for terrestrial vegetation (see Section 10.2). Solar energy is absorbed by vegetation during the process of photosynthesis and this stored energy can be likened to a battery (see Section 5.2.1). Estimates of the proportion of photosynthetically active radiation (PAR) that is absorbed by vegetation are used to quantify both carbon dioxide usage and water loss due to evapotranspiration. Such estimates are further discussed in Section 7. Monitoring of vegetation productivity is particularly important as an indicator of the sustainability of environments, land management practices and lifestyles (see Sections 7.4 and 19).

It is hard for us to accept that the way natural ecosystems work is exemplary: plants synthesise nutrients which feed herbivores; these in turn become food for carnivores, which produce significant quantities of organic waste which give rise to new generations of plants. But our industrial system, at the end of its cycle of production and consumption, has not developed the capacity to absorb and re-use waste and by-products. We have not yet managed to adopt a circular model of production capable of preserving resources for present and future generations, while limiting as much as possible the use of non-renewal resources, moderating their consumption, maximising their efficient use, re-using and recycling them.

(Pope Francis, 2015)

1.3 Terrestrial Ecosystems

1.3.1 Biogeography and biodiversity

Biogeography addresses the question of why plants grow where they do. This discipline combines aspects of biology and geography to determine how organisms are distributed in space and time. An understanding of the patterns of biogeography enables biodiversity to be protected.

The term 'biodiversity' describes the collective variety within all forms of life on Earth. The highest levels of biodiversity generally occur in warm, moist environments. On a global scale, the highest levels of biodiversity, in terms of both marine and terrestrial plants and animals, occur at the equator, then biodiversity declines with latitude. Across the landscape, biodiversity is highest near coastlines and declines towards the interior of most land masses.

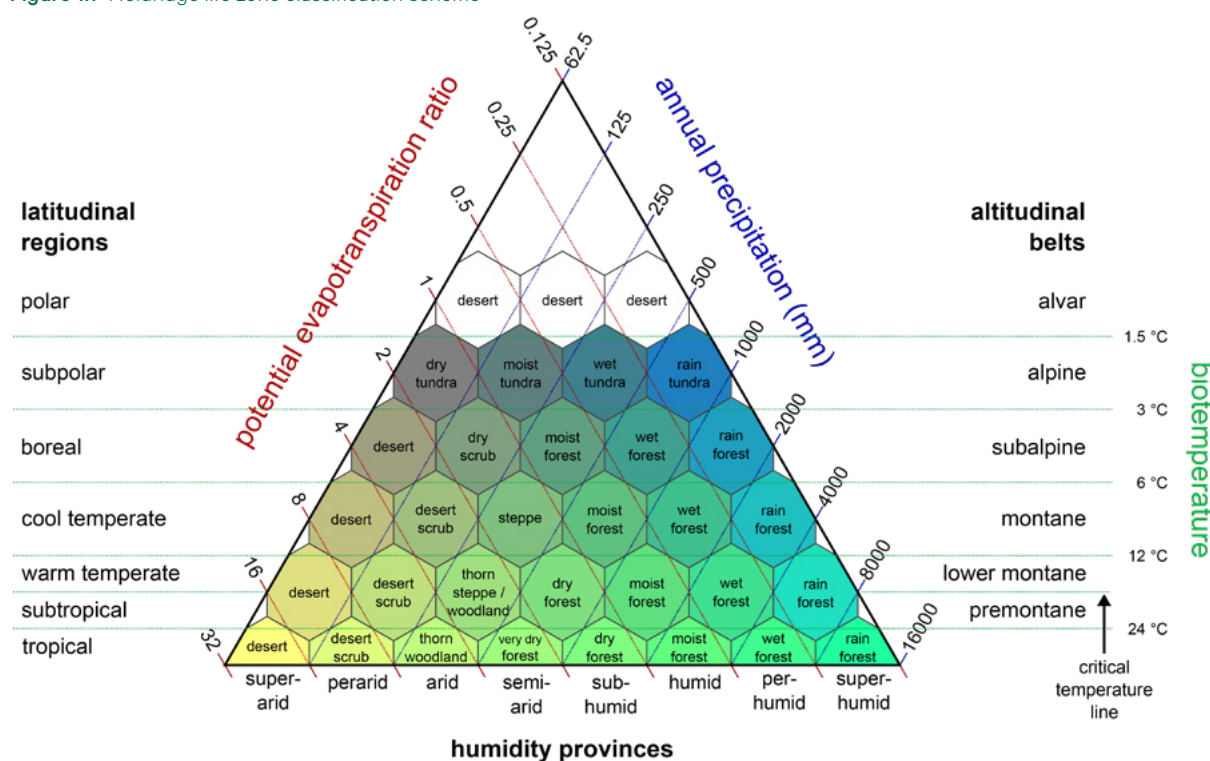
Biodiversity indicates both the stability and productivity of an ecosystem. Stable environments, such as large tropical islands, maintain high levels of biodiversity, and high species richness enhances the efficient use of resources and therefore productivity (Fjeldsa and Lovett, 1997). However, the conservation of biodiversity may not necessarily be maximised by prioritising management efforts in stable environments. Ecosystems exposed to more variable environmental conditions may contain species with greater tolerance of extremes and higher resilience to a rapidly changing climate (see Section 1.1.2.3).

1.3.2 Major habitat zones

Biomes are contiguous areas with similar climate and geography and as such they represent major habitat types. A variety of schemes have been developed to describe ecosystem zones on the basis of climatic and topographic factors such as latitude and humidity, and sometimes altitude. The categories defined by Holdridge (1947) are illustrated in Figure 1.1. Temperature gradients are strongly related to changes in latitude and altitude, so temperature and precipitation alone are often used to map the distribution of vegetation as in Whittaker's classification (Whittaker, 1962; see Figure 1.2).

*All are but parts of one stupendous whole,
Whose body Nature is, and God the soul.
(Alexander Pope, from 'An Essay on Man', 1733)*

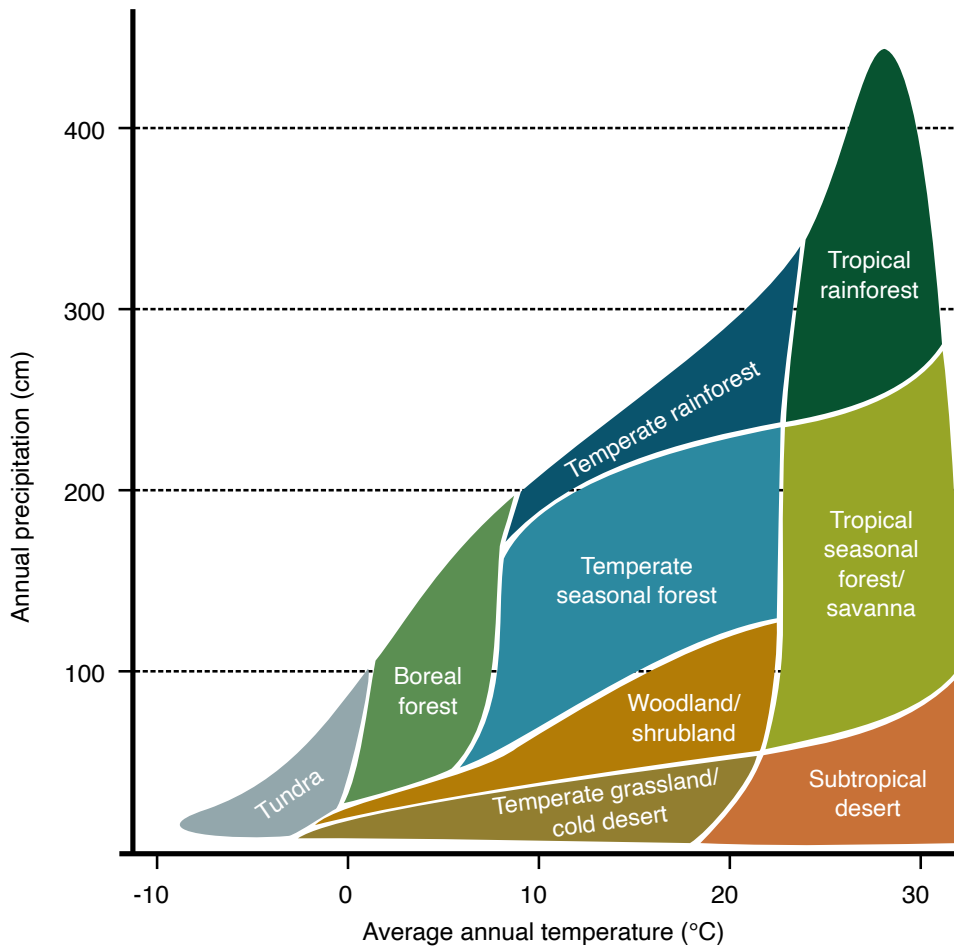
Figure 1.1 Holdridge life zone classification scheme



Source: Peter Halasz, Wikimedia Commons. (Retrieved from https://commons.wikimedia.org/wiki/File:Lifezones_Pengo.svg)

Figure 1.2 Whittaker's biome classification

Average annual temperature and precipitation needed for different categories of common terrestrial biomes



Source: Navarras, Wikimedia Commons. (Retrieved from https://commons.wikimedia.org/wiki/File:Climate_influence_on_terrestrial_biome.svg)

The Terrestrial Ecoregions of the World (TEOW) project offered a biogeographic regionalisation of terrestrial biodiversity on Earth (Olson *et al.*, 2001). This World Wildlife Fund (WWF) product defines 14 major habitat types, or biomes, which were further sub-divided into 867 terrestrial ecoregions. The major habitat types are listed in Table 1.4. These ecoregion categories form the basis of the Interim Biogeographical Regionalisation of Australia (IBRA) as illustrated in Figure 2.13. Eight of these major habitat types exist in Australia.

A biome-based, global land cover map derived from MODIS imagery was released by the International Geosphere-Biosphere Program (IGBP, 1990; Friedl *et al.*, 2010a, 2010b; Channan *et al.*, 2014—see Section 1.4). This series of global mosaics use the MODIS land cover product (MCD12Q1) in the IGBP Land Cover Type classification of 17 terrestrial vegetation categories. The Global Environmental Stratification (GEnS), a high resolution bioclimate stratification based on multivariate statistical clustering (Metzger *et al.*, 2013; Metzger, 2018), has been proposed as an appropriate framework for global monitoring networks (Jongman *et al.*, 2017; see Section 19.3). More recently, a global stratification of World Ecosystems, derived from the integration of temperature, moisture, landform, and vegetation/land use datasets, was developed by Sayre *et al.* (2020) and used to assess the representation of ecosystems in global protected areas (see Section 19).

Table 1.4 Terrestrial biomes

Biome		Description	
Number	Name	Latitude	Humidity
1	Tropical and subtropical moist broadleaf forest	Tropical, Subtropical	Humid
2	Tropical and subtropical dry broadleaf forest	Tropical, Subtropical	Semi-humid
3	Tropical and subtropical coniferous forest	Tropical, Subtropical	Semi-humid
4	Temperate and broadleaf and mixed forest	Temperate	Humid
5	Temperate coniferous forest (Northern Hemisphere only)	Temperate	Humid to semi-humid
6	Boreal	Sub-arctic	Humid
7	Tropical and subtropical grasslands, savannas and shrublands	Tropical, Subtropical	Semi-arid
8	Temperate grasslands, savannas and shrublands	Temperate	Semi-arid
9	Flooded grasslands and shrublands	Temperate to Tropical	Fresh or brackish water inundated
10	Montane grasslands and shrublands	Temperate to Tropical	Alpine to Montane
11	Tundra	Polar	Arid
12	Mediterranean forests, woodlands and scrub or sclerophyll forests	Temperate Warm	Semi-humid to semi-arid with winter rainfall
13	Deserts and xeric shrublands	Temperate to Tropical	Arid
14	Mangrove	Subtropical, Tropical	Saltwater inundated

1.3.3 A dynamic tapestry

Perhaps the most significant characteristic of our planet is that it is constantly changing. The ceaseless processes of growth and decay, erosion and deposition, precipitation and evaporation are driven by diurnal, lunar, seasonal, and annual cycles, irregularly punctuated by disturbances. Everything changes with time; some changes just take more time than others.

To cope with the inevitable changes in abiotic components of the environment, individual species need to adapt to the changes or become vulnerable to more competitive species. Mechanisms for adaptation for a given species include reordering its existing genetic resources to create new gene combinations that would be better suited to the changed environment or developing new genes via mutations in a process known as genetic drift.

A community or ecosystem can be thought of as developing via the gradual, and somewhat theoretical, process of ecological succession. As detailed in Section 6.6, this process involves a variable series of stages:

- a pioneer community colonises a new area; then
- one or more seral communities replace the previous community; until
- a climax community reaches a form of homeostasis which persists for a relatively long time period.

- The number of seral communities, the lifespan of each stage, and the degree of homeostasis varies with individual ecosystems. Ecologists also distinguish between primary succession (very long term development on new landscapes) and secondary succession (shorter term development on disturbed landscapes).

One part of analysing vegetation dynamics involves reconstructing former distributions. Palynology analyses pollen and spores found in fossils and sediments to track the composition and diversity of past landscapes.

The dynamic nature of the Earth somewhat complicates the task of natural resource mapping and necessitates regular revision of maps to quantify the type and extent of change. Knowledge of where and how changes are occurring can contribute to an understanding of why they occur and, possibly, how the extent of change can be managed. One approach that has emerged in recent decades for exploring the dynamic nature of Earth is Earth System Science (ESS; see Excursus 1.2). This integrated view of our planet is particularly valuable when observing large scale processes and relates readily to the perspective of Earth Observation (EO).

The only constant in life is change.

Excursus 1.2—Earth System Science

Further Information: Xiao *et al.* (2019)

Earth System Science (ESS) is a multidisciplinary approach to understanding the structure and function of Earth as an integrated system (Steffen *et al.*, 2020). Large scale monitoring of our planet is closely related to the concept of Earth being an essentially closed system, and comprising four integrated spheres:

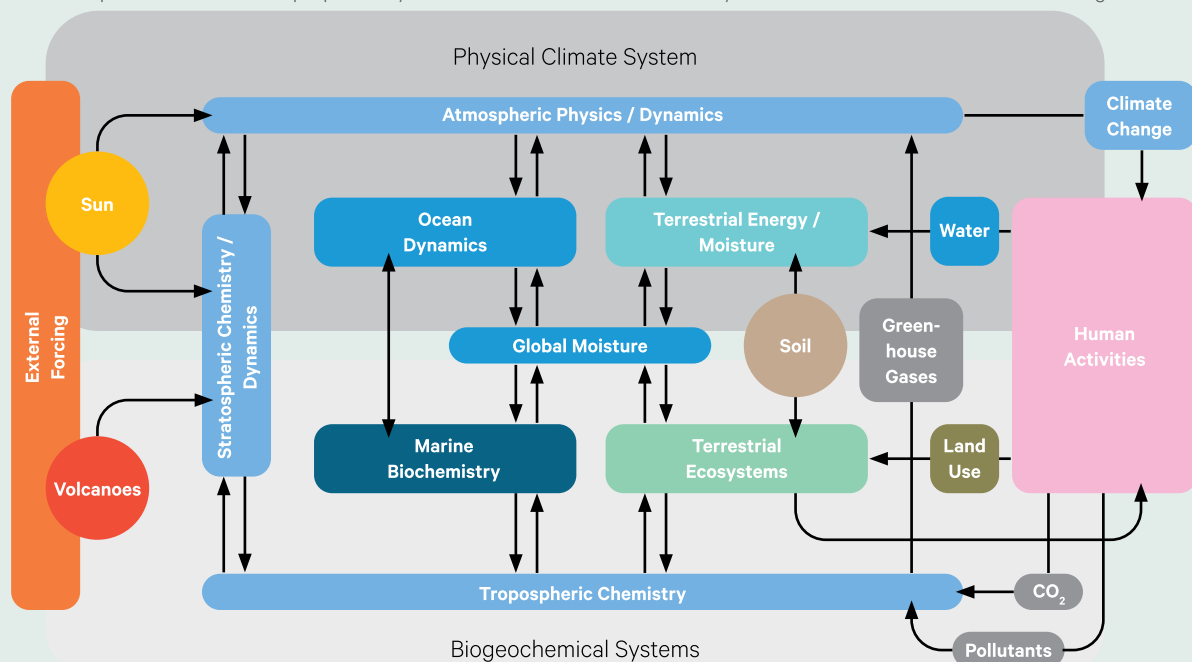
- atmosphere—gaseous protective envelope;
- hydrosphere—surface water, groundwater and atmospheric water;
- geosphere—solid components of Earth (land and under water); and
- biosphere—all forms of life (see Volume 1A—Section 4.1).

These spheres exchange energy and matter via the ongoing cycling of energy, water, and minerals (see Volume 1A—Section 4.2). One conceptual framework that links major Earth components with the processes that impact them is shown in Figure 1.3 (NRC, 1986). Since all processes on Earth are interrelated and impacted by human activities, updated representations show human activity (anthroposphere) as a fully integrated and interacting sphere (Steffen *et al.*, 2020).

Of particular relevance to terrestrial vegetation is the terrestrial carbon cycle which describes the continual exchange of carbon between the biosphere, the geosphere, and the atmosphere (see Volume 1A—Section 4). As detailed in Section 17 below, the typical components of this process are usefully described in terms of carbon fluxes (flows) and stocks (volume of reserves; see Figure 1.4). EO-based analyses can be used to estimate the carbon fluxes of gross primary production (GPP), ecosystem respiration (ER), net primary production (NPP), net ecosystem production (NEP), and net biome production (NBP), and the carbon stocks of aboveground biomass (AGB) and soil organic carbon (SOC; Xiao *et al.*, 2019). The use of EO to quantify and monitor the terrestrial carbon cycle is detailed in Sections 7.4, 10.2.2, and 17 below.

Figure 1.3 Processes and interactions within Earth System Science

This conceptual framework was proposed by Francis Bretherton and is commonly referenced as the NASA Bretherton diagram.



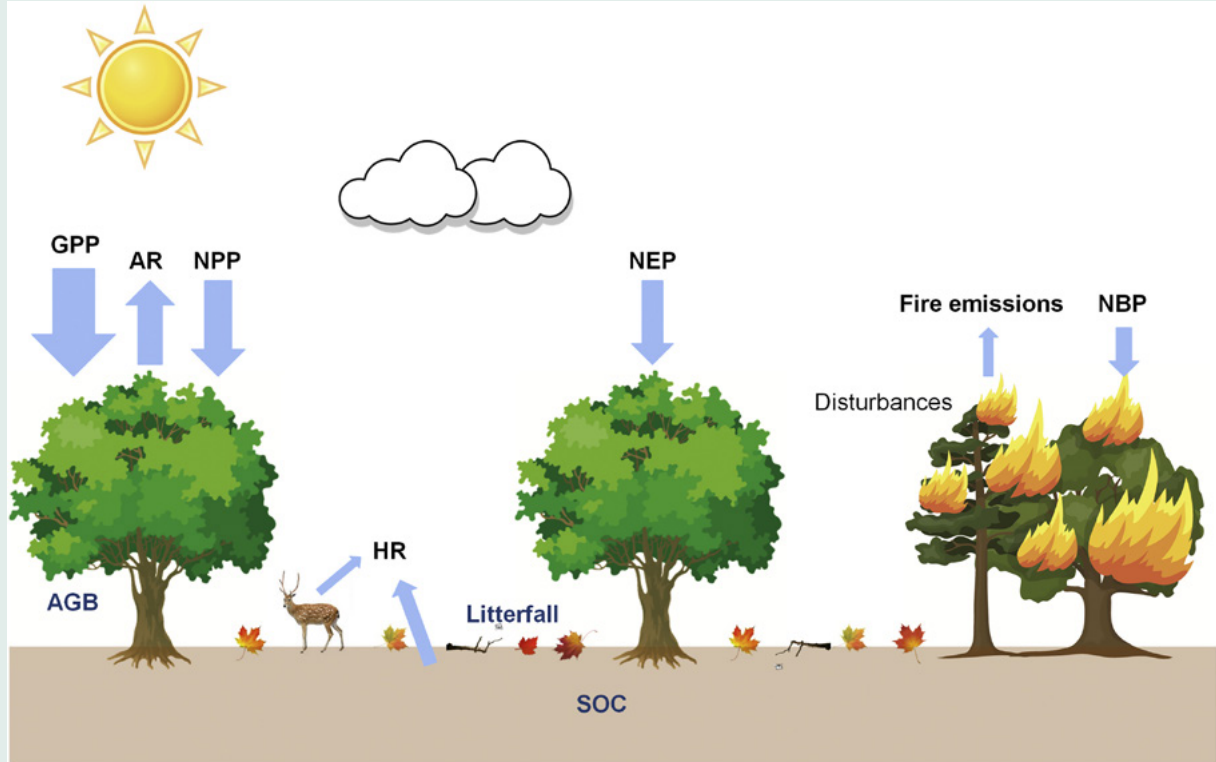
Adapted from: NASA at <http://education.gsfc.nasa.gov/experimental/all98invproject.site/pages/tr/inv4-3.abstract.html>

Figure 1.4 Terrestrial carbon cycle

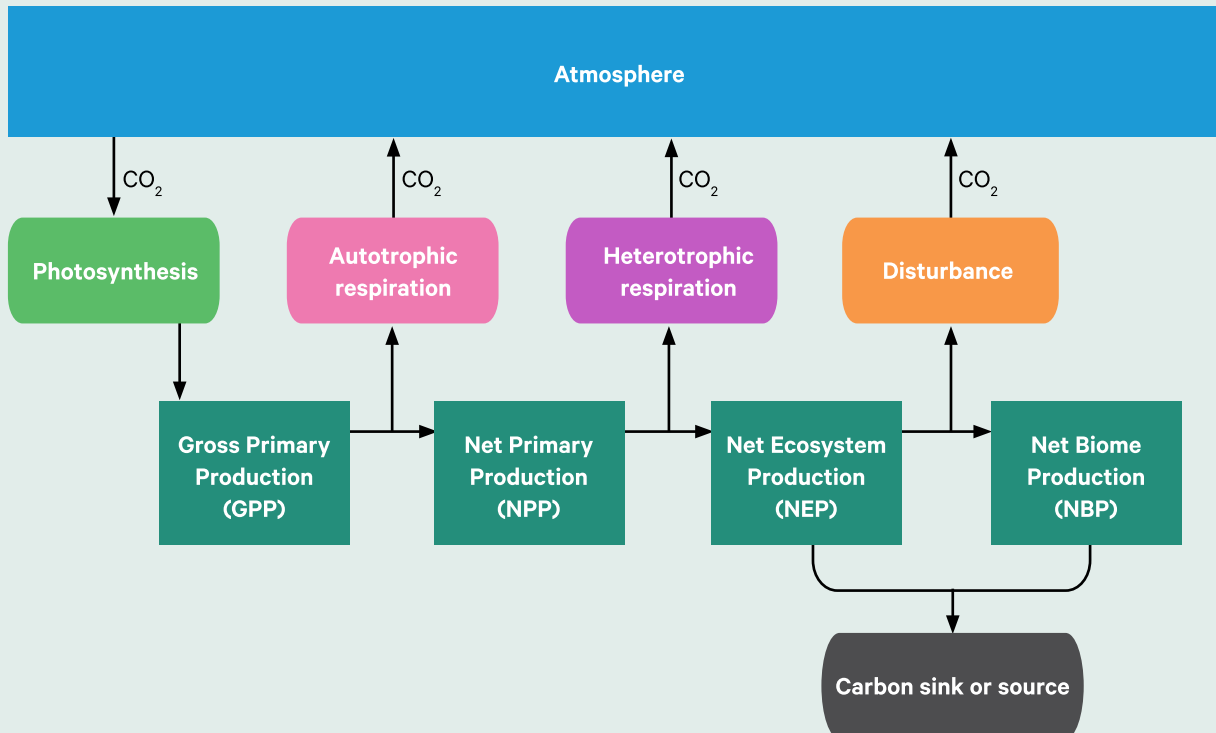
a. Carbon fluxes and stocks

Fluxes: GPP: Gross Primary Productivity; AR: Autotrophic Respiration; NPP: Net Primary Productivity; HR: Heterotrophic Respiration; NEP: Net Ecosystem Productivity; NBP: Net Biome Productivity;

Stocks: AGB: Above Ground Biomass; SOC: Soil Organic Carbon;



b. Computation of fluxes

Source: a. Xiao *et al.* (2019) Figure 1

1.4 Further Information

Global Climate Map

Global Environmental Stratification: <https://datashare.is.ed.ac.uk/handle/10283/3089>

Global Terrestrial Ecosystem Maps

IGBP: IGBP (1990)

Friedl *et al.* (2010)

Global Land Cover Facility: <http://glcf.umd.edu/data/lc/>

WWF: Olson *et al.* (2001)

Terrestrial ecoregion definitions: <https://www.worldwildlife.org/biome-categories/terrestrial-ecoregions>

Map: https://c402277.ssl.cf1.rackcdn.com/publications/347/files/original/Ecoregions_Map.pdf?1345734390

Global ecological zones: <http://www.fao.org/geonetwork/srv/en/main.home?uuid1/42fb209d0-fd34-4e5e-a3d8-a13c241eb61b>

1.5 References

- Aber, J.D., and Melillo, J.M. (1991). *Terrestrial Ecosystems*. Saunders College Publ., Holt, Rinehard and Winston Inc, Orlando, Florida.
- Billings, W.D. (1970). *Plants, Man and the Ecosystem*. 2nd Edn. Wadsworth Publ. Co., Belmont. 160pp. ISBN 0-333-14633-6.
- Bowman, D., and Wood, S.W. (2009). Fire-driven land cover change in Australia and W.D. Jackson's theory of fire ecology of southwest Tasmania. Chapter 8 in *Tropical Fire Ecology: Climate change, land use, and ecosystem dynamics* (Ed: Cochrane, M.). pp 87–106. Springer, New York. doi:10.1007/978-3-540-77381-8_4
- Bowman, D.M.J.S, and Haberle, S.G. (2010). Paradise burnt: how colonizing humans transform landscapes with fire. *PNAS*, 107(50), 21234–21235. doi:10.1073/pnas.1016393108
- Campbell, N.A., Reece, J.B., and Meyers, N. (2006). *Biology*. 7th edn. Pearson Education Australia. ISBN 1 74103 386 1.
- Channan, S., Collins, K., and Emanuel, W.R. (2014). *Global mosaics of the standard MODIS land cover type data*. University of Maryland and the Pacific Northwest National Laboratory, College Park, Maryland, USA.
- Fjeldsa, J., and Lovett, J.C. (1997). Biodiversity and environmental stability. *Biodiversity and Conservation*, 6(3), 315–323.
- Friedl, M.A., Sulla-Menashe, D., Tan, B., Schneider, A., Ramankutty, N., Sibley, A., and Huang, X. (2010a). MODIS Collection 5 global land cover: Algorithm refinements and characterization of new datasets. *Remote sensing of Environment*, 114(1), 168–182.
- Friedl, M.A., Strahler, A.H., Hodges, J., Hall, F.G., Collatz, G.J., Meeson, B.W., Los, S.O., Brown De Colstoun, E., and Landis, D.R. (2010b). *ISLSCP II MODIS (Collection 4) IGBP Land Cover, 2000–2001*. ORNL DAAC, Oak Ridge, Tennessee, USA. <https://doi.org/10.3334/ORNLDAAC/968>
- Green, J.K., Konings, A.G., Alemohammad, S.H., Berry, J. Entekhabi, D., Kolassa, J., Lee, J.E., Gentine, P. (2017). Regionally strong feedbacks between the atmosphere and terrestrial biosphere. *Nature Geoscience*, 10(6), 410–414. doi:10.1038/NGEO2957
- Holdridge, L.R. (1947). Determination of world plant formations from simple climatic data. *Science*, 105(2727), 367–368. doi:10.1126/science.105.2727.367. PMID 17800882.
- Hutchinson, G.E. (1953). The Concept of Pattern in Ecology. *Proceedings of the Academy of Natural Sciences of Philadelphia*, 1–12.
- IGBP (1990). *The International Geosphere–Biosphere Programme: A study of global change—The initial core projects, IGBP Global Change Report no. 12*. International Geosphere–Biosphere Programme. Stockholm, Sweden.
- Jackson, W.D. (1968). Fire, air, water and earth—an elemental ecology of Tasmania. *Proceeding of Ecological Society of Australia*, 3, 9–16.
- Jongman, R.H.G., Skidmore, A.K., (Sander) Mücher, C.A., Bunce, R.G., Metzger, M.J. (2017). Global Terrestrial Ecosystem Observations: Why, Where, What and How?. In: *The GEO Handbook on Biodiversity Observation Networks* (Eds: Walters M., and Scholes R.). Springer, Cham.
- Jurskis, V. (2015). *Firestick Ecology*. Connor Court Publishing, Ballarat.
- Li, Y., Piao, S., Li, L.Z.X., Chen, A., Wang, X., Ciais, P., Huang, L., Lian, X., Peng, S. Zeng, Z. Wang, K., and Zhou, L. (2018). Divergent hydrological responses to large-scale afforestation and vegetation greening in China. *Sciences Advances*, 4(5), eaar4182. doi:10.1126/sciadv.aar4182
- Kerner von Mariluan, A. (1895). *The natural history of plants: Their forms, Growth, Reproduction, and Distribution*. Translated by Oliver, F.W. (1902) and published by Blackie and Son, Ltd, Glasgow and Dublin. <https://doi.org/10.5962/bhl.title.18169>

- Kessell, S.R. (1979). *Gradient Modelling: Resource and Fire Management*. Springer-Verlag, New York.
- Laseron, C.F. (1953). *The Face of Australia*. Angus and Robertson. 244 p.
- Metzger, M.J. (2018). *The Global Environmental Stratification: A high-resolution bioclimate map of the world* [dataset]. The University of Edinburgh. <https://doi.org/10.7488/ds/2354>.
- Metzger, M. J., Brus, D. J., Bunce, R. G. H., Carey, P. D., Gonçalves, J., Honrado, J. P., Jongman, R.H.G., Trabucco, A., and Zomer, R. (2013). Environmental stratifications as the basis for national, European and global ecological monitoring. *Ecological Indicators*, 33, 26–35.
- Möbius, K. (1877). *Die Auster und die Austernwirtschaft*. Hempte and Parey, Berlin.
- NRC (1986). *Earth System Science. Overview: A Program for Global Change*. National Research Council. National Academies Press.
- Odum, E.P. (1969). The Strategy of Ecosystem Development. *Science*, 164(3877), 262–270.
- Odum, E.P. (1971). *Fundamentals of Ecology*. 3rd edn. W.B. Saunder Co., Philadelphia.
- Olson, D.M., Dinerstein, E., Wikramanayake, E.D., Burgess, N.D., Powell, G.V.N., Underwood, E.C., D'Amico, J.A., Itoua, I., Strand, H.E., Morrison, J.C., Loucks, C.J., Allnutt, T.F., Ricketts, T.H., Kura, Y., Lamoreux, J.F., Wettengel, W.W., Hedao, P., and Kassem, K.R. (2001). Terrestrial ecoregions of the world: a new map of life on Earth. *Bioscience*, 51(11), 933–938.
- Patten, B.C. (1991). Network ecology: indirect determination of the life–environment relationship in ecosystems. In *Theoretical Ecosystem Ecology: The Network Perspective* (Eds: Higashi, M., and Burns, T.P.), London, Cambridge University Press. pp. 288–351.
- Pianka, E.R. (2011). *Evolutionary Ecology*. 7th edn. Eric R. Pianka.
- Polechova, J., and Barton, N.H. (2015). Limits to adaptation along environmental gradients, *Proceedings of the National Academy of Sciences*, 112(20), 6401–6406.
- Pope Francis (2015). *Laudato Si': On Care for Our Common Home*. Catholic Truth Society, London.
- Puzachenko, J. (2008). Biogeocoenosis as an Elementary Unit of Biogeochemical Work in the Biosphere. In *Global Ecology, Volume 1 of Encyclopedia of Ecology* (Eds: S.E. Jørgensen and B.D. Fath). Elsevier, Oxford. pp. 396–402
- Raunkiær, C. (1904). Om biologiske Typer, med Hensyn til Planternes Tilpasninger til at overleve ugunstige Aarstider. *Botanisk Tidsskrift*. 26 p. XIV.
- Sayre, R., Karagulle, D., Frye, C., Boucher, T., Wolff, N.H., Breyer, S., Wright, D., Martin, M., Butler, K., Van Graafeiland, K., Touval, J., Sotomayor, L., McGowan, J., Game, E.T., and Possingham, H. (2020). An assessment of the representation of ecosystems in global protected areas using new maps of World Climate Regions and World Ecosystems. *Global Ecology and Conservation*, 21, e00860. <https://doi.org/10.1016/j.gecco.2019.e00860>
- Sheil, D., and Murdiyarto, D. (2009). How forests attract rain: an examination of a new hypothesis. *BioScience*, 59(4), 341–347. <https://doi.org/10.1525/bio.2009.59.4.12>
- Steffen, W., Richardson, K., Rockström, J., Schellnhuber, H.J., Dube, O.P., Dutreuil, S., Lenton, T.M., and Lubchenco, J. (2020). The emergence and evolution of Earth System Science. *Nature Reviews Earth and Environment*, 1, 54–63. <https://doi.org/10.1038/s43017-019-0005-6>
- Sukachev, V.N. (1944). Principles of genetic classification in biogeocoenology. *Zhurnal Obshchei Biologii*, 5(4), 213–227, Moscow.
- Tansley, A.G. (1935). The use and abuse of vegetational terms and concepts. *Ecology*, 16(3), 284–307. doi:10.2307/1930070
- Taylor, S.A., Larson, E.L., and Harrison, R.G. (2015). Hybrid zones: windows on climate change. *Trends in Ecology and Evolution*, 30(7), 398–406.
- UNEP (2003). *Monitoring and indicators: designing national-level monitoring programmes and indicators*. Note by the Executive Secretary. Subsidiary Body on Scientific, Technical and Technological Advice, Convention on Biological Diversity, UNEP/CBD/SBSTA/9/10.
- Walker, B. (2019). *Finding Resilience*. CSIRO, Melbourne.
- Walker, B. (2020). Resilience: what it is and is not. *Ecology and Society*, 25(2), 11. <https://doi.org/10.5751/ES-11647-250211>
- Whittaker, R.H (1962) Classification of Natural Communities. *Botanical Review*, 28(1), 1–239. Reprinted (1977) New York, Arno Press.
- Xiao, J., Chevallier, F., Gomez, C., Guanter, L., Hicke, J.A., Huete, A.R., Ichii, K., Ni, W., Pang, Y., Rahman, A.F., Sun, G., Yuan, W., Zhang, L., Zhang, X. (2019). Remote sensing of the terrestrial carbon cycle: A review of advances over 50 years. *Remote Sensing of Environment*, 233, 111383. <https://doi.org/10.1016/j.rse.2019.111383>.



2 The Australian Environment

The Australian mainland is both the largest island and the smallest continent in the world, as well as the lowest and flattest land mass (see Section 2.1). In terms of land area, Australia is the sixth largest country after Russia, Canada, China, the USA and Brazil, and the only one of these to be encircled by water (GA, 2020a). Some basic information about Australia's location, dimensions, features and population is summarised in Table 2.1 (see also Figure 2.1).

Australia spans 31° of latitude, centred on 27.5° S (just below the Tropic of Capricorn, 23.43657° S—see Volume 2B—Figure 1.14), so experiences a wide range of climates, which can vary significantly from one year to the next (BoM, 2020a). Drought, floods, and cyclones are a natural part of Australia's climatic variation (see Section 2.2).

The Commonwealth of Australia is governed as a federation of six states (see Figure 2.1b; Western Australian: WA, South Australia: SA, Tasmania: TAS, Victoria: VIC, New South Wales: NSW, and Queensland: QLD), each of which is responsible for local land management and many public services. Territories that are not directly administered by specific states are either under federal control or granted the right to self-government (as occurs in the Northern Territory: NT, and the Australian Capital Territory: ACT; AG, 2020). The Commonwealth also governs some 12,000 smaller islands within its marine jurisdiction (see Volume 3B). Land in Australia is either:

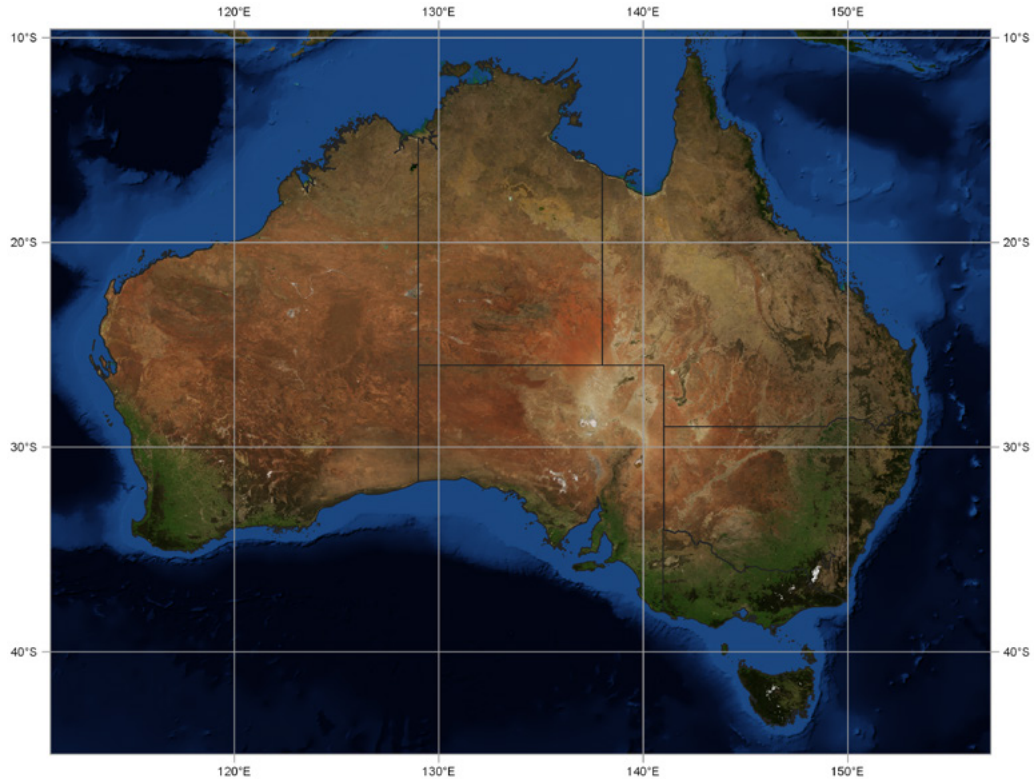
- owned by the 'crown' or government—crown land covers almost a quarter of the total land mass and is regulated by relevant State government legislation;
- leased by the crown to specified users for a defined purpose, such as mining or pastoral activities—leasehold land comprises around half the land area; or
- privately owned, including indigenous land tenure—freehold tenure accounts for nearly 30% of the land in Australia (Austrade, 2020).

In the sub-sections below, we introduce aspects of Australia's topography (see Section 2.1), climate (see Section 2.2), biota (see Section 2.3), ecoregions and fire patterns (see Section 2.4), and land use (see Section 2.5).

*... Flood, fire, and cyclone in successive motion
Complete the work the pioneers began
Of shifting all the soil into the ocean.
(James McCauley, from 'The True Discovery of Australia')*

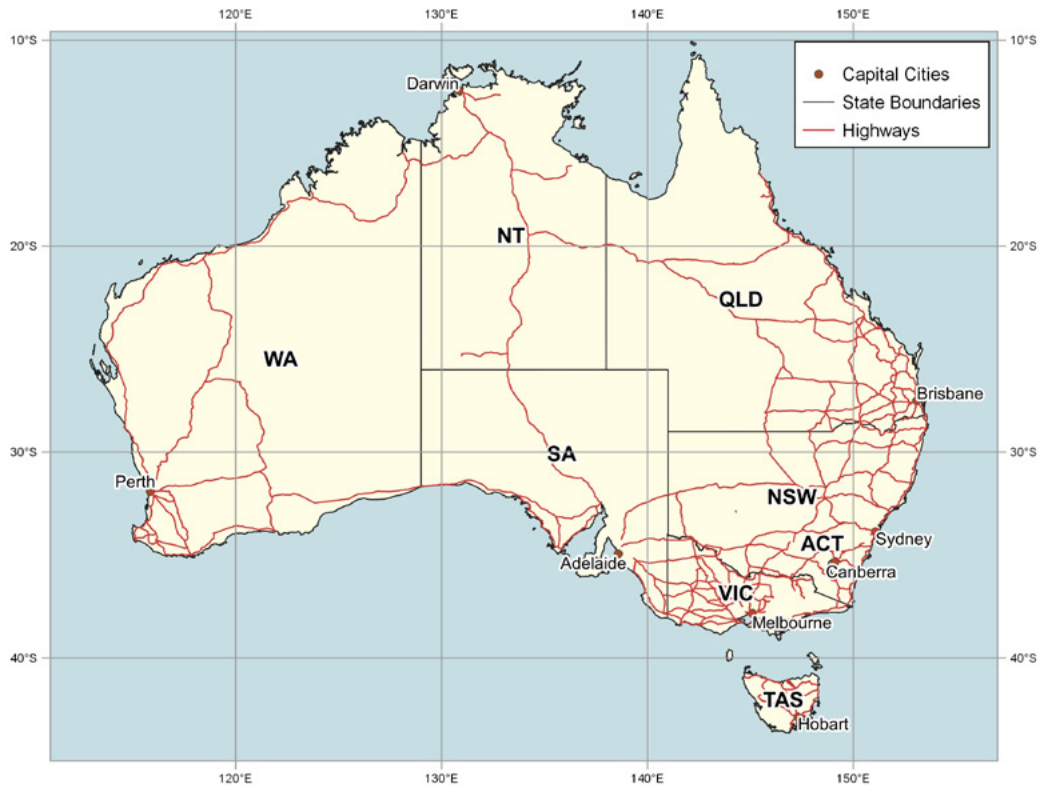
Figure 2.1 Australia

a. Next generation Blue Marble Image with topography and bathymetry, August 2004



b. Locational map (see also Volume 2B—Figure 1.14)

WA: Western Australian; SA: South Australia; TAS: Tasmania; VIC: Victoria; NSW: New South Wales; QLD: Queensland; NT: Northern Territory; ACT: Australian Capital Territory (not labelled but surrounds Canberra)



Source: Tony Sparks, Icon Water, using NASA Visible Earth imagery for figure a, and GA (2002) data for roads in figure b

Table 2.1 Geography and settlement of Australia

Characteristic		Details	Value
Area (sq. km; GA, 2020a)	Total, including islands	6th largest in world	7,688,287
	States and Territories, including islands	Western Australia (WA)	2,527,013
		Queensland	1,729,742
		Northern Territory (NT)	1,347,791
		South Australia (SA)	984,321
		New South Wales (NSW)	801,150
		Victoria	227,444
		Tasmania	68,401
		Australian Capital Territory (ACT) (including Jervis Bay)	2,452
Location	Northern Extremity	Cape York (Queensland)	10° 41' 21" S, 142° 31' 50" E
	Eastern Extremity	Cape Byron (NSW)	28° 38' 15" S, 153° 38' 14" E
	Southern Extremity	South East Cape (Tasmania)	43° 38' 40" S, 146° 49' 30" E
	Western Extremity	Steep Point (WA)	26° 09' 05" S, 113° 09' 18" E
Altitude	Highest	Mount Kosciuszko (NSW)	2,228 m
	Lowest	Lake Eyre (SA)	15 m below mean sea level
Climate	Annual Rainfall	Average	165 mm
	Temperature Extremes	Maximum recorded range	-23°C to 50.7°C
Water Features	Longest River	River Murray	2508 km
	Largest Lake	Lake Eyre (salt)	9690 sq. km
Land Cover	Arid and Semi-arid land	< 500 mm annual rainfall	~70%
	Arable land	Agricultural production	~6%
	Native Vegetation Cover	Including sparse arid vegetation	~90%
	Dominant land cover	Hummock Grasslands	23%
Population at 30/9/2019 (ABS, 2020)	Total	Australian Bureau of Statistics (ABS)	25,464,100
	States and Territories	New South Wales (NSW)	8,118,000
		Victoria (VIC)	6,629,000
		Queensland (QLD)	5,115,500
		Western Australia (WA)	2,630,600
		South Australia (SA)	1,756,500
		Tasmania (TAS)	535,500
		Australian Capital Territory (ACT)	428,100
Northern Territory (NT)	245,600		

2.1 Topography and Hydrology

A well-known Australian poetess, Dorothea Mackellar, aptly describes Australia as a ‘wide brown land’ (see Section 15.1). With an average elevation of less than 300 m, barely 6% of the continent exceeds 600 m. The current topography of Australia has been formed from ongoing erosion and sedimentation by wind and water over hundreds of millennia, resulting in large areas of flat, infertile land (see image on page before Section 1). The topography of mainland Australia can be described in terms of four major landform regions (see Figure 2.2):

- coastal plains—narrow, sandy fringes along the east coast. These plains are relatively fertile and well-irrigated.
- eastern highlands—adjacent to the coastal plains, these run continuously for nearly 4,000 km from northern Queensland through NSW and into Victoria, and ultimately reappear in Tasmania. On the Australian mainland, these highlands are known as the Great Dividing Range, which directs rain onto the coastal plains and separates east-flowing from west-flowing rivers.
- central lowlands—stretch from the Gulf of Carpentaria in the north to the Great Australian Bight in the south, and include large parts of western Queensland and NSW, northwest Victoria and most of SA. These constitute 25% of the mainland, comprise flat, sedimentary material and contain large areas of desert.
- western plateau—or peneplain, covering one third of the continent and large parts of SA, NT, and WA, and composed of igneous and metamorphic rocks.

The distribution of soils in the Australian landscape has been mapped in terms of major soil types using the Australian Soil Resource Information System (ASRIS; McKenzie *et al.*, 2012; CSIRO, 2014; see Figure 2.3 and Section 3.3.1), or as soil attributes in the Soil and Landscape Grid of Australia (TERN, 2020). The Australian Soil Classification defines a national standard for classifying soils (Isbell and NCST, 2021).

National DEM available for Australia are listed in Table 2.2. The Australian Hydrological Geospatial Fabric (more commonly referred to as ‘the Geofabric’; BoM, 2020b; see Section 2.6 and Volume 2D—Excursus 13.2) defines important hydrological features including rivers, waterbodies, catchments, and aquifers. By accurately defining the spatial locations and dimensions of these features and their interconnections, water storage, movement, and use through the landscape can be monitored and modelled. In particular, by enforcing drainage conditions based on an accurate, national Digital Elevation Model (DEM) within a hierarchy of drainage areas, the boundaries of topographic drainage divisions and river regions are reliably mapped at a range of scales (see Figure 2.4). Two major drainage basins are:

- Lake Eyre Basin—Australia’s largest endorheic (closed) drainage basin, covering around 1.2 million km² in SA, NT, Queensland and NSW (DAWE, 2019); and the
- Murray-Darling Basin—the largest and most permanent river system in southeastern Australia, within SA, Queensland, NSW and Victoria (MDBA, 2013).

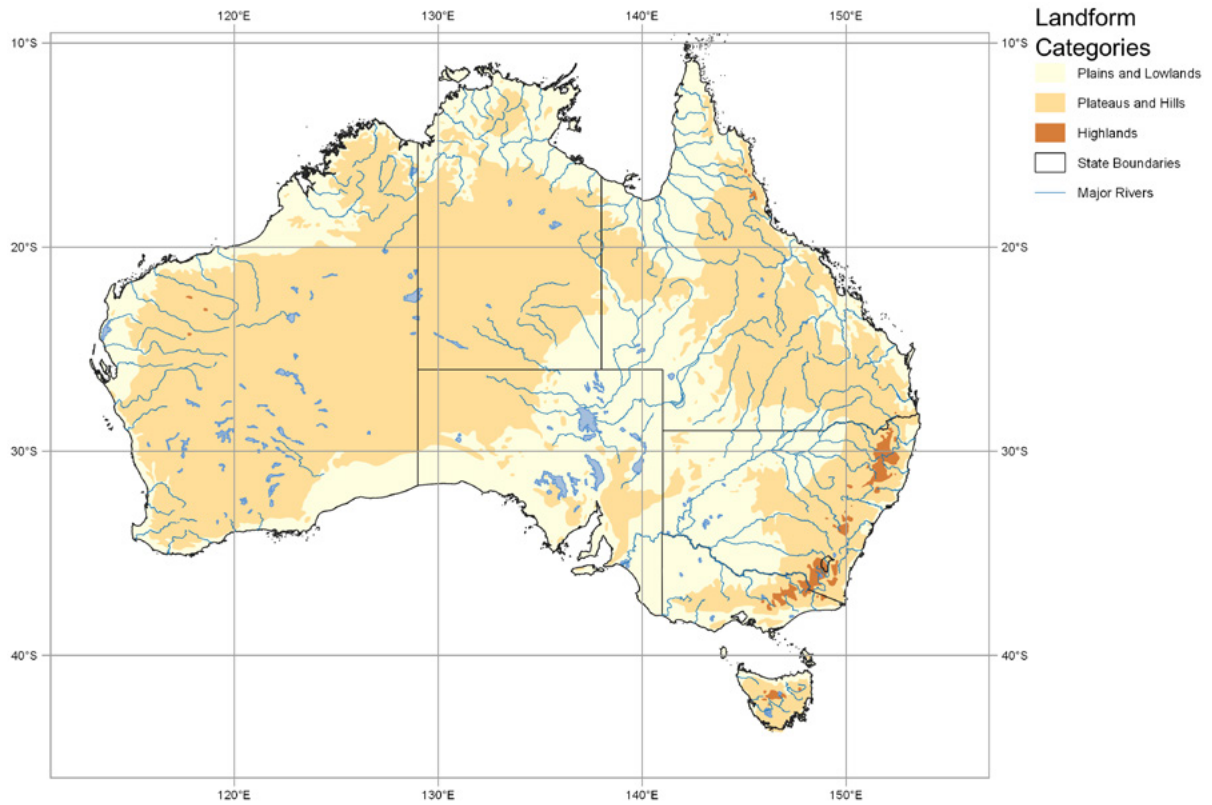
Table 2.2 Australian DEM

Name	Spatial resolution (m)	Based on
GEODATA 9-second DEM and D8 Flow Direction Grid 2008 (DEM-9S) v3	250	Elevation data at 1:100,000 and 1:250,000 cartographic scales
SRTM 3-second DEM v1.0	90	Shuttle Radar Topographic Mission, 2000
SRTM, 1-second DEM v10	30	Shuttle Radar Topographic Mission, 2000
Lidar 25 m grid	25	236 Lidar surveys between 2001 and 2015
Lidar 5 m grid	5	236 Lidar surveys between 2001 and 2015

Source: GA (2019)

Figure 2.2 Major landform categories

Note that the blue waterbodies in central Australia are ephemeral salt lakes.



Source: Tony Sparks, Icon Water, using data from GA (2002) for waterbodies

25

Figure 2.3 Australian Soil Resource Information System (ASRIS)

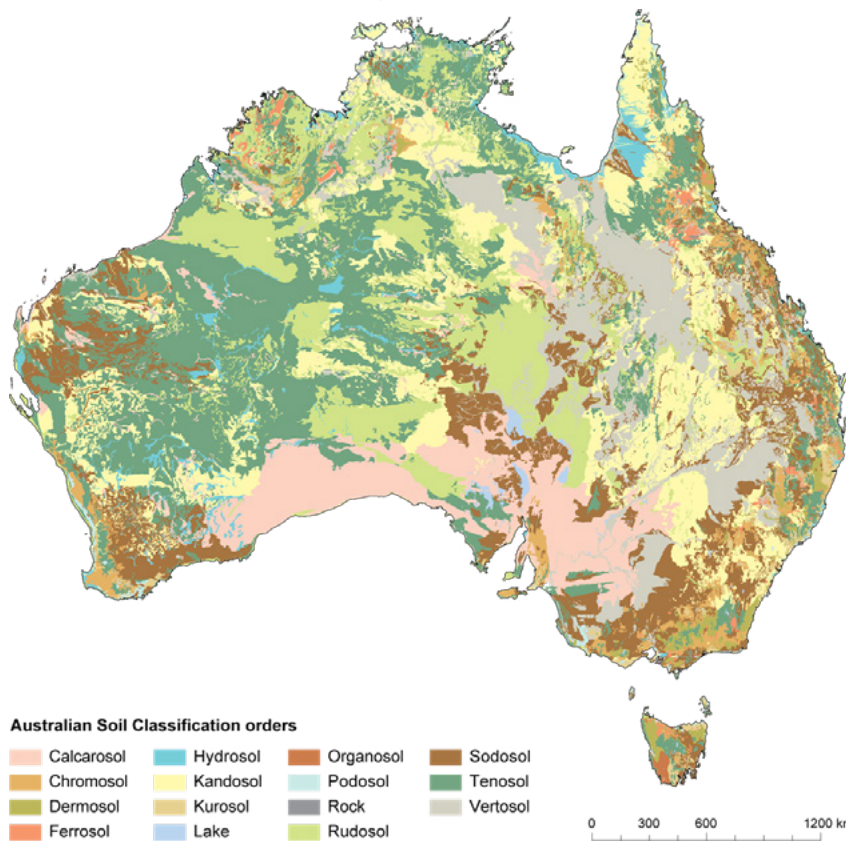
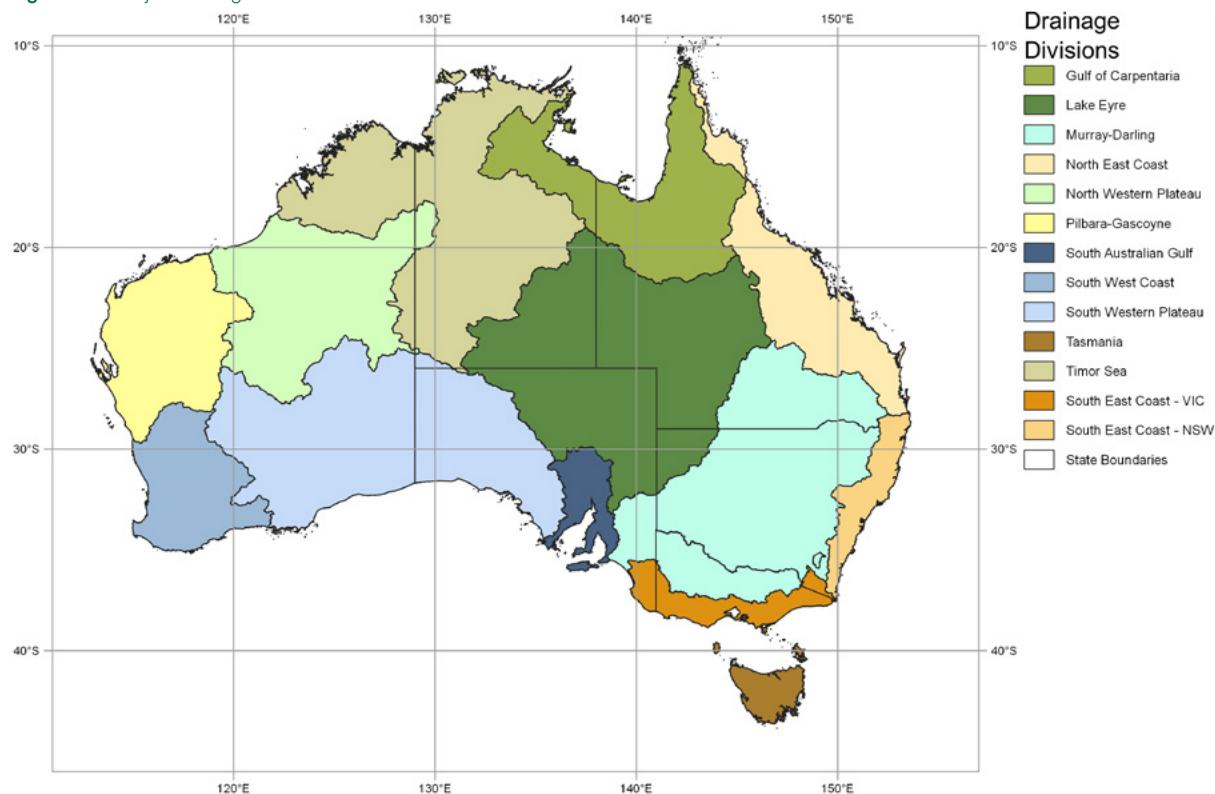


Figure 2.4 Major drainage basins



Source: Tony Sparks, Icon Water, using data derived from the Geofabric Hydrology Reporting Catchments product (BoM, 2020c)

Most of Australia’s rivers do not carry a permanent supply of water and around half drain inland, often terminating in ephemeral salt lakes (see Volume 1A—Excursus 5.1). The major river system, formed by the Murray, Darling, and Murrumbidgee Rivers, is in southeast Australia and forms part of the boundary between NSW and Victoria (see Figure 2.2). The catchment for this river system, the Murray-Darling Basin (MDB; see Figure 2.4), serves as Australia’s major food production region (see Section 12.1 and 13). The MDB covers around one-seventh of the Australian landmass, including the whole ACT, most of NSW, half of Victoria, and smaller portions of Queensland and SA.

... the eastern coastlands exhibit marked juvenile topography, while the rest of Australia is more or less senile throughout
 (Taylor, 1927)

The Great Artesian Basin (GAB) is the largest groundwater aquifer in Australia, underlying nearly one quarter of Australia in SA, NT, Queensland, and NSW (Booth and Tubman, 2011; see Figure 2.5). It spans 1.7 million km², contains an estimated 64,900 million Ml of water, and provides a permanent water supply for much of the arid interior (GA, 2020b; see Section 15.1.2). Water in the GAB is up to 2 million years old. To ensure long term sustainable use of this important resource across Australia's arid interior, careful land management is needed to balance extraction and replenishment (see Section 15.1.2). Accordingly, the Great Artesian Basin Sustainability Initiative (GABSI) was funded by federal and state government agencies from 1999 to 2017 to improve spring pressure and manage water more sustainably within the GAB. During its activity, GABSI upgraded > 750 bores, decommissioned > 21,000 km of bore drains, installed > 31,000 km of new, efficient pipe drains and saved > 250Gl of water per year (DAWE, 2020a).

Figure 2.5 Great Artesian Basin

Lambert conformal conic projection with standard latitudes 18°S and 36°S, centred on 136°E and 24°S, and based on revised Great Artesian Basin Jurassic-Cretaceous sequence boundary from Ransley and Smerdon (2012)



Source: Wikimedia: https://upload.wikimedia.org/wikipedia/commons/8/8d/Great_Artesian_Basin.png

2.2 Climate

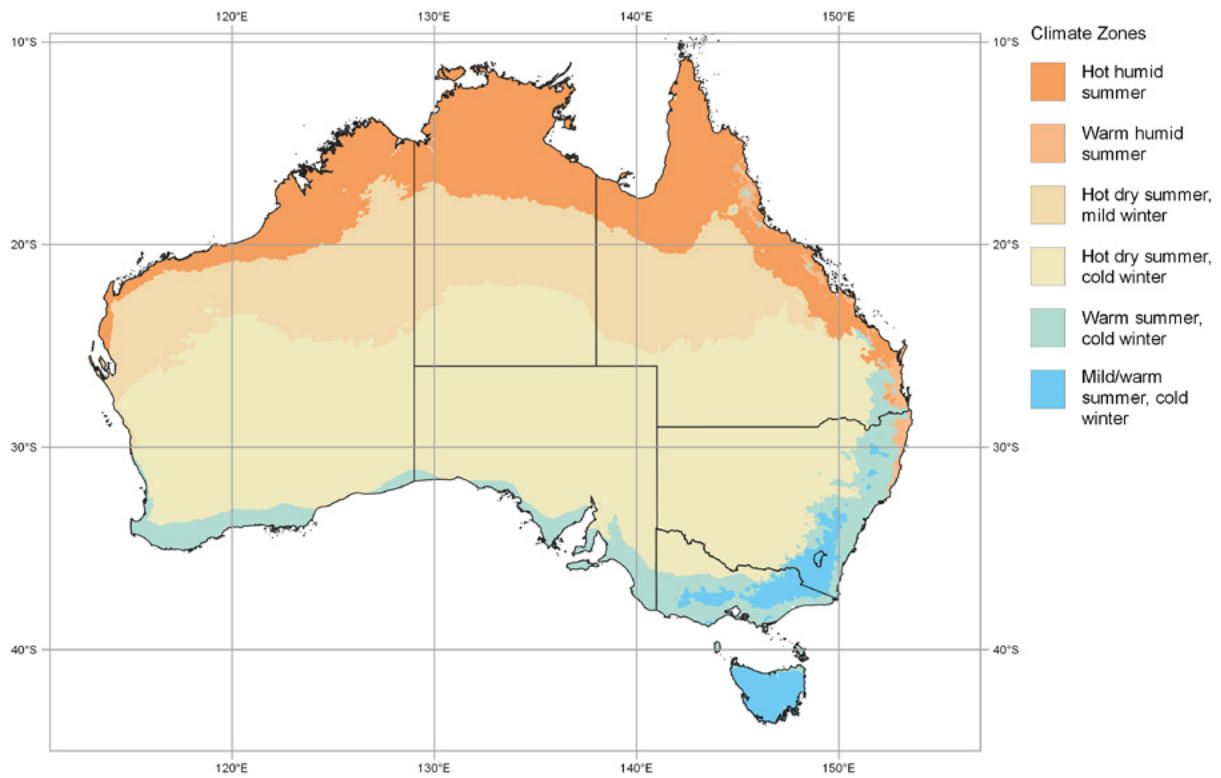
2.2.1 Weather patterns

The Australian mainland is the driest inhabited continent on Earth, with Antarctica being the only continent with a lower rainfall (BoM, 2020a). The combined impact of temperature and humidity creates climate zones that are largely stratified by latitude (see Figure 2.6). 70% of the Australian land mass receives less than 500 mm of rain annually (GA, 2020c), with half of that area being defined as arid (< 250 mm annual rain; see Figure 2.7). Temperatures can also vary significantly, both diurnally and seasonally, especially in the arid central region (see Figure 2.8).

The dry central regions have high levels of evaporation (see Figure 2.9a). The combined impact of rainfall and temperature on land cover is summarised by evapotranspiration (ET), the release of water vapour from vegetated and non-vegetated land into the atmosphere (see Figure 2.9b). In most of Australia, the potential ET is greater than precipitation, with only an estimated 10% of actual ET contributing to groundwater recharge and surface flows (Glenn *et al.*, 2011).

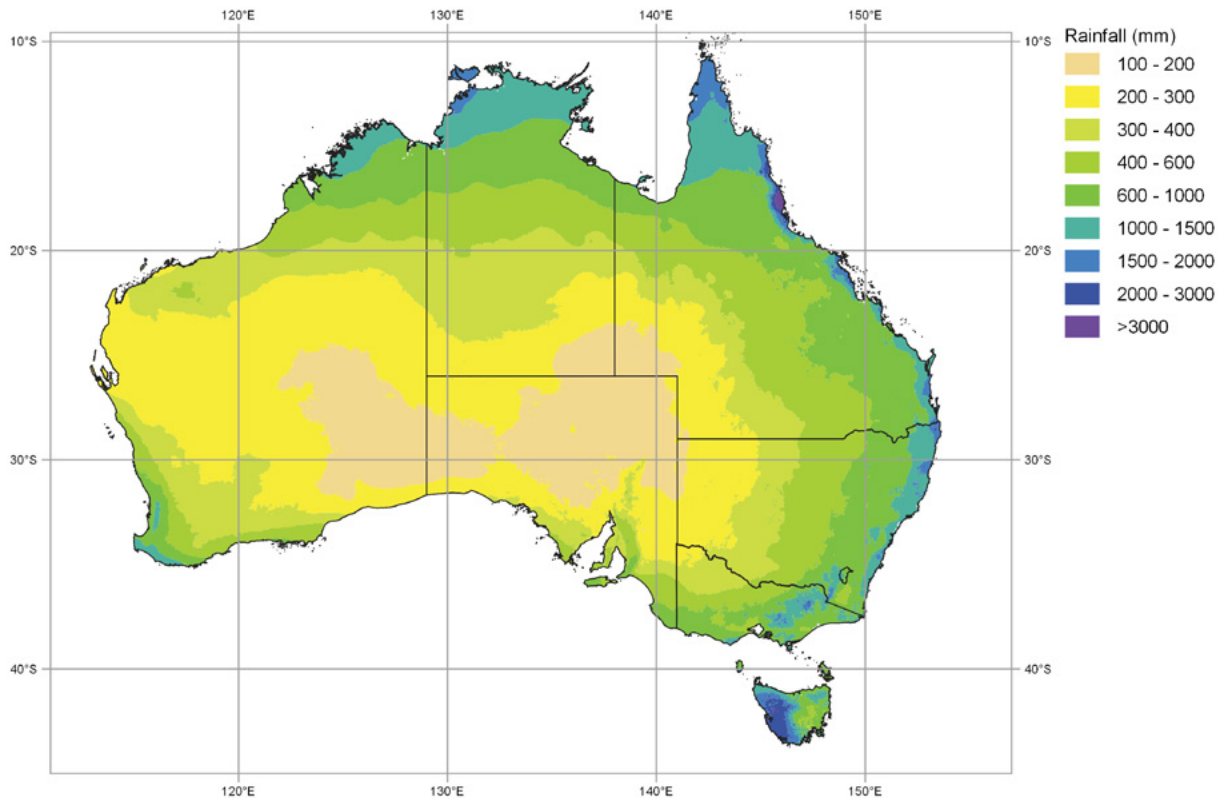
Of all countries the primitive areas of Australia are the safest for mankind. Natural hazards are at a minimum. Possible hunger and thirst and the fear of getting lost are the greatest.
(Charles F. Laseron, 1953)

Figure 2.6 Climate zones derived from humidity and temperature



Source: Tony Sparks, Icon Water, using gridded data from BoM (2020a) based on a standard 30-year climatology (1961–1990)

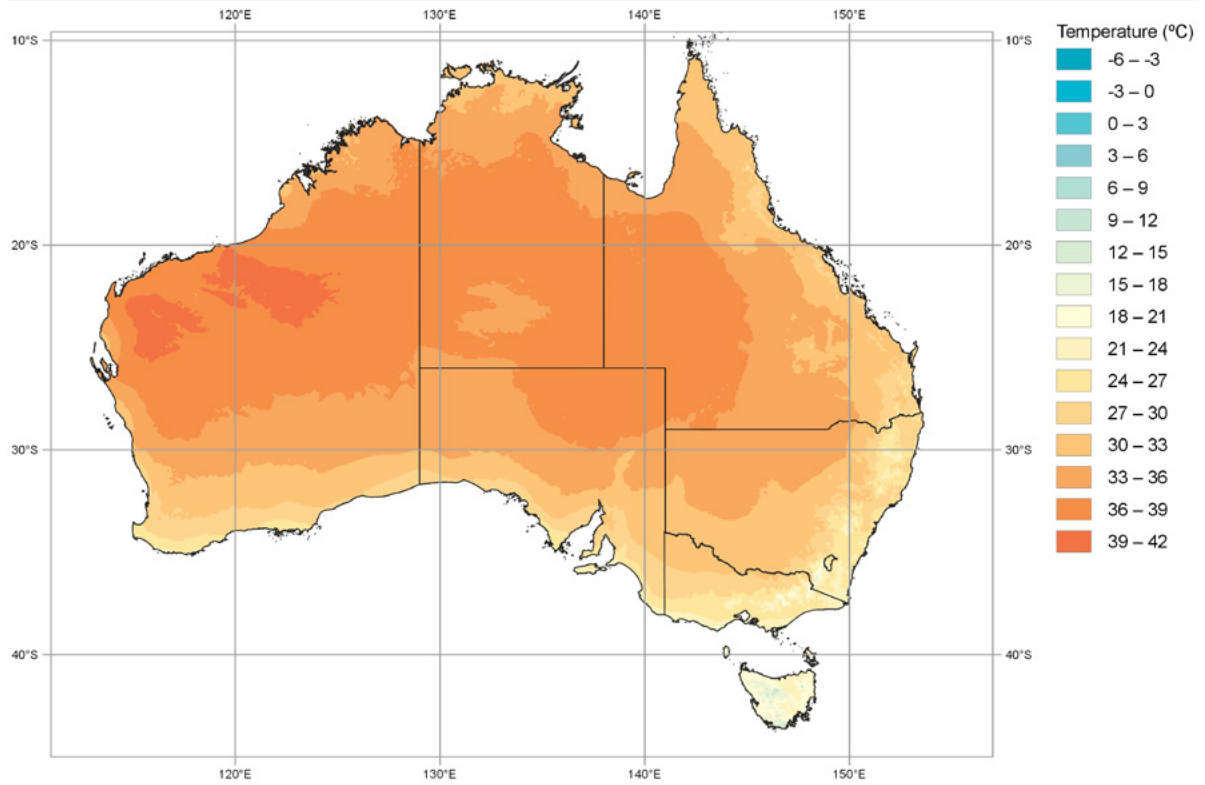
Figure 2.7 Average annual rainfall



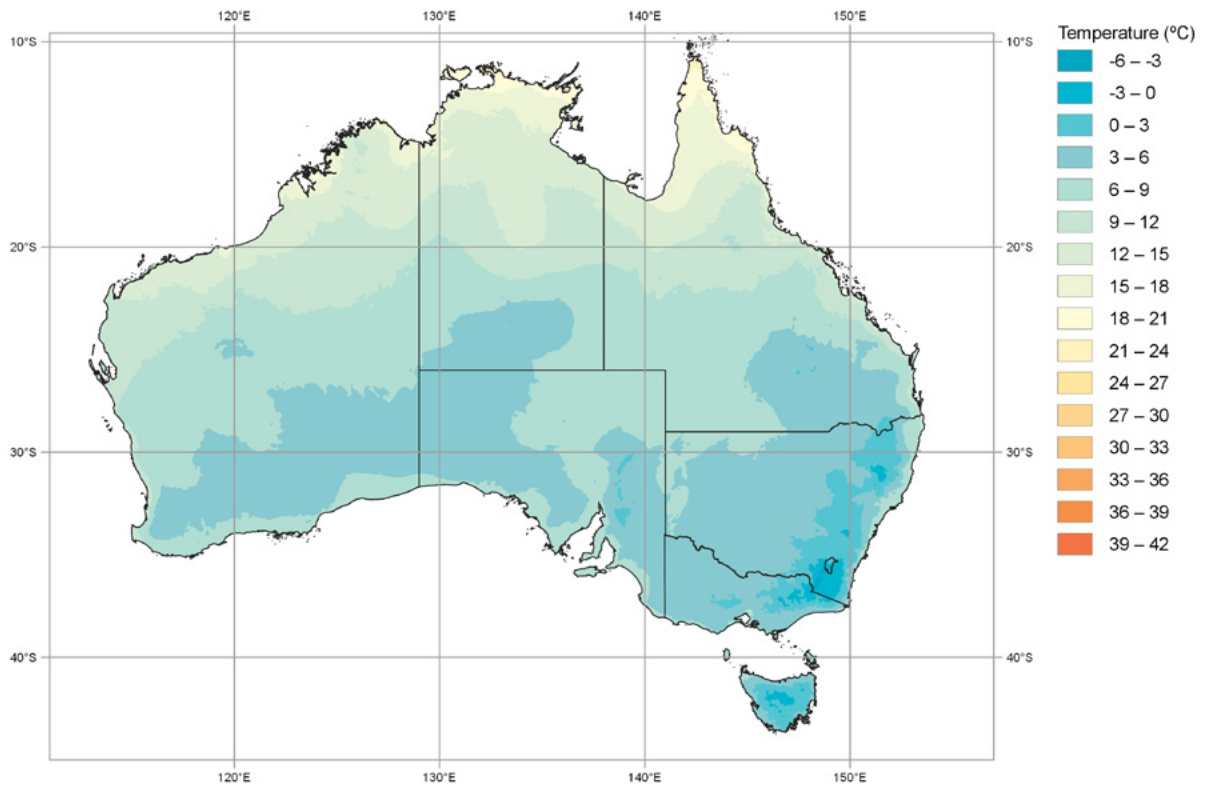
Source: Tony Sparks, Icon Water, using gridded data from BoM (2020a) based on a standard 30-year climatology (1961–1990)

Figure 2.8 Seasonal temperature variations in Australia

a. Summer average daily maximum temperature



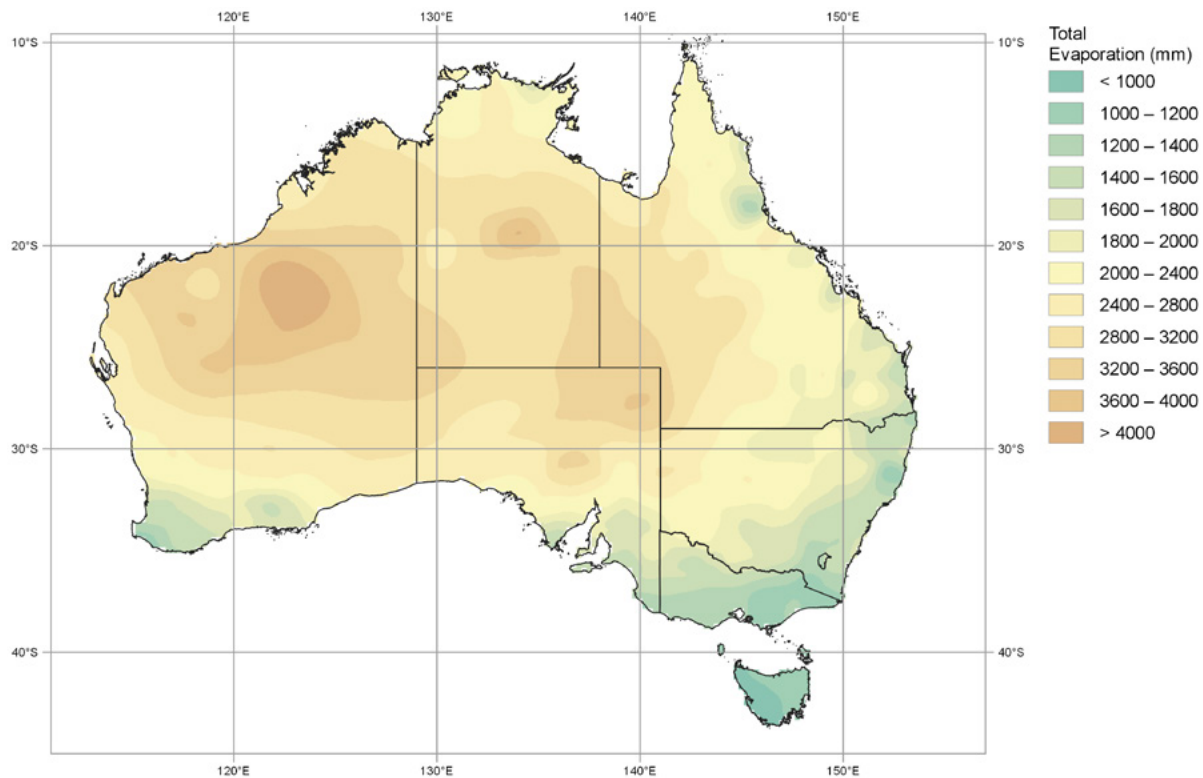
b. Winter average daily minimum temperature



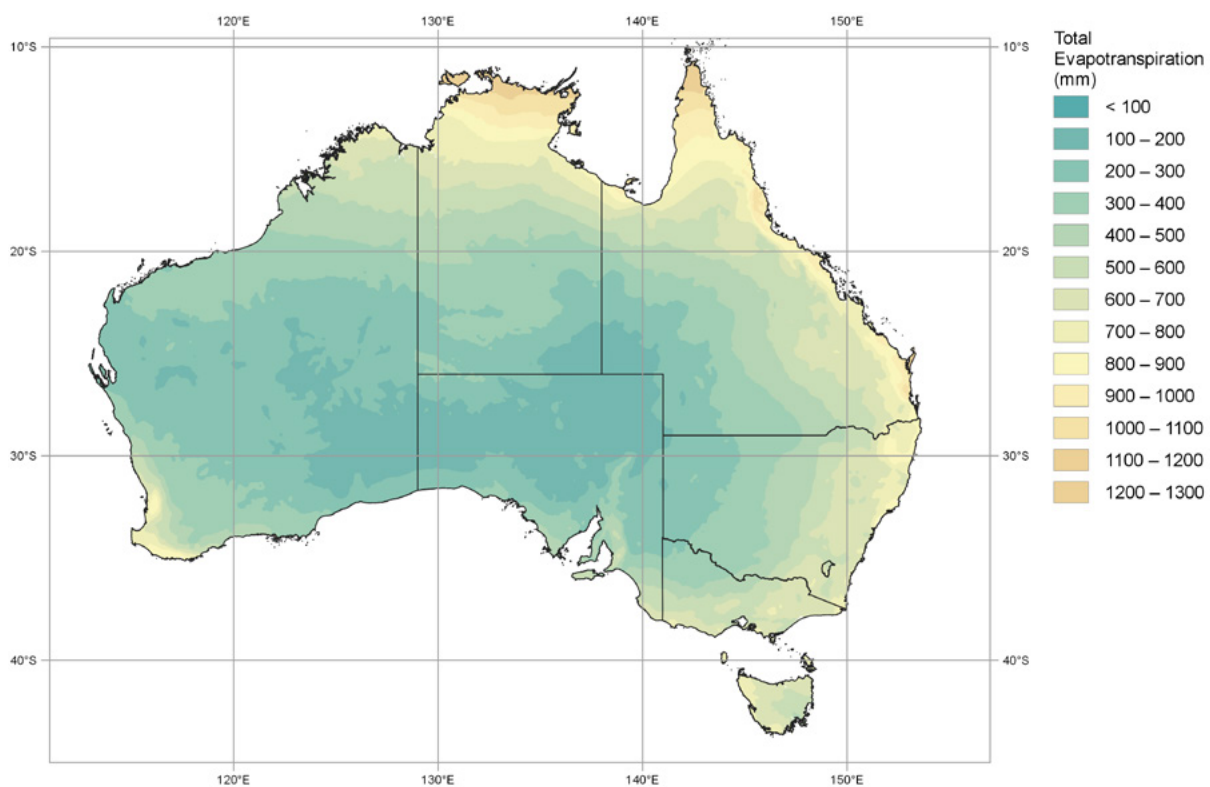
Source: Tony Sparks, Icon Water, using gridded data from BoM (2020a) based on a standard 30-year climatology (1961–1990)

Figure 2.9 Evaporation and evapotranspiration over Australia

a. Average pan evaporation based on at least 10 years of records (1975–2005)



b. Average areal actual evapotranspiration based on a standard 30-year climatology (1961–1990)



Source: Tony Sparks, Icon Water, using gridded data from BoM (2020a)

2.2.2 Climatic drivers

Australian climatic conditions are driven by the major air and water circulation patterns in the Southern Hemisphere. There are two main atmospheric circulation patterns that influence our climate:

- warm, moist equatorial air is drawn towards Northern Australia as the continent heats up in the warmer months, resulting in monsoonal rains in the tropics and a ridge of warm dry air in the sub-tropics. Movement of this sub-tropical ridge induces Australia's seasonal rainfall pattern: summer rainfall in the north and winter rainfall in the south; and
- warm air in the Pacific Ocean is moved into eastern Australia via southeast trade winds which carry moisture during the La Niña phase and drier air during the El Niño phase. This is part of the Walker circulation, which describes the large scale, atmospheric circulation over the Pacific Ocean driven by movement of deep, equatorial waters in the cooler eastern Pacific towards the warmer western Pacific Ocean (Lau and Yang, 2002).

As detailed in Volume 3B, three ocean currents significantly impact the Australian climate:

- a cold current from the southern Indian Ocean moves northward along the WA coast during summer;
- the warm Leeuwin Current moves towards the South Pole along the west and south coasts of Australia with significant effects on marine ecosystems (Feng *et al.*, 2009); and
- a warm Eastern Australian Current moves down the east coast (FAO, 2009).

2.2.3 Climate classifications

The Thornthwaite classification system for climate was proposed in 1931 and revised in 1948 (Thornthwaite, 1931, 1948). The final system was based on the interplay between local moisture and temperature, with the view that temperature was a driver for potential evapotranspiration (see Section 7.6). This system derived indices for humidity and aridity from water balance indicators:

$$\text{humidity} = \frac{\text{water surplus}}{\text{water need}}$$

$$\text{aridity} = \frac{\text{water deficit}}{\text{water need}}$$

where for annual estimates:

$$\text{water surplus} = \text{precipitation} - \text{actual evapotranspiration};$$

$$\text{water deficit} = \text{potential evapotranspiration} - \text{actual evaporation}; \text{ and}$$

$$\text{water need} = \text{potential evapotranspiration}.$$

Geographic regions are classified on the basis of their Thornthwaite Moisture Index (M):

$$M = \text{humidity} - 0.61 \times \text{aridity}$$

or

$$M = \frac{100 \times \text{water surplus} - 60 \times \text{water deficit}}{\text{water need}}$$

In Australia, the Thornthwaite Moisture Index has been used to define six types of climate that are commonly referenced for infrastructure planning (Austroads, 2004; Philp and Taylor, 2012; see Table 2.3).

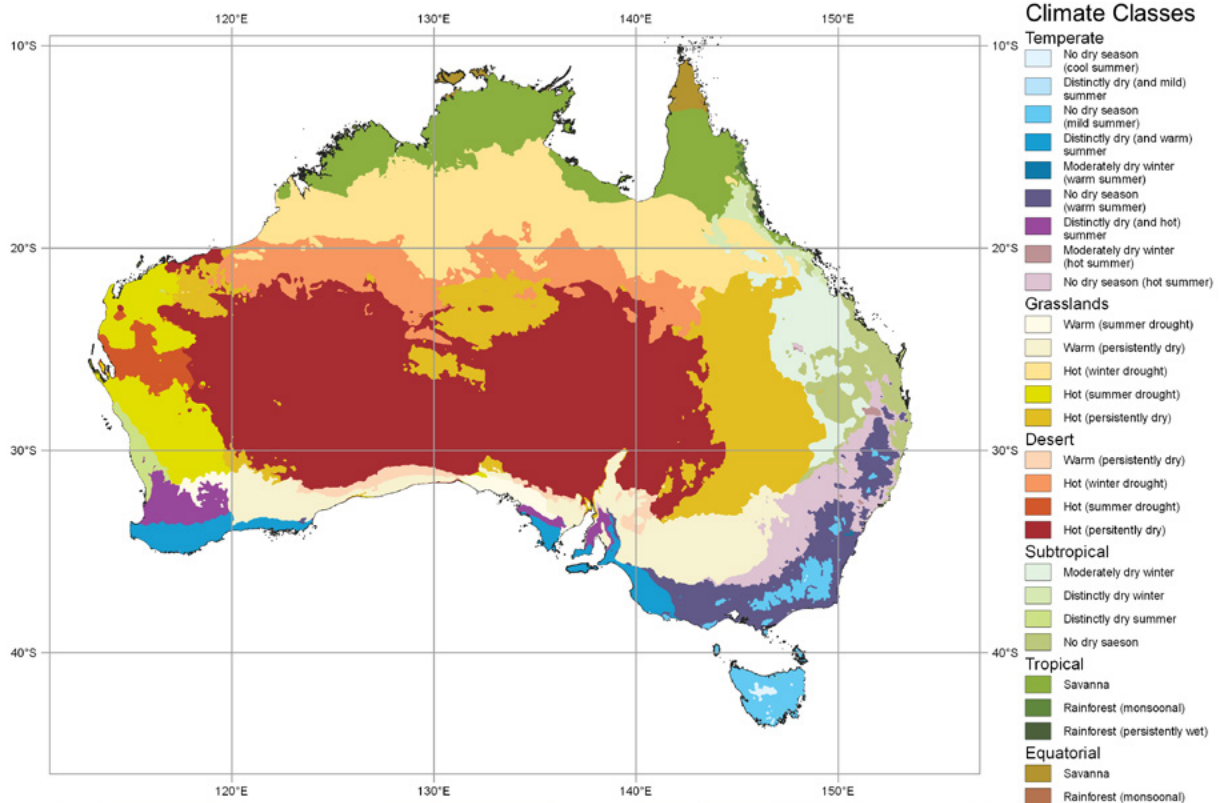
Table 2.3 Australian climate types

Climate Types		Thornthwaite Moisture Index
i	Alpine/coastal	> 40
ii	Wet temperate	10 to 40
iii	Temperate	-5 to 10
iv	Dry temperate	-25 to -5
v	Semi-arid	-40 to -25
vi	Arid	< -40

Source: Philp and Taylor (2012)

Figure 2.10 Modified Köppen climate classification

This classification of Australian climatic regions was derived from 0.025° × 0.025° resolution mean rainfall, mean maximum temperature, and mean minimum temperature gridded data. All means are based on a standard 30-year climatology (1961–1990).



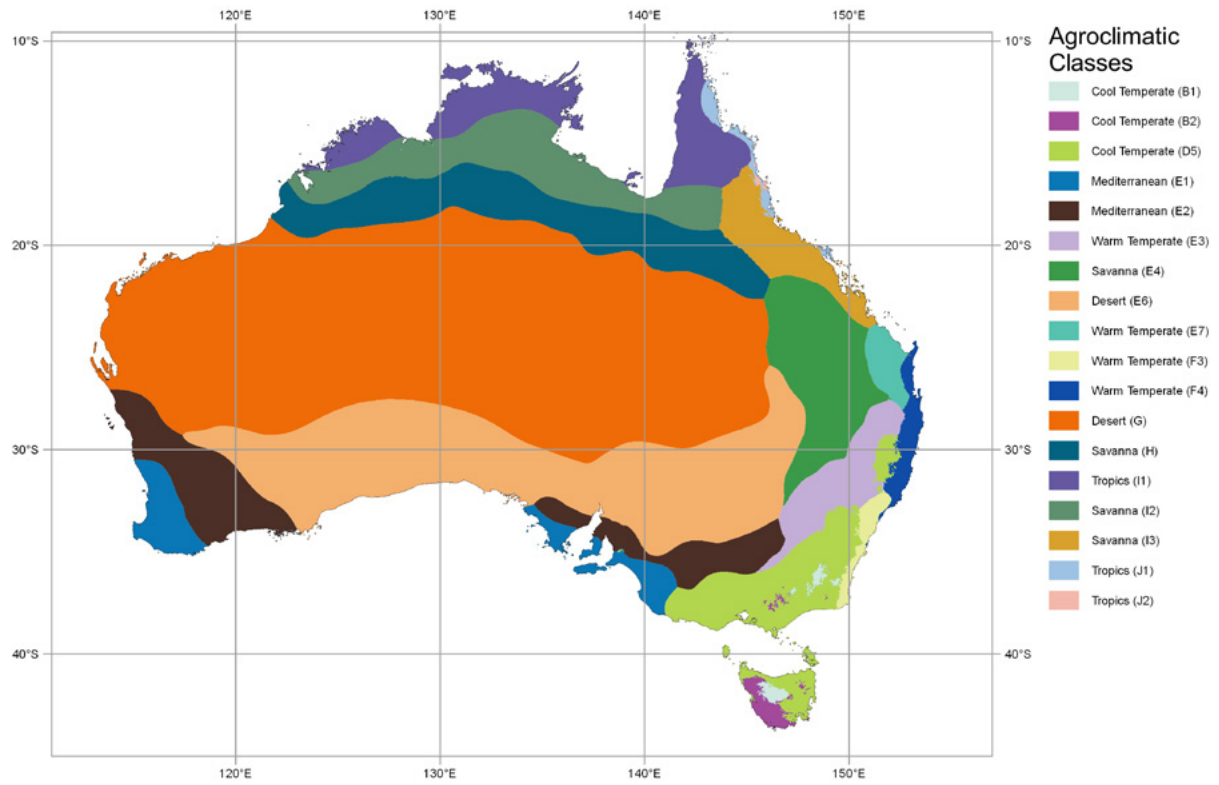
Source: Tony Sparks, Icon Water, using gridded data from BoM (2020a)

Temperature and rainfall data have been used to classify Australia into six broad climatic classes and 27 sub-divisions (see Figure 2.10). These zones are based on a modified Köppen classification (Köppen, 1931; Stern *et al.*, 1999) and are strongly correlated with topography, land cover, and land use.

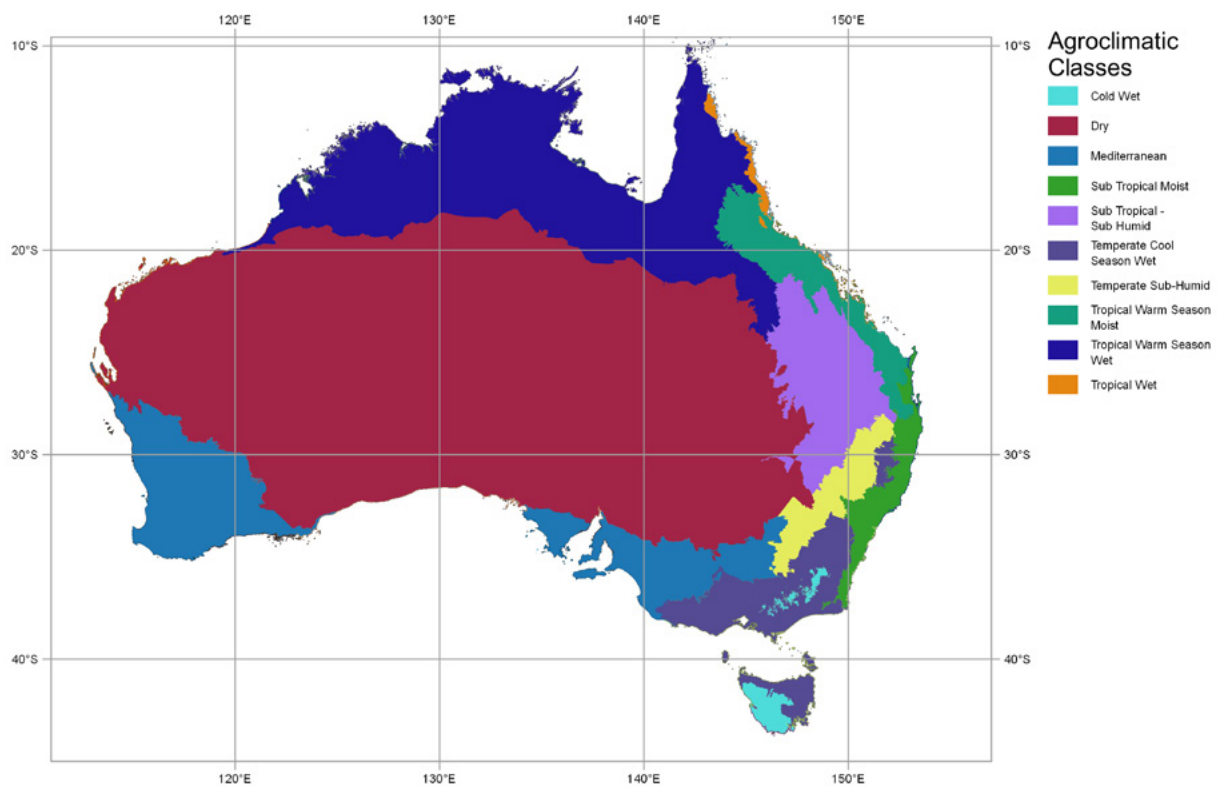
An alternate agroclimatic classification, derived from climate and topography, and aligned with bioregion data, was developed by Hutchinson *et al.* (2005). These 18 classes are illustrated in Figure 2.11a and described in Table 2.4. This classification was subsequently modified by Hobbs and McIntyre (2005) to 10 classes. More recently, Thackway and Freudenberger (2016; see Figure 2.11b) adjusted selected bioregion boundaries and merged them with the agroecological regions defined by Williams *et al.* (2002) to better reflect recent changes in climatic patterns, especially in tropical savanna regions.

Figure 2.11 Agroclimatic classifications

a. 18 classes



b. 10 classes



Source: a. Tony Sparks, Icon Water, using data from Hutchinson *et al.* (2005) Figure 3, b. Tony Sparks, Icon Water, using data from Thackway and Freudenberger (2016) Figure 1a and Table S2

Table 2.4 Agroclimatic class descriptions for Figure 2.11

18 class code	Agroclimate	Location	Land use	10 class label
B1	Very cold winters with summers too short for crop growth	Alpine areas of NSW, Victoria and Tasmania.	Water harvesting, hydroelectricity, tourism and nature conservation	Cold wet
B2	Less severe winters and longer moist summers suitable for some crops	Tasmanian highlands.		
D5	Moisture availability high in winter-spring, moderate in summer, most plant growth in spring	Tasmanian lowlands, southern Victoria, southern and northern Tablelands of NSW.	Forestry, cropping, horticulture, improved and native pastures	Temperate cool season wet
E1	Classic "Mediterranean" climate with peaks of growth in winter and spring and moderate growth in winter	Southwest WA and southern SA.	Forestry, horticulture, winter cropping, improved pastures	Mediterranean
E2	"Mediterranean" climate, but with drier cooler winters and less growth than E1	Inland of E1 in southwest WA, southern SA, northwest Victoria and southern NSW.	Horticulture, winter cropping, improved pastures	
E3	Most plant growth in summer, although summers are moisture limiting; temperature limits growth in winter	Western slopes of NSW and part of the North Western Plains.	Winter cereals and summer crops, grazing	Temperate sub-humid
E4	Growth is limited by moisture rather than temperature and the winters are mild; growth is relatively even through the year	Unique in the world to sub-tropical continental eastern Australia and associated with the brigalow belt of QLD and NSW.	Winter cereals (after summer fallowing), summer crops (including cotton) and sown pastures	Sub-tropical to sub-humid
E6	Semi-arid climate that is too dry to support field crops; soil moisture tends to be greatest in winter	Southern edge of the arid interior in WA, SA, NSW and QLD.	Rangeland	Dry
E7	Moisture is the main limit on crop growth; growth index lowest in spring	Maritime sub-tropical areas in southern QLD.	Sugar, crops and cattle grazing	Tropical warm season moist
F3	Cooler end of the warm, wet sub-tropical climates	The Sydney Basin and the NSW south coast.	Cooler temperatures slightly favour temperate crops and sown pastures	Sub-tropical moist
F4	Warmer and wetter than F3	NSW north coast, extending to southern QLD and the Great Sandy province.	Horticulture, sown pasture and tourism. Potential for wheat, cotton and maize	
G	Desert, supporting very little plant growth due to water limitation	Central Australia.	Cropping possible only with irrigation. Rangeland, wildland	Dry
H	Semi-arid, with some growth in the warm season, but too dry for cropping	Transition between the wet/dry tropics and the arid interior in WA, NT and QLD.	Rangeland	Tropical warm season wet
I1	Strongly developed wet and dry seasons with plant growth determined by moisture availability	NT, northern WA and Cape York Peninsula.	Predominately rangeland. Potential for tropical field crops	
I2	Temperature and moisture are more seasonal than for I1 and the growing season is shorter	Occurs inland of I1	Some crop potential, but predominantly rangeland	Tropical warm season moist
I3	This has cooler winters than I1 and I2 with a growing season lasting at least six months	Occurs in the coastal and hinterland areas of northeast QLD, south of Cape York Peninsula.	Sugar, cropping and rangelands	
J1	Moisture and temperature regime supports growth for 8–9 months of the year, with a 3–4 month dry season	Limited areas in the central Mackay coast and the Wet Tropics.	Sugar cane and horticulture	Tropical wet
J2	As for J1 but with a shorter dry season	Limited areas on the east coast of Cape York Peninsula		

Source: Hutchinson *et al.* (2005) Table 1; Thackway and Freudenberger (2016)

2.3 Biota

Australia supports a diverse and unique range of indigenous plants and animals. Being an isolated continent, Australia's terrestrial biota largely evolved independently from the rest of the world with over 80% of its angiosperms, mammals, reptiles, and frogs, and over half of its birds, being unique. The remainder migrated during prehistoric times, before land bridges with then adjacent continents were submerged by rising sea levels. Fossil evidence suggests that marsupial (but not placental) mammals arrived via Antarctica, and placental rats and bats came from Asia (Cox, 2000).

In addition to these naturally-occurring species, thousands of plants and hundreds of animals have been introduced to the Australian landscape in recent centuries, some of which now produce most of our agricultural income. A significant number of species, however, have become invasive and present serious threats to natural ecosystems and agricultural activities. In 2012, feral animals and invasive weeds were identified as the two major threats to sustainable natural resource management (NRM) in all NRM regions in Australia (NRM, 2019). Changes in land management practices since European settlement, which started with the arrival of the First Fleet in 1788, have also modified the populations and distributions of some indigenous biota, resulting in some species becoming endangered or extinct and others having a greater impact on the environment (Burrows, 2018).

The following sub-sections introduce aspects of Australia's biota that have direct relevance to EO-based studies of terrestrial vegetation:

- vegetation classification systems (see Section 2.3.1);
- weeds (see Section 2.3.2); and
- indigenous and feral animals (see Section 2.3.3).

2.3.1 Classifying vegetation

The intricate composition of natural vegetation and the gradual transitions that occur between different types of vegetation complicate the task of defining discrete vegetation classes. While many different approaches have been used to classify vegetation, three basic attributes of vegetation underpin most classification systems, namely growth form, foliage cover, and floristic composition. Plants can also be grouped into functional groups or plant functional types (PFT) on the basis of their function in an ecosystem and their resource usage (Smith *et al.*, 1997; see Sections 4.1.2, 4.2.1, and 7.4).

Current vegetation classification systems define labels on the basis of specific, measurable attributes rather than descriptive criteria. The standard methods and terminology for field survey of land and soil attributes, including vegetation, in Australia are detailed in NCST (2009). While this approach cannot solve the problems associated with attempts to classify the complexities of natural vegetation, it does reduce ambiguity in class nomenclature.

The first systematic floristic classification for Australia's vegetation, including origins, development, and composition, was published by Beadle (1981). Since 1973, the Australian Biological Resources Study (ABRS, 2012) has been compiling the definitive reference on taxonomy for Australian flora based on the Cronquist system (Cronquist, 1968, 1981). Keith (2017) reviews the development of nomenclature to map and classify Australian vegetation, describes significant ecological processes, and provides details of each major vegetation type.

Criteria useful in the description of vegetation include: life form; size; density of individual plants; shape, size and texture of leaves; and whether evergreen or deciduous. Each of these criteria includes several classes which differ in kind (e.g. life form and leaf attributes) or in degree (e.g. size and density), and the possible number of combinations of all these classes is so large as to lead to an unworkable system so far as classification is concerned, although any particular plant community can be defined with accuracy by such a system. A workable system necessarily must select among possible criteria and make arbitrary divisions among characteristics which are continuous in magnitude; in so far as it does this it cannot define the many combinations met with in nature. (Specht, 1970).

Table 2.5 Common definitions for Australian vegetation

Specht Land Cover Label	Equivalent Label	Rainfall (mm)	Species Composition	Height (m)	Foliage Projective Cover (%)
Closed Forest	Rainforest	> 900	Wide range of rainforest trees and understorey plants	15–40	70–100
Tall Open Forest	Wet Sclerophyll	> 900	Mostly <i>Eucalyptus</i> plus ferns, and shrubs/small trees with soft foliage	> 30	30–70
Low Open Forest	Dry Sclerophyll	> 900	Mostly <i>Eucalyptus</i> plus grasses/shrubs with hard leaves	5–30	30–70
Woodland	Savanna	< 900	Mostly <i>Eucalyptus</i> plus <i>Callitrus</i> , <i>Casuarina</i> and <i>Acacia</i> species	5–25	10–30
Open Woodland	Open savanna	400–500	<i>Eucalyptus</i> and <i>Corymbia</i> , plus <i>Callitrus</i> , <i>Casuarina</i> and <i>Acacia</i> species	< 10	0–10
Shrublands	Heath	< 400	Mostly <i>Acacia</i> species, e.g. Mulga	2–8	30–100
Shrub Steppe	Low Shrubland	< 200	Mostly mallee eucalypts	< 2	10–30
Closed Grassland	Alpine Meadows, Herbland	< 400	<i>Poa</i>	< 1	30–100
Tussock Grassland	Mitchell Grasslands, Bluegrass Grasslands	400–700	Perennial grasses, rushes, sedges, <i>Lomandra</i> species	< 1	< 70
Hummock Grassland	Spinifex Grasslands	200–300	<i>Triodia</i>	< 2	10–30
Desert	Bare, Exposed	< 250	<i>Acacia aneura</i> , <i>Eremophila glabra</i> , <i>Atriplex vesicaria</i> , <i>Swainsona formosa</i>	< 2	0–10

Source: Specht (1970); Florence (1985); DEWR (2007)

The descriptive labels commonly used in Australia for vegetation were originally defined on the basis of rainfall, species composition and biomass density (measured as Foliage Projective Cover, FPC), which is defined as the “vertically projected percentage cover of photosynthetic foliage of all strata of the forest stand” (Specht, 1983), that is, the percentage of ground area occupied by the vertical projection of woody vegetation foliage. As summarised in Table 2.5, this approach tended to embrace alternative, and sometimes ambiguous, labels and imprecise boundary conditions (Gillison and Anderson, 1981). For example, one of the earliest national vegetation maps for Australia, compiled by Williams (1959) and derived from aerial photography and expert knowledge, used category labels based on structure and cover.

A widely used classification system for Australian vegetation, attributed to Specht (1970), is based on two structural features that are characteristic of most natural Australian flora—namely that the largest proportion of total biomass is contained in the upper stratum of vegetation and that biomass can be reasonably estimated from FPC plus height or growth form (see Section 3.2.1 and 5.1.1)—to define the 28 categories indicated in Table 2.6. This system for classifying vegetation is compatible with the ISO standards for terrestrial vegetation and has been adopted by several Australian land cover mapping projects.

In more recent decades, however, Australian vegetation classification systems explicitly derive vegetation class names from the structural formation of the vegetation (for example, see Excursus 6.1), in addition to the floristic association of the dominant species, rather than using labels that imply these characteristics (Walker and Hopkins, 1990; Thackway *et al.*, 2008; Hnatiuk *et al.*, 2009). In this context, a formation is defined as a “synthetic structural unit to which are referred all climax communities exhibiting the same structural form, irrespective of floristic composition” (Beadle and Costin, 1952), such as a tropical forest. A sub-unit of a formation, with two or more dominant species, is called an association (see Section 6.1). The Australian Vegetation Attribute Manual (NVIS Technical Working Group, 2017) includes the new attribute standard for compiling non-native and non-vegetated cover types. This new standard enables monitoring and reporting of the whole landscape and will complement monitoring land cover changes using the FAO Land Cover Classification (see Section 3).

Table 2.6 Structural classification of Australian vegetation

Growth form of tallest stratum	Foliage cover of tallest stratum			
	> 70%	30–70%	10–30%	< 10%
Tall trees (> 30 m)	Tall closed forest (T4)	Tall open forest (T3)	Tall Woodland (T2)	–
Medium trees (10–30 m)	Closed forest (M4)	Open forest (M3)	Woodland (M2)	Open woodland (M1)
Low trees (< 10 m)	Low closed forest (L4)	Low open forest (L3)	Low woodland (L2)	Low open woodland (L1)
Tall shrubs (> 2 m)	Closed scrub (S4)	Open scrub (S3)	Tall shrubland (S2)	Tall open shrubland (S1)
Low Shrubs (< 2 m)	Closed heath (Z4)	Open heath (Z3)	Low shrubland (Z2)	Low open shrubland (Z1)
Hummock grasses	–	–	Hummock grassland (H2)	–
Tussocky or Tufted grasses or Graminoids	Closed tussock grassland or closed sedgeland (G4)	Tussock grassland or sedgeland (G3)	Open tussock grassland (G2)	Sparse open tussock grassland (G1)
Other herbaceous plants	Dense sown pasture (F4)	Sown pasture (F3)	Open herbfield (F2)	Sparse open herbfield (F1)

The National Vegetation Information System (NVIS; NVIS Technical Working Group, 2017; DAWE, 2020b) is an ongoing collaborative initiative between the Australian federal, state, and territory governments to manage national vegetation data and has become the standard system for all Australian federal, state and territory government land management agencies. NVIS was developed to improve vegetation planning and management within Australia, and assist in managing a range of ecosystem services and practices (see Section 20.3), such as conserving biodiversity, controlling salinity, improving water quality, and managing vegetative fuel loads.

NVIS classifies Australian vegetation types at the sub-formation, association and sub-association levels using structural and floristic criteria (see Table 2.7 and Volume 2D—Excursus 12.1 for details). The NVIS Version 5.1 map product defines 33 Major Vegetation Groups (MVG; see Figure 2.12) and 85

sub-groups, which comprehensively describe the extent and distribution of vegetation in Australia, for both estimated pre-1750 and extant vegetation. A complementary national database, the National Forest Inventory (NFI), focuses on the productivity and sustainability of Australia's forests (see Section 16.1).

NVIS has enabled a nationally consistent vegetation dataset to be compiled from data collected by various state and territory jurisdictions. The recommended data collection level is Level 5 or better, with Levels 1–4 generated algorithmically for consistency (see Table 2.7). All NVIS data—both spatial data and the underlying vegetation attribute information—is open source. The classification systems used by relevant Australian federal state and territory authorities for mapping native vegetation are summarised in Table 2.8. Further information on some of these systems is provided in Sections 2.6 and 3.3.

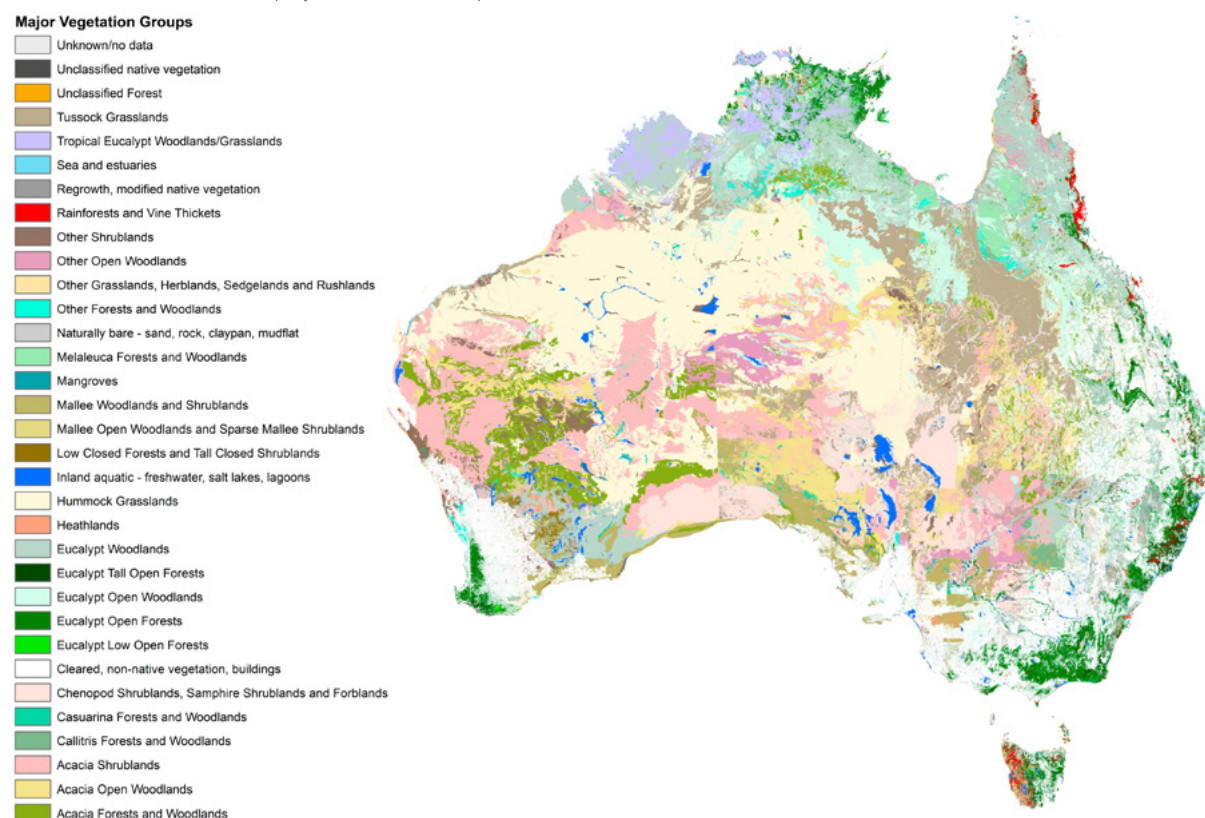
Table 2.7 NVIS information hierarchy

Level 5 (association) is recommended as the minimum level of input for input data to NVIS. Hnatiuk *et al.* (2009) refer to Level 1 as Formation.

Level	Category	Description
1	Class	Dominant growth form for the structurally dominant stratum
2	Structural formation	Dominant growth form, cover and height for the structurally dominant stratum
3	Broad floristic formation	Dominant genus (or genera) plus growth form, cover and height for the structurally dominant stratum
4	Sub-formation	Dominant genus (or genera) plus growth form, cover and height for each of the three main strata. (Upper, Mid, and Ground)
5	Association	Dominant growth form, height, cover and species (to a maximum of 3 species) for each of the three main strata. (Upper, Mid, and Ground)
6	Sub-association	Dominant growth form, height, cover, and species (to a maximum of 5 species) for each of the substrata

Source: NVIS Technical Working Group (2017)

Figure 2.12 Major Vegetation Groups derived from NVIS Version 3
 EPSG:3577 Australian Albers projection with 30 m spatial resolution



Source: Scarth *et al.* (2019) Figure 2 (from DEWR, 2007)

Table 2.8 Native vegetation classification systems

Jurisdiction	Categories
Federal	33 Major Vegetation Groups (MVG; DAWE, 2020b) 85 Major Vegetation Subgroups (MVS; DAWE, 2020b)
ACT	Ecological Communities (ACT EPSDD, 2020)
NSW	16 Vegetation Formations (Keith, 2004) 99 Vegetation Classes (Keith, 2004) ~1500 NSW Plant Community Types (PCT) in BioNet Vegetation Classification (NSW DPIE, 2020) State Vegetation Type Mapping (SVTM; see Excursus 8.2)
NT	Vegetation Associations (NT EPA, 2013; Brocklehurst <i>et al.</i> , 2007) 174 Vegetation Types (Lewis <i>et al.</i> , 2008; NTNVIS, 2020)
Queensland	16 Broad Vegetation Groups (BVG) (Queensland Government, 2020a; Neldner <i>et al.</i> , 2019) 1384 Regional Ecosystems (RE) (Queensland Government, 2020b)
SA	NVIS Framework (SA DEWNR, 2019)
Tasmania	~ 158 TASVEG Vegetation Communities (Harris and Kitchener, 2005)
Victoria	28 Bioregions (DELWP, 2020) 897 Ecological Vegetation Classes (EVC)
WA	819 Vegetation Associations (Shepherd <i>et al.</i> , 2002)

Source: Richard Thackway, Australian National University

2.3.2 Weeds

Weeds or invasive plants are defined as “any plant that requires some form of action to reduce its effect on the economy, the environment, human health and amenity” (DEE, 2019a). Many weeds in Australia were introduced by European settlers, but natives species can also become weeds, either when their native habitat changes favourably, or when they wander into ‘new’ ecosystems with suitable conditions. The introduction of any exotic vegetation has the potential to become a weed problem. Ecosystems can be permanently changed by the invasion of exotic weeds, which can transform faunal habitats, food sources, and fire regimes. Further, native vegetation may not be equipped to compete with invasive weeds, which can form dense, smothering thickets.

Weeds reproduce readily, usually through an abundance of seeds, and rapidly colonise disturbed sites. They impact urban, rural, and natural environments, including surface waters, deserts, and alpine regions. Despite active control measures being enforced by legislation in all levels of government, weeds are still spreading in Australia (DEE, 2019b). As such, they are considered to be a serious threat to both Australian agriculture and conservation areas (DEE, 2019a).

3,480 of the 28,000 plant species introduced into Australia since European settlement are now classified as weeds (Lesslie *et al.*, 2011). Of these weeds, 32 have been identified as ‘Weeds of National Significance’ on the basis of their “invasiveness, potential for spread and environmental, social and economic impacts” (DEE, 2019c). Specific lists of noxious weeds—those posing the greatest threat to native species and agricultural productivity—are also ranked and administered by each state and territory government for areas within its jurisdiction.

The average cost of weed impact and control was estimated as \$4,989.2 million for Australian agricultural industries in 2018 (McLeod, 2018). In order to prevent land degradation in the longer term, weed control is viewed by farmers as one of their highest priorities (Lesslie *et al.*, 2011). While weed management is a significant problem throughout Australia, it is most challenging in the arid areas (Scott *et al.*, 2018), where both population density and productivity are low (see Section 15).

Weeds contaminate crops, displace pasture plants and compete with crop and pasture plants for water and nutrients. Weeds also harbour diseases and insect pests, reduce livestock carrying capacity and condition and can be toxic to livestock.
(Lesslie *et al.*, 2011)

2.3.3 Indigenous and feral animals

While Australia’s unique fauna adapted to its environment in isolation from the rest of the world, human management of the Australian landscape has modified the composition and distribution of fauna for millennia (Gammage, 2012; Pascoe, 2018). At the time of European settlement, the only widespread and large carnivorous animal on the Australian mainland was the dingo, which may have been introduced from Papua New Guinea some 5,000 years ago (Ardalan *et al.*, 2012). All other indigenous mammals were non-ungulate (non-hoofed) herbivores, and their distributions were managed by the culture and activities of their indigenous custodians (see Section 2.5.1).

As with indigenous flora, Australia’s native fauna has competed with a wide variety of introduced faunal species in recent centuries (see Section 2.3.2). While these exotic species were initially introduced for the

purposes of grazing, hunting, fishing, and transport, several quickly adapted to their new environment and continue to successfully compete with native animals for food, shelter and territory. Some introduced species also prey on native fauna (Clarke, 2001; Denny and Dickman, 2010), destroy their habitats (McKenzie *et al.*, 2006), and/or spread diseases (Henderson, 2009). Additionally, ungulate (hoofed) species, such as horses, sheep, goats, deer, and cattle, introduced significant soil compaction and ‘erosion’ problems (Lunt *et al.*, 2007), and extensively damage riparian zones. This is due, in part, to total grazing pressure, that is, competition for limited resources between domestic stock and native herbivores.

Feral animals have permanently transformed Australia.
(Norris *et al.*, 2005)

Environmentalists cannot be animal liberationists. Animal liberationists cannot be environmentalists. The environmentalist would sacrifice the lives of individual creatures to preserve the authenticity, integrity and complexity of ecological systems. The liberationist—if the reduction of animal misery is taken seriously as a goal—must be willing, in principle, to sacrifice the authenticity, integrity and complexity of ecosystems to protect the rights, or guard the lives, of individual animals.
(Mark Sagoff, 1984)

Exotic species typically have a number of competitive advantages in new territory and can severely impact native biodiversity. In Australia, these advantages included few natural predators, few fatal diseases and conditions favorable to high rates of reproduction. Accordingly their populations increased quickly (DEE, 2019d) and wild populations of over 80 species of exotic vertebrate animals have now become established in Australia (Lesslie *et al.*, 2011). Of these, more than 30 are considered pests to agriculture and/or the environment. In the 2013–14 financial year, the annual economic impact of pest animals in Australia was estimated as approaching \$600 million (McLeod, 2016).

The term ‘feral’ is used for wild animals that have descended from domestic animals. The most significant impacts of feral animals in Australia include:

- rabbits, goats, buffalo, donkeys, horses, camels, deer, and cattle—grazing and land degradation;
- dogs, foxes, pigs, and cats—livestock and native fauna predation; and
- mice and birds—damage to grain and horticultural crops.

Land management practices also changed rapidly after European settlement, which both positively and negatively impacted the populations of native fauna. As the number of grazing animals (both pastoral species and native herbivores) increased, so did predation of dingoes, foxes, and feral dogs on stock, resulting in a 5,400 km dingo-proof fence being erected nearly continuously from the west coast of SA to the east coast of northern NSW (PIRSA, 2019). As pastures were improved and extended and watering points were installed, the numbers of kangaroos, wallabies, and feral herbivores also increased, especially in southeast Australia where the dingo had been fenced out (Eldridge *et al.*, 2016).

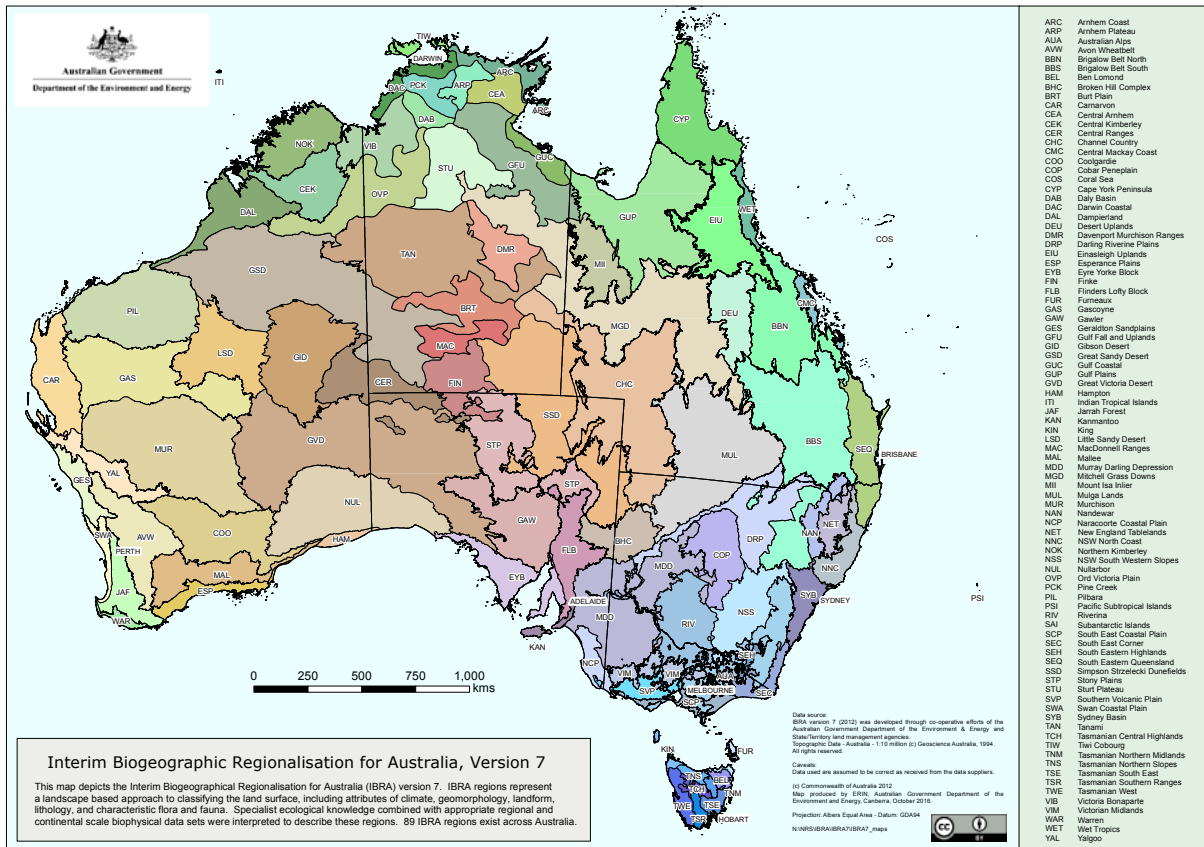
The impact of feral animals in the rangelands of Australia is significant in terms of biodiversity and productivity, and the geographic range of eight feral species is expanding (Norris *et al.*, 2005). As well as devouring crops and livestock, feral animals have degraded large areas of habitat, resulting in the loss of native mammals, irreversible erosion, and invasion by weeds, which further threatens rare biota (Burrows, 2018). While accurate estimates of feral animal distribution and abundance is lacking in this sparsely-populated region, potential solutions are further confounded by lack of rigorous knowledge about regional biodiversity and the impacts of feral animals on rangeland ecosystems (Norris *et al.*, 2005). These concerns are further considered in Section 15.

2.4 Ecoregions and Fire Patterns

Fire in the Australian landscape is frequent and recurrent, especially following drought conditions. Fire extent and intensity can vary dramatically with differences in vegetation composition and age, and ambient weather conditions (see Section 18). Recovery from fire also varies with fire intensity and vegetation type, with younger vegetation often being more susceptible. Severe and extensive fires can thus change the age distribution of vegetation and potentially increase future fire risk.

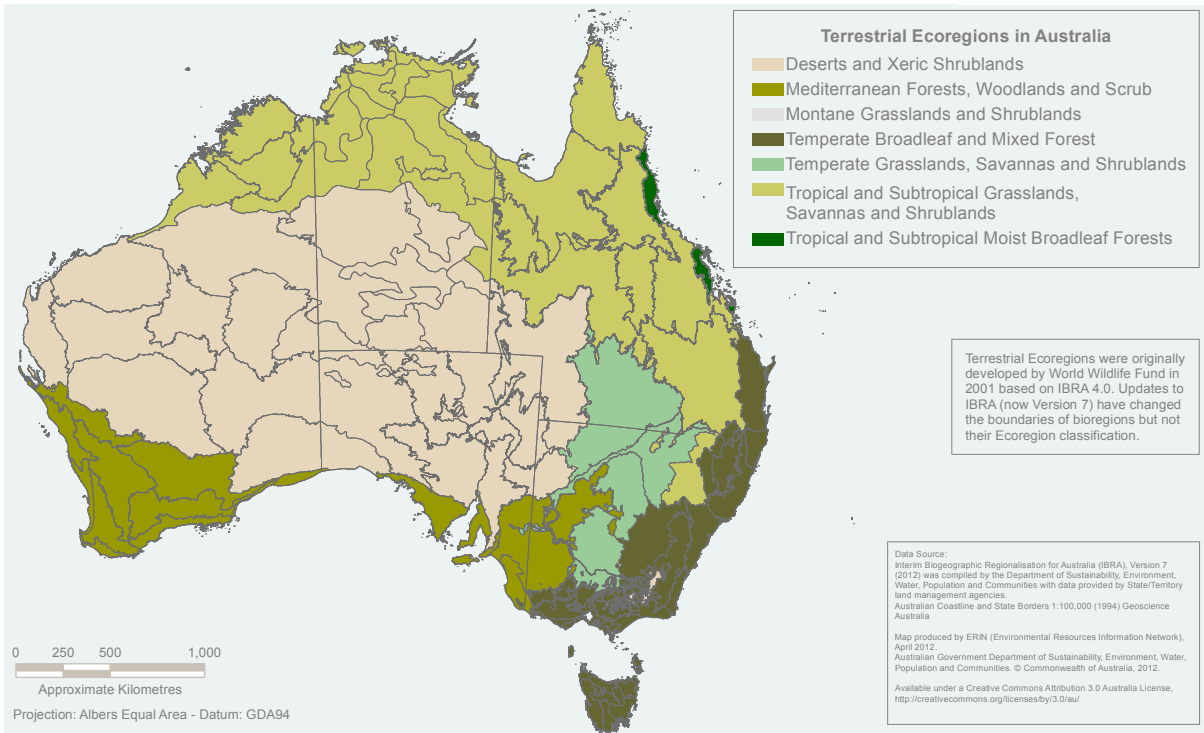
Ecological regions, or ecoregions, are biogeographic units that attempt to categorise the natural distribution of biodiversity (Olson *et al.*, 2001). Each ecoregion is a geographically distinct assemblage of fauna, flora, and ecosystems, with similar geology, lithology, landform, and climate. Ecoregions are separated by distinct geographic features, such as oceans or mountain ranges. Associated with their vegetation patterns, ecoregions have characteristic fire patterns, in terms of both frequency and severity, which significantly impact vegetation structure and extent.

Figure 2.13 Interim Biogeographic Regionalisation of Australia (IBRA) Version 7



Source: DAWE (2020c)

Figure 2.14 Terrestrial Ecoregions in Australia



Source: ERIN (2012)

In the whole country I scarcely saw a place without the marks of a fire; whether these had been more or less recent—whether the stumps were more or less black, was the greatest change which varied the uniformity, so wearisome to the traveller's eye.
(Charles Darwin's description of NSW, from 'The Voyage of the Beagle', 1845)

Similarly, the Interim Biogeographic Regionalisation for Australia (IBRA; Thackway and Cresswell, 1995; see Figure 2.13) classifies landscapes in Australia “into 89 large geographically distinct bioregions based on common climate, geology, landform, native vegetation and species information” (DAWE, 2020c). This forms part of a global, hierarchical classification of 14 terrestrial habitats or biomes (Olson *et al.*, 2001), eight of which occur in Australia (DAWE, 2020d). IBRA has been simplified into seven broad habitats by the Terrestrial Ecoregions classification (see Figure 2.14; note that the eighth habitat, Tundra, only occurs in Subantarctic islands).

IBRA acts as the planning framework for the National Reserve System (NRS), and ecoregion descriptions in the following sub-sections have been derived from the NRS to provide an overview of the Australian landscape and its response to fire (Harrison and Bradstock, 2010 and Section 18). The following descriptions are based on the estimated pre-European extents of these ecoregions and do not discuss their modification or fragmentation.

2.4.1 Deserts and xeric shrublands

Arid and semi-arid landscapes cover 70% of the Australian continent, including over half of WA, SA and NT, and smaller portions of western Queensland and NSW. This ecoregion varies greatly in the amount of annual rainfall received, with evaporation generally exceeding rainfall. Temperature extremes characterise most deserts, resulting in hot days and cold nights. These harsh, but diverse, climatic conditions support a rich array of habitats, many of which are ephemeral (DAWE, 2020d). Vegetation types include hummock grasslands, tussock grasslands, chenopod shrublands, and *Acacia* woodlands.

In arid Australia, rainfall is not only low, but irregular, and vegetation has adapted to these conditions. Significant, sporadic rainfall events trigger rapid growth, resulting in dramatic changes in vegetation extent and greenness. The fire distribution trends have been observed to follow latitude-based rainfall gradients, with most wildfires occurring in spring (late dry season), due to higher fuel loads and temperatures, coupled with reduced fuel moisture

(Allan *et al.*, 2003). The fire return interval varies regionally between three and 30 or more years and is considered to be directly related to fuel accumulation following antecedent rainfall (Allan and Southgate, 2002; Russell-Smith *et al.*, 2003). Patchiness of fires is related to the heterogeneity of fire ‘ages’ in a region (Allan and Southgate, 2002), so prescribed burning using patchy, early dry season fires is encouraged to avoid later conflagrations. In this landscape, fire footprints are clearly visible on satellite EO imagery and persist for a long time, which can result in overlapping fire scars over several years.

2.4.2 Mediterranean forests, woodlands and scrub

Mediterranean ecoregions feature hot, dry summers, cool, moist winters, and regular periods of drought, and generally occur in areas of low topography. These conditions only occur in five regions globally and, together, they support over 10% of the known species of flora. The Fynbos (in South Africa) and shrublands in southwest Australia have greater biodiversity than the other Mediterranean ecoregions. In southwest WA, southeast SA, and western Victoria, Mediterranean vegetation has been heavily fragmented by land clearing. Some large, intact areas of Mediterranean woodlands and scrub still exist in sparsely populated areas, such as the Great Western woodlands in WA. Vegetation in the Mediterranean ecoregion includes heath, mallee, and forest.

Most plants endemic to this ecoregion are adapted to, and dependent on, fire. Heath vegetation, which also occurs in tropical and temperate climates, is particularly fire prone. Fires are seasonal, predominantly occurring in summer with lightning being the primary cause, and often follow drought. Fire frequency estimates vary from five to 30 years, with large fires occurring every 20–30 years (Bradstock and Cohn, 2002). Since rainfall, and hence fuel moisture content, is generally low during summer in this climate, fire risk is primarily related to fuel load. High severity burns in this ecoregion can be accurately delineated in EO imagery.

Bushfires have a fundamental and irreplaceable role in sustaining many of Australia's natural ecosystems and ecological processes and are a valuable tool for achieving land management objectives. However, if they are too frequent or too infrequent, too severe or too mild, or mistimed, they can erode ecosystem health and biodiversity and compromise other land management goals.

(Ellis et al., 2004)

2.4.3 Montane grasslands and shrublands

This ecoregion includes high elevation (montane and alpine) grasslands and shrublands. In Australia, montane grassland and shrublands are restricted to the mountainous regions of southeastern Australia above 1300 m, in which trees do not grow. This region occupies less than 3% of the Australian landmass and straddles the borders of the ACT, Victoria, and NSW on the Australian mainland, with a significant element occurring in Tasmania (DAWE, 2020d).

Fires are rare in montane grasslands and usually follow extreme drought. Fire is limited by fuel load and moisture content, with montane shrubland species being more flammable than grassland species. These areas are believed to burn naturally only once or twice a century (Ross Bradstock, *pers. comm.*). While rare, however, fires in this region of Australia can be massive and uncontrollable, as occurred in 1938/39, 2002/03 and 2019/20.

2.4.4 Temperate broadleaf and mixed forest

Temperature and precipitation vary widely in temperate forests. These forests generally comprise four layers of vegetation (upper and lower canopies plus shrub and ground layers), with biodiversity being highest near the forest floor. *Eucalyptus* and *Acacia* species typify the composition of the temperate broadleaf and mixed forests in Australia. This ecoregion also includes areas of temperate rainforest. In Australia, these forests stretch along the Great Dividing Range and coastal regions from southeast Queensland, through NSW and the ACT into Victoria. The moderate climate and high rainfall of this region support unique *Eucalyptus* forests and open woodlands. The temperate rainforests and mixed forests of Tasmania are also extraordinarily complex (DAWE, 2020d).

These forests generally occur in mountainous landscapes where topography affects vegetation density and composition and, in turn, fuel volume and exposure. In this ecoregion, topography and fuel load have been identified as the most important factors influencing fire propagation and severity

(Bradstock et al., 2010). Fires in temperate forests are linked to irregular drought conditions, with megafires following periods of extreme drought (Bartlett et al., 2007).

The predominant fuel in these forests is leaf litter so most fires occur in hotter, drier seasons. In wetter areas, the natural fire frequency is estimated to be 50–100 years, while drier areas may experience fire every 10–20 years. In recent years, there has been an increased frequency of large fires in these regions with several major fire seasons resulting in 4 million ha being burned between 2000 and 2010 (Ross Bradstock, *pers. comm.*) and more in 2019/20 (see Section 18.1). Most major towns and cities in southeast Australia are situated near temperate forests so their populations are directly and indirectly affected by wildfires occurring in these regions.

While the relatively dense canopies in these forests obscure understory vegetation in imagery from passive EO sensors, crown fires can be clearly discerned in these datasets.

2.4.5 Temperate grasslands, savannas and shrublands

This ecoregion has cooler and more varied annual temperatures than tropical grasslands. Trees tend to only occur along streams and rivers. Located between temperate forests and the arid interior of Australia, the southeast Australian temperate savannas span a broad north-south swath on the drier side of the Great Dividing Range through Queensland, NSW and Victoria, and into Tasmania. Since European settlement, most of this ecoregion has been converted to sheep and wheat farms so that only small fragments of the original vegetation remains (DAWE, 2020d).

Distinct fire seasons occur in this ecoregion, which are related to grassland curing. Southern areas with winter rainfall experience summer fires and northern areas of summer rainfall are most likely to burn in late winter and spring. In these relatively flat regions with scattered tree cover, fires are clearly delineated in EO imagery.

2.4.6 Tropical and subtropical grasslands, savannas and shrublands

The tropical and subtropical grasslands, savannas, and shrublands are characterised by rainfall levels between 900–1500 mm per year, following a predictable, seasonal pattern of wet summers and extended, warm, dry winters. The abrupt onset of the dry season, evidenced by a sudden decline in atmospheric and surface moisture, signals the start of fire weather.

Tropical savannas occupy 25% of Australia, covering about 200 million ha in northern WA, the top half of NT, and inland of the Great Dividing Range in Queensland. These biologically diverse regions do not receive sufficient rainfall to support extensive tree cover. Patches of dry rainforest also occur throughout this ecoregion.

Fire is extensive and frequent, with both extent and frequency varying regionally, and is predominantly initiated by human activity. Conversely, population and infrastructure are sparse. New fire footprints are clearly discernible in EO data in this landscape. Given its dynamic nature, the timing of EO data acquisition is particularly important for mapping fire effects in this ecoregion. The relatively simple and open structure of savanna vegetation with predominately grassy understoreys, which quickly recover from fire, means that the focus for fire mapping is on burned area rather than severity. The rate of regrowth of grasslands can also result in overlap of fire scars within a fire season.

2.4.7 Tropical and subtropical moist broadleaf forests

These forests are generally found in large, discontinuous patches in tropical latitudes. They are characterised by low variability in annual temperature and high annual rainfall (> 2000 mm). Forest structure comprises five layers (three canopy layers plus shrub and ground layers) with greatest biodiversity generally occurring in the canopy. Species composition in these forests is dominated by semi-evergreen and evergreen deciduous trees.

In Australia, small and scattered areas of this type of forest only occur in Queensland. These forests are noted for their southern location and their highly endemic fauna and flora. Subtropical moist forests with high levels of plant and bird endemism also occur on Lord Howe Island and Norfolk Island (DAWE, 2020d).

Fire risk is low in rainforest areas due to the high fuel moisture content. Some research has noted expansion of rainforest vegetation in recent decades, possibly due to the absence of fire (Jurskis, 2015).

Eucalyptus was excellent at extracting and hoarding precious nutrients, but so were most of the Australian flora. What made it special was its extraordinary opportunism, a relationship reinforced by fire. Eucalypts accepted wretched soils and tolerated drought, but they thrived amid fire.
(Pyne, 1992).

2.5 Land Use

Today, the vast majority of Australians live in, and derive their livelihood from, the coastal fringe. The highest population densities occur in southeast Australia, spanning from Brisbane to Adelaide, and in the southwest of WA around Perth (see Table 2.1 and Figure 2.15). 71% of Australians live in major cities, and another ~10% live in small towns (ABS, 2020).

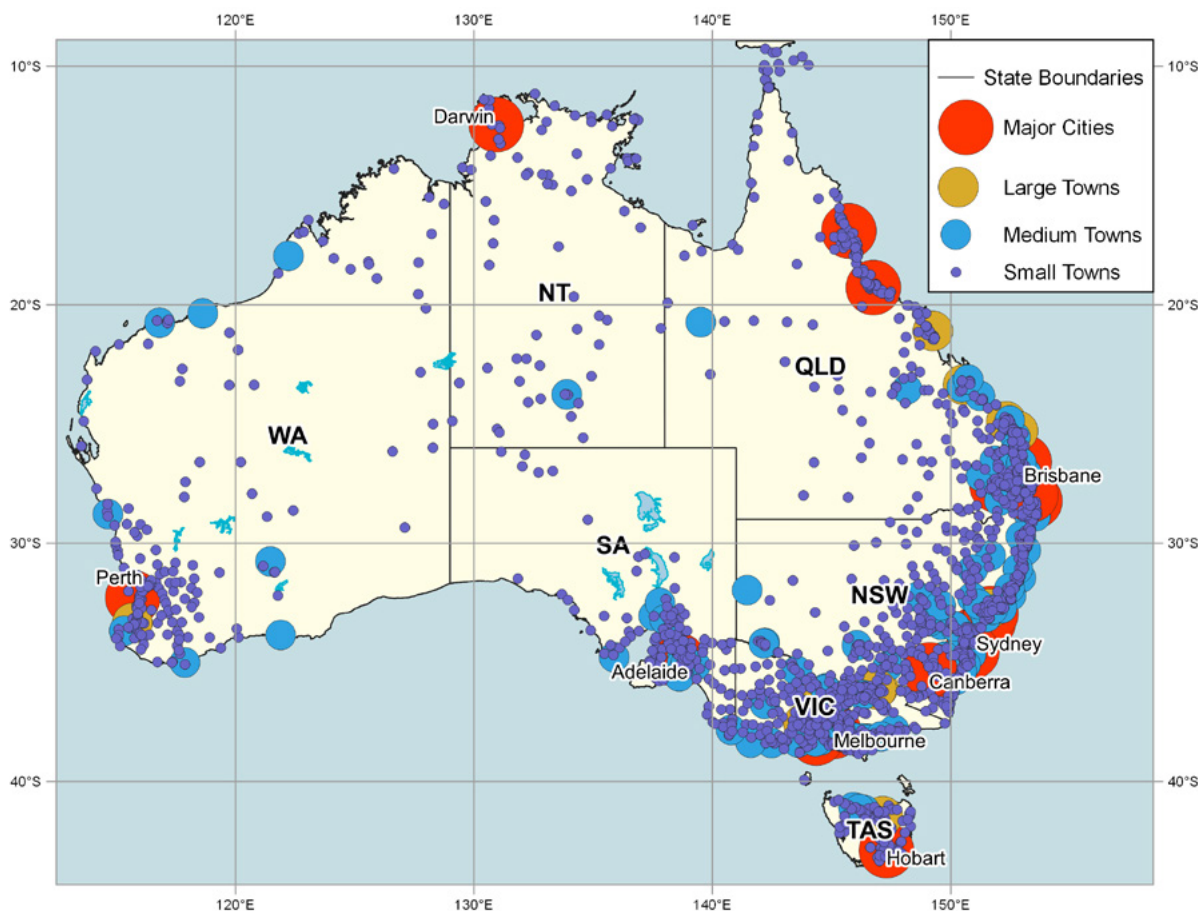
However, this has not always been the case. Below we consider traditional indigenous land use patterns (see Section 2.5.1), the changes that followed European settlement (see Section 2.5.2), and the methods that are currently used to map and monitor land use in Australia (see Section 2.5.3).

Land use in Australia today is a legacy of patterns of land occupation since European settlement—from early pastoralism, agriculture and prospecting through to today's major agricultural, forest and mining industries, reserve landscapes and urban communities. For most of the past 200 years, land use change has been driven by relatively unrestricted access to land, technological change and growth in productivity and population.

(Lesslie et al., 2011)

Figure 2.15 Australia's towns by population size groupings, 2016

In this classification, major cities > 100,000 residents, large towns 50,000–100,000 residents, medium towns 10,000–50,000 residents and small towns < 10,000 (and generally > 200) residents.



Source: Tony Sparks, Icon Water, using gridded data from ABS (2016)

2.5.1 Indigenous patterns

For scores of millennia, the Australian landscape supported an indigenous population that may have numbered more than one million people (ABS, 2008). For most of the last two centuries, these people of Australia's first nations were believed to have followed a semi-nomadic lifestyle based on hunting and gathering. More recently, analysis of reports by early settlers and explorers has cast a different light on the lifestyles of these indigenous communities (Tindale, 1974; Gerritsen, 2008). Gammage (2012) summarises the Aboriginal land management 'law' in terms of three rules:

- ensure that all life flourishes;
- make plants and animals abundant, convenient and predictable; and
- think universal, act local.

Early reports of Australian coastal vegetation, such as “the whole country or at least a great part of it might be cultivated without being obliged to cut down a single tree”³ or “the country looked very pleasant and fertile; and the trees, quite free from underwood, appeared like plantations in a gentleman's park”,⁴ describe a rather different landscape from the one that exists today. Numerous other descriptions—both narratives and artworks—by early settlers and explorers support the view that portions of Australia's landscape (particularly higher rainfall areas of open woodlands and woodlands, and some drier open forests) have changed significantly since European settlement, partly by overgrazing and partly by underburning (Gammage, 2012).

Traditional land management practices included the use of fire to reduce vegetative fuel loads, which helped to shape the distribution of native vegetation until the time of European settlement: “For more than 40,000 years, Aborigines lit mostly mild fires that consumed dead wood and dry herbage, killed seedlings, reduced some saplings back to ground level and scorched the leaves of some small trees and large shrubs. These fires allowed annual herbs to germinate and perennials to flush with new growth. They recycled nutrients from dead and dry into new growth. They maintained a diverse, open, safe and productive environment. After European settlers disrupted Aboriginal burning, dead wood, litter, and dry herbage accumulated. Too many seedlings and saplings grew into trees or bushes. Delicate herbage was smothered and nutrient cyclings was disrupted. Megafires, chronic decline of eucalypts, scrub invasion, pestilence, loss of biodiversity and socio-economic distress have been the result.” (Jurskis, 2015)

Figure 2.16 Aboriginal grain harvest map

Grassland areas managed by aborigines as important sources of grain food, with names of some tribes overlaid.



Adapted from: Tindale (1974) Figure 31

Tindale (1974) compiled evidence suggesting that, prior to European settlement, most of the continent was managed to harvest grains, tubers, and fruits, including complex systems of aquaculture. For example, grassland regions from which Aboriginal tribes harvested grains are shown in Figure 2.16. It is interesting to compare this area with the extent and distribution of the current grain production zones shown in Figure 2.17 and Figure 11.1. Except in southwest and southeast Australia, the locations of grains harvested by indigenous peoples do not coincide with current grain production zones.

... it may perhaps be doubted whether any section of the human race has exercised a greater influence on the physical condition of any large portion of the globe than the wandering savages of Australia.
(Edward Curr, 1883)

3 James Cook (1770) quoted by Gammage (2012) page 5

4 Sydney Parkinson (1770) quoted by Gammage (2012) page 5

*They live in a tranquillity which is not disturbed by the inequality of condition;
the earth and sea of their own accord furnishes them with all things necessary for life;
... they live in a warm and fine climate and enjoy a very wholesome air ...
in my opinion ... they think themselves provided with all the necessities of life
and that they have no superfluities
(James Cook, 1770, from Endeavour Journal)*

2.5.2 European settlement patterns

European settlement patterns in Australia have been driven, and continue to be limited, by the availability of water and pastoral lands. The vast majority of the current population, estimated at more than 25 million (see Table 2.1), live in capital cities within the high rainfall zone (see Section 2.2). The advent of European culture introduced clearing and thinning of vegetation for agriculture, mining, and urban development, and modification of waterways for townships and irrigation. Since the First Fleet arrived in 1788, around one third of the traditionally vegetated land has been cleared or thinned for various land use purposes (AUSLIG, 1990), predominantly cropping and intensive pasture production (see Figure 2.12).

The agricultural regions, in which different forms of agricultural activity are considered to be viable, are closely related to topography and climate (see Sections 2.1 and 2.2 respectively) and broadly follow the coastal plains (see Sections 2.5.3 and 11.1). Within these regions, soil type tends to determine the most appropriate agricultural approach (FAO, 2009; see Figure 2.3).

In higher rainfall zones in the south and east of the continent, land management practices have both decreased the extent and density of natural vegetation and accelerated soil erosion, land degradation, and salinity (McKenzie *et al.*, 2006). In recent decades, regulations governing stocking rates, land clearing and cultivation practices, with controls on feral animals and chemical usage, have reduced the rate of soil degradation (see Sections 3.4 and 11.4).

2.5.3 Current land use

Current land use is mapped and monitored nationally by the Australian Land Use and Management (ALUM) classification system (DAWE, 2020e; see Section 3.3.4), based on a scheme proposed by Baxter and Russell (1994). This dataset compiles relevant federal, state, and territory data to indicate the dominant land use in each 50 m by 50 m grid cell. The relative proportions of area occupied by the major categories of land use in 2010–11 are listed in Table 2.9. A simplified map of these classes is shown in Figure 2.17. The latest datasets are available from DAWE (2020f). Land use mapping and monitoring, and details of the ALUM categories, are further discussed in Sections 3.3.4 and 3.4.2.

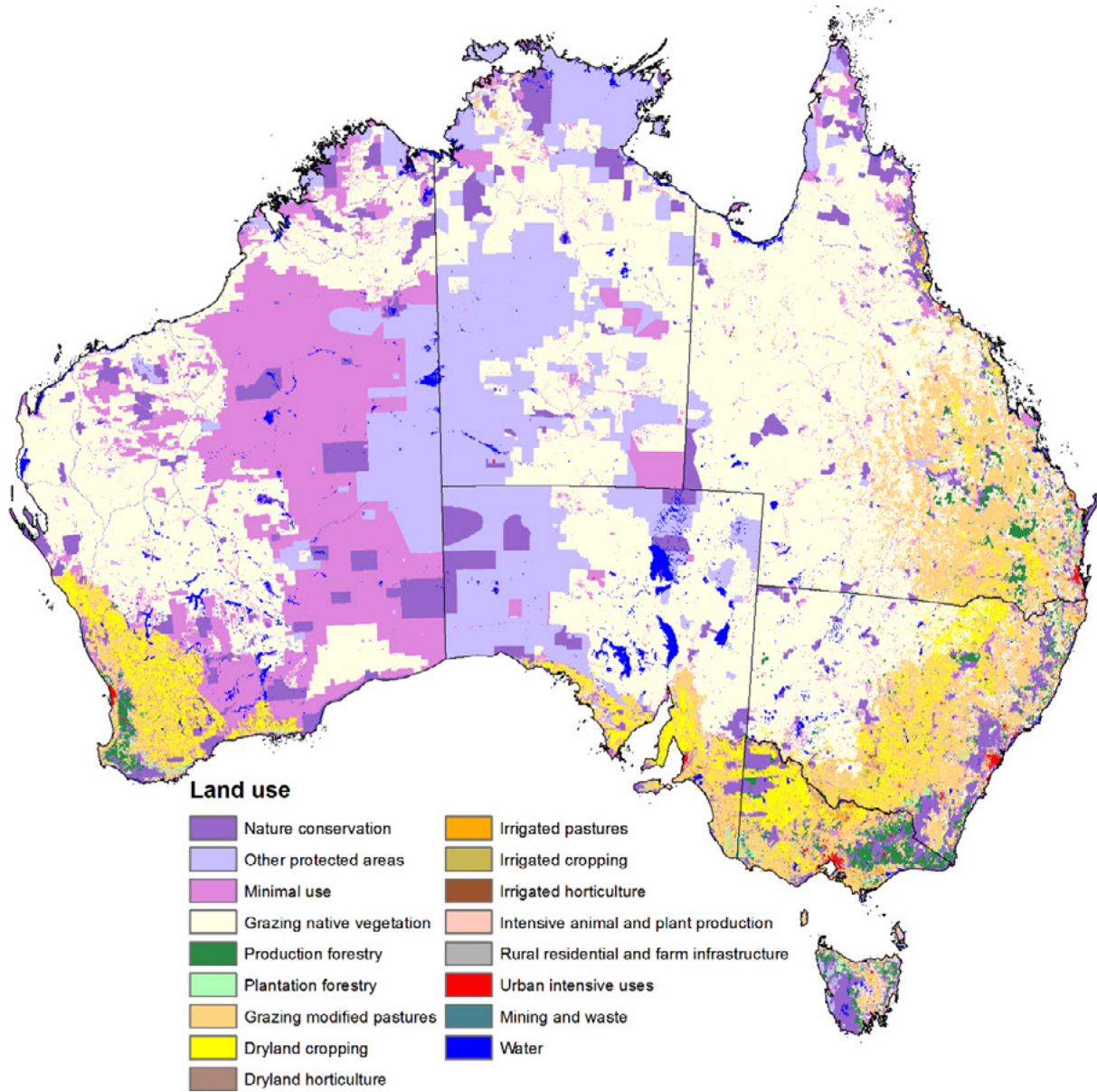
Table 2.9 Land uses in Australia 2010–11

Land use	Area (sq.km)	Percent (%)
Nature conservation	604,671	7.87%
Other protected areas including Indigenous uses	1,163,676	15.14%
Minimal use	1,172,679	15.26%
Grazing natural vegetation	3,448,896	44.87%
Production forestry	103,494	1.35%
Plantation forestry	25,752	0.34%
Grazing modified pastures	710,265	9.24%
Dryland cropping	275,928	3.59%
Dryland horticulture	743	0.01%
Irrigated pastures	6,048	0.08%
Irrigated cropping	9,765	0.13%
Irrigated horticulture	4,552	0.06%
Intensive animal and plant production	1,414	0.02%
Intensive uses (mainly urban)	13,806	0.18%
Rural residential	17,632	0.23%
Waste and mining	1,860	0.02%
Water	125,542	1.63%
No data	401	0.005%
Total	7,687,124	100.00%

Source: ABARES (2020)

Figure 2.17 Land use in Australia for 2010–11

17 class summary of land use derived using a modelling approach based on agricultural statistics, satellite imagery, and other land use information.



Source: ABARES (2020)

The Australian is fortunate that close to the main cities there still lie areas of virgin bush where it is possible to find direct contact with nature. There are few who have not boiled a billy under the gum-trees.
(Charles F. Laserson, 1953)

2.6 Further Information

About Australia

Overview: <https://www.australia.gov.au/about-australia/our-country>

Natural Environment: <https://www.australia.gov.au/about-australia/our-country/our-natural-environment>

National Location Information: <https://www.ga.gov.au/scientific-topics/national-location-information>

ANUDEM: <https://fennerschool.anu.edu.au/research/products/anudem>

Geofabric V3.2 products, documentation and tutorials: <http://www.bom.gov.au/water/geofabric/>

Australian Ecosystem and Climate Datasets

TERN Data Discovery Portal: <https://portal.tern.org.au/#/e8fbc61b>

Australian Soil Datasets

Australian Soil Resource Information System (ASRIS): <https://www.asris.csiro.au/>

Soil and Landscape Grid of Australia: TERN (2020)

ALUM Datasets

Land use data download: <http://www.agriculture.gov.au/abares/aclump/land-use/data-download>

Indigenous Land Use

Tindale (1974)

Gerritsen (2008)

Gammage (2012)

Invasive Species

Invasive Species CRC: <https://invasives.com.au/our-publications>

Vegetation Resources

Australia:

Keith (2017)

NVIS: <http://www.environment.gov.au/land/native-vegetation/national-vegetation-information-system>

New South Wales:

NSW State Vegetation Type Mapping (SVTM): see Excursus 8.2; <https://www.environment.nsw.gov.au/vegetation/state-vegetation-type-map.htm>

BioNET vegetation (biodiversity data repository): <http://www.bionet.nsw.gov.au>

Native Vegetation publications: <https://www.environment.nsw.gov.au/vegetation/OtherPublications.htm>

Queensland:

Dept. Science and Environment: <https://environment.des.qld.gov.au/maps-imagery-data/online/>

Queensland Herbarium: <https://www.qld.gov.au/environment/plants-animals/plants/herbarium/mapping-ecosystems>

Tasmania:

Barker (2001)

Kitchener and Harris (2013)

TASVEG: [https://dpiwve.tas.gov.au/conservation/development-planning-conservation-assessment/planning-tools/monitoring-and-mapping-tasmanias-vegetation-\(tasveg\)/tasveg-the-digital-vegetation-map-of-tasmania](https://dpiwve.tas.gov.au/conservation/development-planning-conservation-assessment/planning-tools/monitoring-and-mapping-tasmanias-vegetation-(tasveg)/tasveg-the-digital-vegetation-map-of-tasmania)

Victoria:

Newell *et al.* (2006)

Sinclair *et al.* (2012)

Habitat hectares: <https://www.ari.vic.gov.au/research/modelling/mapping-vegetation-extent-and-condition>

Western Australia:

Shepherd *et al.* (2002)

Native Vegetation Extent: <https://catalogue.data.wa.gov.au/dataset/native-vegetation-exten>

2.7 References

- ABARES (2020). *Land Use in Australia—At a Glance* brochure, Australian Bureau of Agricultural and Resource Economics and Sciences website: <https://www.agriculture.gov.au/sites/default/files/abares/aclump/documents/Land%20use%20in%20Australia%20at%20a%20glance%202016.pdf>
- ABRS (2012). *Flora of Australia Online*. Australian Biological Resources Study, Canberra. <http://www.environment.gov.au/biodiversity/abrs/online-resources/flora/main/index.html>
- ABS (2008). Aboriginal and Torres Strait Islander Population. *Year Book Australia, 2008*. Australian Bureau of Statistics. <https://www.abs.gov.au/ausstats/abs@nsf/0/68AE74ED632E17A6CA2573D200110075?opendocument>
- ABS (2010). *Year Book Australia, 2009-10*. Australian Bureau of Statistics. <https://www.abs.gov.au/AUSSTATS/abs@Nsf/7d12b0f6763c78caca257061001cc588/bb322d1ad0d30a7fca25773700169c19!OpenDocument>
- ABS (2016). *Census of Population and Housing* webpage, Australian Bureau of Statistics website: <https://www.abs.gov.au/ausstats/abs@nsf/Lookup/by%20Subject/2071.0~2016~Main%20Features~Small%20Towns~113>
- ABS (2020). *Australian Demographic Statistics, Sep 2019* webpage, Australian Bureau of Statistics website: <https://www.abs.gov.au/AUSSTATS/abs@nsf/Latestproducts/3101.0Main%20Features1Sep%202019?opendocument&tabname=Summary&prodno=3101.0&issue=Sep%202019&num=&view=>
- ACT EPSDD (2020). *Conservation and Ecological Communities* webpage, Environment, Planning and Sustainable Development Directorate, ACT government website: https://www.environment.act.gov.au/cpr/conservation_and_ecological_communities
- AG (2020). *How Government Works* webpage, Australian Government website: <https://info.australia.gov.au/about-government/how-government-works>
- Allan, G., and Southgate, R. (2002). Fire regimes in the spinifex landscapes of Australia. In: *Flammable Australia: the Fire Regimes and Biodiversity of a Continent* (Eds: R. Bradstock, J. Williams and A. Gill) pp. 145–176. Cambridge University Press, Cambridge.
- Allan, G., Johnson, A., Cridland, S., and Fitzgerald, N. (2003). Application of NDVI for predicting fuel curing at landscape scales in northern Australia: Can remotely sensed data help schedule fire management operations? *International Journal of Wildland Fire*, 12(4), 299–308. doi:10.1071/WF03016
- Ardalan, A., Oskarsson, M., Natanaelsson, C., Wilton, A.N., Ahmadian, A., and Savolainen, P. (2012). Narrow genetic basis for the Australian dingo confirmed through analysis of paternal ancestry. *Genetica*, 140 (1–3), 65–73. doi:10.1007/s10709-012-9658-5
- Austrade (2020). *Land Tenure* webpage, Australian Trade and Investment Commission website: <https://www.austrade.gov.au/land-tenure/Land-tenure/about-land-tenure>
- AUSLIG (1990). *Atlas of Australian Resources (Third Series) Volume 6: Vegetation*. Australian Land and Surveying Information Group, AUSMAP, Department of Administrative Services, Canberra. 64 p.
- Austrroads (2004). *Impact of Climate Change on Road Infrastructure*. Austrroads Inc, Sydney. ISBN 0 85588 692 7 http://www.bitre.gov.au/publications/2004/files/cr_001_climate_change.pdf
- Barker, P. (2001). *A Technical Manual for Vegetation Monitoring*. Department of Primary Industries, Water and Environment, Hobart.
- Bartlett, T. Leonard, M., and Morgan, G. (2007). The mega-fire phenomenon: some Australian perspectives. In: *The 2007 Institute of Foresters of Australia and New Zealand Institute of Forestry Conference: Programme, Abstracts and Papers*. Institute of Foresters of Australia, Canberra.
- Baxter, J.T., and Russell, L.D. (1994). *Land use mapping requirements for natural resource management in the Murray-Darling Basin, Project M305: Task 6*. Victorian Department of Conservation and Natural Resources, Melbourne.
- Beadle, N.C.W. (1981). *The Vegetation of Australia*. Cambridge University Press, Cambridge. 690p.
- Beadle, N.C., and Costin, A.B. (1952). Ecological Classification and Nomenclature. *Proceedings of Linnaeus Society NSW*, 77(1–2), 61–82.
- BoM (2020a). *Long-range weather and climate* webpage. Bureau of Meteorology website: <http://www.bom.gov.au/climate/averages/maps.shtml>
- BoM (2020b). *About the Geofabric* webpage. Bureau of Meteorology website: <http://www.bom.gov.au/water/geofabric/about.shtml>

- BoM (2020c). *Topographic Drainage Basins and River Regions* webpage. Bureau of Meteorology website: <http://www.bom.gov.au/water/about/riverBasinAuxNav.shtml>
- Booth, C., and Tubman, W. (2011). *Water Down Under: Understanding and Managing Australia's Great Artesian Basin*. Department of Sustainability, Environment, Water, Populations and Communities., Canberra. ISBN: 978-1-921733-19-2.
- Bradstock, R.A., and Cohn, J (2002). Fire regimes and biodiversity in semi-arid mallee ecosystems. In *Flammable Australia: The Fire Regimes and Biodiversity of a Continent*. (Eds: R.A. Bradstock, J.E. Williams, and M.A. Gill) Cambridge University Press, Cambridge.
- Bradstock, R.A., Hammill, K.A., Collins, L., and Price, O. (2010). Effects of weather, fuel and terrain on fire severity in topographically diverse landscapes of south-eastern Australia. *Landscape Ecology*, 25(4), 607–619. doi:10.1007/s10980-009-9443-8
- Brocklehurst, P., Lewis, D., Napier, D., and Lynch, D. (2007). *Northern Territory Guidelines and Field Methodology for Vegetation Survey and Mapping*. Technical Report No. 02/2007D. Department of Natural Resources, Environment and the Arts, Palmerston, Northern Territory.
- Burrows, N.L. (2018). Feral Animals in the Semi-arid and Arid Regions of Australia: Origins, Impacts and Control. In *On the Ecology of Australia's Arid Zone*. (Ed: H. Lambers). Springer, Cham. <https://doi.org/10.1007/978-3-319-93943-8>
- Clarke, G.M. (2001). *Environmental pest species in Australia*. Australian Government, Environment Australia, Canberra.
- Cox, C.B. (2000). Plate Tectonics, Seaways and Climate in the Historical Biogeography of Mammals. *Memórias do Instituto Oswaldo Cruz*, 95(4), 509–516. <https://doi.org/10.1590/S0074-02762000000400012>
- Cronquist, A. (1968). *The Evolution and Classification of Flowering Plants*. Houghton Mifflin, Boston.
- Cronquist, A. (1981). *An Integrated System of Classification of Flowering Plants*. Columbia University Press, New York. 1262pp.
- CSIRO (2014). *Australian Soil Resource Information System*. www.asris.csiro.au
- Curr, E.M. (1883). *Recollections of Squatting in Victoria Then called the Port Phillip District (From 1841 to 1851)*. George Robertson, Melbourne. <http://classic.austlii.edu.au/au/journals/AUCollLawMon/1883/1.pdf>
- DAWE (2019). *About Kati Thanda—Lake Eyre Basin* webpage, Department of Agriculture, Water and the Environment website: <https://www.agriculture.gov.au/water/national/lake-eyre-basin/about>
- DAWE (2020a). *Great Artesian Basin Sustainability Initiative* webpage. Department of Agriculture, Water and the Environment website: <https://www.agriculture.gov.au/water/national/great-artesian-basin/great-artesian-basin-sustainability-initiative>
- DAWE (2020b). *NVIS Data Products* webpage, Department of Agriculture, Water and the Environment website: <http://www.environment.gov.au/land/native-vegetation/national-vegetation-information-system/data-products#nvis31>
- DAWE (2020c). *Australia's bioregions (IBRA)* webpage, Department of Agriculture, Water and the Environment website: <https://www.environment.gov.au/land/nrs/science/ibra>
- DAWE (2020d). *Australia's ecoregions* webpage, Department of Agriculture, Water and the Environment website: <https://www.environment.gov.au/land/nrs/science/ibra/australias-ecoregions>
- DAWE (2020e). *Australian Land Use and Management Classification Version 8 (October 2016)* webpage, Department of Agriculture, Water and the Environment website: <https://www.agriculture.gov.au/abares/aclump/land-use/alum-classification>
- DAWE (2020f). *Land Use and Management Information for Australia* webpage, Department of Agriculture, Water and the Environment website: <https://www.agriculture.gov.au/abares/aclump>
- DELWP (2020). *Bioregions and EVC benchmarks* webpage, Victorian Department of Environment, Land, Water and Planning website: <https://www.environment.vic.gov.au/biodiversity/bioregions-and-ecv-benchmarks>
- DEE (2019a). *Weeds in Australia* webpage, Department of Environment and Energy website: <https://www.environment.gov.au/biodiversity/invasive/weeds/>
- DEE (2019b). *Weeds in Australia/Grants and Government/Roles and Responsibilities* webpage, Department of Environment and Energy website: <https://www.environment.gov.au/biodiversity/invasive/weeds/government/roles/index.html>
- DEE (2019c). *Weeds in Australia/About weeds/National weeds list* webpage, Department of Environment and Energy website: <https://www.environment.gov.au/biodiversity/invasive/weeds/weeds/lists/index.html>

- DEE (2019d). *Feral Animals in Australia* webpage, Department of Environment and Energy website: <https://www.environment.gov.au/biodiversity/invasive-species/feral-animals-australia>
- Denny, E.A., and Dickman, C.R. (2010). *Review of cat ecology and management strategies in Australia*. Invasive Animals Cooperative Research Centre, Canberra. ISBN: 978-0-9806716-6-7
- DEWR (2007). *Australia's Native Vegetation: A summary of Australia's Major Vegetation Groups, 2007*. Department of the Environment and Water Resources, Canberra, ACT.
- Eldridge, D.J., Poore, A.G., Ruiz-Colmenero, M., Letnic, M., and Soliveres, S. (2016). Ecosystem structure, function, and composition in rangelands are negatively affected by livestock grazing. *Ecological Applications*, 26(4), 1273–1283.
- Ellis, S., Kanowski, P., and Whelan, R. (2004). *National Inquiry on Bushfire Mitigation and Management*. Commonwealth of Australia, Canberra.
- ERIN (2012). *Terrestrial Ecoregions in Australia* (map based on IBRA7). Environmental Resources Information Network, Department of Sustainability, Environment, Water, Population and Communities. https://www.environment.gov.au/system/files/pages/1716eb1c-939c-49a0-9c0e-8f412f04e410/files/ecoregions_1.pdf
- FAO (2009). Country Pasture/Forage Resource Profiles: Australia. Prepared by Edwin Wolfe. Food and Agriculture Organisation of the United Nations. <http://www.fao.org/ag/agp/AGPC/doc/Counprof/Australia/australia.htm>
- Feng, M., Weller, E., Hill, K. (2009). The Leeuwin Current. In *A Marine Climate Change Impacts and Adaptation Report Card for Australia*. (Eds. E.S. Poloczanska, A.J. Hobday and A.J. Richardson), NCCARF Publication 05/09. ISBN 978-1-921609-03-9.
- Florence, R.G. (1985). Eucalypt Forests and Woodlands. In *Think Trees, Grow Trees*, AGPS, Canberra.
- GA (2002). *GEODATA TOPO 10M 2002* webpage, Geoscience Australia website: <https://ecat.ga.gov.au/geonetwork/srv/eng/catalog.search#/metadata/60803>
- GA (2019). Geoscience Australia website, *Digital Elevation Data* webpage: <http://www.ga.gov.au/scientific-topics/national-location-information/digital-elevation-data>
- GA (2020a). *Area of Australia—States and Territories* webpage, Geoscience Australia website: <https://www.ga.gov.au/scientific-topics/national-location-information/dimensions/area-of-australia-states-and-territories>
- GA (2020b). *Great Artesian Basin* webpage, Geoscience Australia website: <http://www.ga.gov.au/scientific-topics/water/groundwater/gab>
- GA (2020c). *Deserts* webpage, Geoscience Australia website: <https://www.ga.gov.au/scientific-topics/national-location-information/landforms/deserts#:~:text=Apart%20from%20Antarctica%2C%20Australia%20is,arid%2C%20or%20semi%20Darid.>
- Gammage, B. (2012). *The Biggest Estate on Earth*. Allen and Unwin, Sydney.
- Gerritsen, R. (2008). *Australia and the Origins of Agriculture*. British Archaeological Reports International Series 1874, Oxford.
- Gillison, A.N., and Anderson, D.J. (1981). *Vegetation Classification in Australia*. CSIRO, Canberra. <https://openresearch-repository.anu.edu.au/bitstream/1885/114747/2/b12586894.pdf>
- Glenn, E., Doody, T.M., Guerschman, J.P., Huete, A.R., King, E.A., McVicar, T.R., van Dijk, A.I.J.M., van Niel, T.G., Yebra, M., and Zhang, Y. (2011). Actual evapotranspiration estimation by ground and remote sensing methods: the Australian experience. *Hydrological Processes*, 25(26), 4103–4116. doi:10.1002/hyp.8391
- Harris, S., and Kitchener, A. (2005). *From Forest to Fjaeldmark: Descriptions of Tasmania's Vegetation* (edition 1). Department of Primary Industries, Parks, Water and Environment. Printing Authority of Tasmania, Hobart.
- Harrison, B.A., and Bradstock, R.A. (2010). *Current Use of Remote Sensing to Map and Monitor Fire in Australia*. Report by CERMB, University of Wollongong for NSW Rural Fire Service.
- Henderson, W.R. (2009). *Pathogens in invasive animals of Australia*. Invasive Animals Cooperative Research Centre, Canberra. ISBN: 978-0-9806716-4-3.
- Hnatiuk R.J., Thackway R., and Walker J. (2009). *Vegetation*. In: *Australian Soil and Land Survey: Field Handbook* (3rd Edn). (Ed. National Committee on Soil and Terrain) pp. 73–125. CSIRO Publishing, Melbourne.
- Hobbs, R.J., and McIntyre, S. (2005). Categorizing Australian landscapes as an aid to assessing the generality of landscape management guidelines. *Global Ecology and Biogeography*, 14, 1–15.

- Hutchinson, M.F., McIntyre, S., Hobbs, R.J., Stein, J.L., Garnett, S., and Kinloch, J. (2005). Integrating a global agro-climatic classification with bioregional boundaries in Australia. *Global Ecology and Biogeography* 14, 197–212.
- Isbell, R.F., and NCST (2021). *The Australian Soil Classification*, 3rd edn. Volume 4 of Australian Soil and Land Survey Handbooks Series, National Committee on Soil and Terrain. CSIRO Publishing, Melbourne.
- Jurskis, V. (2015). *Firestick Ecology*. Connor Court Publishing, Ballarat.
- Keith, D.A. (2004). *From ocean shores to desert dunes: the vegetation of New South Wales and the ACT*. Department of Environment and Conservation, Hurstville.
- Keith, D.A. (2017). *Australian Vegetation*. 3rd edn. Cambridge University Press, Cambridge. ISBN 978-1-107-11843-0
- Kitchener, A., and Harris, S. (2013). *From Forest to Fjaeldmark: Descriptions of Tasmania's Vegetation*. 2nd Edn. Department of Primary Industries, Parks, Water and Environment, Tasmania.
- Köppen, W. (1931). *Klimakarte der Erde. Grundriss der Klimakunde*, 2nd Ed., Berlin and Leipzig.
- Laseron, C.F. (1953). *The Face of Australia*. Angus and Robertson. 244 p.
- Lau, K.-M., and Yang, S. (2002). *Walker Circulation*. NASA, USA. http://meteo.fisica.edu.uy/Materias/climatologia/teorico_climatologia_2013/LauWalkercirculation.pdf
- Lesslie, R., Mewett, J., and Walcott, J. (2011). *Landscapes in transition: Tracking land use change in Australia. Science and Economic Insights, 2.2*. Australian Bureau of Agricultural and Resource Economics and Sciences, Canberra, ACT.
- Lewis, D.L., Brocklehurst, P.B., Thackway, R., and Hill, J.V. (2008). Adopting national vegetation guidelines and the National Vegetation Information System (NVIS) framework in the Northern Territory. *Cunninghamia*, 10(4), 557–567.
- Lunt, I., Eldridge, D.J., Morgan, J.W., and Witt, G.B. (2007). Turner Review No. 13: A framework to predict the effects of livestock grazing and grazing exclusion on conservation values in natural ecosystems in Australia. *Australian Journal of Botany*, 55, 401–415. doi:10.1071/BTO6178
- McKenzie, N.L., Burbidge, A.A., Baynes, A., Brereton, R.N., Dickman, C.R., Gordon, G., Gibson, L.A., Menkhorst, P.W., Robinson, A.C., Williams, M.R., and Woinarski, J.C.Z. (2006). Analysis of factors in the recent decline of Australia's mammal fauna. *Journal of Biogeography*, 34, 597–611. <https://doi.org/10.1111/j.1365-2699.2006.01639.x>
- McKenzie, N.J., Jacquier, D.W., Maschmedt, D.J., Griffin, E.A., and Brough, D.M. (2012). *The Australian Soil Resource Information System (ASRIS) Technical Specifications Revised Version 1.6*, June 2012. The Australian Collaborative Land Evaluation Program. <http://www.asris.csiro.au/downloads/ASRIS%20Tech%20Specs%201.6.pdf>
- McLeod, R. (2016). *Cost of Pest Animals in NSW and Australia, 2013–14*. eSYS Development Pty Ltd, Sydney. ISBN 978-0-6480750-3-5 (online) <https://invasives.com.au/wp-content/uploads/2019/01/Cost-of-weeds-report.pdf>
- McLeod, R. (2018). *Annual Costs of Weeds in Australia*. eSYS Development Pty Ltd, Sydney. <https://invasives.com.au/wp-content/uploads/2019/01/Cost-of-weeds-report.pdf>
- MDBA (2013). *Murray Darling Basin Authority website*: <http://www.mdba.gov.au/about-basin>
- NCST (2009). *Australian Soil and Land Survey Field Handbook*. 3rd edn. National Committee on Soil and Terrain, CSIRO, Canberra. 264p.
- Neldner, V.J., Niehus, R.E., Wilson, B.A., McDonald, W.J.F., Ford, A.J., and Accad, A. (2019). *The Vegetation of Queensland. Descriptions of Broad Vegetation Groups*. Version 4.0. Queensland Herbarium, Department of Environment and Science.
- Newell, G., White, M., Griffioen, P., and Conroy, M. (2006). Vegetation condition mapping at a landscape-scale across Victoria. *Ecological Management and Restoration*, 7, S65–S68.
- Norris, A., Low, T., Gordon, I., Saunders, G., Lapidge, S., Lapidge, K., Peacock, T., and Pech, G. (2005). *Review of the management of feral animals and their impact on biodiversity in the Rangelands. A resource to aid NRM planning*. Pest Animal Control CRC Report 2005, Pest Animal Control CRC, Canberra.
- NRM (2019). *Biosecurity webpage, NRM Regions Australia website*: <http://nrmregionsaustralia.com.au/biosecurity/>
- NSW DPIE (2020). *BioNet Vegetation Classification webpage, NSW Department of Planning, Industry and Environment*: <https://www.environment.nsw.gov.au/research/Visclassification.htm>

- NT EPA (2013). *Guidelines for Assessment of Impacts on Terrestrial Biodiversity*. Version 2.0. Northern Territory Environment Protection Authority. https://ntepa.nt.gov.au/_data/assets/pdf_file/0004/287428/guideline_assessment_terrestrial_biodiversity.pdf
- NTNVIS (2020). *NVIS Version 3.1, National Vegetation Information System, NT Data Compilation*: http://www.ntlis.nt.gov.au/metadata/export_data?metadata_id=2DBC771207006B6E040CD9B0F274EFE&type=html
- NVIS Technical Working Group (2017). *Australian Vegetation Attribute Manual: National Vegetation Information System, Version 7.0*. (Eds: Bolton, M.P., deLacey, C., and Bossard, K.B.). Department of the Environment and Energy, Canberra.
- Olson, D.M., Dinerstein, E., Wikramanayake, E.D., Burgess, N.D., Powell, G.V.N., Underwood, E.C., D'Amico, J.A., Itoua, I., Strand, H.E., Morrison, J.C., Loucks, C.J., Allnutt, T.F., Ricketts, T.H., Kura, Y., Lamoreux, J.F., Wettengel, W.W., Hedao, P., and Kassem, K.R. (2001) Terrestrial ecoregions of the world: a new map of life on Earth. *Bioscience*, 51(11), 933–938.
- Philp, M., and Taylor, M. (2012). *Beyond Agriculture: Exploring the application of the Thornthwaite Moisture Index to infrastructure and possibilities for climate change adaptation*. ACCARNSI Discussion Paper X, National Climate Change Adaptation Research Facility.
- PIRSA (2019). *The Dog Fence in South Australia* webpage, Primary Industry and Regions, South Australia: https://www.pir.sa.gov.au/biosecurity/weeds_and_pest_animals/animal_pests_in_south_australia/established_pest_animals/wild_dogs/dog_fence?SQ_VARIATION_299639=0
- Pyne, S.J. (1992). *The Burning Bush: A Fire History of Australia*. Allen and Unwin, Sydney. 520pp. ISBN: 1863731946
- Queensland Government (2020a). *Broad vegetation groups* webpage: <https://www.qld.gov.au/environment/plants-animals/plants/ecosystems/broad-vegetation>
- Queensland Government (2020b). *Regional ecosystems* webpage: <https://www.qld.gov.au/environment/plants-animals/plants/ecosystems>
- Ransley, T.R., and Smerdon, B.D. (Eds) (2012). *Hydrostratigraphy, hydrogeology and system conceptualisation of the Great Artesian Basin*. A technical report to the Australian Government from the CSIRO Great Artesian Basin Water Resource Assessment. CSIRO Water for a Healthy Country Flagship, Australia.
- Russell-Smith, J., Yates, C., Edwards, A., Allan, G.E., Cook, G.D., Cooke, P., Craig, R., Heath, B., and Smith, R. (2003) Contemporary fire regimes of northern Australia, 1997-2001: change since Aboriginal occupancy, challenges for sustainable management. *International Journal of Wildland Fire*, 12, 283–297.
- SA DEWNR (2019). *Native Vegetation Floristic Areas (NVIS)* webpage, SA Department of Environment, Water and Natural Resources: http://location.sa.gov.au/lms/Reports/ReportMetadata.aspx?p_no=898+&pa=dewnr
- Sagoff, M. (1984). Animal liberation and environmental ethics: bad marriage, quick divorce. *Osgoode Hall Law Journal*, 22, 297–307.
- Scarth, P., Armston, J., Lucas, R., and Bunting, P. (2019). A Structural Classification of Australian Vegetation Using ICESat/GLAS, ALOS PALSAR, and Landsat Sensor Data. *Remote Sensing*, 11(2), 147. <https://doi.org/10.3390/rs11020147>
- Scott, J.K., Friedel, M.H., Grice, A.C., and Webber, B.L. (2018). Weeds in Australian Arid Regions. In *On the Ecology of Australia's Arid Zone*. (Ed: H. Lambers). Springer, Cham. <https://doi.org/10.1007/978-3-319-93943-8>
- Shepherd, D.P, Beeston, G.R, and Hopkins, A.J. (2002). *Native vegetation in Western Australia : extent, type and status*. Department of Agriculture and Food, Western Australia, Perth. Report 249.
- Sinclair, S.J., White, M.D., Medley, J., Smith, E., and Newell, G.R. (2012). Mapping the past: constructing a digital land-use history map for Victoria, Australia. *Proceedings of the Royal Society of Victoria*, 124(3), 193–206.
- Smith, T.M., Woodward, I.A., Shugart, H.H. (Eds) (1997). *Plant Functional Types: Their Relevance to Ecosystem Properties and Global Change*. Cambridge University Press. England.
- Specht, R.L. (1970). Vegetation. In *The Australian Environment*. 4th Edn. (Ed: Leeper, G.W.) CSIRO, Melbourne.
- Specht, R.L. (1983). Foliage projective covers of overstorey and understorey strata of mature vegetation in Australia. *Austral Ecology*, 8, 433–439. doi:10.1111/j.1442-9993.1983.tb01340.x
- Stern, H., de Hoedt, G., and Ernst, J. (1999). *Objective classification of Australian climates*. 8th Conference on Aviation, Range and Aerospace Meteorology, Amer. Meteor. Soc., Dallas, Texas, 10-15 Jan., 1999. http://www.bom.gov.au/climate/environ/other/koppen_explain.shtml

- Taylor, G. (1927). The Topography of Australia. Feature Article in *Year Book Australia, 1927*. <https://www.abs.gov.au/AUSSTATS/abs@.nsf/Previousproducts/1301.0Feature%20Article20601927?opendocument&tabname=Summary&prodno=1301.0&issue=1927&num=&view=>
- TERN (2020). Soil and Landscape Grid option on TERN Data Discovery Portal: <https://portal.tern.org.au/#/e8fbc61b>
- Thackway, R., and Cresswell, I.D. (1995). *An Interim Biogeographic Regionalisation for Australia: a Framework for Establishing the National System of Reserves, Version 4.0*. Australian Nature Conservation Agency, Canberra.
- Thackway, R., and Freudenberger, D. (2016). Accounting for the Drivers that Degrade and Restore Landscape Functions in Australia. *Land*, 5, 40. doi:10.3390/land5040040
- Thackway, R., Neldner, J., and Bolton, M. (2008). Vegetation. In: *Australian Soil and Land Survey Handbook Guidelines for Conducting Surveys* (2nd Edition). (Eds: N.J. McKenzie, M.J. Grundy, R. Webster, and A.J. Ringrose-Voase). CSIRO Publishing, Melbourne.
- Thorntwaite, C.W. (1931). The climates of North America according to a new classification. *Geographical Review*, 21, 633–655.
- Thorntwaite, C.W. (1948). An approach toward a rational classification of climate. *Geographical Review*, 38, 55–94
- Tindale, N.B. (1974). *Aboriginal Tribes of Australia: Their Terrain, Environmental Controls, Distribution, Limits, and Proper Names*. ANU Press, Canberra. ISBN: 0-7081-0741-9
- Walker, J., and Hopkins, M.S. (1990). *Vegetation. Australian Soil and Land Survey Handbook: Guidelines for Conducting Surveys*. (Eds: R.H. Gunn, J.A. Beattie, R.E. Reid and R.H.M. v.d. Graaff). Inkata Press, Melbourne. pp 58–86.
- Williams, R.J. (1959). Vegetation map of Australia in *The Australian Environment*. 3rd Edition. CSIRO, Melbourne. Reproduced with changed legend in *The Australian Environment*. 4th Edition (Ed: G.W. Leeper, 1970) CSIRO, Melbourne.
- Williams, J., Hook, R.A., and Hamblin, A. (2002). *Agro-Ecological Regions of Australia, Methodologies for Their Derivation and Key Issues in Resource Management*. CSIRO Land and Water, Canberra, Australia.



3 Mapping Vegetated Landscapes

In this section we differentiate between mapping the extent, type, condition, and use of vegetated landscapes. Initially we will consider some key concepts that underpin landscape mapping (see Section 3.1) and methods used to map land cover (see Section 3.2), before discussing specific approaches used to map (see Section 3.3) and monitor (see Section 3.4) terrestrial vegetation in the Australian landscape.

3.1 Key Concepts in Landscape Mapping

The terms ‘vegetation type’, ‘vegetation condition’, ‘land cover’, and ‘land use’ are frequently encountered in landscape mapping applications. In the following two sub-sections we distinguish between these terms in the context of mapping the Australian terrestrial landscape.

3.1.1 Vegetation type versus vegetation condition

Traditional vegetation maps show the type, or variety, of vegetation in a particular location. While this information is a useful summary of the diversity of terrestrial vegetation in a landscape, it does not indicate the condition or ‘quality’ of that vegetation against some defined ‘benchmark’ or reference state. Information about the extent and condition of each vegetation type is critical for monitoring rates of loss and gain in different types of vegetation and across defined regions (such as IBRA regions or different jurisdictions). More recently, several federal, state, and territory mapping projects in Australia have considered approaches to benchmarking vegetation condition as well as defined the vegetation type. As a benchmark for assessing the condition of current vegetation, these projects infer the likely condition of each vegetation type in the year 1750—that is, before European settlement (see Figure 2.12 and Excursus 8.2). This benchmark is derived from:

- observations of recent changes in vegetation patterns; and
- models that consider those changes in conjunction with coincident changes in relevant environmental variables.

The value of such a benchmark is twofold as it provides:

- a picture of vegetation distribution and condition before European settlement; and
- a consistent baseline for measuring future vegetation changes.

Vegetation condition mapping has particular relevance in the context of monitoring compliance of land owners to environmental legislation governing land clearing in Australia (see Volume 2D—Excursus 14.3 and Excursus 19.2 below). Specific examples of mapping and monitoring vegetation type and condition in Australia are given in Sections 3.3 and 3.4 respectively. We note here that spatial mapping of changes and trends is not the same as site-based monitoring of changes and trends, although there is close relationship between directly-measured attributes and indicators and mapping these as classes of vegetation condition.

Land cover is a convenient label for that part of the biosphere that is critical for the continued existence of all terrestrial life.
(Graetz et al., 1992)

Background image: Astronaut photograph of Kangaroo Island, SA, taken from the International Space Station on 21 November 2002. Source: NASA Gateway to Astronaut Photography of Earth

3.1.2 Land cover versus land use

A wide variety of land cover inventories have been conducted by human civilisations over several millennia. This information has allowed societies to understand their environment, and plan and monitor their opportunities for development and sustainability.

Land cover is an excellent indicator of the resilience—or fragility—of the Earth’s biophysical resources, including soils, nutrients, water, plants, and wildlife (ANRA, 2009). Mapping and monitoring of existing land cover enable the impact of specific land uses and management practices to be observed and quantified. Land cover assessment may also indicate the suitability of potential land uses (such as nature conservation, urban development, agriculture, or mining) in a particular area. Additionally, long term monitoring of land cover is invaluable for understanding the impacts of climate variability and relating these to patterns of severe climate events including wildfire, droughts, floods, and cyclones.

Natural vegetation patterns are largely determined by climate (especially rainfall), elevation (plus slope and aspect), and soil type, such that, in a pristine environment, natural land covers can often be modelled from these environmental attributes (Nix, 1982; see Section 2). Once these natural patterns have been modified by human activities, however, land cover cannot necessarily be inferred from such models but needs to be surveyed, measured, and/or inferred in some way.

Although the terms ‘land cover’ and ‘land use’ are sometimes used interchangeably, they do refer to different characteristics of land. Land cover is defined as the “observed (bio)physical cover on the Earth’s surface” (Di Gregorio, 2005). Strictly speaking, while this definition only includes vegetation and man-made features, the term is generally accepted to embrace water surfaces, bare rock, and exposed soil as well. Examples of common land covers include grass, shrubs, trees, water, bare ground, artificial surfaces, and buildings.

The simplest definition of resilience is the ability to cope with shocks and to keep functioning in much the same kind of way. It is a measure of how much an ecosystem, a business, a society can change before it crosses a tipping point into some other kind of state that it then tends to stay in.

(Walker, 2020)

By contrast, land use has been described as the “arrangements, activities and inputs people undertake in a certain land cover type to produce, change or maintain it” (Di Gregorio, 2005). Thus, land use describes the impact of human occupation on an environment rather than simply its biophysical components (Fisher *et al.*, 2005). A single land use can involve multiple land cover features, and multiple land uses can contain the same single land cover. For example, the term ‘rangelands’ describes land used to graze livestock, but may comprise different land covers, such as trees, shrubs, and grasses (see Section 15). Conversely, the land cover type ‘trees’ may be used for timber production or nature conservation. Accordingly, land use is not readily discriminated by EO of specific land cover features but can often be inferred by combining land cover information with data from other sources.

The importance of land use and land cover (LULC) datasets has been recognised by several major international research programs (Cihlar, 2000; DeFries and Belward, 2000), including the International Geosphere–Biosphere Program (IGBP; (IGBP, 1990); Lambin and Geist, 2006). Similarly, the Group on Earth Observations (GEO) determined land cover to be the fifth most important parameter derived from satellite datasets (GEO, 2012).

Land use refers to the purpose to which the land cover is committed, including the production of goods (such as crops, timber and manufactures) and services (such as defence, recreation, biodiversity and natural resources protection). Some uses, such as cropping, have a distinctive land cover pattern, and are regular inclusions in land cover classifications. Others, such as nature conservation, are not readily identified from a characteristic land cover pattern. For example, where the land cover is forest, land use may be timber production or nature conservation. A single land cover class may support multiple uses and a single land use may involve several land cover conditions.

(ABARES, 2010)

3.2 How Do We Map Land Cover?

A land cover map represents the spatial distribution of a selected set of land covers. Creating a land cover map involves two fundamental considerations, namely, how do we define the:

- categories of land cover to map—or the classification scheme (see Section 3.2.1); and the
- boundaries for these land cover categories—or the mapping method (see Section 3.2.2).

However, these considerations raise several difficulties, the first being the inevitable diversity and complexity of any natural resource, and the unavoidable outcome that no classification can truly represent the vast array of ‘classes’ that exist in nature. Another difficulty in classifying and mapping land cover is that most natural land covers, especially vegetation, transition gradually from one type to another rather than at readily defined boundaries (Kessell, 1979). For example, the transition from woodland to open forest is often gradual, such that it can be difficult to precisely locate where one land cover becomes another. Inevitably, when classifying natural resources, the final decisions on class boundaries are somewhat arbitrary. The process of defining the transition point does, however, provide a valuable reference datum for consistent use of each class label.

Natural vegetation types do not generally change from one type to another at a given location over time. What does change are some attributes associated with the type such as cover/density, age class, height, strata, and to some extent composition (see Section 2.3.1). These changes are driven by changes in climate patterns, episodic severe climate events, and recurring land management regimes.

Another significant difficulty with land cover classification is the method used to name classes, that is, its nomenclature. In many traditional systems for mapping land cover, labels were not defined precisely and could easily be assumed to have a different meaning in a different context or community. For example, early settlers in Australia used the term ‘scrub’ to describe rainforest in eastern Australia, drier Mallee vegetation in southern Australia and the more open Mulga vegetation in arid Australia (Specht, 1970). Where labels were defined, they were not necessarily used consistently in different classification systems. As a result, a single land cover label could have multiple interpretations and a single land cover could have multiple labels—precisely the opposite outcome desired of such classifications, namely that a single land cover would have a single, unambiguous label.

3.2.1 Classification schemes

Although by its nature land cover can be described in many different ways, the essential goal of any classification of land cover is that the categories are unique, so that a single land cover will always be represented by a single category. All classification methods attempt to identify similar features and represent them as a particular group or class (see Volume 2E). The number of classes in a classification needs to be sufficient to allow discrimination of the significant differences between features, but no greater than is necessary to enable efficient analysis of variations between classes. Efficiency is particularly important when dealing with very large datasets, as are required for continental or global coverage (see Volume 2D).

Many classification systems have been developed to categorise land cover. These systems group the major similarities and differences in natural land cover types by selected attributes, such as:

- Vegetation: colour, type, density, structure, and condition/health;
- Water: depth, colour, quality, and temperature; and
- Bare rock and soil: colour, mineralogy, and texture.

Similarly, man-made land cover types can be grouped by characteristics such as:

- Artificial surfaces: colour and texture; and
- Constructions: colour, density, and height.

A wide variety of methods and data sources have been used to describe and group land cover features. In many cases these have focused on individual land cover attributes, such as floral characteristics, vegetation density, or indicators of land degradation. Some approaches to classifying land cover focus on specific attributes that directly relate to a particular end use. The datasets resulting from such activities are not readily comparable with other land cover classifications and may not be useful for other purposes. Other classification approaches attempt to define a comprehensive set of criteria that could be used to define all possible land covers. The latter approach allows land cover data collected at different times and locations, by different methods, to conform to a common set of underlying definitions of land cover attributes. As such, the results of these surveys can be easily applied to a range of analyses and readily compared with other datasets.

Table 3.1 Structure of FAO Land Cover Classification System

First Level	Second Level	Third Level	Example Land Cover
Primarily vegetated	Terrestrial	Managed/Cultivated	Cropping, Forestry
		Natural/Semi-natural	Native vegetation
	Aquatic or regularly flooded	Managed/Cultivated	Aquaculture
		Natural/Semi-natural	Native aquatic vegetation
Primarily non-vegetated	Terrestrial	Managed/Cultivated	Artificial surfaces
		Natural/Semi-natural	Bare land
	Aquatic or regularly flooded	Managed/Cultivated	Artificial waterbodies, snow and ice
		Natural/Semi-natural	Natural waterbodies, snow and ice

The Food and Agriculture Organisation of the United Nations (FAO) developed a Land Cover Classification System (LCCS; Di Gregorio, 2005) to standardise global land cover mapping. It allows scale-independent classes to be defined using discrete diagnostic criteria, which are arranged hierarchically in two phases:

- primary—defines three classification levels leading to eight basic land cover classes as shown in Table 3.1; and
- secondary—uses criteria, or ‘classifiers’, specific to each of the eight basic classes to further differentiate land cover types (see Excursus 3.1 for details)

While the biophysical environment cannot be fully or accurately represented by any classification system, the consistency and stability resulting from a standardised system improves communication between users and increases the utility of the classified data (Yang *et al.*, 2017). Accordingly, a standardised land cover system allows classified data from different sources to be compared and integrated with confidence, especially for national and international datasets (see Volume 2D).

A number of EO-based systems have implemented the LCCS taxonomy for land cover classification, including the Earth Observation Data for Ecosystem Monitoring (EODESM; EcoPotential, 2021; see Section 20.5). In Australia, the LCCS has been applied nationally to describe land cover categories in the Dynamic Land Cover Dataset (DLCD; Lymburner *et al.*, 2011). The capacity and conceptual framework of EODESM has also been demonstrated within Digital Earth Australia (DEA; see Volume 2D—Section 11.2) for two time periods across four test sites (Lucas *et al.*, 2019).

Nature is a tireless sculptor, forever fashioning new masterpieces, yet, as if unsatisfied, commencing their destruction from the very moment of their completion. Something of the old always remains to be built into the new. The shape of a hill, the contour of a waterfall, the rocky ledges on the sides of a gully, the meanderings of a river, the alluvium of a plain are all links with the past, and within them lies the story of what has gone before.
(Charles F. Laseron, 1953)

Excursus 3.1—FAO Land Cover Classification System

Further Information: Di Gregario (2005, 2016); Di Gregario and Jansen (2000)

The land cover classification system (LCCS) developed by the UN Food and Agriculture Organisation (FAO) is a hierarchical system that classifies land covers in two phases (Di Gregario, 2005):

- a primary, dichotomous phase which uses three classifiers to define eight major land cover types as summarised in Table 3.2; and
- a secondary, modular-hierarchical phase which refines the eight major land cover types into specific land cover classes using pre-defined classifiers tailored to each major type. In addition, environmental attributes (such as climate, landform, or soil type) or specific technical attributes (such as floristic characteristics) can also be used to define detailed classes in this phase. The pre-defined classifiers and attributes for each major land cover type are summarised in Table 3.3 and Table 3.4.

In order to define an international standard for land cover classification systems, FAO submitted the LCCS to the ISO Technical Committee 211 on Geographic Information in 2003. Although ISO had previously only defined standards for more abstract standards with established rules, a general classification system (ISO 19144-1 Classification Systems) and a land cover classification system (ISO 19144-2 Land Cover Meta Language: LCML) were approved in 2012 as official international ISO standards. The LCML characterises geographic features using an open, object-oriented system. Fundamentally, LCML uses a predefined set of biotic and abiotic elements (see Section 1.1) arranged in different ‘patterns’ to describe a wide range of land cover ‘situations’. This “allows not only an unambiguous description of real world features more consistent with the logic and structure of modern databases but also enlarges the capability of the system to describe phenomena related to inputs and activities peoples undertake on a certain land cover feature typical of agriculture” (Di Gregario, 2016).

Table 3.2 Dichotomous phase classifiers and land cover types

Classifier	Presence of Vegetation	Edaphic Condition	Artificiality of Cover	
Decision	Is vegetative cover > 4% for woody and/or herbaceous vegetation, or > 25% for lichen/mosses, during at least two months each year?	Is the environment significantly influenced by the presence of water for extensive periods of time?	Is the land cover significantly modified by human activity?	
Land Cover Types	A: Primarily Vegetated Areas (see Table 3.3)	A1: Terrestrial Primarily Vegetated Areas	A11: Cultivated and Managed Terrestrial Areas	
		A2: Aquatic or Regularly Flooded Primarily Vegetated Areas	A12: Natural and Semi-Natural Vegetation	
	B: Primarily Non-Vegetated Areas (see Table 3.4)	B1: Terrestrial Primarily Non-Vegetated Areas	A23: Cultivated Aquatic or Regularly Flooded Areas	A24: Natural and Semi-Natural Aquatic or Regularly Flooded Vegetation
			B15: Artificial Surfaces and Associated Areas	B16: Bare Areas
		B2: Aquatic or Regularly Flooded Primarily Non-Vegetated Areas	B27: Artificial Waterbodies, Snow and Ice	B28: Natural Waterbodies, Snow and Ice

Source: Di Gregario and Jansen (2000)

Table 3.3 LCCS classification of primarily vegetated areas

LCCS land cover type	Type of classifier	Classification level	Characteristics used to refine classes
A11: Cultivated and Managed Terrestrial Areas Natural vegetation has been removed or modified and replaced by other vegetation by human activity. Such vegetation requires long term maintenance and is planted with a view to harvesting. Example land covers include crops (with seasonal variation in cover), orchards, and plantations	'Pure' land cover classifiers	I	Life Form + Spatial Aspects
		II	Crop Combination
		III	Cover-related Cultural Practice
	Environmental attributes	IV	Landform + Lithology/Soils + Climate
		V	Altitude + Erosion + Cover/Density
	Specific technical attributes	VI	Crop Type
A12: Natural and Semi-natural Vegetation Natural vegetated areas are defined as areas where the vegetative cover is in balance with the abiotic and biotic forces of its biotope. Semi-natural vegetation is defined as vegetation not planted by humans but influenced by human actions. Example land covers include grazing, selective logging, and abandoned or shifting cultivation	'Pure' land cover classifiers	I	Life Form and Cover + Height + Macro Pattern
		II	Leaf Type and Leaf Phenology
		III	Stratification
	Environmental attributes	IV	Landform + Lithology/Soils
		V	Climate + Altitude + Erosion
	Specific technical attributes	VI	Floristic Aspect
A23: Cultivated Aquatic or Regularly Flooded Areas This category includes areas where an aquatic crop is purposely planted, cultivated and harvested, and which is standing in water over extensive periods during its cultivation period (such as paddy rice, tidal rice, and deepwater rice, but not irrigated cultivation).	'Pure' land cover classifiers	I	Life Form + Spatial Aspects
		II	Water Seasonality
		III	Cover-related Cultural Practice
		IV	Crop Combination
	Environmental attributes	V	Landform + Lithology/Soils + Climate
		VI	Altitude + Erosion + Cover/Density
	Specific technical attributes	VII	Crop Type
A24: Natural and Semi-natural Aquatic or Regularly Flooded Areas Transitional areas between pure terrestrial and aquatic systems and where the water table is usually at or near the surface, or the land is covered by shallow water, are included in this class. Examples include mangroves, marshes, swamps, and aquatic beds.	'Pure' land cover classifiers	I	Life Form and Cover + Height
		II	Water Seasonality
		III	Leaf Type + Leaf Phenology
		IV	Stratification
	Environmental attributes	V	Landform + Lithology/Soils + Climate
		VI	Altitude + Erosion + Cover/Density
	Specific technical attributes	VII	Floristic Aspect

Source: Di Gregario and Jansen (2000)

LCML acts as a method to bring the LC community together to create a common understanding of LC nomenclatures with the aim to produce global, regional and national data sets able to be reconciled at different scales, level of detail and geographic location. The LCML provides a general framework of rules from which more exclusive conditions can be derived to create specific legends. It is a language based on physiognomy and stratification of both biotic and abiotic materials. The system may be used to specify any LC feature anywhere in the world, using a set of independent diagnostic criteria that allow correlation with existing classifications and legends.
 (Di Gregario, 2016)

Table 3.4 LCCS classification of primarily non-vegetated areas

LCCS land cover type	Type of classifier	Classification level	Characteristics used to refine classes
B15: Artificial Surfaces and Associated Areas Areas that have an artificial cover as a result of human activities such as construction (cities, towns, transportation), extraction (open mines and quarries) or waste disposal	'Pure' land cover classifiers	I	Surface Aspect
	Environmental attributes	II	Landform + Climate + Altitude
	Specific technical attributes	III	Built-Up Object
B16: Bare Areas Areas that do not have an artificial cover as a result of human activities (such as bare rock areas, sands, and deserts), including areas with less than 4% vegetative cover.	'Pure' land cover classifiers	I	Surface Aspect
		II	Macro-pattern
	Environmental attributes	III	Landform + Climate
		IV	Altitude + Erosion + Water Quality
Specific technical attributes	V	Soil Type/Lithology	
B27: Artificial Waterbodies, Snow and Ice Areas that are covered by water only as a result of the construction of artefacts such as reservoirs, canals, or artificial lakes	'Pure' land cover classifiers	I	Physical Status + Persistence
		II	Depth + Sedimentation
	Environmental attributes	III	Climate + Altitude + Vegetation
	Specific technical attributes	IV	Salinity
B28: Natural Waterbodies, Snow and Ice Areas naturally covered by water (such as lakes, rivers, snow, or ice)	'Pure' land cover classifiers	I	Physical Status + Persistence
		II	Depth + Sedimentation
	Environmental attributes	III	Climate + Altitude + Vegetation
	Specific technical attributes	IV	Salinity

Source: Di Gregorio and Jansen (2000)

3.2.2 Mapping methods and accuracy assessment

All methods for mapping land cover utilise data from at least one of three primary sources:

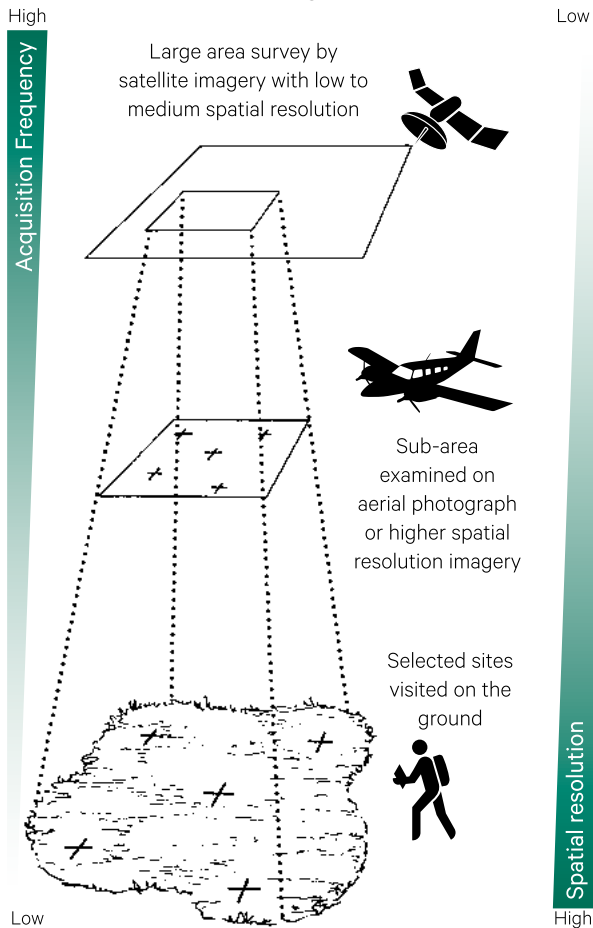
- ground-based survey;
- aerial photography; and/or
- satellite imagery, or Earth Observation from Space (EOS).

Ground-based surveys require trained teams to visit field sites and record the land cover types encountered at precise locations (see Volume 2D—Section 12.1). Surveys generally involve measurements of pre-defined attributes for a range of land

covers (Avery, 1975; TERN Australia, 2018). These measurements can involve the use of instrumentation and/or rely on the experience and judgement of the survey team. Different forms of ground-based survey have been used to map various types of land cover for thousands of years, and these have become increasingly standardised in recent decades. For example, the standard Australian methods and terminology for surveying land and soil attributes in the field are detailed in NCST (2009). In recent decades, however, given the labour-intensive and time-consuming nature of field data collection, this is generally limited to checking the accuracy of more synoptic data sources that can be acquired remotely (see Figure 3.1).

Figure 3.1 Multi-level EO

Analysis of low and medium resolution imagery can be more easily related to ground data through high resolution imagery. Low resolution imagery tends to be acquired more quickly and cover a larger extent, so is most appropriate for large area surveys. Selected locations within the surveyed area would typically be checked using data with higher spatial resolution, such as aerial photography. Some of these locations would then be visited in the field to verify the image analysis. This scaled approach enables the results of expensive and time-consuming field work to be extended to a larger area.



Adapted from: Harrison and Jupp (1989) Figure 39

It seems inevitable that, with increasing auto-scanning and data handling, as our knowledge of land increases, and as the demands of the land user become more specialised, that parametric analysis will become general practice
(Mabbutt, 1968)

Aerial photography interpretation (API) has been used internationally to map different types of land cover for well over a century (see Volume 1A—Section 11). The Australian archive of aerial photography dates from 1928 and has supported various detailed inventories of natural resources with panchromatic, colour, and infrared photography. While still used to survey land cover in Australia for some applications, aerial imagery is now more frequently used to validate broader area analyses from space-based data (see Figure 3.1).

As detailed in Volume 1, EO datasets offer a range of approaches to observe and measure Earth surface properties. Space-based data have been available internationally for over five decades and offer a unique source of Earth surface data by recording:

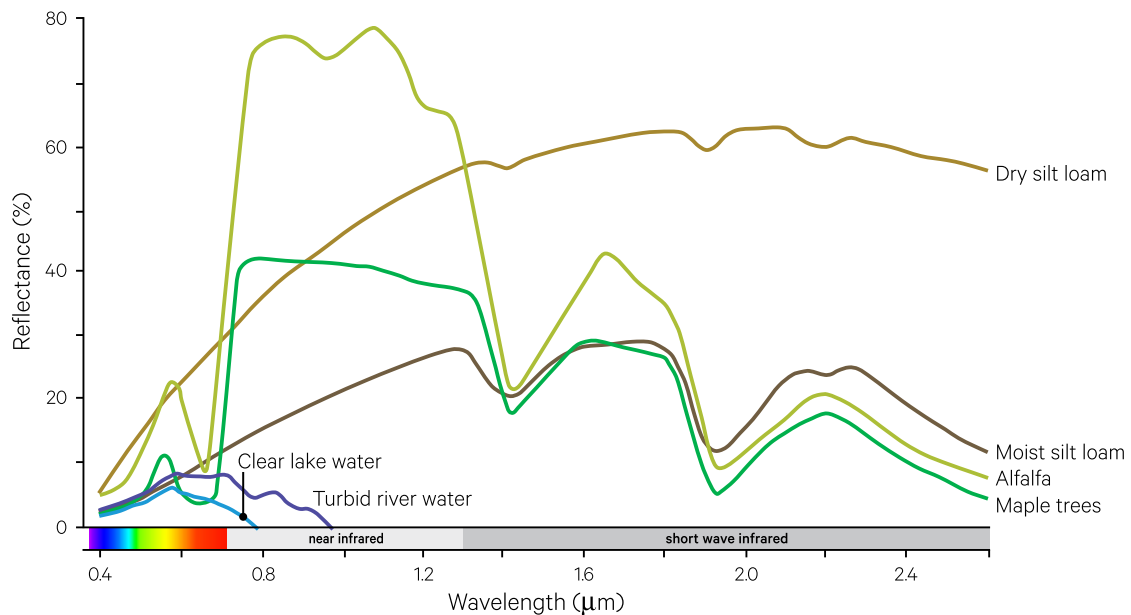
- accurate geo-locations for contiguous target areas;
- objective, consistent measurements of physical properties of the land surface that can be interpreted to define its features and condition; and
- repeated coverage to enable detection of changes in features and/or their condition.

As introduced in Volume 1, different land and water cover features have varying, and often characteristic, reflectance in different wavelengths of the EM spectrum (see Figure 3.2). For any land cover to be discernible in EO, both the resolution and extent of the remote measurements need to be appropriate for the measurable properties of that land cover (see Volume 1B—Section 1). To separate one land cover from others, these measurements must also be able to discriminate between the differences in radiation from those land covers (Townshend, 1992).

A wide variety of statistics have been developed to exploit the similarities and differences between reflectance characteristics of different land covers, most of which highlight the high near infrared (NIR) reflectance and low red reflectance of healthy vegetation. Some of the standard image processing options used with EO data are described in Volumes 2A and 2C and reviewed in Section 8.1. The expanding archive of EO imagery now enables sophisticated time series analyses, which are being used to further quantify landscape dynamics, highlight the environmental drivers in natural processes, monitor compliance with resource usage regulations, and address issues related to climatic variations (Wulder *et al.*, 2018; see Volume 2D and Section 9).

Figure 3.2 Idealised spectral signatures

Reflectance from different Earth surface features varies for different wavelengths. Characteristic spectral reflectance curves can be created for different features to indicate a 'typical' shape over a particular range of wavelengths. This information can be used to differentiate between different surface features on the basis of their observed reflectance characteristics.



Adapted from: Harrison and Jupp (1989) Figure 6

A complete EO exercise usually involves the integration of imagery at several different 'levels' of resolution with data from other sources, such as maps or aerial photography. Within a large region represented in a satellite image, certain areas are usually selected for comparison with aerial photography, some of which would be visited in the field, or compared with field data. The concept of a multi-level approach is illustrated in Figure 3.1. This approach was implemented in the BigFoot Project, in which EO and field datasets with a variety of scales were analysed to characterise relationships between leaf area Index, net primary productivity, and carbon allocation within and between biomes, and validate relevant, landscape scale, EO-based products (NASA, 1999; see Section 7.4).

Accuracy assessments tend to assume that one dataset represents 'truth' and, thus, can be used to measure the 'value' of the other. In any landscape scale mapping exercise, few datasets can be viewed this way, so discrepancies in cross-comparison may show deficiencies in either dataset, or a lack of commonality in their intrinsic 'world views'.

Thus, when relating EO radiance to a reference dataset, correlation will depend on how accurately each dataset represents surface features. A lack of correlation does not necessarily imply that EO imagery cannot be used to map relevant landscape attributes but suggests that it may not differentiate them in the same way as the reference dataset. Any analysis of results must retain an awareness of this situation (see Volume 2E). Procedures for validation of EO analyses are detailed in TERN Australia (2018) and Malthus *et al.* (2013).

For example, since API largely relies on pattern interpretation by trained operators, it tends to generate maps that cleanly delineate regions characterised by internal heterogeneity. This approach contrasts with the pixel-based, spectral classification methods used with EO datasets (see Volume 2E). However, neither the results of API nor EO image analysis actually represent the whole 'truth'. When discrepancies between these two representations are being compared, the differences in their provenances should be considered.

In recent decades, a number of global and regional datasets have been derived from EO imagery to monitor land cover. For example, 21 global products and 43 regional products are reviewed by Grekousis *et al.* (2015). These freely available products cover different spatial and temporal scales, depending on the imagery used to generate them. Some examples include⁵:

- GlobCover (ESA with JRC, EEA, FAO, UNEP, GOCF-GOLD and IGBP)—annual global land cover maps derived from various satellite image sources at 300 m from 1992 to 2015 (ENVISAT; <http://cci.esa.int/content/land-cover-annual-global-land-cover-maps-v207-dataset-release>); Bontemps *et al.* (2011);
- Global Land Survey (NASA/USGS Land Cover Institute)—based on 30 m Landsat imagery, from

2009 to 2011 (https://www.usgs.gov/land-resources/nli/landsat/global-land-survey-gls?qt-science_support_page_related_con=0#qt-science_support_page_related_con);

- MODIS Land Cover (University of Maryland)—IGBP Land Cover Type classification (16 vegetation classes plus water) from 2001 to 2012 reprojected to geographic coordinates in WGS 1984 (EPSG: 4326) in two resolutions: 0.5° and 5' square pixels (<http://glcf.umd.edu/data/lc/>); and
- GLC2000 (EC coordinated consortium of researchers)—global and regional classifications of land cover derived from SPOT VEGETATION imagery (SPOT-4) for the year 2000 (http://forobs.jrc.ec.europa.eu/products/glc2000/data_access.php; Bartholomé and Belward, 2007).

3.3 Mapping Approaches

Classifying landscapes in terms of their biophysical characteristics allows geographers, land managers, and decision makers to focus on the similarities and differences between different regions. This information provides insight into the processes that determine these characteristics and allows the impact of land management practices to be evaluated objectively. Such data and classifications are used for a range of activities, including conservation planning, resource assessment, and agricultural management.

The interrelationship between land cover and environmental factors, such as climate, topography, and soil substrate, is well-established for the Australian environment (Graetz *et al.*, 1992). As outlined in Section 2, the distribution of natural vegetation in Australia is strongly dependent on rainfall, aspect, and soil type. Since World War II, numerous classifications of landscape biodiversity have been developed for both research and operational use in Australia. These have involved varying methods, scales, products, and coverage. Some of these systems are summarised in Table 3.5. While these efforts have substantially contributed to the current knowledge of Australia's biophysical resources and have each delivered iterative improvements in terms of reliability and accessibility, none currently offers consistent land cover information over the Australian landmass that can be updated readily.

Below, we will consider the existing landscape classifications in terms of four categories:

- land evaluation based on mapping units (see Section 3.3.1);
- actual distribution of current vegetation (see Section 3.3.2);
- probable distribution of natural vegetation (see Section 3.3.3); and
- actual distribution of current land use (see Section 3.3.4).

3.3.1 Land evaluation based on mapping units

The CSIRO Land Systems project (Christian and Stewart, 1953, 1968) developed the first landscape classification system to be based on 'mapping units'. Reconnaissance surveys were conducted in northern and central Australia and Papua New Guinea from 1946 to 1977, to identify and map land resources and the potential for regional development. To integrate the various types of landscape data, a new system of land evaluation was required. Each area or group of areas characterised by a recurring pattern of topography, soils, and vegetation was identified as a discrete mapping unit or 'land system'. Initial mapping of land systems was generally based on patterns identified from aerial photography, in conjunction with supporting information available from topographic and thematic maps, reports and other documents, and expert knowledge. Successive surveys used more advanced classifications of soils, vegetation, and terrain as these became available. The results of these surveys are still used as a reference data source in other mapping exercises.

⁵ ESA: European Space Agency; JRC: Joint Research Centre (EC); EEA: European Economic Area; FAO: UN Food and Agriculture Organisation; UNEP: UN Environment Program; GOCF-GOLD: Global Observations of Forest Cover and Land Dynamics; IGBP: International Geosphere-Biosphere Programme

A similar approach to land evaluation was used to develop the Interim Biogeographic Regionalisation for Australia (IBRA; DAWE, 2020a; see Figure 2.13), part of a nested series of bioregionalisations used to define global terrestrial habitats and world ecoregions by the World Wildlife Fund (WWF; Olson *et al.*, 2001; see Section 1.3.2). This classification was developed for conservation planning and represents Australia's landscapes as geographically distinct bioregions on the basis of climate, geology, landform, and native flora (see Section 2.4). Each bioregion has been subdivided into more homogeneous geomorphological units or subregions. In IBRA7, 89 bioregions and 419 subregions collectively describe the Australian landmass and selected marine areas.

A hierarchy of mapping units was also used to compile the Australian Soil Resource Information System (ASRIS; CSIRO, 2014; see Figure 2.3). This provides online access to consistent soil and land resource information across Australia in a seven-tiered hierarchy. Different attributes are used to map each level in the hierarchy, as deemed appropriate to each mapping scale, based on the most recent publicly available data. This system can be used to summarise the soil and landscape properties for other classifications, such as IBRA.

Land, then, is not merely soil; it is a fountain of energy flowing through a circuit of soils, plants, and animals.
(Aldo Leopold)

Table 3.5 Australian landscape mapping approaches

Name	Description	Coverage	Further Information
CSIRO Land Systems	First systematic approach to land evaluation in Australia, conducted from 1946–1977, based on evolving classifications of soils, vegetation and terrain	Primarily northern and central Australia, approximately 50% of continental Australia	Christian and Stewart (1953, 1968); www.publish.csiro.au/nid/289.htm
Vegetation Map of Australia	Probable distribution of major natural vegetation groups	16 categories across the Australian landmass	Williams (1959)
Major Vegetation Types in Australia	Probable distribution of major vegetation groups prior to European settlement based on Specht structural types and Beard and Webb (1974) notation	1977—1:12,000,000 1988—1:5,000,000	Carnahan (1976, 1988)
Present Vegetation (Atlas of Australian Resources, 3rd Edition)	First continental map of actual vegetation based on Landsat MSS satellite imagery with input from existing maps, reports, and expert knowledge.	24 broad structural categories with supplementary codes Australian landmass; 1:5,000,000	AUSLIG (1990)
Interim Biogeographic Regionalisation of Australia (IBRA)	Divides Australia into geographically distinct areas with common characteristics (such as geology, landform patterns, climate, and ecology) as a broad framework for conservation planning	Digital data for 89 bioregions and 419 sub-regions across Australian land mass and selected marine areas	Thackway and Cresswell (1995); https://www.environment.gov.au/land/nrs/science/ibra
Australian Soil Resource Information System (ASRIS)	Online access to best available soil and land resources information using a seven-tiered hierarchy of mapping units	Digital data for Australian landmass	McKenzie <i>et al.</i> (2012); www.asris.csiro.au
National Vegetation Information System (NVIS)	National collaboration of state and federal datasets that combines floristic and structural parameters to describe all layers of native vegetation, both current and pre-1750.	National hierarchical framework for inventory and monitoring of vegetation type and extent. Dataset covers the Australian landmass and contains over 9,000 distinct vegetation types	https://www.environment.gov.au/land/native-vegetation/national-vegetation-information-system
Major Vegetation Groups (MVG)	Aggregations of NVIS 4.1 vegetation types to estimate major groups of vegetation in Australia, both current and pre-1750.	33 Major Vegetation Groups and 85 sub-groups over Australian landmass	DE (2012) https://data.gov.au/data/dataset/57c8ee5c-43e5-4e9c-9e41-fd5012536374
Australian Land Use and Management Classification (ALUM)	National scale land use classification using modelling approach to integrate agricultural commodity data, satellite data, and other land use data	1:2,500,000	http://www.agriculture.gov.au/abares/aclump/land-use/alum-classification
Catchment Scale Land Use of Australia (CLUM)	A seamless raster dataset that combines land use data for all state and territory jurisdictions, at a resolution of 50 m, by combining state cadastre, public land databases, fine scale satellite data, other land cover and use data, and information collected in the field	1:5,000 to 1:25,000 for irrigated and peri-urban; 1:100,000 for broadacre cropping; 1:250,000 for semi-arid and arid pastoral zone.	http://data.daff.gov.au/anrdl/metadata_files/pb_luAusg9abll20171114_11a.xml

3.3.2 Actual distribution of current vegetation

The first national scale map of actual vegetation in Australia based on satellite imagery was produced by Carnahan (1988) for the Australian Surveying and Land Information Group (AUSLIG) publication series Atlas of Australian Resources (AUSLIG, 1990). This two-part dataset mapped both natural (pre-European settlement; see Section 3.3.3) and present (current) vegetation at 1:1 million scale. The 'present vegetation' map, which showed both native and exotic vegetation, was based on visual interpretation of Landsat MSS satellite imagery with reference to existing maps, reports and expert knowledge (especially for crop and pasture classes). Land cover labels were based on eight growth forms and four categories of foliage cover for the tallest stratum, resulting in 22 broad categories for terrestrial vegetation with two additional classes for wetland vegetation and bare areas. Supplementary mapping detail describing floristic type and vegetation in the lower stratum was added using alphanumeric codes and shading patterns. Each major vegetation type was also detailed and mapped in AUSLIG (1990).

The National Land and Water Resources Audit (NLWRA) was founded in 1997 to collate information relating to Australia's natural resources and finished operation in 2008 (Land and Water Australia, 2009). One of its collaborative projects with state agencies was the Australian Native Vegetation Assessment 2001 (NLWRA, 2001), the first Australia-wide, regional level, assessment of type, extent, and change in Australia's native vegetation cover since European settlement. Included in this project was the development of a consistent national classification framework, based on Walker and Hopkins (1990) Figure 8, which became known as the National Vegetation Information System (NVIS; see Section 2.3.1 and Volume 2D—Excursus 12.1). Over 10,000 distinct vegetation types are contained in the NVIS database (NVIS Technical Working Group, 2017). In NVIS Version 5.1, these detailed data records are aggregated into 33 Major Vegetation Groups (MVG) and 85 Major Vegetation Subgroups (MVS) for Australia on the basis of similarity in structure and floristic composition in the dominant stratum (see Section 2.3.1). These datasets have been used to map both current (extant) and pre-1750 vegetation in Australia (see Figure 2.12 and Section 3.3.3).

3.3.3 Probable distribution of natural vegetation

Since the spatial distribution of natural vegetation is largely determined by climate (principally precipitation and temperature) and moderated by factors relating to soils and topography (especially aspect and slope) (Graetz *et al.*, 1992), the probable distribution of vegetation prior to European settlement in Australia has been modelled on the basis of these variables (Nix, 1982). Current vegetation, however, has been modified by anthropogenic influences and can only be determined using surveying and modelling methods. Several maps showing the likely distribution of Australian vegetation before European settlement have been produced using expert knowledge (from field surveys, existing maps, and reports). Natural vegetation maps showing the probable state of Australia's vegetation around 1788 (Carnahan, 1976, 1988) were produced for AUSLIG (1990). The earliest of these maps was based on API and other data sources, while the latter map was compiled from visual interpretation of Landsat MSS imagery and all relevant information (see Table 3.5). Such maps have allowed the impact of land cover change since European settlement to be identified and quantified.

It should be noted that, at the state level, numerous maps of potential natural vegetation have been also produced, including for WA, SA, Tasmania, NSW, and Queensland. These maps are generally produced at a coarser scale than maps of present or actual native vegetation.

Using assumptions about undisturbed land condition and the environmental drivers for landscape change, the probable distribution of natural vegetation can also be inferred from the distribution of current vegetation. This type of mapping has been applied to NVIS (NVIS Technical Working Group, 2017; see Figure 2.12) and several state-based vegetation maps (see Section 19.5). For such approaches to operate reliably, however, it is essential that the back-engineering models (which simulate vegetation type and condition in the pre-European landscape from those existing in the present landscape) be based on accurate benchmarks for all ecosystems within the study area, for each jurisdiction.

3.3.4 Actual distribution of current land use

The distinction between ‘land cover’ and ‘land use’ was discussed in Section 3.1.2 above. Identification of land use is critical for planning and managing land resources, both for productive industries and environmental protection.

Australian Land Use and Management (ALUM; see Section 2.5.3) is a land use classification system that comprises a three-tiered hierarchy of classes, broadly structured by their potential for disturbance. The primary level in this hierarchy includes six classes, with classes 1 to 5 being ordered by increasing modification to the natural landscape:

1. Conservation and natural environments—land that has a relatively low level of human intervention. The land may be formally reserved by government for conservation purposes, or conserved through other legal or administrative arrangements. Areas may have multiple uses, but nature conservation is the prime use. Some land may be unused as a result of a deliberate decision of government or landowner, or due to circumstance.
2. Production from relatively natural environments—land that is subject to relatively low levels of intervention. The land may not be used more intensively because of its limited capability. The structure of the native vegetation generally remains intact despite deliberate use, although the floristics of the vegetation may have changed markedly. Where the native vegetation structure is, for example, open woodland or grassland, the land may be grazed.
3. Production from dryland agriculture and plantations—land that is used principally for primary production, based on dryland farming systems. Native vegetation has largely been replaced by introduced species through clearing, the sowing of new species, the application of fertilisers or the dominance of volunteer species. The range of activities in this category includes plantation forests, pasture production for stock, cropping and fodder production, and a wide range of horticultural production.
4. Production from irrigated agriculture and plantations—agricultural land uses where water is applied to promote additional growth over normally dry periods, depending on the season, water availability and commodity prices.
5. Intensive uses—land uses that involve high levels of interference with natural processes, generally in association with closer residential settlement, commercial or industrial uses.
6. Water—water features are regarded as an essential aspect of the ALUM classification, primarily as a cover type (ABARES, 2016).

The three levels in this hierarchical classification system are summarised in Table 3.6. The range of secondary and tertiary classes indicates the diversity of land uses in Australia. In this system, agricultural activities are further differentiated by their dependence on irrigation, extent of land disturbance, and current status of activity. Two scales of land use map are generated from ALUM:

- national scale (1:2,500,000)—integrates agricultural commodity data, satellite imagery, and other land use information using a modelling approach; and
- catchment scale (1:5,000–1:25,000 for irrigated and peri-urban, 1:100,000 for broadacre cropping and 1:250,000 for semi-arid and arid pastoral zone)—combines state cadastre, public land databases, high spatial resolution satellite data, other land cover and use data, and field data (Figure 2.17). Overall attribute accuracy of catchment scale maps is assessed as greater than 80% (ABARES, 2011).

While national scale land use maps (1:2,500,000) have been available biennially since 1992/93, continental coverage at catchment scale was first completed in 2008. The ALUM dataset is updated periodically to reflect changes in land use and serves as a valuable national and regional monitoring tool (see Section 3.4.2). The current national map, updated in December 2018 from CLUM data, features 18 broad land use classes and 33 ALUM secondary classes (DAWE, 2020b), with interactive viewing of recent maps being available via the National Map tool (see Volume 2D—Excursus 13.1).

ALUM is managed by the Australian Collaborative Land Use and Management Program (ACLUMP), which is overseen by the National Committee for Land Use and Management Information (NCLUMI—a consortium of federal, state and territory government partners seeking to develop nationally consistent land use and land management information for Australia; DAWE, 2020c). In addition to compiling land use maps, ACLUMP produces guidelines for land use mapping and handbooks for field measurement (see Section 3.5).

The way in which land is used has a profound effect on Australia's unique climate, soil, water, vegetation and biodiversity resources (Thackway and Freudenberger, 2016). There is a strong link between spatial and temporal patterns of land use and prevailing environmental, economic and social conditions. Therefore, information on land use and management is fundamental to the development and implementation of land use policy and planning. (Thackway, 2018)

Table 3.6 ALUM classification

Notes: Classes 1.1.1–1.1.6 are based on the Collaborative Australian Protected Areas Database (CAPAD) classification (Cresswell and Thomas, 1997) and can be translated to IUCN (2008) categories I to V. Class 1.1.7 covers additional forms of nature conservation protection, including heritage agreements, voluntary conservation arrangements, registered property agreements, and recreation areas with primarily native cover. Classes 1.2.1–1.2.4 are based on the CAPAD classification (IUCN, 2008 Category VI).

Primary class	Secondary class	Tertiary class	Area (%) 2010–11	Area (%) 2010–11
1. Conservation and natural environments	1.1 Nature conservation	1.1.1 Strict nature reserve 1.1.2 Wilderness area 1.1.3 National park 1.1.4 Natural feature protection 1.1.5 Habitat/species management area 1.1.6 Protected landscapes 1.1.7 Other conserved area	7.86	38.26
	1.2 Managed resource protection	1.2.1 Biodiversity 1.2.2 Surface water supply 1.2.3 Groundwater 1.2.4 Landscape 1.2.5 Traditional indigenous land uses	15.14	
	1.3 Other minimal use	1.3.1 Defence land—natural areas 1.3.2 Stock route 1.3.3 Residual native cover 1.3.4 Rehabilitation	15.26	
2. Production from relatively natural environments	2.1 Grazing native vegetation		44.87	46.22
	2.2 Production native forests	2.2.1 Wood production forestry 2.2.2 Other forest production	1.35	
3. Production from dryland agriculture and plantations	3.1 Plantation forests	3.1.1 Hardwood plantation forestry 3.1.2 Softwood plantation forestry 3.1.3 Other forest plantation 3.1.4 Environmental forest plantation	0.34	13.18
	3.2 Grazing modified pastures	3.2.1 Native/exotic pasture mosaic 3.2.2 Woody fodder plants 3.2.3 Pasture legumes 3.2.4 Pasture legume/grass mixtures 3.2.5 Sown grasses	9.24	
	3.3 Cropping	3.3.1 Cereals 3.3.2 Beverage and spice crops 3.3.3 Hay and silage 3.3.4 Oilseeds 3.3.5 Sugar 3.3.6 Cotton 3.3.7 Alkaloid poppies 3.3.8 Pulses	3.59	
	3.4 Perennial Horticulture	3.4.1 Tree fruits 3.4.2 Olives 3.4.3 Tree nuts 3.4.4 Vine fruits 3.4.5 Shrub berries and fruits 3.4.6 Perennial flowers and bulbs 3.4.7 Perennial vegetables and herbs 3.4.8 Citrus 3.4.9 Grapes	0.01	
	3.5 Seasonal horticulture	3.5.1 Seasonal fruit 3.5.2 Seasonal flowers and bulbs 3.5.3 Seasonal vegetables and herbs		
	3.6 Land in transition	3.6.1 Degraded land 3.6.2 Abandoned land 3.6.3 Land under rehabilitation 3.6.4 No defined use 3.6.5 Abandoned perennial horticulture	0.00	13.18

Primary class	Secondary class	Tertiary class	Area (%) 2010–11	Area (%) 2010–11
4. Production from irrigated agriculture and plantations	4.1 Irrigated plantation forests	4.1.1 Irrigated hardwood plantation forestry 4.1.2 Irrigated softwood plantation forestry 4.1.3 Irrigated other forest plantation 4.1.4 Irrigated environmental forest plantation	0.00	0.27
	4.2 Grazing irrigated modified pastures	4.2.1 Irrigated woody fodder plants 4.2.2 Irrigated pasture legumes 4.2.3 Irrigated legume/grass mixtures 4.2.4 Irrigated sown grasses	0.08	
	4.3 Irrigated cropping	4.3.1 Irrigated cereals 4.3.2 Irrigated beverage and spice crops 4.3.3 Irrigated hay and silage 4.3.4 Irrigated oilseeds 4.3.5 Irrigated sugar 4.3.6 Irrigated cotton 4.3.7 Irrigated alkaloid poppies 4.3.8 Irrigated pulses 4.3.9 Irrigated rice	0.12	
	4.4 Irrigated perennial horticulture	4.4.1 Irrigated tree fruits 4.4.2 Irrigated olives 4.4.3 Irrigated tree nuts 4.4.4 Irrigated vine fruits 4.4.5 Irrigated shrub berries and fruits 4.4.6 Irrigated perennial flowers and bulbs 4.4.7 Irrigated perennial vegetables and herbs 4.4.8 Irrigated citrus 4.4.9 Irrigated grapes	0.03	
	4.5 Irrigated seasonal horticulture	4.5.1 Irrigated seasonal fruits 4.5.2 Irrigated seasonal flowers and bulbs 4.5.2 Irrigated seasonal vegetables and herbs 4.5.4 Irrigated turf farming	0.02	
	4.6 Irrigated land in transition	4.6.1 Degraded irrigated land 4.6.2 Abandoned irrigated land 4.6.3 Irrigated land under rehabilitation 4.6.4 No defined use—irrigation 4.6.5 Abandoned irrigated perennial horticulture	0.00	
5. Intensive uses	5.1 Intensive horticulture	5.1.1 Production nurseries 5.1.2 Shadehouses 5.1.3 Glasshouses 5.1.4 Glasshouses—hydroponic 5.1.5 Abandoned intensive horticulture	0.00	0.41
	5.2 Intensive animal production	5.2.1 Dairy sheds and yards 5.2.2 Feedlots 5.2.3 Poultry farms 5.2.4 Piggeries 5.2.5 Aquaculture 5.2.6 Horse studs 5.2.7 Saleyards/stockyards 5.2.8 Abandoned intensive animal production	0.01	
	5.3 Manufacturing and industrial	5.3.1 General purpose factory 5.3.2 Food processing factory 5.3.3 Major industrial complex 5.3.4 Bulk grain storage 5.3.5 Abattoirs 5.3.6 Oil refinery 5.3.7 Sawmill 5.3.8 Abandoned manufacturing and industrial	0.01	
	5.4 Residential and farm infrastructure	5.4.1 Urban residential 5.4.2 Rural residential with agriculture 5.4.3 Rural residential without agriculture 5.4.4 Remote communities 5.4.5 Farm buildings/infrastructure	0.33	
	5.5 Services	5.5.1 Commercial services 5.5.2 Public services 5.5.3 Recreation and culture 5.5.4 Defence facilities—urban 5.5.5 Research facilities	0.04	

Primary class	Secondary class	Tertiary class	Area (%) 2010–11	Area (%) 2010–11
5. Intensive uses (cont.)	5.6 Utilities	5.6.1 Fuel powered electricity generation 5.6.2 Hydro electricity generation 5.6.3 Wind electricity generation 5.6.4 Solar electricity generation 5.6.5 Electricity substations and transmission 5.6.6 Gas treatment, storage and transmission 5.6.7 Water extraction and transmission	0.00	0.41
	5.7 Transport and communication	5.7.1 Airports/aerodromes 5.7.2 Roads 5.7.3 Railways 5.7.4 Ports and water transport 5.7.5 Navigation and communication	0.00	
	5.8 Mining	5.8.1 Mines 5.8.2 Quarries 5.8.3 Tailings 5.8.4 Extractive industry not in use	0.02	
	5.9 Waste treatment and disposal	5.9.1 Effluent pond 5.9.2 Landfill 5.9.3 Solid garbage 5.9.4 Incinerators 5.9.5 Sewage/sewerage	0.00	
6. Water	6.1 Lake	6.1.1 Lake–conservation 6.1.2 Lake–production 6.1.3 Lake–intensive use 6.1.4 Lake–saline	1.13	1.63
	6.2 Reservoir/dam	6.2.1 Reservoir 6.2.2 Water storage—intensive use/farm dams 6.2.3 Evaporation basin	0.07	
	6.3 River	6.3.1 River–conservation 6.3.2 River–production 6.3.3 River–intensive use	0.06	
	6.4 Channel/aqueduct	6.4.1 Supply channel/aqueduct 6.4.2 Drainage channel/aqueduct 6.4.3 Stormwater	0.00	1.63
	6.5 Marsh/wetland	6.5.1 Marsh/wetland–conservation 6.5.2 Marsh/wetland–production 6.5.3 Marsh/wetland–intensive use 6.5.4 Marsh/wetland–saline	0.12	
	6.6 Estuary/coastal waters	6.6.1 Estuary/coastal waters–conservation 6.6.2 Estuary/coastal waters–production 6.6.3 Estuary/coastal waters–intensive use	0.25	

Source: ABARES (2016)

Landscapes have been transformed by harvesting native food and fibre, removing vegetation and regolith to extract minerals, removing vegetation to provide housing and urban infrastructure, draining floodplains to create productive agricultural soils, [and] irrigating previously dryland native vegetated areas. Landscapes have also been transformed inadvertently through the combined effects of feral animals, weeds and changed fire regimes. (Thackway et al., 2015)

3.4 Monitoring Landscape Change

Any landscape mapping exercise needs to consider the fact that landscapes change. Variations in landscape features may occur as part of natural cycles or may result from disturbances in the natural balance. In this section we will consider those factors in a landscape that can change land cover condition (see Section 3.4.1) and/or land use (see Section 3.4.2).

Biotic and abiotic factors in the environment are introduced in Section 1.1. Changes in these factors can modify the vegetated landscape of any environment. In the Australian context, critical factors include fire (see Sections 2.4 and 18), weeds (see Section 2.3.2), and feral animals (see Section 2.3.3). Changes in climate patterns (see Section 2.2) also impact vegetation directly by varying temperatures, wind exposure, and rainfall as well as indirectly by altering the distribution of predators. Land use activities can accelerate natural erosion patterns, reduce runoff, and alter drainage systems (see Sections 2.1 and 11.4). Finally tectonic activity can have a dramatic effect on topography and any vegetation it supports (see Volume 1A—Section 3.2).

In the last two centuries, the condition of native vegetation in the Australian landscape has changed significantly (Gammage, 2012), creating fragmentation of ecosystems in many regions. In Central Australia, where population pressure is much lower than

along the coastal fringe, changes in grazing and fire management practices have also transformed native vegetation (Thackway *et al.*, 2015).

Now that various forms of environmental legislation govern land clearing in Australia, it is important that changes in land cover can be assessed accurately and consistently. Understanding change patterns in the landscape helps to predict future distribution and condition of plants and animals, and also enables modelling of the likely distribution of biodiversity in the past.

The National Landcare Program (and its numerous predecessors) has federally funded natural resource management in Australia for several decades to protect and rehabilitate our environment (NLP, 2017), with the specific goal of improving soil, water, and biodiversity (see Table 3.7). This program involves collaboration between landowners, researchers, local communities, and the 56 regional natural resource management (NRM) groups (NRM, 2019a, 2019b) to ensure that Australia satisfies both national and international obligations that are relevant to the environment (NLP, 2019). As part of this program, a number of online tools, based on EO and other spatial datasets, have been developed to assist landowners towards sustainable land management (see Sections 3.5 and 19).

Table 3.7 National Landcare Program

Phase One (2014/15–2017/18) of the National Landcare Program defines the four strategic objectives listed below.

Objective	Outcome	Contribution to obligations
Communities are managing landscapes to sustain long term economic and social benefits from their environment.	Maintain and improve ecosystem services through sustainable management of local and regional landscapes	Protection and restoration of ecosystem function, resilience and biodiversity Appropriate management of invasive species which threaten ecosystems, habitats or native species
Farmers and fishers are increasing their long term returns through better management of the natural resource base.	Increase in the number of farmers and fishers adopting practices that improve the quality of the natural resource base, and the area of land over which those practices are applied	Sustainable management of agriculture and aquaculture to conserve and protect biological diversity and reduce greenhouse gas emissions and increase carbon stored in soil
Communities are involved in caring for their environment.	Increase engagement and participation of the community, including landcare, farmers, and Indigenous people, in sustainable natural resource management	Build community awareness of biodiversity values, skills, participation and knowledge, including Indigenous knowledge and participation, to promote conservation and sustainable use of biological diversity
Communities are protecting species and natural assets.	Increase restoration and rehabilitation of the natural environment, including protecting and conserving nationally and internationally significant species, ecosystems, ecological communities, places, and values	Reduce the loss of natural habitats, degradation and fragmentation Protect or conserve 'Matters of National Environmental Significance' including management of World Heritage Areas, Ramsar wetlands, national heritage, etc Reduce the number of nationally threatened species and improve their conservation status

Source: NLP (2017) Table 1

3.4.1 Changes in land condition

While the type of vegetation in an area may essentially stay the same over time, the condition of that vegetation may change (see Section 3.1.1). Methods to objectively and consistently assess vegetation condition—as well as vegetation type—have been developed for Australia in recent years. For example, Thackway *et al.* (2015) propose a seven step process based on Sbrocchi (2013) to account for the condition of native vegetation as an example of an environmental ‘asset’:

1. Document the environmental assets;
2. Select environmental indicators;
3. Determine reference benchmarks;
4. Collect data;
5. Calculate indicator condition scores;
6. Calculate environmental condition index; then
7. Submit for accreditation.

To streamline the accounting process for native vegetation at the property and regional levels, this seven step process was refined by Butler *et al.* (2020) to four steps:

1. Defining the accounting area;
2. Compile existing published standardised data for native vegetation types;
3. Stratifying accounting area into assessment units; and
4. Measure indicators.

The environmental condition index (*Econd*TM; see Section 20.5) is derived to allow comparison of the relative condition of different assets. This index ranges from pre-industrial condition (100) to absent (0). Indicators of change need to efficiently reflect ecological productivity and resilience, and involve measures of both the quality (condition) and quantity (extent) of native vegetation, as well as its composition (the functional and structural integrity and landscape complexity).

One system that has been developed to monitor changes in the condition of vegetated landscapes is the Vegetation Assets, States and Transitions (VAST; see Excursus 3.2). The VAST system offers “a structured way to record observed, measured responses of native plant communities against historic and contemporary land use and land management practices relative to a reference state” (Thackway *et al.*, 2015). The key indicators and key functional, structural, and composition criteria that are identified by VAST Version 2 (VAST-2) are summarised in Table 3.8.

The national VAST-2 dataset is shown in Figure 3.3, which emphasises characteristic patterns of vegetation condition in different jurisdictions:

- very large areas of residual and modified vegetation in the rangelands of central and northern Australia;
- large areas of residual and modified vegetation in temperate regions that are less suited to agriculture;
- replaced vegetation occurs in fertile, moist regions, principally being used for cropping and improved pasture;
- extensive modified and transformed vegetation in arid and semi-arid rangelands due to grazing; and
- small areas of removed vegetation in coastal margins due to human settlement (Lessie *et al.*, 2010).

This approach to mapping the condition of vegetated landscapes offers “a simple communication and reporting metric that can assist in describing, valuing, and evaluating anthropogenic modification of native vegetation” (Lessie *et al.*, 2010). Such datasets can closely track the way vegetation responds to land management practices, quantify changes in vegetation type and extent, and monitor progress towards defined vegetation targets.

Table 3.8 VAST-2 diagnostic components, criteria and indicators

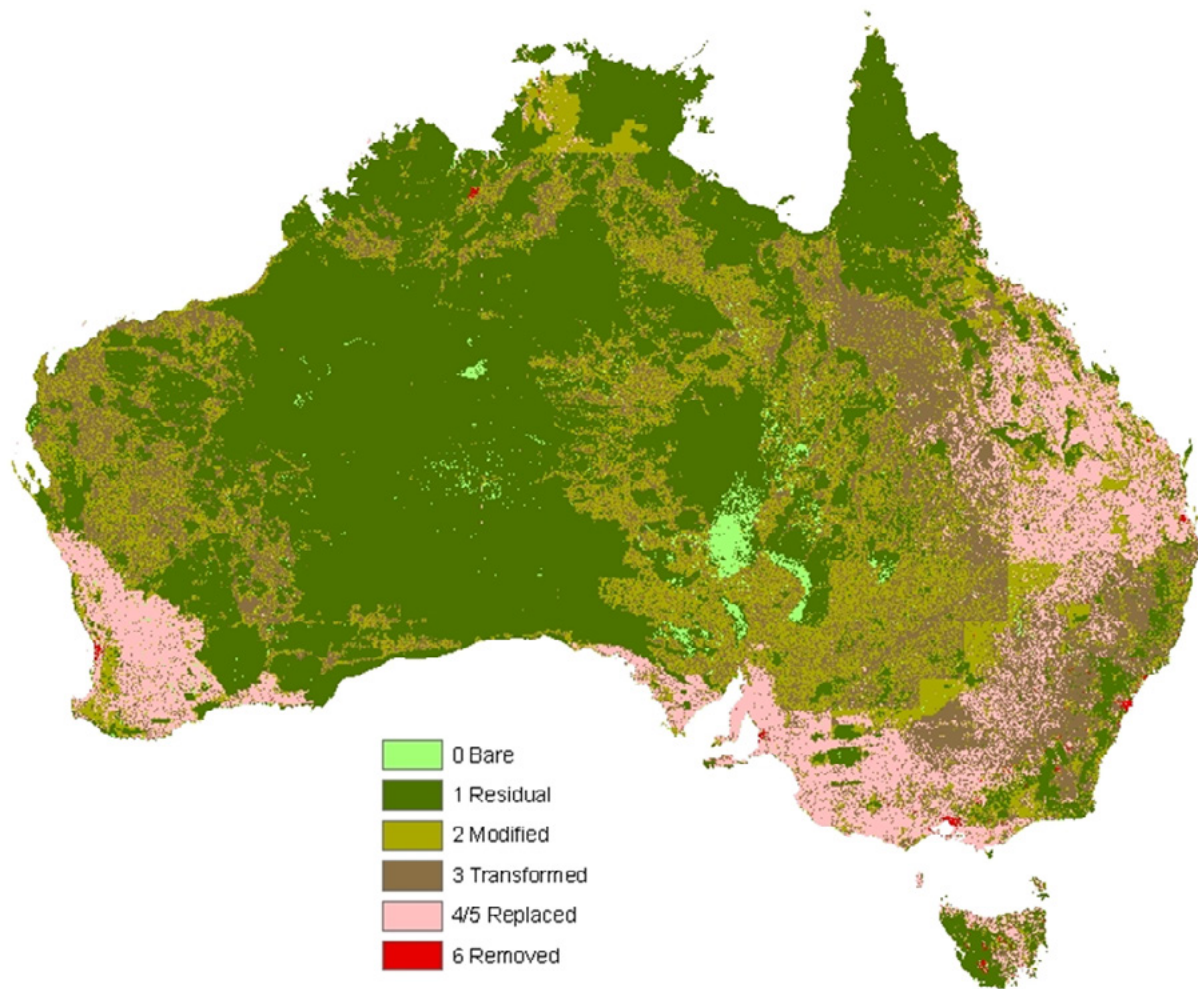
Diagnostic components	Key criteria	Key indicators
Regenerative capacity	1. Fire regime	1. Area/size of fire footprints
		2. Interval between fire starts
	2. Soil hydrology	3. Plant available water holding capacity
		4. Groundwater dynamics
	3. Soil physical state	5. Effective rooting depth of soil profile
		6. Bulk density of soil through changes to soil structure or soil removal
	4. Soil nutrient state	7. Nutrient stress—rundown (deficiency) relative to reference soil fertility
		8. Nutrient stress—excess (toxicity) relative to reference soil fertility
	5. Soil biological state	9. Organisms responsible for maintaining soil porosity and nutrient recycling
		10. Surface organic matter, soil crusts
	6. Reproductive potential	11. Reproductive potential of overstorey structuring species
		12. Reproductive potential of understorey structuring species
Vegetation structure	7. Overstorey structure	13. Overstorey top height (mean) of plant community
		14. Overstorey Foliage Projective Cover (mean) of the plant community
		15. Overstorey structural diversity (i.e. a diversity of age classes) of the stand
	8. Understorey structure	16. Understorey top height (mean) of plant community
		17. Understorey ground cover (mean) of the plant community
		18. Understorey structural diversity (i.e. a diversity of age classes) of the stand
Species composition	9. Overstorey composition	19. Densities of overstorey species functional groups
		20. Richness—number of indigenous overstorey species relative to the number of exotic species
	10. Understorey composition	21. Densities of understorey species functional groups
		22. Richness—number of indigenous understorey species relative to the number of exotic species

Source: Thackway (2014)

Condition information is needed to inform regional priorities, to establish policies, and to design and evaluate natural resource management programs for maintaining, restoring and rehabilitating native vegetation assets to improve the health of rivers, wetlands and estuaries, protect degraded landscapes against soil erosion, mitigate against dryland salinity, and improve habitat for Australia's unique native plants and animals.

(Thackway et al., 2015)

Figure 3.3 National VAST-2 dataset



Source: ABARES (2008)

Excursus 3.2—Vegetation Assets, States and Transitions (VAST)

Source: Lesslie *et al.* (2010); Thackway and Lesslie (2006, 2008); Thackway (2014); Thackway and Freudenberger (2016)

VAST classifies vegetation condition by assessing the degree of anthropogenic modification from a benchmark reference state (I) through five states of increasing human modification, where states I, II, and III represent native vegetation cover and states IV, V, and VI represent non-native vegetation cover. The VAST framework includes reporting the condition of native vegetation at regional and national scales, accounting for changes in the status and condition of vegetation, and describing the consequences of land management on vegetation condition (Thackway and Lesslie, 2006). VAST-2 (VAST Version 2) vegetation condition classes were developed from national spatial datasets (1995 to 2006) on a 1 km by 1 km grid, in conjunction with an expert model comparing

land management effects relative to a benchmark of pristine vegetation condition (assumed pre-1750; Lesslie *et al.*, 2010). Primary datasets used were:

- biophysical naturalness disturbance information forming part of the Australian Land Disturbance Database (ALDD; previously known as the National Wilderness Inventory, NWI; Lesslie and Maslen, 1995); updated in temperate forested environments in the Comprehensive Regional Assessment and Regional Forest Agreement (CRA-RFA) process (JANIS, 1997);
- land use datasets developed by the Australian Collaborative Land Use Mapping Program (BRS, 2006; Lesslie *et al.*, 2006);

- bare ground cover derived from MODIS satellite imagery (2004); and
- native vegetation extent baseline (2004) compiled from datasets collected by the states and territories (Thackway *et al.*, 2010).

For example, a study by Thackway and Freudenberger (2016) selected ten sites that are representative of Australia's agroclimatic regions (see Section 2.2.3), to systematically examine the response of plant communities to land management regimes over the past 250 years. The VAST framework was used to track changes in regenerative capacity, vegetation structure, species composition, and overall vegetation status. To demonstrate the information that can be derived from such analyses, Table 3.9 summarises relevant information for three of these sites. The impact of fragmentation and the extent of site modification for all ten sites are summarised in Figure 3.4.

All sites observed in this study occurred in intact landscapes during the early stages of rural development. While site 1 currently represents an intact landscape (> 90% vegetation retained and mostly unmodified), site 7 occurs in a variegated landscape (60–90% native vegetation retained, but mostly modified), and site 3 occurs in a relictual landscape (< 10% native vegetation retained). These condition assessments can be translated to estimates of the resilience of each site, from highest for site 1, to medium for site 7, to lowest for site 3. This type of landscape model is valuable for monitoring and reporting vegetation changes with a view to better understanding ecosystem resilience. Such understanding will allow appropriate management interventions to be prioritised for sites with low resilience and thus avoid further degradation into the future.

Table 3.9 Selected site attributes

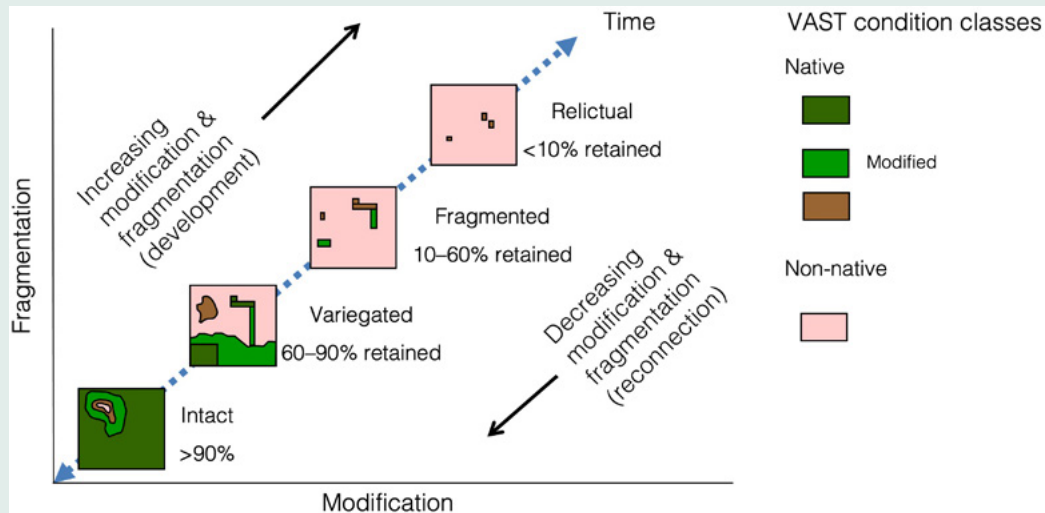
Vegetation condition dynamics indicate status score of change relative to reference state.

Attribute	Site Reference Number		
	1. Rocky Valley, Bogong High Plains	2. Wirilda, Harrogate	3. Conkerberry Paddock, Victoria River Research Station
Agroclimatic region	Cold-wet	Mediterranean	Tropical warm season wet
Bioregion	Victorian Alps (Victoria)	Kanmantoo (SA)	Ord Victoria Plain (NT)
Plant community	<i>Poa</i> tussock grassland	<i>Callitris</i> , eucalypt low mallee woodland	Eucalypt open woodland
Vegetation condition dynamics	10% loss due to livestock grazing then recovery to near reference conditions	70% loss due to clearing, then significant recovery by active restoration	50% loss due to livestock and feral herbivore grazing with modest recovery due to improved grazing management and increasing woody cover due to climate change
Government policies	State government reduction, then prohibition of livestock grazing, then creation of a national park	Various regulations that required clearing, then fertiliser subsidies to increase intensification More recently, agri-environmental schemes support farmers to restore native vegetation	Government-managed livestock reserve, and subsidies for artificial watering points and fencing, then research into improved range management
Markets	Rapid development of national and international markets for meat and wool	Domestic and international demand for grains, meat and wool	Domestic and particularly international demand, including live cattle exports
Technological changes	Domestic livestock	Broadscale cropping and exotic pasture systems, domestic livestock, fencing, and feral rabbits No till cropping into dormant native pasture with cell-based sheep grazing	Artificial watering points (bores), then fencing to improve grazing management, improved roads and transport, introduction of <i>Bos indicus</i> breeds of cattle
Climate variation	Periods of drought that increased livestock grazing pressure on alpine grassland	Drought and wildfire were a stimulus for land management change coupled with localised rising groundwater that was saline.	Large seasonal fluctuations in rainfall affecting livestock and feral herbivore numbers, but overall increasing rainfall over a longer season
Cultural	Total indigenous displacement by Western European values and land management practices	Total indigenous displacement by Western European values and land management practices	Total indigenous displacement by Western European values and land management practices; a conditional land claim was granted in 1990, enabling continued use of the area as a research station

Source: Thackway and Freudenberger (2016) Tables 3 and S1

Figure 3.4 Landscape change summary

Both the landscape alteration levels and VAST classes are shown for ten sites.



Source: Thackway and Freudenberger (2016) Figure 12

3.4.2 Changes in land use

The diversity of land use activities being undertaken in Australia is introduced in Sections 2.5.3 and 3.3.4. Information about land use change is needed to determine trends in agricultural activities and assess the management of natural resources, both in terms of regional and national changes (Lesslie and Mewett, 2013). Land use changes can have long term impacts on agricultural sustainability, food security, water availability, air quality, and biodiversity, all of which need to be monitored in terms of their social, economic and environmental consequences (Lesslie *et al.*, 2011). Thoughtful reviews of various aspects of land use practices and policies in Australia are presented in Thackway (2018).

Some of the drivers for changing land uses have been summarised as:

- resource scarcity leading to an increase in the pressure of production on resources;
- changing opportunities created by markets (such as production, infrastructure and transport costs);
- outside policy intervention (such as subsidies, taxes, property rights, infrastructure, governance);
- loss of adaptive capacity and increased vulnerability (such as exposure to natural hazards); and
- change in social organisation, attitudes, and access to resources (Lambin *et al.*, 2003).

Specific examples of events and conditions in each of these driver categories are listed in Table 3.10.

*Land use and land use change are central to our understanding of human impacts on the environment
(Clancy *et al.*, 2018)*

Table 3.10 Drivers of land use change

Driver	Example events and conditions determining rate of change	
	Slow	Fast
Resource scarcity	Natural population growth Inappropriate land uses reduce land productivity Degraded environmental resources	Forced population displacement (e.g. refugees) Allocation of previously productive land to other land uses
Market changes	Increased commercialisation and agro-industrialisation Improved access to land (e.g. new roads) Changes in prices of inputs/outputs Alternative employment opportunities	Capital investment in new land use(s) Price changes due to macro economics or trade conditions New technologies for intensification of resource use New commodities and land use activities
Government intervention	Economic development programs Inappropriate subsidies, taxes, price distortions, incentives Poor governance and corruption Insecurity of land tenure	Rapid policy changes (e.g. devaluation) Government instability War
Increased vulnerability	Impoverishment; Increased dependence on welfare Social discrimination	Internal conflicts Epidemics Natural hazards
Social changes	Institutional changes in resource management Increased urbanisation Extended family breakdown Increased materialism Reduced public awareness of environmental degradation	Expropriation of communal resources and/or private property Ecological marginalisation of the poor

Adapted from: Lambin *et al.* (2003) Table 4 and Thackway (2018)

Specific approaches to land use monitoring will vary with the intended end use and the spatial and temporal resolutions of available data. Most land use change reporting by ABARES, for example, relies on the ALUM time series (see Sections 2.5.3 and 3.3.4) and agricultural statistics from the Australian Bureau of Statistics (ABS; Mewett *et al.*, 2013). While ACLUMP aims for 80% accuracy in overall spatial and thematic attributes when a land use map is released (ABARES, 2015), this accuracy will inevitably reduce with time as land uses change.

Approaches that may be used to maintain the accuracy of land use maps include:

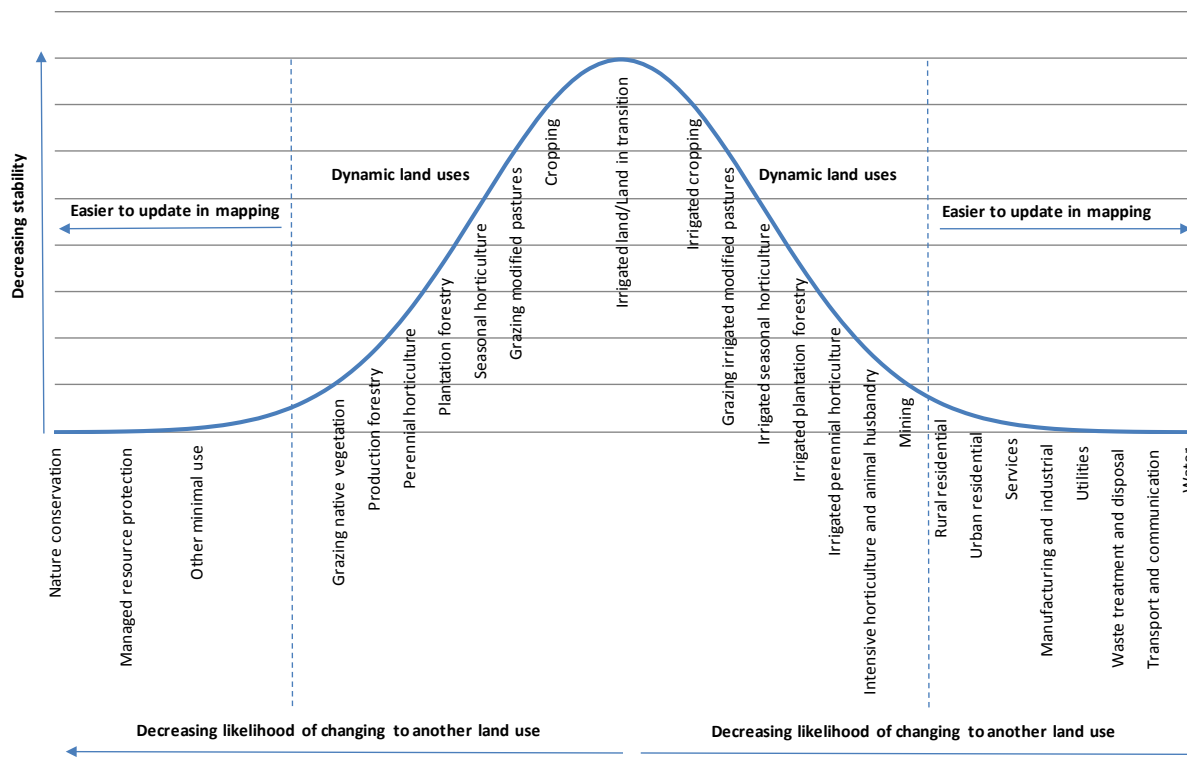
- update all areas at appropriate intervals (such as every five years for intensive agriculture regions and every ten years for pastoral and rangelands areas);
- use authoritative ancillary datasets to update specific land uses and/or regions as needed; or
- prioritise areas to update based on assessed likelihood of land use changes (see Figure 3.5; ABARES, 2015).

EO datasets are being used by some Australian state land use mapping agencies (e.g. QLUMP, 2017; Lawrence *et al.*, 2018) to identify areas of change in land use and land cover annually. Only those areas identified as changed are then updated in the relevant land use maps (ABARES, 2015; Hicks, 2018).

Land use planning has never been widely popular in democracies, as it is seen to impinge on the rights of the individual. However, a shift from rights to responsibilities is long overdue.
(Henry Nix, 2018)

Figure 3.5 Likelihood of ALUM land use change

These likelihoods are based on a national assessment, and will vary by region.



Source: ABARES (2015) Figure 4

The patterns of land use change can be variously described in terms of:

- area—spatial extent;
- productivity—efficiency associated with converting inputs to outputs;
- intensification—increased consumption of inputs (such as nutrients, water, and energy); and
- innovation—improvements aimed at ‘better’ outcomes such as greater productivity, more efficient use of inputs, or reduced degradation of landscape (Lesslie *et al.*, 2011).

For example, the intensification of agricultural land use, expressed in terms of the cost of production per unit area during the two decades from 1985/86 to 2005/06, was mapped by Leslie *et al.* (2011; see map 4).

Monitoring of land use change is closely coupled to monitoring of land cover (see Section 3.1.2) and increasingly relies on the use of EO datasets in combination with cadastre and ancillary spatial datasets. For example, ABARES coordinated a national Ground Cover Monitoring project that developed the Fractional Cover Product (see Excursus 8.3) to monitor soil erosion, and ultimately management practices, in cropped areas of Australia.

In combination with historical land use patterns, and datasets tracking climatic variables, such products may eventually enable the development of methods for forecasting land use changes, and thereby improve our understanding of resource utilisation across Australia. Spatial Decision Support Systems (DSS), such as the Multi-Criteria Analysis Shell for Spatial Decision Support (MCAS-S, 2018; Lesslie, 2013; Lesslie *et al.*, 2008), will assist this process by manipulating vast quantities of spatial data and highlighting the relevance of their patterns and interactions. To maximise the capabilities of available resources and best serve the interests of relevant stakeholders in Australia, an organising framework has been proposed to integrate land use and land resources information within a virtual centre (Clancy and Lesslie, 2013; Clancy *et al.*, 2018). Such an integrated framework would greatly simplify the process of monitoring land use changes in Australia.

3.5 Further Information

Australian Land Use

Land use data downloads: <https://www.agriculture.gov.au/abares/aclump/land-use/data-download>

ALUM (Australian Land Use and Management Classification system): <http://www.agriculture.gov.au/abares/aclump/land-use/alum-classification>

CLUM (Catchment scale Land Use for Australia): <https://www.agriculture.gov.au/abares/aclump/land-use/catchment-scale-land-use-of-australia-update-december-2018>

Australian Vegetation

NVIS: <https://www.environment.gov.au/land/native-vegetation/national-vegetation-information-system>

Major Vegetation Groups (based on NVIS): <https://data.gov.au/data/dataset/57c8ee5c-43e5-4e9c-9e41-fd5012536374>

New South Wales Vegetation/Land Cover

Bionet: <http://www.bionet.nsw.gov.au/>

SEED (NSW): <https://www.seed.nsw.gov.au>

SVTM: <https://www.environment.nsw.gov.au/vegetation/state-vegetation-type-map.htm>

Victoria Vegetation/Land Cover

Habitat Hectares: Parkes *et al.* (2003); McCarthy *et al.* (2004);

<https://www.environment.vic.gov.au/native-vegetation/native-vegetation/biodiversity-information-and-site-assessment>

<https://www.ari.vic.gov.au/research/modelling/mapping-vegetation-extent-and-condition>

EO-based Study of Land Cover Change

Graetz, D., Fisher, R., and Wilson, M. (1992). *Looking Back: The Changing Face of The Australian Continent, 1972–1992*. CSIRO Division of Wildlife and Ecology, Canberra.

Interactive Maps for Australian Resources

National Map: <https://nationalmap.gov.au/>

NEII (National Environmental Information Infrastructure): <http://neii.gov.au/data-viewer>

AURIN (Australian Urban Research Infrastructure Network): <https://map.aurin.org.au>

AREMI (Australian Renewable Energy Agency): <https://nationalmap.gov.au/renewables/>

Investor Map (locates opportunities for mining, tourism and agriculture): <https://nationalmap.gov.au/investormap/>

State of Environment maps: <https://soe.terria.io>

NRM Tools

FarmMap4D Spatial Hub (formerly NRM Spatial Hub; see Volume 1B—Excursus 10.4): <https://www.farmmap4d.com.au/>

VegMachine: <https://vegmachine.net/> (see Excursus 15.1 below)

Earth Observation Data for EcoSystem Monitoring (EODESM)

EODESM classifies land cover and change by combining essential environmental descriptors using the FAO LCCS taxonomy: <https://www.ecopotential-project.eu/products/eodesm.html>

Global Land Cover and Ecosystem Products

NASA Land Cover/Land Use Change Program (LCLUC): <https://lcluc.umd.edu/>

GLC2000: Global Land Cover 2000 database. European Commission, Joint Research Centre, 2003. http://forobs.jrc.ec.europa.eu/products/glc2000/data_access.php

GlobCover: http://due.esrin.esa.int/page_globcover.php

MODIS Land Cover: <http://glcf.umd.edu/data/lc/>

Sayre *et al.* (2020)

IUCN Red List of Ecosystems (RLE) Global Ecosystems Typology: <https://iucnrle.org/about-rle/ongoing-initiatives/global-ecosystem-typology/>

3.6 References

- ABARES (2008). *National Scale Vegetation Assets, States and Transitions (VAST Version 2)—2008*. Australian Bureau of Agricultural and Resource Economics and Sciences, Department of Agriculture and Water Resources. http://data.daff.gov.au/anrdl/metadata_files/pa_vast_g9abll0032008_11a.xml
- ABARES (2010). *Land Use and Land Management Information for Australia. Workplan of the Australian Collaborative Land Use and Management Program*. Australian Bureau of Agricultural and Resource Economics and Sciences, Canberra.
- ABARES (2011). *Guidelines for land use mapping in Australia: principles, procedures and definitions*. 4th edn. Australian Bureau of Agricultural and Resource Economics and Sciences, Canberra.
- ABARES (2015). *Addendum to the guidelines for land use mapping in Australia: Principles, procedures and definitions* 4th edn. Australian Bureau of Agricultural and Resource Economics and Sciences, Canberra, ACT. http://data.daff.gov.au/data/warehouse/pe_abares99001806/AddendumGuidelinesLandUseMapping2015_v1.0.0.pdf
- ABARES (2016). *The Australian Land Use and Management Classification Version 8*. Australian Bureau of Agricultural and Resource Economics and Sciences, Canberra.
- ANRA (2009). *Australian Natural Resources Atlas*. www.anra.gov.au
- AUSLIG (1990). *Atlas of Australian Resources (Third Series) Volume 6: Vegetation*. Australian Land and Surveying Information Group, AUSMAP, Department of Administrative Services, Canberra. 64 p.
- Avery, T.E. (1975). *Natural Resources Measurements* 2nd edn. McGraw-Hill, New York.
- Bartholomé, E., and Belward, A.S. (2007). GLC2000: a new approach to global land cover mapping from Earth Observation data. *International Journal of Remote Sensing*, 9, 1959–1977. doi.org/10.1080/01431160412331291297
- Beard, J.S., and Webb, M.J. (1974). *Vegetation Survey of Western Australia: Great Sandy Desert—Part I. Aims, Objectives and Methods*. University of Western Australia Press, Nedlands, WA.
- Bontemps, S., Defourny, P., Van Bogaert, E., Arino, O., Kalogirou, V., and Perez, J.R. (2011). *Globcover 2009. Products Description and Validation Report*. ESA/UCL. http://due.esrin.esa.int/files/GLOBCOVER2009_Validation_Report_2.2.pdf
- BRS (2006). *Guidelines for Land Use Mapping in Australia: Principles, Procedures and Definitions*. 3rd edn. Bureau of Rural Sciences, Canberra.
- Butler, D., Thackway, R., and Cosier, P. (2020). *Technical Protocol for Constructing Native Vegetation Condition Accounts Version 1.0 - May 2020*. Accounting for Nature Limited, Sydney, Australia. <https://static1.squarespace.com/static/5dc38cde1d028031235ca3cf/t/5fa246b73c71c92e01513cc7/1604470479988/AfN+Native+Vegetation+Technical+Protocol+ACCREDITED.pdf>
- Carnahan, J.A. (1976). Natural Vegetation map with commentary. *Atlas of Australian Resources, Second Series*. Department of Natural Resources, Canberra.
- Carnahan, J.A. (1988). Present Vegetation map. In *Atlas of Australian Resources, Second Series*. Department of Natural Resources, Canberra.
- Christian, C.S., and Stewart, G.A. (1953). *General report on survey of Katherine-Darwin region, 1946*. CSIRO, Melbourne.
- Christian, C.S., and Stewart, G.A. (1968). Methodology of integrated surveys. In *Aerial surveys and integrated studies. Proceedings of Toulouse Conference of 1964*. UNESCO, Paris.
- Cihlar, J. (2000). Land cover mapping of large areas from satellites: Status and research priorities, *International Journal of Remote Sensing*, 21, 1093–1114.
- Clancy, T.F., and Lesslie, R.G. (2013). *A needs assessment for a national research centre addressing land use and food security issues*. ABARES Report to client prepared for the International Agricultural Cooperation Program, Trade and Market Access Division of the Department of Agriculture, Canberra.
- Clancy, T., Bryan, B.A., and Guru, S.M. (2018). The Future for Land Use Mapping: National E-Infrastructure, Modelling Analytics, Synthesis and Securing Institutional Capacity. Ch. 10 in *Land Use in Australia: Past, Present and Future*. (Ed: Thackway, R.). ANU eVIEW, Canberra. ISBN: 9781921934421
- Cresswell, I., and Thomas, G. (1997). *Terrestrial and Marine Protected Areas in Australia (1997)*. Environment Australia, Biodiversity Group, Canberra.
- CSIRO (2014). *Australian Soil Resource Information System*. www.asris.csiro.au

- DAWE (2020a). *Australia's bioregions (IBRA)* webpage, Department of Agriculture, Water and the Environment website: <https://www.environment.gov.au/land/nrs/science/ibra>
- DAWE (2020b). *Catchment scale land use for Australia—Update December 2018* webpage, Department of Agriculture, Water and the Environment website: <https://www.agriculture.gov.au/abares/aclump/land-use/catchment-scale-land-use-of-australia-update-december-2018>
- DAWE (2020c). *Australian Land Use and Management Classification Version 8 (October 2016)* webpage, Department of Agriculture, Water and the Environment website: <https://www.agriculture.gov.au/abares/aclump/land-use/alum-classification>
- DE (2012). *Australia—Present Major Vegetation Groups: NVIS Version 4.1 (Albers 100m analysis product)*. Bioregional Assessment Source Dataset, Department of the Environment. <http://data.bioregionalassessments.gov.au/dataset/57c8ee5c-43e5-4e9c-9e41-fd5012536374>.
- DeFries, R.S., and Belward, A.S. (2000). Global and regional land cover characterization from satellite data: An introduction to the special issue. *International Journal of Remote Sensing*, 21, 1083–1092.
- Di Gregorio, A. (2005). *Land Cover Classification System: Classification Concepts and User Manual. Software version 2*. FAO Environment and Natural Resources Service Series, No. 8. FAO, Rome. 208 p.
- Di Gregorio, A. (2016). *Land Cover Classification System Software version 3*. FAO, Rome. ISBN 978-92-5-109017-6 <http://www.fao.org/3/a-i5232e.pdf>
- Di Gregorio, A., and Jansen, L.J.M. (2000). *Land Cover Classification System (LCCS): Classification Concepts and User Manual*. FAO. ISBN 92-5-104216-0 http://www.fao.org/3/x0596e/X0596e00.htm#P-1_0
- EcoPotential (2021). *EODESM: Earth Observation Data for Ecosystem Monitoring* webpage, EcoPotential website: <http://www.ecopotential-project.eu/products/eodesm.html>
- Fisher, P., Comber, A.J., and Wadsworth, R. (2005). Land Use and Land Cover: Contradiction or Complement. In *Representing GIS*. (Eds: R. Fisher and D. Unwin). John Wiley and Sons Ltd.
- Gammage, B. (2012). *The Biggest Estate on Earth*. Allen and Unwin, Sydney.
- GEO (2012). *Task US-09-01a: Critical Earth Observation Priorities*. Final Report (2nd edition). Group on Earth Observations. https://www.wmo.int/pages/prog/sat/meetings/documents/ARCH-3_Inf_02_GEO-US-09-01a-final-report.pdf
- Graetz, D., Fisher, R., and Wilson, M. (1992). *Looking Back. The changing face of the Australian continent, 1972–1992*. CSIRO, Canberra.
- Grekousis, G., Mountrakis, G., Kavouras, M. (2015). An overview of 21 global and 43 regional land-cover mapping products. *International Journal of Remote Sensing*, 36(21), 5309–5335. doi.org/10.1080/01431161.2015.1093195
- Harrison, B.A., and Jupp, D.L.B. (1989) *Introduction to Remotely Sensed Data: Part ONE of the microBRIAN Resource Manual*. CSIRO, Melbourne. 156 p.
- Hicks, R. (2018). Responding to Land Use Pressures: A State and Territory Perspective. Ch. 6 in *Land Use in Australia: Past, Present and Future*. (Ed: Thackway, R.). ANU eVIEW, Canberra. ISBN: 9781921934421
- IGBP (1990). *The International Geosphere–Biosphere Programme: A study of global change—The initial core projects*. IGBP Global Change Report no. 12. International Geosphere–Biosphere Programme, Stockholm, Sweden.
- IUCN (2008). *Guidelines for applying protected area management categories*. International Union for Conservation of Nature, Switzerland. http://www.iucn.org/sites/dev/files/import/downloads/iucn_assignment_1.pdf.
- JANIS (1997). *Nationally Agreed Criteria for the Establishment of a Comprehensive, Adequate and Representative Reserve System for Forests in Australia*. A report by the Joint ANZECC–MCFFA, National Forest Policy Statement Implementation Sub-committee. Commonwealth of Australia, Canberra. 20 p.
- Kessell, S.R. (1979). *Gradient Modelling: Resource and Fire Management*. Springer-Verlag, New York.
- Lambin, E.F., Geist, H.J., and Lepers, E. (2003). Dynamics of land-use and land-cover change in tropical and subtropical regions. *Annual Review of Environmental Resources*, 28, 205–241.
- Lambin, E.F., and Geist, H.J. (Eds) (2006). *Land-Use and Land-Cover Change: Local Processes and Global Impacts*. The IGBP Series. Springer-Verlag, Berlin.

- Land and Water Australia (2009). *National Land and Water Audit*. <http://lwa.gov.au/programs/national-land-and-water-resources-audit>
- Lawrence, P., Shephard, C., Norman, P., Jones, C., and Witte, C. (2018). Monitoring and Reporting Land Use Change and Its Effects on the Queensland Environment. Ch. 13 in *Land Use in Australia: Past, Present and Future*. (Ed: Thackway, R.). ANU eVIEW, Canberra. ISBN: 9781921934421
- Lesslie, R. (2013). Mapping our priorities—innovation in spatial decision support. In *Innovation for 21st century conservation* (Eds: P. Figgis, J. Fitzsimons and J. Irving). Australian Committee for the International Union of Conservation of Nature, Sydney, NSW. pp. 156–163.
- Lesslie, R.G. and Maslen, M.A. (1995). *National wilderness inventory Australia : handbook of procedures, content, and usage*. AGPS, Canberra.
- Lesslie, R., and Mewett, J. (2013). *Land use and management: The Australian context*. Australian Bureau of Agricultural and Resource Economics and Sciences Research Report 13.1. Canberra, ACT.
- Lesslie, R., Barson, M., and Smith, J. (2006). Land use information for integrated natural resources management—a coordinated national mapping program for Australia. *Journal of Land Use Science*, 1(1), 45–62.
- Lesslie, R.G., Hill, M.J., Hill, P., Cresswell, H.P., and Dawson, S. (2008). The application of a simple spatial multi-criteria analysis shell for natural resource management decision making. In *Landscape analysis and visualisation: Spatial models for natural resource management and planning*. (Eds: C. Pettit, W. Cartwright, I. Bishop, K. Lowell, D. Pullar and D. Duncan). Springer, Berlin. pp. 73–96. doi.org/10.1007/978-3-540-69168-6_5
- Lesslie, R., Thackway, R., and Smith, J. (2010). *A national-level Vegetation Assets, States and Transitions (VAST) dataset for Australia (version 2.0)*. Bureau of Rural Sciences, Canberra. ISBN 978-1-921192-48-7
- Lesslie, R., Mewett, J., and Walcott, J. (2011). *Landscapes in transition: Tracking land use change in Australia*. *Science and Economic Insights*, 2.2. Australian Bureau of Agricultural and Resource Economics and Sciences, Canberra, ACT.
- Lucas, R., Mueller, N., Siggins, A., Owers, C., Clewley, D., Bunting, P., Kooymans, C., Tissott, B., Lewis, B., Lymburner, L., and Metternicht, G. (2019). Land Cover Mapping using Digital Earth Australia. *Data*, 4, 143. [doi:10.3390/data4040143](https://doi.org/10.3390/data4040143)
- Lymburner, L., Tan, P., Mueller, N., Thackway, R., Thankappan, M., Islam, A., Lewis, A., Randall, L., and Senarath, U. (2011). *The National Dynamic Land Cover Dataset - Technical report*. Record 2011/031. Geoscience Australia, Canberra. ISBN 978-1-921954-30-6 http://cmi.ga.gov.au/dlcd_25_1.0.0
- Mabbutt, J.A. (1968). Review of concepts of land classification. In *Land Evaluation* (Ed: A.G. Stewart) Macmillan, Melbourne. pp 11–28.
- McCarthy, M.A., Parris, K.M., van der Ree, R., McDonnell, M.J., Burgman, M.A., Williams, N.S.G., McLean, N., Harper, M.J., Meyer, R., Hahs, A., and Coates, T. (2004). The habitat hectares approach to vegetation assessment: An evaluation and suggestions for improvement. *Ecological Management and Restoration*, 5(1), 24–27.
- Malthus, T.J., Barry, S., Randall, L.A., McVicar, T., Bordas, V.M., Stewart, J.B., Guerschman, J.-P., and Penrose, L. (2013). *Ground cover monitoring for Australia: Sampling strategy and selection of ground control sites*. CSIRO, Australia.
- MCAS-S (2018). *Multi-criteria analysis (MCAS-S)* webpage: <http://www.agriculture.gov.au/abares/aclump/multi-criteria-analysis>
- McKenzie, N.J., Jacquier, D.W., Maschmedt, D.J., Griffin, E.A., and Brough, D.M. (2012). *The Australian Soil Resource Information System (ASRIS) Technical Specifications Revised Version 1.6*, June 2012. The Australian Collaborative Land Evaluation Program. <http://www.asris.csiro.au/downloads/ASRIS%20Tech%20Specs%201.6.pdf>
- Mewett, J., Paplinska, J., Kelley, G., Lesslie, R., Pritchard, P., and Atyeo, C. (2013). *Towards national reporting on agricultural land use change in Australia*. ABARES technical report, Canberra.
- NASA (1999). *BigFoot. Characterizing Land Cover, LAI, and NPP at the Landscape Scale for EOS/MODIS Validation. Field Manual Version 2.1*. National Aeronautics and Space Administration, ORNL/TM-1999/216.
- NCST (2009). *Australian Soil and Land Survey Field Handbook*. 3rd edn. National Committee on Soil and Terrain, CSIRO, Canberra. 26 pp.
- Nix, H. (1982). Environment determinants of biogeography and evolution in Terra Australis. In *Evolution of the Flora and Fauna of Arid Australia*. (Eds: W.R. Barker and P.J.M. Greenslade). Peacock Publications, Frewville. pp. 47–66.
- Nix, H. (2018). Foreword in *Land Use in Australia: Past, Present and Future*. (Ed: Thackway, R.). ANU eVIEW, Canberra. ISBN: 9781921934421

- NLP (2017). *The Report on the Review of the National Landcare Program*. Commonwealth of Australia.
- NLP (2019). *National Landcare Program Phase One* webpage: <http://www.nrm.gov.au/national-landcare-programme/phase-one>
- NLWRA (2001). *Australian Native Vegetation Assessment 2001*. National Land and Water Resources Audit, Land and Water Australia, Canberra. ISBN: 0 642 37128 8
- NRM (2019a). *What is NRM?* webpage, NRM Regions Australia website: <http://nrmregionsaustralia.com.au/what-is-nrm/>
- NRM (2019b). *NRM regional model* webpage, NRM Regions Australia website: http://nrmregionsaustralia.com.au/nrm_regional_model/
- NVIS Technical Working Group (2017). *Australian Vegetation Attribute Manual: National Vegetation Information System, Version 7.0*. (Eds: Bolton, M.P., deLacey, C., and Bossard, K.B.). Department of the Environment and Energy, Canberra.
- Olson, D.M., Dinerstein, E., Wikramanayake, E.D., Burgess, N.D., Powell, G.V.N., Underwood, E.C., D'Amico, J.A., Itoua, I., Strand, H.E., Morrison, J.C., Loucks, C.J., Allnutt, T.F., Ricketts, T.H., Kura, Y., Lamoreux, J.F., Wettengel, W.W., Hedao, P., and Kassem, K.R. (2001). Terrestrial ecoregions of the world: a new map of life on Earth. *Bioscience*, 51(11), 933–938.
- Parkes, D., Newell, G., and Cheal, D. (2003). Assessing the quality of native vegetation: The 'habitat hectares' approach. *Ecological Management and Restoration*, 4, S29–S38.
- QLUMP. (2017). *Queensland land use mapping program (QLUMP)*. Queensland Government. <https://www.qld.gov.au/environment/land/management/mapping/statewide-monitoring/qlump>
- Sayre, R., Karagulle, D., Frye, C., Boucher, T., Wolff, N.H., Breyer, S., Wright, D., Martin, M., Butler, K., Van Graafeiland, K., Touval, J., Sotomayor, L., McGowan, J., Game, E.T., and Possingham, H. (2020). An assessment of the representation of ecosystems in global protected areas using new maps of World Climate Regions and World Ecosystems. *Global Ecology and Conservation*, 21, e00860. <https://doi.org/10.1016/j.gecco.2019.e00860>
- Sbrocchi, C. (2013). *Guidelines for Constructing Regional Environmental (Asset Condition) Accounts: Quick Guide*. Wentworth Group of Concerned Scientists, Sydney.
- Specht, R.L. (1970). Vegetation in *The Australian Environment*. 4th edn. (Ed: Leeper, G.W.). CSIRO, Melbourne.
- TERN Australia (2018). *Effective Field Calibration and Validation Practices: A practical handbook for calibration and validation satellite and model-derived terrestrial environmental variables for research and management*. A TERN Landscape Assessment Initiative, NCRIS. ISBN 978-0-646-94137-0. <https://www.tern.org.au/NEW-CalVal-handbook-for-remote-sensing-bgp4370.html>
- Thackway, R. (Ed.) (2018). *Land Use in Australia: Past, Present and Future*. ANU eVIEW, Canberra. ISBN: 9781921934421
- Thackway, R., and Cresswell, I.D. (1995). *An Interim Biogeographic Regionalisation for Australia: a Framework for Establishing the National System of Reserves*, Version 4.0. Australian Nature Conservation Agency, Canberra.
- Thackway, R., and Lesslie, R. (2006). Reporting vegetation condition using the Vegetation Assets, States, and Transitions (VAST) framework. *Ecological Management and Restoration*, 7(1), 53–62.
- Thackway, R., and Lesslie, R. (2008). Describing and mapping human-induced vegetation change in the Australian landscape. *Environmental Management*, 42, 572–590.
- Thackway, R., Wilson, P., Hnatiuk, R., Bordas, V., and Dawson, S. (2010). *Establishing a national baseline (2004) to assess change in native vegetation extent*. Bureau of Rural Sciences, Canberra.
- Thackway, R. (2014). VAST-2 Tracking the Transformation of Vegetated Landscapes, *Handbook for Recording Site-based Effects of Land Use and Land Management Practices on the Condition of Native Plant Communities*, version 3.0. The University of Queensland, Brisbane. 35 p.
- Thackway, R., Cosier, P., McIntosh, E., Saunders, D., Possingham, H., and Sbrocchi, C.D. (2015). *Draft Protocol for Constructing a Native Vegetation Condition Account*. Australian Regional Environmental Accounts Working Paper Series (1/5). Wentworth Group of Concerned Scientists, Sydney.
- Thackway, R., and Freudenberger, D. (2016). Accounting for the drivers that degrade and restore landscape functions in Australia. *Land*, 5(4), 40. doi.org/10.3390/land5040040
- Townshend, J.R. (1992). Land Cover. *International Journal of Remote Sensing*, 13(6–7), 1319–1328.
- Walker, B. (2020). Resilience: what it is and is not. *Ecology and Society*, 25(2), 11. <https://doi.org/10.5751/ES-11647-250211>

Walker, J., and Hopkins, M.S. (1990). *Vegetation. Australian Soil and Land Survey Handbook: Guidelines for Conducting Surveys*. (Eds: R.H. Gunn, J.A. Beattie, R.E. Reid and R.H.M. v.d. Graaff). Inkata Press, Melbourne. pp 58–86.

Williams, R.J. (1959). Vegetation map of Australia in *The Australian Environment*. 3rd edn. CSIRO, Melbourne. Reproduced with changed legend in *The Australian Environment*. 4th edn (Ed: G.W. Leeper, 1970). CSIRO, Melbourne.

Wulder, M.A., Coops, N.C., Roy, D.P., White, J.C., and Hermosilla, T. (2018). Land cover 2.0. *International Journal of Remote Sensing*, 39(12), 4254–4284. doi:10.1080/01431161.2018.1452075

Yang, H., Li, S., Chen, J., Zhang, X., Xu, S.(2017). The standardization and harmonization of land cover classification systems towards harmonized datasets: a review. *International Journal of Geo-Information*, 6, 154–170.

Measurable Properties of Terrestrial Vegetation



Most of the terrestrial surfaces on Earth are covered by vegetation of some description. Given that waterbodies cover over 70% of the Earth's surface (see Volume 3B), vegetation has been estimated to cover some 20% of the total surface of our planet.

An enormous diversity of vegetation exists on Earth, exhibiting major differences in appearance, life cycle, and growth requirements (see Section 1.3.2). Different plants are best suited to particular climates and landscapes and most tend to flourish in association with 'friends' and 'healthy competition', forming unique communities of species that are mutually supportive (see Section 1.2). This synergy contributes to recovery from external changes and enriches the environment for other organisms.

Our planet is dynamic at a variety of scales (see Section 1.3.3). The characteristics of vegetation cover on Earth vary not only over space but also with the passage of time. Change can occur in cycles, resulting from natural rhythms related to the movement of the Earth and the Moon relative to the Sun, or as a consequence of 'irregular' events such as natural disasters or anthropogenic activities. Natural changes are fundamental to the Earth's stability and resilience, and enable natural resources to be recycled and sustained. Anthropogenic changes, however, can outstrip the intrinsic timeframes of landscape recovery, so require prudent monitoring and management.

Botany is concerned with classifying and understanding plants (see Excursus 1.1). The characteristics of vegetation that botanists use to identify plants, however, are not necessarily directly related to EO image interpretation. The following sections discuss particular characteristics of individual plants and groups of plants that are relevant to categorising vegetation using EO datasets:

- attributes of foliage (Section 4);
- attributes of individual plants (Section 5);
- attributes of communities (Section 6); and
- attributes of ecosystems (Section 7).

Contents

4	Attributes of Foliage	89
5	Attributes of Individual Plants	107
6	Attributes of Plant Communities	125
7	Attributes of Ecosystems	141

4 Attributes of Foliage

Plant leaves are collectively called foliage. Leaves are the primary site for photosynthesis, and occur in a wide variety of colours, sizes, shapes, and textures. Foliage is one of the principal characteristics of vegetation that is used to identify individual species. Several aspects of foliage that are relevant to analysing EO images are discussed in the following sub-sections:

- structure and shape (see Section 4.1);
- chemical composition (see Section 4.2);
- spectral reflectance properties (see Section 4.3); and
- aerodynamic forces (see Section 4.4).

4.1 Structure and Shape

Leaf structure and shape are discussed below in terms of:

- anatomy—internal structure (see Section 4.1.1);
- morphology—external shape and orientation (Section 4.1.2);
- texture—external surfaces (Section 4.1.3); and
- strength—vulnerability to external forces (Section 4.1.4).

4.1.1 Anatomy

A ‘typical’ plant leaf comprises multiple layers with characteristic functions. As illustrated in Figure 4.1, when traversed from the top surface to the bottom surface, specialised cell types can be distinguished:

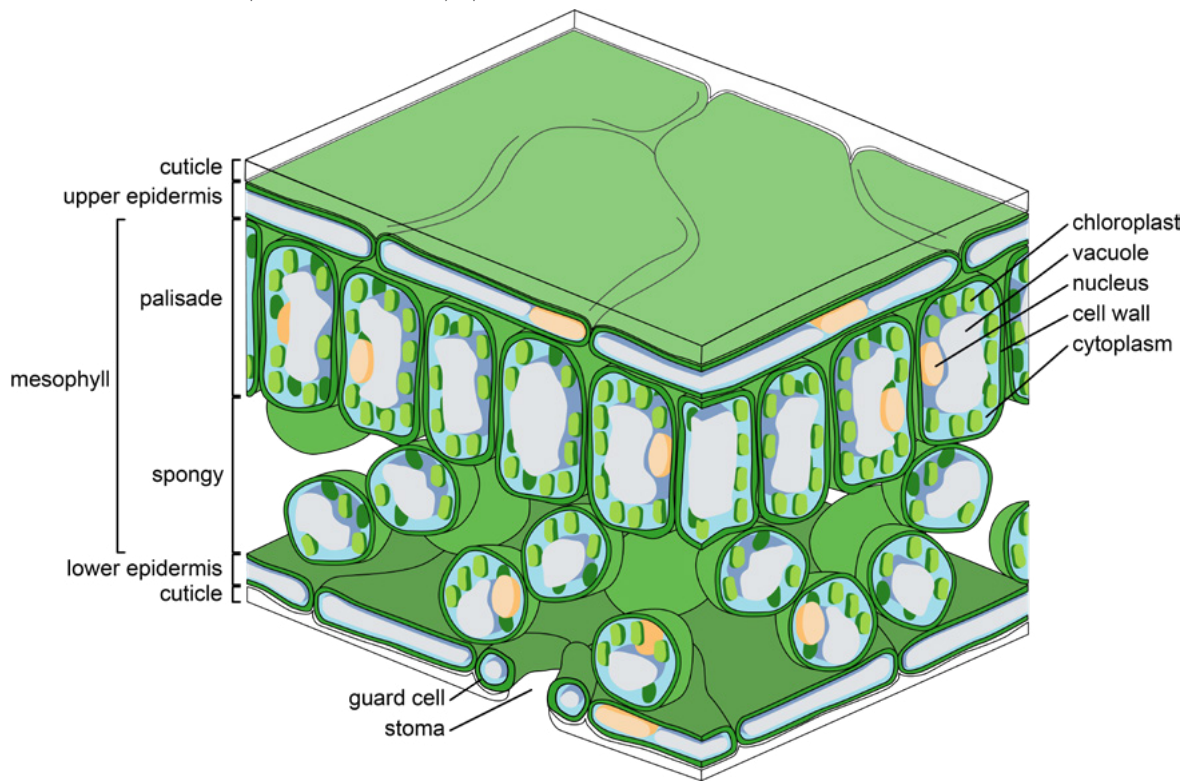
- upper epidermis (and often cuticle)—top outer layer with waxy, waterproof coating;
- mesophyll—containing chloroplast and comprising:
 - ◆ palisade parenchyma—elongated cells adjacent to epidermis; and
 - ◆ spongy mesophyll parenchyma—looser irregular cells bordered by palisade parenchyma; and
- lower epidermis (and often cuticle)—bottom surface with guard cells that open and close stomata (pores) to control transpiration and carbon dioxide (CO₂) exchange (Esau, 1965).

In many plants, the epidermis secretes a waxy coating called the cuticle, which protects the leaf from pests and predators, such as insects and bacteria, and water loss (Yeats and Rose, 2013). The cuticle surface diffuses light and has low reflectivity. Most of the sunlight reaching the cuticle is transmitted through the epidermis to the palisade cells, with shaded leaves having thinner cuticles and shorter palisade cells than leaves in direct sunlight (see Section 4.1.2). The epidermis can contain trichomes (hair cells), which offer further protection against predators and reduce the intensity of sunlight on the leaf (Esau, 1965; see Section 4.1.3).

The palisade mesophyll cells have a high concentration of chloroplasts and act as ‘pipes’ that direct light towards their pigment molecules for photosynthesis (Croft and Chen, 2017). These cells are generally arranged in rows, with plants growing in full sun having more layers than those growing in shade. In some plants whose leaves hang vertically, such as adult eucalypts, palisade cells are adjacent to both the upper and lower epidermis and thus form a sandwich around the spongy mesophyll cell layer (Evans and Vogelmann, 2006).

Figure 4.1 Typical leaf cell structure

The fine scale structure of an angiosperm leaf featuring the major tissues: the upper and lower epithelia (and associated cuticles); the palisade and spongy mesophyll; and the guard cells of the stoma. Vascular tissue (veins) is not shown. Key plant cell organelles (the cell wall, nucleus, chloroplasts, vacuole, and cytoplasm) are also shown.



Source: Richard Wheeler, Zephyris, Wikimedia Commons. (Retrieved from https://en.wikipedia.org/wiki/Leaf#/media/File:Leaf_Tissue_Structure.svg)

Air spaces between the smaller spongy mesophyll cells allow gas exchange of water vapour, CO₂, and oxygen with the atmosphere via stomata. The guard cells control stomatal opening to conserve water and heat within the leaf. In most plants, stomata are often more numerous on the lower than the upper leaf surface and also in plants from cooler climates (Harrison *et al.*, 2020).

A network of veins throughout the leaf transport food, water, and minerals to and from the rest of the plant. The vein pattern, or venation, of a leaf is characteristic of its species. Veins comprise vascular tissue located within the spongy mesophyll layer. A vein includes two types of conducting cells: xylem, which transports water and minerals from the roots to the leaf; and phloem, which moves photosynthetic products from the leaf to the rest of the plant. These conducting structures are surrounded by a sheath of lignin, which increases leaf rigidity.

The three mechanisms for photosynthesis, namely C₃, C₄, and CAM are introduced in Section 5.2.1. Most plants use C₃ carbon fixation for photosynthesis. Those that use the C₄ or CAM metabolic pathways have slightly different leaf anatomy (Edwards, 2019).

4.1.2 Morphology

Most leaves are flat, but some are folding or bulbous; most are photosynthetic, but in some plants this function has been adopted by other structures, such as cladodes in *Casuarina* species. Leaf allometry considers the impact of the size characteristics of leaves on their anatomy and physiology (Niklas, 1994; John *et al.*, 2013). Some of the major foliage differences that occur between and within plant species include the size of the leaf blade, the overall leaf shape, the extent of dissection into leaflets, the shape on leaf/leaflets margins, the pattern of veins (venation), the size of the leaf stem (petiole), the arrangement and orientation of leaves along a branching stem, and/or the arrangement of leaves on the petiole. The composite impact of leaf shape, size, arrangement, and orientation is particularly relevant to water and light availability (see Section 4.2.2).

A number of plant classification systems rely on plant functional traits (PFT)—“morphological, biochemical, physiological, structural, phenological, or behavioural characteristics that are expressed in phenotypes of individual organisms” (Violle *et al.*, 2007)—rather than their taxonomic characteristics (see

Section 1.1). These traits define the ecological role of species—their interaction with the environment and other species. An understanding of the costs and benefits of these traits also provides insight into vegetation changes along physical geography gradients (Westoby and Wright, 2006). Several PFT have been nominated for this purpose, with simplicity of measurement being an advantage. Below we will consider leaf size, area, shape, and orientation.

Leaf size, measured as the one-sided projected surface area of a fresh leaf (as mm²), impacts leaf energy production, carbon assimilation, and water balance. Variations in leaf size between species have been related to climatic variation, geology, altitude, and latitude, with environments involving the stresses of heat, cold, drought, and fire showing a preference towards smaller leaves. Plants with larger leaves tend to live in warmer, sunnier, and moister climates, with small leaves offering more control over the loss of heat and water. For a given species, however, shaded leaves tend to become both larger and thinner than their sunlit counterparts, presumably endeavouring to capture more sunlight with a larger surface area (Larcher, 1980). Compound leaves may enable better air exchange over the leaf surface and thus improve the efficiency of heat transfer within a plant (Xu *et al.*, 2009). Larger and thicker leaf types are more ‘expensive’ for the plant to make and maintain, that is they require a greater investment in non-productive infrastructure, so they need to be more durable to justify their production (Milla *et al.*, 2008). Similarly, leaf temperature and evaporative demand both increase with leaf size (Gates, 1980; Givnish, 1979).

Specific Leaf Area (SLA) is computed as the ratio of the leaf size to its oven-dry mass (leaf dry matter content) in m²/kg. It indicates the leaf area available for photosynthesis per unit of biomass and appears to be indicative of the potential relative growth rate of a plant. It is also used to estimate stomatal density. SLA can be expressed as a function of leaf dry matter content (LDMC; see Section 4.2.1) and leaf thickness (Perez-Harguindeguy *et al.*, 2013). Lower values of SLA tend to correspond to plants with structural leaf defence mechanisms and high leaf longevity, although SLA is typically lower in evergreen than in deciduous species (Reich *et al.*, 1997; Ackerly *et al.*, 2002) and in sun leaves compared with shade leaves (Lichtenthaler, 2009). Higher SLA values occur in permanently or temporarily resource-rich environments and also in selected shade-tolerant understorey species. Larger leaves, with a smaller proportion of photosynthetically active material per unit mass, generally have lower SLA than smaller leaves, although variations in this relationship can

occur when leaf thickness changes are unrelated to leaf cell density (Milla *et al.*, 2008). SLA is considered to be more indicative of resource usage by plants than LDMC in sand dune environments (Li *et al.*, 2005) and may be indicative of climate response, CO₂ response, nutrient response, competitive strength, plant defence, and biogeochemical cycles, and related to flammability (Cornelissen *et al.*, 2003; Perez-Harguindeguy *et al.*, 2013). When CO₂ levels increase, SLA and stomatal density decrease (Juneau and Tarasoff, 2012).

Leaf shape can be considered in terms of the degree of dissection (number of leaflets per leaf) and lobation (number of lobes or segments). One measure of leaf shape and complexity is the Dissection Index (DI), which is standardised to a value of one for a circle (McLellan and Endler, 1998):

$$DI = \frac{\text{perimeter}}{\sqrt{\text{area}}}$$

Leaf shape characteristics have been related to hydraulic resistance in plants (Sisó *et al.*, 2001), photosynthetic rates and optimal temperature range (Nicotra *et al.*, 2008), and also climatic distribution (Royer *et al.*, 2005). Lobation effectively reduces the active leaf area and offers plants particular advantages in terms of controlling water and temperature balance (Williams *et al.*, 2004). For example, lobed leaves demonstrate greater efficiency in thermal control in calm weather (Vogel, 1970).

Leaf orientation also differs between species and can vary with plant age. For example, eucalypt seedlings start life with juvenile leaves, which can intercept maximum sunlight for rapid growth. Such leaves are often round and grow horizontally from the plant structure. As the tree matures (at around seven years old) the leaves of most species change form and orientation, becoming long, thin, and pendulous (Jacobs, 1955). With this shape and orientation, adult leaves intercept less solar radiation but conserve moisture, which is essential for survival in many regions of Australia (James and Bell, 2000). Orientation, size, and density of leaves determine their shading value to understorey species and, hence, the extent of cast shadows for a given Sun position. The degree of shading projected by leaves (and stems) can be used to indicate leaf volume as detailed in Section 5.1.2.

4.1.3 Texture

Leaf texture can significantly impact the way light interacts with foliage, and hence its appearance. The surface of a leaf can include a range of textural features, including hairs, spikes, coatings, patterns, and bumps, which modify light reflection properties (Esau, 1965). The flatness of a leaf also affects the way light will reflect and refract from its surface. The texture of the uppermost (adaxial) leaf surface often differs from that of the underside (abaxial). All these factors contribute to the intensity and wavelengths of light reflected by a leaf and also influence the radiation that is allowed to reach underlying vegetation (see Section 4.3).

The texture of a leaf also affects its function in terms of heat transfer, ultraviolet (UV) protection, photosynthetic efficiency, moisture loss, and susceptibility to both biotic and abiotic factors (see Section 1.1). Frost damage can be reduced by leaf coatings and hairs, while some predators can be discouraged by rough and prickly textures. While the propensity of a species towards a particular leaf texture is related to genetic traits, its manifestation in individual plants can be significantly varied by environmental factors (Roy *et al.*, 1999).

The cuticle layer on the epidermis protects the leaf from gaining or losing too much water and from invasion by a range of potential pathogens, such as fungi. This microcrystalline structure mostly comprises waterproof waxes (lipids), but also contains a much smaller proportion of polysaccharide compounds, such as cellulose and pectin, that attract water (hydrophilic). Microfibrils into the leaf selectively transport water and mineral salts between the leaf surface and internal tissues (Popp *et al.*, 2005), thus avoiding excessive leaching of plant metabolites in damp environments. This structure also allows the leaf to release volatile solutions to deter pests or attract insects. Natural leaf coatings can vary in thickness and appear shiny, glaucous, rough, or smooth. Various leaf coatings for crop protection are based on disguising or enhancing the natural leaf surface (Walters, 2006).

Hairs on plant leaves can vary in terms of number, density, width, length, colour, and orientation. Plants with leaf hairs are termed pubescent; those without are called glabrous. The presence of leaf hairs varies with plant species, location, and function. Pubescent leaves are generally less palatable to predators and less susceptible to frost damage. Most leaf hairs allow solar radiation to be transmitted through the cuticle layer to the photosynthetic cells. A dense covering of hairs, however, protects underlying cells from intense solar radiation, and thus effectively insulates

the leaf from burning (Karabourniotis *et al.*, 1995). By reducing leaf absorptance (the effectiveness with which it absorbs radiant energy), pubescence tends to lower both the leaf temperature (relative to ambient air temperature) and transpiration, which is advantageous in windy locations. Not surprisingly, pubescence is particularly common among leaves of desert and drought-tolerant plants (Ehleringer, 1984; Grammatikopoulous and Manetas, 1994). A negative correlation has been observed between leaf size and leaf hair density, with smaller leaves having a higher density of hair (Roy *et al.*, 1999). This relationship may result from cumulative stresses, such that both smaller leaf size and increased pubescence offer greater protection to the plant. The cost of this protection, however, is reduced absorption of light for photosynthesis (Ehleringer and Mooney, 1978).

Other potential leaf protuberances include spinose structures, such as thorns (modified stems), spines (modified leaves and stipules), and prickles (modified hairs). Spinosity deters herbivores and other predators. A range of leaf bumps or irregular thickenings can also result from interactions with pathogens. These features change the air flow around (see Section 4.4) and reflectance properties (see Section 4.3) of foliage and, in some instances, shade the leaf.

Another leaf variant that can impact texture is the scale and symmetry of internal patterns, largely resulting from venation (see Section 4.1.1). Variations in size, density, and topology of veins influence plant performance, ultimately favouring certain plants in particular environments (Sack and Scoffoni, 2013). Leaves with more complex outlines tend to have more primary veins and experience less shrinkage when dried, whereas simpler leaves tend to show more secondary veins and greater shrinkage potential (Holbrook and Zwieniecki, 2005). Venation also determines leaf flatness, which directly affects leaf reflectance and scattering properties.

4.1.4 Strength

Leaves endure various forms of mechanical stress, including gravity, rubbing, wind, rain, and predators (Niklas, 1992). Stronger leaves are more resistant to such stresses, which may reduce leaf loss and increase the leaf lifespan (Reich *et al.*, 1991). Leaves growing in shaded positions are typically less dense to allow better light transmission and absorption (see Section 4.1.1). Plants with an ample supply of nutrients generally grow larger, more nitrogen-rich leaves with a shorter lifespan, and more photosynthetic proteins (Evans, 1989).

The mechanical resistance of a leaf affects not only its lifespan but also its rate of decomposition, and its interactions with both the abiotic environment and potential consumers. Leaf fracture properties can be measured by shearing, punching, or tearing tests and expressed in terms of leaf lamina strength (the maximum force per unit area required to fracture the leaf), toughness (the work required to fracture the leaf), and stiffness (the resistance against deformation; Onoda, 2017). All leaf strength properties

have been observed to increase with the availability of light, such that leaves in full sun were more resistant to fracture than those growing in shaded positions. Sun leaves demonstrated greater Leaf Mass per Area (LMA), while shade leaves showed greater punch strength per leaf mass. Since cell walls provide most of the mechanical strength in leaves, containing 60% of the total leaf carbon, this characteristic of shade leaves is attributed to the more reinforced structure of their cell walls (Onoda *et al.*, 2008).

4.2 Chemical Composition

The chemical composition of foliage is determined by both environmental factors, such as soil fertility, and plant genetic traits. The foliar concentration of various biochemicals is directly related to essential biochemical processes in plants, including photosynthesis, respiration, evapotranspiration, and decomposition (Curran, 1989; Curran *et al.*, 2001; see Section 5.2). Foliar chemistry is particularly relevant to herbivore survival, with variations in forage quality directly impacting the distribution, diversity, and abundance of animal species. Plant chemical composition can thus be indicative of soil nutrient availability, habitat quality, and ecosystem processes (Youngtob *et al.*, 2012).

Analytical techniques such as atomic absorption spectrophotometry or chromatography can be used to identify and quantify the chemical components in foliage. While the specific chemical composition of plants varies between species and locations, the major constituent by weight in green leaves is water (Weisz and Fuller, 1962). Below we further discuss the chemical composition of leaves in terms of their most significant components:

- water—the heaviest component in green foliage (see Section 4.2.1);
- inorganic components—minerals (see Section 4.2.2); and
- organic components (see Section 4.2.3):
 - ◆ carbohydrates—energy storage and structural elements ;
 - ◆ lipids—waterproofing and structure;
 - ◆ proteins and nucleoproteins—structure and genetic codes; and
 - ◆ pigments—colour.

4.2.1 Water

Water is the major constituent of plant tissue, comprising over 75% of most green foliage and governing most plant processes (Weisz and Fuller, 1962). The internal moisture content of leaves varies enormously both between and within species with variations in ambient climatic and edaphic factors, especially water availability, and significant variations in leaf moisture content can occur during diurnal, seasonal, and phenological cycles. Water also acts as a solvent to transfer gases, minerals, and other solutes between plant cells and organs, as a reactant in photosynthesis, and as a substrate in hydrolytic processes. It maintains the turgor of living plants, controls cell growth and stomatal opening, and directly supports the form of herbaceous plants. As water content decreases, leaves wilt—they reduce photosynthesis rates, close stomata, and stop cell enlargement—until a critical threshold is reached when cells begin to die (Kramer and Boyer, 1995).

Leaf moisture content is indicative of plant stress, productivity, and evapotranspiration, as well as the availability of moisture in the soil and atmosphere. As such, leaf water content has been used as an indicator for scheduling irrigation and assessing the risk of drought and fire (Peñuelas *et al.*, 1993, 1996; see Sections 13 and 18). Plants adapt to water stress by either using water more efficiently or reducing water loss (Dudley, 1996). Both these adaptations can be achieved by reducing leaf size, as smaller leaves typically have fewer stomata and higher hair density (see Section 4.1.3). Water stress is increased in saline environments since the presence of salt reduces water potential in the plant root zone, resulting in loss of turgidity in plant tissue (Pasternak, 1987).

... many biochemical processes, such as photosynthesis, respiration, evapotranspiration and decomposition are related to the foliar concentration of biochemicals such as chlorophyll, water, nitrogen, lignin and cellulose. (Curran, 2001).

Water does not occur in its pure form in plants, but as a solution, which modifies some of its basic properties (Salisbury and Ross, 1969). It moves within plants primarily via osmosis, that is, diffusion through a permeable membrane (such as a cell wall) from a less concentrated (hypotonic) to a more concentrated (hypertonic) solution. Since this movement represents a form of energy, solutions can be viewed in terms of their osmotic potential. It is a characteristic of water that it moves to achieve equilibrium across a permeable membrane such that the water potentials on both sides are equivalent (isotonic). By contrast, osmotic pressure is the pressure required on a solution to stop water diffusing across a semi-permeable membrane, that is, to act against osmosis (Kramer and Boyer, 1995).

The concentration of fluids determines their chemical potential—the force they can exert. In plants, the cell water potential derives from the cumulative potentials of solutes, porous solids, pressure, and gravity. As a cell dehydrates, its contents become more concentrated and its water volume decreases, so its cell water potential decreases—it is less likely to force water out of the cell. The extent of cell shrinkage during dehydration, however, is also determined by the cell wall elasticity, with greater changes in cell water potential being observed in cells with more rigid walls. Leaf water potential is correlated with its net CO₂ assimilation rate and stomatal conductance to water vapour. Plant and soil water potentials are expected to be in equilibrium before dawn for non-transpiring plants, enabling plant water potential at that time to be used as a surrogate for soil water availability (Ehlers and Goss, 2003).

A leaf begins to lose moisture when it is removed from a plant, resulting in reduced turgidity in cells and generalised shrinking. Leaves with high initial water content are more likely to shrink in storage than those with low water content. Complex leaves generally have more structural support against shrinkage than simple leaves. Leaf cell structure determines the impact of water loss on leaf appearance, with those plants containing elastic cell walls withstanding up to 40% of water loss before contracting, while those with inelastic cell walls wilting after losing only 1–3% (Weatherley, 1965). Most crop species wilt when leaf water content is around 60–70%. This is an important consideration for leaf sample collection and measurement during field work (Juneau and Tarasoff, 2012; TERN Australia, 2018).

The water status of a plant can be described in terms of physical characteristics, such as its chemical potential within the plant cells, or in terms of its water content, that is, the proportion of water relative to plant tissue. Both approaches require destructive sampling of individual leaves. Since chemical potential and pressure are related, a thermocouple psychrometer, which detects vapour pressure, can be used to measure cell water potential in leaves. Other methods for measuring water potential involve using a pressure chamber (which determines the tension on water in the xylem) and a pressure probe (which quantifies the turgor pressure of single cells; Boyer, 1995). Water potential is directly related to the energy status of plant water but does not account for osmotic adjustment, which conserves cell moisture in drought conditions. Accordingly measures of water content are considered more appropriate in this context.

Water content is expressed either as a mass or a volume. Both are determined by drying a leaf sample and comparing the dried and fresh quantities. This approach underlies a number of EO-based indices, including Water Content (WC), Live Foliar Moisture Content (LFMC), Relative Water Content (RWC), and Equivalent Water Thickness (EWT; see Sections 8.1.5 and 9.5). WC (also called Gravimetric Water Content, GWC) actually determines the ratio of leaf water to leaf dry weight, where leaf water is computed as the difference between fresh and dry weights:

$$WC = \frac{FW - DW}{DW}$$

where

FW is fresh leaf weight (g); and
DW is oven dried leaf weight (g).

Live Foliar Moisture Content (LFMC) computes the same ratio as a percentage. A similar measure is succulence, which compares the water mass with leaf area:

$$\text{Succulence} = \frac{FW - DW}{\text{area}}$$

A related metric is the Leaf Dry Matter Content (LDMC, in mg/g):

$$\text{LDMC} = \frac{DW}{FW}$$

LDMC is currently in favour as a PFT to differentiate plants on the basis of their ecological behaviour. LDMC and SLA (specific leaf area, see Section 4.1.2) together represent the balance achieved by plants between rapid biomass production and efficient nutrient management (Garnier *et al.*, 2001).

RWC or ‘relative turgidity’ (Barr and Weatherley, 1962) compares the difference between the water mass of a sample leaf with its fully hydrated water content:

$$\text{RWC} = \frac{\text{FW} - \text{DW}}{\text{TW} - \text{DW}}$$

RWC is a preferred measure of leaf water content as it is invariant within a leaf and changes in proportion to leaf turgor. EWT represents the volume of water per unit area of leaf (g/cm^2). This measure has been most closely approximated by analysis of spectral properties of leaves in the short wave infrared (SWIR) and near infrared (NIR) wavelengths (see Section 4.3).

Various studies have observed differences in both the leaf water content and leaf dry matter content (LDMC) of species that are enabled with strategies to regenerate after fire (Trabaud, 1987, 1991; Keeley, 1995). Common fire survival strategies include the capacity to resprout from adventitious shoots (resprouters) and/or produce abundant fire-hardy seed (seeders). Resprouting species were found to have consistently higher measurements of LDMC throughout the year compared with seeders, while seeders were observed to be more drought tolerant (Saura-Mas and Lloret, 2007).

Leaf wetness is a measure of meteorological precipitation (water from clouds) and dew (water from condensation near the ground) on the leaf surface. It is difficult to quantify directly, but a number of sensors rely on measuring the dielectric constant of the adaxial surface (Magarey *et al.*, 2005). Leaf wetness is also estimated by artificial leaf surface sensors, which electronically log the moisture that accumulates on a prepared surface. In conjunction with air temperature, leaf wetness duration (LWD) is important for control of fungal diseases in agriculture (Yarwood, 1978; Huber and Gillespie, 1992; Rowlandson *et al.*, 2015).

The water status of foliage is not only indicative of the physiological status and productivity of a plant, but at a landscape scale it is also informative for assessing drought conditions, scheduling irrigation, and rating fire risk. Net Primary Productivity (NPP; above ground) correlates directly with actual evapotranspiration (AET) for a range of biomes (see Section 7.6), with both estimates being indicative of the availability of water and solar energy (Rosenzweig, 1968).

While it is possible to scale up from leaf porometer measurements to canopy estimates of water content, most studies have found this approach to be problematic (Jarvis, 1985; Rollin and Milton, 1998). Leaf optical properties contribute to canopy reflectance, but so too do structural characteristics, background strata and viewing configuration factors (Jacquemoud and Ustin, 2003). EO-based techniques for mapping and monitoring water content of vegetation are further discussed in Sections 8 and 9.

4.2.2 Inorganic components

Mineral solids generally comprise 1–2% of living foliage (Weisz and Fuller, 1962). Most plant minerals exist in solution, but some can also occur as crystals. Minerals can occur freely or as part of organic compounds. For an individual species, low foliar nutrient content generally indicates low site mineral availability.

Terrestrial vegetation requires a range of inorganic minerals, which are absorbed from the growing medium. At least 14 minerals are considered essential for plant nutrition: six macronutrients (nitrogen, phosphorus, potassium, calcium, magnesium, and sulphur), which are required in large amounts, and eight micronutrients (chlorine, boron, iron, manganese, copper, zinc, nickel, and molybdenum). These and other minerals, when present in high concentrations in the growing medium, can be toxic to plant growth, including sodium, chlorine, boron, iron, manganese, and aluminium (White and Brown, 2010).

The most limiting nutrient for growing crops in many agricultural areas is nitrogen. This mineral is important for herbivores but exists in relatively low concentrations in some genera such as *Eucalyptus*. Nitrogen Use Efficiency (NUE) indicates the efficiency of nitrogen usage by plants for food production (see Section 5.3.5).

All mineral nutrients and trace elements—both essential and non-essential—detected in an organism define its ‘ionome’ (Salt *et al.*, 2008). Since the leaf ionome indicates the interactions between the plant and its environment, especially soil composition, ionic characteristics are being analysed to understand phenotypic variation within species (Stein *et al.*, 2017).

4.2.3 Organic components

With the exception of compounds from mineral origins, such as CO₂ and carbonic acid, compounds containing carbon are collectively considered as organic. Some organic components support plant structure while others are dissolved or suspended in water in plant cells. The actual proportions of different organic compounds vary between species and locations. The major categories of organic compounds that occur in foliage with relevance to EO studies are carbohydrates, proteins, fats, and pigments:

- Carbohydrates account for around 20% of the mass of living plants (Weisz and Fuller, 1962) or 50–80% of the total dry weight of most plants (Salisbury and Ross, 1969). These compounds occur as sugars, polysaccharides, and the more complex configurations of the elements carbon, hydrogen, and oxygen. A simple sugar molecule is based on a 6-carbon structure resulting from photosynthesis. Two of these sugars can combine into a double sugar (12-carbon or disaccharide), and multiple sugars can combine to form a polysaccharide, such as cellulose, glycogen, or starch. The carbohydrates primarily function as energy reserves but also contribute to the structure of organelles. Structural carbohydrate derivatives include pectin, lignin, hemicellulose, and chitin. Cellulose and lignin, the most abundant renewable carbon resources on Earth, work together to strengthen cell walls and water transportation networks in vascular plants, thereby providing mechanical support for stems and leaves.
- Proteins are formed from long chains of amino acids. They occur in greater variety than any other organic components (with every type of living organism developing a different, and characteristic, type of protein) but only comprise a small proportion of living plant matter by weight (< 2%; Weisz and Fuller, 1962). Protein chains can be broken (denatured) by heat, pressure, electricity, and radiation. They provide the main structural material in plants, supply enzymes in cells, and help to form other organic compounds such as nucleoproteins that are built from nucleic acid and proteins. The two major nucleic acids are ribose nucleic acid (RNA) and deoxyribose nucleic acid (DNA). RNA exists throughout cells while DNA only occurs within the cell nucleus as a structural component of genes.
- Lipids include fats, fatty acids, glycerine, waxes, and sterols that do not dissolve in water. These compounds are formed from varying combinations and configurations of the elements of carbon, hydrogen, and oxygen and are generally insoluble in water. They form the framework for cell membranes and release energy when decomposed. Fat derivatives, such as cutin, act as a waterproofing agent in the leaf cuticle and are believed to reduce transpiration (see Section 4.1). Lipids occur in small quantities (< 2% of dry weight) in plant leaves, stems and roots (Salisbury and Ross, 1969).
- Pigments are molecules that absorb light, and the colour of a leaf is determined by its pigment composition. These compounds selectively absorb some wavelengths of electromagnetic radiation (EMR) and reflect others, such that those wavelengths that are reflected determine the apparent colour of a pigment (see Volume 1B—Section 6). While chlorophyll a is the primary photosynthetic pigment in all photosynthetic plants, most organisms contain multiple pigments to absorb energy across a wider range of wavelengths (see Excursus 4.1). This is particularly important to vegetation that does not have direct access to sunlight, such as understory or submersed plants. The precise pigment composition within an individual leaf results from its generic heritage, its age, and its vigour, as well as its location with respect to intercepting direct sunlight. The latter will be impacted by latitude and aspect for all plants, and either horizontal layering for terrestrial plants or depth below water surface for aquatic plants.

Excursus 4.1—Plant Pigments

Further information: Salisbury and Ross (1969), Croft and Chen (2017)

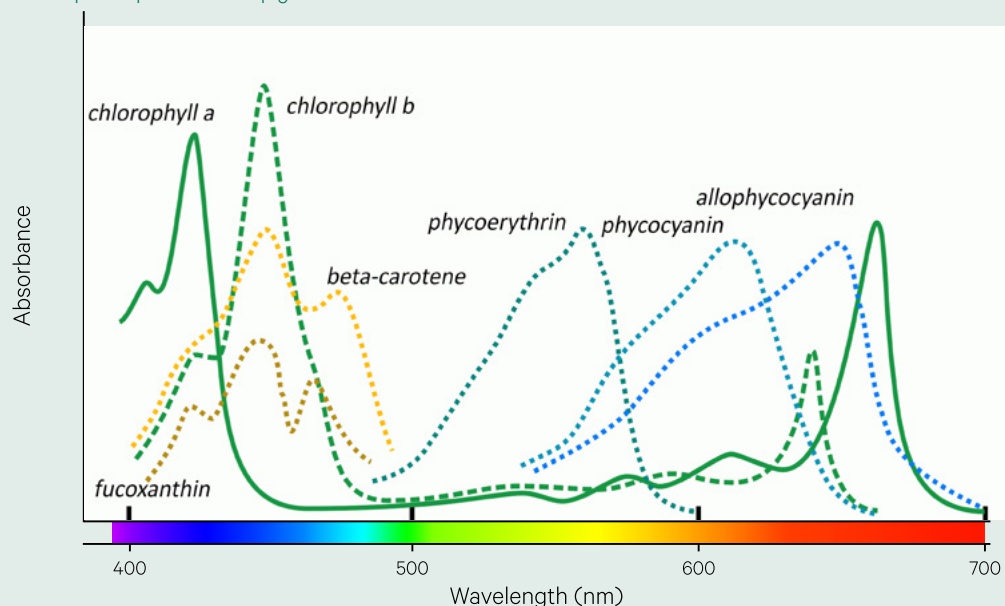
The EMR wavelengths that are absorbed by some major leaf pigments are illustrated in Figure 4.2. The precise absorption characteristics of pigments can be determined by various biochemical and photochemical analyses (Lichtenthaler, 1987; Lichtenthaler and Buschmann, 2001; Croft and Chen, 2017). Leaf absorption characteristics can also be approximated by field instruments, such as spectrophotometers, and by hyperspectral remote sensing (Curran, 1989; Blackburn, 2007). Relevant characteristics of photosynthetic pigments are listed in Table 4.1. These pigments are contained in plastids, the major organelles in plants and algae. In addition, non-photosynthetic plant pigments occur in the cell vacuole (see Figure 4.1), or sap.

Chlorophyll pigments are produced by chloroplasts (green plastids; see Figure 4.1) and are responsible for photosynthesis. They absorb blue and red light and reflect green wavelengths, so appear green. Chlorophyll molecules are large, stable, nutrient-rich, and repel water. All forms of chlorophyll have the same basic molecular structure based on a chlorin (tetrapyrrole) ring with a central magnesium ion (Croft and Chen, 2017). Being the primary pigment

for photosynthesis, chlorophyll a is the most abundant, with 2.5 to 4.0 times more chlorophyll a than chlorophyll b in photosynthetic plants. The other forms of chlorophyll are accessory pigments which collaborate with chlorophyll a by capturing a wider range of wavelengths. Chlorophyll c, chlorophyll d, and chlorophyll e only occur in aquatic algae and chlorophyll d primarily exists in organisms living in deeper waters. Photosynthetic bacteria contain a modified form of chlorophyll known as bacteriochlorophylls, which exists as a range of compounds (see Volume 3B).

Phycobilins are attached to water-soluble proteins (phycobiliproteins) and absorb a wider range of wavelengths than chlorophyll. This is particularly useful for organisms growing in water. These molecules comprise a chain of pyrrole rings. Phycoerythrin is the main phycobilin in red algae which can photosynthesise using dim blue-green light, and the proportion of this phycobilin relative to chlorophyll increases with water depth. Blue-green algae that grows in surface waters, and some terrestrial algae, contain a greater proportion of Phycocyanin.

Figure 4.2 Absorption spectra of leaf pigments



Adapted from: Goodwin and Mercer (1990) by Qiaoyun Xie, University of Technology Sydney. (Original retrieved from http://biologywiki.apps01.yorku.ca/index.php?title=File:Pigment_spectra.png)

Carotenoids are long molecules created in chromoplasts (pigmented plastids). They mostly absorb blue wavelengths, so generally appear as yellow-orange colours in petals, fruits, and leaves. These carbon-based compounds do not dissolve in water. While carotenoids help to capture a greater range of solar wavelengths than chlorophyll, they are considered to be accessory pigments for photosynthesis since this energy needs to be transferred to chlorophyll for photosynthesis to occur. Carotenes are hydrocarbons, with the three common forms being stereoisomers of the same molecular formula. Xanthophylls (or carotenols) also contain oxygen as a hydroxyl, carbonyl, or carboxyl group.

Anthocyanins are a type of water-soluble flavonoid that vary in colour from red to purple and blue depending on pH. They absorb blue-green wavelengths and are predominantly found in petals and fruit, where they attract pollinators, but are also responsible for red juvenile and autumn leaves. Red anthocyanins are believed to offer pharmacological benefit as antioxidants. The production of anthocyanins uses carbohydrate reserves in a plant. They are produced in the leaf as it dies, possibly as

a defence against pests which would be attracted to the declining chlorophyll levels, or to enable efficient resorption of foliar nutrients (see Section 5.3.3). This group of pigments also act as a natural sunscreen for plants by trapping excessive solar radiation, with production increasing in response to ultraviolet (UV) light, and provide photostability during leaf expansion (Close and Beadle, 2003; Liakopoulos *et al.*, 2006). Another group of vacuole pigments (see Figure 4.1) includes tannins, which occur in leaf, bud, seed, root, and stem tissues. Tannins are water soluble and coloured brown. When leached from nearby vegetation (such as eucalypts), they contribute to the dark water colour of many inland waterbodies in Australia. Tannins are astringent to taste and play a defensive role against plant predators.

Higher concentrations of chlorophyll a generally mask the presence of other pigments in leaves. As light levels fall with the approach of winter, the volume of chlorophyll a decreases in deciduous plants, allowing other pigments to become more visible. A similar process occurs as plants senesce. The precise colours of autumn leaves depend on the pigment composition in the leaves of different plant species.

Table 4.1 Photosynthetic pigments

Absorption peaks (in nm) are approximate values only.

Pigment Group	Pigment	Colour/spectral region	Characteristic Absorption Peaks	Occurrence
Chlorophyll	Chlorophyll a	Blue-green	435, 675	All photosynthetic organisms except bacteria
	Chlorophyll b	Yellow-green	480, 650	All green plants, green algae and some prokaryotes
	Chlorophyll c	Golden-brown	~645	Chromista, dinoflagellates, brown algae
	Chlorophyll d	Far red	~740	Red algae, blue-green algae
	Chlorophyll e	Golden-yellow	415, 654	Golden-yellow algae
Bacterioviridin	Chlorobium chlorophyll	Far red	750/770	Green bacteria
Bacteriochlorophyll	Bacteriochlorophyll a	Far red, NIR	800, 850, 890	Purple and green bacteria
	Bacteriochlorophyll b	NIR	1,017	<i>Rhodospseudomonas</i> (purple bacteria)
Phycobilin	Allophycocyanin	Blue-red	654	Red algae, blue-green algae,
	Phycocerythrin	Red	490, 546, 576	
	Phycocyanin	Blue-green	618	
	Phycourobilin	Orange	~495	
Carotene	α -carotene	Yellow-orange	420, 440, 470	Green leaves and some bacteria and fungi
	β -carotene	Yellow-orange	425, 450, 480	Main carotene in most plants
	γ -carotene	Brown	440, 460, 495	Green sulphur bacteria; some amounts in other plants
Xanthophyll	Luteol	Pale yellow	425, 445, 475	Green leaves, green algae and red algae
	Violaxanthol	Brown	425, 450, 475	Main carotenol in green leaves, green algae and red algae
	Fucoxanthol	Brown	425, 450, 475	Brown algae, diatoms
	Spirilloxanthol		464, 490, 524	Purple bacteria

Sources: Rabinowitch and Govindjee (1969) and Lichtenthaler and Buschmann (2001)

4.3 Spectral Properties

Electromagnetic radiation (EMR), originating from the Sun or an artificial light source, is either absorbed, reflected, or transmitted by foliage, where

$$\begin{aligned} \text{incident energy} &= \text{reflected energy} \\ &+ \text{transmitted energy} + \text{absorbed energy} \end{aligned}$$

For convenience, names are assigned to the various regions of the electromagnetic spectrum, but there are no precise divisions between these regions—they are generally defined by the sensing method by which they are detected (see Volume 1A—Section 5). Commonly accepted ranges for the EMR spectral regions that are most relevant to EO are:

- visible: 0.38–0.7 μm (380–700 nm);
- infrared (IR): 0.7–1,000 μm ;
- microwave: > 1 mm–1 m.

Infrared wavelengths are often sub-divided into the regions:

- near infrared (NIR): 0.7–1.3 μm ;
- short wave infrared (SWIR): 1.3–3 μm ;
- middle infrared (MIR) or mid-wavelength (or medium wave) infrared (MWIR): 3–8 μm ;
- thermal infrared (TIR) or long wavelength infrared (LWIR): 8–15 μm ; and
- far infrared (FIR): 15–1,000 μm .

Reflectance of an object is defined as the proportion of incident energy it reflects:

$$\text{reflectance} = \frac{\text{reflected energy}}{\text{incident energy}}$$

with similar definitions for transmittance and absorptance, so that:

$$\text{reflectance} + \text{transmittance} + \text{absorptance} = 1$$

A typical reflectance curve for green vegetation is shown in Figure 4.3a. Absorption of visible and NIR wavelengths of EMR results from energy transfer to molecules, atoms, or electrons whereas SWIR and TIR wavelengths produce molecular vibrations in leaves, largely due to the presence of water (see Volume 1). However, the precise interaction for an individual leaf with a radiation source will depend on the wavelength(s) of radiation and the physical structure (morphology) and chemical composition of the leaf, as well as its orientation and surface features. Accordingly, reflectance spectra can vary for different species in a genus (see Figure 4.3b) and different leaves on the one plant.

UV to visible wavelengths excite electrons and determine the apparent colour of foliage, that is, those wavelengths that it reflects rather than absorbs. Chlorophyll molecules, for example, absorb blue

and red wavelengths and reflect green, resulting in the characteristic colour of vegetation, while other photosynthetic pigments absorb different wavelengths. In terrestrial vegetation, the range of wavelengths that can be absorbed for photosynthesis approximately spans from 400–700 nm and is called Photosynthetically Active Radiation (PAR). The major groups of pigments associated with photosynthesis can be grouped in terms of their chemical structure:

- Tetrapyrrols:
 - ◆ Chlorophylls—enable photosynthesis in plants and algae;
 - ◆ Bacteriochlorophylls—enable photosynthesis in bacteria;
 - ◆ Phycobilins—accessory pigment for photosynthesis in aquatic algae; and
- Carotenoids—carotenes and xanthophylls—accessory pigment for photosynthesis in plants, algae, and bacteria (see Excursus 4.1).

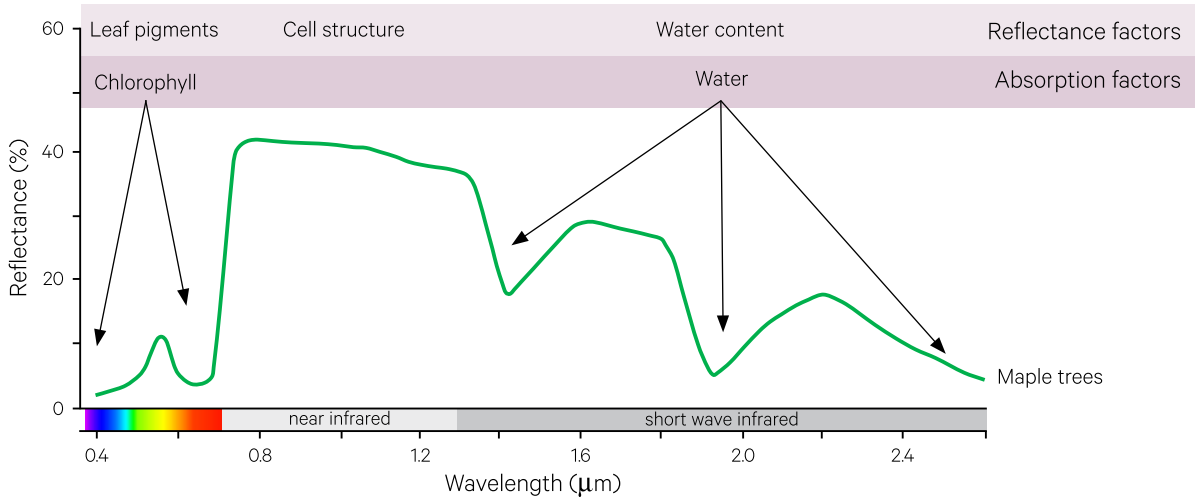
While leaf optical properties have been researched for well over a century, there are still a number of unknowns. We know that reflectance and transmittance characteristics result from both the concentration of compounds that absorb light and the internal scattering of the light that is not absorbed. A healthy leaf absorbs:

- violet and blue wavelengths—due to the presence of chlorophyll, carotenoid, and xanthophyll pigments;
- red wavelengths—due to the presence of chlorophyll pigment(s); and
- SWIR—due to the presence of water with characteristic absorption peaks near 1450 nm and 1900 nm (see Figure 4.3).

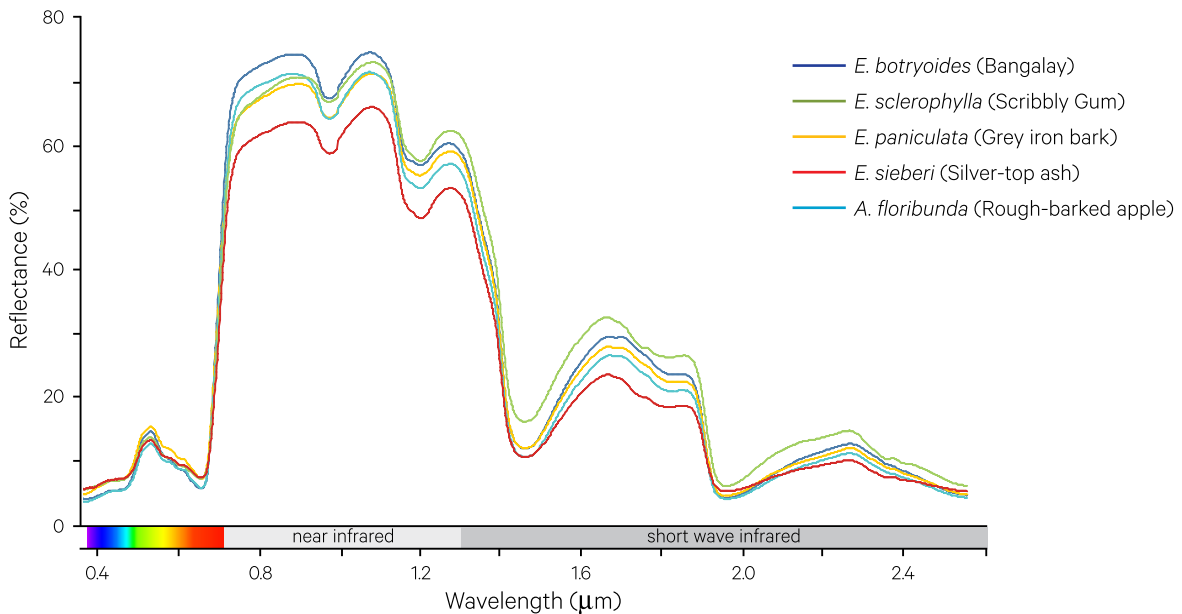
These characteristics produce reflectance peaks for those wavelengths that are not absorbed, namely green and NIR, with two ‘bumps’ in SWIR wavelengths that are not absorbed by water, and reflectance troughs for those wavelengths that are absorbed (namely blue, red, and SWIR wavelengths). The NIR reflectance plateau (700–1100 nm) results from structural biochemicals and multiple scattering from structures and air spaces within the leaf (see Figure 4.1). Water absorption in the SWIR region produces primary reflectance dips at 1450 nm, 1940 nm, and 2500 nm, and secondary dips at 980 nm and 1240 nm (Carter, 1991). In addition, various aspects of the physical morphology of leaves will impact reflectance properties (see Section 4.1.2). In particular, the leaf surface shape, size, orientation, and texture all affect the way it intercepts and reflects light.

Figure 4.3 Reflectance of green foliage

a. Reflectance properties of green vegetation primarily derive from leaf pigments in visible wavelengths, cell structure in NIR wavelengths and water content in SWIR wavelengths. Characteristic absorption features occur in visible wavelengths (due to chlorophyll) and SWIR wavelengths (due to water content).



b. Reflectance spectra varies for different species. Below is shown the mean reflectance spectra for four species of *Eucalyptus* and one species of *Angophora*.



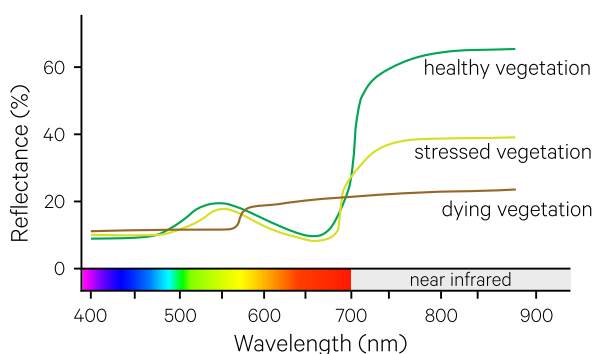
Source: a. Based on Harrison and Jupp (1989) Figure 30; b. Laurie Chisholm, University of Wollongong

Spectral properties of leaves are also known to vary with various forms of plant stress, including dehydration, flooding, freezing, herbicides, competition, disease, predators, and deficiencies. As foliage dries, the spectral absorption features in SWIR and TIR wavelengths are less dominated by water and those resulting from its biochemical components become more evident. Stressed plants

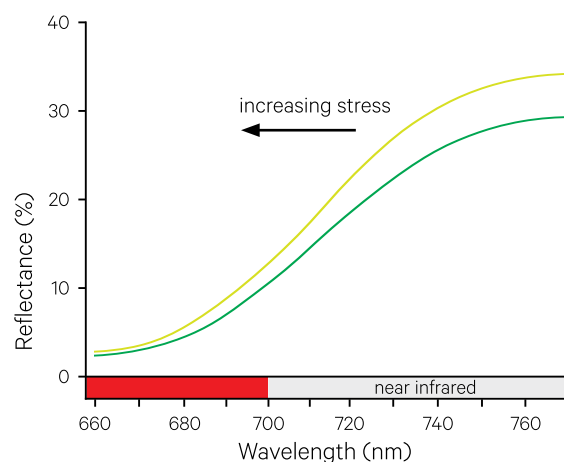
have increased transmittance and decreased absorbance of wavelengths near 700 nm, resulting from changes in leaf chlorophyll concentration (Carter and Knapp, 2001). As the chlorophyll concentration reduces in a leaf, either from abscission or stress, the leaf colour also changes (Jacquemoud and Ustin, 2014; see Section 5.3.3).

Figure 4.4 Leaf reflectance changes with stress

a. In the initial stages of disease, NIR reflectance is reduced. As disease progresses, NIR reflectance continues to decrease and the colour of foliage changes markedly.



b. Increasing plant stress shifts the 'red edge' towards shorter wavelengths



Adapted from: a. Barrett and Curtis (1976) Figure 15.1b; b. Cho *et al.* (2012)

The onset of stress, senescence, or disease in plants reduces reflectance in both green and NIR wavelengths and shifts the transition between red absorption and NIR reflectance (see Figure 4.4a). In green leaves, the transition from low red reflectance to high NIR reflectance corresponding to the spectral range 680–780 nm is referred to as the 'red edge'. Changes in vegetation vigour affect the precise position and slope of the red edge (see Figure 4.4b).

Many spectral indices developed for EO datasets focus on changes in these spectral regions (see Section 8.1) and are used to determine the chlorophyll content of foliage (Croft and Chen, 2017). Physical and mathematical models that simulate the spectral consequences of variations in leaf biochemical and physical composition are introduced in Sections 9 and 10.

4.4 Boundary layer

A boundary layer results from aerodynamic forces between a fluid and an object. This can occur when either an object moves through a fluid or a fluid moves past an object. The speed and shape of the object together with the mass, viscosity, and compressibility of the fluid determine the magnitude of the aerodynamic forces. The net effect of these forces is a layer at the boundary of the fluid that is most strongly affected by its viscosity, that is the resistance of the fluid to its flow. Boundary layers occur on the surfaces of many moving vehicles and in the transition zone between fluid layers. Some commonplace examples of boundary layers include the air zone around aerofoils, such as aircraft wings, the water zone around aerofoils, such as ship hulls, and the interface between the Earth and its atmosphere. They also surround leaf surfaces and can impact essential physiological processes.

Within the boundary layer, the velocity of the fluid is reduced as some of the fluid attaches to the surface of the object, creating shearing stresses within the fluid. Movement within the boundary layer can be either laminar (flowing in layers), or turbulent (mixing

across layers), or a transition between the two. Mixing across layers involves non-laminar currents called eddies. These typically create swirling movement within fluids, and often result from diversion around some obstacle. Eddies occur at various scales between and within fluid layers in the ocean and in the atmosphere (see Volume 3B).

Between a fluid and an object's surface, turbulence can result from surface roughness, uneven fluid flow, and/or increased distance from the object's leading edge. In fluid dynamics, the degree of turbulence is quantified by the dimensionless Reynolds Number (RN):

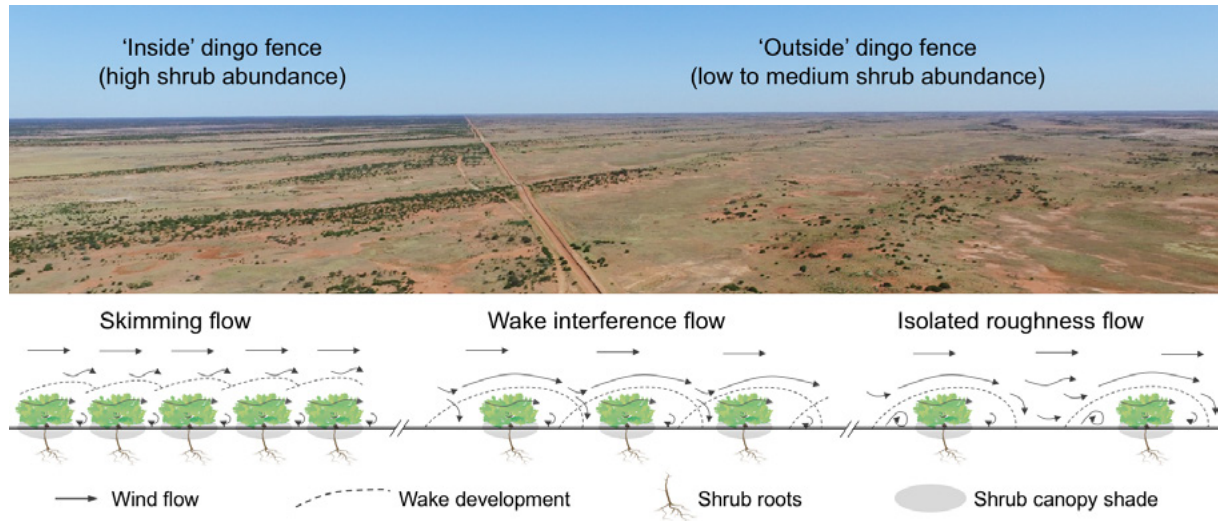
$$RN = \frac{\text{density} \times \text{velocity} \times \text{diameter}}{\text{viscosity}}$$

where

RN < 100,000 indicates laminar flow;
 RN > 1,000,000 indicate turbulent flow; and
 100,000 < RN < 1,000,000 indicates a transition between laminar and turbulent flow.

Figure 4.5 Impact of vegetation density on wind flow

This aerial photograph of the dingo-proof fence in the Strzelecki Desert, Australia, shows increased woody shrub density where dingoes have been removed. The diagram below demonstrates predicted wind flow regimes—'isolated roughness' and 'wake interference' at low to medium shrub density; 'skimming flow' at high shrub density—and increased root structure and canopy shade at high shrub density.



Source: Lyons *et al.* (2018)

A boundary layer surrounds any leaf surface, providing a thin interface of relatively stationary air between the leaf and the atmosphere. Within the boundary layer, turbulence is effectively reduced by friction and the thickness of this layer is modified by a number of factors, including:

- leaf texture—dense hairs effectively create a windbreak, which increases the thickness of the boundary layer and reduces transpiration rates, while sparse hairs may increase turbulence (Jones, 1992);
- stomatal structure—recessed stomata increase the boundary layer thickness;
- leaf size—the boundary layer increases with leaf size and distance from the leading edge of the leaf (Grace and Wilson, 1976) and with variations in leaf shape that effectively reduce leaf size (for example leaf lobes and serration also reduce the thickness of the boundary layer; Schuepp, 1993); and
- atmospheric turbulence—wind will reduce the thickness of the boundary layer.

The boundary layer between leaves and the atmosphere directly impacts the rate of plant water loss via transpiration (see Section 5.2.3) and the transfer of heat into the atmosphere (see Section 5.2.4). The density of foliage and plants also impacts wind flow regimes (see Figure 4.5). This effect is particularly relevant in dryland regions with patchy vegetation, where higher plant densities reduce wind erosion and sediment transport (Mayaud *et al.*, 2016) and encourage more stable dune formations (Lyons *et al.*, 2018).

4.5 Further Information

Physiology

Taiz *et al.* (2015): www.plantphys.net

Pigments

Light and photosynthetic pigments: <https://www.khanacademy.org/science/biology/photosynthesis-in-plants/the-light-dependent-reactions-of-photosynthesis/a/light-and-photosynthetic-pigments>

4.6 References

- Ackerly, D.D., Knight, C.A., Weiss, S.B., Barton, K., and Starmer, K.P. (2002). Leaf size, specific leaf area and microhabitat distribution of chaparral woody plants: contrasting patterns in species level and community level analyses. *Oecologia*, 130(3), 449–457.
- Barr, H.D., and Weatherley, P.E. (1962). A re-examination of the relative turgidity technique for estimating water deficit in leaves. *Australian Journal of Biological Science*, 15, 413–428.
- Barrett, E.C., and Curtis, L.F. (1976). *Introduction to Environmental Remote Sensing*. Chapman and Hall, London.
- Blackburn, G.A. (2007). Hyperspectral remote sensing of plant pigments. *Journal of Experimental Botany*, 58(4), 855–867.
- Boyer, J.S. (1995). *Measuring the Water Status of Plants and Soils*. Academic Press, San Diego. <http://udspace.udel.edu/handle/19716/2828>
- Carter, G.A. (1991). Primary and secondary effects of water content on the spectral reflectance of leaves. *American Journal of Botany*, 78(7), 916–924.
- Carter, G.A., and Knapp, A.K. (2001). Leaf optical properties in higher plants: linking spectral characteristics to stress and chlorophyll concentration. *American Journal of Botany*, 88(4), 677–684.
- Cho, M.A., Debba, P., Mutanga, O., Dudeni-Tlhone, N., Magadla, T., and Khuluse, S.A. (2012). Potential utility of the spectral red-edge region of SumbandilaSat imagery for assessing indigenous forest structure and health. *International Journal of Applied Earth Observation and Geoinformation*, 16, 85–93. doi:<http://dx.doi.org/10.1016/j.jag.2011.12.005>
- Close, D.C., and Beadle, C.L. (2003). The ecophysiology of foliar anthocyanin. *The Botanical Review*, 69, 149–161.
- Cornelissen, J.H.C., Lavorel, S., Garnier, E., Díaz, S., Buchmann, N., Gurrich, D.E., Reich, P.B., ter Steege, H., Morgan, H.D., van der Heijden, M.G.A., Pausas, J.G., and Poorter, H. (2003). A handbook of protocols for standardised and easy measurement of plant functional traits worldwide. *Australian Journal of Botany*, 51, 335–380.
- Croft, H., and Chen, J.M. (2017). Leaf Pigment Content. In *Comprehensive Remote Sensing Volume 3, Reference Module in Earth Systems and Environmental Sciences* (Ed: Liang, S.). Elsevier. pp 117–142. <https://doi.org/10.1016/B978-0-12-409548-9.10547-0>
- Curran, P.J. (1989). Remote sensing of foliar chemistry. *Remote Sensing of Environment*, 29, 271–278.
- Curran, P. (2001). Imaging spectroscopy for ecological applications. *International Journal of Applied Earth Observation and Geoinformation*, 3(4), 305–312.
- Curran, P.J., Dungan, J.L., and Peterson, D.L. (2001). Estimating the bio-chemical concentration of leaves with reflectance spectrometry: testing the Kokaly and Clark methodologies. *Remote Sensing of Environment*, 76, 349–359.
- Dudley, S.A. (1996). Differing selection on plant physiological traits in response to environmental water availability: a test of adaptive hypotheses. *Evolution*, 50, 92–102.
- Edwards, E.J. (2019). Evolutionary trajectories, accessibility and other metaphors: the case of C4 and CAM photosynthesis. *New Phytologist*, 223(4), 1742–1755. <https://doi.org/10.1111/nph.15851>
- Ehleringer, J. (1984). Ecology and ecophysiology of leaf pubescence in North American desert plants. In: *Biology and Chemistry of Plant Trichomes* (Eds: E. Rodrigues, P.L. Healey and I. Mehta) pp 113–132. Plenum, New York.
- Ehleringer, J.R., and Mooney, H.A. (1978). Leaf Hairs: Effects on Physiological Activity and Adaptive Value to a Desert Shrub. *Oecologia*, 37, 183–200.
- Ehlers, W., and Goss, M.J. (2003). *Water Dynamics in Plant Production*. CABI Publishing, Oxon. ISBN 0-85199-694-9
- Esau, K. (1965). *Plant Anatomy*. 2nd edn. John Wiley and Sons, New York.
- Evans, J.R. (1989). Photosynthesis and nitrogen relationships in leaves of C₃ plants. *Oecologia*, 78, 9–19.
- Evans, J.R., and Vogelmann, T.C. (2006). Photosynthesis within isobilateral *Eucalyptus pauciflora* leaves. *New Phytology*, 171(4), 771–782. doi:[10.1111/j.1469-8137.2006.01789.x](https://doi.org/10.1111/j.1469-8137.2006.01789.x)

- Garnier, E., Shipley, B., Roumet, C., and Laurent, G. (2001). A standardized protocol for the determination of specific leaf area and leaf dry matter content. *Functional Ecology*, 15, 688–695.
- Gates, D.M. (1980). *Biophysical Ecology*. Springer-Verlag, New York.
- Givnish, T.J. (1979). On the adaptive significance of leaf form. In: *Topics in Plant Population Biology* (Eds: O.T. Solbrig, S. Jain, G.B. Johnson, and P.H. Raven) pp. 375–407. Columbia University Press, New York.
- Goodwin, T.W., and Mercer, E.I. (1990). *Introduction to Plant Biochemistry*. Pergamon Press.
- Grace, J., and Wilson, J. (1976). The boundary layer over a Populus leaf. *Journal of Experimental Botany*, 27, 231–241.
- Grammatikopoulous, G., and Manetas, Y. (1994). Direct absorption of water by hairy leaves of *Phlomis fruticosa* and its contribution to drought avoidance. *Canadian Journal of Botany*, 72, 1805–1811.
- Harrison, B.A., and Jupp, D.L.B. (1989) *Introduction to Remotely Sensed Data: Part ONE of the microBRIAN Resource Manual*. CSIRO, Melbourne. 156pp.
- Harrison, E.L., Arce Cubas, L., Gray, J.E., and Hepworth, C. (2020). The influence of stomatal morphology and distribution on photosynthetic gas exchange. *The Plant journal : for cell and molecular biology*, 101(4), 768–779. <https://doi.org/10.1111/tpj.14560>
- Holbrook, N.M., and Zwieniecki, M.A. (2005). *Vascular transport in plants*. Elsevier Academic Press, Burlington MA. 564 p.
- Huber, L., and Gillespie, T.J. (1992). Modeling Leaf Wetness in Relation to Plant Disease Epidemiology. *Annual Review of Phytopathology*, 30(1), 553–577.
- Jacobs, M. (1955). *Growth Habit of the Eucalypts*. CSIRO, Canberra. (Reprinted in 1986 by IFA).
- Jacquemoud, S., and Ustin, S.L. (2003). Application of radiative transfer models to moisture content estimation and burned land mapping. *Proceedings of 4th International Workshop on Remote Sensing and GIS Applications to Forest Fire Management*. pp 3–12. (Eds: E. Chuvieco, P. Martin and C Justice). Ghent (Belgium), 5–7 June, 2003.
- Jacquemoud, S., and Ustin, S.L. (2014). Modeling Leaf Optical Properties. In *Photobiological Sciences Online* (Ed: S.C. Smith). American Society of Photobiology. <http://www.photobiology.info/>
- James, S.A., and Bell, D.T. (2000). Leaf orientation, light interception and stomatal conductance of *Eucalyptus globulus* ssp. *globulus* leaves. *Tree Physiology*, 20, 815–823.
- Jarvis, P.G. (1985). Transpiration and assimilation of tree and agricultural crops: the ‘omega factor’. In *Attributes of Trees as Crop Plants* (Eds: M.G.R. Cannell and J.E. Jackson). Institute of Terrestrial Ecology. pp 460–480.
- John, G.P., Scoffoni, C., and Sack, L. (2013). Allometry of cells and tissues within leaves. *American Journal of Botany*, 100(10), 1936–1948. doi:10.3732/ajb.1200608
- Jones, H.G. (1992). *Plants and Microclimate*. Cambridge, Cambridge University Press.
- Juneau, K.J., and Tarasoff, C.S. (2012). Leaf area and water content changes after permanent and temporary storage. *PLoS ONE*, 7(8), e42604. <https://doi.org/10.1371/journal.pone.0042604>
- Karabourniotis, G., Kotsabassidis, D., and Manetas, Y. (1995). Trichome density and its protective potential against ultra-violet-B radiation damage during leaf development. *Canadian Journal of Botany*, 73, 376–383.
- Keeley, J.E. (1995) Seed-germination patterns in fire-prone Mediterranean climate regions. In: *Ecology and biogeography of Mediterranean eco- systems in Chile, California, and Australia*. (Eds: Arroyo, M.T.K., Zedler, P.H., Fox, M.D.) New York, Springer-Verlag. pp. 239–73.
- Kramer, P.J., and Boyer, J.S. (1995). *Water relations of plants and soils*. Academic Press, San Diego. <http://udspace.udel.edu/handle/19716/2830>
- Larcher, W. (1980). *Plant Physiological Ecology*. Springer-Verlag, Berlin.
- Li, Y., Johnson, D.A., Su, Y., Cui, J., and Zhang, T. (2005). Specific leaf area and leaf dry matter content of plants growing in sand dunes. *Botanical Bulletin of Academia Sinica*, 46, 127–134
- Liakopoulos, G., Nikolopoulos, D., Klouvatou, A., Vekkos, K.A., Manetas, Y., and Karabourniotis, G. (2006). The photoprotective role of epidermal anthocyanins and surface pubescence in young leaves of grapevine (*Vitis vinifera*). *Annals of Botany*, 98, 257–265.
- Lichtenthaler, H.K. (1987). Chlorophylls and carotenoids: Pigments of photosynthetic biomembranes. Ch 34 in *Methods in Enzymology*. Volume 148 in *Plant Cell Membranes* (Eds: Packer, L., and Douce, R.). Academic Press. pp. 350–382. [https://doi.org/10.1016/0076-6879\(87\)48036-1](https://doi.org/10.1016/0076-6879(87)48036-1)
- Lichtenthaler, H.K. (2009). Biosynthesis and Accumulation of Isoprenoid Carotenoids and Chlorophylls and Emission of Isoprene by Leaf Chloroplasts. *Bulletin of the Georgian National Academy of Sciences*, 3(3), 81–94.

- Lichtenthaler, H.K., and Buschmann, C. (2001). Chlorophylls and Carotenoids: Measurement and Characterization by UV-VIS Spectroscopy. *Current Protocols in Food Analytical Chemistry*, F4.3.1-F4.3.8.
- Lyons, M.B., Mills, C.H., Gordon, C.E., and Letnic, M. (2018). Linking trophic cascades to changes in desert dune geomorphology using high-resolution drone data. *Journal of the Royal Society Interface*, 15(144), 20180327.
- Magarey, R.D., Seem, R.C., Weiss, A., Gillespie, T., and Huber, L. (2005). Estimating Surface Wetness on Plants. Ch 10 in *Micrometeorology in Agricultural Systems*, Agronomy Monograph 47, American Society of Agronomy. <https://digitalcommons.unl.edu/cgi/viewcontent.cgi?article=1696&context=agronomyfacpub>
- Mayaud, J.R., Wiggs, G.F.S., and Bailey, R.M. (2016). Dynamics of skimming flow in the wake of a vegetation patch. *Aeolian Research*, 22, 141–151. doi:10.1016/j.aeolia.2016.08.001
- McLellan, T., and Endler, J.A. (1998). The relative success of some methods for measuring and describing the shape of complex objects. *Systematic Biology*, 47, 264–281.
- Milla, R., Reich, P.B., Niinemets, U., and Castro-Díez, P. (2008). Environmental and developmental controls on specific leaf area are little modified by leaf allometry. *Functional Ecology*, 22(4), 565–576. doi:10.1111/j.1365-2435.2008.01406
- Nicotra, A., Cosgrove, M., Cowling, A., Schlichting, C., and Jones, C. (2008). Leaf shape linked to photosynthetic rates and temperature optima in South African *Pelargonium* species. *Oecologia*, 154, 625–635.
- Niklas, K.J. (1992). *Plant biomechanics: an engineering approach to plant form and function*. University of Chicago Press. 607 p. <https://hdl.handle.net/1813/28577>
- Niklas, K.J. (1994). *Plant allometry*. University of Chicago Press, Chicago, Illinois, USA.
- Onoda, Y. (2017). Fracture Toughness. *Prometheus Wiki*, CSIRO Publishing. <http://prometheuswiki.org/tiki-index.php?page=Fracture+toughness>
- Onoda, Y., Schieving, F., and Anten, N.P.R. (2008). Effects of light and nutrient availability on leaf mechanical properties of *Plantago major*: A conceptual approach. *Annals of Botany*, 101, 727–736.
- Pasternak, D. (1987). Salt tolerance and crop production—a comprehensive approach. *Annual Review of Phytopathology*, 25, 271–291.
- Peñuelas, J., Gamon, J.A., Griffin, K.L., and Field, C.B. (1993). Assessing type, biomass, pigment composition and photosynthetic efficiency of aquatic vegetation from spectral reflectance. *Remote Sensing of Environment*, 46, 110–118.
- Peñuelas, J., Filella, I., Serrano, L., and Save, R. (1996). Cell wall elasticity and water index (r970nm/r900nm) in wheat under different nitrogen availabilities. *International Journal of Remote Sensing*, 17, 373–382.
- Pérez-Harguindeguy, N., Díaz, S., Garnier, E., Lavorel, S., Poorter, H., Jaureguiberry, P., Bret-Harte, M.S., Cornwell, W.K., Craine, J.M., Gurvich, D.E., Urcelay, C., Veneklaas, E.J., Reich, P.B., Poorter, J.L., Wright, I.J., Ray, P., Enrico, L., Pausas, J.G., de Vos, A.C., Buchmann, N., Funes, G., Quétier, F., Hodgson, J.G., Thompson, K., Morgan, H.D., ter Steege, H., van der Heijden, M.G., Sack, A.L., Blonder, B., Poschold, P., Vaieretti, M.V., Conti, G., Staver, A.C., Aquino, S., and Cornelissen, J.H.C. (2013). New handbook for standardised measurement of plant functional traits worldwide. *Australian Journal of Botany*, 61, 167–234.
- Popp, C., Burghardt, M., Friedmann, A., and Riederer, M. (2005). Characterization of hydrophilic and lipophilic pathways of *Hedera helix* L. cuticular membranes: permeation of water and uncharged organic compounds. *Journal of Experimental Botany*, 56(421), 2797–2806.
- Rabinowitch, E., and Govindjee, R. (1969). *Photosynthesis*. Wiley, New York.
- Reich, P.B., Uhl, C., Walters, M.B., and Ellsworth, D.S. (1991). Leaf lifespan as a determinant of leaf structure and function among 23 amazonian tree species. *Oecologia*, 86, 16–24. <https://doi.org/10.1007/BF00317383>
- Reich, P.B., Walters, M.B., and Ellsworth, D.S. (1997). From tropics to tundra: global convergence in plant functioning. *PNAS*, 94, 13730–13734.
- Rollin, E.M., and Milton, E.J. (1998). Processing of high spectral resolution reflectance data for the retrieval of canopy water content information. *Remote Sensing of Environment*, 65, 86–92.
- Rosenzweig, M. (1968). Net Primary Productivity of Terrestrial Communities: Prediction from Climatological Data. *The American Naturalist*, 102(923), 67–74.
- Rowlandson, T., Gleason, M., Sentelhas, P., Gillespie, T., Thomas, C., and Hornbuckle, B. (2015). Reconsidering leaf wetness duration determination for plant disease management. *Plant Disease*, 99(3), 310–310.

- Roy, B.A., Stanton, M.L., and Eppley, S.M. (1999). Effects of environmental stress on leaf hair density and consequences for selection. *Journal of Evolutionary Biology*, 12, 1089–1103.
- Royer, D.L., Wilf, P., Janesko, D.A., Kowalski, E.A., and Dilcher, D.L. (2005). Correlations of climate and plant ecology to leaf size and shape: potential proxies for the fossil record. *American Journal of Botany*, 9, 1141–1151.
- Sack, L., and Scoffoni, C. (2013). Leaf venation: structure, function, development, evolution, ecology and applications in the past, present and future. *New Phytologist*, 198, 983–1000.
- Salisbury, F.B., and Ross, C. (1969). *Plant Physiology*. Wadsworth Publishing Company, Belmont.
- Salt, D.E., Baxter, I., and Lahner, B. (2008). Ionomics and the Study of the Plant Ionome. *Annual Review of Plant Biology*, 59, 709–733.
- Saura-Mas, S., and Lloret, F. (2007). Leaf and Shoot Water Content and Leaf Dry Matter Content of Mediterranean Woody Species with Different Post-fire Regenerative Strategies. *Annals of Botany*, 99, 545–554.
- Schuepp, P.H. (1993). Tansley Review No. 59. Leaf boundary layers. *New Phytologist*, 125, 477–507.
- Sisó, S., Camarero, J., and Gil-Pelegrín, E. (2001). Relationship between hydraulic resistance and leaf morphology in broadleaf *Quercus* species: a new interpretation of leaf lobation. *Trees—Structure and Function*, 15, 341–345.
- Stein, R.J., Höreth, S., de Melo, J.R.F., Syllwasschy, L., Lee, G., Garbin, M.L., Clemens, S., and Krämer, U. (2017). Relationships between soil and leaf mineral composition are element-specific, environment-dependent and geographically structured in the emerging model *Arabidopsis halleri*. *New Phytologist*, 213, 1274–1286. doi:10.1111/nph.14219
- Taiz, L., Zeiger, E., Moller, I.M., and Murphy, A. (2015). *Plant Physiology and Development*. 6th edn online. Sinauer Associates. www.plantphys.net
- TERN Australia (2018). *Effective Field Calibration and Validation Practices: A practical handbook for calibration and validation satellite and model-derived terrestrial environmental variables for research and management*. A TERN Landscape Assessment Initiative, NCRIS. ISBN 978-0-646-94137-0. <https://www.tern.org.au/NEW-CalVal-handbook-for-remote-sensing-bgp4370.html>
- Trabaud, L. (1987). Fire and survival traits of plants. In *The role of fire in ecological systems*. (Ed: Trabaud, L.) The Hague, SPB Academic Publishing. pp. 65–89.
- Trabaud, L. (1991). Fire regimes and phytomass growth dynamics in a *Quercus coccifera* garrigue. *Journal of Vegetation Science*, 2, 307–14.
- Violle, C., Navas, M.L., Vile, D., Kazakou, E., Fortunel, C., Hummel, I., and Garnier, E. (2007). Let the concept of trait be functional! *Oikos*, 116, 882–892.
- Vogel, S. (1970). Convective cooling at low airspeeds and the shapes of broad leaves. *Journal of Experimental Botany*, 21, 91–101.
- Walters, D.R. (2006). Disguising the leaf surface: the use of leaf coatings for plant disease control. *European Journal of Plant Pathology*, 114, 255–260.
- Weatherley P (1965). The state and movement of water in the leaf. *Symposia of the Society for Experimental Biology*, 19, 157–184.
- Weisz, P.B., and Fuller, M.S. (1962). *The Science of Botany*. McGraw-Hill, New York.
- Westoby, M., and Wright, I.J. (2006). Land-plant ecology on the basis of functional traits. *Trends in Ecology and Evolution*, 21(5), 261–268.
- White, P.J., and Brown, P.H. (2010). Plant nutrition for sustainable development and global health. *Annals of Botany*, 105(7), 1073–1080.
- Williams, M., Woodward, F.I., Baldocchi, D.D., and Ellsworth, D. (2004). CO₂ capture from the leaf to the landscape, In: *Photosynthetic Adaptation: Chloroplast to Landscape* (Eds: W.K. Smith, T.C. Vogelmann and C. Critchley). Ecological Studies 178, Springer.
- Xu, F., Guo, W., Xu, W., Wei, Y., and Wang, R. (2009). Leaf morphology correlates with water and light availability: What consequences for simple and compound leaves? *Progress in Natural Science*, 19, 1789–1798.
- Yarwood, C.E. (1978). Water and the infection process. In *Water deficits and plant growth. Volume V. Water and plant disease*. (Ed: T.T. Kozlowski). Academic Press, New York. pp. 141–173.
- Yeats, T.H., and Rose, J.K. (2013). The formation and function of plant cuticles. *Plant physiology*, 163(1), 5–20. <https://doi.org/10.1104/pp.113.222737>
- Youngentob, K.N., Renzullo, L.J., Held, A.A., Jia, X., Lindenmayer, D.B., and Foley, W.J. (2012). Using imaging spectroscopy to estimate integrated measures of foliage nutritional quality. *Methods in Ecology and Evolution* 3, 416–426. doi:10.1111/j.2041-210X.2011.00149.x

5 Attributes of Individual Plants

Plants supply food, oxygen, medicines, clothing, shelter, and fuel for human populations. They also modulate local atmospheric conditions, recharge groundwater, and stabilise and enrich soils. The following sub-sections describe specific attributes of plants that are relevant to the interpretation of EO datasets:

- structure (see Section 5.1)—shape, size and volume;
- physiological processes (see Section 5.2)—photosynthesis, respiration, transpiration, and thermal stability; and
- growth (see Section 5.3)—life cycle, phenology, abscission, photomorphogenesis, and nutrient use efficiency.

5.1 Structure

Within any organism, groups of similar cells form tissue, which become specialised for particular functions. For example, xylem tissues transport fluids within a plant. Likewise, groups of tissues with a common function form organs, such as roots, stems, leaves, or flowers. The plant organs determine its internal and external structure. The stems or trunks of plants not only provide their structural scaffolding, but also enclose the vascular pipeline, which distributes water and nutrients from the roots to plant leaves, flowers, and fruit, and circulates energy resources from leaves to other parts of the plant. Below we consider two structural attributes of plants that are relevant to EO: growth form (see Section 5.1.1) and biomass (see Section 5.1.2).

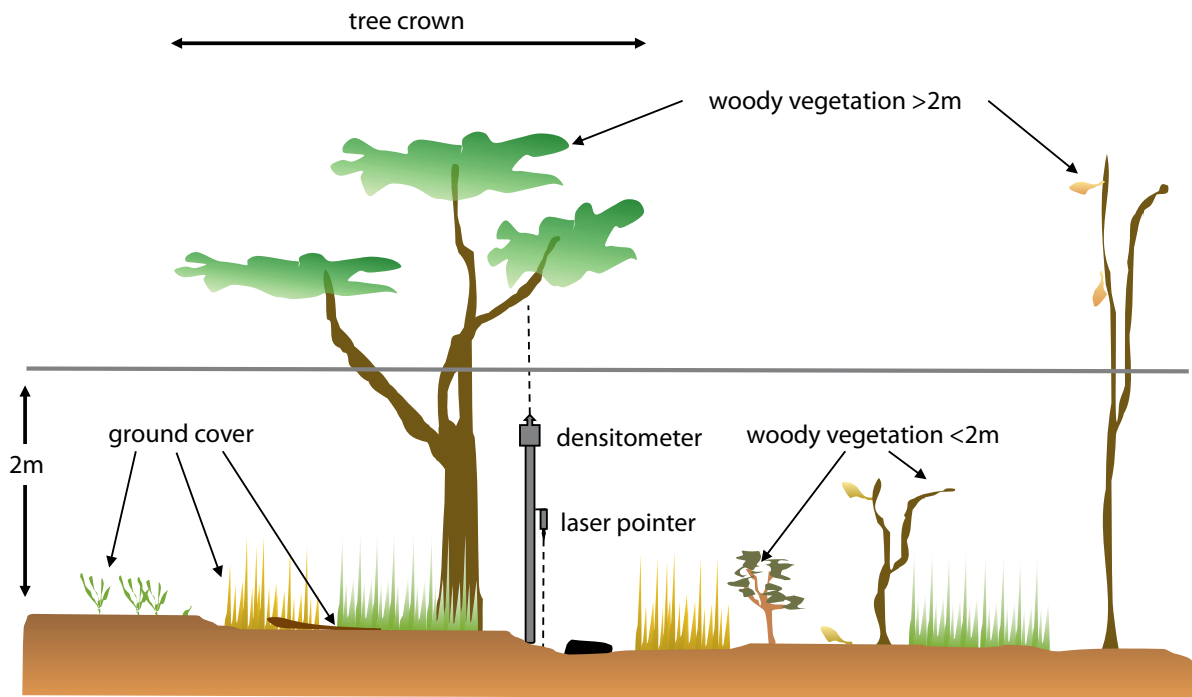
5.1.1 Growth form

Growth form, or habit, describes the overall dimensions and branching, or structural characteristics, of plants, and results from both hereditary and environmental factors. Some plant classification systems refer to growth form as life form (see Section 1.1), while others use that term to differentiate between woody and non-woody vegetation (Hnatiuk *et al.*, 2009). The broadest categories for growth form are:

- trees—large, woody plants supported on a main stem or trunk with secondary branches;
- shrub (or bush)—smaller woody plant with multiple stems;
- vine—woody or herbaceous plant with climbing or twining stem; and
- ground covers:
 - ◆ forbs—herbaceous, broad-leaved plant, often with conspicuous flowers; and
 - ◆ grass—herbaceous plant with slender leaves (blades) and inconspicuous flowers.

These categories are often further sub-divided into height classes and/or described in terms of their vertical position in the canopy relative to their neighbouring plants, that is, overstorey, midstorey, or understorey (see Figure 5.1).

Figure 5.1 Vegetation cover classes



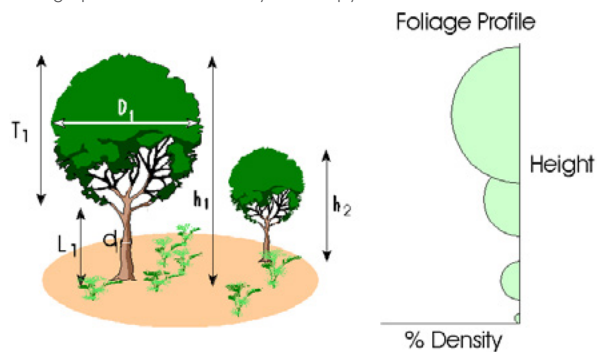
Source: Muir *et al.* (2011) Figure 10

Taller and heavier plants generally require the support of a woody structure, either as part of its own habit or provided by a host plant. Woody plants are characterised by thickened xylem tissue, such as occurs in trees, shrubs, palms, and some cycads, ferns, and vines. The standard Australian system for describing growth forms in vegetation is detailed in Hnatiuk *et al.* (2009). This system has been used extensively for national classifications of vegetation, such as NVIS (see Section 2.3.1).

Plant height can be measured in absolute or relative terms (see Section 5.1.2). Actual plant height can be estimated from trigonometry using a clinometer or sensed remotely using lidar equipment (see Excursus 5.1 and Section 16.5). The vertical distribution of vegetation can also be represented as foliage profile diagrams for either individual plants or groups of plants (see Figure 5.2). This provides more information than just the maximum height as it shows where most foliage will intercept incoming radiation and has been related to various aspects of plant ecology (Yokozawa and Hara, 1995). Vegetation profiles can vary with species and development stages and are indicative of wildlife habitat.

Figure 5.2 Foliage profile

Foliage profile for a multi-layer canopy



Source: Jupp and Lovell (2007) Figure 2.4

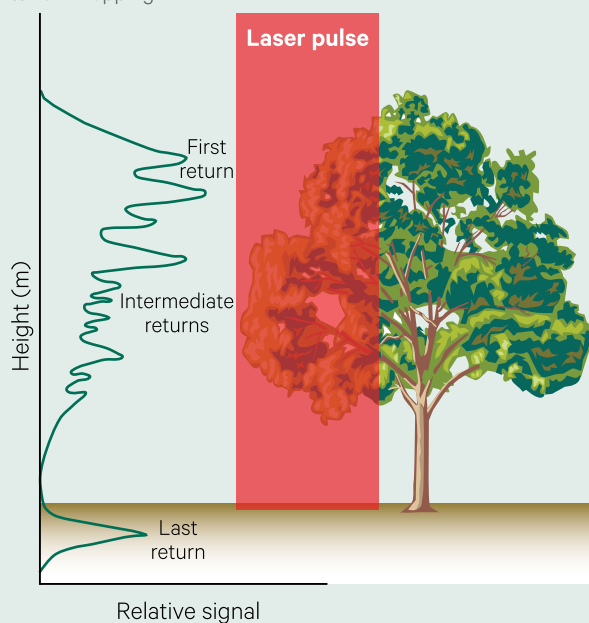
Excursus 5.1—Lidar

Source: Nicholas Coops, University of British Columbia, and Glenn Newnham, CSIRO

Lidar (Light Detection and Ranging) imaging systems can operate on a range of EO platforms (see Volume 1A—Section 15.1). These active remote sensing systems emit pulses of light to determine the distance (or range) to a target. Transmission of each emitted pulse is precisely timed, as is the time when its return (or echo) from the target is detected. Using the speed of light and the elapsed time between transmission and return of the pulse, the distance between the sensor and the target can be calculated. Based on the known trajectory of the laser beam, a three-dimensional point cloud can also be computed (Lim *et al.*, 2003; see Volume 1A—Excursus 15.1).

Figure 5.3 Lidar operation

A continuous waveform sensor would record the continuous height profile shown on the left of tree in the diagram below. Multiple discrete return sensors record the heights of discrete targets intercepted by the laser pulse. A first-return sensor would only record the height of the first target encountered, which in this example is the height of the first intercepted branch. A last-return sensor would only record the distance to the last object encountered by the laser beam, so is useful for terrain mapping.



A lidar system comprises three major components: a laser device, an inertial navigational measurement unit (IMU), and a Global Positioning System (GPS) unit. Lidar systems can be classified as either small footprint or large footprint systems, and sample with either:

- discrete return—recording up to five returns per laser footprint (Lim *et al.*, 2003) and optimised to derive terrain surface heights with sub-metre accuracy (Blair *et al.*, 1999, Schenk *et al.*, 2001); or
- full waveform—acquiring a fully digitised, returned pulse for continuous, sub-metre, vertical profiles (see Figure 5.3).

Small footprint lidar systems for both discrete return and full waveform sampling are widely available and, as the number of returns recorded per emitted pulse increases with new sensor developments, these systems provide increasingly detailed structural information. For a given species, small footprint lidar measurement error has been demonstrated to be:

- < 1.0 m for individual tree heights (Persson *et al.*, 2002);
- < 0.5 m for plot-based estimates of maximum and mean canopy height with full canopy closure (Magnussen and Boudewyn, 1998; Magnussen *et al.*, 1999; Næsset, 2002); and
- more precise than manual, field-based measurements (Næsset and Økland, 2002).

Large footprint, full waveform systems are less common but systems such as the Scanning Lidar Imager of Canopies by Echo Recovery (SLICER) and Laser Vegetation Imaging Sensor (LVIS) instruments (Harding *et al.*, 2001; Blair *et al.*, 1999) have been proven for mapping forest structure (Lefsky *et al.*, 2005).

Airborne

Airborne platforms used for Earth Observation (EO) include manned and unmanned aeroplanes and helicopters (see Volume 1A—Section 11 for details). Airborne Laser Scanning (ALS) systems can be carried on any of these platforms. Unmanned Aerial Vehicles (UAV) potentially offer greater flexibility, increased spatial resolution, and more rapid assessment of vegetated landscapes than manned aircraft (although current systems are restricted both by weight and flying time and, to some extent, aviation restrictions). For example, Wallace *et al.* (2012a, 2012b) describe the development of a low-cost UAV lidar system that includes a discrete return lidar and high definition video camera. This system was capable of acquiring extremely dense lidar point clouds (62 points per m^2), from which detailed measurements of tree locations, heights and crown dimensions could be derived. Point cloud density also varies with flying height and speed, so for a given lidar system, there is a trade-off between data density and extent of coverage. An increasing range of portable lidar scanning units are becoming available, often including smart interfaces to avoid potential collisions and providing localisation, navigation, and flight control when GPS is not available.

Satellite

Satellite laser sensors such as the Geoscience Laser Altimeter System (GLAS), which was onboard the Ice, Cloud and land Elevation Satellite (ICESat), acquired global waveform data over forests from 2003 to 2009 with a large footprint spanning over 90 m (see Excursus 6.1). Two additional spaceborne lidar systems have been launched and are acquiring lidar data in 2020. Specifically, both the full waveform Global Ecosystem Dynamics Investigation (GEDI) on the International Space Station (ISS) and single photon lidar system on ICESAT2 are beginning to provide valuable space-based data for vegetation assessments (Hancock *et al.* 2019; Markus *et al.*, 2017).

Terrestrial

While ALS systems are relatively cost-effective for large areas (Næsset and Nelson, 2007; Wulder *et al.*, 2008), the structure of understorey components is often obscured by taller vegetation from an overhead perspective (Lovell *et al.*, 2003), and information about tree trunks is not directly visible to the scanner. Accordingly, to complement airborne lidar data, a number of studies have used ground-based lidar (or Terrestrial Laser Scanning, TLS) systems, which observe the canopy structure from below (Henning and Radtke, 2006; Hilker *et al.*, 2010; Jupp *et al.*, 2009). These systems can be mounted on tripods or moving vehicles to acquire data for all or selected portions of the hemispherical field of view (Hyypä *et al.*, 2012). TLS instruments mounted on a tripod can scan forest stands out to radial distances of hundreds of metres (Calders *et al.*, 2020) depending on vegetation density, and have been installed on a permanent basis at selected locations to monitor growth following disturbances.

TLS allows extremely dense point clouds to be acquired (see Figure 5.4) which can be used to generate very detailed, three-dimensional models of vegetation structure for individual trees (see Section 16.5.2). Established methods exist to derive tree height, diameter at breast height (DBH), and above ground biomass (AGB) from TLS (Calders *et al.*, 2015a, 2015b; see Section 16.5). Thus, TLS already delivers information on forest structure that cannot be derived from plot-based forest surveys (Newnham *et al.*, 2015) and promises to enable full, three-dimensional mapping of ecosystem structure (Calders *et al.*, 2020).

Figure 5.4 TLS-based three-dimensional complexity of forest

Grey shades in image below indicate distance from RIEGL VZ-400 TLS instrument to vegetation elements in a simple notophyll vine forest at Robson Creek, Queensland. The graph shows derived plant area volume density as a function of canopy height using method outlined by Calders *et al.* (2015b).



Source: Calders *et al.* (2020) Figure 1

5.1.2 Biomass

Any biological matter from organisms that are alive or decomposing is called biomass (see Section 7.4 for related productivity terms). Biomass predominantly comprises carbon, hydrogen, and oxygen, with lesser amounts of nitrogen and other elements. It represents the solar energy stored in organic matter and, as such, can be used for fuel. In ecological terms, biomass estimates express the mass of biological organisms per unit area and can be referenced for individual species or communities (see Section 7.4).

Depending on the location and state of decomposition of biomass, it can be differentiated into four categories:

- above ground biomass—all living plant matter above the soil surface, including foliage, stems, branches, bark, flowers, and seeds;
- below ground biomass—all living roots below the soil surface, including:
 - ◆ fine roots (< 2 mm diameter);
 - ◆ small roots (2–10 mm diameter); and
 - ◆ large roots (> 10 mm diameter);
- litter—all dead plant material on the soil surface that is less than some specified diameter⁶, usually decomposing; and
- dead mass—all other dead woody biomass both above and below the soil surface.

Plant biomass is an indicator of plant vigour (see Section 9.6), site productivity (see Sections 7.4 and 10.2.2), carbon stocks (see Section 17), and fire risk (see Section 18). It is traditionally measured by destructive sampling of selected plants and expressed in terms of fresh and/or dry weight. Biomass measurements are reported in terms of Fresh Biomass (FBM), Oven-dried Biomass (DBM), or Dry Matter Content (DMC). Litter traps are commonly

used to non-destructively measure falling plant parts, such as fruit, leaves, flowers, and petioles. Other non-destructive methods for measuring biomass include visual obstruction sampling, vertical and horizontal image analysis, radiation reflectance measurement, allometric relationships, scaled digital image of plant silhouettes, aerial and terrestrial laser scanning (see Excursus 5.1), and analysis of EO imagery (Tanaka *et al.*, 1998; Montes *et al.*, 2000; Holzgang, 2001; Tomasel *et al.*, 2001; Vermeire and Gillen, 2001; Thursby *et al.*, 2002; Tackenberg, 2007; Zehm *et al.*, 2003). Detailed reviews of biomass sampling methods are provided by Catchpole and Wheeler (1992) and Schaefer (2018).

Biomass monitoring is used to derive estimates of net primary production (NPP; see Section 7.4) and analyse plant growth (Cornelissen *et al.*, 2003; Perez-Harguindeguy *et al.*, 2013). The vertical biomass distribution can be derived from sampling at defined cutting heights (Tackenberg, 2007). While this profile is indicative of the competitive vigour of particular species (Schwinning and Weiner, 1998), it is not commonly measured (Tackenberg, 2007).

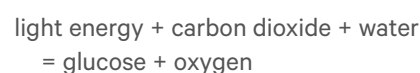
EO measures of biomass offer an efficient mechanism to generate landscape scale estimates of biomass. Optical reflectance data have been reliably related to foliage biomass (see Section 8) and SAR data has been used to infer woody biomass for forest carbon tracking (Mitchell *et al.*, 2010, 2012; Lehmann *et al.*, 2012) and pasture biomass (Schmidt *et al.*, 2016; see Sections 13 and 15). Lidar instruments, by effectively constructing a three-dimensional model of a target (see Excursus 5.1), furnish valuable information on vegetation structure, and both terrestrial laser scanning (TLS) and airborne laser scanning (ALS) are gaining popularity for estimating woody biomass in forestry and environmental surveys (Jupp and Lovell, 2007; Schaefer, 2018; see Section 16).

5.2 Physiological Processes

Plants function via a number of physiological processes. The following processes have direct relevance to EO-based studies: photosynthesis (see Section 5.2.1); respiration (see Section 5.2.2); transpiration (see Section 5.2.3); and thermal stability (see Section 5.2.4).

5.2.1 Photosynthesis

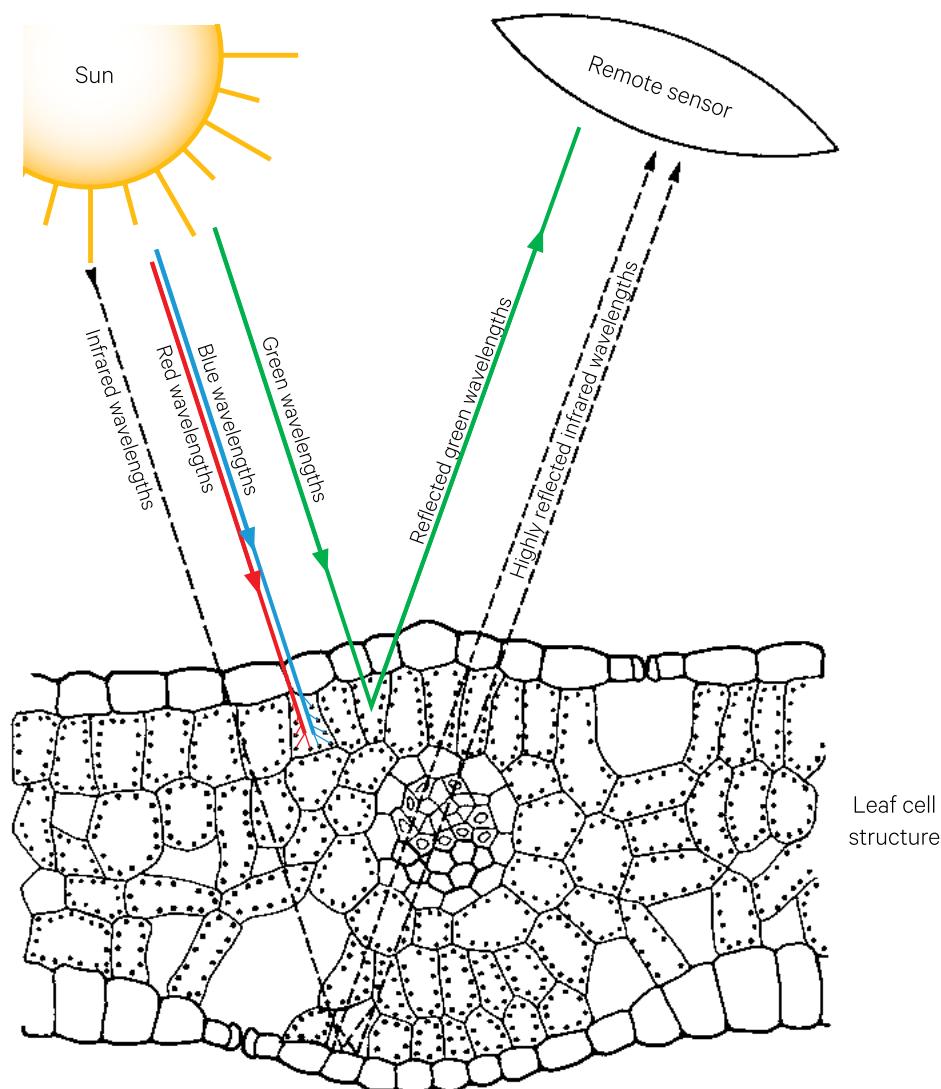
Photosynthesis is the primary energy capture mechanism in the biosphere. This process transforms light energy into chemical energy. Photosynthetic organelles, principally chloroplasts in leaves (see Figure 4.1), convert light and carbon dioxide (CO₂) and water into glucose and oxygen:



⁶ For example 10 cm—specified by individual countries (Schaefer, 2018)

Figure 5.5 Reflectance characteristics of typical green leaf structure

Chloroplasts reflect green wavelengths but absorb blue and red wavelengths for use in photosynthesis. Spongy mesophyll cells strongly reflect infrared wavelengths.



Source: Harrison and Jupp (1989) Figure 5

Principally blue and red wavelengths from the Sun's energy are absorbed by plant pigments during this process (see Section 4.3), with green and NIR wavelengths being reflected (hence the green colour of most living vegetation; see Figure 4.3 and Figure 5.5). As introduced in Section 4.1.1 above, gaseous exchange of water and CO₂ between the leaf surface and the atmosphere occurs via the stomata, whose opening and closing are controlled by guard cells. The plant sugars resulting from photosynthesis form an energy store, which is either consumed by the plant (to fuel internal metabolic processes and growth) or by external heterotrophs.

In simplistic terms, the rate of photosynthesis determines plant growth and vigour and, below species-specific thresholds, increased levels of CO₂, sunlight and heat can increase photosynthetic activity. As the name implies, photosynthesis is a photochemical reaction, that is, one that is initiated by the absorption of light energy (Rabinowitch and Govindjee, 1965). The speed of this process is limited by the:

- intensity of light—low intensities reduce the speed of photosynthesis;
- concentration of CO₂—low concentrations limit photosynthetic activity; and
- ambient temperature—extreme conditions, too hot or too cold, limit photosynthesis.

Table 5.1 Photosynthetic pathways

Characteristic	Photosynthetic Pathway		
	C ₃	C ₄	CAM
Name	First stable product from CO ₂ is a 3-carbon compound	First stable product from CO ₂ is a 4-carbon compound	Process discovered in Crassulaceae family CO ₂ initially stored as 4-carbon acid
Carbon Fixation	In single chloroplast using RuBisCO enzyme	In chloroplast of thin-walled mesophyll cell using phosphoenol pyruvate (PEP) enzyme	In chloroplast at night using PEP enzyme then stored in cell vacuole as malate
Calvin Cycle	In same chloroplast	In chloroplast of thick-walled bundle sheath cell	In same chloroplast during daytime
Stomata	Open during day and generally close at night	Open during day and generally close at night	Open during the night and generally closed during the day
Advantages	Better performance with ample water and sunshine	Better performance when CO ₂ levels are low Highest growth rates, comprising 25% of terrestrial photosynthesis Withstand higher light levels plus salinity and dryness No photorespiration Stomata open for shorter periods for CO ₂ intake so less transpiration	Use less water than C ₃ or C ₄ plants Better recovery from drought stress Can assimilate CO ₂ during day with abundant moisture
Disadvantage	Photorespiration	Energy used to move intermediate products to different cell locations	Low rates of photosynthesis; slow growth and low yield
Location	Throughout leaf (and some stems)	Inner leaf cells with Kranz anatomy	Thick, fleshy leaves and stems
Occurrence	~85% plants; Mostly in cooler temperate regions	> 19 families including sugar cane, saltbush, corn, summer annuals, and many grasses Mostly in tropical and subtropical grasslands and savannas	~10% plants: cacti, agaves, some orchids, ferns, and bromeliads Mostly in arid environments

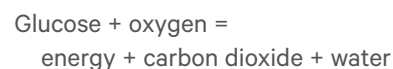
Photosynthesis involves two fundamental biochemical processes:

- carbon fixation—CO₂ is converted into a stable intermediate product; then the
- Calvin Cycle—sugar is produced from the intermediate product.

Three metabolic pathways for photosynthesis have been identified: C₃, C₄, and CAM (Crassulacean Acid Metabolism). While most plants use the C₃ process, both the C₄ and CAM processes offer efficiency advantages to plants growing in arid environments. C₄ plants compartmentalise the intermediate processing steps to photosynthesise at a faster rate than C₃ plants and thus avoid photorespiration (see Section 5.2.2 below), while CAM plants can delay the Calvin Cycle to conserve energy. C₄ plants are very productive, comprising only 3% of vascular plants but conducting 25% of terrestrial photosynthesis (Sage, 2004), and have been observed to be more dominant geographically as temperature increases and rainfall decreases (Hattersley, 1983). Since photosynthesis in C₄ plants requires less nitrogen, these plants can also thrive in less fertile soils. Relevant characteristics of these three photosynthetic pathways are summarised in Table 5.1.

5.2.2 Respiration

The opposite process to photosynthesis is respiration, that is, the energy stored in the sugar product is released in the presence of oxygen, to produce CO₂ and water:



By consuming oxygen, this can be viewed as an oxidation reaction. Unlike photosynthesis, respiration occurs in most plant cells and is not dependent on light.

Respiration fuels plant metabolic processes and permits growth. In most plants, the rates of both photosynthesis and respiration increase with temperature up to a species-dependent threshold, at which point respiration occurs more rapidly than photosynthesis. In bright, hot conditions, stomata close and the ambient CO₂ levels in a plant can drop. If photosynthesis continues when the concentration of CO₂ levels drop below 50 ppm, oxygen is fixed instead of CO₂. This process is called photorespiration and is less efficient in terms of energy production for the plant.

5.2.3 Transpiration

Transpiration releases water from plants via stomata, the leaf pores that permit water vapour from the leaf to transfer into the atmosphere and CO₂ from the atmosphere to enter the leaf. Guard cells surround each stomate to control its opening and closing, and hence are an important factor in determining the rate of transpiration (see Section 4.1.1). In hot and dry conditions plants generally close their stomata to avoid excessive moisture loss. Most water loss from plants results from transpiration, but there is also a small volume of water lost via evaporation from leaf surfaces. Water stress restricts transpiration, reduces photosynthetic efficiency, and limits plant productivity (Salisbury and Ross, 1969).

The transpiration process achieves three essential functions in plants:

- water provides both the solvent and the vehicle to transport:
 - ◆ minerals from the roots to plant stems and leaves via xylem cells; and
 - ◆ sugars from the leaves to the rest of the plant via phloem cells;
- turgor pressure in plant cells is maintained by water, providing both structural support and controlling the operation of guard cells (see Section 4.2.1); and
- evaporative cooling from transpiration delivers most of the cooling provided by a shade tree (with an increase in vegetative cover of 10% in urban areas reducing the land surface temperature by 1.2°C; Coutts *et al.*, 2016).

The rate of transpiration is determined by the balance between two primary forces:

- water potential differential between the soil and atmosphere around the plant—dry air will encourage more water to leave the plant and hence increase transpiration; and
- resistance of leaf cuticle, stomata, and the leaf boundary layer to water movement—leaves slow down water loss from transpiration by closing stomata and increasing cuticle thickness. The boundary layer comprises a thin, stationary layer of air surrounding the leaf surface through which leaf water must diffuse to enter moving air (see Section 4.4).

Thus, transpiration rates increase in response to several environmental conditions:

- light—stomata open in bright light to allow CO₂ into the leaf for photosynthesis;
- temperature—due to evaporation and diffusion of water at higher temperatures;
- wind—windy conditions quickly remove water vapour and speed up diffusion;
- soil moisture—plants with access to adequate soil moisture will transpire more than those in dry soil; and decreases with
- humidity—humid conditions slow diffusion of water vapour from the leaf.

The rate of transpiration (in mols of water/cm²/sec) can be expressed as the equation:

$$TR = \frac{LW \text{ potential} - \text{ambient AW potential}}{\text{resistance}}$$

where TR is transpiration rate, LW is leaf water, and AW is atmospheric water.

Leaf transpiration is either measured directly using a leaf porometer or indirectly via leaf temperature (Leinonen *et al.*, 2006). Models of transpiration rates at the level of individual leaves have been developed from detailed measurements of conductance characteristics, including CO₂ capture (involving a porometer or infrared gas analyser; Jones, 1992) and boundary layer properties (Brenner and Jarvis, 1995). Whole plant transpiration can also be measured via thermal sensors that monitor xylem sap fluxes from the root system to the canopy (Granier, 1987; Bush *et al.*, 2010). The Bowen ratio (ratio of sensible to latent heat flux; see Section 5.2.4) is used to estimate whole ecosystem evapotranspiration (see Sections 4.4 and 7.6). Optical spectroscopy has also been used in conjunction with chemometric methods to determine leaf water content (Zhang *et al.*, 2012).

5.2.4 Thermal stability

The temperature of a material is indicative of its energy content. Thermal energy is exchanged between plants and their environment by:

- conduction and convection;
- absorption and emission; and
- evaporation of moisture.

Only a small proportion (3–6%) of the solar energy intercepted for photosynthesis is actually converted into chemical energy (FAO, 1997). The harvested energy that is not converted into biomass is dissipated as heat or chlorophyll fluorescence.

Within any biological system, the net (or stored) energy is the difference between the energy input and energy output. At equilibrium, the energy balance sums to zero, that is, energy input equals energy output, so that no energy is stored. The energy produced and/or consumed in metabolic processes within a leaf is relatively insignificant in comparison with other heat exchange processes in leaves. While convective heat transfer is encouraged by windy conditions or when the air temperature is higher than the leaf temperature, little heat is lost by conduction. Evaporation provides a generous mechanism for heat dissipation, especially in hot, dry conditions.

The boundary layer surrounding a leaf resists heat transfer from the leaf to the surrounding air (see Section 4.4), so impacts leaf temperature. If the adjacent air is cooler than the leaf surface, air circulates around the leaf and removes some heat by convection, but high boundary layer conductances resist this transfer of heat and water vapour (Martin *et al.*, 1999). Leaf temperature depends on the leaf energy balance and can be expressed as a function of the temperature, humidity, density, water vapour pressure, and specific heat capacity of the ambient air, and the isothermal radiation absorption, boundary layer resistance, and stomatal resistance of the leaf (Jones, 1992).

The metabolic processes that enable plants to survive only operate within a restricted range of temperatures, with different plants being suited to different temperature ranges. Leaf temperatures generally track within 2°C of the diurnal cycle of air temperatures but may be much higher in full sunlight with little air movement, especially when water stressed (Nelson and Bugbee, 2015). Both within a single plant, and between plants of the same species in different locations, however, individual leaves are exposed to differing amounts of sunlight and wind. To enable all leaves within a plant to maintain comparable temperatures, sunlit foliage in the upper canopy of trees and shrubs intercepts light less efficiently than shaded foliage. Variations can occur in leaf shape and orientation, as well as transpiration rates, with the result that more exposed leaves are generally smaller and have a greater perimeter than less exposed ones (see Section 4.1.2). Nonetheless, being composed largely of water, leaves exposed to full sunlight carry a high heat load. Much of this load is dissipated by:

- sensible (meaning perceptible) heat loss as thermal EMR (or emitted energy: E_R); and
- evaporative (or latent energy: E_L) heat loss, or evaporation.

The ratio of sensible and evaporative heat losses is called the Bowen Ratio (BR; Lewis, 1995):

$$BR = \frac{\text{sensible heat loss}}{\text{latent heat loss}}$$

This ratio is high when the supply of water is limited (low evaporation) and low for well-watered plants. Accordingly, BR is typically higher for dry ecosystems such as deserts and lower for tropical vegetation. Some plants, such as cactii, have adapted to dry climates by minimising transpiration and enduring high leaf temperatures. Such adaptations are usually associated with slow growth rates. When air and leaf temperatures are very similar, as occur for irrigated grass in calm conditions, BR values are close to zero. Canopy measurements of evapotranspiration can be derived from BR, net incident radiation, soil heat loss, and gradients in temperature and water vapour above the canopy (Taiz *et al.*, 2015; see Section 7.6).

Leaf temperature is important as an indicator of transpiration rate and is frequently monitored for irrigation scheduling (see Sections 9.4 and 9.5). Studies employing suites of proximal sensors to quantify plant water status have demonstrated that leaf temperature is strongly correlated with stem water potential, air temperature, relative humidity, photosynthetically active radiation, and wind speed, especially for shaded leaves (Udompetaikul *et al.*, 2011).

The temperature of a leaf can be measured using a thermocouple (generally attached to shaded side; Tarnopolsky and Seginer, 1999), infrared thermometer (Blad and Rosenberg, 1976), or thermal imaging (Hartz *et al.*, 2006; Leuzinger *et al.*, 2010). For example, WaterWise is a smart irrigation tool that uses proximal infrared thermometers to detect when a plant is approaching stress (CSIRO, 2019). Such monitoring is being integrated with weather forecasts, soil moisture status, and other crop data to optimise the water use efficiency and yield of high-value crops (see also Section 9.5). Thermal imagery (8–14 μm ; Volume 1B—Section 7) can also be used to monitor evapotranspiration and water deficit stress (see Section 9.4).

Certain metabolic processes associated with heat dissipation in plants, including xanthophyll pigment interconversion, have been related to variations in leaf absorption characteristics near wavelength 531 nm (Demmig-Adams, 1990). EO-based spectral indices such as the Photochemical Reflectance Index (PRI) have been proposed to assess the efficiency of photosynthetically active radiation usage when plants are water stressed (Peñuelas *et al.*, 1997; see Section 8.1.4).

5.3 Growth

Most fundamental characteristics of plant species are determined by their genetic inheritance, but environmental factors such as the availability of nutrients, sunlight, moisture, and CO₂ can accelerate and enhance plant growth. Likewise, the presence of predators and adverse environmental conditions (excess moisture, wind, heat, or cold) can impede growth. Table 5.2 summarises the principal factors that are responsible for the quantity and quality of plant growth. These primary factors are related by the sequence (Kramer and Boyer, 1995):

Hereditary Potential + Environmental Factors →
Plant Processes and Conditions →
Quantity and Quality of Growth

The following sub-sections consider plant growth in the context of plant life cycle (see Section 5.3.1), phenology (see Section 5.3.2), abscission (see Section 5.3.3), photomorphogenetic (light-dependent) processes (see Section 5.3.4), and nutrient use efficiency (see Section 5.3.5).

Table 5.2 Plant growth factors

Primary Factor	Components
Hereditary Potential	Root system—depth, extent
	Leaves—size, shape, area, thickness
	Stomata—number, location, behaviour
Environmental Factors	Soil—texture, structure, depth, chemical composition, pH, aeration, temperature, water holding capacity, water conductivity
	Atmospheric—precipitation (amount and seasonal distribution), evaporation, CO ₂ concentration, radiant energy, temperature, wind, vapour pressure
	Biotic—competing plants, pathogens, predators
Plant Processes and Conditions	Water absorption, distribution, transpiration
	Internal water balance—water potential, turgidity, stomatal opening, cell enlargement
	Chemical composition—pigments, growth regulators, nutrients
	Metabolic processes—photosynthesis, respiration, nutrient cycling
Quantity and Quality of Growth	Size of cells, organs, plant
	Dry weight, succulence, chemical composition
	Root to shoot ratio
	Vegetative versus reproductive growth

Adapted from: Kramer and Boyer (1995) Figure 1.1

5.3.1 Life cycle

The life cycle of all plants spans from germination to death, with a wide range of variations between species in terms of modes of reproduction and stages of maturation. Annual plants complete their life cycle within a single year and generally expend more energy on seed production than establishment. Biennial plants grow and die within two years, using the first growing season for growth and the second for reproduction. Perennial plants live for more than two years and generally become stronger and larger plants that produce seed over many years.

Different plants use different mechanisms to create their next generation. Reproduction can occur asexually, creating genetically identical offspring, via cuttings, runners, stolons, or suckers, or division of rhizomes, bulbs, and corms. Alternatively, sexual reproduction combines genes from both male and female parent plants to produce genetically different offspring. This mechanism is used by most seed and spore producing plants and enables greater biological diversity.

The life cycle of a typical angiosperm, for example, can be summarised in terms of several consecutive stages. For a tree, a seed germinates, grows through the seedling stage into a sapling or young tree, develops into a mature tree, then produces seed-bearing fruit of some form. During these stages of growth, the size, shape, and structure of the tree changes. At senescence the tree dies, shedding limbs and leaves to create compost for future generations. Growth stages of groups of plants is further discussed in Section 6.5.

5.3.2 Phenology

Phenology studies the relationships between life cycle stages in biota (plants and animals) and weather and climate (Schwartz, 2013). Plant phenology considers plant life cycles and their interactions with seasonal, climatic, and other rhythms. Seasons are largely driven by variations in the amount of solar radiation that reaches the Earth's surface at different locations (see Volume 1A—Section 3). Recurring events within plant life cycles are triggered by periodic environmental changes, particularly those related to seasonal changes in ambient temperature and light levels. In order to better understand and manage plant growth, phenology attempts to identify these trigger factors and relies heavily on chronology, that is, the analysis of historical records relating to the dates of key events. Indeed, indigenous communities have traditionally used phenological indicators as a climatic almanac.

For annual plants, the stages of growth are clearly delineated within an annual cycle by the extent of green plant cover (see Sections 5.1.2 and 9.1). Four key event dates can be identified in the growth of annual plants:

- greening—green leaves become visible as photosynthesis begins;
- maturity—growing leaves attain maximum green leaf area;
- senescence—brown leaves appear as photosynthesis rapidly decreases; and
- dormancy—end of cycle when photosynthesis ceases.

Broad scale phenological changes are most obvious during leaf emergence and senescence. Plants respond to both diurnal variations in light levels, temperature and precipitation, and seasonal changes in day length, or photoperiodism. The latter often operates in conjunction with a chilling threshold for many temperate species. Similarly, the developmental responses of some plants are affected by the ratio of red to far red light in different seasons, whereas the growing cycles of crops are more closely related to changes in temperature and precipitation.

While the dates of key phenological events can vary from season to season and from year to year, they provide valuable insight into longer term vegetation responses to climatic variations. Inter-seasonal and interannual variations in phenology affect different parts of the biosphere in different ways, so an understanding of phenological trigger factors is fundamental to understanding the spatiotemporal dynamics of carbon, water, and thermal cycles of Earth (Schwartz, 2013). Thus, phenology is relevant to studies of vegetation distribution (Chuine, 2010), agricultural management (Chmielewski, 2003; Keatinge *et al.*, 1998), food web interactions (Straile, 2002), ecosystem productivity dynamics (Myneni *et al.*, 1997, 2007), land surface modelling (Richardson *et al.*, 2012), biosphere-atmosphere interactions (Flanagan, 2009), and epidemiology (Luvall *et al.*, 2011; Malone *et al.*, 2019).

5.3.3 Abscission

For efficiency reasons, plants shed, or abscise, any part of their structure that is no longer required. Deciduous plants produce leaves that only last one seasonal cycle, whereas evergreen leaves are designed to function for many years. These two types of leaves offer distinct advantages and disadvantages in particular environments. The key factors that appear to determine whether deciduous or evergreen species dominate or intermix in a geographic region are photosynthetic capacity, nutrient availability, and winter desiccation (Smith, 1993).

To replace their photosynthetic system each year, deciduous plants expend more nutrient resources than evergreen plants, whose leaves are replaced gradually. Deciduous plants typically have greater capacity for both photosynthesis and transpiration. They accumulate food reserves in warm weather, which are stored in roots and stems to enable survival through winter. The productivity of such plants is driven by seasonal or climatic changes. In cold environments, it is easier for plants to abscise their leaves than to protect them from the drying impact of freezing in winter. Abscission usually involves significant resorption of soluble nutrients, such as phosphorus, nitrogen, and potassium, from senescing tissue. Routine abscission also discourages parasites, pathogens, and predators.

Rather than shed their leaves, evergreen species have developed various mechanisms to protect their leaves from winter temperatures, such as converting free water in cells into a gel which will not freeze. However, evergreen plants lose more water during winter and are more susceptible to predators.

In temperate regions, deciduous plants abscise leaves in response to seasonal temperature changes, so are dormant during winter. In subtropical areas, leaf drop is triggered by non-seasonal rainfall patterns with foliage being shed to reduce water loss. The longevity of leaves in woody plants has obvious relevance to measuring foliage attributes in different seasons and localities. Plants that maintain green leaves throughout the year are categorised as Persistent Green Vegetation (see Section 9.1), that is, evergreen perennials such as vascular plants with deep roots and slow rates of biomass growth and decay (Donohue *et al.*, 2009).

5.3.4 Photomorphogenesis

In addition to pigments, plants contain a number of photoreceptors that are sensitive to particular wavelengths of EMR, such as phytochrome (red and far red), cryptochrome (blue and UVa), and phototropin (blue; Casal, 2000; Briggs and Olney, 2001). While the concentrations of these photoreceptors are much lower than those of the major plant pigments (see Section 4.3), they have distinct absorption spectra and impact the reflectance spectra of leaves (Blackburn, 2007).

Apart from photosynthesis, many processes involved with plant growth and development are dependent on the presence or absence of light (Sullivan and Deng, 2003). Photomorphogenetic processes include:

- germination of seeds in response to red light;
- leaf development in dicotyledon seedlings in red light;
- photoperiodism in older plants triggers seasonal changes, such as flowering after extended periods of long nights;
- phototropism—bending plant organs towards (blue) light source due to rapid cell growth on shaded side of plant; and
- nyctinastic movements (diurnal changes controlled by circadian rhythms and light reception) in higher plants in low, ‘far red’ (700–750 nm) light levels (such as folding leaves or flower petals at night).

5.3.5 Nutrient use efficiency

One measure of the efficiency of nutrient usage in plants is the proportion of organic matter produced per unit of absorbed nutrient. For short-lived plants, this has been observed to be inversely correlated with the nutrient concentration in plant tissue, with plants growing on less fertile soils having higher nutrient concentrations than the same plants grown on more fertile sites (Chapin, 1980). Long-lived perennials, however, are more likely to recycle nutrients as leaves senesce, so for these plants nutrient use efficiency is inversely related to the concentration of nutrients in above ground litterfall, root turnover, and live organic matter (Vitousek, 1982).

The minerals nitrogen, phosphorus, and calcium are more likely to be removed from forest trees in the fine litter fraction (comprising leaves, twigs, small branches, flowers, fruit, and seeds), while potassium tends to be leached by rain as throughfall. Nitrogen Use Efficiency (NUE), the ratio of nitrogen output to nitrogen input, is used as an indicator of the efficiency of nutrient usage in food production (EU Nitrogen Expert Panel, 2015). NUE varies between different types of plants, with plants growing on less fertile soils typically using nitrogen more efficiently in active leaves and/or resorbing more nitrogen from senescing leaves, and as stem wood transitions to heartwood. The rate of nitrogen release from decomposing plant matter is highly correlated with its C:N ratio, such that slower rates of litter decomposition are observed when N levels are low (Vitousek, 1982).

5.4 Further Information

Photosynthesis

Rabinowitch and Govindjee (1965, 1969)

Bowen Ratio

Lewis (1995): ftp://195.37.229.5/pub/outgoing/jwinder/BowenRatioLiterature/Lewis_BullAmeriMeteoSoc_1995.pdf

Plant Physiology Protocols

Prometheus Wiki, CSIRO: http://prometheuswiki.publish.csiro.au/tiki-custom_home.php

5.5 References

- Blackburn, G.A. (2007). Hyperspectral remote sensing of plant pigments. *Journal of Experimental Botany*, 58(4), 855–867.
- Blad, B.L., and Rosenberg, N.J. (1976). Measurement of crop temperature by leaf thermocouple, infrared thermometry and remotely sensed thermal imagery. *Agronomy Journal*, 68, 635–641.
- Blair, J.B., Rabine, D.L., and Hofton, M.A. (1999). The Laser Vegetation Imaging Sensor (LVIS): A medium-altitude, digitization-only, airborne laser altimeter for mapping vegetation and topography. *ISPRS Journal of Photogrammetry and Remote Sensing*, 54, 115–122.
- Brenner, A.J., and Jarvis, P.G. (1995). A heated leaf replica technique for determination of leaf boundary layer conductance in the field. *Agricultural and Forest Meteorology*, 72, 261–275.
- Briggs, W.R., and Olney, M.A. (2001). Photoreceptors in Plant Photomorphogenesis to Date. Five Phytochromes, Two Cryptochromes, One Phototropin, and One Superchrome. *Plant Physiology*, 125(1), 85–88. <https://doi.org/10.1104/pp.125.1.85>
- Bush, S.E., Hultine, K.R.J.S., Sperry, J.S., and Ehleringer, J.R. (2010). Calibration of thermal dissipation sap flow probes for ring- and diffuse-porous trees. *Tree Physiology*, 30, 1545–1554.
- Calders, K., Newnham, G., Burt, A., Murphy, S., Raumonon, P., Herold, M., Culvenor, D., Avitabile, V., Disney, M., Armston, J., and Kaasalainen, M. (2015a). Nondestructive estimates of above-ground biomass using terrestrial laser scanning. *Methods in Ecology and Evolution*, 6, 198–208. doi:10.1111/2041-210X.12301
- Calders, K., Schenkels, T., Bartholomeus, H., Armston, J., Verbesselt, J., and Herold, M. (2015b). Monitoring spring phenology with high temporal resolution terrestrial LiDAR measurements. *Agricultural and Forest Meteorology*, 203, 158–168. <https://doi.org/10.1016/j.agrformet.2015.01.009>
- Calders, K., Adams, J., Armston, J., Bartholomeus, H., Bauwens, S., Patrick Bentley, L., Chave, J., Danson, F.M., Demol, M., Disney, M., Gaulton, R., Krishna Moorthy, S.M., Levick, S.R., Saarinen, N., Schaaf, C., Stovall, A., Terry, L., Wilkes, P., Verbeeck, H. (2020). Terrestrial laser scanning in forest ecology: Expanding the horizon. *Remote Sensing of Environment*, 251, 112102. <https://doi.org/10.1016/j.rse.2020.112102>
- Casal, J.J. (2000). Phytochromes, Cryptochromes, Phototropin: Photoreceptor Interactions in Plants. *Photochemistry and Photobiology*, 71(1), 1–11. [https://onlinelibrary.wiley.com/doi/pdf/10.1562/0031-8655\(2000\)0710001PCPPII2.0.CO2](https://onlinelibrary.wiley.com/doi/pdf/10.1562/0031-8655(2000)0710001PCPPII2.0.CO2)
- Catchpole, W.R., and Wheeler, C.J. (1992). Estimating plant biomass: A review of techniques. *Australian Journal of Ecology*, 17, 121–31.
- Chapin, S.F. (1980). The Mineral Nutrition of Wild Plants. *Annual Review of Ecology and Systematics*, 11, 233–60.
- Chmielewski, F.-M. (2003). Phenology and Agriculture, In: *Phenology: An Integrative Environmental Science, Tasks for Vegetation Science*. (Ed: M.D. Schwartz) Springer, Netherlands. pp. 505–522.
- Chuine, I. (2010). Why does phenology drive species distribution? *Philosophical Transactions of the Royal Society B Biological Sciences*, 365, 3149–3160. doi:10.1098/rstb.2010.0142
- Cornelissen, J.H.C., Lavorel, S., Garnier, E., Díaz, S., Buchmann, N., Gurvich, D.E., Reich, P.B., ter Steege, H., Morgan, H.D., van der Heijden, M.G.A., Pausas, J.G., and Poorter, H. (2003). A handbook of protocols for standardised and easy measurement of plant functional traits worldwide. *Australian Journal of Botany*, 51, 335–80.
- Coutts, A.M., Harris, R.J., Phan, T., Livesley, S.J., Williams, N.S.G., and Tapper, N.J. (2016). Thermal infrared remote sensing of urban heat: Hotspots, vegetation, and an assessment of techniques for use in urban planning. *Remote Sensing of Environment*, 186, 637–651.

- CSIRO (2019). *WaterWise* webpage, Digiscape Future Science Platform website: <https://research.csiro.au/digiscape/digiscapes-projects/waterwise/>
- Demmig-Adams, B. (1990). Carotenoids and photoprotection: a role for the xanthophyll zeaxanthin. *Biochimica et Biophysica Acta*, 1020, 1–24.
- Donohue, R.J., McVicar, T.R., and Roderick, M.L. (2009). Climate-related trends in Australian vegetation cover as inferred from satellite observations. 1981–2006. *Global Change Biology*, 15(4), 1025–39.
- EU Nitrogen Expert Panel (2015). *Nitrogen Use Efficiency (NUE)—an indicator for the utilization of nitrogen in agriculture and food systems*. Wageningen University, Alterra, PO Box 47, NL-6700 Wageningen, Netherlands. <http://www.eunep.com/wp-content/uploads/2017/03/Report-NUE-Indicator-Nitrogen-Expert-Panel-18-12-2015.pdf>
- FAO (1997). Renewable biological systems for alternative sustainable energy production. *FAO Agricultural Services Bulletin*. <http://www.fao.org/docrep/w7241e/w7241e05.htm#1.2.1>
- Flanagan, L.B. (2009). Phenology of Plant Production in the Northwestern Great Plains: Relationships with Carbon Isotope Discrimination, Net Ecosystem Productivity and Ecosystem Respiration. In: *Phenology of Ecosystem Processes: Applications in Global Change Research*. Springer, New York, USA, pp. 169–185. doi:10.1007/978-1-4419-0026-5_7
- Granier, A. (1987). Evaluation of transpiration in a Douglas-Fir stand by means of sap flow measurements. *Tree Physiology*, 3, 309–319.
- Hancock, S., Armston, J., Hofton, M., Sun, X., Tang, H., Duncanson, L.I., Kellner, J.R., and Dubayah, R. (2019). The GEDI simulator: a large-footprint waveform Lidar simulator for calibration and validation of spaceborne missions. *Earth and Space Science*, 6(2), 294–310.
- Harding, D.J., Lefsky, M.A., Parker, G.G., and Blair, J.B. (2001). Laser altimeter canopy height profiles. Methods and validation for closed-canopy, broadleaf forests. *Remote Sensing of Environment*, 76, 283–297.
- Harrison, B.A., and Jupp, D.L.B. (1989). *Introduction to Remotely Sensed Data: Part ONE of the microBRIAN Resource Manual*. CSIRO, Melbourne. 156pp.
- Hartz, D.A., Prasad, L., Hedquist, B.C., Golden, J., and Brazel, A.J. (2006). Linking satellite images and hand-held infrared thermography to observed neighborhood climate conditions. *Remote Sensing of Environment*, 10, 190–200.
- Hattersley, P.W. (1983). The distribution of C3 and C4 grasses in Australia in relation to climate. *Oecologia*, 57, 113–128.
- Holzgang, O. (2001). Assessing above-ground phytomass in an alpine region using a hand-held radiometer. *Botanica Helvetica*, 111, 73–85.
- Hnatiuk R.J., Thackway R., and Walker J. (2009). Vegetation. In: *Australian Soil and Land Survey: Field Handbook* (3rd Edn). (Ed: National Committee on Soil and Terrain) pp. 73–125. CSIRO Publishing, Melbourne.
- Jones, H.G. (1992). *Plants and Microclimate*. Cambridge, Cambridge University Press.
- Jupp, D.L.B., and Lovell, J.L. (2007). *Airborne and ground-based lidar systems for forest measurement: background and principles*. CSIRO Marine and Atmospheric Research, Canberra. 151 p. <https://doi.org/10.4225/08/58615c112f355>
- Keatinge, J.D.H., Qi, A., Wheeler, T.R., Ellis, R.H., and Summerfield, R.J. (1998). Effects of temperature and photoperiod on phenology as a guide to the selection of annual legume cover and green manure crops for hillside farming systems. *Field Crops Research*, 57 (2), 139–152.
- Kramer, P.J., and Boyer, J.S. (1995). *Water relations of plants and soils*. Academic Press, San Diego. <http://dspace.udel.edu:8080/dspace/handle/19716/2830>
- Lefsky, M.A., Harding, D.J., Keller, M., Cohen, W.B., Caraba-jal, C.C., Del Bom Espirito-Santo, F., Hunter, M.O., and de Oliveira Jr., R. (2005). Estimates of forest canopy height and aboveground biomass using ICESat. *Geophysical Research Letters*, 32, L22S02. doi:10.1029/2005GL023971.
- Lehmann, E.A., Caccetta, P.A., Zhou, Z-S., McNeill, S.J., Wu, X., and Mitchell, A.L. (2012). Joint processing of Landsat and ALOS PALSAR data for forest mapping and monitoring. *IEEE Transactions on Geoscience and Remote Sensing*, 50, (1), 55–67.
- Leinonen, I., Grant, O.M., Tagliavia, C.P.P., Chaves, M.M., and Jones, H.G. (2006). Estimating stomatal conductance with thermal imagery. *Plant Cell and Environment*, 29, 1508–1518.
- Leuzinger, S., Vogt, R., and Korner, C. (2010). Tree surface temperature in an urban environment. *Agricultural and Forest Meteorology*, 150, 56–62.
- Lewis, J.M. (1995). The Story behind the Bowen Ratio. *Bulletin of the American Meteorological Society*, 76(12), 2433–2443. ftp://195.37.229.5/pub/outgoing/jwinder/BowenRatioLiterature/Lewis_BullAmeriMeteoSoc_1995.pdf
- Lim, K., Treitz, P., Wulder, M., St-Onge, B., and Flood, M. (2003). LiDAR remote sensing of forest structure. *Progress in Physical Geography*, 27, 88–106.

- Luvall, J.C., Sprigg, W.A., Levetin, E., Huete, A., Nickovic, S., Pejanovic, G.A., Vukovic, A., Van deWater, P.K., Myers, O.B., Budge, A.M., Zelicoff, A.P., Bunderson, L., Crimmins, T.M. (2011). Use of MODIS satellite images and an atmospheric dust transport model to evaluate *Juniperus* spp. Pollen phenology and dispersal. Proceedings of *WG VIII/2: Advances in Geospatial Technologies for Health, ISPRS 34*, Santa Fe, New Mexico, USA.
- Magnussen, S., and Boudewyn, P. (1998). Derivations of stand heights from airborne laser scanner data with canopy-based quantile estimators. *Canadian Journal of Forest Research*, 28, 1016–1031.
- Magnussen, S., Eggermont, P., and LaRiccia, V. (1999). Recovering tree heights from airborne laser scanner data. *Forest Science*, 45, 407–422.
- Malone, J.B., Bergquist, R., Martins, M., and Luvall, J.C. (2019). Use of Geospatial Surveillance and Response Systems for Vector-Borne Diseases in the Elimination Phase. *Tropical medicine and infectious disease*, 4(1), 15. <https://doi.org/10.3390/tropicalmed4010015>
- Martin, T.A., Hinckley, T.M., Meinzer, F.C., and Sprugel, D.G. (1999). Boundary layer conductance, leaf temperature and transpiration of *Abies amabilis* branches. *Tree Physiology*, 15, 435–443.
- Mitchell, A.L., Milne, A.K., Tapley, I., Lowell, K., Caccetta, P., Lehmann, E., and Zhou, Z-S. (2010). Wall-to-wall mapping of forest extent and change in Tasmania using ALOS PALSAR data. *Proceedings of IGARSS*, July, 2010, Hawaii.
- Mitchell, A.L., Tapley, I., Milne, A.K., Williams, M., and Lowell, K. (2012). *Radar processing methodologies for the generation of wall-to-wall mosaics*. CRC Spatial Information. <http://www.crcsi.com.au/assets/Uploads/Files/1-IFCIRA-SARproc.pdf>
- Montes, N., Gauquelin, T., Badri, W., Bertaudiere, V., and Zaoui, E.H. (2000). A non-destructive method for estimating above-ground forest biomass in threatened woodlands. *Forest Ecology and Management*, 130, 37–46.
- Muir, J., Schmidt, M., Tindall, D., Trevithick, R., Scarth, P., and Stewart, J., (2011). *Guidelines for Field measurement of fractional ground cover: a technical handbook supporting the Australian collaborative land use and management program*. Tech. rep., Queensland Department of Environment and Resource Management for the Australian Bureau of Agricultural and Resource Economics and Sciences, Canberra. http://data.daff.gov.au/data/warehouse/pe_hbgcm9abll07701/HndbkGrndCovMontring2011_1.0.0_HR.pdf
- Myneni, R.B., Keeling, C.D., Tucker, C.J., Asrar, G., and Nemani, R.R. (1997). Increased plant growth in the northern high latitudes from 1981 to 1991. *Nature*, 386(6626), 698. doi:10.1038/386698a0
- Myneni, R.B., Yang, W., Nemani, R.R., Huete, A.R., Dickinson, R.E., Knyazikhin, Y., Didan, K., Fu, R., Negrón Juárez, R.I., Saatchi, S.S., Hashimoto, H., Ichii, K., Shabanov, N.V., Tan, B., Ratana, P., Privette, J.L., Morisette, J.T., Vermote, E.F., Roy, D.P., Wolfe, R.E., Friedl, M.A., Running, S.W., Votava, P., El-Saleous, N., Devadiga, S., Su, Y., Salomonson, V.V. (2007). Large seasonal swings in leaf area of Amazon rainforests. *Proceedings of the National Academy of Science*, 104, 4820–4823.
- Næsset, E. (2002). Predicting forest stand characteristics with airborne scanning laser using a practical two-stage procedure and field data. *Remote Sensing of Environment*, 80(1), 88–99.
- Næsset, E., and Økland, T. (2002). Estimating tree height and tree crown properties using airborne scanning laser in a boreal nature reserve. *Remote Sensing of Environment*, 79, 105–115.
- Næsset, E., and Nelson, R. (2007). Using airborne laser scanning to monitor tree migration in the boreal-alpine transition zone. *Remote Sensing of Environment*, 110, 357–369.
- Nelson, J.A., and Bugbee, B. (2015). Analysis of Environmental Effects on Leaf Temperature under Sunlight, High Pressure Sodium and Light Emitting Diodes. *PloS one*, 10(10), e0138930. <https://doi.org/10.1371/journal.pone.0138930>
- Newnham, G.J., Armston, J.D., Calders, K., Disney, M.I., Lovell, J.L., Schaaf, C.B., Strahler, A.H., and Danson, F.M. (2015). Terrestrial Laser Scanning for Plot-Scale Forest Measurement. *Current Forestry Reports*, 1, 239–251. doi:10.1007/s40725-015-0025-5
- Penuelas, J., LLusia, J., Pinol, J., and Filella, I. (1997). Photochemical reflectance index and leaf photosynthetic radiation-use-efficiency assessment in Mediterranean trees. *International Journal of Remote Sensing*, 18(13), 2863–2868.
- Pérez-Harguindeguy, N., Díaz, S., Garnier, E., Lavorel, S., Poorter, H., Jaureguiberry, P., Bret-Harte, M.S., Cornwell, W.K., Craine, J.M., Gurvich, D.E., Urcelay, C., Veneklaas, E.J., Reich, P.B., Poorter, J.L., Wright, I.J., Ray, P., Enrico, L., Pausas, J.G., de Vos, A.C., Buchmann, N., Funes, G., Quétier, F., Hodgson, J.G., Thompson, K., Morgan, H.D., ter Steege, H., van der Heijden, M.G., Sack, A.L., Blonder, B., Poschlod, P., Vaieretti, M.V., Conti, G., Staver, A.C., Aquino, S., and Cornelissen, J.H.C. (2013). New handbook for standardised measurement of plant functional traits worldwide. *Australian Journal of Botany*, 61, 167–234.

- Persson, A., Holmgren, H., and Söderman, U. (2002). Detecting and measuring individual trees using an airborne Laser scanner. *Photogrammetric Engineering and Remote Sensing*, 68, 925–932.
- Rabinowitch, E.I., and Govindjee, R. (1965). The role of chlorophyll in photosynthesis. *Scientific American*, 213(1), 74–83. doi:10.1038/scientificamerican0765-74
- Rabinowitch, E., and Govindjee, R. (1969). *Photosynthesis*. Wiley, New York.
- Richardson, A.D., Anderson, R.S., Arain, M.A., Barr, A.G., Bohrer, G., Chen, G., Chen, J.M., Ciais, P., Davis, K.J., Desai, A.R., Dietze, M.C., Dragoni, D., Garrity, S.R., Gough, C.M., Grant, R., Hollinger, D.Y., Margolis, H.A., McCaughey, H., Migliavacca, M., Monson, R.K., Munger, J.W., Poulter, B., Raczka, B.M., Ricciuto, D.M., Sahoo, A.K., Schaefer, K., Tian, H., Vargas, R., Verbeeck, H., Xiao, J., Xue, Y. (2012). Terrestrial biosphere models need better representation of vegetation phenology: results from the North American Carbon Program Site Synthesis. *Global Change Biology*, 18, 566–584. doi:10.1111/j.1365-2486.2011.02562.x
- Sage, R.F. (2004). The evolution of C-4 photosynthesis. *New Phytologist*, 161, 341–370.
- Salisbury, F.B., and Ross, C. (1969). *Plant Physiology*. Wadsworth Publishing Company, Belmont.
- Schaefer, M.T. (2018). Measurement of above ground biomass. Ch 12 in *Effective Field Calibration and Validation Practices: A practical handbook for calibration and validation satellite and model-derived terrestrial environmental variables for research and management*. Version 1.3. TERN Australia, ISBN 978-0-646-94137-0.
- Schenk, T., Seo, S., and Csatho, B. (2001). Accuracy study of airborne laser scanning data with photogrammetry. International Archives of Photogrammetry and Remote Sensing, Volume XXXIV, Part 3/W4. Pp. 113–118 in *Land Surface Mapping and Characterization Using Laser Altimetry*, ISPRS III/3 and III/6 Workshop, Annapolis, MD.
- Schmidt, M., Carter, J., Stone, G., and O'Reagain, P. (2016). Integration of Optical and X-Band Radar Data for Pasture Biomass Estimation in an Open Savannah Woodland. *Remote Sensing*, 8, 989. doi:10.3390/rs8120989
- Schwartz, M.D. (Ed) (2013). *Phenology: An Integrative Environmental Science*. 2nd Edn. Springer Verlag, The Netherlands. 610p. doi:10.1007/978-94-007-6925-0
- Schwinning, S., and Weiner, J. (1998). Mechanisms determining the degree of size asymmetry in competition among plants. *Oecologia*, 113, 447–455.
- Smith, F.C. (1993). Evergreen vs. Deciduous Woody Plants: Which Wins Where. *Maine Naturalist*, 1(4), 205–212.
- Straile, D. (2002). North Atlantic Oscillation synchronizes food-web interactions in central European lakes. *Proceedings of the Royal Society of London B Biological Sciences*, 269, 391–395. doi:10.1098/rspb.2001.1907
- Sullivan, J.A., and Deng, X.W. (2003). From seed to seed: the role of photoreceptors in Arabidopsis development. *Developmental Biology*, 260(2), 289–297. [https://doi.org/10.1016/S0012-1606\(03\)00212-4](https://doi.org/10.1016/S0012-1606(03)00212-4)
- Tackenberg, O. (2007). A New Method for Non-destructive Measurement of Biomass, Growth Rates, Vertical Biomass Distribution and Dry Matter Content Based on Digital Image Analysis. *Annals of Botany*, 99(4), 777–83.
- Taiz, L., Zeiger, E., Moller, I.M., and Murphy, A. (2015). *Plant Physiology and Development*. 6th edn online. Sinauer Associates. www.plantphys.net
- Tanaka, T., Yamaguchi, J., and Takeda, Y. (1998). Measurement of forest canopy structure with a laser plane range-finding method—development of a measurement system and applications to real forests. *Agricultural and Forest Meteorology*, 91, 149–60.
- Tarnopolsky, M., and Seginer, I. (1999). Leaf temperature error from heat conduction along thermocouple wires. *Agricultural and Forest Meteorology*, 93, 185–194.
- TERN Australia (2018). *Effective Field Calibration and Validation Practices: A practical handbook for calibration and validation satellite and model-derived terrestrial environmental variables for research and management*. A TERN Landscape Assessment Initiative, NCRIS. ISBN 978-0-646-94137-0. <https://www.tern.org.au/NEW-CalVal-handbook-for-remote-sensing-bgp4370.html>
- Thursby, G.B., Chintala, M.M., Stetson, D., Wigand, C., and Champlin, D.M. (2002). A rapid, non-destructive method for estimating aboveground biomass of salt marsh grasses. *Wetlands*, 22, 626–30.
- Tomasel, F.G., Paruelo, J.M., Abras, G., Ballarin, V., and Moler, E. (2001). A chromaticity-based technique for estimation of above-ground plant biomass. *Applied Vegetation Science*, 4, 207–212.
- Udompetaikul, V., Upadhyaya, S.K., Slaughter, D., Lampinen, B., and Shackel, K. (2011). Plant Water Stress Detection Using Leaf Temperature and Microclimatic Information. *Proceedings of 2011 ASABE Annual International Meeting*. Paper 1111555, 7–10 August, Louisville.

- Vermeire, L.T., and Gillen, R.L. (2001). Estimating herbage standing crop with visual obstruction in tallgrass prairie. *Journal of Range Management*, 54, 57–60.
- Vitousek, P. (1982). Nutrient Cycling and Nutrient Use Efficiency. *The American Naturalist*, 119(4), 553–572.
- Yokozawa, M., and Hara, T. (1995). Foliage Profile, Size Structure and Stem Diameter-Plant Height Relationship in Crowded Plant Populations. *Annals of Botany*, 76, 271–285.
- Zehm, A., Nobis, M., and Schwabe, A. (2003). Multiparameter analysis of vertical structure based on digital image processing. *Flora*, 198, 142–160.
- Zhang, Q., Li, Q., and Zhang, G. (2012). Rapid determination of leaf water content using VIS/NIR Spectroscopy Analysis with Wavelength Selection. *Journal of Spectroscopy*, 27, 93–105.

6 Attributes of Plant Communities

Plants tend to grow with friends, and individual species are frequently found in association with a predictable range of friends, through both facilitative and competitive mechanisms. Groups of plants can be characterised by a number of attributes such as their species composition, their spacing, their foliage volume, their canopy texture and colour, and their dynamics (see Section 2.3.1).

Often in vegetation science there is a need to more formally define plant communities into a classification scheme, so that the classification can serve as a surrogate for biodiversity (Margules and Pressey, 2000). Typically, the primary goal is to arrange a set of observations into groups based on various floristic and environmental attributes, many of which are discussed in this section. The groups have several purposes, but a common purpose in this context is to serve as a mapping classification scheme (see Section 2.3.1). The methods for creating the groups in the classification scheme can be directed by expert knowledge, numerical analysis, or some combination of both (De Caceres and Wiser, 2012). Expert knowledge employs *a priori* subjective knowledge to manually devise the groups and allocate observations to those groups. Numerical methods typically employ some form of supervised or unsupervised clustering approach, which group observations by analysing pattern and structure in the community attribute data (usually floristics and/or environmental information; see Volume 2E for details of classification methods).

Various methods have been devised to sample vegetation communities. Such methods are often based on quadrats, predefined areas within which vegetation attributes of a small number of plants are measured to infer traits that are representative of the larger population (see Volume 2D—Section 12). Quadrats are sometimes located along a sampling transect. Detailed guidelines for vegetation surveys in Australia are provided in Hnatiuk *et al.* (2009) and Muir *et al.* (2011).

The following sub-sections describe attributes of plant communities that are relevant to EO analyses:

- formations—combinations and permutations of different plants (see Section 6.1);
- horizontal spacing and pattern—layout of plants (see Section 6.2);
- density and cover—number and spread of plants (see Section 6.3);
- canopy colour and texture—how plant canopies blend (see Section 6.4);
- growth stages and phenology—how plants age and interact with seasonal variations (see Section 6.5); and
- succession—how associations change with time (see Section 6.6).

If we concentrate on any one particular species our impression will be one of flux and hazard, but if we concentrate on total community properties (such as biomass in a given trophic level) our impression will be of pattern and steadiness.
(May, 1974)

6.1 Formations

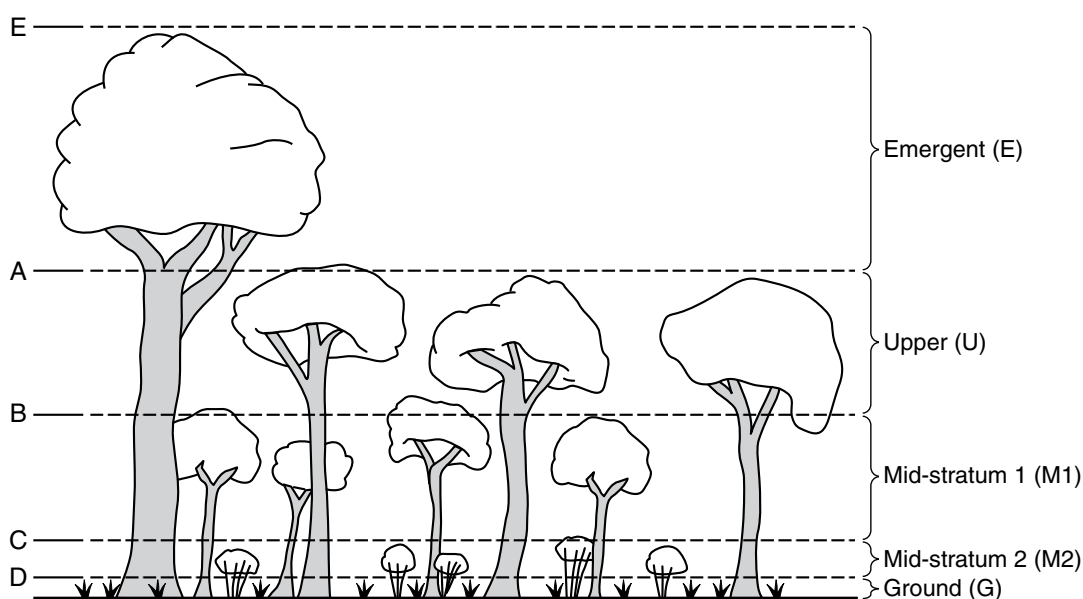
Floristic composition, or association, indicates the variety of botanical species within a particular community. While botanical classification of individual plants involves visual comparison with standardised descriptive keys, which rely on both structural and floristic characteristics (see Section 5.1), structural classification of groups of plants is largely based on their growth form, vertical stratification, and spacing.

Any vegetation grouping can contain multiple growth forms, such as trees and ground covers, which tend to coexist as discrete layers or strata, with the tallest, or upper, stratum often typifying the group (see Figure 5.1). A hierarchical Australian system of classifying vegetation type on the basis of structural and floristic attributes was presented by Hnatiuk *et al.*, (2009) and is summarised in Table 6.1. In this system, the broad floristic formation is defined by, and named after, the major species or genera that characterise the dominant stratum. In the nomenclature of NVIS (see Section 2.3.1), an association expands on the broad floristic formation to nominate three dominant or co-dominant species in each stratum (see Table 2.7).

Many vegetation classification systems stratify the vertical distribution of plants into height classes, where vegetation layers, or strata, are defined to differentiate between and within growth forms (see Table 6.2 and Figure 6.1). Such categories are relative to each association rather than corresponding to predefined heights.

Vegetation height is often correlated with biome, being an indication of both climatic extremes and edaphic resources. Since the diverse range of biomes in Australia complicates the task of defining absolute height classes, relative classes, which can be consistent within regional assessment areas, are recommended (NCST, 2009). An Australian implementation of relative height classes is given in Table 6.3. An integrated, structural classification that has been developed using optical and microwave datasets to map biomass across Australia is described in Excursus 6.1.

Figure 6.1 Height strata



Source: Hnatiuk *et al.* (2009) Figure 8

Table 6.1 Vegetation formations

Vegetation Attributes	Vegetation Category		
	Formation	Structural Formation	Broad Floristic Formation
Life form (woody/non-woody)	✓	✓	✓
Crown separation	✓	✓	✓
Crown type		✓	✓
Growth forms in each stratum		✓	✓
Height of each stratum		✓	✓
Foliage cover of lower stratum		✓	✓
Cover and height of emergents		✓	✓
Characteristic species of dominant stratum			✓
Example	Dense woody plants	Very tall, dense trees	Very tall, dense <i>Eucalyptus</i> trees

Source: Hnatiuk *et al.* (2009)**Table 6.2** Height strata

Stratum	Description	Example
Emergent	Tallest plants above canopy, which may be dominant layer in sparse vegetation	E
Upper or Dominant	Vegetation forming canopy layer that has greatest ecological impact is generally the tallest stratum	U
Middle	Vegetation between canopy and ground layer when present	M1 M2
Ground	Vegetation close to ground and is usually < 2 m (may be the dominant layer, as in grasslands).	G

Adapted from Hnatiuk *et al.* (2009)**Table 6.3** Height classes

Height (m)		Life Form	
Min	Max	Woody	Non-Woody
50	–	Giant	–
35	50	Extremely tall	–
20	35	Very tall	–
10	20	Tall	–
5	10	Medium	Giant
2	5	Low	Extremely tall
1	2	Dwarf	Very tall
0.5	1	Miniature	Tall
0.25	0.5	Micro	Medium
0.05	0.25	Nano	Low
–	0.05	–	Dwarf

Source: Hnatiuk *et al.* (2009)

Excursus 6.1—Vegetation Height and Structure Map

Source: Scarth *et al.* (2019)**National structure map:** <http://auscover.org.au/purl/icesat-vegetation-structure>**Biomass library:** <http://www.auscover.org.au/purl/biomass-plot-library>**Further information:** <https://www.tern.org.au/satellite-eye-on-australias-vegetation/>

A detailed national map of vegetation structure (height and cover) has been developed for Australia based on EO datasets (see Table 6.4). This 30 m resolution structure map of Australian forest and woodland structure was derived from:

- Landsat TM/ETM+ imagery (30 m resolution; dry season 1987–2010) processed to Foliage Projective Cover (FPC);
- ALOS (Advanced Land Observing System) PALSAR (Phased Arrayed L-band Synthetic Aperture Radar) L-band Fine Beam Dual (HH and HV) mosaic product (25 m resolution) for 2010; and
- ICESat (Ice, Cloud and land Elevation satellite) GLAS (Geoscience Laser Altimeter System) L2 GLA14 (Global Land Surface Altimetry), acquired 2003–2009.

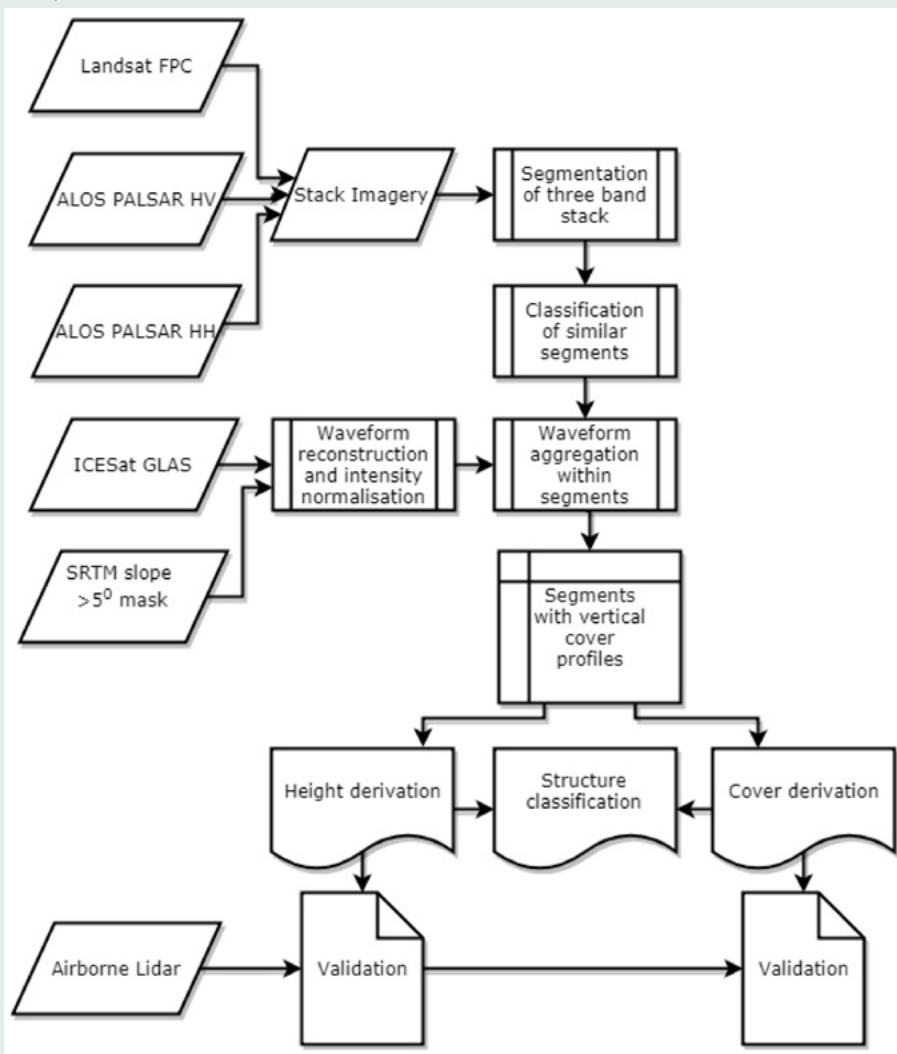
Table 6.4 Summary of structural classes

Structural formations used in the national structure map are adapted from NVIS (DEWR, 2007), Specht (1970), and Specht and Specht (1999)—see Section 2.3.1 and Table 2.6.

Lifeform and height of tallest stratum	Foliage Projective Cover (FPC) or Crown Cover (CC) of the tallest plant layer			
	Dense (70–100% FPC; > 80% CC)	Mid-dense (30–70% FPC; 50–80% CC)	Sparse (10–30% FPC; 20–50% CC)	Very Sparse/Isolated (< 10% FPC; 0.25–20% CC)
Trees > 30 m	Tall closed forest	Tall open forest	Tall woodland	Tall open woodland
Trees 10–30 m	Closed forest	Open forest	Woodland	Open woodland
Trees 5–10 m	Low closed forest	Low open forest	Low woodland	Low open woodland
Shrubs 2–8 m	Closed scrub	Open scrub	Tall shrubland	Tall open shrubland
Shrubs 0–2 m	Closed heath	Open heath	Low shrubland	Low open shrubland

Source: Scarth *et al.* (2019)

Figure 6.2 Processing overview



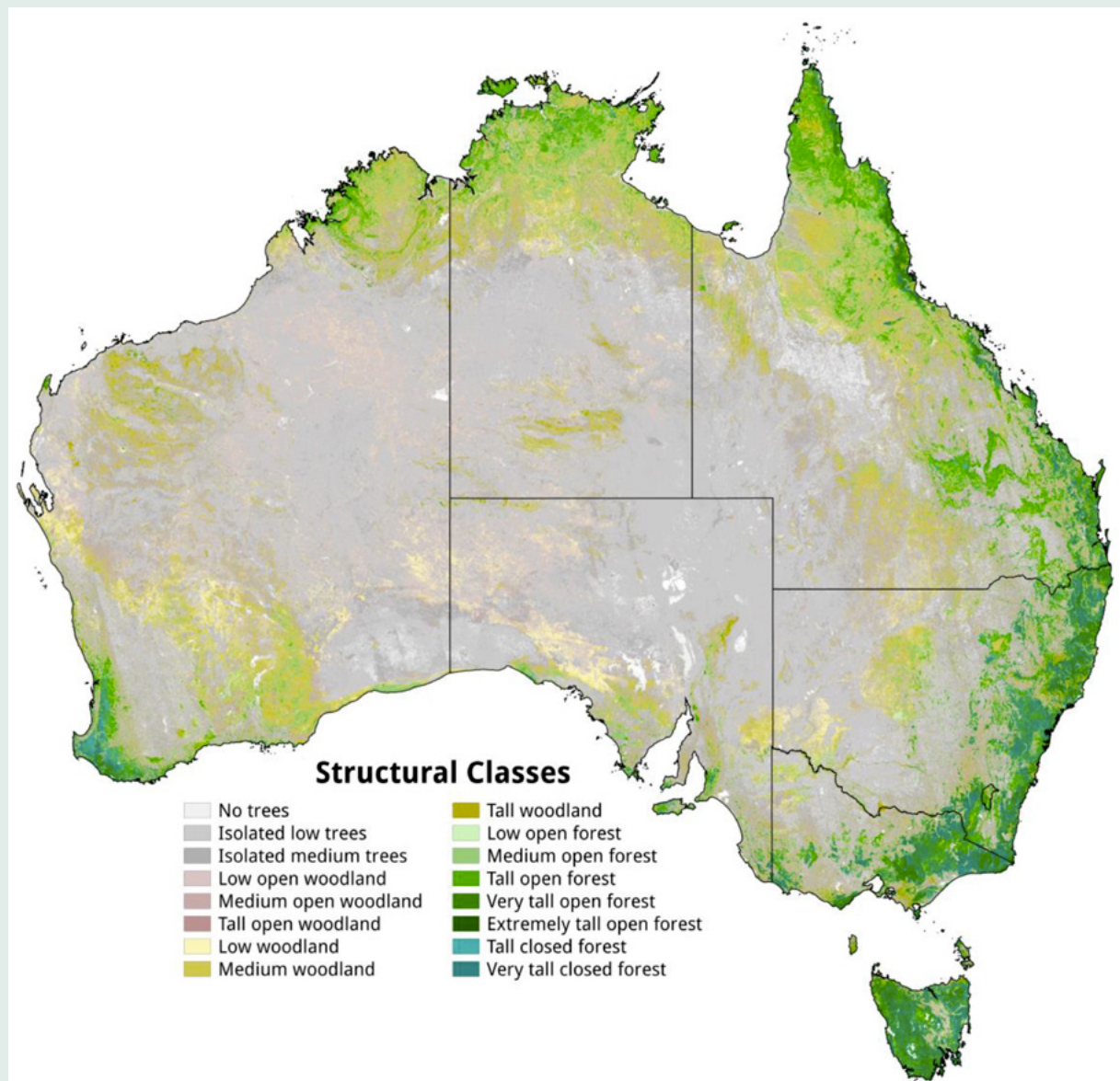
Source: Scarth *et al.* (2019) Figure 3

ALOS PALSAR data were integrated with Landsat-derived FPC data to produce a unique segmentation of the landscape into regions with similar vegetation structure. These regions were classified and associated with vertical plant profiles derived from ICESat GLAS waveforms to characterise vegetation height. Airborne lidar data was used to validate a range of forest structural types. The processing steps are summarised in Figure 6.2, with the resulting map being shown in Figure 6.3.

The Biomass library was constructed by methodically collating tree level data from over 15,000 plots located in all states, comprising over 1 million diameter measurements of individual trees. The biomass of each tree was estimated using a suite of allometric equations (Paul *et al.*, 2016, 2019) and biomass estimates for each plot were scaled to a per hectare metric. Both the structure map and the National Biomass Library are available online from TERN Australia (see Section 6.7).

Figure 6.3 Vegetation height and structure

Vertical plant profiles for the Australian continent, including height, cover, age class, and L-band backscatter characteristics based on the ICESat and Landsat time series and ALOS PALSAR datasets.



Source: Scarth *et al.* (2019) Figure 11

6.2 Horizontal Spacing and Pattern

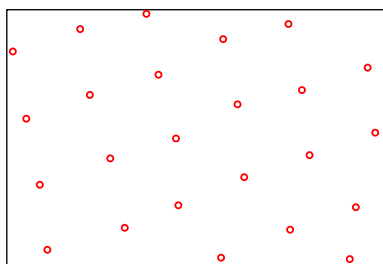
Spacing of plants depends on their frequency and arrangement. Frequency indicates the likelihood of locating a particular species at a specific location and is indicative of its abundance. Estimates of species frequency are determined using field sampling of presence/absence counts within quadrats. Since frequency is often related to vegetation pattern and density, it can be misrepresented by quadrat methods when the quadrat size is inappropriate. The horizontal pattern formed by plants can be generalised into three types:

- random—unpredictable spacing, often resulting from wind dispersal of seed;
- regular—uniform distribution, usually resulting from controlled planting by *Homo sapiens*; or
- clumped—common for seedlings growing near a seed plant (see Figure 6.4).

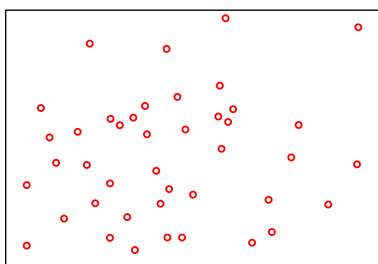
Most natural vegetation associations create random or clumped patterns, such as uneven-aged forests, resulting from a continuous cycle of plant establishment and senescence. After a major disturbance however, such as a fire, natural regeneration can be arranged in random clumps of uniform age. By contrast, man-made forests are often planted in a regular pattern at one time, forming an even-aged forest, in which the range of tree ages is generally within 20% of the rotation age. The underlying pattern of plants directly influences the canopy texture (see Section 6.4).

Figure 6.4 Population distribution patterns

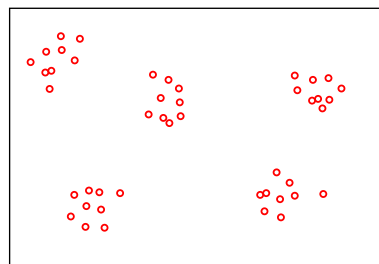
a. Regular distribution



b. Random distribution



c. Clumped distribution



Source: Yerpo, Wikimedia Commons. (Retrieved from http://en.wikipedia.org/wiki/Species_distribution#mediaviewer/File:Population_distribution.svg)

6.3 Density and Cover

Vegetation density indicates the number of individual plants per unit area. Cover is the proportion of ground occupied by vegetation. Given the overlapping nature of vegetation, the combined cover for all plants in a given area can exceed 100%. Vegetation cover can be estimated from field sampling, aerial photography, or satellite imagery. Traditional measures of vegetation cover include foliage cover (see Section 6.3.1), cover-abundance (see Section 6.3.2), leaf area index (LAI—see Section 6.3.3), fraction of absorbed photosynthetically active radiation (fAPAR—see Section 6.3.4), basal area (BA—see Section 6.3.5), and fractional cover (see Section 6.3.6).

6.3.1 Foliage cover

Foliage cover, or leaf density, represents the amount of photosynthetic material, or biomass, of green vegetation within a given area. This has been measured in various ways, some of which include both foliage and branches, rather than just foliage. The term foliage cover is often reserved for estimates of foliage (and branch) material in ground layer vegetation (Hnatiuk *et al.*, 2009).

Some traditionally used measures attempt to estimate cover on the basis of vertical projection, that is, the proportion of ground beneath plants that would be shaded when the Sun is directly overhead:

- Foliage Cover %—the percentage of a sample site covered by the vertical projection of foliage (and branches for woody vegetation; Carnahan, 1977)
- Foliage Projective Cover (FPC)—the proportion of ground covered by the vertical projection of foliage only (Specht *et al.*, 1974).

These measures involve estimation of the extent of ground shadowing resulting from overhead foliage and have proved to be variable between estimators. More recent measures of vegetation density have attempted to reduce the subjectivity of field measurements by focusing on crown extent, rather than the foliage density. Within a defined sample area, % crown cover records the percentage of area covered by a vertical projection of the crown and is the recommended measure for plants higher than 1.5 m (Hnatiuk *et al.*, 2009). The Crown Separation Ratio (CSR; Walker *et al.*, 1988; Penridge and Walker, 1988) is computed as:

$$\text{CSR} = \frac{\text{mean distance between crowns}}{\text{mean crown width}}$$

This is best measured separately for each vegetation stratum and assumes approximately circular crowns. When measured in accordance with guidelines, CSR is directly related to crown cover %. Estimates of foliage density can subsequently be incorporated to convert crown projection estimates to foliage projection estimates. This process typically involves matching the actual tree crowns to photos of crown openness (Hnatiuk *et al.*, 2009):

$$\% \text{ foliage cover} = \% \text{ crown cover} \times \text{crown type}$$

The term foliage cover is often reserved for estimates of foliage (and branch) volume in ground layer vegetation (Hnatiuk *et al.*, 2009). For a measured distance, % foliage cover is the percentage covered by the vertical projection of plant material.

6.3.2 Cover-abundance

Cover-abundance estimates the quantity of individual species in a given sample area. The Braun-Blanquet Cover-Abundance Scale (Mueller-Dombois and Ellenberg, 1974) is commonly used to record vegetation cover-abundance on the basis of either:

- cover estimate—where vegetation covers more than 5% of the sample area; or
- plant count—when vegetation cover is less than 5%.

This method has been shown to be more efficient than density sampling methods, especially for baseline studies such as environmental impact analyses (Wikum and Shanholtzer (1978).

6.3.3 Leaf area index (LAI)

Leaf Area Index (LAI) attempts to quantify the extent of leaf overlap so varies with plant growth. It represents the total area of leaves (one-sided) projecting into a given vertical column and is computed as:

$$\text{LAI} = \frac{\text{total leaf area (one surface)}}{\text{ground area}}$$

This dimensionless parameter is considered to characterise the interface between canopy and atmosphere. Since the area of foliage that can intercept solar radiation essentially drives the microclimates within and beneath canopies, LAI is also indicative of canopy energy exchange processes, water interception and transpiration rates, and stand productivity (Bréda, 2003; see Section 7).

LAI estimates have traditionally required destructive, time-consuming sampling of leaves (see Section 5.1.2). Direct and semi-direct methods of measuring leaf area are reviewed by Bréda (2003). Indirect methods include the use of optical instruments that measure radiation transmission through the canopy, which can be subsequently converted to Plant Area Index (PAI) or Surface Area Index (SAI). Both of these measures implicitly include both foliage and woody elements of the canopy. Where multiple optical instruments are available, the canopy gap fraction (“the fraction of view that is unobstructed by canopy in any particular direction”; Welles and Cohen, 1996) can be computed (Schaefer *et al.*, 2018). PAI/LAI estimates can also be derived using terrestrial laser scanning (Jupp *et al.*, 2009; Strahler *et al.*, 2008; see Excursus 5.1).

LAI is used to model the growth and yield of crops and forests (see Sections 12, 14, and 16). Many methods for deriving LAI assume that leaves are randomly distributed, so do not consider clumping or overlapping arrangements that commonly occur in nature. LAI models also need to consider the impact of leaf size (relative to the canopy extent) and leaf orientation, since these factors vary in different types of vegetation and modify how much radiation is transmitted through the canopy (Hill *et al.*, 2006a, 2006b). Various adjustments have been proposed for these factors (such as Chen *et al.*, 1997), but many authors recommend use of direct LAI measurements to calibrate any indirect estimates of canopy LAI in Australian ecosystems (Coops *et al.*, 2004; Schaefer *et al.*, 2018). Further, given the vertical leaf inclination of most *Eucalyptus* species, projective foliage cover has demonstrated closer correlation with some satellite-based LAI products than indirect LAI estimates (Hill *et al.*, 2006a).

Given the functional link between LAI and the spectral reflectance of plant canopies, numerous techniques have been developed to derive LAI estimates from EO data (see Section 8.1). Procedures for validating LAI products derived from satellite imagery are detailed in Schaefer *et al.* (2018).

6.3.4 Fraction of absorbed photosynthetically active radiation (fAPAR)

Photosynthetically Active Radiation (PAR) is defined as EMR with wavelengths in the range 400–700 nm and includes both direct and diffuse light. Incident PAR represents the amount of PAR that reaches the top of a vegetation canopy. As detailed in Volume 1A, this varies with geographic location, season and atmospheric conditions. The Intercepted PAR (IPAR) is the amount of PAR reaching layers within the canopy as the light penetrates through the top layer. The amount of light that is actually absorbed by vegetation is called Absorbed PAR (APAR). The fraction of APAR (fAPAR) indicates the proportion of PAR that is absorbed by all vegetation layers within a canopy and is commonly estimated from transmittance measurements using the generalised relationship:

$$fAPAR = \frac{APAR}{PAR}$$

fAPAR includes:

- photosynthetically active vegetation components (PAV)—mostly chloroplasts;
- non-photosynthetically active vegetation components (NPV)—mostly senescent foliage, branches, and stems; and
- non-photosynthetic components in leaves—veins and cell walls (Xiao *et al.*, 2004).

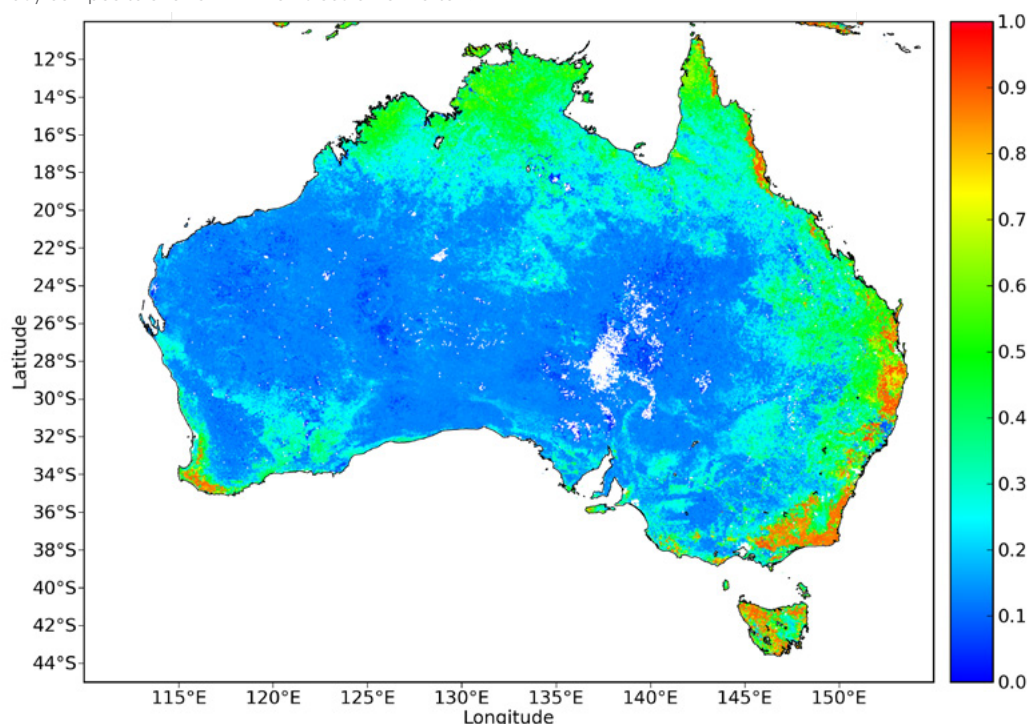
Thus, fAPAR is the proportion of PAR absorbed by both photosynthetic (PAV) and non-photosynthetic (NPV) components of vegetation:

$$fAPAR = fAPAR_{PAV} + fAPAR_{NPV}$$

It should be noted that the proportion of fAPAR deriving from PAR varies in different ecosystems. For example, in communities with sparse canopies, such as savannas and shrublands, $fAPAR_{NPV}$ can increase fAPAR by 10% to 40% (Asner *et al.*, 1998). Accordingly, transmittance measurements may need to be taken at different heights within different ecosystems (Restrepo-Coupe *et al.*, 2018). fAPAR can be viewed as representing the energy absorption capacity of a vegetation community (Fensholt *et al.*, 2004) and is frequently expressed as a function of LAI (Baret and Guyot, 1991; Myneni and Williams, 1994; Ruimy *et al.*, 1994, 1999). fAPAR can also be derived using quantum sensors, directional measurements, or three-dimensional models of canopy optics. fAPAR estimates can be impacted by solar zenith angle, diffuse radiation levels, canopy architecture, and variations in soil albedo (Gower *et al.*, 1999). Methods for validating fAPAR products derived from EO imagery are reviewed by Baret *et al.* (2013) and Schaefer *et al.* (2018). An example of an EO-based fAPAR map of Australia is shown in Figure 6.5.

Figure 6.5 Fraction of Absorbed Photosynthetically Active Radiation (fAPAR)

fAPAR derived from MODIS/Terra imagery (LPDAAC MOD15A2 mosaic) acquired between 1 and 8 January 2016 (inclusive). This gridded 8-day composite shows fAPAR on a scale from 0 to 1.



Source: TERN AusCover. (Retrieved from <http://www.auscover.org.au/purl/lpdaac-mosaic-mod15a2-v5>)
AusCover is the remote sensing data products facility of the Terrestrial Ecosystem Research Network (TERN; <http://www.tern.org.au>)

6.3.5 Basal area (BA)

Forest development can be characterised by its canopy, the combined leaves, twigs, and branches of all tree crowns in a stand, or the stand structure, the size and frequency of stems within a given area. Measurement of the latter is readily achievable and directly related to timber production (see Section 16.5). Tree volume is also indicative of carbon stores and woody biomass (see Section 17).

Basal area (BA), or cross-sectional area, indicates the proportion of area occupied by the base of a plant, such as a tree trunk, and is computed as:

$$\text{BA} = \frac{\text{sum of trunk areas at breast height}}{\text{ground area}}$$

Basal area has been traditionally computed from manual measurements of individual trees using a calibrated tape measure or caliper at a trunk height of 1.3 m (or 1.4 m in some countries⁷). Estimates of basal area can also be derived using lidar instruments (see Excursus 5.1 and Volume 1A—Section 15.1). When combined with laser altimetry, surface lidar instruments enable accurate canopy structure measurements to be derived for forests (see Excursus 6.1 and Section 16).

6.3.6 Fractional cover

Functionally, all vegetative material can be described as either photosynthetic—green, photosynthesising leaves—or non-photosynthetic—dead plant material (above ground), woody material, and litter (Guerschman *et al.*, 2009). Many sparsely vegetated landscapes, such as savanna and grassland ecosystems, can simplistically be classified in terms of three ground components:

- photosynthetic vegetation;
- non-photosynthetic vegetation; and
- bare ground (soil, gravel, rock).

Fractional cover represents the ground area covered by each of these components as a percentage of a given area. Since the structure and scale of vegetation is closely tied to water and energy balance in these landscapes, estimates of fractional cover are valuable for a range of analyses relating to carbon and nutrient uptake, water and energy cycling, and fire and erosion potential (see Sections 7 and 9.1).

Traditionally, fractional cover estimates have been derived from ground-based measurements “using a variety of qualitative and quantitative approaches centred on plots or transects, where the locations have been chosen to be representative of vegetation communities, ecosystem types or management practices” (Scarth *et al.*, 2018). However, more recently, accurate estimates of fractional cover can be determined from EO imagery, where individual image pixels form the area unit for which vegetation fractions are estimated (see Excursus 8.3).

6.4 Canopy Colour and Texture

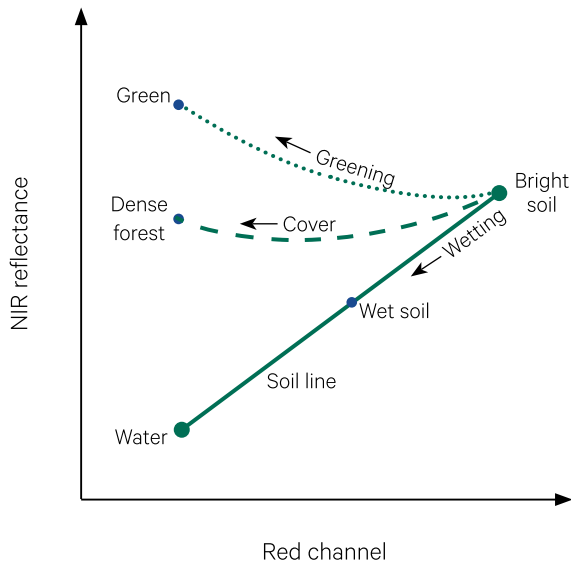
Both the colour and texture of a vegetation canopy are indicative of plant type(s), density, age, and condition. The composite ‘colour’ of a canopy is readily summarised in EO imagery, with each reflectance measurement being integrated over the area of an optical pixel (see Volume 1B—Section 1.2). As detailed in Section 4 above, the canopy reflectance in particular wavelengths can be indicative of the vegetation composition, condition, density, structure, and/or age. For example, when the spectral characteristics of surface features are plotted on a crossplot of red versus NIR reflectance, green vegetation forms a characteristic triangular shape (Kauth and Thomas, 1976; see Section 8.1.1). Bare soil typically plots in a line along the base of the vegetation triangle while vegetation plots above the soil line, with its greenness and cover determining distance from the line (see Figure 6.6).

Monitoring the changes in canopy colour through time can differentiate between vegetation with varying phenological cycles and allow vegetation types to be identified more accurately (see Section 9.2). For example, vegetation that stays green throughout the year is characterised by smaller annual variations in colour than deciduous or annual vegetation (see Section 9.1).

The imaged texture within a canopy is directly dependent on image scale relative to the plant crown diameter (see Volumes 1 and 2). Textural variations within a canopy can be indicative of changes to vegetation condition or structure (see Volume 2C—Section 6.1). Textural characteristics within an EO image can also be exploited to delineate individual tree crowns and estimate biomass (Cabello-Leblic, 2018).

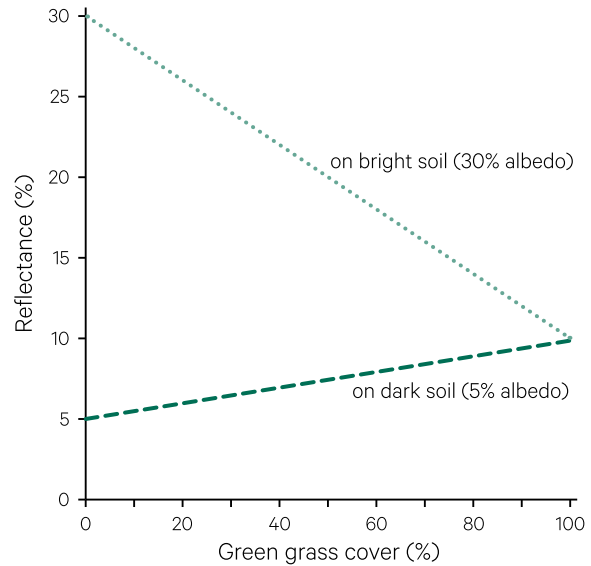
⁷ Breast height is fixed at 1.3 m in Australia, UK, Canada and continental Europe, and at 1.4 m in the USA, New Zealand, Burma, India, Malaysia and South Africa.

Figure 6.6 Vegetation cover triangle



Source: Harrison and Jupp (1990) Figure 92

Figure 6.7 Simulated reflectance for increasing grass cover



Adapted from: McVicar *et al.* (2002)

When a vegetation canopy is not continuous, the ‘colour’ measured by a remote sensor will result from a blend of the vegetation colour and the background colour (see Volume 1B—Section 6.6). As such, different densities of vegetation cover will appear as different ‘colours’ when grown on different coloured soils. One example of the impact of soil colour on the reflectance from a grassy ground cover is provided by McVicar *et al.* (2002) based on work by Roderick *et al.* (2000). Using an unshaded, Lambertian surface, the variations in albedo were modelled as grass cover (with 10% albedo) increased on both light and dark soils. As illustrated in Figure 6.7, while full grass cover produces the same canopy reflectance on both soil colours, the gradations from full cover to bare soil resulted in markedly different reflectances, both in terms of the overall reflectance values for equivalent partial grass coverage and the rate of reflectance change between gradations. In this simulation, a 20% increase in green grass cover raised the overall albedo by 1% on dark soil, but the same increase in grass cover resulted in a 4% decrease in total albedo on bright soil.

While this model simplifies many aspects of imaging a real canopy, it demonstrates the reality of composite reflectance interactions within an EO pixel. The relative reflectance range corresponding to increased grass cover on dark soil is effectively narrower than the corresponding range on bright soil. This situation is particularly relevant to selecting the radiometric resolution required to detect a given gradation of change in canopy density. As detailed in Table 6.5, an 8% variation in grass cover on dark soil would vary the imaged reflectance by 1 digital number in 8-bit data, whereas only 2% variation in grass cover on bright soil would result in the same difference in imaged reflectance values. Again, while these simulated figures do not account for many of the complexities involved with imaging with remote sensors, they rightly indicate the discriminatory advantages of sensors with increased radiometric resolution (see Volume 1B—Section 1).

Table 6.5 Effect of sensor quantisation on radiometric sensitivity

Quantisation	Number of grey levels	Precision (1/level)	Change in green grass cover (%)	
			On dark soil	On bright soil
7 bit	128	0.007813	15.63	3.91
8 bit	256	0.003906	7.812	1.953
10 bit	1024	0.000977	1.954	0.489
12 bit	4096	0.000244	0.488	0.122

Source: McVicar *et al.* (2002)

The transfer of EMR through a vegetative canopy has been simulated by radiative transfer modelling, which uses information about the shape, size, and density of plants to determine how incoming radiation

is reflected, absorbed, or transmitted by the canopy (see Volume 1B—Section 5). Analyses of sub-pixel components to derive fractional cover estimates are described in Sections 8.3.

6.5 Growth Stages

Within a group of plants, a growth stage describes the prevalent life cycle development phase. Various growth stages have been defined for different types of plants. For example, the following five stages are commonly used to describe the growth of Australian native vegetation (Hnatiuk *et al.*, 2009):

- early regeneration—small juvenile plants of variable density, possibly associated with occasional older, emergent plants;
- advanced regeneration—well-developed immature plants of variable density, generally not reproducing;
- uneven age—reproducing plants of mixed size and age, often forming two or more vertical strata;
- mature—reproducing plants at maximum height with full, healthy crowns; and
- senescent—over-mature plants showing signs of aging.

These stages are typically sampled for the dominant vegetation type and condition at each sample site. For forests, leaf area and twig volume tend to stabilise during early growth stages, so that wood growth is the major component of increased biomass for older forests (see Section 16). Environmental disturbances, such as fire or windthrow, often trigger the demise of an aging generation of plants and assist the establishment of the next generation. For example, the timing of growth stages for a eucalypt forest could be described as:

- disturbance, germination and early growth: 0–5 years;
- saplings and regrowth: 5–100 years;
- mature: 100–250 years; and
- senescent: > 250 years (Jacobs, 1955).

Other factors driving the cyclic nature of vegetation succession are detailed in Section 6.6.

6.6 Succession

Previous sections have introduced the concepts of the life cycle for individual plants (see Section 5.3) and growth stage assessment for groups of plants (see Section 6.5). Like all forms of life, plants age, and their form and interactions with the environment change as they age. Ecological succession considers how plants establish, thrive, and reproduce at particular locations through time and attempts to identify those factors that determine both their survival and their successors.

The term ‘primary succession’ is used to describe the process of succession on pristine, bare earth, possibly resulting from lava flows, whereas ‘secondary succession’ follows a disturbance to a previously vegetated site, as might occur after fire, flood, or landslide. Secondary succession is more common than primary succession, and also more rapid due to the presence of seed and organic matter, taking decades for grasslands or centuries for forests, rather than millennia.

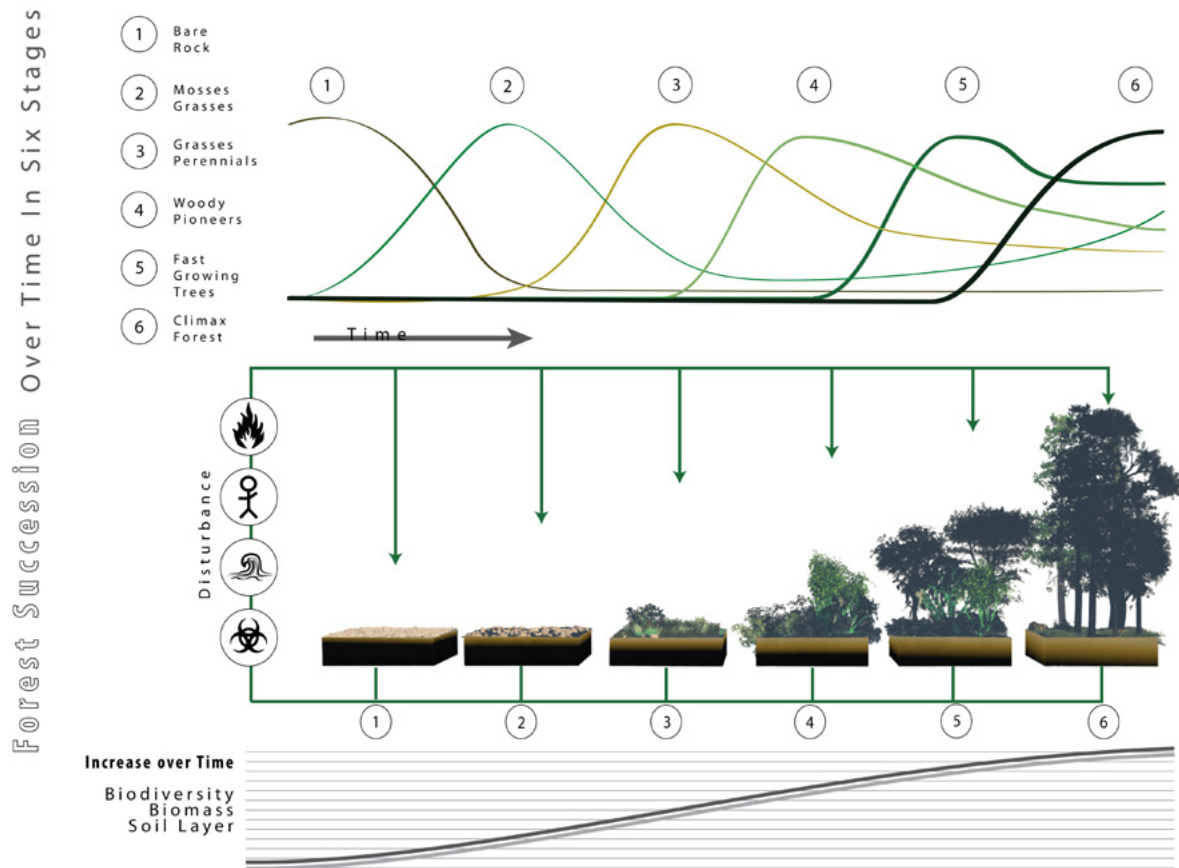
The general mechanism of succession was described by Clements (1916) in terms of six transitional phases:

1. nudation—starting point is a bare site resulting from disturbance or natural history;
2. migration—propagules arrive to enable plant establishment;
3. ecesis—vegetation establishes and grows;
4. competition—between growing and reproducing plants for space, light, and nutrients;
5. reaction—environmental changes resulting from presence of plants; and
6. stabilisation—climax community when plant interactions are in equilibrium with environment.

This process typically involves a wide range of species, some of which are best suited to rapidly colonising new areas with low nutrient levels (pioneer species), followed by a series of transitional species with increasingly more complex structures and requirements (seral species), until finally a stable, but not static, community is formed (climax species). For example, the factors involved with forest succession are illustrated in Figure 6.8.

Figure 6.8 Forest succession

An abstract diagram showing forest succession over time. Increase in biomass, biodiversity and soil thickness are also shown, as well as the fluctuation of different plant communities over the process of succession.



Source: Lucas Martin Frey, Wikimedia Commons. (Retrieved from http://upload.wikimedia.org/wikipedia/commons/4/41/Forest_succession_depicted_over_time.png)

Ecological theory implies that the climax community is balanced, independent, and resilient. This phase could theoretically continue indefinitely without external disturbance and is characterised by stability in terms of energy input and output, nutrient uptake and recycling, and species composition (Clements, 1916; Tansley, 1935; Whittaker, 1953). Nature, however, does not always comply with theories so, while succession is continuous in any situation, the neatly defined phases may not always be apparent or spatially coherent at a given location or instance in time (Connell and Slatyer, 1977). A mature forest, for example, can comprise a patchwork of communities at varying stages of succession. In concert with increasing vegetation cover and height through primary succession, richer and deeper soils are slowly

formed until climax communities occur on 'mature' soils. The interrelationships between temperature and moisture in the processes of vegetation and soil succession can be seen to underlie many climatic classification systems (see Sections 1 and 2.2.3).

An understanding of succession underlies ecosystem dynamics and is important for assessing and managing any vegetation resource (see Section 7). As the structural complexity of successive stages increases, the capacity of a vegetation community to provide a greater range of habitats and food sources for fauna also increases. The successional stage of a vegetation community can thus be indicative of faunal composition and diversity, and provide valuable information for managing a range of terrestrial resources.

*An understanding of ecological succession provides a basis for resolving man's conflict with nature.
(Odum, 1969)*

6.7 Further Information

Field Guides

NCST (2009)

TERN Australia (2018)

Guerschman *et al.* (2018)

Ecology

Pianka, E.R. (2011). *Evolutionary Ecology*. 7th Edn. Eric R. Pianka.

Miller, G.T.Jr, and Spoolman, S.E. (2009). *Essentials of Ecology*, 5th edn. Brooks/Cole Cengage Learning. ISBN-13: 978-0-495-55795-1 https://www.academia.edu/40164243/Essentials_of_Ecology

Vegetation Height and Structure Map of Australia

National structure map: <http://auscover.org.au/purl/icesat-vegetation-structure>

Biomass library: <http://www.auscover.org.au/purl/biomass-plot-library>

6.8 References

- Asner, G.P., Wessman, C.A., and Archer, S. (1998). Scale Dependence of Absorption of Photosynthetically Active Radiation in Terrestrial Ecosystems. *Ecological Applications*, 8, 1003–1021. doi:10.1890/1051-0761(1998)008[1003:SDOAP]2.0.CO;2
- Baret, F., and Guyot, G. (1991). Potentials and limits of vegetation indices for LAI and APAR assessment. *Remote Sensing of Environment*, 35, 161–173. [https://doi.org/10.1016/0034-4257\(91\)90009-U](https://doi.org/10.1016/0034-4257(91)90009-U)
- Baret, F., Weiss, M., Lacaze, R., Camacho, F., Makhmara, H., Pacholczyk, P., and Smets, B. (2013). GEOV1: LAI and FAPAR essential climate variables and FCOVER global time series capitalizing over existing products. Part 1: Principles of development and production. *Remote Sensing of Environment*, 137, 299–309.
- Bréda, N.J.J. (2003). Ground-based measurements of leaf area index: a review of methods, instruments and current controversies. *Journal of Experimental Botany*, 54 (392), 2403–2417.
- Cabello-Leblic, A. (2018). Tree crown delineation. Ch 11 in *Effective Field Calibration and Validation Practices: A practical handbook for calibration and validation satellite and model-derived terrestrial environmental variables for research and management*. A TERN Landscape Assessment Initiative, NCRIS. ISBN 978-0-646-94137-0.
- Carnahan, J.A. (1977). 'Natural Vegetation' map with commentary. *Atlas of Australian Resources, Second Series*. Department of Natural Resources, Canberra.
- Chen, J.M., Rich, P.M., Gower, S.T., Norman, J.M., and Plummer S. (1997). Leaf area index of boreal forests: theory, techniques and measurements, *Journal of Geophysical Research*, 102(D24), 29429–29443.
- Clements, F.E. (1916). *Plant Succession: Analysis of the Development of Vegetation*. Carnegie Institution of Washington Publication Sciences. <http://dx.doi.org/10.5962/bhl.title.56234>
- Connell, J.H., and Slatyer, R.O. (1977). Mechanisms of Succession in Natural Communities and Their Role in Community Stability and Organization. *The American Naturalist*, 111(982), 1119–1144.
- Coops, N.C., Smith, M.L., Jacobsen, K.L., Martin M., and Ollinger, S. (2004). Estimation of plant and leaf area index using three techniques in a mature eucalypt canopy, *Austral Ecology*, 29, 332–341.
- De Caceres, M., and Wiser, S.K. (2012). Towards consistency in vegetation classification. *Journal of Vegetation Science*, 23, 387–393.
- Fensholt, R., Sandholt, I., and Rasmussen, M.S. (2004). Evaluation of MODIS LAI, fAPAR and the relation between fAPAR and NDVI in a semi-arid environment using *in situ* measurements. *Remote Sensing of Environment*, 91(3–4), 490–507.
- Gower, S.T., Kucharik, C.J., and Norman, J.M. (1999). Direct and Indirect Estimation of Leaf Area Index, fapar and Net Primary Production of Terrestrial Ecosystems, *Remote Sensing of Environment*, 70, 29–51.
- Guerschman, J.P., Hill, M.J., Renzullo, L.J., Barrett, D.J., Marks, A.S., and Botha, E.J. (2009). Estimating fractional cover of photosynthetic vegetation, non photosynthetic vegetation and bare soil in the Australian tropical savannah region upscaling Hyperion and MODIS sensors. *Remote Sensing of Environment*, 113, 928–945.

- Guerschman, J., Leys, J., Rozas Larraondo, P., Henrikson, M., Paget, M., and Barson, M. (2018). *Monitoring groundcover: an online tool for Australian regions*. CSIRO, Canberra. <https://doi.org/10.25919/5bf84026e556d>
- Harrison, B.A., and Jupp, D.L.B. (1990) *Introduction to Image Processing: Part TWO of the microBRIAN Resource Manual*. CSIRO, Melbourne. 256 p.
- Hill, M.J., Senarath, U., Lee, A., Zeppel, M., Nightingale, J.M., Williams, R., and McVicar, T.R. (2006a). Assessment of the MODIS LAI product for Australian ecosystems, *Remote Sensing of Environment*, 101, 495–518.
- Hill, M.J., Held, A.A., Leuning, R., Coops, N.C., Hughes, D., and Cleugh, H.A. (2006b). MODIS spectral signals at a flux tower site: Relationships with high-resolution data, and CO₂ flux and light use efficiency measurements. *Remote Sensing of Environment*, 103, 351–368.
- Hnatiuk R.J., Thackway R., and Walker J. (2009). *Vegetation*. In: *Australian Soil and Land Survey: Field Handbook* (3rd edn). (Ed: National Committee on Soil and Terrain) pp. 73–125. CSIRO Publishing, Melbourne.
- Jacobs, M. (1955). *Growth Habit of the Eucalypts*. CSIRO, Canberra. (Reprinted in 1986 by IFA).
- Jupp, D.L.B., Culvenor, D.S., Lovell, J.L., Newnham, G.J., Strahler, A.H., and Woodcock, C.E. (2009). Estimating forest LAI profiles and structural parameters using a ground-based laser called ‘Echidna®’. *Tree Physiology*, 29, 171–181.
- Kauth, R.J., and Thomas, G.S. (1976). The Tasselled Cap—a graphic description of the spectral-temporal development of agricultural crops as seen by Landsat. *Proceedings of Symposium on Machine Processing of Remotely Sensed Data*. Purdue University, West Lafayette, Indiana, 4B41-4B51. http://docs.lib.purdue.edu/lars_symp/159
- McVicar, T.R., Davies, P.J., Qinke, Y., and Zhang, G. (2002). An Introduction to Temporal-Geographic Information Systems (TGIS) for Assessing, Monitoring and Modelling Regional Water and Soil Processes. In *Regional Water and Soil Assessment for Managing Sustainable Agriculture in China and Australia* (Eds: T.R. McVicar, Li Rui, J. Walker, R.W. Fitzpatrick, and Liu Changming) ACIAR Monograph No. 84, 205–223.
- Margules, C.R., and Pressey, R.L. (2000). Systematic conservation planning. *Nature*, 405, 243–253.
- May, R.M. (1974). *Stability and Complexity in Model Ecosystems*. 2nd edn. Princeton University Press, Princeton, New Jersey.
- Mueller-Dombois, D., and Ellenberg, H. (1974). *Aims and methods of vegetation ecology*. John Wiley and Sons, New York.
- Muir, J., Schmidt, M., Tindall, D., Trevithick, R., Scarth, P., and Stewart, J. (2011). *Guidelines for Field measurement of fractional ground cover: a technical handbook supporting the Australian collaborative land use and management program*. Tech. rep., Queensland Department of Environment and Resource Management for the Australian Bureau of Agricultural and Resource Economics and Sciences, Canberra. http://data.daff.gov.au/data/warehouse/pe_hbgcm9abl107701/HndbkGrndCovMontring2011_1.0.0_HR.pdf
- Myneni, R.B., and Williams, D.L. (1994). On the relationship between FAPAR and NDVI. *Remote Sensing of Environment*, 49, 200–211. [https://doi.org/10.1016/0034-4257\(94\)90016-7](https://doi.org/10.1016/0034-4257(94)90016-7)
- NCST (2009). *Australian Soil and Land Survey Field Handbook*. 3rd edn. National Committee on Soil and Terrain, CSIRO, Canberra. 264 p.
- Odum, E.P. (1969). The Strategy of Ecosystem Development. *Science*, 164(3877), 262–270.
- Paul, K. I., Roxburgh, S. H., Chave, J., England, J. R., Zerihun, A., Specht, A., Lewis, T., Bennett, L. T., Baker, T. G., Adams, M. A., Huxtable, D., Montagu, K. D., Falster, D. S., Feller, M., Sochacki, S., Ritson, P., Bastin, G., Bartle, J., Wildy, D., Hobbs, T., Larmour, J., Waterworth, R., Stewart, H. T., Jonson, J., Forrester, D. I., Applegate, G., Mendham, D., Bradford, M., O’Grady, A., Green, D., Sudmeyer, R., Rance, S. J., Turner, J., Barton, C., Wenk, E. H., Grove, T., Attiwill, P. M., Pinkard, E., Butler, D., Brooksbank, K., Spencer, B., Snowdon, P., O’Brien, N., Battaglia, M., Cameron, D. M., Hamilton, S., McAuthur, G., and Sinclair, J. (2016). Testing the generality of above-ground biomass allometry across plant functional types at the continent scale. *Global Change Biology*, 22 (6), 2106–2124. doi:10.1111/gcb.13201
- Paul, K., Larmour, J., Specht, A., Zerihun, A., Ritson, P., Roxburgh, S., Sochacki, S., Lewis, T., Barton, C.V.M., England, J.R., Battaglia, M., O’Grady, A.P., Pinkard, E.A., Applegate, G., Jonson, J., Brooksbank, K., Sudmeyer, R., Wildy, D.T., Montagu, K., Bradford, M.G., Butler, D.W., and Hobbs, T. (2019). Testing the generality of below-ground biomass allometry across plant functional types. *Forest Ecology and Management*, 432, 102–114. doi:10.1016/j.foreco.2018.08.043
- Penridge, L., and Walker, J. (1988). The crown-gap ratio and crown cover: derivation and simulation study. *Australian Journal of Ecology*, 13, 1090–1120.

- Restrepo-Coupe, N., Huete, A., and Davies, K. (2018). Satellite Phenology Validation. Ch 9 in *Effective Field Calibration and Validation Practices: A practical handbook for calibration and validation satellite and model-derived terrestrial environmental variables for research and management*. A TERN Landscape Assessment Initiative, NCRIS. ISBN 978-0-646-94137-0.
- Roderick, M.L., Chewings, V., and Smith, R.C.G. (2000). Remote sensing in vegetation and animal studies. In *Field and Laboratory Methods for Grassland and Animal Production Research*. (Eds: L. Mennetje and R.M. Jones) Wallingford UK, CABI, pp. 205–225.
- Ruimy, A., Saugier, B., and Dedieu, G. (1994). Methodology for estimation of terrestrial net primary production from remotely sensed data. *Journal of Geophysical Research*, 99, 5263–5283. <https://doi.org/10.1029/93JD03221>
- Ruimy, A., Kergoat, L., Bondeau, A., and Potsdam NPP Model Intercomparison Participants. (1999). Comparing global models of terrestrial net primary productivity (NPP): analysis of differences in light absorption and light-use efficiency. *Global Change Biology*, 5 (Suppl. 1), 56–64. doi:10.1046/j.1365-2486.1999.00007.x
- Scarath, P., Guerschman, J.P., Clarke, K., and Phinn, S. (2018). Validation of Australian Fractional Cover Products from MODIS and Landsat Data. Ch 7 in *Effective Field Calibration and Validation Practices: A practical handbook for calibration and validation satellite and model-derived terrestrial environmental variables for research and management*. A TERN Landscape Assessment Initiative, NCRIS. ISBN: ISBN 978-0-646-94137-0. <https://www.tern.org.au/NEW-CalVal-handbook-for-remote-sensing-bgp4370.html>
- Scarath, P., Armston, J., Lucas, R., and Bunting, P. (2019). A Structural Classification of Australian Vegetation Using ICESat/GLAS, ALOS PALSAR, and Landsat Sensor Data. *Remote Sensing*, 11(2), 147. <https://doi.org/10.3390/rs11020147>
- Schaefer, M.T., Farmer, E., Soto-Berelov, M., Woodgate, W., and Jones, S. (2018). Overview of ground based techniques for estimating LAI. Ch 6 in *AusCover Good Practice Guidelines: Effective Field Calibration and Validation Practices: A practical handbook for calibration and validation satellite and model-derived terrestrial environmental variables for research and management*. A TERN Landscape Assessment Initiative, NCRIS. ISBN 978-0-646-94137-0.
- Specht, R.L., and Specht, A. (1999). *Australian plant communities : dynamics of structure, growth and biodiversity*. Oxford University Press, Melbourne. ISBN 019553705X
- Specht, L., Roe, E., and Boughton, V. (eds) (1974). Conservation of major plant communities in Australia and Papua New Guinea. *Australian Journal of Botany Supplement*, 7.
- Strahler, A.H., Jupp, D.L.B., Woodcock, C.E., Schaaf, C.B., Yau, T., Zhau, F., Yang, X., Lovell, J., Culvenor, D., Newnham, G., Ni-Miester, W., and Boykin-Morris, W. (2008) Retrieval of forest structural parameters using a ground-based lidar instrument (Echidna®). *Canadian Journal of Remote Sensing*, 34(2), S426–S440.
- Tansley, A.G. (1935). The use and abuse of vegetational concepts and terms. *Ecology*, 16, 284–307.
- TERN Australia (2018). *Effective Field Calibration and Validation Practices: A practical handbook for calibration and validation satellite and model-derived terrestrial environmental variables for research and management*. A TERN Landscape Assessment Initiative, NCRIS. ISBN 978-0-646-94137-0. <https://www.tern.org.au/NEW-CalVal-handbook-for-remote-sensing-bgp4370.html>
- Walker, J., Crapper, P., and Penridge, L. (1988). The crown-gap ratio I and crown cover: the field study. *Australian Journal of Ecology*, 13, 101–108.
- Welles, J.M., and Cohen, S. (1996). Canopy structure measurement by gap fraction analysis using commercial instrumentation. *Journal of Experimental Botany*, 47(9), 1335–1342. <https://doi.org/10.1093/jxb/47.9.1335>
- Whittaker, R.H. (1953). A consideration of climax theory: the climax as a population and pattern. *Ecological Monographs*, 23(1), 41–78. <https://doi.org/10.2307/1943519>
- Wikum, D.A., and Shanholtzer, G.F. (1978). Application of the Braun-Blanquet Cover-Abundance Scale for Vegetation Analysis in Land Development Studies. *Environmental Management*, 2(4), 323–329.
- Xiao, X., Zhang, Q., Braswell, B., Urbanski, S., Boles, S., Wofsy, S., Moore III, B., and Ojima, D. (2004). Modeling gross primary production of temperate deciduous broadleaf forest using satellite images and climate data. *Remote Sensing of Environment*, 91, 256–270. doi:10.1016/j.rse.2004.03.010



7 Attributes of Ecosystems

The concept of an ecosystem—comprising all biotic and abiotic factors in an environment—is introduced in Section 1.2.3. The distribution of a species and the productivity of an ecosystem both depend on the success or failure of individual plants, while the success or failure of each plant largely results from the influence of the environment on the rates of its vital processes (see Section 5). Vegetation is thus a delicate integrator of environmental conditions and can be viewed as indicative of those conditions (Billings, 1970).

The interactions that exist between an organism and its environment are both complex and interrelated—or ‘holocoenotic’. The various environmental factors described in Section 1.1 not only interact with the organism but also among themselves. As such, it is difficult to isolate and change one part of the environment without affecting the other parts; should the normal pattern of one factor be altered, the others will also change until a comparable balance is achieved. Conversely, while vegetation establishment needs certain environmental prerequisites, once this has happened further modification to the environment may then occur as the vegetation exerts its influence on the locality.

Given the gradual changes that often occur between ecosystems, it can be difficult to precisely define their boundaries and extent (Kessell, 1979). Gradual changes in soil moisture, elevation, humidity, and soil

fertility typically result in corresponding changes in vegetation height, density, and species composition. For example, a major factor driving woody vegetation change in Australia is soil fertility, with poor soils typically supporting open (dry sclerophyll) forest, better soils supporting tall open (wet sclerophyll) forests, and high fertility soils supporting rainforests (IFA, 1985).

The following sub-sections consider measurable properties of ecosystems in terms of:

- biodiversity (see Section 7.1);
- stability and equilibrium (see Section 7.2);
- function and condition (see Section 7.3);
- productivity (see Section 7.4);
- energy balance (see Section 7.5); and
- water balance (see Section 7.6)

The unique features that define individual ecosystem types are scale-dependent. The four key elements of an ecosystem type may be organised on spatial, temporal and thematic scales. Spatially, ecosystems vary in extent and grain size from water droplets to oceans, with boundaries delimited physically or functionally. Temporally, ecosystems may develop, persist and change over time frames that vary from hours to millennia. They appear stable at some temporal scales, while undergoing trends or fluctuations at others. Thematic scale refers to similarity of features within and between ecosystems, their degree of uniqueness in composition and processes, which may be depicted hierarchically.

(Keith et al., 2013)

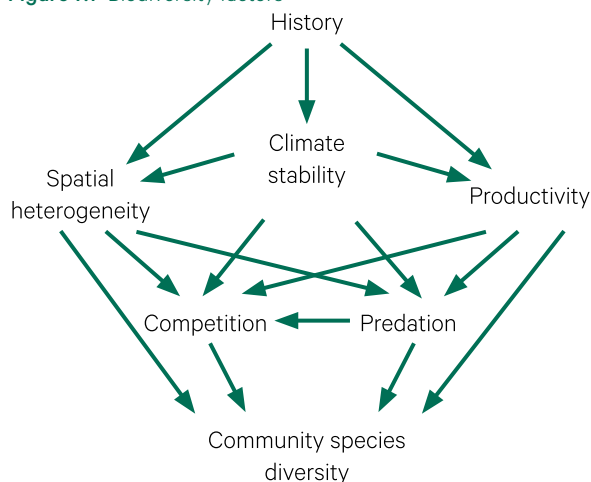
7.1 Biodiversity

Section 1 above introduced the integrated nature of ecology. The interactions between environmental factors and plant genetics result in a diverse range of combinations and permutations of species within plant associations and communities in nature. The extent of heterogeneity may not always be apparent, with variations still occurring in the chemical composition of foliage when species composition and density appear to be homogeneous. Such variations are particularly relevant to herbivores whose distribution and abundance is directly related to forage quality (Youngtob *et al.*, 2012).

Terrestrial biodiversity tends to be greatest near the equator and decreases towards the polar regions, forming latitudinal gradients (see Section 1.3). While a wide range of indicators of biodiversity have been proposed (see Section 3.4.1), species diversity is a commonly used measure. A greater range of species in a community results in a greater range of resources for consumers. Many environmental factors, such as climatic stability, predation, and competition, contribute to species diversity, and can interact in complex ways (Pianka, 1971; see Figure 7.1).

Species richness (or species density) refers to the number of species present in a given area. The relative importance of individual species, however, is not always based on abundance, and can vary both within and between communities and ecosystems. Species diversity encapsulates the concepts of species density and relative importance and represents the likelihood of predicting the species of a randomly selected individual. In a monoculture, for example, species diversity is low since it would be easy to predict the species for any individual.

Figure 7.1 Biodiversity factors



Adapted from: Pianka (1971)

While increased ecosystem diversity has traditionally been considered to coincide with greater ecological stability and resilience (MacArthur, 1955), recent studies have suggested that relatively simple ecosystems are more likely to be stable than complex ones. In some ecosystem models, the likelihood of achieving a stable equilibrium point actually decreased with increases in the number of species, the strength of interaction between species, and the frequency of that interaction (May, 1973). Empirical studies both support and reject this hypothesis. Studies based on vegetation diversity suggest that more complex communities stabilised ecosystem processes and were more resilient after perturbations, such as drought, but did not stabilise population processes, with reduced interannual biomass variability for higher biodiversity (Tilman, 1996; Tilman *et al.*, 1998). In contrast, herbivore populations appeared to be more stable when feeding on a restricted range of species (Watt, 1968). It should be noted that the concept of equilibrium also varies with spatial scale (see Section 7.2). The use of EO datasets to monitor global and Australian biodiversity is detailed in Section 19.

Resilience and transformation are not opposites. They can be complementary. Maintaining resilience at one scale can require transformational changes at other scales. ... Resilience includes knowing when an unwanted transformation is inevitable and instead deliberately transforming all or parts of the system such that the new system delivers what is valued and wanted. ... It's about learning where not to go rather than perfectly controlling where to go.
(Walker, 2020)

7.2 Stability and Equilibrium

Ecosystems and landscapes constantly change. As part of the natural cycle of our environment, plants grow, water courses change, soil moves and air circulates—the environment keeps changing. Natural disasters, such as fire, flood, drought, and tectonic activity can impose massive and sudden changes on landscapes and ecosystems (see Section 1.1.2.3). Earth's inhabitants, who are all part of the ecosystem, superimpose other changes, such as land clearing, cropping or afforestation, urban developments, mining, dam building, and other engineering works. The sum total of all these changes is a very dynamic planet (see Section 1.3.3).

Landscape disturbances can result from natural and anthropogenic causes (see Section 3.4.1). When changes occur suddenly, both the cause and impact are clearly evident. However, when changes are gradual, the driving factors can be more difficult to identify. One of the challenges for observing landscape dynamics is the lack of a clear baseline which defines 'stability' or 'balance'. Indeed, both the rate and extent of 'normal' landscape changes differ in different ecosystems, with some ecosystems rapidly recovering from major disturbances, and others showing scars for extended periods.

Separating the effects of 'natural' disturbance from anthropogenic changes presents a further challenge in many landscapes (see Section 15). More recently, ecosystem changes have been described by their impact on human populations. This perspective considers ecosystems in terms of the services they deliver and encourages sustainable management of resources in order to maintain those ecosystem services (see Section 20.3).

An ecosystem is a dynamic complex of plant, animal, and microorganism communities and the nonliving environment interacting as a functional unit.
(MEA, 2005)

Coupled with landscape stability is the concept of equilibrium. As introduced in Section 6.6, ecological succession assumes that plant communities progressively establish themselves on a given site until a state of equilibrium is achieved between competing components. This view of the landscape was accepted for most of the twentieth century, with agricultural management regimes aiming to maintain equilibrium by defining appropriate capacities for grazing animals and/or crop rotations. While the linear succession model can be observed to apply to some vegetated landscapes, it has been found wanting in resource-limited environments such as drylands, where plant growth is controlled by abiotic factors (see Section 15).

Excursus 7.1 introduces some equilibrium and non-equilibrium models that have been developed to simulate ecosystem dynamics in grazed landscapes.

An ecosystem functions by continually cycling energy and materials through living organisms that grow, reproduce and then die. This cycling of energy and materials through living organisms has evolved in response to a mix of disturbances (e.g. fires or floods), stresses (e.g. droughts or diseases) and ecological interactions (e.g. competition or predation) over millions of years. Recent changes in the frequency and intensity of these disturbances and stresses raises important issues about the ability of species and ecosystems to survive and adapt.
(DEWHA, 2010)

Excursus 7.1—Modelling Grazed Landscapes

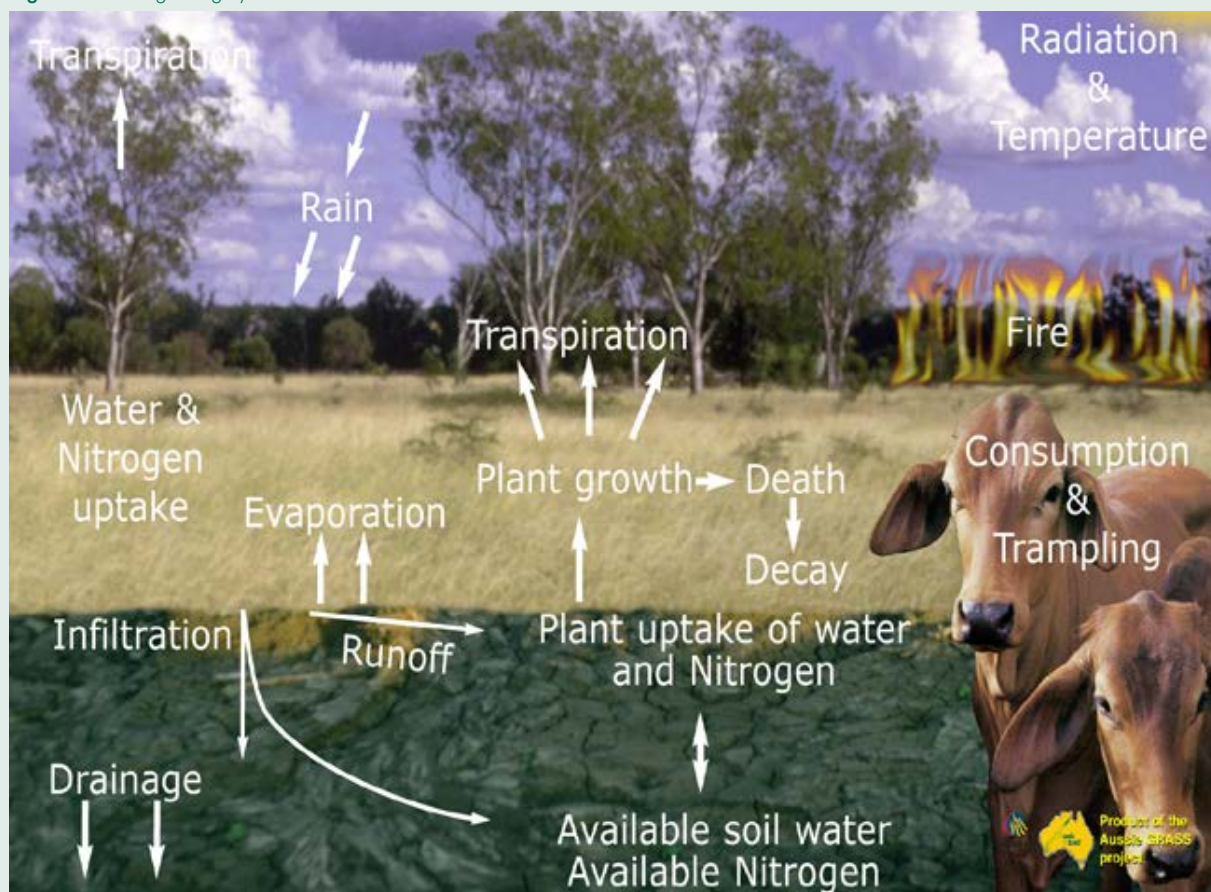
The grazing system in grasslands and rangelands can be represented as the interaction of multiple environmental factors as illustrated in Figure 7.2. The traditional view of ecosystem dynamics assumes an equilibrium state as the endpoint of succession, which is maintained by the interactions between its components (see Section 7.3). This situation applies where plant growth is mostly constant over time, with continuous consumption by herbivores.

However, drylands, which occupy most of the Australian continent, are landscapes with complex environmental interactions, where plant growth rate is strongly controlled by rainfall, which is highly variable in both space and time. In these landscapes the equilibrium theory has proven to be inadequate for predicting the likely outcomes of natural or

anthrogenic disturbances (Stringham *et al.*, 2003). As an alternative, a non-equilibrium framework has been used to conceptualise vegetation dynamics in terms of multiple successional pathways and steady states, change thresholds, and discontinuous and irreversible transitions (Westoby *et al.*, 1989; Stringham *et al.*, 2003).

Characteristics of equilibrium and non-equilibrium modelling frameworks are summarised in Table 7.1. In a non-equilibrium system the carrying capacity of the system is too dynamic for close tracking between the climate and populations, since rather than cycles being limit-driven, they are controlled by abiotic factors. Most rangeland ecosystems occupy an intermediate position somewhere between equilibrium and non-equilibrium behaviour.

Figure 7.2 The grazing system



Source: McKeon and Carter (2015) Figure 1.1

For example, over the past century, a series of ecological models have been applied to rangeland environments around the world (see Table 7.2). For most of the twentieth century, “the rangelands were viewed as equilibrium systems potentially disturbed by grazing” (Pickup *et al.*, 1994), with the corollary that equilibrium could be restored by adjusting carrying capacity (Illius and O’Connor, 1999). Range models assume that the species composition of plant communities results from the opposing forces of plant succession and grazing intensity. In this modelling context, grazing is viewed as slowing, stopping, or reversing secondary succession, such that plant communities are produced that differ in species composition from the historical climax plant community, which would represent the single reference (equilibrium) point (Briske *et al.*, 2005, 2017). However, the expansion of woody weeds could not be reversed by the removal of grazing (Westoby *et al.*, 1989) and during prolonged droughts plant production and livestock numbers were rarely balanced. These observations led to the adoption of a non-equilibrium approach for modelling rangelands. Indeed, recent evidence suggests that grazing and other disturbances can disrupt the natural state for decades after grazing is removed (Sims *et al.*, 2019).

Humans interact with nature through the use of simplified and incomplete perceptions of its structure, interrelationships, and dynamics.
(Briske *et al.*, 2017)

Table 7.1 Equilibrium versus nonequilibrium systems

Characteristic	Equilibrium system	Nonequilibrium system
Ecological metaphor	‘Balance of nature’	‘Flux of nature’
Abiotic patterns	Relatively constant	Stochastic/variable
Plant-herbivore interactions	Tight coupling	Weak coupling
	Biotic regulation	Abiotic drivers
Population patterns	Density dependence	Density independence
	Populations track carrying capacity	Dynamic carrying capacity limits population tracking
Community/ecosystem	Competitive structuring	Competition not expressed
	Internally regulated	External drivers

Adapted from: Briske *et al.* (2017) Table 6.1

By comparison, the State-and-Transition Modelling (STM) approach to managing natural resources considers the complexities of vegetation dynamics under a variable climate with changing stressors, such as grazing and fire (see Table 7.3 for terminology). Although originally introduced as ‘management language’ rather than ecological theory, STM models are now widely used to understand ecosystem response to disturbances in rangeland environments and can represent all known or anticipated stable states that may occupy a given site (Briske *et al.*, 2017). While STM theory accommodates discontinuous and non-reversible vegetation change and is relevant to many grazed savanna land types, it may be inadequate for the more arid and semi-arid regions experiencing highly variable, often episodic, rainfall with consequent unpredictable vegetation responses under grazing. Moreover, its conceptual nature means that the framework often fails to adequately deal with the spatial realities of paddock heterogeneity and uneven grazing distribution (Ash *et al.*, 1994). Nonetheless, STM models are useful both in terms of organising data and portraying landscape function.

Table 7.2 Rangeland management models

Name	Description	Metric	References
Range model	Envisioned vegetation dynamics to occur along a single axis on which grazing intensity linearly counteracts secondary succession	Range condition rating derived from comparison of species composition with a reference site, which is used to infer production goals and ecological assessments	Dyksterhuis (1949) Joyce (1993)
Non-equilibrium persistent model	Livestock maintain equilibrium with forage in key resource areas but may not do so when forage is abundant in the wet season	Rainfall variability metric defined the non-equilibrium point	Ellis and Swift (1988) Illius and O’Conner (1999)
State-and-Transition model	Organised as a collection of all recognised or anticipated stable states that individual ecological sites may support	Change direction of ecological indicators used to modify state resilience	Westoby <i>et al.</i> (1989) Bestelmeyer <i>et al.</i> (2017) Stringham <i>et al.</i> (2003)

Source: Briske (2017)

Table 7.3 State-and-Transition model terms

Term	Definition
State	A state is a recognisable, resistant, and resilient complex of two components, the soil base and the vegetation structure. The vegetation and soil components are necessarily connected through integrated ecological processes which interact to produce a sustained equilibrium that is expressed by a specific suite of vegetative communities.
Ecological indicators	Characteristics or attributes of phenomena that are being monitored, that is, inventoried over time.
Trend	Overall temporal or spatial trajectory of an indicator, statistically measured in terms of direction, strength, and rate.
Benchmark	A benchmark reference, or standard, is a baseline value of a measurement indicator by which an indicator can be compared and judged.
Disturbance	Discrete event in time, such as drought or fire, that significantly reduces the abundance of a natural resource and can be characterised in terms of the magnitude of its impact.
Transitions	A trajectory of system change away from the current stable state that is triggered by natural events, management actions, or both. The primary difference between the reversible and irreversible property of a transition is defined by the ability or inability of the system to repair itself.
Threshold	Boundary in space and time between any and all states, or along irreversible transitions, such that one or more of the primary ecological processes has been irreversibly changed and must be actively restored before return to a previous state is possible.
Resilience	Capacity of a system to return to a former configuration following a disturbance, that is, how far a system can be displaced from equilibrium before return to equilibrium is precluded. Ecological resilience is the degree, manner and pace of recovery of indicators after a disturbance.
Resistance	Capacity of a system to remain unchanged by a disturbance, that is, it indicates the ability of a system to remain at or near its equilibrium condition by maintaining control of its ecological processes.
Feedback mechanisms	Ecological processes that influence the rate of change among system variables.

Source: Stringham *et al.* (2003); Briske *et al.* (2017); Washington-Allen and Ravi (2012)

A good example of the practical application of STM to rangeland management in Australia, including monitoring, is the Grazing Land Management (GLM) package (DAFF, 2013). GLM provides guidelines to assist northern beef producers in understanding and better managing their grazing practices. ‘Grazing land condition’ is defined as “the capacity of land to respond to rain and produce useful forage, and is a measure of how well the grazing ecosystem is functioning” (MLA, 2006). One or more defined vegetation and soil characteristics are used to relate land condition to a particular state or condition class (see Table 7.4). These characteristics are expected to remain relatively stable within a range of climatic variations, grazing pressures and other forms of disturbance, such as fire. An increase in grazing pressure for the same set of seasonal conditions (or maintaining the same stocking rate in a drought) may cause the landscape to transition to a more degraded state, depending on its inherent stability and/or resilience, where the latter is characterised by the ability of vegetation to recover when more favourable conditions return.

Resilience-based management, which specifically “acknowledges both the dependence and impact human populations have on natural resources and ecosystem services” (Briske, 2017), is gaining popularity in a variety of natural resource management fields and reflects our philosophical shift from being consumers of natural resources to being their stewards (see Sections 19 and 21.4).

Table 7.4 Grazing land condition classes

The ABCD framework in the Grazing Land Management (GLM) defines four condition classes based on the listed features. 3P: perennial, productive, and palatable).

Class	Features
A	High density and good cover of perennial grasses dominated by 3P species for a particular land type Little bare ground (usually < 30%) Few or no weeds Good soil condition—no erosion and good surface condition; High organic matter Little woody thickening.
B	Some decline in the health and/or density of 3P grasses An increase in other less favoured or weed species Some decline in soil condition Some signs of previous erosion and/or increased bare ground (usually > 30% but < 60%).
C	Moderate to low density of preferred grasses or moderate density of intermediate grasses Mainly annual grasses and forbs Many weeds Some erosion Often poor ground cover (< 60%) Some woody thickening.
D	General lack of any perennial grasses or palatable forbs Severe erosion or scalding, resulting in restricted plant growth; Ground cover mainly comprises weeds and annuals Thickets of woody plants or weeds cover most of the area Restoration to a better condition is reliant on high inputs of time, energy and money and land in this condition will not recover in the short term by excluding grazing.

Source: MLA (2011) Table 1

7.3 Function and Condition

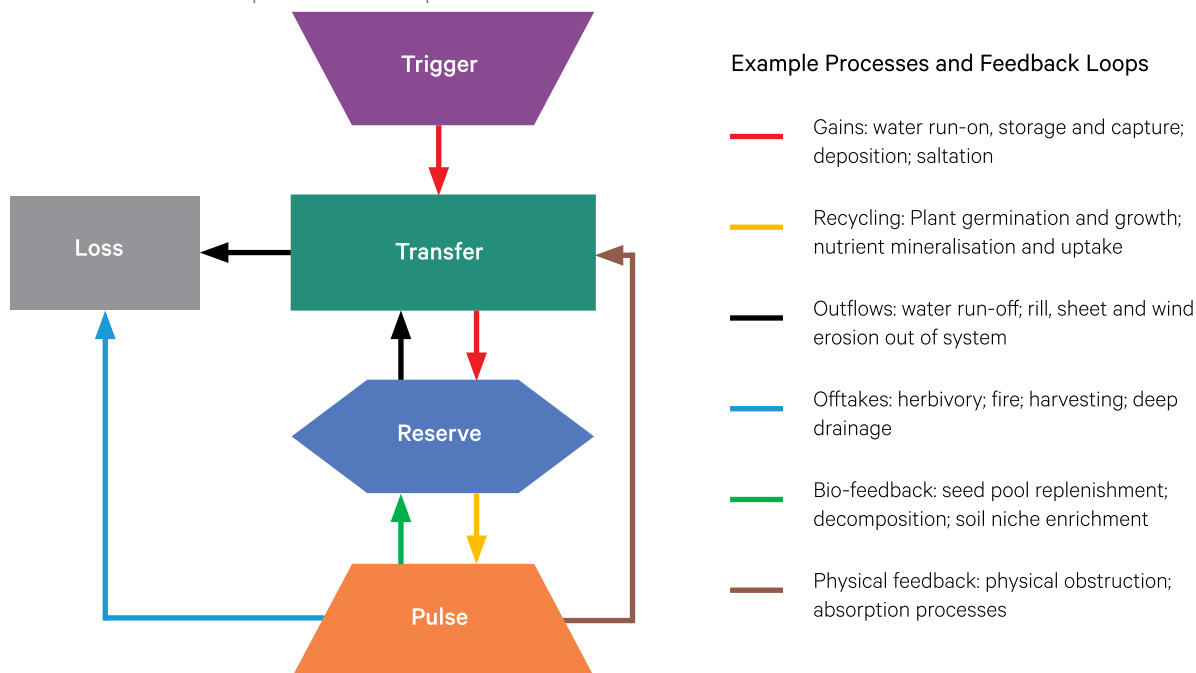
Traditionally, ecosystems have been assessed in terms of their biological composition and structure. Landscapes can also be usefully described, however, in terms of their function, that is, their ecosystem processes, such as the transport, usage, and cycling of resources in space and time (Ludwig and Tongway, 1997).

One conceptual framework for landscape functionality is the Trigger-Transfer-Reserve-Pulse (TTRP) ecosystem model, which defines a sequence of processes that 'maintain' a landscape. In this framework, resource 'losses' from the landscape are offset by resource inputs and feedback mechanisms (see Figure 7.3). An example input, or trigger, would be rainfall, which may become runoff that is either lost or absorbed into the soil as reserve to support future plant growth. That plant growth may then be removed by consumption, recycled back into the reserve, or act as a physical obstruction to modify subsequent transfer processes (Tongway and Hindley, 2004). This whole framework has also been depicted as resting on a fulcrum to emphasise the need for balance between internal feedback processes and resource extraction (Tongway and Ludwig, 2006).

Landscape function describes how well the landscape's biophysical system operates. This can be represented as a continuum of regulated resources, which is an objective assessment, independent of social and economic values. When a landscape loses function, it can be viewed as 'leaking' out of 'boundaries'; conversely, when control over resource loss is increased, landscape function is boosted (Tongway and Hindley, 2004). However, once we start to consider how well a landscape might be suited to a particular purpose or land use, the emphasis has moved from its objective function to its subjective 'condition' (see Figure 7.5). The 'condition' of something can be equated to its 'state of being' or 'health'. Clearly, such relative terms will vary with the purpose of the assessment. For example, a landscape condition that is acceptable for pastoral activities may be less acceptable for carbon sequestration goals and unacceptable for biodiversity conservation. One of the advantages of monitoring ecological condition is to be able to project future condition states based on defined states relating to management practices and/or climatic variations, such as potential trajectories of change for a grazed landscape based on the current land condition and differing future management strategies (Lunt *et al.*, 2007).

Figure 7.3 Ecosystem processes and feedback loops

This conceptual framework for the Trigger-Transfer-Reserve-Pulse (TTRP) ecosystem model represents sequences of ecosystem processes and feedback loops within a landscape.



Adapted from: Tongway and Hindley (2004) Figure 5 and Tongway and Ludwig (2006) Figure 1

Figure 7.4 Landscape function examples

On the left of these photographs, where the ground is covered by vegetation and litter, the soil is protected from rain and wind. In contrast on the right, unfenced side, the unprotected soil surface allows sediments to 'leak' from the landscape.

a. Upper Burdekin Catchment, Queensland, 22 May 2003



b. Near boundary of Herbert and Burdekin shires, Queensland, 3 December 2003



Source: John Ludwig, CSIRO

An example of landscape function being lost at a grazing site is shown in Figure 7.4. On the left of these photographs, where grazing animals have been excluded, dense vegetation and litter cover over the soil surface, retain rainwater, and prevent wind erosion. By contrast, on the grazed side of the fencelines, the soil has been bared and shows surface damage from animal movements. Such unprotected soil surfaces allow soil sediments to 'leak' from the landscape. A healthy—or functional—landscape conserves its water and soil resources while a 'leaky'—or dysfunctional—one loses these resources (Tongway and Ludwig, 1997a, 1997b). Since vegetation cover and its spatial patterns strongly impact landscape function, metrics that represent the patchiness of vegetation cover and/or the condition and undulations of the soil surface can then be used as indicators of landscape function both for ecological and hydrological purposes (Wilcox *et al.*, 2003; Ludwig *et al.*, 2005).

An indicator is a convenient or useful substitute for something that is difficult to measure, such as land condition. In Australian rangelands, for example, useful indicators are related to soil losses via eco-hydrological processes (Ludwig *et al.*, 2007), which are directly impacted by management practices (Pickup and Chewings, 1994). Other indicators of land condition from a pastoral perspective include:

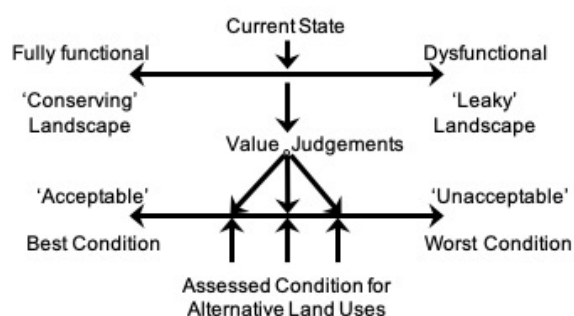
- ground cover, and particularly basal cover—that part of the herbage layer rooted in the ground, which protects the soil surface against erosion from overland flow of water in heavy or intense rainfall;
- pasture biomass—particularly available forage;
- herbage composition—including the proportion of palatable, perennial grasses⁸;
- woody-layer dynamics—any long term change in tree and shrub density;
- accelerated soil erosion; and the
- presence of weeds.

For example, ground cover is a useful indicator of the state of grazed rangelands because it protects the soil surface against erosion, provides some information about landscape 'leakiness', approximates pasture biomass (available forage) in some vegetation types, infers carbon dynamics (particularly the effectiveness with which organic matter is being returned to the soil through litter), and indicates habitat quality where entirely native species are present, which may be of value for inferring biodiversity condition (Fisher and Kutt, 2006). In this environment, when information is known about the composition and palatability of pasture species and appropriate cover-mass relationships, ground cover estimates can be used to infer pasture biomass (see Sections 14 and 15).

8 Pasture grasses are classified as 2P (perennial and palatable) or 3P (perennial, productive and palatable).

Figure 7.5 Landscape function versus landscape condition

This diagram clarifies the differences between landscape (or ecosystem) functionality, that is its 'state', from its suitability for a particular purpose, that is its 'condition'. While functionality is an objective description, condition is fundamentally based on value judgements, which will vary for different purposes. For example, the land use goals of pastoral productivity, biodiversity, or carbon sequestration may apply different value judgements to a given landscape state and, as a consequence, derive different assessments of its condition.



Source: Ludwig *et al.* (1997)

In some environments, landscape function could be envisaged as a continuum between a 'conserving' landscape and a 'leaky' landscape (see Figure 7.5). For example, this 'leakiness' indicator has been used to monitor the health of arid and semi-arid landscapes in Australia (Ludwig *et al.*, 2007; see Section 8.1.6). It also provides an axis along which the potential consequences of alternative land uses can be evaluated (see Sections 8.1.6 and 15). The framework illustrated in Figure 7.5 shows how an indicator of the functional state of a landscape, currently positioned midway along a continuum, may lead, through a 'values prism' (Gibbons and Freudenberger, 2006), to different assessments of its condition, depending on how different stakeholders value this level of functionality relative to their specific land use goals (Ludwig and Bastin, 2008).

For example, in Australian rangelands (see Section 15), environmental stakeholders who are predominantly interested in either pastoral production or biodiversity as land use goals would assess landscape condition using different criteria. In this context, contrasting expressions for indicators that singularly, or in combination, suggest better or poorer land condition are listed in Table 7.5 below. Using appropriate indicators, the question of 'what is the condition of the landscape?' (interpreted as 'how healthy is it?') becomes two questions:

- how functional is it for the intended/desired purpose? and
- how do its relevant indicators compare or interrelate?

Such criteria rely on the selection of appropriate indicators, that is, convenient, quantifiable aspects of land condition. As noted above, one indicator of landscape function is leakiness—its capacity to capture and retain rainwater, soils, and their nutrients on site, rather than lose them to the surrounding landscape(s) (see Figure 7.3 and Figure 7.5). These resources are not only vital for plant and animal growth, but provide food and shelter for the providers of numerous ecosystem 'services', such as pollination (see Section 20.3).

The degree to which the comparative terms in Table 7.5 apply at a particular location can only really be judged by comparison with appropriate reference or benchmark sites. To monitor land condition in grazed landscapes, for example, it may be possible to physically locate useful reference areas, such as water-remote locations, exclosures, or other small paddocks protected from continuous grazing. However, suitable reference areas may not be available where land types are highly preferred for grazing and/or are well watered. It is also necessary to account for any spatial differences in the amount and timing of rainfall when using information from reference areas.

Table 7.5 Examples of land condition indicators

Pastoral assessment		Biodiversity assessment	
Better condition	Poorer condition	Better condition	Poorer condition
More feed for livestock	Less or no feed for livestock	More feed for native fauna	Less or no feed for native fauna
More palatable perennials	Few or no perennials	Wide range of 'desirable' perennials	Few or no 'desirable' perennials
More ground cover and litter	Low ground cover or no litter	Wide range of ground covers and litter	Low ground cover or no litter
Lower utilisation—less grazing pressure	Higher utilisation—more grazing pressure	Plant growth ≥ grazing	Plant growth < grazing
No or few feral herbivores	Presence of feral herbivores	Wide range of herbivores	Small range of herbivores, mostly feral
Appropriate balance between trees and grasses	Too many or too few trees and shrubs	Diversity of trees and shrubs for faunal habitats	Small range of trees and shrubs

Source: Ludwig *et al.* (1997)

7.4 Productivity

The rate at which energy is stored by photosynthesis can be used as an indication of the productivity of an ecosystem, or its rate of biomass production (see Section 5.1.2). This process can be considered as a sequence of four energy flows within the terrestrial carbon cycle (see Excursus 1.2 and Figure 1.4):

- Gross Primary Productivity (GPP)—total amount of energy fixed in an ecosystem in unit time (including energy used in respiration). This equals the biomass produced per unit area in a given time.
- Net Primary Productivity (NPP)—amount of stored organic matter in plant tissue, after respiration, that is necessary for its production. This equals GPP minus autotrophic respiration, that is, the biomass available to consumers.
- Net Ecosystem Productivity (NEP)—amount of stored organic matter that is not consumed by heterotrophs (namely, NPP minus heterotrophic respiration).

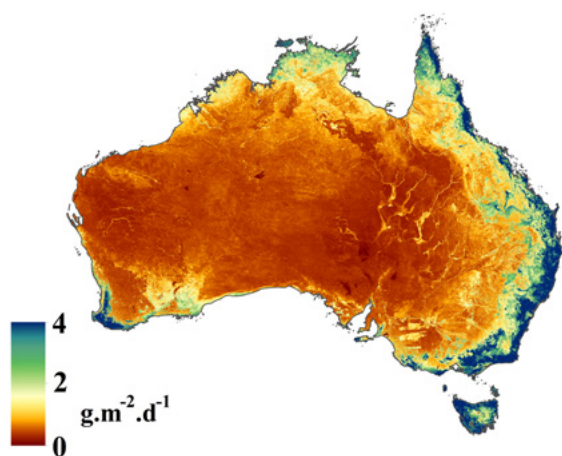
- Secondary Productivities (such as Net Biome Productivity, NBP)—equals NEP minus consumption, that is, the energy stored at the consumer level (Odum, 1971).

GPP equates with the carbon removed from the atmosphere by plants, while NPP is defined as the difference between carbon gained by photosynthesis and the carbon lost by respiration (McCallum *et al.*, 2009; see Section 5.2). Since NPP effectively quantifies the conversion of atmospheric carbon (CO₂) into plant biomass, it can be viewed as the first step in carbon accumulation (Running *et al.*, 2004). Alarming, the human appropriation of net primary production (HANPP), which quantifies the human impact on the biosphere, is estimated to have doubled from 13% to 25% of global NPP between 1910 and 2005 (Krausman *et al.*, 2013; see Sections 20 and 21.2).

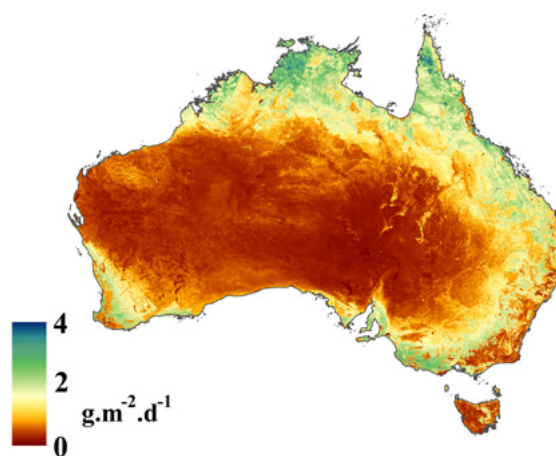
Figure 7.6 GPP over Australia

Mean monthly GPP was derived from MODIS imagery from January 2001 to December 2019 using methods detailed in Donohue *et al.* (2014).

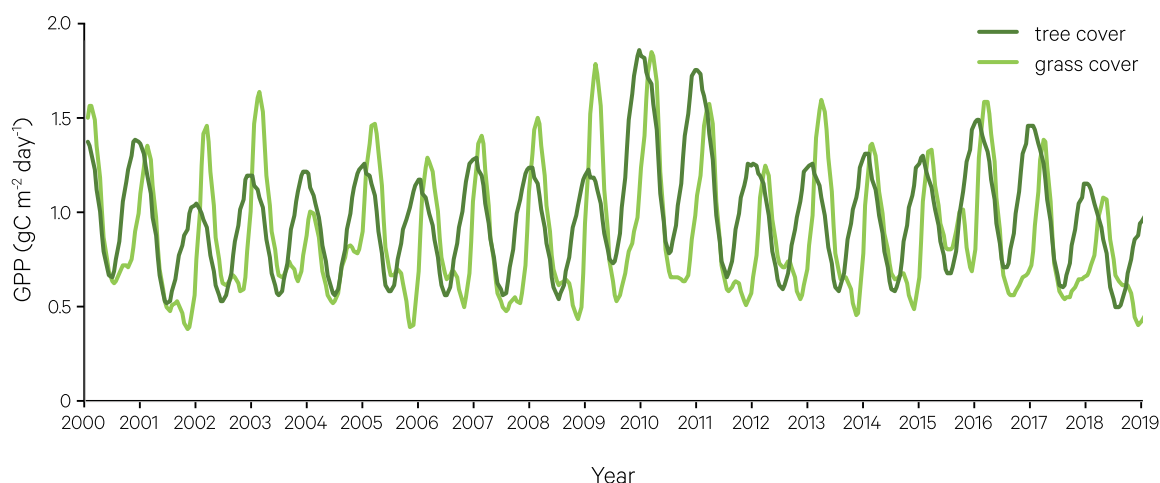
a. Tree cover



b. Grass cover



c. GPP time series



Source: Randall Donohue, CSIRO

As light levels, temperature, water availability, and nutrient supply fluctuate with diurnal and seasonal cycles, GPP also varies (see Figure 7.6). Annual GPP differences between ecosystems largely result from differences in canopy coverage and the duration of photosynthetic activity. Daily measurements (or estimates) of absorbed photosynthetic radiation (APAR; see Section 6.3.4) can be integrated over longer time periods, such as a growing season, to summarise the radiation available to a given plant canopy (Donohue *et al.*, 2014). Estimates of annual APAR effectively integrate diurnal and seasonal variations in solar radiation through changing atmospheric conditions to determine the amount of radiation absorbed by a vegetated canopy and, by inference, quantify the area of leaf cover that absorbs that radiation (see Sections 6.3 and 8.1).

Monteith (1972, 1977) observed the relationship between the rate of vegetative productivity and the rate of canopy light absorption, and proposed a straightforward modelling approach to estimate GPP and NPP from measurements of canopy reflective properties:

$$\text{GPP} = \text{PAR} \times f\text{APAR} \times (\text{LUE} \times \text{carbon}_{\text{dry}}) \\ \times \text{environmental constraints}$$

$$\text{NPP} = \text{GPP} - \text{autotrophic respiration}$$

where $f\text{APAR}$ is the fraction of absorbed photosynthetically active radiation (see Section 6.3.4). The efficiency with which plants utilise light to store carbon via photosynthesis varies as they grow. This characteristic, called photosynthetic Light Use Efficiency (LUE), can be computed as:

$$\text{LUE} = \frac{\text{GPP}}{\text{APAR}}$$

As such, LUE effectively estimates the amount of carbon fixed via photosynthesis for each unit of APAR. LUE underlies the many production efficiency models (PEM) that have been developed in recent decades. Such models initially assumed that photosynthetic carbon uptake by plants is proportional to the radiation absorbed by canopies, but recent studies have questioned this relationship, with variations being observed between plant functional types (PFT; see Sections 4.1.2 and 4.2.1) and photosynthetic pathways (see Section 5.2.1). LUE has also been observed to vary with species composition, nutrient availability, water stress, temperature, frost, and phenological stage (McCallum *et al.*, 2009), and increase with a greater proportion of diffuse to direct radiation (Gu *et al.*, 2002).

In global estimates of productivity, conversion efficiency parameters are determined for each type of biome and can be varied to account for changes in vegetation type and/or climatic conditions (see Section 17). Conversion efficiency parameters are used to convert estimates of APAR (as units of energy) to NPP (as units of biomass; Running *et al.*, 2004). PEM rely heavily on satellite observations for estimates of LUE, and meteorological data and $f\text{APAR}$ to estimate daily to yearly productivity at a range of spatial scales. For example, the BigFoot modelling approach (Running *et al.*, 1999; Cohen *et al.*, 2003) applies a biogeochemistry model to each cell of coregistered spatial datasets to derive NPP. In this model, the drivers are solar radiation and precipitation/temperature etc, with LAI and land cover being used for model initialisation. Other metrics related to productivity include:

- standing crop—a measure of the total amount of living organic matter, or biomass, in a given area at a given time, generally expressed as calories or g/m^2 ;
- turnover—the ratio of standing crop to production; and
- maintenance: structure ratio—indicative of turnover or energy flow rate = R/B

where

R is the total community respiration; and
B is the total community biomass.

Sellers (1985, 1987) explored the relationships between canopy reflectance and the leaf processes of photosynthesis and transpiration. This work integrated leaf models to estimate canopy photosynthetic activity and observed a near linear relationship between the ratio of NIR and red reflectances, as measured by remote sensors, and APAR, for high canopy covers. As the canopy cover decreases and the soil surface is visible to the remote sensor, this relationship becomes non-linear, especially for bright soils (see Section 6.4). Given that the canopy biophysical characteristics of photosynthetic capacity and bulk stomatal resistance are similarly related to the passage of PAR through the canopy, these characteristics also share a linear relationship with canopy reflectance in NIR and red wavelengths (see Sections 8.1.4 and 10.2.2).

7.5 Energy Balance

Plants and ecosystems can be viewed as thermodynamic engines whose energy source is the Sun (see Section 1). The First Law of Thermodynamics applies when the input energy equals the output energy, that is, the system is at equilibrium (see Volume 1A—Section 2.10.3). The Second Law of Thermodynamics, which observes that we don't live in a perfect world and that some energy is 'wasted' whenever useful energy is produced, also applies to plants and ecosystems (Monteith, 1972). The energy balance of ecosystems can be modelled to determine their stability in successional terms and their productivity in both ecological and economic terms.

Land surface temperature (LST) is commonly derived using EO datasets (see Volume 1B—Section 7.6). Canopy temperature is sometimes used as a surrogate for transpiration, but its relationship with air temperature and transpiration rate involves complex interactions of atmospheric, soil, and plant properties (see Section 5.2.4). Canopy temperature has also been useful as an indicator of drought resistance since those genotypes that maintain transpiration rates with lower canopy temperatures are more likely to withstand drought conditions (Blum, 2017; see Section 5.2.3). At the canopy or ecosystem level, a combination of instruments is used to estimate thermal energy balance, including:

- radiometers—measure upwelling and downwelling longwave and shortwave radiation (e.g. thermal sensors; see Volume 1B—Sections 7 and 8);
- heat flux sensors—measure heat transfer into the ground (e.g. ground heat flux plates and soil temperature probes); and
- eddy-covariance estimates of latent heat exchanges (evaporative flux) from anemometer and water vapour gas analyser measurements. Measurement of atmospheric factors using flux towers, as coordinated by the global consortium FLUXNET, is described in Excursus 7.2.

A range of models has been proposed to represent the fluxes of energy, water, and carbon between the biosphere, atmosphere, hydrosphere, and geosphere (see Excursus 1.2 and Section 7.6). Such models include Land Surface Models (LSM) that describe the energy balance at the interface between terrestrial surfaces and the atmosphere:

$$\begin{aligned} \text{Net radiation} = & \\ & (\text{downwelling SWIR EMR} \times (1 - \text{SWIR albedo})) \\ & + \text{downwelling thermal EMR} \\ & - \text{upwelling thermal EMR} \end{aligned}$$

Over the surface of the globe, these energy components achieve equilibrium, but not at a local scale. Different land surfaces store different amounts of energy in different cycles (diurnal, seasonal, and longer term). The local imbalances in these components drive the Earth's climate.

Section 5.2.4 introduced the terms sensible and latent heat fluxes. The net radiation equation above can also be written in the form:

$$R_n = H + \lambda E + G + F$$

where

- R_n is the net radiation;
- H is the sensible heat flux derived from the difference between surface and air temperatures, aerodynamic resistance, density of air, and specific heat of air;
- λ is the latent heat of vaporisation;
- E is evapotranspiration;
- G is the soil flux; and
- F is the chemical energy flux stored in photosynthesis.

Aerodynamic resistance depends on the wind speed and surface roughness length, which in turn is related to vegetation height since taller vegetation, such as forest trees, allow more exchange of turbulent heat fluxes than shorter vegetation, such as grass (see Section 13). These components are interrelated and changes in one component flow on to other components (Pitman, 2003) and also affect the exchange of materials and gases, such as CO_2 .

LSM have progressed from simple models based on uniform surfaces to multi-layer, EO-based models, that include multiple vegetation and soil characteristics, to detailed foliage models that account for cell structure and biochemical processes (see Section 10.2).

Energy is indeed present in all things. Living organisms draw it from their environment, as plants take it from the sun in photosynthesis and animals take chemical energy from their food through digestion and respiration. They accumulate it in their own bodies and use it to power their movements and behaviour. When they die, the energy accumulated in their bodies is released to continue on its way in other forms. The flow of energy on which your body and your brain depend at this very moment is part of the cosmic flux, and the energy within you will flow on after you are dead and gone, taking endless new forms.

(Rupert Sheldrake, 1994)

Excursus 7.2—Flux Towers

Source: Beringer *et al.* (2016); Isaac *et al.* (2017); van Gorsel *et al.* (2018)

Within atmospheric boundary layers, vertical turbulence is measured using the eddy flux technique, also known as eddy covariance or eddy correlation (EC). This statistical technique is used to compute the flux (or flow) of various gases through the atmosphere from continuous micrometeorological measurements at selected locations. Such measurements track the vertical and horizontal movement of air parcels by eddies and are typically taken from mobile or fixed towers known as Flux Towers.

A global network of over 500 flux towers is coordinated by FLUXNET to measure the exchanges of CO₂, water vapour and energy between the biosphere and the atmosphere (FLUXNET, 2018; Williams *et al.*, 2009; Oliphant, 2012). This network provides continuous, long term micrometeorological measurements for monitoring the state of ecosystems globally (see Volume 1A—Section 10.1). In Australia and New Zealand, data from nearly 30 flux towers, managed by a dozen institutions, are collated by TERN Ecosystem Processes (formerly TERN OzFlux and TERN Supersites), as part of FLUXNET (see Figure 7.7). OzFlux was established to provide the Australian and global modelling communities with consistent observations of energy, carbon and water exchange between the atmosphere and the key ecosystems of Australia and New Zealand: tropical rainforest and savanna, sclerophyll forest and woodland, alpine meadow, peatland, semi-arid woodland, savanna, grasslands, croplands, and pastures (Beringer *et al.*, 2016).

The flux towers measure CO₂ flux as well as sensible and latent heat flux. Processed data from the flux tower network is available from a number of places (see Section 7.7) and include Net Ecosystem Exchange (NEE), Gross Primary Productivity (GPP) and Ecosystem Respiration (ER) in addition to evapotranspiration (ET), precipitation, and the components of the surface energy balance (see Figure 7.7b). Using flux measurements in conjunction with models and EO datasets, ecosystem dynamics (productivity, respiration, evapotranspiration, water-use efficiency) can be explored within the context of climate fluctuations, meteorological drivers, phenology, and management activities. Broad science outcomes from analyses of EC data provided by the flux tower network include:

- improved methods for observations and interpretation (Beringer *et al.*, 2016; Isaac *et al.*, 2017; McHugh *et al.*, 2017);
- upscaling of ecosystem scale measurements to regional and larger scales using EO and physical modelling (Haverd *et al.*, 2016; Laubach *et al.*, 2016;

Restrepo-Coupe *et al.*, 2016; Trudinger *et al.*, 2016; Whitley *et al.*, 2016); and

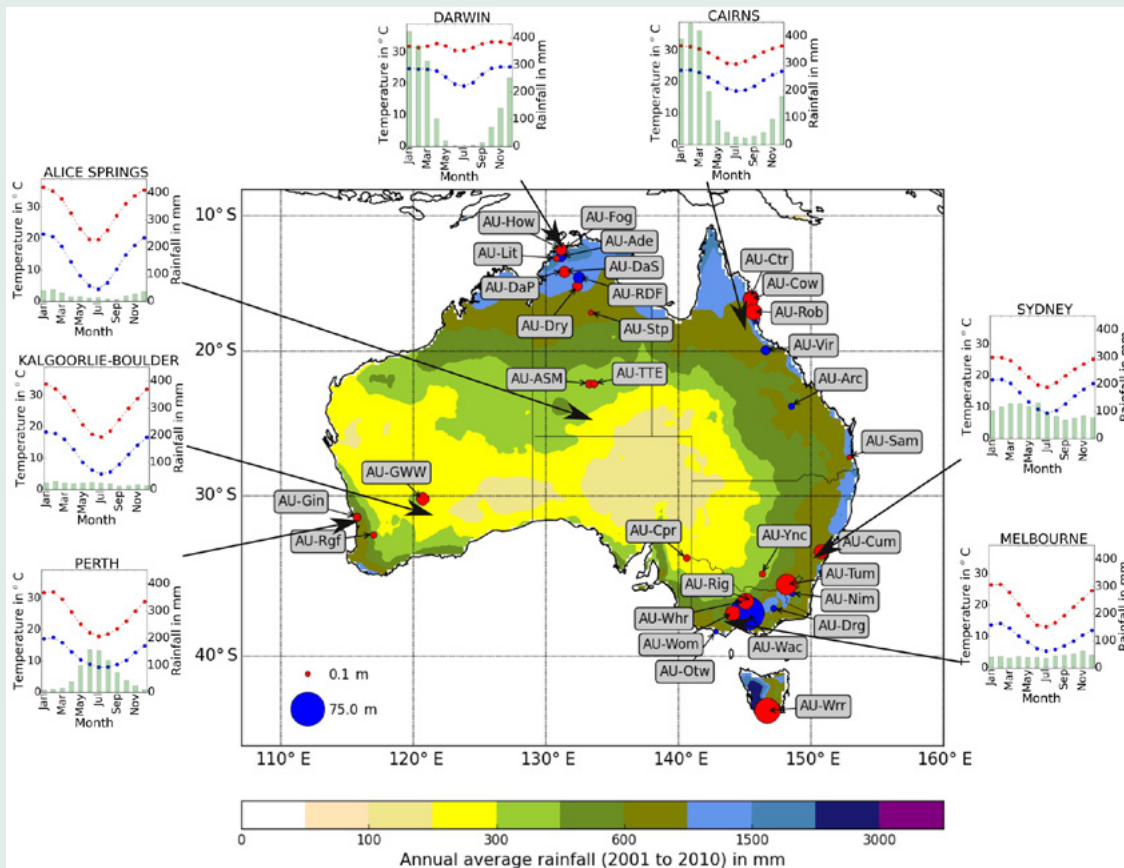
- better understanding of the interactions between carbon, water and energy cycles and their responses to changes related to land use, climate, extreme weather, and fire (Bristow *et al.*, 2016a; Hinko-Najera *et al.*, 2017; Hunt *et al.*, 2016; Moore *et al.*, 2016a; van Gorsel *et al.*, 2016; Fest *et al.*, 2017).

By directly quantifying sensible heat and moisture fluxes in and around vegetation canopies, EC moisture flux towers provide reliable measures of Actual Evapotranspiration (AET) over large areas (hundreds to thousands of m²; Drexler *et al.*, 2004), and are commonly used with catchment water balance data to validate EO-based estimates of AET (Glenn *et al.*, 2011). While the accuracy of EC measurements have been assessed as being 15–30%, which impacts the accuracy of any studies they are used to validate (Allen *et al.*, 2011), they deliver important, ecosystem level information about the factors that impact AET (Glenn *et al.*, 2011) and expand our understanding of ecological, biogeochemical and hydrological processes in terrestrial ecosystems. Nonetheless, uncertainty exists in all methods, and EC towers are currently one of the best means of measuring AET at the ecosystem scale via an *in situ*, non-destructive approach. Beringer *et al.* (2016) identify four key benefits from these flux towers for Australia:

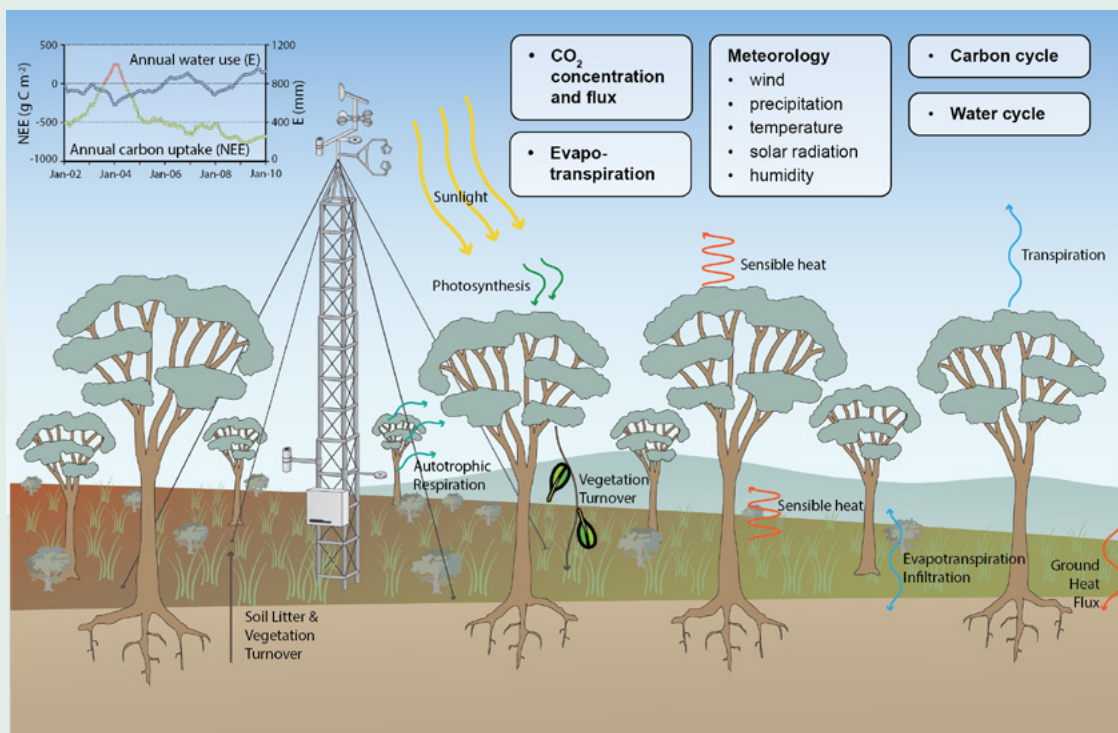
- providing accurate, continuous half-hourly to annual estimates of sinks and sources of greenhouse gases and water from ecosystems for carbon accounting and water management that are particularly important in an arid country like Australia (Hutley *et al.*, 2005; Raupach *et al.*, 2013);
- evaluating the effects of disturbance, topography, biodiversity, stand age, insect/pathogen infestation, and extreme weather on carbon and water fluxes, particularly cyclone, fire, and heat waves in the Australian environment (Beringer *et al.*, 2014; Bowman *et al.*, 2009; van Gorsel *et al.*, 2016; Hutley *et al.*, 2013);
- examining the effects of land management practices, such as harvest, fertilisation, irrigation, tillage, thinning, cultivation, and clearing, especially for agricultural activities (Bristow *et al.*, 2016b; Campbell *et al.*, 2015; Cleverly *et al.*, 2020); and
- producing important ground truth data for parameterizing, validating, and improving satellite EO and global inversion products (Anav *et al.*, 2015; Running *et al.*, 1999; Schimel *et al.*, 2015), particularly for phenology (Ma *et al.*, 2013; Moore *et al.*, 2016b) and water balance.

Figure 7.7 Flux tower distribution and site data

a. Locations of flux tower sites are shown in red for active sites and blue for inactive sites. The thumbnail plots show monthly average air temperature and precipitation at Bureau of Meteorology sites that are representative of the tower locations. The diameter of the symbol marking the tower locations is proportional to the canopy height (see scale at bottom left of map).



b. Site diagram for an individual flux tower



Source: a. Isaacs *et al.* (2017) Figure 1; b. Mark Grant, TERN

7.6 Water Balance

Each year more than half a million cubic kilometres of water is moved around the Earth's surface, between the surface and sub-surface storage, and between the surface and the atmosphere (see Volume 3B).

This cycling of water is referred to as the hydrological cycle (see Volume 1A—Section 4.2.2). Water balance modelling attempts to understand the interactions of components within the hydrological cycle:

- within atmosphere—solar radiation and moisture transport;
- from atmosphere to surface—various forms of precipitation;
- surface to atmosphere transfers—evaporation from land and water surfaces, and transpiration from plants; and
- surface and sub-surface transfers—runoff, infiltration and percolation into soil layer, deep seepage to groundwater, and groundwater discharge to lakes, streams, and seas.

The Australian climate has highly variable rainfall and runoff, and these components of the hydrological cycle vary widely in both space and time (see Section 2.2). These factors make water balance modelling particularly challenging for the Australian environment (Zhang *et al.*, 2002).

Transpiration describes the process of water entering the atmosphere from plants (see Section 5.2.3) while evapotranspiration (ET) collectively refers to the transfer of water vapour to the atmosphere from both vegetated and unvegetated surfaces (see Section 2.2.1). Evapotranspiration is a major determinant of water balance in dry continents such as Australia and varies with the:

- availability of water in the landscape;
- climatic conditions, such as temperature, cloudiness, humidity, and wind speed; and
- rates of transpiration by individual plants.

Evapotranspiration increases with temperature, so is regulated by the same drivers that regulate temperature, namely latitude, altitude, cloud cover, and topography (see Section 5.2.4). Potential ET (PET) defines a theoretical water volume for an ecological system, which represents the water that can be 'extracted' from it for known inputs of solar energy and precipitation. The Actual ET (AET) is often less than the potential when water supply is limited. AET can be viewed as the reciprocal of precipitation, although only 90% of precipitation returns to the atmosphere via evapotranspiration (NWC, 2007). On a regional basis, when PET exceeds precipitation, there is a water deficit; when precipitation exceeds PET, there is a water surplus. During times of water surplus, water may be stored by plants, by soil, or by the water table, for use during times of water deficit.

Water balance modelling "is based on the law of conservation of mass: any change in the water content of a given soil volume during a specified period must equal the difference between the amount of water added to the soil volume and the amount of water withdrawn from it" (Zhang *et al.*, 2002). Water balance can be considered at a range of scales, such as the root zone for a small number of plants, for a whole catchment, for a continent or the whole globe. At a catchment scale, the water balance equation can be given as:

$$\Delta S = P - ET - Q - R$$

where all components are spatially averaged for the catchment:

- S is the water storage;
- P is precipitation;
- ET is evapotranspiration;
- Q is surface runoff; and
- R is recharge (Zhang *et al.*, 2002).

Water balance models need to be tailored to specific climates and landscapes and may be integrated with other process models (see Section 7.5). For example, the WAVES model (Dawes and Short, 1993; Zhang *et al.*, 1996) simulates the energy, water, carbon, and solute balances of a one-dimensional soil-canopy-atmosphere system (Zhang *et al.*, 2002). EO-based water balance models are further discussed in Sections 9.4 and 10.2.3, and Excursus 10.2.

7.7 Further Information

Global NPP Image Composites

https://neo.sci.gsfc.nasa.gov/view.php?datasetId=MOD17A2_M_PSN

TERN Ecosystem Processes

<http://www.tern.org.au/OzFlux-pg17729.html>

Processed data from the flux tower network is available from <http://data.ozflux.org.au/portal/home.jsp> and <http://dap.ozflux.org.au/thredds/catalog.html> for example, including Net Ecosystem Exchange (NEE), Gross Primary Productivity (GPP), and Ecosystem Respiration (ER) in addition to evapotranspiration (ET), precipitation, and the components of the surface energy balance (see Excursus 7.2).

7.8 References

- Allen, R.G., Pereira, L.S., Howell, T.A., Jensen, M.E. (2011). Evapotranspiration information reporting: I. Factors governing measurement accuracy. *Agricultural Water Management*, 98, 899–920.
- Anav, A., Friedlingstein, P., Beer, C., Ciais, P., Harper, A., Jones, C., Murray-Tortarolo, G., Papale, D., Parazoo, N. C., Peylin, P., Piao, S., Sitch, S., Viovy, N., Wiltshire, A., and Zhao, M. (2015). Spatiotemporal patterns of terrestrial gross primary production: A review. *Reviews of Geophysics*, 53, 785–818. doi:10.1002/2015RG000483,
- Ash, A.J., Bellamy, J.A., and Stockwell, T.G.H. (1994). State and transition models for rangelands. 4. Application of state and transition models to rangelands in northern Australia. *Tropical Grasslands*, 28, 223–228.
- Beringer, J., Hutley, L.B., Abramson, D., Arndt, S. K., Briggs, P., Bristow, M., Canadell, J.G., Cernusak, L.A., Eamus, D., Evans, B.J., Fest, B., Goergen, K., Grover, S.P., Hacker, J., Haverd, V., Kanniah, K., Livesley, S. J., Lynch, A., Maier, S., Moore, C., Raupach, M., Russell-Smith, J., Scheiter, S., Tapper, N.J., and Uotila, P. (2014). Fire in Australian Savannas: from leaf to landscape. *Global Change Biology*, 11, 6641. doi:10.1111/gcb.12686
- Beringer, J., Hutley, L.B., McHugh, I., Arndt, S.K., Campbell, D., Cleugh, H.A., Cleverly, J., Resco de Dios, V., Eamus, D., Evans, B., Ewenz, C., Grace, P., Griebel, A., Haverd, V., Hinko-Najera, N., Huete, A., Isaac, P., Kanniah, K., Leuning, R., Liddell, M.J., Macfarlane, C., Meyer, W., Moore, C., Pendall, E., Phillips, A., Phillips, R.L., Prober, S. M., Restrepo-Coupe, N., Rutledge, S., Schroder, I., Silberstein, R., Southall, P., Yee, M.S., Tapper, N.J., van Gorsel, E., Vote, C., Walker, J., and Wardlaw, T. (2016). An introduction to the Australian and New Zealand flux tower network—OzFlux. *Biogeosciences*, 13, 5895–5916. <https://doi.org/10.5194/bg-13-5895-2016>
- Bestelmeyer, B.T., Brown, J.R., Havstad, K.M., Alexander, R., Chavez, G., and Herrick, J.E. (2003). Development and use of state-and-transition models for rangelands. *Journal of Range Management*, 56, 114–126.
- Bestelmeyer, B.T., Ash, A., Brown, J.R., Densambuu, B., Fernández-Giménez, M., Johanson, J., Levi, M., Lopez, D., Peinetti, R., Rumpff, L., and Shaver, P. (2017). State and Transition Models: Theory, Applications, and Challenges. Ch 9 in *Rangelands Systems* (Ed: Briske, D.D.). Springer Series on Environmental Management. https://doi.org/10.1007/978-3-319-46709-2_9
- Billings, W.D. (1970). *Plants, Man and the Ecosystem*. 2nd Edn. Wadsworth Publ. Co., Belmont. 160 p. ISBN 0-333-14633-6.
- Blum, A. (2017). Osmotic adjustment is a prime drought stress adaptive engine in support of plant production. *Plant, Cell and Environment*, 40, 4–10.
- Bowman, D.M.J.S., Balch, J.K., Artaxo, P., Bond, W.J., Carlson, J.M., Cochrane, M.A., D’Antonio, C.M., DeFries, R.S., Doyle, J.C., Harrison, S.P., Johnston, F.H., Keeley, J.E., Krawchuk, M.A., Kull, C.A., Marston, J.B., Moritz, M.A., Prentice, I.C., Roos, C.I., Scott, A.C., Swetnam, T.W., van der Werf, G.R., and Pyne, S.J. (2009). Fire in the Earth System. *Science*, 324, 481–484. doi:10.1126/science.1163886
- Briske, D.D. (2017) (Ed). *Rangelands Systems*. Springer Series on Environmental Management. https://doi.org/10.1007/978-3-319-46709-2_9
- Briske, D.D., Fuhlendorf, S.D., and Smeins, F.E. (2005). State-and-transition models, thresholds, and rangeland health: A synthesis of ecological concepts and perspectives. *Rangeland Ecology and Management*, 58, 1–10.

- Briske, D.D., Illius, A.W., and Anderies, J.M. (2017). Nonequilibrium Ecology and Resilience Theory. Ch 6 in *Rangelands Systems* (Ed: Briske, D.D.). Springer Series on Environmental Management. doi:10.1007/978-3-319-46709-2-6
- Bristow, M., Hutley, L.B., Beringer, J., Livesley, S.J., Arndt, S.K., and Edwards, A.C. (2016a). Greenhouse gas emissions from tropical savanna deforestation and conversion to agriculture. *Biogeosciences*, 13, 6285–6303.
- Bristow, M., Hutley, L.B., Beringer, J., Livesley, S.J., Edwards, A.C., and Arndt, S.K. (2016b). Quantifying the relative importance of greenhouse gas emissions from current and future savanna land use change across northern Australia. *Biogeosciences*, 13, 6285–6303. <https://doi.org/10.5194/bg-13-6285-2016>.
- Campbell, D.I., Wall, A.M., Nieveen, J.P., and Schipper, L.A. (2015). Variations in CO₂ exchange for dairy farms with year-round rotational grazing on drained peatlands. *Agriculture, Ecosystems and Environment*, 202, 68–78. doi:10.1016/j.agee.2014.12.019, 2015.
- Cleverly, J., Vote, C., Isaac, P., Ewenz, C., Harahap, M., Beringer, J., Campbell, D.I., Daly, E., Eamus, D., He, L., Hunt, J., Grace, P., Hutley, L.B., Laubach, J., McCaskill, M., Rowlings, D., Rutledge Jonker, S., Schipper, L.A., Schroder, I., Teodosio, B., Yu, Q., Ward, P.R., Walker, J.P., Webb, J.A., Grover, S.P.P. (2020). Carbon, water and energy fluxes in agricultural systems of Australia and New Zealand. *Agricultural and Forest Meteorology*, 287, 107934. doi:10.1016/j.agrformet.2020.107934.
- Cohen, W.B., Turner, D.P., Running, S.W., and Gower, S.T. (2003). Comparisons of land cover and LAI estimates derived from ETM+ and MODIS for four sites in North America: a quality assessment of 2000/2001 provisional MODIS products. *Remote Sensing of Environment*, 88, 233–255.
- DAFF (2013). *Grazing BMP self-assessment: Grazing land management, Northern Australian module*. Department of Agriculture, Fisheries and Forestry, Queensland.
- Dawes, W.R., and Short, D.L. (1993). *The efficient numerical solution of differential equations for coupled water and solute dynamics: the WAVES model*. Technical Memorandum 93/18, CSIRO Division of Water Resources, Canberra.
- DEWHA (2010). *Ecosystem Services: Key Concepts and Applications*. Occasional Paper No 1, Department of the Environment, Water, Heritage and the Arts, Canberra.
- Donohue, R.J., Hume, I.H., Roderick, M.L., McVicar, T.R., Beringer, J., Hutley, L.B., Gallant, J.C., Austin, J.M., van Gorsel, E., Cleverly, J.R., Meyer, W.S., and Arndt, S.K. (2014). Evaluation of the remote-sensing-based DIFFUSE model for estimating photosynthesis of vegetation. *Remote Sensing of Environment*, 155, 349–365.
- Drexler, J.Z., Snyder, R.L., Spano, D., Paw, K.T.U. (2004). A review of models and micrometeorological methods used to estimate wetland evapotranspiration. *Hydrological Processes*, 18, 2071–2101.
- Dyksterhuis, E.J. (1949). Condition and management of rangeland based on quantitative ecology. *Journal of Range Management*, 2, 104–105.
- Ellis, J.E., and Swift, D.M. (1988). Stability of African pastoral ecosystems: Alternate paradigms and implications for development. *Journal of Range Management*, 41, 450–459.
- Fest, B.J., Hinko-Najera, N., Wardlaw, T., Griffith, D.W.T., Livesley, S.J., and Arndt, S.K. (2017). Soil methane oxidation in both dry and wet temperate eucalypt forests shows a near-identical relationship with soil air-filled porosity. *Biogeosciences*, 14, 467–479. <https://doi.org/10.5194/bg-14-467-2017>
- Fisher, A., and Kutt, A. (2006). *Biodiversity and Land Condition in Tropical Savanna Rangelands: Summary Report*. Tropical Savannas CRC, Darwin, NT.
- FLUXNET (2018). *FLUXNET* webpage, ORNL DAAC NASA website: <http://fluxnet.ornl.gov/>
- Gibbons, P., and Freudenberger, D. (2006). An overview of methods used to assess vegetation condition at the scale of the site. *Ecological Management and Restoration*, 7, S10–S17.
- Glenn, E., Doody, T.M., Guerschman, J.P., Huete, A.R., King, E.A., McVicar, T.R., van Dijk, A.I.J.M., van Niel, T.G., Yebra, M., and Zhang, Y. (2011). Actual evapotranspiration estimation by ground and remote sensing methods: the Australian experience. *Hydrological Processes*, 25(26), 4103–4116. doi:10.1002/hyp.8391
- Gu, L., Baldocchi, D., Verma, S.B., Black, T.A., Vesala, T., Falge, E.M., and Dowty, P.R. (2002). Advantages of diffuse radiation for terrestrial ecosystem productivity. *Journal of Geophysical Research*, 107(D6). doi:10.1029/2001JD001242.

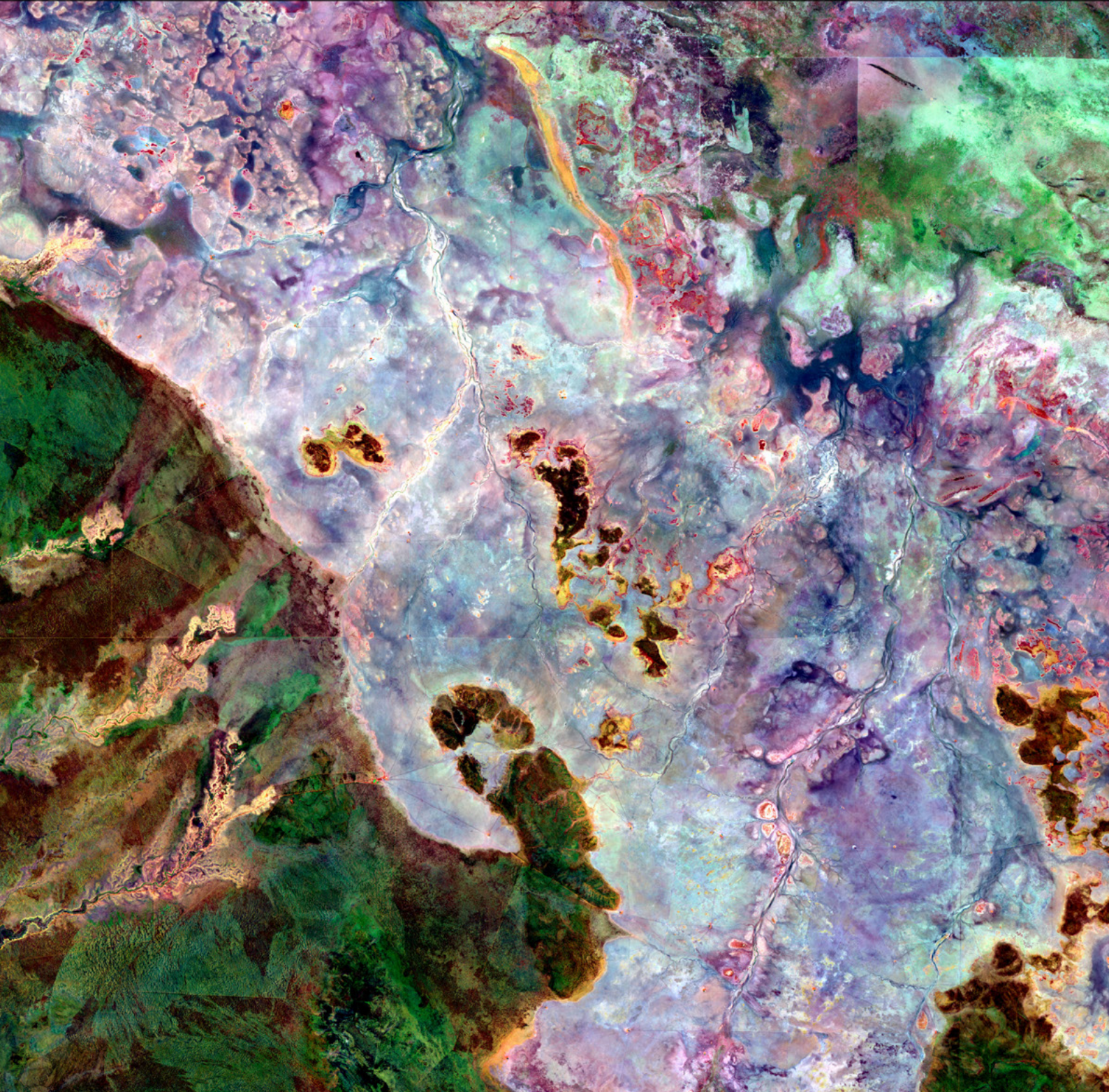
- Haverd, V., Smith, B., Raupach, M., Briggs, P., Nieradzki, L., Beringer, J., Hutley, L., Trudinger, C.M., and Cleverly, J. (2016). Coupling carbon allocation with leaf and root phenology predicts tree–grass partitioning along a savanna rainfall gradient. *Biogeosciences*, 13, 761–779. <https://doi.org/10.5194/bg-13-761-2016>
- Hinko-Najera, N., Isaac, P., Beringer, J., van Gorsel, E., Ewenz, C., McHugh, I., Exbrayat, J.-F., Livesley, S.J., and Arndt, S.K. (2017). Net ecosystem carbon exchange of a dry temperate eucalypt forest. *Biogeosciences*, 14, 3781–3800. <https://doi.org/10.5194/bg-14-3781-2017>
- Hunt, J.E., Laubach, J., Barthel, M., Fraser, A., and Phillips, R.L. (2016). Carbon budgets for an irrigated intensively grazed dairy pasture and an irrigated winter-grazed pasture. *Biogeosciences*, 13, 2927–2944. <https://doi.org/10.5194/bg-13-2927-2016>
- Hutley, L.B., Leuning, R., Beringer, J., Cleugh, H.A. (2005). The utility of the eddy covariance techniques as a tool in carbon accounting: tropical savanna as a case study. *Australian Journal of Botany*, 53, 663–675.
- Hutley, L.B., Evans, B.J., Beringer, J., Cook, G.D., Maier, S.M., and Razon, E. (2013). Impacts of an extreme cyclone event on landscape-scale savanna fire, productivity and greenhouse gas emissions. *Environmental Research Letters*, 8, 045023. doi:10.1088/1748-9326/8/4/045023
- IFA (1985). *Think Trees, Grow Trees*. Dept. Arts, Heritage and Environment/Institute of Foresters of Australia. AGPS, Canberra.
- Illius, A.W., and O'Connor, T.G. (1999). On the Relevance of Nonequilibrium Concepts to Arid and Semiarid Grazing Systems. *Ecological Applications*, 9(3), 798–813.
- Isaac, P., Cleverly, J., McHugh, I., van Gorsel, E., Ewenz, C., and Beringer, J. (2017). OzFlux data: network integration from collection to curation. *Biogeosciences*, 14, 2903–2928. <https://doi.org/10.5194/bg-14-2903-2017>
- Joyce, L.A. (1993). The life cycle of the range condition concept. *Journal of Range Management*, 46, 132–138.
- Keith, D.A., Rodríguez, J.P., Rodríguez-Clark, K.M., Nicholson, E., Aapala, K., Alonso, A., Asmussen, M., Bachman, S., Basset, A., Barrow, E.G., Benson, J.S., Bishop, M.J., Bonifacio, R., Brooks, T.M., Burgman, M.A., Comer, P., Comín, F.A., Essl, F., Faber-Langendoen, D., Fairweather, P.G., Holdaway, R.J., Jennings, M., Kingsford, R.T., Lester, R.E., Nally, R. Mac, McCarthy, M.A., Moat, J., Oliveira-Miranda, M.A., Pisanu, P., Poulin, B., Regan, T.J., Riecken, U., Spalding, M.D., and Zambrano-Martínez, S. (2013). Scientific Foundations for an IUCN Red List of Ecosystems. *PLoS ONE*, 8(5), e62111. doi:10.1371/journal.pone.0062111
- Kessell, S.R. (1979). *Gradient Modelling: Resource and Fire Management*. Springer-Verlag, New York.
- Krausman, F., Erb, K.-H., Gingrich, S., Haberl, H., Bondeau, A., Gaube, V., Lauk, C., Plutzer, C., and Searchinger, T.D. (2013). Global human appropriation of net primary production doubled in the 20th century. *Proceedings of the National Academy of Sciences of the USA*, 110(25), 10324–10329. <https://doi.org/10.1073/pnas.1211349110>
- Laubach, J., Barthel, M., Fraser, A., Hunt, J.E., and Griffith, D.W.T. (2016). Combining two complementary micrometeorological methods to measure CH₄ and N₂O fluxes over pasture. *Biogeosciences*, 13, 1309–1327. <https://doi.org/10.5194/bg-13-1309-2016>
- Ludwig, J.A., and Bastin, G.N. (2008). Rangeland condition: its meaning and use. A Discussion Paper prepared for the Australian Collaborative Rangelands Information System (ACRIS) Management Committee. ACRIS. <https://www.environment.gov.au/system/files/resources/09f881fe-8119-4719-bfa0-6a2a55e90a1b/files/rangeland-condition-meaning-use.pdf>
- Ludwig, J.A., and Tongway, D.J. (1997). A landscape approach to rangeland ecology. Ch 1 in *Landscape Ecology, Function and Management: Principles from Australia's Rangelands*. (Eds. J. Ludwig, D. Tongway, D. Freudenberger, J. Noble, and K. Hodgkinson). pp. 1–12. CSIRO Publishing, Melbourne.
- Ludwig, J.A., Tongway, D.J., Freudenberger, D.O., Noble, J.C., and Hodgkinson, K.C. (Eds) (1997). *Landscape Ecology, Function and Management: Principles from Australia's Rangelands*. CSIRO Publishing, Melbourne, Australia.
- Ludwig, J.A., Wilcox, B.P., Breshears, D.D., Tongway, D.J., and Imeson, A.C. (2005). Vegetation patches and runoff-erosion as interacting ecohydrological processes in semiarid landscapes. *Ecology*, 86, 288–297.

- Ludwig, J.A., Bastin, G.N., Chewings, V.H., Eager, R.W., and Liedloff, A.C. (2007). Leakiness: A new index for monitoring the health of arid and semiarid landscapes using remotely sensed vegetation cover and elevation data. *Ecological Indicators*, 7, 442–454.
- Lunt, I., Eldridge, D.J., Morgan, J.W., and Witt, G.B. (2007). Turner Review No. 13: A framework to predict the effects of livestock grazing and grazing exclusion on conservation values in natural ecosystems in Australia. *Australian Journal of Botany*, 55, 401–415. doi:10.1071/BTO6178
- Ma, X., Huete, A., Yu, Q., Coupe, N. R., Davies, K., Broich, M., Ratana, P., Beringer, J., Hutley, L. B., Cleverly, J., Boulain, N., and Eamus, D. (2013). Spatial patterns and temporal dynamics in savanna vegetation phenology across the North Australian Tropical Transect. *Remote Sensing of Environment*, 139, 97–115. doi:10.1016/j.rse.2013.07.030
- Macarthur, R. (1955). Fluctuations of Animal Populations and a Measure of Community Stability. *Ecology*, 36(3), 533–536.
- May, R.M. (1973). *Stability and complexity in model ecosystems*. Princeton University Press, Princeton.
- McCallum, I., Wagner, W., Schmulilius, C., Shvidenko, A., Obersteiner, M., Fritz, S., and Nilsson, S. (2009). Satellite-based terrestrial production efficiency modelling. *Carbon Balance and Management*, 4, 8. doi:10.1186/1750-0680-4-8
- McHugh, I.D., Beringer, J., Cunningham, S.C., Baker, P.J., Cavagnaro, T.R., Mac Nally, R., and Thompson, R.M. (2017). Interactions between nocturnal turbulent flux, storage and advection at an “ideal” eucalypt woodland site. *Biogeosciences*, 14, 3027–3050. <https://doi.org/10.5194/bg-14-3027-2017>.
- McKeon, G., and Carter, J. (2015). AussieGRASS: An Operational National Pasture Model. Ch 1 in *AussieGRASS Environmental Calculator—Product Descriptions v1.5*. Department of Science, Information Technology and Innovation, Queensland.
- MEA (2005). *Ecosystems and Human Well-being: Synthesis*. Millennium Ecosystem Assessment, Island Press, Washington, DC.
- MLA (2006). *Grazing Land Management. Sustainable and productive natural resource management*. Meat and Livestock Australia Ltd. ISBN 1 74036 9343
- MLA (2011). *Biodiversity Condition Assessment for Grazing Lands*. Meat and Livestock Australia Ltd, North Sydney. ISBN 9781741916393
- Monteith, J.L. (1972). Solar Radiation and Productivity in Tropical Ecosystems. *Journal of Applied Ecology*, 9(3), 747–766.
- Monteith, J.L. (1977). Climate and the efficiency of crop production in Britain. *Philosophical Transactions of The Royal Society B: Biological Sciences*, 281(980), 294–294. doi:10.1098/rstb.1977.0140.
- Moore, C.E., Beringer, J., Evans, B., Hutley, L.B., McHugh, I., and Tapper, N.J. (2016a). The contribution of trees and grasses to productivity of an Australian tropical savanna. *Biogeosciences*, 13, 2387–2403. doi:10.5194/bg-13-2387-2016
- Moore, C.E., Brown, T., Keenan, T.F., Duursma, R.A., van Dijk, A.I.J.M., Beringer, J., Culvenor, D., Evans, B., Huete, A., Hutley, L.B., Maier, S., Restrepo-Coupe, N., Sonntag, O., Specht, A., Taylor, J.R., van Gorsel, E., and Liddell, M.J. (2016b). Reviews and syntheses: Australian vegetation phenology: new insights from satellite remote sensing and digital repeat photography. *Biogeosciences*, 13, 5085–5102. doi:10.5194/bg-13-5085-2016
- NWC (2007). *Australian Water Resources 2005*. National Water Commission, Canberra. ISBN: 978-1-921107-48-1
- Odum, E.P. (1971). *Fundamentals of Ecology*. 3rd edn. W.B. Saunder Co., Philadelphia.
- Oliphant, A.J. (2012). Terrestrial Ecosystem-Atmosphere Exchange of CO₂, Water and Energy from FLUXNET; Review and Meta-Analysis of a Global in-situ Observatory. *Geography Compass*, 6(12), 689–705. doi:10.1111/gec3.12009
- Pianka, E.R. (1971). Species diversity. In *Topics in the Study of Life: The Bio Source Book*. pp 401-406. Harper and Row, New York.
- Pickup, G., and Chewings, V.H. (1994). A grazing gradient approach to land degradation assessment in arid areas from remotely-sensed data. *International Journal of Remote Sensing*, 15, 597–617.
- Pickup, G., Bastin, G.N., and Chewings, V.H. (1994). Remote-sensing-based Condition Assessment for Nonequilibrium Rangelands under Large-Scale Commercial Grazing. *Ecological Applications*, 4(3), 497–517.
- Pitman, A.J. (2003). The Evolution of, and Revolution in, Land Surface Schemes designed for Climate Models. *International Journal of Climatology*, 23, 479–510.
- Raupach, M.R., Haverd, V., and Briggs, P.R. (2013). Sensitivities of the Australian terrestrial water and carbon balances to climate change and variability. *Agriculture and Forest Meteorology*, 182–183, 277–291. doi:10.1016/j.agrformet.2013.06.017

- Restrepo-Coupe, N., Huete, A., Davies, K., Cleverly, J., Beringer, J., Eamus, D., van Gorsel, E., Hutley, L.B., and Meyer, W.S. (2016). MODIS vegetation products as proxies of photosynthetic potential along a gradient of meteorologically and biologically driven ecosystem productivity. *Biogeosciences*, 13, 5587–5608. doi:10.5194/bg-13-5587-2016
- Running, S.W., Baldocchi, D.D., Turner, D.P., Gower, S.T., Bakwin, P.S., and Hibbard, K.A. (1999). A global terrestrial monitoring network integrating tower fluxes, flask sampling, ecosystem modeling and EOS satellite data. *Remote Sensing of Environment*, 70, 108–127.
- Running, S.W., Nemani, R.R., Heinsch, F.A., Zhao, M., Reeves, M., and Hashimoto, H. (2004). A continuous satellite-derived measure of global terrestrial primary production. *Biosciences*, 54(6), 547–560.
- Schimel, D., Pavlick, R., Fisher, J. B., Asner, G. P., Saatchi, S., Townsend, P., Miller, C., Frankenberg, C., Hibbard, K., and Cox, P. (2015). Observing terrestrial ecosystems and the carbon cycle from space. *Global Change Biology*, 21, 1762–1776. doi:10.1111/gcb.12822.
- Sellers, P.J. (1985). Canopy reflectance, photosynthesis and transpiration. *International Journal of Remote Sensing*, 6(8), 1335–1372.
- Sellers, P.J. (1987). Canopy Reflectance, Photosynthesis, and Transpiration. II. The Role of Biophysics in the Linearity of Their Interdependence. *Remote Sensing of Environment*, 21, 143–183.
- Sheldrake, R. (1994). *The rebirth of Nature: The Greening of Science and God*. Park Street Press, Rochester, Vermont. 272 p.
- Sims, R.J., Lyons, M., and Keith, D.A. (2019). Limited evidence of compositional convergence of restored vegetation with reference states after 20 years of livestock exclusion. *Austral Ecology*, 44(4), 734–746. <https://doi.org/10.1111/aec.12744>
- Stringham, T.K., Krueger, W.C., and Shaver, P.L. (2003). State and transition modeling: An ecological process approach. *Journal of Range Management*, 56, 106–113.
- Tilman, D. (1996) Biodiversity: Population Versus Ecosystem Stability. *Ecology*, 77(2), 350–363.
- Tilman, D., Lehman, C.L., and Bristow, C.E. (1998) Diversity-Stability Relationships: Statistical Inevitability or Ecological Consequence? *The American Naturalist*, 151(3), Notes and Comments.
- Tongway, D.J., and Hindley, N. (2004). *Landscape function analysis: procedures for monitoring and assessing landscapes. With special reference to minesites and rangelands*. CSIRO Sustainable Ecosystems, Canberra.
- Tongway, D.J., and Ludwig, J.A. (1997a). The nature of landscape dysfunction in rangelands. In *Landscape Ecology, Function and Management: Principles from Australia's Rangelands*. (Eds: Ludwig, J.A., Tongway, D.J., Freudenberger, D.O., Noble, J.C., Hodgkinson, K.C.). CSIRO Publishing, Melbourne.
- Tongway, D.J., and Ludwig, J.A. (1997b). The conservation of water and nutrients within landscapes. In *Landscape Ecology, Function and Management: Principles from Australia's Rangelands*. (Eds: Ludwig, J.A., Tongway, D.J., Freudenberger, D.O., Noble, J.C., Hodgkinson, K.C.) CSIRO Publishing, Melbourne.
- Tongway, D.J., and Ludwig, J.A. (2006). *Assessment of Landscape Function as an Information Source for Mine Closure*. Mine Closure (Eds: Fourie, A., and Tibbett, M.). Perth. ISBN 0-9756756-6-4 ISBN 0-9756756-6-4
- Trudinger, C.M., Haverd, V., Briggs, P.R., and Canadell, J.G. (2016) Interannual variability in Australia's terrestrial carbon cycle constrained by multiple observation types. *Biogeosciences*, 13, 6363–6383. <https://doi.org/10.5194/bg-13-6363-2016>
- van Gorsel, E., Wolf, S., Cleverly, J., Isaac, P., Haverd, V., Ewenz, C., Arndt, S., Beringer, J., Resco de Dios, V., Evans, B., Griebel, A., Hutley, L.B., Keenan, T., Kljun, N., Macfarlane, C., Meyer, W.S., McHugh, I., Pendall, E., Prober, S.M., and Silberstein, R. (2016). Carbon uptake and water use in woodlands and forests in southern Australia during an extreme heat wave event in the “Angry Summer” of 2012/2013. *Biogeosciences*, 13, 5947–5964. <https://doi.org/10.5194/bg-13-5947-2016>
- van Gorsel, E., Cleverly, J., Beringer, J., Cleugh, H., Eamus, D., Hutley, L. B., Isaac, P., and Prober, S. (2018). Preface: OzFlux: a network for the study of ecosystem carbon and water dynamics across Australia and New Zealand. *Biogeosciences*, 15, 349–352. <https://doi.org/10.5194/bg-15-349-2018>.
- Walker, B. (2020). Resilience: what it is and is not. *Ecology and Society*, 25(2), 11. <https://doi.org/10.5751/ES-11647-250211>
- Washington-Allen, R.A., and Ravi, S. (2012). Dryland Analysis and Monitoring. In *Encyclopedia of Life Support Systems* (Ed: Squires, V.R.). UNESCO-EOLSS, Oxford.
- Watt, K.E.F. (1968). *Energy and Resource Management*. McGraw-Hill, New York.
- Westoby, M., Walker, B., and Noy-Meir, I. (1989). Opportunistic management for rangelands not at equilibrium. *Journal of Rangeland Management*, 42(4), 266–274.

- Whitley, R., Beringer, J., Hutley, L.B., Abramowitz, G., De Kauwe, M.G., Duursma, R., Evans, B., Haverd, V., Li, L., Ryu, Y., Smith, B., Wang, Y.-P., Williams, M., and Yu, Q. (2016). A model inter-comparison study to examine limiting factors in modelling Australian tropical savannas. *Biogeosciences*, 13, 3245–3265. <https://doi.org/10.5194/bg-13-3245-2016>
- Wilcox, B.P., Breshears, D.D., and Allen, C.D. (2003). Ecohydrology of a resource-conserving semiarid woodland: effects of scale and disturbance. *Ecological Monographs*, 73(2), 223–239.
- Williams, M., Richardson, A.D., Reichstein, M., Stoy, P.C., Peylin, P., Verbeeck, H., Carvalhais, N., Jung, M., Hollinger, D.Y., Kattge, J., Leuning, R., Luo, Y., Tomelleri, E., Trudinger, C.M., and Wang, Y.-P. (2009). Improving land surface models with FLUXNET data. *Biogeosciences*, 6, 1341–1359. <https://doi.org/10.5194/bg-6-1341-2009>.
- Youngentob, K.N., Renzullo, L.J., Held, A.A., Jia, X., Lindenmayer, D.B., and Foley, W.J. (2012). Using imaging spectroscopy to estimate integrated measures of foliage nutritional quality. *Methods in Ecology and Evolution*, 3, 416–426. doi:10.1111/j.2041-210X.2011.00149.x
- Zhang, L., Dawes, W.R., and Hatton, T.J. (1996). Modelling hydrological processes using a biophysically based model—application of WAVES to FIFE and HAPEX-MOBILHY. *Journal of Hydrology*, 185, 147–169.
- Zhang, L., Walker, G.R., and Dawes, W.R. (2002). Water balance modelling: concepts and applications. In *Regional Water and Soil Assessment for Managing Sustainable Agriculture in China and Australia* (Eds: McVicar, T.R., Li Rui, Walker, J., Fitzpatrick, R.W., and Liu Changming). ACIAR Monograph No. 84, pp 31–47.

EO Methods



Mapping, monitoring, and modelling of terrestrial landscapes are complementary activities, with shared benefits as summarised in the table below (see also Volume 2D—Section 1.5), where:

- mapping describes the collation of geographic information about a given landscape as a consistent spatial coverage, which implicitly represents a single point in time;
- monitoring describes changes in the landscape relative to a defined baseline; and
- modelling extends current knowledge to predict or infer landscape condition at some future time and/or for a specified set of conditions.

Complementary benefits of mapping, monitoring, and modelling

Relationship	Benefits
Mapping→monitoring	Spatial framework for selecting representative sites; System for spatial extrapolation of monitoring results; and Broad assessment of resource condition.
Monitoring→mapping	Quantifies and defines important resource variables for mapping; and Assesses land suitability over time (including risk assessments for recommended land management).
Modelling→monitoring	Determines whether trends in specific land attributes can be successfully detected with monitoring; and Identifies key components of system behaviour that can be measured in a monitoring program.
Monitoring→modelling	Validates model results; and Provides data for modelling.
Modelling→mapping	Allows spatial and temporal prediction of landscape processes.
Mapping→modelling	Provides data for modelling; and Provides spatial association of input variables.

Source: McKenzie *et al.* (2008a) Table 1.1

Sections 8 to 10 below review EO-based methods that can be used to map, monitor, and model terrestrial vegetation. The image processing procedures that underlie many of these methods are detailed in Volume 2. Applications of EO-based mapping, monitoring, and modelling are introduced in Volume 2D—Section 14. The EO-based methods described in the following three sections are furthered exemplified in the context of specific Australian applications areas in Sections 11 to 20.

Contents

8 Mapping	165
9 Monitoring	191
10 Modelling	213



8 Mapping

EO-based mapping relates to identifying and labelling surface features in EO imagery at a single instance in time (see Volume 1). Imagery to be used for mapping of terrestrial vegetation requires accurate geometric and radiometric calibration as detailed in Volumes 2A, 2B, and 2D.

EO images can vary in terms of their spectral, spatial, radiometric, and temporal resolutions and extents (see Table 8.1, and Volumes 1B and 2D). The scale of any EO data source largely determines its suitability to a particular study:

- spatial scale dictates the sizes of features that might be discerned;
- spectral scale indicates the types of features that can be identified;
- temporal scale is particularly relevant to phenological studies (see Section 5.3.2) and longer term changes in land cover or condition; and
- radiometric scale relates to intrinsic data quality and determines the magnitude of surface reflectance differences that can be discerned.

Sensor design constraints do not allow high resolution data to be acquired in all dimensions simultaneously (see Volume 1A—Section 13.3 and Volume 1B—Section 1). While high spatial resolution imagery is valuable for detailed analyses, it supplies data volumes that would be unmanageable for landscape scale analyses. However, as spatial resolution decreases, more pixels will cover multiple ground features so that their spectral values will not be unique to a single surface feature. Such mixtures can also create characteristic patterns and textures that are valuable for land cover inventories (see Section 8.3 and Volume 2E).

Interpretation of EO data for inventory purposes involves a variety of image processing techniques, including:

- spectral indices—combining two or more bands (or channels) into a single plane of data to focus on a particular characteristic (see Section 8.1);
- spectral classification—grouping spectrally similar pixels into classes to represent ground features (see Section 8.2); and
- sub-pixel analyses—determining the proportions of basic ground components within each pixel (see Section 8.3).

Other approaches that analyse EO imagery for mapping purposes include:

- spatial analyses—exploiting the image spatial patterns to delineate objects and gradients, such as tree crown delineation (Ke and Quackenbush, 2011) or Geographic Object-Based Image Analysis (GEOBIA; see Volume 2A—Excursus 10.1); and
- structural analyses—modelling the three-dimensional structure of surface features, such as Geometric-Optical Modelling (see Volume 2X—Excursus 1.1) or Point Cloud Modelling of lidar data (Burt *et al.*, 2018; see Excursus 5.1).

Background image: MODIS/Terra global composite image showing the Normalised Difference Vegetation Index (NDVI) for October 2016 (derived from MOD13C1/ MOD13C2 products), with deeper shades of green indicating higher photosynthetic activity. (Note: the vertical extent of this composite image has been clipped and the aspect ratio changed.) Source: NASA Earth Observations. (Retrieved from https://neo.sci.gsfc.nasa.gov/view.php?datasetId=MOD_NDVI_M)

Table 8.1 Sampling dimensions in EO imagery

Dimension	Characteristic		
	Resolution	Density	Extent
Spectral	Width of each wavelength channel	Number of channels detected by sensor	Range of wavelengths covered by all channels
Spatial	Ground area imaged per optical pixel	Number of pixels and lines in image	Area covered by image
Radiometric	Smallest change in detected energy that would be represented as a different image brightness level	Number of gradations (grey levels) used to represent full range of radiances that could be detected by sensor	Actual range of radiances detected in each channel
Temporal	Time period over which each image is acquired	Frequency of successive image acquisitions	Total time period for which this imagery is available

Adapted from: Emelyanova *et al.* (2012)

8.1 Spectral Indices

A wide range of spectral indices has been proposed to improve image interpretation. These indices highlight the spectral response that is characteristic of particular surface features such as vegetation greenness, water content, or fire footprints (see Volume 2C). They also offer the advantage of reducing the volume of large datasets. Numerous studies have either demonstrated the efficacy of these indices to represent environmental gradients and/or compared spectral indices derived from different sensors (for example Huete, *et al.*, 1997, 2002; Liu, 2004, 2008). Indices based on ratios of image spectral bands offer a robust data compression tool, with the advantages of simplified comparisons between multi-date imagery and possible cross-calibration between different sensor systems (Glenn *et al.*, 2008a).

Some vegetation spectral indices have been shown to have strong positive correlation with the fraction of photosynthetically active radiation (fAPAR) absorbed by a canopy (see Section 6.3.4 and 7.4). Accordingly, these have proven most reliable for mapping vegetative features that are directly related to canopy light absorption, such as vegetation condition and density (see Sections 8.1.1–8.1.3). In addition, when accurate validation data are available, indices have been developed to monitor processes related to fAPAR (such as productivity; see Section 8.1.4), assess water content (see Section 8.1.5), and highlight landscape ‘leakiness’ (see Section 8.1.6).

Spectral indices have also been used to estimate various attributes related to canopy architecture, such as fractional vegetation cover, leaf area index (LAI), emissivity, and albedo (see Section 6.3). However, unlike features directly related to canopy absorption, the relationships between spectral indices and these attributes are less direct and reliable, and derived results can be misleading (Glenn *et al.*, 2008a).

8.1.1 Greenness

The green colour of vegetation results from absorption of red and blue wavelengths by the chlorophyll pigment for photosynthesis and reflection of green wavelengths (see Section 4.3). However, it is the combined ‘colour’ resulting from the chlorophyll content of foliage, the area covered by leaves, and the density and structure of the canopy that determines the optical ‘greenness’ for a given patch of vegetation as measured by a remote sensor.

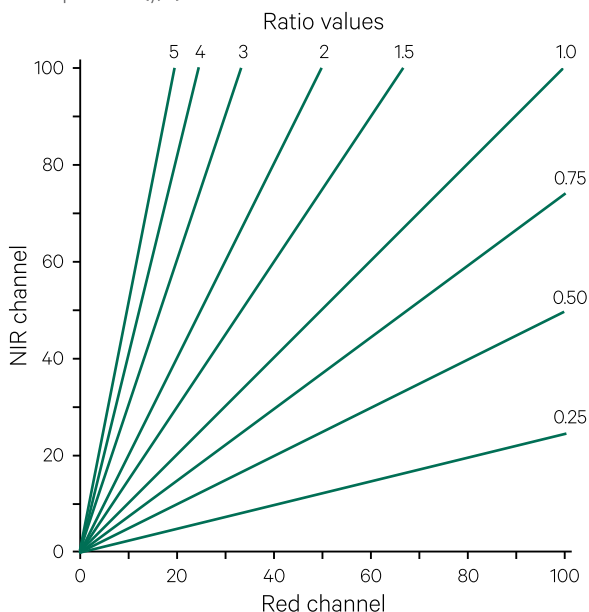
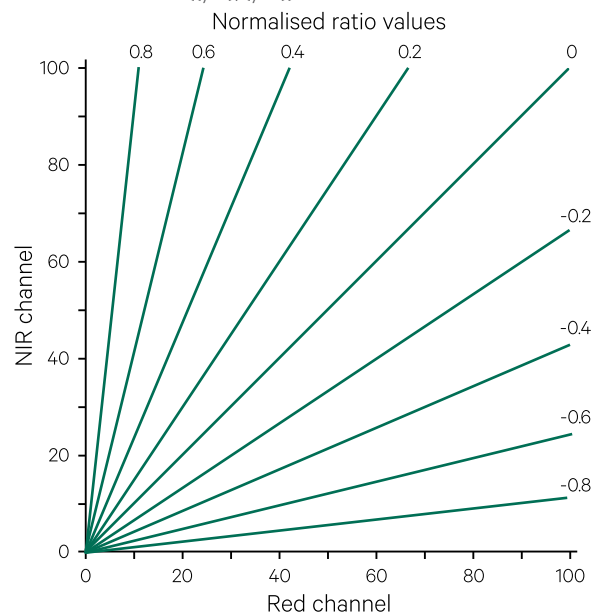
Greenness indices rely upon highlighting the characteristically high near infrared (NIR) reflectance and low red reflectance of healthy, green foliage (see Figure 5.5). Reflectance values in NIR and red are differenced or ratioed to emphasise those pixels that are likely to contain a high proportion of photosynthetic material (see Volume 2C—Section 11). The simplest greenness index involves ratioing red and NIR reflectances and is commonly referenced as the Simple Ratio (SR; see also Volume 2C—Sections 10 and 11):

$$SR = \frac{NIR}{red}$$

where NIR is near infrared reflectance (ρ_{NIR}) and red is ρ_{red} .

One of the most common indices, the Normalised Difference Vegetation Index (NDVI; see Volume 2C—Section 11), is based on the simple difference of NIR (ρ_{NIR}) and red (ρ_{red}) reflectance, normalised by the equation (Rouse *et al.*, 1973; Tucker, 1979):

$$NDVI = \frac{\rho_{NIR} - \rho_{red}}{\rho_{NIR} + \rho_{red}}$$

Figure 8.1 Normalisation effect in 'Normalised Difference Vegetation Index' (NDVI)a. Simple ratio (y/x)b. Normalised ratio $((y-x)/(y+x))$ 

Source: Harrison and Jupp (1990) Figure 94

As illustrated in Figure 8.1, the normalising of NDVI values results in a controlled range of raw ratio values between -1 and 1 and thus greatly simplifies the scaling of output data and comparison of multi-temporal imagery. Since NDVI is functionally equivalent to SR via the equation:

$$\text{NDVI} = \frac{\text{SR} - 1}{\text{SR} + 1}$$

then $\text{SR} = 1$ is equivalent to $\text{NDVI} = 0$, and $\text{SR} = 4$ is the same as $\text{NDVI} = 0.60$, and so on.

NDVI has been related to a range of vegetation characteristics, including cover and condition, which may indicate crop yield in agricultural systems (see Sections 11 to 14). NDVI derived from airborne image spectrometry data has also been used to infer forage quality for herbivores at a landscape scale, with higher NDVI pixels being indicative of more nutritious foliage (Youngentob *et al.*, 2012). Not only can spectral indices be normalised for comparison between multiple images, but they can be differenced between two images to show temporal changes in greenness (see Volume 2D). For example, since fire reduces the amount of green vegetation, greenness indices have been used to map fire footprints, infer burn severity, and monitor recovery (see Sections 9.2.1 and 18). Such indices are also used to determine fire risk by mapping the curing status of grasslands and the fire-prone nature of woody vegetation (Chuvieco *et al.*, 2003; Lasaponara, 2005; see Section 18.3.1.2).

Various studies have observed that NDVI saturates for dense vegetation (Carlson and Ripley, 1997; Huete *et al.*, 1985), with NDVI reportedly approaching maximum value for fractional covers as low as 60% (Jiang *et al.*, 2006). Felderhof (2007) observed limitations of NDVI in arid and semi-arid Australia where bare soil and senescent vegetation affect NDVI and restrict its usefulness in mapping spinifex fuel load. Dilley *et al.* (2004) observed an exponential relationship between NDVI computed from AVHRR imagery and grassland curing. Other researchers have observed a linear relationship between EO-based NDVI and grassland curing for selected soil types (Allan *et al.*, 2003).

A variant of NDVI is the green NDVI (GNDVI; Gitelson *et al.*, 1996a), which substitutes the green band for the red band, and is more sensitive to chlorophyll a concentration in foliage and less impacted by atmospheric effects:

$$\text{GNDVI} = \frac{\rho_{\text{NIR}} - \rho_{\text{green}}}{\rho_{\text{NIR}} + \rho_{\text{green}}}$$

For sugar and horticultural crops, GNDVI has been shown to be better correlated with yield than NDVI (see Section 12).

Transformed Vegetation Index (TVI) is a modified version of NDVI which avoids operating with negative NDVI values and introduces a normal distribution (Deering *et al.*, 1975):

$$TVI = \sqrt{\frac{\rho_{NIR} - \rho_{red}}{\rho_{NIR} + \rho_{red}}} + 0.5$$

Many other variations of NDVI have been proposed, including the Enhanced Vegetation Index (EVI; Huete *et al.*, 1999, 2002; Liu and Huete, 1995; Jiang *et al.*, 2008), which attempts to reduce saturation by accounting for effects due to atmosphere and background, though not necessarily topographic effects (Matsushita *et al.*, 2007):

$$EVI = G \times \left(\frac{\rho_{NIR} - \rho_{red}}{\rho_{NIR} + C_1 \times \rho_{red} + C_2 \times \rho_{blue} + L} \right)$$

where

ρ_{red} and ρ_{NIR} are corrected values for MODIS bands 1 (red) and 2 (NIR) respectively;

ρ_{blue} is the corrected value for MODIS band 3 (blue—500 nm);

G is a gain factor ($G=2.5$; Huete *et al.*, 1994, 1997);

L is an adjustment for the canopy background ($L=1$); and

C_1 and C_2 are coefficients for aerosol resistance ($C_1=6$, $C_2=7.5$).

EVI was designed to reduce interference from atmospheric and vegetated canopy characteristics that can impact NDVI and produce a clearer signal for green vegetation (Huete *et al.*, 2002). Accordingly, EVI is more sensitive to variations in canopy structure (Gao *et al.*, 2000) and thus has been more responsive for land covers with high biomass, such as tropical forests (Huete *et al.*, 2002) and crops (Wardlow *et al.*, 2007). It has also been shown to be a useful indicator of tree richness (Waring *et al.*, 2006). EVI uses data from the 500 nm (blue) band to remove the effects of smoke, aerosols, and thin clouds, and masks out cloud, cloud shadows, marine (as opposed to inland) waters, and aerosols (Huete *et al.*, 2011). A variant of EVI, called EVI2, that is computed using only two spectral bands, has also been proposed for sensors without a blue band (Jiang *et al.*, 2008). Both NDVI and EVI products are routinely and freely available at global and regional scales (see Volume 2D—Excursus 10.1). Their use for phenological studies is discussed in Section 9.3.

Other indices have been proposed to reduce the effects of atmospheric scattering, such as the Atmospherically Resistant Vegetation Index (ARVI; Kaufman and Tanre, 1992), or the soil background, such as the Soil Adjusted Vegetation Index (SAVI; Huete, 1988):

$$ARVI = \frac{\rho_{NIR} - (\rho_{red} + \gamma(\rho_{blue} - \rho_{red}))}{\rho_{NIR} + (\rho_{red} + \gamma(\rho_{blue} - \rho_{red}))}$$

where γ usually ~ 1 .

$$SAVI = \left(\frac{\rho_{NIR} - \rho_{red}}{\rho_{NIR} + \rho_{red} + L} \right) (1+L)$$

where L is a soil brightness correction factor (where $L=0.5$). The Optimised Soil Adjusted Vegetation Index (OSAVI; Rondeaux *et al.*, 1996) uses a different value for L to minimise soil effects:

$$OSAVI = \left(\frac{\rho_{800} - \rho_{670}}{\rho_{800} + \rho_{670} + L} \right) (1+L)$$

where $L=0.16$

The Visible Atmospherically Resistant Index (VARI) was found to be minimally sensitive to atmospheric effects (Gitelson *et al.*, 2002):

$$VARI = \left(\frac{\rho_{green} - \rho_{red}}{\rho_{green} + \rho_{red} - \rho_{blue}} \right)$$

Both atmospheric and soil corrections are combined in the Soil and Atmospherically Resistant Vegetation Index (SARVI; Kaufman and Tanre, 1992), in which red reflectance is replaced by a linear combination of both red and blue reflectance. The EVI formulation is based on SARVI and the merging the SAVI with ARVI equations.

An Absolute Greenness index (Gabs) was proposed to distinguish the weather-related variations in NDVI from longer term temporal variability (such as curing) within a selected time period (Eidenshink *et al.*, 1990):

$$Gabs = \left(\frac{\text{observed NDVI} - \text{min NDVI}}{\text{max NDVI}} \right)$$

A normalised NDVI or Relative Greenness index (RG), which ranks the current NDVI of each pixel relative to its minimum and maximum NDVI over a specified period of time, was found to better distinguish the volume of dead fuel from live fuel (Burgan and Hartford, 1993):

$$RG = \left(\frac{\text{observed NDVI} - \text{min NDVI}}{\text{max NDVI} - \text{min NDVI}} \right) \times 100$$

The Fire Potential Index (FPI), based on RG of AVHRR data and fuel modelling, was developed for regional scale fire danger assessment (Burgan *et al.*, 1998) and demonstrated strong correlation with actual fire occurrence and predicting fire potential. Fiorucci *et al.* (2007) used a similar methodology, involving SPOT VEGETATION imagery integrated with meteorological forecasts, to improve the accuracy of assessing fire danger.

Another type of vegetation index is based on a linear combination of visible and NIR channels to highlight their differences in terms of transformed dimensions relating to brightness, greenness, and yellowness (see Volume 2C—Section 11.1.3). The vegetation cover triangle (see Figure 6.6) effectively corresponds to one plane in this transformed space. A popular example of this approach is the Kauth-Thomas Greenness (or Tasseled Cap) Transformation, which was developed for Landsat MSS by Kauth and Thomas (1976) and adapted to other sensors by Crist and Cicone (1984), Cicone and Metzler (1984) and Roberts *et al.* (2018). These indices have been most relevant to agricultural applications (see Sections 11 to 14).

A range of composite image products based on greenness indices are now available from EO time series datasets (see Excursus 8.1). Since the spectral bands observed by different sensors often span similar wavelength ranges, the opportunity exists to merge their spectral information. For example, as detailed in Volume 2D—Section 6.2, Emelyanova *et al.* (2012, 2013) demonstrated the blending of Landsat ETM+ and MODIS imagery, thus providing surrogate imagery with MODIS frequency and Landsat spatial resolution. Such techniques, however, may not be appropriate for imagery from all sensors. Composite imagery derived from multiple sensors is introduced in Volume 2D—Section 10.2.

Man must rise above Earth, to the top of the atmosphere and beyond, for only thus will he fully understand the world in which he lives.
(Socrates)

Excursus 8.1—Composite Image Products

Composite EO image products are introduced in Volume 2D—Section 10, including a discussion of compositing methods and their constraints. A number of such products are now routinely available to provide a summary image representing a given time period for a selected spectral index (see Section 8.1.1). While these composite images are useful for large area coverage, and rapid assessment of surface condition, changes and long term monitoring of trends, it is important to consider their provenance and any consequent constraints when interpreting results.

For example, the MOD13Q1 product suite is based on a composite of 250 m resolution imagery over a 16-day period (see Volume 2D), which is corrected for atmospheric effects (see Volume 1B—Section 3.5). The impact of viewing and illumination angles becomes increasingly significant in imagery with larger pixel sizes, such as MODIS, especially for tall vegetation with multiple sources of shadow. The MOD13Q1 product does not currently normalise reflectance values to an observer in zenith position, so its time series potentially comprises imagery acquired with varying viewing geometry.

Gill *et al.* (2009) investigated the use of two VI products within the MOD13Q1 product, namely NDVI and EVI, to assess the impact of variations in viewing geometry on the estimation of tree and grass cover. Their results indicated that MODIS EVI was more sensitive to variations in view angle than NDVI, and hence vegetation structure (as also proposed by Gao *et al.*, 2000), and more sensitive to monitoring change in high biomass vegetation (Huete *et al.*, 1994). Variations in EVI were found to be greatest in more complex land covers, such as tropical rainforest, eucalypt woodland, and semi-arid woodland.

Other comparisons between MODIS NDVI and EVI composite images showed that, while both indices agreed with monthly precipitation patterns, there were significant differences between their values, with NDVI generally being higher, especially for shaded backgrounds, and better suited to mapping savanna and deciduous vegetation (Silveira *et al.*, 2007). Foliage Projective Cover (FPC; see Section 2.3.1) is believed to be proportional to evergreen vegetation (Lu *et al.*, 2003) and MODIS NDVI was considered more appropriate to estimate FPC in low biomass vegetation (Gill *et al.*, 2009). In studies of vegetation phenology in Amazonia, vegetation fraction for open tropical forest showed a strong positive correlation with EVI, but not with NDVI (Anderson *et al.*, 2011). Wardlow and Egbert (2010) reported high thematic accuracy from both EVI and NDVI when used to map large area cropping in Kansas. Moura *et al.* (2012) compared EVI derived from both MODIS and MISR imagery for tropical forest sites. Results from these analyses demonstrated significant variability in both intra-annual and interannual trends within MODIS EVI time series datasets, that were not directly related to canopy photosynthetic activity, but were associated with view and illumination effects. EVI was considered to be more sensitive to view angle and view direction than NDVI.

The use of MODIS data for large area crop classifications is reviewed by Wardlow and Egbert (2010). Both MODIS EVI and NDVI showed high correlation with crops in the US Central Great Plains. EVI appeared to be more sensitive to biomass differences during the growing season with NDVI being more sensitive to lower biomass levels during early greening and late senescence.

8.1.2 Hyperspectral indices

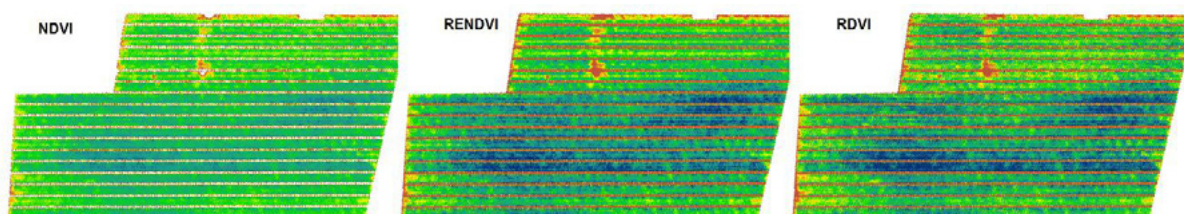
In addition to the broad band spectral indices introduced in Section 8.1.1, the narrow bands of hyperspectral data can be used to compute a range of indices that highlight subtle changes in vegetation type, health, and density (Xue and Su, 2017). In particular, reflectance variations in the ‘red edge’ range (see Section 4.3) are highlighted by many hyperspectral ratios. For example, the Normalised Difference Red Edge index (NDRE), substitutes the red edge band for the red band in the NDVI equation:

$$\text{NDRE} = \frac{\rho_{\text{NIR}} - \rho_{\text{red-edge}}}{\rho_{\text{NIR}} + \rho_{\text{red-edge}}}$$

Since the red edge band can penetrate a leaf more deeply than the red band, it is more sensitive to higher chlorophyll contents. As such, it correlates more closely with crop health than NDVI when a crop is close to harvest. It is also used to map within-crop variability of foliar nitrogen. A derivative of this index is the Canopy Chlorophyll Content Index (CCCI; Barnes *et al.*, 2000), which has strong correlation with foliar nitrogen:

$$\text{CCCI} = \frac{\text{NDRE} - \text{NDRE}_{\min}}{\text{NDRE}_{\max} - \text{NDRE}_{\min}}$$

Figure 8.2 Within field crop variability



Source: Suarez *et al.* (2018) Figure 18

When combined with the Canopy Nitrogen Index (CNI; originally the nitrogen stress index, NSI; Rodriguez *et al.*, 2006), a much stronger correlation was derived for rainfed wheat (Fitzgerald *et al.*, 2010; Cammarano *et al.*, 2011). CCCI has also been used to differentiate between high and low levels of leaf nitrogen in Victorian pear crops (APAL, 2019).

Another popular hyperspectral index is the Red Edge Normalised Difference Vegetable Index (RENDVI; Gitelson *et al.*, 1996b; Sims and Gamon, 2002):

$$\text{RENDVI} = \frac{\rho_{750} - \rho_{705}}{\rho_{750} + \rho_{705}}$$

Whereas most of the greenness indices described in Section 8.1.1 are based on broad differences in vegetation biomass, RENDVI is more sensitive to differences in pigment concentration. This sensitivity is particularly useful as a crop approaches maturity and its photosynthetic capacity is reduced (Suarez *et al.*, 2018; see Figure 8.2).

Two narrow absorption features at 505 nm and 531 nm have been related to the xanthophyll pigments, violaxanthin, antheraxanthin, and zeaxanthin, and can be used to detect changes in pigment concentration (see Excursus 4.1). The Photochemical Reflectance Index (PRI) compares absorption at 531 nm with a xanthophyll-insensitive reference at 570 nm (Gamon *et al.*, 1992, 1997):

$$\text{PRI} = \frac{\rho_{531} - \rho_{570}}{\rho_{531} + \rho_{570}}$$

PRI measures the light use efficiency (LUE) of foliage (see Sections 7.4 and 8.1.4), thus indicates water stress and CO₂ uptake by plants (see Section 17.4.5).

8.1.3 Vegetation cover and condition

In regions with sparse vegetation, such as much of central Australia, vegetation may not be the dominant component of the landscape (see Figure 2.1). In arid landscapes the soil background is the dominant feature at a range of scales, from the regional view to an field quadrat. For medium scale EO imagery, any given pixel is likely to comprise multiple landscape features, which renders indices based on vegetation greenness less useful in such environments.

Furthermore, the dominant vegetation in many of these environments often comprises mixes of green, dry, and woody material, with little contrast between red and infrared (IR) reflectance.

Accordingly, a range of spectral indices has been proposed for vegetation features other than greenness. One index that was developed to map vegetation—both dry and green—in arid rangelands is called PD54 (Pickup *et al.*, 1993). PD54 was developed for Landsat MSS imagery and is based on green and red reflectance (bands 4 and 5 respectively). This index maps vegetation cover as the scaled perpendicular distance from a predefined soil line and is similar to the perpendicular vegetation index (PVI; Richardson and Wiegand, 1977). More recently, the fractional cover methods introduced in Sections 8.3 and Excursus 8.3 are used in these environments.

Cellulose Absorption Index (CAI) describes the relative depth of the lignocellulose absorption feature at 2100 nm and can be used to quantify crop residues (Daughtry *et al.*, 1996; Daughtry, 2001) and plant litter (Nagler *et al.*, 2003). Daughtry *et al.* (2005) computed CAI as:

$$\text{CAI} = \left(\frac{\rho_{2031} + \rho_{2211}}{2} \right) - \rho_{2101}$$

The Anthocyanin Reflectance Index (ARI; Gitelson *et al.*, 2001) ratios the green and red edge reflectances to indicate the physiological status of vegetation:

$$\text{ARI} = \frac{1}{\rho_{561}} - \frac{1}{\rho_{706}}$$

ARI was subsequently modified (MARI) to include NIR reflectance include consideration of variability in leaf thickness (Gitelson *et al.*, 2006):

$$\text{MARI} = \left(\frac{1}{\rho_{561}} - \frac{1}{\rho_{706}} \right) \times \rho_{780}$$

These indices have been successfully used for non-destructive estimation of anthocyanin content in grapevine leaves (Steele *et al.*, 2009). However, they also require precise spectral bands as acquired by hyperspectral sensors rather than multispectral sensors.

The Land Condition Index (LCI), inspired by CAI, is based on the normalised difference of MODIS bands 6 and 7 (Clarke *et al.*, 2011). Since this ratio yields relatively high values for both photosynthetic and non-photosynthetic vegetation but low values for bare soil, it highlights exposed ground. This is particularly useful for “measuring the severity and duration of soil exposure over extensive cropping areas” (Clarke *et al.*, 2011). LCI also showed closer correlation with fractional soil cover (see Excursus 8.3) than NDVI. A continental LCI product is available from TERN Australia as MODIS 16-day composites from 2000 to 2011 at 500 m spatial resolution (see Section 8.4).

8.1.4 Plant productivity

The concepts of plant and ecosystem productivity are introduced in Sections 5.1.2 and 7.4. Various metrics can be considered to be indicative of the productivity of vegetation, such as LAI (see Section 6.3.3), fAPAR (see Section 6.3.4), and LUE (see Section 7.4). Such metrics summarise the capacity of groups of plants to produce energy via photosynthesis. That capacity is related to the density of leaf cover, the concentration of chlorophyll in leaves, and a range of other factors determining plant health (see Sections 5.2 and 5.3). Seasonal and phenological variations in fAPAR are informative for identifying ecosystems and monitoring ecosystem health and integrity (see Section 7).

Various greenness indices have been related to APAR, fAPAR, and LAI. It should be noted, however, that LAI is related to canopy light interception but is not linearly related to fAPAR (see Section 6.3.4). NDVI has been used to estimate LAI for uniform canopies of monocultures, such as crops and irrigated pastures, but is not appropriate to derive LAI for more complex and/or mixed canopies (Glenn *et al.*, 2008).

In particular, SR and NDVI (see Section 8.1.1) have been used extensively for canopy productivity studies. Since,

$$fAPAR = \frac{APAR}{PAR}$$

Gross Ecosystem Productivity (GEP, which is commonly used interchangeably with GPP) is often modelled from estimates of LUE, fAPAR, and PAR (see Section 6.3):

$$GEP = LUE \times fAPAR \times PAR$$

A number of indices with sensitivity to non-chlorophyll plant pigments have also been proposed (see Section 4.3). The Photochemical Reflectance Index (PRI; see Section 8.1.2) is sensitive to plant xanthophyll levels, so can be considered to be indicative of the efficiency of PAR usage and also soil moisture and nutrient status (Peñuelas *et al.*, 1995, 1997a). This has been related to carbon fluxes and GPP (Gamon *et al.*, 1990, 1992; see Section 17), and selectively correlated with LUE (with variations related to differences in vegetation age, type, and leaf persistence; Grace *et al.*, 2007). Net Primary Productivity (NPP; see Section 7.4) has also been mapped from NDVI imagery. For example, Raupach *et al.* (2001) used AVHRR NDVI imagery to compute NPP, over Australia based on available data for climate and agricultural inputs (such as irrigation and nutrients). Similar maps were produced to include carbon stored in growing plants (leaf, wood, and root), and growing plants plus litter. These maps show close correlation with the land cover patterns highlighted in vegetation index imagery and captured in land cover classes. More recently, Donohue *et al.* (2014) used the generic DIFFUSE model to estimate GPP for trees, C3 and C4 plants in Australia from MODIS time series datasets (see Figure 7.6), verified against eddy flux tower-derived estimates (see Excursus 7.2).

It should be noted that the relationship between reflectance and LAI is direct, but the relationship between reflectance and productivity, or biomass, is indirect (Hill, 2004). Canopies with different volumes of biomass may result in the same LAI measurement due to variations in canopy structure, density, and composition. Accordingly, biomass estimates from optical EO data perform best for canopies with simpler structures that are dominated by green, actively growing vegetation. This occurs, for example, in grasslands managed for pasture, where growth is initiated by seasonal variations in temperature and/or rainfall, and steadily continues until it reaches maximum greenness (Hill, 2004; see Section 14).

Measurement of above ground biomass to validate EO analyses is detailed in Schaefer (2018). The use of airborne and ground-based lidar (see Excursus 5.1) to derive estimates of forest biomass is described in Section 16 and models for estimating plant productivity in the context of carbon cycling are detailed in Section 17.

8.1.5 Water content

Attributes of foliage water content were introduced in Section 4.2.1. One indicator of moisture content in vegetation is chlorophyll content (see Section 8.1.1), but variations in chlorophyll concentration can also result from other factors, including species differences, phenological status, atmospheric pollution, nutrient deficiency, toxicity, pathology, and radiation stress (Ceccato *et al.*, 2001). Good indicators of plant water content need to be independent of these factors. It should be noted, however, that water stress can induce changes in plant architecture as well as water content, so modelling approaches that incorporate information on plant structure may be more appropriate for some applications (Jacquemoud and Ustin, 2003).

Equivalent Water Thickness (EWT; Green *et al.*, 1991; Gao and Goetz, 1995; see Section 4.2.1) and radiative transfer simulations (Jacquemoud *et al.*, 1996; Zarco-Tejada *et al.*, 2003) have been related to the relative water content of vegetation (Dennison *et al.*, 2003). EO data can also be used to quantify the water content of vegetation by relying on the liquid water absorption features in optical wavelengths (see Section 13). Since NIR and SWIR reflectance is influenced to varying degrees by internal leaf structure, water content, and dry matter content, reflectance data in both these wavelength regions are needed to determine water content (see Section 4.3). Various studies have selected wavelengths in both of these spectral regions to compute ratios and normalised ratios, which have demonstrated good correlation with EWT, with double ratios providing stronger correlations (Colombo *et al.*, 2008). EWT can also be estimated using the Normalised Difference Infrared Index (NDII; Hardinsky *et al.* 1983):

$$\text{NDII} = \frac{\rho_{870} - \rho_{1650}}{\rho_{870} + \rho_{1650}}$$

and the Normalised Difference Water Index (NDWI; Gao, 1996; Serrano *et al.*, 2000; see Volume 3B—Section 11):

$$\text{NDWI} = \frac{\rho_{870} - \rho_{1240}}{\rho_{870} + \rho_{1240}} = \frac{\text{red} - \text{SWIR}}{\text{red} + \text{SWIR}}$$

WI and NDWI derived from AVIRIS imagery have been shown to account for most of the variation in canopy relative water content, though results are dependent on vegetation species (Serrano *et al.*, 2002). Datt (2012) developed two semi-empirical indices for *Eucalyptus* species, which demonstrated much stronger correlations with EWT and less sensitivity to radiation scatter than other indices:

$$\frac{\rho_{850} - \rho_{2218}}{\rho_{850} + \rho_{1928}}$$

and

$$\frac{\rho_{850} - \rho_{1788}}{\rho_{850} + \rho_{1928}}$$

Other indices that have been proposed to infer vegetation moisture properties from EO imagery include the Normalised Difference Moisture Index (NDMI):

$$\text{NDMI} = \frac{\rho_{\text{NIR}} - \rho_{\text{SWIR}}}{\rho_{\text{NIR}} + \rho_{\text{SWIR}}}$$

and the Moisture Stress Index (MSI), which was originally formulated for Landsat TM bands 5 and 4 (Hunt and Rock, 1989; Ceccato *et al.* 2001):

$$\text{MSI} = \frac{\rho_{1650}}{\rho_{820}}$$

and the Water Index (WI; Peñuelas *et al.*, 1997b):

$$\text{WI} = \frac{\rho_{900}}{\rho_{2218}}$$

Some of the other spectral indices that have been proposed to represent plant water content include:

- Plant Water Index (PWI) = $\frac{\rho_{970}}{\rho_{900}}$; Peñuelas *et al.*, 1997b);
- Relative Depth Index (RDI; Rollin and Milton, 1998);
- Global Vegetation Moisture Index (GVMI; Ceccato *et al.*, 2002a, 2002b);
- Simple Ratio Water Index (SRWI) = $\frac{\rho_{860}}{\rho_{1240}}$; Zarco-Tejada *et al.*, 2003); and
- Canopy Structure Index (CSI; Sims and Gamon, 2003).

The water absorption features that are prominent in EO measurements of vegetation enable an invaluable landscape scale measure of plant water content (see Section 9.4). Colombo *et al.* (2008) obtained more robust estimates of both leaf and canopy EWT from hyperspectral indices than from inversion of leaf and canopy radiative transfer models (see Section 10.2). As discussed in Section 18.3.1.2, various studies have evaluated the capacity of using water content indices derived from EO data to infer fuel moisture for fire risk prediction (Verbesselt *et al.*, 2002, 2007; Chuvieco *et al.*, 2002; Dennison *et al.*, 2003, 2005; Yebra *et al.*, 2008; Caccamo *et al.*, 2011a). Caccamo *et al.* (2011b) found NDII based on MODIS band 6 offered best results for drought monitoring of high biomass vegetation.

8.1.6 Landscape 'leakiness'

The concept of landscape function, and the tendency of a dysfunctional landscape to 'leak' soil and water resources, was introduced in Section 7.3. An EO-based Leakiness Index (LI) that indicates the potential of a landscape to leak, that is not retain, soil sediments was developed by Ludwig *et al.* (2002, 2007):

$$LI = 1 - \left(\frac{L_{max} - L_{calc}}{L_{max} - L_{min}} \right)^k$$

where

LI ranges from 0.0 (non-leaky) to 1.0 (totally leaky);

L_{calc} is determined with reference to EO pixel values and DEM data by modelling surface flows to and from adjacent pixels (using the T-HYDRO model; Ostendorf and Reynolds, 1993), based on the assumption that pixels with greater vegetation cover are more likely to retain water and soil resources, and slow their flow to pixels at lower elevations;

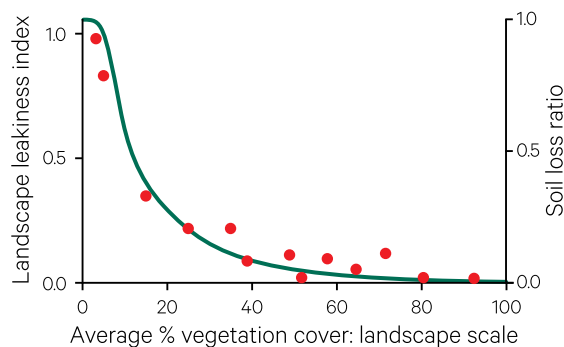
L_{max} is defined as the value of L_{calc} when all pixel covers are zero;

L_{min} is the minimum leakiness value (and is typically set to zero for simplicity); and

k defines the shape and steepness of the relationship between LI and vegetation cover.

Figure 8.3 Leakiness index

The leakiness index relates vegetation cover to soil loss based on field site measurements.



Adapted from: Ludwig *et al.* (2007) Figure 1b

EO-based vegetation cover estimates are calibrated against field site data, with appropriate consideration of scaling differences. Values of LI decrease non-linearly with increasing vegetation cover (see Figure 8.3). LI has been used to successfully monitor the condition of rangeland sites using EO datasets over several decades (Ludwig *et al.*, 2007; see Section 15).

8.2 Spectral Classification

Traditionally, one of the most commonly used image processing techniques for analysing EO imagery is classification. Image classification is introduced in Volume 2A—Section 9, while extensive details of this process, and its many variations, are provided in Volume 2E.

Images are classified in a wide range of application areas to identify and delineate 'classes', that is, to separate the image into a set of categories that contain 'similar' pixels. In this context, the definition of 'similar' will depend on the selected input data, the selected processing method, and the intended purpose of the classification. The use of appropriate image data is paramount to a credible classification result. An understanding of the selected classification process is also essential to ensure that the resulting classes capture the intrinsic variation in the image (see Volume 2E).

Probably the most common end-product from classifying an EO image is a map which aims to describe 'land cover' (see Section 3). Such maps typically have a range of categories which differentiate geographic regions using characteristics of their vegetation, soils, and landforms. The

successful mapping of such regional differences using EO data requires that the selected categories are differentiated somehow in the data itself and can be extracted cleanly using image classification and segmentation methods (see Volume 2E).

Supervised image classification can be viewed as both an art and a science. Volume 2E mostly addresses issues relating to the science. The art of this area of analysis involves both identifying those characteristics of image data that most effectively distinguish between the required categories, then determining a processing pathway that most efficiently produces a reliable land cover map. A key issue in these two activities is to establish the level of detail with which the categories can be reliably differentiated in the image.

As detailed in Volume 1, EO data records levels of radiation being reflected from, or emitted by, the Earth's surface, such that each pixel value represents some pre-defined type and level of radiation for a given area on the Earth's surface at one instant in time. Accordingly, certain categories may be differentiable in one EO image but not in another. If the characteristics defining the categories exhibit

seasonal variation, this may also be true for two images acquired at different times from the same sensing system. The likelihood of a given category of interest being differentiated by image classification can be most readily determined using the exploratory image analysis tools discussed in Volumes 2A, 2C, and 2E. Time spent becoming familiar with an image is usually reimbursed by uncovering a clear and efficient processing pathway through the subsequent stages of classification. These initial analyses also indicate those image channels that provide the best discrimination, and can assist in the selection of transformations to highlight category differences and/or reduce data volume. As discussed in Volume 2E, the choice of allocation algorithms generally depends on the number of categories required and the processing resources (in terms of both interpreter's time and computing facilities) available for the study.

However, image classification should not be viewed solely as a means for interpolating and extrapolating known categories over a given area. By recording objective and consistent measurements of surface radiation, EO data provide an ideal basis for such analyses. However, the imagery should also be considered as an additional source of information that may highlight patterns or occurrences of surface features which are not discernible by other means or anticipated by the interpreter's classes. By forcing a classification to follow a strictly supervised pathway (which effectively assumes that the interpreter already knows everything there is to know about the study area and is simply assessing how well these features can be mapped from an image), useful additional information that is available from the image may be ignored. The Mosaic Model approach introduced in Volume 2A—Section 9 and recommended in Volume 2E attempts to combine supervised and unsupervised techniques during image classification to derive maximum information from the image.

Various categorisations of land use/land cover for classifying EO data have been proposed. One of the more commonly used systems was proposed by Anderson *et al.* (1976). As detailed in Excursus 3.1, this system describes a four level hierarchy of categories which was developed by USGS (United States Geological Survey). The higher levels are necessarily generalised to apply to a range of environments and describe land cover in terms of geographical, and somewhat academic, labels. Many classifications require a set of labels which are specifically tailored to the application problem being studied, so would correspond to Level III or Level IV in the Anderson system.

The following sub-sections discuss characteristics of EO data and processing algorithms which are relevant to classifying several major land cover categories: vegetation, geology and soils, water, and urban features.

8.2.1 Vegetation

Well-established reflectance characteristics for vegetation provide a good starting point for determining the expected parameters for classes relating to vegetation in EO images. As detailed in Sections 4.3 and 8.1, high NIR and low red reflectance values are reliably used to identify healthy green vegetation (see Figure 4.3). As vegetation condition deteriorates, the NIR reflectance decreases before, and more dramatically than, the green decreases and red increases (see Figure 4.4). The 'red edge', the sharp increase in reflectance between red and NIR wavelengths, also occurs at shorter wavelengths as plant health declines. The latter change is a subtle one though, only detectable by sensors with high spectral resolution (see Section 8.1.2).

These heuristic observations can guide selection of the most appropriate image channels to use for mapping vegetation. Most typically red, NIR, and SWIR channels are considered to provide the best discrimination of vegetation types. In most cases, the red and IR channels usually provide best separation between different land cover types. Various vegetation indices have been proposed to highlight gradients within vegetation in EO images (see Section 8.1). These are most commonly based on red and NIR reflectance channels and generally combine channels using ratios or differences. Drawing on 22 years of published hyperspectral studies, a review of wavebands for vegetation class discrimination found that visible and red edge channels were the most frequently selected, followed by portions of the SWIR, then NIR spectral regions (Hennessy *et al.*, 2020).

Seasonal effects need careful consideration when selecting EO imagery for mapping vegetation (see Volume 1B—Section 1.4 and Volume 2D). For example, known characteristics of crop development may define a stage of growth when the crop will be markedly different from surrounding vegetation (see Sections 5.3.2 and 9.3). This may occur at full greenness for an irrigated crop which is growing near slower-maturing or later-sown crops, or non-irrigated areas, or at the crop's haying stage if it is mixed with later-maturing crops (see Section 12). Similarly, as native grasslands dry off, trends within wooded vegetation often become easier to differentiate (see Section 9.1). For example, in tropical environments, at the end of the wet season all vegetation is so lush that EO measurements cannot easily distinguish between different types. A few months after the start of the dry season however, most vegetation has dried out and a much greater range of vegetation types can be delineated.

A major problem for vegetation mapping in many Australian environments is the extent of bushfires, which result in prominent, dark scars in EO imagery (see Section 18), which can be spectrally similar to the edges of waterbodies. In the wet/dry tropics, image dates need to be carefully selected to allow some ‘drying’ of vegetation after the wet season, but preferably precede most fires in the dry season. In temperate woodlands and forests, understorey shrubs (such as acacias) may have flowering characteristics which alter their EO reflectance. The greenness of grasses, and possibly lichens and/or mosses, vary more rapidly with moisture availability than woody vegetation, and can also modify imaged values in woodlands and open forest (see Section 9.1). Leaf and bark colour, and the leaf volume of trees themselves, can also change with the seasons, so need to be considered if tree mapping is an important aspect of the classification (see Section 5.3.2). Sun angle becomes significant for forest and woodland vegetation, with higher Sun angles (closer to midday and the summer solstice) resulting in less shadowing of the background in imaged scenes (see Volume 1B—Section 3.5 and Volume 2X—Excursus 1.1).

One example of classifying vegetation type using EO datasets to determine vegetation condition relative to a defined benchmark (see Section 3.2.2) is presented in Excursus 8.2.

8.2.2 Geology and soils

As with vegetation, various factors can alter the ‘typical’ reflectance for exposed soil or rock surfaces (see Figure 3.2). These factors were introduced in Volume 1B—Section 6.3 and include:

- moisture—wet soils have greater absorption, hence lower reflectance, for all wavelengths;
- organic matter—reflectance of visible to NIR wavelengths can be reduced by up to 60% by organic matter in soils (5% organic matter content results in darker soils, with higher proportions of organic matter resulting in minimal reflectance reductions);
- surface texture and roughness—determined by grain size and structure of aggregated grains. In general, the rougher a soil surface, the more shadowing and darker its appearance. For example, coarse grained sands reflect less strongly than fine grained sands. Strongly structured soils, with high clay content, often form a rougher surface than weaker structured sands which further reduces reflectance; and
- mineral content:
 - ◆ ferric iron-bearing oxides and oxyhydrides (or limonites) have an absorption band centred on ultraviolet wavelengths which results in lower reflectance up to about 550 nm, and

can have shallow absorption in 850–950 nm. Their relatively high reflectance in yellow/red wavelengths causes the characteristic reddish colours of iron-rich soils;

- ◆ carbonate minerals and silicates containing hydroxyl ions (such as micas and clay minerals) exhibit absorption peaks in the wavelength range 2.1–2.5 μm ; and
- ◆ increasing silica content causes the characteristic absorption peak in 8–14 μm range to occur at shorter wavelengths.

Geological analyses often aim to identify linear features and patterns in images so tend to use enhancement techniques rather than classification methods. Filtering techniques can be used to highlight lineaments or directional patterns (see Volume 2C—Section 5). Some enhancements concentrate maximum image information into three channels for visual interpretation such as:

- Hue Saturation Intensity (HSI) transformations; see Volume 2C—Section 8);
- Principal Components Analysis (PCA; see Volume 2C—Section 9); and
- decorrelation stretching (see Volume 2C—Section 9.4).

A range of spectral indices have also been developed to discriminate surface minerals (see Volume 2C—Excursus 10.1), especially for ASTER imagery (Cudahy, 2012).

While multispectral satellite imagery can be used to discriminate and identify surface features related to lithology and soils, applications that are particularly concerned with discriminating geological features often use hyperspectral imagery (Jupp and Datt, 2004) and/or EO sensors that detect energy sources other than EMR, such as radioactivity or magnetism (see Volume 1A—Sections 6 and 7).

An impediment to using EO for geological applications is that the surface layer can often mask underlying geology. Since vegetation cover often conceals the soil surface, a ‘software defoliant’ was developed by Fraser and Green (1987) for geological analyses, which significantly removed the vegetation component in woodland images (see Volume 2C—Section 9). Alternatively, geobotany attempts to link anomalies in vegetation type and growth patterns to characteristics of soil geochemistry (Goetz *et al.*, 1983), but can be confounded by many climate-related factors such as fire (Simpson, 1990). The spectral response of exposed rock surfaces can also be modified by lichen cover, iron-rich coatings, and deep weathering. For example, past chemical weathering events in Australia are reported to have altered surface materials to depths of hundreds of metres over a large proportion of the continent (Simpson, 1990).

Thermal infrared (TIR) information can also be useful for mapping hydrogeology, geology, and soil type and condition (see Volume 1B—Section 7). In particular, the difference in temperature between daytime and nighttime images indicates the rate at which surface materials heat and cool. This phenomena is referred to as thermal inertia and has been shown to be principally related to moisture content and

lithology. Classification of thermal inertia images offer a useful summary of these features. Daytime thermal imagery in conjunction with meteorological data can be used to estimate evapotranspiration (ET), which is a significant parameter in plant growth and the hydrologic cycle (see Sections 5.2.3 and 7.6 respectively).

Excursus 8.2—NSW State Vegetation Type Map (SVTM)

Source: NSW DPIE (2019)

Further information: <https://www.environment.nsw.gov.au/vegetation/state-vegetation-type-map.htm>

The NSW State Vegetation Type Map (SVTM) locates Plant Community Types (PCT) on a consistent base over NSW. This product uses EO image products to extrapolate known landscape characteristics from thousands of survey sites across NSW. Based on the datasets and processes described below, each map unit is finally coded in terms of three hierarchical attributes:

- formations;
- classes; and
- PCT—indicate the species assemblage at local and regional scales.

Vegetation map outputs comprise pre-1750 (before European clearing) PCT coverage and extant PCT coverage. Specific datasets used to create these regional scale maps include:

- high resolution aerial photography (ADS40/80: 50 cm resolution for vegetation classification across eastern and central NSW);
- satellite time series imagery (SPOT-5: 2.5 m resolution, 2005–2013 for vegetation classification across western NSW; Shuttle Radar Topography Mission (SRTM); Landsat TM/ETM+: 25 m resolution, 1989–2008);
- relevant botanical and environmental variables recorded at survey sites (primarily based on pre-existing, full floristic survey data in the Bionet Flora Survey database and augmented by additional surveys to fill data gaps);
- statewide (continuous and categorical) environmental layers covering geology, climate, topography, and water; and
- archival mapping and other historical references, and other compatible regional scale mapping.

The process flow used to create SVTM is consistent with the NVIS methodology (Thackway *et al.*, 2008). As summarised in Table 8.2, this process flow follows parallel pathways for analysing the site-based and image datasets. In the fifth stage (Spatial Product Development), these datasets are analysed jointly using the following processes:

- use expert interpretation and GIS technology to assign pre-1750 vegetation photo patterns to all polygons in imagery based on GEOBIA segmentation (see Volume 2A—Excursus 10.1), environmental layers, and site survey data;
- model the distribution of plant communities within geographical constraints created by vegetation photo patterns and label each polygon as a PCT (unless a non-PCT class, such as rock or water);
- use expert interpretation to review and edit modelling outputs to complete the pre-1750 vegetation coverage; and
- mask out areas which are no longer native vegetation to create an extant vegetation coverage.

The map resulting from this processing sequence is available online (see Section 8.4) and can be accessed in terms of available sub-regions. The SVTM system has been designed to incorporate new data when available, thus maintaining currency of this product.

Table 8.2 SVTM workflow

Site-based data	Spatial data
1. Acquire field data and determine plant type	2. Acquire spatial data
3. Classification and allocation	4. Image processing
5. Spatial product development	
6. Publish maps	

8.2.3 Water

Known reflectance characteristics are again a good starting point for selecting appropriate channels to use for mapping water features. As introduced in Volume 1B—Section 6.4 and detailed in Volume 3B, water has higher reflectance of shorter wavelengths, with reflectance decreasing as wavelength increases up to the NIR region where radiation is totally absorbed (see Figure 3.2). NIR channels are useful to delineate water from land, while the rate of decrease in radiation from blue to IR can be related to water depth. TIR measurements have also been correlated with algal concentrations and thermal pollution. Calibrated EO time series, such as Digital Earth Australia (DEA; see Volume 2D—Section 11.2), have been valuable for delineating persistent and ephemeral watercourses in Australia (Mueller *et al.*, 2016; see Volume 1A—Excursus 5.1) and mapping tidal variations in shorelines (see Volume 3B). Volume 3B reviews processing techniques and applications for these and other EO applications to surface waters, including water quality.

Snow cover exhibits characteristically high reflectance in visible wavelengths, though some reduction in reflectance occurs with age and impurities (see Volume 1B—Section 6.5). Reflectance is lower for IR wavelengths, especially for older snow and glacier ice, with NIR wavelengths (in the range 1.0–1.3 μm) being sensitive to grain size (Dozier, 1984). Thermal wavelengths can be confusing for mapping snow and generally offer less contrast than visible and IR wavelengths (Salomonson, 1983). Engman and Gurney (1991) recommend the use of visible channels from satellite imagery for identifying and mapping snow, preferably selecting a channel close to IR wavelengths (such as Landsat TM3), since there is greater difference between snow and non-snow at those wavelengths. Snow and cloud can be most easily separated in SWIR bands, with snow having much lower values than cloud (Dozier, 1984).

8.2.4 Urban features

Urban here refers to the man-made environment of buildings and roads with small pockets of vegetation. Being monochromatic, many urban materials such as concrete and asphalt have uniform levels of reflectance across the visible (and NIR) wavelengths. As with bare soil, moisture lowers these reflectances. Shadows can also reduce reflectance levels averaged over several objects and can result in well-defined directional patterns in images featuring buildings.

The extent of spatial intermixing of different surface materials that occurs in urban areas is a major problem when using standard classification algorithms. This problem exists at two levels: firstly the spatial resolution of most EO data is of a size which combines multiple surface components, such as vegetation, roofs, and pavement in a single pixel; secondly the categories of interest often pertain to land uses (such as residential areas) that are defined in terms of spatial patterns rather than distinct spectral values. The increasing spatial resolution of both airborne and spaceborne EO sensors is encouraging greater use for monitoring of water usage, drainage, construction, tree removal, and thermal efficiency in urban areas. EO measurements in the 8–14 μm TIR window highlight urban concentrations since these generally emit more thermal energy than natural features in the environment (see Volume 1B—Section 7). Within urban centres, the SWIR window of 3.5–5.5 μm can identify points of high thermal radiation such as mills, power plants, or fires. Features with differing thermal inertia characteristics, such as roads/paving, vegetation, and water, can also be differentiated by the change between their daytime and nighttime temperatures.

*A cloak of loose, soft material, held to the earth's hard surface by gravity,
is all that lies between life and lifelessness.*
(Wallace H. Fuller)

8.3 Sub-pixel Analyses

One image feature extraction approach, which was originally applied to multispectral imagery (Adams and Adams, 1985; Smith *et al.*, 1990) and is now widely used for hyperspectral imagery, is variously called mixture analysis, endmember analysis, or spectral unmixing (Keshava and Mustard, 2002; Keshava, 2003). This approach attempts to quantify the proportion of pre-defined ground components within each pixel. Many variants of ‘sub-pixel’ analysis have been adapted to a wide range of applications (Somers *et al.*, 2011), including mapping the proportion or fraction of vegetation cover, or fractional cover (Guerschman *et al.*, 2009), within each pixel. Sub-pixel analysis is essentially based on a number of assumptions:

- a finite number of ground components can be defined, such as photosynthetic vegetation, non-photosynthetic vegetation, and bare soil, which describe the spectral variation in an EO image;
- each ground component is spectrally distinct and can be represented by their spectral value(s) or ‘endmembers’;
- a ‘pure’ image pixel could contain just one type of ground component, in which case its spectral value(s) could be directly associated with that ground component;
- most image pixels are mixed pixels, comprising different areal proportions (or ‘fractions’) of each ground component; and
- the spectral value(s) of mixed pixels are indicative of the proportions of its ground components.

A block of ‘pure’ pixels for a given component would therefore appear as a single ‘colour’ (or set of spectral value/s) with no variance. A block of ‘mixed’ pixels with the same ‘mix’ of components would appear to be a similar, but variable, colour. Most image classification methods use image ‘colour’ (as spectral values) to associate each image pixel with one from a selected set of feature (or ground cover) classes. By contrast, sub-pixel methods rely on image variance to determine the varying proportions of a small number of pre-defined ground components in each pixel. There are two key issues to consider in this scenario:

- how are the endmembers defined, both in terms of the full set of ground components and their spectral value(s)? and
- how are their proportions determined, that is, the contribution that each component makes towards the pixel spectral value/s (Hapke, 1981, 1984, 1986)?

A number of models have been proposed to describe how the unique spectral value(s) of each ground component is combined into a single set of mixed pixel values for an individual pixel. These models can be grouped into two broad categories based on the way ground component spectral values(s) are combined to produce the value(s) of a given pixel:

- linear mixture models (LMM; also commonly known as Spectral Mixture Analysis: SMA)—assume that the ground components present within a given pixel combine as a simple addition of their spectral values(s) in proportion to the area of the pixel they occupy. LMM are relatively straightforward mathematically but ignore the numerous interactions that can occur between ground components within a pixel and also the variations that can occur within an image, both of which can result in the situation where a given set of ground components could occur in the same proportions in two different pixels yet result in different spectral value(s); or
- non-linear mixture models (NLMM)—recognise that incident light can be scattered both within and between ground components before their combined reflectance is measured by the sensor, so their combination would not be linear (Keshava and Mustard, 2002). NLMM attempt to account for these intra-pixel variations but invariably introduce mathematical complexity for model implementation and greater uncertainty in the modelled results.

LMM can be seen to work when, for a given pixel, the incident light only interacts with one ground component and the components are mixed at a ‘macroscopic scale’. An example of this situation would be a checkerboard pattern. In this case, the reflected light from multiple ground components is only mixed at the sensor. Since ground components rarely contribute equally to the measured radiance from a mixed pixel, with some components simply being more reflective than others (see Figure 3.2), the pixel radiance is unlikely to be a simple additive combination of either the mass or cross-sectional area of the proportional radiances of its ground components (see Section 6.4 and Volume 1B—Section 6.6). However, numerous studies have yielded results which indicate that LMM offer an acceptable model for many real world scenarios (Bioucas-Dias *et al.*, 2012) and many algorithms have been developed to implement these models (Zare and Ho, 2014). Variations of LMM include multiple endmember spectral mixture analysis (MESMA), which extends SMA to permit endmembers to vary, in both number and type, for different image pixels (Roberts *et al.*, 1998).

Mathematically, in LMM the pixel signature (r_s) is assumed to be a linear sum of reflectances from each of n endmembers weighted in proportion to its cover (k_j) in the pixel:

$$r_s = \sum_{j=1}^n k_j R_j$$

where

the pixel signature, r_s , is the linear sum of the reflectances of each cover type (R_j) weighted by its proportion (k_j) in the pixel;

$k_j \geq 0$ for $j=1, n$; and

$$\sum_{j=1}^n k_j = 1$$

Sub-pixel or endmember analysis seeks to invert this mixing by deriving the proportions (k_j) of each component in the pixel signature. This can feasibly be derived from the EO data provided that, if there are n components (trees, shrubs, grass, etc.), then there are at least $(n-1)$ channels of data that separate the endmembers spectrally. There has been considerable work aimed at deriving endmembers from hyperspectral imagery (Boardman, 1990), spectral libraries and/or spectral measurements in the field (TERN Australia, 2018). Some limitations to this approach include:

- broad-band signatures of ground components (such as the tree and shrub crowns over much of Australia) are not markedly spectrally distinct;
- where spectrally distinct crowns exist, their distinction is confounded by the effects of shadowing within crowns and cast shadow on the background, with bigger plants shading smaller plants. This makes the signature of the endmembers difficult to estimate as the signature depends on the proportions of crowns and shadows present and variations in Sun and look angles; and
- relatively low covers of trees and shrubs, together with shadowing, introduce such high spectral variance into the data relative to the spectral contrasts between endmembers that the numerical methods used in the endmember analysis become highly unstable.

Shadow effects obviously depend primarily on the Sun angle (see Volume 1B—Section 3.5). Although the crown cover is the same, lower Sun angles clearly decrease image brightness. Differences due to shadowing can be taken into account in endmember analysis, provided the endmember values are recalculated for each temporal image and one or more components labelled ‘shade’ are added to the list. However, its successful application still depends on an assumption of linear scaling along cover gradients due to changes in Sun position and sensor view angle. These assumptions in practice are erroneous in structured vegetation (that is, vegetation with discontinuous cover of trees or shrubs), which may limit the application of such methods to general synoptic estimates of change in cover (see Volume 2X—Excursus 1.1).

Sub-pixel analysis is being used to derive a number of standard image products from EO data in Australia, such as fractional cover (see Excursus 8.3) and persistent green vegetation (see Section 9.1).

Excursus 8.3—Fractional Cover

Source: TERN Australia: http://www.auscover.org.au/dataset_categories/land-cover-dynamics-and-phenology/

Further information: Guerschman *et al.* (2009, 2015); Muir *et al.* (2011); Stewart *et al.*, (2014); Scarth *et al.* (2018); Guerschman and Hill (2018)

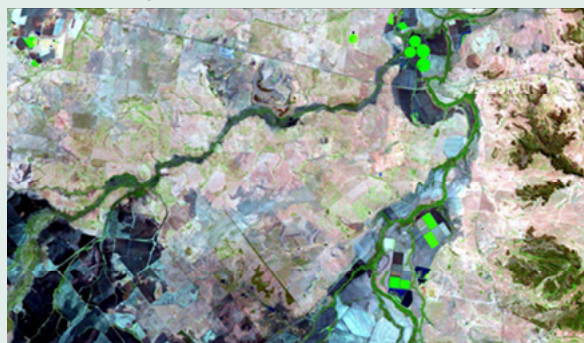
Fractional cover represents the percentages of photosynthetic vegetation (F_{pv}), non-photosynthetic vegetation (F_{npv}), and bare soil (F_{bs}) in a given area (see Section 6.3.6 and Figure 8.4). These proportions are particularly valuable for a range of regional and continental monitoring programs, including estimation of:

- total biomass—for ecosystem studies of carbon and nutrient uptake, surface albedo, and heat exchange between the land surface and the atmosphere (Guerschman *et al.*, 2009, 2015);
- ground cover monitoring—to assess pastures and crops (Muir *et al.*, 2011; Stewart *et al.*, 2014);
- landscape condition—by observing regional soil exposure dynamics (Clarke *et al.*, 2014) and managing stubble to achieve zero tilling;
- compliance monitoring—to detect removal of woody vegetation (see Volume 2D—Excursus 14.3);
- fuel loads that impact fire frequency and intensity (Tindall *et al.*, 2014; He *et al.*, 2019); and
- susceptibility to wind and water erosion (DustWatch, 2019).

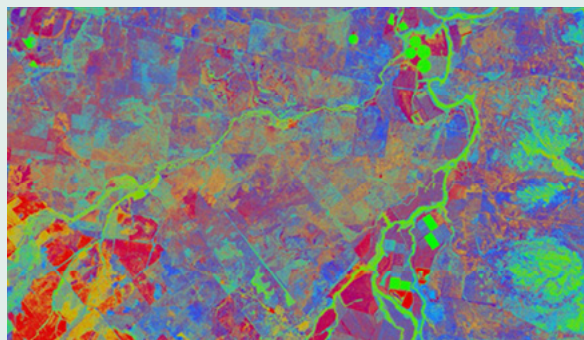
Along with standing biomass and growth rate, fractional cover represents one of three vital inputs for assessment of sustainable global rangeland productivity. (Guerschman and Hill, 2018)

Figure 8.4 Fractional cover index image

a. Example image in true colour



b. The fractional vegetation cover image showing the photosynthetic ('green'), non-photosynthetic ('non-green'), and bare ground fractions. For example, vigorously growing crops in centre pivots at the top right of the image are shown in green, and bare/fallow crops in the lower left are shown in red.



c. Thematic colour key based on three endmembers



Source: Tindall *et al.* (2014)

Fractional cover methods rely on reflectance spectra at defined sites for calibration and validation (Scarath *et al.*, 2018). These methods are based on the image processing approaches of spectral indices (see Section 8.1) and linear unmixing/spectral mixture analysis (see Section 8.3 and Volume 2E). Australian variants of fractional cover products that are available from TERN Australia (see Section 8.4) include:

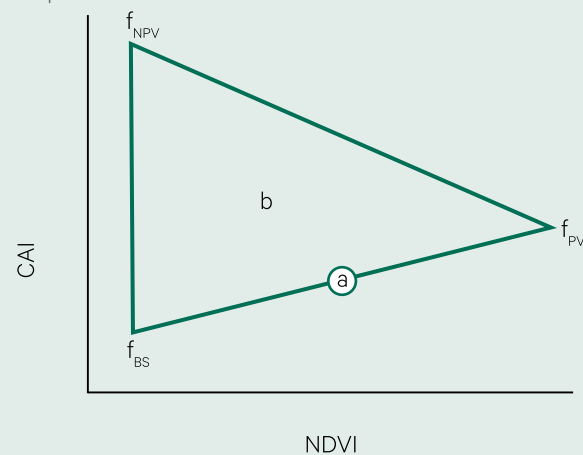
- MODIS fractional cover derived from all bands of the MODIS MCD43A4 collection 6 daily product, using a linear unmixing methodology (Guerschman *et al.*, 2015), with calibration and validation from 3022 field observations (Guerschman and Hill, 2018). This 8-day fractional cover product is available in 500 m spatial resolution from 2000 to the present and maintains consistency with previous Australian versions (Guerschman *et al.*, 2009, 2015; Gill *et al.*, 2014). A suite of derivative products is also produced including:
 - ◆ monthly fractional cover (aggregated from the 8-day composites using the medoid method);
 - ◆ total vegetation cover (photosynthetic + non-photosynthetic); and
 - ◆ anomaly of total cover against the time series (difference between total vegetation cover in a given month and the mean total vegetation cover for that month in all years available).

This product is being upgraded to use MODIS Collection 6.1 products for compatibility with GEOGLAM-RaPP global fractional cover datasets (see Excursus 11.1).

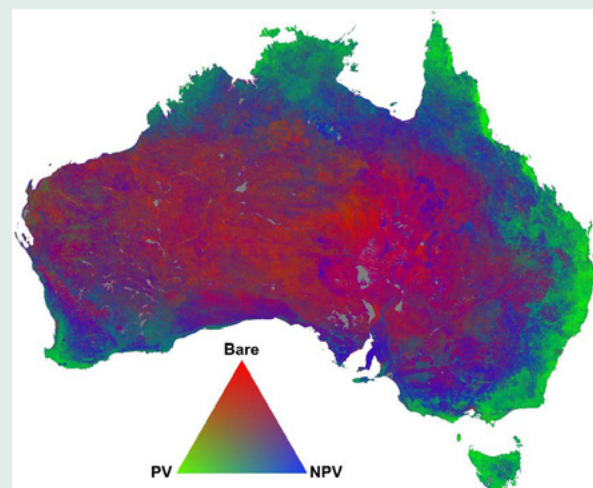
- MODIS 16-day composites based on Relative Spectral Mixture Analysis (RSMA; Okin *et al.*, 2007), Spectral Mixture Analysis Time Series (SMATS; Okin *et al.*, 2013), and Absolute Relative Spectral Mixture Analysis (ARSMA; Clarke *et al.*, 2011) methods, which measure changes in fractional covers relative to a baseline date at 500 m spatial resolution.
- Landsat seasonal fractional cover based on constrained linear spectral unmixing (Scarath *et al.*, 2010; see Section 8.3). This product is available from Digital Earth Australia (DEA; see Volume 2D—Section 11.2) at 25 m spatial resolution from 1986 to the present.

Figure 8.5 Fractional cover endmembers

a. Conceptual approach for locating the endmembers for 'pure' photosynthetic vegetation (f_{PV}), non-photosynthetic vegetation (f_{NPV}), and bare soil (f_{BS}) in a crossplot of NDVI versus CAI. In this example, point (a) represents a ground site halfway between f_{BS} and f_{PV} , while point (b) represents an equal mix of all three components.



b. MODIS Fractional cover for Australia in April 2015



Source: a. Based on Guerschman *et al.* (2009) Figure 2; b. TERN Australia (2018) Figure 7.8

8.4 Further Information

Spectral Indices

Index Database for remote sensing indices: <https://www.indexdatabase.de/>

Fractional Cover Products

TERN Australia (2018): http://www.auscover.org.au/dataset_categories/vegetation-structural-properties-biomass/

DEA: https://docs.dea.ga.gov.au/notebooks/02_DEA_datasets/Introduction_to_Fractional_Cover.html; https://d28rz98at9flks.cloudfront.net/79676/Fractional_Cover_FC25_v1_5.PDF

NSW State Vegetation Type Mapping

SVTM: <https://www.environment.nsw.gov.au/vegetation/state-vegetation-type-map.htm>

8.5 References

- Adams, J.B., and Adams, J.D. (1984). Geologic mapping using LANDSAT MSS and TM images: Removing vegetation by modeling spectral mixtures. In *Third Thematic Conference Remote Sensing for Exploration Geology*, ERIM, Colorado Springs, CO, Vol. 2. pp. 615–622.
- Allan, G., Johnson, A., Cridland, S., and Fitzgerald, N. (2003). Application of NDVI for predicting fuel curing at landscape scales in northern Australia: can remotely sensed data help schedule fire management operations? *International Journal of Wildland Fire*, 12(4), 299–308.
- Anderson, J.R., Hardy, E.E., Roach, J.T., and Witmer, R.E. (1976). *A Land Use and Land Cover Classification System for Use with Remote Sensor Data*. USGS Professional Paper 964. 28p.
- Anderson, L.O., Aragão, L.E.O.C., Shimabukuro, Y.E., Almeida, S., and Huete, A. (2011). Fraction images for monitoring intra-annual phenology of different vegetation physiognomies in Amazonia. *International Journal of Remote Sensing*, 32(2), 387–408.
- Barnes, E.M., Clarke, T.R., Richards, S.E., Colaizzi, P.D., Haberland, J., Kostrzewski, M., Waller, P., Choi, C., Riley, E., Thompson, T., Lascano, R.J., Li, H., and Moran, M.S. (2000). Coincident detection of crop water stress, nitrogen status and canopy density using ground based multispectral data. In *Proceedings of 5th International Conference on Precision Agriculture*, Bloomington, Minnesota, USA.
- Bioucas-Dias, J.M., Plaza, A., Dobigeon, N., Parente, M., Du, Q., Gader, P., and Chanussot, J. (2012). Hyperspectral unmixing overview: Geometrical, statistical, and sparse regression-based approaches. *IEEE Journal of Selected Topics in Applied Earth Observations and Remote Sensing*, 5(2), 354–379.
- Boardman, J. (1990). Inversion of high spectral resolution data. *Proceedings of SPIE, 1298, Imaging Spectroscopy and Terrestrial Environment*. Orlando, Florida. pp 222–223.
- Burgan, R.E., and Hartford, R.A. (1993). *Monitoring vegetation greenness with satellite data*. USDA, Forest Service, General Technical Report INT-297, Intermountain Research Station, Ogden, UT, 43 pp.
- Burgan, R.E., Klaver, R.W., and Klaver, J.M. (1998). Fuel models and fire potential from satellite and surface observations. *International Journal of Wildland Fire*, 8(3), 159–170.
- Burt, A., Disney, M., and Calders, K. (2018). Extracting individual trees from lidar point clouds using treeSeg. *Methods in Ecology and Evolution*, 10, 438–445. doi.org/10.1111/2041-210X.13121
- Caccamo, G., Chisholm, L.A., Bradstock, R.A., Puotinen, M.L., and Phippen, B.G. (2011a). Monitoring live fuel moisture content of heathland, shrubland and sclerophyll forest in south-eastern Australia using MODIS data. *International Journal of Wildland Fire*, 21(3), 257–269.
- Caccamo, G., Chisholm, L.A., Bradstock, R.A., and Puotinen, M.L. (2011b). Assessing the sensitivity of MODIS to monitor drought in high biomass ecosystems. *Remote Sensing of Environment*, 115, 2626–2639.

- Carlson, T., and Ripley, D. (1997). On the relation between NDVI, fractional vegetation cover, and leaf area index. *Remote Sensing of Environment*, 62, 241–252.
- Ceccato, P., Flasse, S., Tarantla, S., Jacquemoud, S., and Grégoire, J.-M. (2001). Detecting vegetation leaf water content using reflectance in the optical domain. *Remote Sensing of Environment*, 77, 22–33.
- Ceccato, P., Gobron, N., Flasse, S., Pinty, B., and Tarantola, S. (2002a). Designing a spectral index to estimate vegetation water content from remote sensing data: Part 1: Theoretical approach. *Remote Sensing of Environment*, 82(2–3), 188–197. doi:10.1016/S0034-4257(02)00037-8
- Ceccato, P., Flasse, S., and Grégoire, J.-M. (2002b). Designing a spectral index to estimate vegetation water content from remote sensing data: Part 2: Validation and applications. *Remote Sensing of Environment*, 82(2–3), 198–207. [https://doi.org/10.1016/S0034-4257\(02\)00036-6](https://doi.org/10.1016/S0034-4257(02)00036-6)
- Chuvieco, E., Riano, D., Aguado, I., and Cocero, D. (2002). Estimation of fuel moisture content from multitemporal analysis of Landsat Thematic Mapper reflectance data: application in fire danger assessment. *International Journal of Remote Sensing*, 23(11), 2145–2162.
- Chuvieco, E., Aguado, I., Cocero, D., And, D., and Rian, O. (2003). Design of an empirical index to estimate fuel moisture content from NOAA-AVHRR images in forest fire danger studies. *International Journal of Remote Sensing*, 24, 1621–1637.
- Cicone, B.C., and Metzler, M.D. (1984). Comparison of Landsat MSS, Nimbus-7, CZCS, and NOAA-7 AVHRR features for land-use analysis. *Remote Sensing of Environment*, 14, 257–265.
- Clarke, K., Lewis, M., Dutkiewicz, A., Forward, G., and Ostendorf, B. (2011). *Spatial and Temporal Monitoring of Soil Erosion Risk with Satellite Imagery*. Land Condition Monitoring Reports #4. University of Adelaide, Report for the South Australian Department for Environment and Natural Resources. Adelaide.
- Clarke, K., Lawley, E., Raja Segaran, R., and Lewis, M. (2014). *Spatially-explicit environmental indicators for regional NRM planning for climate change*. The University of Adelaide, Report for Natural Resources SA Arid Lands. Adelaide,
- Colombo, R., Meroni, M., Marchesi, A., Busetto, L., Rossini, M., Giardino, C., and Panigada, C. (2008). Estimation of leaf and canopy water content in poplar plantations by means of hyperspectral indices and inverse modeling. *Remote Sensing of Environment*, 112, 1820–1834.
- Crist, E.P., and Cicone, R.C. (1984). Application of the Tasseled Cap concept to simulated Thematic Mapper data. *Photogrammetric Engineering and Remote Sensing*, 50, 343–352.
- Cudahy, T. (2012). *Satellite ASTER Geoscience Product Notes for Australia*. CSIRO ePublish No. EP-30-07-12-44. <https://publications.csiro.au/rpr/download?pid=csiro:EP125895&dsid=DS4>
- Datt, B. (2012). Visible/near infrared reflectance and chlorophyll content in *Eucalyptus* leaves. *International Journal of Remote Sensing*, 20(14), 2741–2759. doi:10.1080/014311699211778
- Daughtry, C.S.T. (2001). Discriminating crop residues from soil by short-wave infrared reflectance. *Agronomy Journal*, 93, 125–131.
- Daughtry, C.S.T., McMurtrey III, J. E., Chappelle, E. W., Hunter, W. J., and Steiner, J. L. (1996). Measuring crop residue cover using remote sensing techniques. *Theoretical and Applied Climatology*, 54, 17–26.
- Daughtry, C.S.T., Hunt, E.R.Jr., Doraiswamy, P.C., and McMurtry, III J.E. (2005). Remote sensing the spatial distribution of crop residues. *Agronomy Journal*, 97, 864–871.
- Deering, D. W., Rouse, J. W., Haas, R. H., and Schell, J. A. (1975). Measuring Forage Production of Grazing Units from Landsat MSS Data. *10th International Symposium on Remote Sensing of Environment*, 2, 1169–1178.
- Dennison, P.E., Roberts, D.A., Thorgusen, S.R., Regelbrugge, J.C., Weise, D., and Lee, C. (2003). Modelling Seasonal Changes in Live Fuel Moisture and Equivalent Water Thickness using a Cumulative Water Balance Index. *Remote sensing of Environment*, 88(4), 442–452. doi:10.1016/j.rse.2003.08.015
- Dennison, P.E., Roberts, D.A., Peterson, S.H., and Rechel, J. (2005). Use of Normalized Difference Water Index for monitoring live fuel moisture. *International Journal of Remote Sensing*, 26(10), 1035–1042.
- Dilley, A.C., Millie, S., O'Brien, D.M., and Edwards, M. (2004). The relation between Normalized Difference Vegetation Index and vegetation moisture content at three grassland locations in Victoria, Australia. *International Journal of Remote Sensing*, 25(19), 3913–3930. doi:10.1080/01431160410001698889

- Donohue, R.J., Hume, I.H., Roderick, M.L., McVicar, T.R., Beringer, J., Hutley, L.B., Gallant, J.C., Austin, J.M., van Gorsel, E., Cleverly, J.R., Meyer, W.S., and Arndt, S.K. (2014). Evaluation of the remote-sensing-based DIFFUSE model for estimating photosynthesis of vegetation. *Remote Sensing of Environment*, 155, 349–365.
- Dozier, J. (1984). Snow reflectance from Landsat-4 Thematic Mapper. *IEEE Transactions on Geoscience and Remote Sensing*, 22, 323–328.
- DustWatch (2019). *Community DustWatch* webpage, NSW Department of Planning, Industry and Environment website: <https://www.environment.nsw.gov.au/topics/land-and-soil/soil-degradation/wind-erosion/community-dustwatch>
- Eidenshink J. C., Burgan, R. E., and Haas, R. H. (1990). Monitoring fire fuels condition by using time series composites of Advanced Very High Resolution Radiometer (AVHRR) data. *Proceedings of Resource Technology 90*. Washington, DC, ASPRS, 68–82.
- Emelyanova, I.V., McVicar, T.R., Van Niel, T.G., Li, L.T., and van Dijk, A.I.J.M. (2012). *On blending Landsat–MODIS surface reflectances in two landscapes with contrasting spectral, spatial and temporal dynamics*. WIRADA project 3.4: Technical report. Australia: CSIRO Water for a Healthy Country Flagship. <https://doi.org/10.4225/08/5852dc6879ab8>
- Emelyanova I.V., McVicar, T.R., Van Niel, T.G., Li, L.T., and van Dijk, A.I.J.M. (2013). Assessing the accuracy of blending Landsat-MODIS surface reflectances in two landscapes with contrasting spatial and temporal dynamics: A framework for algorithm selection. *Remote Sensing of Environment*, 133, 193–209.
- Engman, E.T., and Gurney, R.J. (1991). *Remote Sensing in Hydrology*. Chapman and Hall, London. 255 p.
- Felderhof, L. (2007). *The Fire Patchiness Paradigm: A Case Study in Northwest Queensland*. Ph. D thesis, James Cook University, Townsville, Queensland, Australia.
- Fiorucci, P., Gaetani, F., Lanorte, A., and Lasaponara, R. (2007). Dynamic fire danger mapping from satellite imagery and meteorological forecast data. *Earth Interactions*, 11(7), 1–17. doi:10.1175/EI199.1
- Fraser, S.J., and Green, A.A. (1987). A software defoliant for geological analysis of band ratios. *International Journal of Remote Sensing*, 8, 525–532.
- Gamon, J.A., Field, C.B., Bilger, W., Bjorkman, O., Fredeen, A.L., and Peñuelas, J. (1990). Remote sensing of the xanthophyll cycle and chlorophyll fluorescence in sunflower leaves and canopies. *Oecologia*, 85, 1–7.
- Gamon, J.A., Peñuelas, J., Field, C.B. (1992). A narrow-waveband spectral index that tracks diurnal changes in photosynthetic efficiency. *Remote Sensing of Environment*, 41, 35–44.
- Gamon, J.A., Serrano, L., and Surfus, J.S. (1997). The photochemical reflectance index: an optical indicator of photosynthetic radiation use efficiency across species, functional types, and nutrient levels. *Oecologia*, 112, 492–501.
- Gao, B.C. (1996). NDWI—a normalised difference water index for remote sensing of vegetation liquid water from space. *Remote Sensing of Environment*, 58, 257–266.
- Gao, B.C., and Goetz, A.F.H. (1995). Retrieval of equivalent water thickness and information related to biochemical components of vegetation canopies from AVIRIS data. *Remote Sensing of Environment*, 52(3), 155–162. doi:10.1016/0034-4257(95)00039-4
- Gao, X., Huete, A. R., Ni, W., and Miura, T. (2000). Optical–biophysical relationships of vegetation spectra without background contamination. *Remote Sensing of Environment*, 74, 609–620.
- Gallaudet, T.C., and Simpson, J.J. (1991). Automated cloud screening of AVHRR imagery using split-and-merge clustering. *Remote Sensing of Environment*, 38, 77–121.
- Gill, T.K., Phinn, S.R., Armston, J.D., and Pailthorpe, B.A. (2009). Estimating tree-cover change in Australia: challenges of using the MODIS vegetation index product. *International Journal of Remote Sensing*, 30(6), 1547–1565.
- Gill, T., Heidenreich, S., and Guerschman, J.P. (2014). *MODIS Monthly Fractional Cover: Product Creation and Distribution*. Joint Remote Sensing Research Program Publication Series. http://www.gpem.uq.edu.au/cser-web/docs/JRSRP_Publication_Series/gillt.2014.modis_monthly_cover.pdf
- Gitelson, A.A., Kaufman, Y.J., and Merzlyak, M.N. (1996a). Use of a green channel in remote sensing of global vegetation from EOS-MODIS. *Remote Sensing of Environment*, 58, 289–298.
- Gitelson, A.A., Merzlyak, M.N., and Lichtenhaler, H.K. (1996b). Detection of Red Edge Position and Chlorophyll Content by Reflectance Measurements near 700 nm. *Journal of Plant Physiology*, 148(3–4), 501–508. [https://doi.org/10.1016/S0176-1617\(96\)80285-9](https://doi.org/10.1016/S0176-1617(96)80285-9)

- Gitelson, A.A., Merzlyak, M.N., Chivkunova, O.B. (2001). Optical properties and nondestructive estimation of anthocyanin content in plant leaves. *Photochemical Photobiology*, 74(1), 38–45.
- Gitelson, A.A., Kaufman, Y.J., Stark, R., and Rundquist, D. (2002). Novel algorithms for remote estimation of vegetation fraction. *Remote Sensing of Environment*, 80(1), 76–87.
- Gitelson, A.A., Keydan, G.P., and Merzlyak, M.N. (2006). Three-band model for non-invasive estimation of chlorophyll assessment in higher plant leaves. *Journal of Plant Physiology*, 160, 271–282.
- Glenn, E.P., Huete, A.R., Nagler, P.L., and Nelson, S.G. (2008a). Relationship between remotely-sensed vegetation indices, canopy attributes and plant physiological processes: what vegetation indices can and cannot tell us about the landscape. *Sensors*, 8, 2136–2160.
- Goetz, A.F.N., Rock, B.N., and Rowan, L.C. (1983). Remote sensing for exploration: an overview. *Economic Geology*, 78, 5773–5790.
- Grace, J., Nichol, C., Disney, M., Lewis, P., Quaife, T., and Bowyer, P. (2007). Can we measure terrestrial photosynthesis from space directly, using spectral reflectance and fluorescence? *Global Change Biology*, 13, 1484–1497.
- Green, R.O., Conel, J.E., Margolis, J.S., Brugge, C.J., and Hoover, G.L. (1991). An inversion algorithm for the retrieval of atmospheric and leaf water absorption from AVIRIS radiance with compensation for atmospheric scattering, *Proceedings of 3rd Annual Airborne Visible/Infrared Imaging Spectrometer (AVIRIS) Workshop*, Pasadena, California, JPL Publication 91-28, pp. 51–61.
- Guerschman, J.P., and Hill, M.J. (2018). Calibration and validation of the Australian fractional cover product for MODIS collection 6. *Remote Sensing Letters*, 9(7), 696–705. doi:10.1080/2150704X.2018.1465611
- Guerschman, J.P., Hill, M.J., Renzullo, L.J., Barrett, D.J., Marks, A.S., and Botha, E.J. (2009). Estimating fractional cover of photosynthetic vegetation, non photosynthetic vegetation and bare soil in the Australian tropical savannah region upscaling Hyperion and MODIS sensors. *Remote Sensing of Environment*, 113, 928–945.
- Guerschman, J. P., Scarth, P. F., McVicar, T. R., Renzullo, L. J., Malthus, T. J., Stewart, J. B., Rickards, J.E., and Trevithick, R. (2015). Assessing the effects of site heterogeneity and soil properties when unmixing photosynthetic vegetation, non-photosynthetic vegetation and bare soil fractions from Landsat and MODIS data. *Remote Sensing of Environment*, 161, 12–26. doi:10.1016/j.rse.2015.01.021
- Hapke, B.W. (1981). Bidirectional reflectance spectroscopy. 1. Theory. *Journal of Geophysical Research*, 86, 3039–3054.
- Hapke, B.W. (1984). Bidirectional reflectance spectroscopy. 3. Correction for macroscopic roughness. *Icarus*, 59, 41–59.
- Hapke, B.W. (1986). Bidirectional reflectance spectroscopy. 4. The extinction coefficient and the opposition effect. *Icarus*, 67, 264–280.
- Hardisky, M. A., Klemas, V., & Smart, R. M. (1983). The influence of soil salinity, growth form, and leaf moisture on the spectral radiance of *Spartina alterniflora* canopies. *Photogrammetric Engineering and Remote Sensing*, 49, 77–83.
- Harrison, B.A., and Jupp, D.L.B. (1990) *Introduction to Image Processing: Part TWO of the microBRIAN Resource Manual*. CSIRO, Melbourne. 256 p.
- He, J., Loboda, T.V., Jenkins, L., and Chen, D. (2019). Mapping fractional cover of major fuel type components across Alaskan tundra. *Remote Sensing of Environment*, 232, 111324. <https://doi.org/10.1016/j.rse.2019.111324>
- Hennessy, A., Clarke, K., and Lewis, M. (2020). Hyperspectral classification of plants: A review of waveband selection generalisability. *Remote Sensing*, 12(1), 113.
- Hill, M.J. (2004). Grazing agriculture—Managed Pasture, Grassland and Rangeland. In *Manual of Remote Sensing, Volume 4, Remote Sensing for Natural Resource Management and Environmental Monitoring*. (Ed: S.L. Ustin). Wiley International, New York. 768 p.
- Huete, A.R. (1988). A soil-adjusted vegetation index (SAVI). *Remote Sensing of Environment*, 25, 295–309.
- Huete, A, Jackson, R., and Post, D. (1985). Spectral response of a plant canopy with different soil backgrounds. *Remote Sensing of Environment*, 17, 37–53.
- Huete, A., Justice, C., and Liu, H. (1994). Development of vegetation and soil indices for MODIS–EOS. *Remote Sensing of Environment*, 49, 224–234.

- Huete, A.R., Liu, H.Q., Batchily, K., and Leeuwen, W. (1997). A comparison of vegetation indices over a global set of TM images for EOS-MODIS. *Remote Sensing of Environment*, 59, 440–451.
- Huete, A., Justice, C., and van Leeuwen, W. (1999). *MODIS vegetation index (MOD 13) algorithm theoretical basis document (ATBD) Version 3.0*. EOS Project Office, NASA Goddard Space Flight Center, Greenbelt, MD.
- Huete, A.R., Didan, K., Miura, T., Rodriguez, E.P., Gao, X., and Ferreira, L.G. (2002). Overview of the radiometric and biophysical performance of the MODIS vegetation indices. *Remote Sensing of Environment*, 83, 195–213.
- Huete, A., Didan, R., van Leeuwen, W., Miura, T., and Glenn, E. (2011). MODIS Vegetation Indices. Ch 26 in *Land Remote Sensing and Global Environmental Change*, Remote Sensing and Digital Image Processing Volume 11, Springer Science+Business Media, LLC. ISBN 978-1-4419-6748-0.
- Hunt, E.R., Jr, and Rock, B.N. (1989). Detection of changes in leaf water content using near- and middle-infrared reflectances. *Remote Sensing of Environment*, 30, 43–54.
- Jacquemoud, S., and Ustin, S.L. (2003). Application of radiative transfer models to moisture content estimation and burned land mapping. *Proceedings of 4th International Workshop on Remote Sensing and GIS Applications to Forest Fire Management*. pp 3–12. (Eds: E. Chuvieco, P. Martin and C Justice). 5–7 June, 2003, Ghent, Belgium.
- Jacquemoud, S., Ustin, S.L., Verdebout, J., Schmuck, G., Andreoli, G., and Hosgood, B. (1996). Estimating leaf biochemistry using the PROSPECT leaf optical properties model. *Remote Sensing of Environment*, 56, 194–202.
- Jiang, Z., Huete, A., Chen, J., Chen, Y., Li, J., Yan, G., and Zhang, X. (2006). Analysis of NDVI and scaled difference vegetation index retrievals of vegetation fraction. *Remote Sensing of Environment*, 101, 366–378.
- Jiang, Z., Huete, A., Didan, K., and Miura, T. (2008). Development of a two-band enhanced vegetation index without a blue band. *Remote Sensing of Environment*, 112(10), 3833–3845. <https://doi.org/10.1016/j.rse.2008.06.006>
- Jupp, D.L.B., and Datt, B. (Eds) (2004). *Evaluation of the EO-1 Hyperion Hyperspectral Instrument and its Applications at Australian Validation Sites 2001–2003*. CSIRO Earth Observation Centre, Canberra.
- Kaufman, Y. J., and D. Tanre (1992). Atmospherically resistant vegetation index (ARVI) for EOS-MODIS. *IEEE Transactions on Geoscience and Remote Sensing*, 30(2), 261–270.
- Kauth, R.J., and Thomas, G.S. (1976). The Tasselled Cap—a graphic description of the spectral-temporal development of agricultural crops as seen by Landsat. *Proceedings of Symposium on Machine Processing of Remotely Sensed Data*. Purdue University, West Lafayette, Indiana, 4B41–4B51. http://docs.lib.purdue.edu/lars_symp/159
- Ke, Y., and Quackenbush, L.J.L. (2011). A review of methods for automatic individual tree-crown detection and delineation from passive remote sensing. *International Journal of Remote Sensing*, 32, 4725–4747.
- Keshava, N. (2003). A Survey of Spectral Unmixing Algorithms. *Lincoln Laboratory Journal*, 14(1), 55–78.
- Keshava, N., and Mustard, J.F. (2002). Spectral Unmixing. *Signal Processing Magazine, IEEE*, 19(1), 44–57. doi:10.1109/79.974727
- Lasaponara, R., (2005). Inter-comparison of AHVRR-based fire susceptibility indicators for the Mediterranean ecosystems of Southern Italy. *International Journal of Remote Sensing*, 26, 853–870.
- Liu, H.Q., and Huete, A.R. (1995). A feedback based modification of the NDVI to minimize canopy background and atmospheric noise. *IEEE Transactions on Geoscience and Remote Sensing*, 33, 457–465.
- Liu, G.-R., Liang, C.-K., Kuo, T.-H., Lin, T.-H., and Huang, S.-J. (2004). Comparison of the NDVI, ARVI and AFRI Vegetation Index, along with their relations with the AOD using SPOT-4 Vegetation data. *TAO* 15(1), 15–31.
- Liu, J., Miller, J.R., Haboudane, D., Pattey, E., and Hochheim, K. (2008). Crop fraction estimation from casi hyperspectral data using linear spectral unmixing and vegetation indices. *Canadian Journal of Remote Sensing*, 34, S124–S138.
- Lu, H., Raupach, M.R., McVicar, T.R., and Barrett, D.J. (2003). Decomposition of vegetation cover into woody and herbaceous components using AVHRR NDVI time series. *Remote Sensing of Environment*, 86, 1–18.
- Ludwig, J.A., Eager, R.W., Bastin, G.N., Chewings, V.H., and Liedloff, A.C. (2002). A leakiness index for assessing landscape function using remote sensing. *Landscape Ecology*, 17, 157–171.

- Ludwig, J.A., Bastin, G.N., Chewings, V.H., Eager, R.W., and Liedloff, A.C. (2007). Leakiness: A new index for monitoring the health of arid and semiarid landscapes using remotely sensed vegetation cover and elevation data. *Ecological Indicators*, 7, 442–454.
- Matsushita, B., Yang, W., Chen, J., Onda, Y., and Qiu, G. (2007). Sensitivity of the Enhanced Vegetation Index (EVI) and Normalized Difference Vegetation Index (NDVI) to Topographic Effects: A Case Study in High-Density Cypress Forest. *Sensors*, 7, 2636–2651.
- Moura, Y.M., Calvão, L.S., dos Santos, J.R., Roberts, D.A., and Breunig, F.M. (2012). Use of MISR/Terra data to study intra- and inter-annual EVI variations in the dry season of tropical forest. *Remote Sensing of Environment*, 127, 260–270.
- Muir, J., Schmidt, M., Tindall, D., Trevithick, R., Scarth, P., and Stewart, J. (2011). *Guidelines for Field measurement of fractional ground cover: a technical handbook supporting the Australian collaborative land use and management program*. Technical report, Queensland Department of Environment and Resource Management for the Australian Bureau of Agricultural and Resource Economics and Sciences, Canberra. http://data.daff.gov.au/data/warehouse/pe_hbgcm9abll07701/HndbkGrndCovMontring2011_1.0.0_HR.pdf
- Mueller, N., Lewis, A., Roberts, D., Ring, S., Melrose, R., Sixsmith, J., Lymburner, L., McIntyre, A., Tan, P., Curnow, S., and Ip, A. (2015). Water observations from space: Mapping surface water from 25 years of Landsat imagery across Australia. *Remote Sensing of Environment*, 174, 341–352. <https://doi.org/10.1016/j.rse.2015.11.003>
- Nagler, P.L., Inoue, Y., Glenn, E.P., Russ, A.L., and Daughtry, C.S.T. (2003). Cellulose absorption index (CAI) to quantify mixed soil-plant litter scenes. *Remote Sensing of Environment*, 87, 310–325.
- NSW DPIE (2019). *State Vegetation Type Map* webpage, NSW Department of Planning, Industry and Environment website: <https://www.environment.nsw.gov.au/vegetation/state-vegetation-type-map.htm>
- Okin, G.S. (2007). Relative spectral mixture analysis—A multitemporal index of total vegetation cover. *Remote Sensing of Environment*, 106(4), 467–479. doi:10.1016/j.rse.2006.09.018
- Okin, G.S., Clarke, K.D., and Lewis, M.M. (2013). Comparison of methods for estimation of absolute vegetation and soil fractional cover using MODIS Normalized BRDF-Adjusted Reflectance Data. *Remote Sensing of Environment*, 130, 266–279. doi:10.1016/j.rse.2012.11.021
- Ostendorf, B., and Reynolds, J.F. (1993). Relationships between a terrain-based hydrologic model and patch-scale vegetation patterns in an arctic tundra landscape. *Landscape Ecology*, 8, 229–237.
- Peñuelas, J., Filella, I., and Gamon, J.A. (1995). Assessment of photosynthetic radiation-use efficiency with spectral reflectance. *New Phytology*, 131, 291–96.
- Peñuelas, J., Llusia, J., Piñol, J., and Filella, I. (1997a). Photochemical reflectance index and leaf photosynthetic radiation-use efficiency assessment in Mediterranean trees. *International Journal of Remote Sensing*, 18, 2863–2868.
- Peñuelas, J., Piñol, J., Ogaya, R., and Filella, I. (1997b). Estimation of plant water concentration by the reflectance water Index WI (R900/R970). *International Journal of Remote Sensing*, 18, 2869–2875.
- Pickup, G., Chewings, V.H., and Nelson, D.J. (1993). Estimating changes in vegetation cover over time in arid rangelands using Landsat MSS data. *Remote Sensing of Environment*, 43, 243–263. [https://doi.org/10.1016/0034-4257\(93\)90069-A](https://doi.org/10.1016/0034-4257(93)90069-A)
- Raupach, M.R., Kirby, J.M., Barrett, D.J., and Briggs, P.R. (2001). *Balances of Water, Carbon, Nitrogen and Phosphorus in Australian Landscapes: (1) Project Description and Results*. CSIRO Land and Water Technical Report 40/01, Canberra.
- Richardson, A.J., and Wiegand, C.L. (1977). Distinguishing Vegetation from Soil Background Information. *Photogrammetric Engineering and Remote Sensing*, 43(12), 1541–1552.
- Roberts, D., Gardner, M., Church, R., Ustin, S., Scheer, G., and Green, R.O. (1998). Mapping chaparral in the Santa Monica mountains using multiple endmember spectral mixture models. *Remote Sensing of Environment*, 65, 267–279.
- Roberts, D., Dunn, B., and Mueller, N. (2018). Open Data Cube Products Using High-Dimensional Statistics of Time Series. *Proceedings of 2018 IGARSS*, 22–27 July, Valencia Spain.
- Rollin, E.M., and Milton, E.J. (1998). Processing of high spectral resolution reflectance data for the retrieval of canopy water content information. *Remote Sensing of Environment*, 65, 86–92.
- Rondeaux, G., Steven, M., and Baret, F. (1996). Optimisation of Soil-Adjusted Vegetation Indices. *Remote Sensing of Environment*, 55, 95–107
- Rouse, J.W., Haas, R.H., Schell, J.A., and Deering, D.W. (1973). Monitoring vegetation systems in the Great Plains with ERTS. *Proceedings of the 3rd ERTS Symposium*, NASA SP-351 I, 309–317.

- Salomonson, V.V. (1983). Water Resources Assessment. In *Manual of Remote Sensing*. (Ed: R.N. Colwell). 2nd Edn. American Society of Photogrammetry and Remote Sensing, Falls Church, Virginia.
- Scarth, P., Röder, A., and Schmidt, M. (2010). Tracking grazing pressure and climate interaction—the role of Landsat fractional cover in time series analysis. In *Proceedings of the 15th Australasian Remote Sensing and Photogrammetry Conference (ARSPC)*, 13–17 September, Alice Springs, Australia. Alice Springs, NT. doi:10.6084/m9.figshare.94250
- Scarth, P., Guerschman, J.P., Clarke, K., and Phinn, S. (2018). Validation of Australian Fractional Cover Products from MODIS and Landsat Data. Ch 7 in *Effective Field Calibration and Validation Practices: A practical handbook for calibration and validation satellite and model-derived terrestrial environmental variables for research and management*. A TERN Landscape Assessment Initiative, NCRIS. ISBN: ISBN 978-0-646-94137-0. <https://www.tern.org.au/NEW-CalVal-handbook-for-remote-sensing-bgp4370.html>
- Schaefer, M.T. (2018). Measurement of above ground biomass. Ch 12 in *Effective Field Calibration and Validation Practices: A practical handbook for calibration and validation satellite and model-derived terrestrial environmental variables for research and management*. A TERN Landscape Assessment Initiative, NCRIS. ISBN 978-0-646-94137-0.
- Serrano, L., Ustin, S.L., Roberts, D.A., Gamon J.A., and Peñuelas, J. (2000). Deriving water content of chaparral vegetation from AVIRIS data. *Remote Sensing of Environment*, 74(3), 570–581.
- Serrano, L., Peñuelas, J., and Ustin, S.L. (2002). Remote sensing of nitrogen and lignin in Mediterranean vegetation from AVIRIS data. *Remote Sensing of Environment*, 81, 355–364. doi:10.1016/S0034-4257(02)00011-1
- Silveira, E.M., de O., Carvalho, L.M.T., Acerbi Jr., F.W., and de Mello, J.M. (2007). The Assessment of Vegetation Seasonal Dynamics using Multitemporal NDVI and EVI images derived from MODIS. *IEEE Workshop on Analysis of Multi-temporal Remote Sensing Images*, 14(2), 177–184. 18–20 July 2007, Belgium.
- Simpson, C.J. (1990). Deep weathering, vegetation and fireburn. Significant obstacles for geoscience remote sensing in Australia. *International Journal of Remote Sensing*, 11(11), 2019–2034. DOI:10.1080/01431169008955158
- Sims, D.A., and Gamon, J.A. (2002). Relationships between leaf pigment content and spectral reflectance across a wide range of species, leaf structures and developmental stages. *Remote Sensing of Environment*, 81, 337–354.
- Sims, D.A., and Gamon, J.A. (2003). Estimation of vegetation water content and photosynthetic tissue area from spectral reflectance: A comparison of indices based on liquid water and chlorophyll absorption features. *Remote Sensing of Environment*, 84(4), 526–537. doi:10.1016/S0034-4257(02)00151-7
- Smith, M.O., Ustin, S.L., Adams, J.B., and Gillespie, A.R. (1990). Vegetation in deserts: I. A regional measure of abundance from multispectral images. *Remote Sensing of Environment*, 31(1), 1–26. [https://doi.org/10.1016/0034-4257\(90\)90074-V](https://doi.org/10.1016/0034-4257(90)90074-V).
- Somers, B., Asner, G.P., Tits, L., and Coppin, P. (2011). End member variability in Spectral Mixture Analysis: A review. *Remote Sensing of Environment*, 115, 1603–1616.
- Steele, M.R., Gitelson, A.A., Rundquist, D.C., and Merzlyak, M.N. (2009) Nondestructive estimation of Anthocyanin Content in Grapevine Leaves. *American Journal of Enology and Viticulture*, 60(1), 87–92.
- Stewart, J.B., Rickards, J.E., Randall, L.A., McPhee, R.K., and Paplinska, J.Z. (2014). *Ground cover monitoring for Australia: Final report July 2012 to June 2013, ABARES Technical report 14.1*. Australian Bureau of Agricultural and Resource Economics and Sciences, Canberra, May 2014.
- Suarez, L.A., McPhee, J., O'Halloran, J., van Sprang, C., and Robson, A. (2018). *Adoption of precision systems technology in vegetation production*. Literature Review for VG16009, Horticulture Innovation Australia, Queensland.
- TERN Australia (2018). *Effective Field Calibration and Validation Practices: A practical handbook for calibration and validation satellite and model-derived terrestrial environmental variables for research and management*. A TERN Landscape Assessment Initiative, NCRIS. ISBN: ISBN 978-0-646-94137-0. <https://www.tern.org.au/NEW-CalVal-handbook-for-remote-sensing-bgp4370.html>
- Thackway, R., Neldner, J., and Bolton, M. (2008). Vegetation. In: *Australian Soil and Land Survey Handbook Guidelines for Conducting Surveys* (2nd Edition). (Eds: N.J. McKenzie, M.J. Grundy, R. Webster, and A.J. Ringrose-Voase). CSIRO Publishing, Melbourne.

- Tindall, D., Trevithick, R., Scarth, P., Collett, L., Goodwin, N., Denham, R., and Flood, N. (2014). *Ground cover and fire in the grazing lands*. RP64G Synthesis Report, Department of Science, Information Technology, Innovation and the Arts. Brisbane.
- Tucker, C.J. (1979). Red and photographic infrared linear combinations for monitoring vegetation. *Remote Sensing of Environment*, 8(2), 127–150.
- Verbesselt, J., Fleck, S., and Coppin, P. (2002). Estimation of fuel moisture content towards Fire Risk Assessment: A review. In: *Forest Fire Research and Wildland Fire Safety* (Ed: Viegas), Millpress. Rotterdam. ISBN 90-77017-72-0.
- Verbesselt, J., Somer, B., Lhermitte, S., Jonckheere, I., van Aardt, J., and Coppin, P. (2007). Monitoring herbaceous fuel moisture content with SPOT VEGETATION time-series for fire risk prediction in savanna ecosystems. *Remote Sensing of Environment*, 108, 357–368.
- Wardlow, B.D., and Egbert, S.L. (2010). A comparison of MODIS 250-m EVI and NDVI data for crop mapping: a case study for southwest Kansas. *International Journal of Remote Sensing*, 31(3), 805–830.
- Wardlow, B.D., Egbert, S.L., and Kastens, J.H. (2007). Analysis of time-series MODIS 250 m vegetation index data for crop classification in the U.S. Central Great Plains. *Remote Sensing of Environment*, 108, 290–310.
- Waring, R.H., Coops, N.C., Fan, W., and Nightingale, J.M. (2006). MODIS enhanced vegetation index predicts tree species richness across forested ecoregions in the contiguous U.S.A. *Remote Sensing of Environment*, 103, 218–226.
- Xue, J., and Su, B. (2017). Significant Remote Sensing Vegetation Indices: A Review of Developments and Applications. *Journal of Sensors*, 1–17. doi:10.1155/2017/1353691
- Yebra, M., Chuvieco, E., and Riano, D. (2008). Estimation of live fuel moisture content from MODIS images for fire risk assessment. *Agricultural and Forest Meteorology*, 148, 523–536.
- Youngentob, K.N., Renzullo, L.J., Held, A.A., Jia, X., Lindenmayer, D.B., and Foley, W.J. (2012). Using imaging spectroscopy to estimate integrated measures of foliage nutritional quality. *Methods in Ecology and Evolution*, 3, 416–426. doi:10.1111/j.2041-210X.2011.00149.x
- Zarco-Tejada, P.J., Rueda, C.A., and Ustin, S. L. (2003). Water content estimation in vegetation with MODIS reflectance data and model inversion methods. *Remote Sensing of Environment*, 85, 109–124.
- Zare, A., and Ho, K.C. (2014). Endmember Variability in Hyperspectral Analysis. *IEEE Signal Processing Magazine*, 31(1), 95–104.



9 Monitoring

One of the great promises of EO was the prospect of using ‘objective’ measurements to monitor changes in land cover and condition over selected time periods (Singh, 1989). In the context of terrestrial vegetation, various applications of environmental monitoring can be readily listed:

- identifying and quantifying land use changes (see Section 3.4.2);
- measuring the extent and rate of deforestation and afforestation (see Section 16);
- tracking land degradation (see Section 11.4);
- highlighting stress conditions in vegetation (due to biotic and abiotic factors; see Sections 9.5 and 9.6);
- showing the extent of damage from disaster events, such as fire or flood (see Section 18 and Volume 3B); and
- gauging long term changes in vegetative cover due to recurrent drought and other climatic variations (see Sections 3.4.1, 9.2.2, 11.3 and 15).

Of all the questions which can come before this nation, short of the actual preservation of its existence in a great war, there is none which compares in importance with the great central task of leaving this land even a better land for our descendants than it is for us.
(Theodore Roosevelt)

However, in some areas, the application of this technology has hitherto fallen short of its promise. Like most technological solutions, using EO for environmental monitoring presents its own set of problems. While images represent ‘objective’ measurements of surface energy that can be related to different surface features, the measurements can vary with a number of factors which are independent of changes in those features. For example, the calibration of imaging sensors can vary over time, so that the same physical radiance level in a selected wavelength band could result in (slightly) different recorded values in different overpasses (see Volume 2A—Section 3). Changes in Sun position

with diurnal and annual cycles directly affect surface illumination, and hence any remote measurements of reflected energy (see Volume 1B—Section 3). Similarly, scattering by atmospheric particles can modify the surface radiance levels recorded by an airborne or spaceborne sensor (see Volume 1B—Section 4). Short-term surface conditions, such as increased soil moisture after a rainfall event, can also reduce radiance levels. Finally, digital comparison of multiple images generally requires that images are precisely registered geometrically (see Volumes 2B and 2D). This process can introduce spatial errors which could be falsely interpreted as land cover changes.

Background image: MODIS global composite image showing Land Surface Temperature (LST) anomaly for October 2016 (based on science datasets from MOD11C1, MOD11C2, and MOD11C3 products). Colour scale ranging from blue (-12°C) to red (+12°C) indicates the deviation of monthly temperature in October 2016 from the average monthly temperature between 2001–2010. (Note: the vertical extent of this composite image has been clipped and the aspect ratio changed.) **Source:** NASA Earth Observations. (Retrieved from https://neo.sci.gsfc.nasa.gov/view.php?datasetId=MOD_LSTAD_M)

‘Real’ land cover changes still need to be interpreted in an informed way. For example, spectral variation between successive growing seasons for cultivated crops may initially appear to be related to seasonal productivity, but may also be due to cultivation factors (such as a planting pattern, or timing of fertiliser application), differences in maturity (due to changes in crop variety or soil condition), or differences in weather or irrigation (such as stress from heat, cold, wind damage, or excessive or insufficient moisture). The multivariate nature of the environment, combined with variable land use practices, suggest that methodologies for accurately monitoring land cover may never be fully automated. Nevertheless, EO does offer relatively inexpensive, regularly acquired, and internally consistent datasets for investigating changes in land cover, use and/or condition, especially when calibrated and validated as Analysis Ready Data (ARD; see Volume 2D—Section 3.2).

In the context of EO, monitoring relies upon the availability of multiple images for a given location. Two or more coincident images are required to detect changes in land cover or condition, and the increasing archive of EO time series imagery offers greater choice of image resolutions and extents than ever before. Image processing methods that are relevant to environmental monitoring using time series datasets are detailed in Volume 2D. As introduced in Volumes 1 and 2, EO imagery enables the creation of global maps showing vegetation greenness. Spectral indices derived from EO datasets (see Section 8.1) have been related to a range of ecological parameters, which attempt to quantify trends in vegetation cover and structure in space and time, including:

- Foliage Projective Cover (FPC)—fraction of ground surface vertically covered by photosynthetically active components of vegetation (that is, excluding stems and branches; see Sections 6.3.1);
- Leaf Area Index (LAI)—ratio of upper green leaf surface area to ground area (see Section 6.3.3, 8.1.1 and 8.1.4);
- fraction of Absorbed Photosynthetically Active Radiation (fAPAR)—proportion of photosynthetically active radiation (400–700 nm) used by plants (see Section 6.3.4 and 8.1.4);
- fractional cover—proportions of photosynthesising vegetation, non-photosynthetic vegetation, and bare soil within a given area (see Section 6.3.6 and Excursus 8.3) and
- Net Primary Productivity (NPP)—the availability of carbon or biomass in a landscape (see Sections 7.2, 8.1.4 and 17).

Table 9.1 Potential reference site measurements

Environmental factor	Attribute	Measurement
Vegetation	Structure	Height, density, layers, spatial configuration
	Species	Abundances, ages
	Litter	Size, volume, distribution
Soil	Type	Texture, mineral content
	Depth	Topsoil and subsoil layers
	Nutrient status	Proportions of major and minor nutrients
Climate	Precipitation	Diurnal, seasonal, annual, and longer term ranges
	Temperature	
	Humidity	
	Aerosols	Density, type

Monitoring landscape condition necessarily relies on reference sites, at which a range of detailed measurements can be made. Examples of relevant quantitative measurements at these sites are listed in Table 9.1. Of particular relevance to Australian terrestrial ecosystem studies is the Terrestrial Ecosystem Research Network (TERN), which is introduced in Volume 2D—Excursus 12.2. Detailed guidelines for measuring vegetation and soil parameters for environmental inventory and monitoring are provided in TERN Australia (2018), McKenzie *et al.* (2008), and NCST (2009). Integration of EO data with other spatial datasets, including site-based data, is introduced in Volume 2D—Sections 12–14.

The following sub-sections consider monitoring applications using EO imagery in the specific contexts of:

- vegetation types—such as annual versus perennial (see Section 9.1);
- change indices—for fire and other disturbances (see Section 9.2);
- phenology—monitoring changes in vegetation growth stage and condition (see Section 9.3);
- evapotranspiration—quantifying regional moisture loss due to evaporation and transpiration (see Section 9.4);
- plant water stress—monitoring water stress in vegetation, particularly to optimise irrigation scheduling (see Section 9.5); and
- plant vigour—nutritional status, pests and diseases (see Section 9.6).

9.1 Vegetation types

Various EO-based methods have been developed to monitor changes in different types of terrestrial vegetation. For many applications, accurate maps of perennial (mostly woody) vegetation are valuable. For example, some operational systems that monitor perennial vegetation in Australia include:

- Statewide Landcover and Trees Study (SLATS) has been used operationally in Queensland since 1995 and in NSW since 2006 (see Volume 2D—Excursus 14.3 for details). The SLATS methodology identifies woody vegetation changes at intervals of 1–2 years using a well-defined processing workflow, and produces annual reports and maps detailing the location and extent of change across each state (Scarath *et al.*, 2008; Danaher *et al.*, 2011). Near real time detection of vegetation change has been recently implemented using EO datasets with higher spatial and temporal resolutions.
- LandMonitor is a collaborative monitoring project in WA that was initially developed in 1988 to map salinity and vegetation in southwest WA from Landsat imagery (Allen and Beetson, 1999). It now delivers state-wide maps of vegetation extent and change in perennial vegetation cover (Landgate, 2019). This EO-based time series is integrated with DEM and other spatial datasets to allow vegetation history and salinity risk to be monitored efficiently (McFarlene and Wallace, 2019).
- A persistent green vegetation product (Gill *et al.*, 2017, 2018) was derived from the photosynthetic vegetation component of the Landsat fractional cover product (see Excursus 8.3) for the decade from 2000 to 2010. This product maps the density and extent of woody vegetation in Australia with an overall accuracy of 82%.

Annual or deciduous vegetation exhibits a larger annual change in photosynthetic activity and canopy reflectance than evergreen vegetation (see Section 5.3.3). Monitoring of vegetation colour throughout the year can help to separate areas of deciduous and evergreen vegetation cover. Using data collected over several years, persistently green vegetation can similarly be differentiated from vegetation that is susceptible to seasonal or weather-related browning in hot weather. Some advantages of mapping persistently green vegetation include highlighting reliable areas of fodder, locating potential groundwater resources, indicating areas with high fire risk, and identifying useful checkpoints for monitoring vegetation dynamics (Johansen *et al.*, 2012). Perennial and annual plants also have significantly different ecohydrological characteristics as summarised in Table 9.2, with some variations due to plant age (McVicar *et al.*, 2010). These characteristics have been shown to influence catchment water balance at sub-catchment scales (Donohue *et al.*, 2010a).

Time series analysis of EO-based vegetation indices has been used to differentiate between vegetation that is persistently green and vegetation that browns off during the annual cycle (Lu *et al.*, 2003, Donohue *et al.*, 2008). For example, Donohue *et al.* (2009) used a calibrated AVHRR Normalised Difference Vegetation Index (NDVI) time series dataset from 1981 to 2006 (Donohue *et al.*, 2008) to analyse fAPAR trends for Australia in terms of

- slowly varying, persistent vegetation—perennial, woody; and
- rapidly varying, recurrent vegetation—annual, herbaceous, and ephemeral (see Figure 9.1).

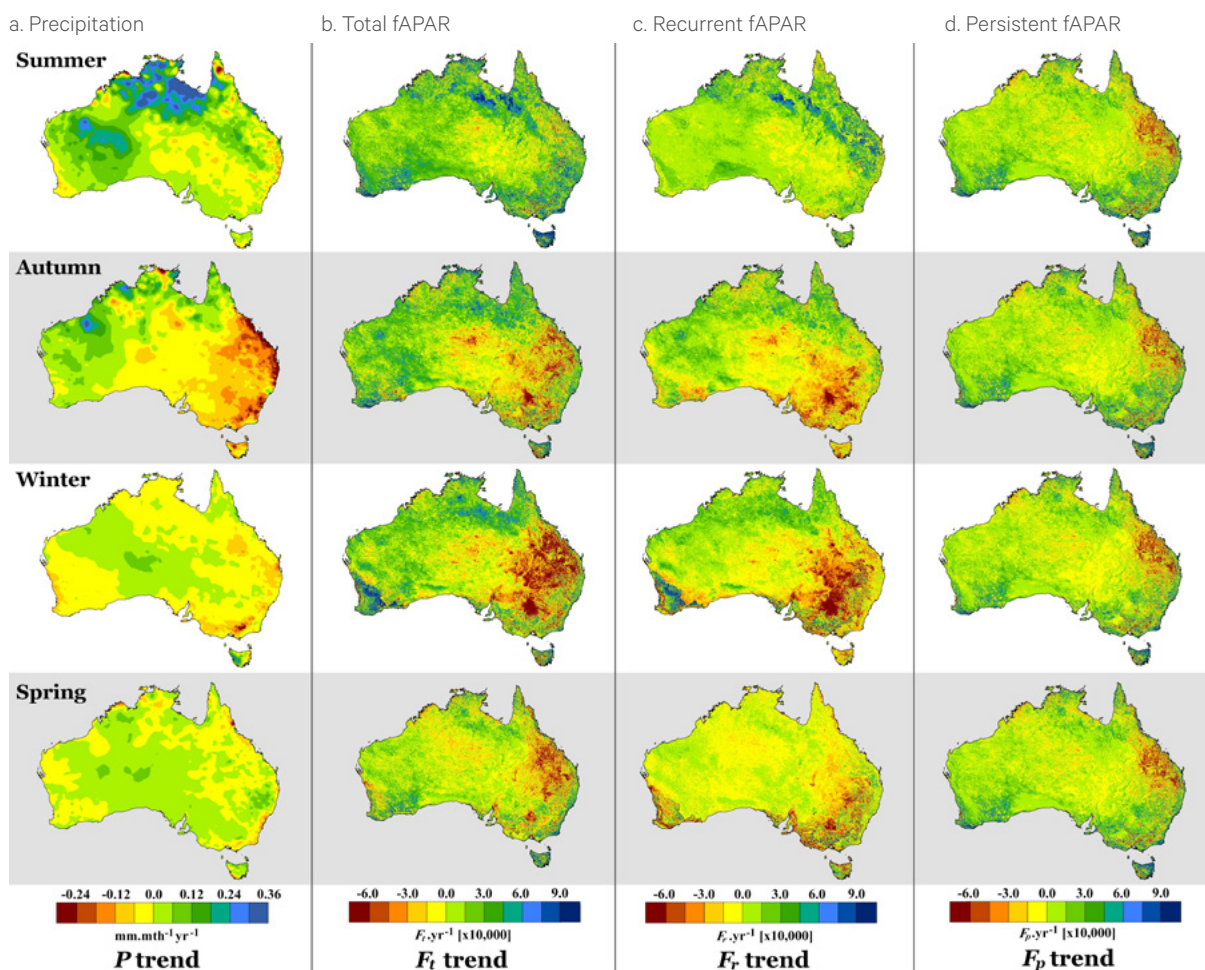
fAPAR trends were compared with climate records to observe an increase in vegetation cover in Australia of 7.8% from 1981 to 2006, which corresponded to a 7% increase in precipitation during the same time period. In terms of vegetation categories, however, this analysis reported that persistent vegetation increased over 21%, while recurrent vegetation decreased by 7% (see Volume 2D—Excursus 8.1).

Table 9.2 Ecohydrological characteristics of perennial and annual vegetation

Vegetation type	Root depth	Photosynthetic rate	Leaf area change	Water use
Annual/ephemeral	Shallow	High	Fast	Alternately high and low
Perennial/non-deciduous	Deep	Low	Slow	Generally constant and moderate

Source: McVicar *et al.* (2010) Table 1

Figure 9.1 Seasonal vegetation trends derived from AVHRR NDVI data 1981–2006



Source: Donohue *et al.* (2009) Figure 5 © Wiley. Used with permission.

9.2 Change Indices

A number of spectral indices have been developed to quantify landscape changes based on a pair of images acquired before and after a change event. As with all monitoring approaches, timing of imagery is important to ensure that the pair capture changes resulting from a specific event (see Volume 2D). For reliable results, these analyses require cloud-free images that are not separately impacted by other environmental conditions such as drought. Below we consider two examples of particular relevance to the Australian environment: fire footprints (see Section 9.2.1) and ecosystem disturbance (see Section 9.2.2).

9.2.1 Fire footprints

A frequent impetus for monitoring land cover change in many parts of Australia is fire. A number of methods for mapping both the extent and severity of fires have been developed, which are discussed in detail in Section 18. Fire indices, however, can saturate in the Australian landscape, resulting in little distinction between areas impacted by high fire severity and those that were completely burnt out (Tony Sparks, *pers. comm.*).

A popular method for mapping fire severity was proposed by Key and Benson (2002, 2006) for Landsat TM/ETM+ imagery based on the Normalised Burn Ratio:

$$\text{NBR} = \frac{\text{TM4} - \text{TM7}}{\text{TM4} + \text{TM7}}$$

Since Landsat TM Band 4 (NIR) is sensitive to changes in vegetation vigour and biomass and Band 7 (SWIR) is sensitive to the visibility and character of soils (Cocke *et al.*, 2005; Key and Benson, 2002), a Normalised Burn Ratio difference image (dNBR), which shows change in NBR due to fire, is then calculated from:

$$\text{dNBR} = \text{NBR}_{\text{prefire}} - \text{NBR}_{\text{postfire}}$$

Although originally developed for Landsat TM imagery, the ratio has been adapted for use with other EO data with similar spectral channels. Uses and limitations of this method for mapping fire severity are described in Section 18.

Miller and Thode (2007) reported higher accuracy in mapping high fire severity areas using a Relative dNBR index (RdNBR) and suggested that a relative index offers a more consistent basis for comparing fires across space and time:

$$\text{RdNBR} = \frac{\text{NBR}_{\text{prefire}} - \text{NBR}_{\text{postfire}}}{\sqrt{\left| \frac{\text{NBR}_{\text{prefire}}}{1000} \right|}}$$

Other indices have been developed for mapping fire footprints, including the Mid-infrared Bi-spectral Index (MIRBI), which was derived from MODIS MIR channels 6 and 7 to detect burned savanna vegetation (Trigg and Flasse, 2001):

$$\text{MIRBI} = 10 \times \text{MODIS Band 7} - 9.8 \times \text{MODIS Band 6} + 2$$

As detailed in Section 18, different methods for mapping fire footprints have also been compared in several studies (Trigg and Flasse, 2001; Roman-Cuesta *et al.*, 2005; Holden *et al.*, 2005; Smith *et al.*, 2007).

9.3 Phenology

Phenology, the interaction between plant life cycles and seasonal, climatic and other rhythms, is introduced in Section 5.3.2 above. A range of metrics is used to identify and compare phenological stages. As indicated in Table 9.3, these are based on either the dates associated with particular stages of greenness or the magnitude of greenness. Different metrics have been demonstrated to be most effective in assessing different types of vegetation and/or different vegetation characteristics.

9.2.2 Ecosystem disturbance

Major disturbances to terrestrial ecosystems, such as fire, floods, storm damage, and insect epidemics, typically destroy large areas of vegetation, resulting in marked changes to the global carbon cycle (see Section 17). Observing the timing, location, extent, and severity of such disturbances is important both to optimise response and recovery efforts, and understand the impact of these events on ecosystem dynamics.

The MODIS Global Disturbance Index (MGDI; Mildrexler *et al.*, 2007, 2009) detects changes in vegetation greenness and land surface temperature (LST) such that:

- greenness, as measured by the MODIS/Terra Enhanced Vegetation Index (EVI; MOD13A1), is expected to decrease after a major disturbance due to reduction in vegetation cover; and
- LST, as measured by MODIS/Aqua LST (MYD11A2), is expected to increase due to reduction in evapotranspiration from less vegetation cover:

$$\text{CCCI} = \frac{\text{NDRE} - \text{NDRE}_{\text{min}}}{\text{NDRE}_{\text{max}} - \text{NDRE}_{\text{min}}}$$

$$\text{MGDI} = (\text{LST}_{\text{max}}/\text{EVI}_{\text{max}})/(\text{LST}_{\text{mean}}/\text{EVI}_{\text{mean}})$$

where

- LST_{max} is the annual maximum of eight-day composite LST;
- EVI_{max} is annual maximum of 16-day EVI;
- LST_{mean} is the multiyear mean of LST_{max} ; and
- EVI_{mean} is multiyear mean of EVI_{max} .

MODIS imagery from 2001 to 2013 were analysed to generate an experimental version of this product for Australia (TERN AusCover, 2014). This has been validated using fire events, but could be used to assess any major landscape event and the associated subsequent regeneration (see Section 9.7).

Phenological studies have employed three principal tools: *in situ* observations, bioclimatic models, and EO. *In situ* observations, such as field measurements (see Volume 2D—Section 12), automatic sensor networks, and phenocams (Brown *et al.*, 2012, 2016), are essential to validate both bioclimatic models and EO analyses, but are expensive, time-consuming, and invariably introduce inconsistencies over large areas. Most bioclimatic models tend to be specific to selected species and local scales and do not readily extend to larger areas. EO offers the only viable option to scale up *in situ* observations for regional and global coverage (Cleland *et al.*, 2007).

Table 9.3 Significant phenological metrics

Basis	Name of Metric	Application
Greening Dates	Start of growing season (SGS)	Indicate sensitivity of ecosystem productivity to phenology and climate change (Ma <i>et al.</i> , 2013; Richardson <i>et al.</i> , 2010);
	End of growing season (EGS)	
	Peak period of growing season (PGS)	
Magnitude of Greenness	First derivatives of seasonal greenness profile	Asymmetry between rate of green-up and rate of senescence used to characterise ecosystem type Variations in rates indicative of vegetation health
	Annual integrals of seasonal greenness profile	Variations related to ecosystem productivity
	Amplitude of seasonal greenness profile	Minimum dry season baseline related to persistent green vegetation cover (Donohue <i>et al.</i> , 2009) Amplitude (PGS minus baseline) related to recurrent vegetation cover

Source: Restrepo-Coupe *et al.* (2018)

As with other time series datasets, annual, interannual, and longer term patterns need to be differentiated in phenological observations (see Section 5.3.2 and Volume 2D—Section 8 and 9). Changes in phenological metrics between years can result from short-term climatic fluctuations (Elmore *et al.*, 2003) or localised anthropogenic changes (White *et al.*, 2002). Longer-term changes in annual cycles may result from major climate variations or regional anthropogenic influences (Myneni *et al.*, 1997; Potter *et al.*, 2003; Tucker *et al.*, 2001).

EO techniques have proven to be a reliable method of assessing plant phenological status, since vegetation canopy greenness is closely related to the generalised growth stages of emergence, development, maturity, and senescence (or harvest) for most forests, grasslands, and wetlands, as well as most agricultural crops (see Figure 6.6). In particular, time series imagery has enabled new insights into vegetation dynamics and land surface changes (see Section 10 and Volume 2D).

The majority of EO-based phenological studies have analysed changes in vegetation ‘greenness’ as represented by spectral indices (see Section 8.1). Analyses of historical imagery have allowed models for growing season parameters to be established, and perturbations induced by climatic or anthropogenic factors to be detected (Myneni *et al.*, 1997; Huete *et al.*, 2006). Validation methods for satellite image-based phenology analyses are detailed in Restrepo-Coupe *et al.* (2018). Zeng *et al.* (2020) review vegetation phenological metrics derived from EO time series datasets both in terms of existing methods and emerging techniques.

Most of the large area studies of seasonal vegetation dynamics have been based on the extensive archives of AVHRR, MODIS, or VIIRS imagery, although Landsat imagery has also been used for regional analyses. AVHRR data provides the longest, continuous time series of global imagery, but this dataset has known limitations for detailed vegetation analyses, including problems with radiometric and geometric precision (Goward *et al.*, 1991; Teillet *et al.*, 2000). Comparisons between time series from different sensors yielded similar results in terms of phenological trends between NDVI derived from MODIS and SPOT-Vegetation datasets, but disagreement with NDVI trends from AVHRR GIMMS (Yin *et al.*, 2012).

Since the extent of green plant cover is indicative of phenological stages in annual plants (see Section 6.5), the key transition dates between greening, maturity, senescence, and dormancy can be identified using a greenness index. When the greenness values for each image pixel are plotted against the calendar date, the trend in greenness is clearly visible as increasing during the greening phase, most constant during the maturity phase and decreasing during the senescing phase (see Table 9.4 and Figure 9.2). The dates of these transitions correspond to the inflexion points in an EO-based greenness plot, that is, the dates when the slope of the greenness trend changes (Zhang *et al.*, 2003; see Section 14.3). Changes in meteorological and environmental conditions or plant varieties, however, may vary the precise temporal trajectory of pixel values throughout the growing season from year to year in terms of duration, amplitude, baseline, and start and end dates, (see Volume 2D—Section 9).

While phenological changes in woodlands are less dramatic than in herbaceous plant communities, they can also be observed. For example, a typical annual cycle in NDVI values for pine plantations in southeast NSW shows high winter values correlating with winter rainfall and low summer values corresponding to low rainfall during the summer months (Verbesselt *et al.*, 2009). Since the impacts of variations in tree vigour are maximised in terms of NDVI during the more stressful summer months, they can be summarised by the normalised difference between winter and summer values (Coops *et al.*, 2009), which has been successfully used to map tree mortality these plantations (Verbesselt *et al.*, 2009).

To clearly identify surface features in a thematic classification, the temporal trends associated with each feature type need to be understood, modelled and labelled appropriately. White and Nemani (2006) suggest five principles that should be observed in phenological analyses based on EO:

- results do not apply to individual pixels;
- pixels with similar time patterns should be treated as a group;
- sequences should not be filled, fitted, or smoothed;
- changes in land surface phenology may not correspond to known vegetation events; and
- variability and/or uncertainty measures should be included.

A range of approaches have been used to determine the time of vegetation greening and browning based on EO greenness indices for regional studies of annual plants (see Section 8.1.1) including thresholds for specific levels (White *et al.*, 1997), largest change (Kaduk and Heimann, 1996), backward-looking moving averages (Reed *et al.*, 1994), and empirical equations (Moulin *et al.*, 1997).

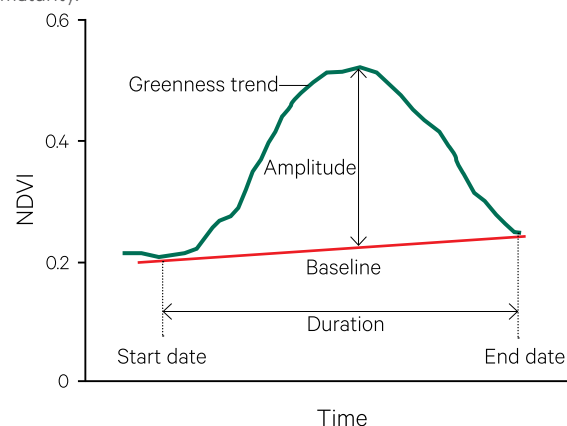
Table 9.4 Phenological stages of rice crop

Growth stage		EO greenness
Vegetative	Transplanting	Initial seedling
	Tillering	Increasing greenness for 60–100 days depending on variety
	Stem elongation	
Reproductive	Panicle initiation	Maximum greenness
	Booting/heading	
	Flowering	
Ripening	Milk stage	Decreasing greenness often takes 30 days
	Dough stage	
	Mature	Harvest

Adapted from: Mosleh *et al.* (2015) Figure 1

Figure 9.2 Greenness changes in annual plants

Annual plants typically follow a temporal pattern of increasing greenness during growth then a reduction in greenness after maturity.



Adapted from: Lhermitte *et al.* (2011) Figure 1

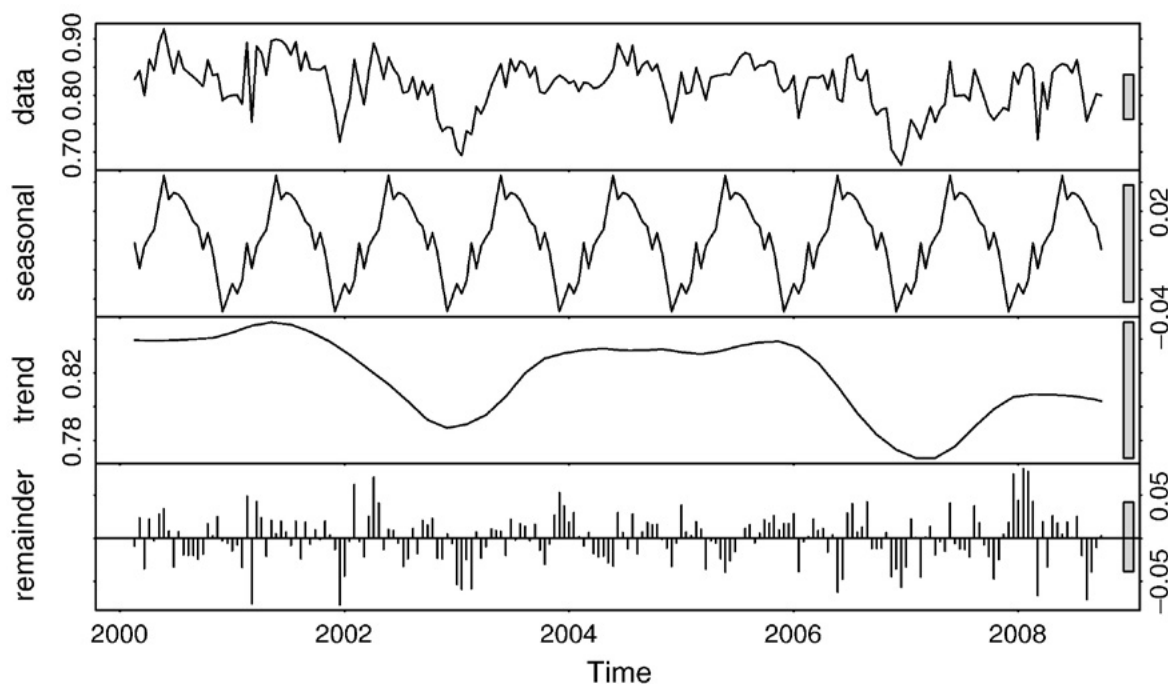
As introduced in Volume 2D—Section 9, various mathematical models can be fitted to EO time series datasets. The following functions have been used to identify phenological transition dates from global imagery archives:

- major changes in curvature for a piecewise logistic function fitted to EVI time series data (Zhang *et al.*, 2003);
- Gaussian forms (Jönsson and Eklundh, 2002, 2004); and
- high order splines (Hermance *et al.*, 2007; Bradley *et al.*, 2007).

Since the phenological status of vegetation impacts energy exchange between the Earth's surface and atmosphere, the relationship between phenology and climate is of prime importance to global monitoring. A Growing Season Index (GSI) was proposed by Jolly *et al.* (2005) to summarise the relative phenological performance of vegetation. At a global scale, this index distinguished major differences in regional phenological controls and could be used both to reconstruct historical variation and forecast future phenological responses to climatic changes. More recent developments include real time monitoring and short term forecasting of phenological changes (White and Nemani, 2006; Zhang *et al.*, 2012), and integration with other models (Nemani *et al.*, 2009). Excursus 9.1 introduces an Australian EO-based product, which monitors phenology.

Figure 9.3 NDVI time series of pine plantation

A 16-day NDVI time series of a pine plantation is decomposed into seasonal, trend, and irregular components. Right hand bars show comparable data ranges. Seasonal amplitude range is around 0.1 NDVI.



Source: Verbesselt *et al.* (2010) Figure 2

Excursus 9.1—Australian Phenology Product

Source: Qiaoyun Xie, University of Technology Sydney

Further information: Broich *et al.* (2014, 2015); <https://www.tern.org.au/australian-phenology-product/>

Data download: <http://www.auscover.org.au/purl/modis-phenology-uts>

Knowing how different parts of Australia's vegetative land cover are growing and developing with the change of seasons is vital information for environmental scientists, land managers and those in the agricultural and horticultural sectors. The Australian Phenology Product provides detailed information on the seasonal growth and development of Australia's vegetation at continental scale (see Figure 9.2). Potential applications include:

- quantifying ecosystem resilience to climate change;
- estimating bushfire fuel accumulation;
- assessing native vegetation condition;
- monitoring airborne allergens; and
- informing agricultural management decisions and crop yields.

This product has been developed from MODIS Enhanced Vegetation Index (EVI) data and a suite of additional data collected and made available by TERN's facilities. The Version 1 product was released in 2015, providing phenological metrics from 2000 to 2015 at 0.05° spatial resolution using MOD13C1

data as input. MYD13A1 data is now being used to transition the product into the VIIRS era. It quantifies vegetation life cycle dynamics, such as episodes of greening and browning, and analyses how these are influenced by seasonal and interannual variations in climate. Phenological cycles are defined as a period of EVI-measured greening and browning that may occur at any time of the year, extend across the end of a year, skip a year (not occur for one or multiple years) or occur more than once a year. Multiple phenological cycles within a year can occur in the form of double cropping in agricultural areas or be caused by aseasonal rain events in water-limited environments.

Based on per-pixel greenness trajectories measured by MODIS EVI, phenological cycle curves were modelled and their key properties, in the form of phenological curve metrics, were derived including: the first and second minimum point, peak, start and end of cycle; length of cycle, and; the amplitude of the cycle. Integrated EVI under the curve between the start and end of the cycle time for each cycle is calculated as a proxy of productivity (Broich *et al.*, 2015).

When applied to the Version 1 product (0.05° resolution) from 2000 to 2013, results showed high inter- and intra-annual variability in phenological cycles across Australia (Broich *et al.*, 2014). The peak of phenological cycles occurred not only during the austral summer, but also at any time of the year, with their timing varying by more than a month in the interior of the continent. The magnitude of the phenological cycle peak and the integrated greenness were most significantly correlated with monthly SOI within the preceding 12 months. Correlation patterns occurred primarily over northeastern Australia and within the Murray Darling Basin, predominantly over natural land cover and particularly in floodplain and wetland areas. Integrated greenness of the phenological cycles (surrogate of vegetation productivity) in Figure 9.5 showed negative anomalies over most of northern and eastern Australia in 2003 and positive anomalies over most of eastern Australia in 2009–2010, which coincided with the transition from the El Niño-induced decadal droughts to flooding caused by La Niña.

Figure 9.4 Australian Phenology Product

Timing of maximum vegetation index in 2018 at 500 m resolution

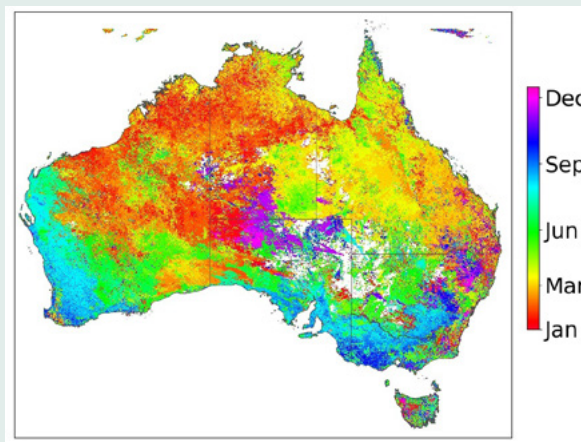
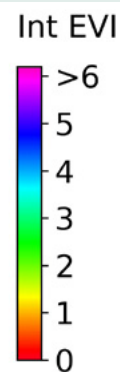
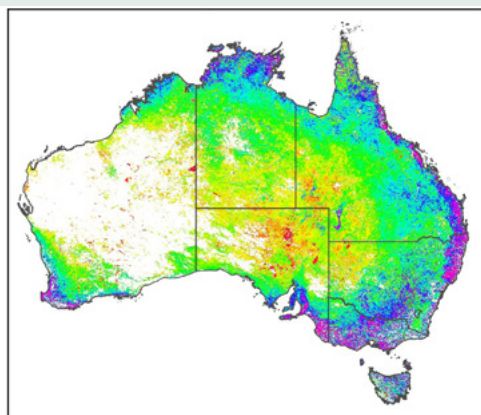
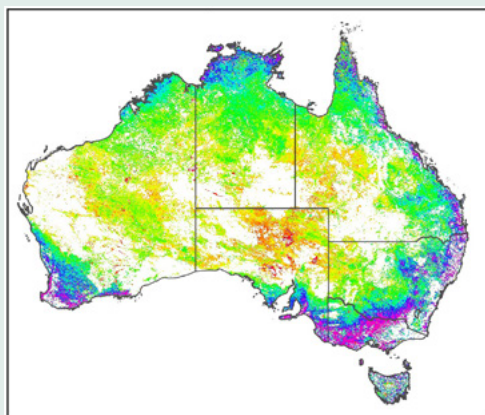


Figure 9.5 Seasonally-integrated EVI from Australian Phenology Product

Seasonally-integrated EVI (the first season) from Australian Phenology Product using MYD13A1 data as input at 500 m resolution for 2003 El Niño dry year case and 2010 La Niña wet year case. White pixels represent areas without detectable vegetation growth.

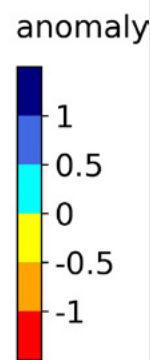
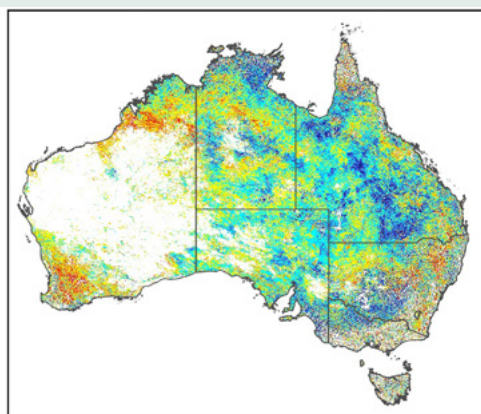
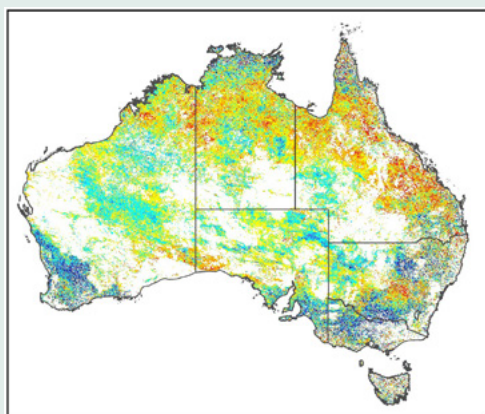
a. Seasonally-integrated EVI in 2003

b. Seasonally-integrated EVI in 2010



c. Seasonally-integrated EVI in 2003 subtracted by climatology from 2003 to 2018

d. Seasonally-integrated EVI in 2010 subtracted by climatology from 2003 to 2018



9.4 Evapotranspiration

Evapotranspiration (ET) describes the combined transfer of water vapour to the atmosphere by evaporation and transpiration from the Earth's surface (see Sections 2.2, 5.2.3, and 7.6). Understanding and managing ET is one of the most important biophysical challenges facing natural and man-made ecosystems, and its behaviour can change dramatically with the scale and nature of particular situations. The approaches and solutions to problems relating to ET will rely on increasing use of EO technologies to cope with issues of scale, and will need diverse, customised approaches to tackle problems at farm, district, and continental scales (see Section 13). Accepted methods for estimating large area, actual ET (AET) using ground-based data (Glenn *et al.*, 2011) include:

- EC flux towers (see Excursus 7.2);
- sap flux sensors (see Section 5.2.3); and
- Budyko framework for catchment water balance (Budyko, 1958, 1974; see Excursus 9.2).

EC flux towers are the most commonly used method for validating EO-based studies of ET. Upscaling of data from sap flux sensors to landscape scale analyses is problematic, but

such sensors have been useful in focused studies (Doody and Benyon, 2011), woody agricultural crops (Blaike *et al.*, 2001), and when combined with EC methods (Silberstein *et al.*, 2001). The Budyko framework is popular for catchment scale studies (see Excursus 9.2) and has been used in conjunction with estimates of total water storage change derived from GRACE satellite data (Long *et al.*, 2014; see Volume 3B—Excursus 1.1).

In many ecosystems, the proportion of the land surface covered by vegetation is closely related to water balance and landscape dynamics, especially the capability to retain precipitation (see Section 7.6). In savanna ecosystems, which comprise sparse vegetation and bare soil, evapotranspiration controls the water balance. Photosynthetically active vegetation in these landscapes cycles annually between the wet season of moist, green growth, and the dry season of desiccated grasses, dry litter, and groundwater-dependent trees (Guerschman *et al.*, 2009). In this situation, monitoring of photosynthetic vegetation cover provides information about the water cycle as well as ecosystem dynamics (see Section 7).

Excursus 9.2—Budyko Framework

Source: Donohue *et al.* (2007)

Further Information: Budyko (1958, 1974)

Budyko (1958, 1974) describes the partitioning of average precipitation into average evapotranspiration and average run-off based on simple physical relationships now known as the 'Budyko curve'. This curve describes the patterns observed between climate, evapotranspiration, and run-off, and has proven to be a useful model for predicting catchment energy and water balances. The Budyko framework assumes catchments are at steady-state and are driven by the macro-climate. These two conditions depend on the scales of application, such that the framework's reliability is greatest when applied using long term averages (much greater than one year) and to large catchments (> 10,000 km²).

Budyko described the hydrology of a catchment using a supply-demand framework and a simple bucket model where net drainage is assumed to be negligible. The water balance (see Section 7.6) was defined as:

$$\frac{dS_w}{dt} = P - E - Q$$

where P, E, and Q are catchment-wide estimates of precipitation, evapotranspiration, and run-off fluxes respectively (in kg s⁻¹), and S_w (kg) is the soil water storage. A catchment is in steady-state when changes in S_w are zero. In reality, the water balance is almost continually varying due to fluctuations in P, E, and Q, and steady-state conditions are typically established in analyses by integrating the above equation over a finite time period (τ) that is larger than the timescale of fluctuations in S_w:

$$\int_0^\tau \frac{dS_w}{dt} dt = \int_0^\tau P dt - \int_0^\tau E dt - \int_0^\tau Q dt$$

In finite form we have the catchment mass balance:

$$\Delta S_w = \bar{P}\tau - \bar{E}\tau - \bar{Q}\tau$$

or

$$\frac{\Delta S_w}{\tau} = \bar{P} - \bar{E} - \bar{Q}$$

We can convert to the familiar depth units by dividing both sides by the catchment area (A_c , in m^2) and the density of liquid water (ρ_w , as $kg\ m^{-3}$):

$$\frac{\Delta S_w}{\rho_w A_c \tau} = \bar{P} - \bar{E} - \bar{Q}$$

The framework can be further extended by noting that soil water depends on the volume of the bucket (V , m^3) and the mass concentration of water in the bucket ($[S_w]$, $kg\ m^{-3}$):

$$S_w = V[S_w]$$

An upper limit to $[S_w]$ is set by the pore space within the soil, which is a function of soil texture and structure (Craze and Hamilton, 1991). Soil water can change because of a change in the volume of the bucket or a change in mass concentration within the volume. To the first order we have:

$$\Delta S_w = [S_w]\Delta V + V\Delta[S_w]$$

The volume of the bucket depends on the catchment area and bucket depth (z , m):

$$V = A_c z$$

For a given catchment, the area is fixed and the volume of the bucket can only change because of the change in depth (Δz) so that:

$$\frac{1}{\rho_w} \left([S_w] \frac{\Delta z}{\tau} + z \frac{\Delta[S_w]}{\tau} \right) = \frac{\bar{P} - \bar{E} - \bar{Q}}{\rho_w A_c}$$

Formulating the water balance in this way allows links to be made between vegetation characteristics and the spatial analysis scales, as well as the 'flux components' (Q and E) and the 'steady-state components' of the water balance (see Donohue *et al.*, 2007). Fluxes of both mass and energy are involved in evapotranspiration and this provides a critical link between the water and energy balances (see Section 7.5). The catchment-wide energy balance is given by:

$$\Delta S_e = R_n - \lambda E - H$$

where the change in energy storage (S_e) is the balance between net radiation (R_n) and the fluxes of latent (λE) and sensible (H) heat (all in $J\ s^{-1}$) where λ (in $J\ kg^{-1}$) is the latent heat of vaporisation. Note that the sign convention used in the above equation assumes that λE and H are positive away from the surface while R_n is positive into the surface. Using the same form as the previous equation gives:

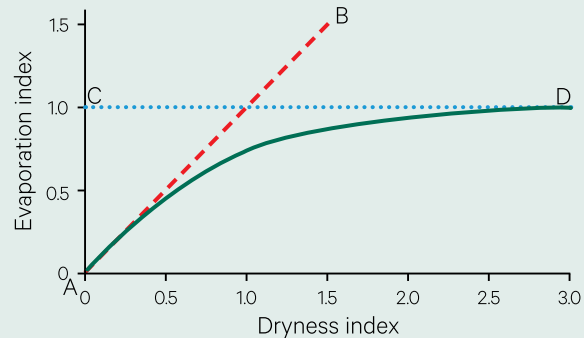
$$[S_e] \frac{\Delta z_e}{\tau} + z_e \frac{\Delta[S_e]}{\tau} = \frac{\bar{R}_n - \lambda \bar{E} - \bar{H}}{A_c}$$

where z_e (m) is the depth to which energy can be stored. Over annual timescales energy storage can usually be omitted from the energy balance.

Evapotranspiration is limited by the supply of either water or energy. At steady-state, when water is limiting ($R_n / \lambda > P$), the maximum possible E is P , at which $Q=0$. Similarly, the maximum possible E when energy is limiting is R_n / λ at which $H=0$. Evapotranspiration approaches one of these two limits as water or energy, respectively, become increasingly limiting. This framework of mass and energy balances and supply and demand-limited evapotranspiration is the key component of Budyko's work. The type and degree of limitation is determined by the radiative index of dryness (Φ), which is the ratio of R_n / λ to P . Values of $\Phi < 1$ represent energy-limited environments, and those where $\Phi > 1$ are water-limited. Intermediate environments occur where $\Phi \sim 1$.

Figure 9.6 Budyko's framework and curve

The curve (green line) describes the relationship between the dryness index and the evaporative index. Line A–B defines the energy-limit to evapotranspiration, and line C–D defines the water-limit.



Adapted from: Donohue *et al.* (2007) Figure 1

Catchment scale annual (or longer) evapotranspiration is usually estimated for gauged catchments by assuming that S_w is 0 and hence E is the difference between measured values of P and Q . The need for a simple means of estimating E from ungauged catchments prompted Budyko to develop the ‘equation of relationship’ that describes the dependency of E on the variables P and R_n / λ :

$$\bar{E} = \left(\frac{\bar{R}_n \bar{P}}{\lambda} \tanh \frac{1}{\Phi} \left(1 - \cosh \Phi + \sinh \Phi \right) \right)^{0.5}$$

This curvilinear relationship, which built on the works of Schreiber (1904) and Ol’dekop (1911), has become known as the Budyko curve (see Figure 9.6).

The assumptions inherent in Budyko’s hydrological model are that:

- catchments are at steady-state (that is, $\Delta S_w \approx 0$)—to a large degree, this condition depends on τ ; and that
- at large spatial scales ($A_c \gg 1000 \text{ km}^2$), only macro-climatic variables are required to describe catchment water balances.

When applied over long timescales and to large catchments, Budyko’s curve reliably predicts catchment water balances. However, when applied to small spatiotemporal scales the inherent assumptions can be violated. In these circumstances, incorporating vegetation into the framework is expected to enhance the framework’s predictive capacity (see Donohue *et al.* (2007) for details).

EO-based approaches for predicting ET from vegetated surfaces are reviewed by Glenn *et al.* (2011) and Nouri *et al.* (2013). EO imagery offers the opportunity to monitor the spatiotemporal variability of ET using:

- thermal estimation—the difference between air temperature and thermal infrared (TIR)-derived surface temperature has been used to compute the sensible heat flux (H ; see Section 7.5) in the equation:

$$LE = R_n - G - H$$

where LE is the latent heat flux associated with AET, R_n is the net radiation, and G is the ground heat flux (Glenn *et al.*, 2011). Using EO or ground-based estimates of the other parameters, LE can be computed as a surrogate for AET. Various models have been proposed on this basis (Li and Lyons, 1999), from simple regression relationships (see Section 13) to sophisticated, surface energy balance models (see Section 10.2.3). While such models have known limitations (Glenn *et al.*, 2007; Kalma *et al.*, 2008), with appropriate processing reasonable agreement has been achieved between modelled and ground-based estimates (McVicar and Jupp, 2002, Mc Vicar *et al.*, 2007); or

- vegetation indices (VI; see Section 8.1)—estimates of LAI or vegetation cover, primarily from AVHRR and MODIS imagery, have been used as inputs to ET models at regional and continental scales (Glenn *et al.*, 2010; see Section 7.6). LAI and canopy conductance can be derived using VI where estimates of maximal stomatal conductance, and the constraints of stomatal conductance, are available from ground measurements of AET, meteorological data, and/or appropriate physiological models, although the bare soil

component of AET must be estimated separately (Glenn *et al.*, 2011). The Penman-Monteith equation is then used to calculate AET by using EO-based estimates of canopy conductance (see Section 13.4.2). This approach relies on empirical relationships, which can be impractical to rescale spectrally, temporally, or spatially (Donohue *et al.*, 2010b; Abuzar *et al.*, 2014; see Volume 2D—Section 4.3). However, simplified models of landscape ET derived from empirical relationships are an essential starting point when dealing with the challenges associated with data sparse, rainfed conditions, where rainfall deficits, vegetation type and cover, and evaporative demand interact to determine landscape ET (see Section 7.6).

Alternative conceptual approaches for estimating AET from VI were categorised by Yebra *et al.* (2013) as:

- estimating actual or maximum, leaf level, stomatal conductance;
- using LAI as a surrogate for AET to scale from stomatal to canopy conductance;
- using an empirical relationship to estimate either canopy conductance or surface conductance (including soil evaporation); and
- developing direct empirical equations between the VI and AET measurements.

Some of these approaches rely on spatial and/or temporal scaling from site-specific measurements to regional and continental scale models (see Section 10). Again, uncertainties in ET estimates can result when the scales of underlying datasets are poorly matched (van Niel *et al.*, 2011). Examples of EO-based indices that have been developed to map and monitor evapotranspiration (ET) for

drought assessment include the Drought Severity Index (DSI; Su *et al.*, 2003) and Evaporative Drought Index (EDI; Anderson *et al.*, 2007; Yao *et al.*, 2010; Bayarjargal *et al.*, 2006).

Surface energy balance models that have been proposed to estimate AET include SEBAL (Surface Energy Balance Algorithm for Land, Bastiaanssen *et al.*, 1998; Bastiaanssen, 2000) and METRIC (Mapping Evapotranspiration at High Resolution with Internal Calibration, Allen *et al.*, 2007). In Australia, these models have been successfully used to monitor crop water requirements (see Section 13) and wetland AET (Khan *et al.*, 2009).

9.5 Plant Water Stress

As introduced in Sections 4.2.1, 5.2.3, and 5.2.4, plant water stress is signalled by increasing plant temperature and reducing transpiration rates. Since air temperature, relative humidity, wind speed, and incoming irradiance can also impact canopy temperature, a normalised index was developed to account for such factors (Idso *et al.*, 1981). The Crop Water Stress Index (CWSI) was proposed by Jackson (1981, 1988) to map variations in canopy water status using remotely sensed temperature:

$$\text{CWSI} = \frac{\text{canopy temp.} - \text{reference temp.}}{\text{maximum temp.} - \text{reference temp.}}$$

where

reference temperature is measured from comparable, non-stressed vegetation; and maximum temperature is the upper temperature tolerated without transpiration.

CWSI values range from zero for a fully transpiring plant to one for a non-transpiring plant with leaf temperature 4–6°C above the air temperature. As with similar indices, the validity of the CWSI is critically dependent on the selection of appropriate reference data. Field measurements of leaf thermal properties can be problematic, with variations continually being induced by fluctuations in irradiance and air currents. View angle variations will also result in different temperature measurements (Jones *et al.*, 2002).

King *et al.* (2011) evaluated continental AET products for Australia, and concluded that estimates based on water balance modelling (Raupach *et al.*, 2009, van Dijk, 2010) proved to be most reliable in regions where AET depends on precipitation, but EO-based methods (Guerschman *et al.*, 2009), which accounted for surface and groundwater contributions, were more appropriate in areas where vegetation is dependent on other water sources. EO-based estimates of ET have become essential inputs to national water resources assessment processes in Australia (van Dijk and Renzullo, 2011; see Excursus 10.2).

CWSI has been widely used for monitoring water stress and scheduling irrigation in a range of cereal and horticultural crops (Alderfasi and Nielsen, 2000; Irmak *et al.*, 2000; Orta *et al.*, 2003; Taghvaeian *et al.*, 2012; Poblete-Echeverria *et al.*, 2017; Alghory and Yazar, 2019). For example, Park *et al.* (2017) acquired high resolution thermal imagery using UAV to map variability of plant water stress in nectarine and peach orchards in Victoria. Stem water potential and stomatal conductance were measured directly on the ground. An adaptive CWSI, derived from crop pixels only (isolated from soil background), showed better agreement with the direct measurements than the conventional CWSI.

At a regional scale, McVicar and Jupp (2002) used the Normalised Difference Temperature Index (NDTI) to monitor moisture availability from integrated meteorological and EO datasets:

$$\text{NDTI} = \frac{T_{\max} - T_s}{T_{\max} - T_{\min}}$$

where

T_s is the observed surface temperature for an EO pixel with a given NDVI value; and T_{\max} and T_{\min} are respectively the highest and lowest surface temperatures for pixels with the same NDVI value.

A Resistance Energy Balance Model (REBM) was used to calculate NDTI from meteorological station records, which were then interpolated using EO-based covariates (see Section 10.1.2). These authors considered NDTI as a 'specific time-of-day version of CWSI'.

At global, regional and country levels, the FAO Agricultural Stress Index System (ASIS) monitors agricultural areas that are very likely to experience water stress or drought (Rojas, 2015; FAO, 2020). This system relies on the Agricultural Stress Index (ASI; Rojas *et al.*, 2011), which compares the Vegetation Health Index (VHI) with the seasonal VHI average, where the crop season is defined using a phenological model derived from NDVI. VHI is one of several global products generated by NOAA/NESDIS since 1981 to map vegetation health. Derived from AVHRR and VIIRS imagery, VHI is a global, validated, weekly composite with 4 km spatial resolution based on proxies for the relative moisture and thermal conditions:

$$VHI = a \times VCI + (1 - a) \times TCI$$

where

VCI (Vegetation Condition Index) indicates the moisture condition of vegetation, derived from NDVI time series imagery:

$$VCI_i = 100 \times \frac{NDVI_i - NDVI_{min}}{NDVI_{max} - NDVI_{min}}$$

TCI (Thermal Condition Index) indicates the thermal condition of vegetation, derived from brightness temperature (BT) time series imagery:

$$TCI_i = 100 \times \frac{BT_i - BT_{min}}{BT_{max} - BT_{min}}$$

a is a coefficient that determines the relative contributions of VCI and TCI to the health status of vegetation (NOAA STAR, 2019). Typically $a=0.5$ unless the contribution of moisture and temperature status to vegetation health is known (Rojas *et al.*, 2011).

In the calculation of VCI and TCI, the NDVI and BT time series are filtered to remove high frequency noise and adjusted for land surface non-homogeneity (Kogan, 1997). VHI, VCI, and TCI are used to define drought conditions (where all indices < 40) as well as the risk of fire and malaria. The VHI product suite has been used for early drought detection, assessing drought area coverage, duration, and intensity, and for monitoring drought impacts on vegetation and agricultural crops (NOAA STAR, 2019; see Section 11.2). ASI has been used to historically identify major droughts and their impact on the African continent (Rojas *et al.*, 2011). ASIS has been incorporated into the Global Information and Early Warning System (GIEWS; FAO, 2020; see Section 11.2) to indicate regions that are currently water-stressed and may be facing drought conditions (Fritz *et al.*, 2019).

9.6 Plant Vigour

Characteristics of leaf optical reflectance that change with variations in plant vigour are introduced in Section 4.3. In terms of EO, thermography, chlorophyll fluorescence and hyperspectral imaging have been the most promising approaches to identify and quantify plant diseases (Mahlein *et al.*, 2012).

Approaches used to measure plant biochemistry, and thus plant vigour, based on spectroscopic measurement can be grouped into two categories (Ustin *et al.*, 2004):

- empirical—using linear and non-linear combinations of spectral bands, which highlight canopy characteristics (Hall *et al.*, 1995; Price, 1992b); and
- analytical and semi-analytical—using canopy reflectance (CR) models, based on radiative transfer theory and leaf optical simulation (Meroni *et al.*, 2004), which can be inverted to estimate leaf and canopy parameters (Privette *et al.*, 1996; Bicheron and Leroy, 1999; Jacquemoud *et al.*, 2009).

Some of the most important biochemical compounds involved in carbon, water and nutrient cycling include the light absorbing pigments (principally chlorophylls and carotenoids; see Excursus 4.1) and nitrogen, which are directly related to the photosynthetic capacity in plants (see Section 5.2.1; Gitelson *et al.*, 2006, 2009; Ollinger and Smith, 2005). In particular, leaf chlorophyll content varies with the photosynthetic capacity, productivity, stress, age, and development stage of a plant (Curran *et al.*, 1990; Ustin *et al.*, 1998).

Various plant stress factors modify the proportion of light-absorbing pigments to reduce light absorption, which further decreases leaf chlorophyll content (Zarco-Tejada *et al.*, 2000). As introduced in Section 4.3, leaf absorption of wavelengths in the spectral region from 550 nm to 700 nm (visible red) is closely related to the concentration of chlorophyll pigments (Thomas and Gausman, 1977; Carter and Knapp, 2001; Devlin and Witham, 1983). As chlorophyll concentration increases, the red absorption feature both broadens and deepens, which moves the ‘edges’

of that feature (Horler *et al.*, 1983). Of greatest significance is the movement of its ‘red edge’ (that is, EMR wavelengths from around 690 nm to 740 nm) towards longer wavelengths as chlorophyll content increases (Rock *et al.*, 1988, Curran *et al.*, 1990; Ustin *et al.*, 1998). Accordingly, when red reflectance is standardised by a non-absorbing waveband, it is strongly correlated with leaf pigment changes (Curran, 1989; Curran *et al.*, 1997), especially leaf chlorophyll concentration (Turrell *et al.*, 1961; Thomas and Gausman, 1977; Everitt *et al.*, 1985).

Various indices have been designed to capture the position and shape of the ‘red edge’ (see Section 8.1.2), many of which can be used to track chlorophyll concentration (Horler *et al.*, 1983; Curran *et al.*, 1991; Miller *et al.*, 1991; Filella and Penuelas, 1994; Curran *et al.*, 1995; see Section 8.1). Changes in plant vigour, due to nutritional status, pests, and/or diseases, has been monitored using EO datasets for several decades (see Sections 11 to 16).

9.7 Further Information

TERN Auscover products

Ecosystem Disturbance Index: <http://www.auscover.org.au/purl/modis-disturbance-index>

Phenology: <http://www.auscover.org.au/purl/modis-phenology-uts>

National Vegetation Information System

NVIS: <http://www.environment.gov.au/land/native-vegetation/national-vegetation-information-system>

<http://www.environment.gov.au/land/native-vegetation/national-vegetation-information-system/data-products>

NVIS Technical Working Group (2017) Australian Vegetation Attribute Manual: National Vegetation Information System, Version 7.0. Department of the Environment and Energy, Canberra. Prep by Bolton, M.P., deLacey, C., and Bossard, K.B. (Eds)

<https://www.environment.gov.au/land/native-vegetation/national-vegetation-information-system/data-products#mvg51>

New South Wales

Statewide Landcover and Trees Study (SLATS): <https://www.environment.nsw.gov.au/topics/animals-and-plants/native-vegetation/reports-and-resources>

NSW Report on Native Vegetation 2014–16: <https://www.environment.nsw.gov.au/vegetation/reports.htm>

NSW Fire Extent and Severity Mapping (annual monitoring and reporting framework): <https://www.environment.nsw.gov.au/topics/animals-and-plants/native-vegetation/landcover-monitoring-and-reporting/fire-extent-and-severity-maps>

DustWatch: <https://www.environment.nsw.gov.au/topics/land-and-soil/soil-degradation/wind-erosion/community-dustwatch>

Queensland

Ground cover monitoring: <https://www.qld.gov.au/environment/land/management/mapping/statewide-monitoring/groundcover>

Ground cover disturbance index: <http://qldspatial.information.qld.gov.au/catalogue/custom/detail.page?fid={E2021208-DBCB-4963-A0F7-D4C7FD3150F2}>

Statewide Landcover and Trees Study (SLATS): <https://www.qld.gov.au/environment/land/management/mapping/statewide-monitoring/slats>

Victoria

Habitat Hectares: https://www.environment.vic.gov.au/_data/assets/pdf_file/0016/91150/Vegetation-Quality-Assessment-Manual-Version-1.3.pdf

Spatial data for Victoria: https://www2.delwp.vic.gov.au/maps?_ga=2.6531511.420315026.1549698228-873342548.1549698228

Western Australia

LandMonitor: <https://landmonitor.landgate.wa.gov.au/home.php>

9.8 References

- Abuzar, M., Sheffield, K., Whitfield, D., O'Connell, M., and McAllister, A. (2014). Comparing Inter-Sensor NDVI for the Analysis of Horticulture Crops in South-Eastern Australia. *American Journal of Remote Sensing*, 2, 1–9. <http://doi.org/10.11648/j.ajrs.2014.0201.11>
- Alderfasi, A.A., and Nielsen, D.C. (2001). Use of crop water stress index for monitoring water status and scheduling irrigation in wheat. *Agricultural Water Management*, 47, 69–75. [https://doi.org/10.1016/S0378-3774\(00\)00096-2](https://doi.org/10.1016/S0378-3774(00)00096-2)
- Alghory, A., and Yazar, A. (2019). Evaluation of crop water stress index and leaf water potential for deficit irrigation management of sprinkler-irrigated wheat. *Irrigation Science*, 37, 61–77. <https://doi.org/10.1007/s00271-018-0603-y>
- Allen, A., and Beetsom, B. (1999). The Land Monitor Project; A Multi-agency project of the Western Australian Salinity Action Plan supported by the Natural Heritage Trust. *Proceedings of WALIS Forum 1999*, Perth, WA, March 1999. pp. 74–77. https://landmonitor.landgate.wa.gov.au/reports/walis_1999.pdf
- Allen R.G., Tasumi, M., and Trezza, R. (2007). Satellite-Based Energy Balance for Mapping Evapotranspiration with Internalized Calibration, METRIC, Model. *Journal of Irrigation and Drainage Engineering*, 133, 380–394.
- Anderson, M.C., Norman, J.M., Mecikalski, J.R., Otkin, J.A., and Kustas, W.P. (2007). A climatological study of evapotranspiration and moisture stress across the continental United States based on thermal remote sensing: 2. Surface moisture climatology. *Journal of Geophysical Research*, 112, D1111.
- Bastiaanssen, W.G.M. (2000). SEBAL-based sensible and latent heat fluxes in the irrigated Gediz Basin, Turkey. *Journal of Hydrology*, 229, 87–100.
- Bastiaanssen, W.G.M., Menenti, M., Feddes, R.A., and Holtslag, A.A.M. (1998). A remote sensing surface energy balance algorithm for land (SEBAL). 1. Formulation. *Journal of Hydrology*, 212–213, 198–212.
- Bayarjargal, Y., Karnieli, A., Bayasgalan, M., Khudulmur, S., Gandush, C., and Tucker, C.J. (2006). A comparative study of NOAA–AVHRR derived drought indices using change vector analysis. *Remote Sensing of Environment*, 105, 9–22.
- Bicheron, P., and Leroy, M. (1999). A method of biophysical parameter retrieval at global scale by inversion of a vegetation reflectance model. *Remote Sensing of Environment*, 67, 251–266.
- Blaikie, S.J., Chacko, E.K., Lu, P., and Muller, W.J. (2001). Productivity and water relations of field-grown cashew: a comparison of sprinkler and drip irrigation. *Australian Journal of Experimental Agriculture*, 41, 663–673.
- Bradley, B.A., Jacob, R.W., Hermance, J.F., and Mustard, J.F. (2007). A curve fitting procedure to derive inter-annual phenologies from time series of noisy satellite NDVI data. *Remote Sensing of Environment*, 106(2), 137–145.
- Broich, M., Huete, A., Tulbure, M. G., Ma, X., Xin, Q., Paget, M., Restrepo-Coupe, N., Davies, K., Devadas, R., and Held, A. (2014). Land surface phenological response to decadal climate variability across Australia using satellite remote sensing. *Biogeosciences*, 11, 5181–5198. <https://doi.org/10.5194/bg-11-5181-2014>
- Broich, M., Huete, A., Paget, M., Ma, X., Tulbure, M., Restrepo Coupe, N., Evans, B., Beringer, J., Devadas, R., Davies, K., and Held, A. (2015). A spatially explicit land surface phenology data product for science, monitoring and natural resources management applications. *Environmental Modelling and Software*, 64, 191–204. <https://doi.org/10.1016/j.envsoft.2014.11.017>
- Brown, T.B., Zimmermann, C., Panneton, W., Noah, N., and Borevitz, J. (2012). High-resolution, time-lapse imaging for ecosystem-scale phenotyping in the field. Ch 7 in *High Throughput Phenotyping in Plants: Methods and Protocols, Methods in Molecular Biology*. (Ed: Normanly, J.). Springer-Science, New York. ISBN 978-1-61779-995-2
- Brown, T.B., Hultine, K.R., Steltzer, H., Denny, E.G., Denslow, M.W., Granados, J., Henderson, S., Moore, D., Nagai, S., SanClements, M., Sánchez-Azofeifa, A., Sonnetta, O., Tazik, D., and Richardson, A.D. (2016). Using phenocams to monitor our changing Earth: toward a global phenocam network. *Frontiers in Ecology and the Environment*, 14(2), 84–93. [doi:10.1002/fee.1222](https://doi.org/10.1002/fee.1222)
- Budyko, M.I. (1958). *The heat balance of the earth's surface*. U.S. Dept. of Commerce, Washington.
- Budyko, M.I. (1974). *Climate and life*. Academic, New York.
- Carter, G.A., and Knapp, A.K. (2001). Leaf optical properties in higher plants: linking spectral characteristics to stress and chlorophyll concentration. *American Journal of Botany*, 88(4), 677–684. <https://doi.org/10.2307/2657068>

- Cleland, E.E., Chuine, I., Menzel, A., Mooney, H.A., and Schwartz, M.D. (2007). Shifting plant phenology in response to global change. *Trends in Ecology and Evolution*, 22(7), 357–365. <https://doi.org/10.1016/j.tree.2007.04.003>
- Cocke, A.E., Fulé, P.Z., and Grouse, J.E. (2005). Comparison of burn severity assessments using Differenced Normalised Burn Ratio and ground data. *International Journal of Wildland Fire*, 14, 189–198. doi:10.1071/WFO4010
- Coops, N.C., Waring, R.H., Wulder, M.A., and White, J.C. (2009). Prediction and assessment of bark beetle-induced mortality of lodgepole pine using estimates of stand vigour derived from remotely sensed data. *Remote Sensing of Environment*, 113, 1058–1066.
- Craze, B., and Hamilton, G.J. (1991). Soil physical properties. In *Soils - Their Properties and Management*. (Eds: Charman, P.E.V., and Murphy, B.W.) Sydney University Press, South Melbourne. pp 147–164.
- Curran, P.J. (1989). Remote sensing of foliar chemistry. *Remote Sensing of Environment*, 30, 271–278.
- Curran, P.J., Dungan, J.L., and Gholz, H.L. (1990). Exploring the relationship between reflectance red-edge and chlorophyll content in slash pine. *Tree Physiology*, 7, 33–48.
- Curran, P.J., Dungan, J.L., Macler, B.A., and Plummer, S.E. (1991). The effect of a red leaf pigment on the relationship between red edge and chlorophyll concentration. *Remote Sensing of Environment*, 35, 69–76.
- Curran, P.J., Windham, W.R., and Gholz, H.L. (1995). Exploring the relationship between reflectance red edge and chlorophyll concentration in slash pine leaves. *Tree Physiology*, 15, 203–206.
- Curran, P.J., Kupiec, I.A., and Smith, G.M. (1997). Remote sensing the biochemical composition of a slash pine canopy. *IEEE Transactions on Geoscience and Remote Sensing*, 35, 415–420.
- Danaher, T., Scarth, P., Armston, J., Collett, L., Kitchen, J., and Gillingham, S. (2011). Remote Sensing of Tree-Grass Systems: The Eastern Australian Woodlands. In *Ecosystem Function in Savannas: Measurement and Modelling at Landscape to Global Scales*. (Eds: Hill, M.J., and Hanan, N.P.) CRC Press, Boca Raton, pp. 175–194.
- Devlin, R.M., and F.H. Witham, F.H. (1983). *Plant physiology*. 4th Edn. Willard Grant Press, Boston, 497 p.
- Donohue, R.J., Roderick, M.L., and McVicar, T.R. (2007). On the importance of including vegetation dynamics in Budyko's hydrological model. *Hydrology and Earth System Sciences*, 11, 983–995.
- Donohue, R.J., Roderick, M.L., McVicar, T.M. (2008). Deriving consistent long-term vegetation information from AVHRR reflectance data using a cover-triangle based framework. *Remote Sensing of Environment*, 112, 2938–2949.
- Donohue, R.J., McVicar, T.R., Roderick, M.L. (2009). Climate-related trends in Australian vegetation cover as inferred from satellite observations, 1981–2006. *Global Change Biology*, 15, 1025–1039.
- Donohue, R.J., Roderick, M.L., McVicar, T.R. (2010a). Can dynamic vegetation information improve the accuracy of Budyko's hydrological model? *Journal of Hydrology*, 390, 23–34.
- Donohue, R.J., McVicar, T.R., and Roderick, M.L. (2010b). Assessing the ability of potential evaporation formulations to capture the dynamics in evaporative demand within a changing climate. *Journal of Hydrology*, 386, 186–197. <http://doi.org/10.1016/j.jhydrol.2010.03.020>
- Doody, T., and Benyon, R. (2011). Quantifying water savings from willow removal in Australian streams. *Journal of Environmental Management*, 92, 926–935.
- Elmore, A.J., Mustard, J.F., and Manning, S.J. (2003). Regional patterns of plant community response to changes in water: Owens Valley, California. *Ecological Applications*, 13(2), 443–460.
- Everitt, J.H., Richardson, A.J., and Gaussman, H.W. (1985). Leaf reflectance—nitrogen-chlorophyll relations in buffelgrass. *Photogrammetric Engineering and Remote Sensing*, 51, 463–466.
- FAO (2020). *Earth Observation* webpage, UN Food and Agriculture Organisation website: <http://www.fao.org/giews/earthobservation/index.jsp?lang=en>
- Filella, I., and Peñuelas, J. (1994). The red edge position and shape as indicators of plant chlorophyll content, biomass and hydric status. *International Journal of Remote Sensing*, 15, 1459–1470.
- Fritz, S., See, L., Bayas, J.C.L., Waldner, F., Jacques, D., Becker-Reshef, I., Whitcraft, A., Baruth, B., Bonifacio, R., Crutchfield, J., Rembold, F., Rojas, O., Schucknecht, A., Van der Velde, M., Verdin, J., Wu, B., Yan, N., You, L., Gilliams, S., Mûcher, S., Tetrault, R., Moorthy, I., and McCallum, I. (2019). A comparison of global agricultural monitoring systems and current gaps. *Agricultural Systems*, 168, 258–272. <https://doi.org/10.1016/j.jagsy.2018.05.0>

- Gill, T., Johansen, K., Phinn, S., Trevithick, R., Scarth, P., and Armston, J. (2017). A method for mapping Australian woody vegetation cover by linking continental-scale field data and long-term Landsat time series. *International Journal of Remote Sensing*, 38(3), 679–705. Doi: 10.1080/01431161.2016.1266112
- Gill, T., Johansen, K., Scarth, P., Armston, J., Trevithick, R., and Flood, N. (2018). Persistent Green Vegetation Fraction. Ch 8 in *Effective Field Calibration and Validation Practices: A practical handbook for calibration and validation satellite and model-derived terrestrial environmental variables for research and management*. A TERN Landscape Assessment Initiative, NCRIS. ISBN 978-0-646-94137-0.
- Gitelson, A.A., Keydan, G.P., and Merzlyak, M.N. (2006). Three-band model for non-invasive estimation of chlorophyll assessment in higher plant leaves. *Journal of Plant Physiology*, 160, 271–282.
- Gitelson, A.A., Chivkunova, O.B., and Merzlyak, M.N. (2009). Nondestructive estimation of anthocyanins and chlorophylls in anthocyanic leaves. *American Journal of Botany*, 96(10), 1861–1868.
- Glenn, E.P., Huete, A.R., Nagler, P.L., Hirschboeck, K.K., and Brown, P. (2007). Integrating remote sensing and ground methods to estimate evapotranspiration. *Critical Reviews in Plant Sciences*, 26, 139–168.
- Glenn, E.P., Nagler, P.L., and Huete, A.R. (2010). Vegetation Index methods for estimating evapotranspiration by remote sensing. *Surveys in Geophysics*, 31(6), 531–555. doi:10.1007/s10712-010-9102-2
- Glenn, E., Doody, T.M., Guerschman, J.P., Huete, A.R., King, E.A., McVicar, T.R., van Dijk, A.I.J.M., van Niel, T.G., Yebra, M., and Zhang, Y. (2011). Actual evapotranspiration estimation by ground and remote sensing methods: the Australian experience. *Hydrological Processes*, 25(26), 4103–4116. doi:10.1002/hyp.8391
- Goward, S. N., Markham, B., Dye, D.G., Dulaney, W., and Yang, A.J. (1991). Normalized difference vegetation index measurements from the Advanced Very High Resolution Radiometer. *Remote Sensing of Environment*, 35, 257–277.
- Guerschman, J.P., Van Dijk, A.I.J.M., Mattersdorf, G., Beringer, J., Hutley, L.B., Leuning, R., Pipunic, R.C., and Sherman, B.S. (2009). Scaling of potential evapotranspiration with MODIS data reproduces flux observations and catchment water balance observations across Australia. *Journal of Hydrology*, 369, 107–119.
- Hall, F. G., Townshend, J. R., and Engman, E. T. (1995). Status of remote sensing algorithms for estimation of land surface state parameters. *Remote Sensing of Environment*, 51, 138–156.
- Hernance, J.F., Jacob, R.W., Bradley, B.A., and Mustard, J.F. (2007). Extracting phenological signals from multiyear AVHRR NDVI time series: Framework for applying high-order annual splines with roughness damping. *IEEE Transactions on Geoscience and Remote Sensing*, 45(10), 3264–3276.
- Holden, Z.A., Smith, A.M.S., Morgan, P., Rollins, M.G., and Gessler, P.E. (2005). Evaluation of novel thermally enhanced spectral indices for mapping fire perimeters and comparisons with fire atlas data. *International Journal of Remote Sensing*, 26(21), 4801–4808.
- Horler, D.N.H., Dockray, M., and Barber, J. (1983). The red edge of plant leaf reflectance. *International Journal of Remote Sensing*, 4(2), 273–288. doi: 10.1080/01431168308948546
- Huete, A.R., Didan, K., Shimabukuro, Y.E., Ratana, P., Saleska, S.R., Hutya, L.R., Yang, W., Nemani, R.R., and Myneni, R. (2006). Amazon rainforests green-up with sunlight in dry season. *Geophysical Research Letters*, 33(6), L06405. <https://doi.org/10.1029/2005GL025583>.
- Idso, S.B., Jackson, R.D., Pinter, P.J., Jr., Reginato, R.J., and Hatfield, J.L. (1981). Normalizing the Stress-Degree-day parameter for environmental variability. *Agricultural Meteorology*, 24, 45–55. [https://dx.doi.org/10.1016/0002-1571\(81\)90032-7](https://dx.doi.org/10.1016/0002-1571(81)90032-7)
- Irmak, S., Haman, D.Z., and Bastug, R. (2000). Determination of Crop Water Stress Index for Irrigation Timing and Yield Estimation of Corn. *Agronomy Journal*, 92, 1221–1227.
- Jackson, R.D., Idso, S.B., Reginato, R.J., and Pinter, P.J. (1981). Canopy temperature as a crop water stress indicator. *Water Resources Research*, 17(4), 1133–1138.
- Jackson, R.D., William, P.K., and Choudhury, B.J. (1988). A Reexamination of the Crop Water Stress Index. *Irrigation Science*, 9, 309–317.
- Jacquemoud, S., Verhoef, W., Baret, F., Bacour, C., Zarco-Tejada, P.J., Asner, G.P., François, C., and Ustin, S.L. (2009). PROSPECT plus SAIL models: a review of use for vegetation characterization. *Remote Sensing of Environment*, 113, S56–S66.
- Johansen, K., Gill, T., Trevithick, R., Armston, J., Scarth, P., Flood, N., and Phinn, S. (2012). Landsat based Persistent Green-Vegetation Fraction for Australia. *Proceeding of 16th Australasian Remote Sensing and Photogrammetry Conference*. Melbourne.

- Jolly, W.M., Nemani, R., and Running, S.W. (2005). A generalized, bioclimatic index to predict foliar phenology in response to climate. *Global Change Biology*, 11, 619–632. doi:10.1111/j.1365-2486.2005.00930.x
- Jones, H.G., Stoll, M., Santos, T., de Sousa, C., Chaves, M.M., and Grant, O.M. (2002). Use of infrared thermography for monitoring stomatal closure in the field: application to grapevine. *Journal of Experimental Botany*, 53(378), 2249–2260. doi:10.1093/jxb/erf083
- Jönsson, P., and Eklundh, L. (2002). Seasonality extraction by function fitting to time-series of satellite sensor data. *IEEE Transactions on Geoscience and Remote Sensing*, 40(8), 1824–1832.
- Jönsson, P., and Eklundh, L. (2004). TIMESAT—a program for analysing time-series of satellite sensor data. *Computers and Geosciences*, 30, 833–845.
- Kaduk, J., and Heimann, M. (1996). A prognostic phenology model for global terrestrial carbon cycle models. *Climate Research*, 6, 1–19.
- Kalma, J.D., McVicar, T.R., McCabe, M.F. (2008). Estimating land surface evaporation: A review of methods using remotely sensed surface temperature data. *Surveys in Geophysics*, 29, 421–469.
- Key, C.H., and Benson, N.C. (2002). *Measuring and remote sensing of burn severity*. USGS Wildland Fire Workshop, 31 October to 3 November 2000. Los Alamos, NM. USGS Open-File Report 02-11.
- Key, C.H., and Benson, N.C. (2006). *Landscape Assessment: Sampling and Analysis Methods*. USDA Forest Service, Rocky Mountain Research Station General Tech. Rep. RMRS-GTR-164-CD. Odgen, UT.
- Khan, S., Hafeez, M., Abbas, A., and Ahmad, A. (2009). Spatial assessment of water use in an environmentally sensitive wetland. *Ambio*, 38, 157–165.
- King, E.A., van Niel, T.G., van Dijk, A.I.J.M., Wang, Z., Paget, M.J., Raupach, T., Guerschman, J., Haverd, V., McVicar, T.R., Miltenberg, I., Raupach, M.R., Renzullo, L.J., and Zhang, Y. (2011). *Actual Evapotranspiration Estimates for Australia Intercomparison and Evaluation*. Water for a Healthy Country National Research Flagship, CSIRO, Canberra.
- Kogan, F.N. (1997). Global Drought Watch from Space. *Bulletin of the American Meteorological Society*, 78(4), 621–636.
- Landgate (2019). *Landmonitor* webpage, Landgate website: <https://landmonitor.landgate.wa.gov.au/home.php>
- Lhermitte, S., Verbesselt, J., Verstraeten, W.W., and Coppin, P. (2011). A comparison of time series similarity measures for classification and change detection of ecosystem dynamics. *Remote Sensing of Environment*, 115, 3129–3152.
- Li, F.Q., and Lyons, T.J. (1999). Estimation of regional evapotranspiration through remote sensing. *Journal of Applied Meteorology*, 38, 1644–1654.
- Long, D., Longuevergne, L., and Scanlon, B.R. (2014). Uncertainty in evapotranspiration from land surface modelling, remote sensing, and GRACE satellites. *Water Resources Research*, 50(2), 1131–1151. <https://doi.org/10.1002/2013WR014581>
- Lu, H., Raupach, M.R., McVicar, T.R., and Barrett, D.J. (2003). Decomposition of vegetation cover into woody and herbaceous components using AVHRR NDVI time series. *Remote Sensing of Environment*, 86, 1–18.
- Ma, X., Huete, A., Yu, Q., Coupe, N.R., Davies, K., Broich, M., Ratana, P., Beringer, J., Hutley, L.B., Cleverly, J., Boulain, N., Eamus, D. (2013). Spatial patterns and temporal dynamics in savanna vegetation phenology across the North Australian Tropical Transect. *Remote Sensing of Environment*, 139, 97–115. doi:10.1016/j.rse.2013.07.030
- Mahlein, A.K., Oerke, E.C., Steiner, U., and Dehne, H.W. (2012). Recent advances in sensing plant diseases for precision crop protection. *European Journal of Plant Pathology*, 133(1), 197–209. doi:10.1007/s10658-011-9878-z
- McFarlane, D.J., and Wallace, J.F. (2019). *Measuring native vegetation extent and condition using remote sensing technologies—a review and identification of opportunities*. The Western Australian Biodiversity Science Institute, Perth.
- McKenzie, N.J., Grundy, M.J., Webster, R., and Ringrose-Voase, A.J. (Eds) (2008). *Guidelines for Surveying Soil and Land Resources*. Australian Soil and Land Survey Handbook Series. CSIRO Publishing, Melbourne.
- McVicar, T.R., and Jupp, D.L.B. (2002). Using covariates to spatially interpolate moisture availability in the Murray-Darling Basin: a novel use of remotely sensed data. *Remote Sensing of Environment*, 79, 199–212.
- McVicar, T.R., Van Niel, T.G., Li, L.T., Hutchinson, M.F., Mu, X.M., Liu, Z.H. (2007). Spatially Distributing Monthly Reference Evapotranspiration and Pan Evaporation Considering Topographic Influences. *Journal of Hydrology*, 338, 196–220.

- McVicar, T.R., Donohue, R.J., O'Grady, A.P., and Li, L. (2010). *The effects of climatic changes on plant physiological and catchment ecohydrological processes in the high-rainfall catchments of the Murray-Darling Basin: A scoping study*. Water for a Healthy Country National Research Flagship, CSIRO. 95 p.
- Meroni, M., Colombo, R., and Panigada, C. (2004). Inversion of a radiative transfer model with hyperspectral observations for LAI mapping in popular plantations. *Remote Sensing of Environment*, 92(2), 195–206.
- Mildrexler, D.J., Zhao, M., Heinsch, F.A., and Running, S.W. (2007). A New Satellite Based Methodology for Continental Scale Disturbance Detection. *Ecological Applications*, 17, 235–250.
- Mildrexler, D.J., Zhao, M., and Running, S.W. (2009). Testing a MODIS Global Disturbance Index across North America. *Remote Sensing of Environment*, 113(10), 2103–2117. doi:10.1016/j.rse.2009.05.016
- Miller, J.D., and Thode, A.E. (2007) Quantifying burn severity in a heterogeneous landscape with a relative version of the delta Normalised Burn Ratio (dNBR). *Remote Sensing of Environment*, 109, 66–80.
- Miller, J.R., Wu, J., Boyer, M.G., Belanger, M., and Hare, E.W. (1991). Seasonal patterns in leaf reflectance red-edge characteristics. *International Journal of Remote Sensing*, 12, 1509–1523.
- Mosleh, M.K., Hassan, Q.K., and Chowdhury, E.H. (2015). Application of remote sensors in mapping rice area and forecasting its production: A review. *Sensors*, 15.1, 769–791.
- Moulin, S., Kergoat, L., Viovy, N., and Dedieu, G. G. (1997). Global-scale assessment of vegetation phenology using NOAA/AVHRR satellite measurements. *Journal of Climate*, 10, 1154–1170.
- Myneni, R.B., Keeling, C.D., Tucker, C.J., Asrar, G., and Nemani, R.R. (1997). Increased plant growth in the northern high latitudes from 1981 to 1991. *Nature*, 386, 698–702.
- NCST (2009). *Australian Soil and Land Survey Field Handbook*. 3rd edn. National Committee on Soil and Terrain (Australia). CSIRO Publishing, Melbourne. 246 p.
- Nemani, R., Hashimoto, H., Votava, P., Melton, F., Wang, W., Michaelis, A., Mutch, L., Milesi, C., Hiatt, S., and White, M. (2009). Monitoring and forecasting ecosystem dynamics using the Terrestrial Observation and Prediction System (TOPS). *Remote Sensing of Environment*, 113, 1497–1509.
- NOAA STAR (2019). STAR—*Global Vegetation Health Products: Background and Explanation* webpage, NOAA Center for Satellite Applications and Research website: https://www.star.nesdis.noaa.gov/smc/emb/vci/VH/VH-Syst_10ap30.php
- Nouri, H., Beecham, S., Kazemi, F., Hassanti, A.M., and Anderson, S. (2013). Remote sensing techniques for predicting evapotranspiration from mixed vegetated surfaces. *Hydrology and Earth System Sciences*, 10, 3879–3925.
- Ol'dekop, E. M. (1911). On evaporation from the surface of river basins. *Transactions on meteorological observations*, 4. Tartu, Estonia.
- Ollinger, S.V., and Smith, M.L. (2005). Net Primary Production and Canopy Nitrogen in a temperate forest landscape: an analysis using imaging spectrometry, modeling and field data. *Ecosystems*, 8, 760–778.
- Orta, A.H., Erdem, Y., and Erdem, T. (2003). Crop water stress index for horticulture. *Scientia Horticulturae*, 98(2), 121–120.
- Park, S., Ryu, D., Fuentes, S., Chung, H., Hernández-Montes, E., and O'Connell, M. (2017). Adaptive Estimation of Crop Water Stress in Nectarine and Peach Orchards Using High-Resolution Imagery from an Unmanned Aerial Vehicle (UAV). *Remote Sensing*, 9, 828. <https://doi.org/10.3390/rs9080828>
- Poblete-Echeverría, C., Espinace, D., Sepúlveda-Reyes, D., Zúñiga, M., and Sanchez, M. (2017). Analysis of crop water stress index (CWSI) for estimating stem water potential in grapevines: comparison between natural reference and baseline approaches. *Acta Horticulturae*, 1150, 189–194. <https://doi.org/10.17660/ActaHortic.2017.1150.27>
- Potter, C., Tan, P.N., Steinbach, M., Klooster, S., Kumar, V., Myneni, R., and Genovese, V. (2003). Major disturbance events in terrestrial ecosystems detected using global satellite data sets. *Global Change Biology*, 9(7), 1005–1021.
- Price, J.C. (1992b). Estimating Leaf Area Index from Remotely Sensed Data. *Proceedings of IGARSS '92*, Houston. Vol. 1. pp. 1500–1502.
- Privette, J.L., Emery, W.J., and Schimel, D.S. (1996). Inversion of a vegetation reflectance model with NOAA AVHRR data. *Remote Sensing of Environment*, 58, 187–200.
- Raupach, M.R., Briggs, P.R., Haverd, V., King, E.A., Paget, M.J., and Trudinger, C.M. (2009). *Australian Water Availability Project (AWAP), CSIRO Marine and Atmospheric Research Component: Final Report for Phase 3*. CAWCR Technical Report No. 013, Canberra, Australia. 67 p.

- Reed, B.C., Brown, J.F., VanderZee, D., Loveland, T.R., Merchant, J.W., and Ohlen, D.O. (1994) Measuring phenological variability from satellite imagery. *Journal of Vegetation Science*, 5, 703–714.
- Restrepo-Coupe, N., Huete, A., and Davies, K. (2018). Satellite Phenology Validation. Ch 9 in *Effective Field Calibration and Validation Practices: A practical handbook for calibration and validation satellite and model-derived terrestrial environmental variables for research and management*. A TERN Landscape Assessment Initiative, NCRIS. ISBN 978-0-646-94137-0.
- Richardson, A.D., Black, T.A., Ciais, P., Delbart, N., Friedl, M.A., Gobron, N., Hollinger, D.Y., Kutsch, W.L., Longdoz, B., Luysaert, S., Migliavacca, M., Montagnani, L., Munger, J.W., Moors, E., Piao, S., Rebmann, C., Reichstein, M., Saigusa, N., Tomelleri, E., Vargas, R., Varlagin, A. (2010). Influence of spring and autumn phenological transitions on forest ecosystem productivity. *Philosophical Transactions of the Royal Society B Biological Sciences*, 365, 3227–3246. doi:10.1098/rstb.2010.0102
- Rock, B.N., Hoshizaki, T., and Miller, J.R. (1988). Comparison of *in situ* and airborne spectral measurements of the blue shift associated with forest decline. *Remote Sensing of Environment*, 24, 109–127.
- Rojas, O. (2015). *Protocol for Country-Level ASIS: Calibration and National Adaptation Process*. Technical report. Food and Agriculture Organization of the United Nations.
- Rojas, O., Vrieling, A., Rembold, F. (2011). Assessing drought probability for agricultural areas in Africa with coarse resolution remote sensing imagery. *Remote Sensing of Environment*, 115, 343–352. <http://dx.doi.org/10.1016/j.rse.2010.09.006>.
- Roman-Cuesta, R.M., Retana, J., Gracia, M., and Rodriguez, R. (2005) A quantitative comparison of methods for classifying burned areas with LISS-III imagery. *International Journal of Remote Sensing*, 26(9), 1979–2003.
- Scarth, P., Gillingham, S., and Muir, J. (2008). Assimilation of spectral information and temporal history into a statewide woody cover change classification. *Proceedings of the 14th Australasian Remote Sensing and Photogrammetry Conference*. Darwin, Australia.
- Schreiber, P., (1904). Über die Beziehungen zwischen dem Niederschlag und der Wasserführung der Flüsse in Mitteleuropa. *Meteorologische Zeitschrift*, 21, 1904.
- Silberstein, R., Held, A., Hatton, T., Viney, N., and Sivapalan, M. (2001). Energy balance of a natural jarrah (*Eucalyptus marginata*) forest in Western Australia: Measurements during the spring and summer. *Agricultural and Forest Meteorology*, 109, 79–104. doi:10.1016/S0168-1923(01)00263-5
- Singh, A. (1989). Digital change detection techniques using remotely-sensed data. *International Journal of Remote Sensing*, 10, 989–1003.
- Smith, A.M.S., Drake, N.A., Wooster, M.J., Hudak, A.T., Holden, Z.A., and Gibbons, C.J. (2007). Production of Landsat ETM+ reference imagery of burned areas within Southern African savannas: comparison of methods and application to MODIS. *International Journal of Remote Sensing*, 28(12), 2753–2775.
- Su, Z., Yacob, A., Wen, J., Roerink, G., He, Y., Gao, B., Boogaard, H., and van Diepen, C. (2003). Assessing relative soil moisture with remote sensing data: Theory, experimental validation, and application to drought monitoring over the North China Plain. *Physics and Chemistry of the Earth (B)*, 28(1-3), 89–101.
- Taghvaeian, S., Chávez, J.L., and Hansen, N.C. (2012). Infrared Thermometry to Estimate Crop Water Stress Index and Water Use of Irrigated Maize in Northeastern Colorado. *Remote Sensing*, 4, 3619–3637. doi:10.3390/rs4113619
- Teillet, P.M., Saleous, N.E., Hansen, M.C., Eidenshink, J.C., Justice, C.O., and Townshend, J.R.G. (2000). An evaluation of the global 1-km AVHRR land dataset. *International Journal of Remote Sensing*, 21, 1987–2021.
- TERN AusCover (2014). *Ecosystem Disturbance Index* webpage, Terrestrial Ecosystem Research Network website: <http://www.auscover.org.au/purl/modis-disturbance-index>
- TERN Australia (2018). *Effective Field Calibration and Validation Practices: A practical handbook for calibration and validation satellite and model-derived terrestrial environmental variables for research and management*. A TERN Landscape Assessment Initiative, NCRIS. ISBN 978-0-646-94137-0. <https://www.tern.org.au/NEW-CalVal-handbook-for-remote-sensing-bgp4370.html>
- Thomas, J.R., and Gausman, H.W. (1977). Leaf reflectance vs leaf chlorophyll and carotenoid concentrations for eight crops. *Agronomy Journal*, 69, 799–811.
- Trigg, S., and Flasse, S. (2000). Characterizing the spectral-temporal response of burned savannah using *in situ* spectroradiometry and infrared thermometry. *International Journal of Remote Sensing*, 21(16), 3161–3168.

- Tucker, C.J., Slayback, D.A., Pinzon, J.E., Los, S.O., Myneni, R.B., and Taylor, M.G. (2001). Higher northern latitude normalized difference vegetation index and growing season trends from 1982 to 1999. *International Journal of Biometeorology*, 45, 184–190.
- Turrell, F.M., Weber, J.R., and Austin, S.W. (1961). Chlorophyll content and reflection spectra for citrus leaves. *Botanical Gazette*, 123, 10–16.
- Ustin, S.L., Smith, M.O., Jacquemoud, S., Verstraete, M.M., and Govaerts, Y. (1998). Geobotany: vegetation mapping for earth sciences. In: *Manual of Remote Sensing: Remote Sensing for the Earth Sciences*. Vol. 3, 3rd Edn. Ed. A.N. Rencz. John Wiley, New York. pp 189–248.
- Ustin, S.L., Jacquemoud, S., Zarco-Tejada, P.J., and Asner, G.P. (2004). Remote sensing of the environment: state of the science and new directions, in *Manual of Remote Sensing. Volume 4: Remote Sensing for Natural Resource Management and Environmental Monitoring* (Ed: S.L. Ustin). John Wiley and Sons. pp. 679–729.
- Van Dijk, A.I.J.M. (2010). *AWRA Technical Report 3. Landscape Model (version 0.5) Technical Description*. WIRADA / CSIRO Water for a Healthy Country Flagship, Canberra.
- Van Dijk, A.I.J.M., and Renzullo, L.J. (2011). Water resource monitoring systems and the role of satellite observations. *Hydrological and Earth System Sciences*, 15, 39–55.
- Van Niel, T.G., McVicar, T.R., Roderick, M.L., Van Dijk, I.J.M., Renzullo, L.J., and Van Gorsel, E. (2011). Correcting for systematic error in satellite-derived latent heat flux due to assumptions in temporal scaling: Assessment from flux tower observations. *Journal of Hydrology*, 409, 140–148. doi:10.1016/j.jhydrol.2011.08.011
- Verbesselt, J., Robinson, A., Stone, C., and Culvenor, D. (2009). Forecasting tree mortality using change metrics derived from MODIS-satellite data. *Forest Ecology and Management*, 258, 1166–1173.
- Verbesselt, J., Hyndman, R., Newnham, G., and Culvenor, D. (2010). Detecting trend and seasonal changes in satellite image time series. *Remote Sensing of Environment*, 114 (1), 106–115.
- White, M.A., and Nemani, R.R. (2006). Real-time monitoring and short-term forecasting of land surface phenology. *Remote Sensing of Environment*, 104, 43–49.
- White, M.A., Thornton, P.E., and Running, S.W. (1997). A continental phenology model for monitoring vegetation responses to interannual climatic variability. *Global Biogeochemical Cycle*, 11, 217–234.
- White, M.A., Nemani, R.R., Thornton, P.E., and Running, S.W. (2002). Satellite evidence of phenological differences between urbanized and rural areas of the eastern United States deciduous broadleaf forest. *Ecosystems*, 5, 260–273.
- Yao, Y., Liang S., Qin Q., and Wang, K. (2010). Monitoring drought over the conterminous United States using MODIS and NCEP Reanalysis-2 data. *Journal of Applied Meteorology and Climatology*, 49(8), 1665–1680. doi:10.1175/2010JAMC2328.1.
- Yebra, M., Van Dijk, A.I.J.M., Leuning, R., Huete, A., and Guerschman, J.P. (2013). Evaluation of optical remote sensing to estimate actual evapotranspiration and canopy conductance. *Remote Sensing of Environment*, 129, 250–261.
- Yin, H., Udelhoven, T., Fensholt, R., Pflugmacher, D., and Hoster, P. (2012). How Normalised Difference Vegetation Index (NDVI) Trends from Advanced Very High Resolution Radiometer (AVHRR) and Système Probatoire d’Observation de la Terre VEGETATION (SPOT VGT) Time Series Differ in Agricultural Areas: An Inner Mongolian Case Study. *Remote Sensing*, 4, 3364–3389.
- Zarco-Tejada, P.J., Miller, J.R., Mohammed, G.H., and Noland, T.L. (2000). Chlorophyll fluorescence effects on vegetation apparent reflectance. I. Leaf-level measurements and model simulation. *Remote Sensing of Environment*, 74, 582–595.
- Zeng, L., Wardlow, B.D., Xiang, D., Hu, S., and Li, D. (2020). A review of vegetation phenological metrics extraction using time-series, T multispectral satellite data. *Remote Sensing of Environment*, 238, 111511. <https://doi.org/10.1016/j.rse.2019.111511>
- Zhang, X., Friedl, M.A., Schaaf, C.B., Strahler, A.H., Hodges, J.C.F., Gao, F., Reed, B.C., and Huete, A. (2003). Monitoring vegetation phenology using MODIS. *Remote Sensing of Environment*. 84, 471–475.
- Zhang, X., Goldberg, M.D., and Yu, Y. (2012). Prototype for monitoring and forecasting fall foliage coloration in real time from satellite data. *Agricultural and Forest Meteorology*, 158–159, 21–29. doi:10.1016/j.agrformet.2012.01.013

10 Modelling

EO imagery offers a unique perspective for landscape scale analyses with a range of resolutions (see Volumes 1 and 2). For terrestrial vegetation, this perspective allows ecophysiological information relating to photosynthetic activity, biomass, productivity, water content, phenology, soil moisture, and nutrient status to be acquired and analysed consistently and repeatedly over large areas. Modelling based on EO datasets aims to use this perspective to improve our understanding of environmental processes, with the ultimate goal of predicting the future environmental impact of changes in current conditions.

Depending on the underlying questions to be answered, models can be simple or complex (Robins *et al.*, 2003). All models approximate reality, and greater functionality means greater complexity. Understandably, more complex questions require more complex models, which deliver more detailed explanations of the underlying processes and drivers. More complex models also require more data and more processing, as well as a deeper understanding of the resource being modelled.

However, models only estimate parameters—they do not supply absolute answers (Robins *et al.*, 2003). As complexity increases, systematic error, resulting from overly simplified assumptions, decreases, but calibration error, due to poorly fitted parameters, increases (Zhang *et al.*, 2002; see Figure 10.1). As a general rule, a model should only be as complex as it needs to be to achieve its defined goal. The reliability of modelled results can be determined by comparison with historical measurements, field validation (see Volume 2D), or sensitivity analysis, where input parameters and/or assumptions are varied slightly to assess the extent of change in modelled values (Robins *et al.*, 2003).

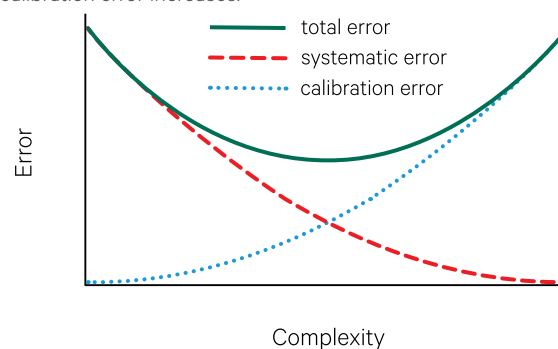
The most appropriate criteria for evaluating a model will depend on its purpose. For example, a common example of an applied plant productivity model based on EO datasets is a crop yield model, which typically correlates a relevant EO-based statistic (such as vegetation greenness—see Section 8.1.1) with a ground-based measure of crop productivity.

Such models, which are intended to reduce the risks inherent in food supply, need to be reliable, objective, timely, consistent, simple, and cost-effective (see Sections 10.2.2 and 12).

In this section, we will revisit the EO analysis framework, which underlies modelling of terrestrial vegetation (see Section 10.1), then introduce three commonly used scales of EO-based modelling for vegetated landscapes (see Section 10.2). EO datasets are also valuable for terrestrial ecosystem models to define model drivers, validate model results, and quantify uncertainty (Pasetto *et al.*, 2018).

Figure 10.1 Modelling error

As complexity increases, systematic error decreases and calibration error increases.



Source: Zhang *et al.* (2002) Figure 5

Background image: MODIS global composite showing Net Primary Productivity (NPP) for November 2016, with deeper shades of green indicating higher productivity to a maximum of 6.5 gC/m²/day. (Note: the vertical extent of this composite image has been clipped and the aspect ratio changed.)

Source: NASA Earth Observations. (Retrieved from https://neo.sci.gsfc.nasa.gov/view.php?datasetId=MOD17A2_M_PSN)

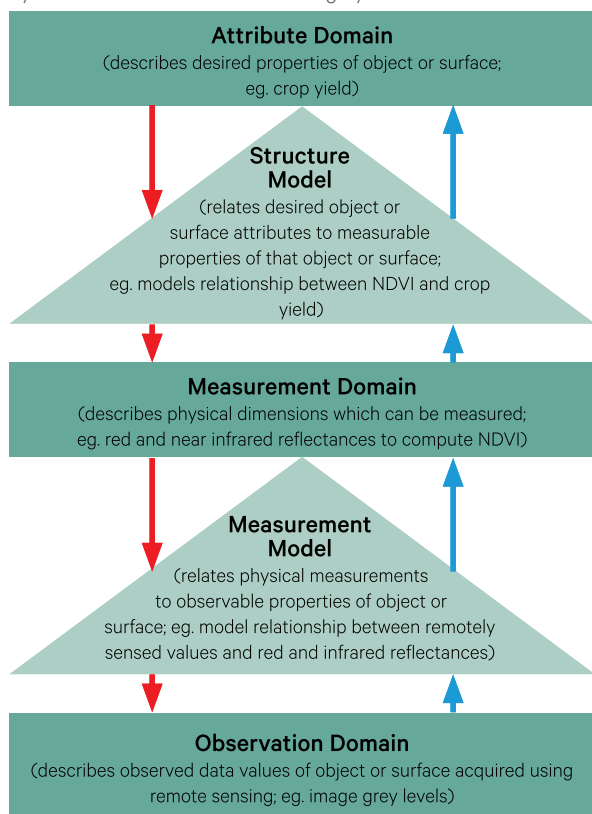
10.1 Modelling Considerations

Modelling allows future conditions to be predicted for a given scenario. It can also be used to predict the impact of potential changes in current conditions, such as resource characteristics, land uses, or management policies. Volume 2A—Section 2.3 introduces three generic modelling approaches that can be used in the context of EO:

- empirical or analytical models—simple relationships, such as regression analysis, between empirical measurements of surface attributes with EO measurements;
- semi-empirical or semi-analytical models—use prior knowledge, including assumptions and generalisations, to tailor an EO model to a specific situation; and
- physics-based models—rely on physical relationship between the surface attributes and the EO measurements. These models are generally more flexible, transferable and computationally intensive.

Figure 10.2 Measurement and analysis of image features

Interpreting imagery from EO sensors is an indirect process, whereby a measurement model is used to transform EO observations to measurements of some measurable property, and a structure model is used to relate those measurements to application-specific attributes. Forward modelling is indicated by red arrows and inverse modelling by blue arrows.



Adapted from: Harrison and Jupp (1989) Figure 33

Some fundamental concepts regarding modelling in the context of EO datasets are introduced in Volumes 2D and 2E. In Section 10.1.1 below we review those concepts that are particularly relevant to modelling of terrestrial vegetation then consider interpolation and extrapolation of data (see Section 10.1.2), appropriate scaling (see Section 10.1.3), and spatial patterns (see Section 10.1.4).

10.1.1 Underlying EO model

As detailed in Volume 1A—Section 1 and Volume 2D—Section 1.1, the relationship between a feature in an EO image and its quantifiable attributes of the Earth's surface is an indirect one. This relationship is illustrated in Figure 10.2 and implicitly involves two modelling stages:

- the measurement model—relates EO-based observations to empirical measurements. Examples of measurements models include image calibration processes that correct for radiometric and geometric distortions in the acquired EO dataset (see Volume 1B—Section 2, Volume 2A—Section 3, Volume 2B, and Volume 2D—Section 3). The measurement model also accounts for distortions in image values resulting from the interaction between the imaging process and the landscape and its component features (see Volume 1B—Section 3 and Volume 2D—Section 1); and
- the structure model—relates calibrated EO-based measurements to attributes of the Earth's surface (see Volumes 2C, 2D and 2E). This section describes approaches to developing structure models using EO datasets for terrestrial vegetation.

The downward and upward arrows in Figure 10.2 distinguish between forward (red) and inverse (blue) models (see Volume 2A—Section 2.3 and Volume 2D—Section 14.3). Forward models infer EO measurements from surface attributes. For example, a forward model for terrestrial vegetation may use measurements of specific plant attribute(s) to model its EO reflectance or emission value(s). Conversely, inverse models infer surface attributes from EO measurements. An example of an inverse model for terrestrial vegetation would be to use EO reflectance or emission value(s) to model specific plant attribute(s).

A model is a tool that helps us predict changes in a particular system before they happen. Models are used for all sorts of purposes: from trying to predict the weather, to trying to predict the stock market.
(Robins et al., 2003)

10.1.2 Interpolation and extrapolation

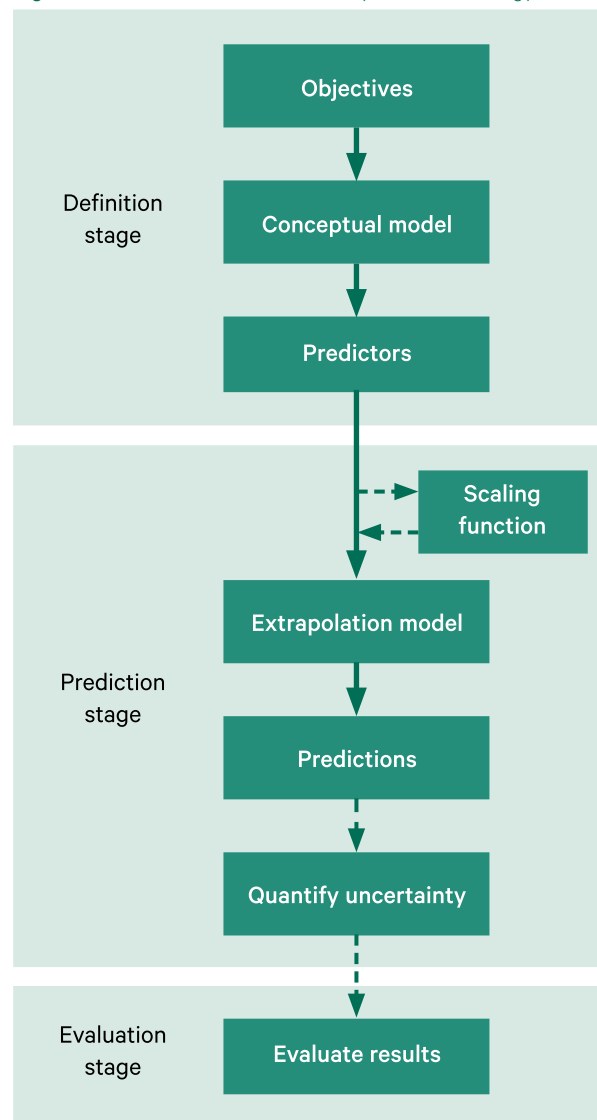
Interpolation estimates new, intermediate data points within a discrete set of known values, whereas extrapolation estimates new data points beyond the range of existing points. Methods for spatial and temporal interpolation of time series datasets were discussed in Volume 2D. Interpolation methods assume strong correlation between the known data points.

Extrapolation assumes some continuity, correspondence, or parallelism between the known and the unknown. Predictive models extrapolate known values in time by assuming that current trends will continue into the future. Spatial extrapolation may be valid where the relationship between a spatially limited dataset and a dataset covering a larger area is known, and this relationship can be used to infer likely values of the limited data into the larger area. In ecology, spatial extrapolation generally follows the framework outlined in Figure 10.3.

When working with sparse spatial datasets, modellers can either interpolate the data before modelling or apply the model to the sparse data then interpolate the modelled results. These approaches are often called 'interpolate then calculate' (IC) and 'calculate then interpolate' (CI) respectively. For very sparse spatial datasets, such as meteorological records, CI has been shown to be more robust (Stein *et al.*, 1991).

Spatially rich (or comprehensive) and temporally stable datasets, such as elevation, can also be used as a covariate when extrapolating sparse datasets. McVicar and Jupp (2002) used AVHRR imagery as a covariate for meteorological records to map moisture availability over the Murray-Darling Basin (MDB). Normalised Difference Temperature Index (NDTI) was derived from temperature data acquired at spatially insulated meteorological stations then extrapolated using covariates derived from AVHRR imagery and interpolated meteorological data (see Section 9.5). Using the EO imagery ensured 'stability' in the interpolated results and avoided direct interpolation, with its inherent problems, from sparse meteorological data (see Volume 2D—Section 13.3).

Figure 10.3 Basic framework for extrapolation in ecology



Adapted from: Miller *et al.* (2004) Figure 1

215

Many environmental variables influence the signals that reach a remote sensor. If we wish to use these remotely sensed signals to estimate environmental variables then we need to ensure that the number of remotely sensed signals is greater than the number of environmental signals that are causing those signals to vary.
(Curran, 2001)

10.1.3 Scaling

An understanding of scale is important for all landscape mapping, monitoring, and modelling activities. Mismatches in the scales of measurement, estimation and prediction for landscape features have long presented challenges to cartographers, geographers, and EO scientists (Gallant *et al.*, 2008) and are particularly relevant to image selection for EO analyses. To address such problems, multi-scale approaches have been proposed for many applications (see Volume 2D—Section 1.4; see Figure 3.1), and EO archives now offer a spatially and temporally extensive range of datasets for terrestrial vegetation studies (see Volume 2D—Section 2). Selection of the most appropriate EO imagery for a given application is considered in Volume 2D—Section 1.2 and the concept of ‘intrinsic scale’ is discussed in Volume 2D—Section 1.4. In some cases, it may be appropriate to increase the temporal frequency of time series datasets by using image blending methods (Emelyanova *et al.*, 2013; see Volume 2D—Excursus 6.2).

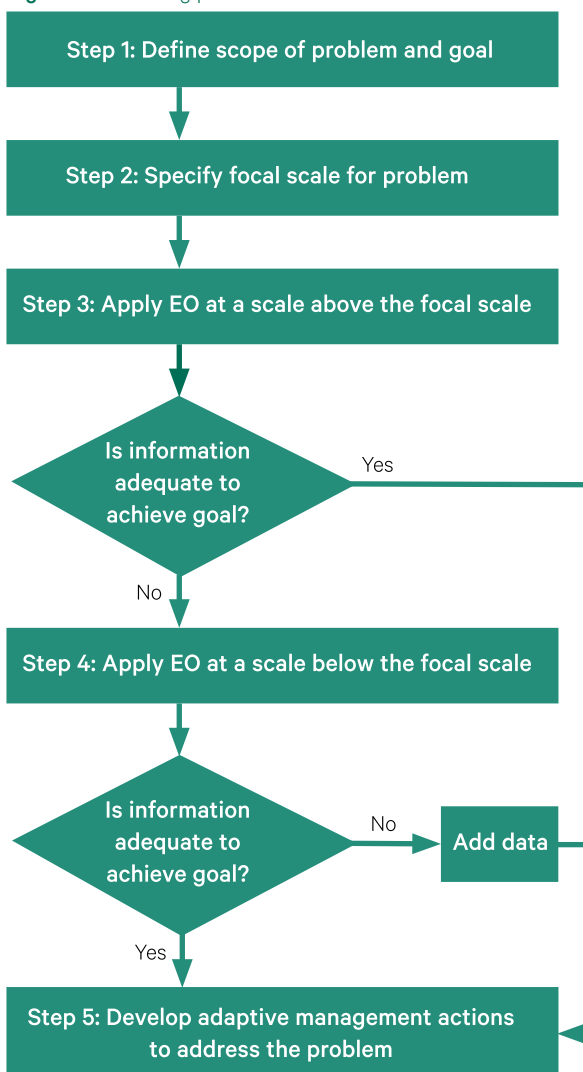
Upscaling and downscaling of EO datasets are described in Volume 2D—Section 4.3. As geographical terms:

- upscaling implies moving up the scale hierarchy, that is, to a larger extent with less detail; and
- downscaling implies moving down the scale hierarchy, that is, to a smaller extent with more detail.

Similarly, with appropriate prerequisites and constraints, terrestrial vegetation models can be developed for a particular spatial scale then upscaled to cover larger areas. For example, a model for the diffusion of CO₂ from the atmosphere to the interior of a single leaf has been aggregated to simulate CO₂ transfer at the scale of vegetated canopies, or even the entire globe (Williams *et al.*, 2004). Such scaling has enabled a range of EO-based models to be incorporated in regional and global vegetation studies (see Section 10.2.3).

Scaling up—extrapolating monitoring from small plots to larger, more representative landscapes—is a significant challenge. Ludwig *et al.* (2007) propose a five-step procedure that is based on scaling to determine when EO analyses require additional data sources to assess landscape health (see Figure 10.4). This procedure defines the focal scale as ‘the size of the area over which the core problem occurs’, then uses smaller and larger scales to check for cross-scale interactions in landscape patterns and processes.

Figure 10.4 Scaling procedure



Adapted from: Ludwig *et al.* (2007) Figure 1

Increasing the complexity of a model does not necessarily lead to a more accurate model and it is essential that model complexity matches the availability of data.
(Zhang *et al.*, 2002)

10.1.4 Spatial patterns

From a statistical viewpoint, any given landscape is merely one manifestation of numerous, equally probable, landscapes that may have occurred at a particular location. This perspective enables stochastic models to be developed, which generate potential variations for each actual landscape or ecosystem. For example, if a specific process operates in the landscape, particular patterns are more likely to occur (Fortin *et al.*, 2003). In Figure 10.5, three hypothetical landscapes are shown with varying spatial patterns, but the same number of patches and the same edge density. Differentiation between these landscape patterns obviously requires consideration of pattern alignment and scale.

The growing body of geographical data, principally from EO sources, provides the opportunity to examine, identify, and quantify spatial processes within actual landscapes. The increasing archives of time series datasets further enables such processes to be analysed over time (see Volume 2D). A number of statistical tools have been proposed to understand these processes, including multivariate statistics, ordination methods, spatial statistics, geostatistics, and landscape pattern indices (Fortin *et al.*, 2003). Spatial pattern analysis essentially attempts to quantify the composition and configuration of landscape components (Rempel and Csillag, 2003). Some specific EO methods to map and monitor landscape patterns are described in Sections 8 and 9.

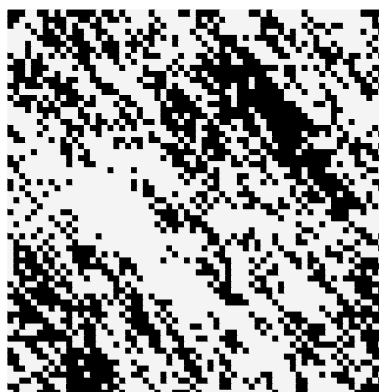
Figure 10.5 Hypothetical landscape patterns

These simulated landscapes of two components have the same number of patches, contagion, landscape shape index, edge density, and proportion of components, yet display different degrees of spatial autocorrelation.

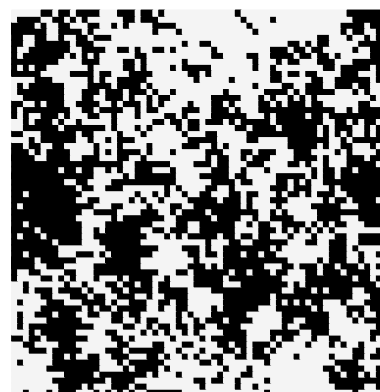
a. Random—purely random stochastic pattern



b. Noodles—elongated narrow patches



c. Bumpy—larger contiguous patches



Adapted from: Rempel and Csillag (2003) Figure 1

Landscapes are spatially heterogeneous areas characterised by a mosaic of patches that differ in size, shape, contents, and history. When spatial heterogeneity is considered, the explicit treatment of scale becomes necessary and hierarchies emerge.

Landscape ecology is the science of studying and improving the relationship between spatial pattern and ecological processes on a multitude of scales and organisational levels.

(Wu, 2013)

10.2 EO-based Models for Terrestrial Vegetation

A diverse range of modelling approaches have been proposed for EO datasets. Many models have been developed to determine plant productivity for various applications, including food crops and pasture (see Sections 11 to 15), forestry (see Sections 16), carbon sequestration (see Section 17), and fire management (see Section 18). Others have been developed to estimate crop water requirements (see Section 13), fuel moisture (see Section 18) and biodiversity risk (see Section 19). The following sub-sections introduce selected approaches that are particularly relevant to studies of terrestrial vegetation at three broad spatial scales:

- leaf models (see Section 10.2.1);
- plant productivity models (see Section 10.2.2); and
- global and regional models (see Section 10.2.3).

10.2.1 Leaf models

The structure, composition and functions of plant leaves are introduced in Section 4. Of particular relevance to EO is the interaction between leaves and the ambient EMR (see Section 4.3). The optical properties of leaves are directly related to their biochemical composition (primarily pigments), enabling EO datasets to be used to estimate leaf pigment concentrations for both individual leaves and canopies using either:

- statistical models based on spectral indices, regression relationships, or machine learning (see Section 8); or
- radiative transfer models (see Volume 1B—Section 5) for:
 - ♦ leaves, which simulate spectral reflectance and transmittance based on leaf biochemistry, such as the popular PROSPECT model (Jacquemoud and Baret, 1990); and
 - ♦ canopies, which (for known optical properties of leaf and soil, vegetation architecture, and acquisition conditions) simulate spectral and bidirectional reflectance (Féret *et al.*, 2017), such as SAIL (Scattering by Arbitrary Inclined Leaves; Verhoef, 1984, 1985; derived from the one-dimensional model by Suits, 1972).

A number of physical and mathematical models have been developed to simulate the spectral consequences of variations in leaf biochemical and physical composition. Some of these are detailed in OPTICLEAF (2020) and reviewed by Ustin *et al.* (2004) and Jacquemoud and Ustin (2019). Jacquemoud and Ustin (2014) describe computer simulations models for leaves in terms of six categories (ordered by increasing complexity) as summarised in Table 10.1. Only the radiative transfer models may be iteratively inverted to derive leaf anatomical or biochemical components from spectral data (Jacquemoud and Ustin, 2001). For example, the contribution of chlorophyll, water, dry matter, and structure to leaf spectral properties was simulated by Ceccato *et al.* (2001) and Bacour *et al.* (2002) using the PROSPECT model.

As well as furthering our understanding of leaf optical properties, leaf models have been integrated with canopy models. For example, PROSAIL combines the PROSPECT leaf model with the canopy model SAIL (Baret *et al.*, 1992; Jacquemoud *et al.*, 2009). PROSPECT requires input parameters for leaf structure and biochemical content to simulate directional-hemispherical reflectance and transmittance for the wavelength range 400–2500 nm whereas SAIL models canopy architecture from bidirectional reflectance measurements. This integrated modelling approach allowed the precise relationship between the reflectance from a canopy and its biophysical and biochemical properties to be examined and quantified for specific wavelength ranges. These models are used operationally in precision agriculture to monitor crop growth, allowing fertiliser application to be restricted to areas of lowered productivity (see Section 12.6). In natural vegetation canopies, such models enable mapping of ecosystem functionality, vegetation health, and fuel moisture (Jacquemoud *et al.*, 2009). For example, Punalekar *et al.* (2018) used proximal hyperspectral data from Sentinel-2A 10 m imagery with the radiative transfer model PROSAIL to estimate LAI and biomass for dairy farms in southern England, and reported that this approach outperformed NDVI-based estimates.

Ecosystem models that elegantly represent salient ecological processes deliver the capacity to monitor and predict change, estimate risks of ecosystem collapse and explore alternative future management scenarios. Such models can be parameterised, initiated, or validated with remote sensing data. ... Remote sensing data therefore has great potential for parameterizing a wide variety of ecosystem models, and is increasingly being used to assess the skill of models at reproducing ecosystem dynamics.

(Murray *et al.*, 2018)

Table 10.1 Leaf models

Model	Models	Example
Plate Model (Allen <i>et al.</i> , 1969)	Cumulative hemispherical reflectance/refraction from internal and external surfaces of leaf blades modelled as stacks of absorbing plates	PROSPECT (Jacquemoud and Baret, 1990; Baret and Fourty, 1997; Féret <i>et al.</i> , 2008, 2017)
Compact Spherical Particle Model	Radiative transfer model to simulate optical properties of conifer needles based on interaction of light with powders (Melamed, 1963)	LIBERTY (Leaf Incorporating Biochemistry Exhibiting Reflectance and Transmittance Yields; Dawson <i>et al.</i> , 1998)
N-flux Models	Leaf as slabs of absorbing and diffusing material	Two-flux model (Kubelka and Munk, 1931; Allen and Richardson, 1968; Vargas, 1999; Cordon and Lagorio, 2007);
		Four-flux model (Fukshansky <i>et al.</i> , 1991; Martinez von Remisowsky <i>et al.</i> , 1992; Richter and Fukshansky, 1996)
Radiative Transfer Equation	Optical Scattering Model based on leaf as turbid homogeneous plate	LEAFMOD (Leaf Experimental Absorptivity Feasibility MODEL; Ganapol <i>et al.</i> , 1998)
Stochastic Approach	Radiative transfer simulation based on optical properties on leaf tissues simulated by Markov chain	LFMOD1 (Tucker and Garatt, 1977)
		SLOP (Stochastic model for Leaf Optical Properties; Maier <i>et al.</i> , 1999)
Ray Tracing Models	Complex Internal Leaf Structure model based on internal leaf structure and optical constants of constituents	RAYTRAN (Govaerts and Verstraete, 1998)

Adapted from categories in Jacquemoud and Ustin (2014)

10.2.2 Plant productivity models

Plant productivity indicates the rate at which plants store energy—and accumulate biomass—via photosynthesis (see Section 7.4). While a wide range of environmental factors can impact the productivity of terrestrial vegetation (see Sections 1.1 and 4 to 7), the major factors influencing plant growth can be grouped in terms of:

- defining factors—determine the potential growth under ideal conditions, but include factors that we cannot directly control such as CO₂, radiation, temperature, and crop characteristics (physiology, phenology, and canopy architecture);
- limiting factors—indicate the attainable growth under controlled conditions. These factors can be controlled to increase production, such as water and nutrients; and
- reducing factors—impact actual growth under real conditions, such that production is reduced if these factors (such as weeds, diseases, pests, and pollutants) are not controlled (Bouman *et al.*, 1996).

Plant productivity models have traditionally attempted to differentiate between these factors on the basis of their impact on plant production and the extent to which they can be ‘controlled’. A commonly encountered model to track changes in particular types of terrestrial vegetation is a crop simulation model (CSM). A CSM uses information about physics, plant physiology, and ecology to mimic crop growth and development using a range of parameters (such as weather, soil conditions, and management practices) in order to forecast various crop productivity metrics (such as yield, date of

maturity for harvest, and fertiliser efficiency). More sophisticated models, tailored to specific crops, can advise on fertiliser and irrigation requirements during crop growth and assess the expected impact of different scenarios on crop yield, such as changes in sowing dates, crop varieties or weather conditions. These models typically rely on historical records and ground measurements but can only practically be tested at a limited number of ground sites. All such modelling predictions are made under the assumption that the crop will not be impacted by unforeseen factors, such as severe frosts or extreme weather events, before harvest.

A well-established CSM that was developed in Australia is the Agricultural Production Systems sIMulator (APSIM) modelling framework (APSIM, 2020; Keating *et al.*, 2003). APSIM comprises plant, soil, animal, and climate models that simulate relevant processes and, where appropriate, their responses to various interactions and external stresses (Holzworth *et al.*, 2014, 2018). EO-based modelling of crop growth is often integrated with CSM to spatially and temporally extrapolate the results from field test sites, thus constraining crop forecasts by current growing conditions (FAO, 2016; see Section 11.2). For example, APSIM is used by agricultural monitoring systems, such as Yield Prophet, a decision support tool which models the growth of major grain crops (BCG, 2017), and Graincast™ (see Excursus 12.1). Another operational cropping system model is WOFOST (World Food Studies; de Wit *et al.*, 2019; see Section 11.6), which is implemented in the European MARS crop yield forecasting system.

Specific EO-based models to estimate plant productivity have been developed for Australian cereal and horticultural crops (see Section 11), including sugar cane (see Volume 1B—Excursus 1.1), peanuts (see Volume 1B—Excursus 9.1), and tree crops (see Section 12.7), as well as pasture growth (see Section 13), forest biomass (see Section 16), and carbon dynamics (see Section 17). For example, the AussieGRASS model combines EO-based water balance and plant growth models to forecast pasture growth (see Excursus 10.1). This type of model is used by governments and industries to manage climatic influences, such as drought, on grazing lands (Nikolova *et al.*, 2013).

From modest beginnings in the mid-1900s, agricultural systems models have greatly benefitted from the confluence of growing environmental awareness, increased global multidisciplinary cooperation, and significant improvements in data acquisition and processing technologies (Jones *et al.*, 2017). Advanced models now relate biophysical and meteorological processes to economic and ecological outcomes, and dynamically estimate the impacts of various land management scenarios on agricultural resources from local to global scales (FAO, 2017; see Section 11).

10.2.3 Global and regional models

A wide variety of models relying on EO datasets have been developed to monitor terrestrial vegetation at regional and global scales. Large scale monitoring of our planet is closely related to the concept of Earth being an essentially closed system, which comprises four integrated spheres (atmosphere, hydrosphere, geosphere, and biosphere; see Excursus 1.2 and Volume 1A—Section 4.1). These spheres exchange energy and matter via four fundamental cycles (energy, water, earth, and carbon; see Volume 1A—Section 4.2). This global view enables a multidisciplinary approach to understanding Earth systems and their processes in a range of spatial and temporal scales. A sufficient network of *in situ* sensors to monitor these systems and processes is impractical in terms of both cost and time, leaving EO datasets as the only feasible, relevant, and cost-effective source for this information. Examples of global models include Terrestrial Ecosystem Models (TEM) and General Circulation Models (GCM).

TEM primarily track vegetation productivity in terms of Net Primary Productivity (NPP; see Section 7.4). Specific examples of these models, in the context of carbon dynamics, are given in Section 17. Major categories of TEM are:

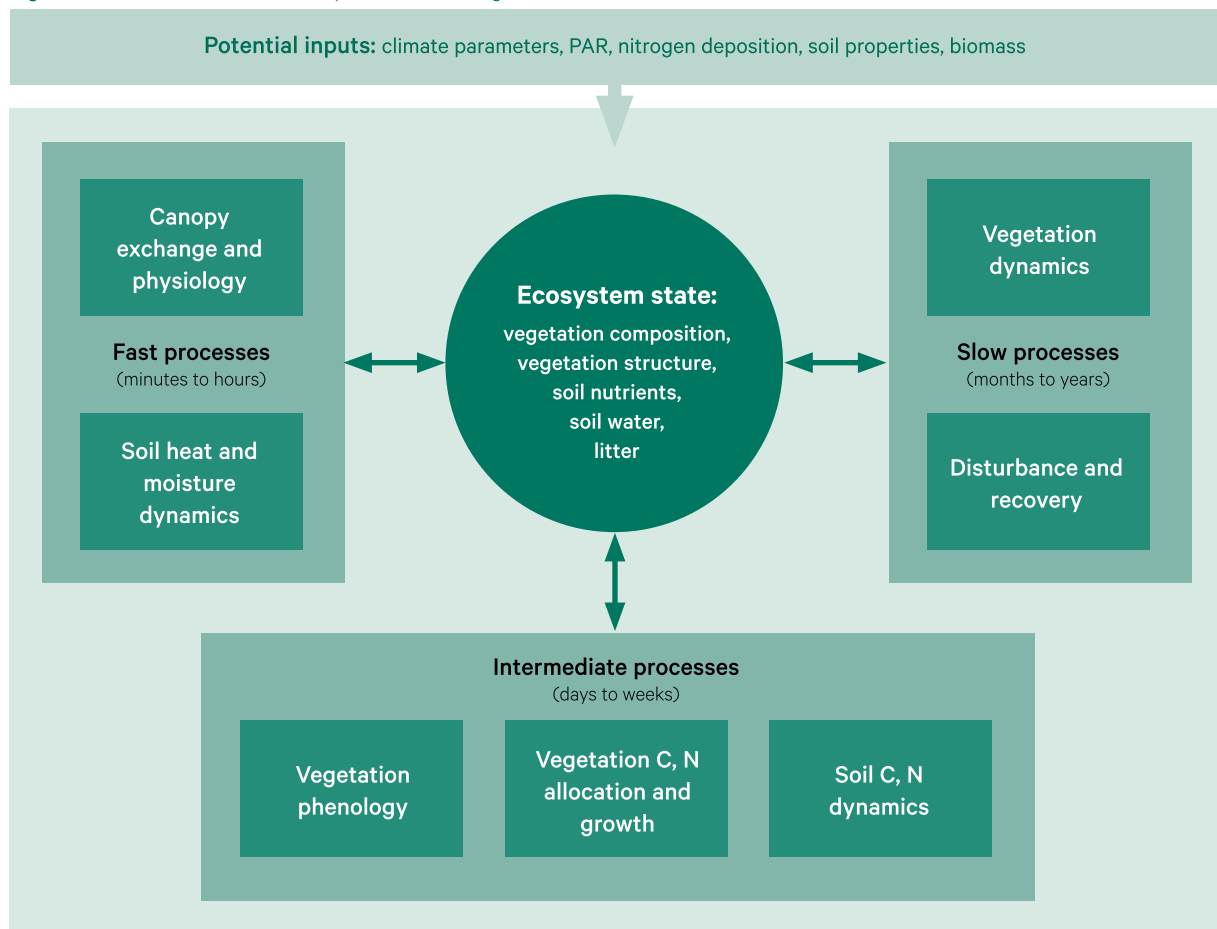
- Dynamic Global Vegetation Models (DGVM)—process-based models of global biogeochemical fluxes and vegetation dynamics to better understand terrestrial biosphere processes and their interactions with other Earth spheres (Prentice *et al.*, 2007; Sitch *et al.*, 2008; Boit *et al.*, 2019); and
- Production Efficiency Models (PEM)—describe the productivity of vegetation by assuming a linear relationship between canopy photosynthesis and the fraction of absorbed photosynthetically active radiation (fAPAR) to monitor NPP (Monteith, 1972, 1977).

GCM simulate the global climate system by representing physical circulation patterns and processes in and between the atmosphere, ocean, cryosphere, and the land surface. Relevant components of GCM include:

- energy balance models—link climate and biophysical models to describe energy and mass transfers between the Earth's surface and the atmosphere (see Section 7.5). Examples of Land Surface Models (LSM) include soil-vegetation-atmosphere transfer (SVAT) models and surface energy balance (SEB) models; and
- water balance models—describe the movement of water through the water cycle (see Section 7.6). An Australian implementation of EO-based water balance modelling to support regulatory monitoring of water resources is summarised in Excursus 10.2.

These large scale models have a multidisciplinary focus. Their development has only been possible in recent decades with the advent of high speed computing and sophisticated algorithms to manage large datasets. DGVM, for example, integrate research from plant geography, biophysics, vegetation dynamics, plant physiology and biogeochemistry, and anthropogenic activities, to simulate the interactions between ecosystem state variables, ecosystem processes, and driving variables (Prentice *et al.*, 2007; see Figure 10.6).

Figure 10.6 Modular structure of Dynamic Global Vegetation Models



Adapted from: Prentice *et al.* (2007) Figure 15.2

Dynamic Global Vegetation Models (DGVMs) offer the possibility of integrating large amounts of geospatial data to quantify and project a large range of ecological variables important for ecosystem service provisioning under future scenarios.

*(Boit *et al.*, 2019)*

Excursus 10.1—AussieGRASS

Source: John Carter, Queensland Department of Environment and Science; <https://www.longpaddock.qld.gov.au/aussiegrass/>

Further information: McKeon and Carter (2015); DSITI (2015)

The AussieGRASS model monitors key biophysical processes associated with pasture growth (such as degradation and recovery) at regional scales (for example, local government areas, or bioregions). Its companion system, FORAGE, extends the implementation to property and paddock scale (Zhang and Carter, 2018; see Section 15.4). AussieGRASS provides time series of rainfall and pasture growth information, as well as projections for the season ahead. The projections are useful for forage budgeting, assessing the impacts of drought, and forecasting bushfire risk.

AussieGRASS is an advanced spatial water balance and plant growth model, producing output on a daily timestep across Australia (Carter *et al.*, 2000). The model was initially built on the point scale GRASP (GRASS Production) simulation model (Rickert *et al.*, 2000), using the SILO climate data base (Jeffrey *et al.*, 2001), and calibrated using satellite data, plus over 600,000 field pasture biomass observations (Hassett *et al.*, 2000). The AussieGRASS system has been operational on an Australia-wide basis since 1996.

Within the AussieGRASS framework, GRASP is run on a daily timestep (1890–current). The observed climate data are spatially interpolated to construct gridded datasets on a regular $0.05^\circ \times 0.05^\circ$ grid (approximately 5×5 km) across Australia. The spatial framework includes inputs of key climate variables (rainfall, evaporation, temperature, vapour pressure, and solar radiation), soil and pasture types, tree and shrub cover, domestic livestock, and other herbivore numbers. In simulating continental pasture response to climate variability, calibration has relied on EO-based datasets to estimate green vegetation cover, coupled with extensive ground truthing across Australia since 1994 (Hassett *et al.* 2000).

Various forms of validation have been conducted with independent datasets (Carter *et al.*, 2003) and inter-model comparisons (McKeon and Carter, 2015). EO-based input datasets include fire scars, tree density, flooded area, and land use maps. Fractional photosynthetic and non-photosynthetic cover (Scarath *et al.*, 2010) from the entire Australian Landsat TM archive is used as a primary EO calibration dataset (see Excursus 8.3). This is supplemented with data from radar and gravity satellites for soil moisture, plus EO of chlorophyll fluorescence and atmospheric CO_2 .

Many challenges exist with modelling the EO signals due to issues like time and space scaling. These include sensed versus modelled depth of soil water, variations in mass to cover relationships with vegetation structure, obscured cover, and using a single observation at one time in the day versus a modelled daily integral.

AussieGRASS provides a platform for translating seasonal climate outlooks into estimates of future plant growth, including the impacts of total grazing pressure from domestic stock and other herbivores. It is a powerful tool for value-adding to climate information, as it takes into account current condition (e.g. soil moisture, ground cover, nitrogen status, and grass basal cover) to provide a probabilistic view of plant growth for the coming three-month period. AussieGRASS outputs are also being increasingly used for various environmental analyses, such as drought analysis, estimating plant net primary production for soil carbon mapping, providing soil moisture as an initial condition for air pollution models, analysing how stock numbers influence the potential amount of biomass which can be burnt, analysing conditions suitable for dust storms, and estimating the impact of removing tree cover on deep soil water infiltration.

Excursus 10.2—Water Resources Assessment

Further Information: BoM (2008, 2013); Frost *et al.* (2018)

Water is a very precious resource in Australia (see Volume 3B). Current and accurate information about the distribution, storage, availability, and use of water is necessary to manage this resource, especially at regional and continental scales. The Water Act 2007 assigned responsibility to the Bureau of Meteorology (BoM) for regular reporting on the status and usage of Australia's water resources (BoM, 2008). These statutory functions include:

- issuing national water information standards;
- collecting and publishing water information;
- conducting regular national water resources assessments;
- publishing an annual National Water Account;
- providing regular water availability forecasts;
- advising on matters relating to water information; and
- enhancing understanding of Australia's water resources.

These assessments help water resource managers and policy makers understand past and present practices governing water management. In line with the National Water Initiative (NWI), which outlines “a shared commitment by governments to increase the efficiency of Australia's water use, leading to greater certainty for investment and productivity, for rural and urban communities and for the environment” (DAWR, 2018), they also help to formulate future policies and practices. The Australian Water Resource Assessment Modelling System (AWRAMS) has been developed to generate two major information products for this purpose (see Section 10.3):

- the annual National Water Account (NWA: www.bom.gov.au/water/nwa)—water accounting for nationally significant urban and rural regions, including information on water stores and flows, water rights, and water use (BoM, 2013; see Section 20.5); and
- Australian Water Resources Assessment (AWRA) reports—daily, monthly and annual estimates of water balance parameters (Hafeez *et al.*, 2015).

The AWRA system is a spatial water resources monitoring system to capture and model the major water flow processes at regional and national scales. It comprises two integrated modules which collectively represent the Australian terrestrial water cycle:

- AWRA-L—models hydrological processes between the atmosphere and the landscape, including groundwater (Van Dijk, 2010; Viney *et al.*, 2015; Frost *et al.*, 2018); and
- AWRA-R—a conceptual hydrological model that simulates processes between the atmosphere and rivers (Dutta *et al.*, 2015).

This operational system includes major water storages and the fluxes in and between component models based on a 0.05° grid. AWRA-L simulates the daily flow of water through each grid cell in the landscape, with the hydrological response of deep-rooted and shallow-rooted vegetation being modelled separately (Frost *et al.*, 2018). Inputs to AWRA-L include *in situ* datasets routinely collected by BoM, estimates from the OzFlux network (see Excursus 7.2), and parameters derived from EO time series imagery (Frost and Wright, 2018—see Figure 2 therein). Ongoing, daily AWRA-L gridded outputs include soil moisture, evapotranspiration, surface runoff, and groundwater recharge/storage/lateral flow. These parameters have also been modelled retrospectively, providing a simulation of the Australian terrestrial water cycle for over a century (Hafeez *et al.*, 2015). AWRAMS has been released for public access, including a community modelling system (AWRA CMS; see Section 10.3).

10.3 Further Information

Modelling Leaf Optical Properties

http://www.photobiology.info/Jacq_Ustin.html

Terrestrial Observation and Prediction System (TOPS)

<https://ecocast.arc.nasa.gov/>

Water Resource Modelling

Bureau of Meteorology: <http://www.bom.gov.au/water/index.shtml>

Australian Landscape Water Balance: <http://www.bom.gov.au/water/landscape/#/sm/Actual/day/-28.4/130.4/3/Point////2020/8/24/>

AWRA Community Modelling System (AWRA CMS): https://github.com/awracms/awra_cms

National Water Account (NWA): www.bom.gov.au/water/nwa

10.4 References

- Allen, W.A., and Richardson, A.J. (1968). Interaction of light with a plant canopy. *Journal of the Optical Society of America*, 58(8), 1023–1028.
- APSIM (2020). *Agricultural Production Systems sIMulator* website: <https://www.apsim.info/apsim-model/>
- Bacour, C., Jacquemoud, S., Tourbier, Y., Dechambre, M., and Frangi, J.P. (2002). Design and analysis of numerical experiments to compare four canopy reflectance models. *Remote Sensing of Environment*, 79, 72–83.
- Baret, F., Jacquemoud, S., Guyot, G., and Leprieur, C. (1992). Modeled analysis of the biophysical nature of spectral shifts and comparison with information content of broad bands. *Remote Sensing of Environment*, 41, 133–142.
- Baret, F., and Fourty, T. (1997). Estimation of leaf water content and specific leaf weight from reflectance and transmittance measurements. *Agronomie*, 17(9–10), 455–464.
- BCG (2017). *Yield Prophet* website, Birchip Cropping Group: <https://www.yieldprophet.com.au/yp/Home.aspx>
- Boit, A., Sakschewski, B., Boysen, L., Cano-Crespo, A., Clement, J., Alaniz, N.G., Kok, K., Kolb, M., Langerwisch, F., Rammig, A., Sachse, R., van Eupen, M., von Bloh, W., Zemp, D.C., and Thonicke, K. (2019). Using Dynamic Global Vegetation Models (DGVMs) for Projecting Ecosystem Services at Regional Scales. In *Atlas of Ecosystem Services* (Eds: Schröter M., Bonn A., Klotz S., Seppelt R., Baessler C.). Springer, Cham. https://doi.org/10.1007/978-3-319-96229-0_10
- BoM (2008). *The Water Act 2007 and the Bureau of Meteorology*. Bureau of Meteorology, April 2008. http://www.bom.gov.au/water/regulations/document/water_act_2007.pdf
- BoM (2013). *The National Water Account. Companion Guide*. Bureau of Meteorology, Melbourne. <http://www.bom.gov.au/water/nwa/document/companion-guide.pdf>
- Bouman, B.A.M., van Keulen, H., van Laar, H.H., and Rabbinge, R. (1996). The ‘School of de Wit’ crop growth simulation models: A pedigree and historical overview. *Agricultural Systems*, 52(2–3), 171–198. [https://doi.org/10.1016/0308-521X\(96\)00011-X](https://doi.org/10.1016/0308-521X(96)00011-X)
- Carter, J.O., Hall, W.B., Brook, K.D., McKeon, G.M., Day, K.A., and Paull, C.J. (2000). AussieGRASS: Australian Grassland and Rangeland Assessment by Spatial Simulation. In *Applications of seasonal climate forecasting in agricultural and natural ecosystems—the Australian experience*. (Eds. G. Hammer, N. Nicholls and C. Mitchell), Kluwer Academic Press, Netherlands. pp 229–249.
- Carter, J.O., Bruget, D., Hassett, R., Henry, B., Ahrens, D., Brook, K., Day, K., Flood, N., Hall, W., McKeon, G., and Paull, C. (2003). Australian Grassland and Rangeland Assessment by Spatial Simulation (AussieGRASS) In *Science for Drought, Proceedings of the National Drought Forum 2003*. (Eds: Stone, R., and Partridge, I.). Department of Primary Industries, Queensland. pp 152–159.
- Ceccato, P., Flasse, S., Tarantla, S., Jacquemoud, S., and Grégoire, J.-M. (2001). Detecting vegetation leaf water content using reflectance in the optical domain. *Remote Sensing of Environment*, 77, 22–33.
- Cordon, G.B., and Lagorio, M.G. (2007). Absorption and scattering coefficients: A biophysical-chemistry experiment using reflectance spectroscopy. *Journal of Chemical Education*, 84(7), 1167–1170.
- Curran, P.J. (2001). Imaging spectrometry for ecological applications. *International Journal of Applied Earth Observation and Geoinformation*, 3(4), 305–312. doi:10.1016/S0303-2434(01)85037-6

- DAWR (2018). Department of Agriculture and Water Resources website. *National Water Initiative* webpage: <http://www.agriculture.gov.au/water/policy/nwi>
- Dawson, T.P., Curran, P.J., and Plummer, S.E. (1998). LIBERTY—Modeling the Effects of Leaf Biochemical Concentration on Reflectance Spectra. *Remote Sensing of Environment*, 65, 50–60.
- De Wit, A., Boogaard, H., Fumagalli, D., Janssen, S., Knapen, R., van Kraalingen, D., Supit, I., van der Wijngaart, van Diepen, K. (2019). 25 years of the WOFOST cropping systems model. *Agricultural Systems*, 168, 154–167. <https://doi.org/10.1016/j.agsy.2018.06.018>
- DSITI (2015). *AussieGRASS Environmental Calculator—Product Descriptions v1.5*. Department of Science, Information Technology and Innovation, Queensland. https://data.longpaddock.qld.gov.au/static/about/publications/pdf/agrass_product_descriptions.pdf
- Dutta, D., Kim, S., Hughes, J., Vaze, J., and Yang, A. (2015). *AWRA-R version 5.0 Technical Report*. CSIRO Land and Water, Canberra. <https://publications.csiro.au/rprt/download?pid=csiro:EP154523&dsid=DS2>
- Emelyanova I.V., McVicar, T.R., Van Niel, T.G., Li, L.T., and van Dijk, A.I.J.M. (2013). Assessing the accuracy of blending Landsat-MODIS surface reflectances in two landscapes with contrasting spatial and temporal dynamics: A framework for algorithm selection. *Remote Sensing of Environment*, 133, 193–209.
- FAO (2016). *Crop Yield Forecasting: Methodological and Institutional Aspects*. UN Food and Agricultural Organisation, Rome. http://www.amis-outlook.org/fileadmin/user_upload/amis/docs/resources/AMIS_CYF-Methodological-and-Institutional-Aspects_web.pdf
- FAO (2017). *Review of the Available Remote Sensing Tools, Products, Methodologies and Data to Improve Crop Production Forecasts*. UN Food and Agriculture Organization, Rome. ISBN 978-92-5-109840-0.
- Féret, J.B., François, C., Asner, G.P., Gitelson, A.A., Martin, R.E., Bidet, L.P.R., Ustin, S.L., le Maire, G., and Jacquemoud, S. (2008). PROSPECT-4 and 5: Advances in the leaf optical properties model separating photosynthetic pigments. *Remote Sensing of Environment*, 112(6), 3030–3043.
- Féret, J.B., Gitelson, A.A., Noble, S.D., and Jacquemoud, S. (2017). *Remote Sensing of Environment*, 193, 204–215. doi:10.1016/j.rse.2017.03.004
- Fortin, M.-J., Boots, B., Csillag, F., and Rimmel, T.K. (2003). On the Role of Spatial Indices in Understanding Landscape Indices in Ecology. *Oikos*, 102(1), 203–212.
- Frost, A.J., and Wright, D.P. (2018). *Evaluation of the Australian Landscape Water Balance model: AWRA-L v6*. Bureau of Meteorology. http://www.bom.gov.au/water/landscape/assets/static/publications/AWRALv6_Model_Evaluation_Report.pdf
- Frost, A.J., Ramchurn, A., and Smith, A. (2018). *The Bureau's Operational AWRA Landscape (AWRA-L v6) Model: Technical description of the Australian Water Resources Assessment Landscape model version 6*. Bureau of Meteorology. http://www.bom.gov.au/water/landscape/assets/static/publications/AWRALv6_Model_Description_Report.pdf
- Fukshansky, L., Fukshansky-Kazarinova, N., and Martinez v. Remisowsky, A. (1991). Estimation of optical parameters in a living tissue by solving the inverse problem of the multiflux radiative transfer. *Applied Optics*, 30(22), 3145–3153.
- Gallant, J.C., McKenzie, N.J., and McBratney, A.B. (2008). Scale. Ch 3 in *Guidelines for Surveying Soil and Land Resources*. Australian Soil and Land Survey Handbook Series. (Eds: McKenzie, N.J., Grundy, M.J., Webster, R., and Ringrose-Voase, A.J.) CSIRO Publishing, Melbourne.
- Ganapol, B.D., Johnson, L.F., Hammer, P.D., Hlavka, C.A., and Peterson D.L. (1998). LEAFMOD: a new within-leaf radiative transfer model. *Remote Sensing of Environment*, 63(2), 182–193.
- Govaerts, Y., and Verstraete, M.M. (1998). Raytran: a Monte Carlo ray-tracing model to compute light scattering in three-dimensional heterogeneous media. *IEEE Transactions on Geoscience and Remote Sensing*, 36(2), 493–505.
- Hafeez, F., Frost, A., Vaze, J., Dutta, D., Smith, A., and Elmahdi, A. (2015). A new integrated continental hydrological simulation system. *Water: Journal of the Australian Water Association*, 42(3), 75–82.
- Harrison, B.A., and Jupp, D.L.B. (1989) *Introduction to Remotely Sensed Data: Part ONE of the microBRIAN Resource Manual*. CSIRO, Melbourne. 156 p.
- Hassett, R.C., Wood, H.L., Carter, J.O., and Danaher, T.J. (2000). A field method for statewide ground-truthing of a spatial pasture growth model. *Australian Journal of Experimental Agriculture*, 40, 1069–1079.

- Holzworth, D.P., Huth, N.I., deVoil, P.G., Zurcher, E.J., Herrmann, N.I., McLean, G., Chenu, K., van Oosterom, E.J., Snow, V., Murphy, C., Moore, A.D., Brown, H., Whish, J.P.M., Verrall, S., Fainges, J., Bell, L.W., Peake, A.S., Poulton, P.L., Hochman, Z., Thorburn, P.J., Gaydon, D.S., Dalgliesh, N.P., Rodriguez, D., Cox, H., Chapman, S., Doherty, A., Teixeira, E., Sharp, J., Cichota, R., Vogeler, I., Li, F.Y., Wang, E., Hammer, G.L., Robertson, M.J., Dimes, J.P., Whitbread, A.M., Hunt, J., van Rees, H., McClelland, T., Carberry, P.S., Hargreaves, J.N.G., MacLeod, N., McDonald, C., Harsdorf, J., Wedgwood, S., Keating, B.A. (2014). APSIM—evolution towards a new generation of agricultural systems simulation. *Environmental Modelling and Software*, 62, 327–350. <https://doi.org/10.1016/j.envsoft.2014.07.009>
- Holzworth, D., Huth, N.I., Fainges, J., Brown, H., Zurcher, E., Cichota, R., Verrall, S., Herrmann, N.I., Zheng, B., and Snow, V. (2018). APSIM Next Generation: Overcoming Challenges in Modernising a Farming Systems Model. *Environmental Modelling and Software*, 103, 43–51. <https://doi.org/10.1016/j.envsoft.2018.02.002>
- Jacquemoud, S., and Baret, F. (1990). PROSPECT: A Model of Leaf Optical Properties Spectra. *Remote Sensing of Environment*, 34, 75–91.
- Jacquemoud, S., and Ustin, S.L. (2001). Leaf Optical Properties: A State of the Art. *Proceedings of 8th International Symposium Physical Measurements and Signatures in Remote Sensing*. pp 223–232. Aussois (France), 8-12 January, 2001. CNES.
- Jacquemoud, S., Verhoef, W., Baret, F., Bacour, C., Zarco-Tejada, P.J., Asner, G.P., Francois, C., and Ustin, S.L. (2009). PROSPECT + SAIL Models: a review of use for vegetation characterization. *Remote Sensing of Environment*, 113, S56–S66.
- Jacquemoud, S., and Ustin, S.L. (2014). Modeling Leaf Optical Properties. In *Photobiological Sciences Online* (Ed: S.C. Smith). American Society of Photobiology. <http://www.photobiology.info/>
- Jacquemoud, S., and Ustin, S. (2019). *Leaf Optical Properties*. Cambridge University Press, Cambridge. doi:10.1017/9781108686457
- Jeffrey, S.J., Carter, J.O., Moodie, K.B., and Beswick, A.R. (2001). Using spatial interpolation to construct a comprehensive archive of Australian climate data. *Environmental Modelling and Software*, 16/4, 309–330.
- Jones, J.W., Antle, J.M., Basso, B., Boote, K.J., Conant, R.T., Foster, I., Godfray, H.C.J., Herrero, M., Howitt, R.E., Janssen, S., Keating, B.A., Munoz-Carpena, R., Porter, C.H., Rosenzweig, C., and Wheeler, T.R. (2017). Brief history of agricultural systems modeling. *Agricultural Systems*, 155, 240–254. <https://doi.org/10.1016/j.agsy.2016.05.014>
- Keating, B.A., Carberry, P.S., Hammer, G.L., Probert, M.E., Robertson, M.J., Holzworth, D., Huth, N.I., Hargreaves, J.N., Meinke, H., and Hochman, Z. (2003). An overview of APSIM, a model designed for farming systems simulation. *European Journal of Agronomy*, 18(3–4), 267–288.
- Kubelka, P., and Munk, F. (1931). Ein beitrag zur optik der farbanstriche. *Zeitschrift fur Technische Physik*, 12, 593–601.
- Ludwig, J.A., Bastin, G.N., Wallace, J.F., and McVicar, T.R. (2007). Assessing landscape health by scaling with remote sensing: when is it not enough? *Landscape Ecology*, 22, 163–169. doi:10.1007/s10980-006-9038-6
- Maier, S.W., Lüdeker, W., and Günther, K.P. (1999). SLOP: a revised version of the stochastic model for leaf optical properties. *Remote Sensing of Environment*, 68(3), 273–280.
- Martinez von Remisowsky, A., McClendon, J.H., and Fukshansky, L. (1992). Estimation of the optical parameters and light gradients in leaves: multi-flux versus two-flux treatment. *Photochemistry and Photobiology*, 55(6), 857–865.
- McKeon, G., and Carter, J. (2015). AussieGRASS: An Operational National Pasture Model. Ch 1 in *AussieGRASS Environmental Calculator—Product Descriptions v1.5*. Department of Science, Information Technology and Innovation, Queensland.
- McVicar, T.R., and Jupp, D.L.B. (2002). Using covariates to spatially interpolate moisture availability in the Murray-Darling Basin: a novel use of remotely sensed data. *Remote Sensing of Environment*, 79, 199–212.
- Melamed, N.T. (1963). Optical properties of powders: Part I. Optical absorption coefficients and the absolute value of the diffuse reflectance. *Journal of Applied Physics*, 34, 560–570. <https://doi.org/10.1063/1.1729309>
- Miller, J.R., Turner, M.G., Smithwick, E.A.H., Dent, C.L., and Stanley, E.H. (2004). Spatial Extrapolation: The Science of Predicting Ecological Patterns and Processes. *BioScience*, 54(4), 310–320. [https://doi.org/10.1641/0006-3568\(2004\)054\[0310:SETSOP\]2.0.CO;2](https://doi.org/10.1641/0006-3568(2004)054[0310:SETSOP]2.0.CO;2)

- Monteith, J.L. (1972). Solar Radiation and Productivity in Tropical Ecosystems. *Journal of Applied Ecology*, 9(3), 747–766.
- Monteith, J.L. (1977). Climate and the efficiency of crop production in Britain. *Philosophical Transactions of The Royal Society B: Biological Sciences*, 281(980), 294–294. doi:10.1098/rstb.1977.0140.
- Murray, N.J., Keith, D.A., Bland, L.M., Ferrari, R., Lyons, M.B., Lucas, R., Pettorelli, N., Nicholson, E. (2018). The role of satellite remote sensing in structured ecosystem risk assessments. *Science of the Total Environment*, 619–620, 249–257. <https://doi.org/10.1016/j.scitotenv.2017.11.034>
- Nikolova, S., Bruce, S., Randall, L., Barrett, G., Ritman, K., and Nicholson, M. (2012). *Using remote sensing data and crop modelling to improve crop production forecasting: a scoping study*. ABARES technical report 12.3. Australian Bureau of Agricultural and Resource Economics and Sciences, Canberra.
- OPTICLEAF (2020). *OPTICLEAF The database on leaf optical properties* website: <http://opticleaf.ipgp.fr/index.php?page=home>
- Pasetto, D., Arenas-Castro, S., Bustamante, J., Casagrandi, R., Chrysoulakis, N., Cord, A.F., Dittrich, A., Domingo-Marimon, C., El Serafy, G., Karnieli, A., Kordelas, G.A., Manakos, I., Mari, L., Monteiro, A., Palazzi, E., Poursanidis, D., Rinaldo, A., Terzago, S., Ziemba, A., and Ziv, G. (2018). Integration of satellite remote sensing data in ecosystem modelling at local scales: practices and trends. *Methods in Ecology and Evolution*, 9, 1810–1821.
- Prentice, I.C., Bondeau, A., Cramer, W., Harrison, S.P., Hickler, T., Lucht, W., Sitch, S., Smith, B., and Sykes, M.T. (2007). Dynamic Global Vegetation Modeling: Quantifying Terrestrial Ecosystem Responses to Large-Scale Environmental Change. In *Terrestrial Ecosystems in a Changing World* (Eds: Canadell, J.G., Pataki, D.E., and Pitelka, L.F.). Springer-Verlag, Heidelberg.
- Punalekar, S.M., Verhoef, A., Quaife, T.L., Humphries, D., Bermingham, L., and Reynolds, C.K. (2018). Application of Sentinel-2A data for pasture biomass monitoring using a physically based radiative transfer model. *Remote Sensing of Environment*, 218, 207–220.
- Rommel, T.K., and Csillag, F. (2003). When are two landscape pattern indices significantly different? *Journal of Geographic Systems*, 5, 331–351.
- Richter, T., and Fukshansky, L. (1996). Optics of a bifacial leaf: 1. A novel combined procedure for deriving the optical parameters. *Photochemistry and Photobiology*, 63(4), 507–516.
- Rickert, K.G., Stuth, J.W., and McKeon, G.M. (2000). Modelling pasture and animal production. In *Field and Laboratory Methods for Grassland and animal Production Research*. (Eds: Mannelje, L.T., and Jones, R.M.). CABI publishing, New York. pp 29–66.
- Robins, L., Freebairn, D., and Sedger, A. (2003). *Groundwater Models. A Community Guide to Better Understanding*. Murray-Darling Basin Commission, Canberra. ISBN: 1 876830 45 X
- Scarth, P., Röder, A., and Schmidt, M. (2010). Tracking grazing pressure and climate interaction the role of Landsat fractional cover in time series analysis. In *Proceedings of Australasian Remote Sensing and Photogrammetry Conference*, Alice Springs, 13–17 September. figshare.com/articles/Tracking_Grazing_Pressure_and_Climate_Interaction_-_The_Role_of_Landsat_Fractional_Cover_in_Time_Series_Analysis/94250/1
- Sitch, S., Huntingford, C., Gedney, N., Levy, P.E., Lomas, M., Piao, S.L., Betts, R., Ciais, P., Cox, P., Friedlingstein, P., Jones, C.D., Prentice, I.C., and Woodward, F.I. (2008). Evaluation of the terrestrial carbon cycle, future plant geography and climate-carbon cycle feedbacks using five Dynamic Global Vegetation Models (DGVMs). *Global Change Biology*, 14(9), 2015–2039. <https://doi.org/10.1111/j.1365-2486.2008.01626.x>
- Stein, A., Staritsky, I.G., Bouma, J., Van Eijsbergen, A.C., and Bgegt, A.K. (1991). Simulation of moisture deficits and areal interpolation by universal cokriging. *Water Resources Research*, 27, 1963–1973.
- Suits, G.H. (1972). The calculation of the directional reflectance of a vegetative canopy. *Remote Sensing of Environment*, 2, 117–125.
- Tucker, C.J., and Garratt, M.W. (1977). Leaf optical system modeled as a stochastic process. *Applied Optics*, 16(3), 635–642.
- Ustin, S.L., Jacquemoud, S., Zarco-Tejada, P.J., and Asner, G.P. (2004). Remote sensing of the environment: state of the science and new directions, in *Manual of Remote Sensing. Volume 4: Remote Sensing for Natural Resource Management and Environmental Monitoring* (Ed: S.L. Ustin). John Wiley and Sons. pp. 679–729.
- Van Dijk, A.I.J.M. (2010). *AWRA Technical Report 3. Landscape Model (version 0.5) Technical Description*. WIRADA / CSIRO Water for a Healthy Country Flagship, Canberra.
- Vargas, W.E. (1999). Two-flux radiative transfer model under nonisotropic propagating diffuse radiation. *Applied Optics*, 38(7), 1077–1085.

- Verhoef, W. (1984). Light scattering by leaf layers with application to canopy reflectance modeling: the SAIL model. *Remote Sensing of Environment*, 16, 125–141.
- Verhoef, W. (1985). Earth observation modeling based on layer scattering matrices. *Remote Sensing of Environment*, 17, 165–178.
- Viney, N., Vaze, J., Crosbie, R., Wang, B., Dawes, W., and Frost, A. (2015). *AWRA-L v5.0: technical description of model algorithms and inputs*. CSIRO, Australia.
- Williams, M., Woodward, F.I., Baldocchi, D.D., and Ellsworth, D. (2004). CO₂ capture from the leaf to the landscape, In *Photosynthetic Adaptation: Chloroplast to Landscape* (Eds: W.K. Smith, T.C. Vogelmann and C. Critchley) Ecological Studies 178, Springer.
- Wu, J. (2013). Landscape Ecology. In *Ecological Systems* (Ed: Leemans R.). Springer, New York. https://doi.org/10.1007/978-1-4614-5755-8_11
- Zhang, B., and Carter, J. (2018) FORAGE—An online system for generating and delivering property-scale decision support information for grazing land and environmental management. *Computers and Electronics in Agriculture*, 150, 302–311.
- Zhang, L., Walker, G.R., and Dawes, W.R. (2002). Water balance modelling: concepts and applications. In *Regional Water and Soil Assessment for Managing Sustainable Agriculture in China and Australia* (Eds: McVicar, T.R., Li Rui, Walker, J., Fitzpatrick, R.W., and Liu Changming). ACIAR Monograph No. 84. pp 31–47.

Observing Agriculture



In this context, ‘agriculture’ describes a land use, an activity, a segment of economics, even a political portfolio. In Australia, both the state and federal political systems have their own unique departments of agriculture. Like many other developed countries, agriculture in Australia often describes the demarcation between urban and rural areas. Agriculture also defines the ancestral origins of most Australians.

The earliest EO sensors enabled scientists to assess, monitor, and measure plant material on a regular basis, with significantly more advanced sensors becoming available over time (see Volume 1A—Sections 12 and 13 and Volume 1B—Section 10). An overview of agriculture in Australia and its ongoing challenges is presented in Section 11. Subsequent sections consider the use of satellite, airborne and proximal EO datasets to observe vegetation in the Australian landscape for specific agricultural applications:

- monitor crop type, condition, extent, and yield (see Section 12);
- model crop water use in irrigated horticulture (see Section 13);
- estimate pasture biomass and growth rates (see Section 14);
- assess condition and distribution of pasture species, including woody perennial vegetation, in rangelands (see Section 15); and
- observe the biomass and condition of both native forests and plantations (see Section 16).

Contents

11	Agriculture Overview	231
12	Crops	249
13	Irrigated Horticulture	263
14	Pastures	281
15	Rangelands	299
16	Forestry	323



11 Agriculture Overview

The increased scales of operations on modern farms present major challenges for monitoring the water, nutrient, pest, and disease status of various crops to ensure that products are suited to market requirements. EO-based forecasting of crop yield or pasture growth has become an essential part of modern agriculture, which enables efficient marketing and distribution of produce. This involves monitoring pest infestations and fertiliser requirements during growth, determining the best time to harvest crops, then managing its storage and sale. Reliable monitoring and forecasting—with an emphasis on Early Warning Systems (EWS)—are also critically important for shaping food policy and addressing food security concerns around the world (FAO, 2017).

An integrated suite of timely EO technologies is required at a range of scales to meet the management requirements of food and fibre crops in Australia. Recent advances in EO technologies, particularly the advent of Digital Earth Australia (DEA; see Volume 2D), have transitioned this field from a promising research tool to a practical management necessity for many Australian agricultural activities. For example, a collaborative project between Geoscience Australia (GA) and the Australian Bureau of Statistics (ABS) is merging ABS agricultural census/survey data (de-identified) with DEA images to rapidly develop regional maps of crops and land covers. Such maps then form an ideal basis for assessing the impact of natural disasters, determining crop suitability in changing environmental conditions, and estimating crop yield for financial and actuarial applications (ABS, 2020b).

An overview of Australian agricultural activities is presented in Section 11.1. The remainder of this section reviews four pivotal topics for using EO datasets to map, monitor, and model agricultural activities both globally and in Australia, namely, defining essential agricultural variables (see Section 11.2), monitoring managed landscapes (see Section 11.3), understanding land degradation (see Section 11.4) and addressing food security (see Section 11.5). The following five sections describe EO-based methods that are being developed or used operationally for specific Australian agricultural sectors.

For about two million years humans lived by gathering, herding and hunting. Then in the space of a few thousand years a radically different way of life emerged based on a major alteration to natural ecosystems in order to produce crops and provide pasture for animals. This more intensive system of food production was developed separately in three core areas of the world and marked the most important transition in human history. Because it was capable of providing much greater quantities of food it made possible the evolution of settled, complex, hierarchical societies and a much faster growth in human population. By about 2000 BC all the major crops and animals that make up the contemporary agricultural systems of the world had been domesticated.

....

Agriculture is most definitely not an easier option than gathering and hunting. It requires far more effort in clearing land, sowing, tending and harvesting crops and in looking after domesticated animals. It does not necessarily provide more nutritious food, nor does it offer greater security because it selects and depends on a far smaller range of plants and animals. The one advantage agriculture has over other forms of subsistence is that in return for a greater degree of effort it can provide more food from a smaller area of land.

(Ponting, 1991)

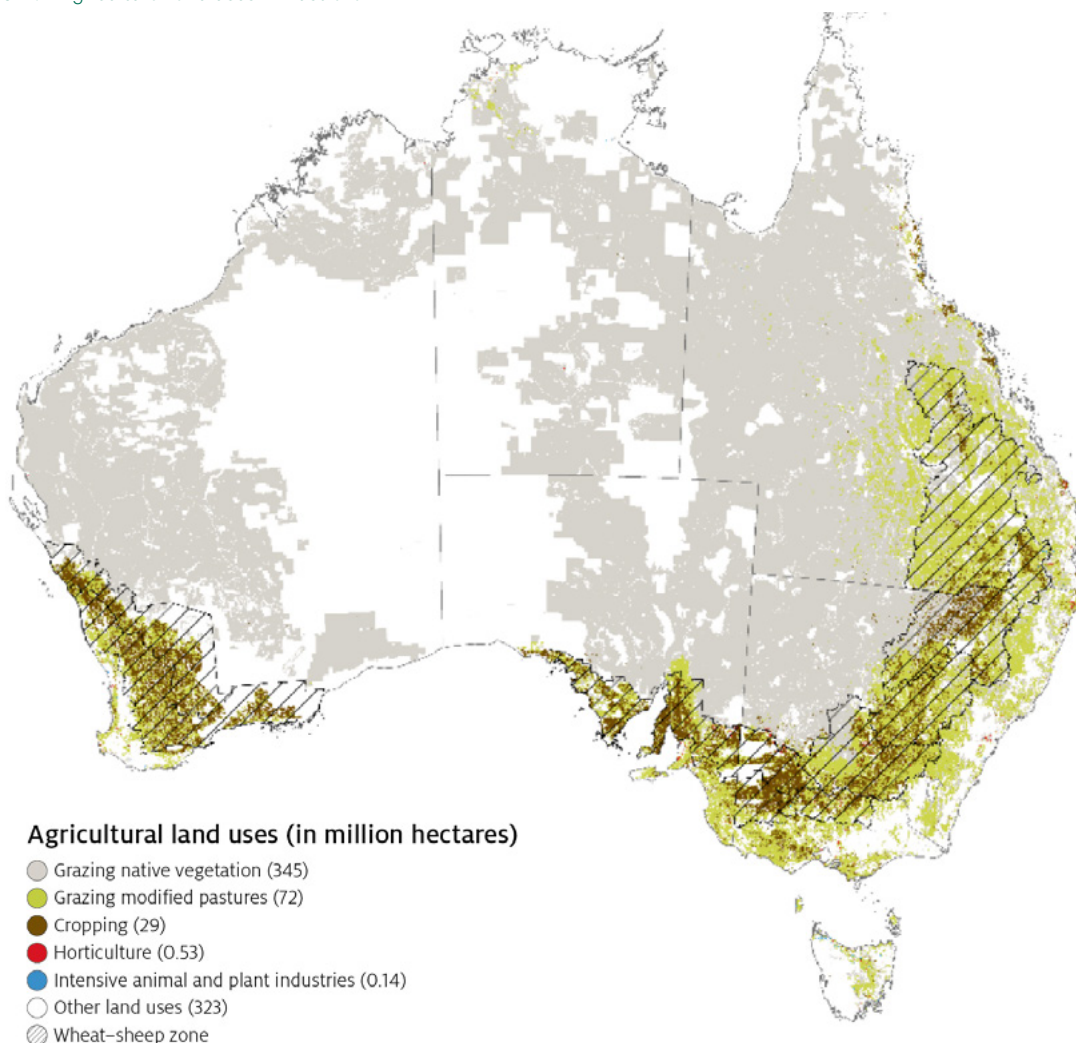
Background image: Landsat-8 OLI image over the mixed agricultural district of Kerang, Victoria, acquired on 2 July 2018. This image is displayed using bands 4, 3, 2 as RGB and clearly differentiates irrigated and non-irrigated crops (see also Volume 2C—Excursus 11.1). **Source:** Norman Mueller, Geoscience Australia

11.1 Agriculture in Australia

The mainland of Australia is the sixth largest continent in the world and has the dubious honour of being the driest, with the majority of its land area receiving less than 500 mm of rainfall per year (see Figure 2.7). Approximately 97% of the Australian population live outside the lower rainfall zone, that is, within 15% of Australia's land area (see Figure 2.15). It can be easily extrapolated from these figures that of the whole continent (a little less than the size of the USA), when areas of dense urban populations (including the advancing peri-urban regions) are excluded, only a very small area remains with access to sustainable water reserves that is suitable for intensive farming. Given Australia's hugely varied rainfall patterns, ranging from summer rainfall in the north to predominantly spring rainfall in the south (see Section 2.2), other factors, such as soil types, determine viable agricultural activities (see Section 2.5.2).

Each of the 89,400 agricultural landholdings in Australia (ABS, 2020a), from any production sector and/or locality, is unique in terms of its size, soil, topography, climate, vegetation cover, economic security, and/or proximity to market. Since the majority of landholdings are privately owned and work from a low economic base, farmers and graziers are often obliged to rely on less expensive processes to improve efficiency and profitability.

Figure 11.1 Agricultural land uses in Australia



Source: ABARES (2020b). (Retrieved from <https://www.agriculture.gov.au/sites/default/files/images/agricultural-production-zones.png>)

Australian agricultural areas devoted to food production include broad-acre cropping (cereals, legumes, and oil; see Section 12), irrigated horticulture (see Section 13), grasslands (see Section 14), and rangelands (see Section 15). In addition, both native forests and exotic plantations are managed for timber production (see Section 16). Just over half of the 769 million ha of land in Australia is used for agricultural holdings (ABS, 2020c), of which around 87% is grazed (see Figure 11.1). Grazing predominantly occurs on arid and semi-arid native pastures, known as rangelands, with improved pasture only covering around 10% of the grazing area.

The gross value of Australian agricultural production in 2020/21 is estimated as \$61 billion with approximately 75% of produce being exported (ABARES, 2020a). Australian agriculture accounts for:

- 59% of water extractions (9,434 gigalitres used by agriculture in 2015/16);
- 11% of goods and services exports in 2018/19; and
- 2.2% of value added (GDP) and 2.6% of employment in 2018/19 (ABARES, 2020b).

In 2019, the Australian Bureau of Statistics (ABS) reported that the Australian population exceeded 25 million and by 2050 this number may have increased by 50%. In addition to the anticipated demand resulting from population growth in neighbouring countries, this population increase may strain the capacity of farmers to meet the projected domestic food requirements (see Section 11.5).

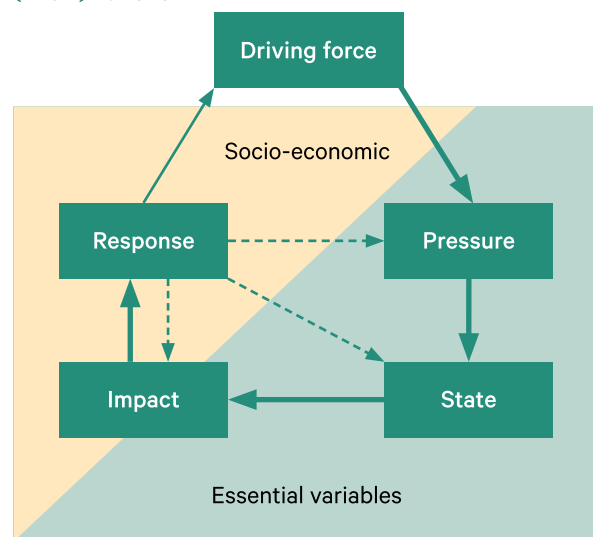
The primary source of agricultural commodity statistics, with a focus on aggregated production, is the five-yearly ABS Agricultural Census, which is sent to 170,000 farms whose agricultural activities have an estimated value exceeding \$5,000. In non-census years, the ABS survey 30,000 farms. The Australian Bureau of Agricultural and Resource Economics and Sciences (ABARES) also survey around 70% of farms in the broadacre cropping, grazing and dairy industries each year (~2,000 farms) for detailed information on finances, which is extrapolated to produce regional, state, and national crop production estimates in February, June, September, and December (Nikolova *et al.*, 2012).

Amidst the goodwill towards Australia's productive landscapes, clever farmers and strong agricultural research sector, there is often a lack of recognition that the underlying resource base of soils and biodiversity has been gripped in a cycle of decline for decades.
(Ogilvy, 2020)

11.2 Essential Agricultural Variables

A relatively recent focus in EO considers 'essential variables' (EV), that is, a minimal, streamlined, yet comprehensive set of independent, constraining variables that can be derived from EO datasets, which collectively characterise the state, trend, and future evolution of the integrated Earth System (Masó *et al.*, 2020; see Excursus 1.2) based on its energy and matter cycling (Whitcraft *et al.*, 2019; see Section 10.2.3). EV effectively define a set of common, geo-referenced measurements of physical, chemical, and/or biological attributes that can be acquired on a regular basis to efficiently analyse relevant drivers, pressures, states, impacts, and responses in a range of Earth System disciplines, or 'domains' (Masó *et al.*, 2020).

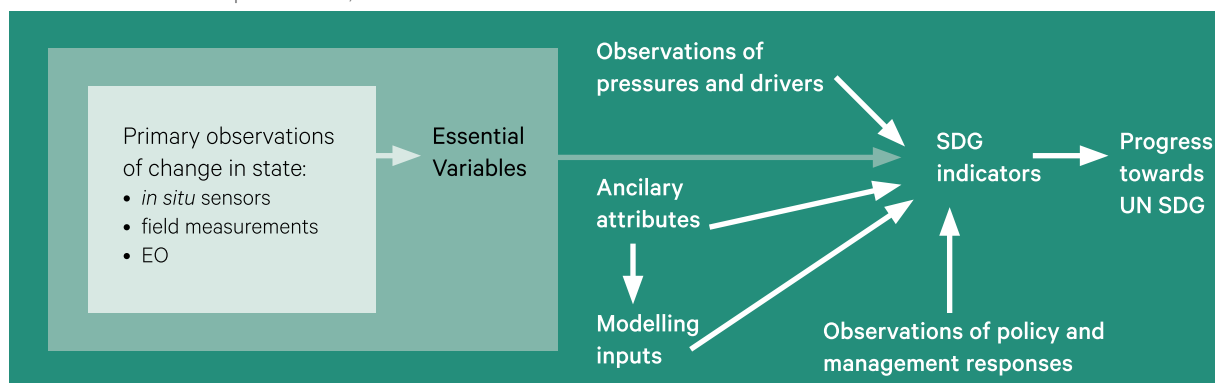
Figure 11.2 Driving force–pressure–state–impact–response (DPSIR) framework



Adapted from: Mace and Baillie (2007) Figure 2 and Masó *et al.* (2020) Figure 3

Figure 11.3 Essential Variables in the context of UN Sustainable Development Goals

SDG: Sustainable Development Goals; EO: Earth Observation



Adapted from: Masó *et al.* (2020) Figure 4

As well as maximising cost-effectiveness, recommended criteria for EV include being relevant to purpose, readily communicated to target audiences, and able to differentiate between measures of pressure, state, and response (Mace and Baillie, 2007). The driving force–pressure–state–impact–response (DPSIR) framework (OECD, 1993) is often used to construct and evaluate sets of indicators (see Figure 11.2). This conceptual framework classifies indicators as measures of pressure, state, impact, or response in social-environmental systems, and offers a convenient tool to analysing the socio-economic impacts of anthropogenic activities on the environment, including causal relationships (Burkhard and Müller, 2008). For example, social changes can be viewed as drivers which apply pressure to the environment, resulting in impacts on people or ecosystems. In response, policies are introduced to relieve pressure and restore the desired state. Since indicator development is inevitably an evolutionary process, this framework highlights potential gaps in current indicator sets, enables the impact of changes in components and their interactions to be assessed, and helps to retain focus on achievable implementation targets (Mace and Baillie, 2007).

Existing EV include Essential Climate Variables (ECV; Bojinski *et al.*, 2014; see Volume 1A—Section 1.5.2), Essential Ocean Variables (EOV; Moltmann *et al.*, 2019; see Volume 3B), and Essential Biodiversity Variables (EBV; Pereira *et al.*, 2013; see Section 19.3). These standardised variables have particular value for global monitoring applications towards the United Nations (UN) Sustainable Development Goals (SDG; see Section 20.4), such as food security (Patias *et al.*, 2019; see Figure 11.3 and Section 11.5).

One of the activities of the Group on Earth Observation (GEO) Global Agricultural Monitoring initiative (GEOGLAM) is to develop a set of globally-relevant Essential Agricultural Variables (EAV) that are relevant to agricultural activities (Whitcraft *et al.*, 2019; GEO, 2019). EAV will help standardise EO-based products for regional and global agricultural monitoring (see Excursus 11.1) and further integrate EO datasets into operational systems designed to reduce land degradation (see Section 11.4), alleviate food insecurity (see Section 11.5), and monitor crop condition and yield (see Section 12).

Resilience describes the capacity of a system to maintain its equilibrium in the face of impacts or pressures that arise from natural or human-made interactions or events. 'Resilience' comes from the Latin word 'resilire', which means to 'leap back' after adversity. A resilient system has the capacity to absorb disturbance and essentially retain the same function, structure and feedbacks. ... Modified ecosystems are generally ecologically simpler and therefore have less resilience to external pressures (eg. variations in climate) than complex ecosystems.
(DEWHA, 2010)

11.3 Monitoring Managed Landscapes

To ensure the health of both soil and vegetation, monitoring is an integral part of the adaptive management of cultivated and grazed natural resources. For example, EO-based systems to monitor pasture productivity and condition have been established for decades in Australia (see Excursus 14.1 and Section 15.4). Similarly, an international, EO-based system, GEOGLAM RaPP (see Excursus 11.1), observes the condition of pastures and rangelands on a global scale to estimate biomass dynamics and productivity (see Sections 13 and 15), and reduce land degradation (see Section 11.4).

The ‘condition’ of land has been described as a concept in which “specific indicators like vegetation cover, production, or composition ... at a particular location (are compared with) the assumed potential for that attribute within that vegetation type or compared to other locations” (Friedel *et al.*, 2000; see also Sections 7.2 and 7.3 above). In the context of rangelands for example, to monitor condition means “to determine to what extent human factors (e.g. grazing management) have caused departure from the assumed potential” (Bastin and Ludwig, 2006).

Land condition is analogous to human health and the rating (or rank) given to an area is often subjective, and can be contentious (see Section 7.3). This uncertainty is increased in the arid rangelands where large fluctuations in the amount and timing of rainfall can produce considerable natural variation in the vegetation attributes used to determine condition. As such, it is often difficult to know which parts of the grazed rangelands are remaining stable, or are improving or deteriorating over time. Since drought is part of the normal climatic variation experienced by the Australian rangelands, land condition can only be assessed in these landscapes in the context of the variation between the episodic drought years and the infrequent years of high rainfall.

Figure 11.4 Seasonal quality matrix

This matrix summarises site level change in condition indicators with respect to rainfall amount. The upper left and lower right ‘traffic light’ colours focus attention on those groups of sites showing change that is contrary to seasonal expectations.

Seasonal conditions	Decline	No change	Increase
Above average			~
Average		~	
Below average	~		

The term ‘seasonal quality’ has been used to indicate the relative value of rainfall to vegetation (Bastin *et al.* 2008) and can assist with understanding landscape change. The seasonal quality matrix (see Figure 11.4) focuses attention on unexpected change. Here, site level change based on indicators is interpreted with respect to recent ‘seasonal quality’. In this case recent seasonal conditions may be classified as above average, average, or below average, based on rainfall prior to the most recent assessment. A decline in indicator value following above average rainfall, or an increase following below average rainfall, strongly suggest non-rainfall related causes. The former is often associated with enhanced fire activity, while the latter suggests favourable land management practices. The seasonal quality matrix also underpins the development and application of EO-based methods for monitoring land condition in these landscapes (see Section 15).

Landscape Functional Analysis (LFA; Tongway and Hindley, 2004; see Section 7.3 above) was developed to quantify degradation and recovery in drylands. Its conceptual framework is the Trigger-Transfer-Reserve-Pulse (TTRP) model (see Figure 7.3), which describes ecosystem function in terms of the transport, usage, and cycling of scarce natural resources (such as water, topsoil, organic matter, seeds) in space and/or time:

- triggers are climatic drivers, management interventions or disturbances;
- transfers are processes such as wind and water erosion that move nutrients into reserves;
- reserves are zones or patches (above or below ground) where nutrients are stored; and
- pulses are increased floral or faunal productivity resulting from the stored nutrients and available soil moisture.

While traditional approaches assess vegetation characteristics, such as composition and structure, LFA focuses on landscape function to understand the regulation of resource outputs versus inputs and internal feedbacks (Reinhart, 2009). The loss of resources from the landscape, such as by erosion or runoff, indicates its ‘leakiness’ (see Sections 7.3 and 8.1.6), whereas gains in resources may indicate increased capacity in its ‘reserve’ zones, possibly due to successful restoration activities, and therefore a more tightly coupled system. The distribution of reserve zones in dryland landscapes is characteristically patchy and discontinuous with different resources occurring at different patch scales in both space and time (Tongway and Hindley, 2004). These concepts are further explored in Section 15.

Excursus 11.1—GEOGLAM RaPP

Source: Guerschman *et al.* (2018)

Further information: <https://www.geo-rapp.org>

Reporting tool: <https://map.geo-rapp.org/>

An integrated system for observing the condition of Earth's pastures and rangelands is being established by the Group on Earth Observation (GEO) Global Agricultural Monitoring initiative (GEOGLAM; see Section 21.3). In particular, the GEOGLAM Rangeland and Pasture Productivity (RaPP) aims to enable the condition of rangelands and pasture lands to be monitored routinely at global, regional, and national scales, with the goal of estimating biomass dynamics and productivity. The Australian component of this system uses MODIS imagery to map fractional cover (FC: photosynthetic vegetation, non-photosynthetic vegetation, and bare soil) on a monthly basis at 500 m spatial resolution (see Excursus 8.3). In regions with < 20% trees cover, ground cover can be represented as the sum of photosynthetic and non-photosynthetic vegetation, or the total vegetation cover (see Figure 5.1).

These EO-based products extend the community-based work of Leys *et al.* (2008) in NSW in the development of the DustWatch program, which monitors wind erosion risk (see Section 11.6). Much of Australia's agricultural land has a significant risk of wind erosion (see Section 11.4), which can result in localised loss of soil and nutrients and a reduction in regional air quality (see Figure 11.5). Water erosion on hillslopes is also a risk in some rangeland and cropping regions, with subsequent impact on water quality. One of the primary factors in controlling soil erosion is the retention of a protective cover layer over the soil surface, including vegetation, litter, biological crusts, and stones. To avoid wind erosion, more than half the soil surface needs to be covered (Leys, 1991), while to prevent water erosion, over 70% ground cover is required (Lang, 2005). Thus, higher levels of total vegetation cover can be used to indicate lower soil erosion risk.

A range of spatial datasets are integrated by RaPP (see Table 11.1 and Leys *et al.*, 2020) to provide interactive tools that can be applied to a defined region, including:

- change in ground cover for a defined time interval;
- time series plot of mean ground cover; and
- statistical comparisons of current ground cover with previous conditions and 'normal' state.

These tools assist users to visualise changes in total vegetation cover and distribution through time at a variety of scales over the entire Australian land mass.

The main objective of GEOGLAM is to reinforce the international community's capacity to produce and distribute relevant, timely, and accurate information on agricultural land use and production at national, regional, and global scales, using Earth observation (EO) data, toward enhancing knowledge and improving sustainable decisions related to agriculture and food security.
(GEO, 2019)

Table 11.1 RaPP spatial datasets

FC: Fractional Cover; TV: Total Vegetation; GC: Ground Cover; PGC: Persistent Ground Cover; CHIRPS: Climate Hazards Group InfraRed Precipitation with Station data (<https://www.chc.ucsb.edu/data/chirps>); CLUM: Catchment scale Land Use for Australia (see Section 3.3.4 and 3.5);

Data type	Source	Description
EO time series	MODIS Fractional Cover (FC)	Monthly (FC, TV, TV anomalies, TV deciles) 8-day (FC, TV)
	Seasonal Landsat/Sentinel FC	Landsat (FC, GC, PGC—see Section 9.1)
		Sentinel-2 (FC)
Climate	Rainfall	Totals (CHIRPS), Monthly anomalies
Land use and land cover	CLUM (2017)	See Section 3.3.4
	Land use of Australia	National scale (2010–11)
	Ramsar wetlands	See Volume 3B
	IBRA 7.0 regions and subregions	See Sections 2.4 and 3.3.2
	Collaborative Australian Protected Areas Database (CAPAD)	CAPAD (2018)
	Major vegetation subgroups	NVIS (see Section 2.3.1)
	Vegetation height and structure	See Excursus 6.1
Boundaries	Australian rangelands	See Section 15
	NRM regions 2017	See Section 3.4
	Local Government Areas 2016	Australian Bureau of Statistics
	Census Mesh Blocks 2011	
	State Suburbs (SSC) 2016	
	Census Statistical area level	
	River regions	Bureau of Meteorology

Source: Guerschman *et al.* (2018) Table 2; see also Leys *et al.* (2020)

Land degradation is actually generally a slow process therefore it's the cumulative impact of both rapid and prolonged effects that cause land degradation. Perennial woody vegetation such as trees and shrubs generally change over periods of months, years or decades; except when major disturbance events occur such as fire, cyclones or land clearing. The non-woody ground cover is generally more dynamic and can change over much shorter time periods (e.g. weeks to months), in response to rainfall events and land management practices such as grazing and cropping. It can therefore be a useful indicator of land management, particularly if it is understood in the context of local or regional climate patterns and landscape variability (i.e. soil types and landform pattern).
(Guerschman et al., 2018)

11.4 Land Degradation

At a global scale, land degradation is not a new problem (see Excursus 11.2). In Australia, the majority of agricultural lands have been actively degraded since European settlement and this trend still continues in parts of the country. The challenge now is to learn from history before it is too late (see Section 21).

Wind and water erosion continually relocate soil in Australia, with soil erosion rates due to water exceeding the rate of soil formation by orders of magnitude. Soil erosion on Australian cropping land has been assessed as unsustainable (Bui et al., 2010), delivering excessive volumes of sediments and nutrients to inland and coastal watercourses and waterbodies. Wind erosion removes topsoil, sometimes in sufficient volume to create dust storms (see Volume 1B—Section 4), which present a significant hazard to human health, vegetation, infrastructure, and aviation, and inflict substantial economic costs to the affected communities (Tozer and Leys, 2013; see Figure 11.5). Since bare land is most susceptible to soil loss from both agents, the first step towards controlling this problem

involves retaining ground cover on grazing lands and minimising soil disturbance on cropping land (SOE, 2016a). Both local systems such as DustWatch (Leys et al., 2018) and global systems such as GEOGLAM RaPP (see Excursus 11.1) utilise EO datasets to monitor potential and actual erosion. Meteorological datasets and models are also instrumental in understanding dust transport pathways in Australia and developing a dust trajectory climatology (O'Loingsigh et al., 2017).

Despite this erosion potential, an estimated 35% of Australian agricultural land is currently overgrazed and/or over-cultivated (Ogilvy, 2020). While drought—like fire (see Section 18)—is a characteristic of the Australian landscape, when coupled with overgrazing the resulting environmental degradation can be long term (Hendy et al., 2003; see Section 15). For example, McKeon et al. (2004) document and analyse eight extended droughts up until the end of the 20th century that occurred in different parts of Australia (see Table 11.2), each of which resulted in significant land degradation.

There is an intimate relationship between the landscape, its geological and climatic history, weathered and transported soil types, groundwater and the hazard posed by salt load within the soil.
(Spies and Woodgate, 2005)

Excursus 11.2—Learning from History

Source: Ponting (1991), Carson (1962)

To be ignorant of what occurred before you were born is to always remain a child. For what is the worth of human life, unless it is woven into the life of our ancestors by records of history.
(Marcus Tullius Cicero)

Ecosystems provide a variety of essential resources for human inhabitants, primarily food, water, clothing, shelter, and energy (see Section 20.3). However, humans are a unique species—they have spread into every ecosystem on Earth, yet repeatedly demonstrate the capacity to destroy the ecosystems that support them. History offers numerous examples of societies that have developed, flourished, specialised, foundered, then collapsed as a result of overexploitation, mismanagement, degradation, and/or pollution of their available natural resources (including other humans). This sequence has played out to different extents and over different time periods—largely depending on the resilience of the natural ecosystem—all around the globe, most notably in Mesopotamia, the Indus Valley, ancient Egypt, the Maya, and Easter Island (Ponting, 1991).

Agricultural practices change natural ecosystems by clearing land, introducing new species, exposing soil to erosion, changing nutrient recycling, and possibly developing irrigation methods (Asner *et al.*, 2004). Agriculture necessitates settled communities and population growth, which generally requires further clearing of forests for construction and fuel. To support these communities, additional mechanisms are then needed to supply water, dispose of wastes and revitalise the soil between crops. This transformation from natural to managed ecosystems has intensified in recent centuries, with the support of technological advances in machinery for clearing and tilling land, and the availability of an increasing array of chemical agents to promote the growth of food plants and animals and discourage pests and disease (Ramankutty *et al.*, 2018). Such agents include artificial fertilisers, insecticides, herbicides, and soil treatments, which deliver short term economic benefits, but their longer term cost—in terms of pollution, species depletions, human health, water quality, and disruptions to the food web—is still being accounted (Carson, 1962).

Environmental degradation is not a new problem for human communities, but it is now becoming more widespread and more urgent on a global basis (see Sections 19 and 20). Recent understanding of the processes of degradation are prompting effective control of this problem in some parts of the world, including Australia (McKeon *et al.*, 2004). For example, since the mid-1900s, soil erosion has declined in many regions due to better land management practices, including control of feral animals, rotational grazing, minimum tilling, regenerative agriculture, and a focus on sustainable development.

EO is playing a key role in optimising the use of agricultural chemicals through precision farming and avoiding over-grazing through programs such as GEOGLAM RaPP (see Excursus 11.1). A range of spatial technologies now provide essential information to farmers and bureaucrats to guide their stewardship of land resources in both tactical and strategic decisions at a range of scales in time and space. EO datasets are also being used to monitor the global status of terrestrial vegetation across a range of application areas (see Section 21). Hopefully, these examples demonstrate that we have started to learn from history.

What has been, that will be; what has been done, that will be done. Nothing is new under the sun.
(Book of Ecclesiastes 1:9)

Figure 11.5 Dust storm

This landscape view of the approaching ‘Red Dawn’ dust storm was taken around 1 pm on 23 September 2009 at Kars Station, 60 km east of Broken Hill, NSW. Red dust that had been collected in central Australia was quickly transported across the continent leading to an estimated loss of 2.54 Mt of soil (Leys *et al.*, 2011). Along the eastern coastline the plume extended in a 3000 km swath, from the Gulf of Carpentaria, Queensland, to Eden, in southeast NSW (see Volume 1B—Figure 4.6b). Red Dawn ultimately shrouded an area spanning 840,000 km², significantly reduced air quality (with a total dust load between 12.1 Mt and 17.5 Mt), and resulted in an estimated cost of A\$299 million to NSW (Tozer and Leys, 2013).



Source: Fred Hughes, Kars Station

To mitigate the impact of drought in impoverished communities, insurance schemes based on EO analyses have been developed for Africa, such as Index-based Livestock Insurance (IBLI). For example, since 2010, the International Livestock Insurance Institute (ILRI) have offered index-based insurance to protect vulnerable pastoralists from asset losses related to climatic conditions, particularly those located in drought-prone, arid and semi-arid lands in Kenya and Ethiopia (ILRI, 2020). ILRI relies on Early Warning Systems (EWS; see Section 12.3), which use EO and meteorological datasets to predict natural

disasters such as drought (CTA, 2018). Based on historical trends, the index approach uses NDVI imagery to highlight years when forage will be inadequate for stock. By allowing farmers to claim assistance through dry seasons they avoid grazing dry soils and thereby increasing erosion, so conserve the natural resources for better growing seasons in the future. This approach also discourages the consumption of seed reserves or breeding stock in lean years, which would ultimately intensify poverty into the future (Barnett and Mahul, 2007).

Table 11.2 Eight extended droughts in Australia

In each case the start of the drought period is defined as the first year with rainfall less than 70% of the mean.

Period	Location	Environmental Impact	Social/Government Consequence
1898/99 to 1902/03	Western NSW	Soil erosion, woody weed infestation, rabbit plagues	Substantial financial losses and financial hardship resulting in the Royal Commission of 1901
1925/26 to 1929/30	South Australia and Western NSW	Substantial loss of perennial vegetation and soil erosion	Government legislation for regulation of carrying capacity and soil conservation
1935/36 to 1940/41	Gascoyne region of Western Australia	Substantial loss of perennial shrubs, soil erosion and animal losses	Royal Commission of 1940
1941/42 to 1944/45	Western NSW	Substantial dust storms and animal losses	Paintings (Russell Drysdale)
1958/59 to 1965/66	Central Australia	Wind and water erosion	Extensive surveys and reassessment of carrying capacity
1964/65 to 1967/68	Western NSW	Large increases in woody weeds	Reduced carrying capacity and income in 1960s
1964/65 to 1967/68	Southwest Queensland	Soil erosion and woody weed infestation	Government-sponsored Southwest Strategy supporting review of recommended carrying capacities and property amalgamation
1984/85 to 1987/88	Northeast Queensland	Soil erosion and loss of ‘desirable’ perennial grasses	Extensive government-sponsored surveys and dramatic grazier response

Adapted from: McKeon *et al.* (2004) Table 1

Table 11.3 Total economic value of ecosystem services

Value	Type	Examples
Use	Direct	Agricultural produce, fuel, transport
	Indirect	Flood mitigation, pollination, pest control
	Option	Genetic resources with potential future value
Non-use	Existence	Value of existence of other species
	Bequest	Value of functional ecosystem to future generations

Source: DEWHA (2010) Box 4

A significant soil degradation problem in Australia is salinity. Anthropogenic salinity is not a new problem globally however, having occurred in ancient agricultural settlements, such as Mesopotamia, and contributed to the demise of numerous civilisations (Jacobson and Adams, 1958; see Excursus 11.2). Salinity occurs when water tables rise to ground level and bring natural salts to the soil surface. In addition to some naturally saline land, vegetation clearing and inappropriate irrigation have induced salinity problems in several regions of Australia. Salinity reduces water and soil quality and can lead to reduced biodiversity of both plants and invertebrates in low lying agricultural lands (Beresford *et al.*, 2001; Clarke *et al.*, 2002). In the most recent comprehensive survey (NLWRA, 2001), dryland (non-irrigated) salinity affected 5.7 million ha in Australia, primarily in southwest WA and Victoria, and this is expected to increase to 17 million ha by 2050 (SOE, 2016b). Globally, soil salinity is estimated to impact nearly 1 billion ha, or around 7% of the land surface, especially in arid and semi-arid regions (Ghassemi *et al.*, 1995), and at least 20% of irrigated land (Pitman and Läuchli, 2002). A number of EO-based approaches have been proposed to map and monitor salinity using sensors that detect electromagnetic radiation (EMR), electromagnetic induction (EMI), and geophysical attributes (see Volume 1A—Sections 5–9), with an emphasis on data fusion and data integration methods, and adequate ground truthing (Metternicht and Zinck, 2003; Spies and Woodgate, 2005).

Soil acidification is an even more widespread problem than salinity, due to the use of agricultural fertilisers on light soils with low pH, which can lead to unhealthy changes in soil biota, increased leaching of selected nutrients, loss of clay particles, erosion, and reduced Net Primary Productivity and carbon sequestration. Acid soils are more likely to release heavy metals into watercourses and the food chain, and increase siltation and eutrophication of waterbodies (see Volume 3B). NLWRA (2001) estimated that around 50 million ha of Australia's agricultural land and about 23 million ha of subsoil are affected by soil acidity, with most of these areas occurring in WA and NSW (SOE, 2016b).

The concept of ecosystem services, that is, the services that ecosystems deliver to human society, is described in Section 7.3. The total economic value of ecosystem services includes both use and non-use values (see Table 11.3). For example, a study of the relationship between soil condition in Australian agricultural lands, their management practices, and the ecosystem services they provide (Cork *et al.*, 2012), concluded that the practices of increasing soil carbon, reducing surface soil acidity, and maintaining ground cover on agricultural soils not only improved financial returns from agricultural activities, but also resulted in fewer dust storms, cleaner water from catchments, less reliance on agricultural chemicals, and an enhanced 'sense of place, mental wellbeing and acquisition of knowledge'.

Monitoring in drylands used primarily for commercial and subsistence livestock operations, typically concentrates on indicators related to plant-herbivore interactions and soil stability in relation to trampling. Most monitoring in drylands concentrates first on vegetation attributes and secondarily on soils attributes where vegetation attributes, such as cover, usually serve as a proxy for soil attributes, such as soil erosion. This is due to an observed negative linear correlation between declining vegetation cover and increased erosion. Assessment requires time series data of the drivers of change, including human and herbivore population and demographics, climate, and fire data.

(Washington-Allen and Ravi, 2012)

11.5 Food Security

Food security is not a new problem. For most of human history, the majority of the world's population has lived on the brink of starvation, with high rates of infant mortality, short lifespans, ongoing malnutrition, and the recurrent dangers of famine and disease. Some fortunate societies have only managed to escape this lifestyle in recent centuries, mostly by exploiting the resources of colonies (Ponting, 1991).

Of the Earth's total land surface (13.2×10^9 ha), just over half (7×10^9 ha) is considered arable (Zaman *et al.*, 2018). However, as land degradation reduces the area of arable land around the world, less land is available to grow food (see Section 11.4). In the face of growing population pressures—and the need for land for other purposes—we are faced with a situation where more food is required but less land is available to grow it. This situation simply repeats the pattern of demise witnessed in many civilisations throughout human history (see Excursus 11.2).

The UN defines food security as the global situation “when all people, at all times, have physical, social and economic access to sufficient, safe and nutritious food that meets their dietary needs and food preferences for an active and healthy life” (FAO, 2020a). Despite food being a basic human need and right, around 10% of the world's population have inadequate food supplies on a daily basis. At the same time, current estimates indicate that up to 30% of all food produced is lost or wasted. In this context, losses can occur at each stage in the supply chain between the grower and the consumer (FAO, 2020a). Thus food security involves more than just food availability, but also access to, utilisation of, and stability of food supplies:

- availability—food supply and trade, not just quantity but also the quality and diversity of food. Improving availability requires sustainable productive farming systems, well-managed natural resources, and policies to enhance productivity.
- access—economic and physical access to food. Improving access requires better market access for smallholders allowing them to generate more income from cash crops, livestock products, and other enterprises.

- utilisation—how the human body uses the various nutrients in food. Improving utilisation requires improving nutrition and food safety, increasing diversity in diets, reducing post-harvest loss, and adding value to food.
- stability—being food secure at all times. Food insecurity can be transitory due to weather, employment, conflict, and market fluctuations. Social networks can play an important role in supporting people through transitory food insecurity (AIFSRC, 2014).

Australia is currently one of the lucky nations, producing far more food than it consumes, and only importing around 10% of consumed food and beverages (ABARES, 2020c). As such it enjoys the status of being ranked as “the world's equal lowest level of undernourishment” (ABARES, 2020c based on FAO, 2020b). However, 4% of Australians are viewed as food insecure (Lindberg *et al.*, 2015), including children (McCrinkle, 2017), with an increasing number of diet-related problems becoming apparent in the wider population (Farmar-Bowers *et al.*, 2013). Recommendations to improve food security in Australia include:

- improving efficiency in food production, processing, and distribution;
- reducing wastage and minimise costs; and
- encouraging greater productivity in agriculture and food processing (PMSEIC, 2010).

In addition to the land degradation factors described above that are directly related to agricultural activities, land use pressures from a growing population are also actively shrinking the area of land available to agriculture in Australia. Despite only 6% of Australian landscapes being deemed suitable for cultivated crops and pastures, these areas are also considered to be the most appropriate for energy production and other developments. Urban encroachment, mining, conservation, and other land uses have already reduced the area of productive land in Australia by 9% in the last two decades (Ogilvy, 2020). If we continue to degrade the available agricultural resource and allocate productive land for other land uses, food security will become a more urgent problem for our nation.

*Wealth and vegetation go together, and that exacerbates environmental injustice.
The poor bear the burden of degraded environments.
(Natalie Jeremijenko)*

Soil is a non-renewable resource, its preservation is essential for food security and our sustainable future.
(FAO)

At a global level, much effort is being expended to increase and monitor food production. FAO (2009) estimated that to feed the world's population by 2050, we will need 70% more food (AIFSRC, 2014). Recommendations to avoid increased inequality, energy usage, and land degradation globally, have included trading safety nets, appropriate environmental policy, and consumer education (Martin and Laborde, 2018). By delivering information on global agricultural production that is timely, objective, and repeatable, EO datasets are contributing to numerous efforts to both improve food security (e.g. Song *et al.*, 2017; see Section 12.3) and reduce disaster risk (see Section 11.4). For example, the Vegetation Health Index (VHI; see Section 9.5) underpins several monitoring systems being used to ensure future food security (Kogan, 2019).

With food security being one of the UN SDGs (see Section 20.4), a number of global, EO-based systems, such as the CropWatch system (Wu *et al.*, 2014), have been developed towards this goal. These systems continually monitor food crops and provide early warning of potential food crises (see Section 12.5). EWS rely on EO datasets to detect signs of looming drought and flood conditions, often in conjunction with financial relief schemes, such as IBLI (see Section 11.4). Such schemes alleviate current hardship, avoid extending food security ramifications into future seasons, and reduce the potential for further land degradation.

One aspect of food security that is often overlooked is the essential ecosystem service of pollination (see Section 20.3 and Table 20.6). Since nearly 90% of wild flowering plants require animal pollination (particularly by wild pollinator species), pollinators not only sustain biodiversity and ecosystem functions that help to stabilise the biosphere (see Volume 1A—Section 4.1.4), but their abundance and diversity also impacts crop yield and/or quality (Kearns *et al.*, 1998; IPBES, 2017). 5–8% of global food production relies on pollination services and around 75% of food crops are directly impacted by animal pollination, with these crops supplying an estimated 35% of the global food stock (Klein *et al.*, 2007; Potts *et al.*, 2016). While recent decades have seen a significant increase in the cultivation of pollinator-dependent crops (Aizen *et al.*, 2009), the yield of these crops has increased at a lower rate than that of other crops and also demonstrated greater variability (based on FAO data for 1961–2008; Garibaldi *et al.*, 2011).

A wide range of studies suggest that the populations of pollinators—both wild and managed—are declining. Potential reasons for this decline include the direct and indirect impacts of both agricultural chemicals and genetically modified crops on pollinators, biodiversity loss (see Section 19), and climatic variability (IPBES, 2017). While EO is currently used to monitor related indicators of pollination, such as crop health and production, regional biodiversity, and remnant habitat extent, it could also be used to gain insight into pollination services (Galbraith *et al.*, 2015), as well as the interactions between pollination and plant health, and their impacts on the spatial and temporal variability of yield in pollinator-dependent crops (Willcox *et al.*, 2018).

On some estimates, there is almost 20% more food available per person now than there was three decades ago, nearly 30% more calories per person per day than necessary, and as much as one third of food produced globally (1.3 billion tonnes) is lost or wasted each year.
(Ogilvy *et al.*, 2015)

11.6 Further Information

Global EO-based Agricultural Statistics

GSARS (2017). *Handbook on Remote Sensing for Agricultural Statistics*. Global Strategy to improve Agricultural and Rural Statistics, Rome.

GSARS (2015). *Handbook on Master Sampling Frames for Agricultural Statistics: Frame Development, Sample Design and Estimation*. Global Strategy to Improve Agricultural and Rural Statistics, UN Statistical Commission, Rome. <http://gsars.org/wp-content/uploads/2016/02/MSF-010216-web.pdf>

Erosion in Australia

NSW Community Dustwatch: <https://www.environment.nsw.gov.au/topics/land-and-soil/soil-degradation/wind-erosion/community-dustwatch>

Soils for Life: <https://soilsforlife.org.au/>

Food Security in Australia

Clancy and Lesslie (2013)

Australian Department of Foreign Affairs and Trade: <https://www.dfat.gov.au/aid/topics/investment-priorities/agriculture-fisheries-water/agriculture-food-security/Pages/agriculture-food-security-initiatives>

International Food Sustainability

GEOGLAM Rangeland and Pasture Productivity (RaPP) tool:

Australia: <https://map.geo-rapp.org/#australia>

Global: <https://www.geo-rapp.org>

Information: <https://www.csiro.au/en/Research/LWF/Areas/Landscapes/Earth-observation/RAPP-Map-GEOGLAM>

CropWatch reports: <http://www.cropwatch.com.cn/html/en/index.shtml>

Crop Monitor: Cropmonitor.org

SERVIR: <http://servir.rcmr.org/>

EO4SD (Earth Observation for Sustainable Development) is a new ESA initiative which aims to achieve a step increase in the uptake of satellite-based environmental information in the IFIs regional and global programs: <https://eo4sd.esa.int/>

World Food Studies—WOFOST: [https://www.wur.nl/en/Research-Results/Research-Institutes/Environmental-Research/Facilities-Products/Software-models-and-databases/WOFOST.htm#:~:text=WOFOST%20\(WORLD%20FOOD%20STUDIES\)%20IS,production%20of%20annual%20field%20crops.&text=In%20the%20Global%20Yield%20Gap,available%20soil%20and%20water%20resources.](https://www.wur.nl/en/Research-Results/Research-Institutes/Environmental-Research/Facilities-Products/Software-models-and-databases/WOFOST.htm#:~:text=WOFOST%20(WORLD%20FOOD%20STUDIES)%20IS,production%20of%20annual%20field%20crops.&text=In%20the%20Global%20Yield%20Gap,available%20soil%20and%20water%20resources.)

11.7 References

- ABARES (2020a). *Agricultural overview: June quarter 2020* (Howden, M., Nelson, R., and Cameron, A.) Department of Agriculture, Water and the Environment website: <https://www.agriculture.gov.au/abares/research-topics/agricultural-outlook/agriculture-overview>
- ABARES (2020b). *Snapshot of Australian Agriculture 2020* (Jackson, T., Hatfield-Dodds, S., and Zammit, K. Department of Agriculture, Water and the Environment website: <https://www.agriculture.gov.au/abares/publications/insights/snapshot-of-australian-agriculture-2020>
- ABARES (2020c). *Analysis of Australia's food security and the COVID-19 pandemic* webpage, Department of Agriculture, Water and the Environment website: <https://www.agriculture.gov.au/abares/publications/insights/australian-food-security-and-COVID-19#what-is-food-security>
- ABS (2020a). *Improving agricultural crop statistics using satellite data*, 2020 webpage, Australian Bureau of Statistics website: <https://www.abs.gov.au/ausstats/abs@.nsf/0/13BE1A5F2BDE7E9FCA2585920016C460?OpenDocument>
- ABS (2020b). *Agricultural Commodities, Australia, 2018–19* webpage, Australian Bureau of Statistics website: <https://www.abs.gov.au/ausstats/abs@.nsf/mf/7121.0>
- ABS (2020c). *Land Management and Farming in Australia, 2016–17* webpage, Australian Bureau of Statistics website: <https://www.abs.gov.au/AUSSTATS/abs@.nsf/mf/4627.0>
- AIFSRC (2014). *Australian International Food Security Research Centre* website: <https://aifsc.aciar.gov.au/food-security-and-why-it-matters.html>
- Aizen, M.A., Garibaldi, L.A., Cunningham, S.A., and Klein, A.M. (2009). How much does agriculture depend on pollinators? Lessons from long-term trends in crop production. *Annals of Botany*, 103, 1579–1588.

- Asner, G.P., Elmore, A.J., Olander, L.P., Martin, R.E., and Harris, A.T. (2004). Grazing Systems, Ecosystem Responses, and Global Change. *Annual Review of Environment and Resources*, 29, 261–299.
- Barnett, B., and Mahul, O. (2007). Weather Index Insurance for Agriculture and Rural Areas in Lower-Income Countries. *American Journal of Agricultural Economics*, 89(5), 1241–1247. <https://doi.org/10.1111/j.1467-8276.2007.01091.x>
- Bastin, G.N., and Ludwig, J.A. (2006). Problems and prospects for mapping vegetation condition in Australia's arid rangelands. *Ecological Management and Restoration*, 7, S71–S74.
- Bastin, G., and the ACRIS Management Committee (2008). *Rangelands 2008—Taking the Pulse*. National Land and Water Resources Audit, Canberra. doi:10.1071/RJ08072
- Beresford, Q., Phillips, H., and Bekle, H. (2001). The salinity crisis in Western Australia: a case of policy paralysis. *Australian Journal of Public Administration*, 60(4), 30–38.
- Bojinski, S., Verstraete, M., Peterson, T.C., Richter, C., Simmons, A., and M. Zemp, M. (2014). The Concept of Essential Climate Variables in Support of Climate Research, Applications, and Policy. *Bulletin of the American Meteorological Society*, 95, 1431–1443.
- Bui, E.N., Hancock, G.J., Chappell, A., and Gregory, L.J. (2010). *Evaluation of tolerable erosion rates and time to critical topsoil loss in Australia*. CSIRO Sustainable Agriculture Flagship, Canberra.
- Burkhard, B., and Müller, F. (2008). Drivers-Pressure-State-Impact-Response. In *Ecological Indicators. Volume 2 of Encyclopedia of Ecology* (Eds: Jorgensen, S.E., and Fath, B.D.). Elsevier. ISBN 978-0-08-045405-4
- CAPAD (2018). *Collaborative Australian Protected Area Database*: <https://www.environment.gov.au/land/nrs/science/capad>
- Carson, R. (1962). *Silent Spring*. Penguin, Reading, UK.
- Clarke, C.J., George, R.J., Bell, R.W., and Hatton, T.J. (2002). Dryland salinity in south-western Australia: its origins, remedies, and future research directions. *Australian Journal of Soil Research*, 40(1), 93–1113.
- Clancy, T.F., and Lesslie, R.G. (2013). *A scoping assessment for a national research centre addressing land use and food security issues*. Canberra, ACT: Department of Agriculture, Fisheries and Forestry.
- CLUM (2017). *Catchment Scale Land Use of Australia—Update September 2017*. Australian Bureau of Agriculture and Resource Economics and Sciences: <https://data.gov.au/dataset/ds-dga-c128490d-fb8f-49eb-9757-3ca1350b87c8/details>
- Cork, S., Eadie, L., Mele, P., Price, R., and Yule, D. (2012). *The relationships between land management practices and soil condition and the quality of ecosystem services delivered from agricultural land in Australia*. Kiri-ganai Research Pty Ltd, Canberra.
- CSIRO (2020). *ePaddocks™* webpage, Commonwealth Scientific and Industrial Research Organisation website: <https://research.csiro.au/digiscape/digiscapes-projects/epaddocks-mapping-every-paddock-across-the-australian-grain-region/>
- CTA (2018). *Index-Based Livestock Insurance as an Innovation Tool against Drought Loss*. Technical Centre for Agricultural and Rural Cooperation. ISBN 978-92-9081-636-2
- DEWHA (2010). *Ecosystem Services: Key Concepts and Applications*. Occasional Paper No 1, Department of the Environment, Water, Heritage and the Arts, Canberra.
- FAO (2009). *How to Feed the World in 2050*. UN Food and Agriculture Organization: http://www.fao.org/fileadmin/templates/wsfs/docs/expert_paper/How_to_Feed_the_World_in_2050.pdf
- FAO (2017). *Review of the Available Remote Sensing Tools, Products, Methodologies and Data to Improve Crop Production Forecasts*. UN Food and Agriculture Organization, Rome. ISBN 978-92-5-109840-0.
- FAO (2020a). *The State of Food Security and Nutrition in the World 2020*. UN Food and Agriculture Organization, Rome. <http://www.fao.org/3/ca9692en/online/ca9692en.html>
- FAO (2020b). *Suite of food security indicators: domestic food price volatility (index)/value*. UN Food and Agriculture Organization, Rome. <http://www.fao.org/faostat/en/#data/FS>
- Farmar-Bowers, Q., Higgins, V, and Millar, J. (Eds) (2013). *Food Security in Australia*. Springer. 476 p. doi:10.1007/978-1-4614-4484-8
- Friedel, M.H., Laycock, W.A, and Bastin, G.N. (2000). Assessing rangeland condition and trend. In *Field and Laboratory Methods for Grassland and animal Production Research*. (Eds: Mannelje, L.T., and Jones, R.M.). CABI publishing, New York. pp 29–66.
- Galbraith, S.M., Vierling, L., and Bosque-Pérez, N. (2015). Remote sensing and ecosystem services: current status and future opportunities for the study of bees and pollination-related services. *Current Forestry Reports*, 1(4), 261–274. doi:10.1007/s40725-015-0024-6

- Garibaldi, L.A., Aizen, M.A., Klein, A.M., Cunningham, S.A., and Harder, L.D. (2011). Global growth and stability of agricultural yield decrease with pollinator dependence. *Proceedings of National Academy of Science*, 108, 5909–5914. <https://doi.org/10.1073/pnas.1012431108>
- GEO (2019). *Essential Agricultural Variables for GEOGLAM—White Paper*. Group on Earth Observations, Draft, 27 March 2019. http://earthobservations.org/geoglam_resources/3%20Earth%20Observation%20Data%20Coordination/Draft%20EAV%20White%20Paper.pdf
- Ghassemi, F., Jakeman, A. J., & Nix, H. A. (1995). *Salinisation of land and water resources: human causes, extent, management and case studies*. The Australian National University, Canberra, Australia; CAB International, Wallingford, Oxon, UK.
- Guerschman, J., Leys, J., Rozas Larraondo, P., Henrikson, M., Paget, M., and Barson, M. (2018). *Monitoring groundcover: an online tool for Australian regions*. CSIRO, Canberra. <https://doi.org/10.25919/5bf84026e556d>
- Hendy, E.J., Gagan, M.K., and Lough, J.M. (2003). Chronological control of coral records using luminescent lines and evidence for non-stationary ENSO teleconnections in northeast Australia. *Holocene*, 13, 187–199.
- ILRI (2020). *International Livestock Research Institute website*: <https://www.ilri.org/about-us>
- IPBES (2017). *Assessment Report on Pollinators, Pollination and Food Production*. Intergovernmental Science-Policy Platform on Biodiversity and Ecosystem Services, Zenodo. <http://doi.org/10.5281/zenodo.3402857>
- Jacobson, T., and Adams, R.M. (1958). Salt and silt in ancient Mesopotamian agriculture. *Science*, 128(3334), 1251–1258.
- Kearns, C.A., Inouye, D.W., and Waser, N. (1998). Endangered mutualisms: the conservation of plant-pollinator interactions. *Annual Reviews of Ecological Systems*, 29, 83–112. doi:10.1146/annurev.ecolsys.29.1.83
- Klein, A.M., Vaissiere, B.E., Cane, J.H., Steffan-Dewenter, I., Cunningham, S.A., Kremen, C., and Tscharntke, T. (2007). Importance of pollinators in changing landscapes for world crops. *Proceedings of Royal Society B*, 274, 303–313.
- Kogan, F. (2019). *Remote Sensing for Food Security*. Springer International Publishing, Switzerland. ISBN 978-3-319-96255-9
- Lang, D. (2005). Maintaining groundcover to reduce erosion and sustain production. *Agfacts P2.1.14*, NSW Department of Primary Industries. https://www.dpi.nsw.gov.au/_data/assets/pdf_file/0018/162306/groundcover-for-pastures.pdf
- Leys, J.F. (1991). The threshold friction velocities and soil flux rates of selected soils in south-west New South Wales. Australia. *Acta Mechanica*, 2, 103–112.
- Leys, J., McTainsh, G., Strong, C., Heidenreich, S., Biesaga, K. (2008). DustWatch: using community networks to improve wind erosion monitoring in Australia. *Earth Surface Processes and Landforms*, 33, 1912–1926. <https://doi.org/10.1002/esp.1733>
- Leys, J.F., Heidenreich, S.K., Strong, C.L., McTainsh, G.H., and Quigley, S. (2011). PM10 concentrations and mass transport during ‘Red Dawn’ Sydney September 2009. *Aeolian Research*, 3, 327–342. doi:10.1016/j.aeolia.2011.06.003
- Leys, J., Strong, C., Heidenreich, S., and Koen, T. (2018). Where She Blows! A Ten Year Dust Climatology of Western New South Wales Australia. *Geosciences*, 8, 232. doi:10.3390/geosciences8070232
- Leys, J.F., Howorth, J.E., Guerschman, J.P., Bala, B., and Stewart, J.B. (2020). *Setting targets for National Landcare Program monitoring and reporting vegetation cover for Australia*. NSW Department of Planning, Industry, and Environment.
- Lindberg, R., Lawrence, M., Gold, L., Friel, S., and Pegram, O. (2015). Food insecurity in Australia: Implications for general practitioners. *Australian Family Physician*, 44(11), 859–862. <https://www.racgp.org.au/afp/2015/november/food-insecurity-in-australia-implications-for-general-practitioners/#2>
- Mace, G.M., and Baillie, J.E.M. (2007). The 2010 Biodiversity Indicators; Challenges for Science and Policy. *Conservation Biology*, 21(6), 1406–1413.
- Martin, W., and Laborde, D. (2018). The free flow of goods and food security and nutrition. Ch 3 in *2018 Global food policy report*. pp. 20–29. Washington, DC: International Food Policy Research Institute (IFPRI). https://doi.org/10.2499/9780896292970_03
- Masó, J., Serral, I., Domingo-Marimon, C., and Zabala, A. (2020). Earth observations for sustainable development goals monitoring based on essential variables and driver-pressure-state-impact-response indicators. *International Journal of Digital Earth*, 13(2), 217–235. <https://doi.org/10.1080/17538947.2019.1576787>
- McCrindle (2017). *Foodbank Hunger Report 2017*. https://2qean3b1j1d1s87812ool5ji-wpengine.netdna-ssl.com/wp-content/uploads/2018/04/Foodbank_HungerReport_McCrindle_Oct2017_Digital.pdf

- McKeon, G.M., Hall, W.B., Henry, B.K., Stone, G.S., and Watson, I.W. (2004). *Pasture Degradation and Recovery in Australia's Rangelands: Learning From History*. Queensland Department of Natural Resources, Mines and Energy, Brisbane.
- Metternicht, G.I., and Zinck, J.A. (2003). Review article. Remote sensing of soil salinity: potentials and constraints. *Remote Sensing of Environment*, 85, 1–20.
- Moltmann, T., Turton J., Zhang, H.-M., Nolan, G., Gouldman, C., Griesbauer, L., Willis, Z., Piniella, Á.M., Barrell, S., Andersson, E., Gallage, C., Charpentier, E., Belbeoch, M., Poli, P., Rea, A., Burger, E.F., Legler, D.M., Lumpkin, R., Meinig, C., O'Brien, K., Saha, K., Sutton, A., Zhang, D., and Zhang, Y. (2019). A Global Ocean Observing System (GOOS), Delivered Through Enhanced Collaboration Across Regions, Communities, and New Technologies. *Frontiers in Marine Science*, 6, 291. <https://www.frontiersin.org/article/10.3389/fmars.2019.00291>
- Nikolova, S., Bruce, S., Randall, L., Barrett, G., Ritman, K., and Nicholson, M. (2012). *Using remote sensing data and crop modelling to improve crop production forecasting: a scoping study*. ABARES technical report 12.3. Australian Bureau of Agricultural and Resource Economics and Sciences, Canberra.
- NLWRA (2001). *Australian dryland salinity assessment 2000: extent, impacts, processes, monitoring and management options*. National Land and Water Resources Audit, Canberra.
- OECD. (1993). *OECD Core Set of Indicators for Environmental Performance Reviews. A Synthesis Report by the Group on the State of the Environment*. OCDE/GD(93)179. Organisation for Economic Co-operation and Development, Paris. 35 p
- Ogilvy, S. (2020). *Toward a methodology for incorporating ecological capital into the accounts of individual entities*. Ph.D. Thesis, ANU. <https://openresearch-repository.anu.edu.au/handle/1885/204830>
- Ogilvy, S., Kulkarni, A., and Hurley, S. (2015). *From vicious to virtuous cycles: a sustainable future for Australian agriculture*. CPD discussion paper, August 2015. <https://cpd.org.au/wp-content/uploads/2015/08/Vicious-to-virtuous-cycles-2015.pdf>
- O'Loingsigh, T., Chubb, T., Baddock, M., Kelly, T., Tapper, N.J., De Deckker, P., and McTainsh, G. (2017). Sources and pathways of dust during the Australian "Millennium Drought" decade. *Journal of Geophysical Research: Atmospheres*, 122, 1246–1260. doi:10.1002/2016JD025737.
- Patias, P., Verde, N., Tassopoulou, M., Georgiadis, C., and Kaimaris, D. (2019). Essential variables: describing the context, progress, and opportunities for the remote sensing community. *Proceedings of Society of Photo-Optical Instrumentation Engineers (SPIE) 11174*, Seventh International Conference on Remote Sensing and Geoinformation of the Environment (RSCy2019),111740C (27 June 2019). <https://doi.org/10.1117/12.2533604>
- Pereira, H.M., Ferrier, S., Walters, M., Geller, G.N., Jongman, R.H.G., Scholes, R.J., Bruford, M.W., Brummitt, N., Butchart, S.H.M., Cardoso, A.C. (2013). Essential biodiversity variables. *Science*, 339, 277–278.
- Pitman, M.G., and Läuchli, A. (2002). *Global Impact of Salinity and Agricultural Ecosystems*. Ch 1 in *Salinity: Environments—Plants—Molecules*. (Eds: Läuchli, A., and Lüttige, U.). Kluwer Academic Publishers, Netherlands.
- PMSEIC (2010). *Australia and Food Security in a Changing World. Can we feed ourselves and help feed the world in the future?* The Prime Minister's Science, Engineering and Innovation Council, Canberra, Australia. https://www.chiefscientist.gov.au/sites/default/files/FoodSecurity_web.pdf
- Ponting, C. (1991). *A Green History of the World*. Penguin.
- Potts, S.G., Imperatriz-Fonseca, V., Ngo, H.T., Zizen, M.A., Biesmeijer, J.C., Breeze, T.D., Dicks, L.V., Garibaldi, L.A., Hill, R., Settele, J., and Vanbergen, A.J. (2016). Review: Safeguarding pollinators and their value to human well-being. *Nature*, 540, 220–229. <https://doi.org/10.1038/nature20588>
- Ramankutty, N., Mehrabi, Z., Waha, K., Jarvis, L., Kremen, C., Herrero, M., and Rieseberg, L.H. (2018). Trends in Global Agricultural Land Use: Implications for Environmental Health and Food Security. *Annual Review of Plant Biology*, 69(1), 789–815.
- Reinhart, K.O. (2009). Rangeland Communities: Structure, Function and Classification. Ch 6 in *Range and Animal Sciences and Resources Management*. Eolss Publishers, Oxford, UK.
- SOE (2016a). *Soil: Formation and erosion*, State of Environment 2016 website: <https://soe.environment.gov.au/theme/land/topic/2016/soil-formation-and-erosion>
- SOE (2016b). *Soil: Salinity and acidification* webpage, State of Environment 2016 website: <https://soe.environment.gov.au/theme/land/topic/2016/soil-salinity-and-acidification>

- Song, X.-P., Potapov, P.V., Krylov, A., King, L., Di Bella, C.M., Hudson, A., Khan, A., Adusei, B., Stehman, S.V., and Hansen, M.C. (2017). National-scale soybean mapping and area estimation in the United States using medium resolution satellite imagery and field survey. *Remote Sensing of Environment*, 190, 383–395.
- Spies, B., and Woodgate, P. (2005). *Salinity Mapping Methods in the Australian Context*. Report prepared for Programs Committee of Natural Resource, Department of Environment, Heritage, Agriculture, Fisheries and Forestry, Canberra. ISBN: 0 642 55128 6
- Tongway, D.J., and Hindley, N.L. (2004). *Landscape Function Analysis Manual: Procedures for Monitoring and Assessing Landscapes with Special Reference to Minesites and Rangelands, Version 3.1*. CD-ROM. CSIRO Sustainable Ecosystems, Canberra.
- Tozer, P., and Lees, J. (2013). Dust storms—what do they really cost?. *The Rangelands Journal*, 35, 131–142.
- Waldner, F., and Diakogiannis, F. I. (2020). Deep learning on edge: extracting field boundaries from satellite images with a convolutional neural network. *Remote Sensing of Environment*, 245, 111741.
- Washington-Allen, R.A., and Ravi, S. (2012). Dryland Analysis and Monitoring. Ch in *Range and Animal Sciences and Resources Management—Volume II*. UNESCO-EOLSS.
- Whitcraft, A.K., Becker-Reshef, I., Justice, C.O., Gifford, L., Kavvada, A., and Jarvis, I. (2019). No pixel left behind: Toward integrating Earth Observations for agriculture into the United Nations Sustainable Development Goals framework. *Remote Sensing of Environment*, 235, 111470. <https://doi.org/10.1016/j.rse.2019.111470>
- Willcox, B.K., Robson, A.J., Howlett, B.G., and Rader, R. (2018). Toward an integrated approach to crop production and pollination ecology through the application of remote sensing. *PeerJ*, 6:e5806. DOI 10.7717/peerj.5806
- Wu, B., Meng, J., Li, Q., Yan, N., Du, X., and Zhang, M. (2014). Remote sensing-based global crop monitoring: experiences with China's CropWatch system. *International Journal of Digital Earth*, 7(2),113–137. DOI 10.1080/17538947.2013.821185
- Zaman, M., Shahid, S.A., Heng, L. (2018). *Guideline for Salinity Assessment, Mitigation and Adaptation Using Nuclear and Related Techniques*. Springer Open. <https://doi.org/10.1007/978-3-319-96190-3>



12 Crops

Barbara Harrison and Graham Donald

This section focuses on the use of EO datasets to map and monitor food crops, both in Australia and globally. EO technologies now feature in the management of a wide range of Australian crops, including cereals, legumes, vegetables, fruits, nuts, and other seeds.

As introduced in Section 10.2.2, Crop Simulation Models (CSM) simulate the growth, development and yield of crops as a function of soil conditions, weather and management practice (Hoogenboom *et al.*, 2004). These models allow observations at specific ground sites to be extrapolated temporally to improve our understanding of the interactions between physiological processes and agronomic activities.

In conjunction with historical yield datasets and meteorological records, CSM can be used to estimate yield for larger areas (see Section 11.2). EO-based datasets are increasingly being integrated with CSM to derive surrogates of crop growth, such as Leaf Area Index (LAI) (see Section 6.3.3). Some of the methods used to achieve this integration are reviewed in FAO (2017).

Forecasting crop production (and crop yield in particular) has been a constant concern since the beginning of the history of agriculture. Forecasting techniques have evolved, as has agriculture itself and the specifications of the forecasts needed. Those who use forecast data are always seeking greater accuracy, granularity, comparability, and timeliness. Those who produce the data or contribute to their production always operate under financial and technical constraints. Obtaining timely knowledge presents a very real challenge.

(FAO, 2016)

12.1 Crops in Australia

Weather and climatic conditions split the Australian continent into two growing regions (northern and southern) and two growing seasons (summer and winter) for crops (see Figure 2.6, Figure 2.10 and Figure 2.11). The northern region, which spans central and southern Queensland and northern NSW, has summer rains, so grows a dryland summer crop (sorghum, sunflowers, maize, mungbeans, soybeans, cotton, and peanuts) in addition to a winter crop (wheat, barley, oats, chickpeas, triticale, faba beans,

lupins, field peas, canola, millet/panicum, safflower, and linseed). Southern regions, including central NSW to Victoria, Tasmania, southern SA and southwest WA, have a Mediterranean climate with dry summers and winter rainfall. These areas principally grow winter crops (wheat, barley, oats, triticale, cereal rye, lupins, field peas, canola, chickpeas, faba beans, vetch, lentils, and safflower) and require irrigation for summer crops (rice and maize; Australian Grain, 2019a).

Background image: Canola crop near Kojonup, WA, photographed on 28 February 2013. Source: Keith Lightbody, Wikimedia Commons. (Retrieved from https://commons.wikimedia.org/wiki/File:Canola_crop_near_Kojonup.jpg)

Recommended Chapter Citation: Harrison, B.A., and Donald, G.E. (2021). Crops. Ch 12 in *Earth Observation: Data, Processing and Applications. Volume 3A—Terrestrial Vegetation*. CRC SI, Melbourne. pp. 249–262.

An area covering 19 million ha was planted to cereal, legume and oil crops in Australia during 2018, which produced a total of 33 million tonnes (Australian Grain, 2019b)⁹. Over half of this area grew wheat, which delivered around 3% of global production. Wheat is a major export crop for Australia, with only about 30% of production being destined for the domestic market (AEGIC, 2020).

The horticultural industry in Australia produces fruit, vegetables, nuts, flowers, turf, and nursery products for both domestic and international markets (DAWR, 2016). Horticulture comprises the second largest rural production industry after wheat (AuSHS, 2019), with the major crops by area being grapes, apples, bananas, and potatoes (Nikolova *et al.*,

2012). The major horticulture growing areas are located in the naturally well-watered and/or irrigated locations of:

- Goulburn Valley of Victoria;
- Murrumbidgee Irrigation Area of New South Wales (NSW);
- Sunraysia district of Victoria and NSW;
- Riverland region of South Australia;
- northern Tasmania;
- southwest Western Australia; and
- coastal strips of both northern NSW and Queensland (DAWR, 2016; see Figure 11.1).

12.2 EO Sensors for Crops

A range of platforms (proximal, airborne and spaceborne; see Volume 1A—Sections 10–12) and sensors (active and passive; see Volume 1A—Sections 13–16 and Volume 1B—Sections 6–8) are being used to observe terrestrial vegetation. The EO datasets acquired by these sensors vary in terms of their spectral, spatial, radiometric, and temporal resolutions, densities and extents (see Volume 1B—Section 1) and fidelity (see Volume 1B—Section 2.1). Some characteristics of EO sensors that are relevant to studies of agricultural crops are summarised in Table 12.1. As with all EO analyses, validation of results using independent datasets is

essential (see Volume 2D—Section 12 and Volume 2E). Recommended validation procedures to use with EO datasets are detailed in TERN Australia (2018) and Malthus *et al.* (2013).

The major EO sensors used to map and monitor agricultural crops have traditionally detected optical reflectances. The most commonly used approaches for mapping vegetation biomass fundamentally detect the differences between red and near infrared (NIR) reflectance (see Section 8.1.1). EO-based estimates of ET are also used to monitor irrigation requirements (Abuzar *et al.*, 2019; see Sections 9.4, 9.5 and 13).

Table 12.1 EO sensors relevant to crops

TIR: Thermal infrared; SAR: Synthetic Aperture Radar; DEM: Digital Elevation Model; ET: Evapotranspiration

Type	Sensor	Platform	Relevance	Advantages	Disadvantages
Passive optical	Multispectral radiometer	Satellite or airborne	National or regional land cover mapping	Global, recurrent coverage, low cost;	Low accuracy, coarse scale
	Hyperspectral spectroradiometer	Airborne	Crop mapping, intensive agriculture Plant biochemical functioning and health	High spectral resolution, highlight plant stress	High cost, high data volume
	TIR radiometer	Field, satellite or airborne	Soil/canopy temperature, water stress	Surrogate measure for ET	Resolution depends on platform
Active optical	Lidar	Airborne and terrestrial	Crop structure DEM	Detailed structure for plant canopy and soil surface	High cost, specialised processing
	Active optical sensors	Ground vehicles or RPAS	Crop cover and condition mapping	Convenience, low cost, independent of sunlight	Low availability
Active microwave	SAR	Satellite or airborne	Vegetation structure, soil moisture	All weather, operates at night	Data availability, noisy data, complex processing
Proximal	Passive optical sensors (phenocam, hyperspectral), meteorological sensors (including soil moisture)	Ground, tractor or tower-based (see Excursus 7.2 and Volume 2D—Section 12)	Soil, crop, and atmospheric variability, Phenology	Continuous, long term measurements	High cost and require skilled maintenance
Locational	GPS	Portable devices	Locating field sites	Low cost	Coverage in remote regions or below dense canopies

⁹ Please note: The 2018 cropping area was below the average of 22 million ha due to a prolonged drought.

SAR sensors detect characteristics of both soil and vegetation (see Volume 1B—Section 8). Satellite-based SAR is used to monitor agricultural and land cover practices at both global and regional scales, assess soil moisture status, and quantify plant biomass (Zhou *et al.*, 2016). Multi-temporal datasets of integrated optical and SAR imagery have delivered operational inventories of major crops in Canada for a range of cropping systems (McNairn *et al.*, 2008).

Cereal crops in Australia cover thousands of hectares so are often mapped using satellite imagery whereas horticultural crops are grown in smaller areas and generally require imagery acquired by aircraft. The principal satellite sensors that are used for crop mapping and yield estimation are Landsat, MODIS, and Sentinel, all of which are broadband optical sensors with adequate spatial coverage and temporal frequency (see Section 11.2). Accurate monitoring of crop nutrition has been demonstrated using airborne hyperspectral imagery (see Section 9.6 and Volume 1A—Section 14; Pullanagari *et al.*, 2016), which is particularly valuable for varying fertiliser applications in precision agriculture (Cilia *et al.*, 2014).

Traditional EO-based monitoring of agricultural vegetation observes crop greenness and temperature as indicators of biomass, vigour, and water stress (see Sections 8 and 9 above). More recent approaches focus on nutrient status, principally nitrogen, but also phosphorus and potassium (see Section 5.3.5 and 9.6). Aerial and ground-based gamma radiometry have also been trialled for mapping soil properties (Hall *et al.*, 2014; see Volume 1A—Section 6). New proximal sensors, such as soil pH sensors and Electromagnetic Induction (EMI) sensors, are also being deployed to monitor the impact of soil condition on crops. By mapping the apparent electrical

conductivity, electromagnetic induction (EMI) sensors (such as EM38) can be used to highlight the spatial variations in clay, salt, and moisture content of soils (Stanley *et al.*, 2014; Heil and Schmidhalter, 2017).

A range of active and passive sensors that are being used for precision agriculture are reviewed in Suarez *et al.* (2018). Other digital innovations being embraced by precision agriculture, such as using Variable Rate Technology (VRT) rather than the traditional uniform application of fertilisers, are designed to control the efficient use of inputs for maximised outputs (see Section 12.6). Terrestrial Laser Scanning (TLS) and Airborne Laser Scanning (ALS) have also been successfully trialled for mapping tree structure in avocado, macadamia, and mango orchards in Australia (Wu *et al.*, 2020; see Excursus 5.1).

An increasing number of growers are using unmanned aerial vehicles (UAV, commonly called drones; see Volume 1A—Section 11.2), carrying multispectral, hyperspectral, and thermal sensors, to monitor the health, nutrient status, and yield of horticultural crops (see Section 11.5). Since these platforms are typically flown at low altitude for agricultural applications, the acquired sensor measurements are minimally impacted by atmospheric effects. UAV-acquired datasets are also being used to ground truth crop mapping from satellite imagery (Hegarty-Craver *et al.*, 2020).

A new area of research for crops is solar induced chlorophyll fluorescence (SIF), which is a direct measure of photosynthetic activity (Mohammed *et al.*, 2019; see Section 17.3.2). SIF can be detected using optical sensors (especially hyperspectral). Several satellites can currently be used to do this but there are few bespoke SIF systems planned for future launch.

12.3 Crop Type and Agricultural Land Use

Crop type mapping is valuable for a wide range of crops in Australia. Growers, distributors and consumers all directly benefit from efficiencies derived from knowledge of crop extent, timing, vigour, variability, and yield, while indirect benefits extend to efficient responses to biosecurity threats and natural disasters.

A range of EO methods for mapping land cover have been used to map agricultural land uses and different types of crops (see Section 3). Early mapping of agricultural land cover used the Normalised Difference Vegetation Index (NDVI; see Section 8.1.1; Hill *et al.*, 1999) and image classification (Hill *et al.*, 2005). More recently, EO time series datasets have enabled more sophisticated analyses, both for mapping crop type, and also for quantifying crop condition and predicting crop yield (see Section 12.4).

The optimum timing of EO image acquisition to differentiate between crops, and separate yield categories for a single crop, varies considerably with both crop and growing region (Van Niel and McVicar, 2003, 2004). Single date analyses can be misleading if the image date is not indicative of the crop peak growth stage. The best relationships between vegetation indices and crop yield for grain crops have been observed when the image is acquired at the mid grain-filling stage (Shanahan *et al.*, 2001; Panek and Gozdowski, 2020; see Section 9.3). However, temporal characteristics of crops can vary from year to year, depending on sowing dates and other management practices, and also climatic variations between seasons.

Some recent approaches that have been developed to differentiate agricultural crops using EO datasets in Australia include:

- applying geostatistical concepts to EO time series to differentiate broad crop groups (Pringle *et al.*, 2018);
- applying curve fitting methods to EO time series to characterise the phenology of specific crops, then use these characteristics to discriminate between crops and estimate crop areas (Potgieter *et al.*, 2013);
- deriving climate-driven, crop-specific stress indices to explain the influence of agro-environmental heterogeneity in croplands at finer spatial scales (Chen *et al.*, 2020a);
- monitoring fallow dynamics using biased support vector machines (see Volume 2E) with fractional cover images (see Excursus 8.3; Zhao *et al.*, 2020);
- classifying summer cropping in irrigated areas of the Murray-Darling Basin (MDB; see Section 2.1 and Figure 2.4) using a random forest model (see Volume 2E) with EO-based estimates of vegetation phenology and water use (Peña-Arancibia *et al.*, 2014);
- using balancing methods to more accurately classify rare and infrequent crops (Waldner *et al.*, 2019); and
- refining criteria for using blended datasets (see Volume 2D—Section 6) to increase the density of EO time series datasets for crop identification and yield prediction (Chen *et al.*, 2020b).

12.4 Crop Extent, Condition and Production Forecasts

Two of the most established applications of EO datasets are mapping crop area and forecasting crop yield. As crops mature the spectral characteristics of vegetation vary temporally with phenological changes (see Sections 5.3.2 and 9.3). They also vary both temporally and spatially with changes in ambient environmental conditions (see Volume 1B—Section 1). EO datasets allow these variations to be mapped through time to analyse a single growing season and/or trends across several seasons. The spatial variations in EO imagery, within individual crop fields and districts, can highlight infestations of weeds, diseases in plants and soils, and deficiencies in water or nutrients.

Traditionally, such analyses relied on correlations between EO-based greenness indices and crop yield (see Volume 2C—Section 11 and 8.1.1). One of the spectral indices that is commonly used for crop mapping is NDVI (see Section 8.1.1), which is considered a surrogate for LAI or fAPAR (fraction of Absorbed Photosynthetically Active Radiation; see Section 6.3; FAO, 2017). The most appropriate spectral information and algorithms to correlate with crop yield, however, vary with crop type, season, age, condition, and location, with stressed situations being more challenging (Suarez *et al.*, 2018). When based on spectral indices, the most appropriate index is typically selected as the one with the highest correlation with yield data, then index values for a crop image can be classified into appropriate categories such as low, medium, and high (see

Volume 1B—Excursus 9.1). While originally such methods were applied to broadacre cereal crops, principally wheat and rice (Tucker *et al.*, 1980), more recently higher resolution imagery has enabled this approach to be used with a range of fruit, nut, and vegetable crops (see Section 12.6). Other EO-based approaches to yield mapping include image classification (see Volume 2E), machine learning regression methods (Kamir *et al.*, 2020), semi-empirical models (Chen *et al.*, 2020a), and integrated crop models, which combine relevant spectral indices with predictive models (Schut *et al.*, 2009).

For example, Crop-SI is a semi-empirical model that is used to estimate the yield of wheat, barley, and canola crops in the dryland Australian wheatbelt (Chen *et al.*, 2020a). It combines a radiation use efficiency model with meteorology-driven Stress Indices (SI) at critical crop growth stages (e.g. anthesis and grain-filling; see Table 12.2). These crop-specific SI (e.g. drought, heat, and cold stress) help explain the impact of high spatial agro-environmental heterogeneity, which has led to substantial improvement in grain yield prediction.

Another example of EO-based yield forecasting in Australia is SugarMaps, a prototype system which provides automated processing and delivery of EO imagery to over 95% of the sugar industry. Products include crop vigour, derived yield, and qualitative foliar nitrogen concentration maps for most Australian growing regions (UNE CASI, 2020).

Timely and reliable crop production forecasts are crucial to making informed food policy decisions and enabling rapid responses to emerging food shortfalls.

(FAO, 2017)

Table 12.2 Crop-SI model

Approach	Input parameters	Derived parameters	Result
Radiation Use Efficiency (RUE)	Top of atmosphere shortwave irradiance	Photosynthetically Active Radiation (PAR)	Carbon fixation Grain yield estimate
	Ratio of irradiance at sloping surface to that at a horizontal surface		
	Atmospheric transmissivity		
	NDVI	fraction of Absorbed Photosynthetically Active Radiation (fAPAR)	
	Diffuse fraction	RUE	
	Photosynthetic capacity		
Support Vector Machine (SVM) feature selection	Air temperature	Meteorologically-driven Stress Index (SI)	
	Precipitation		

Source: Chen *et al.* (2020) Figure 2

Automated mapping of paddock boundaries helps farmers to monitor productivity and land condition at a relevant scale. A new Digiscape project, ePaddocks™, uses artificial intelligence to interpret high spatial resolution satellite imagery in order to define paddock boundaries (CSIRO, 2020a; Waldner and Diakogiannis, 2020; see page before Section 11). This facility is being applied across the Australian grain region and will be integrated with other EO-based systems to classify land use and identify crop types (see Sections 3 and 12.3). The benefits (to both individual farmers and the wider agricultural sector) of focusing yield forecasts on individual land parcels include land management, harvest logistics, and financial analysis.

For a selected crop in a given season, integrated forecasting systems aim to deliver near real time estimates of crop area, which can be merged with near real time predictions of yield, to determine the likely total production (Nikolova *et al.*, 2012). Traditionally, most estimates of crop yield and production have been derived from climate-driven models, with expert knowledge supplying estimates of planted area and production rates. Such models, however, cannot account for unexpected changes in seasonal conditions during the forecast period, such as natural disasters, and are typically less accurate for winter cropping. In Australia, different crop forecasting methods are used in different regions and jurisdictions, and plans are underway to develop a nationally-consistent approach for all major crops (Nikolova *et al.*, 2012). Increasingly EO-based datasets and biophysical crop growth models are being integrated with agroclimatic models, and crop, soil, and management datasets, to improve the accuracy, frequency, and latency of spatially-explicit, agricultural forecasts at regional, national, and global

scales. Ultimately such systems enable mapping of crop type, area, condition and yield, and forecasting of crop production on a regional and global basis (FAO, 2017; see Section 12.5.).

Meteorological datasets are valuable in crop monitoring, not only to track production but also to warn of potentially damaging weather condition. For example, the Australian Tree Crop Map Severe Weather App integrates live weather data with maps of commercial horticulture tree crops (avocado, banana, citrus, macadamia, mango, and olive) to provide early warning of possible storm damage (see Section 12.7).

The type and precision of crop forecasting varies with the purpose and scale of analysis from global predictions to farm-based estimates (see Table 12.3). In recent years, improvements in near real time crop-specific monitoring at regional and national scales, including crop type mapping and vegetation status, have been achieved using high resolution, satellite-derived EO imagery and automated workflows (Inglada *et al.*, 2015; Defourny *et al.*, 2019). These products provide valuable input to global monitoring initiatives such as GEOGLAM (see Excursus 11.1).

While many existing crop yield models have not scaled up from field to regional scales with sufficient accuracy, some recent, scalable crop yield models are showing promise in this area (Lobell *et al.*, 2015; Donohue *et al.*, 2018). However, the utility of crop models is determined by both their spatial and temporal scales. Since the primary goal of these models is to reduce risk in all steps along the food supply chain from farm to market, timeliness in delivering results—particularly minimum latency—is essential to all users (FAO, 2016). An Australian system that delivers multi-scale, real time forecasting of yield for cereal crops is introduced in Excursus 12.1.

Table 12.3 Scales of crop forecasting

Ground scale	User	Decision	EO spatial resolution
Field	Farmer	Crop and resource management	Very high
Farm	Producers, suppliers	Business, marketing, supply chain	High
Agroecological zone	Districts, farmer co-ops	Economic optimisation, environmental management	Medium
Regional	State/regional agencies	Land use and economic planning, environmental management	Medium
National	Governments	Food security, disaster relief, strategic planning, trade policy, environmental impact and policy	Low
Global	International agencies, multinational companies	International treaties, protocols, global treaties	Very low

Adapted from: FAO (2016) and Potgieter *et al.* (2013) Figure 1

Excursus 12.1—Graincast

Source: CSIRO (2020b)

Graincast™ uses national weather and soils information to estimate the soil moisture that is available to plants on a daily basis, and the crop yield potential for the current season. This estimate can apply to an individual paddock, a farm, a region, or a nation. Graincast™ provides objective information for farmers and land managers to make better informed management decisions in near real time.

Inputs to Graincast™ include:

- daily rainfall, temperature, and solar radiation data at 5 km resolution from the Bureau of Meteorology (BoM, 2020);
- climate data from SILO (Scientific Information for Land Owners) climate database at 5 km resolution (Queensland Government, 2020); and
- soil data from the Soil and Landscape Grid of Australia (SLGA; Grundy *et al.*, 2015) at 90 m resolution.

These data layers are integrated with cadastre, elevation, and/or EO datasets to generate multiple outputs:

- maps of crop species growing in each paddock derived using adaptive learning algorithms applied to available optical and SAR images from the Landsat-8 and Sentinel-2 satellites;
- estimates of yield potential and ‘plant available soil water’ for the current season calculated using the APSIM (Agricultural Production Systems simulator) crop model (Holzworth *et al.*, 2014, 2018; see Section 10.2.2) based on the SLGA and SILO datasets;

- time series of historical water-limited, potential yield estimates for a particular paddock, to assist with benchmarking, diagnosing yield constraints and setting yield targets; and
- seasonal yield forecasts derived using real time crop models based on NDVI computed from multiple satellite images (Donohue *et al.*, 2018).

Since APSIM needs to estimate the daily dynamics of plant available water (PAW) to simulate crop growth under the current seasonal conditions, Graincast™ can also be used to provide an estimate of PAW in real time, without the need for local knowledge of the actual soil type in each paddock. Such estimates of PAW often provide better estimates of soil water than a single, poorly calibrated, standalone, soil water sensor (Freebairn *et al.*, 2018).

At this stage of development, Graincast™ forecasts are based on known conditions to the date of publication and the probable conditions to harvest based on the previous 30 years. Extreme events, such as severe frosts, heat shocks, floods, and hail storms, can have significant local implications that are not included in the forecasts and may result in lower than forecast yields if they are more widespread than usual. Also, forecasts do not account for large scale outbreaks of pests or diseases which may also result in lower than forecast yields.

12.5 Global Crop Monitoring Systems

The original large scale study of global wheat production, the Large Area Crop Inventory Experiment (LACIE; MacDonald *et al.*, 1975; Erickson, 1984), achieved its goals to:

- demonstrate that multispectral, EO from space was economical, timely, and repeatable;
- forecast the global wheat crop area, yield, and production using Landsat-2 MSS imagery and NOAA meteorological data, together with climatological and conventional data sources; and
- validate techniques to deliver timely estimates of crop production (Erickson, 1984).

This pioneering project paved the way for many more precise and accurate EO-based crop models, whose results can be directly interpreted in terms of economic outcomes (see Section 10.2.2). Sophisticated modelling approaches have been developed using EO time series datasets, integrated with meteorological records and soil surveys, to monitor and profile crop productivity through time (FAO, 2016). For example, eight global and regional agricultural monitoring systems, reviewed by Fritz *et al.* (2019), are summarised in Table 12.4. These systems enable early warnings of potential food famines to be coordinated and disseminated efficiently (Atzberger, 2013) by monitoring weather conditions and crop growth, then highlighting anomalies in key indicators such as precipitation, Land Surface Temperature (LST; see Section 7.5), and NDVI (FAO, 2017). In addition to essential input from analysts to vet input data, guide processing, and check results, agricultural monitoring systems now rely on four major sources of information:

- meteorological—e.g. precipitation, temperature, evapotranspiration, solar radiation, relative humidity, wind speed, snow cover, atmospheric pressure (many of these parameters are also derived from EO sensors);
- optical satellite EO—e.g. vegetation indices, soil moisture;
- crop models—e.g. water balance, biophysical; and
- auxiliary datasets—e.g. cadastre, elevation, census, climatic/agroecological zones, soils, crop type, crop calendar (Fritz *et al.*, 2019; see Figure 2 therein).

Typical model outputs include forecasts of crop condition, intensity, yield, and area impacted by critical anomalies. Not surprisingly, forecasts tend to improve during the growing season. While several of these systems supply regular reports and online maps, they are not validated statistically and significant discrepancies exist between the results of different systems. Many of the global land cover mapping products are used as input to define crop type and these also display major differences with respect to cropland (Fritz *et al.*, 2011; Waldner *et al.*, 2015). Similarly, many global crop calendars do not account for detailed spatial variations (Fritz *et al.*, 2019), and refinements in agricultural system models are needed both in terms of data and methods (Jones *et al.*, 2017).

Although EO-based datasets deliver reliable estimates of crop condition and condition anomalies, they do not currently supply the quantitative estimates of crop area or forecasts of crop production required to accurately monitor food security (see Section 11.5). Other areas where these systems could be improved include more consistent calibration and validation protocols, global maps of crop intensity and crop type, additional information on crop management, better access via portable smart devices, and inclusion of crowdsourced and volunteered data (including social media; Fritz *et al.*, 2019).

VRT (Variable Rate Technology) is essentially managing variability within paddocks by adjusting major inputs such as fertiliser to their optimum profit level. A synthesis of previous yield maps, imagery and soils data can be used to define zones within paddocks that warrant varying levels of inputs.
(Agrans Research, 2007)

Table 12.4 Global and regional agricultural monitoring systems

CAS-IRSDE: Institute of Remote Sensing and Digital Earth at the Chinese Academy of Sciences; USDA-FAS: United States Department of Agriculture-Foreign Agricultural Service; WFP: World Food Programme; EC-JRC: European Commission Joint Research Centre

System	Coordinator	Start Date	Purpose	Outputs	Reference
Global information and early warning system (GIEWS)	UN FAO	Early 1970s	Global food crop production, consumption and trade	Quarterly reports and <i>ad hoc</i> briefs plus monthly bulletins on food price trends	http://www.fao.org/giews/en/
			Agricultural Stress Index (ASI) System	Regional hotspot maps of water stressed crops based on ASI every ten days (see Section 9.5)	
Famine early warning systems network (FEWS NET)	USAID	1985	Quantify changes in crop area planted and crop yield	Quarterly outlook reports with monthly updates for selected food insecure countries and alerts on emerging crises	http://www.fews.net/
MARS crop yield forecasting system (MCYFS)	EC-JRC	1992	Operational estimates of area, yield and production at pan-European level for EU member states	Monthly bulletins, maps updated three times per month	https://agri4cast.jrc.ec.europa.eu/
				Visualisations via JRC MARS Explorer	http://www.marsop.info/en/web/mars-explorer/home
CropWatch	CAS-IRSDE	1998	Predictions of crop conditions and production, both within China and globally	Quarterly and annual bulletin with updates for global coverage, regional indicators (VHI, VCI) and detailed national/sub-national estimates	http://www.cropwatch.com.cn/
Crop Explorer	USDA-FAS	2001	Global crop conditions and production estimates, for all major commodities, for all foreign countries	Data visualisation products and numerous maps and charts updated every 10 days	https://www.fas.usda.gov/
Group on Earth Observations Global Agricultural Monitoring Initiative (GEOGLAM)	GEO	2013	Assessment of crop growing conditions, crop status and agroclimatic conditions that may have an impact on global production of wheat, maize, rice, and soy for Agricultural Market Information System (AMIS)	Monthly reports	http://www.geoglam.org/index.php/en/
Seasonal Monitor	WFP	2014	Monitor growing season status and to provide early warning of conditions detrimental to crop and pasture production within WFP regions of interest	Monthly reports	https://www.wfp.org/content/seasonal-monitor
				Dataviz visualisation platform	http://dataviz.vam.wfp.org/
Anomaly Hot Spots of Agricultural Production (ASAP)	EC-JRC	2017	Identify areas where unfavourable growing conditions for both crops and rangelands may represent a potential food security problem	Early warnings every ten days based on rainfall estimates/NDVI with verified hotspots for potential food security updated monthly	https://mars.jrc.ec.europa.eu/asap/

Source: Fritz *et al.* (2019)

12.6 Precision Agriculture

Precision agriculture comprises a range of digital technologies that are designed to monitor variations in the environmental conditions of plant, animal and soil resources in order to optimise their productivity, reduce their environmental impact and enhance food security (Zhang *et al.*, 2002; Mulla, 2013; Bramley and Trengove, 2013). These technologies allow farmers to vary the use of inputs, such as the selection and application of seeds, fertilisers, pesticides, and water, and/or cultivation methods (planting, tillage, harvesting), to match varying soil and crop conditions across a field (Srinivasan, 2006).

Technologies involved with precision agriculture basically rely on EO sensors carried by satellite, airborne (manned and unmanned), and ground platforms. Local platforms, such as low-level aircraft and quad bikes, offer convenience and flexibility for data acquisition in a precision agriculture environment. For example, when equipped with active optical sensors, these two platforms have respectively enabled assessment of plant vigour for cereal crops (Lamb *et al.*, 2009, 2011) and perennial pastures (Trotter *et al.*, 2010).

Examples of location-specific data that can be acquired by relevant sensors include:

- soil moisture, temperature, albedo, nutrient content, compaction, and elevation;
- animal location, digestion, and fertility;
- plant biomass, moisture status, temperature, and nutritional and physiological status; and
- air temperature, humidity, precipitation, and wind speed and direction.

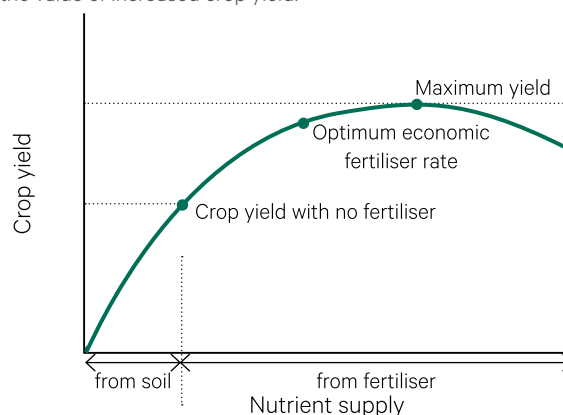
Analysis of soil, plant and atmospheric datasets enables precise application of irrigation water, fertilisers and chemicals to deter pests and weeds. This information also provides early warning of disease, deficiency conditions, or weed infestations at specific locations (Mahlein *et al.*, 2012). Animal tracking devices monitor grazing patterns, and allow graziers to optimise stocking rates and resource usage (see Volume 1A—Excursus 10.1) and implement virtual fencing (Butler *et al.*, 2004; CSIRO, 2020c). Automated plant counts derived from drone imagery are also being trialled to monitor non-overlapping vegetable crops, such as brassicas and lettuce (O'Halloran and van Sprang, 2019).

A wide range of agricultural robots with both remote and proximal sensors are now available to plow, fertilise, treat and harvest crops, while automated imaging systems can deliver rapid analyses of the spatial variations in crop and soil condition, and produce georeferenced yield maps. For ease of access in the field, many of these applications have been adapted to control by smartphone or tablet.

Variable Rate Technology (VRT) are also being embraced by the grains industry to tailor crop management to variations in growing conditions within crops (Suarez *et al.*, 2018). By adjusting agricultural inputs to suit environmental conditions, precision agriculture not only increases the output of agricultural enterprises, but improves the efficiency of resource use with less pollution (Agtrans Research, 2007). This is particularly important for fertiliser use where excessive applications can leach into waterways. Ideally nutrient supply only matches, but does not exceed, crop requirements to achieve maximum profit (see Figure 12.1). For example, Basso *et al.* (2016) analysed high resolution satellite imagery, which had been transformed using the Canopy Chlorophyll Content Index (CCCI; see Section 8.1.2) and validated using hand-held spectrometers, to map the spatial uptake of nitrogen applications by wheat crops. Thus, VRT, coupled with EO datasets, can both reduce potential environmental problems resulting from excessive use of fertiliser and avoid expenses that do not contribute to crop yield.

Figure 12.1 Crop response to fertiliser application

Additional fertiliser increases crop yield only up to a site-specific threshold. However, before this threshold, there may be a break-even point at which the cost of extra fertiliser exceeds the value of increased crop yield.



Adapted from: <http://adlib.everysite.co.uk/adlib/defra/content.aspx?id=2RRVTHNXTS.88UF41WXROOZS>

Selected precision agriculture monitoring datasets have been coupled with crop production models and meteorological records to deliver real time estimates of seasonal yield. In conjunction with a decision support framework, farmers can then assess the seasonal profitability of additional inputs for individual crops. When integrated with Geographic Information Systems (GIS), precision agriculture readily generates 'Paddock to Plate' forecasts to achieve efficient marketing of produce (see Volume 1B—Excursus 9.1).

Precision agriculture allows the performance of a crop and its environmental conditions to be monitored closely throughout its growth cycle and enables harvesting to be timed for maximum yield. This approach also allows growers to focus on crop quality by selective harvesting (Bramley and Trengove, 2013). Especially for horticultural crops, prior knowledge of harvest time allows growers to optimise labour, packaging, and marketing requirements. Some of the agricultural industries in Australia that are adopting precision agriculture include:

- viticulture (Bramley, 2010; Bramley *et al.*, 2011; Bramley and Trengove, 2013; Fuentes *et al.*, 2014);
- broadacre cropping—Australian wheat growers are optimising crop productivity and profit by using the Yield Prophet application (CSIRO, 2020d);
- sugar (see Volume 1B—Excursus 1.1; Rahman and Robson, 2016a, 2016b, Robson *et al.*, 2016a);
- fruit crops (see Volume 1B—Excursus 9.1; APAL, 2019);
- nut crops (Robson *et al.*, 2016b, 2017); and
- vegetable production (Suarez *et al.*, 2018).

12.7 Further Information

Plant Phenomics

<https://www.plantphenomics.org.au/about-us/>

Australian Crop Monitoring

Agricultural Production Systems sIMulator (APSIM):

<https://www.apsim.info/apsim-model/>

Graincast: <https://research.csiro.au/graincast/>

Queensland Crop Mapping: <https://www.qld.gov.au/environment/land/management/mapping/statewide-monitoring/crops>

International Monitoring Systems

Cropwatch: <http://www.cropwatch.com.cn/htm/en/index.shtml>

EuroGEO: e-shape/eurogeo/h2020/eu-cap

GEOGLAM Rangeland and Pasture Productivity (RaPP) tool:

Australia: <https://map.geo-rapp.org/#australia>

Global: <https://www.geo-rapp.org>

Precision Agriculture

Srinivasan (2006)

CSIRO Precision Agriculture webpage: <https://www.csiro.au/en/Research/AF/Areas/Sustainable-farming-systems/Precision-agriculture>

Society of Precision Agriculture Australia (SPAA): www.spaa.com.au

Tree Crops

Australian Tree Crop Map Dashboard:

<https://une-2351.maps.arcgis.com/apps/dashboards/8fd2ce70111e40088127867c63b9127e>

Australian Tree Crop Map Severe Weather App:

Overlays live weather data with the location and extent of commercial horticulture tree crops in Australia. Mapped commodities include: avocado, banana, citrus, macadamia, mango and olive: <https://une-2351.maps.arcgis.com/apps/webappviewer/index.html?id=03c4d068ada9458da2eeb3e44d6f45ad>

12.8 References


- Abuzar, M., Whitfield, D., McAllister, A., and Sheffield, K. (2019). Application of ET-NDVI-relationship approach and soil-water-balance modelling for the monitoring of irrigation performance of treed horticulture crops in a key fruit-growing district of Australia. *International Journal of Remote Sensing*, 40(12), 4724–4742. doi:10.1080/01431161.2019.1573337
- AEGIC (2020). *Wheat* webpage, Australian Export Grains Innovation Centre website: <https://www.aegic.org.au/publications/australian-grains/wheat/>
- Agtrans Research (2007). *An Economic Analysis of the GRDC Investment in Precision Agriculture Variable Rate Technology (VRT)*. Grains Research and Development Corporation Project Code: ATR00002. ISBN 978-1-921779-04-6 https://grdc.com.au/_data/assets/pdf_file/0021/225084/grdc_impact_precisionagricultureanalysis.pdf
- APAL (2019). *Drones deployed to assess nitrogen needs of pears* webpage, (4 September 2019) Apple and Pear Australia Ltd website: <https://apal.org.au/drones-deployed-to-assess-nitrogen-needs-of-pears/>
- AuSHS (2019). *Australian Horticulture* webpage. Australian Society of Horticultural Science website: <http://aushs.org.au/australian-horticulture/>
- Australian Grain (2019a). *The Grain Industry*. Australian Grain website: <http://www.ausgrain.com.au/industry.html>
- Australian Grain (2019b). *Grain Yearbook 2019*. Australian Grain. Greenmount Press. <http://www.ausgrain.com.au/Back%20Issues/287ybgrn19/287ybgrn19.pdf>
- Atzberger, C. (2013). Advances in remote sensing of agriculture: context description, existing operational monitoring systems and major information needs. *Remote Sensing*, 5, 949–981. <http://dx.doi.org/10.3390/rs5020949>
- Basso, B., Fiorentino, C., Cammarano, D., and Schulthess, U. (2016). Variable rate nitrogen fertilizer response in wheat using remote sensing. *Precision Agriculture*, 17(2), 168–182. doi:10.1007/s11119-015-9414-9
- BoM (2020). *Climate Data Online* webpage, Bureau of Meteorology website: <http://www.bom.gov.au/climate/data/>
- Bramley, R., and Trengove, S. (2013). Precision agriculture in Australia: Present status and recent developments. *Engenharia Agricola*, 33(3), 575–588.
- Bramley, R.G.V. (2010). Precision Viticulture: Managing vineyard variability for improved quality outcomes. In: (Ed: Reynolds, A.G.) *Managing wine quality. Viticulture and wine quality*. Woodhead Publishing, Cambridge. pp. 445–480.

- Bramley, R.G.V., Le Moigne, M., Evain, S., Ouzman, J., Florin, L., Fadaili, E.M., Hinze, C.J., and Cerovic, Z.G. (2011). On-the-go sensing of grape berry anthocyanins during commercial harvest: development and prospects. *Australian Journal of Grape and Wine Research*, 17(3), 316–326. doi:10.1111/j.1755-0238.2011.00158.x
- Butler, Z., Corker, P., Peterson, R., and Rus, D. (2004). Virtual Fences for Controlling Cows. *Proceedings of IEEE International Conference on Robotics and Automation, September 2004*. New Orleans, LA, USA. pp. 4429–4436, Volume 5. doi:10.1109/ROBOT.2004.1302415
- Chen, Y., Donohue, R.J., McVicar, T.R., Waldner, F., Mata, G., Ota, N., Houshmandfar, A., Dayal, K., Lawes, R.A. (2020a). Nationwide crop yield estimation based on photosynthesis and meteorological stress indices. *Agricultural and Forest Meteorology*, 284, 107872. <https://doi.org/10.1016/j.agrformet.2019.107872>
- Chen, Y., McVicar, T.R., Donohue, R.J., Garg, N., Waldner, F., Ota, N., Li, L., and Lawes, R. (2020b). To Blend or Not to Blend? A Framework for Nationwide Landsat–MODIS Data Selection for Crop Yield Prediction. *Remote Sensing*, 12(10), 1653. <https://doi.org/10.3390/rs12101653>
- Cilia, C., Panigada, C., Rossini, M., Meroni, M., Busetto, L., Amaducci, S., Boschetti, M., Picchi, V., and Colombo, R. (2014). Nitrogen Status Assessment for Variable Rate Fertilization in Maize through Hyperspectral Imagery. *Remote Sensing*, 6(7), 6549–6565. <https://doi.org/10.3390/rs6076549>
- CSIRO (2020a). ePaddocks™ webpage, Commonwealth Scientific and Industrial Research Organisation website: <https://research.csiro.au/digiscape/digiscapes-projects/epaddocks-mapping-every-paddock-across-the-australian-grain-region/>
- CSIRO (2020b). Graincast™ webpage, Commonwealth Scientific and Industrial Research Organisation website: <https://research.csiro.au/graincast/>
- CSIRO (2020c). Virtual fencing webpage, Commonwealth Scientific and Industrial Research Organisation website: <https://www.csiro.au/en/Research/AF/Areas/Livestock/Virtual-fencing#:~:text=Virtual%20fencing%20is%20an%20animal,need%20for%20an%20actual%20fence.>
- CSIRO (2020d). Yield Prophet® webpage, Commonwealth Scientific and Industrial Research Organisation website: <https://www.csiro.au/en/Research/AF/Areas/Digital-agriculture/Cropping-pastures/Yield-Prophet>
- DAWR (2016). *Horticulture fact sheet*, Department of Agriculture and Water Resources: http://www.agriculture.gov.au/ag-farm-food/hort-policy/horticulture_fact_sheet
- Defourny, P., Bontemps, S., Bellemans, N., Cara, C., Dedieu, G., Guzzonato, E., Hagolle, O., Inglada, J., Nicola, L., Rabaute, T., Savinaud, M., Udroui, C., Valero, S., Bégué, A., Dejoux, J.-F., El Harti, A., Ezzahar, J., Kussul, N., Labbassi, K., Lebourgeois, V., Miao, Z., Newby, T., Nyamugama, A., Salh, N., Shelestov, A., Simonneau, V., Sibiry Traore, P., Traore, S.S., and Koetz, B. (2019). Near real-time agriculture monitoring at national scale at parcel resolution: Performance assessment of the Sen2-Agri automated system in various cropping systems around the world. *Remote Sensing of Environment*, 221, 551–568.
- Donohue, R., Lawes, R., Mata, G., Gobbett, D., and Ouzman, J. (2018). Towards a national, remote-sensing-based model for predicting field-scale crop yield: application to three winter crop species. *Field Crops Research*, 227, 79–90. <https://doi.org/10.1016/j.fcr.2018.08.005>
- Erickson, J.D. (1984). The LACIE Experiment in Satellite Aided Monitoring of Global Crop Production. Ch 8 in *The Role of Terrestrial Vegetation in the Global Carbon Cycle: Measurement by Remote Sensing*. (Ed: G.M. Woodwell). John Wiley and Sons Ltd.
- FAO (2016). *Crop Yield Forecasting: Methodological and Institutional Aspects*. UN Food and Agricultural Organisation, Rome. http://www.amis-outlook.org/fileadmin/user_upload/amis/docs/resources/AMIS_CYF-Methodological-and-Institutional-Aspects_web.pdf
- FAO (2017). *Review of the Available Remote Sensing Tools, Products, Methodologies and Data to Improve Crop Production Forecasts*. UN Food and Agriculture Organization, Rome. ISBN 978-92-5-109840-0.
- Freebairn, D.M., Ghahramani, A., Robinson, J.B., McClymont, D. (2018). A soil water monitoring tool using modelling, on-farm data and mobile technology. *Environmental Modelling and Software*, 104, 55–63. <https://doi.org/10.1016/j.envsoft.2018.03.010>
- Fritz, S., See, L., McCallum, I., Schill, C., Obersteiner, M., van der Velde, M., Boettcher, H., Havlík, P., Achard, F., (2011). Highlighting continued uncertainty in global land cover maps for the user community. *Environmental Research Letters*, 6, 044005. <http://dx.doi.org/10.1088/1748-9326/6/4/044005>
- Fritz, S., See, L., Bayas, J.C.L., Waldner, F., Jacques, D., Becker-Reshef, I., Whitcraft, A., Baruth, B., Bonifacio, R., Crutchfield, J., Rembold, F., Rojas, O., Schucknecht, A., Van der Velde, M., Verdin, J., Wu, B., Yan, N., You, L., Gilliams, S., MÜcher, S., Tetrault, R., Moorthy, I., and McCallum, I. (2019). A comparison of global agricultural monitoring systems and current gaps. *Agricultural Systems*, 168, 258–272. <https://doi.org/10.1016/j.agsy.2018.05.0>

- Fuentes, S., Poblete-Echeverría, C., Ortega-Farías, S., Tyerman, S., and de Bei, R. (2014). Automated estimation of leaf area index from grapevine canopies using cover photography, video and computational analysis methods. *Australian Journal of Grape and Wine Research*, 20(3), 465–473.
- Grundy, M., Viscarra Rossel, R., Searle, R., Wilson, P., Chen, C., and Gregory, L. (2015). The Soil and Landscape Grid of Australia. *Soil Research*, 53, 835–844.
- Hall, D., Galloway, P., Lemon, J., Curtis, B., van Burgel, A., and Kong, K. (2014). *The agronomy jigsaw*. Department of Agriculture and Food, Western Australia. Bulletin 4850. ISSN 1833-7236. <https://www.agric.wa.gov.au/sites/gateway/files/Agronomy%20jigsaw%20bulletin%204850.pdf>
- Hegarty-Craver, M., Polly, J., O’Neil, M., Ujeneza, N., Rineer, J., Beach, R.H., Lapidus, D., and Temple, D.S. (2020). Remote Crop Mapping at Scale: Using Satellite Imagery and UAV-Acquired Data as Ground Truth. *Remote Sensing*, 12, 1984. doi:10.3390/rs12121984
- Heil, K., and Schmidhalter, U. (2017). The Application of EM38: Determination of Soil Parameters, Selection of Soil Sampling Points and Use in Agriculture and Archaeology. *Sensors*, 17(11), 2540. <https://doi.org/10.3390/s17112540>
- Hill, M.J., Vickery, P.J., Furnival, E.P., and Donald, G.E. (1999). Pasture land cover in eastern Australia from NOAA-AVHRR NDVI and classified Landsat TM. *Remote Sensing of Environment*, 67, 32–50 doi:10.1016/S0034-4257(98)00075-3
- Hill, M.J., Ticehurst, C.J., Lee, J.S., Grunes, M.R., Donald, G.E., and Henry, D. (2005). Integration of optical and radar classifications for mapping pasture type in western Australia. *IEEE Transactions on Geoscience and Remote Sensing*, 43, 1665–1681. doi:10.1109/TGRS.2005.846868
- Holzworth, D.P., Huth, N.I., deVoil, P.G., Zurcher, E.J., Herrmann, N.I., McLean, G., Chenu, K., van Oosterom, E.J., Snow, V., Murphy, C., Moore, A.D., Brown, H., Whish, J.P.M., Verrall, S., Fainges, J., Bell, L.W., Peake, A.S., Poulton, P.L., Hochman, Z., Thorburn, P.J., Gaydon, D.S., Dalgliesh, N.P., Rodriguez, D., Cox, H., Chapman, S., Doherty, A., Teixeira, E., Sharp, J., Cichota, R., Vogeler, I., Li, F.Y., Wang, E., Hammer, G.L., Robertson, M.J., Dimes, J.P., Whitbread, A.M., Hunt, J., van Rees, H., McClelland, T., Carberry, P.S., Hargreaves, J.N.G., MacLeod, N., McDonald, C., Harsdorf, J., Wedgwood, S., Keating, B.A. (2014). APSIM—evolution towards a new generation of agricultural systems simulation. *Environmental Modelling and Software* 62, 327–350. <https://doi.org/10.1016/j.envsoft.2014.07.009>
- Holzworth, D., Huth, N.I., Fainges, J., Brown, H., Zurcher, E., Cichota, R., Verrall, S., Herrmann, N.I., Zheng, B., and Snow, V. (2018). APSIM Next Generation: Overcoming Challenges in Modernising a Farming Systems Model. *Environmental Modelling and Software*, 103, 43–51. <https://doi.org/10.1016/j.envsoft.2018.02.002>
- Hoogenboom, G.J., White J.W., and Messina, C.D. (2004). From genome to crop: integration through simulation modelling. *Field Crop Research*, 90, 145–163.
- Inglada, J., Arias, M., Tardy, B., Hagolle, O., Valero, S., Morin, D., Dedieu, G., Sepulcre, G., Bontemps, S., Defournay, P., and Koetz, B. (2015). Assessment of an Operational System for Crop Type Map Production Using High Temporal and Spatial Resolution Satellite Optical Imagery. *Remote Sensing*, 7, 12356–12379. doi:10.3390/rs70912356
- Jones, J.W., Antle, J.M., Basso, B., Boote, K.J., Conant, R.T., Foster, I., Godfray, H.C.J., Herrero, M., Howitt, R.E., Janssen, S., Keating, B.A., Munoz-Carpena, R., Porter, C.H., Rosenzweig, C., Wheeler, T.R. (2017). Toward a new generation of agricultural system data, models, and knowledge products: state of agricultural systems science. *Agricultural Systems*, 155, 269–288. <http://dx.doi.org/10.1016/j.agsy.2016.09.021>
- Kamir, E., Waldner, F., and Hochman, Z. (2020). Estimating wheat yields in Australia using climate records, satellite image time series and machine learning methods. *ISPRS Journal of Photogrammetry and Remote Sensing*, 160, 124–135. <https://doi.org/10.1016/j.isprsjprs.2019.11.008>
- Lamb, D.W., Trotter, M.G., and Schneider, D.A. (2009). Ultra low-level airborne (ULLA) sensing of crop canopy reflectance: A case study using CropCircle™ sensor. *Computers and Electronics in Agriculture*, 69, 86–91.
- Lamb, D.W., Schneider, D.A., Trotter, M.G., Schaefer, M.T., and Yule, I.J. (2011). Extended-altitude, aerial mapping of crop NDVI using an active optical sensor: A case study using a Raptor™ sensor over wheat. *Computers and Electronics in Agriculture*, 77, 69–73.
- Lobell, D.B., Thau, D., Seifert, C., Engle, E., Little, B. (2015). A scalable satellite-based crop yield mapper. *Remote Sensing of Environment*, 164, 324–333. <https://doi.org/10.1016/j.rse.2015.04.021>
- MacDonald, R.B., Hall, F.G., and Erb, R.B. (1975). The Use of LANDSAT Data in a Large Area Crop Inventory Experiment (LACIE). *LARS Symposia*. Paper 46. http://docs.lib.purdue.edu/lars_symp/46

- Mahlein, A.K., Oerke, E.C., Steiner, U., and Dehne, H.W. (2012). Recent advances in sensing plant diseases for precision crop protection. *European Journal of Plant Pathology*, 133(1), 197–209. doi:10.1007/s10658-011-9878-z
- Malthus, T.J., Barry, S., Randall, L.A., McVicar, T., Bordas, V.M., Stewart, J.B., Guerschman, J.-P., and Penrose, L. (2013). *Ground cover monitoring for Australia: Sampling strategy and selection of ground control sites*. CSIRO, Australia.
- McNairn, H., Champagne, C., Shang, J., Holmstrom, D., and Reichert, G. (2008). Integration of optical and Synthetic Aperture Radar (SAR) imagery for delivering operational annual crop inventories. *ISPRS Journal of Photogrammetry and Remote Sensing*, 64(5), 434–449. <https://doi.org/10.1016/j.isprsjprs.2008.07.006>
- Mohammed, G.H., Colombo, R., Middleton, E.M., Rascher, U., van der Tol, C., Nedbal, L., Goulas, Y., Pérez-Priego, O., Damm, A., Meroni, M., Joiner, J., Cogliati, S., Verhoef, W., Malenovský, Z., Gastellu-Etchegorry, J.-P., Miller, J.R., Guanter, L., Moreno, J., Moya, I., Berry, J.A., Frankenberg, C., Zarco-Tejada, P.J. (2019). Remote sensing of solar-induced chlorophyll fluorescence (SIF) in vegetation: 50 years of progress. *Remote sensing of environment*, 231, 111177. <https://doi.org/10.1016/j.rse.2019.04.030>
- Mulla, D.J. (2013). Twenty five years of remote sensing in precision agriculture: key advances and remaining knowledge gaps. *Biosystems Engineering*, 114(4), 358–371. doi:10.1016/j.biosystemseng.2012.08.009
- Nikolova, S., Bruce, S., Randall, L., Barrett, G., Ritman, K., and Nicholson, M. (2012). *Using remote sensing data and crop modelling to improve crop production forecasting: a scoping study*. ABARES technical report 12.3. Australian Bureau of Agricultural and Resource Economics and Sciences, Canberra.
- O'Halloran, J., and van Sprang, C. (2019). Automating plant counts using drone imagery. pp 41–42 in *Vegetables Australia* (May/June 2019), AUSVEG Ltd and Horticulture Innovation Australia Ltd 2019. <http://era.daf.qld.gov.au/id/eprint/7131/1/VG16009%20Final%20Literature%20review.pdf>
- Panek, E., and Gozdowski, D. (2020). Analysis of relationship between cereal yield and NDVI for selected regions of Central Europe based on MODIS satellite data. *Remote Sensing Applications: Society and Environment*, 17, 100286. <https://doi.org/10.1016/j.rsase.2019.100286>
- Peña-Arancibia, J.L., McVicar, T.R., Paydar, Z., Li, L.T., Guerschman, J.P., Donohue, R., Dutta, D., Podger, G., Van Dijk, A., and Chiew, F. (2014). Dynamic identification of summer cropping irrigated areas in a large basin experiencing extreme climatic variability. *Remote Sensing of Environment*, 154, 139–152.
- Potgieter, A.B., Lawson, K., and Huete, A.R. (2013). Determining crop acreage estimates for specific winter crops using shape attributes from sequential MODIS imagery. *International Journal of Applied Earth Observation and Geoinformation*, 23(1), 254–263. <https://doi.org/10.1016/j.jag.2012.09.009>
- Pringle, M.J., Schmidt, M., and Tindall, D.R. (2018). Multi-decade, multi-sensor time-series modelling—based on geostatistical concepts—to predict broad groups of crops. *Remote Sensing of Environment*, 216, 183–200. <https://doi.org/10.1016/j.rse.2018.06.046>
- Pullanagari, R.R., Kereszturi, G., and Yule, I.J. (2016). Mapping of macro and micro nutrients of mixed pastures using airborne AisaFENIX hyperspectral imagery. *ISPRS Journal of Photogrammetry and Remote Sensing*, 117, 1–10. <https://doi.org/10.1016/j.isprsjprs.2016.03.010>
- Queensland Government (2020). *SIL0: Australian climate data from 1889 to yesterday* webpage, Queensland Government website: <https://www.longpaddock.qld.gov.au/silo/>
- Rahman, M.M., and Robson, A.J. (2016a). A Novel Approach for Sugarcane Yield Prediction Using Landsat Time Series Imagery: A Case Study on Bundaberg Region. *Advances in Remote Sensing* 5, 93–102. <http://dx.doi.org/10.4236/ars.2016.52008>
- Rahman, M.M., and Robson, A.J. (2016b). Integrating Landsat-8 and Sentinel-2 Time Series Data for Yield Prediction of Sugarcane Crops at the Block Level. *Remote Sensing*, 12(8), 1313. <https://doi.org/10.3390/rs12081313>
- Robson, A., Rahman, M.M., Falzon, G., Verma, N.K., Johansen, K.J., Robinson, N., Lakshmanan, P., Salter, B., and Skocaj, D. (2016a). Evaluating Remote Sensing Technologies for Improved Yield Forecasting and for the Measurement of Foliar Nitrogen Concentration in Sugarcane. *Proceedings of the 38th Australian Society of Sugar Cane Technologists*, April, Mackay, Queensland.
- Robson, A.J., Rahman, M.M., Muir, J., Saint, A., Simpson, C., and Searle, C. (2016b). Evaluating satellite remote sensing as a method for measuring yield variability in Avocado and Macadamia tree crops, *Proceedings of the Society of Precision Agriculture Australia*, 12 September, Toowoomba, Australia.

- Robson, A.J., Rahman, M.M., and Muir, J. (2017). Using Worldview Satellite Imagery to Map Yield in Avocado (*Persea americana*): A Case Study in Bundaberg, Australia. *Remote Sensing*, 9(12), 1223. <https://doi.org/10.3390/rs9121223>
- Schut, A.G.T., Stephens, D.J., Stovold, R.G.H., Adams, M., and Craig, R.L. (2009). Improved wheat yield and production forecasting with a moisture stress index, AVHRR and MODIS data. *Crop and Pasture Science*, 60(1), 60–70.
- Shanahan, J., Schepers, J.S., Francis, D.D., Varvel, G.E., Wilhelm, W., Tringe, J.M., Schlemmer, M.R., and Major, D.J. (2001). Use of Remote-Sensing Imagery to Estimate Corn Grain Yield. *Agronomy Journal*, 93, 583–589.
- Srinivasan, A. (Ed) (2006). *Handbook of Precision Agriculture: Principles and Applications*. The Haworth Press, New York. ISBN-13: 978-1-56022-945-4.
- Stanley, J.N., Lamb, D.W., Falzon, G., and Schneider, D.A. (2014). Apparent electrical conductivity (Eca) as a surrogate for neutron probe counts to measure soil moisture content in heavy clay soils (Vertosols). *Soil Research*, 52(4), 373–378.
- Suarez, L.A., McPhee, J., O'Halloran, J., van Sprang, C., and Robson, A. (2018). *Adoption of precision systems technology in vegetation production*. Literature Review for VG16009, Horticulture Innovation Australia, Queensland.
- TERN Australia (2018). *Effective Field Calibration and Validation Practices: A practical handbook for calibration and validation satellite and model-derived terrestrial environmental variables for research and management*. A TERN Landscape Assessment Initiative, NCRIS. ISBN 978-0-646-94137-0. <https://www.tern.org.au/NEW-CalVal-handbook-for-remote-sensing-bgp4370.html>
- Trotter, M.G., Lamb, D.W., and Schneider, D.A. (2010). Evaluating an active optical sensor for quantifying and mapping green herbage mass and growth in a perennial grass pasture. *Crop and Pasture Science*, 61, 389–398.
- Tucker, C.J., Holben, B.N., Elgin, J.H. Jr., and McMurtrey, J.E. Jr. III (1980). Remote sensing of total dry matter accumulation in winter wheat. *Remote Sensing of Environment*, 11, 171–189.
- UNE CASI (2020). *SugarMaps* webpage, University of New England Computation Analytics Software Informatic website: <https://casi.une.edu.au/#!/projects>
- Van Niel, T.G., and McVicar, T.R. (2003). A simple method to improve field-level rice identification: toward operational monitoring with satellite remote sensing. *Australian Journal of Experimental Agriculture*, 43, 379–387.
- Van Niel, T.G., and McVicar, T.R. (2004). Determining temporal windows for crop discrimination with remote sensing: a case study in south-eastern Australia. *Computers and Electronics in Agriculture*, 45, 91–108.
- Waldner, F., Fritz, S., Di Gregorio, A., Defourny, P. (2015). Mapping priorities to focus cropland mapping activities: fitness assessment of existing global, regional and national cropland maps. *Remote Sensing*, 7, 7959–7986. <http://dx.doi.org/10.3390/rs70607959>
- Waldner, F., Chen, Y., Lawes, R., and Hochman, Z. (2019). Needle in a haystack: Mapping rare and infrequent crops using satellite imagery and data balancing methods. *Remote Sensing of Environment*, 233, 11375. <https://doi.org/10.1016/j.rse.2019.111375>
- Waldner, F., and Diakogiannis, F. I. (2020). Deep learning on edge: extracting field boundaries from satellite images with a convolutional neural network. *Remote Sensing of Environment*, 245, 111741.
- Wu, D., Johansen, K., Phinn, S., and Robson, A. (2020). Suitability of Airborne and Terrestrial Laser Scanning for Mapping Tree Crop Structural Metrics for Improved Orchard Management. *Remote Sensing*, 12, 1647. doi:10.3390/rs12101647
- Zhang, N., Wang, M., and Wang, N. (2002). Precision agriculture—a worldwide overview. *Computers and Electronics in Agriculture*, 36(2–3), 113–132. doi:10.1016/S0168-1699(02)00096-0
- Zhao, L., Waldner, F., Scarth, P., Mack, B., and Hochman, Z. (2020). Combining fractional cover images with one-class classifiers enables near real-time monitoring of fallows in the northern grains region of Australia. *Remote Sensing*, 12(8), 1337. <https://doi.org/10.3390/rs12081337>
- Zhou, Z.-S., Caccetta, P., Sims, N.C., and Held, A. (2016). Multi-band SAR Data for Rangeland Pasture Monitoring. *Proceedings of IEEE IGARSS 2016*. pp. 170–173, July 2016. doi:10.1109/IGARSS.2016.7729035



13 Irrigated Horticulture

Des Whitfield, Andrew McAllister, Mohammad Abuzar, and Mark O'Connell

Australian horticulture is introduced in Section 11.1. This section focuses on the use of EO datasets to monitor the water requirements of irrigated fruit, nut, and vine crops in southeastern Australia.

Since most of Australia is too dry for commercial, rainfed fruit production, Australian horticultural enterprises, including those in the Riverland and Mallee areas of South Australia and Victoria, respectively, commonly rely on irrigation to supply more than half of the crop water requirements in the majority of seasons. Discretionary irrigation may be practised in other parts of Australia where rainfall routinely provides > 50 % of crop water requirements.

Water needs of crops vary greatly in time and space. Spatial differences are attributable to variations in crop vegetation status (crop type, age, and growth conditions), and temporal differences are associated with seasonal and daily weather conditions, and rainfall contributions to root zone soil water. Irrigators are consequently required to employ sophisticated real time information and analytical tools to ensure that crops receive the requisite amounts of water. Over-irrigation wastes water and results in irrigation runoff and/or deep drainage losses from the root

zone. Over-supply is therefore conducive to nutrient runoff (and/or leaching) and shallow water tables, respectively. Conversely, effects of under-supply are readily seen in reduced rates of crop growth, and lowered yields and product quality. Irrigation should therefore be used to ensure that root zone soil moisture optimally supports the rapid rates of crop growth and water use conducive to high yields of high quality produce, with minimal contributions to nutrient runoff and deep drainage.

Over-allocation of available water resources and over-irrigation are also important at district and regional scales. Over-allocation of resources, where too many irrigators are granted access to a limited resource, leads to district scale water shortages (under-irrigation) in dry years, chronic limits on the availability of environmental water, and elevated water prices where marginal producers and industries are increasingly required to review their participation in irrigated farming.

13.1 Irrigated Horticulture in Southeast Australia

Irrigated fruit and vegetable production on the Murray River in southeast Australia dates back to colonial support for the establishment of irrigation settlements in the region and the arrival of the pioneering Chaffey brothers in the 1890s.

Irrigated horticulture is now expanding rapidly in the southern Murray-Darling Basin (MDB; see Section 2.1). High growth rates are especially evident in the Mallee region of northwest Victoria, where the formative years of irrigation development (1887–1947) accounted for 22,000 ha of crops (principally wine-grapes, dried

grapes, and citrus), another 52,000 ha was added during 1947–1997, with a further 48,000 ha added 1998–2017 (Argus, 2015). Small scale family farm units have been superseded by large scale, highly capitalised farming investments. Irrigated almonds continue to expand into non-traditional 'green-field' areas that were previously used for rainfed grains. The relatively new capability of flying fresh produce into Asian markets has supported the recent rapid expansion of table grapes in the Robinvale-Euston districts on the NSW/Victoria border.

Background image: Apricot trees (c.v. Golden May) planted on Tatura Trellis at the Stonefruit Experimental Orchard, SmartFarm Tatura, Victoria, photographed in August 2019. Source: Mark O'Connell

Recommended Chapter Citation: Whitfield, D., McAllister, A., Abuzar, M., and O'Connell, M. (2021). Irrigated Horticulture. Ch 13 in *Earth Observation: Data, Processing and Applications. Volume 3A—Terrestrial Vegetation*. CRC SI, Melbourne. pp. 263–280.

The routine and severe spring-summer rainfall deficiencies experienced in inland southeast Australia impose an absolute dependence on irrigation to meet the high yield and quality standards required of modern, high value, horticulture enterprises. Notwithstanding, irrigation requirements vary annually, depending on annual variations in spring-summer rainfall deficiencies.

Severe summer rainfall deficits experienced in the southern MDB consequently impose an obligate need for irrigation on horticultural producers in the region. Accordingly, the reliable production of profitable high yielding, high quality produce is intrinsically dependent on the external factors that influence the price and availability of water, and, also, the management factors that govern on-farm water use efficiency. Irrigation licensing regimes in the Mallee, for example, operate on fixed annual allocations of supplementary irrigation that range to maxima of 14 ML/ha for almonds grown in Victoria and to 16 ML/ha for almonds in South Australia. Actual seasonal requirements differ from prescribed license volumes, and Victoria makes provision to adjust licensed volumes for extraordinary seasonal demands. Further expansion of the fruit, nut, and vine industries in the southern MDB will occur against a backdrop of increased regional uncertainty in patterns of autumn and winter rainfall, and the associated risk

that major storage levels in Lakes Eildon, Dartmouth and Burrinjuck fall short of crop demands in summer. There exists, therefore, a strong need to gauge water use and demand in the fruit, nut, and vine industries of the southern MDB to ensure that irrigators are able to match irrigation amounts to crop demand at field and farm scales and, further, that regional resources are optimally employed to satisfy irrigation, social and environmental demands for water. In addition, there is an over-arching requirement to ensure that irrigation-induced rates of root zone drainage do not exacerbate salinity concerns in the Murray River.

In this Section, we present examples of ‘Satellite-based Irrigation Demand Analytics’ for fruit, nut, and vine crops grown in the southern MDB, with focus on:

- relationships between crop water use (evapotranspiration, ET; see Sections 2.2 and 9.4) and crop vegetation status (inferred by the satellite-based Normalised Difference Vegetation Index, NDVI; see Section 8.1.1) in major fruit, nut, and vine crops grown in the southern MDB; and the
- potential use of those data in daily irrigation management and in the assessment of the minimum quantities of water that are needed to produce high yields of high quality horticultural products in the region.

13.2 EO Sensors for Irrigated Horticulture

Mapping and monitoring of irrigated horticulture using EO datasets principally depends upon optical sensors to highlight differences between red and near infrared (NIR) reflectance (see Section 8.1.1). Thermal and passive microwave sensors are also relevant to derive land surface temperature (LST; see Section 7.5

and Volume 1B—Sections 7.6 and 8.1.1). Some of the sensor characteristics that are relevant to studies of irrigated horticulture are summarised in Table 13.1. In particular, drones are being increasingly employed to survey horticultural crops (for example, Gonzalez-Dugo *et al.*, 2013; see Section 12.2).

Table 13.1 EO sensors relevant to irrigated horticulture

TIR: Thermal infrared; GPS: Global Positioning System; RPAS: Remotely piloted aircraft system; DEM: Digital elevation model; ET: evapotranspiration

Type	Sensor	Platform	Relevance	Advantages	Disadvantages
Passive optical	Multispectral radiometer	Satellite or airborne	National or regional land cover mapping	Global, recurrent coverage, low cost	Low accuracy, coarse scale
	Hyperspectral spectroradiometer	Airborne	Plant biochemical functioning and health	High spectral and spatial resolution highlight plant stress and crop nutrition	High cost, high data volume
	TIR radiometer	Field, satellite, or airborne	Soil/canopy temperature, water stress	Surrogate measure for ET	Resolution depends on platform
Active optical	Lidar	Airborne and terrestrial	Crop structure and identification, DEM	Detailed structure for plant canopy and soil surface	High cost, specialised processing
	Active optical sensors	Ground vehicles or RPAS	Crop cover and condition mapping	Convenience, independent of sunlight	Low availability, specialised hardware
Proximal	Passive optical sensors (phenocam, hyperspectral), meteorological sensors (including soil moisture)	Ground, tractor, or tower-based (see Excursus 7.2 and Volume 2D—Section 12)	Soil, crop, and atmospheric variability Phenology	Continuous, long term measurements	High cost and require skilled maintenance
Locational	GPS	Portable devices	Locating field sites	Low cost	Coverage in remote regions or below dense canopies

13.3 Fundamentals of Irrigation Management

Irrigation systems and their management vary widely between regions, crops, and industries in Australia. System options range from traditional gravity or surface irrigation systems to the modern pressurised irrigation systems where water is delivered to crops through pipes, driplines and sprays. Pressure-based systems reliably and precisely deliver small amounts of water at daily and sub-daily intervals, whereas gravity-based systems are characterised by large infrequent deliveries, and are used to replenish root zone soil water stores at intervals of four or more days.

The quantum of water captured in the root zone after gravity irrigation is directly dependent on the soil water deficit in the root zone at the time of irrigation. Gravity-based irrigators must schedule irrigation events based on competing needs to ensure that root zone soil water deficits are large enough to maximise the retention of water applied to bays and furrows, and small enough to support rapid rates of crop growth. Errors in the timing (scheduling) of irrigation events in relation to soil water deficits, and/or the application of irrigation volumes that are poorly related to soil water deficits and crop requirements, cause unacceptable quantities of surface runoff from fields, and excessive root zone drainage. Inefficiencies are amplified when soil water retention is limited by the soil physical properties.

Pressure-based systems are able to deliver precise quantities of water to the soil, and are consequently conducive to fixed-interval irrigation events (such as daily), allowing irrigators to replenish the precise amounts of water used by crops in the intervening time interval (with appropriate allowance for rainfall). The modern pressurised irrigation systems adopted extensively by horticulture industries in southeast Australia in recent decades are commonly used for fixed-interval irrigation and thereby rely on precise estimates/measurements of the quantum of root zone soil water consumed by crops (ET^* ; see Section 13.4.1) over periods ≤ 2 days.

The management of root zone soil water deficits is central in considerations of irrigation water management. Soil water deficits determine the optimal timing and amount of applied water in gravity irrigation and, further, the amount of water delivered at fixed time intervals in pressurised systems. Cahn and Johnson (2017) described contemporary approaches to irrigation scheduling in vegetable crops grown in California. They emphasised that the use of soil moisture monitoring had progressed from limits imposed by sensor accuracy and cost to current demands for large scale whole-farm systems where the labour costs required for the installation and

removal of sensors over multiple fields outweighed the lower cost of modern sensors. They proposed that technical improvements in weather station networks, satellite and aerial imaging, and digital communication networks allow irrigators to combine satellite and weather data to assist in the progression from small to large scale irrigation farming systems.

Many Australian irrigators continue to rely on soil moisture sensors and, with the possible exception of IrriSAT (Hornbuckle, 2014; Montgomery *et al.*, 2015; see Section 13.9), the combined use of satellite and weather data to assist in large scale irrigation management systems is generally regarded as an emerging technology.

Weather-based estimates of irrigation water requirements are widely based on the crop coefficient method, which accounts for both crop and weather effects on water use (Doorenbos and Pruitt, 1974; Allen *et al.*, 1998; Jensen and Allen, 2016). The method relies on an initial measure of evaporative demand ('potential' evaporation), which accounts for the effects of weather on crop water use. The most widely used measure of evaporative demand, known as reference crop evapotranspiration (ET_{ref}), is modified by crop-specific factors incorporated into the crop coefficient to estimate crop water use (see Section 13.4).

Estimates of crop water use by the crop coefficient method are combined with rainfall data in soil water balance models to gauge the net effects of crop water use (ET), weather, and rainfall on the consumption of root zone soil water by crops. Soil water models reveal when soil water deficits become unacceptable for crop growth, and thereby predict both timing of irrigation events and the amounts of water required to maintain an optimal root zone soil water status. The management of multiple fields in large scale whole-farm irrigation management systems is achieved by combining field- and crop-specific satellite data (field/crop-specific estimates of crop coefficient) with an estimate of evaporative demand based on weather data sourced from a local automatic weather station or a web-based weather service. As described by Cahn and Johnson (2017), water use estimates based on satellite and weather data are inherently scalable over numerous fields, and thereby provide a practical basis for affordable whole-farm irrigation management systems.

13.4 Irrigation Requirements of Horticultural Crops

Crop water use is synonymous with ET, which describes the quantities of water evaporated by soil and leaf surfaces (evaporation, E, and transpiration, T, respectively; see Sections 7.6 and 9.4). Estimates of Irrigation Water Requirement (IWR) are therefore based on the amount of water required to compensate for ET losses from the root zone. Models of root zone soil water balance provide an explicit soil water accounting mechanism that allow irrigators to maintain a favourable soil water regime using irrigation to ensure that total water deliveries (irrigation + rainfall) are optimally matched to prevailing field-specific values of well-watered rates of ET (ET*).

13.4.1 Weather-based estimates of soil water status in orchards

Weather-based estimates of root zone soil water status are routinely based on soil water balance calculations where changes in soil moisture, are derived from estimates of ET* and rainfall following irrigation. In general terms, irrigation is required to compensate for rainfall deficits, estimated by:

$$\sum (ET^* - RF_e)$$

where RF_e is 'effective' rainfall in mm (see Table 13.2 for definitions of major water use terms).

Calculations of the crop-specific values of ET* are routinely based on the assumption that ET* is directly proportional to the weather (evaporative demand) experienced by crops (see Section 13.4.2), as modified by crop characteristics (see Section 13.4.3).

Table 13.2 Definition of major water use terms

Parameter Group	Term	Definition
Evapotranspiration	ET	Generic evapotranspiration
	ET*	Well-watered ET
	ET _{ref}	Reference crop ET
	ET _o	'Short' reference crop ET
	ET _r	'Tall' reference crop ET
	ET _F	Fractional ET _r
Crop water use coefficients	K _c	Crop water use coefficient
	K _{cb}	Basal crop coefficient
	K _{co}	Coefficient for 'short' crop
	K _{cr}	Coefficient for 'tall' crop
	K _d	Crop density coefficient
Vegetation	FC	Fractional Cover
	VI	Vegetation Index

13.4.2 Reference crop evapotranspiration

Evaporative demand, defined as the maximum or 'potential' rate of ET under the prevailing weather conditions, depends on solar radiation, humidity, temperature, and windspeed (see Section 7.6). The availability of affordable automatic weather stations has provided widespread access to site-specific estimates of evaporative demand, and an associated increase in the adoption of weather-based, soil moisture modelling approaches in irrigation scheduling and control systems.

Prior to FAO56 (Allen *et al.*, 1998), numerous variants of reference crop ET (ET_{ref}) were used to describe 'potential' rates of ET by crops (for example, FAO24; Doorenbos and Pruitt, 1977). The use of different measures of potential evaporation in reports of crop water use severely compromised the transferability of water use findings between researchers and regions. FAO56 contributors defined the 'short' crop version of ET_{ref} (ET_o) as a standardized measure of evaporative demand and proposed standardised procedures for the computation of ET_{ref} based on estimates of ET* that are appropriate to an extensive uniform sward of short green grass. The grass reference was adopted largely due to the preponderance of global lysimeter studies conducted on grass to that time.

The American Society of Civil Engineers (ASCE) Environmental and Water Resources Institute (EWRI) subsequently complemented short crop ET_{ref} with an optional 'tall' crop ET_{ref} (ET_r), based on alfalfa (ASCE-EWRI, 2005) for use in the USA. The alfalfa standard recognised the long history of alfalfa used in agricultural applications in the USA and provided continuity with the established use of short and tall forms of ET_{ref} in USA (ASCE-EWRI, 2005; Jensen and Allen, 2016).

Table 13.3 Values of C_n and C_d coefficients

Values of coefficients, C_n and C_d, appropriate to daily estimates of ET_o and ET_r, in the equation for ET_{ref} (Allen *et al.*, 2006)

Coefficient	C _d	C _n
'short' crop ET _o	0.34	900
'tall' crop ET _r	0.38	1600

Mathematically, both short and tall versions of ET_{ref} were founded on the Penman-Monteith equation, expressed as:

$$ET_{ref} = \frac{0.408\Delta(R_n - G) + \gamma \frac{C_n}{T + 273} u_2 (e_s - e_a)}{\Delta + \gamma(1 + C_d u_2)}$$

where

- ET_{ref} is reference crop ET (mm/day);
- R_n is net radiation at the crop surface (MJ/m²/day);
- G is soil heat flux density (MJ/m²/day);
- C_n is the numerator constant that changes with reference type (tall/short) and calculation time step in ET_{ref} (see Table 13.3);
- C_d is the denominator constant that changes with reference type (tall/short) and calculation time step in ET_{ref} (see Table 13.3);
- u_2 is wind speed at 2 m (m/s);
- e_s is saturation vapour pressure (kPa);
- e_a is actual vapour pressure (kPa);
- γ is the psychrometric constant (kPa °C⁻¹); and
- T is the mean daily air temperature at 2 m (°C).

The values of C_n and C_d for short and tall reference crops derive from the definition of vegetation characteristics adopted for the respective crops (vegetation height, leaf area index, stomatal resistance), and their impact on the full form Penman-Monteith equation (see Table 13.3). The short reference crop was defined by FAO56 as an hypothetical crop with an assumed height of 0.12 m, a surface resistance of 70 s/m and an albedo of 0.23, and closely resembled the evaporation from an extensive, actively-growing, adequately-watered, green grass sward of uniform height. The tall crop reference was based on an extensive uniform sward of alfalfa with a height of 0.5 m.

13.4.3 Crop characteristics

ET_o and ET_r provide standardised indices of evaporative demand (ASCE-EWRI, 2005). Crop-specific values of ET^* are calculated for 'non-reference' target crops by multiplying measures of ET_{ref} (ET_o , ET_r) by an associated crop coefficient (K_{co} , K_{cr}) as follows:

$$ET^* = K_{co} ET_o = K_{cr} ET_r$$

Crop- and field-specific values of K_{co} and K_{cr} account for all factors that cause crop-specific values of ET^* to differ from the reference estimates, ET_o and ET_r , respectively, that apply to extensive crops of uniform height and complete ground cover. Foliage and ground cover vary with both crop age and seasonal or phenological stages of crop growth in deciduous tree, nut, and vine crops. Typical row-based planting

configurations mean that fruit, nut, and vine crops rarely achieve full cover. Tabulated values of K_{co} for deciduous crops therefore require adjustments for growth (crop age), and seasonal and cultural differences in foliage cover.

In addition, the nominal values of K_{co} tabulated in FAO56 were described as 'typical' values expected for 'standard sub-humid climatic conditions' (average daytime minimum relative humidity (RH) \approx 45%; wind speed \approx 2 m/s), and height-dependent climate corrections were needed in order to apply tabulated values of K_{co} in conditions where average daytime minimum RH < 45% and/or wind speed > 2 m/s. The magnitude of designated climate corrections increased with crop height.

The assignment of tabulated K_{co} values to fruit, nut, and vine crops grown in southeast Australia therefore depends on an adequate accounting for differences in foliage cover due to crop growth/age, seasonal phenological changes, planting configuration, and crop- and height-dependent climate corrections. These and other effects are responsible for a voluminous scientific literature directed to the quantification and understanding of variations in K_{co} attributable to differences in crop characteristics and growth conditions (for example, Guerra *et al.*, 2016). Accordingly, the cost and complexity of establishing a comprehensive range of crop coefficients for the range of crop types, and crop cultural and management variants, is prohibitive for the wide array of crop types and configurations grown in horticultural regions in Australia and elsewhere.

13.4.4 Why two reference crops?

Height-dependent climate adjustments are required if the crop coefficient approach based on short crop ET_{ref} (ET_o) is applied to fruit, nut, and vine crops grown in the warm, dry climate experienced in southeast Australia and the southern MDB. However, the greater roughness of the 'tall' crop alfalfa reference means that measures of ET , approximate peak-season rates of ET^* for most tall crops, including orchards, in warm dry climates, and climate/height adjustments are unnecessary when the alternative 'tall' crop ET_{ref} (ET_r) is used with tall crops under warm, dry climatic conditions (Allen and Pereira, 2009).

ET_o and ET_r are both estimated by the equation for ET^* above, but differ in their numerator and denominator coefficients (C_n and C_d) used for daily estimates of ET_{ref} (see Table 13.3). ET_r tends to be 20–40% larger than ET_o (Allen and Pereira, 2009). K_c values associated with the alternative ET_o and ET_r reference values must be clearly distinguished as K_{co} and K_{cr} , respectively.

13.5 Satellite-based Estimates of ET

The importance of vegetation status in K_c values has been established by many studies relating K_c values, developed in lysimeter studies, to satellite- and ground-based vegetation indices (VI; see Section 8.1; for example Johnson and Trout, 2012). VI have been overwhelmingly based on the red and NIR bands obtained from EO (such as Heilman *et al.*, 1982; Bausch and Neale, 1987; Neale *et al.*, 1989; Hunsacker *et al.*, 2003). As detailed in Volume 2C—Section 11, and summarised in Section 8.1.1 above, NDVI and other VI are strongly related to the vegetation cover of the soil surface (or Fractional Cover: FC; Johnson and Trout, 2012; see Excursus 8.3). For example, Rajan and Maas (2014) modelled ET^* in cotton using satellite-based estimates of FC as a direct surrogate for K_c .

Below we consider satellite-based estimates of ET based on the:

- relationship between the crop water coefficient (K_c) and EO-based VI (see Section 13.5.1);
- relationship between surface temperature (T_s) and VI (see Section 13.5.2); and
- surface energy balance models (see Section 13.5.3).

13.5.1 K_c -VI relationships

Web-based, irrigation scheduling approaches have been developed based on the observed linear relationships between K_c and VI. Global examples include:

- Demeter in Europe (DEMONstration of Earth observation TEchnologies in Routine irrigation advisory services; Belmonte *et al.*, 2005;);
- TOPS-SIMS in USA (Terrestrial Observation and Prediction System Satellite Irrigation Management Support; Cahn and Johnson, 2017; <https://ecocast.arc.nasa.gov/simsi/>); and
- IrriSAT in Australia (Hornbuckle, 2014).

TOPS-SIMS, supported by NASA and USGS, aims to provide contemporary field scale K_c data and real time weather data to support real time, weather-based, irrigation management by combining field-specific values of NDVI and K_c with district ET_0 data for the state of California (Cahn and Johnson, 2017). TOP-SIMS uses ET_0 data sourced from an extensive network of weather stations (CIMIS) operated by the Californian Department of Water Resources.

Reflectance-based K_c -VI approaches (such as TOPS-SIMS, IrriSAT) are founded on relationships linking ET^* to a crop coefficient based on FC and/or NDVI. EO-based measures of the T_s /NDVI relationships in irrigated crops, and/or ET /NDVI relationships based on surface energy balance estimates of ET, potentially play an important role in the development of practical irrigation management systems based on readily-acquired, reflectance-based VI (see Section 9.4).

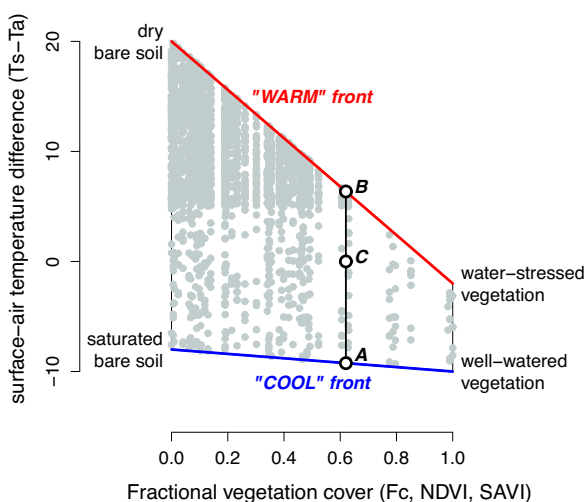
13.5.2 T_s -VI relationships

Remotely sensed values of NDVI are not directly related to vegetation water status or rates of evapotranspiration. Early EO-based studies of vegetation water status and water use (or ET) focused on relationships between surface temperature (T_s) and NDVI on the basis that T_s was inversely related to ET, since evaporative cooling due to ET decreases vegetation temperature and T_s . Remotely sensed T_s /NDVI values were commonly confined within a trapezoidal space described by the approximate limits, $0.1 \leq NDVI \leq 0.9$ (which can be optionally interpreted in terms of FC; $0 \leq FC \leq 1$) and upper and lower 'warm' and 'cool' edges associated with low and high rates of ET, respectively.

The trapezoid/triangle approach proposed by Moran *et al.* (1994, 1996) provided an initial quantitative approach to remotely sensed ET and soil moisture estimation (see Figure 13.1). Weather-dependent rates of ET were ascribed to each of the vertices of the trapezoid (dry, bare soil; water-stressed vegetation; well-watered vegetation; saturated bare soil) based on the Penman-Monteith equation (see first equation in Section 13.4.2). Intermediate pixel scale ET estimates were linearly interpolated based on the proximity of T_s /NDVI values to the warm and cool fronts in the trapezoidal T_s /NDVI distribution (that is, the ratio BC/BA in Figure 13.1).

Figure 13.1 Variation of surface-air temperature differences with vegetation cover

Diagram depicting the trapezoidal distribution of surface-air temperature differences ($T_s - T_a$) relative to values of fractional vegetation cover (FC, SAVI or NDVI) as seen in many vegetation/water stress studies. The 'warm' $T_s - T_a$ front is associated with low rates of ET ($ET=0$), and the 'cool' front depicts well-watered patches of vegetation and/or wet soils ($ET=ET^*$). Moran *et al.* (1994) estimated the ratio ET/ET^* by the ratio BC/BA.



Adapted from: Moran *et al.* (1994, 1996)

13.5.3 Surface energy balance models

Bastiaanssen *et al.* (1998) published the seminal SEBAL model (Surface Energy Balance Algorithm for Land), a satellite-based energy balance approach to estimate land surface ET (see Section 9.4). SEBAL incorporated sub-models to estimate components of the surface energy balance (SEB) equation, expressed as:

$$(R_n - G) = H + LE$$

where,

R_n is net radiation measured above the vegetation (MJ/m²/day);

G is soil heat flux (MJ/m²/day);

H is sensible heat flux (MJ/m²/day); and

LE is latent heat flux (ET).

LE is estimated as the residual:

$$LE = (R_n - G) - H$$

Pixel scale estimates of H are derived by identifying 'wet' and 'dry' endmember pixels, where the sensible heat, H , assumed the values:

- $H = 0$ ($LE = R_n$) for 'wet' endmembers; and
- $H = R_n$ ($LE = 0$) for 'dry' endmembers.

Relative to the trapezoid approach, 'dry' and 'wet' endmember pixels in SEBAL analyses corresponded to the vertices associated with 'large T_s + low NDVI' and 'low T_s + large NDVI' respectively in Figure 13.1.

13.6 METRIC Model: Summer Crops

Tasumi *et al.* (2005) applied the METRIC model to irrigated summer crops grown in Idaho, USA. They employed Landsat imagery to study field scale ET_r/F/NDVI relationships. Data were acquired as a series of snapshots at overpass intervals of approximately 16 days during crop growth periods and the resultant ET_r/F/NDVI data were collated in order to develop seasonal ET_r/F/NDVI relationships for the major irrigated summer crops grown in Magic Valley, Idaho, in 2000. Tasumi *et al.* (2005) made the *a priori* assumption that all irrigated crops were adequately supplied with water (that is, $K_c = ET_r/F$) for the crops in their study.

K_c /NDVI relationships for potato and sugar beets (see Figure 13.2) showed that NDVI values extended over the approximate limits, $0.1 \leq NDVI \leq 0.85$, encompassing the range of FC, $0 \leq FC \leq 1.0$ (from

Bastiaanssen and Allen subsequently collaborated to produce the METRIC model (Mapping Evapotranspiration at High Resolution with Internal Calibration), an adaption of SEBAL that was tailored to irrigation applications (Allen *et al.*, 2007). Whilst METRIC also employed wet and dry endmember pixels, the wet pixel in METRIC is associated with:

$$H = R_n - ET_r$$

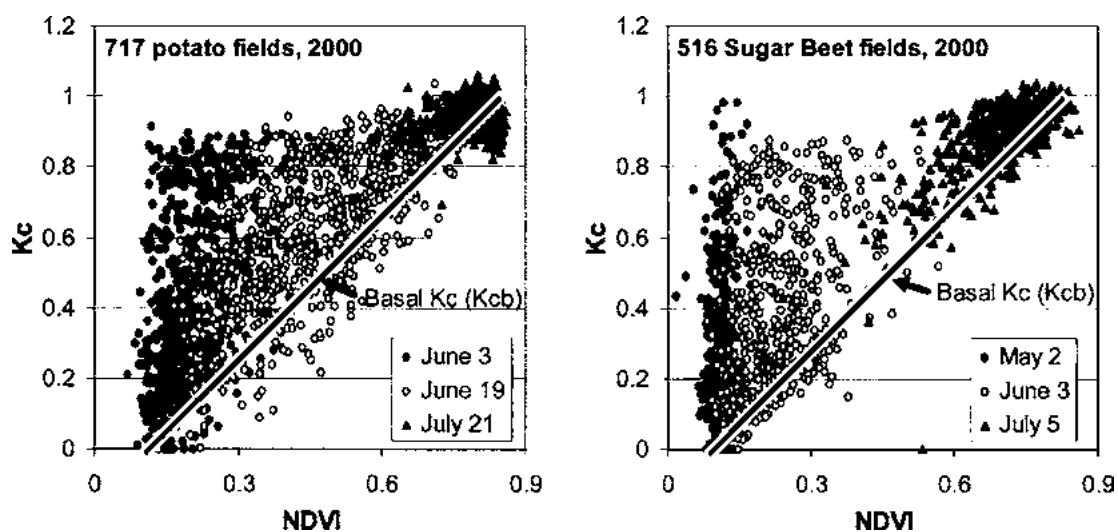
rather than the assumption, $H=0$, used by SEBAL. The use of ET_r to approximate ET at the wet 'anchor' pixel compensated for regional advection effects, and supported the extrapolation of instantaneous satellite-derived values of ET to periods of 24 hours and longer. METRIC can be applied across crop types and growing conditions, and has significant advantages over conventional methods of estimating ET from documented crop calendar curves (see Figure 13.3) in that neither the crop development stages, nor the specific crop type need to be known with METRIC. Allen *et al.* (2011) provide a detailed comparison of the SEBAL and METRIC algorithms.

The energy balance methods employed in SEBAL and METRIC respond to reductions in ET caused by water stress. Values of evaporative fraction (LE/R_n) produced by SEBAL and fractional ET_r ($ET_r/F = ET/ET_r$) from METRIC may be associated with crops that are inadequately supplied with water. Supporting evidence is required before satellite-based SEB estimates of ET can be equated with well-watered values, ET^* . ET_r/F estimates in Section 13.7 (made with the Agriculture Victoria rendition of METRIC) were equated with values of K_{cr} (see first equation, Section 13), based on comparisons with published data for irrigated summer crops grown in USA.

bare ground to full canopy cover; see, for example, Bastiaanssen and Ali, 2003). Tasumi *et al.* (2005) reported that the lower observed limit on K_c (ET_r/F) increased approximately linearly with increases in NDVI over the entire range of NDVI, and consequently equated the lower observed limit on K_c with K_{cb} (the basal crop coefficient), which describes the minimum rate of ET of a crop adequately supplied with water (surface evaporation = 0). K_{cb} is defined as the value of ET_r/F when the soil surface is dry ($E \approx 0$), and transpiration is maintained at maximal rates (Allen *et al.*, 1998). The K_{cb} line has important practical implications, as it represents the irrigation trigger point, beyond which a further reduction in root zone soil water leads to the onset of crop water stress.

Figure 13.2 Crop coefficient variations

Variation in crop coefficients, K_c , estimated as fractional 'tall' crop evapotranspiration (ET_r/F), versus NDVI for potato and sugar beet crops in the Magic Valley area of Idaho for three Landsat dates during crop development in 2000.



Source: Tasumi *et al.* (2005)

Maximum values of K_c were described by $K_c = ET_r/F = 1.0$, over the observed range of NDVI (see Figure 13.2). The limit, $K_c = ET_r/F = 1.0$, complied with energy balance limits on the rates of ET observed in lysimeter studies of dry surface, full cover crops ($ET = ET_r$; Allen *et al.*, 2007; Jensen and Allen, 2016). The dry surface limit, $ET_r/F = 1.0$, extends to an approximate maximum, $ET_r/F \leq 1.20$, in fields where the vegetation and/or soil surface are wet by recent rain or irrigation (Tasumi *et al.*, 2005; Allen *et al.*, 2007). Tasumi *et al.* (2005) attributed the large range in ET_r/F at low NDVI ($0 \leq ET_r/F \leq 1.0$) to variations in surface soil moisture, caused by rain and/or irrigation events, during periods of low plant cover.

K_c (ET_r/F) values were therefore confined to a triangular K_c /NDVI space within K_c and NDVI limits, $K_{cb} \leq K_c \leq 1.0$ and $0.1 \leq NDVI \leq 0.85$, respectively. Rainfall and irrigation-induced increases in ET_r/F were progressively diminished by increases in FC during crop growth.

The range of NDVI in the Idaho ET_r/F /NDVI data encompassed recently sown crops with a vegetation-free soil surface, and fully grown crops with complete canopy cover, and therefore extended across the potential range of FC seen in annual field crops ($0 \leq FC \leq 1$).

13.7 METRIC Model: Irrigated Horticulture

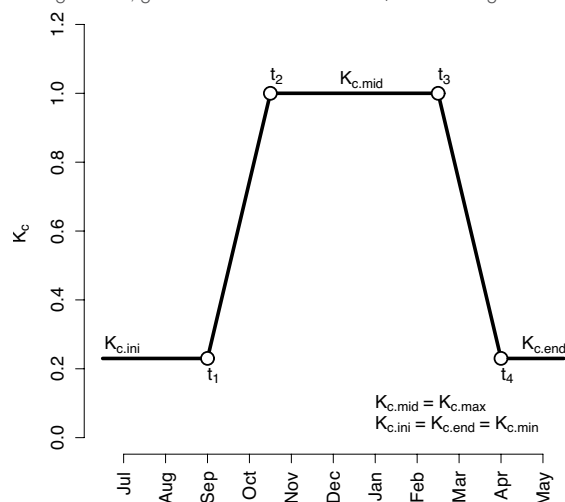
13.7.1 Introduction

Whilst perennial fruit, nut, and vine crops grown in the southern MDB show little physical resemblance to irrigated annual summer crops (see Section 13.6), the hydrologic responses elucidated by the latter provided a comparative, contextual framework for the study and interpretation of ET /NDVI data in horticultural crops grown in the southern MDB. In contrast to perennial fruit, nut, and vine crops, summer annuals are resown into freshly-prepared seedbeds in spring each year ($FC=0$) and crops exhibit an extended period of low plant cover during germination, emergence and establishment stages of growth, then subsequent growth and leaf expansion is rapid under favourable conditions, resulting in near complete cover of the soil surface before crops set

seed, mature and senesce. Conversely, perennial fruit, nut, and vine crops undergo an establishment period of up to seven years before they reach full production. Once established, deciduous horticultural species also show marked seasonal trends in foliage cover: FC typically increases rapidly in spring, followed by a prolonged period of maximal incomplete cover during fruit/nut growth, and harvest in summer or autumn. Deciduous species lose leaves during cooler months, whereas evergreen species, including citrus, maintain a more or less constant foliage cover and water use capability (K_c) throughout the year (see Sections 4 and 5).

Figure 13.3 Typical crop coefficient curve

Typical crop coefficient curve for Southern Hemisphere deciduous tree crops: seasonal changes in the basal crop coefficient (K_{cb}) are approximated by piecewise linear changes on calendar transition dates t_1 , t_2 , t_3 , and t_4 . Peak-season values of K_{cb} (t_2 – t_3) vary depending on the crop age, orchard configuration, growth conditions and tree/vine management.



Source: Mohammed Abuzar, Agriculture Victoria

Seasonal water use of temperate deciduous species (and annual summer crops) is therefore characterised by large temporal variations in K_c that closely follow seasonal changes in foliage cover. To account for the impact of variable vegetation cover and background evaporation from soil in orchards and natural landscapes, Allen *et al.* (1998) introduced the basal crop coefficient (K_{cb}), which is principally the transpiration component of ET, with negligible evaporation from soil. As such, it represents the minimum rate of ET for a crop adequately supplied with water.

Crop ‘calendars’ are used to describe the seasonal progression in K_c values attributable to changes in vegetation cover of deciduous perennial horticultural crops. Calendars for deciduous tree crops in the Southern Hemisphere typically show:

- a small value for the basal crop coefficient, K_{cb} , ($K_{cb,ini}$) in the early stages of foliage development;
- followed by an increase to a maximum ($K_{cb,mid}$) associated with the period of peak foliage cover; and
- a subsequent post-harvest decline and return to the minimum values ($K_{cb,ini}$) seen in winter (see Figure 13.3).

In order to facilitate field operations, vegetation cover of the soil surface is carefully planned and managed in row-based fruit, nut, and vine plantings. Canopy/row configurations may also vary within and between orchards in order to promote yield and quality outcomes. Allen and Pereira (2009) described changes in K_{cb} of orchards as a function of crop

height and canopy cover. They employed a density coefficient (K_d) to account for the increase in K_{cb} (and associated increase in K_c) with increased vegetation cover:

$$K_{cb} = K_{cb,min} + K_d (K_{cb,full} - K_{cb,min})$$

Changes in K_{cb} in the range $K_{cb,min}$ – $K_{cb,full}$ were related to the effects of vegetation cover (FC) and crop height (h) depending on the value of K_d applicable to the target crop. K_d showed a near-linear dependence on FC for low values of FC, and achieved a maximum ($K_{cr}=1$) at sub-maximal values of FC in tall crops ($h > 2m$).

The equation above is consistent with the empirical, satellite-based, linear relationship linking K_{cb} to NDVI derived by Tasumi *et al.* (2005; see Figure 13.2), which described a linear increase in K_{cb} of irrigated summer annual crops ($h < 2m$) with increasing NDVI over the full range of NDVI ($0.1 \leq NDVI \leq 0.85$; Tasumi *et al.*, 2005: $K_{cb} \approx 1.33 \times (NDVI - 0.1)$).

Values of $K_{c,mid}$ (see Figure 13.3) coincide with seasonal maximum values of evaporative demand experienced in the southern MDB, and hence with maximal daily values of IWR. Minimum values of K_{cb} , denoted $K_{c,ini}$ and $K_{c,end}$ in Figure 13.3, apply to deciduous fruit, nut, and vine crops during the autumn-winter period. Seasonal changes in K_{cb} of evergreen citrus species are minor, and the values $K_{cb} = K_{c,mid}$ apply throughout the year.

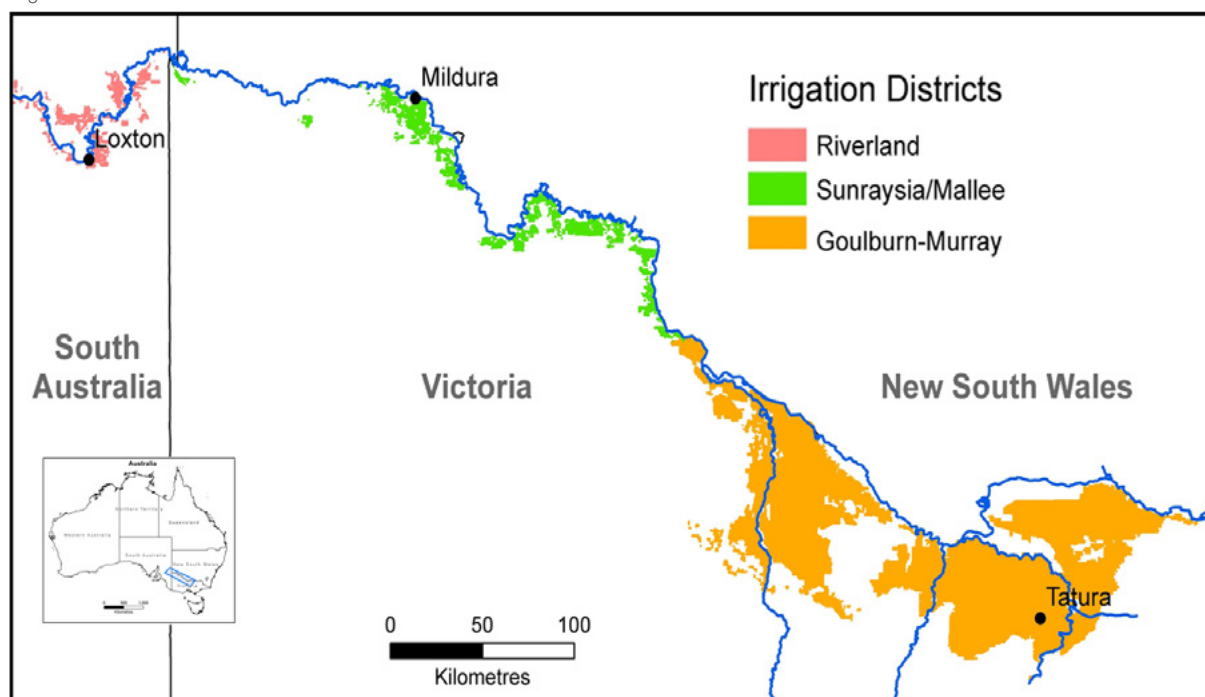
13.7.2 Model implementation

METRIC analyses (Allen *et al.*, 2007) were conducted to investigate $ET_r/NDVI$ relationships seen in perennial fruit, nut, and vine crops grown in the southern MDB during the summer period (peak-season irrigation demand), and to explore the potential relevance of the triangular $ET_r/NDVI$ relationship in those crops. Analyses were undertaken for the period December 2008–February 2010 in the Riverland (RL), Sunraysia/Mallee (SR), and Goulburn-Murray (GM) irrigation districts of SE Australia. These analyses employed Landsat-5 imagery acquired during peak-season irrigation periods (October–April, inclusive). Landsat images were georeferenced to contemporary, field scale, district land use maps (see Table 13.4).

Image-synchronised values of ET_r were computed using district-specific, meteorological data generated by automatic weather stations operated by the Bureau of Meteorology for sites at Loxton (RL), Mildura (SR) and Tatura (GM; see Table 13.5 and Figure 13.4). Values of ET_r were calculated according to standardised ASCE procedures (ASCE EWRI, 2005).

Figure 13.4 Irrigation districts

Map showing the extents of the Riverland, Sunraysia/Mallee and Goulburn-Murray Irrigation Districts in the southern MDB. Representative meteorological data were sourced for the towns of Loxton, Mildura and Tatura, respectively. Inset shows the study region in a continental context.



Source: Des Whitfield, Agriculture Victoria

Table 13.4 Landsat-5 images used in analysis

Clear-sky Landsat-5 images were employed in analyses of ET_f/NDVI relationships in irrigated fruit, nut, and vine crops in the southern MDB. District/date indices were formulated according to irrigation district and date of image acquisition (as doy/year, where doy was day of year, e.g. Jan 1 = doy 1, and year was year of century, e.g. 2000).

Irrigation district	District Code	Acquisition Date	Path/Row	District/Date index	Source of landuse map
Riverland	RL	2010-02-16	96/84	RL047/10	River Murray Irrigated Crops Data (June 2008) produced by the South Australian MDB Resource Information Centre of the South Australian MDB Natural Resources Management Board (SAMDBNRM, 2010)
Sunraysia/Mallee	SR	2008-12-20	95/84	SR355/08	SunRise21 (www.sunrise21.org.au)
		2009-01-05	95/84	SR005/09	
Goulburn-Murray	GM	2008-11-03	93/85	GM308/08	Shepparton Preserving Co. Ltd
		2009-01-22	93/85	GM022/09	
		2009-02-23	93/85	GM054/09	
		2009-03-27	93/85	GM086/09	
		2009-04-12	93/85	GM102/09	

Field scale values of ET_rF (ET_r/ET_c) and NDVI were computed for all fruit, nut, and vine crops grown in each district according to the procedures described in Allen *et al.* (2007)¹⁰. Analytical estimates of momentum roughness length (z_{om}), effects of elevation, and the assignment of hot and cold pixels were as follows:

- The NDVI-albedo (α) approach (see equation 34b in Allen *et al.*, 2007) was used for estimates of z_{om} . We used the relationship published by Teixeira *et al.* (2009) for a mixture of agricultural and natural ecosystems seen in the Sao Francisco River basin, Brazil:

$$z_{om} = \exp\left(0.26\left(\frac{NDVI}{\alpha}\right) - 2.21\right)$$

The NDVI-albedo (α) approach helps to distinguish z_{om} of tall and short vegetation types that have similar NDVI but different albedo (Allen *et al.*, 2007; Teixeira *et al.*, 2009), so avoids the need for crop-specific land cover/vegetation height relationships to describe z_{om} .

- Given the minor variation in elevation across the southern MDB (see Table 13.5), the METRIC model was applied using a constant elevation of 80 m.
- Hot ‘anchor’ pixels ($ET_r = ET_rF = 0$) were identified within low NDVI ($NDVI \leq 0.3$) pixels showing high surface temperature (defined as the upper 2% of T_s), located in non-irrigated fields adjacent to irrigated farms. Cold anchor pixels were selected from fields associated with centre-pivot irrigation of tomatoes (in Riverland district), carrots (in Sunraysia) or lucerne (in Goulburn-Murray). Identified cold-pixel crops closely resembled the theoretical alfalfa crop underpinning estimates of ET_r , with candidate pixels being confined to the upper range of irrigation NDVI, and the lower range of irrigation T_s . Crops were assumed to receive regular, adequate irrigation at intervals of 3–4 days, as observed for lucerne (in Goulburn-Murray). Cold-pixel crops were therefore assumed to be free of surface water (or dry) at the times of satellite overpass, and the value of ET_rF appropriate to dry surface foliage, $ET_rF = 1.0$, was assigned to cold pixels.

Table 13.5 Automatic weather station sites

Site details of automatic weather stations that were used for district METRIC analyses. Station number represents the official designation used by the Bureau of Meteorology, Australia.

District	Site	Station number	Latitude (°S)	Longitude (°E)	Elevation (m asl)
GM	Tatura	81049	36.4378	145.2672	114
SR	Mildura	76031	34.2358	142.0867	51
RL	Loxton	24024	34.4390	140.5978	30

Source: Weatherzone (www.weatherzone.com.au)

Paired pixel scale values of ET_rF /NDVI were attributed to irrigated tree and vine crops based on the delineation of fields in land use maps. Field scale values of ET_rF and NDVI were estimated by respective pixel scale means. Crop-specific analyses were restricted to major crops in each district, and included almond, citrus, and grape crops in both Riverland and Sunraysia districts, and pear, peach, apple and apricot crops in the Goulburn-Murray irrigation area.

ET_rF /NDVI analyses targeted peak-season irrigation periods when fully-grown crops typically experience large rainfall deficits (maximum annual values of evaporative demand coupled with low rainfall). Clear-sky weather conditions provided five scenes for the Goulburn-Murray district in season 2008–09 (see Table 13.4), which allowed for a detailed temporal analysis of the major fruit crops grown in the district.

13.7.3 ET_rF /NDVI relationships

Figure 13.5 shows the peak-season NDVI and ET_rF distributions seen in 29 crop/district/date combinations for fruit, nut, and vine crops grown in the southern MDB within the study period. NDVI was predominantly confined to the range $0.1 \leq NDVI \leq 0.70$, and consequently never achieved the large values ($NDVI > 0.80$) seen in the Idaho data (see Figure 13.2). Reduced maxima in the fruit, nut, and vine data were attributed to row-based plantings in horticultural crops ($FC < 1$). The large variability in peak-season NDVI within the range 0.1–0.70 was attributed primarily to differences in crop age and development, and differences in planting patterns, orchard management, and growth conditions.

¹⁰ Analyses were conducted using ENVI/IDL software (Harris Geospatial, Broomfield CO, USA).

Figure 13.5 also shows relatively few observations of ET_r/F in the range $ET_r/F > 1$, which are expected under conditions where ET is enhanced by direct evaporation of liquid water from wet soil/plant surfaces due to recent irrigation and/or rainfall. Irrigation was employed judiciously during the drought period experienced during the study (Goodwin and O'Connell, 2017), and rainfall events were scarce. Nevertheless, almost all ET_r/F observations exceeded

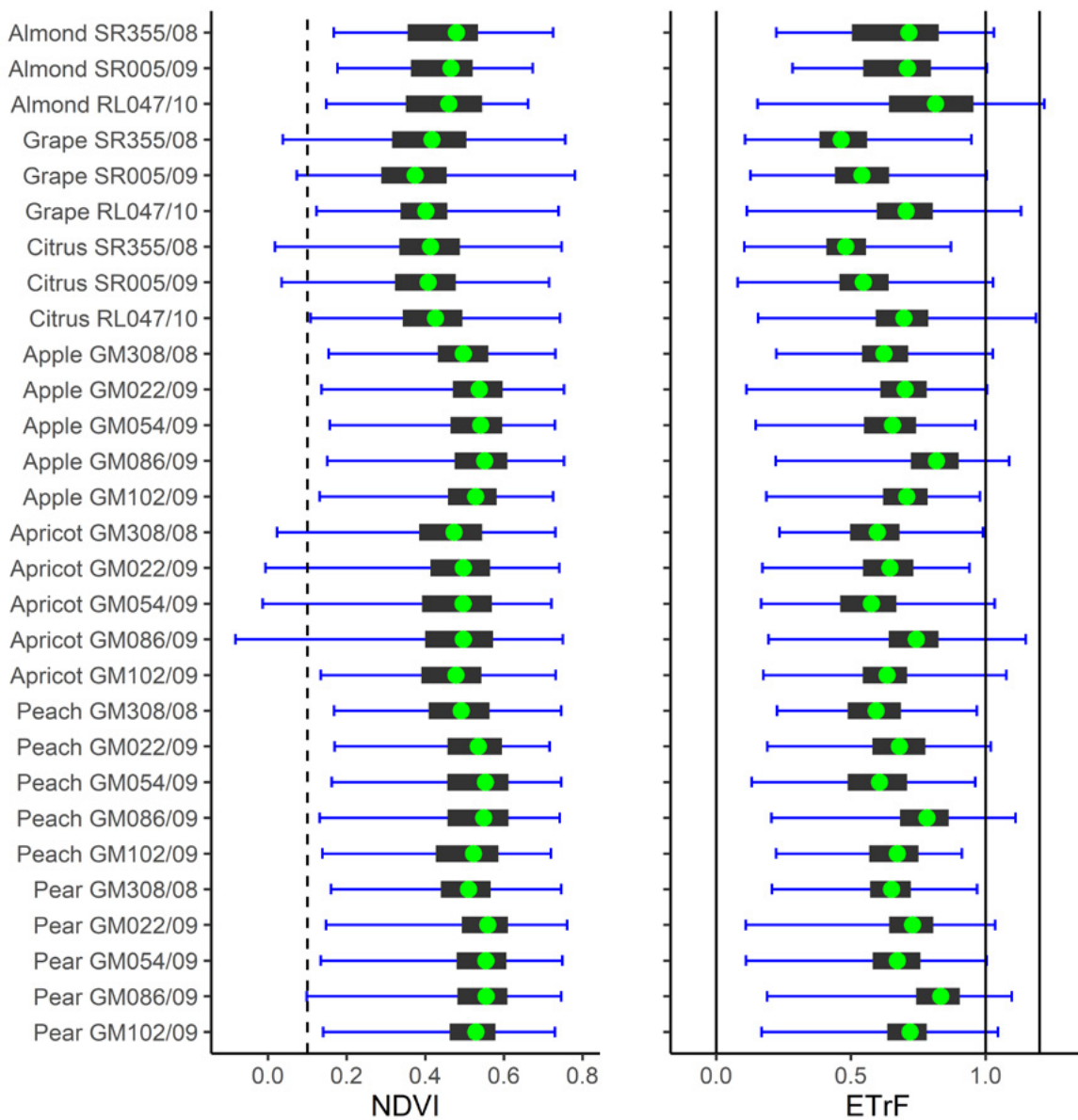
the NDVI-dependent K_{cb} baseline associated with the reference $ET/NDVI$ triangle (see Figure 13.6 and Figure 13.7), providing strong empirical support for the assumption that crops were adequately supplied with water:

$$ET = ET^*$$

$$K_{cr} = ET_r/F (= ET/ET_r)$$

Figure 13.5 Quartile representations

Quartile representations of the distribution of peak-season, field scale values of NDVI and ET_r/F in fruit, nut, and vine crops in the southern MDB irrigation districts in the period 2008–10 inclusive (see Table 13.4 for district/date codes). Blue lines show the range of observed field scale measures of NDVI and ET_r/F , respectively, while solid black bars represent the range of observations in the second and third quartiles. Green dots indicate the median values. Vertical lines demarcate the values $NDVI = 0.1$, $ET_r/F = 0$ and $ET_r/F = 1$.



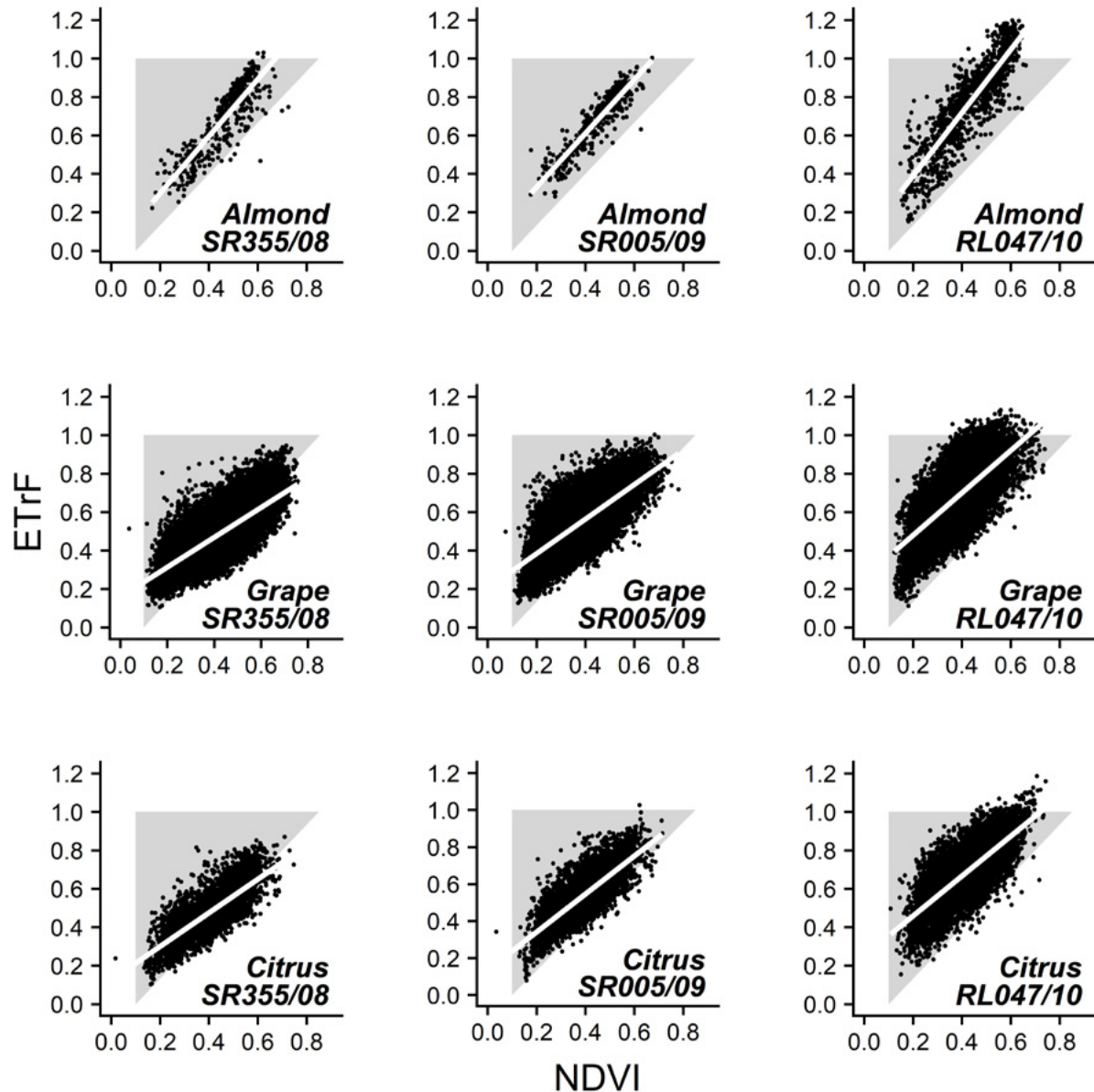
Source: Des Whitfield, Agriculture Victoria

Representative $ET_rF/NDVI$ relationships in Figure 13.6 and Figure 13.7 showed few observations where high rates of ET ($ET_rF > 0.9$) were associated with low NDVI, which is consistent with the scarcity of rainfall events during the study period. $ET_rF/NDVI$

relationships were therefore free of rainfall effects at low NDVI (compared with Figure 13.2 of Tasumi *et al.*, 2005), and ET_rF was consequently significantly related to NDVI ($P < 0.05$) in all 29 crop/district/date combinations available to the study.

Figure 13.6 Relationships for selected crops

Peak-season, field scale $ET_rF/NDVI$ relationships of almond, grape and citrus crops grown in the Sunraysia/Mallee (SR) in 2008/09 irrigation season and Riverland (RL) districts in 2009/10 (see Table 13.4 for district/date codes). Grey triangles represent limits on $ET_rF/NDVI$ values seen in irrigated summer annual crops (Tasumi *et al.*, 2005). White lines represent least squares lines of best fit.



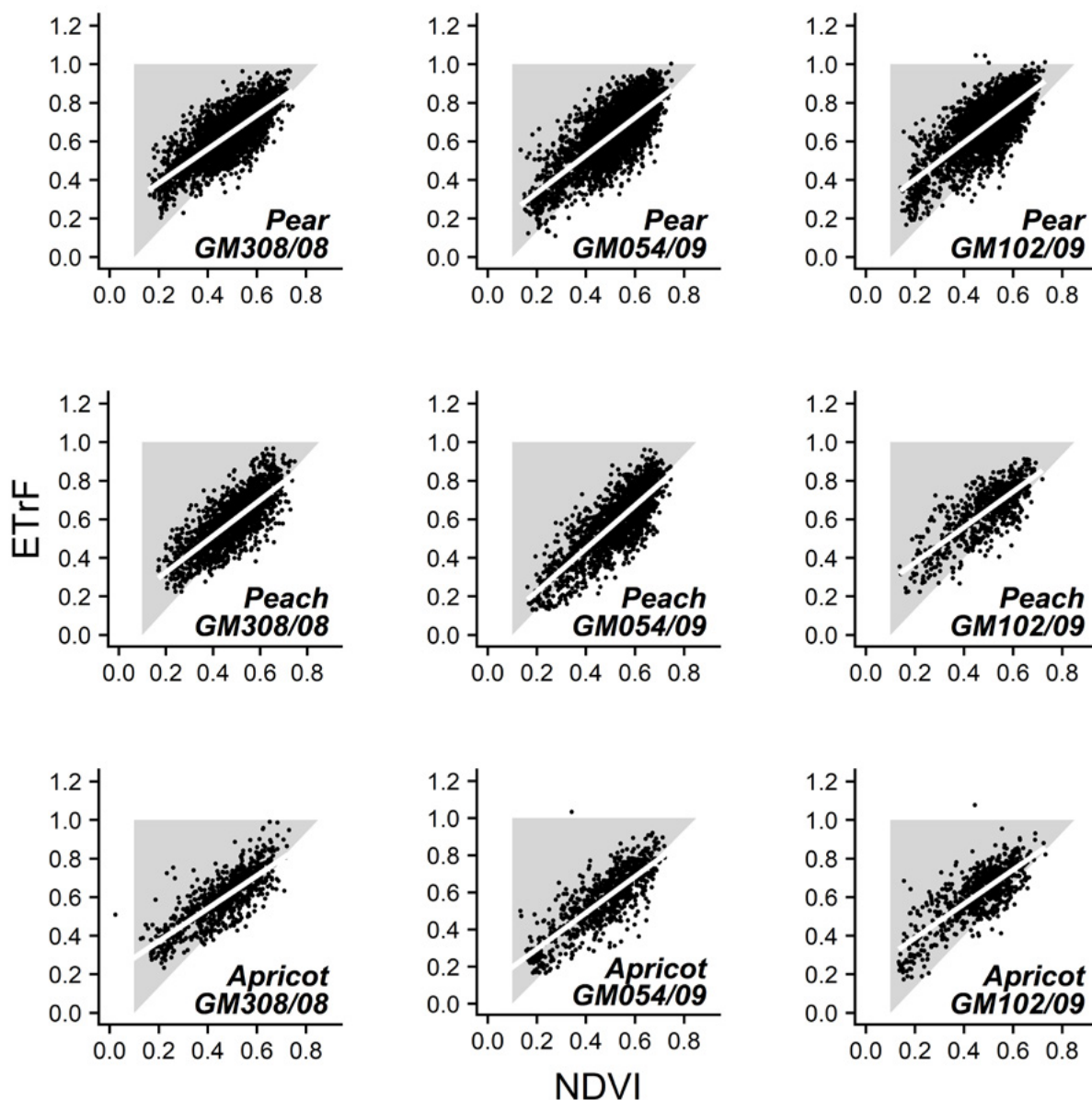
Source: Des Whitfield, Agriculture Victoria

The linear regression relationships shown in Figure 13.6 and Figure 13.7 were appraised by investigating differences in the predicted values of ET_{rF} at endmember values of NDVI (0.1 and 0.85) defined by the $ET_{rF}/NDVI$ reference triangle (using the values $ET_{rF_{min}}$ and $ET_{rF_{max}}$ respectively), along with appropriate 95% fiducial limits, for each crop/district/date combination.

The analysis paralleled the endmember approach adopted by Allen and Pereira (2009), who described changes in K_{cb} of 'tall' horticultural crops in terms of a density coefficient, K_d , for values of K_{cb} within the range, $K_{cb_{min}} - K_{cb_{full}}$ (see equation for K_{cb} in Section 13.7.1).

Figure 13.7 Representative $ET_{rF}/NDVI$ relationships for selected crops

Representative peak-season field scale $ET_{rF}/NDVI$ relationships seen in pear, peach, and apricot crops grown in Goulburn-Murray Irrigation District in 2008/09 irrigation season (see Table 13.4 for district/date codes). Grey triangles represent limits on $ET_{rF}/NDVI$ values seen in irrigated summer annual crops (Tasumi *et al.*, 2005). White lines depict least-squares lines of best fit.



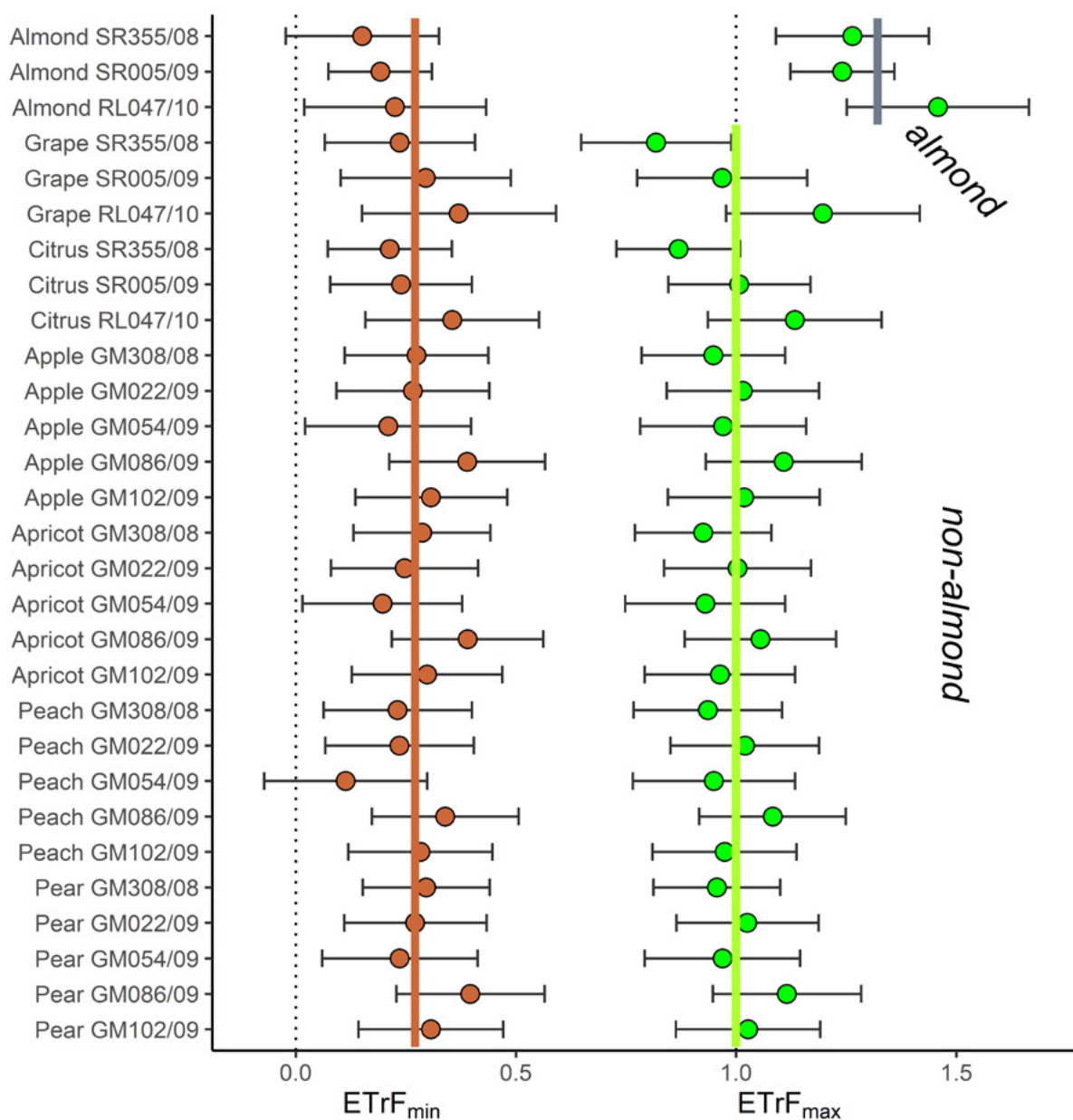
Source: Des Whitfield, Agriculture Victoria

Figure 13.8 shows that regression estimates of ET_rF_{min} were confined to the approximate range $0.1 \leq ET_rF_{min} \leq 0.4$ (fiducial limits $-0.1 \leq ET_rF_{min} \leq 0.6$). The mean value of ET_rF_{min} ($ET_rF_{min} = 0.27$) fell within fiducial limits appropriate to individual crop/district/date combinations.

Figure 13.8 shows that regression estimates of ET_rF_{max} ranged between 0.8 and 1.4 (fiducial limits $0.7 \leq ET_rF_{max} \leq 1.75$). The data clearly demonstrated that the mean value of ET_rF_{max} for almonds exceeded values seen in non-almond crops. The mean value of ET_rF_{max} in non-almond crops was consistent with the estimate $ET_rF_{max} = 1.00$ (see Figure 13.8), whereas the mean value for almonds was $ET_rF_{max} = 1.32$.

Figure 13.8 Endmember regression estimates of ET_rF_{min} and ET_rF_{max}

Predicted values of endmember estimates of ET_rF_{min} (brown) and ET_rF_{max} (green) in crop/district/date combinations (see Table 13.4 for district/date codes) enumerated in the southern MDB in seasons, 2008/09 and 2009/10, and associated fiducial limits (95%). Mean value of the coefficient, ET_rF_{min} , was 0.27 in all fruit, nut, and vine crops (shown as brown vertical line), while mean value of ET_rF_{max} was 1.00 in non-almond crops (shown as green vertical line). ET_rF_{max} assumed the value, $ET_rF_{max} = 1.32$, in almond crops grown in the southern MDB (shown as grey vertical line).



Source: Des Whitfield, Agriculture Victoria

The preceding analysis of satellite-based ET_rF /NDVI relationships for irrigated fruit, nut, and vine crops grown in the southern MDB showed large variations in peak-season values of ET_rF . Derived estimates of $ET_{rF_{min}}$ and $ET_{rF_{max}}$ were attributed to adequately watered crops on the dual basis that:

- satellite-based ET_rF measures were related exclusively to irrigated fields and crops defined by irrigation land use maps; and
- field scale observations of ET_rF overwhelmingly exceeded values associated with the nominal lower limit (K_{cb}) of the ET_rF /NDVI triangle derived from Tasumi *et al.* (2005).

The severe lack of rainfall experienced by irrigation districts during the drought conditions of this study further suggested that estimates of ET_rF shown in Figure 13.5, Figure 13.6, and Figure 13.7 were closely associated with K_{cb} values expected for adequately watered, fruit, nut, and vine crops.

ET_rF showed strong, statistically-significant, linear relationships with NDVI in all peak-season crop/date/district combinations addressed by this study (see Figure 13.6 and Figure 13.7), providing strong independent support for the use of the K_c -VI to determine IWR of horticultural crops grown in the southern MDB. Endmember analyses of linear K_c /NDVI relationships (see Figure 13.8) showed that complex variations in FC, crop height, and tree/vine

planting distributions were described by crop-specific endmember values of ET_rF estimated for the extremes of NDVI, namely NDVI = 0.1 and NDVI = 0.85, according to the ET_rF /NDVI triangle derived from Tasumi *et al.* (2005). Data shown in Figure 13.8 further suggested that linear ET_rF /NDVI relationships applicable to fruit, nut, and vine crops in the range $ET_rF \leq 1$ may be described by:

$$ET_rF = ET_{rF_{min}} + \frac{(NDVI - 0.1)(ET_{rF_{max}} - ET_{rF_{min}})}{0.75}$$

Here, $ET_{rF_{min}}$ described the lower limit on ET_rF at minimal NDVI (NDVI = 0.1), while $ET_{rF_{max}}$ described differences in ET_rF seen at maximal NDVI (NDVI = 0.85). $ET_{rF_{max}}$ varied between species, assuming the values $ET_{rF_{max}} = 1.32$ in almond, and $ET_{rF_{max}} = 1.00$ in all other species included in the range of fruit, nut, and vine crops. Values of ET_rF afforded by the equation above are limited to the maximum rate of ET attributable to well-watered alfalfa ($ET_rF = 1$; Allen *et al.*, 2007; Allen and Pereira, 2009; Jensen and Allen, 2016).

Derived estimates of $ET_{rF_{min}}$ and $ET_{rF_{max}}$ may therefore be combined with weather-based measures of ET_r to estimate rates of ET^* for use in real time, field scale irrigation management, or regional and farm scales in order to ensure an optimal balance between water supply and demand in horticultural crops.

13.8 Application to Irrigated Horticultural Crops in Southeast Australia

Seasonal and annual analyses of regional and farm scale irrigation demand may be conducted by undertaking crop water balance analyses based on weather, and the area and peak-season NDVI of constituent crops. This proposed regional approach contrasts with existing methods, which use census and other data to describe crop type and area, usually without regard to differences in the irrigation water requirements associated with crop age or size, and rely on historic water use data and/or the application of a predefined set of K_c values to describe crop water use capability.

Regional water use assessments are important in districts where crop mix and/or crop area are subject to rapid change. Regular assessments allow water managers to stay abreast of changes in the regional supply/consumption differentials that vary with changes in crop mix, crop area, and climate. Variations in crop mix change the K_c values that determine irrigation intensity (water use per ha), and changes in climate (rainfall deficit) also lead to changes in irrigation intensity. The largest changes in irrigation water use/demand are ultimately attributable to changes in the area of irrigated crops.

Irrigation farmers require a clear understanding of crop-specific water requirements in order to gauge irrigation demand of existing and prospective crops, and are challenged by the need to ensure that irrigation practices satisfy the yield and quality targets of crops, with minimal over-irrigation and consequent impact on the deep drainage to underlying water tables. Thus irrigators are primarily concerned with issues of irrigation intensity, and the need to ensure that irrigation applications are closely aligned to the temporal and spatial variations that arise from the range of crops and fields that contribute to on-farm irrigation demand. Methods described in this chapter provide the potential to define and refine crop-dependent, field scale water use targets and are further suited to turnkey regional supply/demand analytics when assessments of district and farm scale irrigation supply and demand are augmented by EO crop mapping techniques.

Seasonal trends in K_c of deciduous crops are important to farm/district scale assessments of irrigation demand. These may be incorporated in analyses of well-established crops by the use of crop calendars for temporal scaling of in-season values of NDVI (see Figure 13.2). Alternatively, multiple satellite images may be used to undertake real time, field-customised irrigation management (such as IrriSAT; Hornbuckle, 2014; see Section 13.9).

In all cases, estimates of ET^* are readily incorporated in soil water balance analyses to estimate field- and crop-specific irrigation water requirements. Methods described in Section 13.7 therefore provide a formal, objective basis for the irrigation demand analytics needed to ensure that irrigation demand is appropriately matched to irrigation resources at field, farm and district scales in irrigated fruit, nut, and vine crops of the southern MDB.

13.9 Further Information

Australian Horticulture

Australian Department of Agriculture and Water Resources: Horticulture fact sheet: http://www.agriculture.gov.au/ag-farm-food/hort-policy/horticulture_fact_sheet

Australian Society of Horticultural Science (AuSHS):

Australian Horticulture webpage: <http://aushs.org.au/australian-horticulture/> <http://aushs.org.au/australian-horticulture/>

Australian Horticulture Statistics Handbook 2017/18: <https://www.horticulture.com.au/growers/help-your-business-grow/research-reports-publications-fact-sheets-and-more/australian-horticulture-statistics-handbook/>

IrriSAT

Hornbuckle (2014)

Montgomery *et al.* (2015)

<https://irrisat-cloud.appspot.com/>

Evapotranspiration

Allen *et al.* (1998)

ASCE-EWRI (2005)

Jensen and Allen (2016)

13.10 References

- Allen, R.G., Pereira, L.S., Raes, D., and Smith, M. (1998). *Crop evapotranspiration: Guidelines for computing crop water requirements*. United Nations FAO Irrigation and Drainage Paper 56. FAO, Rome. ISBN 92-5-104219-5 <http://www.fao.org/3/X0490E/x0490e00.htm#Contents>
- Allen, R.G., Pruitt, W.O., Wright, J.L., Howell, T.A., Ventura, F., Snyder, R., Itenfisu, D., Steduto, P., Berengena, J., Yrisarry, J.B., Smith, M., Pereira, L.S., Raes, D., Perrier, A., Alves, I., Walter, I., and Elliott, R. (2006). A recommendation on standardized surface resistance for hourly calculation of reference ET_0 by the FAO56 Penman-Monteith method. *Agricultural Water Management*, 81, 1–22.
- Allen, R.G., Tasumi, M., and Trezza, R. (2007). Satellite-Based Energy Balance for Mapping Evapotranspiration with Internalized Calibration, METRIC. Model. *Journal of Irrigation and Drainage Engineering*, 133, 380–394.
- Allen, R.G., and Pereira, L.S. (2009). Estimating crop coefficients from fraction of ground cover and height. *Irrigation Science*, 28, 17–34.
- Allen, R.G., Irmak, A., Trezza, R., Hendrickx, J.M.H., Bastiaanssen, W.H.M., and Kjaersgaard, J. (2011). Satellite-based ET estimation in agriculture using SEBAL and METRIC. *Hydrological Processes*, 25, 4011–4027.
- Argus S. (2015). *Summary report: Irrigated crops of the Lower Murray-Darling: 1997 to 2015*. <https://www.sunrisemapping.org.au>
- ASCE-EWRI (2005). *The ASCE Standardized Reference Evapotranspiration Equation*. Final Report: Environmental and Water Resources Institute of the American Society of Civil Engineers, Virginia, USA. 70 p.
- Bastiaanssen, W.G.M., and Ali, S. (2003). A new crop yield forecasting model based on satellite measurements applied across the Indus Basin, Pakistan. *Agriculture, Ecosystems and Environment*, 94, 321–340.
- Bastiaanssen, W.G.M., Menenti, M., Feddes, R.A., and Holtslag, A.A. (1998). A remote sensing surface energy balance algorithm for land (SEBAL). *Journal of Hydrology*, 212–213, 198–212.

- Bausch, W.C., and Neale, C.M.U. (1987). Crop coefficients derived from reflected canopy radiation: a concept. *Transactions of the American Society of Agricultural Engineers*, 30, 703–709.
- Belmonte, A.C., Jochum, A.M., Garcia, A.C., Rodriguez, A.M., and Fuster, P.L. (2005). Irrigation management from space: Towards user-friendly products. *Irrigation and Drainage Systems*, 19, 337–353.
- Cahn, M.D., and Johnson, L.F. (2017). Review: New Approaches to Irrigation Scheduling of Vegetables. *Horticulturae*, 3, 28.
- Doorenbos, J., and Pruitt, W.O. (1977). *Crop water requirements*. United Nations FAO Irrigation and Drainage Paper Number 24 (rev). 144 p.
- Goodwin, I., and O’Connell, M.G. (2017). Drought water management: an Australian perspective. *Acta Horticulturae*, 1150, 219–232.
- Gonzalez-Dugo, V., Zarco-Tejada, P., Nicolas, E., Nortes, P.A., Alarco, J.J., Intrigliolo, D.S., and Fereres, E. (2013). Using high resolution UAV thermal imagery to assess the variability in water status of five fruit tree species within a commercial orchard. *Precision Agriculture*, 14(6), 660–678. doi:10.1007/s11119-013-9322-9
- Guerra, E., Ventura, F., and Snyder, R. (2016). Crop Coefficients: A Literature Review. *Journal of Irrigation and Drainage Engineering*, 142(3), [06015006]. [https://doi.org/10.1061/\(ASCE\)IR.1943-4774.0000983](https://doi.org/10.1061/(ASCE)IR.1943-4774.0000983)
- Heilman, J.L., Heilman, W.E., and Moore, D.G. (1982). Evaluating the crop coefficient using spectral reflectance. *Agronomy Journal*, 74, 967–971.
- Hornbuckle, J. (2014). *Vineyard Irrigation—delivering water savings through emerging technology*. Final Report, Grape and Wine Research and Development Corporation Project CSL0901, 90 p.
- Hunsaker, D.J., Pinter, P.J., Barnes, E.M., and Kimball, B.A. (2003). Estimating cotton evapotranspiration crop coefficients with a multispectral vegetation index. *Irrigation Science*, 22, 95–104.
- Jensen, M.E., and Allen, R.G. (2016). *Evaporation, evapotranspiration, and irrigation water requirements*. American Society of Civil Engineers. <https://doi.org/10.1061/9780784414057>
- Johnson, L.F., and Trout, T.J. (2012). Satellite NDVI Assisted Monitoring of Vegetable Crop Evapotranspiration in California’s San Joaquin Valley. *Remote Sensing*, 4, 439–455.
- Montgomery, J., Hornbuckle, J., Hume, I., and Vleeshouwer, J. (2015). IrriSAT—weather based scheduling and benchmarking technology. *Proceedings of 17th ASA Conference*, Hobart, Australia. http://www.agronomyaustraliaproceedings.org/images/sampled/2015_Conference/pdf/agronomy2015final00449.pdf
- Moran, M.S., Clarke, T.R., Inoue, Y., and Vidal, A. (1994). Estimating Crop Water Deficit Using the Relation between Surface-Air Temperature and Spectral Vegetation Index. *Remote Sensing of Environment*, 49, 246–263.
- Moran, M.S., Rahman, A.F., Washburne, J.C., Goodrich, D.C., Weltz, M.A., and Kustas, W.P. (1996). Combining the Penman-Monteith equation with measurements of surface temperature and reflectance to estimate evaporation rates of semiarid grassland. *Agricultural and Forest Meteorology*, 80, 87–109.
- Neale, C.M.U., Bausch, W.C., and Heermann, D.F. (1989). Development of reflectance based crop coefficients for corn. *Transactions of the American Society of Agricultural Engineers*, 32, 1891–1899.
- Pereira, L.S., Perrier, A., Allen, R.G., and Alves, I. (1999). Evapotranspiration: Concepts and Future Trends. *Journal of Irrigation and Drainage Engineering*, 125, 45–51.
- Rajan, N., and Maas, S.J. (2014). Spectral crop coefficient approach for estimating daily crop water use. *Advances in Remote Sensing*, 3, 197–207.
- SAMDBNRM, (2010). *Regional Plan, Volume 3: Regulatory and Policy Framework*. South Australian MDB Natural Resources Management Board. 74 p.
- Tasumi, M., Allen, R.G., Trezza, R., and Wright, J.L. (2005). Satellite-Based Energy Balance to Assess Within-Population Variance of Crop Coefficient Curves. *Journal of Irrigation and Drainage Engineering*, 131, 94–109.
- Teixeira, A.H.C., Bastiaanssen, W.G.M., Ahmad, M.D., and Bos, M.G. (2009). Reviewing SEBAL input parameters for assessing evapotranspiration and water productivity for the Low-Middle Sao Francisco River basin, Brazil Part A: Calibration and validation. *Agricultural and Forest Meteorology*, 149, 462–476.
- Yang, Y., Roderick, M.L., Zhang, S., McVicar, T.R., and Donohue, R.J. (2018). Hydrologic implications of vegetation response to elevated CO₂ in climate projections. *Nature Climate Change*, 9, 44–48. doi:10.1038/s41558-018-0361-0



14 Pastures

Graham Donald

This section considers EO methods for extracting information to assist the management of pasture lands in Australia. In this context, the term ‘pasture’ combines the grassland definitions of Hill (2004):

- human-made pastures and grasslands—largely resulting from clearing of forested lands to grow pasture for dairy, meat, or wool production, as occurs in the coastal and hinterland regions of NSW, Victoria, and WA; and
- highly managed natural grasslands—naturally grassy regions now used to graze livestock, such as the semi-improved pastoral regions of eastern Australia.

To be a successful farmer one must first know the nature of the soil.
(Xenophon)

Section 15 below will consider EO methods that are more appropriate for the semi-arid and arid Australian rangelands, where vegetation density and stocking rates are much lower.

At a global level, grasslands are the most prevalent type of vegetation cover (Latham *et al.*, 2014), the second largest terrestrial carbon sink (Derner and Schuman, 2007), and the cheapest source of fodder for livestock (Ali *et al.*, 2016). However, the combined impacts of urbanisation, industrial development, overgrazing, intensive management, and climate change have meant that the area of agricultural land, and particularly permanent pasture cover, has declined in recent decades both on a global basis and in Australia (Poore, 2016; see Figure 14.1).

To assist graziers making management decisions, a number of spatial technologies have become available including EO-based information. Some of the attributes of grasslands that can be retrieved from EO datasets include biomass, forage quality, growth rate,

land cover, and degradation (Ali *et al.*, 2016). These data provide an objective assessment of pasture condition to assist farmers and graziers in resource monitoring and management, and thereby measure the sustainability of agricultural practices over many years. EO-based systems allow graziers and farmers to self-regulate their activities to maintain the health of their pastures, and enable governmental authorities to regulate regional issues such as deforestation and the protection of native grasses.

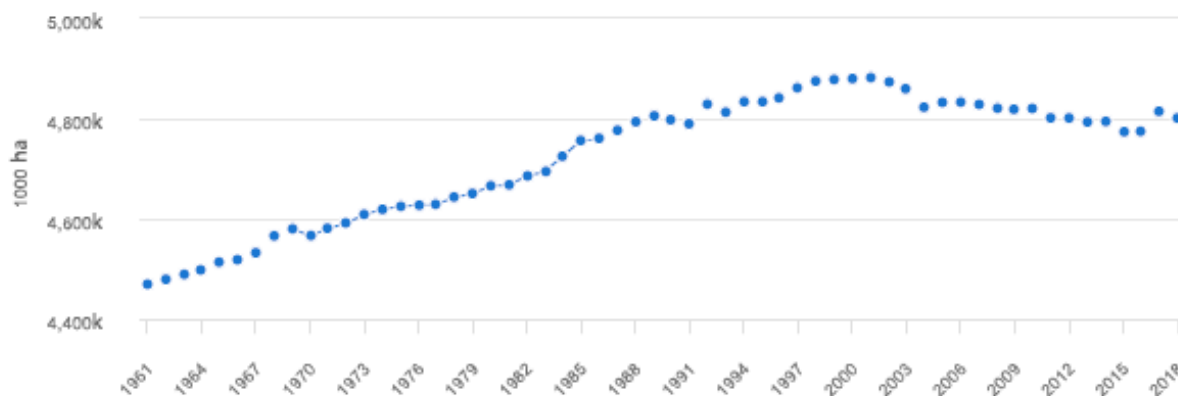
As with many applications, the major improvements with EO data in agriculture are likely to result from its integration with other spatial services and the ‘sense making’ processes that will be derived from complex system modelling. In essence, this includes all the information required for balancing the agricultural, economic, and ecological systems in a sustainable management environment that cannot be otherwise achieved without EO technology (see Section 20).

Background image: Cattle grazing in New England region, NSW. Source: Graham Donald

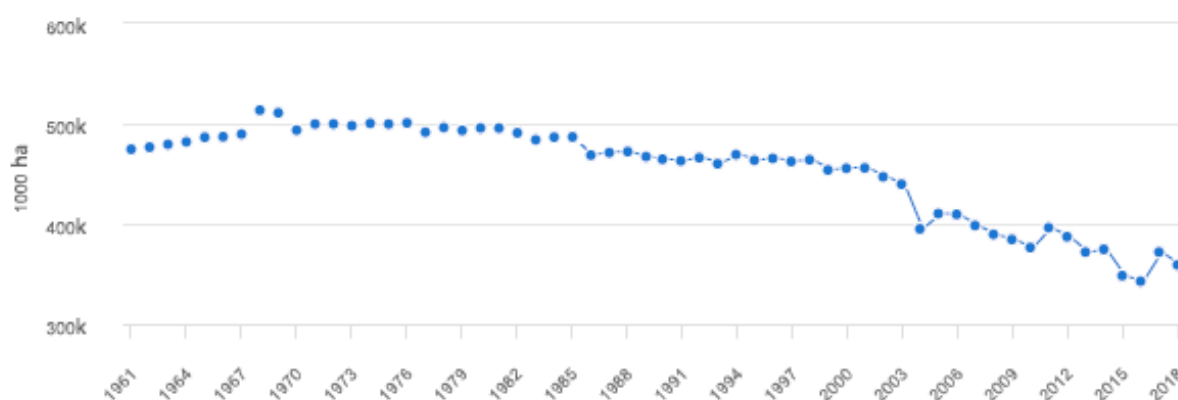
Recommended Chapter Citation: Donald, G.E. (2021). Pastures. Ch 14 in *Earth Observation: Data, Processing and Applications. Volume 3A—Terrestrial Vegetation*. CRCSP, Melbourne. pp. 281–298.

Figure 14.1 Area of agricultural land

a. Global



b. In Australia



Source: FAOSTAT (2019)

14.1 Pastures in Australia

In Australia, pastoral regions are relatively well-vegetated and enjoy a Mediterranean climate (see Sections 2.2 and 2.4). The coastal belt and hinterlands of Queensland, NSW, and Victoria, plus southeast SA, southwest WA, and Tasmania, receive the highest rainfalls so are best suited to dairy farms, horticulture, and fine wool production (see Figure 11.1). In the drier 'wheat-sheep zone', which covers the slopes and plains of NSW, northern Victoria, southern SA, and parts of southwest WA, larger properties grow grain crops, legumes, and oilseeds, often in rotation with grazing by sheep or cattle (McIvor, 2005).

The main livestock grazed commercially in Australia are sheep and cattle. Sheep are primarily grazed for meat in areas with higher rainfall and grown for wool on drier pastures.

The Australian Bureau of Statistics (ABS) regularly collects agricultural census data, with the major unit for aggregation and reporting being the Statistical Local Area (SLA; see Section 11.1). SLA boundaries are based on subdivisions or groupings of Local Government Areas (LGA) or their equivalent. Data are reported at the end of March for each census year, so statistics actually relate to production in the previous year. ABS agricultural census datasets have been used to validate estimates of pasture development and production derived from EO-based greenness indices, such as NDVI (see Section 8.1.1).

14.2 EO Sensors for Pastures

In the last decades of the twentieth century, various data storage and analysis tools, such as Geographic Information Systems (GIS), were embraced by many areas of land management, including agriculture. These systems integrate spatially-defined grids, raster layers, and cadastral datasets, within a variety of geographic coordinate systems, and enable spatial manipulation, merging, and statistical analyses at the national, regional, station/farm, paddock, or even at a point, scale (see Volume 2D—Section 13). They also provide a means to integrate EO data with other datasets and generate derivative products (see Section 8).

A wide range of EO datasets at varying spectral and spatial scales are now being used to map and monitor agricultural activities (see Table 14.1). Satellite imagery has been used in agriculture since the early 1970s and offers an excellent means to monitor land cover at national, regional, and farm scales (see Sections 3 and 12.3). In particular, outside the intensive agricultural areas, medium resolution satellite imagery (such as acquired by Landsat) has been one of the most productive means of identifying seasonal pasture cycles. In general terms, a relationship exists between the spatial resolution of EO imagery and the reliability/accuracy of the prediction, such that, in most cases, a higher image resolution improves the predictive capability. This assumption is related to the farm/station paddock size and the uniformity of biomass composition (see Section 10.1). With the more recent advent of higher resolution, spaceborne sensors, more detailed information is available allowing the horticulture, viticulture, and intensive farming production sectors to make use of this emerging technology (see Sections 12.6 and 13).

Repeated coverage of seasonal events and cycles has also enabled time series analysis of agricultural activities using multiple, accurately-located, EO datasets (see Sections 9 and 10). Time series of EO-based data offer new opportunities for agricultural applications, including identifying crop types, monitoring land cover, and assessing the productivity of land uses relative to their economic return (see Volume 1B—Section 1.4 and Volume 2D). For example, the Landsat NDVI time series dataset has been used to demonstrate the change and content of vegetation and salinity across the southwest region of WA (Caccetta *et al.*, 2000). The power of this vegetation monitoring observation subsequently became a major component in the Land Monitoring Project, extending across Australia (Wallace *et al.*, 2006).

Both spaceborne and airborne hyperspectral sensors provide valuable information for agricultural applications. For example, a ground-based hyperspectral sensor study (Edirisinghe *et al.*, 2004) demonstrated excellent prediction of *in vitro* digestibility and protein content for field pasture. Remotely piloted aircraft (see Volume 1A—Section 11.2) offer great flexibility for data acquisition over small areas.

Within GIS, optical, thermal, and microwave EO data and derived products have been integrated with many other spatial datasets, such as rainfall, temperature, soil, topography, and cadastre. Many GIS and EO data sources also depend on accessing accurate locational information via Global Positioning System (GPS) and the Global Navigational Satellite System (GNSS; see Volume 1B—Section 10).

Table 14.1 EO sensors relevant to pastures

TIR: thermal infrared; SAR: Synthetic Aperture Radar; DEM: Digital Elevation Model; ET: Evapotranspiration

Type	Sensor	Platform	Relevance	Advantages	Disadvantages
Passive optical	Multispectral radiometer	Satellite or airborne	National or regional land cover mapping	Global coverage, low cost	Low accuracy, coarse scale
	Hyperspectral spectro-radiometer	Airborne	Plant biochemical functioning and health	High spectral resolution, highlight plant stress	High cost, high data volume
	TIR radiometer	Satellite or airborne	Soil temperature	Surrogate measure for ET	Low spatial resolution
Active optical	Lidar	Airborne and terrestrial	DEM	Hydrology	High cost, specialised processing
	Active optical sensors	Ground vehicles or RPAS	Cover and condition mapping	Convenience, low cost, independent of sunlight	Specialised hardware
Passive microwave	Microwave radiometer	Satellite	Soil moisture	High temporal frequency, large spatial coverage, cloud penetration	Low spatial resolution
Active microwave	SAR	Satellite or airborne	Plant biomass	All weather, independent of sunlight	Data availability
Locational	GPS	Portable devices	Tracking livestock	Low cost	Low signal reception in remote areas

Microwave imagery, both passive and active, has the advantages of being largely independent of weather and lighting conditions (see Volume 1B—Section 8). Satellite-based Synthetic Aperture Radar (SAR) can be used for monitoring agricultural and land cover practices at a global and regional scales, assessing soil moisture status, and quantifying plant biomass (Zhou *et al.*, 2016). Airborne SAR (C-, L- and P-band) has been used to predict grassland biomass and

the types and heights of grass cover in grass cover monitoring studies (Hill *et al.*, 1996, 1999a, 2005). Since optical EO datasets primarily describe chlorophyll and water content (see Section 4.3), whereas microwave information is more relevant to the structural appearance of pasture, the fusion of optical and radar images can also be valuable (Hill *et al.*, 2005; Schmidt *et al.*, 2016).

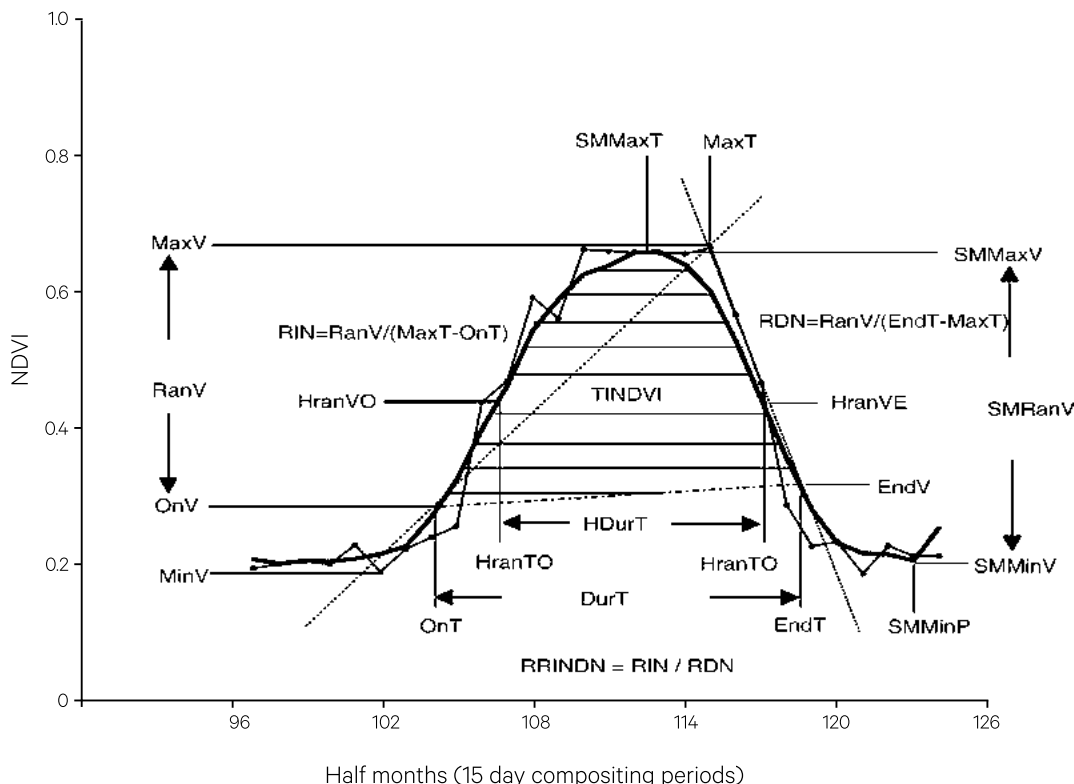
14.3 Phenology and Production

Time series modelling is widely used for deriving phenological metrics (see Section 9.3) and monitoring changes in EO-based indices (see Volume 2D). For example, for a grassland pasture region in southwest Australia, Hill and Donald (2003) extracted agricultural production data from long term ABS agricultural census data (see Sections 11.1 and 14.1) for the period 1983–1997, then compared these data with NOAA AVHRR NDVI 15 day composites (calculated using a maximum value method; Holben, 1986; see Excursus 8.1). Bi-weekly images were processed into an NDVI time series from which a number of metrics were derived (see Figure 14.2, Table 14.2 and Table 14.3).

In this example, the period of lag corresponded approximately to the length of the non-growing period, therefore the forward and backward lag periods were set to 13 intervals corresponding to the non-growing period of 6.5 months. For each NDVI pixel, a time series curve was produced and averaged within each SLA. The resulting metrics were then correlated with the agricultural ABS statistics (Hill and Donald, 2003). The area under the curve, or the integrated NDVI value, represents the accumulated amount of vegetation greenness, or net primary production (NPP; Reed *et al.*, 1994; see Section 7.4), which related well to agricultural production within each SLA. These metrics are most appropriate in highly seasonal grasslands systems, such as those regions with Mediterranean climates in southern Australia (Hill, 2004).

Figure 14.2 Basic metrics

The phenology metrics defined in Table 14.2 and Table 14.3 can be derived from attributes of an NDVI profile (line shown with points) and its smoothed curve.



Adapted from: Hill and Donald (2003) from Reed *et al.* (1994)

Table 14.2 Description of NDVI metrics

Abbreviation	Definition	Metric
OnT	Intersection of forward lag and smooth curve	Starting date of NDVI high period
OnV	Value of NDVI at forwards intersection	NDVI at start of high period
EndT	Intersection of backwards lag and smooth curve	End date of NDVI high period
EndV	Value of NDVI at backwards intersection	NDVI at end of high period
MaxT	Time of maximum raw corrected NDVI	Date of maximum NDVI
MaxV	Maximum value of corrected raw NDVI	Maximum NDVI
DurT	Time from forwards to backwards intersections	Length of NDVI high period
RanV	Difference between minimum and maximum value of smooth curve	Amplitude of season
RIN	Slope of line from forwards intersection to raw maximum	Rate of NDVI increase
RDN	Slope of line from raw maximum value to backwards intersection	Rate of NDVI decrease
TINDVI	Integrated area under smooth NDVI curve	"Magnitude" of season
DurNT	Time from backwards to forwards intersection	Length of NDVI low period

Source: Hill and Donald (2003) Table 1

Table 14.3 Supplementary metrics

Abbreviation	Definition	Metric
RRINDN	Rate of increase/rate of decrease	"Quality" of season
HranTO	Time of half range value at onset—equals $\text{OnV} + (\text{RanV}/2)$ when rising	Start of active growing season
HranVO	Half range value at onset— $\text{OnV} + (\text{RanV}/2)$	NDVI at start of active growing season
HranTE	Time of half range value at end—equals $\text{EndV} + (\text{RanV}/2)$ when falling	End of active growing season
HranVE	Half range value at end— $\text{EndV} + (\text{RanV}/2)$	NDVI at end of active growing season
HdurT	Duration of period from HranTO to HranTE	Duration of active growing season
SMMaxT	Time of maximum smooth NDVI curve	Date of peak of season
SMMaxV	Maximum value of smooth NDVI curve	Value at peak of season
SMMinT	Time of minimum smooth NDVI curve	Date of season minimum
SMMinV	Minimum value of smooth NDVI curve	Value of season minimum

Source: Hill and Donald (2003) Table 1

14.4 Pasture Growth Rate

Pasture Growth Rate (PGR) is a biophysical property of grassland vegetation that represents the daily increase in biomass (measured as kg of total dry matter/ha/day). PGR is influenced by climatic factors and management practices (Ali *et al.*, 2016), and provides valuable information for graziers to determine the ‘feed on offer’ (FOO; Edirisinghe *et al.*, 2000, 2002) for their livestock in the context of individual paddocks.

NDVI time series datasets, in conjunction with estimates of PAR, moisture, and temperature, can be used to model PGR (Hill *et al.*, 2004). Based on a variation of the light use efficiency (LUE) models (Prince, 1991; see Section 7.4), the PGR model requires greater than 60% grass cover to ensure that biomass assumptions are valid. Hill *et al.* (2004) modelled PGR as:

$$\text{PGR} = \text{LUE} \times \text{APAR}$$

where

PGR is in units of g/ha;

LUE is in units of g/MJ; and

APAR is in units of MJ/m².

This model has underpinned the successful Australian application called Pastures from Space (PFS; see Volume 1A—Excursus 14.1), an EO-based system that maps PGR (see Excursus 14.1). PFS, and its successor PFS+, were developed by CSIRO using a range of EO datasets and models (Hill *et al.*, 2004; Donald *et al.*, 2004a; Smith *et al.*, 2011; Donald *et al.*, 2015, 2016). The PFS/PFS+ were hosted by Landgate (WA) as a near real time tool to map pasture productivity at farm and paddock scales from 2000 to 2018. It is now available for Western Australia via DIPRD (WA, see Section 11.6) to deliver FOO and PGR imagery. PFS/PFS+ is a product of a consortium comprising CSIRO, DPIRD (WA), and LandGate (WA).

These online PGR estimates provide a time series record of the changes in Gross Annual Pasture Production (GAPP) for Australian pastures, thus making it a useful tool for monitoring climatic effects on plant production and the impacts of land use. Biweekly estimates of PGR can be averaged to derive annual figures. Annual PGR and NDVI profiles reveal paddock NPP (or total dry matter, TDM) and provide a means to compare the productivity of paddocks over time and identify analogous years. National maps of PGR also provide an input to the supply chain management process, highlight those areas/regions that have responded favourably to climatic changes, and deliver confidence to those purchasing livestock or supplying urban markets.

A dairy farmer was asked about the benefit of satellite EO models of providing ‘feed on offer’ (FOO) and pasture growth rate (PGR) to the farm operations. He replied “What we wish to know is how many days grazing is there and to which paddock the cows should go next”. At a farm/station scale EO-based models can illustrate those pasture types that are more productive and reliable. The moral here is to keep the message simple to assist farmers with their day-to-day decision-making processes.

(Graham Donald)

Excursus 14.1—EO-based Pasture Products

Source: Graham Donald

A number of operational products based on EO datasets are now available to assist farmers and graziers to improve their management techniques and productivity (see Section 14.8). Below we summarise some pioneering Australian systems.

SatMap

One of the first significant EO-based products for pasture management was SatMap (Vickery and Hedges, 1987), which was designed to assist with proposed fertiliser applications. Initially, this farm map defined classes of pasture growth status and provided a fertility index for pastures in the Northern Tablelands of NSW in terms of three levels of pasture ranging from slow (native pastures), medium (semi-improved or degraded), to fast growth (highly improved). In conjunction with the Grassgro DSS (Hill *et al.*, 1999b), a component of the GRAZPLAN DSS (Donnelly *et al.*, 1997), SatMap data provided a soil fertility scalar to spatially simulate pasture production and weaning weights of lambs.

In a long term grazing trial, a set of improved pastures used for sheep grazing were allocated to high and low stocking rates, then half of these were systematically rotated leaving areas to recover. Landsat images of these areas showed significant differences between treatments as management impacts and seasonal conditions took effect (Donald *et al.*, 2013). All Landsat optical bands were processed into clusters and subsequently classified using unsupervised maximum likelihood procedures (using the ISODATA algorithm; see Volume 2E). The resulting classifications showed discrimination across a continuum from sparse, dry pastures to highly improved, green pastures (Vickery *et al.*, 1997). Since satellite surveillance objectively reflects the strengths and weaknesses of a farm unit with respect to its soil types, slope, aspect, and pasture composition, such applications inform decisions relating to renovating pasture, maintaining pasture composition, and continuing soil fertility, as well as adjusting stocking rates and grazing management across every paddock for an entire farm.

Pastures from Space

Pastures from Space (PfS) provides near real time information tools at whole-of-farm and within-paddock levels for Australian pastoral businesses. Using EO datasets PfS estimates pasture production during the growing season to derive pasture biomass, or 'feed on offer', FOO (Edirisinghe *et al.*, 2000, 2002). When combined with climate and soil data, the model forecasts pasture growth rate, PGR. The technology was initially developed in WA and has since been validated across Australia's southern and Mediterranean agricultural regions, and also New Zealand's dairy pastures (CSIRO, 2019).

In 2000, the introduction of the PGR model (Hill *et al.*, 2004) into the southwestern grasslands of WA was met by enthusiasm from farmers (see Volume 1A—Excursus 14.1) and road signs were erected to advertise the local PGR. Prior to this, the WA Department of Agriculture (DAFWA) was in the process of demonstrating to farmers how to manually assess FOO and PGR.

The Australian PGR model (Hill *et al.*, 2004) differentiates itself from related models by the fusion of weekly real time BoM continental 5×5 km gridded climate data and weekly composited daily MODIS 250×250 m NDVI information (Holben *et al.*, 1986; see Section 14.4), incorporating:

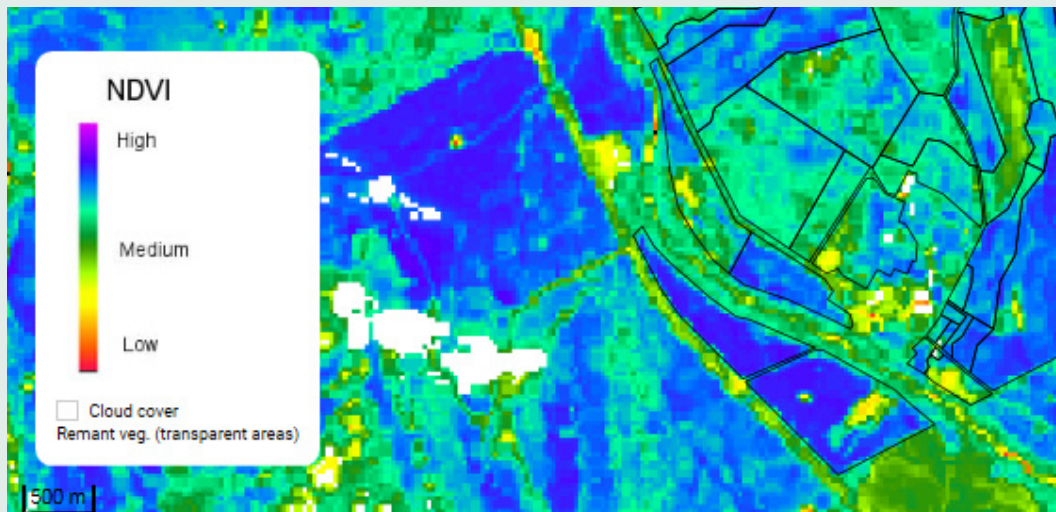
- a light use efficiency index (LUE; Gower *et al.*, 1999);
- fAPAR (Goward *et al.*, 1994);
- a growth index (Nix, 1981, Fitzpatrick and Nix, 1970);
- weekly local climate data (BoM National Climate Centre); and
- MODIS NDVI imagery (LandGate, GA; see Section 8.1.1).

NDVI provides a practical means for determining fAPAR (Goward *et al.*, 1994), which relates to LAI and NPP (see Sections 6.3 and 7.4). This PGR prediction model was calibrated on approximately 50 farms in southwest WA over the years 1995–99, and validated for the next six years (Donald *et al.*, 2004a). DAFWA pasture technicians provided 8–10 geolocated point values for PGR and FOO values in each paddock, for a range of pasture types over the growing season (May to October).

Figure 14.3 Examples of Pasture Growth Rate imagery

This example Landsat image was acquired on 26 July 2016 for a farm in southwest WA.

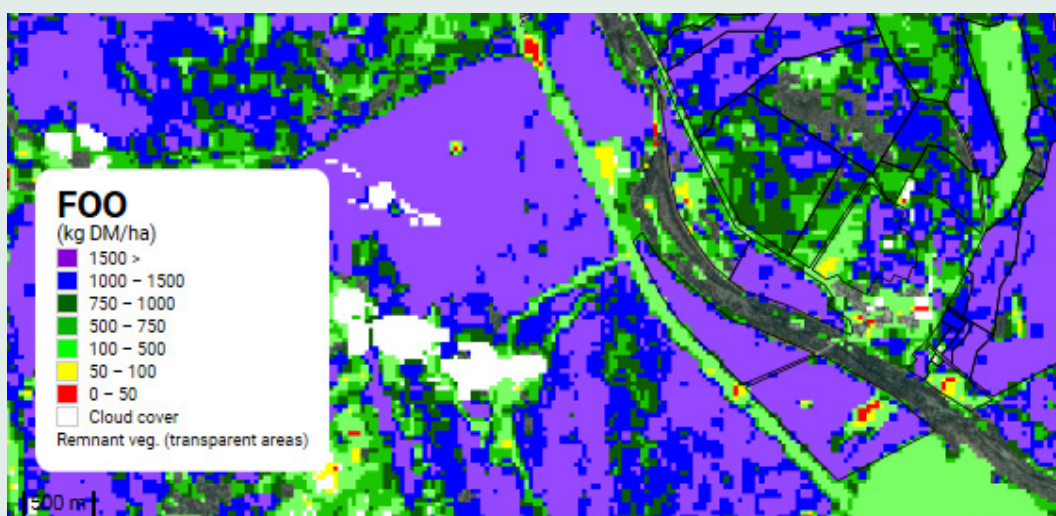
a. Normalised Difference Vegetation Index (NDVI)



b. Farm Pasture Growth Rate (PGR)



c. Feed On Offer (FOO)



Source: PFS+, www.landgate.gov.wa.gov.au

National estimates of FOO, PGR, and NDVI were available online from WA Landgate, as PfS from 1999, and PfS+ from 2016, until 2018 at national, regional, and farm scales (Donald *et al.*, 2004b, Donald *et al.*, 2010a; see Figure 14.3). Since its inception, this product has enjoyed numerous enhancements:

- Smith *et al.* (2011) derived a MODIS NDVI FOO model suitable for the southern temperate pastures where paddock sizes exceed 100 ha.
- Donald *et al.* (2015, 2016) modified the MODIS (and, where possible, included Landsat) NDVI model to assess total green biomass and total accrued biomass as TDM, which is also referred to as gross annual pasture production (GAPP). This modified model was released as Rangewatch (see below). Weekly PGR, TDM, and GAPP are also available as averages for each paddock.
- When intersected with geo-located farm cadastre information, individual real time paddock PGR and biomass data can be extracted. This process was improved by incorporating a national perennial remnant vegetation cover (Furby, 2002) to exclude scrub and forest from paddock and farm estimates.
- Farmers can also input their own localised rainfall if they believe it differs from the BoM integrated estimate. This is useful as generalised BoM data may not pick up local storms that can impact farm management. A secondary benefit provides farmer interaction, which enhances the experience, encourages adoption, and contributes to overall confidence in the product.

The weekly plot of GAPP over time for each paddock, for each growing season, over many years, reflects the productivity capacity of individual paddocks and provides farmers with a tool to highlight those paddocks that may require additional attention. Paddock data can be filtered into FatStock (a livestock module and Smartphone app), which allows farmers to describe the livestock grazed on the selected paddock and provides information relating to the management of these livestock, such as the suggested stocking rate and grazing days. Spatial maps of these data are very useful for other farm activities, such as highlighting the need for fertilisers, proposed fencing, and potential cereal cropping, which may offer a more financial proposition. Sensitivity of NDVI is limited at high LAI, and therefore at high green biomass levels, however moderate relationships have been obtained between biomass and NDVI for grazed rangeland (see RangeWatch product below).

One example of a farmer's application of PfS+ (Foley, 2017), involved applying climate forecasts and replacing MODIS with Landsat NDVI in the PfS model to provide a spatial representation of PGR and a paddock average FOO (Smith *et al.*, 2011). This grazier also used PfS+ to generate the liveweight growth rate of his sheep, which, when combined with climate forecasts, allowed him to adjust the paddock stocking rates to maximise his financial return.

RangeWatch

The Landsat time series datasets provide an opportunity to assess fractional ground cover estimates of bare ground, green vegetation, and non-green vegetation (see Excursus 8.3; Scarth *et al.*, 2010, 2015), with the inference that any increase in bare ground over time could suggest either overstocking or climatic extremes in rangelands (see Section 15). Using this approach, the Rangewatch tool was developed from PfS. This was initially developed in the Kimberley region (Donald *et al.*, 2015, 2016) and validated on a Pilbara cattle station in the northern rangeland regions of WA. This tool gave graziers assistance to maximise production, self-regulate the sustainability of sensitive rangelands, and assess available biomass suitable for livestock. As spectral bands of the MODIS and Landsat sensors are similar, merged spectral information were used to provide more intensive time series spectral information at the Landsat spatial resolution (Emelyanova *et al.*, 2012, 2013; see Volume 2D—Section 6.2). More recent adaptations include a variety of livestock intake requirements and a stocking rate calculator to predict the potential number of grazing days remaining. When combined with livestock tracking, this EO-based information also identified regions on large cattle stations where watering points could be installed.

The imagery from Rangewatch (PfS+) demonstrated the potential benefits of better quality pastures in higher producing regions and suggested where fencing around better quality pastures could improve livestock production (Donald *et al.*, 2015). Another rangelands study (Donald *et al.*, 2016) showed that pasture utilisation (the amount of edible pasture) was less than 20% and in some cases the amount of ground cover was as low as 15%. PfS+ has also provided WA graziers and WARMS (Western Australian Regional Monitoring System—see Section 15.3.2) the ability to independently assess station management.

14.5 Biomass Monitoring

While vegetation greenness indices are valuable for estimating the biomass of green pasture, in many parts of Australia, especially where perennial pasture species are prevalent, grass still provides valuable fodder after it has turned brown (see Section 15). In these environments biomass estimates based on a cover-to-mass relationship can be derived throughout the annual cycle. As introduced in Excursus 8.3, fractional cover (FC) can determine the proportions of green vegetation, non-green vegetation, and bare soil contained within each pixel. With appropriate time series models, persistent vegetation (such as evergreen trees; see Section 9.1.) can be separated from other green vegetation, allowing the ‘non-woody’ non-green and green proportions to be used to estimate biomass. A limitation of approaches relying on the cover-to-mass relationship is that this relationship will change depending on the land type and species mix, allowing only local scale or very generalised global estimates to be made.

To improve the cover-to-mass approach requires either time series integration of the cover fractions and/or inclusion of other data, such as additional spectral bands, indices, and ancillary datasets (for example, climatic and land type information). These improvements have been achieved in recent years with the advent of Sentinel-2 data, with valuable spectral information in the red edge region and a revisit time of five days. One promising way to utilise this additional information is to implement a machine learning (ML) approach based on calibration against field data (see Volume 2E). Using this ML approach, biomass estimates can be derived for each new satellite image to provide a dynamic sequence of biomass snapshots to assist decision making on rural properties. In time, these sequences could be quantified in terms of seasonal and longer term trends in biomass and related to climatic and/or environmental drivers.

A variety of *in situ* data allows these models to be rapidly calibrated and validated to account for differing environmental and/or atmospheric conditions. For example, the farm management app *AgriWebb* enables farmers to photograph and record relevant information about the type and quantity of pasture at specific locations for easy integration with EO-based analyses. Open data kit (ODK) based field applications, as used by TERN and several government organisations, have also been used to collect a large amount of publicly available biomass data. The availability of current, accurately-located, *in situ* data means the generic model can be calibrated for spatial and temporal differences in biomass, then validated independently. This ‘living laboratory’ process allows continual refinement of models, interpretation, and ground data collection to improve both the accuracy and precision of the derived estimates (see Excursus 14.2), which can be directly used to derive carrying capacity by farmers (see Section 15).

Excursus 14.2—Integrated Biomass Estimation

Source: Peter Scarth, cibolabs

Further Information: <https://www.cibolabs.com.au/>

Using a ‘living laboratory’ model of data science tailored to Australian agriculture, estimates of biomass and food on offer (FOO) are now commercially available to graziers at 10 m resolution every five days. Using predictive models based on field calibration data applied to Sentinel-2 imagery from the ESA archives, these estimates allow graziers to monitor biomass in each paddock and property throughout the year.

Over 2,000 field samples of total standing dry matter (TSDM) across northern and eastern Australia were collected over a two-year period (see Figure 14.4). This dataset aims to capture much of the variability across species and land types in the grazing regions. Coincident Sentinel-2 imagery and the associated Landsat-derived persistent green fraction is used to train a three layer, multilayer perceptron regression model using a 50% dropout, a maximum norm constraint, and a robust loss function to avoid open prediction. A national biomass map resulting from this modelling process is shown in Figure 14.5.

33% of the field site data is used for training, with the remainder reserved for validation. To determine the prediction error, the model is trained 100 times for approximately 16,000 epochs before reaching the termination criterion, and results in a median prediction error of 295 ± 8 kg/ha. (Note that in ML terminology, an epoch indicates the number of passes of the entire training dataset the ML algorithm has completed.) In this example, significant outliers can be attributed to missed cloud or shadow, poor tree or shrub cover estimation, significant rainfall events close to the calibration time, or heavy grazing in the week following the field observation.

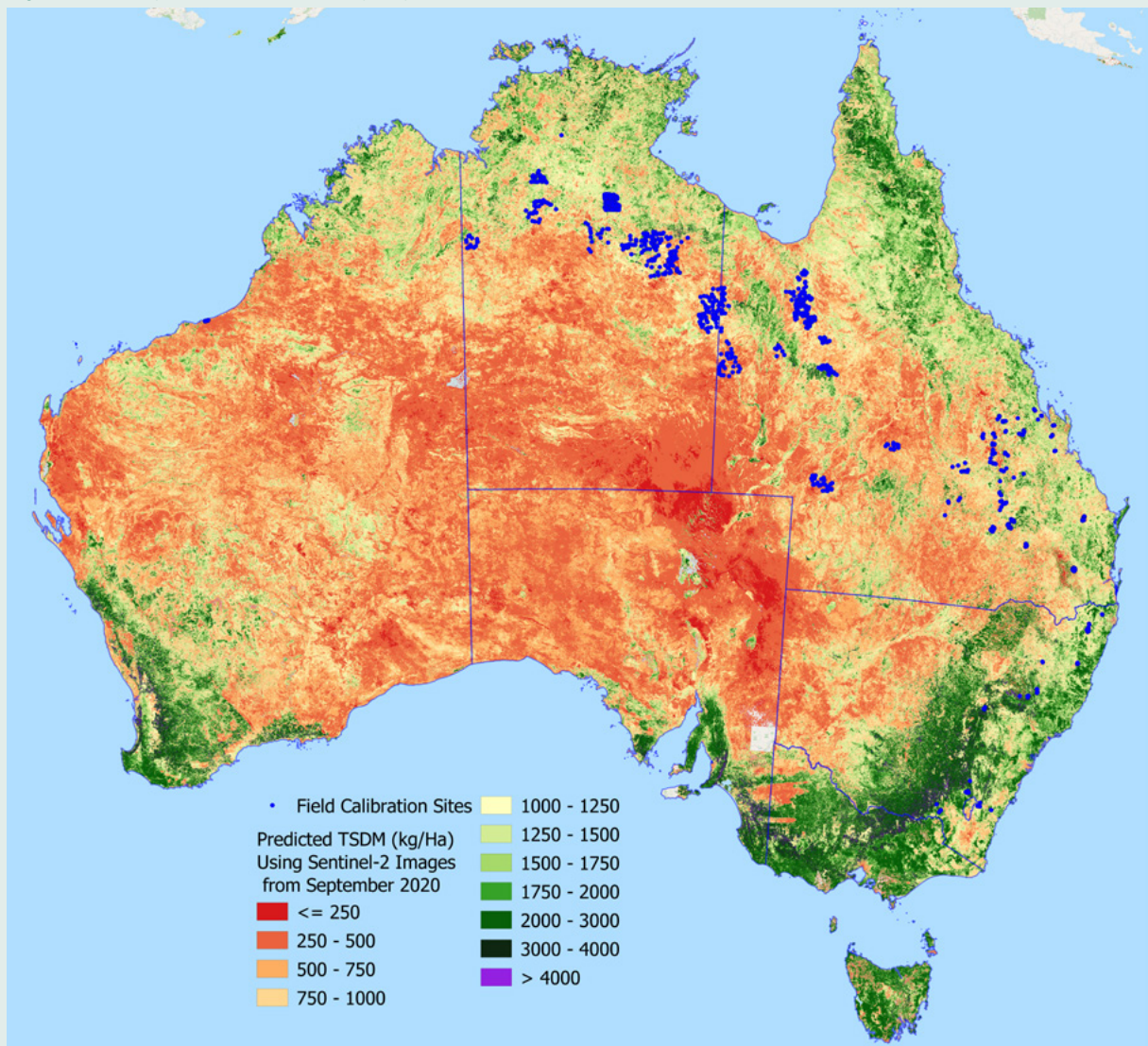
The relative simplicity of this model, coupled with the availability of global imagery in cloud optimised formats, means that biomass estimates can be obtained in either batch mode over large areas in a high performing computing environment, or on demand as a cloud computing function. The typical latency between image capture and delivery is under 24 hours. This enables fast interrogation of individual paddocks from global scale imagery, either in the user’s browser or through integrations with other farm management software, including detailed statistical summaries over space and time.

Figure 14.4 Biomass calibration/validation sites

These photographs sample more than 2000 field calibration sites across Australia. The locations of these sites are shown as blue dots on the map in Figure 14.5. The sites are used to train a machine learning (ML) model which allows per pixel prediction of Total Standing Dry Matter (TSDM) from Sentinel-2 image data.



Figure 14.5 Sample national biomass map, September 2020



14.6 Precision Grazing

There has been an increase in the number farmers and graziers embracing EO-based, precision agriculture technologies to assist with the growing complexity of farm management decisions (see Section 12.6). For example, farmers in rangelands, grasslands, or intensive grazing environments are implementing GPS tracking of livestock (see Volume 1A—Section 10).

Recent perturbed climate events, coupled with insecurity in the economic sector, have made landholders more aware that they need to improve their understanding of farm management. Farmers have the capacity to monitor the locations and movements of their livestock across the farm, which in turn provides information on grazing behaviour (Trotter *et al.*, 2010). For example, satellite-based datasets can provide frequent, up-to-date, biomass assessments of PGR, total biomass and ground cover (see Section 14.4).

Several precision agricultural companies are also developing a range of products for integrated precision agriculture, some of which rely on drones (see Volume 1A—Section 11 and Section 12.6). In combination with GPS tracking, this information provides a powerful tool for managing livestock production in a sustainable manner. In light of these resource and economic factors, farmers have to be more flexible in choosing enterprises from the number of production sectors available.

Biosecurity research (Donald *et al.*, 2010b, Miron *et al.*, 2007) also showed that livestock movements, both on and off farm, were highly correlated to PGR and biomass estimates. This provided inputs into models pre-empting livestock movements within regions, which is necessary for those needing supply chain movements. Results demonstrated a high correlation between the movement of cattle at farm locations and PGR/biomass within six SLAs in southern Queensland.

Livestock tracking is also critically important in the event of an outbreak of an exotic disease, such as foot and mouth. Early detection and identification of an area around infected stock reduces the spread of the disease (Miron *et al.*, 2007). Meat Livestock Australia (MLA), in conjunction with state governments, has introduced a National Livestock Identification Scheme (NLIS) to electronically track the movement of livestock off-farm via radio frequency identification (RFID). This technology will undoubtedly be eventually refined to enable ready integration into a GIS system and thus enable many other uses, including tracking livestock theft.

14.7 Wool Production

The sale of greasy wool is highly dependent on its fibre diameter and tensile strength, with a lesser emphasis on colour, condition, and length. Finer wool has a lower fibre diameter and a higher price by weight.

Throughout the grazing year, pasture nutrition varies with seasons and climatic conditions. Since the fibre diameter profile (FDP) reflects the sheep's nutritional status, the nutritional composition of pasture can impact fibre diameter. A rapid shift in nutrition from poor to high, as can occur at the end of a drought, may cause severe fibre weakening (referred to as 'tender') and reduced yield (Mata and Masters, 2002), which together substantially reduces the value of a fleece. Particularly in the highly prized Saxon merino genotype, where the fleece is valued primarily by its fibre diameter and tensile strength, wool that becomes tender has little or no value.

While wool fibre diameter is not only dependent on nutrition but a number of other factors, including genetics and physical stresses, such as lambing, the yearly variation in the profile of the fibre diameter is mostly attributed to quantity and quality of pasture. The weakest stage of the wool profile occurs at

the change of season when there is an increase in available green pasture. Managing these changes of seasonal pasture growth across the major wool producing regions of Australia will help graziers to maintain the fleece staple strength and achieve a more even diameter profile.

The fibre diameter of wool has been associated with the seasonal environmental nutrition of grazing pastures in a number of wool producing regions (Whelan *et al.*, 2008). This environmental nutritional profile can be easily observed in NDVI imagery. Whelan *et al.* (2008) predicted the average fibre diameter of the wool clip using NDVI and showed that the NDVI profile could be used to indicate when feed availability should be increased or decreased to avoid weakening of the wool staple. NDVI from strategic wool producing regions may forecast wool production with more certainty than rainfall data and expert opinion (Whelan *et al.*, 2007). Thus, combining estimates of sheep numbers with NDVI, FOO, and PGR may provide an ongoing platform to predict the Australian wool supply, and in conjunction with the FDP, its potential economic value.

Using the tools within EO applications such as PFS, farmers can detect changes in PGR across a farm, highlight areas where wool staple strength may be at risk, then decide whether to avoid risking profitability at the next shearing. An example of the efficacy of the

PfS+ model with respect to its application in sheep farming was reported by Foley (2017), a wool producer in the southern region of WA, who was able to improve overall wool production by 60%, increase lambing rates, and double pasture production.

14.8 Further Information

Agricultural Statistics

ABARES (2018). Snapshot of Australian Agriculture.

Insights (1): <https://www.agriculture.gov.au/abares/publications/insights/snapshot-of-australian-agriculture>

UN Food and Agriculture Organisation (FAO): <http://www.fao.org>

EO-based Pasture Models

Pastures from Space:

WA Agriculture and Food: <https://www.agric.wa.gov.au/sheep/understanding-pastures-space-south-west-western-australia>

<https://www.csiro.au/en/Research/AF/Areas/Digital-agriculture/Cropping-pastures/Pastures-from-Space>

CIBO-Labs—Building Solutions for Agriculture: <https://www.cibolabs.com.au>

FarmMap4D Spatial Hub (formerly NRM Spatial Hub; see Volume 1B—Excursus 10.3): <http://www.farmmap4d.com.au/>

14.9 References

- Ali, I., Cawkwell, F., Dwyer, E., Barrett, B., and Green, S. (2016). Satellite remote sensing of grasslands: from observation to management—a review. *Journal of Plant Ecology*, 9(1), 649–671. <https://doi.org/10.1093/jpe/rtw005>
- Caccetta, P.A., Allan, A., and Watson, I. (2000). The land monitor project, *Proc. 10th Australian Remote Sensing and Photogrammetry Conference*, Adelaide, Australia.
- CSIRO (2019). Pastures from Space webpage, Commonwealth Scientific and Industrial Research Organisation website: <https://www.csiro.au/en/Research/AF/Areas/Digital-agriculture/Cropping-pastures/Pastures-from-Space>
- Derner, J.D., and Schuman, G.E. (2007). Carbon sequestration and rangelands: A synthesis of land management and precipitation effects. *Journal of Soil Water Conservation*, 62, 77–85.
- Donald, G.E., Edirisinghe, A., Henry, D.A., Mata, G., Gherardi, S.G., Oldham, C.M., Gittins, S.P., and Smith, R.C.G. (2004a). Pastures from Space—Validation of predictions of pasture growth rates. In *Proceedings of Australian Society of Animal Production*, 25, 232.
- Donald, G.E., Edirisinghe, A., Craig, R., Henry, D.A., Mata, G., Gherardi, S.G., and Stovold, R. (2004b). Advantages of TERRA MODIS imagery over AVHRR to quantitatively estimate pasture growth rate in south west region of Western Australia. *Proceedings of 12th Australian Remote Sensing and Photogrammetry Conference*, Fremantle, Australia.
- Donald, G.E., Edirisinghe, A., Henry, D.A., Gherardi, S.G., Gittins, S., and Mata, G. (2010a). Using MODIS imagery, and climate and soil data to estimate pasture growth rates on properties in the south-west of Western Australia. *Animal Production Science*, 50(6), 611–615
- Donald, G.E., Miron, D.J., Dyall, T., and Garner, M.G. (2010b). Temporal and spatial regional cattle farm turn-off patterns in Eastern Australia. *Animal Production Science*, 50(6), 359–362
- Donald, G.E., Scott, J.M., and Vickery, P.J. (2013). Satellite derived evidence of whole farmlet and paddock responses to management and climate. *Animal Production Science*, 53, 699–710
- Donald, G.E., Mundava, C., Stovold, R., Lamb, D., and Santich, N. (2015). Satellite rangelands monitoring tool for pastoralists. *Australian Rangelands Conference*, 12th April, Alice Springs, NT.
- Donald, G.E., Santich, N., Stovold, R., Abbott, S., and Lamb, D. (2016). RANGEWATCH: An NDVI-light use efficiency based method of estimating forage in northern Australia. A case study in the Pilbara region of Western Australia. *Proceedings of 57th Annual Conference of the Grasslands Society Southern Australia*, 31 Aug–1 Sept, Hamilton, Victoria.

- Donnelly, J.R., Moore, A.D., and Freer, M. (1997). GRAZPLAN: Decision support systems for Australian grazing enterprises. I. Overview of the GRAZPLAN project, and a description of the MetAccess and LambAlive DSS. *Agricultural Systems*, 54(1), 57–76.
- Edirisinghe, A., Hill, M.J., Donald, G.E., Hyder, M., Warren, B., Wheaton, G.A., and Smith, R.C.G. (2000). Estimation of feed on offer and growth rate of pastures using remote Sensing. *Proceedings of 10th Australian Remote Sensing and Photogrammetry Conference*, Adelaide, Australia. Paper No. 112.
- Edirisinghe, A., Donald, G.E., Hill, M.J. (2002). Precision management of feed supply through the timely delivery of biomass and growth rate predictions of Western Australian annual pastures. *Proceedings of 29th International Symposium on Remote Sensing of Environment*, Buenos Aires, Argentina.
- Edirisinghe, A., Donald, G.E., Henry, D.A., and Hulm, E. (2004). Pastures from Space—Assessing forage quality using remote sensing. *Proceedings of 25th Biennial Australian Society of Animal Production*, 4–8 June, Melbourne.
- Emelyanova, I.V., McVicar, T.R., Van Niel, T.G., Li, L.T., and van Dijk, A.I.J.M. (2012). *On blending Landsat-MODIS surface reflectances in two landscapes with contrasting spectral, spatial and temporal dynamics*. WIRADA Project 3.4: Technical report. CSIRO Water for a Healthy Country Flagship, Australia. 72 pp.
- Emelyanova I.V., McVicar, T.R., Van Niel, T.G., Li, L.T., and van Dijk, A.I.J.M. (2013). Assessing the accuracy of blending Landsat-MODIS surface reflectances in two landscapes with contrasting spatial and temporal dynamics: A framework for algorithm selection. *Remote Sensing of Environment*, 133, 193–209.
- FAOSTAT (2019) FAOSTAT Land Use webpage, UN Food and Agriculture Organisation website: <http://www.fao.org/faostat/en/#data/RL/visualize>
- Fitzpatrick, E.A., and Nix, H.A. (1970). The climate factor in Australian grasslands ecology. In *Australian Grasslands*. (Ed: R.M. Moore), pp. 3–26. Canberra, Australian National University Press.
- Foley, M. (2017). Top tech and know how to boost profitability. *LandonLine*, May 2017, Fairfax media.
- Furby, S. (2002). Land Cover Change. Specification for remote sensing analysis. *National Carbon Accounting System, CSIRO, Technical Report No. 9*, 402 p.
- Goward, S.N., Waring, R.H., Dye, D.G., and Yang, J. (1994). Ecological remote sensing at OTTER: Satellite macroscale observations. *Ecological Applications* 4, 322–343.
- Gower, S.T., Kucharik, C.J., and Norman, J.M. (1999). Direct and indirect estimation of leaf area index, fAPAR, and net primary production of terrestrial ecosystems. *Remote Sensing of Environment*, 70, 29–51.
- Hill, M.J. (2004). Grazing agriculture—Managed Pasture, Grassland and Rangeland. In *Manual of Remote Sensing, Volume 4, Remote Sensing for Natural Resource Management and Environmental Monitoring*. (Ed: S. L. Ustin) Wiley International, New York. 768 p.
- Hill, M.J., Vickery, P.J., Donald, G.E., Furnival, E.P., and Mulcahy, C. (1996). Managing the pastoral landscape: Adding a spatial dimension? *Proceedings of 8th Australian Agronomy Conference*, Toowoomba, QLD. pp 309–312.
- Hill, M.J., Donald, G.E., and Vickery, P.J. (1999a). Relating backscatter to biophysical properties of temperate perennial grasslands. *Remote Sensing of Environment* 67, 15–31.
- Hill, M.J., Donald, G.E., Vickery, P.J., Moore, A.D., and Donnelly, J.R. (1999b). Combining satellite data with a simulation model to describe spatial variability in pasture growth at a farm scale. *Australian Journal of Experimental Agriculture*, 39, 285–300.
- Hill, M.J., and Donald, G.E. (2003). Estimating spatio-temporal patterns of agricultural productivity in fragmented landscapes using AVHRR NDVI time series. *Remote Sensing of Environment*, 84, 367–384. doi:10.1016/S0034-4257(02)00128-1
- Hill, M.J., Donald, G.E., Hyder, M.W., and Smith, R.C.G. (2004). Estimation of pasture growth rate in the south west of Western Australia from AVHRR NDVI and climate data. *Remote Sensing of Environment*, 93, 528–545. doi:10.1016/j.rse.2004.08.006
- Hill, M.J., Ticehurst, C.J., Lee, J.S., Grunes, M.R., Donald, G.E., and Henry, D. (2005). Integration of optical and radar classifications for mapping pasture type in western Australia. *IEEE Transactions on Geoscience and Remote Sensing*, 43, 1665–1681. doi:10.1109/TGRS.2005.846868
- Holben, B.N. (1986). Characteristics of maximum-value composite images from temporal AVHRR data. *International Journal of Remote Sensing*, 11, 1417–1434.
- Latham, J., Cumani, R., Rosati, I., and Bloise, M. (2014) *Global Land Cover SHARE (GLC-SHARE): database Beta-Release Version 1.0-2014*. <http://www.fao.org/uploads/media/glc-share-doc.pdf>

- Mata, G., and Masters, D. (2002). Management of intake in winter to control Micron blowout and improve staple strength. *Wool Technology and Sheep Breeding*, 50(3), 471–476.
- Mclvor, J.G. (2005). Australian Grasslands. Ch 9 in *Grasslands of the World*. (Eds: Suttie, J.M., Reynolds, S.G., and Batello, C.). FAO, Rome. <http://www.fao.org/3/y8344e0g.htm#bm16>
- Miron, D.J., Emelyanova, I.V., Donald, G.E., and Garner, G.M. (2007). Agent based model of livestock movements. *International Conference on Complex Systems 2007*, 28 October–2 November, Boston, MA, USA, 2007 <http://necsi.org/events/iccs7/viewpaper.php?id=196>
- Nix, H. (1981). Simplified simulation models based on specified minimum data sets: The CROPEVAL concept. Pp. 151–169 in *Application of Remote Sensing to Agricultural Production Forecasting*. (Eds. A Berg and A. Balkema). Rotterdam.
- Poore, J. (2016). Call for conservation: Abandoned pasture. *Science*, 351, 6269.
- Prince, S. (1991). A model of regional primary production for use with coarse resolution satellite data. *International Journal of Remote Sensing*, 12(6), 1313–1330. doi:10.1080/01431169108929728
- Reed, B.C., Brown, J.F., VanderZee, D., Loveland, T.R., Merchant, J.W., and Ohlen, D.O. (1994). Measuring phenological variability from satellite imagery. *Journal of Vegetation Science* 5, 703–714. <https://doi.org/10.2307/3235884>
- Scarath, P., Roder, A., and Schmidt, M. (2010). Tracking grazing pressure and climate interaction, the role of Landsat fractional cover in time series analysis. *Proc. 15th Australasian Remote Sensing and Photogrammetry Conference*, 13–17 September, Alice Springs, NT.
- Scarath, P., Armston, J., Flood, N., Denham, R., Collett, L., Watson, F., Trevithick, B., Muira, J., Goodwin, N., Tindall, D., and Phinn, S. (2015). Operational application of the Landsat time series to address large area land cover understanding, *International Archives of the Photogrammetry, Remote Sensing and Spatial Information Sciences*, Volume XL-3/W3, ISPRS Geospatial Week 2015, 28 September–3 October, La Grande Motte, France.
- Schmidt, M., Carter, J., Stone, G., and O'Reagain, P. (2016). Integration of Optical and X-Band Radar Data for Pasture Biomass Estimation in an Open Savannah Woodland. *Remote Sensing*, 8, 989. doi:10.3390/rs8120989
- Smith, R., Adams, M., Gittins, S., Gherardi, S., Wood, D., Maier, S., Stovold, R., Donald, G., Khokar, S., and Allen, A. (2011). Near real-time Feed on Offer from MODIS for the early season grazing management of Mediterranean annual pastures. *International Journal of Remote Sensing*, 32, 4445–4460.
- Trotter, M.G., Lamb, D.W., Donald, G.E., and Schneider, D.A. (2010). Active optical sensors for quantifying and mapping pasture biomass: A case study using red and near infrared waveband combinations from a Crop Circle™ in Tall Fescue (*Festuca arundinacea*) pastures. *Crop Pasture Science*, 61, 389–398.
- Vickery, P.J., and Hedges, D.A. (1987). Use of Landsat MSS data to determine the fertiliser status of improved grasslands. *Proceedings of 4th Australasian Remote Sensing Conference* (Ed: D. Bruce). pp.287–96. Floreat, WA.
- Vickery, P.J., Hill, M.J., and Donald, G.E. (1997). Landsat derived maps for pasture growth status: association of classification with botanical composition. *Australian Journal of Experimental Agriculture*, 37, 547–562.
- Wallace, J., Behn, G., and Furby, S. (2006). Vegetation condition assessment and monitoring from sequences of satellite imagery. *Ecological Management and Restoration* 7(S1), S31–S36. <https://doi.org/10.1111/j.1442-8903.2006.00289.x>
- Whelan, M., Cottle, D.J., Gherardi, S., and Clarke, A. (2007). The potential for predicting Australian wool supply using remote sensed data. *International Wool Textile Organisation*, May, Edinburgh.
- Whelan, M.B., Genty, K.G., Cottle, D.J., Lamb, D., and Donald, G.E. (2008). The relationship between a satellite derived vegetative index and wool fibre diameter profiles. *World Congress on Animal Production*, 23–28 November, South Africa.
- Zhou, Z.-S., Caccetta, P., Sims, N.C., and Held, A. (2016). Multi-band SAR Data for Rangeland Pasture Monitoring. *Proceedings of IEEE IGARSS 2016*, pp. 170–173, July 2016. doi:10.1109/IGARSS.2016.7729035



15 Rangelands

Gary Bastin

Arid and semi-arid landscapes, or drylands (aridity index < 0.65), occur in both tropical and temperate latitudes, and cover 41.3% of the land surface of Earth (IUCN, 2019). They are home to a third of the world's population and more than 28% of endangered species globally (IUCN, 2019). They also feature significantly in terms of global biophysical risks identified by the World Economic Forum (WEF, 2018).

Dryland landscapes are predominantly used for grazing and commonly known as 'rangelands'. In Australia, they include (but are not limited to) the ecoregions labelled as deserts and xeric shrublands (see Section 2.4.1), temperate grasslands, savannas and shrublands (see Section 2.4.5), and tropical and subtropical grasslands, savannas, and shrublands (see Section 2.4.6) in Figure 2.14. From Section 2.2 and Table 2.4 it is readily apparent that the majority of the Australian continent is arid or semi-arid and thus considered as rangeland.

Much of the information in the following sections describing the Australian rangelands derives from the Australian Collaborative Rangelands Information System (ACRIS, Bastin *et al.*, 2008, 2009;

DSEWPC, 2013). From 2002 to 2014 ACRIS operated as a partnership between the Australian Government and the state/territory jurisdictions responsible for rangelands, primarily to collate the available, and often disparate, biophysical, and socio-economic datasets to report change in this environment (see Figure 15.1).

The following sub-sections introduce EO of rangelands in terms of:

- Australian conditions (see Section 15.1);
- relevant sensors (see Section 15.2);
- land condition (see Section 15.3);
- operational systems (see Section 15.4); and
- conserving biodiversity (see Section 15.5).

The rangelands encompass tropical woodlands and savannas in the far north; vast treeless grassy plains (downs country) across the mid-north; hummock grasslands (spinifex), mulga woodlands and shrublands through the mid-latitudes; and saltbush and bluebush shrublands that fringe the agricultural areas and Great Australian Bight in the south. Across this gradient, seasonal rainfall changes from summer-dominant (monsoonal) in the north to winter-dominant in the south. Soils are characteristically infertile. Great climate variability and the dominating influence of short growing seasons distinctly characterise rangeland environments.

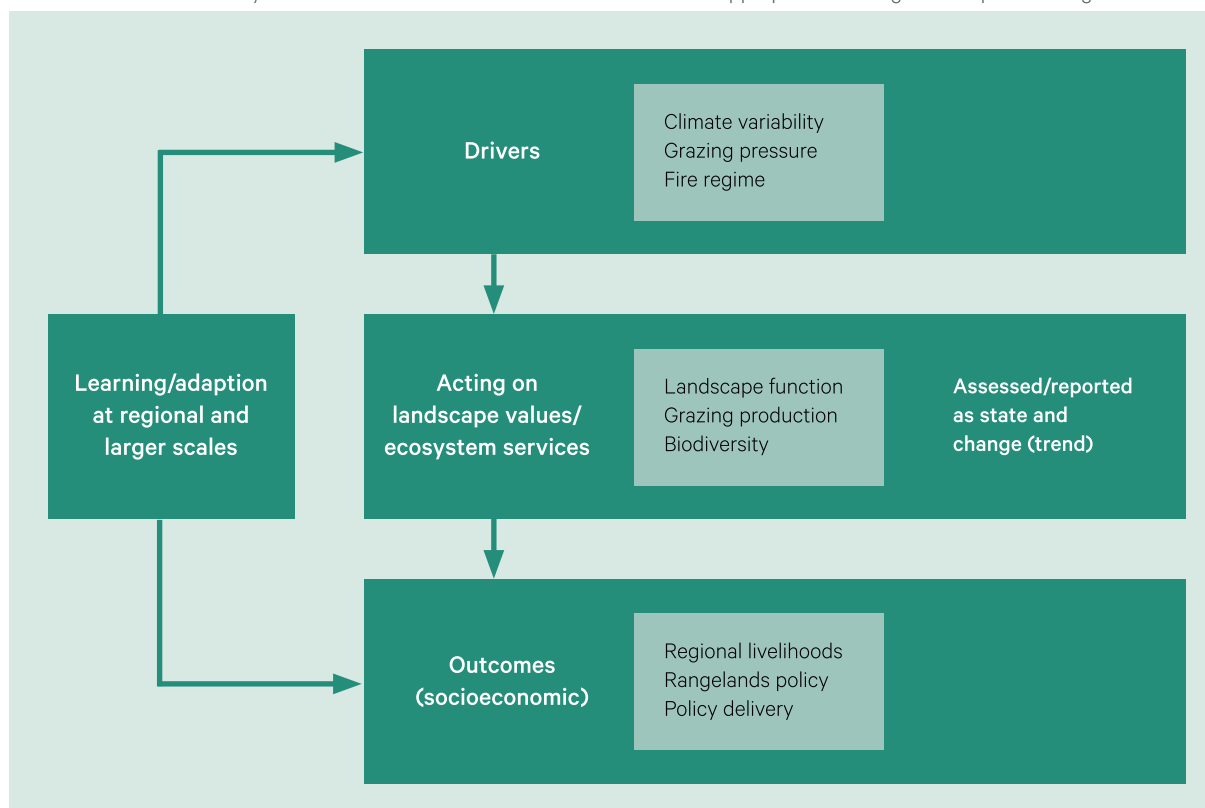
(Bastin et al., 2008)

Background image: The Bokhara Plains Station, 35 km north of Brewarrina, NSW, is a case study in Soils for Life. (For details visit: <https://soilsforlife.org.au/bokhara-plains-reaching-the-real-potential-of-the-nsw-rangelands/>). **Source:** Kirsty Yeates

Recommended Chapter Citation: Bastin, G.N. (2021). Rangelands. Ch 15 in *Earth Observation: Data, Processing and Applications. Volume 3A—Terrestrial Vegetation*. CRCIS, Melbourne. pp. 299–322.

Figure 15.1 Framework for ACRIS reporting

ACRIS attempted to integrate available and suitable biophysical, economic and social data to describe and understand changes in Australia’s rangelands. Key drivers of change are related to their effects on landscape values and their further impact on socio-economic outcomes. Ideally these outcomes then feed back to the drivers via appropriate learning and adaptive management.



Adapted from: Bastin *et al.* (2009) Figure 1

15.1 Rangelands in Australia

The Australian Rangelands Society defines rangelands as ‘all those environments where natural ecological processes predominate and where values and benefits are based primarily on natural resource areas which have not been intensively developed for primary production’ (ARS, 2019). In Australia, rangelands occur where regular cropping is (generally) not possible due to insufficient rainfall and/or poor soils. These areas are principally used for grazing by both domestic livestock and wild fauna. They cover 81% of the country (Bastin *et al.*, 2008; see Figure 15.2) and are popularly referred to as ‘the outback’. They are also home to numerous indigenous communities, who actively support the health and wellbeing of remote, rangeland communities, and play an important role in the stewardship of indigenous cultural heritage (Foran *et al.*, 2019). Rangelands landscapes include savannas, woodlands, shrublands, grasslands, and wetlands, and span latitudes ranging from monsoonal to temperate (Bastin *et al.*, 2008).

Despite being the least populated region in Australia (see Figure 2.15), the economic value realised from rangelands totals nearly \$60 billion annually (ARS, 2019). Most of this revenue is generated from mineral mining, with the remainder mostly being derived from agriculture and tourism. Land uses across Australia’s rangelands in the 2001/2002 financial year are summarised in Figure 15.2.

Australia’s rangelands are characterised by infertile soils, large climatic variations, and short growing seasons (Bastin *et al.*, 2008). Grazing from domestic stock (principally sheep and cattle, plus some goats), native wildlife (principally kangaroos), and feral animals (rabbits, goats, camels, horses, and donkeys), combined with a highly variable rainfall, frequent fires, and exotic weeds, present unique and complex management challenges for maintaining biodiversity and landscape stability in this region. The task of monitoring vegetation change is further exacerbated by highly variable vegetation patterns and remote locations, where permanent landmarks are, quite literally, few and far between.

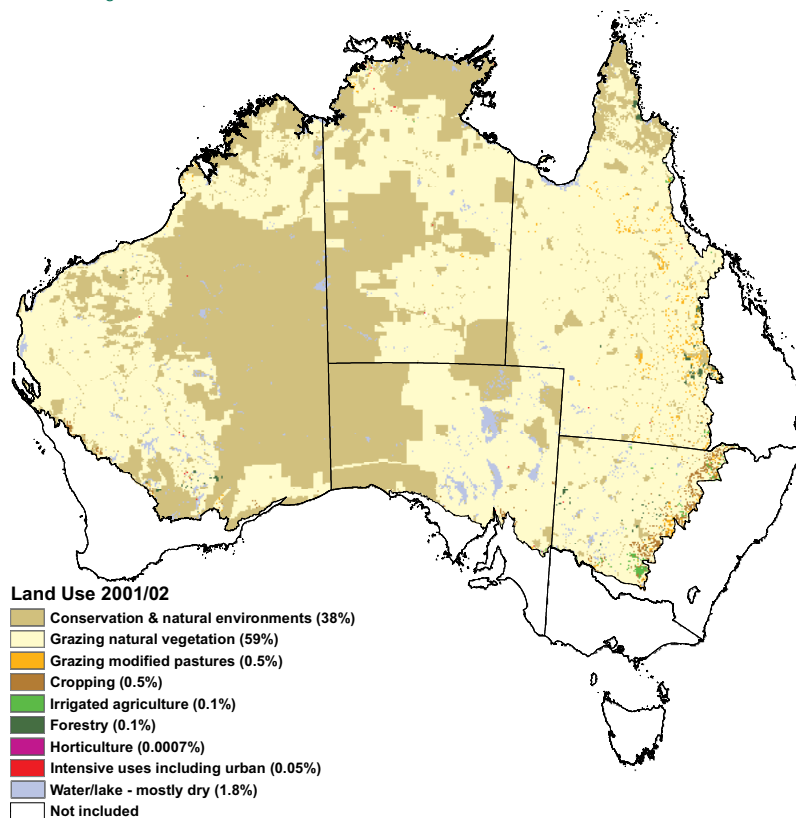
There is no such thing as 'pristine' in the Southern Rangelands [of WA]. The landscape is ever changing and evolving, and being shaped by different processes, including those introduced by humans.
(Pollock, 2019)

Understanding, monitoring, and managing the rangelands as a whole becomes more tractable when they are stratified into components reflecting their biophysical characteristics. A number of classification systems have been used to categorise biogeographic differences in this region, including NVIS (National Vegetation Information System; see Section 2.4.1) and IBRA (Interim Biogeographic Regionalisation of Australia; see Section 2.5). Characteristics, locations, and extents of major vegetation types and their underlying soils are broadly summarised in terms of 52 IBRA bioregions in Bastin *et al.* (2008). Relevant state-based systems include regional ecosystems in Queensland and land systems in other jurisdictions, while SA developed a seamless mapping system relating land systems to component units of bioregions in the rangelands of that state (see Section 2.3.1).

For EO analyses, however, hierarchical categorisations are most useful to allow further stratification for monitoring and assessment of the rangelands landscape. The IBRA bioregions provide a convenient stratification for dealing with the broadly different environments/landscapes within the rangelands and, with their component units, were the preferred regionalisation for the ACRIS Management Committee (Bastin *et al.*, 2008).

Despite decades of grazing, much of the rangelands environment can still be considered as 'natural' (see Figure 3.3 classes I, II and III). Many ecosystems are largely intact but require careful management to maintain biodiversity and, where grazed, their productive value. Potential agents of degradation include the impact of overgrazing by domestic, feral and native herbivores, inappropriate fire regimes, introduced predators, weeds and other invasive biota (DSEWPC, 2013), and poor road design and maintenance in some areas (OAGWA, 2017).

Figure 15.2 Land uses in Australian rangelands



Source: Bastin *et al.* (2008) Figure 3.108 (p130) Updated data can be downloaded from: <http://www.agriculture.gov.au/abares/aclump/land-use/data-download>

15.1.1 Vegetation

Vegetation in rangelands varies from tropical savannas and woodlands in northern Australia to arid environments in central Australia, and semi-arid shrublands in southern regions. Ground-layer species composition can vary greatly in short time periods, particularly in the arid zone. Rangelands encompass a wide variety of vegetation associations, structures and densities, with underlying soils varying from cracking clays to alluvial loam to sand dunes. As in most ecosystems, perennial species act as an environmental anchor, sustaining the landscape by stabilising the soil surface and recycling nutrients.

In rangelands, forage comprises any non-woody plant material. In addition to grasses, many shrub species have leaves that are palatable for stock, and palatable perennial grasses and shrubs sustain livestock into dry times and drought. The ACRIS Management Committee described these palatable perennial species as ‘critical stock forage’ and examples of the results of jurisdictional monitoring for this key indicator of rangeland condition are given in Bastin *et al.* (2008; see pages 42–51). Although some weed species provide valuable pasture, others are spreading rapidly through cleared areas in savanna regions and into the arid zone (see Section 2.3.2). Biodiversity has also been observed to reduce in many rangeland areas that have been colonised by exotic weeds (see Section 15.5).

While droughts can be extended and devastating (see Section 15.1.2), rangeland vegetation responds quickly to most rainfall events. Especially in central and southern Australia, vegetation growth, and subsequently fuel loads, are directly related to antecedent rain (Bastin *et al.*, 2008; Bastin and Allan, 2012).

Recurring periods of higher rainfall can also encourage germination and growth of woody species in the Australian rangelands. This response is not always advantageous for the broader landscape, and has contributed to woody thickening, which may restrict future pasture growth through competition for soil water, nutrients, or light (see Section 15.1.3).

To survive the harsh climatic conditions in arid and semi-arid regions, many plants have adapted to the limited soil nutrients and moisture, and generous exposure to sunlight (see Sections 4.2 and 5.2 above). Such adaptations typically involve:

- reducing water loss by limited transpiration;
- efficient root systems to maximise water uptake;
- controlled or deferred photosynthesis until conditions are favorable;
- conscientious storage and recycling of nutrients; and
- rapid growth and reproduction when circumstances are advantageous (Stafford Smith and McAllister, 2008).

Native vegetation has also adapted to fire—a frequent and harsh environmental broom, particularly in the northern tropical savanna (see Section 18).

While these vegetation communities appear to be robust, having become established in extreme climates, some are fragile, at times balancing between survival and demise. Even where plant communities have adapted to these conditions, they cannot necessarily withstand major changes in their environment (see Section 7). Ecosystems find their own range of stability in managing environmental resources, and significant perturbations can take years or decades of recovery. Additional environmental pressures, whether from grazing, increased fire frequency, extended drought or excessive water usage, can undermine the stability of rangeland ecosystems (see Section 7.2). Once degraded, vegetation recovery can take many years of above average rainfall and low grazing pressure to enable plant populations and perennial root systems to recoup (McKeon *et al.*, 2004; Pollock, 2019), with decades sometimes being required to attain pre-degradation levels of ecosystem ‘health’ and pasture productivity. One example of this process is illustrated in Figure 15.3.

*I love a sunburnt country, a land of sweeping plains,
of ragged mountain ranges, of droughts and flooding rains.
I love her far horizons, I love her jewel-sea,
Her beauty and her terror, the wide brown land for me.
(Dorothea MacKellar, from ‘My Country’)*

Figure 15.3 Vegetation Recovery

This sequence of photos shows the vegetation recovery process at a fixed location in the Victoria River Research Station, 40 km north of Victoria River Downs Homestead and 220 km southwest of Katherine in the Northern Territory.

a. April 1973—extensive areas of bare soil before construction of cattle-proof enclosure



b. June 1978—revegetation with grasses, forbs and the introduced shrub *Calotopis procera* (rubberbush)



c. June 1989—rubberbush has been replaced by native tree and shrub species



d. June 2000—landscape dominated by native perennial black spear grass (*Heteropogon contortus*)



Source: Bastin *et al.* (2008) Figure 2.1

15.1.2 Water

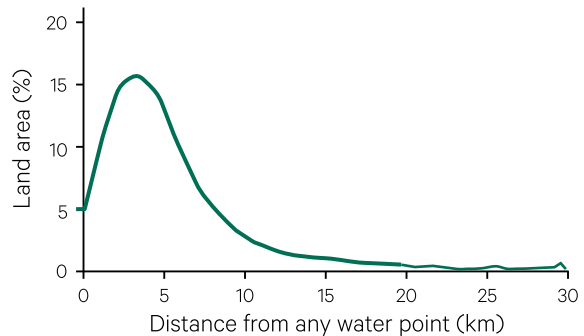
An overriding constraint in most rangelands is water. While major river systems exist around the fringes of the Australian rangelands (see Figure 2.2), rainfall is episodic and ephemeral, and surface water is scarce. Thus, in most of this region, rainfall is the primary driver of landscape change (Bastin *et al.*, 2008). Duration, frequency, volume, and timing of rain are significant for both floral and faunal populations. Droughts—extended periods without rain—have occurred in Australia for millennia (Hendy *et al.*, 2003), but in conjunction with overgrazing can be devastating (see Section 11.4 and Table 11.2).

The Great Artesian Basin (GAB; see Section 2.1 and Figure 2.5), which underlies much of northeastern Australia and extends into central Australia, enables settlement and enterprises in this region. Prior to the first deep bores drilled in the late 19th Century to access the GAB, semi-permanent waterholes and springs along major rivers and mountain ranges, plus a few wells, supplied the only reliable water sources. Now, in addition to surface water in large catchments or drainage basins (such as the Lake Eyre Basin), smaller dams or earthen tanks at paddock scale and localised aquifers accessed by bores or wells provide water for communities, livestock, and limited irrigation (mainly horticulture), but don't promote pasture growth for grazing (Bastin *et al.*, 2008). Tens of thousands of bores, some reticulated using polyphene piping, tanks, and troughs, have now been installed to supply water for stock.

The density and location of these waterpoints is significant for both livestock production and land degradation, as well as biodiversity of native and introduced fauna and flora (James *et al.*, 1999). Landsberg *et al.* (1997) estimated that there are few areas in pastoral rangelands that are located more than 10 km from a source of water (Croft *et al.*, 2007; see Figure 15.4). There is concern that the artificial supply of water in rangelands has impacted biodiversity by biasing the distribution of native vegetation and further encouraging the spread of some exotic flora and fauna (James *et al.*, 1999; DEWHA, 2009), resulting in loss of biodiversity and landscape functionality (Howes and McAlpine, 2008; see Section 15.5).

Figure 15.4 Density of waterpoints

For a typical rangeland region in central Australia, this graph shows the proportion of land area at different distances from a water point (natural and artificial).



Adapted from: Biogroze (2000)

Droughts are inevitable in Australia's rangelands. Yet, despite the physical hardship, the social heartbreak, the animal suffering, the financial and economic consequences, and the environmental damage we know for certain will occur, we appear to be surprised by the next inevitable drought.
(McKeon *et al.*, 2004)

15.1.3 Fire

Fire affects long term changes in vegetation, such that a decreased fire frequency encourages tree growth and an increased fire frequency encourages grass growth. Accordingly, fire has long been used by indigenous land managers to promote pasture (Jurskis, 2015). In some rangeland bioregions, the longterm suppression of fire, either through active management to eliminate or control fire, or the lack of fuel due to grazing, has resulted in an increase in woody biomass in the the semi-arid savannas from both native and exotic shrubs (Burrows *et al.*, 1990; Fuhlendorf *et al.*, 2008). This change is known as woody thickening and considered undesirable for both grazing and habitat balance. Woody thickening has also been observed in Australia's northern tropical savannas (Murphy *et al.*, 2014).

The use of controlled burning to reduce fuel load, and hence the intensity of late season fires, is increasing, particularly in northern rangeland areas (see Section 18). In the savannas of northern Australia, where high (summer monsoonal) rainfall encourages high fuel loads, fire is frequent and extensive. More than half the area of some bioregions can be burnt annually (Bastin *et al.*, 2008). The most extensive fires occur in the late dry season, and these are intense

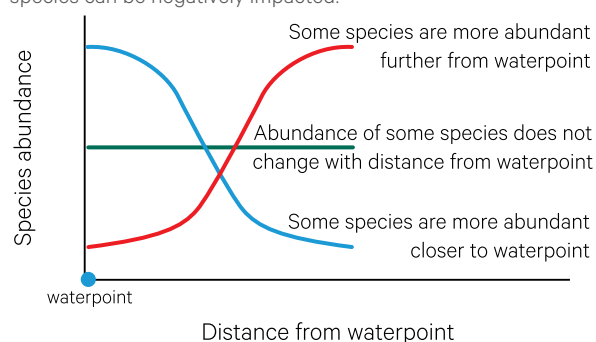
in terms of burn severity and largely uncontrolled. Early dry-season burning using controlled fires, particularly on indigenous-held land, are being promoted to mitigate greenhouse gas emissions and reduce the severity of late season fires (Russell-Smith and Sangha, 2018; see Section 18). In arid and semi-arid central Australia, fires are more episodic and linked to prior rainfall, which stimulates plant growth (Bastin *et al.*, 2008, Bastin and Allan, 2012). Widespread fire, however, is rare in the chenopod shrublands of the southern rangelands.

15.1.4 Grazing

The spatially dominant land use in Australian rangelands is livestock grazing. Bastin *et al.* (2008) reported that nearly 3.7 million km² of native vegetation and 30,000 km² of modied pastures were used for this purpose in 2001/2002, while Foran *et al.* (2019) estimated a slightly smaller area (3.4 million km²) based on figures from ABARES (2017) and URS Australia P/L (2013). Cattle grazing predominates in northern regions, with greater numbers of sheep in southern regions (Foran *et al.*, 2019), however, sheep numbers have declined in recent decades, partly due to problems with dingo control (see Section 2.3.3).

Figure 15.5 Impact of artificial waterpoints on native species

While the presence of artificial waterpoints increases the abundance of some native species of fauna and flora, other species can be negatively impacted.



Adapted from: Biograze (2000)

As a general trend, grazing pressure has been observed to decline with distance from water (Andrew and Lange, 1986). The term 'piosphere' describes the impact of grazing on vegetation and soils in a zone centred on an animal attractant, such as water or mineral licks, with impacts being most concentrated closer to the centre of the zone (Lange, 1969; Andrew and Lange, 1986). Accordingly, in large paddocks, the impact of livestock on vegetation and soils is greatest near waterpoints (Pickup *et al.*, 1994), with 'near' equating to ~3 km for sheep and ~5 km for cattle. Within the piosphere, increased soil erosion is likely with reduced vegetation cover and changes in soil chemistry (Washington-Allen *et al.*, 2004). Soil erosion is greatest within 2–3 km from the water source (Howes and McAlpine, 2008).

Historically, excessive grazing pressure has resulted in land degradation, which manifests as degraded soil structure, increased soil erosion, loss of palatable forage, and an increase in unpalatable woody weeds (see Section 11.4). Although most native species of flora and fauna survive in grazed areas of rangelands, the presence of artificial watering points has altered the composition of some species, with their abundance and extent being largely determined by distance from water (Howes and McAlpine, 2008; see Figure 15.5).

The potential response of vegetation to grazing exclusion varies with the initial site productivity (see Table 15.1). Provided landscapes have not crossed a degradation threshold, either a reduction in grazing pressure or a sequence of wetter years can facilitate recovery to an improved state (Ash *et al.*, 2011). In the arid and semi-arid rangelands, recovering the most degraded state by manipulating grazing pressure alone (such as wet season spelling) is more problematic since extensive erosion and/or woody thickening generally results. Erosion control often requires earthworks to manage flows of rainwater and increase on site infiltration to restore the water cycle. Limited grass growth and fuel accumulation precludes the use of fire for thinning woody thickets.

Table 15.1 Potential responses of vegetation to grazing exclusion

Site degradation	Initial site productivity	
	Low	High
Low	Native dominance	Native dominance
	Small increase in biomass	Large increase in biomass
	Small change in exotic biomass	Potential increases in large exotic species
	Possible minor increase in small scale richness of low biomass species	Decline in small scale plant richness, especially in low biomass species
High	Native: exotic co-dominance	Exotic dominance
	Small increase in biomass	Large increase in biomass
	Possible minor increase in small scale richness of low biomass species	Decline in small scale richness, especially in low biomass species
	Limited increase in native richness owing to propagule constraints	Negligible increase in native diversity owing to competition and propagule constraints

Source: Lunt *et al.* (2007) Table 1

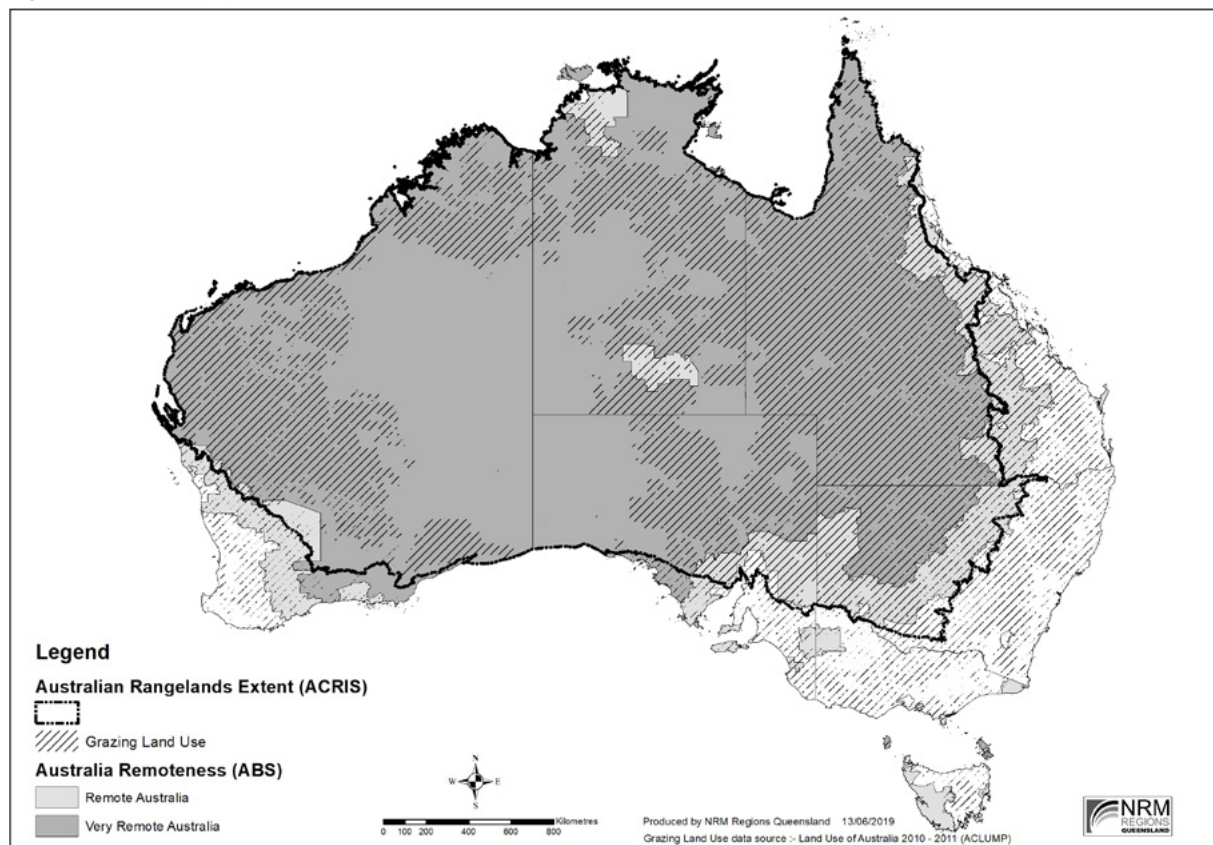
The worst instances of pasture degradation occur when overgrazing is coupled with drought (McKeon *et al.*, 2004; see Section 11.4). Past expectations of carrying capacity, sometimes unwittingly encouraged by government policy, have led to undesired outcomes, in terms of both environmental and social devastation, as landscapes, stock, and communities are impacted by drought (see Table 11.2). For example, until 1992, NT pastoral leases had a minimum stocking covenant and, in some cases, the prescribed number exceeded the inherent carrying capacity of the land types (or land systems) present on the lease. Closer settlement schemes in both Queensland and NSW in the 1900s produced leases which became unviable and were often severely degraded with both climate variability (drought) and changing economic circumstances. Australian literature contains many examples of pastoral families that have faced emotional and financial ruin during severe droughts (e.g., Ker Conway, 1989). With hindsight, it appears these disasters could have been avoided, or at least mitigated, by appropriate management of pastoral resources. For example, the impact of grazing is now considered to be more benign, and difficult to distinguish from the effects of large interannual variability in rainfall.

15.1.5 Socio-economic factors

Human settlement patterns in Australian rangelands are highly variable. Being remote from large urban centres, these communities are often isolated and tend to be distanced from political attention and influence. In Figure 15.6, regions classified as 'remote' by the Australian Bureau of Statistics (ABS) for population census purposes (ABS, 2016) are compared with the accepted boundary of rangelands based on environmental attributes (Bastin *et al.*, 2008) and the extent of grazing (ABARES, 2017).

Some of the areas used for pastoral activities in rangelands are owned under freehold title, but much of the area is crown land and leased to pastoralists with specific conditions and restrictions. Pastoral leases now cover 44% of the Australian mainland (Austrade, 2019) and over half the area defined as rangelands (Foran *et al.*, 2019). These leases are administered by state and territory jurisdictions, who have legislative responsibility to regularly assess and monitor the leased land condition.

Figure 15.6 Remote populations in Australia



Source: Foran *et al.* (2019) Figure 1

Monitoring of rangelands is undertaken at a range of scales, including:

- paddock and property—as part of enterprise management to determine forage budgeting, appropriate stocking rates, etc; and
- regional, usually agency-based—to fulfill legislative responsibilities for leasehold and Crown lands to ensure that natural resources are suitably managed.

Foran *et al.* (2019) outlined the current challenges facing rangeland communities in Australia and proposed some systemic actions that are needed to address these concerns. A national, integrated approach to rangeland monitoring that maximises the value of EO datasets would help the custodians of this environment to understand and maintain its resilience for the benefit of current and future generations (Sparrow, 2017).

15.2 EO Sensors for Rangelands

As indicated by the examples provided in the following sub-sections, the most commonly used EO sensors for observing rangelands detect passive optical wavelengths to discern differences in the land surface and its vegetative cover (see Table 15.2). The scale of the Australian rangelands necessitates reliance on spaceborne rather than airborne sensors.

The optical reflectance of a hypothetical dryland pixel has been described as a function of:

- geometry—viewing and illumination positions (see Volume 1B—Section 3);
- tissue optics for all vegetative components—living and dead (see Sections 4 and 5 above);
- canopy structure—volume and orientation of vegetative tissue including litter (see Sections 5 and 6 above);
- landscape structure—crown size, canopy cover and height (see Section 7 above); and
- soil optics—mineral content, organic matter, surface roughness, grain size distribution, and cryptobiotic soil crusts (Asner, 1998; see Volume 1B—Section 6.4).

The sparse density and high spatial variability of vegetation in rangelands landscapes pose challenges to EO analyses in terms of selecting the optimal spatial scale for imagery (see also Volume 2D). Several aspects of grassland ecosystems relating to scale are particularly relevant to EO monitoring (Hill, 2004):

- scale of sward variation relative to pixel size—grassland ‘texture’ can vary from a uniform monoculture to different mixtures of grasses, tussocks, shrubs, and bare soil;
- persistence of spatial patterns—can be examined using spatial and temporal statistics (see Volume 2A—Section 8) and may be informative to land managers;
- temporal variations may be driven by climate/phenology or management practices—both spatial and temporal variations in vegetation are further complicated by the movements and appetites of grazing animals;
- scale and density of ground sampling relative to pixel size—ground ‘truth’ data need to represent structural and chemical properties, especially for quantitative products, and be sufficiently dense to relate to image pixel size; and
- surveys for ecological, botanical, or production attributes may require different spatial resolutions, revisit frequencies and spectral discrimination capabilities.

The impact of EO image spatial resolution on spatial statistics is introduced in Volume 2A—Section 8.2. In the context of rangelands:

- high resolution (H-resolution) pixels are generally smaller than vegetation entities so depict them against a contrasting background; and
- low resolution (L-resolution) pixels are generally larger than vegetation entities so observe an integrated signal for vegetation and background.

Table 15.2 EO sensors relevant to rangelands

TIR: Thermal infrared; SAR: Synthetic Aperture Radar

Type	Sensor	Platform	Relevance	Advantages	Disadvantages
Passive optical	Multispectral radiometer	Satellite (or airborne)	Mapping vegetation extent, biomass, biodiversity, and productivity Monitoring land degradation	Local to national scale, recurrent coverage with high temporal frequency and extent, low cost;	Cloud contamination
	TIR radiometer	Satellite (or airborne)	Soil/canopy temperature Mapping fire potential, severity, and extent Assessing drought and monitoring regional hydrological changes	Highlight thermal anomalies	Low resolution, low signal to noise ratio
Active microwave	Multi-band SAR	Satellite (or airborne)	Soil characteristics Vegetation structure and biomass Water dynamics	All weather, operates at night	Data availability, noisy data, complex processing

In this sparsely-vegetated landscape, most medium resolution optical sensors image dryland vegetation as L-resolution, with each pixel representing a mixture of different soil types (with varying age, mineralogy, and parent materials) and different vegetation types (with varying growth forms, cluster patterns, and condition, where vegetation condition is defined as the vigour, photosynthetic capacity, or stress of a particular vegetation canopy or cluster; Asner, 2004).

Thus, a given pixel contains multiple landscape components so is well-suited to fractional cover analyses (Scarath *et al.*, 2012; see Section 8.3). Since dryland canopies have low leaf area index (LAI; see Section 6.3.3), leaf level variations are not a major component of canopy reflectance in optical

wavelengths (Asner, 2004). Accordingly, most variations in EO reflectance in rangeland landscapes can be assumed to result from changes in canopy cover (Guerschman *et al.*, 2009). Slow rates of decomposition means that non-photosynthetic material accumulates in these landscapes, which increases spectral reflectance across all optical wavelengths, especially in herbaceous canopies.

In rangeland environments, thermal sensors are also used to monitor fire (see Section 18) and regional hydrology (see Section 7.6 and Excursus 10.2), including drought. Multi-band SAR sensors have also been investigated for mapping the dynamics of above ground biomass in tropical and sub-tropical rangelands (Zhou *et al.*, 2016).

15.3 Rangeland Condition

In more arid regions, a useful indicator of habitat condition is the amount of vegetation versus bare soil covering the ground surface, especially relative to what might be expected for a given rangeland climate and soil type (see Section 7.3). The 'intactness' of vegetation cover in this landscape indicates the structural and functional integrity of habitats, which is critical for maintaining plants and animal populations. There are three key considerations when analysing EO data for the purpose of monitoring land condition in rangelands:

- determining an appropriate and suitably robust index of vegetation cover based on the spectral properties or dimensions of the sensor (see Section 8.1 and Volume 2C);
- examining spatial patterns in the derived index, including typical summary statistics for stratified areas, such as land type/system, paddock, or property (see Volumes 2A and 2E); and
- exploring the temporal dynamics of spatially-summarised data (see Volume 2D).

Approaches that are used to monitor the health of grazed rangelands rely on multiple, reliable indicators that individually, and in combination, provide objective and consistent information from which land condition can be assessed (see Section 7.3). These approaches can be differentiated in terms of their reliance on point, population, or pattern sampling (see Figure 15.7). Conventional ground-based techniques for assessing land condition and its change (trend) utilise a limited number of *point*-based assessments at stratified locations within landscapes and paddocks, which acquire repeated measures at fixed sites (see Figure 15.7a). EO-based methods analyse the spectral properties of the *population* of pixels within an area of interest (landscape type, paddock, or region) with varying levels of sophistication (see Figure 15.7b). Grazing gradient methods (Pickup and Chewings, 1994; Pickup *et al.*, 1994) search for systematic spatial *patterns* in vegetation cover (see Figure 15.7c) that are explicitly related to grazing, such as the persistence of grazing gradients within paddocks (see Section 15.3.1). Methods such as land cover change analysis (Karfs, 2002) examine patterns of change through time (see Section 15.3.1.2). All three approaches can be used to look for change over time (Pickup *et al.*, 1998; Wallace *et al.*, 2006).

The ecological sustainability of pastoral lands is not adequately protected by the State's current system of land monitoring and administration. Pastoral lands have been under threat for over 75 years and during that time there has been limited progress to halt the decline in pastoral land condition. Current knowledge of the environmental condition of individual leases is poor. A reduction in the scope of monitoring since 2009 and limited use of remote sensing tools has contributed to a lack of understanding of land condition at the lease level, and restricted visibility of the extent of land condition issues across the pastoral estate. Future sustainability of the pastoral industry and the Crown's land estate relies on being able to make informed decisions on how to address existing issues and prevent new ones.

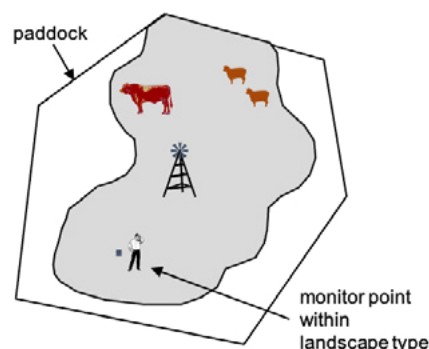
(OAGWA, 2017)

Figure 15.7 Monitoring approaches

Schematic representation of point (ground-based), population (high and low resolution EO-based) and pattern (EO grazing gradients) approaches to monitoring condition and trend, and some of their key characteristics.

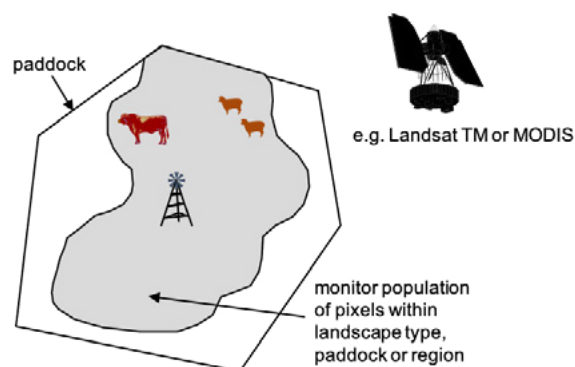
a. Point: ground-based monitoring

- small sample area (generally < 5 ha per site), and few sample sites (1–2 per paddock or 1 per water point)
- rapid subjective assessment or quantitative and descriptive information about plant species and soil; typically includes information about vegetation composition
- problems of measurement error and repeatability
- data can be presented in easily understood tables/charts
- data seem readily interpretable (but dependent on the underlying model of landscape change, which may be poorly developed for some ecosystems)
- generally inadequate spatial or temporal sampling for separating grazing impacts from site-specific and seasonal effects



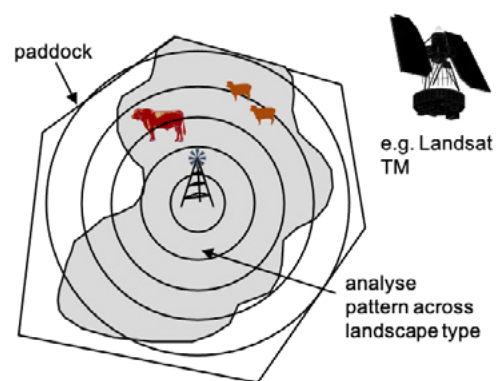
b. Population: satellite data and change over time

- general advantages of satellite data:
 - can analyse total area grazed
 - repeat coverage and selective acquisition
 - historical archive for many sensors
 - range of spatial resolutions
- landscape change expressed through differences in fractional cover over time
- VegMachine and other tools provide tailored, user-friendly software for analysing time series data
- inference based on ancillary data is generally required to separate grazing effects from natural variation



c. Pattern: satellite data and change over space and time—grazing gradient methods

- general advantages as for satellite data above
- search for systematic change in cover related to grazing, reliably identifying grazing effect but requiring larger paddocks
- stratification according to landscape type (e.g. land systems) allows separate grazing effects within large paddocks to be monitored
- uses an explicit definition of land degradation to determine landscape change (ability of vegetation cover to respond to large episodic rainfall events, when received)
- reasonably complex—results not easily understood or accepted by land managers
- broadly applicable to rangelands with < 500 mm annual rainfall



The utility of the pattern approach (see Figure 15.7c) to understanding grazing effects on vegetation cover dynamics is enhanced where the range in rainfall variability is restricted to either above average or below average seasonal conditions (see Figure 11.4). These two constraints correspond, respectively, with ecological analogues of vegetation resilience and persistence (or stability; see Section 7.2).

In the sub-sections below, we consider EO-based approaches that have been developed for monitoring vegetation resilience (see Section 15.3.1), landscape condition and leakiness (see Section 15.3.2), and ground cover persistence (see Section 15.3.3) in the Australian rangelands.

15.3.1 Vegetation resilience

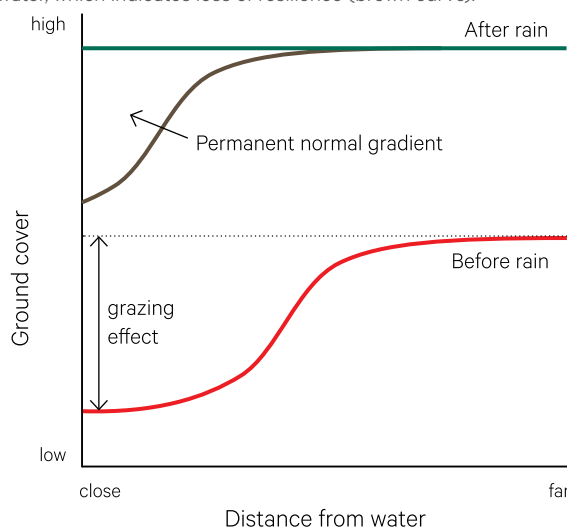
Resilience is “a measure of the persistence of systems and their ability to absorb change and disturbance and still maintain the same relationships between system variables” (Holling 1973). Vegetation resilience, specifically the increase in ground cover after much above average (and often, episodic) rainfall, underpins the grazing gradient methods developed by Pickup *et al.* (1994; see Section 8.1.3).

15.3.1.1 Grazing gradients

As introduced in Section 15.1.4, grazing gradients of vegetation cover develop with increasing distance from stock watering points in large paddocks (> 100 km²—shown as the red line in Figure 15.8). Water-remote areas provide a guide to the expected (reference) cover at any point in time, such that the extent to which ground cover increases (recovers) after large rainfall events indicates the landscape’s capacity to retain its inherent resilience to respond to such events (see Section 7.2). Thus, in Figure 15.8, the horizontal green line shows the expected average level of ground cover in a fully resilient landscape, where all areas at increasing distance from water have similar cover, while the brown curve indicates a permanent effect from grazing with the vegetation cover response closer to water being suppressed, even after substantial rainfall.

Figure 15.8 Stylised grazing gradient based on remotely sensed ground cover

In the grazing gradient methods, the resilience of vegetation cover near stock watering points indicates condition. In this diagram, the red curve indicates vegetation cover relative to distance from water before rain. After substantial rains, vegetation either recovers at all distances from water, which would indicate a fully resilient landscape (green line), or remains sparse closer to water, which indicates loss of resilience (brown curve).



Adapted from: Bastin and Ludwig (2006) Figure 1a

15.3.1.2 Land Cover Change Analysis

Contemporaneous with the application of grazing gradient methods in central Australia (Bastin *et al.*, 1993, 1996, 1998), the ‘land cover change analysis’ (LCCA) method was developed for monitoring grazing effects in WA and the NT (Wallace *et al.*, 1994). This method had its genesis from the observation that a major indicator of condition in many grazing regions was the loss of perennials and their replacement by seasonally-dependent annuals.

In the shrublands and grasslands of WA, multi-temporal Landsat image sequences were used to produce maps of the differential temporal responses of annuals and perennials (see Volume 2D). For example, areas known to be in poor condition have a negative slope over time (indicating cover loss) and increasing seasonal variance (indicating increased presence of annuals). Other meaningful, pixel level, trend summaries include areas of positive slope (increasing cover) and no change (stable cover over time). This analysis was initially based on limited ground knowledge, but subsequent field validation demonstrated that the maps were useful for interpreting condition (Karfs, 2002; Karfs *et al.*, 2004). Long term cover trends from multi-year image sequences also provided information on shrub invasion and cover dynamics, from which aspects of condition could be inferred (Wallace *et al.*, 2006).

Ecosystem resilience is thought to be a product of the diversity of ecosystem functional groups, the diversity of species within those functional groups, and diversity within species and populations (Folke et al. 2004). Resilience has been an important quality of the ecology of Australia’s biodiversity, as ecosystems have had to develop a range of evolutionary strategies to cope with the naturally high variability of rainfall, poor soils, and the long term drying of the continent. (DEWHA, 2010)

The LCCA method was widely tested in the Kimberley (WA), Victoria River (NT) regions and southwest Queensland (Wallace and Thomas, 1998, Karfs *et al.*, 2004), and subsequently developed into 'VegMachine' (Peel *et al.*, 2006, Beutel *et al.*, 2015). This software package assisted graziers and natural resource management staff to summarise and benchmark vegetation cover change, based on EO data, over long periods at user specified locations. VegMachine is now freely available online (Beutel *et al.*, 2015, 2019) and is described in Excursus 15.1.

15.3.2 Landscape condition and leakiness

Mapping land condition in the rangeland environment in Australia is difficult due to the enduring problems of its vast extent coupled with the spatial complexity and temporal variability of arid-zone vegetation. Methods used to map vegetation condition in rangelands need to be (Bastin and Ludwig, 2006):

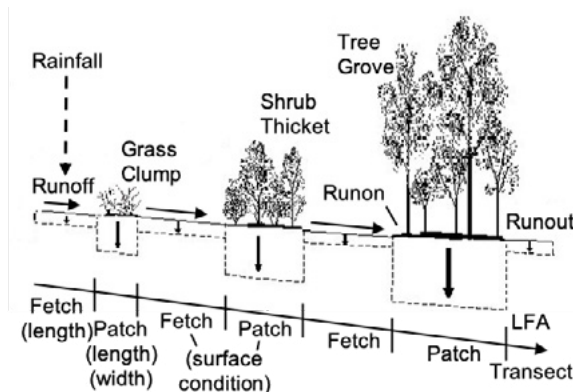
- robust—rigorous methods are needed to differentiate the impact of management decisions on vegetation from its inherent variability over space and time;
- efficient—effective methods must be suited to large area mapping at low cost; and
- general—the complex interactions between vegetation, climate, fire and grazing in rangelands means that methods need to be adaptable to specific environments.

Given debate about the relevance and suitability of current paradigms for understanding vegetation dynamics in parts of the rangelands (see Briske *et al.*, 2003 for a review), some monitoring systems focus on vegetation change over time (see Sections 7.3 and 11.3). This avoids the often fraught process of trying to 'shoe horn' assessments into ill-fitting and often arbitrary condition classes. Causality is a fundamental component of understanding change; in this case, determining the most plausible reasons for observed change, be they related to climatic variations or due to grazing, fire, or other forms of disturbance. For example, the Western Australian Rangeland Monitoring System (WARMS; Watson *et al.*, 2007a, 2007b; Novelly *et al.*, 2008) is a sophisticated site-based monitoring system for reporting regional scale change in perennial vegetation under grazing. WARMS focuses on change and its most probable causes when interpreting monitoring data.

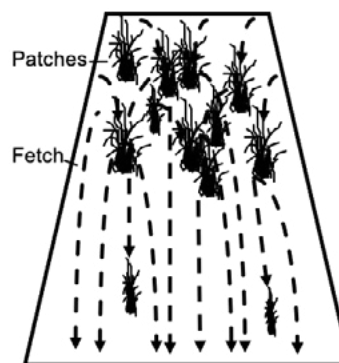
The concept of landscape function—the capacity of a landscape to capture and retain rainwater, soils and their nutrients after rainstorms (Ludwig *et al.*, 2007)—is introduced in Section 7.3 above. The capacity to retain these components depends not just on vegetation cover *per se* but its distribution in the landscape. In Figure 15.9a, the relevant vegetative and surface water components in a rangelands environment are identified. Landscape Function Analysis (LFA) relies on measurement of the sizes of vegetation patches, the inter-patch distances (or fetch), and the soil surface condition of both patches and fetches (Tongway and Hindley, 2004), which in combination demonstrate how rainwater moves through the landscape (see Figure 15.9b). Since its development, this approach has been used for research and land management purposes in a range of landscapes (Eldridge *et al.*, 2020).

Figure 15.9 Landscape function

a. A transect to measure simple indicators of land condition in Landscape Functional Analysis (LFA)



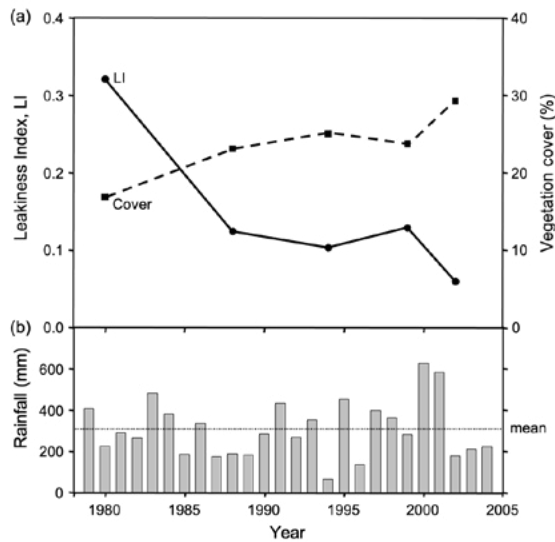
b. The role of vegetation patches as obstructions to surface flows, where a high cover of patches on the upper slopes greatly slows runoff to enhance water retention and a low cover on lower slopes leads to long fetches and loss of water, that is, a 'leaky' landscape.



Source: Bastin and Ludwig (2006) Figures 1b and 1c

Figure 15.10 Leakiness index example

a. Leakiness index for rangeland monitoring site compared with mean levels of persistent vegetation cover for five monitoring periods from 1980 to 2002. b. Annual rainfall from 1979 to 2004 in relation to 305 mm average.



Source: Ludwig *et al.* (2007) Figure 4

The leakiness index (see Section 8.1.6) used EO imagery and DEM data to derive landscape scale values for leakiness (see Figure 15.10). This method has been applied to change in landscape leakiness from 1986 to 2005 for selected sub-catchments of the Fanning River, Queensland (Bastin *et al.*, 2007). Leakiness Index (LI) values were calculated with the Leakiness Calculator (version LI4). In this study changes over time in indicated leakiness of sub-catchments dominated by native perennial-tussock grasses were contrasted with those dominated by an introduced stoloniferous mat-forming grass, Indian couch (*Bothriochloa pertusa*). For example, under the Grazing Land Management (GLM) program in Queensland (FutureBeef, 2020), the former pastures tend to be in good condition and the latter in reduced condition. For the same level of average cover, pastures dominated by Indian couch were deemed to be more leaky than the native tussock grasses. Of critical importance, average cover appeared to decline to relatively low values following a run of poor, wet seasons (such as occurred in the mid 1990s) and, at this time, values of the leakiness index reached relatively high values. While this study was supported by limited ground data, the results demonstrate the importance of:

- maintaining minimum acceptable levels of persistent pasture cover (particularly on hillslopes); and
- managing to improve the density and cover of native perennial-tussock grasses in the pasture.

This method has been used for research purposes in different parts of the rangelands overseas and as a connectivity index to link vegetation patterns with erosion risk (Xu *et al.*, 2018, 2019). However, there are no known applications of the leakiness index as part of jurisdictional monitoring of rangelands in Australia.

15.3.3 Persistence of ground cover

In drier years, retained ground cover is critical for minimising the risk of wind and water erosion. It is reasonable to infer that most of the cover present in drier (and drought) years comprises perennial species (see Section 9.1)

The Dynamic Reference Cover Method (DRCM) automatically calculates an expected (reference) level of ground cover for each Landsat TM pixel in a nominated dry/drought year (Bastin *et al.*, 2012). The difference between the actual and reference cover—the cover deficit—indicates the extent to which an area has been modified by past grazing. Change in cover deficit from one drought period to the next provides an objective and systematic way of determining how ground cover is being managed when its presence is most critical.

Landsat fractional cover (see Excursus 8.3) for repeat dry years between 1988 and 2005 was analysed with DRCM at sub-bioregional scale for approximately 640,000 km² of the Queensland rangelands (Bastin *et al.*, 2014). All 34 sub-regions analysed had similar or increased levels of seasonally-adjusted ground cover at the end of the analysis period (2003 or 2005). Allowing for possible landscape heterogeneity effects on assessed condition, at the first assessment in 1988 the Einasleigh Uplands bioregion was in a comparatively better state at the end of the period and those analysed parts of the Mulga Lands bioregion in poorer state. Most sub-regions of the Cape York Peninsula, Brigalow Belt North, Desert Uplands, Gulf Plains and Mitchell Grass Downs bioregions, lay between these two end-states. Simulated levels of pasture utilisation based on modelled pasture growth and statistically-based grazing pressure supported the results of this regional assessment of land condition.

It is important to remember that remotely sensed ground cover is but one indicator of the functionality of rangelands under grazing use. Information about other indicators is also required, such as the persistence of palatable perennial forage species, the dynamics of the woody layer, and erosion status. Thus ground-based monitoring is required in addition to EO analyses, but the value of the ground component is increased where it complements information available from EO.

A number of operational systems and products have been developed to use EO datasets for monitoring change in woody vegetation cover, including the Statewide Landcover and Tree Study (SLATS; see Volume 2D—Excursus 14.3) and the Persistent Green Vegetation product (see Section 9.1). The routine

monitoring of woody cover dynamics in Australia's arid rangelands is currently limited by the lack of a suitably robust cover index for 'non-green' canopies such as *Acacia* species, however, research is continuing in this area (e.g. Barnetson *et al.*, 2019).

15.4 Operational Systems for Monitoring Rangelands

A range of systems have been developed to monitor Australian rangelands (see Table 15.3). In the absence of a national coordinating body, current details for these programs are difficult to determine, although status reports on pastoral leases are available for some states (such as OAGWA, 2017 and DENR, 2019). These systems have been improved over time and in some states multiple systems are still in use in different regions. For example, FORAGE is an online decision support system developed in Queensland for grazing land managers, which integrates information specific to individual properties including rainfall, pasture growth, seasonal rainfall and pasture growth outlooks, ground cover, Foliage Projective Cover (FPC), soil erodibility, land types, and climate projections (Zhang and Carter, 2018). More generic systems for mapping vegetation and ecosystems at both the state/territory and national level (see Section 2.3.1) complement and support the rangeland-specific systems.

Excursus 15.1 describes an operational, EO-based system that has been specifically developed to monitor the rangeland environment in Australia. The international Group on Earth Observation (GEO) Global Agricultural Monitoring initiative (GEOGLAM; see Section 21.3) is also developing the GEOGLAM Rangeland and Pasture Productivity (RaPP) application to monitor the condition of pastures and rangelands globally (see Excursus 11.1).

Table 15.3 Rangelands in Australia

This table summarises the status of rangelands monitoring in 2008. Current status for most jurisdictions are difficult to update in the absence of a national coordinating body. Reassessment of ground sites varies with jurisdiction between one and 14 years.

State/Territory	% of state as rangelands	Rangeland tenure	Rangeland population (2016)	Permanent monitoring sites	Monitoring system
NSW	60	Mostly leasehold with small areas freehold	52,670	350 sites monitored annually	Rangeland Assessment Program (RAP) SLATS (see Volume 2D—Excursus 14.3)
NT	98	46% pastoral leases	89,444	2333 pastoral monitoring sites	Integrated monitoring program which relates site-based data to Landsat fractional cover (DENR, 2019)
SA	85	60% pastoral leases 40% conservation or regional reserves	62,797	Baseline monitoring on ~400 sites and resource inventories on each of the 328 pastoral leases	Arid Lands Information System (ALIS) based on Grazing gradient assessment in northern leases Land Condition Index (LCI) in southern leases
Queensland	82	75% freehold and leasehold grazing properties	124,050	~1000 pastoral leases	SLATS (see Volume 2D—Excursus 14.3) AussieGRASS (see Excursus 10.1) FORAGE (Zhang and Carter, 2018) VegMachine (see Excursus 15.1)
WA	87	42% pastoral leases	81,341	1622 sites monitored since 1992 on 435 pastoral leases Grassland sites assessed 3 yearly and shrublands assessed 5 yearly	Western Australian Rangelands Monitoring System (WARMS; see also OAGWA, 2017, Table 3)

Source: Bastin *et al.* (2008); Foran *et al.* (2019); NSW DPI (2019); Austrade (2019); OAGWA (2017)

Excursus 15.1—VegMachine

Source: <https://vegmachine.net>

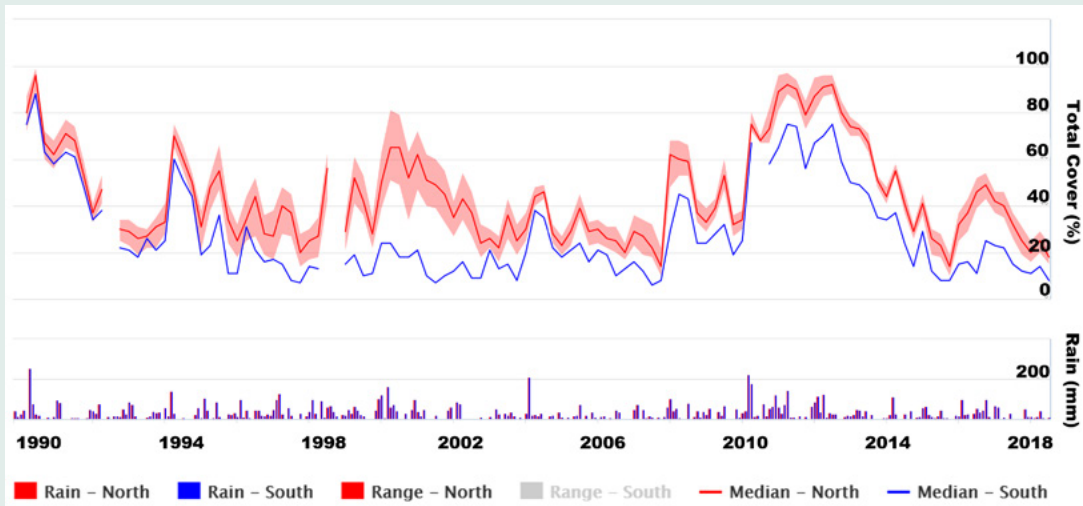
Further Information: Beutel *et al.* (2019)

VegMachine is a free, online tool that uses time series of satellite imagery and derived products to summarise spatial and temporal changes in land cover on Australia's grazing lands. The software has been refined and used by government agencies, Natural Resource Management (NRM) groups and pastoralists since 2002, with the current national website being launched in 2016 (Beutel *et al.*, 2019). Using VegMachine, for selected areas a user can:

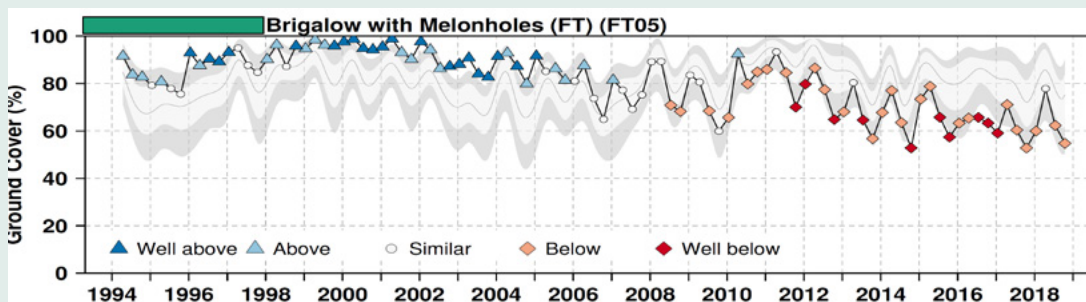
- generate comprehensive ground cover monitoring reports;
- measure land cover change or estimate soil erosion rates;
- view satellite image land cover products; and
- better understand the links between management, climate and cover in grazing land.

Figure 15.11 VegMachine comparisons

a. This partial screenshot compares two adjacent sites that are separated by a fence. The North site (red) has had consistently more ground cover and better land condition than the South site (blue) over that period. Red and blue lines respectively show the median seasonal ground cover at each site, and the red band shows the 'range' (actually 20th to 80th percentile) of ground cover values on the North site. The analysis reflects known conditions at the sites since 2003, and also suggests the observed difference extends back to the early 1990s. Since the two sites are in the same land type with a common rainfall history, management is the most likely cause of the observed differences.



b. This extract from a regional comparison report shows the total ground cover in part of a paddock that has been very heavily grazed from 2005. The pale grey bands show the percentiles of ground cover in the FT05 land type of the surrounding region (5th–20th: lower grey band; 50th: central grey line; 80th–95th: upper grey band). The overlaid time trace shows median ground cover in the same land type within the paddock. The symbols along the time trace classify cover in the paddock relative to the regional cover percentiles (Well below: < 5th; Below: 5th–20th; Similar: 20th–80th; Above: 80th–95th; Well above > 95th). This analysis shows cover in the paddock has declined dramatically since 2005, corresponding to the increased grazing pressure over this period. This trend is evident despite the presence of rainfall-driven fluctuations in regional cover (higher in 2010–2012, and lower in 2004–2007 and 2013–2014).



Source: Beutel *et al.* (2019) Figure 2

The current datasets interrogated by VegMachine date from 1990 and include imagery from Landsat TM/ETM+/OLI and Sentinel-2 as the products: seasonal ground cover (see Section 9.2), fractional cover (see Section 8.3), and persistent green cover (see Section 9.1). These datasets can be viewed as images at a range of scales, and ranked in time and space. Spatial comparisons are particularly

informative for ‘identifying paddocks in need of more attention’ (Brinsmead 2017; QRIScloud, 2018; see Figure 15.11). Paddock-by-paddock and land type-by-land type analyses of ground cover change from 1990 to the present allow graziers to clearly see the impact of management decisions and infrastructure changes on their properties.

15.5 Conserving Biodiversity

The major threats to biodiversity in Australia are considered to be habitat fragmentation, climatic changes, land use change, invasive species, grazing pressure, altered fire regimes, and changed hydrology (DEWHA, 2009), all of which are significant landscape factors in rangelands (see Sections 7.1 and 19). While threatened biota occur in greatest abundance in areas with high population and the highest land use pressures, there is evidence that the numbers of small mammals in tropical savannas are declining. All changes in conservation status of threatened species in recent decades have shown declines and virtually every bioregion includes several threatened taxa.

The Australian rangelands comprise 52 IBRA bioregions and 244 subregions (see Section 2.4). In many of these bioregions, grazing by domestic livestock has resulted in significant impacts on soils, landscape processes, and native biota, with ongoing loss of landscape function, particularly within the piosphere (see Section 15.1.4). Lunt *et al.* (2007) identified six site factors that could be used “to predict, interpret and compare the impacts of grazing on natural ecosystems”:

- soil and ecosystem processes—positive, negative, or no impact of grazing;
- grazing history—including loss of grazing-sensitive species;
- site productivity—in terms of landscape function;
- plant palatability—of dominant native and exotic species;

- plant recruitment—impact on germination and growth; and
- context in the broader landscape—across different spatial scales.

These characteristics were integrated into a hierarchical decision tree, which concluded that “livestock grazing is likely to be detrimental to biodiversity conservation in many ecological contexts” (Lunt *et al.*, 2007; see also Table 15.1).

Although a number of state/territory and federal programs have been undertaken to monitor the condition of rangelands in Australia, these have been disproportionately funded given the extent of the rangeland environment. Monitoring programs include the TERN AusPlots Rangelands program, which uses a standardised approach to sample soil and vegetation characteristics at 442 sites within the rainfall range of 129–1437 mm (White *et al.*, 2012; Guerin *et al.*, 2017). Many state-based programs are tailored to the information needs of local regions and produce data that are difficult to compare across the continent. Also, pastoral monitoring programs, which focus on pastorally productive country, typically collect different data from environmental monitoring programs that aim to assess biodiversity. Although biological assets are declining in Australia, existing data are insufficient to report on biodiversity trends at a national level (DEWHA, 2009).

Locking up the land purely for conservation is not the solution to our environmental problems [in the WA rangelands]. We must do better than that. I have no doubt that if we do lock it up, ecological processes will take over and the land will heal itself into a stable state. But, eventually, those small conservation areas are certain to fail if we do not change the way that we manage the surrounding land. Even if those small pockets of pristine wilderness did manage to persist, the increasing pressure to produce food from dwindling resources would eventually mean that they were overrun in a last-ditch effort to wring the final bit of productivity from the landscape to feed ourselves.

(Pollock, 2019)

Native vegetation is a cost-effective and powerful surrogate for biodiversity. The distribution of threatened species and communities is closely aligned with areas where native vegetation has been extensively cleared.
(DEWHA, 2009)

To understand the impact of grazing on plant biodiversity and composition in Australia—and its consequential impact on fauna—requires a systematic approach to biodiversity monitoring at a landscape scale. Potential frameworks for jurisdictional monitoring of biodiversity in the rangelands were proposed by Eyre *et al.* (2011a) (see Excursus 15.2) and McAlpine *et al.* (2014). To date, however, no rangeland jurisdiction in Australia has implemented this monitoring framework operationally. More studies are required to link habitat condition indicators to those species that are dependent on particular proportions and types of groundcover. Linkages between groundcover and biological diversity have hitherto been based on local sites only. To assess this relationship across our rangelands, broader landscape and regional analyses will be needed (Sparrow, 2017).

Recognising that management improvements for grazing can also benefit biodiversity, tools are being developed to assist rangeland managers to assess land condition in terms of biodiversity. For example, procedures for assessing the biodiversity condition, or BioCondition, of grazing lands in southern Queensland have been defined with support from Meat and Livestock Australia (Eyre *et al.*, 2011b; MLA, 2011, 2012). This complements the Grazing Land Management (GLM) package, which promotes sustainable management by graziers in northern Australia (DPIF, 2006; see Excursus 7.1). BioCondition is designed for rapid assessment of sites and rests on three components:

- a set of site-based and landscape-scaled attributes, which indicate biodiversity (see Table 15.4);
- benchmarks for each attribute derived from reference sites; and a
- rating system for the relative value of attribute to benchmark values.

Similar systems have been developed for other jurisdictions (such as Butler *et al.*, 2020, Table 1; see Section 3.4.1).

Towards avoiding loss of biodiversity, and stressing the importance of maintaining and enhancing landscape heterogeneity, various reviews of biodiversity status that are limited to specific regions have hitherto offered a ‘portfolio of partial solutions’ (Waters and Hacker, 2008). However, in order to effectively manage rangelands across Australia, consistent and objective monitoring protocols are required in all jurisdictions and at all landscape scales to provide reliable answers to the questions:

- where is change occurring?
- how much change is there?
- what is driving that change? (Sparrow, 2017).

The challenge for future land managers will be to balance the requirements of agricultural production for growing human populations with appropriate safeguards for biodiversity conservation. Given the scale of Australian rangelands, EO datasets need to be a significant part of any monitoring solution.

Table 15.4 BioCondition indicators

Indicator	Attribute
Site-based	Regeneration—recruitment of dominant tree species
	Diversity—native plant species richness for four life forms
	Cover/complexity—tree canopy cover and canopy health (%); tree height (m); shrub layer cover (%); native perennial ‘decreaser’ grass species basal area; native perennial forb and non-grass cover (%); native annual grasses, forb, and non-grass cover (%); cryptogram cover
Landscape	Habitat—large trees and hollows; fallen woody material; litter cover
	Weeds—weed cover
	Size of patch
	Context
	Connectivity
	Distance to artificial water

Source: MLA (2011) Table 2

...our ability to report change in biodiversity is limited due to inadequate data
(Bastin *et al.*, 2008)

Excursus 15.2—Rangelands Biodiversity Monitoring Framework

Source: Eyre *et al.* (2011a, 2011b)

A framework for jurisdictional monitoring of biodiversity in the rangelands was proposed by Eyre *et al.* (2011a). This systematic and scaled approach combines field measurements and EO-based methods to integrate:

- direct measures of biodiversity attributes;
- indirect measures of biodiversity (through indicators or surrogates);
- measures of drivers of biodiversity; and
- measures of response indicators.

As detailed in Section 19, changes in biodiversity drivers exert a pressure on biotic attributes, leading to a change in their state (where biotic attributes measure biodiversity either directly, in terms of abundance or extent of a species, or indirectly, as habitat condition). In this context, biodiversity drivers impact environmental attributes at both the local and landscape scales, and include indicators such as climate variations, management practices, and disturbances (Eyre *et al.*, 2011a). This framework follows the multi-resolution approach of relating EO datasets to ground measurements shown in Figure 3.1 and identifies three spatially hierarchical and complementary components that are integrated through research, analysis and modelling:

- Targeted monitoring—localised, field-based monitoring to address specific management questions based on target species that are known to be indicators of change or have been identified as vulnerable. These programs need to be well-defined, focused in terms of spatial extent and stated goals, and reviewed frequently.
- Surveillance monitoring—broad-scale, field-based sampling for a range of species across multiple ecosystems.
- Landscape scale monitoring—regional to national scale information on habitat quality and trends in threats to, or drivers of, biodiversity, using data from systematic ground-based and EO methods with frequent coverage.

Some of the biodiversity driver indicators that would be observed in each layer of this hierarchy include:

- incidence of fire—threatens species habitat or species directly, and varies with ecoregion;
- vegetation clearing and fragmentation—directly threatens habitat for native species, most commonly in tropical savanna environments;
- grazing pressure—threatens habitat and competition for resources, and includes both domestic and feral animals;
- feral predator abundance and distribution—endangers native fauna and domestic stock;
- invasive plant abundance and distribution—threatens habitat quality, competes with native flora, and can change fire regimes;
- climatic data—particularly rainfall and temperature, to provide context for both short and long term variations (Eyre *et al.*, 2011a).

Any biodiversity sampling system also needs to ensure that surveillance sites are stratified by bioregions within jurisdictions (Eyre *et al.*, 2011a).

15.6 Further Information

GEOGLAM Rangeland and Pasture Productivity (RaPP) tool

Australia: <https://map.geo-rapp.org/#australia>

Global: <https://www.geo-rapp.org>

Information: <https://www.csiro.au/en/Research/LWF/Areas/Landscapes/Earth-observation/RAPP-Map-GEOGLAM>

Australian Collaborative Rangelands Information System (ACRIS)

ACRIS: <http://www.environment.gov.au/land/rangelands/acris>

Bastin *et al.* (2008)

Foran *et al.* (2019)

Soils for Life

A not-for-profit charity dedicated to supporting Australian farmers and rural communities in regenerating soils and landscapes to build natural and social capital and transform food systems: <https://soilsforlife.org.au/about/>

FarmMap4D Spatial Hub

Online, subscription tool for mapping, assessing and monitoring property infrastructure, land resources and ground cover: <http://www.farmmap4d.com.au/mapping/>

Northern Territory

DENR (2019). Rangelands Field Monitoring Manual Version 5. Department of Environment and Natural Resources, NT. ISBN 1 920772 93 6

15.7 References

Andrew, M.H., and Lange, R.T. (1986). Development of a new piosphere in arid chenopod shrubland grazed by sheep. 2: Changes to the vegetation. *Australian Journal of Ecology*, 11, 411–424.

ABARES (2017). *Landuse by NRM region*. Australian Bureau of Agricultural and Resource Economics and Sciences website: <http://www.Agriculture.gov.au/abares/aclump/land-use/catchment-scale-land-use-reports>

ABS (2016). *Quickstats—data by geography*. Australian Bureau of Statistics website: <http://www.abs.gov.au/websitedbs/D3310114.nsf/Home/Census?OpenDocument&ref=topBar>

New South Wales

SLATS: <https://www.environment.nsw.gov.au/topics/animals-and-plants/native-vegetation/reports-and-resources>

Queensland

SLATS: <https://www.qld.gov.au/environment/land/management/mapping/statewide-monitoring/slats>

FORAGE: <https://www.longpaddock.qld.gov.au/forage/about/>

Vegmachine: <https://vegmachine.net/>

AussieGRASS: national simulation framework for Australian grasslands and rangelands based on GRASP soil water and pasture growth model: <https://www.longpaddock.qld.gov.au/aussiegrass/>

BioCondition: MLA (2012)

Western Australia

<https://www.agric.wa.gov.au/rangelands/assessing-rangeland-condition>

OAGWA (2017)

WARMS: Watson *et al.*, 2007a, 2007b; Novelly *et al.*, 2008

Rangelands NRM: <https://rangelandswa.com.au>

TERN AusPlots

Rangelands: <https://www.tern.org.au/AusPlots-Rangelands-pg28320.html>

World Atlas of Desertification (3rd edition)

<https://wad.jrc.ec.europa.eu/>

ARS (2019). *Australian Rangelands Society* website, landing page. <https://www.austrangesoc.com.au/>

Ash, A.J., Corfield, J.P., Mclvor, J.G., and Ksiksi, T.S. (2011). Grazing management in tropical savannas: Utilisation and rest strategies to manipulate rangeland condition. *Rangeland Ecological Management*, 64, 223–239. doi:10.2111/REM-D-09-00111.1

Asner, G.P. (1998). Biophysical and biochemical sources of variability in canopy reflectance. *Remote Sensing of Environment*, 64, 234–253.

- Asner, G.P. (2004). Biophysical Remote Sensing Signatures of Arid and Semiarid Ecosystems. Ch. 2 in *Manual of Remote Sensing, Volume 4, Remote Sensing for Natural Resource Management and Environmental Monitoring*. (Ed: Ustin, S.L.) Wiley International, New York. 768 p.
- Austrade (2019). *Pastoral leases* webpage, Austrade website: <https://www.austrade.gov.au/land-tenure/Land-tenure/pastoral-leases>
- Barnetson, J., Phinn, S., and Scarth, P. (2019). Mapping woody vegetation cover across Australia's arid rangelands: utilising a machine-learning classification and low-cost Remotely Piloted Aircraft System. *International Journal of Applied Earth Observation and Geoinformation*, 83, 101909. <https://doi.org/10.1016/j.jag.2019.101909>
- Bastin, G., and Allan, G. (2012). After the smoke has cleared: 2011 fire in central Australia. *Range Management Newsletter*, 12/2, 3–6. Australian Rangeland Society, Australia.
- Bastin, G.N., and Ludwig, J.A. (2006). Problems and prospects for mapping vegetation condition in Australia's arid rangelands. *Ecological Management and Restoration*, 7, S71–S74.
- Bastin, G.N., Pickup, G., Chewings, V.H., and Pearce, G. (1993). Land degradation assessment in central Australia using a grazing gradient method. *The Rangeland Journal*, 15, 190–216. doi:10.1071/RJ9930190
- Bastin, G.N., Pickup, G., and Stanes, A. (1996). Estimating Landscape Resilience from Satellite Data and its Application to Pastoral Land Management. *The Rangeland Journal*, 18(1), 118–135.
- Bastin, G.N., Tynan, R.W., and Chewings, V.H. (1998). Implementing satellite-based grazing gradient methods for rangeland assessment in South Australia. *The Rangeland Journal*, 20, 61–76.
- Bastin, G.N., Abbott, B.N., Chewings, V.H., and Wallace, J. (2007). *Metrics of landscape health for sustainable grazing in the Burdekin Dry Tropics, Queensland*. Project report for the Sustainable Grazing Program Great Barrier Reef catchments node Water for a Healthy Country Flagship, CSIRO. doi:<https://doi.org/10.4225/08/59a70b5a5345c>
- Bastin, G., and the ACRIS Management Committee (2008). *Rangelands 2008—Taking the Pulse*. National Land and Water Resources Audit, Canberra. <http://www.environment.gov.au/land/publications/acris-rangelands-2008-taking-pulse>
- Bastin, G.N., Stafford Smith, D.M., Watson, I.W., and Fisher, A. (2009). The Australian Collaborative Rangelands Information System: preparing for a climate of change. *The Rangeland Journal*, 31, 111–125. doi:10.1071/RJ08072
- Bastin, G., Scarth, P., Chewings, V., Sparrow, A., Denham, R., Schmidt, M., O'Reagain, P., Shepherd, R., and Abbott, B. (2012). Separating grazing and rainfall effects at regional scale using remote sensing imagery: a dynamic reference-cover method. *Remote Sensing of Environment*, 121, 443–457. doi:10.1016/j.rse.2012.02.021
- Bastin, G., Denham, R., Scarth, P., Sparrow, A., and Chewings, V. (2014). Remotely-sensed analysis of ground-cover change in Queensland's rangelands, 1988–2005. *The Rangelands Journal*, 36, 191–204. <http://dx.doi.org/10.1071/RJ13127>
- Beutel, T., Karfs, R., Wallace, J., Trevithick, R., Scarth, P., and Tindall, D. (2015). VegMachine® in Queensland. In *Innovation in the Rangelands. Proceedings of the 18th Australian Rangeland Society Biennial Conference*. Alice Springs, NT. (Ed: Friedel, M.H.) Australian Rangeland Society, Parkside, SA.
- Beutel, T.S., Trevithick, R., Scarth, P., and Tindall, D. (2019). VegMachine.net. online land cover analysis for Australian rangelands. *The Rangeland Journal*, 41, 355–362. <https://doi.org/10.1071/RJ19013>
- Biograze (2000) *Biograze: waterpoints and wildlife*. CSIRO, Alice Springs NT.
- Brinsmead, N. (2017). Let's get technical. Introducing you to VegMachine®. *Envoy*, 2017, 17.
- Briske, D.D., Fuhlendorf, S.D., and Smeins, F.E. (2003). Vegetation dynamics on rangelands: A critique of the current paradigms. *Journal of Applied Ecology*, 40, 601–614.
- Burrows, W.H., Carter, J.O., Scanlan, J.C., and Anderson, E.R. (1990). Management of savannas for livestock production in north-east Australia: contrasts across the tree-grass continuum. *Journal of Biogeography*, 17(4/5), 503–512. doi:10.2307/2845383
- Butler, D., Thackway, R., and Cosier, P. (2020). *Technical Protocol for Constructing Native Vegetation Condition Accounts Version 1.0 - May 2020*. Accounting for Nature Limited, Sydney, Australia. <https://static1.squarespace.com/static/5dc38cde1d028031235ca3cf/t/5fa246b73c71c92e01513cc7/1604470479988/AfN+Native+Vegetation+Technical+Protocol+ACCREDITED.pdf>
- Croft, D.B., Montague-Drake, R., and Dowle, M. (2007). Biodiversity and water point closure: is the grazing piosphere a persistent effect? In *Animals of Arid Australia: out on their own?* (Eds: Dickman, C., Lunney, D., and Burgin, S.) Royal Zoological Society of NSW, Mosman. pp143–171.
- DENR (2019). *NT Pastoral Land Board Annual Reports*: <https://depws.nt.gov.au/boards-and-committees/pastoral-land-board>

- DEWHA (2009). *Assessment of Australia's Terrestrial Biodiversity 2008*. Biodiversity Assessment Working Group of the National Land and Water Resources Audit for the Australian Government, Canberra.
- DEWHA (2010). *Ecosystem Services: Key Concepts and Applications*. Occasional Paper No 1, Department of the Environment, Water, Heritage and the Arts, Canberra.
- DPIF (2006). *The ABCD pasture condition guide: Mulga and Mitchell Grass*. Department of Primary Industries and Fisheries, Charleville. ISSN 0727-6273
- DSEWPC (2013). *The Australian Collaborative Rangelands Information System (ACRIS): Reporting Change in the Rangelands*. Department of Sustainability, Environment, Water, Population and Communities, Canberra. <https://www.environment.gov.au/system/files/resources/46e443c5-673a-4093-948d-d87830cfc2f9/files/acris-reporting-change.pdf>
- Eldridge, D.J., Delgado-Baquerizo, M., Quero, J.L., Ochoa, V., Gozalo, B., Escolar, C., García-Gómez, M., Prina, A., Bowker, M.A., Bran, D.E., Castro, I., Cea, A., Derak, M., Espinosa, C.I., Florentino, A., Gaitán, J.J., Gatica, G., Gómez-González, S., Ghiloufi, W., Gutierrez, J.R., Gusmán-Montalván, E., Hernández, R.M., Hughes, F.M., Muiño, W., Moneris, J., Ospina, A., Ramírez, D.A., Ribas-Fernández, Y.A., Romão, R.L., Torres-Díaz, C., Koen, T.B., and Maestre, F.T. (2020). Surface indicators are correlated with soil multifunctionality in global drylands. *Journal of Applied Ecology*, 57(2), 424–435.
- Eyre, T.J., Fisher, A., Hunt, L.P., and Kutt, A.S. (2011a). Measure it to better manage it: a biodiversity monitoring framework for the Australian rangelands. *The Rangeland Journal*, 33, 239–253.
- Eyre, T.J., Kelly, A.L., Neldner, V.J., Wilson, B.A., Ferguson, D.J., Laidlaw, M., and Franks, A.J. (2011b). *BioCondition: A Condition Assessment Framework for Terrestrial Biodiversity in Queensland. Assessment Methodology Manual*. Department of Environment and Resource Management, Brisbane.
- Folke, C., Carpenter, S., Walker, B., Scheffer, M., Elmqvist, T., Gunderson, L., and Holling, C.S. (2004). Regime shifts, resilience, and biodiversity in ecosystem management. *Annual Review of Ecology and Systematics*, 35, 557–81 doi:10.1146/annurev.ecolsys.35.021103.105711
- Foran, B., Stafford Smith, M., Burnside, D., Andrew, M., Blesing, D., Forrest, K., and Taylor, J. (2019). Australian rangelands futures: time now for systemic responses to interconnected challenges. *The Rangeland Journal*, 41, 271–292. <https://doi.org/10.1017/RJ18105>
- Fuhlendorf, S.D., Archer, S.A., Smeins, F., Engle, D.M., and Taylor, C.A. (2008). The Combined Influence of Grazing, Fire, and Herbaceous Productivity on Tree-Grass Interactions. In *Western North American Juniperus Communities: A Dynamic Vegetation Type*. 196. (Ed: Van Auken, O.W.) Springer, New York, NY. Pp. 219–238.
- FutureBeef (2020). *Grazing land management* webpage, FutureBeef website: <https://futurebeef.com.au/knowledge-centre/grazing-land-management/>
- Guerin, G.R., Sparrow, B., Tokmakoff, A., Smyth, A., Leitch, E., Baruch, Z., and Lowe, A.J. (2017). Opportunities for Integrated Ecological Analysis across Inland Australia with Standardised Data from Ausplots Rangelands. *PLoS ONE*, 12(1), e0170137. <https://doi.org/10.1371/journal.pone.0170137>
- Guerschman, J.P., Hill, M.J., Renzullo, L.J., Barrett, D.J., Marks, A.S., and Botha, E.J. (2009). Estimating fractional cover of photosynthetic vegetation, non photosynthetic vegetation and bare soil in the Australian tropical savannah region upscaling Hyperion and MODIS sensors. *Remote Sensing of Environment*, 113, 928–945.
- Hendy, E.J., Gagan, M.K., and Lough, J.M. (2003). Chronological control of coral records using luminescent lines and evidence for non-stationary ENSO teleconnections in northeast Australia. *Holocene*, 13, 187–199.
- Hill, M.J. (2004). Grazing agriculture–Managed Pasture, Grassland and Rangeland. Ch. 9 in *Manual of Remote Sensing, Volume 4, Remote Sensing for Natural Resource Management and Environmental Monitoring*. (Ed: Ustin, S.L.) Wiley International, New York. 768 p.
- Holling, C.S. (1973). Resilience and stability of ecological systems. *Annual Review of Ecology and Systematics*, 4, 1–23.
- Howes, A.L., and McAlpine, C.A. (2008). *The impact of artificial watering points on rangeland biodiversity: A review*. DKCRC Working Paper 15, The WaterSmart™ Literature Reviews. Desert Knowledge CRC, Alice Springs.
- IUCN (2019). *Global Drylands Initiative* webpage. International Union for Conservation of Nature website: <https://www.iucn.org/theme/ecosystem-management/our-work/global-drylands-initiative>
- James, C.D., Landsberg, J., and Morton, S.R. (1999). Provision of watering points in the Australian arid zone: a review of effects on biota. *Journal of Arid Environments*, 41(1), 87–121. <https://doi.org/10.1006/jare.1998.0467>
- Jurskis, V. (2015). *Firestick Ecology*. Connor Court Publishing, Ballarat.

- Karfs, R. (2002). *Rangeland monitoring in tropical savanna grasslands Northern Territory, Australia: relationships between temporal satellite data and ground data*. Masters Thesis, Research School of Tropical Environment Studies and Geography, James Cook University, Townsville, Queensland.
- Karfs, R.A., Daly, C., Beutel, T.S., Peel, L., and Wallace J.F. (2004). VegMachine—Delivering monitoring information to northern Australia's pastoral industry. *Proceedings of 12th Australasian Remote Sensing and Photogrammetry Conference, Fremantle Western Australia*. RSPAA, Perth.
- Ker Conway, J. (1989). *The Road from Coorain*. Mandarin, London.
- Landsberg, J., James, C.D., Morton, S.R., Hobbs, T.J., Stol, J., Drew, A., and Tongway, H. (1997). *The Effects of Artificial Sources of Water on Rangeland Biodiversity*. Environment Australia and CSIRO, Canberra.
- Lange, R.T. (1969). The piosphere, sheep track and dung patterns. *Journal of Range Management*, 22, 396–400. <http://hdl.handle.net/10150/649971>
- Ludwig, J.A., Bastin, G.N., Chewings, V.H., Eager, R.W., and Liedloff, A.C. (2007). Leakiness: a new index for monitoring the health of arid and semiarid landscapes using remotely sensed vegetation cover and elevation data. *Ecological Indicators*, 7, 442–454. doi:10.1016/j.ecolind.2006.05.001
- Lunt, I., Eldridge, D.J., Morgan, J.W., and Witt, G.B. (2007). Turner Review No. 13: A framework to predict the effects of livestock grazing and grazing exclusion on conservation values in natural ecosystems in Australia. *Australian Journal of Botany*, 55, 401–415. doi:10.1071/BT06178
- McAlpine, C., Thackway, R., and Smith, A. (2014). *Towards an Australian Rangeland Biodiversity Monitoring Framework*. A discussion paper developed from a biodiversity monitoring workshop convened by Australian Collaborative Rangeland Information System (ACRIS) held at the University of Queensland, Brisbane, 30–31 October 2013. University of Queensland, Brisbane. https://espace.library.uq.edu.au/view/UQ:342912/Acris_Report.pdf
- McKeon, G.M., Hall, W.B., Henry, B.K., Stone, G.S., and Watson, I.W. (2004). *Pasture Degradation and Recovery in Australia's Rangelands: Learning From History*. Queensland Department of Natural Resources, Mines and Energy, Brisbane.
- MLA (2011). *Biodiversity Condition Assessment for Grazing Lands*. Meat and Livestock Australia Ltd, North Sydney. ISBN 9781741916393
- MLA (2012). *Biodiversity Condition Toolkit for Grazed Lands*. Meat and Livestock Australia Ltd. ISBN 9781741919240
- Murphy, B.P., Lehmann, C.E.R., Russell-Smith, J., and Lawes, M.J. (2014). Fire regimes and woody biomass dynamics in Australian savannas. *Journal of Biogeography*, 41(1). doi:10.1111/jbi.12204
- Novelly, P.E., Watson, I.W., Thomas, P.W.E., and Duckett, N.J. (2008). The Western Australian Rangeland Monitoring System (WARMS)—operating a regional scale monitoring system. *The Rangeland Journal*, 30, 271–281. doi:10.1071/RJ07047
- NSW DPI (2019). *Rangelands* webpage. NSW Department of Primary Industries website: <https://www.dpi.nsw.gov.au/agriculture/pastures-and-rangelands/rangelands>
- OAGWA (2017). *Management of Pastoral Lands in Western Australia*. Report 17: October 2017. Office fo the Auditor General Western Australia, Perth. [https://www.parliament.wa.gov.au/publications/taledpapers.nsf/displaypaper/4010833a47ac7e4cc25e5b46482581b600166282/\\$file/833.pdf](https://www.parliament.wa.gov.au/publications/taledpapers.nsf/displaypaper/4010833a47ac7e4cc25e5b46482581b600166282/$file/833.pdf)
- Peel, L.J., Beutel, T.S., Bull, A.L., Karfs, R.A., and Wallace, J. (2006). *NBP.315 VegMachine—Extending Integrated Rangeland Monitoring Information to Industry*. Meat and Livestock Australia, North Sydney, NSW.
- Pickup, G., and Chewings, V.H. (1994). A grazing gradient approach to land degradation assessment in arid areas from remotely-sensed data. *International Journal of Remote Sensing*, 15, 597–617.
- Pickup, G., Bastin, G.N., and Chewings, V.H. (1994). Remote-sensing-based Condition Assessment for Nonequilibrium Rangelands under Large-Scale Commercial Grazing. *Ecological Applications*, 4(3), 497–517. <https://doi.org/10.2307/1941952>
- Pickup, G, Bastin, G.N., and Chewings, V.H. (1998). Identifying trends in land degradation in non-equilibrium rangelands. *Journal of Applied Ecology*, 35, 365–377. <https://doi.org/10.1046/j.1365-2664.1998.00319.x>
- Pollock, D. (2019). *The Wooleen Way*. Scribe, Melbourne. ISBN: 9781925849257
- QRIScloud (2018). *QRIScloud delivers satellite data to Australian farmers, government and the public*. <https://www.qriscloud.org.au/about-qriscloud/case-studies/item/82-qriscloud-delivers-satellite-data-to-australian-farmers-govt-and-the-public>
- Russell-Smith, J., and Sangha, K.K. (2018). Emerging opportunities for developing a diversified land sector economy in Australia's northern savannas. *The Rangeland Journal*, 40, 315–330. doi.org/10.1071/RJ18005

- Scarth, P., Röder, A., and Schmidt, M. (2012). Tracking Grazing Pressure and Climate Interaction—The Role of Landsat Fractional Cover in Time Series Analysis. *Proceedings of the 15th Australasian Remote Sensing and Photogrammetry Conference (ARSPC)*, 13–17 September, Alice Springs, Australia. <https://doi.org/10.6084/m9.figshare.94250.v1>
- Sparrow, B. (2017). Monitoring in the Australian Rangelands: Where we've come from and where we should be headed. *Proceedings of the 19th Australian Rangeland Society Biennial Conference*. Australian Rangeland Society, Parkside, SA.
- Stafford Smith, M., and McAllister, R.R.J. (2008). Managing arid zone natural resources in Australia for spatial and temporal variability—an approach from first principles. *The Rangeland Journal*, 30, 15–27.
- Tongway, D.J., and Hindley, N.L. (2004). *Landscape Function Analysis Manual: Procedures for Monitoring and Assessing Landscapes with Special Reference to Minesites and Rangelands, Version 3.1*. CD-ROM. CSIRO Sustainable Ecosystems, Canberra.
- URS Australia P/L (2013). *Sustainable Land Use and Economic Development Opportunities in the Western Australian Rangelands*. Unpublished report prepared for the Department of Agriculture and Food, South Perth, WA. https://d3n8a8pro7vhm.cloudfront.net/modernoutback/pages/515/attachments/original/1472028646/Rangeland_Opportunities_Final_Report_URS_2013.pdf?1472028646
- Wallace, J.F., and Thomas, P.W.E. (1998). *Rangeland monitoring in northern Western Australia using sequences of Landsat imagery*. Report to National Landcare Program Project No. 953024. Agriculture Western Australia, unpublished.
- Wallace, J.F., Holm, A. Mc.R., Novelly, P.E., and Campbell N.A. (1994). Assessment and monitoring of rangeland vegetation composition using multi-temporal Landsat data. In *Proceedings 7th Australian Remote Sensing Conference*, Melbourne, pp. 1102–1109.
- Wallace, J., Behn, G., and Furby, S. (2006). Vegetation condition assessment and monitoring from sequences of satellite imagery. *Ecological Management and Restoration*, 7, S31–S36. <https://doi.org/10.1111/j.1442-8903.2006.00289.x>
- Washington-Allen, R.A., Van Niel, T.G., Ramsey, R.D., and West, N.E. (2004). Remote Sensing-Based Piosphere Analysis. *GIScience and Remote Sensing*, 41(2), 136–154, doi:10.2747/1548-1603.41.2.136
- Waters, C., and Hacker, R. (2008). *Integration of biodiversity and primary production in northern and western New South Wales*. NSW Department of Primary Industries.
- Watson, I.W., Thomas, P.W.E., and Fletcher, W.J. (2007a). The first assessment, using a rangeland monitoring system, of change in shrub and tree populations across the arid shrublands of Western Australia. *The Rangeland Journal*, 29, 25–37. doi:10.1071/RJ07018
- Watson, I.W., Novelly, P., and Thomas, P.W.E. (2007b). Monitoring changes in pastoral rangelands—the Western Australian Rangeland Monitoring System (WARMS). *The Rangeland Journal*, 29, 191–205. doi:10.1071/RJ07008
- WEF (2018). *The global risks report 2018*. World Economic Forum, Geneva, Switzerland. <https://www.weforum.org/reports/the-global-risks-report-2018>
- White, A., Sparrow, B., Leitch, E., Foulkes, J., Flitton, R., Lowe, A.J., and Caddy-Retalic, S. (2012). *AusPlots Rangelands Survey Protocol Manual*. The University of Adelaide Press, Adelaide. ISBN 978-1-922064-38-7
- Xu, S., Zhao, Q., Ding, S., Qin, M., Ning, L., and Ji, X. (2018). Improving Soil and Water Conservation of Riparian Vegetation Based on Landscape Leakiness and Optimal Vegetation Pattern. *Sustainability*, 10, 1571.
- Xu, S., Zhao, Q., Liu, Y., Ding, S., and Qin, M. (2019). Sensitivity and Applicability of Landscape Leakiness Index in Determining Soil and Water Conservation Function of a Subtropical Riparian Vegetation Buffer Zone. *Environmental Engineering Science*, 36(2), 227–236.
- Zhang, B., and Carter, J. (2018). FORAGE—An online system for generating and delivering property-scale decision support information for grazing land and environmental management. *Computers in Electronics in Agriculture*, 150, 302–311. <https://doi.org/10.1016/j.compag.2018.05.010>
- Zhou, Z.-S., Caccetta, P., Sims, N.C., and Held, A. (2016). Multi-band SAR Data for Rangeland Pasture Monitoring. *Proceedings of IEEE IGARSS 2016*, pp. 170–173, July 2016. doi:10.1109/IGARSS.2016.7729035



16 Forestry

Nicholas Coops and Barbara Harrison

The need for accurate, timely, and cost-effective forest information has never been more critical (White *et al.*, 2016). Australia's commitment to sustainable forest management and conservation of biodiversity, as well as a renewed focus on biomass and bioenergy, and increasing awareness of climate change scenarios, all require detailed knowledge of the existing forest resource, and a greater understanding of the dynamic processes of forest growth and stand condition.

Forestry has long-established practices for using airborne EO datasets for timber volume estimation and sampling stratification. However, like other forestry communities around the world, the use of EO in Australia has increased in recent decades in response to the need for accurate, and spatially explicit, information on land cover change, forest health assessment, fire severity and burn scar mapping, and carbon sequestration, as well as estimation of areas planted and harvested.

Traditionally, EO imagery acquired by most state-based forest organisations in Australia comprised medium scale, aerial photography (1:10,000–1:25,000), which was manually interpreted to stratify large heterogeneous forests into smaller, more uniform areas deemed suitable for ground sampling (Smith and Woodgate, 1985). The resulting maps enabled relevant metrics of timber volume and/or environmental health to be determined, recorded, and monitored. The advent of readily available, high spatial resolution, digital EO imagery has seen a shift in forestry EO data usage, enabling more automated processing to derive relevant forest attributes.

The wide range of information needs and users, however, resulted in many different EO data sources and approaches being used for different purposes, with no single EO platform or processing stream being suitable to meet *all* user requirements (Packalen and

Maltamo, 2008). In addition, the complexity of the Australian forest environment makes the development of generalised EO procedures to cover such diversity a difficult task. Australian forest canopies are typically more open than their northern hemisphere counterparts, which means many EO-based methods that were derived overseas may not be appropriate. Extensive shadowing, which is common in most images, is caused by complex topography in most forested landscapes (for example, see banner image for Section 1). This undulating foundation is overlaid with a variety of natural and human disturbance regimes leading to an array of structural and floristic patterns (see Section 2.3.1). The high degree of speciation and intra-species variation in the genus *Eucalyptus* further complicates the situation, as does the canopy geometry of that genus, which features generally vertical leaves and a wide variety of leaf forms, with juvenile to old and insect-damaged leaves sometimes being present on a single tree (Lees and Ritman, 1991). As a result, hybrid methods, which use a combination of technologies, are likely to continue, such as airborne lidar for Digital Elevation Model (DEM) development and volume assessment, coupled with more conventional optical imagery for species and health assessment. In the drier and less productive areas, which are essentially unmanaged, combinations of freely available, satellite-based optical and radar datasets offer viable alternatives.

Background image: Terrestrial scan of an open eucalypt forest at Tumberumba, Australia, acquired using Dual-Wavelength Echidna Lidar (DWEL; Douglas *et al.*, 2015). The image uses a blue–red colour table applied to the normalised difference index (NDI), which is computed from the wavelengths, in nm, as (1064–1548)/(1064+1548). The distinction between woody and non-woody material can clearly be seen in the level of the NDI, irrespective of range from the instrument. Source: Glenn Newnham, CSIRO (from Newnham *et al.*, 2015, Figure 1)

Recommended Chapter Citation: Coops, N.C., and Harrison, B.A. (2021). Forestry. Ch 16 in *Earth Observation: Data, Processing and Applications. Volume 3A—Terrestrial Vegetation*. CRC SI, Melbourne, pp. 323–350.

Vast expanses of Eucalyptus forests present in springtime an unforgettable picture, the straight, clean trunks rising in a blend of tints that range from delicate cream to ochre, from pearl pink to deepest red, a single giant trunk sometimes displaying all of these colours at once.
(Elizabeth Kenny, from 'And They shall Walk')

EO methods that are relevant to assessment of forest vegetation are introduced in earlier sections of this volume. In this section, we discuss the role EO technology can play in improving our understanding of forests across Australia. To do so we focus on assessment of those components commonly considered when describing forest vegetation and managing the forest resource, namely:

- forest type—zonation of plant communities and species (see Section 16.3);
- forest hydrology—catchment and drainage characteristics (see Section 16.4);
- forest structure—plant height and stratification (see Section 16.5);
- forest functionality—forest health and biosecurity (see Section 16.6);
- forest diversity—ecosystem richness (see Section 16.7); and
- forest disturbance—landscape scale changes (see Section 16.8).

Characteristics of Australian forests are introduced in Sections 2.3.1 and 2.4 and detailed in Section 16.1. EO sensors that are relevant to forest mapping and monitoring are summarised in Section 16.2.

Silviculture is the art and science of controlling the establishment, growth, composition and quality, health, protection and utilisation of stands of trees or forests to meet the diverse needs and values of forest owners and society on a sustainable basis. Silvicultural practice embodies a range of treatments to maintain and enhance the utility of the forest for any defined management purpose.
(IFA Forestry Policy Statement 2.9; IFA, 2008)

16.1 Forestry in Australia

In Australia, a forest is defined as:

An area, incorporating all living and non-living components, that is dominated by trees having usually a single stem and a mature or potentially mature stand height exceeding 2 m and with existing or potential crown cover of overstorey strata about equal to or greater than 20%. This includes Australia's diverse native forests and plantations, regardless of age. It is also sufficiently broad to encompass areas of trees that are sometimes described as woodlands.¹¹

Using this definition, Australia contains around 3% of global forests by area (SOFR, 2018). These forests vary significantly in structure and floristic diversity, from dense rainforests, to sparse, multi-stemmed mallee associations, to exotic plantations (see Section 2.3.1).

The area of forest in Australia is monitored by the National Forest Inventory (NFI), which incorporates systematic and validated analyses of multi-temporal Landsat imagery (including data from the National Greenhouse Gas Inventory, formerly known as the National Carbon Accounting System—NCAS) in conjunction with state and territory records and ground surveys. Forests cover 17% of the Australian land mass (134 Mha; SOFR, 2018), the vast majority of which (132 Mha) comprises native hardwood forests, dominated by species from *Eucalyptus* and/or *Acacia*, with relatively small areas of forest being dominated by *Callitris*, *Melaleuca*, and *Casuarina* (see Table 16.1).

¹¹ Forests Australia: <https://www.agriculture.gov.au/abares/forestsaustralia/australias-forests>

Table 16.1 Forest area in Australia

Category	Description	Area ('000 ha)	% Area
Native	Acacia	10,813	8.07
	Callitris	2,011	1.50
	Casuarina	1,236	0.92
	Eucalyptus (including species from <i>Corymbia</i> and <i>Angophora</i>)	101,058	75.40
	Mangrove	854	0.64
	Melaleuca	6,382	4.76
	Rainforest	3,581	2.67
	Other native forest	5,679	4.24
	Total	131,615	98.2
Commercial plantations	Softwood species	1,015	0.77
	Hardwood species	922	0.67
	Unknown or mixed species	11	0.0
	Total	1,949	1.45
Other forests	Non-industrial plantations and various planted forests	474	0.35
Total	All forests	134,037	100

Source: SOFR (2018) Table 1.5

These native forests are largely distributed throughout Tasmania and near the northern, eastern and southern coastal and hinterland regions of continental Australia (see Figure 16.1a). Six tenure categories of native forest are recognised by the NFI (with the proportion by area shown in parentheses below):

- Leasehold forest (35.9%)—Crown land held under leasehold title and generally regarded as privately managed, including land with special conditions for designated Indigenous communities (see Section 2 for definitions of land tenure categories in Australia).
- Private forest (31.2%)—land held under freehold title and private ownership.
- Nature conservation reserve (16.5%)—publicly owned land formally reserved for conservation and recreational purposes including national parks, nature reserves, and state and territory recreation and conservation areas.

- Other Crown land (8.4%)—reserved for purposes including utilities, mining, water catchments, and use by indigenous communities.
- Multiple-use public forest (7.4%)—publicly owned forest on which government agencies manage a range of forest values including wood harvesting, water supply, biodiversity conservation, recreation, and environmental protection.
- Unresolved tenure (0.6%)—areas of unknown tenure (SOFR, 2018).

In Australia, most native forest grows on privately-owned or leasehold land (see Figure 16.1b), which is managed for forestry and/or grazing purposes (see Section 15). In total, around one third of the native forest area (46 Mha) is protected for biodiversity conservation (SOFR, 2018). Many Australian forests also serve an important function as water catchment areas for major cities and towns. Importantly, an estimated 22 million tonnes of carbon were sequestered in Australian forests in 2016 (SOFR, 2018).

Two thirds of the vegetation in the native forest area is commonly described as woodland, with crown cover of 20–50%, while around one quarter is designated open forest (50–80% crown cover), and only 3% as closed forest (see Table 16.2). Native forests are commonly sub-divided by both height and crown cover into nine structural classes as illustrated in Figure 16.2. Around two thirds of native forest are classified as medium height (10–30 m), about 30% as low (2–10 m) and the remainder as tall (> 30 m; SOFR, 2018). Distribution of these structural classes is closely related to moisture availability, past and present land uses, altitude and underlying geology (see Section 2).

Table 16.2 Native forest classes

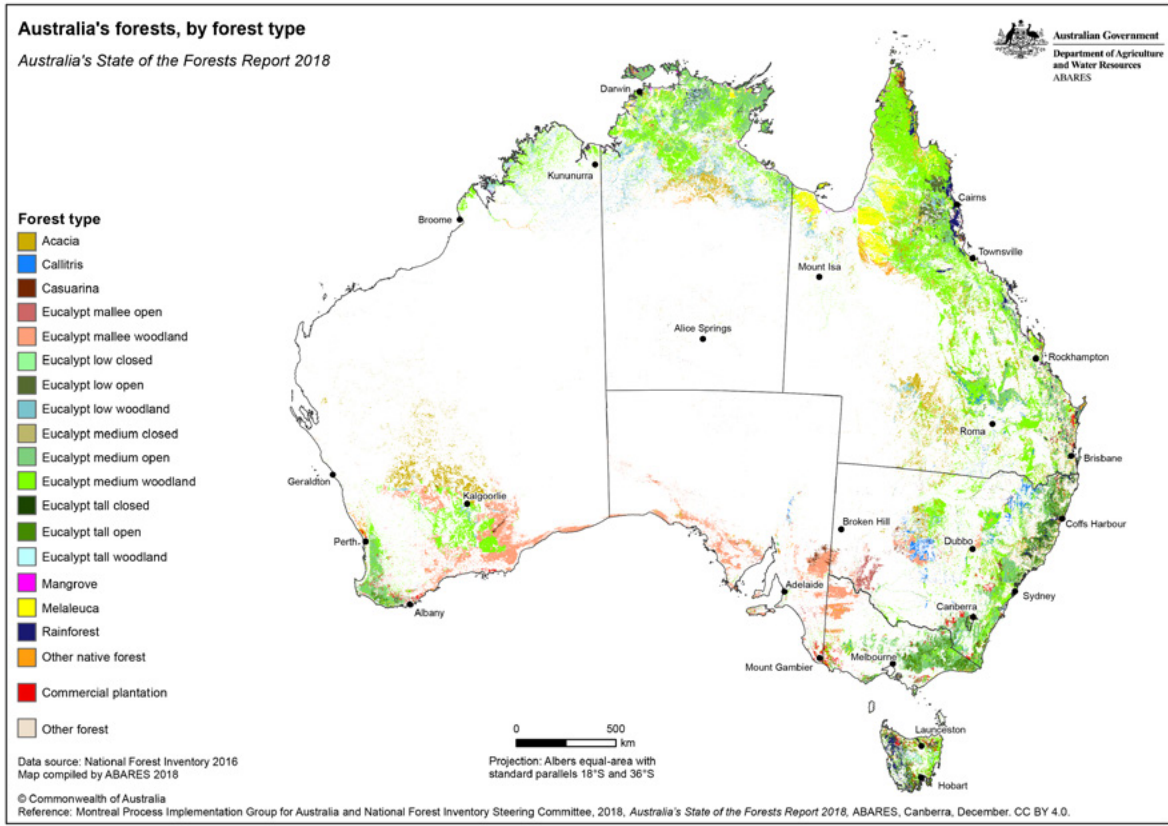
Type	Crown Cover (%)	Area ('000 ha)	% Area
Woodland	20–50	91,455	69
Open forest	50–80	33,962	26
Closed forest	80–100	3,622	3
Unknown	–	2,576	2
Total	–	131,615	100

Source: SOFR (2018)

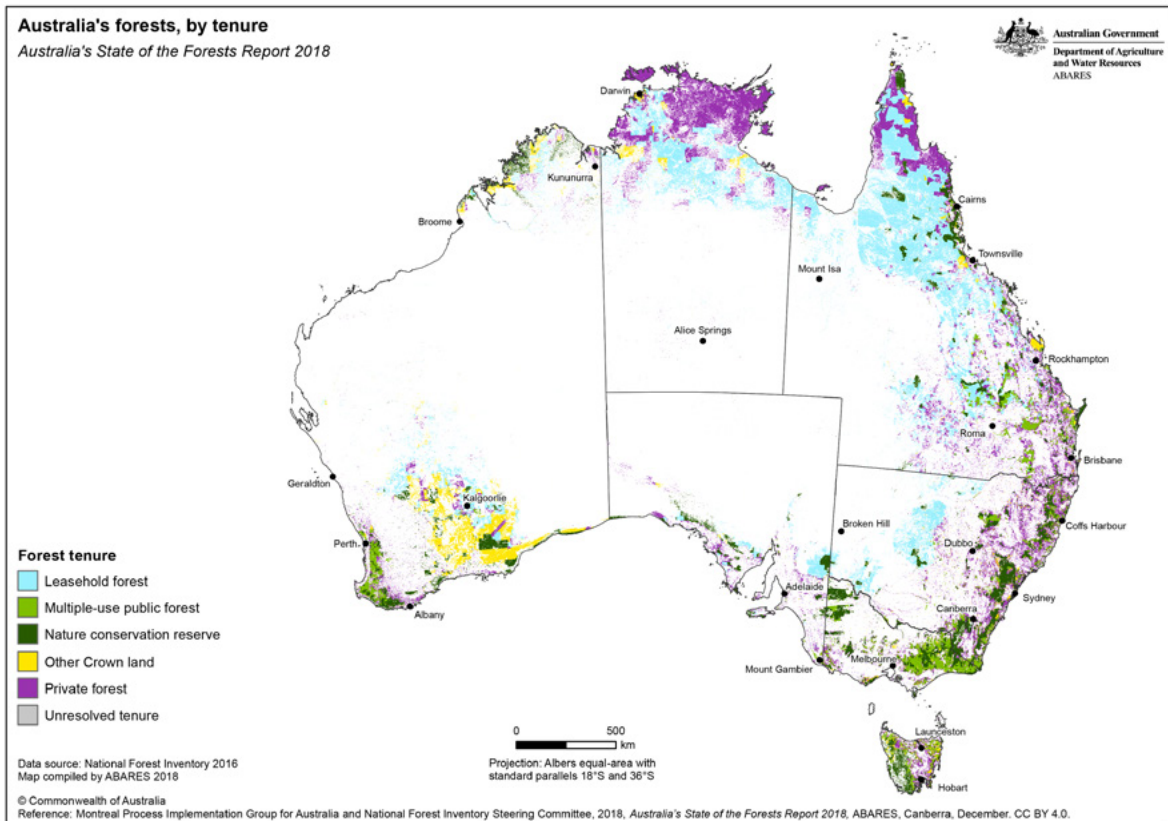
The Australian bush owes its peculiarity, more than anything else, to Eucalyptus. No other continental forest or woodland is so dominated by a single genus. Other biomes on Earth have scleromorphs, most have grasses, and few are spared wholly from fire, but none has the combination that exists in Australia and has given the bush its indelible character.
(Pyne, 1992)

Figure 16.1 Australian forests

a. Forest type



b. Tenure



Source: SOFR (2018) Figures 1.1 and 1.4

Figure 16.2 Native forest categories

Native forests are sub-divided by height and crown cover into nine general categories. The percentages below each diagram represent the proportion of each height/crown cover type within Australia's total area of native forests.



Source: SOFR (2018) Figure 1.2

16.2 EO Sensors for Forestry

Since the launch of the Landsat series of satellites in 1972, numerous studies have been undertaken to map forest area, condition, and structure from satellite imagery (Skidmore *et al.*, 1987). The relevance of different EO sensors to forestry applications is summarised in Table 16.3.

Passive optical sensors (including panchromatic, multispectral, and hyperspectral) are introduced in Volume 1A—Section 14 and their data characteristics are considered in Volume 1B—Section 6. While multispectral imagery acquired by satellite sensors has produced valuable global forest maps, their accuracy and spatial resolution are both low (see Section 16.3). Various studies have also combined passive optical datasets with data derived from other EO and GIS sources for a range of forestry applications (e.g. Hayward and Stone, 2011; Stone *et al.*, 2008).

In recent years, standardised time series of passive optical imagery (see Volume 2D) have enabled a greater understanding of the temporal changes in forested lands around the globe. For example, Digital Earth Australia (DEA) has enabled ready

access to the Landsat archive for monitoring the Australian landscape (see Volume 2D—Section 11.2). Hyperspectral sensors are relevant to understanding spectral covariates for various subtle variations of forest type and condition, and their datasets have been used to deduce plant species and biochemical status (see Section 16.6).

Light Detection and Ranging (lidar, also known as laser scanning; see Excursus 5.1) is an active form of EO that uses light emissions in the form of pulsed lasers to measure the distance from the sensor to a target (see Volume 1A—Section 15.1). These active optical sensors can be mounted in a variety of spaceborne and airborne platforms and also ground-based instruments (see Volume 1A—Section 10), with Airborne Laser Scanning (ALS) being most commonly used for forestry applications. Both forestry and topographic ALS applications rely on pulses of NIR wavelengths, typically at 1064 nm (Lim *et al.*, 2003). Lidar sensors can provide information relevant to describing the three-dimensional distribution of vegetation canopy components as well as the sub-canopy topography (see Section 16.5).

Table 16.3 EO sensors relevant to forestry

SAR: Synthetic Aperture Radar; DEM: Digital Elevation Model

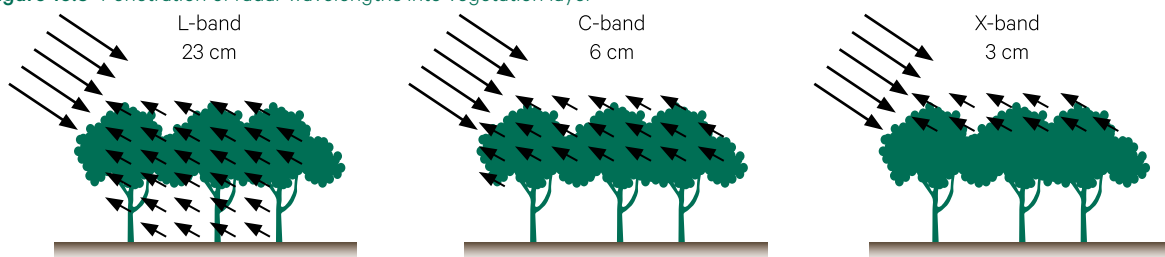
Type	Sensor	Platform	Relevance	Advantages	Disadvantages
Passive optical	Multispectral radiometer	Satellite or airborne	Broad forest type and condition mapping	Global coverage, low cost	Relatively low spectral and spatial resolution
	Hyperspectral spectro-radiometer	Satellite or airborne	Species mapping Plant biochemical functioning and health	High spectral resolution, highlight plant stress	High data volume, specialised processing
Active optical	Lidar	Satellite, airborne and terrestrial	Forest structure Biomass DEM Fuel load	Detailed structure for trees and stands, forestry hydrology	High cost, specialised processing
Active microwave	SAR	Satellite or airborne	Biomass Forest disturbance	All weather, so useful in tropical regions	More complex processing

The application of lidar technology to forestry, both in Australia and internationally, has been rapid. In Australia, various studies have examined the application of lidar data to plantations (Bennett, 2005; Alam *et al.*, 2012), open woodlands, and tall eucalypt forests (Lovell *et al.*, 2003, Lee *et al.*, 2004, Lucas *et al.*, 2006; Jupp and Lovell, 2007; Fedrigo *et al.*, 2018; Fisher *et al.*, 2020). In North America and Europe, lidar is well recognised as a mature EO technology, routinely being applied to forest management and operations (Næsset, 2002, Reutebuch *et al.*, 2005, Wulder *et al.*, 2008, White *et al.*, 2013). For example, the Area Based Approach (ABA; Næsset 2002) has been used operationally for a decade to process lidar point cloud data into spatial metrics for forest inventory applications (Wulder *et al.*, 2008; White *et al.*, 2013). This approach enables precise prediction of a suite of basic forest inventory variables, such as stem volume, basal area, and height. Lidars carried by unmanned aerial vehicles (UAV) are gaining popularity, and advances in this field will likely result in these sensors being more readily available and applicable to tailored forest management applications (Du Toit *et al.*, 2020). In forestry applications, Terrestrial Laser systems (TLS) complement ALS by providing structural information about tree trunks that can be obscured by the vegetation canopy from an airborne sensor (see Excursus 5.1).

Radar sensors are introduced in Volume 1A—Section 15.2 and detailed in Volume 1B—Section 8. These active microwave sensors also offer the potential to map the structure and biomass of Australian forests, both from spaceborne and airborne platforms, especially in the drier eucalypt forests with lower biomass. The majority of studies investigating the use of radar data for biomass estimation have focused either on coniferous forests in the northern hemisphere, particularly in North America and Eurasia, or tropical regions. However, radar-based methods have also been developed in Australia for the UN REDD+ (Reducing Emissions from Deforestation and Forest Degradation) framework (Mitchell *et al.*, 2017; see Section 17.7.3). Since different radar frequency bands penetrate into multi-layered volumes (such as vegetation canopies) to differing depths, L-band data is often preferred for vegetative studies (see Figure 16.3).

Space-based Synthetic Aperture Radar (SAR) technology is rapidly developing, with the imminent launch of new satellites carrying radars that use longer wavelengths than ever before. For example, at the end of 2020, ESA are launching BIOMASS, a satellite with P-band (~68 cm wavelength) radar which can penetrate the canopy and interact with tree trunks and the ground surface. This will be the first of its kind, as P-band has previously been restricted to airborne platforms.

Figure 16.3 Penetration of radar wavelengths into vegetation layer



Source: Bruce Forster and Linlin Ge, Course Notes, UNSW

16.3 Forest Type

Conventionally, most processing of digital satellite imagery for mapping forest type has used various image classification procedures (see Volume 2E for details on classification algorithms). Classification accuracy is usually determined using a confusion matrix, which compares the allocation of a number of randomly selected pixels in the image with a known cover class (derived from independent sources such as maps, photographs, or ground data). The overall classification accuracy is then computed as the ratio of the total number of correctly classified pixels to the total number of pixels in each class (see Volume 2E).

Early forest type classifications from multispectral imagery relied on Landsat MSS data and, while spatially comprehensive and revolutionary at the time, generally resulted in low classification accuracy, with only broad forest types (such as coniferous versus broadleaf) being differentiated reliably (for example, see Section 3.3.2). Landsat MSS was also used to estimate rates of forest clearing in Victoria (Woodgate and Black, 1988). The improved spectral, spatial, and radiometric resolutions of Landsat TM/ETM+/OLI, as well as greater temporal resolution in more recent EO satellites such as Sentinel-2, have proved to be superior for classifying forest information. For example:

- SPOT XS and Landsat TM imagery, in conjunction with ancillary datasets, allowed discrimination of species and age classes in native and exotic vegetation (Skidmore and Turner, 1988, Skidmore, 1989);
- a combination of aerial photography and multi-temporal Landsat TM imagery were used to classify and differentiate various forest type associations

(including dry eucalypt forest, humid eucalypt forest, and littoral rainforest, Yagüe and Garcia, 2006); and

- the performance of metrics derived from Landsat TM imagery with auxiliary terrain and climatic variables were used to predict forest cover across the state of Victoria, delivering an overall accuracy of 96% for forest/non-forest classification (Mellor *et al.*, 2013).

Hyperspectral imagery and lidar data have also been used to map forest type in Australia. Examples include:

- Lucas *et al.* (2008)—outlined an approach for the use of airborne digital hyperspectral imagery (Compact Airborne Spectrographic Imager: CASI) to discriminate and map mixed-species forests at the tree crown/cluster level for use in biodiversity assessment, which identified dominant genera in the central southeast Queensland study area including *Acacia*, *Eucalyptus*, *Angophora*, and *Callitris*.
- Jafari and Lewis (2012)—utilised Hyperion hyperspectral data to discriminate distinct land cover types in an arid landscape in South Australia using endmember analysis (see Volume 2E and Section 8.3 above).
- Fedrigo *et al.* (2018)—used airborne lidar data as inputs to predict the distribution of rainforest and eucalypt stands that was comparable to existing ecological vegetation classes derived manually. The result was highly accurate (84%), allowing identification of small rainforests that had not previously been identified and demonstrating lidar as a key technology for mapping the structural and spatial complexity of these ecosystems.

16.4 Forest Hydrology

One of the most useful and important products of airborne lidar EO data is the generation of highly accurate and detailed DEM, even under forest canopies (see Excursus 5.1). For forest practitioners, lidar-based DEMs can provide detailed information about the underlying hydrology and water access across the forested landscape. Lidar topographic maps are critical for forest managers for operations and access, terrain stability, and erosion assessment, determination of drainage patterns for catchment protection, and engineering and road constructions (Bater and Coops, 2009; Reutebuch *et al.*, 2005; Wulder *et al.*, 2008).

Knowledge of the surface topography is also useful for forest planning and management decisions, such as selecting tree species for planting or determining an appropriate intensity of management. Murphy *et al.* (2011) utilised a lidar-derived DEM to predict a depth-to-water (DTW) index, which was then used to predict soil drainage, soil type, and a number of

additional forest soil properties at Swan Hills, Alberta, Canada. Important indicators of soil moisture content, coarse fragment sand, silt, clay composition, pH, and a range of other nutrients by soil layer type and depth were reliability predicted. Detailed topographic information both identifies and explains those forest ecological processes that are impacted by soil drainage and DTW, including nitrogen loss and forest litter/soil organic matter accumulation from ridge tops to depressions.

As the use of airborne lidar-derived terrain indices is expanding, research is also investigating the application of lidar to the development of predictive landscape ecological site classification modelling, integrating slope, topographic position, water and nutrient availability, as well as vegetation structure more holistically. This is paralleled by the acquisition of new information about the effects of eco-site characteristics on the distribution of wood attributes at different scales (Pokharel *et al.*, 2014).

16.5 Forest Structure

In forest vegetation, a contiguous group of trees within a forest that appears to be uniform in terms of species composition, age, size, structure, density, and/or condition is often referred to as a 'stand'. For silvicultural purposes, a stand is viewed, measured and managed as an integrated unit. Silvicultural practices, such as thinning and harvesting, alter the stand age structure. Accordingly, the distribution of tree diameters (measured by Diameter at Breast Height¹²: DBH) within a stand is closely related to its structure and composition, and indicative of its age and management history (see Section 6). Spatial diversity measures, such as the Stand Variance Index (STVI; Staudhammer and LeMay, 2001), which consider the variance in tree diameter and height within a stand, provide a useful platform to compare the structure of stands.

Desirable forest stand conditions, which meet multiple resource objectives, can generally be expressed in terms of stand structure. A stand structure approach to forest management therefore presents a unifying theme for multiple resource management objectives (O'Hara *et al.*, 1996), providing information to:

- enable sound silvicultural practice (Florence, 1996);
- assess suitability of the forest for wildlife;
- estimate fire risk;
- stratify the forest for more efficient ground-based inventories; and
- facilitate point source data, such as growth plots, to be extrapolated to a wider spatial context.

For silvicultural assessment, stand structure is typically represented in terms of mean DBH, tree height, canopy cover, and/or timber volume (see Sections 5 and 6). Estimates of total biomass and/or carbon content in a forest are also relevant to forest ecological studies and carbon accounting (see Sections 7.4 and 17).

The most common method to obtain estimates of volume and growth in forests is by developing relationships between direct measurements of the size and weight of the plants or plant parts and their corresponding EO-based observations (see Section 10). These relationships are developed by dividing a forest stand into different components, such as trees, shrubs, and ground covers, each of which can then be considered separately. Typically, a forest sampling program involves three types of sample measurements:

- non-destructive (such as DBH and height);
- destructive (such as cutting branches and trees, partitioning them into functional groups, such as leaves, main branches, boles, then estimating their dry weight or volumes); and
- various types of litter fall (see Sections 5.1.2 and 6.3).

Empirical methods, such as regression analysis, can then be used to obtain correlations between a comparatively small destructive sample and a significantly larger sample of non-destructive measurements that are representative of the total forest stand. Advances in TLS technologies (see Section 16.2), however, invite new approaches to using structural information in forest biometrics (Newnham *et al.*, 2015; see Excursus 5.1).

16.5.1 Stand height and cover

The use of ALS (airborne lidar) data to determine tree height is well established (see Excursus 5.1). This attribute is one of the few physical parameters that can directly be measured by lidar instruments. For example, strong correlations between lidar height and ground-measured height were observed in Blackbutt and River Red Gum forests ($r^2=0.95$, Turner, 2006). Other studies in Australian conditions have also shown height correlations in the range 89–97% (Bennett, 2005, Tickle *et al.*, 2001, Weller *et al.*, 2003). Crown cover (see Section 6.3.1) can be computed from ALS data, with lidar-derived estimates showing good correspondence with field data in woodland and open dry eucalypt forest in Queensland ($r^2=0.79$, Lucas *et al.*, 2006). At the same location, Lee and Lucas (2007) found strong relationships between lidar results and field measures of height, ($r^2=0.81$), tree density ($r^2=0.82$), crown cover ($r^2=0.78$), and foliage and branch cover ($r^2=0.89$).

In addition to predicting stand structural metrics, there has been much focus on estimating forest canopy attributes using EO datasets. Foliage Projective Cover (FPC, see Sections 2.3.1 and Excursus 6.1) is a critical attribute in many vegetation classification schemes (see Section 6.3) and is known to be highly dynamic. It is a required dataset at catchment through to continental scales in Australia and other areas around the world. Across Queensland and NSW, the state governments have mapped FPC using EO imagery to derive maps of land cover and land cover change which support government policies. For example, the Statewide Landcover and Trees Study (SLATS) program has been operationally processing Landsat imagery for several decades (SLATS; see Section 9.1 and Volume 2D—Excursus 14.3).

¹² Breast height is fixed at 1.3 m in Australia, UK, Canada and continental Europe, and at 1.4 m in the USA, New Zealand, Burma, India, Malaysia and South Africa.

As part of this program, Armston *et al.* (2009) observed long term trends in woody vegetation in Queensland using Landsat-5 TM and Landsat-7 ETM+ imagery and a combination of modelling approaches. Results indicated that parametric and artificial intelligence models had similar prediction errors (RMSE < 10%), but the latter models had less bias when overstorey FPC was greater than ~60%. All models showed more than 10% bias in plant communities with high herbaceous or understorey FPC.

Two additional biophysical parameters that provide information about the forest canopy and can be accurately estimated using EO approaches are:

- Leaf Area Index (LAI)—a dimensionless unit representing the area of foliage per area of ground (see Section 6.3.3); and
- Fraction of absorbed photosynthetically active radiation (fAPAR)—the fraction of photosynthetically active radiation (PAR) in visible wavelengths that is absorbed by a canopy including overstorey, understorey, and ground cover elements (Gower *et al.*, 1999; see Section 6.3.4).

At the global scale, a range of satellite sensors provides estimates for LAI and fAPAR at broad spatial resolution and fine temporal resolution over the Australian continent, including Advanced Very High Resolution Radiometer (AVHRR), Moderate Resolution Imaging Spectroradiometer (MODIS), and the SPOT VEGETATION sensor (see Volume 1A—Sections 12 and 14). A number of studies have assessed the capacity of these global datasets to measure LAI and fAPAR under Australian conditions (Hill *et al.*, 2006; Sea *et al.*, 2011). For example, Pickett-Heaps *et al.* (2014) investigated the consistency of six fAPAR products (MODIS, MERIS, SeaWiFS, MODIS-TIP, SPOT VEGETATION, and AVHRR) across the Australian continent using multi-year records. Large differences in fAPAR products were observed over much of Australia and these were explained by simple offsets and different sensitivities in fAPAR products to changes in vegetation cover. Relatively high agreement was observed at grassland, shrubland, and agricultural sites, with more significant disagreement occurring at sites classified as forest.

TLS are increasingly being used to measure plot level leaf area and gap fractions within forested landscapes (Zheng and Moskal, 2009; Danson *et al.*, 2007) as well as individual tree dimensions, such as stem diameter (with RMSE ranging between 1.5–3.3 cm from field measurements, Hopkinson *et al.* 2004; Tansey *et al.*, 2009), plus stem taper (Bienert *et al.*, 2007), sweep, and lean (Thies *et al.*, 2004). TLS has also been used

successfully to estimate standing timber volume, branch size, density and configuration, foliage density, and tree growth (Murphy, 2008; Maas *et al.*, 2008, Klemmt *et al.*, 2010; Bucksch and Fleck, 2011). Further, TLS enables the estimation of standing timber volume to be based on the full tree profile (rather than simply the traditional approximations of DBH and tree height) and allows bole size and taper to be predicted (Murphy, 2008; Maas *et al.*, 2008). For example, an Australian TLS system (Echidna®) has been used to accurately estimate LAI, DBH, and tree density in both native and plantation forests (Jupp *et al.*, 2009). Strahler *et al.* (2008) used Echidna® to retrieve a range of forest parameters including mean DBH, stand height, distance to tree, stocking, and foliage area in plantation and native forest stands in NSW. Results indicated that LAI from this TLS system matched favourably with ground-based estimates. Tree stems were clearly delineated, and diameters retrieved very accurately ($r^2=0.99$), with stand basal area and stocking (a practical index of density) being within 2% of field-measured estimates.

16.5.2 Individual trees

Both the growing availability of high spatial resolution imagery and increasing computing power have enabled greater focus on detecting and measuring individual trees as opposed to obtaining stand level statistics. For analysing individual tree crowns in forests, a general rule is that the image spatial resolution should be much greater than the crown size (that is, more than nine pixels per crown), such that an image spatial resolution ranging between 10 cm and 2 m is preferred (Gougeon and Leckie, 2001). A wide variety of tree crown detection and delineation algorithms have been developed in a range of forest types (Cabello-Leblic, 2018), some especially for Australian conditions (such as Culvenor, 2002; Bunting and Lucas, 2006; Held *et al.*, 2001), including wet and dry eucalypt, tropical, deciduous, and mixed species forests. Existing approaches for automated tree crown delineation and tree crown detection can be broadly categorised into four groups (Ke and Quackenbush, 2011):

- local maxima/minima—identifies crown locations based on brightness variations (Pinz, 1991; Walsworth and King, 1999);
- valley following—relies on shading patterns (Gougeon, 1995, 1999);
- region growing—segments the image assuming that treetops are brightest (Culvenor, 2002); and
- watershed segmentation (Serra, 1982; Ticehurst *et al.*, 2001).

Culvenor (2002) found region growing was most suited to crown delineation in pre-mature forest canopies where trees have a well-defined crown shape, noting that individual tree crown delineation from spaceborne EO imagery is not a realistic expectation (even via manual image interpretation) in structurally complex forests. Variations in viewing angle and Sun angle inhibited the ability to achieve repeatable results in multi-temporal imagery (see Volume 1B—Section 3). In a mixed species, dry eucalypt forest in Queensland, Bunting and Lucas (2006) found the accuracy of their approach, when compared to field data, to be ~70% (range 48–88%) for either individual trees, or groups of trees from the same species, having DBH greater than 10 cm, with reduced accuracies associated with dense stands containing several canopy layers.

Lidar-derived branching information, such as the number of branches per whorl (Klemmt *et al.*, 2010), can be used to simulate knot morphology (Duchateau *et al.*, 2013) or detailed tree architecture (Runions *et al.*, 2007; Côté *et al.*, 2009, 2011; Van der Zande *et al.*, 2011). In combination with tree models, such as L-systems (Prusinkiewicz and Hanan, 1990) and quantitative structure models (QSM, Calder *et al.*, 2015), individual trees can also be ‘reconstructed’ accurately (see Figure 16.4).

While many ground-based lidar studies have investigated deriving individual tree structure, the intricate differences between, and complementary features of, TLS and ALS datasets have also been researched (Hilker *et al.*, 2013). The combination of these two perspectives promises to be an effective and efficient tool for measuring the three-dimensional structure of individual trees (Dassot *et al.*, 2011). Given that ground-based measures (such as TLS) focus on the tree trunks whereas airborne data (such as ALS) mainly describe the top of the canopy, there are clear distinctions between TLS and ALS observations. Likewise, TLS data are less suitable for investigating stand structure over larger areas but provide a means for calibrating and validating ALS data, by enabling investigation of changes in the stem density and structure, and branching and understorey characteristics, as a function of overall stand structure. These relationships can then be used to model the relationship between below canopy architecture and the upper canopy light regime (Hilker *et al.*, 2010) and may ultimately allow an indirect retrieval of the complete canopy architecture from ALS measurements across the landscape.

Figure 16.4 TLS-derived tree structure

TLS data was collected for a tree (*Eucalyptus tricarpa*, 21 m tall, in Rushworth forest, Australia) using a RIEGL VZ-400 TLS. The Quantitative Structure Model (QSM) was generated following the procedure described by Calders *et al.* (2015).

a. Point cloud coloured by height b. QSM



Source: Newnham *et al.* (2015) Figure 3

An alternative approach to scaling up TLS-based attributes for individual trees to forest stands and landscapes has been demonstrated by Côté *et al.* (2012), who built three-dimensional libraries of individual trees and then distributed them across the landscape using L-systems approaches, enabling three-dimensional modelling of entire forest stands (Côté *et al.*, 2012).

16.5.3 Geometric-optical models

Spectral and spatial responses in EO data have also been related to forest variables by numerical models that account for the geometry of the tree structure at the time of the satellite overpass (see Volume 1X—Excursus 1.1). This modelling approach views each pixel as mixtures of four basic components: sunlit canopy, shaded canopy, sunlit background, and shaded background.

Strahler and Li (1981, 1984) modelled conifer trees as widely spaced cones and surmised that the different reflectances of forest pixels result from different mixtures of illuminated/shadowed background and illuminated/shadowed tree crowns within each ground pixel. This geometric-optical model was used to estimate tree density and height in sparse to moderately dense ponderosa pine plantations using Landsat MSS data, with the modelled results being within 10% of the ground-based measurements.

This approach was adapted to Australian forests (Jupp *et al.*, 1986; Walker *et al.*, 1986) and used to demonstrate how geometric-optical models could be interfaced with simple process-based models of vegetation function to predict changes in plant

responses to increasing woody weeds (Jupp and Walker, 1996; see Volume 2X—Excursus 1.1). Scarth and Phinn (2000) applied a similar approach to mixed eucalypt forests in Queensland using Landsat TM imagery and found that modelled estimates of crown cover, canopy size, and tree densities had significant agreement with ground validation, but structural successional stage showed less significant correlation. Others have used the approach to better understand patterns of tree density in EO imagery (Coops and Culvenor, 2000) and predict gap probability profiles (Lovell *et al.*, 2012; Haverd *et al.*, 2012).

Spectral mixture analysis (see Section 8.3 and Volume 2E) has also been used to determine the proportions of sunlit canopy and background, and shadowed canopy and background, within each EO pixel, with subsequent inversion based on geometric-optical modelling being used to derive stand structural attributes (Coggins *et al.*, 2013).

16.5.4 Biomass and fuel load

The importance of assessing forest biomass has been recognised both as an indicator for global climate change and to provide insights into the forest carbon storage (see Section 17; Richards and Brack, 2004). The use of passive optical data to map forest biomass has been well-established through the strong correlations of above ground biomass (AGB) with cover and LAI (see Sections 6.3.3 and 14), as well as with active remote sensing systems such as lidar (see Excursus 5.1). For example, using Landsat time series imagery Nguyen *et al.* (2020) developed a robust approach for monitoring forest biomass dynamics associated with forest disturbance and recovery, which allowed a single date conventional inventory to be extrapolated through time. Lidar has also been used for biomass assessment in regrowth Blackbutt forests on the NSW Central Coast, to estimate AGB components by segmenting canopy height data, which yielded results within 9% of the ground-based estimates (Turner, 2006).

The use of both spaceborne and airborne SAR is still an active area of research in Australia (Watt *et al.*, 2012; Richards, 2012). SAR is well-suited to the Australian environment since the majority of Australia's forested area is represented by woodlands, the biomass of which rarely exceeds 100 Mg/ha and is especially low in areas of regeneration (see Section 16.1). C-, L-, and P-band scattering intensity has been shown to saturate at biomass levels of approximately 20–40 Mg/ha, 60–100 Mg/ha, and 150 Mg/ha respectively (see Section 16.2). The biomass of most woodland areas should thus be quantifiable using, as a minimum, single-polarised L-band data, since most of the biomass is below

its threshold of saturation (Milne *et al.*, 2000). For example, at a long term study site in Queensland, Lucas *et al.* (2006) evaluated the use of multi-frequency, radar data for quantifying the AGB of open eucalypt forests and woodlands. Using NASA JPL AIRSAR (POLSAR) data, empirical relationships between AGB and SAR backscatter confirmed that C-, L-, and P-bands saturated at different levels and revealed both a greater strength in the relationship at higher incidence angles and a larger dynamic range and consistency of relationships at HV polarisations. The study concluded that L-band HV backscatter data acquired at incidence angles approaching or exceeding 45° were best suited to estimating the AGB up to the saturation level of 80–85 Mg/ha (Lucas *et al.*, 2006). The availability of P-band SAR data from the BIOMASS mission (see Section 16.2) is expected to provide more information about both tree trunks and the ground surface in forested landscapes.

Another ALS application involves providing spatial layers to forest fuel models, which traditionally have not used significant amounts of EO data due to an inability of spectral data to capture the structural complexity of closed canopies. In the USA, ALS has been used to predict crown bulk density, foliage biomass, and crown volume (Riaño *et al.*, 2003). The US Forest Service has also evaluated the capacity of ALS to predict crown bulk density, canopy base height, and crown fuel weight, demonstrating its effectiveness for characterising landscape level, fuel-related variables (Andersen *et al.*, 2005). Research under Australian conditions has found that, while it is difficult to distinguish surface and 'near surface' fuels using ALS data (Gould and Cruz, 2012), good correlations could be achieved between lidar-derived understorey attributes and elevated fuel load, fuel cover, and fuel volume (Brown *et al.*, 2011). Since understorey vegetation is an important fuel-ladder for crown fires in Australia, mapping of elevated fuel structure is valuable (Turner, 2007).

ALS data has also been used to assess fuels in the wildland-urban interface where wildfires present a significant risk to homes, life, and property. Management of this risk requires current and detailed knowledge of the spatial extent of wildland. ALS has been used to map wildland vegetation based on the combination of a vertically-stratified cover threshold and spatial morphology (Newnham *et al.*, 2012). Results indicated that the proportion of homes destroyed at the wildland-urban interface was greater than previously reported and that there was an exponential decline in the proportion of homes destroyed as a function of distance from wildland (see Section 18).

16.6 Forest Functionality

Plant physiological processes are highly dynamic and can vary over space and time as plants respond to rapidly changing environmental conditions. In the forestry context, plant functionality is closely related to forest health, and EO methods can provide early warning of disease, nutritional imbalance, moisture stress, or increasing predators. Current monitoring programs in Australia are integrating lidar and multispectral data sources to monitor forest biosecurity and manage forest health (NSW DPI, 2015).

Leaf biochemistry is closely related to leaf reflectance characteristics (see Sections 4, 8.1.1, and 9.6), allowing high spatial and spectral resolution imaging techniques to be used to infer information about the chemical composition of a vegetated canopy (Ollinger and Smith, 2005). These relationships only apply to photoactive molecules, such as pigments, and may be obscured by broad leaf water absorption. As detailed in Volume 1A—Section 13, spectrometers measure reflectance in specific, narrow, and often multiple, wavebands allowing imaging spectrometers to be used with ground-based, aerial, or spaceborne platforms for calibration and validation purposes to deliver consistent and contiguous measurements of the Earth's surface.

16.6.1 Plant nutrition

Forest nutrition assessments were amongst the earliest research projects conducted with the hyperspectral scanner, Hyperion, as part of calibration and validation for that instrument in Australia. Coops *et al.* (2003) demonstrated the use of Hyperion image data for mapping nutrient concentrations in *Eucalyptus* and *Pinus* species. These models initially focused on nitrogen but were also shown to be useful for mapping the concentration of additional macronutrients and micronutrients in a southern Australian *P. radiata* estate. Each of these nutrients plays an important role in the physiological functioning of plants and can influence the size and form of plantation trees (see Sections 4.2 and 5.3.5).

In a review of the use of EO technology to map nutrient status and fertiliser requirements in Australian plantations, Sims *et al.* (2013) discussed a number of operational considerations when using EO data. They mapped concentrations of 12 macronutrients and micronutrients in a Queensland exotic pine estate (*P. caribea* and *P. elliotii*) with comprehensive field data collection. They also considered many questions relating to model transferability between species and age classes, including the need for hyperspectral image data, detailed correction approaches, timing of image acquisition, complete sampling of the entire nutrient range in a forest stand, and the impact of stand age and canopy closure.

16.6.2 Plant stress

Factors that impact plant vigour and EO methods to detect stress are described in Sections 9.5 and 9.6. Thus far, the EO approaches that show the most promise for identifying and quantifying plant diseases have been thermography, chlorophyll fluorescence, and hyperspectral imaging (Mahlein *et al.*, 2012).

Various stress factors can induce leaf loss and discolouration (chlorosis and/or redness due to production of anthocyanins; see Excursus 4.1) and reduced leaf and crown sizes in eucalypts (Pook, 1985; Stone and Coops, 2004). Changes in leaf pigment concentrations impact foliar absorption of visible wavelengths, while changes in leaf and crown structure are most obvious in NIR reflectance (Asner, 1998; Gitelson *et al.*, 2002). A range of spectral indices has been developed for vegetation studies that highlight the relative changes in leaf reflectance of red and NIR wavelengths (see Section 8.1 above and Volume 2C). In particular, various vegetation indices have been proposed to identify and monitor stress in different eucalypt species. For example, Datt (1999) developed a series of chlorophyll indices suitable for eucalypt vegetation at both the leaf and stand level. Many of these indices were tested by Coops *et al.* (2002) using CASI-2 imagery, who found that the Datt (1999) indices correlated moderately well with relative leaf chlorophyll content for all dominant eucalypt species in the NSW study area and yielded slightly higher correlation for individual species.

In Australia, forest health has traditionally been surveyed by trained assessors using both ground-based and aerial observations (Carnegie, 2008; Carnegie *et al.*, 2008). Barry *et al.* (2008) used hand-held spectrometers to determine whether spectral analysis methods could detect changes in chlorophyll concentration resulting from stress. Three commercially important species of *Eucalyptus* were observed after defoliation (*E. globulus*) or exposure to cold and nutrient deprivation (*E. pilularis* and *E. grandis*). The resulting leaf loss in both *E. globulus* and *E. pilularis* was strongly correlated with two greenness indices (Modified Chlorophyll Absorption Ratio Index 2: MCARI2 and Modified Triangular Vegetation Index 2: MTVI2) as well as changes in the position and slope of the red edge, while leaf redness induced by stress in *E. grandis* and *E. pilularis* was strongly correlated with the Anthocyanin Reflectance Index (ARI) and the Red-Green Index (RGI; see Section 8.1 above). Stress-related changes in both chlorophyll concentration and leaf loss in *E. pilularis* were more noticeable than in *E. grandis*, possibly due to phenological factors (Stone *et al.*, 2005).

Chisholm (2006) investigated the use of hand-held spectra to assess both chlorophyll and moisture content of *E. camaldulensis* stands subject to a range of moisture stress regimes. Results indicated that moisture stress could be detected using high resolution spectral reflectance data at the leaf level and that the analysis was successful at identifying broad regions of the electromagnetic (EM) spectrum which could be used to discriminate different levels of stress.

In addition to chlorophyll and nitrogen, the past decade has seen advances towards estimation of other plant pigments as indicators of plant stress and light absorption. One of these pigments is xanthophyll, which is produced in a leaf during a process known

as photo-protection (see Section 4.2.3). Briefly, while plants can use most of the energy they absorb for photosynthesis, in strong illumination, the photochemical reaction tends to be limited by factors such as temperature, water, or nutrient availability. A change in the concentration of xanthophyll in foliage is indicative of Light Use Efficiency (LUE), which in turn is related to Gross Primary Productivity (GPP; see Section 7.4). Advances in estimation of LUE and GPP from spaceborne sensors have focused on imagery from MODIS or CHRIS-PROBA (Drolet *et al.*, 2008, Hilker *et al.*, 2009, 2011) in readiness for the European FLEX mission (Mohammed *et al.*, 2019), which will measure fluorescence from vegetation, a key attribute for GPP estimation (Coops *et al.*, 2011; see Section 17).

16.7 Forest Diversity

In addition to forest structure and function, the diversity of species within forest stands is often a critical piece of information both for forest management and biodiversity assessment. Species diversity, of course, relates to both flora (see Section 16.7.1) and fauna (see Section 16.7.2).

16.7.1 Floral diversity

In Australian conditions, the classification of native forest species is highly challenging (Shang and Chisholm, 2014; Kumar *et al.*, 2010). This is largely attributed to similarities in structural and chemical properties between species and the architecture of eucalypt leaves. These leaves are characteristically pendulous, forming a generally open canopy structure, so that the spectral reflectance obtained from EO imagery is strongly affected by the background.

Hyperspectral imagery is often viewed as necessary for discriminating the small spectral differences between species. For example, Lucas *et al.* (2008) produced tree species maps (including *Acacia*, *Angophora*, *Callitris*, and *Eucalyptus*) for central southeast Queensland using hyperspectral imagery acquired by CASI. Classification of the dominant species delivered the most accurate result (76%). The fusion of HyMap (airborne hyperspectral) spectra increased the accuracy for some species, principally due to the additional MIR (middle infrared) spectral wavebands. Shang and Chisholm (2014) assessed the potential of hyperspectral EO data to classify Australian forest species at the leaf, canopy and community levels in eastern NSW and obtained the most accurate classification result at the leaf level (94.7%), which reduced to 84% and 75% at the canopy and community levels respectively.

Rather than attempting to directly detect individual tree species, indirect mapping methods utilise environmental parameters and EO data to predict species distributions or associations with the aid of *a priori* knowledge (Coops *et al.*, 2008). Mackey *et al.* (2004) and Berry *et al.* (2007) developed an integrated index to track landscape productivity over the Australian continent using monthly observations of fAPAR during 2003. This index was used to assess how biomass is partitioned and made available as food and other habitat resources for fauna on the premise that, while some animal species reside within a single landscape region, many species are highly mobile, primarily in search of food and habitat. Mobile species often move large distances on a regular (mostly driven by seasonal changes) or irregular (dispersive or nomadic movement reflecting less predictable changes) basis (Gilmore *et al.*, 2007). Variations in mean annual, minimum, and seasonal patterns of fAPAR were related to vegetation production and seasonality, which in turn provided insights into species habitat and forage conditions for that year. The integrated index provided useful information about the structure and cover of Australian vegetation and demonstrated that vegetation-related habitat resource availability can readily be tracked through time using EO data and can be quantified in terms of carbon or energy assimilation over ecologically relevant timeframes (Berry *et al.*, 2007).

An alternative approach is that of Palmer *et al.* (2002), who proposed the spectral variation hypothesis whereby species richness can be inferred from the variations in the spectral characteristics of an EO image, that is, more unique spectra indicate greater species diversity. A number of studies have tested this approach by comparing field-based, species richness measures to image spectral heterogeneity using both multispectral and hyperspectral imagery (Rocchini *et al.*, 2004, 2007; White *et al.*, 2010).

Asner and Martin (2009) proposed a ‘spectranomics’ approach to forest biodiversity monitoring that can be used to link the chemistry, spectroscopy, taxonomy, and ecology of canopies. Initial work has been undertaken examining the leaf spectral and chemical properties of 162 canopy species in tropical forest sites in Queensland. They concluded that, within a site, leaf chemistry varied more strongly among species rather than along a climate gradient and did not aggregate well along genus or family levels, highlighting the spectral and species diversity and complexity in these stands (Asner *et al.*, 2009). This work has expanded into the Carnegie Spectranomics Project described by Asner and Martin (2016; see Excursus 16.1).

Excursus 16.1—Carnegie Spectranomics Project

Source: Asner and Martin (2016)

Spectranomics is an approach to conceptually and geographically link plant canopy species and their functional traits to their ‘spectral-optical’ properties. With the long term goal of advancing EO in the biodiversity science arena, the Carnegie Spectranomics Project has generated tree-of-life, or phylogenetically-based, connections between the spectral properties of plants and their canopy functional traits for more than 13,000 canopy tree and liana specimens in over 3 million tissue samples. This sample represents around 10,000 species, mostly tropical, and focuses on canopy species growing in full sunlight.

Canopy functional traits refer to a constellation of elemental and molecular properties, some of which support growth, such as nitrogen and photosynthetic pigments (which are functionally related), and others that provide defence, like polyphenols and lignin, which have evolved in plant canopy leaves (see Section 4.2). This chemical make-up of plant canopies, and its similarity and uniqueness among species, is called ‘chemical phylogeny’. These functional traits mediate leaf processes, whole plant function, and ecosystem dynamics, are often differentially formulated at the species level, and are an essential component of Spectranomics (see Figure 16.5a).

In this context, spectral properties of plant canopies describes the mostly invisible interactions between plant foliage and solar radiation. Between the EM wavelengths from ultraviolet to short wave infrared (350–3500 nm), this interaction is strongly determined by 21 or more chemicals (Asner *et al.*, 2011) that underpin plant evolution, and which power the biosphere. Chemometric studies determine how these chemicals relate to reflectance spectra, with methods ranging from traditional spectroscopic assays to new machine learning approaches (Feilhauer *et al.*, 2015; Serbin *et al.*, 2014; Wold *et al.*, 2001; see Figure 16.5b). Spectral properties also provide a tantalising pathway forward to scale up from leaves to landscapes (Ustin *et al.*, 2004) and to the planetary level (Jetz *et al.*, 2016; see Section 10.2), but only if we can accurately and repeatedly measure and interpret the spectra of plants over increasingly larger portions of Earth (see Figure 16.5c,d).

The Spectranomics database has become increasingly useful for quantitatively testing the relationships between plant phylogeny, canopy traits, and spectral properties at nested biographic scales, whether in tree communities, on mountains, or between continents. It has also transitioned to a forecasting tool to predict what can be remotely mapped and monitored using spectral EO instruments. These insights are feeding back to more focused field studies and improved EO sensor design (Asner *et al.*, 2012).

Figure 16.5 Spectranomics Database elements

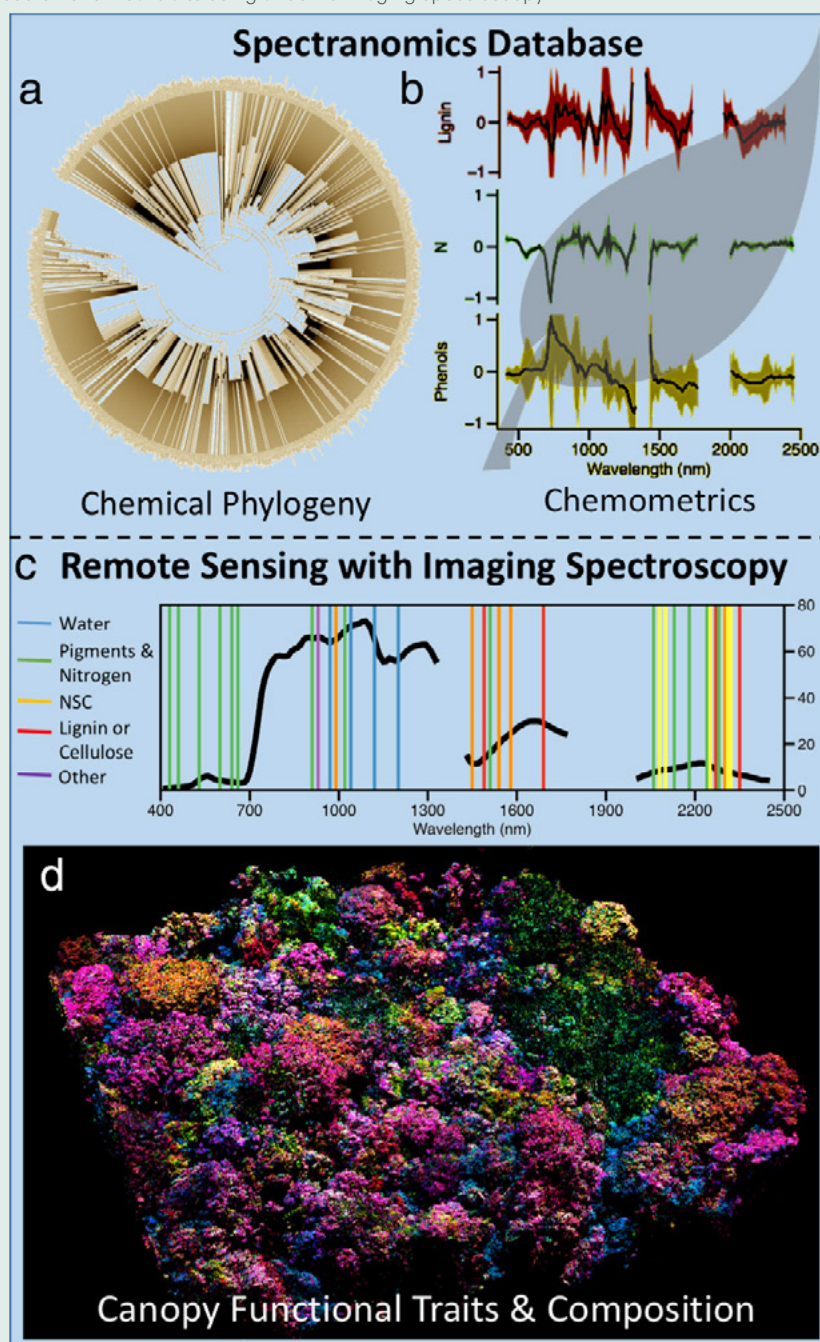
The essential interactive elements of the Spectranomics Database include phylogenetic, chemical, and spectral information on canopy species.

a. 21 foliar chemical traits are collected, organised and analysed phylogenetically, producing a tree-of-life based on the relatedness of functional trait signatures. This generic phylogeny shows the chemical relatedness of thousands of species in the Spectranomics Database.

b. Chemometric equations are derived to quantitatively relate canopy functional traits (chemicals) to spectral data. Example relationships are shown for foliar lignin, nitrogen (N), and polyphenols. The x-axis indicates spectral wavelength from 400–2500 nm; the y-axis indicates relative importance of the spectrum to each example chemical constituent.

c. An example remotely sensed canopy reflectance spectrum of one species is shown along with indicators of key chemical contributions to the spectrum (Curran, 1989; Kokaly *et al.*, 2009; Ustin *et al.*, 2009).

d. Oblique three-dimensional view of a one hectare portion of lowland Amazonian forest canopy. Different colors indicate different species detected based on chemical traits using airborne imaging spectroscopy.



Source: Asner and Martin (2016) Figure 1

16.7.2 Faunal monitoring

In Australian forestry conditions, Coops and Catling (1997) described how airborne video data, if correctly pre-processed, could be used to accurately predict the suitability of the forest for ground-dwelling fauna. They used habitat quality ratings to develop maps of habitat quality across the landscape. It was concluded that these spatial predictions could then be used to stratify the landscape into regions that would predict the distribution and abundance of some faunal groups. These predictions were then verified in the field, with actual species abundances being accurately predicted in over 70% of situations (Catling and Coops, 1999).

Using hyperspectral EO imagery, Youngentob *et al.* (2012) developed relationships between foliage nutritional quality and HyMap imagery acquired with 3.5 m pixels over native eucalypt and plantation forest in NSW. An integrated measure of foliage nutritional quality (available nitrogen) was related to the spectra using continuum removal and derivative analysis. Regression relationships were developed with a range of accuracies ($r^2=0.55-0.78$). The significant majority of spectral bands selected by the regression analysis related to known foliage pigments and nutrient absorption features. The results indicated the potential of hyperspectral imagery to be used to map variations in foliar constituents across forested landscapes. These types of spatial predictions can then be used to estimate the presence and abundance of folivores (herbivores that specialise in consuming leaves), such as the greater glider.

16.8 Forest Disturbance

Monitoring and quantifying forest disturbance is valuable for a range of forestry activities, including timber harvesting and reforestation. Forest changes can also result from natural disasters such as fire, windthrow, lightning, drought and floods. Other factors that can disturb forests include pollution, predators, and disease, all of which may be introduced by other anthropogenic activities (see Section 9.6). At a landscape scale, such disturbances change forest patterns, and those changes can be delineated in appropriate EO datasets (see Section 9.2).

EO provides an ideal basis to identify forest disturbance, and monitor forest regrowth (Kennedy *et al.*, 2010; Zhu *et al.*, 2012). Approaches which map and monitor landscape disturbance are highly scale-dependent however, both spatially and temporally (see Volume 2D). As such, the landscape patterns and processes that are discernible within any particular image source will be dependent on the target of interest—that is, individual trees or a whole stand—and the spatial, spectral, radiometric, and temporal characteristics of the image data (Turner, 1989; Perera and Euler, 2000; see Volume 1B—Section 1). Disturbances that are non-stand replacing and heterogeneous over the landscape, such as defoliation or partial harvesting, are generally more difficult to detect with EO data than larger and more spatially contiguous, stand-replacing disturbances, such as fire or land clearing (Coops *et al.*, 2006). Hislop *et al.* (2019) utilised Landsat time series data over a 29-year period to map abrupt disturbances in Victorian sclerophyll forests. Using an ensemble approach, they found an overall error rate of 7% and developed annual disturbance maps for 9 million ha of forest for this time period.

16.8.1 Insect damage

At a broad spatial scale, the high radiometric quality and frequent temporal resolution of MODIS can allow non-stand replacing disturbances, such as insect-induced tree mortality, to be detected. Verbesselt *et al.* (2009) used a MODIS time series (250 m; 16-day composite) to assess *Pinus radiata* plantation mortality in southern NSW (see Section 9.3). Results indicated that NDVI images were more effective for assessing tree mortality than the Enhanced Vegetation Index (EVI) or the Normalised Difference Infrared Index (NDII; see Section 8.1).

The more recent development of the Harmonised Landsat-Sentinel Data processing methodology is now allowing sub-weekly, global multispectral observations at 30 m resolution. This resource opens the way for finer scale insect damage assessments in the future (Claverie *et al.*, 2018; see Volume 2D—Section 10.2).

16.8.2 Fire monitoring

EO assessment of fire severity is one of the major success stories in disturbance observation (see Section 18). EO of burn extent has two major advantages over traditional methods of field assessment: cost-effectiveness and global coverage in remote areas. Most commonly, with spectral bands that are sensitive to fire disturbance and being freely available globally, Landsat TM/ETM+/OLI imagery is well-suited to the task of studying fire severity. As detailed in Section 18.5.1, extensive research has demonstrated that fire severity can be assessed using the:

- Normalised Burn Ratio (NBR)—normalised ratio of the NIR and SWIR spectral bands; and the
- Normalised Burn Ratio difference (dNBR; or Differenced NBR)—post-fire NBR is subtracted from a pre-fire NBR (Key and Benson, 2006; see Section 9.2.1).

dNBR has been shown to be particularly useful for forest and ecological research and land management projects as the index accounts for both pre- and post-fire conditions, making the overall approach more transferable across ecosystems (Kasischke *et al.*, 2008; Soverel *et al.*, 2011).

In Australia, Landsat imagery has been used for several decades to derive a more comprehensive understanding of fire histories (Russell-Smith *et al.*, 1997) and seasonality (see Figure 18.1). For example, Goodwin and Collett (2014) developed a new, fully automated approach to classifying burnt areas across Queensland based on different Landsat TM/ETM+ spectral combinations. In their approach time series imagery (rather than just a pair of images pre-and post-fire) is developed and the thermal, reflective and contextual characteristics of landscape patches are assessed through time. The results indicated an overall producer's accuracy of 85% and user's accuracy of 71% (see Volume 2E). Areas frequently misclassified were most often areas of cropping or inundated land, with variations in moisture and ground cover on dark soil. Other approaches to mapping fire severity and extent are detailed in Section 18.5.1.

If there were no Forestry in Australia, beyond mere fire-prevention, the benefits to the country would be incalculable. ... For complete fire-protection three measures are necessary:

1. Watch-towers and a good look-out.
2. Fire-paths.

3. Extra watchers during the fire season.

(David E. Hutchins, from 'A Discussion of Australian Forestry', 1916)

16.8.3 Environmental monitoring

EO datasets have also been used to monitor land use changes for various purposes (see Section 3.4). For example, Furby *et al.* (2008) describe the use of over 5,000 Landsat scenes to map land use changes associated with agriculture and forestry across Australia as part of the NCAS Land Cover Change Project. Dry season Landsat MSS, TM and ETM+ imagery was used to detect land cover change and discriminate between forest and non-forest cover from 1972 onwards. The program was then expanded to map a number of other land cover change attributes such as detection of new hardwood and softwood plantations, forest density classes, and sparse vegetation cover mapping.

The opening up of the complete Landsat archive (Wulder *et al.* 2012) has led to the development of many more monitoring approaches focusing on multi-temporal and pixel-based analyses of EO time series data (Kennedy *et al.*, 2010; see Volume 2D). These approaches move beyond scene-based analysis to compositing algorithms which select the best available pixel (BAP) from multiple images acquired within a pre-defined time interval (Roy *et al.*, 2010), thus allowing pixel level tracking of forest disturbance through time (Zhu *et al.*, 2012). Common to many of these approaches is the derivation of information from spectral changes in Landsat reflectance at a given location over time using what are broadly known as temporal trajectory methods (Hermosilla *et al.*, 2016; see Volume 2D—Section 9). For example, Lehmann *et al.* (2013) applied this type of approach to a Landsat time series for continental scale monitoring of disturbances within forested regions of Australia to produce the National Forest Trend (NFT), which identifies within-forest vegetation changes (disturbance and recovery) over time using imagery acquired from 1989 to 2006. By examining the spectral trajectory of a vegetation cover index, this approach can identify processes affecting forests that are of interest to ecologists and forest managers. Trend information along the trajectory, such as the slope curvature, is calculated to highlight areas of forest decline or recovery, which are critical for environmental reporting. Other EO-based monitoring approaches for forest vegetation, such as BFAST (Breaks for Additive Season and Trend) Monitor (Verbesselt *et al.*, 2012), are described in Volume 2D.

16.9 Further Information

Australian Forestry

State of the Forests Report (SOFR) 2018: <https://www.agriculture.gov.au/abares/forestsaustralia/sofr/sofr-2018>

Australia's forests at a glance 2019: with data to 2017–18. Australian Bureau of Agricultural and Resource Economics and Sciences, Canberra. <https://doi.org/10.25814/5dc8d577976b8>

Australia's forests webpage, ABARES website: <https://www.agriculture.gov.au/abares/forestsaustralia/australias-forests>

Department of Agriculture: <http://www.agriculture.gov.au/forestry>

Institute of Foresters Australia (IFA)—<http://www.forestry.org.au/>

National Forest Inventory (NFI)—<http://www.agriculture.gov.au/abares/forestsaustralia/australias-national-forest-inventory>

Statewide Landcover and Trees Study (SLATS)

SLATS Queensland: <https://www.qld.gov.au/environment/land/management/mapping/statewide-monitoring/slats>

SLATS NSW: <https://www.environment.nsw.gov.au/topics/animals-and-plants/native-vegetation/reports-and-resources>

16.10 References

Alam, M.M., Strandgard, M.N., Brown, M.W., and Fox, J.C. (2012). Improving the productivity of mechanised harvesting systems using remote sensing. *Australian Forestry*, 75(4), 238–245. doi:10.1080/00049158.2012.10676408

Andersen, H.E., McGaughey, R.J., and Reutebuch, S.E. (2005). Estimating forest canopy fuel parameters using lidar data. *Remote Sensing of Environment*, 94, 441–449.

Armston, J.D., Denham, R.J., Danaher, T.J., Scarth, P.F., and Moffiet, T.N. (2009). Prediction and validation of foliage projective cover from Landsat-5 TM and Landsat-7 ETM+ imagery. *Journal of Applied Remote Sensing*, 3(1), 033540. <https://doi.org/10.1117/1.3216031>

Asner, G.P. (1998). Biophysical and biochemical sources of variability in canopy reflectance. *Remote Sensing of Environment*, 64, 234–253.

Asner, G.P., and Martin, R.E. (2009). Airborne spectranomics: mapping canopy chemical and taxonomic diversity in tropical forests. *Frontiers in Ecology and the Environment*, 7, 269–276. <http://dx.doi.org/10.1890/070152>

Asner, G.P., and Martin, R.E. (2016). Spectranomics: Emerging science and conservation opportunities at the interface of biodiversity and remote sensing. *Global Ecology and Conservation*, 8, 212–219. <https://doi.org/10.1016/j.gecco.2016.09.010>

Asner, G.P., Martin, R.E., Ford, A.J., Metcalfe, D.J., and Liddell, M.J. (2009). Leaf chemical and spectral diversity in Australian tropical forests. *Ecological Applications*, 19, 236–253. <http://dx.doi.org/10.1890/08-0023.1>

Asner, G.P., Martin, R.E., Knapp, D.E., Tupayachi, R., Anderson, C., Carranza, L., Martinez, P., Houcheime, M., Sinca, F., Weiss, P. (2011). Spectroscopy of canopy chemicals in humid tropical forests. *Remote Sensing of Environment*, 115, 3587–3598.

Asner, G.P., Knapp, D.E., Boardman, J., Green, R.O., Kennedy-Bowdoin, T., Eastwood, M., Martin, R.E., Anderson, C., Field, C.B. (2012). Carnegie Airborne Observatory-2: Increasing science data dimensionality via high-fidelity multi-sensor fusion. *Remote Sensing of Environment*, 124, 454–465.

AUSLIG (Australian Land and Surveying Information Group) (1990). *Atlas of Australian Resources (3rd Series) Volume 6: Vegetation*. AUSMAP, Department of Administrative Services, Canberra. 64 p.

Barry, K.M., Stone, C., Mohammed, C.L. (2008). Crown-scale evaluation of spectral indices for defoliated and discoloured eucalypts. *International Journal of Remote Sensing*, 29, 47–69.

Bater, C., and Coops, N.C. (2009). Evaluating error associated with lidar-derived DEM interpolation under dense forest canopy. *Computers and Geoscience*, 35, 289–300.

Bennett, L. (2005). *Evaluating the cost effectiveness of various Lidar acquisition specifications on estimates of Dominant Tree Height in Tasmanian Eucalypt Plantations and Single Aged Regrowth*. GIS Project KGA 385, Centre for Spatial Information Science, School of Geography and Environmental Studies, University of Tasmania. 21 p.

- Berry, S., Mackey, B., and Brown, T. (2007). Potential applications of remotely sensed vegetation greenness to habitat analysis and the conservation of dispersive fauna. *Pacific Conservation Biology*, 13(2), 120–127.
- Bienert, A., Scheller, S., Keane, E., Mohan, F., and Nugent, C. (2007). Tree detection and diameter estimations by analysis of forest terrestrial laserscanner point clouds. *International Archives of Photogrammetry, Remote Sensing and Spatial Information Sciences*, Vol. XXXVI, Part 3/ W52.
- Brown, C., Scherl, T., Chylinski, T., and Burns, J. (2011). The use of LiDAR in fuel hazard characterisation and stratification within the Sugarloaf Catchment Area. *AFAC and Bushfire CRC Conference*, Sydney, NSW, 29 August–1 September, 2011.
- Bucksch, A., and Fleck, S. (2011). Automated Detection of Branch Dimensions in Woody Skeletons of Fruit Tree Canopies. *Photogrammetric Engineering and Remote Sensing*, 77(3), 229–240.
- Bunting, P., and Lucas, R. (2006). The delineation of tree crowns in Australian mixed species forests using hyperspectral Compact Airborne Spectrographic Imager (CASI) data. *Remote Sensing of Environment*, 101, 230–248.
- Cabello-Leblic, A. (2018). Tree Crown Delineation. Ch 11 in *Effective Field Calibration and Validation Practices: A practical handbook for calibration and validation satellite and model-derived terrestrial environmental variables for research and management*. A TERN Landscape Assessment Initiative, NCRIS. ISBN 978-0-646-94137-0.
- Calders, K., Newnham, G., Burt, A., Murphy, S., Raunonen, P., Herold, M., Culvenor, D., Avitabile, V., Disney, M., Armston, J., and Kaasalainen, M. (2015). Nondestructive estimates of above-ground biomass using terrestrial laser scanning. *Methods in Ecology and Evolution*, 6, 198–208. doi:10.1111/2041-210X.12301
- Carnegie, A.J. (2008). A decade of forest health surveillance in Australia: an overview. *Australian Forestry*, 71, 161–163.
- Carnegie, A., Eldridge, R., and Cante, R. (2008). Forest health surveillance in New South Wales, Australia. *Australian Forestry*, 71, 164–195.
- Catling, P.C., and Coops, N.C. (1999). Prediction of the distribution and abundance of small mammals in the eucalypt forests of south-eastern Australia from airborne videography. *Wildlife Research*, 26, 641–650.
- Chisholm, L.A. (2006). Detection of moisture stress in *Eucalyptus camaldulensis* using leaf-level spectral reflectance: implications for remote sensing. *International Journal of Geoinformatics*, 2(1), 79–92.
- Claverie, M., Ju, J., Masek, J.G., Dungan, J.L., Vermote, E.F., Roger, J.-C., Skakun, S.V., and Justice, C. (2018). The Harmonized Landsat and Sentinel-2 surface reflectance data set. *Remote Sensing of Environment*, 219, 145–161
- Coggins, S.B., Coops, N.C., Hilker, T., and Wulder, M.A. (2013). Augmenting forest inventory attributes with geometric optical modelling in support of regional susceptibility assessments to bark beetle infestations. *International Journal of Applied Earth Observation and Geoinformation*, 21, 444–452.
- Coops, N.C., and Catling, P.C. (1997). Predicting the complexity of habitat in forests from airborne videography for wildlife management. *International Journal of Remote Sensing*, 18(12), 2677–2686.
- Coops, N.C., and Culvenor, D. (2000). Utilizing local variance of simulated high-spatial resolution imagery to predict spatial pattern of forest stands. *Remote Sensing of Environment*, 71(3), 248–260.
- Coops, N.C., Stone, C., Culvenor, D.S., Chisholm, L., and Merton, R. (2002). Predicting Chlorophyll Content in Eucalypt Vegetation at the Leaf and Canopy Level using High Spectral Resolution Imagery. *Tree Physiology*, 23, 23–31.
- Coops, N.C., Smith, M., Martin, M.E., and Ollinger, S.V. (2003). Prediction of eucalypt foliage nitrogen content from satellite-derived hyperspectral data. *IEEE Transactions on Geoscience and Remote Sensing*, 41, 1338–1346.
- Coops N.C., White J.C., and Wulder, M.A. (2006). Identifying and describing forest disturbance and spatial pattern. In: *Understanding forest disturbance and spatial pattern: Remote sensing and GIS approaches*. (Eds: T. Wulder and S.E. Franklin). CRC Press, Taylor and Francis, Boca Raton. Pp 31-61.
- Coops, N., Hilker, T., Wulder, M., St-Onge, B., Siggins, A., Newnham, G., and Trofymow, J.A. (2007). Estimating Canopy Structure of Douglas-fir forest stands from discrete-return LIDAR. *Trees: Structure and Function*, 21(3), 295–310.
- Coops, N.C., Wulder, M.A., Duro, D.C., Han, T., and Berry, S. (2008). The development of a Canadian dynamic habitat index using multi-temporal satellite estimates of canopy light absorbance. *Ecological Indicators*, 8, 754–766.

- Coops, N.C., Nilker, T., Hall, F.G., Nichol, C.J., Drolet, G.G. (2011). Estimation of Light-use Efficiency of Terrestrial Ecosystem from Space: A Status Report. *Bioscience*, 60(10), 788–797.
- Côté, J.-F., Widlowski, J.-L., Fournier, R.A., and Verstraete, M.M. (2009). The structural and radiative consistency of three-dimensional tree reconstruction from terrestrial lidar. *Remote Sensing of Environment*, 113, 1067–1081.
- Côté, J.-F., Fournier, R.A., and Egli, R. (2011). An architectural model of trees to estimate forest structural attributes using terrestrial LiDAR. *Environmental Modelling and Software*, 26, 761–777.
- Côté, J.-F., Fournier, R.A., Frazer, G.W., and Niemann, K.O. (2012). A fine-scale architectural model of trees to enhance LiDAR-derived measurements of forest canopy structure. *Agricultural and Forest Meteorology*, 166–167, 72–85.
- Culvenor, D.S. (2002). TIDA: an algorithm for the delineation of tree crowns in high spatial resolution remotely sensed imagery. *Computers and Geoscience*, 28(1), 33–44.
- Curran, P.J. (1989). Remote sensing of foliar chemistry. *Remote Sensing of Environment*, 30, 271–278.
- Danson, F.M., Hetherington, D., Morsdorf, F., Koetz, B., and Allgower, B. (2007). Forest canopy gap fraction from terrestrial laser scanning. *IEEE Transactions on Geoscience and Remote Sensing Letters*, 4 (1), 157–160.
- Dassot M., Constant T., and Fournier M. (2011). The use of terrestrial LiDAR technology in forest science: application fields, benefits and challenges, *Annals of Forest Science*, 68, 959–974. <http://dx.doi.org/10.1007/s13595-011-0102-2>.
- Datt, B. (1999). A new reflectance index for remote sensing of chlorophyll content in higher plants: tests using *Eucalyptus* leaves. *Journal of Plant Physiology*, 154, 30–36.
- Douglas, E.S., Martel, J., Li, Z., Howe, G., Hewawasam, K., Marshall, R.A., Schaaf, C.L., Cook, T.A., Newnham, G.J., Strahler, A., and Chakrabarti, S. (2015). Finding leaves in the forest: the dual-wavelength Echidna lidar. *IEEE Geoscience and Remote Sensing Letters*, 12, 776–80.
- Drolet, G.G., Middleton, E.M., Huemmrich, K.F., Hall, F.G., Amiro, B.D., Barr, A.G., Black, T.A., McCaughey, J.H., and Margolis, H.A. (2008). Regional mapping of gross light-use efficiency using MODIS spectral indices. *Remote Sensing of Environment*, 112, 3064–3078.
- Du Toit, F., Coops, N.C., Tompalski, P., Goodbody, T.R.H., El-Kassaby, Y.A., Stoehr, M., Turner, D., and Lucieer, A. (2020). Characterizing variations in growth characteristics between Douglas-fir with different genetic gain levels using airborne laser scanning. *Trees*, 34, 649–664. <https://doi.org/10.1007/s00468-019-01946-y>
- Duchateau, E., Longuetaud, F., Mothe, F., Ung, C., Auty, D., and Achim, A. (2013). Modelling knot morphology as a function of external tree and branch attributes. *Canadian Journal of Forest Research*, 43(3), 266–277.
- Fedrigo, M., Newnham, G., Coops, N., Culvenor, D., Bolton, D., and Nitschke, C. (2018). Predicting temperate forest stand types using only structural profiles from discrete return airborne lidar. *ISPRS Journal of Photogrammetry and Remote Sensing*, 136(1) 106–119. <https://doi.org/10.1016/j.isprsjprs.2017.11.018>
- Feilhauer, H., Asner, G.P., and Martin, R.E. (2015). Multi-method ensemble selection of spectral bands related to leaf biochemistry. *Remote Sensing of Environment*, 164, 57–65.
- Fisher, A., Armston, J., Goodwin, N., and Scarth, P. (2020). Modelling canopy gap probability, foliage projective cover and crown projective cover from airborne lidar metrics in Australian forests and woodlands. *Remote Sensing of Environment*, 237, 111520. <https://doi.org/10.1016/j.rse.2019.111520>
- Florence, R.G. (1996). *Ecology and silviculture of eucalypts*. CSIRO Publishing, Melbourne, Australia.
- Furby, S.L., Caccetta, P.A., Wu, X., and Chia, J. (2008). Continental Scale Land Cover Change Monitoring in Australia using Landsat Imagery, *Proceedings of Studying, Modeling and Sense Making of Planet Earth*. 1-6 June 2008, Department of Geography, University of the Aegean, Mytilene, Lesvos, Greece.
- Gilmore, S., Mackey, B., and Berry, B. (2007). The extent of dispersive movement behaviour in Australian vertebrate animals, possible causes, and some implications for conservation. *Pacific Conservation Biology*, 19, 93–103.
- Gitelson, A.A., Kaufman, Y.J., Stark, R., and Rundquist, D. (2002). Novel algorithms for remote estimation of vegetation fraction. *Remote Sensing of Environment*, 80(1), 76–87.
- Goodwin, N.R., and Collett, L.J. (2014). Development of an automated method for mapping fire history captured in Landsat TM and ETM time series across Queensland, Australia. *Remote Sensing of Environment*, 148, 206–221. <http://dx.doi.org/10.1016/j.rse.2014.03.021>

- Gougeon, F.A. (1995). A crown-following approach to the automatic delineation of individual tree crowns in high spatial resolution aerial images. *Canadian Journal of Remote Sensing*, 21, 274–28.
- Gougeon, F.A. (1999). Automated individual tree crown delineation using a valley-following algorithm and rule-based system. *Proceedings of International forum: Automated interpretation of high spatial resolution digital imagery for forestry* (Eds: D.A. Hill and D.G. Leckie) February 10–12, 1998, Victoria, British Columbia. Natural Resources Canada, Canadian Forest Service, Pacific Forestry Centre, Victoria, BC. pp 11–23.
- Gougeon, F.A., and Leckie, D.G. (2001). Individual tree crown image analysis—a step towards precision forestry. *First International Precision Forestry Symposium*, Seattle, Washington, 17–20 June 2001.
- Gould, J., and Cruz, M. (2012). *Australian Fuel Classification: Stage II*. Ecosystem Sciences and Climate Adaptation Flagship. CSIRO, Canberra Australia.
- Gower, S.T., Kucharik, C.J., and Norman, J.M. (1999). Direct and Indirect Estimation of Leaf Area Index, fAPAR and Net Primary Production of Terrestrial Ecosystems, *Remote Sensing of Environment*, 70, 29–51.
- Haverd, V., Lovell, J.L., Cuntz, M., Jupp, D.L.B., Newnham, G.J., and Sea, W. (2012). The Canopy Semi-analytic P_{gap} And Radiative Transfer (CanSPART) model: Formulation and application. *Agricultural and Forest Meteorology*, 160, 14–35. doi:10.1016/j.agrformet.2012.01.018
- Haywood, A., and Stone, C. (2011). Semi-automating the stand delineation process in mapping natural eucalypt forests, *Australian Forestry*, 74(1), 13–22. doi:10.1080/00049158.2011.10676341
- Held, A., Ticehurst, C., Lymburner, L. (2001). Hyperspectral mapping of rainforests and mangroves, in: IGARSS 2001. Scanning the Present and Resolving the Future. *Proceedings of IEEE International Geoscience and Remote Sensing Symposium*. pp. 2787–2789.
- Henning, J.G., and Radtke, P.J. (2006). Ground-based laser imaging for assessing three-dimensional forest canopy structure. *Photogrammetric Engineering and Remote Sensing*, 72, 1349–1358.
- Hermosilla, T., Wulder, M.A., White, J.C., Coops, N.C., Hobart, G.W., and Campbell, L.B. (2016). Mass data processing of time series Landsat imagery: pixels to data products for forest monitoring. *International Journal of Digital Earth*, 9(11), 1035–1054. doi:10.1080/17538947.2016.1187673
- Hilker, T., Lyapustin, A., Hall, F.G., Wang, Y.J., Coops, N.C., Drolet, G., and Black, T.A. (2009). An assessment of photosynthetic light use efficiency from space: Modeling the atmospheric and directional impacts on PRI reflectance. *Remote Sensing of Environment*, 113, 2463–2475.
- Hilker, T.M., van Leeuwen, M., Coops, N.C., Wulder, M.A., Newnham, G., Culvenor, D.S., Jupp, D.L.B. (2010). Comparing canopy metrics derived from terrestrial and airborne laser scanning in a Douglas-fir dominated forest stand. *Trees: Structure and Function*, 24, 819–832. doi:10.1007/s00468-010-0452-7
- Hilker, T., Coops, N.C., Hall, F.G., Nichol, C.J., Lyapustin, A., Black, T.A., Wulder, M.A., Leuning, R., Barr, A., Hollinger, D.Y., Munger, B., and Tucker, C.J. (2011). Inferring terrestrial photosynthetic light use efficiency of temperate ecosystems from space. *Journal of Geophysical Research*, 116, G03014.
- Hilker, T., Frazer, G.W., Coops, N.C., Wulder, M.A., van Leeuwen, M., Newnham, G.J., Culvenor, D.S., and Stewart, J.D. (2013). Prediction of wood fiber attributes from LiDAR-derived forest canopy indicators. *Forest Science*, 59(2), 231–242. <http://dx.doi.org/10.5849/forsci.11-074>
- Hill, M.J., Senarath, U., Lee, A., Zeppel, M., Nightingale, J.M., Williams, R., and McVicar, T.R. (2006). Assessment of the MODIS LAI product for Australian ecosystems, *Remote Sensing of Environment*, 101, 495–518.
- Hislop, S., Jones, S., Soto-Berelev, M., Skidmore, A., Haywood, A., and Nguyen, T. (2019). A fusion approach to forest disturbance mapping using time-series ensemble techniques. *Remote Sensing of Environment*, 221, 188–197.
- Hopkinson, C., Chasmer, L., Young-Pow, C., and Treitz, P. (2004). Assessing forest metrics with a ground-based scanning lidar. *Canadian Journal of Forest Research*, 34, 573–583. <http://dx.doi.org/10.1139/x03-225>.
- Hyypä, J., Yu, X., Hyypä, H., Vastaranta, M., Holopainen, M., Kukko, A., Kaartinen, H., Jaakkola, A., Vaaja, M., Koskinen, J., and Alho P. (2012). Advances in forest inventory using airborne laser scanning. *Remote Sensing*, 4, 1190–1207. <http://dx.doi.org/10.3390/rs4051190>.
- IFA (2008). *Silviculture in Australia's Native Forests*. Institute of Foresters of Australia Policy Statement 2.9, IFA. http://www.forestry.org.au/pdf/pdf-public/policies/Statement%20%201%20%20-%20Silviculture%20in%20Native%20Forests%20Approved%2007-08-08_%20-%20Web%20%209_.pdf

- Jafari, R., and Lewis, M.M. (2012). Arid land characterisation with EO-1 Hyperion hyperspectral data. *International Journal of Applied Earth Observation and Geoinformation*, 19, 298–307.
- Jetz, W., Cavender-Bares, J., Pavlick, R., Schimel, D., Davis, F.W., Asner, G.P., Guralnick, R., Kattge, J., Latimer, A.M., Moorcroft, P. (2016). Monitoring plant functional diversity from space. *Nature Plants*, 2(3), [16024]. <https://doi.org/10.1038/NPLANTS.2016.24>
- Jupp, D.L.B., and Lovell, J.L. (2007). Airborne and ground-based lidar systems for forest measurement: background and principles. *CSIRO Marine and Atmospheric Research Paper 17*. 151 p.
- Jupp, D.L.B., and Walker, J. (1996). Detecting structural and growth changes in woodlands and forests: the challenge for remote sensing and the role of geometric optical modelling. In: *The Use of Remote Sensing in the Modeling of Forest Productivity at Scales from the Stand to the Globe*. (Eds: Gholz, H.L., Nakane, K., and Shimoda, H.). Kluwer Academic Publishers, Dordrecht.
- Jupp, D.L.B., Walker, J., and Penridge, L.K. (1986). Interpretation of vegetation structure in Landsat MSS imagery: a case study in disturbed semi-arid eucalypt woodland. Part 2. Model based analysis. *Journal of Environmental Management*, 23, 35–57.
- Jupp, D.L.B., Culvenor, D.S., Lovell, J.L., Newnham, G.J., Strahler, A.H., and Woodcock, C.E. (2009). Estimating forest LAI profiles and structural parameters using a ground-based laser called 'Echidna®'. *Tree Physiology*, 29(2), 171–181.
- Kasischke, E.S., Turetsky, M.R., Ottmar, R.D., French, N.H.F., Shetler, G., Hoy, E., and Kane, E.S. (2008). Evaluation of the Composite Burn Index for Assessing Fire Severity in Black Spruce Forests. *International Journal of Wildland Fire*, 17(4), 515–526.
- Ke, Y., and Quackenbush, L.J.L. (2011). A review of methods for automatic individual tree-crown detection and delineation from passive remote sensing. *International Journal of Remote Sensing*, 32, 4725–4747.
- Kennedy, R.E., Yang, Z., and Cohen, W.B. (2010). Detecting trends in forest disturbance and recovery using yearly Landsat Time Series: 1. LandTrendr—Temporal segmentation algorithms. *Remote Sensing of Environment*, 114, 2897–2910.
- Key, C.H., and Benson, N.C. (2006). *Landscape Assessment: Sampling and Analysis Methods*. USDA Forest Service, Rocky Mountain Research Station General Technical Report RMRS-GTR-164-CD. Ogden, UT.
- Klemmt, H.-J., Seifert, T., Seifert, S., Kunneke, A., Wessels, B., and Pretzsch, H. (2010). Assessment of branchiness in a *Pinus pinaster* plantation by terrestrial laser scanner data as a link between exterior and interior wood properties. *Proceedings SilviLaser 2010*. 14–17 September, 2010. Freiburg. pp 253–264.
- Kokaly, R.F., Asner, G.P., Ollinger, S.V., Martin, M.E., Wessman, C.A. (2009). Characterizing canopy biochemistry from imaging spectroscopy and its application to ecosystem studies. *Remote Sensing of Environment*, 113, S78–S91.
- Kumar, L., Skidmore, A.K., and Mutanga, O. (2010). Leaf level experiments to discriminate between *Eucalyptus* species using high spectral resolution reflectance data: use of derivatives, ratios and vegetation indices. *Geocarto International*, 25, 327–344. doi:10.1080/10106040903505996
- Lee, A., Lucas, R., and Brack, C. (2004). Quantifying vertical forest stand structure using small footprint LiDAR to assess potential stand dynamics. *International Archives of Photogrammetry, Remote Sensing and Spatial Information Science*, XXXVI-8/W2, 213–217.
- Lee, A., and Lucas, R.M. (2007). A LiDAR-derived canopy density model for tree stem and crown mapping in Australian woodlands. *Remote Sensing of Environment*, 111, 493–518.
- Lees, B.G., and Ritman, K. (1991). Decision-tree and rule-induction approach to integration of remotely sensed and GIS data in mapping vegetation in disturbed or hilly environments. *Environmental Management*, 15, 823–831.
- Lehmann, E.A., Wallace, J.F., Caccetta, P.A., Furby, S.L., and Zdunic, K. (2013). Forest cover trends from time series Landsat data for the Australian continent. *International Journal of Applied Earth Observation and Geoinformation*, 21, 453–462.
- Lim, K., Treitz, P., Wulder, M., St-Onge, B., and Flood, M. (2003). LiDAR remote sensing of forest structure. *Progress in Physical Geography*, 27, 88–106.
- Lovell, J.L., Jupp, D.L.B., Culvenor, D.S., and Coops, N.C. (2003). Using airborne and ground-based ranging LIDAR to measure canopy structure in Australian forests. *Canadian Journal of Remote Sensing*, 29(5), 607–622.
- Lovell, J.L., Haverd, V., Jupp, D.L.B., and Newnham, G.J. (2012). The Canopy Semi-analytic P_{gap} And Radiative Transfer (CanSPART) model: Validation using ground based lidar. *Agricultural and Forest Meteorology*, 158–159, 1–12. doi:10.1016/j.agrformet.2012.01.020

- Lucas, R.M., Cronin, N., Lee, A., Moghaddam, M., Witte, C., and Tickle, P. (2006). Empirical relationships between AIRSAR backscatter and LiDAR-derived forest biomass, Queensland, Australia, *Remote Sensing of Environment*, 100, 407–425
- Lucas, R., Bunting, P., Paterson, M., and Chisholm, L. (2008). Classification of Australian forest communities using aerial photography, CASI and HyMap data, *Remote Sensing of Environment*, 112(5), 2088–2103. <http://dx.doi.org/10.1016/j.rse.2007.10.011>.
- Maas, H.G., Bienert, A., Scheller, S., and Keane, E. (2008). Automatic forest inventory parameter determination from terrestrial laser scanner data. *International Journal of Remote Sensing*, 29, 1579–1593.
- Mackey, B.G., Bryan, J., and Randall, L. (2004). Australia's Dynamic Habitat Template 2003. *Proceedings of MODIS Vegetation Workshop II*, University of Montana.
- Mahlein, A.K., Oerke, E.C., Steiner, U., and Dehne, H.W. (2012). Recent advances in sensing plant diseases for precision crop protection. *European Journal of Plant Pathology*, 133(1), 197–209. doi:10.1007/s10658-011-9878-z
- Markus, T., Neumann, T., Martino, A., Abdalati, W., Brunt, K., Csatho, B., Farrell, S., Fricker, H., Gardner, A., Harding, D., Jasinski, M., Kwok, R., Magruder, D., Lubin, D., Luthcke, S., Morison, J., Nelson, R., Neuenschawander, A., Palm, S., Popescu, S., Shum, C.K., Schutz, B.E., Smith, B., Yang, Y., Jasinski, M. (2017). The Ice, Cloud, and land Elevation Satellite-2 (ICESat-2): science requirements, concept, and implementation. *Remote Sensing of Environment*, 190, 260–273. <https://doi.org/10.1016/j.rse.2016.12.029>
- Mellor, A., Haywood, A., Stone, C., and Jones, S. (2013). The Performance of Random Forests in an Operational Setting for Large Area Sclerophyll Forest Classification. *Remote Sensing*, 5(6), 2838–2856. <https://doi.org/10.3390/rs5062838>
- Milne, T. (2000). Forest and Woodland Biomass and Classification using Airborne and Spaceborne Radar Data. *International Archives of Photogrammetry and Remote Sensing*, Vol. XXXIII, Part B7. Amsterdam 2000.
- Mitchell, A.L., Rosenqvist, A., and Mora, B. (2017). Current remote sensing approaches to monitoring forest degradation in support of countries measurement, reporting and verification (MRV) systems for REDD+. *Carbon Balance and Management*, 12(1), 9. <https://doi.org/10.1186/s13021-017-0078-9>
- Mohammed, G.H., Colombo, R., Middleton, E.M., Rascher, U., van der Tol, C., Nedbal, L., Goulas, Y., Pérez-Priego, O., Damm, A., Meroni, M., Joiner, J., Cogliati, S., Verhoef, W., Malenovský, Z., Gastellu-Etchegorry, J.-P., Miller, J.R., Guanter, L., Moreno, J., Moya, I., Berry, J.A., Frankenberg, C., Zarco-Tejada, P.J. (2019). Remote sensing of solar-induced chlorophyll fluorescence (SIF) in vegetation: 50 years of progress. *Remote sensing of environment*, 231, 111177. <https://doi.org/10.1016/j.rse.2019.04.030>
- Murphy, G. (2008). Determining Stand Value and Log Product Yields Using Terrestrial Lidar and Optimal Bucking: A Case Study. *Journal of Forestry*, 106(6), 317–324.
- Murphy, P.N.C., Ogilvie, J., Meng, F.-R., White, B., Bhatti, J.S., and Arp, P.A. (2011). Modelling and mapping topographic variations in forest soils at high resolution: A case study. *Ecological Modelling*, 222(14), 2314–2132.
- Næsset, E. (2002). Predicting forest stand characteristics with airborne scanning laser using a practical two-stage procedure and field data. *Remote Sensing of Environment*, 80(1), 88–99.
- Newnham, G.J., Siggins, A.S., Bianchi, R.M., Culvenor, D.S., Leonard, J.E., and Mashford, J.S. (2012). Exploiting three dimensional vegetation structure to map wildland extent. *Remote Sensing of Environment*, 123, 155–162.
- Newnham, G.J., Armston, J.D., Calders, K., Disney, M.I., Lovell, J.L., Schaaf, C.B., Strahler, A.H., and Danson, F.M. (2015). Terrestrial Laser Scanning for Plot-Scale Forest Measurement. *Current Forestry Reports*, 1, 239–251. doi:10.1007/s40725-015-0025-5
- Nguyen, T.H., Jones, S.D., Soto-Berelov, M., Haywood, A., and Hislop, S. (2020). Monitoring aboveground forest biomass dynamics over three decades using Landsat time-series and single-date inventory data. *International Journal of Applied Earth Observation and Geoinformation*, 84, 101952. <https://doi.org/10.1016/j.jag.2019.101952>
- NSW DPI (2015). *Forest Biosecurity and Resource Assessment*. <http://www.dpi.nsw.gov.au/research/areas/fhr>
- O'Hara, K.L., Latham, P.A., Hessburg, P., and Smith, B.G. (1996). A structural classification for inland northwest forest vegetation. *Western Journal of Applied Forestry*, 11(3), 97–102.
- Ollinger, S.V., and Smith, M.L. (2005). Net Primary Production and Canopy Nitrogen in a temperate forest landscape: an analysis using imaging spectrometry, modeling and field data. *Ecosystems*, 8, 760–778.

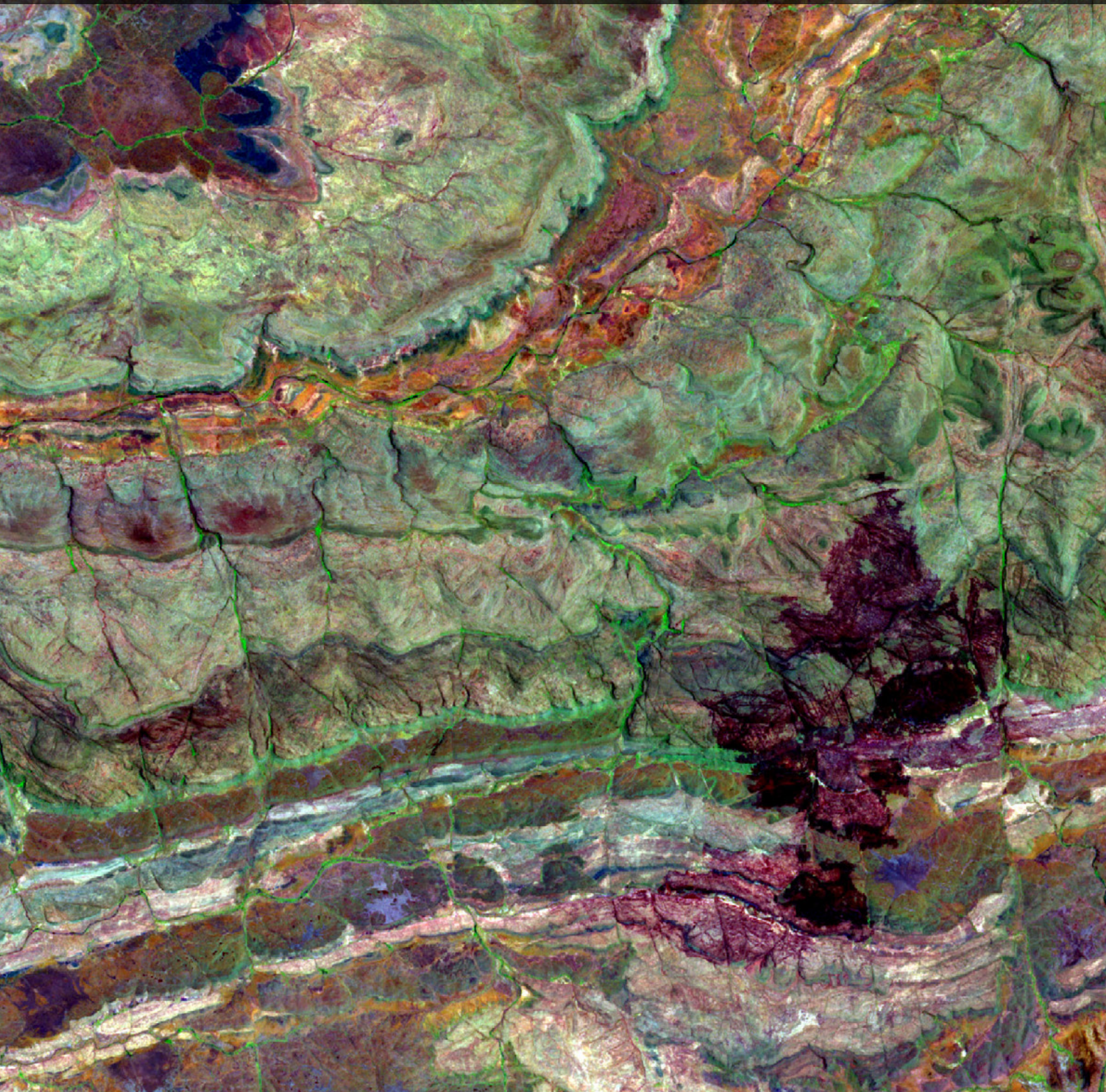
- Packalen, P., and Maltamo, M. (2008). Estimating Species-Specific Diameter Distributions and Saw Log Recoveries of Boreal Forests from Airborne Laser Scanning Data and Aerial Photographs: A Distribution-Based Approach. *Canadian Journal of Forest Research*, 38, 1750–1760.
- Palmer, M.W., Earls, P.G., Hoagland, B.W., White, P.S., and Wohlgemuth, T. (2002). Quantitative tools for perfecting species lists. *Environmetrics*, 13, 121–137.
- Perera, A.H., and Euler, D.L. (2000). Landscape ecology in forest management: An introduction. In: *Ecology of a Managed Terrestrial Landscape: Patterns and Processes of Forest Landscapes in Ontario*. (Eds: A.H. Perera, D.L. Euler and I. D. Thompson). Ontario Ministry of Natural Resources/ UBC Press, Vancouver, BC. pp. 3–11.
- Pickett-Heaps, C.A., Canadell, J.G., Briggs, P.R., Gobron, N., Haverd, V., Paget, M.J., Pinty, B., and Raupach, M.R. (2014). Evaluation of six satellite-derived Fraction of Absorbed Photosynthetic Active Radiation (FAPAR) products across the Australian continent. *Remote Sensing of Environment*, 140, 241–256.
- Pinz, A.J. (1991). A computer vision system for the recognition of trees in aerial photographs. NASA, Goddard Space Flight Center, *Multisource Data Integration in Remote Sensing* pp. 111–124. (SEE N91-1561507-43).
- Pokharel, B., Dech, J.P., Groot, A., and Pitt, D. (2014). Ecosite-based predictive modeling of black spruce (*Picea mariana*) wood quality attributes in boreal Ontario. *Canadian Journal of Forest Research*, 475, 465–475.
- Pook, E.W. (1985). Canopy dynamics of *Eucalyptus maculata* Hook. 3. Effects of drought. *Australian Journal of Botany*, 33, 65–79.
- Prusinkiewicz, P., and Hanan, J. (1990). Visualization of botanical structures and processes using parametric L-systems. In: *Scientific Visualization and Graphics Simulation* (Ed: D. Thaimann) pp. 183–201. John Wiley and Sons.
- Pyne, S.J. (1992). *The Burning Bush: A Fire History of Australia*. Allen and Unwin, Sydney. 520 p. ISBN: 1863731946
- Reutebuch, S., Andersen, H., and McGaughey, R. (2005). Light Detection and Ranging (LIDAR): An emerging tool for multiple resource inventory. *Journal of Forestry*, 103(6), 286–292.
- Riaño, D., Meier, E., Allgower, B., Chuvieco, E., and Ustin, S.L. (2003). Modeling airborne laser scanning data for the spatial generation of critical forest parameters in fire behavior modeling. *Remote Sensing of Environment*, 86, 177–186.
- Richards, J. (2012). *Australia and SAR: A Road Map*. CRCSI, Melbourne.
- Richards, G.P., and Brack, C. (2004). A continental biomass stock and stock change estimation approach for Australia. *Australian Forestry*, 67(4), 284–288. doi:10.1080/00049158.2004.10674948
- Rocchini, D., Chiarucci, A., and Loiselle, S.A. (2004). Testing the spectral variation hypothesis by using satellite multispectral images. *Acta Oecologica*, 26, 117–120.
- Rocchini, D., Ricotta, C., and Chiarucci, A. (2007). Using satellite imagery to assess plant species richness: The role of multispectral systems. *Applied Vegetation Science*, 10, 325–331.
- Roy, D.P., Ju, J., Kline, K., Scaramuzza, P.L., Kovalsky, V., Hansen, M., Loveland, T.R., Vermote, E., and Zhang, C. (2010). Web-enabled Landsat Data (WELD): Landsat ETM+ composited mosaics of the conterminous United States. *Remote Sensing of Environment*, 114, 35–49.
- Runions, A., Lane, B., and Prusinkiewicz, P. (2007). Modeling Trees with a Space Colonization Algorithm. *Proceedings of Eurographics Workshop on Natural Phenomena* (Eds: D. Ebert, and S. Mérillou). <http://www.algorithmicbotany.org/papers/colonization.egwnp2007.pdf>
- Russell-Smith, J., Ryan, P.G., and Durieu, R. (1997). A Landsat MSS-derived fire history of Kakadu National Park. *Journal of Applied Ecology*, 34, 748–766.
- Scarth, P., and Phinn, S. R. (2000). Determining forest structural attributes using an inverted geometric-optical model in mixed eucalypt forests, Southeast Queensland, Australia. *Remote Sensing of Environment*, 71 (2), 141–157. doi:10.1016/S0034-4257(99)00066-8
- Sea, W.B., Choler, P., Beringer, J., Weinmann, R.A., Hutley, L.B., and Leuning, R. (2011). Documenting improvement in leaf area index estimates from MODIS using hemispherical photos for Australian savannas. *Agricultural and Forest Meteorology*, 151, 1453–1461.
- Serbin, S.P., Singh, A., McNeil, B.E., Kingdon, C.C., Townsend, P.A. (2014). Spectroscopic determination of leaf morphological and biochemical traits for northern temperate and boreal tree species. *Ecological Applications*, 24, 1651–1669.
- Serra, J. (1982). *Image Analysis and Mathematical Morphology*. Academic Press, London, New York.

- Shang, X., and Chisholm, L.A. (2014). Classification of Australian Native Forest Species Using Hyperspectral Remote Sensing and Machine-Learning Classification Algorithms. *IEEE Journal of Selected Topics in Applied Earth Observations and Remote Sensing*, 7(6), 2481–2489.
- Sims, N.C., Culvenor, D.S., Newnham, G., Nicholas C. Coops, N.C., and Hopmans, P. (2013). Towards the Operational Use of Satellite Hyperspectral Image Data for Mapping Nutrient Status and Fertilizer Requirements in Australian Plantation Forests. *IEEE Journal of Selected Topics in Applied Earth Observations and Remote Sensing*, 6(2), 320–328.
- Skidmore, A.K. (1989). Unsupervised training area selection in forests using a non-parametric distance measure and spatial information. *International Journal of Remote Sensing*, 10, 133–146.
- Skidmore, A.K., and Turner, B.J. (1988). Forest mapping accuracies are improved using a supervised nonparametric classifier with SPOT data. *Photogrammetric Engineering and Remote Sensing*, 54, 1415–1421.
- Skidmore, A.K., Wood, G.B., and Shepherd, K.R. (1987). Remotely sensed digital data in forestry: a review, *Australian Forestry*, 50(1), 40–53. doi:10.1080/00049158.1987.10674493
- Smith, R.B., and Woodgate, P.W. (1985). Appraisal of fire damage and inventory for timber salvage by remote sensing in mountain ash forests in Victoria. *Australian Forestry*, 48, 252–263.
- SOFR (2018). Australia's State of the Forests Report 2018. Montreal Process Implementation Group for Australia and National Forest Inventory Steering Committee 2018, ABARES, Canberra. <https://www.agriculture.gov.au/abares/forestsaustralia/sofr/sofr-2018>
- Soverel, N.O., Coops, N.C., Perrakis, D.B., Daniels, L., and Gergel, S. (2011). The transferability of a dNBR derived model to predict burn severity across ten wildland fires in Western Canada. *International Journal of Wildland Fire*, 20, 1–14.
- Staudhammer, C.L., and LeMay, V.M. (2001). Introduction and evaluation of possible indices of stand structural diversity. *Canadian Journal of Forest Research*, 31(7), 1105–1115.
- Stone, C., and Coops, N.C. (2004). Assessment and monitoring of damage from insects in Australian eucalypt forests and commercial plantations. *Australian Journal of Entomology*, 43, 283–292.
- Stone, C., Chisholm, L., and McDonald, S. (2005). Effects of leaf age and psyllid damage on the spectral reflectance properties of *Eucalyptus saligna* foliage. *Australian Journal of Botany*, 53, 45–54.
- Stone, C., Turner, R., and Verbesselt, J. (2008). Integrating plantation health surveillance and wood resource inventory systems using remote sensing, *Australian Forestry*, 71(3), 245–253. doi:10.1080/00049158.2008.10675043
- Strahler, A.H., and Li, X. (1981). An invertible coniferous forest canopy reflectance model. *Proceedings of 15th International Symposium on Remote Sensing of the Environment*, Ann Arbor, Michigan, May, 1981. pp. 1237–1243.
- Strahler, A.H., and Li, X. (1984). Spatial/spectral modeling of conifer forest reflectance, *Proc. Third Australasian Remote Sensing Conference*, Queensland, Australia. pp. 88–90.
- Strahler, A.H., Jupp, D.L.B., Woodcock, C.E., Schaaf, C.B. Yao, T., Zhao, F., Yang, X., Lovell, J., Culvenor, D., Newnham, G., Ni-Miester, W., and Boykin-Morris, W. (2008). Retrieval of forest structural parameters using a ground-based lidar instrument (Echidna). *Canadian Journal of Remote Sensing*, 34, Supplement 2, S426–S440.
- Tansey, K., Selmes, N., Anstee, A., Tate, N.J., and Denniss, A. (2009). Estimating tree and stand variables in a Corsican Pine woodland from terrestrial laser scanner data. *International Journal of Remote Sensing*, 30, 5195–5209.
- TERN Australia (2018). *Effective Field Calibration and Validation Practices: A practical handbook for calibration and validation satellite and model-derived terrestrial environmental variables for research and management*. A TERN Landscape Assessment Initiative, NCRIS. ISBN 978-0-646-94137-0. <https://www.tern.org.au/NEW-CalVal-handbook-for-remote-sensing-bgp4370.html>
- Thies, M., Pfeifer, N., Winterhalder, D., and Gorte, B.G.H. (2004). Three-dimensional reconstruction of stems for assessment of taper, sweep and lean based on laser scanning of standing trees. *Scandinavian Journal of Forest Research*, 19, 571–581.
- Ticehurst, C., Lymburner, L., and Held, A. (2001). Mapping tree crowns using hyperspectral and high spatial resolution imagery. In: *Third International Conference on Geospatial Information in Agriculture and Forestry*. Denver, Colorado.

- Tickle, P.K., Witte, C., Lee, A., Lucas, R.M., Jones, K., and Austin, J. (2001). The use of airborne scanning LIDAR and large scale photography within a strategic forest inventory and monitoring framework. *Proceedings of IEEE International Geoscience and Remote Sensing Symposium. IGARSS 2001*, 9–13 July 2001, Sydney, Australia. IEEE Inc. Piscataway, N.J.
- Turner, M. (1989). Landscape Ecology: The Effect of Pattern on Process. *Annual Review of Ecology and Systematics*, 20, 171–197.
- Turner, R. (2006). *An airborne lidar canopy segmentation approach for estimating above-ground biomass in Coastal Eucalypt forests*. PhD thesis. School of Biological, Earth and Environmental Sciences. UNSW, Sydney.
- Turner, R. (2007). An overview of Airborne LIDAR applications in New South Wales state forests. *ANZIF Conference*, Coffs Harbour, June 2007.
- Ustin, S.L., Roberts, D.A., Gamon, J.A., Asner, G.P., Green, R.O. (2004). Using imaging spectroscopy to study ecosystem processes and properties. *BioScience*, 54, 523–534.
- Ustin, S.L., Gitelson, A.A., Jacquemoud, S., Schaepman, M., Asner, G.P., Gamon, J.A., Zarco-Tejada, P. (2009). Retrieval of foliar information about plant pigment systems from high resolution spectroscopy. *Remote Sensing of Environment*, 113, S67–S77.
- Van der Zande, D., Stuckens, J., Verstraeten, W.W., Mereu, S., Muys, B., and Coppin, P. (2011). 3D modeling of light interception in heterogeneous forest canopies using ground-based LiDAR measurements. *International Journal of Applied Earth Observation*, 13, 792–800, doi:10.1016/j.jag.2011.05.005.
- Verbesselt, J., Robinson, A., Stone, C., and Culvenor, D. (2009). Forecasting tree mortality using change metrics derived from MODIS satellite data. *Forest Ecology and Management*, 258, 1166–1173.
- Verbesselt, J., Zeileis, A., and Herold, M. (2012). Near real-time disturbance detection using satellite image time series. *Remote Sensing of Environment*, 123, 98–108. <https://doi.org/10.1016/j.rse.2012.02.022>
- Walker, J., Jupp, D.L.B., Penridge, L.K., and Tian, G. (1986). Interpretation of vegetation structure in Landsat MSS imagery: a case study in disturbed semi-arid eucalypt woodlands. Part 1. Field data analysis. *Journal of Environmental Management*, 23, 19–33.
- Wallace, L., Lucieer, A., Watson, C., and Turner, D. (2012a). Development of a UAV-LiDAR System with Application to Forest Inventory. *Remote Sensing*, 4(6), 1519–1543. doi:10.3390/rs4061519
- Wallace, L., Lucieer, A., and Watson, C.S. (2012b). Assessing the feasibility of UAV-based LiDAR for high resolution forest change detection. *Proceedings of ISPRS Congress*, 25 August–1 September 2012, Melbourne. ISPRS International Archives of the Photogrammetry, Remote Sensing and Spatial Information Sciences XXXIX-B7, pp. 499–504. http://www.terraluma.net/downloads/Wallace_ISPRS2012.pdf
- Walsworth, N., and King, D. (1999). Image modelling of forest changes associated with acid mine drainage. *Computers and Geoscience*, 25(5), 567–580.
- Watt, M., Milne, T., Williams, M., and Mitchell, A. (2012). *Robust Imaging from Space: Satellite SAR (Synthetic Aperture Radar)*. CRCSI. <http://www.crcsi.com.au/library/resource/robust-imaging-from-space>
- Weller, D., Denham, R., Witte, C., Mackie, C., and Smith, D. (2003). Assessment and monitoring of foliage projected cover and canopy height across native vegetation in Queensland, Australia, using laser profiler. *Canadian Journal of Remote Sensing*, 29, 578–591.
- White, J.C., Gómez, C., Wulder, M.A., and Coops, N.C. (2010). Characterizing temperate forest structural and spectral diversity with Hyperion EO-1 data. *Remote Sensing of Environment*, 114, 1576–1589.
- White, J.C., Wulder, M.A., Varhola, A., Vastaranta, M., Coops, N.C., Cook, B.D., Pitt, D., and Woods, M. (2013). *A best practices guide for generating forest inventory attributes from airborne laser scanning data using an area-based approach*. Natural Resources Canada, Canadian Forest Service, Canadian Wood Fibre Centre, Victoria, BC. Information Report FI-X-010.
- White, J.C., Coops, N.C., Wulder, M.A., Vastaranta, M., Hilker, T., and Tompalski, P. (2016). Remote Sensing Technologies for Enhancing Forest Inventories: A Review. *Canadian Journal of Remote Sensing*, 42(5), 619–641.
- Wold, S., Sjostrom, M., Eriksson, L. (2001). PLS-regression: a basic tool of chemometrics. *Chemometrics and Intelligent Laboratory Systems*, 58, 109–130.
- Woodgate, P., and Black, P. (1988). *Forest cover changes in Victoria: 1869–1987*. Dept. of Conservation Forests and Lands, Melbourne.

- Wulder, M.A., Bater, C.W., Coops, N.C., Hilker, T., White, J.C. (2008). The role of lidar in sustainable forest management. *The Forestry Chronicle*, 84(6), 807–826.
- Wulder, M.A., Masek, J.G., Cohen, W.B., Loveland, T.R., and Woodcock, C.E. (2012). Opening the archive: How free data has enabled the science and monitoring promise of Landsat. *Remote Sensing of Environment*, 122, 2–10.
- Yagüe, J., and Garcia, P. (2006). A remote sensing survey of vegetation communities adjacent to Myall Lakes, NSW, Australia. *Global developments in environmental earth observation from space. Proceedings of 25th EARSeL Symposium*. Porto, Portugal, 2005. pp 355–365.
- Youngentob, K.N., Renzullo, L.J., Held, A.A., Jia, X., Lindenmayer, D.B., and Foley, W.J. (2012). Using imaging spectroscopy to estimate integrated measures of foliage nutritional quality. *Methods in Ecology and Evolution*, 3, 416–26. doi:10.1111/j.2041-210X.2011.00149.x
- Zheng, G., and Moskal, L.M. (2009). Retrieving leaf area index (LAI) using remote sensing: Theory, method, and sensors. *Sensors*, 9(4), 2719–2745.
- Zhu, Z., Woodcock, C.E., and Olofsson, P. (2012). Continuous monitoring of forest disturbance using all available Landsat imagery. *Remote Sensing of Environment*, 122, 75–91.

Observing Carbon Dynamics



The carbon cycle is introduced in Volume 1A—Section 4.2.4 and Excursus 1.2 above. The following sections consider the use of EO to map and monitor the Australian landscape in two areas that are relevant to carbon studies:

- carbon cycling (see Section 17); and
- fire (see Section 18).

Contents

17 Carbon Cycling	353
18 Fire	389



17 Carbon Cycling

Alfredo Huete

Carbon is the foundation and primary energy source of all life on Earth—from the food that sustains us to the fossil fuels that drives the global economy. Carbon, as an important greenhouse gas, is intertwined with the Earth's climate by helping to regulate the Earth's temperature. Human activities such as the burning of fossil fuels, and land use and land cover modifications, are greatly raising the amounts of carbon dioxide (CO₂) in the atmosphere with associated impacts on global temperatures and climate.

The carbon cycle describes the flow and storage of carbon among the land, ocean, and atmosphere carbon reservoirs (see Figure 17.1, Excursus 1.2 above, and Volume 1A—Section 4.2.4). Most of the carbon is stored in geologic rocks and sediments, including fossil carbon, while the rest is present in the ocean, atmosphere, land, and living organisms. The carbon cycle functions across a wide range of timescales and includes:

- a relatively 'slow' carbon cycle—geologic processes, such as the weathering of rocks, soil formation, sedimentation, and deep ocean storage of carbon; and
- a more active, 'fast' carbon cycle—biologic processes absorb CO₂ from the atmosphere to sustain life and release CO₂ when organisms die, and in the ocean, there are also chemical exchanges of carbon between surface waters and the atmosphere (see Excursus 1.1).

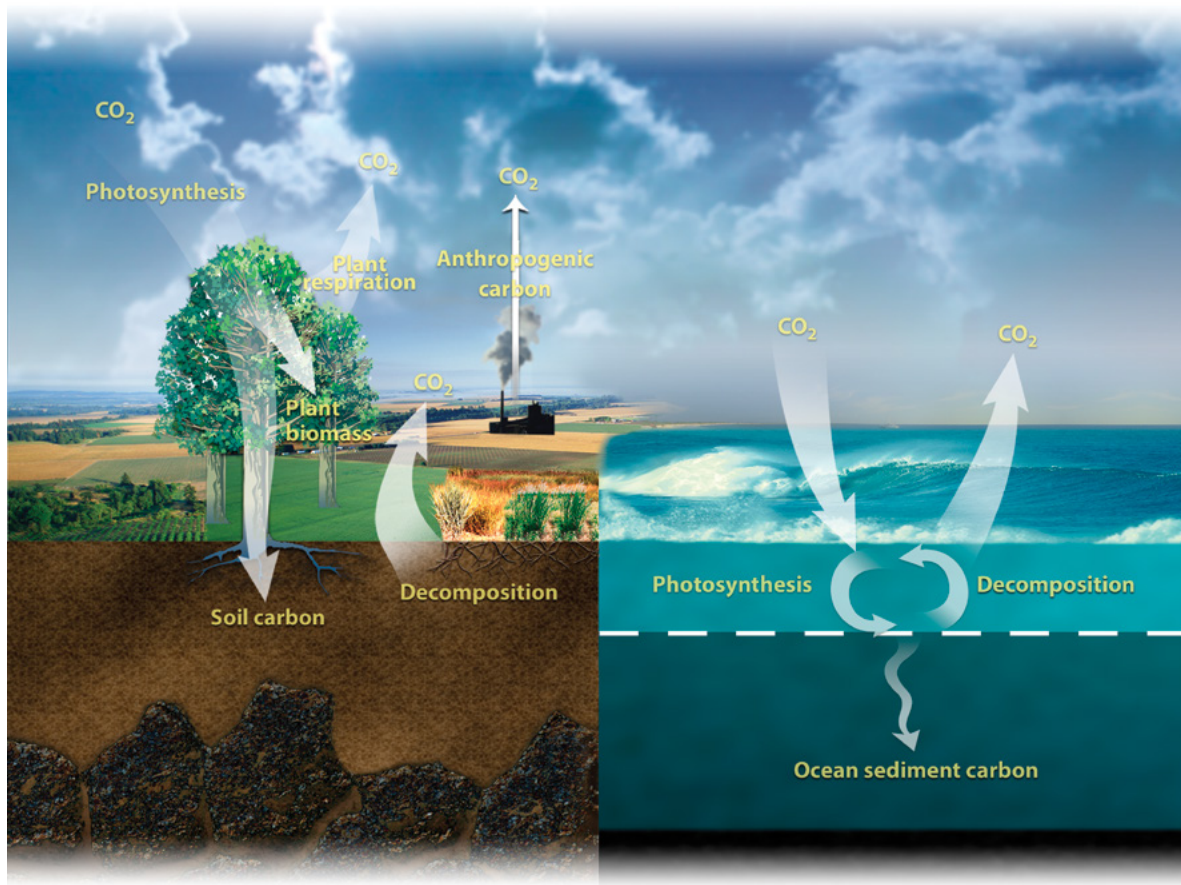
Accurate estimates of carbon pools and fluxes in the biosphere are necessary for quantifying carbon balances across space and time, and at regional to global scales, but are quite challenging to accomplish (Schimel, 1995; Baldocchi *et al.*, 2001). The determination of productivity across diverse landscapes is traditionally carried out in various, often inconsistent ways, that include field and plot scale biomass measurements, plant harvests, micrometeorological flux measurements, EO, and empirical and process-based models that may involve field, micrometeorological, and EO data inputs (see Excursus 17.2).

We cannot hope to either understand or to manage the carbon in the atmosphere unless we understand and manage the trees and the soil too.
(Freeman Dyson)

Background image: Major bushfires in southeastern Australia photographed on 18 January 2003 from the International Space Station. Winds direct smoke plumes eastward off the Australian coast, north of Cape Howe, near the NSW/Victoria border. The agricultural valleys of the Murrumbidgee and Murray Rivers give way to the burning, darker bush areas of the mountains, with the extreme eastern coastline of Victoria visible on the right of this image. **Source:** NASA-JSC. (Retrieved from https://eol.jsc.nasa.gov/Collections/EarthObservatory/articles/Australian_Bushfires.htm)

Recommended Chapter Citation: Huete, A.R. (2021). Carbon Cycling. Ch 17 in *Earth Observation: Data, Processing and Applications. Volume 3A—Terrestrial Vegetation*. CRCIS, Melbourne. pp. 353–388.

Figure 17.1 The carbon cycle between land, atmosphere, and oceans



Source: NASA

Carbon is the currency of life. The rapid formation of carbon-rich topsoil is the greatest priority and opportunity of our time.
(Rattan Lal)

Excursus 17.1—The Carbon Cycle

Source: Alfredo Huete, University of Technology, Sydney

The carbon cycle—the flow and storage of carbon among the land, ocean, and atmosphere carbon reservoirs—is introduced in Excursus 1.2 above (see also Volume 1A—Section 4.2.4) and illustrated in Figure 17.1.

Carbon Reservoirs (Pools)

Carbon reservoirs refer to the major storage areas of carbon on the Earth, distributed among land, ocean, and atmosphere (see Figure 17.1). Global quantities of these carbon reservoirs are uncertain. Most of

Earth's carbon (estimated at 65,500 Pg, where 1 Pg=1 billion metric tons) is stored in rocks, while the rest is present in the ocean, atmosphere, land surface (vegetation, soil), and fossil fuels, and include:

- atmosphere carbon—as CO₂ and CH₄, carbon gases is estimated at 800 Gt;
- ocean carbon—in the surface ocean (1,000 Gt), deep ocean (37,000 Gt), and reactive sediments (6,000 Gt); and
- terrestrial carbon—as plant biomass (550 Gt), soil (2,300 Gt), and fossil carbon (10,000 Gt).

Slow Carbon Cycle

The slow carbon cycle occurs at geologic timescales (> 1 million years), in which processes of rock weathering, soil formation, and sedimentation of carbonates in oceans move carbon among rocks, soil, ocean, and atmosphere. On average, 0.01–0.10 Pg of carbon move through the slow carbon cycle every year. Carbon moves from the atmosphere to the lithosphere (rocks) as carbonic acid in rainfall. The acid dissolves rocks and initiates the process of chemical weathering, which, along with physical weathering, contributes to soil formation. Chemical weathering releases calcium and other nutrients, which may be transported to the ocean and combine with bicarbonate ions to form calcium carbonate.

In the oceans, calcium carbonate shells from marine organisms, such as corals and plankton produce layers of calcium carbonate that sink to the seafloor, which over time, are cemented together and turn to rock, storing the carbon in limestone, and other carbon-containing rocks. Organic carbon may also be embedded in layers of mud which, under heat and pressure, compress the mud and carbon over millions of years to form sedimentary rock such as shale. In special cases, when dead plant matter builds up faster than it can decay, layers of organic carbon become oil, coal, or natural gas instead of sedimentary rock like shale.

Over time, carbon eventually returns to the atmosphere through volcanoes. At the ocean surface, CO₂ gas dissolves in and ventilates out of the ocean in a steady exchange with the atmosphere. Once in the ocean, the CO₂ gas reacts with water to make the ocean more acidic, and reacts with carbonate from rock weathering to produce bicarbonate ions.

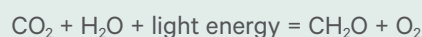
This complex and integrated carbon cycle system maintains a balance among the land-atmosphere-ocean carbon pools that prevents excessive carbon accumulation in the atmosphere or excessive carbon stored in rocks. For example, increases in CO₂ in the atmosphere from volcanic activity, will lead to rising temperatures which will result in more rainfall that increases the weathering of rocks, that will eventually deposit more carbon on the ocean floor. This rebalances the slow carbon cycle through chemical weathering over a period of a few hundred thousand years. This buffering of carbon behaves as a thermostat and helps to maintain the quantity of CO₂ in the atmosphere and keep the Earth's temperature relatively stable. As Earth's climate is intimately tied to atmospheric concentrations of carbon (CO₂ and CH₄), an understanding of the carbon cycle is essential for dealing with current climate change problems, as well as modelling and predicting Earth's future carbon-climate system.

Fast Carbon Cycle

The fast carbon cycle operates at diurnal, annual and decadal timescales, where carbon is exchanged between the land, ocean, and the atmosphere, through the relatively fast processes of photosynthesis and respiration (autotrophic and heterotrophic), fire, and land use and land cover change. Plants, marine biota, soil microbes, and human activities are the main components of the fast carbon cycle and 10–100 Gt of carbon move through this cycle every year through land and ocean uptake of atmosphere CO₂ through photosynthesis, CO₂ diffusion into the ocean, and the release of CO₂ in respiration, decomposition, fire, and air-sea gas exchange.

Photosynthesis

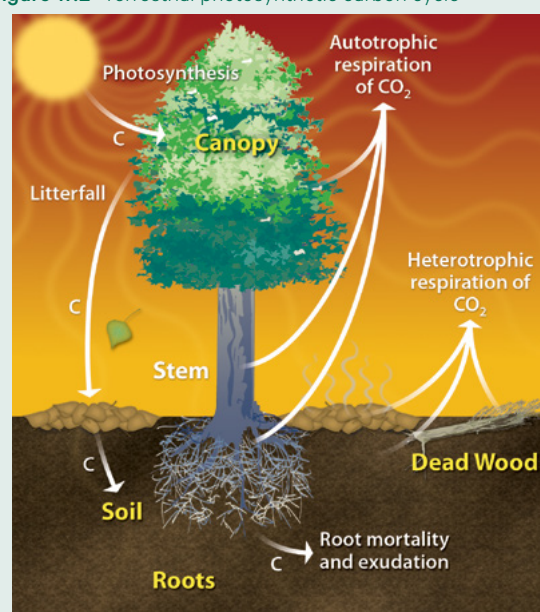
In the process of photosynthesis, plants absorb CO₂ from the atmosphere and use sunlight to combine it with water to form sugar molecules (CH₂O) and oxygen (O₂; see Figure 17.2 and Section 5.2.1). The chemical reaction is:



The organic compounds produced by plants are assimilated for building plant structures (leaves, stems, wood branches, trunks, and roots) and stored in biomass.

The rate of carbon fixation by the biosphere, or total organic carbon produced per unit of time and over a defined area is termed gross primary productivity (GPP; see Section 7.4). GPP is the basis for food, fibre, and wood production, and has important implications for human welfare. It is the largest carbon flux between the terrestrial biosphere and the atmosphere and is a key measure of ecosystem metabolism.

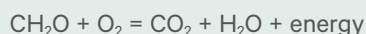
Figure 17.2 Terrestrial photosynthetic carbon cycle



Source: <https://public.ornl.gov/site/gallery/>

Respiration

Part of the carbon fixed in photosynthesis by plants is returned to the atmosphere through the process of respiration (autotrophic respiration; see Section 5.2.2). The energy content of the organic carbon molecules is an excellent source of energy for all living things. Oxygen combines with sugar to release water, CO₂ and energy. The basic chemical reaction is:



There are various mechanisms by which the biosphere-fixed organic carbon molecules return to the atmosphere, but all involve the same chemical reaction. Plants and phytoplankton may break down the sugar to get the energy they need to grow (autotrophic respiration). The plants or phytoplankton may also be consumed by higher organisms, along food chains, and break down the plant sugar to get energy (heterotrophic respiration).

Growing season carbon processes

At seasonal to annual timescales, plants and phytoplankton may die and decay at the end of the growing season, and carbon moves from plants and animals to the atmosphere and soils through microbial decomposition and heterotrophic respiration. Litterfall, plant materials that fall to the ground (leaves, branches, flowers, and fruits), contributes to the buildup of the soil carbon pool. The size of the soil organic carbon pool will be a function of carbon inputs from litterfall, root exudation, and mortality, and the release of carbon during decomposition (Wang *et al.*, 2018; Gray *et al.*, 2015). Fire may also consume plants and stored carbon and release it into the atmosphere (see Section 18).

The fast carbon cycle is tightly coupled between the atmosphere and biosphere, as can be seen by CO₂ fluctuations in the atmosphere with the changing seasons. When the large land masses of the Northern Hemisphere green up during spring and summer, atmospheric CO₂ decreases as carbon is removed from the atmosphere in the process of photosynthesis. This cycle peaks in August, with about 2 ppm of CO₂ drawn out of the atmosphere. In the autumn and winter, many plants senesce and decay with GPP declining while decomposition and heterotrophic respiration increase, thus returning CO₂ back to the atmosphere.

Resource Constraints

Productivity is generally limited by spatially and temporally varying resource constraints (e.g. nutrients, light, water, and temperature; Field *et al.*, 1995; Churkina and Running 1998; Nemani *et al.*, 2003). GPP and microbial respiration will thus be limited by water availability in arid regions and by cold temperatures at very high latitudes and elevations. This results in spatially distributed high biomass, carbon rich ecosystems as well as low biomass areas (e.g. deserts) with low carbon contents over the planet in response to climatic, geologic (nutrient), and topographic variations. The same occurs in the oceans in which primary productivity varies along coastlines and areas of warm and cool ocean currents (see Volume 3B).

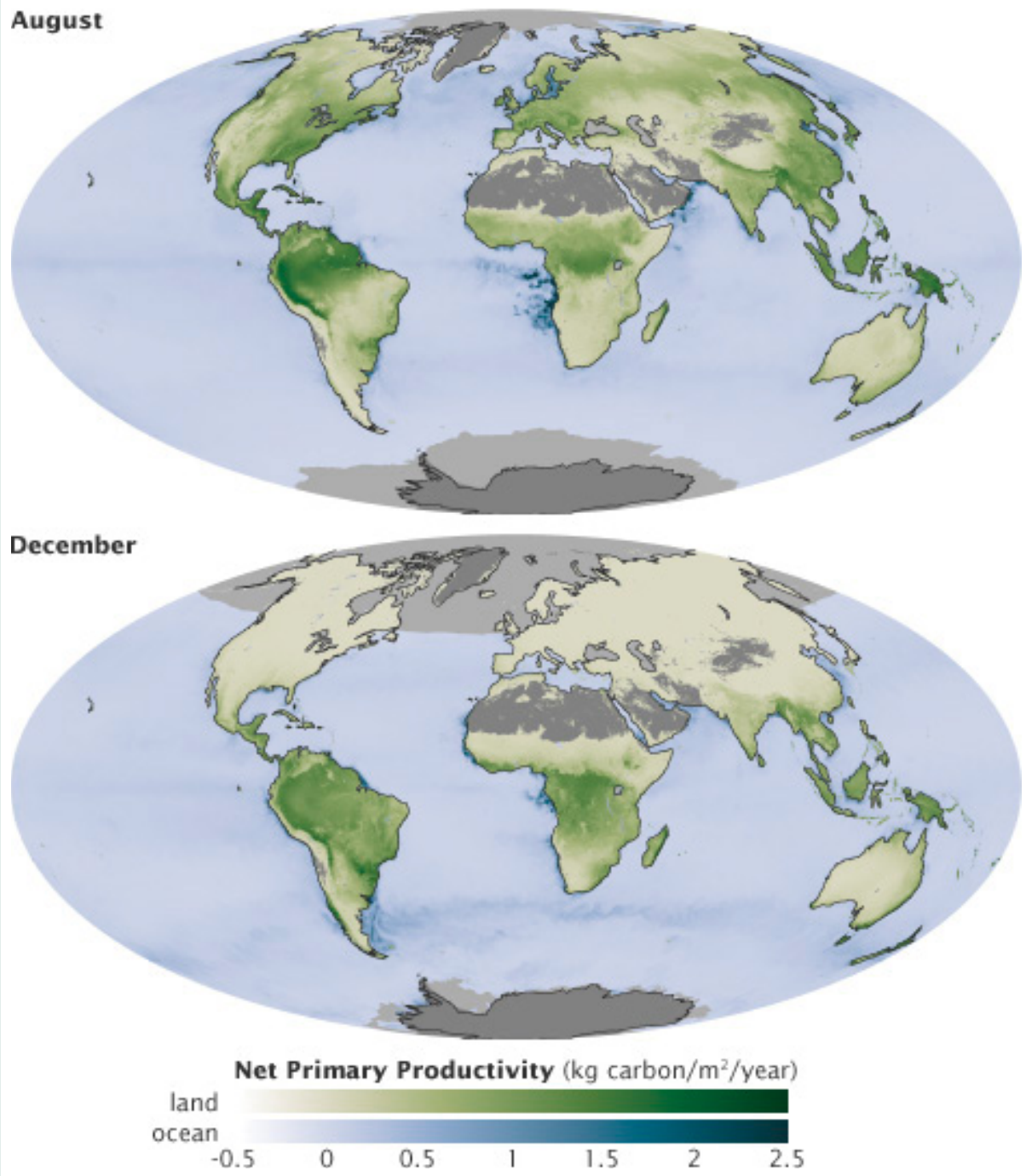
Photosynthesis or primary production is essentially an integrator of resource availability, and according to the resource optimisation theory (Field *et al.*, 1995), ecological processes tend to adjust plant characteristics over time periods of weeks or months to match the capacity of the environment to support photosynthesis and maximise growth.

Productivity terms

The net balance between photosynthesis and respiration is defined as net productivity of an area and determines whether an area is source or a sink of CO₂ to the atmosphere (see Section 7.4). Productivity forms the basis of biosphere functioning and carbon, energy, and water budgets. There are various ways to express productivity, including:

- Net primary productivity (NPP), defined as the difference between GPP, or photosynthesis, and autotrophic respiration. Terrestrial net primary productivity (NPP) is the amount of carbon fixed by plants and accumulated as biomass (Cramer *et al.*, 1999).
- Net ecosystem productivity (NEP) is defined as GPP minus ecosystem respiration (ER), which is the sum of autotrophic and heterotrophic respiration. This includes photosynthesis by plants and respiration from soils, and plants, including litter.
- Net biome productivity (NBP) is defined as the overall net ecosystem carbon balance, and includes other processes such as deforestation, harvest, and fire that lead to the loss of, and changes in, carbon.

Figure 17.3 Seasonal variations in photosynthesis (GPP) between hemispheres



Source: NASA Earth Observatory <https://earthobservatory.nasa.gov/features/CarbonCycle/page3.php>

Excursus 17.2—Measuring Biosphere Productivity

Source: Alfredo Huete, University of Technology, Sydney

In Situ Methods

In situ measures of carbon stocks and productivity involve sampling methods that will vary with biome type, and can include tree inventories, litter traps, grassland forage estimates, destructive sampling, cropland harvests, and market statistics. Field inventory plots and plot networks have been established for carbon monitoring of forests at the national scale (FAO, 2007). The plots enable direct carbon measurements and systematic data collection of forest information over small areas of forest, and although they can be difficult to maintain, they provide valuable *in situ* information on carbon stocks over time (Chambers *et al.*, 2009).

Established long term experimental plots further enable cross-site production comparisons. Plot level methods generally measure above ground net primary production (ANPP), from which gross primary production (GPP) can be estimated by correcting for respiratory losses (Field *et al.*, 1995). Agricultural yield statistics combined with maps of cropland areas provide large scale ANPP estimates from local to national level census statistics (Monfreda *et al.*, 2008; Guanter *et al.*, 2014). These methods are amenable to many uncertainties due to differences in site-based procedures, and in some cases, inconsistent sampling methods over time at a given site (Moran *et al.*, 2014). For example, established procedures for biomass clipping of grass sampling plots can vary in timing from either the peak of the growing season or the end of the growing season (see Moran *et al.*, 2014).

Eddy covariance flux towers

A global network of over 500 micrometeorological tower sites, known as FLUXNET (see Excursus 7.2), provide continuous measurements of carbon and water flux exchanges between ecosystems and the atmosphere (Baldocchi, 2001). The eddy covariance method is used to directly measure fluxes at a spatial scale of hundreds of metres, by computing the covariance between the vertical velocity and target scalar mixing ratios at each tower site. The carbon gas flux measured is the net amount resulting from autotrophic and soil heterotrophic respiration and photosynthesis, and is termed net ecosystem exchange production (NEE):

$$\text{NEE} = \text{GPP} + \text{Respiration}$$

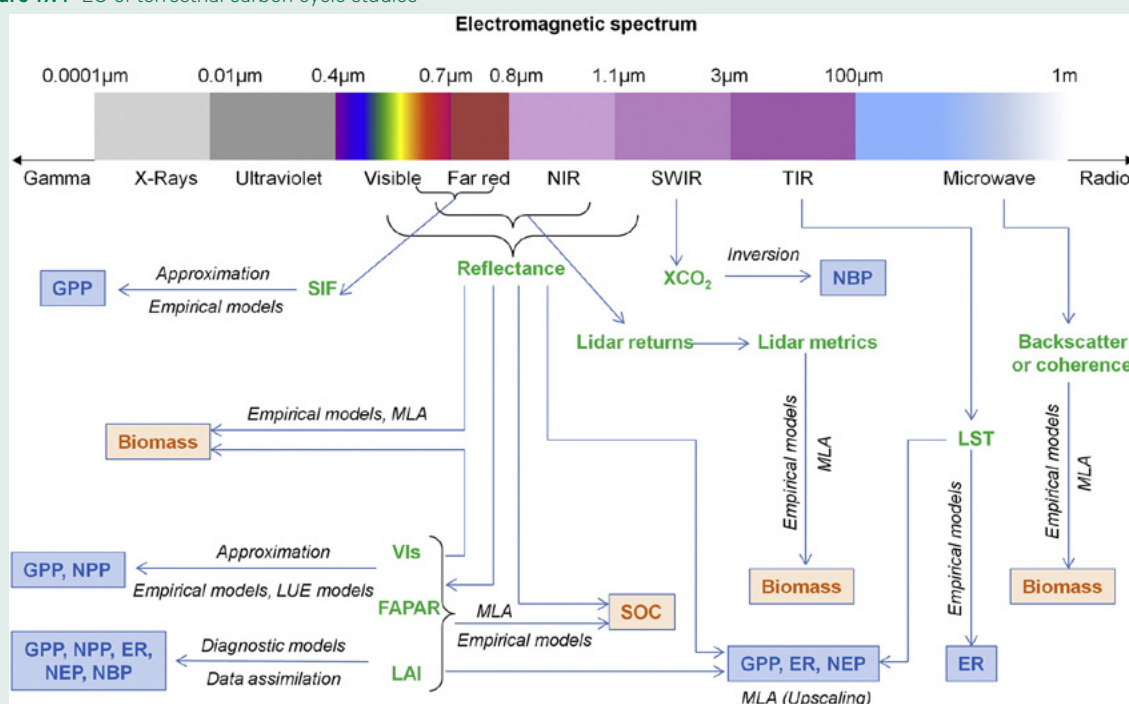
This yields information on diurnal, daily, and seasonal dynamics plus interannual variations of NEE of CO₂ between the land surface and the atmosphere (Baldocchi *et al.*, 2001; Verma *et al.*, 2005). GPP is the residual calculated from the direct measurements of NEE and estimates of respiration. This generates valuable *in situ* information for validating EO-based productivity products and for carbon model development and independent evaluation and assessment of their uncertainties.

Earth Observation

Over the last four decades, EO has played an increasingly important role in global (terrestrial and marine) carbon cycle studies. Satellite imaging sensors offer synoptic scale observations of ecosystem states and landscape dynamics, and are seen as invaluable tools to help fill the large spatial gaps and restrictive coverage afforded by *in situ* measurements (experimental plots and eddy covariance flux towers) to better constrain and improve the accuracies of models (see Section 10). EO provides much needed data and information of under-sampled critical regions (e.g. tropical and arctic/boreal environments) and facilitates broadscale patterns of ecosystem functioning. A strategic combination of satellite observations and *in situ* data, can provide the dense sampling in space and time required to characterise the heterogeneity of ecosystem structure and function (Schimel *et al.*, 2015).

As illustrated in Figure 17.4, carbon fluxes assessed with EO data include gross primary production (GPP), ecosystem respiration (ER), net primary production (NPP), net ecosystem production (NEP), and net biome production (NBP). The carbon stocks that are quantified by EO include above ground biomass (AGB), litter, and soil organic carbon (SOC).

Figure 17.4 EO of terrestrial carbon cycle studies



Source: Xiao *et al.* (2019) Figure 2

17.1 Carbon Cycling in Australia

National and regional carbon budgets are important for providing information on spatial and temporal variations in carbon fluxes and stocks in response to climate variability, fire activity, and land use and land cover changes. Haverd *et al.* (2013) performed a comprehensive assessment of the terrestrial carbon budget for Australia over a decadal period from 1990 to 2011. They combined a regional biogeochemical model (BIOS2) and a land surface model (CABLE) constrained by published emissions data and multiple types of observations, including satellite measures of vegetation cover, leaf area index (LAI), and burnt areas from AVHRR and MODIS sensors.

The national carbon budget assessments included the mean, variance, and uncertainty estimates of the following land-atmosphere carbon flux components (Haverd *et al.*, 2013):

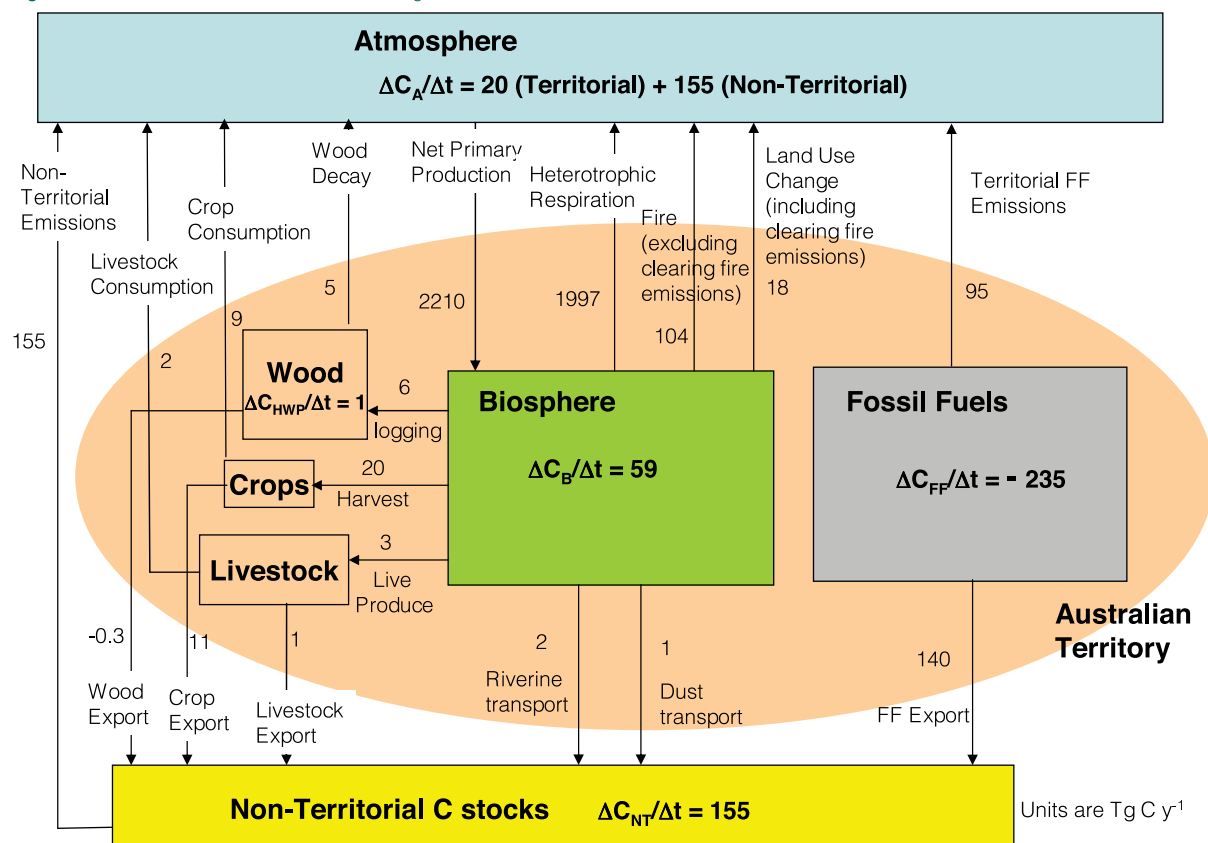
- net primary production (NPP) and net ecosystem production (NEP);
- fires and land use change;
- riverine export, dust export, and harvest (wood, crop and livestock); and
- fossil fuel emissions (both territorial and non-territorial).

Their findings demonstrated the Australian terrestrial carbon cycle is characterised by extreme variability in carbon uptake by vegetation, emissions from

fires, and land use changes (see Figure 17.5). Overall, Australian ecosystems were absorbing carbon (NEP) by 80 TgC yr^{-1} , with climate variability accounting for 12 TgC yr^{-1} and rising CO_2 levels accounting for 68 TgC yr^{-1} . The relative contributions of the climate and CO_2 forcings (or drivers) varied greatly across bioclimatic regions. In the desert areas of central Australia, CO_2 fertilisation and very high rainfall in 1990–2011 together generated a strong positive NEP response, while in the cool temperate regions the CO_2 fertilisation effect was offset by long term drought (1990–2011) and its negative impact on NEP. The response of NPP to rising CO_2 also varied regionally, being higher for regions where gross primary production (GPP) was strongly influenced by high vapour pressure deficit (VPD).

Moreover, the positive ecosystem gains in NEP (80 TgC yr^{-1}) were partially offset by fire emissions (26 TgC yr^{-1}) and land use change (18 TgC yr^{-1}), resulting in a net biome productivity (NBP) of 36 TgC yr^{-1} . Thus, the aggregate Australian ecosystem net positive NBP offset averaged fossil fuel emissions of 95 TgC yr^{-1} , by 38% (Haverd *et al.*, 2013). The interannual variability (IAV) in the Australian carbon budget was dominated by interannual variability in ecosystem NEP, and exceeded Australia's total fossil fuel carbon emissions. Lateral transport of carbon in rivers accounted for 0.1% of NPP, while net export of carbon by dust was smaller at 0.05%.

Figure 17.5 Australian territorial carbon budget 1990–2011



Source: Haverd *et al.* (2013) Figure 1

Australia has also been an active partner in international agreements to track global carbon emissions resulting from forest degradation, including the Reducing Emissions from Deforestation and Forest Degradation in Developing Countries (REDD+)

and the UN Global Forest Observations Initiative (GFOI; see Section 17.9). The current EO-based approaches for national measurement, reporting, and verification within the REDD+ framework are reviewed by Mitchell *et al.* (2017).

17.2 EO Sensors for Carbon Cycling

A wide variety of satellite sensors and techniques have been used to quantify carbon fluxes (Running *et al.*, 2004; Xiao *et al.*, 2019) and stocks (Saatchi *et al.*, 2011) at various spatial and temporal scales (see Table 17.1). These include sensors in the optical, thermal, and microwave regions of the electromagnetic (EM) spectrum, and include measures of land and ocean chlorophyll content, leaf area, biomass, solar-induced chlorophyll fluorescence (SIF), canopy height and structure, and atmosphere carbon gases (see Figure 17.4). This combination renders EO a powerful tool for studying vegetation productivity at local, regional, and global scales (Gitelson *et al.*, 2006; Schimel *et al.*, 2015).

Historically, the availability of satellite observations since the 1970s has enabled the assessments of the magnitude, spatial patterns, interannual variability, and long term trends of carbon dynamics at landscape, regional, and global scales. Recent satellites with high resolution spectrometers, which can retrieve concentrations of key atmospheric gases (such as the Orbiting Carbon Observatory-2; OCO-2), are providing valuable insights into global variations in, and sources of, greenhouse gases (see Section 17.6).

Table 17.1 EO sensors relevant to carbon cycling

SAR: Synthetic Aperture Radar

Type	Sensor	Platform	Relevance	Advantages	Disadvantages
Passive optical	Multispectral radiometer	Satellite or airborne	Carbon fluxes and stocks	Long archives, short revisit frequency, global coverage, readily available at a range of spatial scales	Impacted by cloud cover
	Spectrometer	Satellite	Terrestrial chlorophyll fluorescence GPP Drought and heat stress sensitivity	Unique global coverage	Coarse spatial resolution
	Meteorological	Satellite	Atmospheric carbon and energy fluxes	Global coverage	Coarse spatial resolution
Active optical	Lidar	Satellite, airborne, and terrestrial	Forest biomass Fuel load	Detailed structure for trees and stands	High cost, specialised processing
Active microwave	SAR	Satellite or airborne	Biomass Forest disturbance	All weather, available since early 1990s	Medium-coarse resolution
Proximal	Passive optical sensors (phenocam, hyperspectral); meteorological sensors	Ground and tower-based (see Excursus 7.2 and Volume 2D—Section 12)	Ecosystem and atmospheric variability Carbon dynamics Phenology	Continuous, long term measurements	High cost, high data volume, require skilled maintenance

17.3 Biosphere productivity

Vegetation productivity is directly related to the interaction of solar radiation with the plant canopy (see Section 7.4). As plants and phytoplankton grow, the productivity gain resulting from their conversion of CO₂ into biomass through photosynthesis, can be quantified with EO approaches involving vegetation indices (VIs), solar-induced chlorophyll fluorescence (SIF), and light use efficiency (LUE) models. Spectral measures of vegetation growth include vegetation and chlorophyll indices, LAI and fractional vegetation cover (see Section 8). VIs are the most empirical spectral measure of productivity, however, they do not measure photosynthesis fluxes directly. EO complements the detailed information available from *in situ* sensors, such as from flux tower sites (see Excursus 7.2), through broad spatial-temporal coverage and extension, and further enables intercomparisons of vegetation across space and time (see Volume 2D).

Monteith and Unsworth (1990) noted that spectral VIs can legitimately be used to estimate the rate of processes that depend on absorbed light, such as photosynthesis. EO-based estimates of Gross Primary Productivity (GPP) have been implemented at global scales, based on the LUE equation that defines the amount of carbon fixed through photosynthesis as proportional to the solar energy absorbed by green vegetation multiplied by the efficiency with which the absorbed light is used in carbon fixation:

$$\text{GPP} = \varepsilon_{\text{par}} \times \text{APAR} = \varepsilon_{\text{par}} \times f\text{APAR} \times \text{PAR}$$

where

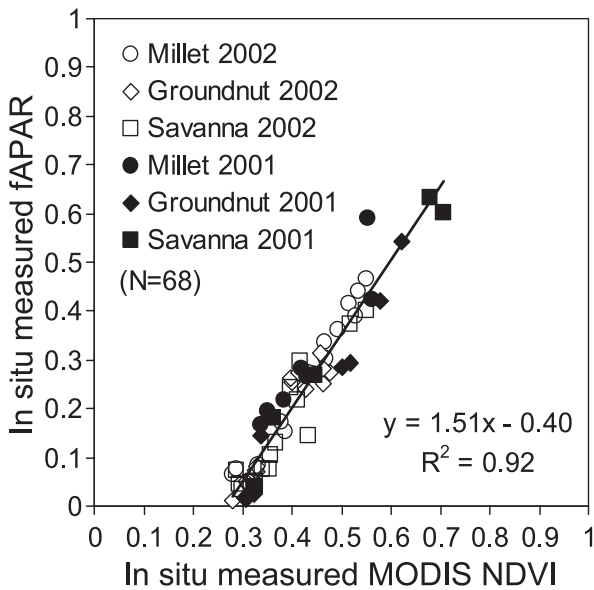
ε_{par} is the efficiency of conversion of absorbed light into above ground biomass (AGB), or LUE;
 PAR is the photosynthetically active radiation;
 APAR is the absorbed PAR integrated over a time period; and
 fAPAR is the fraction of APAR to the PAR available.

Monteith (1972) suggested that productivity of stress-free annual crops would be linearly related to vegetation absorbed PAR.

Asrar *et al.* (1984) showed the Normalised Difference Vegetation Index (NDVI; see Section 8.1.1) was linearly related with vegetation absorption of light energy, APAR, and thereby related to productivity through the potential capacity of vegetation to absorb light for photosynthesis (see Figure 17.6). The linear relationship between NDVI and fAPAR has been documented through field measurements (Fensholt *et al.*, 2004) and theoretical analyses (Sellers, 1985; Goward and Huemmrich, 1992; Myneni and Williams, 1994), although these relationships were not universal, and appeared to be unique to vegetation type, structure, soil optics. EO products, such as NDVI, were then used to map GPP globally, providing estimates of GPP that approximated eddy covariance (EC) estimates (Schimel *et al.*, 2015).

Figure 17.6 NDVI-APAR relationship

A linear relationship exists between NDVI and vegetation absorption of light energy (APAR) or fraction of APAR across multiple cropland and biome sites in Africa.



Source: Fensholt *et al.* (2004) Figure 10

17.3.1 Relationships between EO and flux tower GPP estimates

The advent of global, flux tower networks (see Excursus 7.2) has provided the opportunity to validate remotely sensed retrievals of productivity with *in situ* GPP estimates derived from the tower flux measures of net ecosystem exchange (NEE). This has been useful for validating EO spectral measures and carbon models, and to cross-calibrate EO-based methods. With the measurement footprint of flux towers at least partially overlapping the pixel size of daily return satellites (e.g. 250 m for MODIS), EO can simplify the upscaling of ecosystem processes, such as photosynthesis, from the network of flux towers to larger landscape units and to regional scales. Today, the integration of independently derived tower measured carbon fluxes with satellite data is the focus of many investigations across many ecosystems (Glenn *et al.*, 2008).

Several studies have suggested that EO products, such as VIs, are able to estimate GPP with relatively good accuracy, thus potentially simplifying carbon balance models and offering opportunities for region-wide upscaling of carbon fluxes (Glenn *et al.*, 2008). As top-of canopy measurements, flux towers do not require knowledge of LAI or details of canopy architecture to estimate fluxes facilitating their comparisons with satellite spectral index measures that similarly involve community properties resulting from integrative, top-of-canopy radiation interactions.

Rahman *et al.* (2005) initially reported that the Enhanced Vegetation Index (EVI; see Section 8.1.1) provided reasonably accurate estimates of GPP across a wide range of North American ecosystems. The strength of the linear relationships between EVI and tower GPP in temperate forests was greater in seasonally contrasting deciduous forests compared with more aseasonal evergreen forests (Rahman *et al.*, 2005; Sims *et al.*, 2006). Strong correlations between EVI and GPP were reported across Northern Europe (Olofsson *et al.*, 2008), across African tropical savanna ecosystems (Sjostrom *et al.*, 2011), and in dry to humid tropical forest sites in Southeast Asia and the Amazon (Xiao *et al.*, 2005; Huete *et al.*, 2006, 2008). Ma *et al.* (2013) observed good convergences between MODIS EVI and tower GPP across mesic and xeric tropical savannas in northern Australia.

The relationships between EVI and tower GPP are partly a result of fairly good correlations between LUE and EVI that make an independent estimate of LUE less necessary. Sims *et al.* (2006) reported that LUE derived from nine flux towers in North America was well-correlated with EVI ($r^2=0.76$), while Wu *et al.* (2011) reported moderate correlation between EVI and tower LUE in temperate and boreal forest ecosystems in North America. Further, the 16-day averaging period removes much of the influences of short term fluctuations in solar radiation and other environmental parameters, thereby minimising the need for climatic drivers.

Sims *et al.* (2006) further noted that when data from the winter period of inactive photosynthesis was excluded by use of land surface temperature (LST) observations below 0° , the EVI-tower GPP relationship improved. This demonstrates a limitation of spectrally-based satellite products for GPP estimations, in that spectral measurements record evergreen coniferous forests to remain 'green', even when temperatures inhibit photosynthesis (GPP).

Distinct differences in VI relationships with tower GPP were found between phenology-driven and meteorologically-driven Australian ecosystems. Restrepo-Coupe *et al.* (2016) found that in primarily meteorologically-driven (e.g. PAR, temperature, and/or precipitation) and relatively aseasonal ecosystems, there were no statistically significant relationships between GPP and MODIS vegetation products (LAI, fAPAR, VIs). The poor correlations were observed where meteorology and phenology were asynchronous (e.g. Mediterranean ecosystems). On the other hand, in phenology-driven ecosystems, changes in the vegetation status can be well-represented by VIs, and highly correlated VI-GPP relationships can be found in locations where key meteorological variables and vegetation phenology were synchronous.

The validation of satellite-based productivity products remains challenging due to a variety of spatial and temporal scaling issues. These include the matching of large satellite pixels (~1 km) with field plot scale measurements in both time and space. Li *et al.* (2007) demonstrated limitations associated with disparate footprints between satellite and tower flux measurements and the need for Landsat spatial resolutions for flux footprint matching, particularly in non-forested canopies. However, tower data of fluxes potentially offer much more than simply validating and/or calibrating EO products and models. An understanding of why satellite–flux tower relationships hold, or do not hold, will greatly advance and contribute to our comprehension of the carbon cycle mechanisms and scaling factors at play.

17.3.2 Solar-induced chlorophyll fluorescence (SIF) as proxy for GPP

More recent capabilities to measure solar-induced chlorophyll fluorescence (SIF) from airborne and space-based platforms now provides a more direct approach for estimating GPP (Frankenberg *et al.*, 2011; Joiner *et al.*, 2011). The PAR absorbed by chlorophyll in leaves is used to drive photosynthesis, but some radiation is also dissipated as heat or emitted back into the atmosphere at longer wavelengths (650–850 nm; see Volume 1A—Section 5). This re-emitted red and near infrared (NIR) light from illuminated plants as a by-product of photosynthesis, or SIF, has been found to strongly correlate with GPP (Baker, 2008; Meroni *et al.*, 2009). Chlorophyll fluorescence may be conceptualised as:

$$\text{SIF} = \varepsilon_f \times \text{PAR} \times \text{fAPAR}$$

where ε_f is the fAPAR photons that are re-emitted from the canopy as SIF photons, or yield of fluorescence photons.

17.4 Net Primary Productivity

17.4.1 VIs as proxies for ANPP

Vegetation indices (VIs) may be more appropriate measures of net primary productivity, NPP, the balance between GPP and plant autotrophic respiration, that is, VIs measure the vegetation remaining after respiration (R_a):

$$\text{NPP} = \text{GPP} - R_a$$

At short timescales, plants respond to the dynamics of environmental variables through stomatal closure and other diurnal adjustments that cannot be easily sensed by satellite-derived VIs and other LAI, fAPAR, or fractional cover products (see Section 8).

SIF data provide information on both the light absorbed and the efficiency with which it is being used for photosynthesis. It is an independent measurement, linked to chlorophyll absorption, providing unique information on photosynthesis relative to VIs. The SIF expression can be combined with the GPP-based LUE equation to yield:

$$\text{GPP} = \frac{\varepsilon_{\text{par}}}{\varepsilon_f} \times \text{SIF}$$

Empirical studies at the leaf and canopy scale indicate that the two LUE terms tend to covary under the conditions of the satellite measurement (Flexas *et al.*, 2002). SIF is seen as one way to increase the effective remotely sensed temporal resolution of vegetation photosynthesis, with near real time capabilities. SIF has been found to be more dynamic than greenness measures, and respond more quickly to environmental stress, through both change in stress-induced LUE and canopy light absorption (Porcar-Castell *et al.*, 2014; Schimel *et al.*, 2015). Vegetation indices, on the other hand, sense long and medium term changes (weeks to months) in canopy chlorophyll, related to canopy stress, phenology, and photosynthetic capacity of the vegetation (Glenn *et al.*, 2008).

As SIF responds to both incoming radiation and fluorescence yield, one may also normalise SIF by PAR (SIF/ PAR) to better relate SIF signals to canopy properties (Shen *et al.*, 2020). Shen *et al.* (2020) also combined SIF and EVI, as measure of SIF per unit greenness. Current sensors with capabilities to measure SIF include, NASA's Orbiting Carbon Observatory-2 (OCO-2) satellite, the Global Ozone Monitoring Instrument (GOME-2), and the more recent TROPospheric Monitoring Instrument (TROPOMI) on board the Copernicus Sentinel-5.

Variations in GPP and LUE are likely to be significant over shorter, daily time frames when water or temperature stress develops. At moderate to longer (e.g. weekly to monthly) timescales, plants tend to increase leaf foliage under favorable environments as an investment of resources into their photosynthetic apparatus, and reduce leaf foliage under stress when leaves are expensive to produce and maintain. Thus, at longer timescales, there is a convergence of satellite greenness vegetation signals with biologic and structural canopy properties (Glenn *et al.*, 2008).

Several studies have suggested that ecosystem NPP can be captured with an annual VI integral, that integrates growing season production through VI relationships with APAR. Goward *et al.* (1985) found good relationships between above ground NPP (ANPP) and integrated NDVI from AVHRR, over annual growing periods of North American biomes. Wang *et al.* (2004) found that the NDVI integral over the early growing season was strongly correlated to *in situ* forest measurements of diameter increase and tree ring width in the U.S. central Great Plains.

The integrated Enhanced Vegetation Index (iEVI) was also found to be a good proxy of ANPP. Ponce-Campos *et al.* (2013) compiled *in situ* field measures of ANPP over a range of North American and Australian biomes, and found iEVI to be an effective surrogate to estimate ANPP:

$$\text{ANPP} = 51.42 \times \text{iEVI} \times 1.15$$

where a log–log relation accounted for the uneven distribution of ANPP estimates over time.

The annual integrated VI offers a robust approximation of vegetation productivity, because, in general, VIs provide both a measure of the capacity to absorb light energy, as well as reflect recent environmental stress acting on the canopy, with stress forcings showing up as reductions in VI expressed as either less chlorophyll and/or less foliage (Running *et al.*, 2004).

17.4.2 Ecosystem respiration

Whereas optical EO data acquired in the visible, NIR, and short wave infrared (SWIR) wavelengths are used to determine ecosystem fluxes, GPP, and NPP, ecosystem respiration (ER) is more commonly measured using LST observations from thermal infrared (TIR) wavelengths (Rahman *et al.*, 2005; see Volume 1B—Section 7). ER is a combined measure of autotrophic and heterotrophic respiration and is a large carbon flux from the Earth’s surface to the atmosphere.

Since the main controlling factor of microbial activity is air and surface (soil, water) temperature, using remotely sensed measurements of land surface temperature (LST) has the potential to provide information on the spatial and temporal estimates or retrievals of ER. Rahman *et al.* (2005) found a strong correlation between MODIS-derived LST and EC tower-derived ER over North American sites (especially forests), and Schubert *et al.* (2012) found good relationships over peat lands in Sweden. Others have combined LST with either EVI or a water index in order to obtain better estimates of GPP or NEE, which were then used to derive ER. For

example, MODIS LST was combined with EVI in a modified Temperature-Greenness (T-G) model (Sims *et al.*, 2008; see Section 17.5.3) to investigate ER in insect-infested forests (Moore *et al.*, 2013). Tang *et al.* (2011) combined MODIS LST with a water index to model ER in a mixed temperate forest. Kimball *et al.* (2009) used LST derived from the Advanced Microwave Scanning Radiometer for EOS (AMSR-E) sensor and found it to be an effective surrogate for soil respiration (heterotrophic respiration and root respiration) across a broad range of boreal forest, grassland, and tundra sites in the boreal and arctic biomes. Methods to constrain ER estimates with other drivers, such as soil moisture, vegetation production, or nutrient limitations will further improve EO-based estimates of ER (Jagermeyr *et al.*, 2014).

17.4.3 Net ecosystem productivity and net biome productivity

Net ecosystem productivity (NEP) and net biome productivity (NBP) both estimate net ecosystem carbon uptake/release. The fluxes contributing to NEP are GPP and autotrophic (R_a) and heterotrophic (R_h) respiration, while NBP is mainly determined by NEP minus the loss of carbon by processes such as fire and harvest:

$$\text{NEP} = \text{GPP} - R_a - R_h$$

$$\text{NBP} = \text{NEP} - \text{fire} - \text{harvest}$$

The recent availability of column CO_2 concentration retrievals from newly launched satellites has made it feasible to quantify NEP and NBP from satellite observations. These satellites use high resolution spectrometers to measure the intensity of sunlight, at different wavelengths, for retrievals of columnar CO_2 and CH_4 concentrations. For example, NASA’s OCO-2 (launched in 2014) provides comprehensive, global measurements of CO_2 in the atmosphere, including seasonal fluctuations of the greenhouse gas and their spatial sources and sinks. This enables a better understanding of how ecosystems absorb and release CO_2 , both seasonally and across years in response to interannual climate variability. Basu *et al.* (2013) estimated the global distribution of CO_2 fluxes using column CO_2 measurements from the GOSAT instrument. Inversions of satellite CO_2 observations provide useful constraints on terrestrial carbon sinks and sources.

17.4.4 Growing season phenology

Numerous efforts have been made to improve upon the characterisation of the plant growing, or productivity, season at regional scales using satellite-based phenology models (see Section 9.3).

The phenological life cycles of plant species and communities have large effects on their rates of photosynthesis and annual productivity (Tucker *et al.*, 1986) and VIs are able to provide seasonal and annual growing season metrics of plant productivity (see Section 8.1). Phenological factors such as leaf age and life expectancy play important roles in productivity (Wilson *et al.*, 2001) with some vegetation production models explicitly incorporating phenophase periods, such as bud burst to full leaf expansion, and full expansion to dormancy (Xiao *et al.*, 2004). LST satellite data and/or meteorological air temperature data (T_a) are also used to identify biologically inactive seasonal periods, for example, masking cold temperature time intervals from the VI integrals.

Generally, *in situ* measures of productivity are made at discrete times within the growing season and there is a need to synchronise the satellite measurements with scheduled or variable destructive or harvesting sampling dates to reduce *in situ* ANPP-VI uncertainties. Often it is difficult to predict and sample at peak productivity and greenness periods. Continuous VI growing season productivity profiles allow one to better synchronise VI temporal values with actual *in situ* sampling periods. For example, Moran *et al.* (2014) found significant improvements in productivity–iEVI relationships across a range of grassland sites, when the EVI was only partially integrated from the beginning to the peak of the growing season period (rather than the full season). This was due to the synchronisation of time periods to peak biomass periods when grassland ANPP destructive sampling is typically conducted (see Section 5.1.2). In such cases, EO data provides better temporal stability and opportunities to reduce productivity uncertainties.

17.5 Carbon Models

There are many empirical, diagnostic, and process-based models that have been developed over the past few decades to quantify land and ocean productivity, with many of these methods integrating independently derived carbon flux measurements from satellite data, EC tower fluxes, and field measurements (see Excursus 17.2). Estimates of daily GPP and annual NPP are now routinely produced operationally over the global terrestrial surface at 1 km spatial resolution through production efficiency models (PEM) with near real time satellite data inputs from MODIS (Turner *et al.*, 2006; see Section 10.2.3).

EO-based modelling approaches focus on the fAPAR term (see Section 6.3.4), which is derived through spectral VI relationships (Asrar *et al.*, 1984; Sellers, 1985; Goward and Huemmrich, 1992; see Section 8.1.4). The

17.4.5 Photochemical Reflectance Index

The Photochemical Reflectance Index (PRI; Gamon *et al.*, 1997; see Section 8.1.2) derived from tower-based spectral measurements and MODIS data (Middleton *et al.*, 2018) provides a scaled LUE measure based on light absorption processes by carotenoids (see Section 4.3 and Excursus 4.1), which has been shown to be a good proxy for LUE:

$$\text{PRI} = \frac{\rho_{531} - \rho_{570}}{\rho_{531} + \rho_{570}}$$

The potential of PRI as an EO-based proxy for LUE has been demonstrated (Goerner *et al.*, 2009). The spectral variations at 531 nm are associated with dissipation of excess light energy by xanthophyll pigments (a major carotenoid group of yellow pigments; see Section 4.3) in order to protect the photosynthetic leaf apparatus. Carotenoids function in light absorption in plants as well as protecting plants from the harmful effects of high light conditions, hence lower carotenoid/chlorophyll ratios, indicate lower physiological stress. However, the PRI has also been shown to be very sensitive to canopy structure, gap fraction, background, viewing angle, and LAI, which complicates the association between PRI and LUE (Middleton *et al.*, 2018). In addition, although the short term variation in leaf level PRI appears indeed to be controlled by non-photochemical quenching (NPQ), the seasonal variation in leaf level PRI seems to be controlled by the slow changes in pigment pools rather than NPQ. The mechanistic link between the PRI and LUE appears to be highly dependent on scale and remains to be fully elucidated.

fundamental basis for these models is the LUE equation that defines the amount of carbon fixed through photosynthesis (GPP), as proportional to the PAR from solar energy that is absorbed by vegetation multiplied by the efficiency with which the absorbed light is used in carbon fixation (see Sections 7.4 and 17.3):

$$\text{GPP} = \epsilon_{\text{par}} \times \text{APAR} = \epsilon_{\text{par}} \times \text{fAPAR} \times \text{PAR}$$

This simple LUE-based productivity equation comprises a large amount of biological complexity, resulting in numerous productivity modelling approaches that tend to emphasise either the fAPAR equation term or LUE (ϵ). The LUE approach has been one of the most important methods to map GPP and NPP regionally or globally (Potter *et al.*, 1993; Running *et al.*, 2004).

17.5.1 EO-based LUE models

The LUE concept has been widely adopted by the EO community to assess and extrapolate carbon processes through knowledge of two conversion coefficients:

- fAPAR (see Section 6.3.4); and
- LUE or ϵ (see Section 7.4).

EO data play a significant role in the LUE approach by providing information on vegetation type, growth status, and environmental conditions. fAPAR is readily estimated using remotely sensed 'greenness' measures (see Section 8.1.1), or through satellite MODIS-FPAR products (Zhao *et al.*, 2005). Longer term GLASS-FAPAR products (Xiao *et al.*, 2015) extend the temporal coverage of FAPAR back to 1982 and can potentially lead to long term GPP estimates.

LUE (ϵ) however is very difficult to measure as it dynamically varies with plant functional type, vegetation phenophase, and different environmental stress conditions (Ruimy *et al.*, 1995; Turner *et al.*, 2004; Sims *et al.*, 2006; Jenkins *et al.*, 2007). As a result, there are scarce measurements of LUE available, particularly at the landscape scale, and potential or maximum LUE values have only been specified for a limited set of biome types, with these values down-regulated by environmental stress scalars derived from meteorological inputs (Zhao *et al.*, 2005; Heinsch *et al.*, 2006).

EO also provides measures of two other inputs of LUE models, namely water stress (Jones *et al.*, 2017) and incident radiation (Zhang *et al.*, 2014), as well as spatially explicit information on land cover type (Friedl *et al.*, 2010) that determines maximum LUE and other model parameters.

17.5.2 Greenness and radiation (G-R) models

The fraction of PAR absorbed by chlorophyll throughout the canopy (fAPAR_{chl}) could lead to more accurate cropland GPP estimates than the MODIS-FPAR (Zhang *et al.*, 2014). VIs are commonly used, but chlorophyll indices can also be coupled with measures of light energy, PAR, to provide robust estimates of GPP. Canopy level chlorophyll represents a community property that is most relevant in quantifying the amount of absorbed radiation used for productivity. Gitelson *et al.* (2006) showed that for the same LAI amount, the chlorophyll content during the green-up stage might be more than two times higher than the chlorophyll content in leaves in the reproductive and senescence stages:

$$GPP = VI_{chl} \times PAR_{toc}$$

where

PAR_{toc} is the top-of-canopy measured PAR (MJ m⁻² day⁻¹); and

VI_{chl} is a chlorophyll-related spectral index.

Peng *et al.* (2013) described two types of chlorophyll spectral indices:

- commonly used VIs, such as EVI and the Wide Dynamic Range Vegetation Index (WDRVI), which indirectly indicate total chlorophyll content through 'greenness' estimates; and
- chlorophyll indices, such as the MERIS Terrestrial Chlorophyll Index (MTCI), which directly represent the leaf chlorophyll content.

The WDRVI equation is:

$$WDRVI = \frac{a \times \rho_{NIR} - \rho_{red}}{a \times \rho_{NIR} + \rho_{red}}$$

where a is a weighing coefficient with value between 0.1 and 0.2 (Gitelson, 2004; Gitelson *et al.*, 2006).

MTCI is the ratio of the difference in reflectance between an NIR and red edge band and the difference in reflectance between red edge and red band as:

$$MTCI = \frac{\rho_{753.75} - \rho_{708.75}}{\rho_{708.75} + \rho_{681.25}}$$

where $\rho_{753.75}$, $\rho_{708.75}$, and $\rho_{681.25}$ are reflectances in the centre wavelengths of the MERIS narrow-band channel settings (Dash and Curran, 2004). In the Greenness and Radiation (G-R) model, both fAPAR and LUE are driven by total chlorophyll content with strong correlations between GPP/PAR and canopy chlorophyll content (Gitelson *et al.*, 2006; Peng *et al.*, 2011).

Ma *et al.* (2014) found significant improvements in the use of G-R models, relative to EVI alone, for predicting tower GPP, demonstrating the importance of this quantity as a critical driver of savanna vegetation productivity (Whitley *et al.*, 2011; Kanniah *et al.*, 2013a). The G-R model has been successfully applied in estimating GPP in natural ecosystems (Sjostrom *et al.*, 2011; Wu *et al.*, 2011, 2014) and croplands, including maize, soybeans, and wheat (Wu *et al.*, 2010; Peng *et al.*, 2011).

Two definitions of LUE become apparent in G-R models, with this term either defined as the ratio of GPP to APAR, or the ratio of GPP to PAR (Gower *et al.*, 1999), with the latter sometimes referred to as ecosystem-LUE or eLUE:

$$\epsilon = \frac{GPP}{APAR}$$

$$eLUE = \frac{GPP}{PAR} = fAPAR \times \epsilon$$

An advantage of using chlorophyll-based VIs in G-R models is that the biological drivers of photosynthesis, fAPAR and ϵ resulting from environmental stress and leaf age phenology, are combined into eLUE, thereby simplifying EO-based productivity estimates.

Other measures of PAR that have been used include 'potential' PAR, or maximal clear-sky PAR ($PAR_{\text{potential}}$; Peng *et al.*, 2013; Rossini *et al.*, 2015) and top-of-atmosphere PAR (PAR_{toa}). $PAR_{\text{potential}}$ can be calibrated from long term PAR_{toc} measurements or modelled using an atmosphere radiative transfer code (Kotchenova and Vermote, 2007). Gitelson *et al.* (2014) found an improved performance of $PAR_{\text{potential}}$ relative to PAR_{toc} noting that decreases in PAR_{toc} during the day do not always imply a decrease in GPP. Further, Kanniah *et al.* (2013) showed that the negative forcings of wet season cloud cover over Australian tropical savannas were partly compensated by enhanced LUE resulting from a greater proportion of diffuse radiation. Ma *et al.* (2014) found that coupling of EVI with PAR_{toa} better predicted GPP than coupling EVI with PAR_{toc} and attributed this to tower sensor-based measurement uncertainties of PAR_{toc} , as well as better approximations of meteorological controls on GPP by PAR_{toa} .

17.5.3 Temperature-Greenness (T-G) model

Although potentially useful in certain cases, the simple VI 'greenness' model—defined as the straightforward relationship between VIs and GPP—exhibits various limitations due to its inability to always recognise between-growth and inactive-growth periods, in which spectral 'greenness' may show little change. These inactive periods are associated with evergreen vegetation in winter months with low temperatures, as well as evergreen vegetation growing in Mediterranean climates in which high temperature, vapor pressure deficit, and soil drought limit growth (Sims *et al.*, 2008; Vickers *et al.*, 2012).

For these reasons, Sims *et al.* (2008) introduced the temperature and greenness (T-G) model, using combined daytime LST and EVI products from MODIS. They found the T-G model substantially improved the correlation between predicted and measured GPP at 11 EC flux tower sites across North American biomes compared with the MODIS GPP product or MODIS EVI alone, while keeping the model based entirely on remotely sensed variables without any ground-based meteorological inputs (Sims *et al.*, 2008). The T-G model may be described as follows:

$$GPP = EVI_{\text{scaled}} \times LST_{\text{scaled}} \times m$$

$$LST_{\text{scaled}} = \min \left[\left(\frac{LST}{30} \right); \left(2.5 - (0.05 \times LST) \right) \right]$$

$$EVI_{\text{scaled}} = EVI - 0.10$$

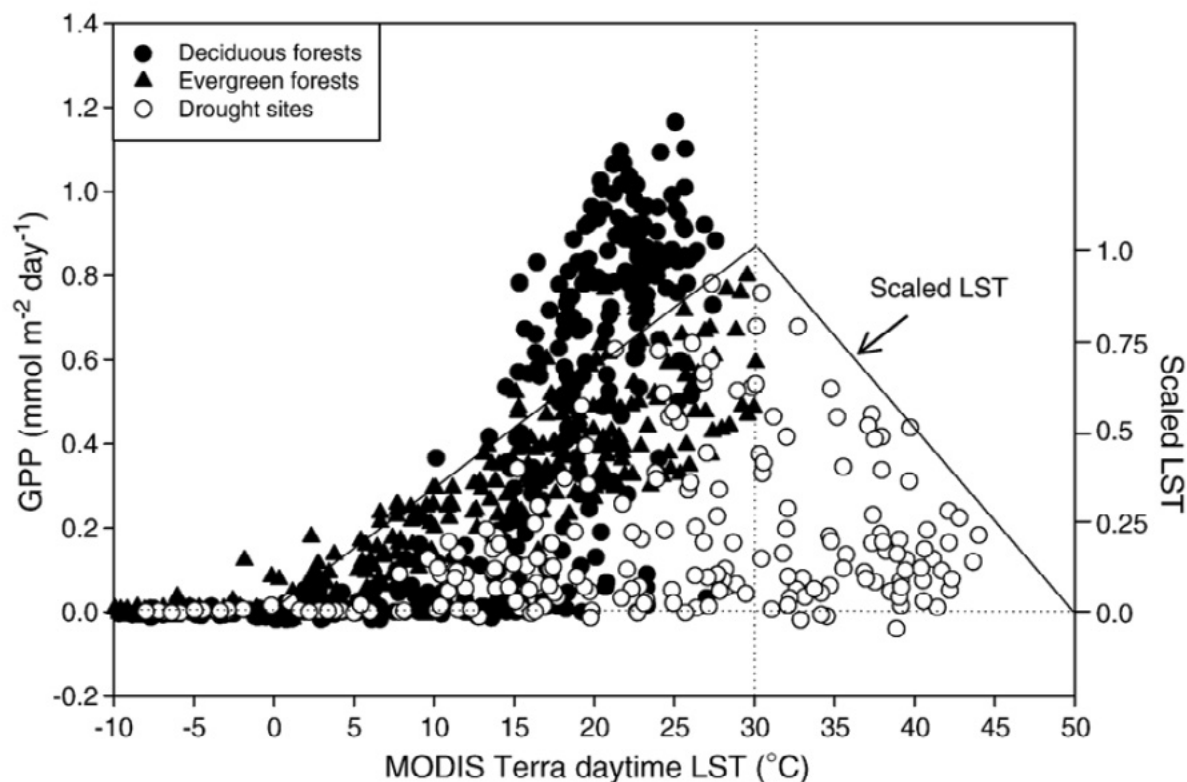
where

- LST_{scaled} sets GPP to zero when LST is less than zero, and defines the inactive winter period;
- EVI_{scaled} adjusts EVI values to a zero baseline value in which GPP is known to be zero;
- m is a scalar that varies between deciduous and evergreen sites, with units of $\text{mol C m}^{-2} \text{ day}^{-1}$; and
- LST_{scaled} also accounts for low temperature limitations to photosynthesis when LST is between 0°C and 30°C , and accounts for high temperature and high VPD stress in sites that exceed LST values of 30°C (Sims *et al.*, 2008; see Figure 17.7).

LST is closely related to VPD and thus can provide a measure of drought stress, consistent with the BIOME-BGC model, where temperature and VPD are used as scalars directly modifying LUE (Running *et al.*, 2004). LST is a useful measure of physiological activity of the upper canopy leaves, provided that leaf cover is high enough that LST is not significantly affected by soil surface temperature. Thus, the T-G model has been found less useful in sparsely vegetated ecosystems (e.g. shrublands) where soil surface temperatures significantly influence derived LST values, rendering them less useful as indicators of plant physiology. As an example, Ma *et al.* (2014) found coupling EVI with LST showed no improvements in predicting savanna GPP compared with using EVI alone over the relatively open tropical savannas in northern Australia, with appreciable soil exposure. This may also be due to temperature not being a limiting factor or significant driver of photosynthesis in tropical savannas (Leuning *et al.*, 2005; Cleverly *et al.*, 2013; Kanniah *et al.*, 2013).

Figure 17.7 Combined temperature-greenness model

GPP is enhanced by increasing temperatures up to 30°C. Solid line is scaled LST from the T-G model.



Source: Sims *et al.* (2008) Figure 2

17.5.4 Carbon modelling

Modelling of carbon, water, and energy fluxes between terrestrial surfaces and the atmosphere are increasingly important for hydrological and climate studies. Ecophysiological information relating to photosynthetic activity, biomass, productivity, water content, phenology, soil moisture, and nutrient status may be acquired and analysed consistently and repeatedly over large areas.

The BIOME-BGC (BioGeochemical Cycles) model calculates daily GPP as a function of incoming solar radiation, conversion coefficients, and environmental stresses (Running *et al.*, 2004). This was implemented as the first operational standard satellite product for MODIS (MOD17), providing global estimates of GPP, expressed as follows:

$$GPP = \epsilon_{\max} \times 0.45 \times SW_{\text{rad}} \times fAPAR \times f(VPD) \times f(T_{\min})$$

where

ϵ_{\max} is the maximum LUE (g C MJ⁻¹) obtained from a biome properties lookup table (BPLUT);

SW_{rad} is shortwave downward solar radiation (MJ⁻¹ day⁻¹), of which 45% is assumed to be PAR;

$f(VPD)$ and $f(T_{\min})$ are vapor pressure deficit and air temperature reduction scalars for the biome specific ϵ_{\max} values; and

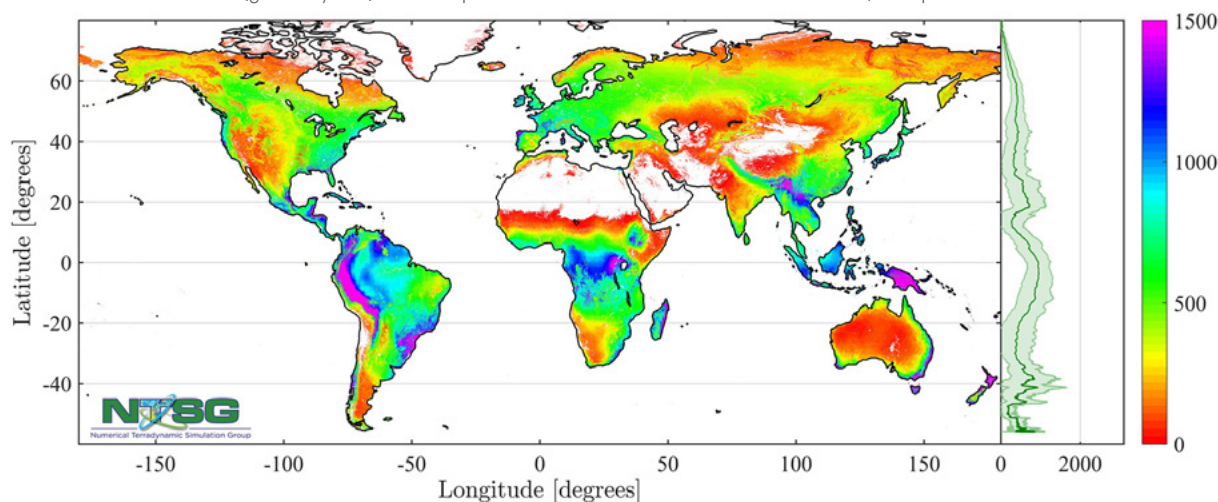
$fAPAR$ is directly input from the MODIS-FPAR (MOD15) product (Running *et al.*, 2004; Zhao *et al.*, 2005).

MODIS-FPAR retrievals are physically-based and use biome specific lookup tables generated using a three-dimensional radiative transfer model (Myneni *et al.*, 2002).

The reduction scalars encompass LUE variability resulting from water stress (high daily VPD) and low temperatures (low daily minimum temperature, T_{\min} ; Running *et al.*, 2004). The MODIS GPP product is directly linked to EO and weather forecast products and can provide near real time information on productivity and the influence of anomalies such as droughts. A consistent forcing meteorology is based upon the NCEP/NCAR (National Centres for Environmental Prediction/National Centre for Atmospheric Research) Reanalysis II datasets (see Figure 17.8).

Figure 17.8 MODIS NPP product based on BIOME-BGC model

Global mean annual NPP ($\text{g C m}^{-2} \text{ year}^{-1}$) over the period 2000–2015 based on the MODIS GPP/NPP product.



Source: Steven W. Running, NTGS (see <http://www.ntsg.umn.edu/project/modis/default.php>)

Using these satellite products, Zhao and Running (2010) found that global NPP declined slightly by 0.55 Pg C due to drought from 2000 to 2009. Ichii *et al.* (2007) used the BIOME-BGC model to simulate seasonal variations in GPP for different rooting depths, 1–10 m, over Amazon forests, then determine which rooting depths best estimated GPP to be consistent with satellite-based EVI. They were subsequently able to map rooting depths at regional scales and improve the assessments of carbon, water, and energy cycles in tropical forests.

The utility and accuracy of MODIS GPP/NPP products have been validated in various FLUXNET studies (see Excursus 7.2), which have also demonstrated the value of independent tower flux measurements to better understand the satellite-based GPP/NPP products (Leuning *et al.*, 2005; Zhao *et al.*, 2005, 2006; Turner *et al.*, 2006). These studies highlight the capabilities of MODIS GPP to correctly predict observed fluxes at tower sites, but also draw attention to some of the uncertainties associated with use of coarse resolution and interpolated meteorology inputs, uncertainties with the LUT-based values, noise and uncertainties in the satellite fAPAR inputs, and difficulties in constraining the LUE term (Zhao *et al.*, 2005; Heinsch *et al.*, 2006; Yuan *et al.*, 2010). Since meteorological inputs are often not available at sufficiently detailed temporal and spatial scales, they can introduce substantial errors into the carbon exchange estimates.

Turner *et al.* (2006) concluded that although the MODIS NPP/GPP products are generally responsive to spatial–temporal trends associated with climate, land cover, and land use, they tend to overestimate GPP at low productivity sites and underestimate GPP at high productivity sites. Similarly, Sjöström *et al.* (2011) found that although MODIS GPP described seasonality at 12 African flux tower sites quite well, it tended to underestimate tower GPP at the dry sites in the Sahel region due to uncertainties in the meteorological and fAPAR input data and the underestimation of ϵ_{\max} . Jin *et al.* (2013) reported the MODIS GPP product to substantially underestimate tower GPP during the greening up phase at a woodland savanna site in Botswana, while overestimating tower-GPP during the browning down phase.

Some studies have found that when properly parameterised with site level meteorological measurements, MODIS GPP becomes more closely aligned with flux tower derived GPP (Turner *et al.*, 2003; Kanniah *et al.*, 2009). Kanniah *et al.* (2011), however, found that utilizing site-based meteorology could only improve GPP estimates during the wet season over northern Australian savannas, and suggested the MODIS GPP product has a systematic limitation in the estimation of savanna GPP in arid and semi-arid areas due to the lack of the representation of soil moisture. Sjöström *et al.* (2011) also found soil moisture information to be quite important for accurate GPP estimates in drier African savannas.

17.5.5 Vegetation Photosynthesis Model (VPM)

Xiao *et al.* (2004) developed a mostly satellite-based vegetation photosynthesis model (VPM) that estimates GPP using satellite inputs of EVI and the land surface water index (LSWI):

$$GPP = \epsilon \times fAPAR_{chl} \times PAR_{toc}$$

$$\epsilon = \epsilon_{max} \times T_{scalar} \times W_{scalar} \times P_{scalar}$$

where

$fAPAR_{chl}$ is estimated as a linear function of EVI; PAR_{toc} is measured at the site;

T_{scalar} , W_{scalar} , and P_{scalar} are scalars for the effects of temperature, water, and leaf phenology on vegetation, respectively (see Figure 17.9);

T_{scalar} is based on air temperature and uses minimum, maximum, and optimum temperature for photosynthesis at each time step; and

W_{scalar} is based on satellite-derived LSWI that accounts for the effect of water stress on photosynthesis:

$$W_{scalar} = \frac{1+LSWI}{1+LSWI_{max}}$$

$$LSWI = \frac{\rho_{nir} - \rho_{swir}}{\rho_{nir} + \rho_{swir}}$$

where

ρ_{swir} is the reflectance in a broadband SWIR band (e.g., MODIS, 1580–1750 nm); and

$LSWI_{max}$ is the maximum value for the growing season.

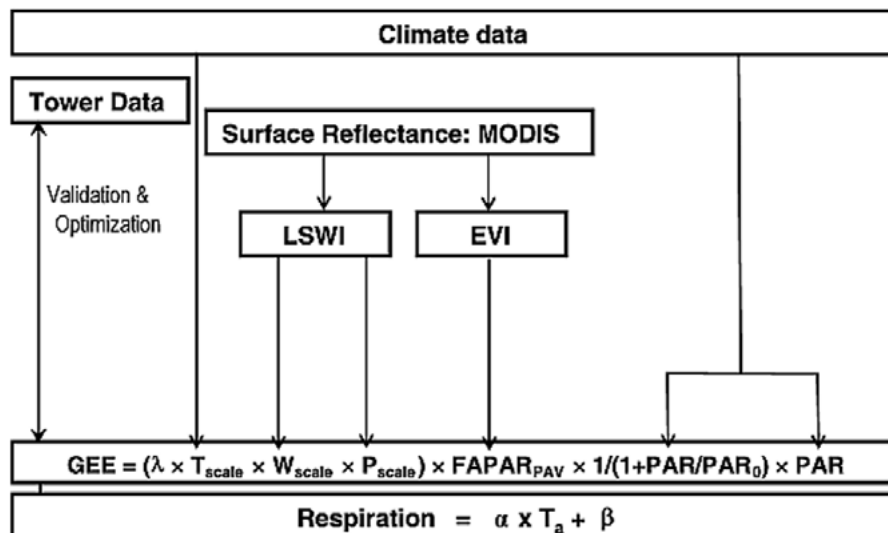
P_{scalar} accounts for the effect of leaf age on photosynthesis and is dependent on the growing season life expectancy of the leaves (Wilson *et al.*, 2001). P_{scalar} is calculated over two phenophases as:

$$P_{scalar} = \frac{1 + LSWI}{2}$$

from bud burst to full leaf expansion, and $P_{scalar}=1$, after full expansion (Xiao *et al.*, 2004).

Figure 17.9 Primarily Satellite-based Vegetation Photosynthesis and Respiration Model (VPRM)

LSWI: Land Surface Water Index; EVI: Enhanced Vegetation Index; Gross Ecosystem Exchange (GEE): light-dependent part of Net Ecosystem Exchange (NEE); Respiration (R): light-independent part of NEE; $FAPAR_{PAV}$: fraction of incident light absorbed by the photosynthetically active vegetation in the canopy; T_{scale} , P_{scale} , and W_{scale} : scalars for temperature, leaf phenology, and canopy water content, respectively; λ , PAR_0 , α , and β : four model parameters, one set per vegetation type.



Source: Mahadevan *et al.* (2008)

The VPM model has been applied to both MODIS and SPOT-4 VEGETATION sensor data to produce tower-calibrated estimates of GPP across a wide range of biomes, including evergreen and deciduous forests, grasslands, and shrub sites in temperate North America and in seasonally moist tropical evergreen forests in the Amazon (Xiao *et al.*, 2005; Mahadevan *et al.*, 2008; Jin *et al.*, 2013).

Mahadevan *et al.* (2008) further developed the vegetation photosynthesis and respiration model (VPRM), a satellite-based assimilation scheme that estimates hourly values of NEE using EVI, LSWI, and high-resolution meteorology observations of sunlight and air temperature (see Figure 17.9). NEE represents

the difference between uptake (photosynthesis) and loss (respiration) processes that vary over a wide range of timescales. The VPRM model provides fine-grained fields of surface CO₂ fluxes for application in inverse models at continental and smaller scales. This capability is presently limited by the number of vegetation classes for which NEE can be constrained using EC tower flux data.

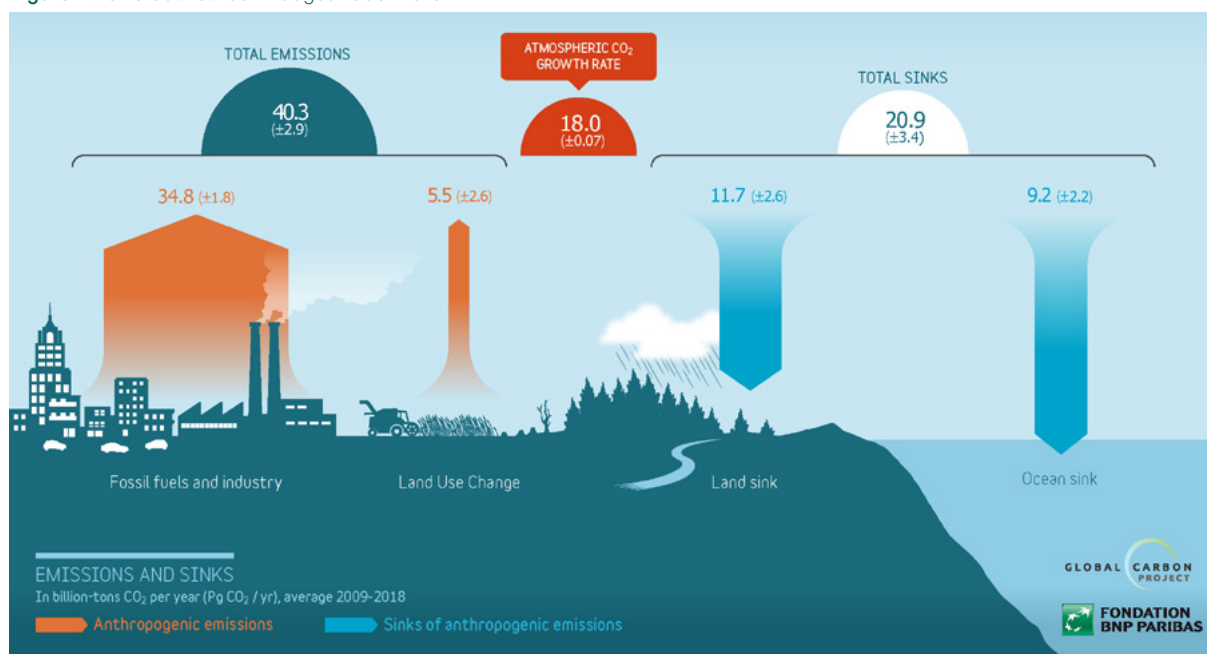
Another popular LUE model for quantifying GPP or NPP, which has incorporated satellite products, is the Carnegie Ames Stanford Approach (CASA) Biosphere model (Potter *et al.*, 1993). CASA has been widely used to simulate carbon dynamics at regional to global scales using NDVI and EVI inputs.

17.6 Anthropogenic carbon emissions

Human activity is significantly altering the global cycling of carbon through the burning of fossil fuels and land cover modifications (including fires—see Section 18), all of which result in more carbon accumulating in the atmosphere. The burning of fossil carbon fuels from coal, oil, and natural gas currently releases over 8 Gt of carbon annually into the atmosphere, representing the primary source of increased atmospheric CO₂ (see Figure 17.10). Land cover modifications and land use changes

currently transfer an additional 1 Gt of carbon into the atmosphere each year. Increases in CO₂ (a greenhouse gas) warms the atmosphere by absorbing TIR energy emitted by the Earth (see Volume 1A—Section 5.2.2) and then re-emitting it in all directions, including towards the Earth's surface, and thereby having a significant impact on the warming of our planet. As a result, average global temperatures have risen 0.8°C since 1880.

Figure 17.10 Global Carbon Budget 2009–2018



Source: Global Carbon Atlas, <http://www.globalcarbonatlas.org/en/content/global-carbon-budget>

17.6.1 CO₂ emissions

Ground-based CO₂ measurements first began in 1958 by Dr. Charles Keeling at Mauna Loa, Hawaii, and have steadily recorded increasing CO₂ concentrations in the atmosphere over time (see Figure 17.11). An increasing number of ground stations now provide a broader view of carbon in the atmosphere, with models and estimates filling in some details. These show the levels of CO₂ in the atmosphere to have increased from about 280 ppm, at the beginning of the Industrial Revolution, to over 400 ppm at present—a greater than 40% increase—significantly exceeding their envelope over the last several million years (Sellers *et al.*, 2018).

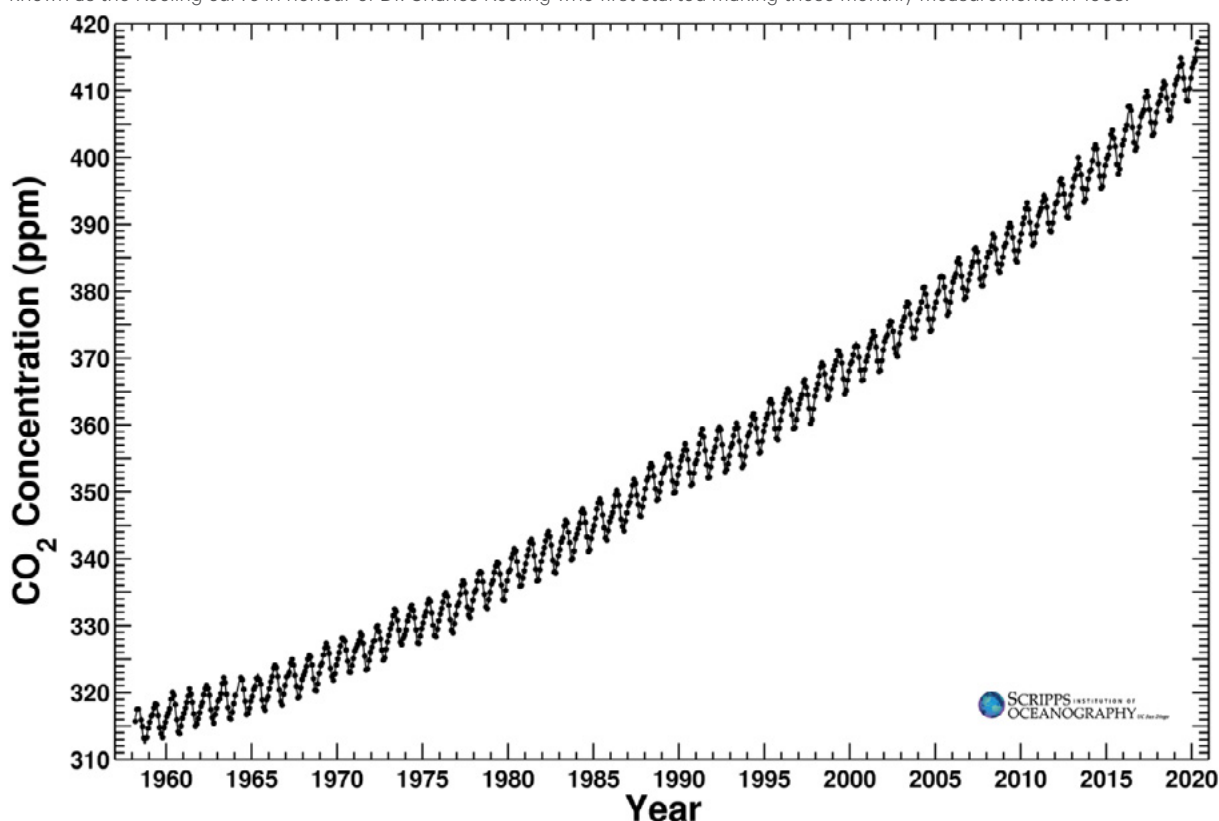
Our knowledge of global CO₂ from ground stations is restricted by the inability to collect sufficient measurements over the oceans and remote land areas, and by incomplete reporting by countries and companies that are monitoring this gas. EO technologies for measuring atmospheric column CO₂ and CH₄ concentrations from space have made many recent advances, enabling inversions of carbon

fluxes from satellite observations with high accuracy and coverage. Remotely sensed greenhouse gas observations provide a significant potential for improving our understanding of the natural carbon cycle and for the monitoring of anthropogenic emissions.

NASA's OCO-2 satellite was designed to study how carbon sources and sinks are distributed and how they change over time. OCO-2 is able to map and monitor areas that have not been observed much before, such as vast ocean areas, remote tropical forests and high latitude tundra areas. This allows the pinpoint location of CO₂ emitting sources and the estimation of the net ecosystem productivity (NEP). OCO-2 is also used to identify emissions from urban areas, biomass burning, volcanoes, and 'hidden' sources. Other current and planned satellite missions include OCO-3, GeoCARB, GOSAT-2, Sentinel-5P, and CO2M. They will enable large scale and consistent measurements with the same instrument over all land and sea surfaces.

Figure 17.11 Changes in carbon dioxide concentration

Interannual and seasonal time series of monthly average atmospheric CO₂ measurements at Mauna Loa Observatory, Hawaii. This is known as the Keeling curve in honour of Dr. Charles Keeling who first started making these monthly measurements in 1958.



Source: Scripps Institute of Oceanography, http://scrippsco2.ucsd.edu/data/atmospheric_co2/primary_mlo_co2_record

17.6.2 Examples of satellite studies of CO₂ emissions and flux inversions

It is a challenge to isolate recent human emissions from natural cycles and long term accumulations, and spatially-temporally attribute specific human CO₂ emissions. Some examples of attempts to do this are mentioned below.

17.6.2.1 El Niño-Southern Oscillation (ENSO)

The El Niño-Southern Oscillation (ENSO) is a recurring climate warming and cooling pattern involving water temperature changes in the Pacific Ocean (see Volume 3B). The oscillation period ranges from two to seven years and is referred to as the ENSO cycle. El Niño and La Niña are the extreme phases of the ENSO cycle, representing the warming and cooling phases of the ocean surface, respectively. Both phases significantly influence the rainfall distribution patterns, and thereby carbon cycle patterns in many parts of the world, including Australia.

EO has been instrumental in understanding how CO₂ fluctuates during ENSO cycles, and what roles the land and ocean play in this process. During the 2015–2016 El Niño, for instance, droughts, heat, and fires in tropical areas caused plants and soil on three continents to contribute to the largest growth of CO₂ on record. During this event, because of little rain and higher than normal temperatures in South America, Africa, and Asia, some plants did not absorb as much CO₂ while others died and decomposed more quickly, releasing the carbon they had absorbed from the air. During this period, an extra 2.5 Gt of CO₂ was released into the air compared to 2011, when conditions were normal. That extra carbon came from tropical areas in South America, Africa, and Asia—where plants all reacted differently. In South America, the growth of plants was stunted by drought, causing them to extract less CO₂ than usual. In Africa, the heat caused dead plants to decompose more quickly, releasing high amounts of CO₂, and in Asia, drought and heat caused forest fires, which also pumped huge quantities of carbon into the air.

17.6.2.2 Volcanoes and cities

The OCO-2 satellite makes such high resolution measurements that researchers can look at CO₂ concentrations over very small areas, such as a city or a volcano. CO₂ is higher in urban areas, where there are more cars and power plant emissions, than in suburban areas. The findings show that the OCO-2 satellite can quickly scan cities for pollution, complementing ground-based measurements.

OCO-2 data can also be used to monitor active volcanoes, such as the Yasur volcano in Vanuatu, which constantly spews out a plume rich in CO₂. These measurements suggest that Yasur is pumping out 41.6 kt of CO₂ a day. By processing OCO-2 data to account for seasonal changes, as well as the background level (already near 400 ppm), one is left with the signal of emissions from motor vehicles, power plants, and other industrial processes.

17.6.3 Land use and land cover modification

Changes in land cover, land use activities and land use management decisions will have corresponding impacts on carbon absorption and the carbon cycle (see Figure 17.10). The activities of deforestation, land degradation, forest logging and forest conversion to pastures and cropland remove large carbon stocks in woody biomass and replace them with vegetation that has lower carbon storage. The woody carbon that has accumulated over many years is then released back into the atmosphere, either through burning or decomposition (Friedlingstein *et al.*, 2019).

Increasing agricultural expansion activities will have the greatest impact and incursion onto rangelands to meet an ever expanding human population (see Section 15). Carbon emissions also result from disturbances such as fire and insect outbreaks. Agriculture intensification has increased to grow more food on less land (see Section 11.5). These managed agricultural lands release additional greenhouse gases (GHG), including methane (Sellers *et al.*, 2018) whose concentration has risen from 715 ppb in 1750 to 1,774 ppb in 2005.

Whereas deforestation can release large amounts of CO₂ into the atmosphere, forest regrowth acts to remove CO₂. In many areas, abandoned farmland is reverting to forest and drawing carbon out of the atmosphere, and these forests store much more carbon, both in wood and soil, than crops would.

Various EO datasets and approaches have been used to estimate carbon emissions from land use, land cover change, disturbance, and other sources. In particular, time series satellite data from the Landsat satellites, have enabled detailed monitoring of changes in forest cover (Hansen *et al.*, 2013; see Section 16), and land cover modifications resulting from urbanisation and expansion of agricultural lands (see Section 3). MODIS sensors also measure fire activities, and map burned areas and the subsequent regeneration of the landscape (see Section 18).

17.6.4 Effects of Carbon Cycle Changes

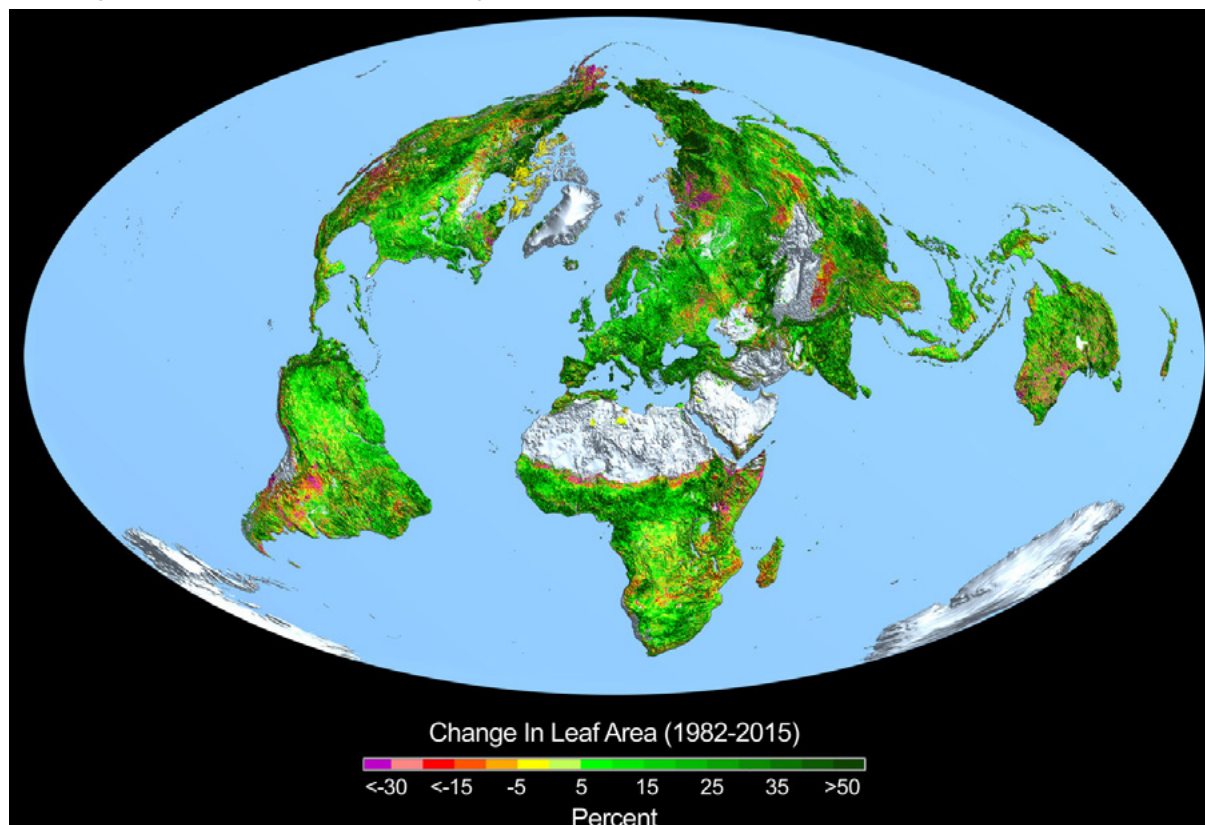
The changes in the carbon cycle impact each of the carbon reservoirs. About half of the fossil carbon emissions into the atmosphere each year are removed by the fast carbon cycle (see Excursus 17.1), but the remainder stays in the atmosphere. Increased carbon in the atmosphere can alter or induce plant growth, either through CO₂ fertilisation and its warming related increase in biological activity and plant growth (see Section 17.6.4.1) or changes in growing season phenology (see Section 17.6.4.2). Through increased levels of photosynthesis, plants have taken up approximately 25% of the CO₂ that humans have put into the atmosphere. This is termed a land cover sink (see Section 17.6.4.3).

17.6.4.1 Carbon fertilisation

With more atmospheric CO₂ available to convert to plant matter in photosynthesis, plants are able to grow more. This increased growth is referred to as carbon fertilisation and was associated with significant changes in global LAI (Myneni *et al.*, 1997; see Figure 17.12). CO₂ fertilisation increases plant growth until the plant reaches another limiting resource, such as water, nutrients, or light. Donohue *et al.* (2013) demonstrated that even in warm arid regions, with the effects of rainfall variations removed, the fertilisation effect was a significant land surface process that accounted for an 11% increase in green cover in the first decade of this century. The amount of carbon that plants take up varies greatly from year to year, but in general, the world's plants have increased the amount of CO₂ they absorb since 1960.

Figure 17.12 Change in global leaf area across 1982–2015

The change in MODIS-derived leaf area across the globe from 1982 to 2015 is associated with CO₂ fertilisation.



Source: <https://www.nasa.gov/feature/goddard/2016/carbon-dioxide-fertilization-greening-earth/>

17.6.4.2 Climate change and variability impacts on the carbon cycle

Interannual variations in climate (precipitation and temperatures) can also cause significant variations in biosphere-atmosphere carbon cycling. GPP is a critical intersection between the terrestrial biosphere and the Earth's climate. The increases of CO₂ and CH₄ and other greenhouse gases shift the Earth's climate on time and space scales that are important to humans (Sellers *et al.*, 2018).

During ENSO cycles (see Section 17.6.2.1), drought and wet years alter the net uptake and release of CO₂. In dry El Niño years, the vegetation is unable to absorb as much CO₂ due to water limitations. Thus CO₂ levels in the atmosphere will be higher than in more normal years. Further, dry years can increase the frequency and intensity of fire activity resulting in greater CO₂ emissions into the atmosphere. The opposite may occur in wet La Niña years, in which less vegetation is water limited and more CO₂ can be absorbed from the atmosphere through photosynthesis.

17.6.4.3 Australian carbon sink anomaly in 2011

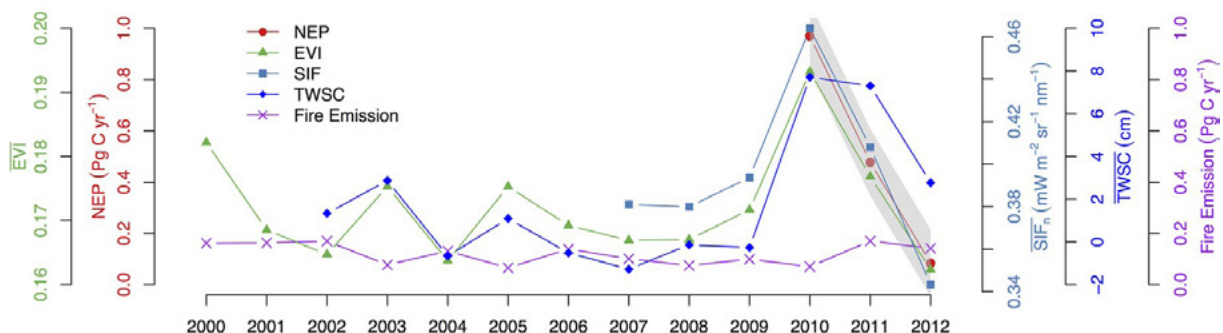
The amount of carbon that plants take up varies greatly from year to year, due to variations in limiting factors that restrict photosynthesis and plant growth. As an example, in an unusual, extremely wet year across Australia in 2011, an exceptionally large land carbon sink anomaly was recorded, of which more than half was attributed to Australia (see Figure 17.13; Ma *et al.*, 2016).

The biggest changes in the land carbon cycle are likely to come because of climate change. Continued global warming can extend the growing seasons and prolong growth, unless water becomes a limiting factor. However, warmer temperatures can also stress plants and, with a longer, warmer growing season, the plants need more water to survive. There is already evidence that plants in the Northern Hemisphere slow their growth in the summer because of warmer temperatures and water shortages (Angert *et al.*, 2005).

EO datasets have been used in a vast number of carbon-climate studies over northern latitudes, Africa, and the Amazon (Tucker *et al.*, 1986; Myneni *et al.*, 1997; Tucker *et al.*, 2001; Zhou *et al.*, 2001; Xiao and Moody, 2005; Saleska *et al.*, 2016). Satellite measurements have helped assess how the global carbon cycle is changing through time. They help us gauge the impact we are having on the carbon cycle by releasing carbon into the atmosphere or finding ways to store it elsewhere. They will show us how our changing climate is altering the carbon cycle, and how the changing carbon cycle is altering our climate. A better understanding of the carbon cycle is essential for improving projections of the Earth's carbon-climate system under future conditions (Schimel *et al.*, 2015).

Figure 17.13 Australian interannual variations in carbon-related indicators

Variations are shown for the continental summation of NEP (Pg C yr⁻¹), continental average of annual integrated EVI, continental average of SIF_n (PAR normalised SIF, mW m⁻² sr⁻¹ nm⁻¹), continental average of Total Water Storage Change (TWSC, cm), and continental total fire carbon emission (Pg C yr⁻¹). NEP is derived from GOSAT atmospheric inversion modeling. The gray shaded area represents the Bayesian uncertainty range of inverted NEP ($\pm 1\sigma$).



Source: Ma *et al.* (2016) Figure 1b

17.7 Carbon stocks

Measurements of carbon stocks, including vegetation biomass and soil organic carbon, are essential in quantifying the carbon cycle, and various optical, microwave, and lidar observations have been employed to quantify these.

17.7.1 Biomass carbon stock

Above ground biomass (AGB; see Section 5.1.2) can be estimated from passive optical EO methods that are sensitive to vegetation canopy properties (see Sections 12, 14, and 16). Coarse spatial resolution satellite data are frequently used to produce biomass estimates at regional or global scales for forest, grassland, and tundra ecosystems (Chopping *et al.*, 2011; John *et al.*, 2018; Epstein *et al.*, 2012), while medium spatial resolution data, such as from Landsat and Sentinel-2, are more frequently used for biomass estimations at local and regional scales (Turner *et al.*, 2004; Friedl *et al.*, 1994; Shoshany and Karnibad, 2011). Fine spatial resolution data (< 5 m) from high spatial resolution imaging sensors such as QuickBird, Ikonos, and WorldView-2/-3 can be used to calculate local tree biomass (Palace *et al.*, 2008; Fuchs *et al.*, 2009) and grass biomass (Sibanda *et al.*, 2017).

Satellite-derived AGB estimates are based on empirical models, machine learning (ML) methods, and allometric models (see Section 10). The variables derived from passive optical EO data for use in these models may include spectral reflectance, VIs, spatial texture, and vegetation canopy attributes (see Section 8). For example, empirical regression models have been developed by associating VIs to field biomass measurements (Roy and Ravan, 1996; Heiskanen, 2006; Cohen *et al.*, 2003). Spatial texture algorithms can improve biomass estimations by quantifying the spatial characteristics of images, such as contrast, objects, edge features, and heterogeneity (Sarker and Nichol, 2011; see Volume 2C—Section 6). Vegetation canopy attributes include fractional cover, clumping, LAI, and shadow fraction, and are used as proxies of AGB (see Section 6). Other important canopy structural quantities in deriving foliage biomass and total standing biomass in forests are tree height, crown size and area, density, and shadow fraction (Franklin and Hiernaux, 1991; Greenberg *et al.*, 2005; Leboeuf *et al.*, 2007; see Section 16). Spectral unmixing models (Hall *et al.*, 1995) and canopy reflectance models, such as the Li–Strahler geometric-optical model, can retrieve crown size, tree shadow, and density in satellite imagery (Li and Strahler, 1985; see Volumes 1X and 2X).

ML algorithms are increasingly being used in biomass estimation efforts (see Section 14.5). These non-parametric approaches have been used to estimate forest AGB with time series MODIS reflectances and environmental data over large regional areas in California (Baccini *et al.*, 2004), Africa (Baccini *et al.*, 2008), and Russia (Houghton *et al.*, 2007), as well as for AGB estimates over grasslands in Mongolia and Inner Mongolia (John *et al.*, 2018). Similarly, random forests were used to calculate biomass at regional scales using many other types of satellite data (Breiman, 2001; Powell *et al.*, 2010; Karlson *et al.*, 2015). However, both empirical and ML approaches for AGB estimations remain impracticable to directly transfer across biomes, or even different vegetation phenological stages, and saturation is a common problem.

Allometric models are a physically-based approach for the estimation of forest AGB. The simplest and most commonly used allometric models relate tree diameter at breast height (DBH) to AGB as a power function (see Section 16.5). More sophisticated models employ a wider range of forest variable measurements (e.g. canopy crown size, crown depth, tree height, and stem diameter) to derive AGB based on field observations (TerMikaelian and Korzukhin, 1997). Although the tree allometric models are generally species-specific and site-specific, they can be generalised to estimate biomass in mixed species across larger regions (Wirth *et al.*, 2004). For example, general allometric models were derived using linear least squares regression from field measurements of conifer, deciduous and mixed trees (Zhang and Kondragunta, 2006).

17.7.2 Soil organic carbon

EO of soil organic carbon (SOC) builds upon laboratory-based spectral measurements of soils in visible-to-SWIR EM wavelengths that have been conducted since the mid-1990s (Ben-Dor *et al.*, 1999; Rossel *et al.*, 2006). Organic matter influences the shape of a soil spectral signature due to vibrations of O-H and C-H bonds linked to lignin and cellulose and laboratory-based spectral measurements have been shown to accurately estimate soil organic carbon (Ben-Dor *et al.*, 1997; see Volume 1B—Section 6.3). Using a fuzzy clustering method to classify over 1500 soil samples, Shi *et al.* (2014) found that the soil clusters generally decreased in their reflectance with increasing SOC content (soil darkening).

Several studies have successfully mapped SOC content at landscape and regional scales using visible-to-SWIR satellite imagery (Jarmer *et al.*, 2010), the hyperspectral Hyperion sensor (Gomez *et al.*, 2008), and hyperspectral

airborne sensors (Hbirkou *et al.*, 2012). Landsat and MODIS data have been used for SOC content mapping, either as spectral bands (Were *et al.*, 2015; Grinand *et al.*, 2017) or through biophysical variables, such as NDVI and percent vegetation cover (Gray *et al.*, 2015; Mishra *et al.*, 2010; Somarathna *et al.*, 2016). Using such satellite sensors, Wang *et al.* (2018) found large variability in the performance of SOC stock estimations over semi-arid rangelands of eastern Australia. Long term MODIS satellite data can also be used to examine the trends in SOC at regional scales (Chen *et al.*, 2019).

Further progress has been made in SOC mapping by incorporating SpectroTransfer Functions (STFs) that link soil properties measured by laboratory analysis with the visible-to-SWIR imagery (Gomez *et al.*, 2008; Stevens *et al.*, 2010). The STFs can only be applied over exposed bare soils, such as croplands during ploughing periods (Bartholomeus *et al.*, 2011), bare soil pixels in arid ecosystems, and exposed soils resulting from ecosystem disturbances (Jarmer *et al.*, 2010). Other studies have successfully estimated SOC content using STFs with laboratory (Rossel and Hicks, 2015; Guo *et al.*, 2019), field (Cambou *et al.*, 2016), and image data (Guo *et al.*, 2019). In another STF approach, each variable associated with SOC stocks (soil organic matter, soil bulk density) is separately estimated followed by an equation linking SOC to these variables (Mishra *et al.*, 2010).

One can also incorporate environmental data with soil properties determined through visible-to-SWIR laboratory analysis by use of SCORPAN (Soil properties, Climate properties, Organisms, Relief setting, Parent material, Age, and the spatial coordinate, N) ML techniques (McBratney *et al.*, 2003). The SCORPAN models are mainly based on random forest and boosted regression trees (Wang *et al.*, 2018). As they use environmental variables indirectly linked to SOC content, they potentially have higher mapping coverage than STF models and can be applied over croplands, rangelands, shrublands, and grasslands. Wang *et al.* (2018) showed that the use of seasonal fractional cover data derived from visible-to-SWIR image data in association with environmental predictors (climate, parent material, and relief) improved the performance of SOC stock prediction.

17.7.3 Microwave EO

Microwave EO sensors, including ‘passive’ radiometers and ‘active’ scatterometers, have been used in forest estimates of AGB since the early 1990’s (see Excursus 6.1 and Section 16.5). Spaceborne SAR can observe under all-weather conditions, and is of particular use for the estimation of forest AGB over

areas covered by cloud all year (see Volume 1B—Section 8). Le Toan *et al.* (1992) observed the strong correlation of L- and P-band SAR backscattering coefficients with red pine biomass, and Dobson *et al.* (1992) reported a strong dependency of the backscatter of airborne polarimetric SAR at P-, L-, and C-bands on AGB of conifer forests. Generally, the penetration of microwaves into the forest varies positively with longer wavelengths, such as L-band (23.5 cm) and P-band (70.0 cm; see Section 16). Later studies estimated forest biomass with multi-band and multi-polarisation SAR data (e.g. Ranson and Sun, 2000; Ni *et al.*, 2016) and interferometric coherence (Luckman *et al.*, 2000). These studies showed that the SAR backscatter increased almost linearly with increasing biomass until it saturates at a biomass level that depends on the radar frequency.

Mitchell *et al.* (2017) conducted a review of methods for assessments of forest degradation and their role in carbon emissions for national reporting within the framework of UN REDD+. Various assessment methods exist employing multi-resolution SAR and/or optical and lidar data. They reviewed two main approaches for monitoring forest degradation, with the first being the detection of changes in canopy cover, and the second involving the quantification of loss (or gain) in AGB. They concluded that improvements in canopy cover change detections were being made through SAR-optical data fusion and the use of very high resolution data, while increased sensitivities to forest structure and biomass were being achieved using repeat SAR with lidar data. They further noted progress in discrimination of forest age and growth stage using data fusion methods and lidar height metrics, and new interferometric SAR and lidar applications in linking changes in forest structure to degradation in tropical forests (Mitchell *et al.*, 2017).

Neither the SAR backscattering coefficients nor the interferometric coherence are a direct measurement of forest AGB, but instead they directly measure the canopy spatial structure, characterised by tree density, tree height, and/or tree diameter at breast height (DBH; see Section 16.5). Novel methods for direct measurements of forest spatial structure employ modern SAR methods, such as Polarimetric Interferometric Synthetic Aperture Radar (PolInSAR) and three-dimensional point cloud tomographic SAR (TomoSAR) data (Frey *et al.*, 2008), that can directly detect the three-dimensional structure of forest, reduce the biomass saturation problem, and provide improved methods for monitoring forest AGB. Currently, PolInSAR and TomoSAR data are only acquired by airborne sensors, however, their potential advantages in AGB estimations will be fully explored with the upcoming BIOMASS (Europe), NISAR (USA, India), and Tandem-L (Germany) missions, scheduled in 2020–2022 timeframes (Le Toan *et al.*, 2011).

17.7.4 Lidar and above ground biomass

Lidar is an active remote sensing technology that offers much potential for terrestrial carbon assessments and for quantifying AGB in forests (Lefsky *et al.* 2005; see Section 16.5), shrublands, and grasslands (Li *et al.*, 2017; see Excursus 5.1). Opportunities to fuse temporally dynamic vegetation optical measurements with lidar have promising potential for better assessments of not only standing wood biomass, but also forest disturbance, biomass loss, and carbon accumulation through forest regrowth (Asner *et al.* 2007). Lidar can also serve as a reliable replacement for inventory plots in areas lacking field data.

Terrestrial laser scanning (TLS; see Excursus 5.1) provides very detailed vertical structure data for forests, enabling separation of points from trunk, branch, and leaves (Liang *et al.*, 2016; see Volume 1A—Section 10). The quantitative, three-dimensional laser point information provided can be used in structural models (Disney *et al.*, 2018) or for development of allometric equations to estimate AGB (Kankare *et al.*, 2013). Thus, lidar integration with field inventory plots can provide calibrated lidar estimates of above ground carbon stocks, which can then be scaled up using satellite data on vegetation cover, topography, and rainfall from satellite data to model carbon stocks.

Airborne laser scanners (ALS) are increasingly being used to estimate larger scale forest AGB, through its capability to quantify height, density, crown width, and crown volume at scales from individual trees to

more extensive forest stands (Popescu *et al.*, 2018; Tao *et al.*, 2014; see Volume 1A—Section 15.1). The larger airborne footprint waveform data has also led to reasonable biomass estimates for a variety of forest types (Drake *et al.*, 2002). The Global Observation of Forest Cover and Land Dynamics (GOFC-GOLD) program recommended the use of ALS data for biomass estimation in local efforts in reducing emissions from deforestation and forest degradation (REDD+; GOFC-GOLD, 2016).

Several spaceborne lidar sensors have also been utilised in larger scale canopy structure studies and for estimates of AGB. The Geoscience Laser Altimeter System (GLAS) aboard the ICESat satellite was shown to be able to estimate forest AGB in pan-tropical and temperate forests (Baccini *et al.*, 2008; Saatchi *et al.*, 2011; Lefsky *et al.*, 2005; see Excursus 6.1). New generation lidar instruments are becoming available, such as the Advanced Topographic Laser Altimeter System (ATLAS) and the Global Ecosystem Dynamics Investigation (GEDI). The GEDI system, launched in December 2018, contains a three-laser system flying on the International Space Station (ISS), and the full waveform lidar has a circular footprint of ~25 m (Stavros *et al.*, 2017). It is the first spaceborne lidar mission specifically designed to study forests and facilitate the estimation of AGB at large scales. As with the airborne instruments, the retrievable structural height and density metrics can be combined with biomass data from field plots or TLS data to build biomass estimation models (Zhao *et al.*, 2009).

17.8 The Future

New space-based observations can strongly complement *in situ* observations in providing required quantitative ecosystem information globally (see Sections 19 and 20). While spaceborne measurements have uncertainty and bias errors of their own, they can help in reducing bias errors associated with relatively sparse *in situ* systems. Given the challenges of long term, *in situ* observations at regional scales, satellite measurements have made increasingly important contributions, complementing the detailed information available *in situ* by providing broad spatial and temporal coverage.

New space-based observations, including fluorescence, hyperspectral, thermal, and lidar are greatly expanding the number of ecosystem properties that can be quantified from space. Many of the key fluxes and stocks shown in Figure 17.1, Figure 17.2 and Figure 17.10, can, or will soon, be estimated using EO instruments and techniques. Combined, they now enable a more thorough

coupling of the environmental conditions that plants experience with improved characterisation of their biophysical states, and with better monitoring capabilities to track plant responses to environmental changes. These advances are providing a better understanding of the dynamics of terrestrial productivity and the use of satellite data to drive productivity models of the land surface.

To have comprehensive knowledge of carbon stocks and fluxes everywhere and over time involves the coordination of *in situ* and remote observations. It still remains a challenge to develop such a coherent set of terrestrial ecosystem observations of the carbon cycle, and be able to develop early warning and prediction capabilities of carbon cycle feedbacks. All of these observations will have the common goal of helping us better understand our planet and understand how it is changing to benefit food, health, and economic security.

17.9 Further Information

Additional Reading

Viscarra Rossel, R.A., Webster, R., Bui, E.N., and Baldock, J.A. (2014). Baseline map of organic carbon in Australian soil to support national carbon accounting and monitoring under climate change. *Global Change Biology*, 20(9), 2953–2970. <https://doi.org/10.1111/gcb.12569>

Angelopoulou, T., Tziolas, N., Balafoutis, A., Zalidis, G., and Bochtis, D. (2019). Remote sensing techniques for soil organic carbon estimation: A review. *Remote Sensing*, 11(6), 1–18. <https://doi.org/10.3390/rs11060676>

Global Projects

UN Global Forest Observations Initiative (GFOI): <http://www.fao.org/gfoi>

Reducing Emissions from Deforestation and Forest Degradation in Developing Countries (REDD+): <https://redd.unfccc.int/>

Australia

National Inventory System (NIS; formerly National Carbon Accounting System: NCAS): <https://www.industry.gov.au/data-and-publications/national-inventory-reports>

National Greenhouse Accounts (Land sector estimates): <https://www.industry.gov.au/data-and-publications/land-sector-estimates-may-2017-update>

Climate Change Strategies: <https://www.industry.gov.au/strategies-for-the-future/australias-climate-change-strategies>

National Greenhouse and Energy Reporting: <http://www.cleanenergyregulator.gov.au/NGER/About-the-National-Greenhouse-and-Energy-Reporting-scheme>

International Forest Carbon Initiative: Australia's IFCI supported global efforts to establish a REDD+ mechanism under the UNFCCC. Jointly administered by the Australian Department of Climate Change and Energy Efficiency and AusAID, the Initiative enabled Australia to work closely with developing countries to find practical ways to reduce forest emissions: <https://www.unredd.net/partners/103-international-forest-carbon-initiative-australia-.html>

Roxburg, S., Karunaratne, S., and Paul, K. (2017). *A revised above-ground maximum biomass layer for Australia's national carbon accounting system*. CSIRO Land and Water, Canberra. <https://publications.csiro.au/rpr/download?pid=csiro:EP181854anddsid=DS1>

NASA

The Carbon Cycle: <https://www.earthobservatory.nasa.gov/features/CarbonCycle/page1.php>

A New Space-Based View of Human Made Carbon Dioxide: <https://www.jpl.nasa.gov/news/news.php?feature=6666>

Orbiting Carbon Observatory-2: <https://ocov2.jpl.nasa.gov/>

17.10 References

Angert, A., Biraud, S., Bonfils, C., Henning, C.C., Buermann, W., Pinzon, J., Tucker, C.J., and Fung, I. (2005). Drier summers cancel out the CO₂ uptake enhancement induced by warmer springs. *Proceedings of the National Academy of Science*, 102(31), 10823–10827.

Asner, G.P., Knapp, D.E., Kennedy-Bowdoin, T., Jones, M.O., Martin, R.E., Boardman, J., and Field, C.B. (2007). Carnegie Airborne Observatory: in-flight fusion of hyperspectral imaging and waveform light detection and ranging (wLiDAR) for three-dimensional studies of ecosystems. *Journal of Applied Remote Sensing*, 1, 013536.

Asrar, G., Fuchs, M., Kanemasu, E.T., Hatfield, J.L. (1984). Estimating absorbed photosynthetic radiation and leaf-area index from spectral reflectance in wheat. *Agronomy Journal*, 76, 300–306.

Baccini, A., Friedl, M.A., Woodcock, C.E., and Warbington, R. (2004). Forest biomass estimation over regional scales using multisource data. *Geophysical Research Letters*, 31, L10501.

Baccini, A., Laporte, N., Goetz, S.J., Sun, M., and Dong, H. (2008). A first map of tropical Africa's above-ground biomass derived from satellite imagery. *Environmental Research Letters*, 3, 045011.

Baker, N.R. (2008). Chlorophyll fluorescence: A probe of photosynthesis in vivo. *Annual Review of Plant Biology*, 59, 89–113.

- Baldocchi, D., Falge, E., Lianhong, G., Olson, R., Hollinger, D., Running, S., Anthoni, P., Bernhofer, C., Davis, K., Evans, R., Fuentes, J., Goldstein, A., Katul, G., Law, B., Xuhui, L., Malhi, Y., Meyers, T., Munger, W., Oechel, W., and Paw U, K.T. (2001). FLUXNET: A New Tool to Study the Temporal and Spatial Variability of Ecosystem-Scale Carbon Dioxide, Water Vapor, and Energy Flux Densities. *Bulletin of the American Meteorological Society*, 82(11), 2415–2434.
- Bartholomeus, H., Kooistra, L., Stevens, A., van Leeuwen, M., van Wesemael, B., Ben-Dor, E., and Tychon, B. (2011). Soil organic carbon mapping of partially vegetated agricultural fields with imaging spectroscopy. *International Journal of Applied Earth Observation and Geoinformation*, 13, 81–88.
- Basu, S., Guerlet, S., Butz, A., Houweling, S., Hasekamp, O., Aben, I., Krummel, P., Steele, P., Langenfelds, R., Torn, M., Biraud, S., Stephens, B., Andrews, A., and Worthy, D. (2013). Global CO₂ fluxes estimated from GOSAT retrievals of total column CO₂. *Atmospheric Chemistry and Physics*, 13, 8695–8717.
- Ben-Dor, E., Inbar, Y., and Chen, Y. (1997). The reflectance spectra of organic matter in the visible near-infrared and short wave infrared region (400–2500 nm) during a controlled decomposition process. *Remote Sensing of Environment*, 61, 1–15.
- Ben-Dor, E., Irons, J.A., and Epema, G.F. (1999). Soil reflectance. In *Manual of Remote Sensing: Remote Sensing for the Earth Sciences*. John Wiley and Sons Inc, New York. pp. 111–189.
- Breiman, L. (2001). Random forests. *Machine Learning*, 45, 5–32.
- Cambou, A., Cardinael, R., Kouakoua, E., Villeneuve, M., Durand, C., and Barthes, B.G. (2016). Prediction of soil organic carbon stock using visible and near infrared reflectance spectroscopy (VNIRS) in the field. *Geoderma*, 261, 151–159.
- Chambers, J.Q., Negrón-Juárez, R.I., Hurtt, G.C., Marra, D.M., and Higuchi, N. (2009). Lack of intermediate-scale disturbance data prevents robust extrapolation of plot-level tree mortality rates for old-growth tropical forests. *Ecology Letters*, 12(12), E22–E5.
- Chen, D., Chang, N.J., Xiao, J.F., Zhou, Q.B., and Wu, W.B. (2019). Mapping dynamics of soil organic matter in croplands with MODIS data and machine learning algorithms. *Science of the Total Environment*, 669, 844–855.
- Chopping, M., Schaaf, C.B., Zhao, F., Wang, Z.S., Nolin, A.W., Moisen, G.G., Martonchik, J.V., and Bull, M. (2011). Forest structure and aboveground biomass in the southwestern United States from MODIS and MISR. *Remote Sensing of Environment*, 115, 2943–2953.
- Churkina, G., and Running, S.W. (1998). Contrasting climatic controls on the estimated productivity of global terrestrial biomes. *Ecosystems*, 1, 2, 206–215.
- Cleverly, J., Boulain, N., Villalobos-Vega, R., Grant, N., Faux, R., Wood, C., Cook, P.G., Yu, Q., Leigh, A., and Eamus, D. (2013). Dynamics of component carbon fluxes in a semi-arid *Acacia* woodland, central Australia. *Journal of Geophysical Research: Biogeosciences*, 118, 3, 1168–1185.
- Cohen, W.B., Maersperger, T.K., Gower, S.T., and Turner, D.P. (2003). An improved strategy for regression of biophysical variables and Landsat ETM+ data. *Remote Sensing of Environment*, 84, 561–571.
- Cramer, W., Kicklighter, D., Bondeau, A., Iii, B.M., Churkina, G., Nemry, B., Ruimy, A., Schloss, A., Intercomparison, T., and Model, P.O.T.P.N. (1999). Comparing global models of terrestrial net primary productivity (NPP): overview and key results. *Global Change Biology*, 5(S1), 1–15.
- Dash, J., and Curran, P.J. (2004). The MERIS terrestrial chlorophyll index. *International Journal of Remote Sensing*, 25, 5403–5413.
- Disney, M.I., Vicari, M.B., Burt, A., Calders, K., Lewis, S.L., Raunonen, P., and Wilkes, P. (2018). Weighing trees with lasers: advances, challenges and opportunities. *Interface Focus*, 8, 20170048.
- Dobson, M.C., Ulaby, F.T., LeToan, T., Beaudoin, A., Kasichke, E.S., and Christensen, N. (1992). Dependence of radar backscatter on coniferous forest biomass. *IEEE Transactions on Geoscience and Remote Sensing*, 30, 412–415.
- Donohue, R.J., Roderick, M.L., McVicar, T.R., and Farquhar, G.D. (2013). Impact of CO₂ fertilization on maximum foliage cover across the globe's warm, arid environments. *Geophysical Research Letters*, 40, 3031–3035.
- Drake, J.B., Dubayah, R.O., Clark, D.B., Knox, R.G., Blair, J.B., Hofton, M.A., Chazdon, R.L., Weishampel, J.F., and Prince, S.D. (2002). Estimation of tropical forest structural characteristics using large-footprint lidar. *Remote Sensing of Environment*, 79, 305–319.
- Epstein, H.E., Reynolds, M.K., Walker, D.A., Bhatt, U.S., Tucker, C.J., and Pinzon, J.E. (2012). Dynamics of aboveground phytomass of the circumpolar Arctic tundra during the past three decades. *Environmental Research Letters*, 7, 015506.

- FAO (2007). *State of the World's Forests*. UN Food and Agriculture Organisation, Rome.
- Fensholt, R., Sandholt, I., and Rasmussen, M.S. (2004). Evaluation of MODIS LAI, fAPAR and the relation between fAPAR and NDVI in a semi-arid environment using *in situ* measurements. *Remote Sensing of Environment*, 91(3–4), 490–507.
- Field, C.B., Randerson, J.T., and Malmstrom, C.M. (1995). Global net primary production: combining ecology and remote sensing. *Remote Sensing of Environment*, 51, 74–88.
- Flexas, J., Escalona, J.M., Evain, S., Gulías, J., Moya, I., Osmond, C.B., and Medrano, H. (2002). Steady-state chlorophyll fluorescence (Fs) measurements as a tool to follow variations of net CO₂ assimilation and stomatal conductance during water-stress in C3 plants. *Physiologia Plantarum*, 114(2), 231–240.
- Frankenberg, C., Fisher, J.B., Worden, J., Badgley, G., Saatchi, S.S., Lee, J.-E., Toon, G.C., Butz, A., Jung, M., Kuze, A., and Yokota, T. (2011). New global observations of the terrestrial carbon cycle from GOSAT: Patterns of plant fluorescence with gross primary productivity. *Geophysical Research Letters*, 38, L17706.
- Franklin, J., and Hiernaux, P.H.Y. (1991). Estimating foliage and woody biomass in Sahelian and Sudanian woodlands using a remote sensing model. *International Journal of Remote Sensing*, 12, 1387–1404.
- Frey, O., Morsdorf, F., and Meier, E. (2008). Tomographic imaging of a forested area by airborne multi-baseline P-band SAR. *Sensors*, 8, 5884–5896.
- Friedl, M.A., Michaelsen, J., Davis, F.W., Walker, H., and Schimel, D.S. (1994). Estimating grassland biomass and leaf area index using ground and satellite data. *International Journal of Remote Sensing*, 15, 1401–1420.
- Friedl, M.A., Sulla-Menashe, D., Tan, B., Schneider, A., Ramankutty, N., Sibley, A., Huang, X.M. (2010). MODIS collection 5 global land cover: algorithm refinements and characterization of new datasets. *Remote Sensing of Environment*, 114, 168–182.
- Friedlingstein P., Jones, M.W., O'Sullivan, M., Andrew, R. M., Hauck, J., Peters, G. P., Peters, W., Pongratz, J., Sitch, S., Le Quéré, C., Bakker, D. C. E., Canadell, J. G., Ciais, P., Jackson, R. B., Anthoni, P., Barbero, L., Bastos, A., Bastrikov, V., Becker, M., Bopp, L., Buitenhuis, E., Chandra, N., Chevallier, F., Chini, L. P., Currie, K. I., Feely, R. A., Gehlen, M., Gilfillan, D., Gkritzalis, T., Goll, D. S., Gruber, N., Gutekunst, S., Harris, I., Haverd, V., Houghton, R. A., Hurtt, G., Ilyina, T., Jain, A. K., Joetzjer, E., Kaplan, J. O., Kato, E., Klein Goldewijk, K., Korsbakken, J. I., Landschützer, P., Lauvset, S. K., Lefèvre, N., Lenton, A., Lienert, S., Lombardozzi, D., Marland, G., McGuire, P. C., Melton, J. R., Metzl, N., Munro, D. R., Nabel, J. E. M. S., Nakaoka, S.-I., Neill, C., Omar, A. M., Ono, T., Peregon, A., Pierrot, D., Poulter, B., Rehder, G., Resplandy, L., Robertson, E., Rödenbeck, C., Séférian, R., Schwinger, J., Smith, N., Tans, P. P., Tian, H., Tilbrook, B., Tubiello, F. N., van der Werf, G. R., Wiltshire, A. J., and Zaehle, S. (2019). Global Carbon Budget 2019. *Earth System Sciences and Data*, 11, 1783–1838.
- Fuchs, H., Magdon, P., Kleinn, C., and Flessa, H. (2009). Estimating aboveground carbon in a catchment of the Siberian forest tundra: combining satellite imagery and field inventory. *Remote Sensing of Environment*, 113, 518–531.
- Gamon, J.A., Serrano, L., and Surfus, J.S. (1997). The photochemical reflectance index: an optical indicator of photosynthetic radiation use efficiency across species, functional types, and nutrient levels. *Oecologia*, 112, 492–501.
- Gitelson, A.A. (2004). Wide dynamic range vegetation index for remote quantification of biophysical characteristics of vegetation. *Journal of Plant Physiology*, 161, 165–173.
- Gitelson, A.A., Viña, A., Verma, S.B., Rundquist, D.C., Arkebauer, T.J., Keydan, G., Leavitt, B., Ciganda, V., Burba, G.G., and Suyker, A.E. (2006). Relationship between gross primary production and chlorophyll content in crops: Implications for the synoptic monitoring of vegetation productivity. *Journal of Geophysical Research: Atmospheres*, 111(D8), D08S11.
- Gitelson, A.A., Peng, Y., Arkebauer, T.J., and Schepers, J. (2014). Relationships between gross primary production, green LAI, and canopy chlorophyll content in maize: Implications for remote sensing of primary production. *Remote Sensing of Environment*, 144, 65–72.

- Glenn, E.P., Huete, A.R., Nagler, P.L., and Nelson, S.G. (2008). Relationship between remotely sensed vegetation indices, canopy attributes and plant physiological processes: what vegetation indices can and cannot tell us about the landscape. *Sensors*, 8, 2136–2160.
- Goerner, A., Reichstein, M., and Rambal, S. (2009). Tracking seasonal drought effects on ecosystem light use efficiency with satellite-based PRI in a Mediterranean forest. *Remote Sensing of Environment*, 113(5), 1101–1111.
- GOFC-GOLD (2016). A sourcebook of methods and procedures for monitoring and reporting anthropogenic greenhouse gas emissions and removals associated with deforestation, gains and losses of carbon stocks in forests remaining forests, and forestation. In *GOFC-GOLD Report Version COP22-1*. GOFC-GOLD Land Cover Project Office, Wageningen University, The Netherlands.
- Gomez, C., Rossel, R.A.V., and McBratney, A.B. (2008). Soil organic carbon prediction by hyperspectral remote sensing and field vis-NIR spectroscopy: an Australian case study. *Geoderma*, 146, 403–411.
- Goward, S.N., Tucker, C.J., and Dye, D.G. (1985). North American vegetation patterns observed with the NOAA-7 advanced very high resolution radiometer. *Vegetatio*, 64, 3–14.
- Goward, S.N., and Huemmrich, K.F. (1992). Vegetation canopy PAR absorptance and the normalized difference vegetation index: an assessment using the SAIL model. *Remote Sensing of Environment*, 39, 119–140.
- Gower, S.T., Kucharik, C.J., and Norman, J.M. (1999). Direct and Indirect Estimation of Leaf Area Index, fAPAR, and Net Primary Production of Terrestrial Ecosystems. *Remote Sensing of Environment*, 70(1), 29–51.
- Gray, J.M., Bishop, T.F.A., and Wilson, B.R. (2015). Factors controlling soil organic carbon stocks with depth in eastern Australia. *Soil Science Society of America Journal*, 79, 1741–1751.
- Greenberg, J.A., Dobrowski, S.Z., and Ustin, S.L. (2005). Shadow allometry: estimating tree structural parameters using hyperspatial image analysis. *Remote Sensing of Environment*, 97, 15–25.
- Grinand, C., Le Maire, G., Vieilledent, G., Razakarnanarivo, H., Razafimbelo, T., and Bernoux, M. (2017). Estimating temporal changes in soil carbon stocks at ecoregional scale in Madagascar using remote-sensing. *International Journal of Applied Earth Observation and Geoinformation*, 54, 1–14.
- Guo, L., Zhang, H., Shi, T., Chen, Y., Jiang, Q., and Linderman, M. (2019). Prediction of soil organic carbon stock by laboratory spectral data and airborne hyperspectral images. *Geoderma*, 337, 32–41.
- Guanter, L., Y. Zhang, M. Jung, J. Joiner, M. Voigt, J. A. Berry, C. Frankenberg, A. Huete, P. Zarco-Tejada, J.-E. Lee, M.S. Moran, G. Ponce-Campos, C. Beer, G. Camps-Valls, N. Buchmann, D. Gianelle, K. Klumpp, A. Cescatti, J.M. Baker, and T.J. Griffis. (2014) Global and time-resolved monitoring of crop photosynthesis with chlorophyll fluorescence. *Proceedings of the National Academy of Sciences*, 111(14), E1327–E1333.
- Hall, F.G., Shimabukuro, Y.E., and Huemmrich, K.F. (1995). Remote sensing of forest biophysical structure using mixture decomposition and geometric reflectance models. *Ecological Applications*, 5, 993–1013.
- Hansen, M.C., Potapov, P.V., Moore, R., Hancher, M., Turubanova, S.A., Tyukavina, A., Thau, D., Stehman, S.V., Goetz, S.J., Loveland, T.R., Kommareddy, A., Egorov, A., Chini, L., Justice, C.O., and Townshend, J.R.G. (2013). High-resolution global maps of 21st-century forest cover change. *Science*, 342, 850–853.
- Haverd, V., Raupach, M., Briggs, P., Canadell, J., Davis, S., Law, R., Meyer, C., Peters, G., Pickett-Heaps, C., Sherman, B. (2013). The Australian terrestrial carbon budget. *Biogeosciences*, 10, 851–869. doi:10.5194/bg-10-851-2013
- Hbirkou, C., Patzold, S., Mahlein, A.K., and Welp, G. (2012). Airborne hyperspectral imaging of spatial soil organic carbon heterogeneity at the field-scale. *Geoderma*, 175, 21–28.
- Heinsch, F.A., Zhao, M.S., Running, S.W., Kimball, J.S., Nemani, R.R., Davis, K.J., Bolstad, P.V., Cook, B.D., Desai, A.R., Ricciuto, D.M., Law, B.E., Oechel, W.C., Kwon, H., Luo, H.Y., Wofsy, S.C., Dunn, A.L., Munger, J.W., Baldocchi, D.D., Xu, L.K., Hollinger, D.Y., Richardson, A.D., Stoy, P.C., Siqueira, M.B.S., Monson, R.K., Burns, S.P., and Flanagan, L.B. (2006). Evaluation of remote sensing based terrestrial productivity from MODIS using regional tower eddy flux network observations. *IEEE Transactions on Geoscience and Remote Sensing*, 44, 1908–1925.
- Heiskanen, J. (2006). Estimating aboveground tree biomass and leaf area index in a mountain birch forest using ASTER satellite data. *International Journal of Remote Sensing*, 27, 1135–1158.

- Houghton, R.A., Butman, D., Bunn, A.G., Krankina, O.N., Schlesinger, P., and Stone, T.A. (2007). Mapping Russian forest biomass with data from satellites and forest inventories. *Environmental Research Letters*, 2, 045032.
- Huete, A.R., Didan, K., Shimabukuro, Y.E., Ratana, P., Saleska, S.R., Hutyra, L.R., Yang, W.Z., Nemani, R.R., and Myneni, R. (2006). Amazon rainforests green-up with sunlight in dry season. *Geophysical Research Letters*, 33, L06405.
- Huete, A.R., Restrepo-Coupe, N., Ratana, P., Didan, K., Saleska, S.R., Ichii, K., Panuthai, S., and Gamo, M. (2008). Multiple site tower flux and remote sensing comparisons of tropical forest dynamics in Monsoon Asia. *Agricultural and Forest Meteorology*, 148, 748–760.
- Ichii, K., Hashimoto, H., White, M.A., Potters, C., Hutyra, L.R., Huete, A.R., Myneni, R.B., and Nemani, R.R. (2007). Constraining rooting depths in tropical rainforests using satellite data and ecosystem modeling for accurate simulation of gross primary production seasonality. *Global Change Biology*, 13, 67–77.
- Jagermeyr, J., Gerten, D., Lucht, W., Hostert, P., Migliavacca, M., and Nemani, R. (2014). A high-resolution approach to estimating ecosystem respiration at continental scales using operational satellite data. *Global Change Biology*, 20, 1191–1210.
- Jarmer, T., Hill, J., Lavee, H., and Sarah, P. (2010). Mapping topsoil organic carbon in nonagricultural semi-arid and arid ecosystems of Israel. *Photogrammetric Engineering and Remote Sensing*, 76, 85–94.
- Jenkins, J.P., Richardson, A.D., Braswell, B.H., Ollinger, S.V., Hollinger, D.Y., and Smith, M.L. (2007). Refining light-use efficiency calculations for a deciduous forest canopy using simultaneous tower-based carbon flux and radiometric measurements. *Agricultural and Forest Meteorology*, 143(1–2), 64–79.
- Jin, C., Xiao, X., Merbold, L., Arneith, A., Veenendaal, E., and Kutsch, W.L. (2013). Phenology and gross primary production of two dominant savanna woodland ecosystems in Southern Africa. *Remote Sensing of Environment*, 135, 189–201.
- John, R., Chen, J.Q., Giannico, V., Park, H., Xiao, J.F., Shirkey, G., Ouyang, Z.T., Shao, C.L., Laforteza, R., and Qi, J.G. (2018). Grassland canopy cover and aboveground biomass in Mongolia and Inner Mongolia: spatiotemporal estimates and controlling factors. *Remote Sensing of Environment*, 213, 34–48.
- Joiner, J., Yoshida, Y., Vasilkov, A.P., Yoshida, Y., Corp, L.A., and Middleton, E.M. (2011). First observations of global and seasonal terrestrial chlorophyll fluorescence from space. *Biogeosciences*, 8, 637–651.
- Jones, L.A., Kimball, J.S., Reichle, R.H., Madani, N., Glassy, J., Ardizzone, J.V., Colliander, A., Cleverly, J., Desai, A.R., Eamus, D., Euskirchen, E.S., Hutley, L., Macfarlane, C., and Scott, R.L. (2017). The SMAP level 4 carbon product for monitoring ecosystem land-atmosphere CO₂ exchange. *IEEE Transactions on Geoscience and Remote Sensing*, 55, 6517–6532.
- Kankare, V., Holopainen, M., Vastaranta, M., Puttonen, E., Yu, X.W., Hyypä, J., Vaaja, M., Hyypä, H., and Alho, P. (2013). Individual tree biomass estimation using terrestrial laser scanning. *ISPRS Journal of Photogrammetry and Remote Sensing*, 75, 64–75.
- Kanniah, K.D., Beringer, J., Hutley, L.B., Tapper, N.J., and Zhu, X. (2009). Evaluation of Collections 4 and 5 of the MODIS Gross Primary Productivity product and algorithm improvement at a tropical savanna site in northern Australia. *Remote Sensing of Environment*, 113(9), 1808–1822.
- Kanniah, K.D., Beringer, J., and Hutley, L.B. (2011). Environmental controls on the spatial variability of savanna productivity in the Northern Territory, Australia. *Agricultural and Forest Meteorology*, 151(11), 1429–1439.
- Kanniah, K.D., Beringer, J., and Hutley, L. (2013). Exploring the link between clouds, radiation, and canopy productivity of tropical savannas. *Agricultural and Forest Meteorology*, 182–183, 304–313.
- Karlson, M., Ostwald, M., Reese, H., Sanou, J., Tankoano, B., and Mattsson, E. (2015). Mapping tree canopy cover and aboveground biomass in Sudano-Sahelian woodlands using Landsat-8 and random forest. *Remote Sensing*, 7, 10017–10041.
- Kimball, J.S., Jones, L.A., Zhang, K., Heinsch, F.A., McDonald, K.C., and Oechel, W.C. (2009). A satellite approach to estimate land-atmosphere CO₂ exchange for boreal and Arctic biomes using MODIS and AMSR-E. *IEEE Transactions on Geoscience and Remote Sensing*, 47, 569–587.
- Kotchenova, S.Y., and Vermote, E.F. (2007). Validation of a vector version of the 6S radiative transfer code for atmospheric correction of satellite data. Part II. Homogeneous Lambertian and anisotropic surfaces. *Applied Optics*, 46(20), 4455–4464.
- Le Toan, T., Beaudoin, A., Riou, J., and Guyon, D. (1992). Relating forest biomass to SAR data. *IEEE Transactions on Geoscience and Remote Sensing*, 30, 403–411.

- Le Toan, T., Quegan, S., Davidson, M.W.J., Balzter, H., Paillou, P., Papathanassiou, K., Plummer, S., Rocca, F., Saatchi, S., Shugart, H., and Ulander, L. (2011). The BIOMASS mission: mapping global forest biomass to better understand the terrestrial carbon cycle. *Remote Sensing of Environment*, 115, 2850–2860.
- Leboeuf, A., Beaudoin, A., Fournier, R.A., Guindon, L., Luther, J.E., and Lambert, M.C. (2007). A shadow fraction method for mapping biomass of northern boreal black spruce forests using Quick Bird imagery. *Remote Sensing of Environment*, 110, 488–500.
- Lefsky, M.A., Harding, D.J., Keller, M., Cohen, W.B., Carabajal, C.C., Espirito-Santo, F.D., Hunter, M.O., and de Oliveira, R. (2005). Estimates of forest canopy height and aboveground biomass using ICESat. *Geophysical Research Letters*, 32, L22S02.
- Leuning, R., Cleugh, H.A., Zegelin, S.J., and Hughes, D. (2005). Carbon and water fluxes over a temperate *Eucalyptus* forest and a tropical wet/dry savanna in Australia: measurements and comparison with MODIS remote sensing estimates. *Agricultural and Forest Meteorology*, 129(3–4), 151–173.
- Li, X.W., and Strahler, A.H. (1985). Geometric-optical modeling of a conifer forest canopy. *IEEE Transactions on Geoscience and Remote Sensing*, 23, 705–721.
- Li, A.H., Dhakal, S., Glenn, N.F., Spaete, L.P., Shinneman, D.J., Pilliod, D.S., Arkle, R.S., and McIlroy, S.K. (2017). Lidar aboveground vegetation biomass estimates in shrublands: prediction, uncertainties and application to coarser scales. *Remote Sensing*, 9, 903.
- Li, Z., Yu, G., Xiao, X., Li, Y., Zhao, X., Ren, C., Zhang, L., and Fu, Y. (2007). Modeling gross primary production of alpine ecosystems in the Tibetan Plateau using MODIS images and climate data. *Remote Sensing of Environment*, 107(3), 510–519.
- Liang, X.L., Kankare, V., Hyyppä, J., Wang, Y.S., Kukko, A., Haggren, H., Yu, X.W., Kaartinen, H., Jaakkola, A., Guan, F.Y., Holopainen, M., and Vastaranta, M. (2016). Terrestrial laser scanning in forest inventories. *ISPRS Journal of Photogrammetry and Remote Sensing*, 115, 63–77.
- Luckman, A., Baker, J., and Wegmuller, U. (2000). Repeat-pass interferometric coherence measurements of disturbed tropical forest from JERS and ERS satellites. *Remote Sensing of Environment*, 73, 350–360.
- Ma, X., Huete, A., Yu, Q., Coupe, N.R., Davies, K., Broich, M., Ratana, P., Beringer, J., Hutley, L.B., Cleverly, J., Boulain, N., and Eamus, D. (2013). Spatial patterns and temporal dynamics in savanna vegetation phenology across the North Australian Tropical Transect. *Remote Sensing of Environment*, 139, 97–115.
- Ma, X., Huete, A., Cleverly, J., Eamus, D., Chevallier, F., Joiner, J., Poulter, B., Zhang, Y., Guanter, L., Meyer, W., Xie, Z., and Ponce-Campos, G. (2016). Drought rapidly diminishes the large net CO₂ uptake in 2011 over semi-arid Australia. *Scientific Reports*, 6, 37747.
- Ma, X., Huete, A., Yu, Q., Restrepo-Coupe, N., Beringer, J., Hutley, L.B., Kanniah, K.D., Cleverly, J., and Eamus, D. (2014). Parameterization of an ecosystem light-use-efficiency model for predicting savanna GPP using MODIS EVI. *Remote Sensing of Environment*, 154, 253–271.
- Mahadevan, P., Wofsy, S.C., Matross, D.M., Xiao, X., Dunn, A.L., Lin, J.C., Gerbig, C., Munger, J.W., Chow, V.Y., and Gottlieb, E.W. (2008). A satellite-based biosphere parameterization for net ecosystem CO₂ exchange: Vegetation Photosynthesis and Respiration Model (VPRM). *Global Biogeochemical Cycles*, 22, GB2005.
- McBratney, A.B., Santos, M.L.M., and Minasny, B. (2003). On digital soil mapping. *Geoderma*, 117, 3–52.
- Meroni, M., Rossini, M., Guanter, L., Alonso, L., Rascher, U., Colombo, R., and Moreno, J. (2009). Remote sensing of solar-induced chlorophyll fluorescence: Review of methods and applications. *Remote Sensing of Environment*, 113(10), 2037–2051.
- Middleton, E.M., Huemmrich, K.F., Zhang, Q., Campbell, P.I.K.E., and Landis, D.R. (2018). Spectral bio-indicators of photosynthetic efficiency and vegetation stress. Ch 5 in Volume 3: *Biophysical and Biochemical Characterization and Plant Species Studies*, pp. 133–179, of *Hyperspectral Remote Sensing of Vegetation* 2nd edn. (Eds: Thenkabail, P.S., Lyon, J.G., and Huete, A.) Taylor and Francis.
- Mishra, U., Lal, R., Liu, D.S., and Van Meirvenne, M. (2010). Predicting the spatial variation of the soil organic carbon pool at a regional scale. *Soil Science Society of America Journal*, 74, 906–914.
- Mitchell, A.L., Rosenqvist, A., and Mora, B. (2017). Current remote sensing approaches to monitoring forest degradation in support of countries measurement, reporting and verification (MRV) systems for REDD+. *Carbon Balance and Management*, 12, 9. <https://doi.org/10.1186/s13021-017-0078-9>

- Monfreda, C., Ramankutty, N., and Foley, J.A. (2008). Farming the planet: 2. Geographic distribution of crop areas, yields, physiological types, and net primary production in the year 2000. *Global Biogeochemical Cycles*, 22, GB1022. <https://doi.org/10.1029/2007GB002947>
- Monteith, J.L. (1972). Solar-radiation and productivity in tropical ecosystems. *Journal of Applied Ecology*, 9, 747–766.
- Monteith, J.L., and Unsworth, M.H. (1990). *Principles of Environmental Physics*, 2nd edn. Antony Rowe Ltd., Eastbourne, U.K.
- Moore, D.J.P., Trahan, N.A., Wilkes, P., Quaife, T., Stephens, B.B., Elder, K., Desai, A.R., Negron, J., and Monson, R.K., (2013). Persistent reduced ecosystem respiration after insect disturbance in high elevation forests. *Ecological Letters*, 16, 731–737.
- Moran, M.S., Ponce-Campos, G.E., Huete, A., McClaran, M.P., Zhang, Y.G., Hamerlynck, E.P., Augustine, D.J., Gunter, S.A., Kitchen, S.G., Peters, D.P.C., Starks, P.J., and Hernandez, M. (2014). Functional response of U.S. grasslands to the early 21st-century drought. *Ecology*, 95, 2121–2133.
- Myneni, R.B., and Williams, D.L. (1994). On the relationship between FAPAR and NDVI. *Remote Sensing of Environment*, 49(3), 200–211.
- Myneni, R.B., Keeling, C.D., Tucker, C.J., Asrar, G., and Nemani, R.R. (1997). Increased plant growth in the northern high latitudes from 1981 to 1991. *Nature*, 386, 698–702.
- Myneni, R.B., Hoffman, S., Knyazikhin, Y., Privette, J.L., Glassy, J., Tian, Y., Wang, Y., Song, X., Zhang, Y., Smith, G.R., Lotsch, A., Friedl, M., Morisette, J.T., Votava, P., Nemani, R.R., and Running, S.W. (2002). Global products of vegetation leaf area and fraction absorbed PAR from year one of MODIS data. *Remote Sensing of Environment*, 83, 214–231.
- Nemani, R.R., Keeling, C.D., Hashimoto, H., Jolly, W.M., Piper, S.C., Tucker, C.J., Myneni, R.B., and Running, S.W. (2003). Climate-driven increases in global terrestrial net primary production from 1982 to 1999. *Science*, 300, 1560–1563.
- Ni, W., Sun, G., Zhang, Z., and Yu, H. (2016). Retrieval of forest aboveground biomass through the synergy of X-band (TeraSAR-X/TandDEM-X) and L-band (PALSAR-2) InSAR data. In *2016 IEEE International Geoscience and Remote Sensing Symposium (IGARSS)*. pp. 5304–5306.
- Olofsson, P., Lagergren, F., Lindroth, A., Lindström, J., Klemedtsson, L., Kutsch, W., and Eklundh, L. (2008). Towards operational remote sensing of forest carbon balance across Northern Europe. *Biogeosciences*, 5(3), 817–832.
- Palace, M., Keller, M., Asner, G.P., Hagen, S., and Braswell, B. (2008). Amazon forest structure from IKONOS satellite data and the automated characterization of forest canopy properties. *Biotropica*, 40, 141–150.
- Peng, Y., Gitelson, A.A., Keydan, G., Rundquist, D.C., and Moses, W. (2011). Remote estimation of gross primary production in maize and support for a new paradigm based on total crop chlorophyll content', *Remote Sensing of Environment*, 115(4), 978–989.
- Peng, Y., Gitelson, A.A., and Sakamoto, T. (2013). Remote estimation of gross primary productivity in crops using MODIS 250m data. *Remote Sensing of Environment*, 128, 186–196.
- Ponce-Campos, G.E., Moran, M.S., Huete, A., Zhang, Y.G., Bresloff, C., Huxman, T.E., Eamus, D., Bosch, D.D., Buda, A.R., Gunter, S.A., Scalley, T.H., Kitchen, S.G., McClaran, M.P., McNab, W.H., Montoya, D.S., Morgan, J.A., Peters, D.P.C., Sadler, E.J., Seyfried, M.S., and Starks, P.J. (2013). Ecosystem resilience despite large-scale altered hydroclimatic conditions. *Nature*, 494, 349–352.
- Popescu, S.C., Zhou, T., Nelson, R., Neuenschwande, A., Sheridan, R., Narine, L., and Walsh, K.M. (2018). Photon counting LiDAR: an adaptive ground and canopy height retrieval algorithm for ICESat-2 data. *Remote Sensing of Environment*, 208, 154–170.
- Porcar-Castell, A., Tyystjarvi, E., Atherton, J., van der Tol, C., Flexas, J., Pfundel, E.E., Moreno, J., Frankenberg, C., and Berry, J.A. (2014). Linking chlorophyll a fluorescence to photosynthesis for remote sensing applications: mechanisms and challenges. *Journal of Experimental Botany*, 65, 4065–4095.
- Potter, C.S., Randerson, J.T., Field, C.B., Matson, P.A., Vitousek, P.M., Mooney, H.A., and Klooster, S.A. (1993). Terrestrial ecosystem production: a process model based on global satellite and surface data. *Global Biogeochemical Cycles*, 7, 811–841.
- Powell, S.L., Cohen, W.B., Healey, S.P., Kennedy, R.E., Moisen, G.G., Pierce, K.B., and Ohmann, J.L. (2010). Quantification of live aboveground forest biomass dynamics with Landsat time-series and field inventory data: a comparison of empirical modeling approaches. *Remote Sensing of Environment*, 114, 1053–1068.
- Pyne, S.J. (1992). *The Burning Bush: A Fire History of Australia*. Allen and Unwin, Sydney. 520 p. ISBN: 1863731946
- Rahman, A.F., Sims, D.A., Cordova, V.D., and El-Masri, B.Z. (2005). Potential of MODIS EVI and surface temperature for directly estimating per-pixel ecosystem C fluxes. *Geophysical Research Letters*, 32(19), L19404.

- Ranson, K.J., and Sun, G. (2000). Effects of environmental conditions on boreal forest classification and biomass estimates with SAR. *IEEE Transactions on Geoscience and Remote Sensing*, 38, 1242–1252.
- Restrepo-Coupe, N., Huete, A., Davies, K., Cleverly, J., Beringer, J., Eamus, D., van Gorsel, E., Hutley, L.B., and Meyer, W.S. (2016). MODIS vegetation products as proxies of photosynthetic potential along a gradient of meteorologically and biologically driven ecosystem productivity. *Biogeosciences*, 13, 5587–5608.
- Rossel, R.A.V., and Hicks, W.S. (2015). Soil organic carbon and its fractions estimated by visible-near infrared transfer functions. *European Journal of Soil Science*, 66, 438–450.
- Rossel, R.A.V., Walvoort, D.J.J., McBratney, A.B., Janik, L.J., and Skjemstad, J.O. (2006). Visible, near infrared, mid infrared or combined diffuse reflectance spectroscopy for simultaneous assessment of various soil properties. *Geoderma*, 131, 59–75.
- Rossini, M., Nedbal, L., Guanter, L., Ac, A., Alonso, L., Burkart, A., Cogliati, S., Colombo, R., Damm, A., Drusch, M., Hanus, J., Janoutova, R., Julitta, T., Kokkalis, P., Moreno, J., Novotny, J., Panigada, C., Pinto, F., Schickling, A., Schuttemeyer, D., Zemek, F., and Rascher, U. (2015). Red and far red Sun-induced chlorophyll fluorescence as a measure of plant photosynthesis. *Geophysical Research Letters*, 42, 1632–1639.
- Roy, P.S., and Ravan, S.A. (1996). Biomass estimation using satellite remote sensing data—an investigation on possible approaches for natural forest. *Journal of Biosciences*, 21, 535–561.
- Ruimy, A., Jarvis, P., Baldocchi, D., and Saugier, B. (1995). CO₂ fluxes over plant canopies and solar radiation: a review. *Advances in Ecological Research*, 26, 1–68.
- Running, S.W., Nemani, R.R., Heinsch, F.A., Zhao, M.S., Reeves, M., and Hashimoto, H. (2004). A continuous satellite-derived measure of global terrestrial primary production. *Bioscience*, 54, 547–560.
- Saatchi, S.S., Harris, N.L., Brown, S., Lefsky, M., Mitchard, E.T.A., Salas, W., Zutta, B.R., Buermann, W., Lewis, S.L., Hagen, S., Petrova, S., White, L., Silman, M., and Morel, A. (2011). Benchmark map of forest carbon stocks in tropical regions across three continents. *Proceedings of the National Academy of Sciences*, 108, 9899–9904.
- Saleska, S.R., Wu, J., Guan, K.Y., Araujo, A.C., Huete, A., Nobre, A.D., and Restrepo-Coupe, N. (2016). Dry-season greening of Amazon forests. *Nature*, 531, E4–E5.
- Sarker, L.R., and Nichol, J.E. (2011). Improved forest biomass estimates using ALOS AVNIR-2 texture indices. *Remote Sensing of Environment*, 115, 968–977.
- Schimel, D.S. (1995). Terrestrial ecosystems and the carbon cycle. *Global Change Biology*, 1, 77–91.
- Schimel, D., Pavlick, R., Fisher, J.B., Asner, G.P., Saatchi, S., Townsend, P., Miller, C., Frankenberg, C., Hibbard, K., and Cox, P. (2015). Observing terrestrial ecosystems and the carbon cycle from space. *Global Change Biology*, 21, 1762–1776.
- Schubert, P., Lagergren, F., Aurela, M., Christensen, T., Grelle, A., Heliasz, M., Klemetsson, L., Lindroth, A., Pilegaard, K., Vesala, T., and Eklundh, L. (2012). Modeling GPP in the Nordic forest landscape with MODIS time series data—Comparison with the MODIS GPP product. *Remote Sensing of Environment*, 126, 136–147.
- Sellers, P.J. (1985). Canopy reflectance, photosynthesis and transpiration. *International Journal of Remote Sensing*, 6, 1335–1372.
- Sellers, P.J., Schimel, D.S., Moore, B., Liu, J., and Eldering, A. (2018). Observing carbon cycle–climate feedbacks from space. *Proceedings of the National Academy of Sciences*, 115(31) 7860–7868.
- Shen, J., Huete, A., Ma, X., Ngoc, N.T., Joiner, J., Beringer, J., Eamus, D., and Yu, Q. (2020). Spatial pattern and seasonal dynamics of the photosynthesis activity across Australian rainfed croplands. *Ecological Indicators*, 108, 104669.
- Shi, Z., Wang, Q.L., Peng, J., Ji, W.J., Liu, H.J., Li, X., and Viscarra Rossel, R.A. (2014). Development of a national VNIR soil-spectral library for soil classification and prediction of organic matter concentrations. *Science China Earth Sciences*, 57, 1671–1680.
- Shoshany, M., and Karnibad, L. (2011). Mapping shrubland biomass along Mediterranean climatic gradients: the synergy of rainfall-based and NDVI-based models. *International Journal of Remote Sensing*, 32, 9497–9508.
- Sibanda, M., Mutanga, O., Rouget, M., and Kumar, L., (2017). Estimating biomass of native grass grown under complex management treatments using WorldView-3 spectral derivatives. *Remote Sensing*, 9(1), 55.

- Sims, D.A., Rahman, A.F., Cordova, V.D., El-Masri, B.Z., Baldocchi, D.D., Bolstad, P.V., Flanagan, L.B., Goldstein, A.H., Hollinger, D.Y., Misson, L., Monson, R.K., Oechel, W.C., Schmid, H.P., Wofsy, S.C., and Xu, L. (2008). A new model of gross primary productivity for North American ecosystems based solely on the enhanced vegetation index and land surface temperature from MODIS. *Remote Sensing of Environment*, 112(4), 1633–1646.
- Sims, D.A., Rahman, A.F., Cordova, V.D., El-Masri, B.Z., Baldocchi, D.D., Flanagan, L.B., Goldstein, A.H., Hollinger, D.Y., Misson, L., Monson, R.K., Oechel, W.C., Schmid, H.P., Wofsy, S.C., and Xu, L. (2006). On the use of MODIS EVI to assess gross primary productivity of North American ecosystems. *Journal of Geophysical Research: Biogeosciences*, 111(G4), G04015.
- Stjostrom, M., Ardo, J., Arneth, A., Boulain, N., Cappelaere, B., Eklundh, L., de Grandcourt, A., Kutsch, W.L., Merbold, L., Nouvellon, Y., Scholes, R.J., Schubert, P., Seaquist, J., and Veenendaal, E.M. (2011). Exploring the potential of MODIS EVI for modeling gross primary production across African ecosystems. *Remote Sensing of Environment*, 115, 1081–1089.
- Somarathna, P.D.S.N., Malone, B.P., and Minasny, B. (2016). Mapping soil organic carbon content over New South Wales, Australia using local regression kriging. *Geoderma Regional*, 7, 38–48.
- Stavros, E.N., Schimel, D., Pavlick, R., Serbin, S., Swann, A., Duncanson, L., Fisher, J.B., Fassnacht, F., Ustin, S., Dubayah, R., Schweiger, A., and Wennberg, P. (2017). ISS observations offer insights into plant function. *Nature Ecology and Evolution*, 1(7), 194.
- Stevens, A., Udelhoven, T., Denis, A., Tychon, B., Liou, R., Hoffmann, L., and van Wesemael, B. (2010). Measuring soil organic carbon in croplands at regional scale using airborne imaging spectroscopy. *Geoderma*, 158, 32–45.
- Tang, X.G., Liu, D.W., Song, K.S., Munger, J.W., Zhang, B., and Wang, Z.M. (2011). A new model of net ecosystem carbon exchange for the deciduous-dominated forest by integrating MODIS and flux data. *Ecological Engineering*, 37, 1567–1571.
- Tao, S.L., Guo, Q.H., Li, L., Xue, B.L., Kelly, M., Li, W.K., Xu, G.C., and Su, Y.J. (2014). Airborne Lidar-derived volume metrics for aboveground biomass estimation: a comparative assessment for conifer stands. *Agricultural and Forest Meteorology*, 198, 24–32.
- TerMikaelian, M.T., and Korzukhin, M.D. (1997). Biomass equations for sixty-five North American tree species. *Forest Ecology and Management*, 97, 1–24.
- Tucker, C.J., Fung, I.Y., Keeling, C.D., and Gammon, R.H. (1986). Relationship between atmospheric CO₂ variations and a satellite-derived vegetation index. *Nature*, 319, 195–199.
- Tucker, C.J., Slayback, D.A., Pinzon, J.E., Los, S.O., Myneni, R.B., and Taylor, M.G. (2001). Higher northern latitude normalized difference vegetation index and growing season trends from 1982 to 1999. *International Journal of Biometeorology*, 45, 184–190.
- Turner, D.P., Urbanski, S., Bremer, D., Wofsy, S.C., Meyers, T., Gower, S.T., and Gregory, M. (2003). A cross-biome comparison of daily light use efficiency for gross primary production. *Global Change Biology*, 9, 3, 383–395.
- Turner, D.P., Ollinger, S.V., and Kimball, J.S. (2004). Integrating remote sensing and ecosystem process models for landscape- to regional-scale analysis of the carbon cycle. *Bioscience*, 54, 573–584.
- Turner, D.P., Ritts, W.D., Cohen, W.B., Gower, S.T., Running, S.W., Zhao, M.S., Costa, M.H., Kirschbaum, A.A., Ham, J.M., Saleska, S.R., and Ahl, D.E. (2006). Evaluation of MODIS NPP and GPP products across multiple biomes. *Remote Sensing of Environment*, 102, 282–292.
- Vickers, D., Thomas, C.K., Pettijohn, C., Martin, J.G., and Law, B.E. (2012). Five years of carbon fluxes and inherent water-use efficiency at two semi-arid pine forests with different disturbance histories. *Tellus B*, 64.
- Wang, J., Rich, P.M., Price, K.P., and Kettle, W.D. (2004). Relations between NDVI and tree productivity in the central Great Plains. *International Journal of Remote Sensing*, 25(16), 3127–3138.
- Wang, B., Waters, C., Orgill, S., Gray, J., Cowie, A., Clark, A., and Liu, D.L. (2018). High resolution mapping of soil organic carbon stocks using remote sensing variables in the semi-arid rangelands of eastern Australia. *Science of the Total Environment*, 630, 367–378.
- Were, K., Bui, D.T., Dick, O.B., and Singh, B.R. (2015). A comparative assessment of support vector regression, artificial neural networks, and random forests for predicting and mapping soil organic carbon stocks across an Afrotropical landscape. *Ecological Indicators*, 52, 394–403.
- Whitley, R.J., Macinnis-Ng, C.M.O., Hutley, L.B., Beringer, J., Zeppel, M., Williams, M., Taylor, D., and Eamus, D. (2011). Is productivity of mesic savannas light limited or water limited? Results of a simulation study. *Global Change Biology*, 17(10), 3130–3149.

- Wilson, K.B., Baldocchi, D.D., and Hanson, P.J. (2001). Leaf age affects the seasonal pattern of photosynthetic capacity and net ecosystem exchange of carbon in a deciduous forest. *Plant, Cell and Environment*, 24(6), 571–583.
- Wirth, C., Schumacher, J., Schulze, E.D. (2004). Generic biomass functions for Norway spruce in Central Europe—a meta-analysis approach toward prediction and uncertainty estimation. *Tree Physiology*, 24, 121–139.
- Wu, C., Chen, J.M., and Huang, N. (2011). Predicting gross primary production from the enhanced vegetation index and photosynthetically active radiation: Evaluation and calibration. *Remote Sensing of Environment*, 115(12), 3424–3435.
- Wu, C., Gonsamo, A., Zhang, F., and Chen, J.M. (2014). The potential of the greenness and radiation (GR) model to interpret 8-day gross primary production of vegetation. *ISPRS Journal of Photogrammetry and Remote Sensing*, 88, 69–79.
- Wu, C., Niu, Z., and Gao, S. (2010). Gross primary production estimation from MODIS data with vegetation index and photosynthetically active radiation in maize. *Journal of Geophysical Research—Atmospheres*, 115, 12.
- Xiao, J., and Moody, A. (2005). Geographical distribution of global greening trends and their climatic correlates: 1982–1998. *International Journal of Remote Sensing*, 26, 2371–2390.
- Xiao, J., Chevallier, F., Gomez, C., Guanter, L., Hicke, J.A., Huete, A.R., Ichii, K., Ni, W., Pang, Y., Rahman, A.F., Sun, G., Yuan, W., Zhang, L., and Zhang, X. (2019). Remote sensing of the terrestrial carbon cycle: A review of advances over 50 years. *Remote Sensing of Environment*, 233, 111383.
- Xiao, X.M., Hollinger, D., Aber, J., Goltz, M., Davidson, E.A., Zhang, Q.Y., and Moore, B. (2004). Satellite-based modeling of gross primary production in an evergreen needleleaf forest. *Remote Sensing of Environment*, 89, 519–534.
- Xiao, X., Zhang, Q., Saleska, S., Hutyra, L., De Camargo, P., Wofsy, S., Froking, S., Boles, S., Keller, M., and Moore, B. (2005). Satellite-based modeling of gross primary production in a seasonally moist tropical evergreen forest. *Remote Sensing of Environment*, 94(1), 105–122.
- Xiao, Z.Q., Liang, S.L., Sun, R., Wang, J.D., and Jiang, B. (2015). Estimating the fraction of absorbed photosynthetically active radiation from the MODIS data based GLASS leaf area index product. *Remote Sensing of Environment*, 171, 105–117.
- Yuan, W., Liu, S., Yu, G., Bonnefond, J.-M., Chen, J., Davis, K., Desai, A.R., Goldstein, A.H., Gianelle, D., Rossi, F., Suyker, A.E., and Verma, S.B. (2010). Global estimates of evapotranspiration and gross primary production based on MODIS and global meteorology data. *Remote Sensing of Environment*, 114(7), 1416–31.
- Zhang, X.Y., and Kondragunta, S. (2006). Estimating forest biomass in the USA using generalized allometric models and MODIS land products. *Geophysical Research Letters*, 33, L09402.
- Zhang, X.T., Liang, S.L., Zhou, G.Q., Wu, H.R., and Zhao, X. (2014). Generating Global Land Surface Satellite incident shortwave radiation and photosynthetically active radiation products from multiple satellite data. *Remote Sensing of Environment*, 52, 318–332.
- Zhao, M.S., Heinsch, F.A., Nemani, R.R., and Running, S.W. (2005). Improvements of the MODIS terrestrial gross and net primary production global data set. *Remote Sensing of Environment*, 95, 164–176.
- Zhao, M., Running, S.W., and Nemani, R.R. (2006). Sensitivity of Moderate Resolution Imaging Spectroradiometer (MODIS) terrestrial primary production to the accuracy of meteorological reanalyses. *Journal of Geophysical Research—Biogeosciences*, 111(G1). <https://doi.org/10.1029/2004JG000004>
- Zhao, M., and Running, S.W. (2010). Drought-Induced Reduction in Global Terrestrial Net Primary Production from 2000 Through 2009. *Science*, 329(5994), 940–943.
- Zhao, K., Popescu, S., and Nelson, R. (2009). Lidar remote sensing of forest biomass: A scale-invariant estimation approach using airborne lasers. *Remote Sensing of Environment*, 113, 182–196.
- Zhou, L.M., Tucker, C.J., Kaufmann, R.K., Slayback, D., Shabanov, N.V., and Myneni, R.B. (2001). Variations in northern vegetation activity inferred from satellite data of vegetation index during 1981 to 1999. *Journal of Geophysical Research—Atmosphere*, 106, 20069–20083.



18 Fire

Rebecca Gibson, Marta Yebra, Barbara Harrison, and Ross Bradstock

EO datasets have been used in many studies related to fire prediction, behaviour, occurrence, and impact (Tian *et al.*, 2005; Lentile *et al.*, 2006; Roy *et al.*, 2013; Chu and Guo 2014; Pettorelli *et al.*, 2014; Mueller *et al.*, 2017; Chuvieco *et al.*, 2020). These studies can be summarised into three broad groups:

- predictive fire analyses: examining pre-fire conditions which would affect fire likelihood and consequence (see Section 18.3);
- active fire analyses: identifying fire occurrence and magnitude to most effectively direct suppression and evacuation (see Section 18.4); and
- retrospective fire analyses: examining conditions after a fire event, which may include pre-fire conditions, to understand fire extent, severity, emissions, behaviour, impact, and recovery (see Section 18.5).

The temporal and spatial resolution of satellite and airborne imagery is constantly advancing (see Volume 1) and access to satellite imagery is continually enhanced as data acquisition, storage, and processing become faster, cheaper, and more accessible (see Volume 2). With rapidly advancing technologies, it is an ongoing challenge to successfully transfer the results of academic research into an operational environment (see Section 18.2). While there are still many limitations involved with the operational use of EO data for fire mapping and monitoring, significant advances have been made in this field in recent decades (see Section 18.6).

The Fire (Katie Ford)

*When a human is asked about a particular fire,
she comes close:
then it is too hot,
so she turns her face—*

*and that's when the forest of her bearable life
appears,
always on the other side of the fire. The fire
she's been asked to tell the story of,
she has to turn from it, so the story you hear
is that of pines and twitching leaves
and how her body is like neither—*

*all the while there is a fire
at her back
which she feels in fine detail,
as if the flame were a dremel
and her back its etching glass.*

*You will not know all about the fire
simply because you asked.
When she speaks of the forest
this is what she is teaching you,*

you who thought you were her master.

Background image: A bushfire at Lancefield, Victoria, on 7 October 2015, was imaged from 20,000 feet altitude. This false colour composite is displayed using thermal infrared (8.5–13 μm) as red, middle infrared (3–5 μm) as green, and visible blue (<0.5 μm) as blue. Source: Robert Norman, Air Affairs Australia Pty Ltd
Recommended Chapter Citation: Gibson, R.K., Yebra, M., Harrison, B.A., and Bradstock, R.A. (2021). Fire. Ch 18 in *Earth Observation: Data, Processing and Applications. Volume 3A—Terrestrial Vegetation*. CRCSI, Melbourne. pp. 389–426.

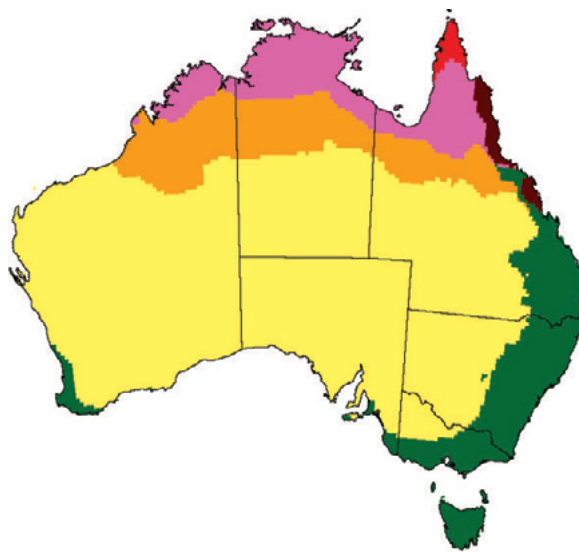
18.1 Fire in Australia

Fire is a major factor in shaping the Australian landscape (Pyne, 1992; Kershaw *et al.*, 2002; Ellis *et al.*, 2004). Fire regimes around Australia differ with the flammability of vegetation, attributes of weather and climate, and characteristics of terrain (see Section 2). The ‘seasonality’ of fires in Australia has been observed to vary with latitude, with northern regions being considered more likely to burn during winter and spring and southern areas being more susceptible to fire in summer and autumn (Luke and McArthur, 1978). These trends are largely governed by rainfall, which drives fuel accumulation (Bradstock, 2010). An EO-based analysis derived from AVHRR (Advanced Very High Resolution Radiometer) imagery (1997–2005) and rainfall data (1969–2004), which mapped the seasonal distribution of recent Australian fires (Russell-Smith *et al.*, 2007), shows a more complex pattern of fire activity (see Figure 18.1).

As introduced in Section 1.1.2.3, many Australian plants have developed mechanisms to recover and/or benefit from fire. Indigenous use of fire prior to European settlement is believed to have been frequent and widespread (Pyne, 1992; see Section 2.5.1). In recent centuries, however, the frequency and severity of bushfires in Australia has changed due to different settlement patterns, land management practices and climatic variations (Bartlett *et al.*, 2007; Jurskis, 2015), often with disastrous consequences to the landscape, local communities, infrastructure, and wildlife (see Table 18.1). A shift to significantly more hazardous fire regimes may be occurring in Australia (and elsewhere), characterised by increasing fire frequency and intensity associated with dynamic fire propagation, and the development of catastrophic ‘fire storms’ (Sharples *et al.*, 2016; Pyne, 2020; Oldenborgh *et al.*, 2020). For example, the unprecedented 2019/20 bushfire season burned nearly 19 million ha nationally, destroyed over 3,000 homes, and resulted in 33 deaths (Filkov *et al.*, 2020; CoA, 2020).

Figure 18.1 Fire seasonality in Australia

This map was derived from AVHRR imagery (1997–2005) and classification of rainfall data (1969–2004). The legend table below this map details the main burning period and average proportion of each coloured region that is burned each year.



Colour	Main burning period	Mean annual burned area (%)
Pink	May–November	35
Red	July–November	27
Orange	August–November	19
Brown	September–November	5
Yellow	September–December	3
Green	December–March	1

Source: Russell-Smith *et al.* (2007) Figure 8c

Occasional, major fires are a long standing part of our ecological furniture, with their imprint hard-wired into the lifecycles of our biota. If we are to live in these environments we must do so on the understanding that we will not eliminate risk.

(Ross Bradstock)

Table 18.1 Major bushfires in Australia

This sample of fire seasons shows the ‘worst’ fire years in recent history based on area burned, number of fires, and/or damage to settlements.

Year(s) [name]	State	Area burned (Million ha)	Deaths	Homes/shops burned	Other losses	Estimated cost at time of fires
1851 [Black Thursday]	Victoria	5	~12	–	25% of state burned; Huge livestock loss	–
1926/27	NSW	>2	8	many	–	> £1 million
1938/39 [including Black Friday]	Victoria	1.52	71	> 700	69 timber mills	–
1944	Victoria	>1	49	500	Huge stock loss	–
1951	Queensland	2.8	–	–	Significant stock loss	£2 million
1951/52	NSW	4.5	11	–	–	£6 million
1957/58	NSW	>2	5	158	Community facilities	–
1960/61	WA	>1.5	–	132	Other buildings	–
1966/67	Tasmania	0.26	64	>1,400	Significant livestock and infrastructure loss	–
1968/69	NT	40	–	–	Remote areas	–
	NSW	>2	14	80	81 buildings	–
1969/70	NT	45	–	–	Remote areas	–
1974/75	NT	45	–	–	Over 100 million ha burned nationally	–
	Queensland	7.3	–	–		–
	NSW	4.5	6	–		–
	SA	16	–	–		–
	WA	29	–	–		–
1983 [Ash Wednesday]	Victoria	0.15	47	1620	> 1,500 other buildings and 32,400 livestock	\$138 million
	SA	0.16	28	383	200 other buildings	\$38 million
1984/85	NSW	3.5	–	5	Livestock and infrastructure	\$40 million
2002	NT	38	–	–	Remote areas	–
2002/03 [Alpine/Canberra]	NSW	1.5	3	86	151 days of severe fire activity	\$12 million
	Victoria	1.1	(1)	41	Livestock	–
	ACT	>0.16	4	488	Plantations, livestock, Observatory, 100 other structures	> \$350 million
2003	WA	15.5	–	–	Remote areas	–
2009 [Black Saturday]	Victoria	>0.4	173	2,029	Community facilities	\$1070 million
2019/20 [Black Summer]	NT	6.8	–	5	> 1 billion vertebrate animals; Global impacts of smoke	\$40 billion
	Queensland	2.5	–	48		–
	NSW	5.6	25	2,475		–
	ACT	0.06	–	–		–
	Victoria	1.5	5	396		–
	Tasmania	0.036	–	2		–
	SA	>0.29	3	186		–
WA	2.2	–	1	–		

Sources: Ellis *et al.* (2004); Filkov *et al.* (2020); ADRKH (2020)

In this fire-prone country, reducing fire risk will be strongly dependent on reducing fire severity, a metric of loss or change in organic matter caused by fire (Keeley, 2009). Major fires typically follow major droughts (as distinct from drier, herbaceous-dominated ecosystems where major fires typically follow major rains), with their impact becoming more devastating when they are adjacent to areas of urban and peri-urban expansion. In recent decades the incidence and severity of megafires, where fire behaviour characteristics exceed all efforts at control, have increased in Australia (Bradstock *et al.*, 2012a).

One of the greatest advantages of using EO datasets in fire studies is the ability to look back on the vegetation, soil and other environmental conditions that preceded fire. While the scale of observation is often deficient in field-based fire studies that focus on single events, EO techniques offer the regional, national, and global scales required to adequately inform fire research and management (see Volume 2D).

For many years, EO imagery has been used globally to identify hotspots—pixels with abnormally high temperatures that may highlight fire ignitions. Hotspot imagery is routinely generated in Australia to enable fire response agencies to investigate small fires before they threaten lives and resources (see Section 18.6.2).

EO datasets are also used to map fire severity. The degree of combustion resulting from a fire is a function of its intensity and duration, as evidenced by the condition of the post-fire landscape. Incomplete combustion leaves a carbon residue (char or black ash), while complete (or near-complete) combustion produces a mineral (incombustible) residue (white ash or silica). Accordingly, the fuel consumption of a fire can be inferred from the proportion of white ash per unit area. For example, black ash is produced during the first 20 minutes of savanna fires, after which time the cumulative fire effects produce white ash (Roy and Landmann, 2005; Smith *et al.*, 2005).

18.2 EO Sensors for Fire

The recent report by the Australian ‘Bushfire Earth Observation Taskforce’ (ASA, 2020) highlighted the fact that the most appropriate combination of imagery and analysis methods for EO of fire will vary with the specific objectives of inquiry (see Table 18.2). For example, sensors used for detection of active fires will have different spatial, spectral, and temporal resolutions (see Volume 1B—Section 1) compared

The volume of white ash has been found to be significantly correlated with surface fuel consumption, thereby indicating fire severity (Hudak, 2013). Increasing availability of hyperspectral and multispectral image capture by remotely piloted aircraft (or drones) provides greater access to the spatial and spectral resolution required to examine the characteristics of ash, an ecologically significant feature related to fire severity (Hamilton *et al.*, 2017)

An initial assessment of fire severity provides a valuable overview of fire impact for land management and planning authorities to plan immediate rehabilitation activities. This has particular value in water catchment areas where post-fire rain can potentially accelerate erosion and reduce water quality. Such analyses also allow environmental scientists to foresee impacts on fauna and flora. Rapid response teams are commonly deployed from land management agencies immediately after a fire is contained. For example, the US Forestry Service (USFS) deploys Burned Area Emergency Response (BAER) teams, and in Australia, most jurisdictions have an equivalent systems of Rapid Risk Assessment Team (RRAT) deployments. These teams assess immediate post-fire landscape conditions in order to identify areas with highest need for site stabilisation treatments.

Identifying factors which can precipitate high fire severity, such as high fuel load, low fuel moisture, terrain liability, and meteorological pre-conditions (Bradstock *et al.*, 2010; Estes *et al.*, 2017), are paramount for predicting fire occurrence and activity (see Section 18.3). Similarly, real time monitoring of high fire intensity during active fires enables mitigation efforts to be directed to areas of greatest need (Keramitsoglou *et al.*, 2004; see Section 18.4). Finally, analysis of fire severity patterns of past fires—and determining their drivers—will allow informed management decisions to reduce the severity of future fires (see Section 18.5).

to sensors for post-fire analysis of fire severity. The many different biogeographic landscapes in Australia may also influence the imagery and analysis methods most appropriate for the type of inquiry. For example, the capacity of passive optical sensors to accurately capture spectral signatures from understory layers is limited under very dense canopies (see Section 18.3.1.3).

Applications using MODIS (Moderate Resolution Imaging Spectroradiometer) data in Australia demonstrate these scale and landscape considerations. A wide range of global MODIS products for fire mapping have been available for over a decade (see Excursus 8.1 and Volume 2D—Excursus 10.1) including:

- MOD14/MYD14/MCD14—a thermal anomalies product that shows active fires and biomass burning. It is available as daily (day and night) images and composites (based on 8 day or monthly data; see Excursus 18.1); and
- MCD64A1—a monthly 500m resolution burned area product that improves on the original algorithm used for MCD64 (Roy *et al.*, 2005; Giglio *et al.*, 2009). Padilla *et al.* (2015) found MCD64A1 to be superior to MCD45A1 for mapping burned area.

In the sparsely-populated, open savanna landscapes of northern Australia, the MODIS active fire product (MOD14) is particularly useful for fires with an active flaming area of 100–300 m² (Maier *et al.*, 2013). While the low spatial resolution of MODIS thermal infrared (TIR) imagery (1 km pixel size) limits its utility in southern regions, where forests are more dense and multi-layered, it can provide a useful cross-check against other fire information sources and helps to locate fires started by lightning in these landscapes (see Sections 18.6 and 18.7).

Similarly, tailored algorithms to estimate fuel moisture content (FMC) from MODIS optical bands with 500 m spatial resolution (Yebra *et al.*, 2018) have been used to characterise fuel condition and flammability across Australia (see Figure 18.2a), which is essential for providing a broadscale sense of fuel dryness (see Section 18.3.1.2). However, when applied to a higher spatial resolution version dataset

(such as Sentinel-2), local FMC gradients in the landscape can be delineated (see Figure 18.2b). These detailed gradients may act as soft containment lines when planning prescribed burns or prepositioning firefighting resources but would not be identifiable using a coarser spatial resolution image product.

However, the pace of technology development is continually increasing, with rapidly evolving improvements in the spatial, temporal, and spectral resolutions of sensors. For example, while geostationary sensors have traditionally had a temporal resolution of imaging the Earth each 1–2 days (see Volume 1A—Section 12), newer sensors supply more frequent imagery. One example is the Advanced Himawari Imager (AHI) on board Himawari-8, which provides hemispherical imagery every 10 minutes at 2 km spatial resolution. This improved temporal resolution greatly increases the likelihood of detecting new fire hotspots (Wickramasinghe *et al.*, 2016; Xu *et al.*, 2017), extracting fire rate of spread (Liu *et al.*, 2018), and even detecting pre-fire fuel condition, such as FMC, at a sub-daily timescale (Quan *et al.*, 2018).

In addition to the EO data available from public good satellites, the International Charter for Space and Major Disasters (ICSMD) supplies EO ‘assets’ from international space agencies and commercial enterprises to assist emergency managers during the disaster response phase (ICSMD, 2020). This initiative supplies data at no charge and also coordinates the acquisition of appropriate datasets at relevant locations. For example, in November 2019 Geoscience Australia (GA) activated the charter on behalf of Emergency Management Australia Crisis Coordination Centre (CCC) and New South Wales Rural Fire Service (NSW RFS) to access additional EO imagery to help with that catastrophic fire season.

Table 18.2 EO sensors relevant to fire-related studies

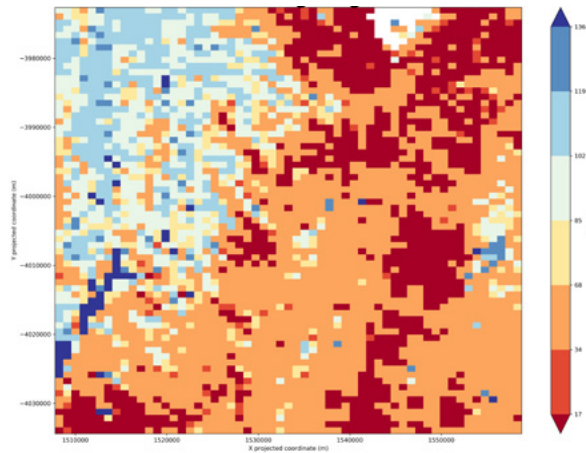
TIR: Thermal infrared; SAR: Synthetic Aperture Radar

Type	Sensor	Platform	Relevance	Advantages	Disadvantages
Passive optical	Multispectral radiometer	Satellite or airborne	Fuel moisture content Fuel type and fire severity Weather monitoring	Global coverage, low cost	Cloud contamination
	Hyperspectral spectro-radiometer	Airborne or terrestrial	Fuel moisture content Fuel type and fire severity	High spectral resolution, highlight plant stress	High cost, high data volume, specialised processing
	TIR radiometer	Satellite or airborne	Fire detection and fuel moisture content Weather monitoring	Global coverage, low cost	Coarse scale, cloud contamination, incapacity to detect small fires
Active optical	Lidar	Satellite, airborne, or terrestrial	Fuel structure and load	High accuracy, penetrates cloud, smoke	Data availability, high cost, specialised processing
Active microwave	SAR	Satellite, airborne, or terrestrial	Fuel structure, load, and moisture content Weather monitoring	All weather, so useful in tropical regions, penetrates cloud, smoke	Data availability, specialised processing

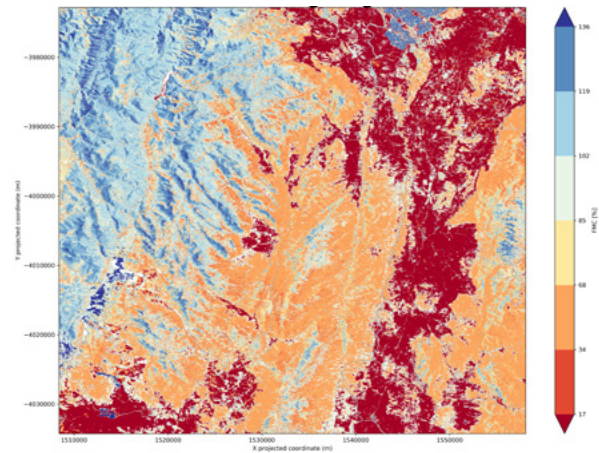
Figure 18.2 Fuel Moisture Content estimates

Local fuel moisture content (FMC) estimates derived using MODIS and Sentinel-2 satellite imagery acquired on 21 November 2019 over the Namadgi National Park, ACT. Both maps were produced using the FMC method described in Yebra *et al.* (2018), with FMC (%) values ranging from 17 (red) to 136 (blue). The higher spatial resolution of the Sentinel-2 imagery is able to detect terrain-driven gradients that are not visible in the MODIS product.

a. MODIS



b. Sentinel-2



Source: Ivan Kotzur, University of Western Sydney

The use of sensors carried by remotely operated aircraft (commonly known as remotely piloted aircraft (RPA), unmanned aerial vehicles (UAV), or drones, and formally labelled Remotely Piloted Aerial Systems (RPAS); see Volume 1A—Section 11.2) is another rapidly evolving technology with applications in fire management and research. There is significant interest by fire management agencies in Australia in using UAV for monitoring active fires, as pioneered in the USA (Wing *et al.*, 2014). Research has recently been conducted in Australia on the use of UAV in fire severity assessments (McKenna *et al.*, 2017). Many opportunities exist to enhance the use of UAV-mounted sensors for fire management in Australia following international developments, such as mapping fuel structure and moisture assessment (Shin *et al.*, 2018; Polinova *et al.*, 2019). A UAV platform can carry a versatile range of sensors, including multispectral, hyperspectral, thermal, and lidar. The capacity for sub-centimeter spatial resolution and lack of cloud contaminated imagery are significant advantages of UAV. However, further development in radiometric and atmospheric corrections (Tu *et al.*, 2018) is needed to enhance the scientific rigour for EO applications of UAV imagery, particularly for broadscale and multi-temporal applications.

Both multispectral and thermal line scan imagery have been acquired for many fires over several decades around Australia. The data is generally used in fire fighting and suppression operations during a fire event, but it has also been investigated in fire behaviour research (Filkov *et al.*, 2018; Storey *et al.*, 2020a, 2020b). Analysis of this imagery has the potential to provide unique insights into

the behaviour and progress of fires in different landscapes and the way fires interact with terrain and weather conditions (Sharples *et al.*, 2012). This understanding will improve fire mitigation efforts for the best possible outcome.

Given the unique biogeographic features of Australia, being able to spectrally characterise land cover changes induced by fire, with high precision, would greatly advance our understanding of Australian ecosystems and their dynamic interaction with fire (see Section 2.4). Hyperspectral imaging provides an opportunity for greater precision due to the narrow bandwidths, compared to the broad spectral bands of multispectral sensors (see Volume 1A—Section 14.3.3). Comparisons of multispectral and hyperspectral data for assessing fire severity using optical wavelengths indicate that fractional cover and burned fraction estimates were significantly better when derived from hyperspectral data (Veraverbeke *et al.*, 2014). However, advanced analysis techniques are required, which may limit the operational capacity. Hyperspectral imagery has not been widely explored for fire extent or severity studies in Australia, however, this sensor type has provided valuable fire-related information in overseas studies (e.g. Kokaly *et al.*, 2007) and warrants further investigation in the Australian fire-prone landscape. A detailed spectral library of Australian land cover components, both pre-fire and post-fire, would significantly improve our understanding of the information provided by EO imagery (see Volume 2D—Section 12.3).

18.3 Predictive Fire Analyses

Predictive analyses are relevant to the pre-fire environment to delineate those areas that are most likely to be vulnerable to fire. The major factors which determine fire behaviour and propagation are:

- fuels (biomass and flammability; see Section 18.3.1);
- weather (see Section 18.3.2); and
- ignitions (see Section 18.3.3).

Climate and terrain have biogeographic influences on these key drivers, which are inevitably interrelated:

- fuel type, structure, volume, and moisture content are dependent on climate and terrain; while
- the interaction between topography and weather creates environmental conditions that are either more or less conducive to fire.

EO data can be used to derive near real time information about fuel load and weather conditions, which can then be readily related to terrain data. Local scale quantitative field measurements, such as fuel type, biomass, and moisture content can be scaled up through models against regional climatic and terrain data (see Section 10 and Volume 2D). Integrated modelling of the factors driving the occurrence of wildfire are used in risk analysis approaches, such as fire danger indices (see Section 18.3.4). These tools allow for efficient management of fire fighting resources and early warning systems to help protect lives and assets.

18.3.1 Fuels

Fuel is the live and dead vegetation that may be consumed by fire. Total biomass and flammability of fuels contribute to the incidence and spread of fire. The specific characteristics of fuel which are relevant to bushfire likelihood include:

- fuel type and structure—size (diameter), horizontal and vertical distribution, and vegetation type (see Section 18.3.1.1);
- fuel moisture content (see Section 18.3.1.2); and
- fuel load (weight per unit area) and density (weight per unit volume; see Section 18.3.1.3).

An understanding of the distribution, volume and flammability of vegetative fuel in the landscape is essential for risk assessment and fuel management. Fuel is the only driver of fire which can be controlled, so fuel reduction is the primary management tool for reducing fire likelihood, although the efficacy of prescribed burning in reducing future fire risk is partial at best, due to the strong influence of fire weather on fire incidence and spread (Bradstock *et al.*, 2012b).

18.3.1.1 Fuel type and structure

The type, density, and structure of fuel vary within and between landscapes and biogeographic regions (see Section 2.4). Some vegetation communities are more prone to fire than others, due to the flammability and volume of fuel they produce and accumulate. While the attributes of vegetation communities are highly variable in Australia, in terms of species composition, structure, and function, the mechanisms influencing fire behaviour can be condensed into a small number of categories. Bradstock *et al.* (2012c) reviewed fire regimes and biodiversity for Australian ecosystems in terms of seven major fuel types:

- **Grasslands** dominate the Australian landscape. This fuel type includes annual or perennial grasses, crops and improved pastures, and open forests and woodlands with a grassy understorey. Weather is generally more significant than fuel load in determining fire intensity and extent in grassy fuel systems (Morgan, 1999). However, fuel load may directly influence fire behaviour in grasslands through the spatial continuity of fuel. For example, heavily grazed grasslands may have scattered patches of bare ground (Bradstock *et al.*, 2012c). Fire frequency and time-since-fire influence grassland composition and structure (Lund and Morgan, 2002), although the abundance of most grassland species is not adversely affected by fire (McDougall and Kirkpatrick, 1994).
- **Spinifex grasslands** occur on low nutrient soils in arid and semi-arid climates and cover about 25% of Australia. Although spinifex species are taxonomically classified as grasses, the fire behaviour they propagate is sufficiently different to warrant a separate fuel class (Bradstock *et al.*, 2012c). Moisture content of spinifex reduces with age, which increases its flammability. Wind speed has been modelled as the major factor in determining fire rate of spread in spinifex grasslands, with fuel quantity and moisture also being significant (Burrows *et al.*, 2006). Fire frequency varies from three to 30 years with fires following antecedent rain (Allan and Southgate, 2002)
- **Shrublands** include *Acacias*, chenopod shrublands and heathlands. This fuel type generally occurs on deficient, acid soils in Mediterranean, temperate, and tropical climates. Shrublands have fine, well-aerated fuels with dead foliage persisting in some species. Without the protection of a canopy layer, fuels are directly exposed to wind and Sun so dry quickly even after rain. Inter-fire periods depend on post-fire fuel density and have been reported to vary from 18 months to 8 years (Keith *et al.*, 2002). Time-since-fire has been modelled as the main determinant of fire spread, with higher fire severity resulting in longer intervals between fires (Bradstock *et al.*, 1998).

- **Mallee-heaths** in semi-arid (200–500 mm), southern Australia, occur in lateritic and aeolian sandplains, dunefields, and flats. These shrublands are characterised by multi-stemmed eucalypts and a Mediterranean climate. Vegetation density, and hence flammability, is affected by soil type, with cover ranging from 20% to 50%. Fuels are often discontinuous and inadequate for fire spread. After sufficient fuel accumulation, large episodic fires can occur in summer initiated by lightning and fanned by changeable winds (Bradstock and Cohn, 2002).
- **Dry sclerophyll forests** dominated by eucalypts cover the Great Dividing Range (GDR) from Queensland to Victoria and into Tasmania. This mountainous landscape features significant variation in topography, with vegetation density increasing in moister areas such as valleys. Leaf litter is the major fire fuel in these forests. Open forests burn more frequently than closed forests due to lower fuel moisture. Research has shown a wide range in fire intensity both within and between fires in these forests (Gill and Catling, 2002). Areas of forest also occur in the Mediterranean climates of southwest WA and southeast SA.
- **Other forests/woodlands:** Prior to European settlement, temperate woodlands covered extensive areas in southeast Australia, predominantly on the drier side of the GDR from Queensland to Victoria and into Tasmania. Much of this fuel type is now used for agriculture and therefore unaccustomed to fire. Similarly, most of the former Mediterranean woodlands in southwest WA have also been cleared for agricultural activities. Mean annual rainfall in these areas varies between 200 mm and 800 mm. Relatively little is known about the floristic composition or fire regimes of these woodlands before European settlement. Litter fuels accumulate more slowly in woodlands than in forests due to both the lower vegetation density and greater termite activity, so fires occur less frequently (Hobbs, 2002).
- **Rainforests** occur in high rainfall areas of nutrient rich, well-drained soils in tropical, sub-tropical, and temperate climates. The absence of fire in some areas is allowing rainforest to expand into wet sclerophyll forest and tropical savannas, and in other areas intense, late dry season fires in tropical savannas are damaging the margins of small patches of rainforest. Recovery of rainforest from fire depends on the frequency and seasonality of fires (Russell-Smith and Stanton, 2002).

Attempts to map multi-layer fuel structure using passive optical datasets have been primarily confounded by the concealing effect of overstorey vegetation. Reasonable fuel structure mapping accuracies have been obtained for grasslands, but dense forest and shrub cover can obscure estimates of the height of surface fuel. Active sensor systems offer the opportunity to measure the three-dimensional structure of vegetation more directly (see Section 16.5). Forest fuel structure has been estimated using various lidar platforms (see Excursus 5.1):

- airborne (or Airborne Laser Scanning, ALS; Hall *et al.*, 2005; Hudak *et al.*, 2008; Chen *et al.*, 2017a), including UAV-based (Wallace *et al.*, 2016); and
- ground-based (or Terrestrial Laser Scanning, TLS; Jupp *et al.*, 2008; Strahler *et al.*, 2008; Chen *et al.*, 2016; Marselis *et al.*, 2016).

Studies using ALS to map Australian forest floristics and structure have produced results comparable to conventional vegetation surveys (Tickle, *et al.*, 2006; Lucas *et al.*, 2008a, Price and Gordon, 2016). While surface and near surface fuels are generally modelled by small footprint lidar with less accuracy compared to elevated fuels (Turner, 2007; see also Section 12), the data may still provide a useful indicator (Price and Gordon, 2016). Recent developments in international research have applied fusion techniques for integrated modelling of forest structure using ALS data with satellite radar and multispectral imagery (Manzanera *et al.*, 2016, Garcia *et al.*, 2018).

18.3.1.2 Fuel moisture content

Fuel moisture is one of the key fire limiting switches that determines the propensity of vegetation to burn (Bradstock, 2010). The moisture content of both live and dead fuels is influenced primarily by temperature, humidity, and soil moisture. EO data has traditionally contributed to the fuel moisture characterisation of live fuel types, while dead fuel types (that is, not photosynthetically active) are generally derived from weather variables. Fuel moisture content (FMC) is inversely related to the flammability of vegetation and fire rate of spread. Traditionally FMC studies have been based on field observation or indirect estimates derived from atmospheric data. EO data offer an internally consistent approach to interpolate available FMC field data over a wide area (Nolan *et al.*, 2016a, 2016b). Alternatively, direct estimates of FMC can be retrieved from EO data based on radiative transfer models (RTM) inversion techniques (Yebra *et al.*, 2013, 2018).

As grasses senesce or become dormant their FMC content gradually decreases and their flammability correspondingly increases. This process is called curing, which is measured as the percentage of grass fuel that is dead. Grasslands that are less than 50% cured are not likely to foster and spread fire, however, when grass is between 70–90% cured, the rate of spread of a fire significantly increases (Cheney and Sullivan, 2008). In Australia, grassland curing is an integral component of the Grassland Fire Danger Index (GFDI; Cheney and Sullivan, 2008). As grasses cure, their spectral reflectance increases in the visible and middle infrared (MIR) wavelengths and decreases in the near infrared (NIR) region (Danson and Bowyer, 2004; see Section 4.3).

Numerous studies have attempted to relate vegetation indices derived from EO data to the curing state of grasslands. The Normalised Differenced Vegetation Index (NDVI) has been used to indicate vegetation greenness in many studies (see Section 8.1.1) and is closely correlated with the moisture content of vegetation. In Australia, Paltridge and Barber (1988) established an inverse exponential relationship between FMC and NDVI derived from AVHRR data. Dilley *et al.* (2004) showed that the relationship between curing and NDVI varied between sites and derived a more accurate relationship between GCI and NDVI. A Relative Greenness approach was then developed using MODIS-derived NDVI (Grassland Curing Index (GCI) algorithm-C; Newnham *et al.*, 2011). This method is used by Landgate to produce Curing Index maps for WA (see Section 18.7). More recently, Martin *et al.* (2015) developed a satellite model for estimating the degree of curing based on EO time series and weekly ground-based observations. Results from these studies are used by the Bureau of Meteorology (BoM) to produce Australia-wide curing maps and a more quantitative curing estimate for computing GFDI¹³.

In forested landscapes, NDVI has been correlated with FMC for fire risk prediction in various locations, including in southern Spain (Aguado *et al.*, 2003), the Canadian boreal forests (Oldford *et al.*, 2006), Mediterranean grasslands and shrublands (Chuvieco *et al.*, 2002), and African savannas (Verbesselt *et al.*, 2007). Several studies have reported significant correlations between live fuel moisture and alternative vegetation indices (such as NDVI < NDWI < VARI; see Section 8.1.1; Stow *et al.*, 2006; Hao and Qu 2007, Caccamo *et al.*, 2012; Garcia *et al.*, 2020). However, empirical studies relating FMC to EO-based vegetation indices have reported variable results (Yebra *et al.*, 2008; Casas *et al.*, 2014), which may be due to sensor and site-dependent effects.

As introduced in Section 10 and Volume 1B—Section 5, RTM are based on physical relationships between spectral reflectance and the biophysical (such as water content) and structural (such as leaf area index, LAI) properties of vegetation (see Sections 5 and 6). Therefore RTM are independent of sensor or site conditions and are generally more universal than empirical modelling (Casas *et al.* 2014; Yebra *et al.* 2013). Yebra *et al.* (2018) derived a continental-wide FMC model for Australia using RTM inversion techniques, based on MODIS imagery (see Figure 18.2). This model was evaluated using high quality field data from around Australia and a flammability index, and indicated reasonable skill in fire risk prediction¹⁴. Ongoing research within the NSW Bushfire Risk Management Research Hub (co-led by the University of Western Sydney and the Australian National University) aims to develop spatially explicit monitoring and forecasting of dead and live fuel moisture in forested landscapes by integrating biophysical and EO modelling.

Emerging alternative approaches to modelling fuel moisture in forested landscapes include the use of radar data. Airborne SAR was used to model live fuel moisture against field data in a semi-arid Australian forest dominated by white cypress pine (Tanase *et al.*, 2014). Sentinel-1 C-band SAR was also used to model fuel moisture against field data in a Juniper, Redberry and Oak forest in central Texas, USA (Wang *et al.*, 2019). Sophisticated integration of radar and optical sensors provide improved accuracies of fuel moisture compared to traditional vegetation indices derived from optical datasets, such as NDVI (Rao *et al.*, 2020). Radar may also provide the opportunity to monitor soil moisture content, which is related to the moisture availability of fine surface fuels (Tanase *et al.*, 2014; Punithraj *et al.*, 2019). The recent and imminent launches of several spaceborne SAR sensors with high temporal revisit times and suitable sensor characteristics provide great opportunities for advancement of current knowledge and operational practices in fuel moisture monitoring for fire risk prediction.

One who neglects or disregards the existence of earth, air, fire, water and vegetation disregards his own existence which is entwined with them.
(Mahavira)

¹³ This data is available from TERN AusCover (see Section 18.7).

¹⁴ Both FMC and Flammability estimates for Australia can be accessed via the Australian Flammability Monitoring website (see Section 18.7).

18.3.1.3 Fuel load and density

A range of EO data sources and methods have been used to estimate fuel load (as t/ha; Roff *et al.* 2005, 2006; Chafer *et al.*, 2004; Chafer, 2007). Many surrogates for forest fuel load, such as biomass or LAI, vary with species composition, tree height, and forest structure. As such, reflectance-based methods may be more appropriate when fuel load is estimated indirectly, using fire extent and/or severity derived from EO to infer fire history (time-since-fire), with ancillary vegetation type data and known fuel accumulation curves subsequently being used to model fuel loads (Brandis and Jacobson, 2003; Duff *et al.*, 2013). Recently, the Vegetation Structure Perpendicular Index (VSPI) derived from Landsat data has been used to estimate stand age by fitting post-fire VSPI time series to an exponential decay curve (Masseti *et al.* 2019). Time-since-fire may be a poor predictor of fuel load in some cases, as interactions between fire severity, vegetation type, and landscape productivity influence both the fuels remaining after fire and the rates of fuel re-accumulation (Price and Gordon, 2016). Direct measures of fuel load from active sensors may reduce such modelling uncertainty.

Active sensors such as lidar have been used to estimate fuel load in Australia and as input into operational hazard mapping (Power, 2006, 2008). The use of active sensors may overcome limitations in estimating fuel load under dense canopies that obstruct the view of understorey layers (see Excursus 5.1 and Section 16.5). For example, predictive models of surface fuel in eucalypt forests in southeastern Australia have been developed using estimates of litter-bed depth derived from TLS, topographical data, and relevant environmental factors including previous fire disturbance (Chen *et al.*, 2017a).

One of the problems with validating EO methods for estimating fuel load is the lack of sufficient and objective field data. Visual assessment methods for estimating fuel load typically involve a qualitative element subject to observer bias, and destructive field sampling is only viable for a small number of sites (see Section 5.1.2). Field assessment methods of fuel load, such as McCarthy *et al.* (1999) and Gould *et al.* (2008), are expensive, time-consuming, complicated and subjective. Furthermore, recent evidence indicates visual assessment overestimated fuel load for very high and extreme fuel hazard categories, compared to destructively sampled surface fuels (McCull-Gausden and Penman, 2017).

Keane *et al.* (2001) discuss other challenges involved with mapping fuel loads, including fuelbed complexity, fuel type diversity, fuel variability, and fuel model generalisations. Multi-scale fuel mapping methods, based on vegetation community, composition, and structure derived from field data, EO and gradient modelling, may help to overcome the limitations of using EO datasets to estimate fuel loads (McCull-Gausden *et al.*, 2019; Jenkins *et al.*, 2020). This methodology was further developed in the LANDFIRE (Landscape Fire and Resource Management Planning Tools) system in the US, which combines fire behaviour and fuel models (Rollins, 2009). Similar systems are operational in Australia, such as FireTools used by NSW National Parks and Wildlife Service, which is used to predict fuel loads and plan prescribed burning. The integrated modelling being developed by the NSW Bushfire Risk Management Research Hub aims to characterise fuels using lidar data, then quantify initial post-fire fuel loads and re-accumulation curves in key fuel types, under varying levels of fire severity (NSW BRMR, 2020).

18.3.2 Weather conditions and topography

A range of weather variables affect fire ignition and propagation, both directly and indirectly, including temperature, relative humidity, precipitation, dew point temperature, solar insolation, wind speed, and wind direction (Rothermel, 1972). The risk of large fires that are difficult to control increases with extreme fire weather, which is the combination of low relative humidity, high temperature, and strong winds. Specific combinations of these conditions exacerbate fire danger in different ways, with wind direction and velocity largely determining the direction and speed of fire spread. Nocturnal temperature inversions can also lead to increased fire behaviour that is unrelated to wind (McRae *et al.*, 2008).

Unstable atmospheric conditions can precipitate extreme fire-atmosphere interactions, such as violent pyrocumulonimbus (pyroCb) storms (Fromm *et al.*, 2010). Pyroconvection can influence widespread flaming and unpredictable fire behavior through strong and erratic changes in surface wind speed and direction, wind shear, mid-level moist instability, latent heating inside the convective cloud, and increased ignition likelihood through lightning (Sharples *et al.*, 2016; Potter, 2012a, 2012b). An increased risk of pyroconvection with future climate change has been identified for southeast Australia during spring and summer, due to decreased vertical atmospheric stability and humidity, combined with more severe, near surface conditions (Dowdy and Pepler, 2018).

Certain interactions between topography and meteorological conditions can escalate fire danger, such as dynamic channelling (Kossmann *et al.*, 2001; Sharples *et al.*, 2012), where fire is directed by terrain to spread down valleys as well as in the major wind direction (Sharples, 2009). The direction and rate of channelling can be predicted by analysis of slope, aspect, and wind regime (McRae, 2004; Sharples *et al.*, 2012). Numerous other complex interactions with slope and wind characteristics have been described with associated effects on fire behaviour, such as:

- atypical lateral fire spread on steep lee-facing slopes, which may be associated with pyroconvective activity (Simpson *et al.*, 2016).
- Foehn winds, the warm dry winds down the lee slopes of mountains caused by adiabatic compression, which can increase the intensity and rate of spread of fires (Sharples *et al.*, 2010).
- mountain wind waves occur as air movement is deflected over a ridge. Lee slope eddies can draw any nearby fire into the channelling zone and circulate embers downwind (Sharples *et al.*, 2009). Terrain can also produce jet-like winds when airflow is accelerated through narrow passes (Stensrud, 1996).
- low level jets may be produced through geostrophic forcing due to horizontal differences in sensible and latent heat fluxes with elevation variation in mountainous regions. The high wind speed and abrupt atmospheric warming and drying increase the potential for fire ignition and propagation (Sharples *et al.*, 2009).

Meteorological terrain interactions are often difficult to predict and therefore present significant risk to firefighters. Satellite imagery captures characteristic cloud patterns produced by some of these phenomena. For example, mountain wind waves and 'dry slots' of low humidity air in the upper atmosphere are visible in water vapour imagery. A range of near real time TIR imagery is also available which shows surface temperature and detects thermal belts (see Volume 1B—Section 7). Meteorological events have been observed in conjunction with several extreme fires in Australia (Mills, 2008a, 2008b, Fromm *et al.*, 2006, Cruz *et al.*, 2012).

The use of EO to detect and predict drivers of the meteorological-terrain conditions that increase fire danger is an active area of research. A better understanding of the interaction between weather and topography on fire intensity and rate of spread will enable suppression agencies to anticipate extreme fire events with more certainty, and to plan and manage resources accordingly.

18.3.3 Ignitions

EO detection of fire ignitions is particularly useful for operational management of active fires, however, predicting ignition risk requires an understanding of the drivers of ignitions. Fire ignition datasets developed from EO products offer spatially consistent, regional scale data to study and model drivers of ignitions. For example, satellite-derived ignition data has been used to model the spatial relationships between anthropogenic land use or disturbance features and ignition for different ecoregions (Fusco *et al.*, 2016; Vilar *et al.*, 2016). Predicting areas prone to lightning-caused ignitions has also been analysed through coupled modelling of EO-based hotspot ignition data and lightning occurrence (Krawchuk *et al.*, 2009).

Line Scanning Systems mounted to aircraft have been used for many years for active firefighting purposes, however, systematic use of this EO data type for fire behaviour analyses has been limited (see Section 18.2). Recently, research has commenced into using line scans in fire behaviour analysis, with recommendations for routine capture of this data source (Filkov *et al.*, 2018). Line scans are being used to understand drivers of increased spotting risk (Storey *et al.*, 2020a, 2020b). Spotting dynamics are known to dominate fire propagation in catastrophic wildfires. For example, during the 2009 Black Saturday fire in Victoria (Cruz *et al.*, 2012; see Table 18.1), prolific short range spotting linked with crown fire propagation in eucalypt forest promoted extremely fast rates of spread. Greater understanding of the circumstances that are conducive to increased spotting risk may enable better forecasting, preparedness, and mitigation.

18.3.4 Risk analysis

Risk assessment includes both the physical probability of fire occurrence (likelihood) and the potential extent of damage (consequence). Analysis of EO data in conjunction with GIS has led to an improved understanding of both fire behaviour and likelihood (Chuvieco *et al.*, 2010, 2014). Being able to identify those locations where fire is likely to occur and, if it occurs, whether it is likely to spread, allows incident management authorities to manage suppression resources most effectively.

Fire danger indices have long been used to estimate the likelihood of fire ignition and propagation (Burgan *et al.*, 1998). These indices are basically derived from measures of weather, topography and fuel dryness. Satellite EO data has been used to compute inputs for these indices for decades (Verbesselt *et al.*, 2002).

Australian fire danger ratings are currently based on two indices:

- Grassland Fire Danger Index (GFDI); and
- Forest Fire Danger Index (FFDI).

Initially developed as analogue meters (McArthur, 1966, 1967), these indices were subsequently expressed as equations by Noble *et al.* (1980). They indicate the likelihood of fire events and the likelihood of fire suppression. Both indices are derived from estimates of average wind velocity, relative humidity, air temperature, and fuel moisture. The latter component should reflect long term fuel moisture, that is, seasonal rather than diurnal variation in moisture content. An estimate of grassland curing is used to represent fuel moisture when computing GFDI, whereas a drought factor is used to compute FFDI. The drought factor is calculated using precipitation data and the Keetch-Byram Drought Index (KBDI; Keetch and Byram, 1968), where KBDI indicates the dryness of soils, deep forest litter, logs, and living vegetation.

Many other indices have been used to assess fire danger. For example, the Haines index (Haines, 1988), which measures lower atmosphere stability and dryness, quantifies the potential for forest fire growth and is used operationally by the USFS. The Continuous Haines Index is modified for more appropriate applications in Australia, due to high values of Haines index occurring very frequently in Australia (Mills and McCaw, 2010). However, a single

index is not expected to precisely indicate the multi-faceted dimensions of fire risk.

A new National Fire Danger Rating System prototype was trialled by the NSW RFS over the summer of 2017/18 to better incorporate extreme fire behaviour. The revised system is based on empirical fire behaviour models and fuel type mapping, as well as meteorological data. This system aims to provide greater ability to understand and predict localised fire danger risk with improved scientific accuracy, rather than applying the same fire danger across large areas (Kenny *et al.*, 2019).

Several international systems have combined EO data with weather and/or topographic data to estimate fire danger (Leblon *et al.*, 2007), ignition potential (Chuvieco *et al.*, 2004), and seasonal fire risk (Manzo-Delgado *et al.*, 2009). In particular, the LANDFIRE Project has produced a comprehensive system which integrates a range of geospatial tools to model various landscape attributes across continental USA, including fire regime condition class (Rollins, 2009). Some Australian fire mitigation agencies produce risk maps to show those areas whose topography and fuel load are associated with a higher likelihood of fire (for example, see <https://www.bnhcrc.com.au/hazardnotes/77>). Bushfire threat has also been analysed in terms of proximity to bushland (Chen and McAneney, 2004, 2005) and changing demographics (Lowell *et al.*, 2009).

18.4 Active Fire Analyses

Active fires typically progress through two stages, flaming then smoldering, which are characterised by different temperatures, intensities, and emissions of aerosol particles. EO imagery from both satellite and airborne platforms has been used to map and monitor active fires. Space photography of extreme fire events graphically demonstrates the impact of the smoke plume on the upper atmosphere.

Several polar orbiting satellites are operationally used to map active fires globally (see Section 18.4.1). Recently, the new generation of geostationary sensors, with greater spatial and temporal resolution, have improved the capacity for active fire detection. This data can be combined with meteorological satellite imagery and prediction models, as well as imagery from airborne sensors, for both tactical and strategic fire suppression and to predict the volume and movement of smoke (see Section 18.4.2).

18.4.1 Satellite imagery

EO TIR bands have varying sensitivities to the temperature ranges associated with flaming and smoldering fires (Dozier, 1981; see Volume 1B—

Section 7). An EO image pixel may comprise a mixture of areas that are unburned, flaming, and smoldering, which complicates detection of fire pixels using satellite imagery (Justice *et al.*, 2006). Change between an active flaming fire front and a low intensity smoldering fire can occur in a short space of time. As such, the revisit frequency of an EO sensor is an important part of the accurate detection of active fires. Differentiation between current fires and the normal land temperature is another major challenge in active fire detection methods. For this reason, detection of smoldering fires from satellite imagery remains a challenge given their relatively low temperatures and small spatial extent compared to flaming fires. Cloud contamination is a general problem in satellite imagery applications, and can obscure the detection of active fires.

Numerous EO methods have been developed to identify pixels containing active fires (see Excursus 18.1). Most algorithms use MIR and TIR bands (such as AVHRR band 3: 3.8 μm ; and band 4: 10.8 μm respectively) with differing sensitivities to flaming and smoldering fires (Giglio and Justice, 2003, Plank *et al.*, 2017). These regions of the electromagnetic spectrum are particularly useful for detecting active

fire because, under normal conditions, the background emission in the TIR range is significantly greater than that in the MIR range. By contrast, when a fire occurs, the emitted radiation becomes more intense at the shorter wavelength in the MIR range (Jones *et al.*, 2017). Other image channels (such as AVHRR band 2, NIR) can also be used to identify and exclude 'bright' non-fire pixels (such as small clouds or bare soil patches), although such masks can also eliminate fire pixels affected by smoke.

Early algorithms compared individual pixels with fixed thresholds. More sophisticated contextual algorithms have been used to determine relative thresholds based on the statistics of neighbouring pixels (Ressl *et al.*, 2009; Plank *et al.*, 2017). Methods using a multi-temporal approach to detecting active fires have also been developed (Koltunov and Ustin, 2007) and some methods use a combination of all three types of algorithms (fixed threshold, contextual, or multi-temporal; Jones *et al.*, 2017). While active fire detection algorithms have been developed for many satellite sensors (Giglio *et al.*, 2000; Calle *et al.*, 2008), MODIS imagery became the preferred image source for detecting hotspots since it offers superior spatial resolution and significantly less saturation of the thermal signal, resulting in fewer false positives (Jones *et al.*, 2017).

An internationally coordinated initiative to produce a globally consistent system that includes fire mapping and monitoring is the Global Observations of Forest Cover and Land Cover Dynamics (GOF-C-GOLD; see Section 18.7). The fire mapping and monitoring program within GOF-C-GOLD aims to develop a real time, global observation network based on geostationary sensors (GOES, MSG and MTSAT) for large area fire detection. Results reported by Calle *et al.* (2008) demonstrated the feasibility of using MSG SEVIRI data to detect and map forest fires at national and global scales.

18.4.2 Airborne imagery

Various airborne sensors have been integrated with inertial measurement units and differential global positioning units for streamlined geo-referencing. Such systems provide detailed, rectified imagery showing location, intensity, and direction of fire fronts and spot fires and their potential targets. Some airborne sensors that are used for fire mapping and monitoring, either singly or in combination, include:

- multispectral scanners, such as Daedalus 1268 ATM (with 12 bands spanning the visible, NIR, short wave infrared (SWIR) and TIR wavelengths), can be used before, during, and after fires to assess fuel and map fire fronts, perimeters, intensity, and impact (see Figure 18.3);
- TIR digital cameras or radiometers (some with selectable temperature ranges) can image the area, perimeter, temperature, and intensity of active fires;
- forward looking infrared (FLIR) scanners can penetrate smoke to locate hotspots and fire edges in active fires, which can be useful to direct suppression or mopping up operations including:
 - ◆ assessing the effort required to black out remote edges using Remote Area Fire Teams (RAFT);
 - ◆ in conjunction with visible imagery, indicating whether ground staff can gain access to remote fires; and
 - ◆ Helicopter-mounted FLIR, providing Air Attack Supervisors and Air Observers additional vision through smoke to see fire perimeters and landmarks for suppression coordination and mapping;
- hyperspectral scanners can capture fire intensity information during active fires (Dennison and Roberts, 2009);
- digital cameras and video cameras can capture valuable aerial views of active fires; and
- radar and lidar systems can be used to detect smoke plumes during active fire.

A variety of sensor platforms are used during active fire image capture, including helicopters and fixed-wing airplanes. Helicopters are more manoeuvrable and can take off and land in more diverse environments, but have higher operational costs and smaller payload capacity than fixed-wing airplanes (Allison *et al.*, 2016). The use of piloted aircraft can be limited in extreme fire conditions due to safety risks. Recent advances in the technology and affordability of UAV show promise in the operational capture of EO imagery during active fires, with reduced risk to personnel safety when compared to manned aircraft (Yuan *et al.*, 2015, Allison *et al.*, 2016). Many of the same sensor types that can be mounted on manned aircraft are available for UAV platforms, including multispectral, hyperspectral and thermal sensors, digital cameras, and video recorders. While operational deployment of UAV is currently not widely adopted, there is increasing reporting of their use during operational fire management in Australia.

Intelligence system which integrate data from EO (scanners plus video) with GIS and downlink in near real time are used in high fire risk areas (Kontoes *et al.*, 2009a, 2009b). These data sources are not only invaluable to fire managers during operational fire containment, but also provide an objective record of fire activity, which can be used to reconstruct time sequences and further understand fire behaviour. For example, imagery from multispectral and thermal sensors mounted on aircraft have been used to observe the direction and rate of channelling (McRae, 2008; Sharples *et al.*, 2012).

Excursus 18.1—Fire Detection Products

Hotspot imagery, which highlights the locations of active fires, has been available for several decades from a range of satellite sensors. Giglio *et al.* (1999) evaluated three algorithms that had been proposed for large area detection of fire using AVHRR data and presented an enhanced algorithm for global monitoring which demonstrated a high probability of detecting small fires and excluding false positives in a range of landscapes. Landgate (WA) developed a hotspot detection method for Australian conditions (Craig *et al.*, 2002) using AVHRR imagery, which detected most hotspots (Smith *et al.*, 2007b)¹⁵. More recently, this process has been modified to identify hotspots using MODIS and Digital Earth Australia (DEA) datasets (GA, 2020).

The MODIS Fire and Thermal Anomalies product (MOD14/MYD14) has been available for over a decade (see Section 18.2). The algorithm used for this global product computes brightness temperatures from two 4 μm channels (21 and 22, which saturate at different temperatures) and channel 31 (11 μm). Other channels may be used to exclude ‘bright’, non-fire pixels (channels 1, 2 and 7) or cloud (channels 1, 2, 7 and 32; Giglio *et al.*, 2003; Justice *et al.*, 2006). Validation of MODIS Fire Products has mostly used higher spatial resolution imagery from sensors such as Landsat and ASTER (Morissette *et al.*, 2005; Schroeder *et al.*, 2008a, 2008b), as well as comparisons with databases maintained by fire management agencies (Benali *et al.*, 2016).

Satellite-based active fire detection systems can show ‘false-alarms’ (false positives or commission error), due to sunglint, forest clearing, desert boundaries, black soil, or hot rocks (Giglio *et al.*, 2016; GA, 2020). False negatives (omission error) from satellite-based systems may be due to small fires, fires of short duration, persistent cloud cover, thick smoke, or topographic shadow effects (de Klerk, 2008;

Hawbaker *et al.*, 2008; Benali *et al.*, 2016; Giglio *et al.*, 2016). Updated algorithms for the MODIS Fire and Thermal Anomalies product (Collection 6) were targeted to address limitations observed with the previous Collection 5 fire product, notably the occurrence of false alarms caused by small forest clearings, and the omission of large fires obscured by thick smoke (Giglio *et al.*, 2016). Ongoing research into the physical properties and processes of fire, and their relation to remotely sensed measurements may help to further reduce these errors in EO of active fires.

Improved fire detection products have recently been developed that build on the well-established MODIS Fire and Thermal Anomalies product. Schroeder *et al.* (2014) describe an algorithm that uses the Visible Infrared Imaging Radiometer Suite (VIIRS), launched in October 2011 aboard the Suomi-National Polar orbiting Partnership (S-NPP) satellite. Initial assessments indicate significant improvements in the mapping capabilities of active fires, compared to the MODIS product, including greater consistency in delineating burned area extent (Schroeder *et al.*, 2014).

Recent advances in geostationary sensors also offer potential improvement in satellite-based active fire detection methods. For example, the Advanced Himawari Imager onboard the Himawari-8 satellite in 2014, provides near real time access to imagery at ten-minute intervals. The high temporal resolution provides an increased volume of data, capturing contextual information to describe background temperature of a landscape in the absence of fire, and increases the opportunity for cloud-free imagery (Hally *et al.*, 2018). Wickramasinghe *et al.* (2016) have developed a multi-spatial resolution approach to the surveillance of active fire lines using data acquired by Himawari-8. In Australia, the DEA Hotspots service routinely delivers hotspot information detected from Himawari-8 imagery (see Section 18.7).

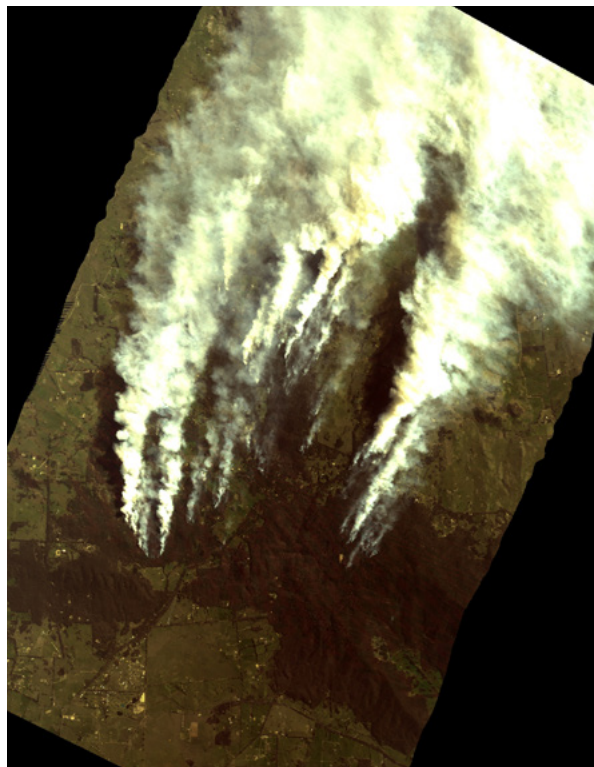
¹⁵ A contextual algorithm based on Lee and Tag (1990) and Flasse and Ceccato (1996) used AVHRR bands 3 and 5, as well as latitude and Sun elevation to classify pixels as ‘fire’ or ‘possibly fire’.

Among the ancient elements, fire is the odd one out. Earth, water, air—all are substances. Fire is a reaction. It synthesises its surroundings, takes its character from its context. It burns one way in peat, another in tallgrass prairie, and yet another through lodgepole pine; it behaves differently in mountains than on plains; it burns hot and fast when the air is dry and breezy, and it might not burn at all in fog. It's a shape shifter.
(Pyne, 2015)

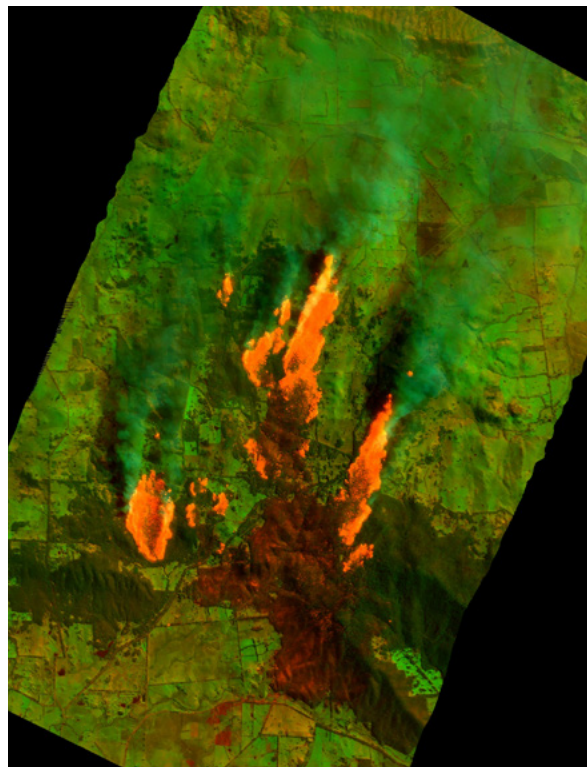
Figure 18.3 Aerial imagery of active fire

A bushfire near Myall Park (western Darling Downs, Queensland) on 5 December 2021 was imaged from 25,000 feet. These true and false colour composites demonstrate the valuable fire information provided by the longer infrared wavelengths that is obscured by smoke in visible wavelengths (see also banner image for Section 18 on page 389).

a. True colour composite



b. False colour composite using 2.2 μm (SWIR) as red, 1.6 μm (SWIR) as green, and $\sim 0.5\mu\text{m}$ (visible blue) as blue.



Source: Robert Norman, Air Affairs Australia Pty Ltd

18.5 Retrospective Fire Analyses

A major advantage of using EO in fire studies is the ability to retrospectively view the environmental conditions that preceded a fire. Standardised EO time series datasets offers this unique ability to obtain pre-fire environmental conditions after a fire event has occurred (see Volume 2D). Equivalent retrospective analyses are generally only possible with field studies prior to planned burns, which may not necessarily burn the area that was measured.

EO-based retrospective fire analyses characterise the effects of fire on the landscape, including removal of vegetation and alteration of vegetation structure. These changes may reveal understory vegetation or soil, and deposition of charcoal and ash. Change detection techniques that capture the difference between pre- and post-fire imagery in relation to reflectance properties of soil, water, and vegetation, are commonly used in EO of fire extent and severity (Miller *et al.*, 2009; Cansler and McKenzie, 2014; see Volume 2D). Pre-processing of EO data is especially pertinent for image differencing techniques (see

Volume 2C). For example, Gitas and Devereux (2006) demonstrated a 40% increase in mapping accuracy of forest fires after using topographic correction. Variations in solar angle and atmospheric influences also have demonstrable effects on the spectral separation of burned and unburned vegetation (Trigg *et al.*, 2005; see Volumes 2A and 2X).

Reflectance properties of land cover may be influenced by fire severity, vegetation, topography, and the spectral and spatial resolutions of the EO sensor (see Volume 1B—Section 6). In general, visible and NIR reflectances decrease after fire due to charring and reduced green vegetation (Trigg and Flasse, 2000). In some cases, the presence of white ash and the exposure of highly reflective soils can increase visible and NIR reflectance (Roy and Landmann, 2005; Huang *et al.*, 2016). A post-fire rise in MIR and SWIR reflectances occurs due to greater soil exposure and changes in vegetation moisture content (Poon and Kinoshita, 2018). Ratios of NIR and SWIR bands therefore enhance the contrast

between burned and unburned areas, although the precise relationship between spectral indices and fire severity is poorly understood (Lentile *et al.*, 2006). To maximise the value of EO, the underlying processes that control fire effects need to be better understood and linked directly to EO measurements.

There are generally two temporal categories for analysing fire effects (Reinhart, 2001):

- First-order or immediate effects—the direct consequence of fire, such as damage to, and death of, vegetation, fuels consumed, and smoke produced; and
- Second-order or delayed effects—the impact of subsequent weather conditions and time, including dispersion of smoke, erosion, and vegetation recovery, changes in species composition, and other ecological responses.

First order effects are only observable for a short period after the fire, while second order effects may be observable for months or years after the fire. The length of time varies with fire severity, seasonality, and productivity of the landscape. First order effects may become undetectable within days in highly dynamic ecosystems during peak growth periods. Similarly, dissipation of ash and charcoal will modify radiance of burned areas (Roy *et al.*, 2002), which may be exacerbated with high post-fire rainfall. Vegetation may start to regrow, with growth rates dependent on primary productivity and environmental factors. Vegetative recovery (second-order effect) has phenological signals that may mask the first-order effects. Field validation may increase confidence that the targeted effects (first or second order) are being captured by the imagery used.

Several authors have noted the lack of standardisation for describing and measuring post-fire effects (Morgan *et al.*, 2001; Lentile *et al.*, 2006; Keeley, 2009). Many commonly used methods are qualitative, so lack an objective basis to consistently apply them to different times, places, and scales. A standardised Australian system would greatly improve data quality and fire management outcomes for assessing fire impacts.

This section will discuss some of the most useful retrospective analyses of fire in EO, including:

- delineating the extent of a fire and classifying the severity of its impact on vegetation (see Section 18.5.1);
- monitoring environmental recovery after fire (see Section 18.5.2); and
- analysing fire history and fire behaviour to understand underlying patterns and major drivers (see Section 18.5.3).

Operational systems that use EO datasets to map fire extent and severity are introduced in Section 18.6.

18.5.1 Fire extent and severity

Fire extent (variously termed fire scar, burned area, fire footprint, and fire perimeter) delineates burned from unburned ground, whereas fire severity measures the loss or change in organic matter caused by fire (Keeley, 2009). Fire severity differs from fire intensity, which is the energy output of the fire. Fire impacts vary regionally due to differences in climate, vegetation, topography, and biogeography, but are generally more heterogeneous in areas of low and moderate severity compared to high severity (Turner *et al.*, 1999). Fire releases carbon stored in living and decaying vegetation so fire severity metrics may also be used to estimate carbon emissions (Chuvieco, 2008; see Section 17).

Fire extent and severity mapping is best suited to a post-fire analysis, as the perimeter and proportions of severity classes continue to change during an active fire (Hudak *et al.*, 2007). Traditional measures of fire severity relied on field determination of the depth of burn in vegetation structure, the volume of scorched vegetation, and changes in soil colour and condition. EO data now provides a cheaper and more extensive basis for evaluating fire extent and severity, with arguably greater standardisation and accuracy compared to either manual hand-digitisation in the field or helicopter-based methods (Kolden and Weisberg, 2007). Fire severity classifications derived from EO are useful for many applications, including:

- understanding post-fire fuel loads and re-accumulation in relation to fire severity and fuel type (Eskelson and Monleon, 2018);
- modelling environmental drivers and landscape patterns of fire severity (King *et al.*, 2008; Estes *et al.*, 2017);
- assessing impacts of fire severity on habitats and ecological processes (Berry *et al.*, 2016; Collins *et al.*, 2019; Walker *et al.*, 2019);
- understanding effects of climate change on fire regimes (Enright *et al.*, 2015; Wang *et al.*, 2015);
- analysing effectiveness of hazard reduction treatments and predicting severity of subsequent wildfires (Bradstock *et al.*, 2010; Price *et al.*, 2012);
- identifying high erosion risk sites when combined with slope and aspect information (Salis *et al.*, 2019);
- calibrating fire behaviour models and exploring patterns of fire occurrence (Diaz-Delgado *et al.*, 2004); and
- predicting ecosystem recovery (Lentile *et al.*, 2009).

Fire severity information is also valuable for operational activities, such as salvaging timber and predicting impacts on water quality within water supply catchments. To map fire extent and fire severity both require the delineation of burned from unburned areas, with severity requiring additional

information about the relative scale of impact within the area burned. Fire extent and severity may be mapped manually by aerial reconnaissance or on the ground. Activities undertaken by many operational fire management organisations, such as the NSW RFS and the USFS, routinely capture aerial and ground-based sketch mapping of fire extents. While suited to the objectives at time of capture, such as emergency incident management, there are accuracy and consistency limitations in using such fire history data for other applications. EO offers a cost-effective, standardised, repeatable, landscape scale view, which is particularly advantageous for remote and inaccessible locations. Digital Earth Australia (DEA; see Volume 2D—Section 11.2) has offered an unprecedented opportunity to develop a continental fire history map for Australia (Renzullo *et al.*, 2019; see Section 18.7).

Accuracy of fire extent and severity mapping using EO imagery is influenced by temporal, spectral and spatial resolution (see Section 18.2 and Volume 1B—Section 1). Temporally, the data needs to image the effects of fire as soon as possible after combustion, once smoke has sufficiently cleared. The date of the post-fire imagery needs to be late enough that the full extent of the fire has been reached (that is, the fire is extinguished), and early enough that post-fire recovery of vegetation has not commenced. Vegetative recovery rates are not well-quantified at a standardised, regional scale. They are likely to be highly variable between vegetation types and climate regions. However, in forest and woodland communities, moderate resolution satellite imagery is typically used to capture immediate post-fire effects for up to 6–8 weeks post-fire. In some landscapes, fire effects are clearly measurable for some time afterwards, so field measurements can still be usefully conducted at a much later date.

Spectrally, EO data needs to be unaffected by smoke and cloud. While smoke and cloud contamination may inhibit suitable acquisition of post-fire imagery, the recent EO satellite launches have significantly increased the frequency of capture of multispectral imagery. The NIR and SWIR spectral wavelengths are important in detecting fire effects and delineating burned from unburned area. The charring and removal of vegetation results in a post-fire reduction in NIR, while soil exposure and increased radiation absorption by the charred vegetation results in a post-fire rise in SWIR (Pereira *et al.*, 1999). Acquisition of SWIR reflectance is generally limited to large satellite-borne sensors, due to the cryogenic cooling systems required, however future developments in technology are likely to eliminate this limitation (Keller, 2019). Radar and other active sensors such as lidar can penetrate cloud and smoke as well as the forest canopy to inform about fire effects in the understorey (see Excursus 5.1 and Volume 1A—Section 15). While

active sensors have demonstrated applications in fire extent and severity mapping (Tanase *et al.* 2014; Hu *et al.*, 2019), passive optical sensors are more commonly used. Current research is being undertaken on the potential for integrating active and passive sensors for fire extent and severity mapping, as well as monitoring post-fire recovery.

Spatially, EO data must be sensitive to the landscape patterns of burned and unburned ground as well as the scale of fire severity. Many EO analyses of fire extent and severity are conducted at a local scale, using imagery from medium scale sensors (such as Landsat TM and Sentinel-2 MSI). For large fires (> 100 ha), accuracies over 80% are common. The accuracy of estimates from coarse spatial resolution data is affected by the spatial patterns of fires. With coarser resolution sensors (such as MODIS) many small, scattered fires can be easily omitted, leading to an underestimation of total area burned, whereas a predominance of large, compact fires can cause overestimation of burned area (Eva and Lambin, 1998; Silva *et al.*, 2005). Higher resolution sensors have the potential for greater precision in mapping fine scale patterns in severity and unburned mosaics within the larger fire extent. Operational products of fire extent and severity are available from a number of international and Australian agencies as detailed in Sections 18.6 and 18.7. Several studies have highlighted deficiencies in these products (Bradley and Millington, 2006) while some have reported consistency with other image-based maps (Boschetti *et al.*, 2008). National scale, fire severity mapping programs are not currently operational in Australia, and presents a clear gap in Australia's fire mapping capability.

Regardless of the method used to produce a fire severity classification, some form of validation of results is required before it should be used on an operational basis. High resolution aerial photography that is captured immediately post-fire provides a surrogate for field observation data to independently validate EO-based fire extent and severity mapping products. Although not routinely captured after all fires in most jurisdictions in Australia, land and fire management agencies often commission large or otherwise notable fires to be flown for high resolution aerial photography. Various satellites are also able to capture high resolution imagery suitable for independent validation techniques (see Volume 1A—Section 12). While this data is not freely available, high resolution post-fire imagery can be a worthwhile investment for many applications when compared to the time and cost invested in traditional field validation. High resolution imagery is also suitable for broadscale landscape studies and validation of various EO-modelled fire mapping products (such as Vanderhoof *et al.*, 2017, Collins *et al.*, 2018, Gibson *et al.*, 2020).

18.5.1.1 Normalised Burn Ratio

A commonly used reflectance index in fire extent and severity mapping is the differenced normalised burn ratio (dNBR), which highlights the differences between pre- and post-fire imagery to detect the fire-induced spectral response in the NIR and SWIR wavelengths (Lopez Garcia and Caselles, 1991; Key and Benson, 1999; see Section 9.2.1 for equations). This index has been shown many times to be more effective than NDVI for this application. Initially developed for Landsat TM imagery, the dNBR is also suited to data with similar spectral bandwidths, such as Sentinel-2 MSI. The dNBR is used in national fire extent and severity mapping programs, such as the US Monitoring Trends in Burn Severity (MTBS; Eidenshink *et al.*, 2007), and has been shown to produce reasonable accuracy compared to field validation for severity within a single fire, across a range of vegetation communities (for example, approximately 60–70% accuracy; Miller and Thode, 2007; Soverel *et al.*, 2010; see Section 18.6.3). Miller and Thode (2007) also produced higher accuracy maps, especially for high fire severity classes in heterogeneous landscapes, using dNBR relativised for the pre-fire NBR (the RdNBR; see Section 9.2.1; also Miller *et al.*, 2009).

Many studies have compared alternative reflectance indices against the dNBR, which has been widely reported to be more sensitive to fire effects than dNDVI and NDVI (Hudak *et al.* 2007, Escuin *et al.*, 2008). Other studies have reported that NBR and its variants were insensitive to some post-fire spectral changes soon after fire occurrence (Roy *et al.*, 2006; Lewis *et al.*, 2007). Variations in NBR can occur due to changes in seasonal solar elevation and topographic shadowing in high latitudes (Verbyla *et al.* 2008, French *et al.* 2008). Many spectral indices are confounded by dark soil backgrounds, which become indistinguishable from burned areas. In forest communities with understorey/mid-storey structural layers, reflectance indices in general have greater accuracies in quantifying canopy fire effects than sub-canopy fire effects, which is an expected limitation of passive optical EO approaches.

The dNBR, like many other fire severity reflectance indices, have limited accuracy when thresholded into standardised severity classes for comparison between different fires, due to the influence of pre-fire vegetation structure, soil type, and vegetation moisture (Miller and Thode, 2007; Kolden *et al.*, 2015). A combination of multiple indices may provide more complete and accurate information than any single index (Miller and Thode, 2007). Indices measuring the relative sub-pixel cover of photosynthetic, non-photosynthetic material, and bare ground (such as fractional cover, or spectral unmixing; see Excursus 8.3) may provide a closer estimate of the quantity of organic matter consumed by fire compared to NBR.

18.5.1.2 Composite Burn Index

The Composite Burn Index (CBI), also referred to as the Geometrically-structured Composite Burn Index (GeoCBI), was specifically developed to validate regional classification schemes of EO-derived fire severity data (Cansler and McKenzie, 2014). It is the most commonly used method to field validate and calibrate fire severity reflectance indices (e.g. Strand *et al.*, 2013; McCarley *et al.*, 2017). Measurements of surface and vegetation changes are visually estimated and aggregated into a unitless score and the protocol requires a subjective estimate of pre-fire condition by including field plots in adjacent unburned areas. Miller and Thode (2007) also report that some transformation may be required when dNBR or RdNBR is used to model CBI since NBR is sensitive to soil conditions and CBI is primarily a vegetation severity measurement. CBI reaches a maximum value when there is complete vegetation mortality as opposed to dNBR (which varies in value after complete vegetation mortality, resulting in a nonlinear relationship between dNBR to CBI). Furthermore, CBI correlates poorly to biophysical metrics and to the spectral reflectance of the top surface, which is likely due to the combinations of effects that can result in the same CBI score (Hudak *et al.*, 2007; Miller and Thode, 2007). Keeley (2009) questioned the validity of using a composite field index (such as CBI) that combines attributes of fire severity and ecosystem response, even if it is correlated with spectral measures.

18.5.1.3 Alternative approaches

Spectral unmixing is increasingly being demonstrated as an effective, if somewhat complicated, method for mapping fire extent and severity in EO (see Section 8.3 and Volume 2E). Spectral unmixing uses a calibrated relationship with high quality, quantitative field data (Scarath *et al.*, 2010; Guerschman *et al.*, 2015), which may be more directly analogous to traditional field-based assessment (Lentile *et al.*, 2006; Morgan *et al.*, 2014; Meddens *et al.*, 2016). Spectral unmixing methods have been used with hyperspectral imagery to assess fine scale effects of fire on the soil surface (Robichaud *et al.*, 2007; Lewis *et al.*, 2007). Alencar *et al.* (2011) used a system based on a Monte Carlo mixture modeling approach to define the usual photosynthetic, non-photosynthetic, and bare fractions, plus a fraction called shade/burn (defined as having zero reflectance in all spectral wavelengths) to distinguish the canopy disturbances caused by fire from those caused only by logging. The resulting Burn Scar Index (Alencar *et al.*, 2011) produced a classification accuracy of 88.9% for burned area, and 95.15% for unburned area. Gibson *et al.* (2020) compared the performance of multiple indices (including spectral unmixing of Sentinel-2 data and

reflectance-based indices) in a machine learning framework trained on severity class samples derived from high resolution post-fire aerial photograph interpretation and concluded that the addition of fractional cover-based indices was particularly helpful in delineating burned from unburned areas.

RTM inversion shares some similarities with spectral unmixing (see Section 8.3), with the spectral response of target surface types being obtained through an RTM, rather than from sampling the image directly (Yin *et al.*, 2019). Pixels are subsequently classified as one of the modelled surfaces based on the similarity to the modelled spectral responses. De Santis *et al.* (2010) developed this approach for the purpose of mapping fire severity by using the PROSPECT leaf RTM coupled to the GeoSail canopy RTM to forward model spectra for 30 different surfaces with different fire severity levels (defined by their GeoCBI index; see Section 18.5.1.2) in coastal California. These spectra formed a Look-Up Table (LUT), and for each pixel, the closest match was defined by the ‘spectral angle’ between model and observed reflectances (see Volume 2D—Section 7). The approach showed a strong linear relationship with field-observed GeoCBI values.

Recent advances in computing technology, such as readily accessible cloud-based satellite data and processing services, have opened new frontiers to develop more sophisticated techniques with complex datasets and multiple indices. Recent examples in fire extent severity mapping include principal components analysis (PCA; Aitkaci *et al.*, 2018, Alexandris *et al.*, 2017; see Volumes 2C and 2D), supervised image classification using machine learning (see Volume 2E) and Google Earth engine (Collins *et al.*, 2018), and the integration of reflectance and fractional cover indices in a machine learning framework (Gibson *et al.*, 2020). Some of these techniques have demonstrated greater sensitivity and predictive power compared to traditional approaches, particularly in complex heterogeneous environments.

18.5.2 Fire recovery

Post-fire recovery is a second-order effect of fire, characterised as a successional process towards either the pre-fire community structure and function or to an alternative stable state (Turner *et al.*, 2016). Measuring and monitoring fire severity and subsequent post-fire recovery are essential for understanding the full effects of fire across the landscape. The relationship between fire severity and post-fire recovery rates has long been a focus for ecology and global carbon cycle studies and is becoming a more pressing issue, as the frequency and severity of fire disturbance increases with warmer and drier global climatic conditions (Turner *et al.*, 2016, Meng *et al.*, 2018).

Post-fire forest recovery is closely connected to fire severity, with strong spatial heterogeneity across the landscape (Bolton *et al.*, 2015). The interaction between first-order fire effects (fire extent and severity) and environmental variables, such as rainfall and climate conditions, influence the post-fire recovery trajectory over time, which may be observable for decades after a fire. The rate of ecosystem recovery after fire depends on local and regional weather, the timing and severity of fire, and the type of vegetation affected. In some communities, high severity burns may encourage subsequent weed invasion and erosion, and may destroy seed or vegetative sources. By contrast, in other communities, high severity fires may promote greater rates of resprouting or seedling emergence than lower severity fires. Post-fire vegetation recovery rates may also vary between species within a community and between conspecific individuals (such as age-related variation in resprouting response to fire; Bellingham and Sparrow, 2000). For example, a homogenous area of extreme fire severity (that is, 100% post-fire loss of above ground biomass) may display heterogeneous patterns in the rates of vegetative resprouting in one vegetation community, while another community may display a more even and rapid rate of resprouting or regrowth (for example, a closed forest with a mix of resprouter and obligate seeder plant functional types (see Section 4.2.1) compared to an open grassland). Such variation in recovery from fire can create difficulty in applying and interpreting metrics of fire recovery between different communities. This highlights the importance of local knowledge for interpreting EO fire mapping products.

A wide range of approaches to monitoring post-fire recovery have been explored in the literature, including image classification (see Section 8.2 and Volume 2E), NDVI (Malak and Pausas, 2006), dNBR (Lentile *et al.*, 2007), SAR-based recovery index (Minchella *et al.*, 2009), char fraction (Smith *et al.*, 2007a), and NDVI time series (Hope *et al.*, 2007). Spectral unmixing has also been used for multi-temporal cover change mapping (Okin, 2007), as well as the vegetation structure perpendicular index (VSPI; Massetti *et al.*, 2019). LandTrendr, based on Landsat SWIR data, has also been tested for recovery monitoring applications. However, it requires a recovery curve pattern assumed *a priori* (Kennedy *et al.*, 2010), which may be a limitation for applying the model at a landscape scale without local knowledge.

The limitations of different EO sensors for monitoring post-fire recovery are becoming widely recognised. The key limitation of optical sensors is the difficulty in separating post-fire forest canopy recovery from understorey recovery (Castro *et al.*, 2011; Fisher *et al.*, 2016). While understorey vegetation (including shrubs, herbaceous, and woody) can

recover quickly after a fire event, the structure and function of understorey vegetation may differ from the pre-fire canopy in terms of lifeform, productivity, and capacity for carbon and water storage (Swanson *et al.*, 2011).

Radar sensors can penetrate cloud, haze, and smoke, and are sensitive to forest structure and biomass (see Volume 1A—Section 15.2 and Volume 1B—Section 8). The SAR L-band sensitivity to forest structural parameters allows for differentiation between forest growth and degradation stages, which may be useful for post-fire regrowth monitoring (Joshi *et al.*, 2015), although known soil moisture effects need to be carefully accounted for (Chu and Guo, 2014). Discriminating post-fire recovery from ALOS PALSAR data was observed to be difficult during early stages of regrowth due to saturation effects (Tanase *et al.*, 2011). Multi-sensor integrated approaches for recovery monitoring are becoming more commonly explored, especially as computing power and processing limitations are further reduced with advancing technology.

18.5.3 Fire history and behaviour

Fire extent and severity mapping compiled over many years gives the opportunity for spatiotemporal patterns of fire incidence, frequency, and severity to be examined (Boer *et al.*, 2006, 2008; Tolhurst and McCarthy, 2016; Case and Staver, 2017). Over 40 years of global satellite data are now available to analyse the progression of a wide range of fire events. Various statistics can be derived from such fire history databases, including years burned, years since last burn, extent of burned area, and frequency of fire, which are commonly used by land and fire management agencies to inform prescribed burning plans. Many of these statistics are now available on web-based fire mapping systems (see Section 18.7). Time series analysis techniques are particularly useful in this context to highlight and quantify patterns of change (see Volume 2D—Sections 8 and 9). Time series analyses of fire extent and severity can help to inform the role of fuel treatments and previous wildfire on subsequent fire extent and severity patterns across the landscape (Tolhurst and McCarthy, 2016, Lydersen *et al.*, 2017).

Recent advances in fire behaviour studies have integrated analyses of EO data captured prior to, during and immediately after a fire event. For example, meteorological observations during a fire event may be used to help understand the role of pyro-convection in driving atypical and dangerous fire behaviour (pyroCb storms; Fromm *et al.*, 2010, McRae *et al.*, 2015; see Section 18.3.2). Line scan aerial imagery can help to understand the interaction between wind and terrain on fire behaviour (Sharples *et al.*, 2012) and factors influencing patterns of spotfire dynamics (see Section 18.3.3). A strong understanding of the effects of meteorological conditions on fire behaviour allows the forecasting of violent and dangerous fire conditions (see Section 18.3.4). Maps of hotspots and subsequent fire extents may be compared to model fire progression (see Section 18.4). This approach is particularly useful for large, unimpeded fires, as occur in tropical savanna landscapes.

Fire simulation systems, such as Phoenix Rapidfire in Australia (Tolhurst *et al.*, 2008), offer a fire behaviour analysis tool that is commonly used for decision support by land and fire managers (Miller *et al.*, 2015). Inputs include atmospheric conditions, fuel conditions, topography, and initial fire location, which can be sourced from a range of databases or derived from satellite imagery. However, fire simulation systems generally use rate of spread models generated under moderate conditions (to enable safe control of the experimental fire), and as such may have limited accuracy in predicting the dynamic wildfire behaviours that occur under more extreme fire weather conditions (Filkov *et al.*, 2018).

Recent climatic changes have been associated with increased frequency of extreme fire weather and consequently, extreme fire events (Collins, 2014; Stavros *et al.*, 2014). These changes are increasing the potential for erratic and extreme fire behavior that puts lives and property at greater risk. Under extreme fire weather conditions, fire behaviour can rapidly change with regard to rate of spread and fire intensity, including unusual or unpredictable phenomena such as plume-dominated spread, vorticity-driven lateral spread, and mass spotting events (Sharples *et al.*, 2012). Further research and more sophisticated prediction models of fire behaviour are increasingly more critical to provide early warnings to protect the lives of fire fighters and local communities.

18.6 Operational Systems for Fire Management

EO methods offer a consistent, scientific base from which known measures of fire likelihood can be extrapolated (both fuel ignition and potential). The vast landscapes of the Australian environment make EO the only cost-effective way to achieve the broadscale assessments required for fire management. While EO imagery offers a unique perspective of any landscape, the challenge in Australia is to identify those elements in this perspective which are associated with the potential for fire in our landscape—and its impact.

Hitherto EO has been an underutilised resource for mapping, monitoring, and studying fire in Australia. While most agencies use EO data for some aspects of fire planning and management, the potential benefits of this technology are not being completely realised. Operational use of EO for fire management in Australia is often opportunistic, relying on data, equipment, methods and validation as these become available. Many risk assessment procedures for fire management currently rely upon subjective measures of fuel condition and load, which can vary significantly within and between geographic regions and jurisdictions.

Following the unprecedented bushfire crisis of 2019/20, five recommendations from the NSW Independent Bushfire Inquiry focus on further government investment into EO of fire to improve fire management and emergency response:

- 4—establish a spatial technology acceleration program to maximise the information available from the various EO technologies;
- 18—ensure that there is a single whole-of-government procurement and acquisition program for imagery;
- 22—as part of the spatial technology acceleration program, support deployment of EO and image processing technologies for monitoring and auditing;
- 36—invest in long term ecosystem and land management monitoring, modelling, forecasting, research and evaluation, and harness citizen science, to (among other things) better understanding the influence of different land management practices on landscape flammability; and
- 51—expand the Remotely Piloted Aerial Systems (RPAS) capability of NSW Fire and Rescue.

Recommendations from the Royal Commission into National Natural Disaster Arrangements, 2020, reiterate the need for national coordination and dissemination of relevant spatial information, including EO datasets (CoA, 2020).

Nonetheless, EO datasets are already being used operationally in a number of areas of fire management in Australia. Operational systems implement research that will continue to be enhanced with ongoing development and refinements, including:

- modelling flammability (see Section 18.6.1);
- hotspots to locate active fires (see Section 18.6.2); and
- fire extent and severity following fires (see Section 18.6.3).

18.6.1 Flammability models

The Australian Flammability Monitoring System (AFMS; <http://anuwald.science/afms>) is an experimental, operational, near real time flammability data service developed by the Australian National University (ANU) with funding from the Bushfire and Natural Hazards CRC (BNHCRC) to support fire risk management and fire operation response activities such as hazard reduction burning and pre-positioning firefighting resources and, in the longer term, the new National Fire Danger Rating System (see Table 18.3). The AFMS has been built in consultation with end users to make sure the system is adapted to their needs in terms of, for example, data content and formats. The AFMS provides information on fuel moisture content and flammability across Australia at 500 m resolution. It also displays information on soil moisture content near the surface (0–10 cm) and shallow soils (10–35 cm) as research outcomes from the joint BoM/BNHCRC project entitled ‘Improving land dryness measures and forecast’. The AFMS is the only system of this kind at a continental scale and it is in the process of being transitioned to GA to sustain the system into the longer term.

Table 18.3 Current and potential uses of the Australian Flammability Monitoring System

FMC: Fuel Moisture Content

Stage	Purpose	Usage examples
1. Planning	Assist with scheduling plan prescribed burns	Drier FMC in a forest may indicate more potential to scorch the canopy
		Fuel moisture differential can act as soft control lines
		Long term fuel conditions for the Prescribed Burning Decision Support Tool (PB-DST)
		Emissions assessment and smoke dispersion
2. Preparedness	Amend preparedness levels	These relate to Fire Danger Rating in response to lower/higher than average landscape dryness conditions or exceed set defined thresholds
3. Response	Assist in firefighting and resources allocation	FMC as an input in Spinifex grass fire behaviour
		Highlight potential for anomalies in predicted rate of spread: for lower FMC a fire may spread faster than predicted
		Soft control lines based on fuel moisture differential

Source: Marta Yebra, ANU

18.6.2 Hotspot imagery

Web-based GIS systems are commonly used to provide near real time, end user access to active fire products in order to support natural resource management and operational fire management decisions. A range of web-based platforms have been developed, using different satellite systems to derive end user products for different regions of the world (see Section 18.4.1 and Excursus 18.1).

In Australia, AVHRR and MODIS imagery are incorporated into several web-based active fire monitoring systems to deliver hotspot information in near real time (with 0.5–2 hour delay). As detailed in Section 18.7, such systems include Firenorth, NAFI (North Australian Fire Information), and Landgate FireWatch (WA). The revised Sentinel Hotspots system (now called DEA Hotspots) also incorporates information from the AHI sensor on the Himawari-8 satellite using algorithms developed by Landgate to derive active fire products (GA, 2020). In addition, Australian fire information is available from Sentinel Asia and some global fire mapping systems (see Section 18.7).

18.6.3 Fire extent and severity

National scale estimates of fire extent have been derived from a range of imagery, including AVHRR (Otón *et al.*, 2019) and MODIS (Roy *et al.*, 2002, Roy *et al.*, 2005, Chen *et al.*, 2017b). One of the global MODIS land products (MCD45A1) is a monthly, 500 m, burned area product (Roy *et al.*, 2005), based on an automatic algorithm that uses a “bidirectional reflectance distribution function (BRDF) model-based expectation approach” (Roy *et al.*, 2002). Various updates and refinements to the MODIS burned area algorithms have occurred, with the current version (collection 6) providing considerably

more sensitivity than the original (Giglio *et al.*, 2016). Chuvieco *et al.* (2018) developed an algorithm that uses MODIS red and NIR reflectances and thermal anomalies data, which provides the highest spatial resolution (~250 m) among the existing global burned area datasets.

The Monitoring Trends in Burn Severity (MTBS) project maps the fire extent and severity of all large fires (> 1000 acres in the west; > 500 acres in the east) in the USA using Landsat imagery since 1984 (Eidenshink *et al.*, 2007; see Section 18.7). This work is sponsored by the Wildland Fire Leadership Council (WFLC) and conducted by the USGS Centre for Earth Resources Observation and Science (EROS) and USFS Remote Sensing Applications Centre (RSAC). The project uses dNBR and RdNBR to manually delineate fire extents (see Section 18.5.1.1). Analyst input is required to determine appropriate image thresholds of dNBR and/or RdNBR fire severity classes, based on the method proposed by Key and Benson (2006). Fires in a range of landscapes have been cross-calibrated to maintain consistency. Results are used to determine long term fire trends for policy purposes, pre- and post-fire assessment and monitoring, LANDFIRE data inputs (see Section 18.3.4), and academic fire severity research.

In Australia, automated or semi-automated systems are operational for fire extent mapping over the rangelands of northern Australia, with differing approaches being adopted in different jurisdictions. Queensland government produces an annual burned area map based on Goodwin and Collett (2014). The NAFI burned area methodology involves differencing pre- and post-fire MODIS imagery with a subsequent segmentation and classification step including some supervisor input. Landgate (WA) also deliver burned area maps and fire history products (see Section 18.7).

In NSW, the Department of Planning, Industry and Environment (DPIE) in partnership with the NSW RFS, is in the final stages of testing an operational fire extent and severity mapping system (FESM), based on a Sentinel-2 random forest algorithm (Gibson *et al.*, 2020). The FESM system was used to support NSW and ACT Government rapid response operations during the bushfire crisis of 2019/20.

In Victoria, the Department of Environment, Land, Water and Planning (DELWP), in partnership with La Trobe University, have implemented a severity mapping system that closely aligns with the severity classification framework used in NSW (Collins *et al.*, 2018). This mapping, which uses Landsat and Google Earth Engine, was generated and made publicly available for the Victorian fires following the bushfire crisis of 2019/20.

An automated algorithm for nation-wide burned area and severity mapping using DEA infrastructure (see Volume 2D—Section 11.2) was recently developed and is close to operational. The algorithm includes a sequence of:

- change detection—for individual pixels based on the cosine distance between the observed and geometric median reflectances for preceding years (Roberts *et al.*, 2017);
- change characterisation—uses absolute and relative NBR and cosine distance changes to quantify fire severity and duration;
- region growing—helps to improve classification by contracting pixels with below-threshold evidence of burning; and
- attribution—integrates results with DEA Hotspots (see Section 18.7) and any externally-available fire maps to produce a burned area product with pixels identified as: potential (detected change); corroborated (change coinciding with detected fire); or confirmed (change coinciding with externally provided burn information).

Depending on the objective of fire mapping and the jurisdiction in Australia, there may be a trade-off decision regarding the spectral and spatial resolution of different data types for operational programs of mapping fire extent and severity. For local scales, where high resolution post-fire aerial imagery has been captured, hand digitisation of fire extent and severity may be appropriate. This is routinely undertaken by the Victorian government, for example. However, for broader scales, or where high resolution post-fire aerial photography is not routinely captured, satellite sensors using spectral analysis will be more appropriate. The most suitable data source and mapping strategy is also likely to vary between landscapes, climatic zones, and biogeographic regions (Gregoire *et al.*, 2003). Edwards *et al.* (2013) proposed that fire severity classification in northern Australia, dominated by open savanna woodlands, would be suited to simply differentiating ‘Severe’ from ‘Not-Severe’. By contrast, in forested ecosystems of southern Australia, fire severity is more accurately categorised with a higher number of classes to discriminate varying levels of scorch, and consumption of canopy and understorey layers (McCarthy *et al.*, 2017; Gibson *et al.*, 2020). Approaches to mapping fire extent may also require different solutions in landscapes where fire locations are generally unknown, such as vast remote areas of northern Queensland, Western Australia, and the Northern Territory, compared to NSW and Victoria where 95% of fires have their locations identified and mapped by incident management authorities shortly after ignition.

18.7 Further Information

2020 Royal Commission into National Natural Disaster Arrangements

<https://naturaldisaster.royalcommission.gov.au/publications/html-report>

Geoscience Australia (GA)

Bushfires: <https://www.ga.gov.au/scientific-topics/community-safety/bushfire>

DEA Hotspots is an upgraded version of Sentinel Hotspots originally developed by CSIRO. DEA Hotspots, features a number of contextual layers and interactive functions, including historical fire data, with latency of 17–60 minutes: <https://hotspots.dea.ga.gov.au/>

TERN AusCover

Fire Dynamics and Impact—a range of monthly fire-related maps to track vegetation and landscape changes over time: http://www.auscover.org.au/dataset_categories/fire-dynamics-impact/

Seasonal composites of fractional cover based on Landsat-5, -7 and -8 for every calendar season since 1986 are available from: <http://auscover.org.au/purl/landsat-seasonal-fractional-cover>

Landgate (Western Australia)

Landgate provide several satellite online fire products and services:

- My FireWatch—national hotspot map updated every 2–4 hours: <https://myfirewatch.landgate.wa.gov.au/>
- FireWatch Pro—advanced fire information for management agencies: <https://firewatch-pro.landgate.wa.gov.au/home.php>
- Aurora—fire spread predictions and simulations: <https://aurora.landgate.wa.gov.au/home.php>

Other relevant Landgate products derived from EO datasets include maps of lightning detection, greenness/curing and burned area: www.landgate.wa.gov.au/maps-and-imagery

North Australia Fire Information (NAFI)

The North Australia Fire Information (NAFI) website was designed to meet the bushfire needs of fire managers in northern Australia. NAFI is a MODIS-based fire scar mapping system hosted by Charles Darwin University, which presents near real time hotspots and regularly updated fire scar maps, and includes data related to fire history: <https://www.firenorth.org.au/nafi3/>

New South Wales

NSW DPIE, in conjunction with NSW RFS, have developed a semi-automated fire extent and severity mapping (FESM) approach using Sentinel-2 imagery: <https://datasets.seed.nsw.gov.au/dataset/fire-extent-and-severity-mapping-fesm>

Australian Fire History

ANU WALD/GA DEA: an automated workflow is being developed to map burned area extent for operational use across Australia, with a focus on woody vegetation (Renzullo *et al.*, 2019): <http://wald.anu.edu.au/challenges/bushfires/burn-mapping/>

Victoria: This dataset represents the spatial extent of fires recorded in Victoria since 1903 primarily on public land, including bushfires and DELWP planned burn information. Since 2006 fire severity data has been included in the Fire History dataset. Country Fire Authority (CFA) data on fires occurring on private land has also been included since 2009: <https://discover.data.vic.gov.au/dataset/fire-history-records-of-fires-primarily-on-public-land>

Australian Flammability Monitoring System (AFMS)

AFMS allows users to visualise and interpret national scale information on live fuel moisture content and its uncertainty, a flammability index, and soil moisture content (both near surface and in shallow soil) as maps or graphs: <http://wenfo.org/afms/>

Sentinel Asia

Sentinel Asia is a cooperative led by the APRSAF (Asia-Pacific Regional Space Agency Forum) to share disaster information in the Asia-Pacific region (Held and Kaku, 2007). This region experiences the largest proportion of natural disasters in the world, many of which are observable in real time using satellite EO: <https://sentinel-asia.org/>

The Global Observations of Forest Cover and Land Cover Dynamics (GOFD-GOLD)

Internationally coordinated initiative to produce a globally consistent system that includes fire mapping and monitoring: <http://gofc-fire.umd.edu/>

MODIS Fire Products

modis.gsfc.nasa.gov/data/dataproduct/index.php

Monitoring Trends in Burn Severity (MTBS)

fsgeodata.fs.fed.us/mtbs/

Fire Philosophy Publications

- Bradstock, R.A., Gill, A.M., and Williams, R.J. (2012). *Flammable Australia: Fire Regimes, Biodiversity and Ecosystems in a Changing World*. CSIRO, Melbourne. 333pp.
- Dyer, R., Jacklyn, P., Partridge, I., Russell-Smith, J., and Williams, D. (Eds). (2002). *Savanna Burning Understanding and Using Fire in Northern Australia*. Tropical Savannas Cooperative Research Centre, Darwin. 136pp.
- Jurskis, V. (2015). *Firestick Ecology*. Connor Court Publishing, Ballarat. 335p. ISBN: 9781925138740
- Latz, P. (2007). *The Flaming Desert: Arid Australia—A Fire Shaped Landscape*. Alice Springs, NT. 164pp. ISBN: 9780646481753
- Pyne, S.J. (1992). *The Burning Bush: A Fire History of Australia*. Allen and Unwin, Sydney. 520pp. ISBN: 1863731946
- Pyne, S.J. (2012). *Fire: Nature and Culture*. Reaktion Books, London. 224pp. ISBN: 978 1 78023 046 7.
- Pyne, S.J. (2015a). *The Fire Age*. Aeon essay: <https://aeon.co/essays/how-humans-made-fire-and-fire-made-us-human>
- Pyne, S.J. (2020). *The Still-Burning Bush*. Scribe Short Books, Melbourne. 144pp. ISBN: 1920769757
- Steffensen, V. (2020). *Fire Country, How Indigenous Fire Management Could Help Save Australia*. Explore Australia. 240pp. ISBN: 9781741177268

18.8 References

- ADRKH (2020). *Australian Disaster Resilience Knowledge Hub* website: <https://knowledge.aidr.org.au/about/>
- Aguado, I., Chuvieco, E., Martin, P., and Salas, J. (2003). Assessment of forest fire danger conditions in southern Spain from NOAA images and meteorological indices. *International Journal of Remote Sensing*, 24(8), 1653–1668.
- Aitkaci, M., Gitas, I.Z., Alioua, A., and Khaddaj, T. (2018). Burned area mapping using single-date principal components analysis. In *Recent advances in environmental science from the Euro-Mediterranean and Surrounding Regions. Proceedings of EMCEI-1, Tunisia 2017*. Advances in Science, Technology and Innovation (IEREK Interdisciplinary Series for Sustainable Development) (Eds: A. Kallel, M. Ksibi, B. H. Dhia and N. Khelifi). Springer, Cham, Switzerland. https://doi.org/10.1007/978-3-319-70548-4_507
- Alencar, A., Asner, G.P., Knapp, D., and Zarin, D. (2011). Temporal variability of forest fires in eastern Arizona. *Ecological Applications*, 21(7), 2397–2412.
- Alexandris, N., Koutsias, N., and Gupta, S. (2017). Remote sensing of burned areas via PCA, Part 2: SVD-based PCA using MODIS and Landsat data. *Open Geospatial Data, Software and Standards*, 2(21).
- Allan, G., and Southgate, R. (2002). Fire regimes in the spinifex landscapes of Australia. In: *Flammable Australia: the Fire Regimes and Biodiversity of a Continent* (Eds: R. Bradstock, J. Williams and A. Gill) pp 145–176. Cambridge University Press, Cambridge
- Allison, R.S., Johnston, J.M., Craig, G., and Jennings, S. (2016). Airborne Optical and Thermal Remote Sensing for Wildfire Detection and Monitoring. *Sensors*, 16, 1310.
- ASA (2020). *Bushfire earth Observation Taskforce*. Australian Space Agency, Canberra. <https://naturaldisaster.royalcommission.gov.au/system/files/exhibit/IND.0003.0001.0001.pdf>
- Bartlett, T. Leonard, M., and Morgan, G. (2007). The mega-fire phenomenon: some Australian perspectives. In: *The 2007 Institute of Foresters of Australia and New Zealand Institute of Forestry Conference: Programme, Abstracts and Papers*. Institute of Foresters of Australia, Canberra.
- Bellingham, P.J., and Sparrow, A.D. (2000). Resprouting as a life history strategy in woody plant communities. *Oikos*, 89(2), 409–416.
- Benali, A., Russo, A., Sa, A.C.L., Pinto, R.M., Price, O., Koutsias, N., and Pereira, J.M.C. (2016). Determining fire dates and locating ignition points with satellite data. *Remote Sensing*, 8(326), rs8040326.

- Berry L.E., Lindenmayer D.B., Dennis T.E., Driscoll D.A., Banks S.C. (2016). Fire severity alters spatio-temporal movements and habitat utilisation by an arboreal marsupial, the mountain brushtail possum (*Trichosurus cunninghami*). *International Journal of Wildland Fire*, 25, 1291–1302. <https://doi.org/10.1071/WF15204>
- Boer, M.M., Norris, J., Sadler, R.J., Grierson, P.F. (2006). Ecologically sustainable management of fire-prone landscapes in southern Australia: A complex systems point of view. *Forest Ecology and Management*, 234S, S155.
- Boer, M., Sadler, R., and Grierson, P. (2008). Objective characterisation of fire regimes for science-based management of fire-prone landscapes. *Proceedings of Australasian Fire and Emergency Services Authorities Council conference*, 2008.
- Bolton, D.K., Coops, N.C., and Wulder, M.A. (2015). Characterizing residual structure and forest recovery following high-severity fire in the western boreal of Canada using Landsat time-series and airborne LiDAR data. *Remote Sensing of Environment*, 163, 48–60.
- Boschetti, L., Roy, D., Barbosa, P., Boca, R., and Justice, C. (2008). A MODIS assessment of the summer 2007 extent burned in Greece. *International Journal of Remote Sensing*, 29(8), 2433–2436.
- Bradley, A.V., and Millington, A.C. (2006). Spatial and temporal scale issues in determining biomass burning regimes in Bolivia and Peru. *International Journal of Remote Sensing*, 27(11), 2221–2253.
- Bradstock, R.A. (2010). A biogeographic model of fire regimes in Australia: current and future implications. *Global Ecology and Biogeography*, 19, 145–158.
- Bradstock, R.A., and Cohn, J. (2002). Fire regimes and biodiversity in semi-arid mallee ecosystems. In *Flammable Australia: The Fire Regimes and Biodiversity of a Continent*. (Eds: R.A. Bradstock, J.E. Williams, and M.A. Gill) Cambridge University Press, Cambridge.
- Bradstock, R.A., Bedward, M., Kenny, B.J., and Scott, J. (1998). Spatially explicit simulation of the effect of prescribed burning on fire regimes and plant extinctions in shrublands typical of south-eastern Australia. *Biological Conservation*, 86, 83–95.
- Bradstock, R.A., Hammill, K.A., Collins, L., and Price, O. (2010). Effects of weather, fuel and terrain on fire severity in topographically diverse landscapes of south-eastern Australia. *Landscape Ecology*, 25(4), 607–619. doi:10.1007/s10980-009-9443-8
- Bradstock, R.A., Williams, D.J., and Gill, A.M. (2012a). Future fire regimes of Australian ecosystems: new perspectives on enduring questions of management. Ch 15 in *Flammable Australia: Fire Regimes, Biodiversity and Ecosystems in a Changing World*. CSIRO, Melbourne. pp 307–324.
- Bradstock, R.A., Cary, G.J., Davies, I., Lindenmayer, D.B., Price, O.F., and Williams, R.J. (2012b). Wildfires, fuel treatment and risk mitigation in Australian eucalypt forests: Insights from landscape-scale simulation. *Journal of Environmental Management*, 105, 66–75.
- Bradstock, R.A., Williams, D.J., and Gill, A.M. (Eds) (2012c). *Flammable Australia: Fire Regimes, Biodiversity and Ecosystems in a Changing World*. CSIRO, Melbourne. 333 p.
- Brandis, K., and Jacobson, C. (2003). Estimation of vegetative fuel loads using Landsat TM imagery in New South Wales, Australia. *International Journal of Wildland Fire*, 12, 185–194.
- Burgan, R., Klaver, R., and Klaver, J. (1998). Fuel models and fire potential from satellite and surface observations. *International Journal of Wildland Fire*, 8, 159–170.
- Burrows, N.D., Burbidge, A.A., Fuller, P.J., and Behn, G. (2006). Evidence of altered fire regimes in the Western Desert region of Australia. *Conservation Science Western Australia*, 5(3), 272–284.
- Caccamo, G., Chisholm, L.A., Bradstock, R.A., Puotinen, M.L., and Phippen, B.G. (2012). Monitoring live fuel moisture content of heathland, shrubland and sclerophyll forest in South-Eastern Australia using MODIS data. *International Journal of Wildland Fire*, 21, 257–269.
- Calle, A., Gonzalez-Alonso, F., and Merino de Miguel, S. (2008). Validation of active forest fires detected by MSG-SEVIRI by means of MODIS hot spots and AwiFS images. *International Journal of Remote Sensing*, 29(12), 3407–3415.
- Cansler, C.A., and McKenzie, D. (2014). Climate, fire size and biophysical setting control fire severity and spatial pattern in the northern Cascade Range, USA. *Ecological Applications*, 24(5), 1037–1056.
- Casas, A., Riaño, D., Ustin, S.L., Dennison, P., and Salas, J. (2014). Estimation of water-related biochemical and biophysical vegetation properties using multitemporal airborne hyperspectral data and its comparison to MODIS spectral response. *Remote Sensing of Environment*, 148, 28–41. <http://dx.doi.org/10.1016/j.rse.2014.03.011>

- Case, M.F., and Staver, A.C. (2017). Fire prevents woody encroachment only at higher than historical frequencies in a South African savanna. *Journal of Applied Ecology*, 54, 955–962.
- Castro, J., Allen, C.D., Molina-Morales, M., Marañón-Jiménez, S., Sánchez-Miranda, Á., and Zamora, R. (2011). Salvage Logging Versus the Use of Burnt Wood as a Nurse Object to Promote Post-Fire Tree Seedling Establishment. *Restoration Ecology*, 19, 537–544. <https://doi.org/10.1111/j.1526-100X.2009.00619.x>
- Chafer, C.J., Noonan, M., Macnaught, E. (2004). The post-fire measurement of fire severity and intensity in the Christmas 2001 Sydney wildfires. *International Journal of Wildland Fire*, 13, 227–240.
- Chafer, C.J. (2007). Using Satellite Imagery to Estimate Landscape Fuel Loads in a Diverse Eucalypt Environment on the Central Coast of New South Wales, Australia. A report prepared by SCA for the NSW RFS, March 2007.
- Chen, K., and McAneney, J. (2004). Quantifying bushfire penetration into urban areas in Australia. *Geophysical Research Letters*, 31, L12212. doi:10.1029/2004GL020244
- Chen, K., and McAneney, J. (2005). The bushfire threat in urban areas. *Australian Science*, 14–16.
- Chen, Y., Zhu, X., Yebra, M., Harris, S., and Tapper, N. (2016). Strata-based forest fuel classification for wild fire hazard assessment using terrestrial LiDAR. *Journal of Applied Remote Sensing*, 10(4), 046025.
- Chen, Y., Zhu, X., Yebra, M., Harris, S., and Tapper, N. (2017a). Development of a Predictive Model for Estimating Forest Surface Fuel Load in Australian Eucalypt forests with LiDAR Data. *Environmental Modelling and Software*, 97, 61–71.
- Chen, D., Pereira, J.M.C., Masiero, A., and Priotti, F. (2017b). Mapping fire regimes in China using MODIS active fire and burned area data. *Applied Geography*, 85, 14–26.
- Cheney, P., and Sullivan, A. (2008). *Grassfires—Fuel, Weather and Fire Behaviour*. Melbourne, CSIRO Publishing, Melbourne.
- Chu, T., and Guo, X. (2014). Remote sensing techniques in monitoring post-fire effects and patterns of forest recovery in Boreal forest regions: A review. *Remote Sensing*, 6, 470–520.
- Chuvieco, E. (2008). Satellite Observations of Biomass Burning. In *Earth observation of global change: the role of remote sensing in monitoring the global environment*. (Ed: E. Chuvieco). Springer, NY.
- Chuvieco, E., Riano, D., Aguado, I., and Cocero, D. (2002). Estimation of fuel moisture content from multitemporal analysis of Landsat Thematic Mapper reflectance data: application in fire danger assessment. *International Journal of Remote Sensing*, 23(11), 2145–2162.
- Chuvieco, E., Aguado, L., and Dimitrakopoulos, A.P. (2004). Conversion of fuel moisture content values to ignition potential for integrated fire danger assessment. *Canadian Journal of Forest Research*, 34(11), 2284–2293.
- Chuvieco, E., Aguado, I., Yebra, M., Nieto, H. Salas, J., Martín, M.P., Vilar, L., Martínez, J., Martín, S., Ibarra, P., de la Riva, J., Baeza, M.J., Rodríguez, F., Molina, J.R., Herrera, M.A., and Zamora, R. (2010). Development of a framework for fire risk assessment using Remote Sensing and Geographic Information System technologies. *Ecological Modelling*, 221, 46–58.
- Chuvieco, E., Aguado, I., Jurdao, S., Pettinari, M.L., Yebra, M., Salas, J., de la Riva B, J., Ibarra, P., Rodrigues, M., Echeverría, M., Azqueta, D. Román, M.V., Bastarrika, A., Martínez, S., Recondo, C., Zapico, E., and Martínez-Vega, J. (2014). Integrating geospatial information into fire risk assessment. *International Journal of Wildland Fire*, 23, 606–619.
- Chuvieco, E., Lizundia-Loiola, J., Pettinari, M.L., Ramo, R., Padilla, M., Tansey, K., Mouillot, F., Laurent, P., Storm, T., Heil, A., and Plummer, S. (2018). Generation and analysis of a new global burned area product based on MODIS 250 m reflectance bands and thermal anomalies. *Earth System Science Data*, 10(4), 2015–2031.
- Chuvieco, E., Aguado, I., Salas, J., Garcia, M., Yebra, M., and Oliva, P. (2020). Satellite Remote Sensing Contributions to Wildland Fire Science and Management. *Current Forestry Reports*, 6, 81–96. <https://doi.org/10.1007/s40725-020-00116-5>
- CoA (2020). *Royal Commission into National Natural Disaster Arrangements Report*. Commonwealth of Australia, Canberra. <https://naturaldisaster.royalcommission.gov.au/>
- Collins, B.M. (2014). Fire weather and large fire potential in the northern Sierra Nevada. *Agricultural and Forest Meteorology*, 189–190, 30–35.
- Collins, L., Griffioen, P., Newell, G., and Mellor, A. (2018). The utility of Random Forests for wildfire severity mapping. *Remote Sensing of Environment*, 216, 374–384. <https://doi.org/10.1016/j.rse.2018.07.005>

- Collins, L., Bennett, A.F., Leonard, S.W.J., and Penman, T.D. (2019). Wildfire refugia in forests: Severe fire weather and drought mute the influence of topography and fuel age. *Global Change Biology*, 25(11). <https://doi.org/10.1111/gcb.14735>
- Craig, R., Heath, B., Raisbeck-Brown, N., Steber, M., Marsden, J., and Smith, R. (2002). The distribution, extent and seasonality of large fires in Australia, April 1998–March 2000, as mapped from NOAA-AVHRR imagery. In *Australian Fire Regimes: Contemporary Patterns (April 1998–March 2000) and Changes since European Settlement*. (Eds: Russell-Smith, J., Craig, R., Gill, A.M., Smith, R., and Williams, J.). Australia State of the Environment Second Technical Paper Series (Biodiversity), Department of the Environment and Heritage, Canberra.
- Cruz, M.G., Sullivan, A.L., Gould, J.S., Sims, N.C., Bannister, A. J., Hollis, J.J., and Hurley, R.J. (2012). Anatomy of a catastrophic wildfire: The Black Saturday Kilmore East fire in Victoria, Australia. *Forest Ecology and Management*, 284, 269–285.
- Danson, F.M., and Bowyer, P. (2004). Estimating Live Fuel Moisture Content from Remotely Sensed Reflectance. *Remote Sensing of Environment*, 92, 309–321.
- de Klerk, H. (2008). A pragmatic assessment of the usefulness of the MODIS (Terra and Aqua) 1-km active fire (MOD14A2 and MYD14A2) products for mapping fires in the fynbos biome. *International Journal of Wildland Fire*, 17, 166–178. <https://doi.org/10.1071/WF06040>
- De Santis, A., Asner, G.P., Vaughan, P.J., and Knapp, D.E. (2010). Mapping burn severity and burning efficiency in California using simulation models and Landsat imagery. *Remote Sensing of Environment*, 114, 1535–1545.
- Dennison, P.E., and Roberts, D.A. (2009). Daytime fire detection using airborne hyperspectral data. *Remote Sensing of Environment*, 113, 1649–1657.
- Diaz-Delgado, R., Lloret, F., and Pons, X. (2004). Statistical analysis of fire frequency models for Catalonia (NE Spain, 1975–1998) based on fire scar maps from Landsat MSS data. *International Journal of Wildland Fire*, 13, 89–99.
- Dilley, A., Millie, S., O'Brien, D., and Edwards, M. (2004). The relation between normalised difference vegetation index and vegetation moisture content at three locations in Victoria, Australia. *International Journal of Remote Sensing*, 25(19). 3913–3928.
- Dowdy, A.J., and Pepler, A. (2018). Pyroconvection risk in Australia: Climatological changes in atmospheric stability and surface fire weather conditions. *Geophysical Research Letters*, 45(4), 2005–2013.
- Dozier, J. (1981). A method for satellite identification of surface temperature fields of subpixel resolution. *Remote Sensing of Environment*, 11, 221–229.
- Duff, T.J., Bell, T.L., and York, A. (2013). Predicting continuous variation in forest fuel load using biophysical models: a case study in south-eastern Australia. *International Journal of Wildland Fire*, 22, 318–332.
- Edwards, A.C., Maier, S.W., Hutley, L.B., Williams, R.J., and Russell-Smith, J. (2013). Spectral analysis of fire severity in north Australia tropical savannas. *Remote Sensing of Environment*, 136, 56–65.
- Eidenshink, J., Schwind, B., Brewer, K., Zhu, Z., Quayle, B., and Howard, S. (2007). A project for monitoring trends in burn severity. *Fire Ecology Special Issue*, 3(1), 3–21.
- Ellis, S., Kanowski, P., and Whelan, R. (2004). *National Inquiry on Bushfire Mitigation and Management*. Commonwealth of Australia, Canberra.
- Enright, N.J., Fontaine, J.B., Bowman, D.M.J.S., Bradstock, R.A., and Williams, R.J. (2015). Interval squeeze: altered fire regimes and demographic responses interact to threaten woody species persistence as climate changes. *Frontiers of Ecology and Environment*, 13(5), 265–272.
- Escuin, S., Navarro, R., and Fernandez, P. (2008). Fire severity assessment by using NBR (Normalised Burn Ratio) and NDVI (Normalized Difference Vegetation Index) derived from LANDSAT TM/ETM images. *International Journal of Remote Sensing*, 29(4), 1053–1073.
- Eskelson, B.N.I., and Monleon, V.J. (2018). Post-fire surface fuel dynamics in California forests across three burn severity classes. *International Journal of Wildland Fire*, 27, 114–124.
- Estes, B.L., Knapp, E.E., Skinner, C.N., Miller, J.D., and Preisler, H.K. (2017). Factors influencing fire severity under moderate burning conditions in the Klamath Mountains, northern California, USA. *Ecosphere*, 8(5), e01794. <https://doi.org/10.1002/ecs2.1794>
- Eva, H., and Lambin, E.F. (1998). Remote sensing of biomass burning in tropical regions: sampling issues and multisensor approach. *Remote Sensing of Environment*, 64, 292–315.
- Filkov, A.I., Duff and T.J., Penman, T.D. (2018). Improving fire behaviour data obtained from wildfires. *Forests*, 9(2), 81.

- Filkov, A.I., Ngo, T., Matthews, S., Telfer, S., and Penman, T.D. (2020). Impact of Australia's catastrophic 2019/20 bushfire season on communities and environment. Retrospective analysis and current trends. *Journal of Safety Science and Resilience*, 1(1), 44–56. <https://doi.org/10.1016/j.jnlssr.2020.06.009>
- Fisher, A., Day, M., Gill, T., Roff, A., Danaher, T., and Flood, N. (2016). Large-area, high-resolution tree cover mapping with multi-temporal SPOT-5 imagery, New South Wales, Australia. *Remote Sensing*, 8(6), 515. <https://doi.org/10.3390/rs8060515>
- Flasse, S.P., and Ceccato, P. (1996). A contextual algorithm for AVHRR fire detection. *International Journal of Remote Sensing*, 17, 419–424.
- French, N.H.J., Kasischke, E.S., Hall, R.J., Murphy, K.A., Verbyla, D.L., Hoy, E.E., and Allen, J.L. (2008). Using Landsat data to assess fire and burn severity in the North American boreal forest region: an overview and summary of results. *International Journal of Wildland Fire*, 17(4), 443–462.
- Fromm, M., Tupper, A., Rosenfield, D., Servranckx, R., and McRae, R. (2006). Violent pyroconvective storm devastates Australia's capital and pollutes the stratosphere. *Geophysical Research Letters*, 33(5). <https://doi.org/10.1029/2005GL025161>
- Fromm, M., Lindsey, D.T., Servranckx, R., Yue, G., Trickl, T., Sica, R., Doucet, P., and Goudin-Beekmann, S. (2010). The untold story of pyrocumulonimbus. *Bulletin of American Meteorological Society*, 91, 1193–1209.
- Fusco, E., Abatzoglou, J.T., Balch, J.K., Finn, J.T., and Bradley, B.A. (2016). Quantifying the human influence on fire ignition across the western USA. *Ecological Applications*, 26(8), 2390–2401.
- García, M., Saatchi, S. Ustin, S., and Balzter, H. (2018). Modelling forest canopy height by integrating airborne LiDAR samples with satellite Radar and multispectral imagery. *International Journal of Applied Earth Observation and Geoinformation*, 66, 159–173.
- García, M., Riaño, D., Yebra, M., Salas, J., Cardil, A., Monedero, S., Ramirez, J., Martín, M.P., Vilar, L., Gajardo, J., and Ustin, S. (2020). A Live Fuel Moisture Content Product from Landsat TM Satellite Time Series for Implementation in Fire Behavior Models. *Remote Sensing*, 12, 1714. <https://doi.org/10.3390/rs12111714>
- GA (2020). *Digital Earth Australia Hotspots Product Description*. D2020-64303. Ecat Reference #70869. Geoscience Australia, Canberra. hotspots.dea.ga.gov.au/cache/DEA+Hotspots+-+Product+Description+-+Version+1.6_final.pdf
- Gibson, R., Danaher, T., Hehir, W., and Collins, L. (2020). A remote sensing approach to mapping fire severity in south-eastern Australia using sentinel 2 and random forest. *Remote Sensing of Environment*, 240(111702).
- Giglio, L., and Justice, C.O. (2003). Effect of wavelength selection on characterisation of fire size and temperature. *International Journal Remote Sensing*, 24(17), 3515–3520.
- Giglio, L., Kendall, J.D., and Justice, C.O. (1999). Evaluation of global fire detection algorithms using simulated AVHRR infrared data. *International Journal of Remote Sensing*, 20, 1947–1985.
- Giglio, L., Kendall, J.D., and Tucker, C.J. (2000). Remote sensing of fires with TRMM VIRS. *International Journal Remote Sensing*, 21, 203–207.
- Giglio, L., Descloitres, J., Justice, C.O., Kaufman, Y.J. (2003). An Enhanced Contextual Fire Detection Algorithm for MODIS. *Remote Sensing of Environment*, 87, 273–282.
- Giglio, L., Loboda, T., Roy, D.P., Quayle, B., and Justice, C.O. (2009). An active-fire based burned area mapping algorithm for the MODIS sensor. *Remote Sensing of Environment*, 113, 408–420
- Giglio, L., Schroeder, W., and Justice, C.O. (2016). The collection 6 MODIS active fire detection algorithm and fire products. *Remote Sensing of Environment*, 178, 31–41.
- Gill, M.A., and Catling, P.C. (2002). Fire regimes and biodiversity of forested landscapes of southern Australia. In *Flammable Australia: The Fire Regimes and Biodiversity of a Continent*. (Eds: R.A. Bradstock, J.E. Williams, and M.A. Gill) Cambridge University Press, Cambridge.
- Gitas, I.Z., and Devereux, B.J. (2006). The role of topographic correction in mapping recently burned Mediterranean forest areas from LANDSAT TM images. *International Journal of Remote Sensing*, 27(10), 41–54.
- Goodwin, N.R., and Collett, L. (2014). Development of an automated method for mapping fire history captured in Landsat TM and ETM+ time series. *Remote Sensing of Environment*, 148, 206–221.
- Gould, J.S., McCaw, W.L., Cheney, N.P., Ellis, P.F., and Matthews, S. (2008). *Field Guide: Fire in Dry Eucalypt Forest. Fuel Assessment and Fire Behaviour Prediction in Dry Eucalypt Forest*. CSIRO Publications, Melbourne. 92 p.
- Gregoire, J.-M., Tansey, K., and Silva, J.M.N. (2003). The GBA2000 Initiative: developing a global burnt area database from SPOT-VEGETATION imagery. *International Journal of Remote Sensing*, 24(6), 1369–1376.

- Guerschman, J.P., Scarth, P.F., McVicar, T.R., Renzullo, L.J., Malthus, T.J., Stewart, J.B., Rickards, J.E., and Trevithick, R. (2015). Assessing the effects of site heterogeneity and soil properties when unmixing photosynthetic vegetation, non-photosynthetic vegetation and bare soil fractions for Landsat and MODIS data. *Remote Sensing of Environment*, 161, 12–26.
- Haines, D.A. (1988). A lower atmospheric severity index for wildland fire. *National Weather Digest*, 13(2), 23–27.
- Hall, S.A., Burke, I.C., Box, D.O., Kaufman, M.R., and Stoker, J.M. (2005). Estimating stand structure using discrete-return lidar: an example from low density, fire prone ponderosa pine forest. *Forest Ecology and Management*, 208, 189–209.
- Hally, B., Wallace, L., Reinke, K., Jones, S., and Skidmore, A. (2018). Advances in active fire detection using a multi-temporal method for next-generation geostationary satellite data. *International Journal of Digital Earth*, 12(9), 1030–1045.
- Hamilton, D., Bowerman, M., Colwell, J., Donohoe, G., and Myers, B. (2017). Spectroscopic analysis for mapping wildland fire effects from remotely sensed imagery. *Journal of Unmanned Vehicle Systems*, 5(4), 146–158. doi:10.1139/juvs-2016-0019
- Hao, X., and Qu, J.J. (2007). Retrieval of real-time live fuel moisture content using MODIS measurements. *Remote Sensing of Environment*, 108, 130–137.
- Hawbaker, T.J., Radeloff, V.C., Syphard, A.D., Zhu, Z., and Stewart, S.I. (2008). Detection rates of MODIS active fire products in the United States. *Remote Sensing of Environment*, 112, 2656–2664.
- Hobbs, R. (2002). Fire regimes and their effects in Australian temperate woodlands. In *Flammable Australia: The Fire Regimes and Biodiversity of a Continent*. (Eds: R.A. Bradstock, J.E. Williams, and M.A. Gill) Cambridge University Press, Cambridge.
- Hope, A., Tague, C., and Clark, R. (2007). Characterizing post-fire vegetation recovery of California chaparral using TM/ETM+ time-series data. *International Journal of Remote Sensing*, 28(6), 1339–1354.
- Hu, T., Q. Ma, Y. Su, J. J. Battles, B. M. Collins, S. L. Stephens, M. Kelly and Q. Guo (2019). A simple and integrated approach for fire severity assessment using bi-temporal airborne LiDAR data. *International Journal of Applied Earth Observation and Geoinformation*, 78, 25–38.
- Huang, H., Roy, D.P., Boschetti, L., Zhang, H.K., Yan, L., Kumar, S.S., Gomez-Dans, J., and Li, J. (2016). Separability analysis of Sentinel-2a Multi-Spectral Instrument (MSI) data for burned area discrimination. *Remote Sensing*, 8(10), 873. <https://doi.org/10.3390/rs8100873>
- Hudak, A.T., Morgan, P., Bobbitt, M.J., Smith, A.M.S., Lewis, S.A., Lentile, L.B., Robichaud, P.R., Clark, J.T., and McKinley, R.A. (2007). The relationship of multispectral satellite imagery to immediate fire effects. *Fire Ecology Special Issue*, 3(1), 64–90.
- Hudak, A.T., Crookston, N.L., Evans, J.S., Hall, D.E., and Falkowski, M.J. (2008). Nearest neighbour imputation of species-level, plot-scale forest structure attributes from LiDAR data. *Remote Sensing of Environment*, 112, 2232–2245. [Corrigendum: *Remote Sensing of Environment*, 113, 289–290.]
- Hudak, A.T., Ottmar, R.D., Vihnanek, R.E., Brewer, N.W., Smith, A.M.S., and Morgan, P. (2013). The relationship of post-fire white ash cover to surface fuel consumption. *International Journal of Wildland Fire*, 22(6), 780–785. <https://doi.org/10.1071/WF15074>
- ICSMD (2020). *International Charter for Space and Major Disasters website*: <https://disasterscharter.org/web/guest/home>
- Jenkins, M.E., Bedward, M., Price, O., and Bradstock, R.A. (2020). Modelling bushfire fuel hazard using biophysical parameters. *Forests*, 11(9), 925. <https://doi.org/10.3390/f11090925>
- Jones, S., Reinke, K., Mitchell, S., McConachie, F., and Holland, C. (2017). *Advances in the remote sensing of active fires: a review—detection, mapping and monitoring v1.0*. Bushfire and Natural Hazards CRC, Melbourne.
- Joshi, N., Mitchard, E.T.A., Woo, N., Torres, J., Moll-Rocek, J., Ehammer, A., Collins, M. Jepsen, M.R., and Fensholt, R. (2015). Mapping dynamics of deforestation and forest degradation in tropical forests using radar satellite data. *Environmental Research Letters*, 10(3), [034014].
- Jupp, D.L.B., Culvenor, D.S., Lovell, J.L., Newnham, G.J., Strahler, A.H., and Woodcock, C.E. (2008). Estimating forest LAI profiles and structural parameters using a ground-based laser called Echidna. *Tree Physiology*, 29, 171–181.
- Jurskis, V. (2015). *Firestick Ecology*. Connor Court Publishing, Ballarat.

- Justice, C., Giglio, L., Boschetti, L., Roy, D., Csiszar, I., Morisette, J., and Kaufman, Y. (2006). *MODIS Fire Products (Version 2.3, 1 October 2006)*. Algorithm Technical Background Document. MODIS Science Team, NASA. http://modis.gsfc.nasa.gov/data/atbd/atbd_mod14.pdf
- Keane, R.E., Burgan, R., van Wagtenonk, J. (2001). Mapping wildland fuel for fire management across multiple scales: integrating remote sensing, GIS and biophysical modelling. *International Journal of Wildland Fire*, 10, 301–319.
- Keeley, J.E. (2009). Fire intensity, fire severity and burn severity: a brief review and suggested usage. *International Journal of Wildland Fire*, 18, 116–126.
- Keetch, J.J., and Bryam, G.M. (1968). *A drought index for forest fire control*. U.S.D.A. Forest Service Research Paper SE-38. 32 p.
- Keith, D.A., McCaw, W.L., and Whelan, R.J. (2002). Fire regimes in Australian heathlands and their effects on plants and animals. In *Flammable Australia: The Fire Regimes and Biodiversity of a Continent*. (Eds: R.A. Bradstock, J.E. Williams, and M.A. Gill) Cambridge University Press, Cambridge.
- Keller, J. (2019). Air force readies shortwave infrared sensors for satellites to reveal materials and lasers on the ground. *Military and Aerospace Electronics*. November 20th, 2019. <https://www.militaryaerospace.com/sensors/article/14072398/shortwave-infrared-sensors-satellites>
- Kennedy, R.E., Yang, Z., and Cohen, W.B. (2010). Detecting trends in forest disturbance and recovery using yearly Landsat Time Series: 1. LandTrendr—Temporal segmentation algorithms. *Remote Sensing of Environment*, 114, 2897–2910.
- Kenny, B., Matthews, s., Grootemaat, S., and Hollis, J., Sauvage, S., and Fox-Hughes, P. (2019). Australian Fire Danger Rating System Research Prototype: National fuel map. *Proceedings of the 6th International Fire Behavior and Fuels Conference, April 29–May 3, 2019, Sydney, Australia*. Published by the International Association of Wildland Fire, Missoula, Montana, USA.
- Keramitsoglou, I., Kiranoudis, C.T., Sarimvels, H., and Sifakis, N. (2004). A multidisciplinary decision support system for forest fire crisis management. *Environmental Management*, 33(2), 212–225.
- Kershaw, A.P., Clark, J.S., Gill, A.M., and D’Costa, D.M. (2002). A history of fire in Australia. In *Flammable Australia*. (Eds: R.A. Bradstock, J.E. Williams and A.M. Gill). Cambridge, Cambridge University Press. pp. 3–25.
- Key, C.H., and Benson, N.C. (1999). Measuring and remote sensing of burn severity: the CBI and NBR. *Proceedings of Joint Fire Science Conference and Workshop, Vol. 2, June*, (Eds. L.F. Neuenschwander, K.C. Ryan) pp. 284. University of Idaho, Moscow, ID.
- Key, C.H., and Benson, N.C. (2006). *Landscape Assessment: Sampling and Analysis Methods*. USDA Forest Service, Rocky Mountain Research Station General Tech. Rep. RMRS-GTR-164-CD. Odgen, UT.
- King, K., Marsden-Smedley, J., Cary, G., Allan, G., Bradstock, R., Gill, M. (2008). *Modelling fire dynamics in the West MacDonnell Range area*. Working Paper 20, Desert Knowledge CRC, Alice Springs.
- Koltunov, A., and Ustin, S.L. (2007). Early fire detection using non-linear multitemporal prediction of thermal imagery. *Remote Sensing of Environment*, 110(1), 18–28.
- Kokaly, R.F., Rockwell, B.W., Haire, S.L., and King, T.V.V. (2007). Characterization of post-fire surface cover, soils and burn severity at the Cerro Grande Fire, New Mexico, using hyperspectral and multispectral remote sensing. *Remote Sensing of Environment*, 106, 305–325.
- Kolden, C.A., and Weisberg, P.J. (2007). Assessing accuracy of manually-mapped wildfire perimeters in topographically dissected areas. *Fire Ecology Special Issue*, 3(1), 22–31.
- Kolden, C.A., Abatzoglou, J.T., and Smith, A.M.S. (2015). Limitations and utilisation of monitoring trends in burn severity products for assessing wildfire severity in the USA. *International Journal of Wildland Fire*, 24, 1023–1028.
- Koltunov, A., and Ustin, S.L. (2007). Early fire detection using non-linear multitemporal prediction of thermal imagery. *Remote Sensing of Environment*, 110, 18–28.
- Kontoos, C., Keramitsoglou, I., Sifakis, N., and Konstantinidis, P. (2009a). SITHON: An Airborne Fire Detection System Compliant with Operational Tactical Requirements. *Sensors*, 9, 1204–1220.
- Kontoos, C.C., Poilvé, H., Florisch, G., Keramitsoglou, I., and Paralikidis, S. (2009b). A comparative analysis of a fixed thresholding vs. a classification tree approach for operational burn scar detection and mapping. *International Journal of Applied Earth Observation and Geoinformation*, 11(5), 299–316. doi:10.1016/j.jag.2009.04.001.

- Kossman, R., Sturman, A., Zawar-Reza, P. (2001). Atmospheric influences on bush fire propagation and smoke dispersion over complex terrain. *Proceedings of 2001 Australasian Bushfire Conference, Christchurch, NZ.*
- Krawchuk, M.A., Moritz, M.A., Parisien, M.-A., Van Dorn, J., and Hayhoe, K. (2009). Global pyrogeography: the current and future distribution of wildfire. *PLoS ONE*, 4(4), e5102.
- Leblon, B., Augusto, P., Garcia, F., Oldford, S., Maclean, D.A., Flannigan, M. (2007). Using cumulative NOAA-AVHRR spectral indices for estimating fire danger codes in northern boreal forests. *International Journal of Applied Earth Observation*, 9, 335–342.
- Lee, T. F., and Tag, P. M. (1990). Improved detection of hotspots using the AVHRR 3.7 μm channel. *Bulletin of the American Meteorological Society*, 71, 1722–1730.
- Lentile, L.B., Holden, Z.A., Smith, A.M.S., Falkowski, M.J., Hudak, A.T., Morgan, P., Lewis, S.A., Gessler, P.E., and Benson, N.C. (2006). Remote sensing techniques to assess active fire characteristics and post-fire effects. *International Journal of Wildland Fire*, 15, 319–345.
- Lentile, L.B., Morgan, P., Hudak, A.T., Bobbitt, M.J., Lewis, S.A., Smith, A.M.S., and Robichaud, P.R. (2007). Post-fire burn severity and vegetation response following eight large wildfires across the western United States. *Fire Ecology Special Issue*, 3(1), 91–108.
- Lentile, L.B., Smith, A.M.S., Hudak, A.T., Morgan, P., Bobbitt, M.J., Lewis, S.A., and Robichaud, P.R. (2009). Remote sensing for prediction of 1-year post-fire ecosystem condition. *International Journal of Wildland Fire*, 18(5), 594–608.
- Lewis, S.A., Lentile, L.B., Hudak, A.T., Robichaud, P.R., Morgan, P., and Bobbitt, M.J. (2007). Mapping ground cover using hyperspectral remote sensing after the 2003 Simi and Old wildfires in southern California. *Fire Ecology Special Issue*, 3(1), 109–128.
- Liu, X., He, B., Quan, X., Yebra, M., Qiu, S., Yin, C., Liao, Z., and Zhang, H. (2018). Near Real-Time Extracting Wildfire Spread Rate from Himawari-8 Satellite Data. *Remote Sensing*, 10(10), 1654. <https://doi.org/10.3390/rs10101654>
- López García, M.J., and Caselles, V. (1991). Mapping burns and natural reforestation using thematic mapper data. *Geocarto International*, 1, 31–37. <https://doi.org/10.1080/10106049109354290>
- Lowell, K., Shamir, R., Siqueira, A., White, J., O'Connor, A., Butcher, G., Garvey, M., and Niven, M. (2009). Assessing Capabilities of Geospatial Data to Map Built Structures and Evaluate Their Bushfire Threat. *International Journal of Wildland Fire*, 18(8), 1010–1020. <https://doi.org/10.1071/WF08077>
- Lucas, R., Bunting, P., Paterson, M., and Chisholm, L. (2008a). Classification of Australian forest communities using aerial photography, CASI and HyMap data. *Remote Sensing of Environment*, 112(5), 2088–2103.
- Luke, R., and McArthur, A. (1978). *Bushfires in Australia*. Australian Government Publishing Service, Canberra.
- Lund, I.D., and Morgan, J.W. (2002). The role of fire regimes in temperate lowland grasslands of south-eastern Australia. In *Flammable Australia: The Fire Regimes and Biodiversity of a Continent*. (Eds: R.A. Bradstock, J.E. Williams, and M.A. Gill) Cambridge University Press, Cambridge.
- Lydersen, J. M., B. M. Collins, M. L. Brooks, J. R. Matchett, K. L. Shive, N. A. Povak, V. R. Kane and D. F. Smith (2017). Evidence of fuels management and fire weather influencing fire severity in an extreme fire event. *Ecological Applications*, 27(7), 2013–2030.
- Maier, S.W., Russell-Smith, J., Edwards, A.C., and Yates, C. (2013). Sensitivity of the MODIS fire detection algorithm (MOD14) in the savanna region of the Northern Territory, Australia. *ISPRS Journal of Photogrammetry and Remote Sensing*, 76, 11–16. <https://doi.org/10.1016/j.isprsjprs.2012.11.005>
- Malak, D.A., and Pausas, J.G. (2006). Fire regime and post-fire Normalised Difference Vegetation Index changes in the eastern Iberian peninsula (Mediterranean basin). *International Journal of Wildland Fire*, 407–413.
- Manzanera, J. A., A. Garcia-Abril, C. Pascual, R. Tejera and S. Martin-Fernandez (2016). Fusion of airborne LiDAR and multispectral sensors reveals synergic capabilities in forest structure characterisation. *GIScience and Remote Sensing*, 53(6), 723–728.
- Manzo-Delgado, L., Sanchez-Colon, S., and Alvarez, R. (2009). Assessment of seasonal forest fire risk using NOAA-AVHRR: a case study in central Mexico. *International Journal of Remote Sensing*, 30(19), 4991–5013.
- Marselis, S.M., Yebra, M., Jovanovic, T., and van Dijk, A.I.J.M. (2016). Deriving comprehensive forest structure information from mobile laser scanning observations using automated point cloud classification. *Environmental Modelling and Software*, 82, 142–151.

- Martin, D., Chen, T., Nichols, D. Bessel, R. Kidnie, S. Alexander, J. (2015). Integrated ground and satellite-based observations to determine the degree of grassland curing. *International Journal of Wildland Fire*, 24(3), 329–339.
- Massetti, A., Rüdiger, C., Yebra, M., Hilton, J. (2019). The Vegetation Structure Perpendicular Index (VSPi): a forest condition index for wildfire predictions. *Remote Sensing of Environment*, 224, 167–181. <https://doi.org/10.1016/j.rse.2019.02.004>
- McArthur, A.G. (1966). *Weather and Grassland Fire Behaviour*. Australian Forestry and Timber Bureau Leaflet. 100, 23 p.
- McArthur, A.G. (1967). *Fire Behaviour in Eucalypt Forests*. Australian Forestry and Timber Bureau Leaflet 107, 25 p.
- McCarley, T.R., Kolden, C.A., Vaillant, Andrew N.V., Hudak, A.T., Smith, A.M.S., and Kreitler, J. (2017). Landscape-scale quantification of fire-induced change in canopy cover following mountain pine beetle outbreak and timber harvest. *Forest Ecology and Management*, 391, 164–175, <https://doi.org/10.1016/j.foreco.2017.02.015>
- McCarthy, G.J., Tolhurst, K.G., and Chatto, K. (1999). *Overall fuel hazard guide, 3rd edn*. Research report 47, Fire Management Branch, Department of Natural Resources and Environment, Victoria.
- McCarthy, G., Moon, K., and Smith, L. (2017). Mapping fire severity and fire extent in forest in Victoria for ecological and fuel outcomes. *Ecological Management and Restoration*, 18, 54–64.
- McColl-Gausden, S.C., and Penman, T.D. (2017). Visual assessment of surface fuel loads does not align with destructively sampled surface fuels. *Forests*, 8(11), 408.
- McColl-Gausden, S.C., Bennett, L.T., Duff, T.J., Cawson, J.G., and Penman, T.D. (2019). Climatic and edaphic gradients predict variation in wildland fuel hazard in south-eastern Australia. *Ecography*, 43(3), 443–455. <https://doi.org/10.1111/ecog.04714>
- McDougall, K., and Kirkpatrick, J.B. (1994). *Conservation of Lowland Native Grasslands in South-Eastern Australia*. World Wide Fund for Nature Australia, Sydney.
- McKenna, P., Erskine, P.D., Lechner, A.M., and Phinn, S. (2017). Measuring fire severity using UAV imagery in semi-arid central Queensland, Australia. *International Journal of Remote Sensing*, 38(14), 4244–4264.
- McRae, R. (2004). The Breath of the Dragon—Observations of the January 2003 ACT Bushfires. *Proceedings of 2004 Australasian Bushfire Research Conference, Adelaide*.
- McRae, R. (2008). *2003 ACT Bushfires Fire Behaviour Post-Analysis*. Unpublished report, ACT ESA, Canberra.
- McRae, R., Sharples, J.J., and Weber, R.O. (2008). *High Fire Risk: The Thermal Belt in Australia*. Poster: AFAC/BushfireCRC Conference 2008, Adelaide.
- McRae, R.H.D., Sharples, J.J., and Fromm, M. (2015). Linking local wildfire dynamics to pyroCb development, *Natural Hazards and Earth System Science*, 15, 417–428. <https://doi.org/10.5194/nhess-15-417-2015>
- Meddens, A. J. H., C. A. Kolden and J. A. Lutz (2016). Detecting unburned areas within wildfire perimeters using Landsat and ancillary data across the northwestern United States. *Remote Sensing of Environment*, 186, 275–285.
- Meng, R., Wu, J., Zhao, F., Cook, B.D., Hanavan, R.P., and Serbin, S.P. (2018). Measuring short-term post-fire forest recovery across a burn severity gradient in a mixed pine-oak forest using multi-sensor remote sensing techniques. *Remote Sensing of Environment*, 210, 282–296.
- Miller, J.D., and Thode, A.E. (2007). Quantifying burn severity in a heterogenous landscape with a relative version of the delta Normalized Burn Ratio (dNBR). *Remote Sensing of Environment*, 109, 66–80.
- Miller, J.D., Knapp, E.E., Key, C.H., Skinner, C.N., Isbell, C.J., Creasy, R.M., and Sherlock, J.W. (2009). Calibration and validation of the relative differenced Normalized Burn Ratio (RdNBR) to three measures of fire severity in the Sierra Nevada and Klamath Mountains, California, USA. *Remote Sensing of Environment*, 113, 645–656.
- Miller C., Hilton J., Sullivan A., Prakash M. (2015). SPARK—A Bushfire Spread Prediction Tool. In: *Environmental Software Systems. Infrastructures, Services and Applications*. (Eds: Denzer R., Argent R.M., Schimak G., Hřebíček J.) ISESS 2015. IFIP Advances in Information and Communication Technology, vol 448. Springer, Chamonix.
- Mills, G.A. (2008a). Abrupt surface drying and fire weather Part 1: overview and case study of the South Australian fires of 11 January 2005. *Australian Meteorological Magazine*, 57, 299–309.
- Mills, G.A. (2008b). Abrupt surface drying and fire weather Part 2: a preliminary synoptic climatology in the forested areas of southern Australia. *Australian Meteorological Magazine*, 57, 311–328.

- Mills, G.A., and McCaw, L. (2010). *Atmospheric Stability Environments and Fire Weather in Australia—extending the Haines Index*. CAWCR Technical Report No. 20, Centre for Australian Weather and Climate Research. ISBN: 978-1-921605-56-7
- Minchella, A., Frate, F.D., Capogna, F., Anselmi, S., and Manes, F. (2009). Use of multitemporal SAR data for monitoring vegetation recovery of Mediterranean burned areas. *Remote Sensing of Environment*, 113, 588–597.
- Morgan, J.W. (1999). Defining grassland fire events and the response of perennial plants to annual fire in temperate grasslands of south-eastern Australia. *Plant Ecology*, 144, 127–144.
- Morgan, P., Hardy, C.C., Swetnam, T.W., Rollins, M.G., and Long, D.G. (2001). Mapping fire regimes across time and space: Understanding coarse and fine-scale fire patterns. *International Journal of Wildland Fire*, 10, 329–342.
- Morgan, P., Keane, R.E., Dillon, G.K., Jain, T.B., Hudak, A.T., Karau, E.C., Sikkink, P.G., Holden, Z.A., and Strand, E.K. (2014). Challenges of assessing fire and burn severity using field measures, remote sensing and modelling. *International Journal of Wildland Fire*, 23, 1045–1060.
- Morissette, J., Giglio, L., Csiszar, I., and Justice, C.O. (2005). Validation of the MODIS active fire product over Southern Africa with ASTER data. *International Journal of Remote Sensing*, 26, 4239–4264.
- Mueller, E.V., Skowronski, N., Clark, N., Gallagher, M., Kremens, R., Thomas, J.C., El Houssami, M., Filkov, A., Hadden, R.M., Mell, W., and Simeoni, A. (2017). Utilization of remote sensing techniques for the quantification of fire behaviour in two pine stands. *Fire Safety Journal*, 91, 845–854.
- Newnham, G.J., Verbesselt, J., Grant, I.F., and Anderson, S.A.J. (2011). Relative Greenness Index for assessing curing of grassland fuel. *Remote Sensing of Environment*, 115(6), 1456–1463. <https://doi.org/10.1016/j.rse.2011.02.005>
- Noble, I.R., Bary, G.A.V., Gill, A.M. (1980). McArthur's fire-danger meters expressed as equations. *Australian Journal of Ecology*, 5, 201–203.
- Nolan, R.H., Boer, M.M., Resco de Dios, V., Caccamo, G., and Bradstock, R.A. (2016a). Large scale, dynamic transformations in fuel moisture drive wildfire activity across southeastern Australia. *Geophysical Research Letters*, 43, 4229–4238.
- Nolan, R.H., Resco de Dios, Boer, M.M., Caccamo, G., Goulden, M.L., and Bradstock, R.A. (2016b). Predicting dead fine fuel moisture at regional scales using vapour pressure deficit from MODIS and gridded weather data. *Remote Sensing of Environment*, 174, 100–108.
- NSW BRMR (2020). *NSW Bushfire Risk Management Research Hub* website: <https://www.uow.edu.au/science-medicine-health/research/cermb/nsw-bushfire-risk-management-research-hub/>
- Okin, G.S. (2007). Relative spectral mixture analysis—A multitemporal index of total vegetation cover. *Remote Sensing of Environment*, 106, 467–479.
- Oldford, S., Leblon, B., Maclean, D., and Flannigan, M. (2006). Predicting slow-drying fire weather index fuel moisture codes with NOAA-AVHRR images in Canada's northern boreal forests. *International Journal of Remote Sensing*, 27(18), 3881–3902.
- Otón, G., Ramo, R., Lizundia-Loiola, J., and Chuvieco, E. (2019). Global Detection of Long-Term (1982–2017) Burned Area with AVHRR-LTDR Data. *Remote Sensing*, 11, 2079.
- Padilla, M., Stehman, S.V., Ramo, R., Corti, D., Hantson, S., Oliva, P., Alonso-Canas, I., Bradley, A.V., Tansey, K., Mota, B., Pereira, J.M., Chuvieco, E. (2015). Comparing the accuracies of remote sensing global burned area products using stratified random sampling and estimation. *Remote Sensing of Environment*, 160, 114–121.
- Paltridge, G.W., and Barber, J. (1988). Monitoring grassland dryness and fire potential in Australia with NOAA/AVHRR Data. *Remote Sensing of Environment*, 25(3) 381–394.
- Pereira, J.M.C., Sa, A.C.L., Sousa, A.M.O, Silva, J.M.N., Santos, T.N., and Carreiras, J.M.B. (1999). Spectral characterization and discrimination of burnt areas. In *Remote Sensing of Large Wildfires*. (Ed: E. Chuvieco). Springer-Verlag, Berlin.
- Pettorelli, N., Laurance, W.F., O'Brien, T.G., Wegmann, M., Nagendra, H., and Turner, W. (2014). Satellite remote sensing for applied ecologists: opportunities and challenges. *Journal of Applied Ecology*, 51, 839–848.
- Plank, S., Fuchs, E.-M., and Frey, C. (2017). A Fully Automatic Instantaneous Fire Hotspot Detection Processor Based on AVHRR Imagery—A TIMELINE Thematic Processor. *Remote Sensing*, 9, 30.
- Polinova, M., Wittenberg, L., Kutiel, H., and Brook, A. (2019). Reconstructing pre-fire vegetation condition in the wildland urban interface (WUI) using artificial neural network. *Journal of Environmental Management*, 238, 224–234.

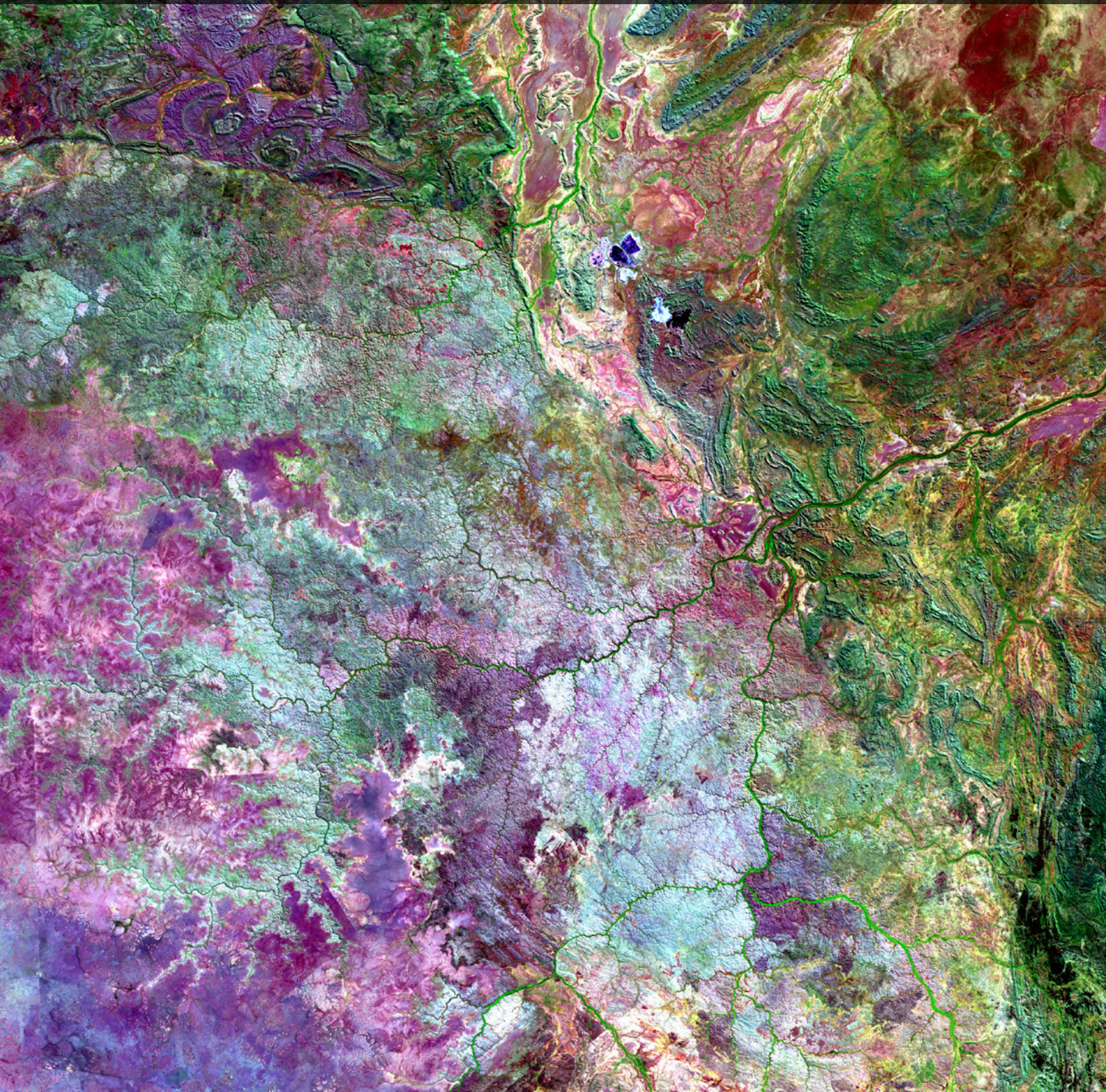
- Poon, P.K., and Kinoshita, A.M. (2018). Estimating evapotranspiration in a post-fire environment using remote sensing and machine learning. *Remote Sensing*, 10, (1728).
- Potter, B.E. (2012a). Atmospheric interactions with wildland fire behaviour—I. Basic surface interactions, vertical profiles and synoptic structures. *International Journal of Wildland Fire*, 21(7), 779–801.
- Potter, B.E. (2012b). Atmospheric interactions with wildland fire behaviour—II. Plume and vortex dynamics. *International Journal of Wildland Fire*, 21(7), 802–817.
- Power, C. (2006). A Spatial Decision Support System for Mapping Bushfire Hazard Potential using Remotely Sensed Data. *Proceedings of Bushfire Conference 2006*. Brisbane, 6–9 June 2009.
- Power, C. (2008). *Fuel Hazard Mapping (Karawatha) Project Report for Brisbane City Council*, Open Space Planning Section.
- Price, O.F., and Bradstock, R.A. (2012). The efficacy of fuel treatment in mitigating property loss during wildfires: insights from analysis of the severity of the catastrophic fires in 2009 in Victoria, Australia. *Journal of Environmental Management*, 113, 146–157. <https://doi.org/10.1016/j.jenvman.2012.08.041>
- Price, O., and Gordon, C.E. (2016). The potential for LiDAR technology to map fire fuel hazard over large areas of Australian forest. *Journal of Environmental Management*, 181, 663–673.
- Punithraj, G., Pruthviraj, U., and Shetty, A. (2019). Surface Soil Moisture Retrieval Using C-Band Synthetic Aperture Radar (SAR) over Yanco Study Site, Australia—A Preliminary Study. In *Applications of Geomatics in Civil Engineering*. (Eds: Ghosh, J.K., and da Silva, I.) Springer Professional. https://doi.org/10.1007/978-981-13-7067-0_8
- Pyne, S.J. (1992). *The Burning Bush: A Fire History of Australia*. Allen and Unwin, Sydney. 520pp. ISBN: 1863731946
- Pyne, S.J. (2015). *The Fire Age*. Aeon essay: <https://aeon.co/essays/how-humans-made-fire-and-fire-made-us-human>
- Pyne, S.J. (2020). *The Still-Burning Bush*. Scribe Short Books, Melbourne. 144pp. ISBN: 1920769757
- Quan, X., He, B., Yebra, M., Liu, X., Liu, X., Zhong, X., and Cao, H. (2018). Retrieval of Fuel Moisture Content from Himawari-8 Product: Towards Real-Time Wildfire Risk Assessment. *IGARSS 2018 - 2018 IEEE International Geoscience and Remote Sensing Symposium*, Valencia, 2018, pp. 7660–7663. doi:10.1109/IGARSS.2018.8517602.
- Rao, K., Park Williams, A., Fortin Flefil, J., and Konings, A.G. (2020). SAR-enhanced mapping of live fuel moisture content. *Remote Sensing of Environment*, 245, 111797.
- Reinhart, E.D., Keane, R.E., and Brown, J.K. (2001). Modeling fire effects. *International Journal of Wildland Fire*, 10, 373–380.
- Renzullo, L.J., Tian, S., van Dijk, A.I.J.M., Rozas Larraondo, P.R., Yebra, M., Yuan, F., and Mueller, N. (2019). Burn extent and severity mapping by spectral anomaly detection in the Landsat data cube. *23rd International Congress on Modelling and Simulation, 1–6 December 2019, Canberra, ACT, Australia*. <https://mssanz.org.au/modsim2019/H7/renzullo.pdf>
- Ressl, R., Lopez, G., Cruz, I., Colditz, R.R., Schmidt, M., Ressler, S., and Jimenez, R. (2009). Operational active fire mapping and burnt area identification applicable to Mexican Nature Protection Areas using MODIS and NOAA-AVHRR direct readout data. *Remote Sensing of Environment*, 113, 1113–1126
- Roberts, D., Mueller, N., and McIntyre, A. (2017). High-Dimensional Pixel Composites From Earth Observation Time Series. *IEEE Transactions on Geoscience and Remote Sensing*, 55(11), 6254–6264. <https://ieeexplore.ieee.org/stamp/stamp.jsp?arnumber=8004469>
- Robichaud, P.R., Lewis, S.A., Laes, D.Y.M., Hudak, A.T., Kokaly, R.F., and Zamudio, J.A. (2007). Postfire soil burn severity mapping with hyperspectral image unmixing. *Remote Sensing of Environment*, 108, 467–480.
- Roff, A., Goodwin, N., and Merton, R. (2005). *Assessing Fuel Loads using Remote Sensing*. NSW RFS Technical Report, University of NSW, Sydney.
- Roff, A.M., Taylor, G.R., Turner, R., Day, M., Mitchell, A., and Merton, R. (2006). Hyperspectral and Lidar Remote Sensing of Forest Fuel Loads in Jilliby State Conservation Area. *Proceedings of 13th Australian Photogrammetric and Remote Sensing Conference*, Canberra, Australia.
- Rollins, M.G. (2009). LANDFIRE: a nationally consistent vegetation, wildland fire, and fuel assessment. *International Journal of Wildland Fire*, 18, 235–249.
- Rothermel, R. (1972). *A mathematical model for predicting fire spread in wildland fuels*. Research Paper INT-115. Ogden, Utah, USDA Forest Service.
- Roy, D.P., and Landmann, T. (2005). Characterizing the surface heterogeneity of fire effects using multi-temporal reflective wavelength data. *International Journal of Remote Sensing*, 26(19), 4197–4218.

- Roy, D.P., Lewis, P., and Justice, C. (2002). Burned area mapping using multi-temporal moderate spatial resolution data—a bi-directional reflectance model-based expectation approach. *Remote Sensing of Environment* 83, 263–286.
- Roy, D.P., Lewis, P., and Justice, C.O. (2005). Prototyping a global algorithm for systematic fire-affected area mapping using MODIS time series data. *Remote Sensing of Environment*, 97, 137–162.
- Roy, D.P., Boschetti, L., and Trigg, S.N. (2006). Remote sensing of fire severity: assessing the performance of the Normalized Burn Ratio. *IEEE Geoscience and Remote Sensing Letters*, 3(1), 112–116.
- Roy, D.P., Boschetti, L., and Smith, A.M.S. (2013). Satellite remote sensing of fires. In *Fire Phenomena and the Earth System: An interdisciplinary guide to fire science*. 1st edn (Ed: C.M. Belcher). John Wiley and Sons, Ltd.
- Russell-Smith, J., and Stanton, P. (2002) Fire regimes and fire management of rainforest communities across northern Australia. In *Flammable Australia: The Fire Regimes and Biodiversity of a Continent*. (Eds: R.A. Bradstock, J.E. Williams, and M.A. Gill) Cambridge University Press, Cambridge.
- Russell-Smith, J., Yates, C.P., Whitehead, P.J., Smith, R., Craig, R., Allan, G.E., Thackway, R., Frakes, I., Cridland, S., Meyer, M.C.P., and Gill, A.M. (2007). Bushfires ‘down under’: patterns and implications of contemporary Australian landscape burning. *International Journal of Wildland Fire*, 16, 361–377.
- Salis, M., Del Giudice, L., Robichaud, P.R., Ager, A., Canu, A., Duce, P., Pellizzaro, G., Ventura, A., Alcasena-Urdiroz, F., Spano, D., and Arca, B. (2019). Coupling wildfire spread and erosion models to quantify post-fire erosion before and after fuel treatments. *International Journal of Wildland Fire*, 28, 687–703. <https://doi.org/10.1071/WF19034>
- Scarth, P., Roder, A., and Schmidt, M. (2010). Tracking grazing pressure and climate interaction—The role of Landsat fractional cover in time series analysis. *Proceedings of the 15th Australasian Remote Sensing and Photogrammetry Conference, Alice Springs, Australia*.
- Schroeder, W., Prins, E., Giglio, L., Csiszar, I., Schmidt, C., Morissette, J., and Justice, C.O. (2008a). Validation of GOES and MODIS active fire detection products using ASTER and ETM+ data. *Remote Sensing of Environment*, 112, 2711–2726.
- Schroeder, W., Ruminski, M., Csiszar, I., Giglio, L., Prins, E., Schmid, C., and Morissette, J. (2008b). Validation of analyses of an operational fire monitoring product: The Hazard Mapping System. *International Journal of Remote Sensing*, 29(20), 6059–6066.
- Schroeder, W., Oliva, P., Giglio, L., and Csiszar, I.A. (2014). The new VIIRS 375m active fire detection data product: Algorithm description and initial assessment. *Remote Sensing of Environment*, 143, 85–96.
- Sharples, J.J. (2009). An overview of mountain meteorological effects relevant to fire behaviour and bushfire risk. *International Journal of Wildland Fire*, 18, 737–754.
- Sharples, J.J., Mills, G.A., McRae, R.H., and Weber, R.O. (2010). Foehn-like winds and elevated fire danger conditions in southeastern Australia. *Journal of Applied Meteorology and Climatology*, 49, 1067–1095.
- Sharples, J.J., McRae, R.H., and Wilkes, S.R. (2012). Wind-terrain effects on the propagation of wildfires in rugged terrain: fire channelling. *International Journal of Wildland Fire*, 21, 282–296.
- Sharples, J.J., Cary, G.J., Fox-Hughes, P., Mooney, S., Evans, J.P., Fletcher, M.S., Fromm, M., Grierson, P., McRae, R., and Baker, P. (2016). Natural Hazards in Australia: extreme bushfire. *Climatic Change*, 139, 85–99.
- Shin, P., Sankey, T., Moore, M.M., and Thode, A.E. (2018). Evaluating unmanned aerial vehicle images for estimating forest canopy fuels in a Ponderosa pine stand. *Remote Sensing*, 10, 1266.
- Silva, J.M.N., Sá, A.C.L., and Pereira, J.M.C. (2005). Comparison of burned area estimates derived from SPOT-VEGETATION and Landsat ETM1 data in Africa: Influence of spatial pattern and vegetation type. *Remote Sensing of Environment*, 96, 188–201.
- Simpson, C.C., Sharples, J.J., and Evans, J.P. (2016). Sensitivity of atypical lateral fire spread to wind and slope. *Geophysiology Research Letters*, 43, 1744–1751.
- Smith, A.M.S., Wooster, M.I., Drake, N.A., Dipotso, F.M., Falkowski, M.J., and Hudak, A.T. (2005). Testing the potential of multi-spectral remote sensing for retrospectively estimating fire severity in African savanna environments. *Remote Sensing of Environment*, 97, 92–115. doi:10.1015/J.RSE-2005.04.014.
- Smith, A.M.S., Lentile, L.B., Hudak, A.T., and Morgan, P. (2007a). Evaluation of linear spectral unmixing and dNBR for predicting post-fire recovery in North American ponderosa pine forest. *International Journal of Remote Sensing*, 28(22), 5159–5166.
- Smith, R., Adams, M., Maier, S., Craig, R., Kristina, A., and Maling, I. (2007b). Estimating the area of stubble burning from the number of active fires detected by satellite. *Remote Sensing of Environment*, 109, 95–106.

- Soverel, N.O., Perrakis, D.D.B., and Coops, N.C. (2010). Estimating burn severity from Landsat dNBR and RdNBR indices across western Canada. *Remote Sensing of Environment*, 114, 1896–1909.
- Stavros, E.N., Abatzoglou, J.T., McKenzie, D., and Larkin, N.K. (2014). Regional projections of the likelihood of very large wildland fires under a changing climate in the contiguous Western United States. *Climatic Change*, 126, 455–468.
- Stensrud, D.J. (1996). Importance of low-level jets to climate: a review. *Journal of Climate*, 9, 1698–1711.
- Storey, M.A., Price, O.F., Sharples, J., and Bradstock, R. (2020a). Drivers of long-distance spotting during wildfires in south-eastern Australia. *International Journal of Wildland Fire*, 29(6), 459–472. <https://doi.org/10.1071/WF19124>
- Storey, M.A., Price, O.F., Bradstock, R.A., and Sharples, J.J. (2020b). Analysis of variation in distance, number, and distribution of spotting in southeast Australian wildfires. *Fire*, 3(2), 10. <http://dx.doi.org/10.3390/fire3020010>
- Stow, D., Niphadkar, M., and Kaiser, J. (2006). *International Journal of Wildland Fire*, 15, 347–360.
- Strahler, A.H., Jupp, D.L.B., Woodcock, C.E., Schaaf, C.B., Yao, T., Zhao, F., Yang, X., Lovell, J., Culvenor, D., Newnham, G., Ni-Miester, W., and Boykin-Morris, W. (2008). Retrieval of forest structural parameters using a ground-based lidar instrument (Echnida). *Canadian Journal of Remote Sensing*, 34, S426–40.
- Strand, E.K., Bunting, S.C., and Keefe, R.F. (2013). Influence of Wildland Fire Along a Successional Gradient in Sagebrush Steppe and Western Juniper Woodlands. *Rangeland Ecology and Management*, 66(6), 667–679. <https://doi.org/10.2111/REM-D-13-00051.1>
- Swanson, M.E., Franklin, J.F., Beschta, R.L., Crisafulli, C.M., DellaSala, D.A., Hutto, R.L., Lindenmayer, D.B., and Swanson, F.J. (2011). The forgotten stage of forest succession: early-successional ecosystems on forest sites. *Frontiers in Ecology and the Environment*, 9, 117–125. <https://doi.org/10.1890/090157>
- Tanase, M., de la Riva, J., Santoro, M., Pérez-Cabello, F., and Kasischke, E. (2011). Sensitivity of SAR data to post-fire forest regrowth in Mediterranean and boreal forests. *Remote Sensing of Environment*, 115(8), 2075–2085.
- Tanase, M.A., Santoro, M., Aponte, C., and de La Riva, J. (2014). Polarimetric properties of burned forest areas at C- and L-band. *IEEE Journal of Selected Topics in Applied Earth Observations and Remote Sensing*, 7(1), 267–276.
- Tian, X., Mcrae, D., Shu, L., Wang, M. (2005). Satellite remote-sensing technologies used in forest fire management. *Journal of Forestry Research*, 16(1), 73–78.
- Tickle, P.K., Lee, A., Lucas, R.M., Austin, J., and Witte, C. (2006). Quantifying Australian forest floristics and structure using small footprint LiDAR and large scale aerial photography. *Forest Ecology and Management*, 223, 379–394.
- Tolhurst, K.G., and McCarthy, G. (2016). Effect of prescribed burning on wildfire severity: a landscape-scale case study from the 2003 fires in Victoria. *Australian Forestry*, 79(1), 1–14.
- Tolhurst, K., Shields, B., and Chong, D. (2008). Phoenix: development and application of a bushfire risk management tool. *The Australian Journal of Emergency Management*, 23, 47–54.
- Trigg, S., and Flasse, S. (2000). Characterizing the spectral-temporal response of burned savannah using *in situ* spectroradiometry and infrared thermometry. *International Journal of Remote Sensing*, 21(16), 3161–3168.
- Trigg, S.N., Roy, D.P., and Flasse, S.P. (2005). An *in situ* study of the effects of surface anisotropy on the remote sensing of burned savannah. *International Journal of Remote Sensing*, 26(21), 4869–4876.
- Tu, Y., Phinn, S., Johansen, K., and Robson, A. (2018). Assessing radiometric correction approaches for multi-spectral UAS imagery for horticultural applications. *Remote Sensing*, 10, 1684.
- Turner, R. (2007). *Assessment of Fuel Loads by Remote Sensing. Sub-report on Airborne Laser Scanner application in the Jilliby Catchment Area*. Final report to NSW RFS 30 March, 2007. Forests New South Wales.
- Turner, M.G., Romme, W.H., and Gardner, R.H. (1999). Prefire heterogeneity, fire severity, and early postfire plant reestablishment in subalpine forests of Yellowstone National Park, Wyoming. *International Journal of Wildland Fire*, 9, 21–36.
- Turner, M.G., Thwaitby, T.G., Tinker, D.B., and Romme, W. (2016). Twenty-four years after the Yellowstone Fires: Are postfire lodgepole pine stands converging in structure and function? *Ecology*, 97(5), 1260–1273.

- van Oldenborgh, G.J., Krikken, F., Lewis, S., Leach, N.J., Lehner, F., Saunders, K.R., van Weele, M., Hausteijn, K., Li, S., Wallom, D., Sparrow, S., Arrighi, J., Singh, R.P., van Aalst, M.K., Philip, S.Y., Vautard, R., and Otto, F.E.L. (2020, in review). Attribution of the Australian bushfire risk to anthropogenic climate change. *Natural Hazards and Earth System Sciences Discussions*. <https://doi.org/10.5194/nhess-2020-69>
- Vanderhoof, M.K., Brunner, N., Beal, Y.G., and Hawbaker, T.J. (2017). Evaluation of the U.S. Geological Survey Landsat Burned Area Essential Climate Variable across the conterminous U.S. using commercial high-resolution imagery. *Remote Sensing*, 9(7), 743.
- Veraverbeke, S., Stavros, E.N., and Hook, S.J. (2014). Assessing fire severity using imaging spectroscopy data from the Airborne Visible/Infrared Imaging Spectrometer (AVIRIS) and comparison with multispectral capabilities. *Remote Sensing of Environment*, 154, 153–163.
- Verbesselt, J., Fleck, S., and Coppin, P. (2002). Estimation of fuel moisture content towards Fire Risk Assessment: A review. In: *Forest Fire Research and Wildland Fire Safety* (Ed: Viegas), Millpress. Rotterdam. ISBN 90-77017-72-0.
- Verbesselt, J., Somer, B., Lhermitte, S., Jonckheere, I., van Aardt, J., and Coppin, P. (2007). Monitoring herbaceous fuel moisture content with SPOT VEGETATION time-series for fire risk prediction in savanna ecosystems. *Remote Sensing of Environment*, 108, 357–368.
- Verbyla, D.L., Kasischke, E.S., and Hoy, E.E. (2008). Seasonal and topographic effects on estimating fire severity from Landsat TM/ETM+ data. *International Journal of Wildland Fire*, 17, 527–534.
- Vilar, L., Camia, A., San-Miguel-Ayanz, J., and Pilar Martín, M. (2016). Modeling temporal changes in human-caused wildfires in Mediterranean Europe based on Land Use-Land Cover interfaces. *Forest Ecology and Management*, 378, 68–78.
- Walker, R.B., Coop, J.D., Downing, W.M., Krawchuk, M.A., Malone, S.L., Meigs, G.W. (2019). How Much Forest Persists Through Fire? High-Resolution Mapping of Tree Cover to Characterize the Abundance and Spatial Pattern of Fire Refugia Across Mosaics of Burn Severity. *Forests*, 10, 782. <https://doi.org/10.3390/f10090782>
- Wallace, L., Lucieer, A., Malenovsky, Z., Turner, D., and Vopenka, P. (2016). Assessment of forest structure using two UAV techniques: a comparison of airborne laser scanning and structure from motion (SfM) point clouds. *Forests*, 7(3), 62.
- Wang, L., Quan, X., He, B., Yebra, M., Xing, M., and Liu, X. (2019). Assessment of the dual polarimetric Sentinel-1A data for forest fuel moisture content estimation. *Remote Sensing*, 11, 1568.
- Wang, X., Thompson, D.K., Marshall, G.A., Tymstra, C., Carr, R., and Flannigan, M.D. (2015). Increasing frequency of extreme fire weather in Canada with climate change. *Climatic Change*, 130(4), 573–586.
- Wickramasinghe, C., Jones, S., Reinke, K., and Wallace, L. (2016). Development of a multi-spatial resolution approach to the surveillance of active fire lines using Himawari-8. *Remote Sensing*, 8(11), 932.
- Wing, M.G., Burnett, J.D., and Sessions, J. (2014). Remote sensing and unmanned aerial system technology for monitoring and quantifying forest fire impacts. *International Journal of Remote Sensing Applications*, 4(1), 18.
- Xu, G., and Zhong, X. (2017). Real-time wildfire detection and tracking in Australia using geostationary satellite: Himawari-8. *Remote Sensing Letters*, 8, 1052–1061.
- Yebra, M., Chuvieco, E., and Riano, D. (2008). Estimation of live fuel moisture content from MODIS images for fire risk assessment. *Agricultural and Forest Meteorology*, 148, 523–36.
- Yebra, M., Chuvieco, E., Danson, M., Dennison, P., Hunt, E.R., Jurdao, S., Riano, D., Zylstra, P. (2013). A global review of remote sensing of live fuel moisture content for fire danger assessment: moving towards operational products. *Remote Sensing of Environment*, 136, 455–468.
- Yebra, M., Quan, X., Riano, D., Rozas-Larraondo, P., van Dijk, A., and Cary, G. (2018). A fuel moisture content and flammability monitoring methodology for continental Australia based on optical remote sensing. *Remote Sensing of Environment*, 212, 260–272.
- Yin, C., He, B., Yebra, M., Juan, X., Edwards, A.C., Liu, X., Liao, Z., Lui, K. (2019). Burn Severity Estimation in Northern Australia Tropical Savannas Using Radiative Transfer Model and Sentinel-2 Data. *IGARSS 2019 (2019 IEEE International Geoscience and Remote Sensing Symposium) Yokohama, Japan*. pp. 6712–6715. doi:10.1109/IGARSS.2019.8899857.
- Yuan, C., Zhang, Y., and Lui, Z. (2015). A survey on technologies for automatic forest fire monitoring, detection and fighting using unmanned aerial vehicles and remote sensing techniques. *Canadian Journal of Forest Research*, 45(7), 783–792.

Observing Ecosystems



Section 1 introduces environmental factors that shape and impact ecosystems and their global distribution. Significant attributes of ecosystems are described in Section 7.

Ecological integrity is said to be “the ability of an ecological system to support and maintain a community of organisms that has species composition, diversity, and functional organisation comparable to those of natural habitats within a region” (Parrish *et al.*, 2003). In the following two sections we consider ecological integrity in terms of biodiversity (see Section 19) and sustainability (see Section 20).

Contents

19 Biodiversity	429
20 Sustainability	451



19 Biodiversity

Biodiversity is a relatively recent term, blended from the Greek word *'bios'*, meaning life, and the Latin word *'diversitas'*, meaning variety or difference. It basically represents the concept of biological diversity and embraces all life forms on Earth (see Sections 1.3.1 and 7.1).

As human populations have expanded, global biodiversity has been observed to decline at both local and global scales (see Section 11.4). Many organisms change their environments to create niches which provide them and their progeny with a competitive advantage over other species in terms of access to, and use of, various resources (Pereira *et al.*, 2012). However, the impact of *Homo sapiens* on global biodiversity vastly exceeds that of other species (see Excursus 11.2). Since the industrial revolution, this impact has accelerated due to massive technological changes and rapid population growth (see Figure 19.1), and has been accompanied by significant pollution of air, water and soil from a wide range of new, toxic materials. The major anthropogenic drivers for biodiversity change (namely, fire, hunting, fishing, agriculture and forest clearing, island invasions, pollution, and anthropogenic climate change) have all been increasing in parallel with population growth over this time period (Pereira *et al.*, 2012). The main threats to biodiversity of mammals, birds and amphibians have been identified (in decreasing order) as:

- habitat changes—urban development, agriculture, mining, transportation;
- overexploitation—fishing, hunting;
- invasive species—introduced exotics;
- climatic variations—temperature and precipitation patterns, sea level rise; and
- pollution—water, air, soil (Pereira *et al.*, 2012; IPBES, 2019).

In response to the global decline in biodiversity, the United Nations Environment Programme (UNEP) developed an international legal instrument called the Convention on Biological Diversity (CBD), which was presented at the 1992 UN Conference on Environment and Development (the Rio 'Earth Summit') and ratified at the end of 1993 with the support of 168 world leaders. The objectives of this convention were:

- conservation of biological diversity;
- sustainable use of the components of biological diversity; and
- fair and equitable sharing of the benefits arising out of the utilisation of genetic resources (CBD, 2020a).

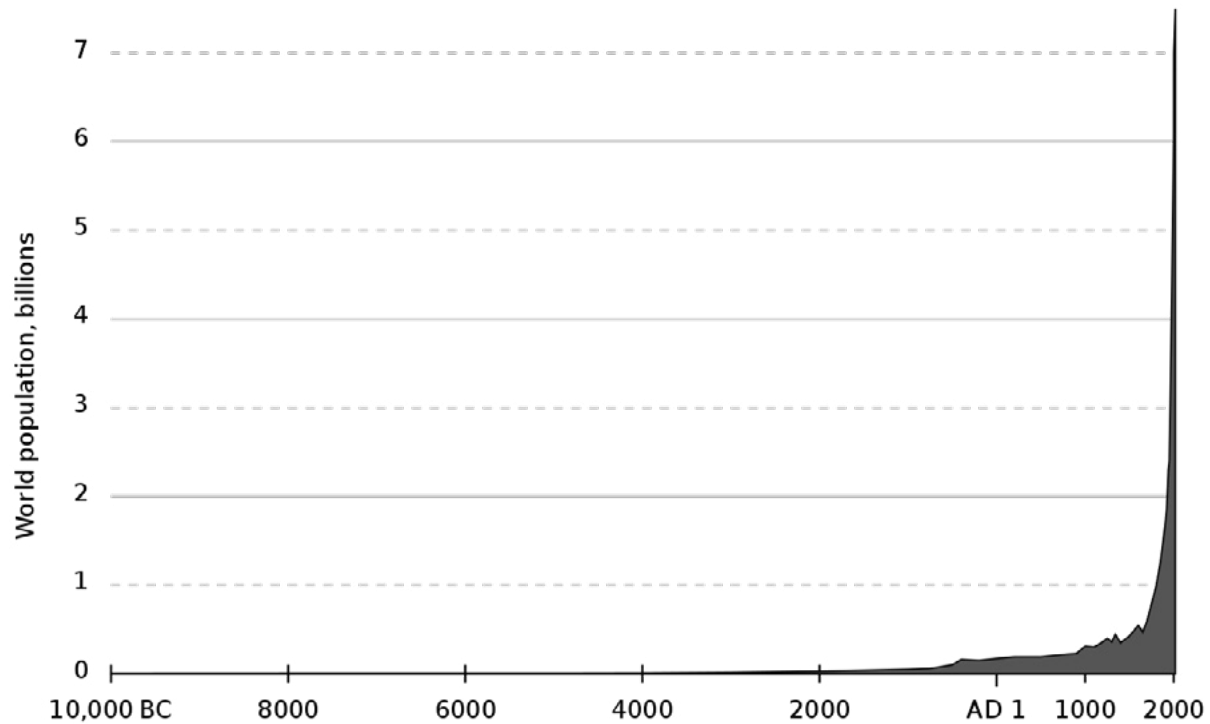
To achieve these objectives, a global strategy was designed, which could be translated into national biodiversity policies and procedures (BIP, 2010). The Strategic Plan for Biodiversity 2011–2020 included the Aichi Biodiversity Targets, which defined five strategic goals:

- A. Address the underlying causes of biodiversity loss by mainstreaming biodiversity across government and society;
- B. Reduce the direct pressures on biodiversity and promote sustainable use;
- C. Improve the status of biodiversity by safeguarding ecosystems, species, and genetic diversity;
- D. Enhance the benefits to all from biodiversity and ecosystem services; and
- E. Enhance implementation through participatory planning, knowledge management, and capacity building (CBD, 2020b).

Background image: Blue Marble Next Generation image with topography and bathymetry for April 2004. (Note: the vertical extent of this composite image has been clipped and the aspect ratio changed.) Source: NASA. (Retrieved from <https://visibleearth.nasa.gov/collection/1484/blue-marble>)

Figure 19.1 Human population growth

Human population growth since 10,000 BC to present day shows an exponential rate of increase since the industrial revolution.



Source: El T, Wikimedia: https://commons.wikimedia.org/wiki/File:Population_curve.svg

Within this set of goals, 20 targets (to be achieved by 2020) were outlined based on measurable indicators of progress (CBD, 2020b). Using the CBD framework, National Biodiversity Strategies and Action Plans (NBSAP), which define policies, planning processes, and research agendas to ensure “consideration of the conservation and sustainable use of biological resources into national decision-making”, are then developed and implemented by all signature nations. A revised Global Biodiversity Framework is currently being prepared by CBD for post-2020.

The International Union for Conservation of Nature (IUCN) defines six categories for protected areas based on management objectives, which are used as a global standard for defining and recording such regions (IUCN, 2020a):

Ia Strict Nature Reserve: Category Ia are strictly protected areas set aside to protect biodiversity and also possibly geological/geomorphical

features, where human visitation, use and impacts are strictly controlled and limited to ensure protection of the conservation values. Such protected areas can serve as indispensable reference areas for scientific research and monitoring.

Ib Wilderness Area: Category Ib protected areas are usually large unmodified or slightly modified areas, retaining their natural character and influence without permanent or significant human habitation, which are protected and managed so as to preserve their natural condition.

II National Park: Category II protected areas are large natural or near natural areas set aside to protect large-scale ecological processes, along with the complement of species and ecosystems characteristic of the area, which also provide a foundation for environmentally and culturally compatible, spiritual, scientific, educational, recreational, and visitor opportunities.

The human appropriation of Earth's natural resources is not only leading to biodiversity loss but also to large alterations of biodiversity distribution, composition, and abundance.
(Pereira et al., 2012)

- III Natural Monument or Feature:** Category III protected areas are set aside to protect a specific natural monument, which can be a landform, sea mount, submarine cavern, geological feature such as a cave or even a living feature such as an ancient grove. They are generally quite small protected areas and often have high visitor value.
- IV Habitat/Species Management Area:** Category IV protected areas aim to protect particular species or habitats and management reflects this priority. Many Category IV protected areas will need regular, active interventions to address the requirements of particular species or to maintain habitats, but this is not a requirement of the category.
- V Protected Landscape/ Seascape:** A protected area where the interaction of people and nature over time has produced an area of distinct character with significant, ecological, biological, cultural and scenic value: and where safeguarding the integrity of this interaction is vital to protecting and sustaining the area and its associated nature conservation and other values.
- VI Protected area with sustainable use of natural resources:** Category VI protected areas conserve ecosystems and habitats together with associated cultural values and traditional natural resource management systems. They are generally large, with most of the area in a natural condition, where a proportion is under sustainable natural resource management and where low-level non-industrial use of natural resources compatible with nature conservation is seen as one of the main aims of the area.”

Global ecosystem maps are necessary to assess the representation of ecosystems in protected areas. In particular, Sayre *et al.* (2020) derived a global dataset with 250 m spatial resolution to map terrestrial ecosystems by combining climate, landform and vegetation information. Of the 431 identified ecosystems, 278 were described as natural/semi-natural. Using Aichi target 11, which defines adequate representation as 17% of the global ecosystem area

being managed for conservation to meet IUCN management categories I–IV (see also Table 3.6), only 19 of the natural/semi-natural ecosystems were adequately represented, 44 were poorly represented (8.5–17% of total area was protected), 206 were very poorly represented (< 8.5%) and 9 were not protected at all. When assessed against IUCN categories 1–VI and including undesignated protected areas, these proportions improved to around one third as adequate, one third as poor and one third as very poor.

In order to monitor biodiversity globally, a set of agreed and appropriate indicators are required “to measure status and trends of biodiversity, sustainable use, threats to biodiversity, ecosystem integrity and ecosystem goods and services, status of knowledge, innovations and practice, and status of resource transfers” (BIP, 2010; see also Section 7.1). Global, EO-based, biodiversity indicators that can be used for standardised monitoring are being developed by the Group for Earth Observations Biodiversity Observation Network (GEOBON; see Section 19.3), which are commonly called ‘Essential Biodiversity Variables’ (EBV; see Section 11.2).

Standardised criteria for assessing the risk of biodiversity loss (see Section 19.4) are needed to improve the management of biodiversity resources and protect ecosystem services (see Section 20.3). Such criteria have been developed by the IUCN for both species and ecosystems (see Excursus 19.1). Despite the bleak outlook for biodiversity risk around the world, in recent decades biodiversity monitoring has shown that some improvements are being achieved by global, regional and national initiatives to conserve specific habitats, reintroduce threatened species, enforce environmental legislation, and increase public awareness (Pereira *et al.*, 2012).

An overview of Australian biodiversity is presented in Section 19.1 and Australian biodiversity monitoring systems based on EO datasets are described in Section 19.5. Some EO sensors that are appropriate for assessing biodiversity are reviewed in Section 19.2.

An understanding of risks to biodiversity is needed for planning action to slow current rates of decline and secure ecosystem services for future human use.
(Keith *et al.*, 2013)

19.1 Biodiversity in Australia

To date, a diverse range of policies and programs have been implemented by different jurisdictions to manage and conserve biodiversity in Australia (see Section 19.5). The central environmental legislation at a federal level is the Environmental Protection and Biodiversity Conservation Act (EPBC) 1999, which “provides a legal framework to protect and manage nationally and internationally important flora, fauna, ecological communities and heritage places as defined in the EPBC Act as matters of national environmental significance” (DAWE, 2020a).

Biodiversity indicators are used for various environmental reporting exercises, including Australian state and federal State of Environment (SoE) reports. For example, the Victorian SoE 2018 report evaluated that, in that state, 75% of the biodiversity indicators had declined or were not known (SoE, 2018), which is consistent with global trends (IPBES, 2019). Land management practices that have been identified as having the greatest impact on biodiversity in Australia are summarised in Table 19.1.

Natural Resource Management (NRM) is the integrated management of the natural resources that make up Australia’s natural landscapes, such as land, water, soil, plants and animals. That is, our land, water and biodiversity assets.
(NRM, 2019)

Table 19.1 Land management practices with ongoing impact on biodiversity in Australia

Land Management Practice	Impacts on biodiversity	Geographic Area
Removing native vegetation Replacing native grasses with improved pasture	Habitat destruction and fragmentation, reduced population sizes, isolation of populations, reduced resilience to other threats, loss of species and diversity, depleted condition and functioning of ecosystems	Ongoing threat to vegetation communities in southeast Queensland and northern NSW, parts of Tasmania and the NT Small scale clearing threatens remnants in all settled areas of Australia
Increasing the intensity of grazing	Habitat depletion and fragmentation, reduced population sizes, isolation of populations, reduced resilience to other threats, loss of species and diversity, depleted condition and functioning of ecosystems	Ongoing pressure across the rangelands, the wheat–sheep zone, and alpine areas, including grazing by livestock, native herbivores, and invasive herbivores
Increasing the intensity of artificial watering points	Habitat destruction, increased competition from invasive species, loss of species and diversity, depleted condition and functioning of ecosystems	Ongoing pressure across much of the rangelands.
Extracting surface and groundwater for irrigation and other uses; Draining wetlands	Depletion of river flows and aquatic habitat, loss of species and diversity, increased vulnerability to invasive species and other threats, depletion of condition, and functioning of aquatic ecosystems	Ongoing threat in all major irrigation areas, especially in the Murray-Darling Basin Groundwater extraction is an ongoing threat to wildlife and natural systems in the Great Artesian basin, southwest Western Australia, and many areas of southern Australia
Converting from livestock to cropping	Habitat destruction and fragmentation, reduced population sizes, isolation of populations, reduced resilience to other threats, loss of species and diversity, depleted condition and functioning of ecosystems, depletion of the condition of aquatic and marine ecosystems	Relatively stable but ongoing threat across the intensive land use wheat–sheep belt of southeastern Australia Ongoing threat to the Great Barrier Reef
Altering natural fire regimes	Depleted composition and structure, reduced resilience to other threats	Australia-wide, but impacts significant in northern savannas and fire-sensitive and fire-dependent communities (e.g. monsoon vine thickets)
Revegetating cleared areas	Increased habitat and reduced fragmentation, increased resilience to other threats	Natural regeneration occurs throughout the country Revegetation programs are primarily implemented in southern Australia Large scale examples aim to link remnants across landscapes.
Reducing the density of livestock	Reduced competition, increased resilience to other threats	Occurs in response to drought throughout grazing lands and in some areas as part of sustainable grazing management programs Newly acquired conservation areas are generally destocked.

Source: DEWHA (2009) Table 5.5

Table 19.2 Biodiversity in Australia's terrestrial vegetation

Key finding	Description
Native vegetation is a key surrogate for biodiversity	Native vegetation is a cost-effective and powerful surrogate for biodiversity. The distribution of threatened species and communities is closely aligned with areas where native vegetation has been extensively cleared.
The extent of native vegetation is known	National mapping of native vegetation has advanced significantly since 2002 with improvements in data and in mapping technologies (e.g. through NVIS). Although important gaps remain (in scale, and in defining some major vegetation groups such as derived native grasslands), we now know the extent of most major vegetation types in the landscape.
Native vegetation has been modified or cleared	Native vegetation has been modified and cleared since European settlement, especially from intensive agricultural and urban areas (particularly in southern and eastern Australia and in southwestern Australia). The losses have been greatest in eucalypt woodlands and have also been significant in eucalypt open forest and mallee woodlands and shrublands. The loss of biota in the cleared and modified areas has been dramatic and continues today (e.g. in woodland birds).
Native vegetation is being lost faster than it is replaced	Broadscale clearing has been reducing since 2002, however nationally, native vegetation is still being cleared and modified faster than it is replaced. A net loss of forest (including native and non-native vegetation) of around 260,000 ha per year occurred between 2000 and 2004 and was primarily attributed to clearing for agriculture and urban development.
We are making progress towards assessing native vegetation condition	Since 2002, there has been progress in the collaboration between national, state, and territory jurisdictions in improving Australia's vegetation information. This includes approaches to modelling, monitoring, and mapping vegetation condition, on both national and more localised scales. Reference-based methodologies are being used in most states for target setting, investment and planning decisions, and reporting.

Source: DEWHA (2009) Table 2

Measures of biodiversity are introduced in Section 7.1. The major indicators for biodiversity assessment in terrestrial ecosystems in Australia are defined as:

- native vegetation extent and distribution;
- changes in native vegetation extent and distribution; and the
- status and trends of native vegetation condition (DEWHA, 2009; see Table 19.2).

Mapping of native vegetation, an effective indicator of biodiversity, has improved in recent decades with systems like NVIS (see Section 2.3.1), although information gaps remain. The available data indicates that native vegetation still grows on 87% of the Australian continent (DEWHA, 2009), however 62% of this area is likely to be modified (Thackway and Lesslie, 2006). Not surprisingly, the greater concentrations of threatened species occur in the eastern, southern and southwestern coastal fringes where population densities are highest.

In order to conserve biodiversity in Australia, a network of conservation parks and reserves has been coordinated by the National Reserve System (NRS) to meet the IUCN principles of 'comprehensiveness, adequacy and representativeness' (CAR):

- comprehensiveness—samples the full range of regional ecosystems recognisable at an appropriate scale within each IBRA bioregion;
- adequacy—at a bioregional scale, consider ecological viability and resilience for each reserve and the reserve system; and
- representativeness—sample regional variability (IBRA sub-region; DEWHA, 2009).

In 2006, 11.6% of the Australian land mass was officially reserved, however, while 49 bioregions satisfied the goals of $\geq 10\%$ representation in reserves, 36 did not (DEWHA, 2009). Although the NRS is a collaborative undertaking between state and federal jurisdictions to provide linked refuges across the landscape, differing priorities and progress towards CAR persist both within and between jurisdictions.

Conservation reserves alone cannot protect the biodiversity of a region. Even if 10% of every ecosystem could be included, which is highly unlikely, in the protected area network, most species would not be included. Any conservation reserve system will fail if the broader land use management practices ignore the conservation of biodiversity in off-reserve areas.
(Tony Brandis, from 'Rescuing the Rangelands')

19.2 EO Sensors for Biodiversity

Passive optical satellite imagery provides the overwhelming majority of EO information to inform biodiversity decision making and legislative instruments, such as mapping and monitoring of land cover, land use, biophysical vegetation properties, and vegetation extent (see Sections 3, 8, and 9). This data source is now available at a range of spatial scales, from pixels spanning centimetres to kilometres, with data archives dating back many decades (see Volume 1A—Section 14). Many of these archives have been calibrated and standardised for ease of use, and reprocessed into a variety of composite image datasets with relevance to biodiversity (see Volume 2D).

Other sources of EO datasets that are relevant to mapping and monitoring biodiversity are summarised in Table 19.3. A growing variety of ground-based sensors are also being utilised to collect *in situ* and near ground data (see Volume 2D—Section 12).

Changes in and the loss of biodiversity directly influences the capacity of an ecosystem to produce and supply essential services, and can affect the long term ability of ecological, economic and social systems to adapt and respond to global pressures. (DEWHA, 2010)

Table 19.3 EO sensors relevant to biodiversity

TIR: Thermal infrared; SAR: Synthetic Aperture Radar; RPAS: Remotely Piloted Aircraft Systems; ET: Evapotranspiration

Type	Sensor	Platform	Relevance	Advantages	Disadvantages
Passive optical	Multispectral radiometer	Predominantly satellite, decreasingly airborne	Local to national scale	Global, recurrent coverage, high temporal frequency and extent, low cost, significant calibration/validation efforts established, many operational processing methods	Some low spatial resolution datasets are not appropriate for detailed studies
	Hyperspectral spectro-radiometer	Predominantly airborne	Species discrimination Plant biochemical functioning and health	High spectral resolution	High cost, high data volume, lower signal to noise ratio, greater processing complexity
	TIR radiometer	Field, satellite or airborne	Soil/canopy temperature	Surrogate measure for ET plus input into EO modelling	Low resolution, low signal to noise ratio
Active optical	Lidar	Predominantly airborne, increasingly terrestrial, emerging satellite	Vegetation structure, volume, and biomass Water balance applications DEM	Highlights detailed structure of plant canopy and soil surface	High cost, specialised processing, longer acquisition times
	Active optical sensor	Ground vehicles or RPAS	Cover and condition mapping Specific property recognition (e.g. disease, optical properties of water)	Convenience, low cost, independent of sunlight	Low availability and limited surface coverage
Passive microwave	Microwave radiometer	Satellite	Soil moisture Climate variables	High temporal frequency, large spatial coverage, cloud penetration	Very low energy targets, very coarse spatial resolution
Active microwave	SAR	Satellite or airborne	Soil characteristics Vegetation structure Water dynamics	All weather, operates at night	Data availability, noisy data, complex processing
Proximal	Passive optical sensor (phenocam, hyperspectral); meteorological	Ground and tower-based (see Excursus 7.2 and Volume 2D—Section 12)	Ecosystem and atmospheric variability Carbon dynamics Phenology	Continuous, long term measurements	High cost, high data volume, require skilled maintenance
Positioning	GPS	Portable devices linked to satellite-based positioning systems	Locating field sites for cal/val	Low cost	Coverage in remote regions or below dense canopies
Citizen Science	Portable, hand-held r	Ground-based	Validation of species occurrence and major phenological events	Low cost, public involvement	Potentially subjective

19.3 Global Biodiversity Indicators

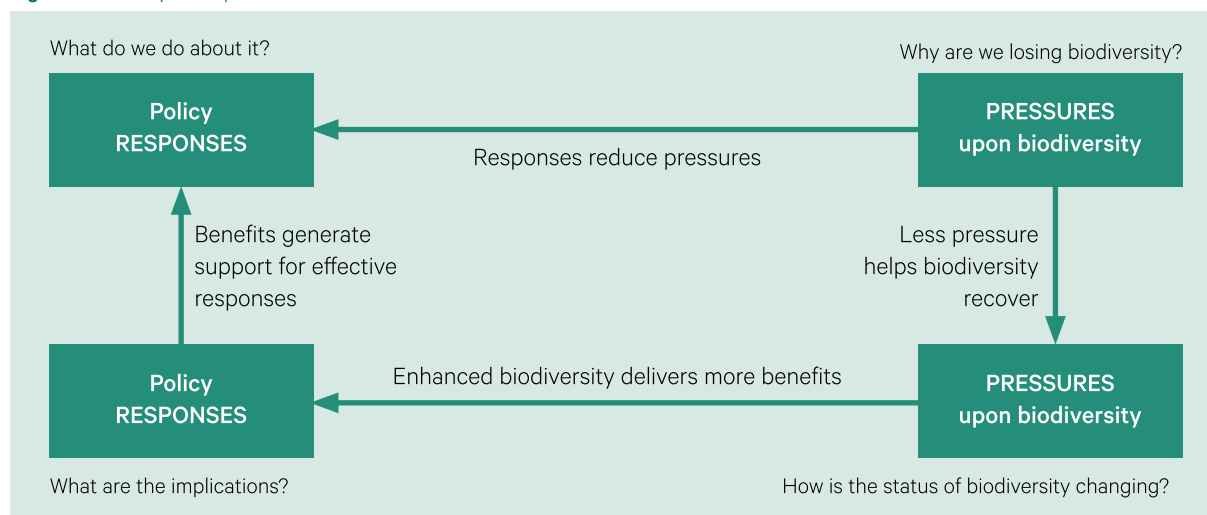
While we are acutely aware of the alarming rate of biodiversity loss worldwide, it is a challenge to quantify the status of global biodiversity change using an approach that is consistent over space and time. There has been considerable debate on the topic of measuring and monitoring biodiversity at a global scale (e.g. EASAC, 2004; Teillard *et al.*, 2016; OECD, 2020). Various sets of global biodiversity indicators have been proposed (BIP, 2019), but many accepted measures, such as the Living Planet Index (LPI; WWF, 1998), have been assessed as failing “to fulfill fundamental scientific requirements” (Böhringer and Jochem, 2007).

One framework that has been proposed to identify and classify appropriate indicators for consistent biodiversity monitoring and evaluation at regional and global scales is the response-pressure-state-benefit framework (Sparks *et al.*, 2011; see Figure 19.2), where the linkages between indicators show the interaction of relevant factors in biodiversity loss (see also Figure 11.2). The function of each indicator is summarised in Table 19.4. This framework underpins the biodiversity monitoring program being implemented in NSW (see Section 19.5).

Major gaps and uncertainties currently exist within the survey data records that are available to monitor global biodiversity (Pereira *et al.*, 2012). There are also significant variations between and within national and regional monitoring programmes. Coupled with insufficient financial resources and a lack of consensus on reliable, scalable biodiversity indicators, these factors have thwarted implementation of an operational ‘global system of harmonised observations’ (Pereira *et al.*, 2013). However, EO offers considerable potential for both direct and indirect assessment of biodiversity (Gillespie *et al.*, 2008) and conservation planning (Rose *et al.*, 2014) at regional to global scales, particularly with the advent of high spatial resolution, spaceborne sensors.

If you can't measure it, you can't manage it.
(Peter Drucker)

Figure 19.2 Response–pressure–state–benefit (RPSB) framework



Adapted from: Sparks *et al.* (2011)

Thus it happens in affairs of state, for when the evils that arise have been foreseen (which it is only given to a wise man to see), they can be quickly redressed, but when, through not having been foreseen, they have been permitted to grow in a way that every one can see them, there is no longer a remedy.
(Machiavelli, from 'The Prince', 1513)

Since raw biodiversity data is typically sparse and heterogeneous, using EO data as covariates with appropriate modelling tools allows the available raw data to be sensibly interpolated both spatially and temporally (Jetz *et al.*, 2019; see Volume 2D). Progress towards a globally-accepted, EO-based set of indicators is being achieved by GEOBON. This international initiative of GEO (Group for Earth Observations, a voluntary intergovernmental partnership; see Volume 1A—Section 1.5) aims to “improve the acquisition, coordination and delivery of biodiversity observations and related services to users including decision makers and the scientific community” and establish an integrated, global network to observe biodiversity in a timely and consistent fashion at a range of scales. This network will help to assess progress towards the CBD Strategic Plan and Aichi Targets (GEOBON, 2020; Walters and Scholes, 2017).

A major focus for GEOBON is defining a set of EBV that can be measured and modelled globally, preferably by integrating EO datasets with *in situ* observations (Pereira *et al.*, 2013; GEOBON, 2020; Masó *et al.*, 2020; see Section 11.2), where an ideal EBV is defined as:

- “able to capture critical scales and dimensions of biodiversity;
- biological;
- a state variable (in general);
- sensitive to change;
- ecosystem agnostic (to the degree possible); and
- technically feasible, economically viable and sustainable in time” (GEOBON, 2020).

Table 19.4 RPSB indicators

Indicator	Function	Example
Response	Measure implementation of policies or actions aimed to prevent or reduce biodiversity loss	Conservation actions including offsets
Pressure	Measure the extent and intensity of the threats to or causes of biodiversity loss	Certain land uses
State	Measure the current condition and status of biodiversity or ecological integrity	Status of threatened species or condition of suitable habitats
Benefit	Quantify the benefits that humans derive from biodiversity	Ecosystem services

Source: Sparks *et al.* (2011); OEH and CSIRO (2019)

The current set of EBV classes and candidates are listed in Table 19.5. Primary observations from *in situ* monitoring and EO systems are preprocessed and combined into EBVs, which represent an intermediate data layer for harmonisation between sampling protocols and measurement systems (see Figure 11.3). All EBV classes should be included in a biodiversity monitoring program. EBVs inform multiple biodiversity and ecosystem service indicators, such as those needed to assess the Aichi Biodiversity targets. Some indicators require the integration of EBVs with other sources of information such as data on ancillary biodiversity attributes (slowly changing variables), drivers and pressures, management and policy responses, and valuation and demand of ecosystem services. Future projections of drivers and policy responses can be used to develop scenarios for biodiversity and ecosystem services using models calibrated and validated with EBVs (Pereira *et al.*, 2013). Further integration between these EBV and appropriate models and infrastructure will support assessment at a range of scales for both policy and research purposes.

Table 19.5 EBV classes and candidates

EBV class	EBV candidate
Genetic composition	Co-ancestry Allelic diversity Population genetic differentiation Breed and variety diversity
Species populations	Species distribution Population abundance Population structure by age/size class
Species traits	Phenology Morphology Reproduction Physiology Movement
Community composition	Taxonomic diversity Species interactions
Ecosystem function	Net primary productivity Secondary productivity Nutrient retention Disturbance regime
Ecosystem structure	Habitat structure Ecosystem extent and fragmentation Ecosystem composition by functional type

Source: GEOBON (2020)

19.4 Risk Assessment

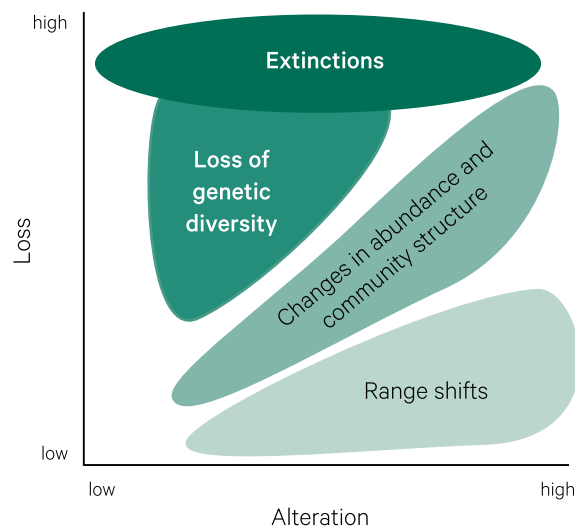
As introduced above, global biodiversity is declining dramatically, especially since the start of the industrial age. These changes include both loss and alteration of biodiversity, in differing proportions (see Figure 19.3). In Australia, one example of this decline is the current extent of Brigalow communities (*Acacia harpophylla* dominant and co-dominant) which before pastoral settlement covered 10.2 million ha in southeast Queensland (Neldner, 2018)¹⁶. By 1940, the extent of brigalow had been reduced to less than 8.5 million ha, and by 1970 it covered half this area (Accad and Neldner, 2015). Various social and political factors contributed to the significant decline for this vegetation group, including subsided ringbarking during the Great Depression and mechanical and chemical clearing following World War 2 (Seabrook *et al.*, 2006). Brigalow now covers only 1.3 million ha and is an EPBC-listed Endangered Ecological Community (Neldner *et al.*, 2017).

The IUCN Red List of Ecosystems (RLE) defines criteria for assessing declining ecosystem biodiversity at a global scale (see Excursus 19.1). These criteria satisfy the IUCN design goals of generality, precision, realism and simplicity (Keith *et al.*, 2015) and have been applied to a wide range of ecosystems around the world. RLE has been used to assess ecosystem risk in Australia for a range of ecosystem types (Keith, 2015), including Alpine herbfields (Williams *et al.*, 2015), lowland rainforests (Metcalf and Lawson, 2015), forests (Burns *et al.*, 2015; Auld and Leishman, 2015), woodlands (Tozer *et al.*, 2015; Wardle *et al.*, 2015), and wetlands (Pisanu *et al.*, 2015). While widespread, these individual case studies do not satisfactorily represent the status of Australian ecosystems. Keith (2015) recommends a comprehensive risk assessment approach comprising:

- a systematic and consistent framework for assessment and scaling with precise differentiation of ecosystems—current typologies for terrestrial vegetation are not consistent with IUCN RLE;
- high to medium resolution spatial data showing ecosystem distribution—EO time series datasets are invaluable here, together with other spatial data (see Volume 2D);
- long term ecological monitoring for assessing and managing ecosystems—such as the TERN Long Term Ecological Research Network (LTERN; see Section 19.6); and
- cross-disciplinary collaboration and cooperation.

Figure 19.3 Biodiversity change in terms of loss and alterations

Loss of biodiversity includes both species extinctions and loss of genetic diversity, while alteration of biodiversity includes changes in species composition and relative abundance, changes in community structure, and changes in species range or extent.



Adapted from: Pereira *et al.* (2012) Figure 1

Many data sources are relevant for ecosystem risk assessment, including those from short and long term monitoring programs, field surveys, and underwater, aerial and satellite sensors. Of these, satellite remote sensing offers the greatest opportunity to evaluate ecosystem change beyond the site level and to scale the risk assessment process to provincial, national and continental jurisdictions.
(Murray *et al.*, 2018a)

¹⁶ <http://www.environment.gov.au/cgi-bin/sprat/public/publicshowcommunity.pl?id=28&status=Endangered>

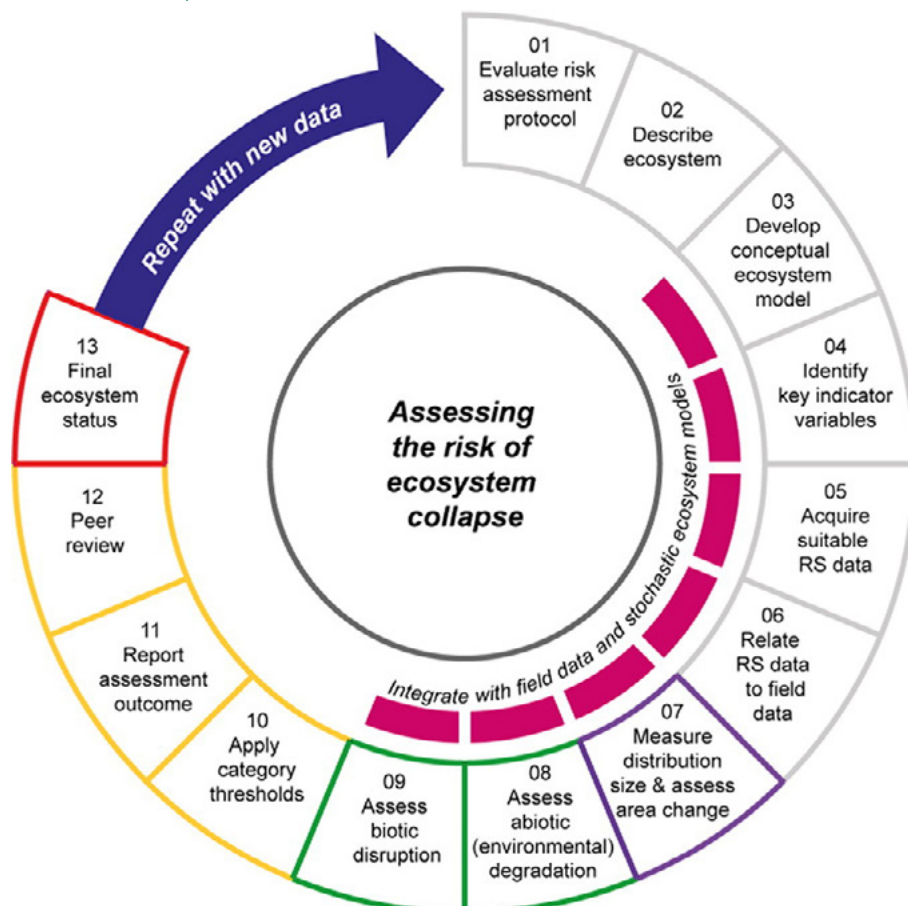
EO datasets are being used increasingly to assess risks to biodiversity, ideally with sufficient spatial and temporal resolutions to represent ecosystem dynamics and detect rapid change. Some of the environmental variables that can be monitored using EO include area loss, biomass change, and disease stress, which can subsequently be used to estimate the spatial extent of biotic and abiotic degradation. EO time series can also be analysed to derive disturbance histories that could further inform forecasts of degradation (Murray *et al.*, 2018a). Appropriate EO data and methods need to be selected for such assessments and repeated as new data become available. For example, Figure 19.4 summarises a framework for using EO datasets to list ecosystems in the RLE:

- evaluate the risk assessment protocol and define assessment unit (01–02);
- develop conceptual ecosystem model and identify indicator variables to monitor with EO (03–06);
- incorporate field data and ecosystem models;
- evaluate ecosystem against risk assessment criteria (07–09);
- summarise and review results (10–12); and
- formally list ecosystem in RLE (13).

An online mapping platform, remap (Remote Ecosystem Assessment and Monitoring Pipeline; Murray *et al.*, 2018b), enables ecosystem status maps to be generated rapidly from freely available EO imagery and other spatial datasets (remap, 2020). This tool is designed for users without specialist knowledge of EO and relies on machine learning algorithms (see Volume 2E) to generate RLE-compatible assessments of ecosystems.

There are risks and costs in a program of action, but they are far less than the long range risks and costs of comfortable inaction.
(John F. Kennedy)

Figure 19.4 EO framework for ecosystem risk assessment



Source: Murray *et al.* (2018a) Figure 2

Excursus 19.1—IUCN Red Lists of Threatened Species and Ecosystems

Source: Keith *et al.* (2013); Rodríguez *et al.* (2015)

Further information: IUCN Red List of Threatened Species: <https://www.iucnredlist.org/>

IUCN Red List of Ecosystems: <https://www.iucn.org/theme/ecosystem-management/our-work/red-list-ecosystems>

IUCN-CEM (2016); Bland *et al.* (2016)

IUCN-CEM Research and development: <https://iucnrle.org/resources/research-development/>

The International Union of Conservation of Nature (IUCN) was established in 1948 to examine the impact of anthropogenic activities on nature. Since its inception it has expanded into a democratic union of 1,400 government and civil organisations around the world, with access to expertise in a wide variety of disciplines related to natural resources. The IUCN has contributed to numerous international conventions, strategies and agreements that address global challenges to conserve nature and achieve sustainable and equitable use of its resources (IUCN, 2020a).

Two of its global achievements are the Red List of Threatened Species and the Red List of Ecosystems.

IUCN Red List of Threatened Species

The IUCN Red List of Threatened Species “provides information about range, population size, habitat and ecology, use and/or trade, threats, and conservation actions that will help inform necessary conservation decisions” (IUCN, 2020b). This list has become the most comprehensive source of information relating to extinction risk status of 116,000 animal, plant, and fungal species globally and is used by a wide range of agencies with interests in land management, education, business, and nature conservation. Its ongoing assessments enable the status of listed species to be monitored and new species to be included with a target of assessing an additional 44,000 species in 2020 (IUCN, 2020b). By 2020, 31,000 species were listed as threatened with extinction (IUCN, 2020c), representing over a quarter of those assessed.

IUCN Red List of Ecosystems (RLE)

In recognition that the ecosystems have changed more rapidly since 1950 due to human impact, a new conservation policy tool was developed by the IUCN to assess the risk of ecosystem collapse. The resulting global standard is called the Red List of Ecosystems Categories and Criteria (RLE) and was accepted by the IUCN in 2014 for application at local, national, regional, and global scales (IUCN-CEM, 2020). All freshwater, marine, terrestrial, and subterranean

ecosystem types of the world at a global level are planned for assessment using RLE by 2025, with periodic updates to monitor progress towards international targets, such as the Aichi Targets (CBD, 2010) or Sustainable Development Goals (UN General Assembly, 2012; see Excursus 20.2).

RLE is a generic method that can be used to assess terrestrial, subterranean, inland and marine waters, and transitional environments. RLE determines ecosystem status in three broad divisions of eight categories:

- least concern—not currently facing significant risk of collapse;
- threatened—critically endangered, endangered or vulnerable; or
- collapse—endpoint of ecosystem decline, “when most of the diagnostic components of the characteristic biota are lost from the system, or when functional components (biota that perform key roles in ecosystem organisation) are greatly reduced in abundance and lose the ability to recruit. Chronic changes in nutrient cycling, disturbance regimes, connectivity, or other ecological processes (biotic or abiotic) that sustain the characteristic biota may also signal ecosystem collapse” (Keith *et al.*, 2013; see Figure 19.5a).

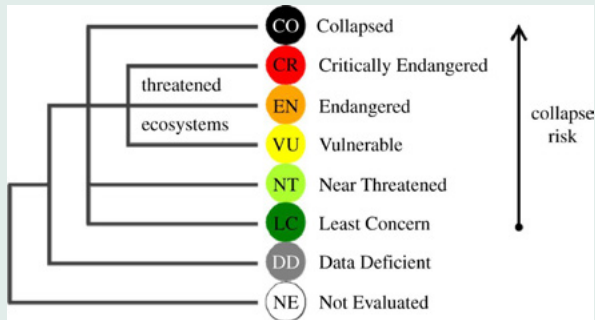
In this context, an ecosystem comprises four essential elements:

- i. a biotic complex or assemblage of species;
- ii. an associated abiotic environment or complex;
- iii. the interactions within and between those complexes; and
- iv. a physical space in which these operate (Tansley, 1935).

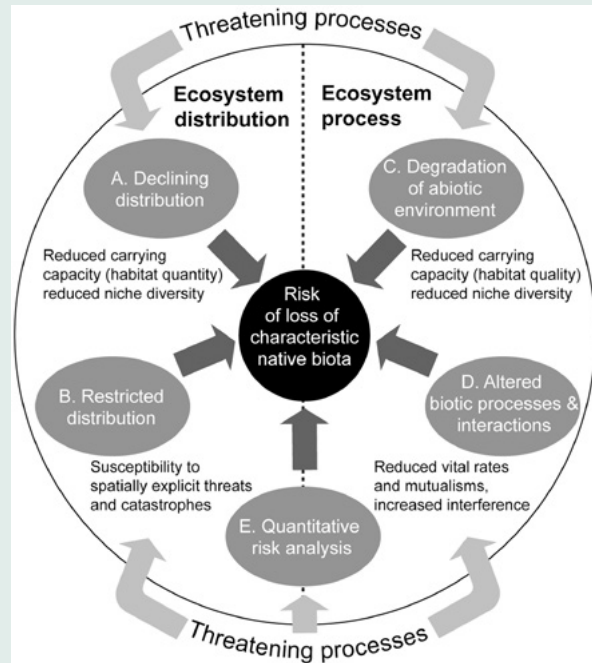
‘Ecosystem type’ is considered to be synonymous with the terms ‘ecological community’, ‘habitat’, and ‘vegetation type’ (Keith *et al.*, 2013). Nicholson *et al.* (2015) review terms used in ecosystem risk assessment.

Figure 19.5 RLE categories and criteria and categories

a. RLE risk categories



b. Mechanisms of ecosystem collapse and symptoms of collapse risk



Source: a. Keith *et al.*, (2013) Figure 2; b. Rodríguez *et al.* (2015) Figure 2

The underlying conceptual model identifies four distributional and functional symptoms of ecosystem risk as the basis for assessment criteria:

- Criterion A: rates of decline in ecosystem distribution—identify each ecosystem type that is currently declining in extent or may decline in the near future using at least two measures of its distribution taken at different points in time and calibrated to the timescales of RLE assessments;
- Criterion B: restricted distributions with continuing declines or threats—evaluate the risk of loss of all occurrences of an ecosystem type by considering the interaction between the spatial extent of threats and the spatial distribution of ecosystem occurrences;
- Criterion C: rates of environmental (abiotic) degradation—evaluate the risk of collapse posed by degradation of the abiotic environment by measuring an appropriate abiotic variable; and
- Criterion D: rates of disruption to biotic processes—evaluate the risk of collapse posed by degradation of the biotic environment by measuring an appropriate biotic variable.

Criterion E is a quantitative estimate of the risk of ecosystem collapse, which enables integrated assessment of multiple processes and provides a conceptual anchor for the other criteria (Keith *et al.*, 2013; see Figure 19.5b). This criterion relies on specific process-based ecosystem models to estimate risk of collapse over a 50 or 100 year timeframe. Criteria A, C, and D assess ecosystem decline over three timeframes:

- current—preceding 50 years;
- future—next 50 years; and
- past—relative to the reference years 1750, which is assumed to be the onset of industrial exploitation of the environment (see Figure 19.6b and Section 3.3.1).

The steps followed to apply the RLE are summarised in Figure 19.6c. In 2018, 1,397 ecosystem units in 100 countries had been assessed following the IUCN RLE protocol (Bland *et al.*, 2018). This approach has been used to assess ecosystem risk in Australia for a range of ecosystem types (Keith *et al.*, 2015; see Section 19.4).

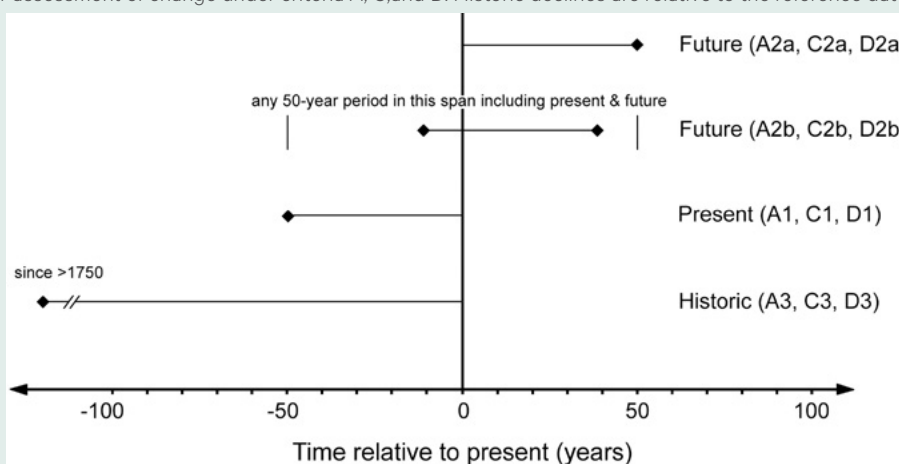
Figure 19.6 Application of RLE

AOO: area of occupancy; EOO: extent of occurrence.

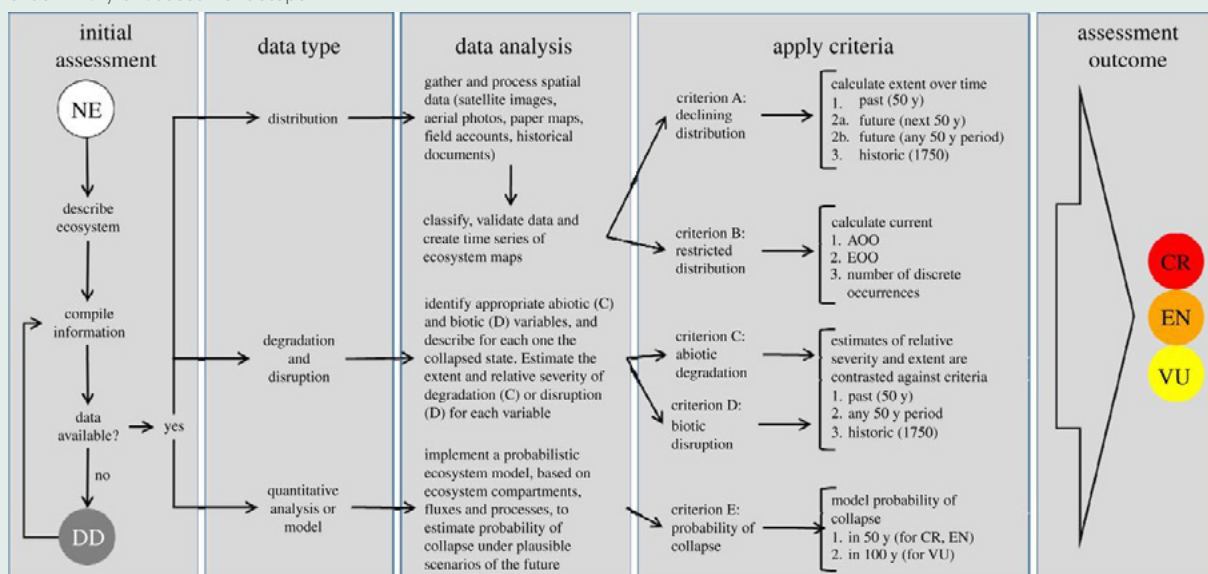
a. Sequence for assessment protocol

Describe ecosystem (characteristic biota, abiota, interactions, location, and spatiotemporal/thematic scale)				
Identify appropriate measure of distribution (maps, sightings)		Describe salient mechanisms of ecosystem dynamics and function (process model)		
		Identify appropriate measure of distribution (maps, sightings)	Identify appropriate measure of biotic interaction	Model ecosystem dynamics
Assess rate of change Criterion A	Assess current extent Criterion B	Assess rate of substrate degradation Criterion C	Assess rate of disruption of interactions Criterion D	Assess risk of collapse Criterion E
A1: present A2: future A3: historic	B1: EOO B2: AOO B3: locations and for B1 and B2: i. Continuing decline ii. Threats (e.g. fragmentation) iii. Number of locations	C1: present C2: future C3: historic	D1: present D2: future D3: historic	

b. Timescales for assessment of change under criteria A, C, and D. Historic declines are relative to the reference date of 1750.



c. Summary of assessment steps.



Source: a. Keith *et al.* (2013) Figure 3; b. Keith *et al.* (2013) Figure 4; c. Rodríguez *et al.* (2015) Figure 3

19.5 Australian Biodiversity Monitoring

The two most significant issues impacting biodiversity management at a national level in Australia have been identified as the lack of systematic monitoring, and limitations in resources available to respond to threats (DEWHA, 2010). Inconsistencies occur both within and between jurisdictions in terms of legislation and regulation related to biodiversity. There is also a trend toward increased private land biodiversity conservation (DEWHA, 2009), such as the Australian Wildlife Conservancy (see Section 20.5). Policy tools that could be used to promote natural resource management and biodiversity conservation in Australia are summarised in Table 19.6.

The Australian Biodiversity Conservation Strategy (ABCS) 2010–2030 (CoA, 2014) identified ten national targets based on the CBD Strategic Plan for Biodiversity 2011–2020 template (see Table 19.7). Progress on the Aichi targets from 2014 to 2018 is reviewed in CoA (2020). The Australian national strategy was updated in 2019 as *Australia's Strategy for Nature 2019–2030* (DAWE, 2020b) to coordinate other federal, state, and territory initiatives in this area, in both the public and private sectors. This strategy includes a dedicated website listing relevant projects, Australia's Nature Hub (see Section 19.6), and rests on three priorities:

- connect all Australians with nature;
- care for nature in all its diversity; and
- share and build knowledge (DAWE, 2020b).

In parallel, the Global Strategy for Plant Conservation (GSPC; also managed by CBD) includes 16 global targets for 2020 (CBD, 2020c). ABCS targets 1, 2, 4, 5, 6 and 7 relate to the GSPC.

Table 19.6 Policy tools

Tool	Options	Example
Suasion	Education	Information to landholders
	Promotion of best practice	Extension programs
	Grants	Community assets
Regulation	Restrictions	Land use planning, compliance monitoring
	Taxes	Carbon tax
Market-based	Pricing	EcoTenders, rebates, LGA rates, revolving funds,
	Quantity regulation	Cap and trade schemes, offsets
	Market friction	Environmental labelling, eco certification

Source: DEWHA (2010)

Under the NSW Biodiversity and Conservation Act 2016, state-wide biodiversity is being assessed using a suite of indicators 'to measure different aspects of biodiversity and ecological integrity' as part of the Biodiversity Indicator program (DPIE, 2020a). The NSW Environmental Monitoring and Assessment and Reporting (eMAR) Framework is used with the RPSB framework as the basis for selecting indicators and grouping them into functional themes (Sparks *et al.*, 2011; see Figure 19.2 and Table 19.8). For terrestrial species and ecosystems, biodiversity indicators are mostly derived from EO datasets and environmental models (OEH and CSIRO, 2019) and supported by *in situ* and related data (such as NSW BioNet; see Section 19.6). The first assessment from this program concluded that in 2013 relative to the reference year of 1750:

- 79–91% of the original, within-species, plant genetic diversity still existed;
- the original habitat effectiveness for supporting native species had reduced to one third; and
- half of the species rated as 'threatened' were likely to be extinct in another century without effective management (DPIE, 2020b).

To retain existing biodiversity within the Australian landscape, several state governments have legislated to limit the area of land that can be cleared of native vegetation. Compliance monitoring for such legislation now relies on EO datasets (see Volume 2D—Section 14.2.2). One operational system for detecting changes in woody vegetation is the Statewide Landcover and Trees Study (SLATS; see Section 9.1 and Volume 2D—Excursus 14.3). An EO-based, hierarchical framework for monitoring biodiversity in rangelands is described in Section 15.5 (Eyre *et al.* 2011; see Excursus 15.2), and floral and faunal components of forest diversity are considered in Section 16.7.

Other approaches for assessing vegetation condition compare current vegetation characteristics with a benchmark representing a mature and long undisturbed state. The benchmark that has been adopted for Australia is the estimated condition of vegetation in 1750, prior to European settlement and industrialisation (see Section 3.1.1). One benchmark-based method that assesses 'vegetation quality' using EO datasets is the Victorian model of Vegetation Quality Assessment (VQA; formerly known as Habitat Hectares), which is described in Excursus 19.2.

Table 19.7 Australian Biodiversity Conservation Strategy 2010–2030 Targets

ABCS Target Number	Target for 2015	Maps to Aichi Targets
1	Achieve a 25% increase in the number of Australians and public and private organisations who participate in biodiversity conservation activities	1, 2, 4, 17
2	Achieve a 25% increase in employment and participation of Indigenous peoples in biodiversity conservation	2, 14, 18
3	Achieve a doubling of the value of complementary markets for ecosystem service	3
4	Achieve a national increase of 600,000 km ² of native habitat managed primarily for biodiversity conservation across terrestrial, aquatic, and marine environments	5, 7, 11
5	1,000 km ² of fragmented landscapes and aquatic systems are being restored to improve ecological connectivity	5, 7, 11, 14, 15
6	Four collaborative continental scale linkages are established and managed to improve ecological connectivity	5, 11, 14, 15
7	Reduce by at least 10% the impacts of invasive species on threatened species and ecological communities in terrestrial, aquatic, and marine environments	9, 10, 12
8	Nationally agreed science and knowledge priorities for biodiversity conservation are guiding research activities	18, 19
9	All jurisdictions will review relevant legislation, policies and programs to maximise alignment with Australia's Biodiversity Conservation Strategy	2, 4, 17
10	Establish a national long term biodiversity monitoring and reporting system	2, 19

Source: CoA (2014)

Table 19.8 NSW Biodiversity Indicator Program

Tool	Theme	Indicator family
Biodiversity	Expected survival of biodiversity	Listed threatened species and ecological communities
		All known and undiscovered species
	State of biodiversity	All known species
		State of biodiversity including undiscovered species
Ecological integrity	Ecosystem quality	Habitat condition
		Pressures
	Ecosystem management	Management responses
		Management effectiveness
		Capacity to sustain ecosystem quality
	Ecosystem integrity	Capacity to retain biological diversity
		Capacity to retain ecological functions

Source: OEH and CSIRO (2019)

The Habitat Condition Assessment System (HCAS) is being developed to provide a nationally consistent coverage of biodiversity habitat condition in Australia (Donohue *et al.*, 2013; Harwood *et al.*, 2016), where habitat condition is defined as “the condition of terrestrial areas in terms of their predicted capacity to support the wildlife expected there under natural conditions” (CSIRO, 2019). This system combines EO and environmental datasets with reference site data and spatial ecological modelling to estimate habitat condition at 250 m resolution across terrestrial Australia.

Many of the mechanisms and symptoms of species vulnerability are relevant to ecosystems, because species are integral parts of ecosystems. Yet ecosystems embody processes and higher-order components of biodiversity that are difficult or impossible to account for in species-by-species assessment. Whereas species risk assessment rests on population theory, ecosystem risk assessment must draw from a wider array of inter-related theories that deal with continua, niches, fractal geometry, succession, resilience, ecological integrity, biodiversity-ecosystem function and insurance, as well as population theory. The success of ecosystem risk assessment therefore rests on a robust synthesis of conservation planning and process ecology to translate theoretical foundations into a practical assessment protocol that can be applied to a wide variety of ecosystems by specialist assessors with differing backgrounds and limited data.

(Keith *et al.*, 2013)

Excursus 19.2—Vegetation Quality Assessment

Source: Parkes *et al.* (2003), DELWP (2017)

Further Information: DSE (2004): https://www.environment.vic.gov.au/_data/assets/pdf_file/0016/91150/Vegetation-Quality-Assessment-Manual-Version-1.3.pdf

To effectively manage native vegetation, information is needed about the:

- vegetation type;
- previous and current ecological processes that shape that vegetation type;
- function of that vegetation type in the local landscape; and
- effectiveness of that function (Parkes *et al.*, 2003).

The Vegetation Quality Assessment (VQA; formerly Habitat Hectares) method has been used across Victoria for over a decade. VQA determines the condition of current vegetation by comparing the existing vegetation features with those of a defined bioregional benchmark that represents “the *average characteristics* of a mature and apparently long-undisturbed stand of the *same* community type” (Parkes *et al.*, 2003). Design characteristics of this method include consistency, objectivity, simplicity, and efficiency across a wide range of vegetation communities. Results from this method also need to be easily communicated to land owners.

Vegetation mapping in Victoria delineates 28 bioregions—landscape scale categories comparable to ecoregions (see Section 2.4). Vegetation characteristics are represented by Ecological Vegetation Classes (EVC), a hierarchical classification that aggregates floristic communities (“defined by a combination of floristics, life form, position in landscape and an inferred fidelity to a particular environment”; DSE, 2004). For VQA, benchmarks relate to a single EVC in one bioregion. Details of field assessment for this method are provided in DSE (2004).

The final score derived for a site combines assessment of ‘site condition’ (largely determined by field work) and ‘landscape context’ (best calculated using GIS) components (see Table 19.9). The final habitat score is the sum of all scores from each site converted from a percent to a decimal, while the final Habitat Hectare score is the product of the decimal habitat score (quality) and the area of vegetation (quantity).

Given the broad categories defined by VQA, this method is not used to quantify change over time. However, the information from 17,000 VQA sites has been extrapolated using EO and other spatial datasets to create a regional scale map showing the condition of native vegetation across Victoria (DSE, 2004; DELWP, 2017).

Table 19.9 VQA scoring

Criteria	Component	Score
Site Condition (derived from field assessment)	Large trees	10
	Tree canopy cover	5
	Understorey	25
	Lack of weeds	15
	Recruitment	10
	Organic litter	5
	Logs	5
Landscape Context (derived from spatial datasets)	Patch size	10
	Neighbourhood	10
	Distance to core area	5
	Total	100

Source: DSE (2004)

*Essentially, this method (‘habitat hectares’) attempts to assess how ‘natural’ a site is by comparing it to the same vegetation type in the absence of major ecosystem changes that have occurred following European settlement of Australia.
(Parkes *et al.*, 2003)*

19.6 Further Information

IUCN Red Lists

IUCN Red List of Threatened Species: <https://www.iucnredlist.org/>

IUCN Red List of Ecosystems: <https://www.iucn.org/theme/ecosystem-management/our-work/red-list-ecosystems>

IUCN-CEM (2016)

IUCN-CEM Research and development: <https://iucnrle.org/resources/research-development/>

Australian Biodiversity Policies and Programs

Review of the EPBC Act: <https://epbcactreview.environment.gov.au/>

National Environmental Science Program: <https://www.environment.gov.au/science/nesp/about>

Biodiversity Information for Australia

Australia's Nature Hub: <https://www.australiasnaturehub.gov.au/>

Department of Agriculture, Water and the Environment: <http://www.environment.gov.au/biodiversity>

Collaborative Australian Protected Area Database: <http://www.environment.gov.au/land/nrs/science/capad>

Common Assessment Method: <https://www.environment.gov.au/biodiversity/threatened/cam>

Australia State of the Environment 2016: <https://soe.environment.gov.au/>

Australia State of the Environment 2016—Biodiversity: <https://soe.environment.gov.au/sites/default/files/soe2016-biodiversity-launch-version2-24feb17.pdf?v=1488792935>

Australian Biological Resources Study: <https://www.environment.gov.au/science/abrs>

Australia's State of the Forest report: <http://www.agriculture.gov.au/abares/forestsaustralia/sofr/sofr-2018>

Atlas of Living Australia: <https://www.ala.org.au/>

Australasian Virtual Herbarium: <https://avh.chah.org.au/>

Terrestrial Ecosystem Research Network (TERN): <https://www.tern.org.au/>

LTERN: <https://www.ltern.org.au/>

Australian Wildlife Conservancy: <https://www.australianwildlife.org/>

Operational Biodiversity Monitoring

New South Wales:

BioNet: <https://www.environment.nsw.gov.au/topics/animals-and-plants/biodiversity/biodiversity-indicator-program>

Victoria:

Habitat Condition Assessment System (HCAS): CSIRO (2019)

<https://research.csiro.au/biodiversity-knowledge/projects/hcas/>

Global Biodiversity

Intergovernmental Panel on Biodiversity and Ecosystem Services: <https://ipbes.net/>

Aichi Targets: www.cbd.int/sp/targets

Sustainable Development Goals: <https://sustainabledevelopment.un.org>

Global Footprint Network: <https://www.footprintnetwork.org/>

Global ecosystems: <https://rmgsc.cr.usgs.gov/outgoing/ecosystems/Global/>

Biodiversity Indicators

European Academies' Science Advisory Council: https://royalsociety.org/~media/royal_society_content/policy/publications/2005/9667.pdf

Nature Serve: <https://www.natureserve.org/biodiversity-science/conservation-topics/biodiversity-indicators#:~:text=Biodiversity%20indicators%20help%20us%20measure,as%20the%20protection%20of%20important>

Ecosystem Assessment

Global Ecosystem and Environment Observation Analysis Research Cooperation (GEOARC): <https://www.earthobservations.org/activity.php?id=144>

ECOPOTENTIAL Project: a large, European-funded H2020 project, focusing on a targeted set of internationally recognised Protected Areas in Europe, European Territories and beyond, and addressing crossscale ecological interactions and landscape-ecosystem dynamics at regional to continental scales, as well as long term and large scale environmental and ecological challenges: <https://www.ecopotential-project.eu/>

EC CORDIS Ecopotential Project: <https://cordis.europa.eu/article/id/254154-earth-observation-data-for-ecosystem-monitoring>

19.7 References

- Accad, A., and Neldner, V.J. (2015). *Remnant Regional Ecosystem Vegetation in Queensland, Analysis 1997–2013*. Queensland Department of Science, Information Technology and Innovation, Brisbane.
- Auld, T.D., and Leishman, M.R. (2015). Ecosystem risk assessment for Gnarled Mossy Cloud Forest, Lord Howe Island, Australia. *Austral Ecology*, 40, 364–372.
- BIP (2010). *Biodiversity indicators and the 2010 Target: Experiences and lessons learnt from the 2010 Biodiversity Indicators Partnership*. Secretariat of the Convention on Biological Diversity, Montréal, Canada. Technical Series No. 53, 196 p.
- BIP (2019). *List of global indicators available for review* webpage, Biodiversity Indicators Partnership website: <https://www.bipindicators.net/list-of-global-indicators-available-for-review>
- Bland, L.M., Keith, D.A., Miller, R.M., Murray, N.J., and Rodríguez, J.P. (Eds.) (2016). *Guidelines for the application of IUCN Red List of Ecosystems Categories and Criteria, Version 1.0*. IUCN, Switzerland. ISBN: 978-2-8317-1769-2
- Bland, L.M., Nicholson, E., Miller, R.M., Andrade, A., Etter, A., Ferrer-Paris, J.R., Kontula, T., Lindgaard, A., Pliscoff, P., Skowno, A., Zager, I., and Keith, D.A. (2018). Impacts of the IUCN Red List of Ecosystems on Conservation Policy and Practice. *Preprints*, 2018120097. doi:10.20944/preprints201812.0097.v1
- Böhringer, C., and Jochem, P.E.P. (2007). Measuring the immeasurable—A survey of sustainability indices. *Ecological Economics*, 63, 1–8.
- Burns, E.L., Lindenmayer, D.B., Stein, J., Blanchard, W., McBurney, L., Blair, D., and Banks, S.C. (2015). Ecosystem assessment of mountain ash forest in the Central Highlands of Victoria, south-eastern Australia. *Austral Ecology*, 40, 386–399.
- CBD (2010). The strategic plan for biodiversity 2011–2020 and the Aichi Biodiversity Targets, decision X/2. In *10th Conference of the Parties, Convention on Biological Diversity*. Montreal, Canada. 13 p.
- CBD (2020a). The Convention on Biological Diversity website: <https://www.cbd.int/convention/>
- CBD (2020b). *Strategic Plan for Biodiversity 2011–2020, including Aichi Biodiversity Targets* webpage, Convention on Biological Diversity website: <https://www.cbd.int/sp/>
- CBD (2020c). *Global Strategy for Plant Conservation* webpage, Convention on Biological Diversity website: <https://www.cbd.int/gspc/>
- CoA (2014). *Australia's Fifth National Report to the Convention on Biological Diversity*. Commonwealth of Australia, Canberra. <https://www.cbd.int/doc/world/au/au-nr-05-en.pdf>
- CoA (2020). *Australia's Sixth National Report to the Convention on Biological Diversity 2014–2018*. Commonwealth of Australia, Canberra. <https://www.cbd.int/doc/nr/nr-06/au-nr-06-en.pdf>
- CSIRO (2019). *The Habitat Condition Assessment System (HCAS). Progress update for stakeholders: June 2019*. CSIRO Land and Water: <https://research.csiro.au/biodiversity-knowledge/wp-content/uploads/sites/69/2019/07/BKP-2HCAS-Factsheet-20190627.pdf>
- DAWE (2020a). *Environment Protection and Biodiversity Conservation Act 1999 (EPBC Act)* webpage, Department of Agriculture, Water and Environment website: <https://www.environment.gov.au/epbc>
- DAWE (2020b). *Australia's Strategy for Nature*. Department of Agriculture, Water and the Environment, Canberra. https://naturehub.govcms.gov.au/sites/default/files/2019-11/Australia_s_Strategy_for_Nature_%20web.pdf
- DELWP (2017). *Biodiversity information explanatory document*. Victorian Department of Environment, Land, Water and Planning, Melbourne.
- DEWHA (2009). *Assessment of Australia's Terrestrial Biodiversity 2008*. Report prepared by the Biodiversity Assessment Working Group of the National Land and Water Resources Audit for the Australian Government, Canberra.
- DEWHA (2010). *Ecosystem Services: Key Concepts and Applications*. Occasional Paper No 1, Department of the Environment, Water, Heritage and the Arts, Canberra. ISBN 978-1-76047-341-9
- Donohue, R.J., Harwood, T.D., Williams, K.J., Ferrier, S., and McVicar, T.R. (2013). *Estimating habitat condition using time series remote sensing and ecological survey data*. CSIRO Earth Observation and Informatics Transformational Capability Platform Client Report EP1311716, CSIRO, Australia. 44 p. <https://publications.csiro.au/rpr/pub?pid=csiro:EP1311716>
- DPIE (2020a). *A Biodiversity Indicator Program for NSW* webpage, NSW Department of Planning, Industry and Environment website: <https://www.environment.nsw.gov.au/topics/animals-and-plants/biodiversity/biodiversity-indicator-program>

- DPIE (2020b). *NSW Biodiversity Outlook Report. Results from the Biodiversity Indicator Program: First assessment*. Department of Planning, Industry and Environment, Sydney. 77p. <https://www.environment.nsw.gov.au/-/media/OEH/Corporate-Site/Documents/Animals-and-plants/Biodiversity/Biodiversity-Indicator-Program/biodiversity-outlook-report-first-assessment-200621.pdf>
- DSE (2004). *Vegetation Quality Assessment Manual—Guidelines for applying the habitat hectares scoring method. Version 1.3*. Victorian Government Department of Sustainability and Environment, Melbourne.
- EASAC (2004). *A users' guide to biodiversity indicators*. European Academies' Science Advisory Council, 29 November 2004. https://royalsocietypublishing.org/~media/royal_society_content/policy/publications/2005/9667.pdf
- Eyre, T.J., Fisher, A., Hunt, L.P., and Kutt, A.S. (2011). Measure it to better manage it: a biodiversity monitoring framework for the Australian rangelands. *The Rangeland Journal*, 33, 239–253.
- GEOBON (2020). *The Groups on Earth Observations Biological Observation Network website*: <https://geobon.org/>
- Gillespie, T.W., Foody, G.M., Rocchini, D., Giorgi, A.P., and Saatchi, S. (2008). Measuring and modelling biodiversity from space. *Progress in Physical Geography*, 32(2), 203–221. doi:10.1177/0309133308093606.
- Harwood, T.D., Donohue, R.J., Williams, K.J., Ferrier, S., McVicar, T.R., Newell, G., and White, M. (2016). Habitat Condition Assessment System: A new way to assess the condition of natural habitats for terrestrial biodiversity across whole regions using remote sensing data. *Methods in Ecology and Evolution*, 7(9), 1050–1059. doi:10.1111/2041-210X.12579.
- IUCN (2020a). *Protected Area Categories* webpage, International Union for Conservation of Nature website: <https://www.iucn.org/theme/protected-areas/about/protected-area-categories>
- IUCN (2020b). *Background and History* webpage for IUCN Red List of Threatened Species. International Union for Conservation of Nature website: <https://www.iucnredlist.org/about/background-history>
- IUCN (2020c). *Summary Statistics* webpage for IUCN Red List of Threatened Species. International Union for Conservation of Nature website: <https://www.iucnredlist.org/resources/summary-statistics#Figure%202>
- Jetz, W., McGeoch, M.A., Guralnick, R., Ferrier, S., Beck, J., Costello, M.J., Fernandez, M., Geller, G.N., Keil, P., Merow, C., Meyer, C., Muller-Karger, F.E., Pereira, H.M., Regan, E.C., Schmeller, D.S., and Turak, E. (2019). Essential biodiversity variables for mapping and monitoring species populations. *Nature Ecology and Evolution*, 3, 539–551. <https://doi.org/10.1038/s41559-019-0826-1>
- Keith (2015). Assessing and managing risks to ecosystem biodiversity. *Austral Ecology*, 40, 337–346.
- Keith, D.A., Rodríguez, J.P., Rodríguez-Clark, K.M., Nicholson, E., Aapala, K., Alonso, A., Asmussen, M., Bachman, S., Basset, A., Barrow, E.G., Benson, J.S., Bishop, M.J., Bonifacio, R., Brooks, T.M., Burgman, M.A., Comer, P., Comín, F.A., Essl, F., Faber-Langendoen, D., Fairweather, P.G., Holdaway, R.J., Jennings, M., Kingsford, R.T., Lester, R.E., Nally, R. Mac, McCarthy, M.A., Moat, J., Oliveira-Miranda, M.A., Pisanu, P., Poulin, B., Regan, T.J., Riecken, U., Spalding, M.D., and Zambrano-Martínez, S. (2013). Scientific Foundations for an IUCN Red List of Ecosystems. *PLoS ONE*, 8(5), e62111. doi:10.1371/journal.pone.0062111
- Keith, D.A., Rodríguez, J.P., Brooks, T.M., Burgman, M.A., Barrow, E.G., Bland, L., Comer, P.J., Franklin, J., Link, J., McCarthy, M.A., Miller, R.M., Murray, N.J., Nel, J., Nicholson, E., Oliveira-Miranda, M.A., Regan, T.J., Rodríguez-Clark, K.M., Rouget, M., and Spalding, M.D. (2015). The IUCN Red List of Ecosystems: Motivations, Challenges, and Applications. *Conservation Letters*, 8, 214–226.
- IPBES (2019). *Global assessment report on biodiversity and ecosystem services of the Intergovernmental Science-Policy Platform on Biodiversity and Ecosystem Services*. (Eds: E.S. Brondizio, J. Settele, S. Díaz, and H. T. Ngo). Intergovernmental Panel on Biodiversity and Ecosystem Services secretariat, Bonn, Germany. <https://ipbes.net/global-assessment>
- IUCN-CEM (2016). *The IUCN Red List of Ecosystems. Version 2016-1*. <https://iucnrl.org/>
- IUCN-CEM (2020). *Global Context* webpage for IUCN Red List of Ecosystem. International Union for Conservation of Nature Commission on Ecosystem Management website: <https://iucnrl.org/about-rle/context/>
- Masó, J., Serral, I., Domingo-Marimon, C., and Zabala, A. (2020). Earth observations for sustainable development goals monitoring based on essential variables and driver-pressure-state-impact-response indicators. *International Journal of Digital Earth*, 13(2), 217–235. <https://doi.org/10.1080/17538947.2019.1576787>

- Metcalfe, D.J., and Lawson, T.J. (2015). Coastal lowland rainforests of the Wet Tropics bioregion, Queensland, Australia. *Austral Ecology*, 40, 373–385.
- Murray, N.J., Keith, D.A., Bland, L.M., Ferrari, R., Lyons, M.B., Lucas, R., Pettorelli, N., Nicholson, E. (2018a). The role of satellite remote sensing in structured ecosystem risk assessments. *Science of the Total Environment*, 619–620, 249–257. <https://doi.org/10.1016/j.scitotenv.2017.11.034>
- Murray, N.J., Keith, D.A., Simpson, D., Wilshire, J.H., Lucas, R.M. (2018b). Remap: An online remote sensing application for land cover classification and monitoring. *Methods in Ecology and Evolution*, 1–9. <https://doi.org/10.1111/2041-210X.13043>
- Neldner, J. (2018). *The Impacts of Land Use Change on Biodiversity in Australia. Ch 8 in in Land Use in Australia: Past, Present and Future.* (Ed: Thackway, R.). ANU eVIEW, Canberra. ISBN: 9781921934421
- Neldner, V.J., Niehus, R.E., Wilson, B.A., McDonald, W.J.F., Ford, A.J., and Accad, A. (2017). *The Vegetation of Queensland. Descriptions of Broad Vegetation Groups. Version 3.0.* Queensland Herbarium, Department of Science, Information Technology and Innovation, Brisbane. publications.qld.gov.au/dataset/redd/resource/78209e74-c7f2-4589-90c1-c33188359086
- Nicholson, E., Regan, T.J., Auld, T.D., Burns, E.L., Chisholm, L.A., English, V., Harris, S., Harrison, P., Kingsford, R.T., Leishman, M.R., Metcalfe, D.J., Pisanu, P., Watson, C.J., White, M., White, M.D., Williams, R.J., Wilson, B., Keith, D.A. (2015). Towards consistency, rigour and compatibility of risk assessments for ecosystems and ecological communities. *Austral Ecology*, 40, 347–363. <https://doi.org/10.1111/aec.12148>.
- NRM (2019). *Biosecurity* webpage, NRM Regions Australia website: <http://nrmregionsaustralia.com.au/biosecurity/>
- OECD (2020). *Biodiversity indicators, valuation and assessments* webpage, Organisation for Economic Co-operation and Development website: <http://www.oecd.org/environment/resources/biodiversity-indicators-valuation-and-assessments.htm>
- OEH and CSIRO (2019). *Measuring Biodiversity and Ecological Integrity in New South Wales: Method for the Biodiversity Indicator Program.* Office of Environment and Heritage NSW and Commonwealth Scientific and Industrial Research Organisation, NSW Government, Sydney.
- Parkes, D., Newell, G., and Cheal, D. (2003). Assessing the quality of native vegetation: The ‘habitat hectares’ approach. *Ecological Management and Restoration*, 4, S29–S38.
- Parrish, J.D., Braun, D.P., and Unnasch, R.S. (2003). Are We Conserving What We Say We Are? Measuring Ecological Integrity within Protected Areas. *BioScience*, 53(9), 851–860. [https://doi.org/10.1641/0006-3568\(2003\)053\[0851:AWCWWS\]2.0.CO;2](https://doi.org/10.1641/0006-3568(2003)053[0851:AWCWWS]2.0.CO;2)
- Pereira, H.M., Navarro, L.M., and Martins, I.S. (2012). Global Biodiversity Change: The Bad, the Good, and the Unknown. *Annual Review of Environmental Resources*, 37, 25–50. <https://www.annualreviews.org/doi/pdf/10.1146/annurev-environ-042911-093511>
- Pisanu P., Kingsford R.T., Wilson B., and Bonifacio R. (2015). Status of connected wetlands of the Lake Eyre Basin, Australia. *Austral Ecology*, 40, 460–71. <https://doi.org/10.1111/aec.12203>
- Pope Francis (2015). *Laudato Si’: On Care for Our Common Home.* Catholic Truth Society, London.
- remap (2020). *remap: Enabling large-scale ecosystem mapping and assessment* website: <https://remap-app.org>
- Rodríguez, J.P., Keith, D.A., Rodríguez-Clark, K.M., Murray, N.J., Nicholson, E., Regan, T.J., Miller, R.M., Barrow, E., Bland, L.M., Boe, K., Brooks, T.M., Oliveira-Miranda, M.A., Spalding, M., and Wit, P. (2015). A practical guide to the application of the IUCN Red List of Ecosystems criteria. *Philosophical Transactions B*, 370, 2014003. <http://dx.doi.org/10.1098/rstb.2014.0003>
- Rose, R.A., Byler, D., Eastman, J.R., Fleishman, E., Geller, G., Goetz, S., Guild, L., Hamilton, H., Hansen, M., Headley, R., Hewson, J., Horning, N., Kaplin, B.A., Laporte, N., Leidner, A., Leimgruber, P., Morissette, J., Musinsky, J., Pintea, L., Prados, A., Radeloff, V.C., Rowen, M., Saatchi, S., Schill, S., Tabor, K., Turner, W., Vodacek, A., Vogelmann, J., Wegmann, M., Wilkie, D., and Wilson, C. (2014). Ten ways remote sensing can contribute to conservation. *Conservation Biology*, 29(2), 350–359. doi:10.1111/cobi.12397.
- Sayre, R., Karagulle, D., Frye, C., Boucher, T., Wolff, N.H., Breyer, S., Wright, D., Martin, M., Butler, K., Van Graafeiland, K., Touval, J., Sotomayor, L., McGowan, J., Game, E.T., and Possingham, H. (2020). An assessment of the representation of ecosystems in global protected areas using new maps of World Climate Regions and World Ecosystems. *Global Ecology and Conservation*, 21, e00860. <https://doi.org/10.1016/j.gecco.2019.e00860>
- Seabrook, L., McAlpine, C., and Fensham, R. (2006). Cattle, crops and clearing: Regional drivers of landscape change in the Brigalow Belt, Queensland, Australia, 1840–2004. *Landscape and Urban Planning*, 78, 373–385. doi.org/10.1016/j.landurbplan.2005.11.007

- SoE (2018). *State of the Environment 2018*. Commissioner for Environmental Sustainability Victoria. <https://www.ces.vic.gov.au/reports/state-environment-2018>
- Sparks, T.H., Butchart, S.H.M., Balmford, A., Bennun, L., Stanwell-Smith, D., Walpole, M., Bates, N.R., Bomhard, B., Buchanan, G.M., Chenery, A.M., Collen, B., Csirke, J., Diaz, R.J., Dulvy, N.K., Fitzgerald, C., Kapos, V., Mayaux, P., Tierney, M., Waycott, M., Wood, L., and Green, R.E. (2011). Linked indicator sets for addressing biodiversity loss. *Oryx*, 45(03), 411–419. doi:10.1017/S003060531100024X.
- Tansley, A.G. (1935). The use and abuse of vegetational concepts and terms. *Ecology*, 16, 284–307.
- Teillard, F., Anton, A., Dumont, B., Finn, J.A., Henry, B., Souza, D.M., Manzano P., Milà i Canals, L., Phelps, C., Said, M., Vijn, S., White, S. (2016). *A review of indicators and methods to assess biodiversity—Application to livestock production at global scale*. Livestock Environmental Assessment and Performance (LEAP) Partnership. FAO, Rome, Italy.
- Thackway, R., and Lesslie, R. (2006). Reporting vegetation condition using the Vegetation Assets, States, and Transitions (VAST) framework. *Ecological Management and Restoration*, 7(1), 53–62.
- Tozer, M.G., Leishman, M.R., and Auld, T.D. (2015). Ecosystem risk assessment for Cumberland Plain Woodland, New South Wales, Australia. *Austral Ecology*, 40, 400–410.
- UN General Assembly (2012) *The future we want*. Resolution adopted by the United Nations (UN) General Assembly on 27 July 2012 (RES/66/288).
- Walters, M., and Scholes, R.J. (2017). *The GEO Handbook on Biodiversity Observation Networks*. Springer, ChamoniX.
- Wardle, G.M., Greenville, A.C., Frank, A.S.K., Tischler, M., Emery, N.J., and Dickman, C.R. (2015). Ecosystem risk assessment of Georgina gidgee woodlands in central Australia (Qld, NT, SA). *Austral Ecology*, 40, 444–459.
- Williams, R.J., Wahren, C.-H., Stott, K.A.J., Camac, J.S., White, M., Burns, E., Harris, S., Nash, M., Morgan, J.W., Venn, S., Papst, W.A., and Hoffmann, A.A. (2015). An IUCN red list ecosystems risk assessment for alpine snow patch herbfields, south-eastern Australia. *Austral Ecology*, 40, 433–443.
- WWF (1998). *Living Planet Report 1998*. World Wildlife Fund.

Ecological culture cannot be reduced to a series of urgent and partial responses to the immediate problems of pollution, environmental decay and the depletion of natural resources. There needs to be a distinctive way of looking at things, a way of thinking, policies, an educational resistance to the assault of the technocratic paradigm. Otherwise, even the best ecological initiatives can find themselves caught up in the same globalised logic. To seek only a technical remedy to each environmental problem which comes up is to separate what is in reality interconnected and to mask the true and deepest problem of the global system.

(Pope Francis, 2015)



20 Sustainability

Sustainability of natural resources implies a balance between their consumption and production. Various trends in the management of natural resources can be observed in recent decades, with the focus moving from ‘productivity’ to ‘conservation’ to ‘sustainability’ to ‘resilience’ over time. Each of these focal points requires consideration when managing natural resources and each requires appropriate environmental indicators to objectively assess and monitor changes in the landscape. Whether one focus is given priority over another is largely a philosophical, if not political, decision. For example, attributes of three different natural resource management models are summarised in Table 20.1. While this specific example applies to rangeland environments, the succession of models from left to right reflects the increasing awareness of ecosystem values in land management in recent decades.

Throughout recorded history, societal attitudes to nature have influenced the management of natural resources. An anthropocentric worldview characterises most ancient, medieval, and modern cultural beliefs, as stated by a wide range of authors, including:

- Xenophon—“the gods have provided everything carefully for the benefit of man”;
- Aristotle—“Nature has made all animals for the sake of man”;
- Genesis—“be fruitful and multiply and replenish the earth and subdue it”;
- Calvin—God “created all things for man’s sake”; and
- Bacon—“the world is made for man, not man for the world”.

Development of the scientific method in the seventeenth century was used to justify these beliefs, with the reductionist approach being applied to nature:

- Descartes—“I do not recognise any difference between the machines made by craftsmen and the various bodies that nature alone composes”; and carried into economics
- Carey—“the earth is a great machine, given to man to be fashioned to his purpose”.

The Darwinism view of ‘survival of the fittest’ reinforced the outlook of humans struggling against nature to survive and control it. Freud wrote of the human need of “taking up the attack on nature, thus forcing it to obey human will, under the guise of science”.

In addition to an anthropogenic worldview, in recent centuries the notion of ‘progress’ has emerged, which envisions science and technology continually improving the productivity of nature and increasing human potential. This perspective, however, is in stark contrast with ancient and medieval beliefs, which tended to view history either as an undirected sequence, or as a process of steady decay from a ‘golden age’ or ‘paradise’ (Ponting, 1991).

The Australian government’s budget for expenditure in 2018–19 was \$488.6 billion. The environmental portfolio stands to receive about \$1.5 billion—about one third of 1% of what we as Australians spend our money on. Is this an accurate representation of how much we value the environment?
(Pollock, 2019)

Table 20.1 Comparison of natural resource management models

Attribute	Management model		
	Steady-state	Ecosystem	Resilience-based
Ecological models	Succession-retrogression	State-and-transition rangeland health	Multiple social-ecological systems/ novel ecosystems
Reference condition	Historic climax plant community	Historic climax plant community, including historical range of variation	Landscapes with maximum options for ecosystem services
Role of humans	Use ecosystems	Part of ecosystems	Direct trajectories of ecosystem change
Ecosystem services	Meat and fibre products	Several ecosystem services	Options for diverse ecosystem services
Management goals	Sustain maximum yield of commodities	Sustain multiple uses	Sustain capacity of social-ecological systems to support human wellbeing
Science-management linkages	Top-down from management agencies	Top-down from management agencies	Multi-scaled social learning institutions
Knowledge systems	Management experience and agricultural experiments	Multidisciplinary science and ecological experiments	Collaborative groups, spatially reference, updatable databases

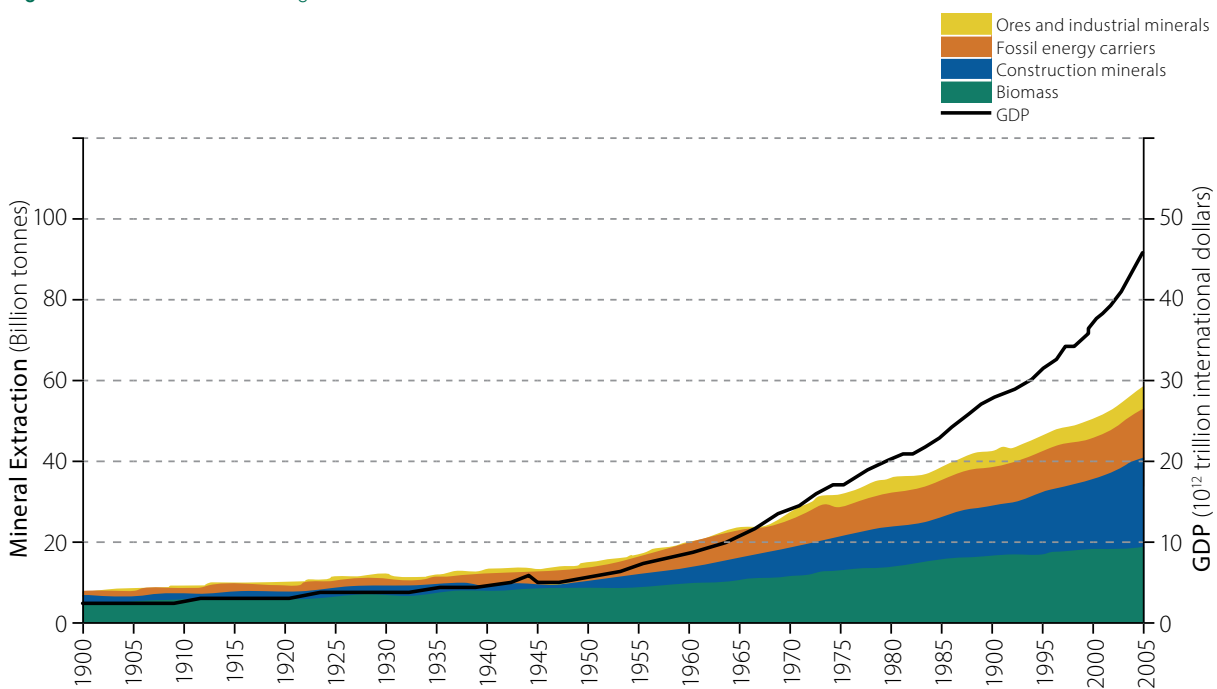
Source: Bestelmeyer and Briske (2012) Table 2

While we are now reaching the limit of our global natural resources, the rate of material extraction continues to accelerate (see Figure 20.1). Clearly it is time to consider more broadly the sustainable role of humankind on Earth and how our resources should be managed into the future. In practical terms at a local scale, better natural resource management decisions are made when managers understand the problem, have the motivation to adopt a changed practice, and have the capacity to implement it (Gordon *et al.*, 2001). Such decisions necessitate the involvement of land custodians and experienced

scientists who understand the landscape firsthand, and can objectively track its processes, productivity, and vulnerabilities over time.

Below we consider aspects of sustainability in Australia in Section 20.1 and suitable EO sensors for observing sustainability in Section 20.2. Assessment of ecosystem services is introduced in Section 20.3, the conundrum of sustainable development is reviewed in the context of EO in Section 20.4, then EO-based environmental-economic accounting is described in Section 20.5.

Figure 20.1 Global GDP versus global material extraction 1900 to 2005



Source: WGCS (2016) Figure 1 (based on Krausmann *et al.*, 2009)

20.1 Sustainability in Australia

We like to think that the terrestrial landscape is both sustainable and resilient, but is that really the case? This section considers how EO is being used to assess sustainability in Australian landscapes.

Australian jurisdictions have generated an impressive array of environmental legislation and policies in recent decades. While there is a growing trend to ‘restructure’, ‘consolidate’, and ‘streamline’ their implementation, especially within politically expedient timeframes, are these changes achieving their intended goals of better management of natural resources?

Logically, in the absence of vested interests and predetermined ideologies, environmental policy is founded objectively on a well-established, scientific understanding of the environment. Such understanding should be derived from data that is appropriate and calibrated, and analysed using methods that are validated, consistent and repeatable (see Volume 2). The driver here is science, which is used to shape and inform policy. Once policy becomes widely accepted however, there is a tendency for policy to drive science, which clearly defeats the assumption of objectivity.

An accounting approach based on relevant economic, environmental, and social datasets, which are consistent through space and time, can be used to derive objective indicators to shape policy. A common base of data, accounts, and indicators will also ensure compatibility between policies and their implementation across jurisdictions and geographic regions. By linking socio-economic and environmental datasets, policy makers can:

- analyse both the impact of economic policies on the environment and the impact of environmental policies on the economy;
- use a quantitative basis for policy design;
- identify socio-economic drivers, pressures, and responses that will impact the environment;
- define environmental regulations and resource management strategies with greater precision; and
- establish integrated indicators for the relationships between the environment and the economy (DEWHA, 2010).

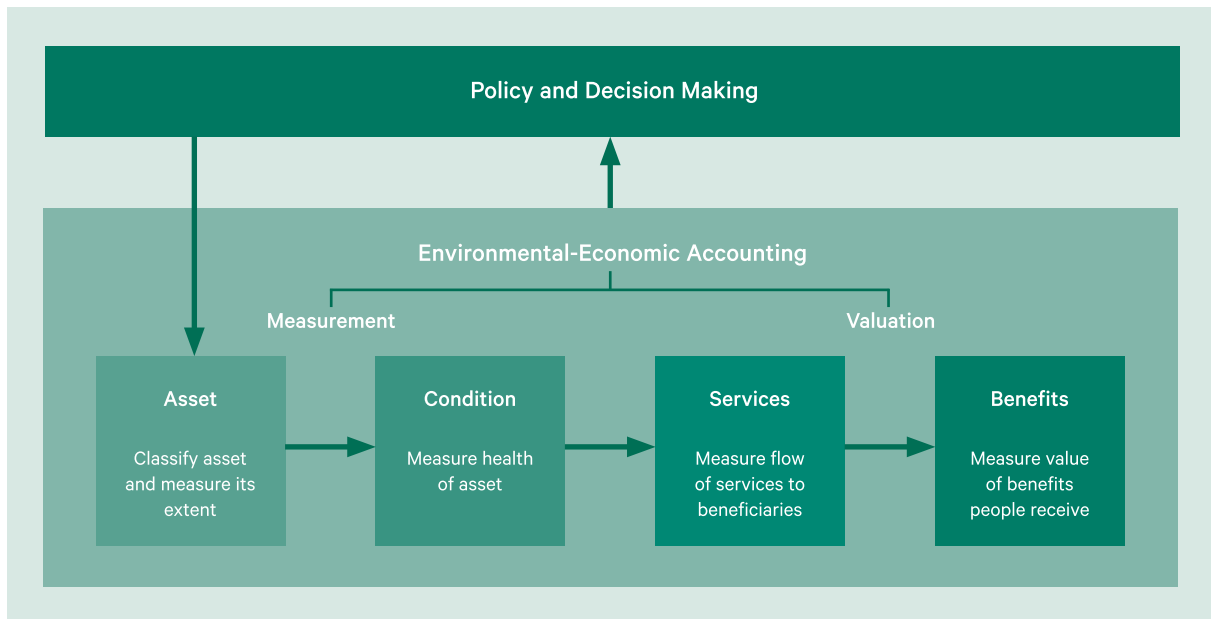
The use of environmental accounting in Australia is introduced in BoM (2013). A global model for environmental-economic accounting has been developed by the System of Environmental Economic Accounting (SEEA; see Figure 20.2 and Excursus 20.4). The SEEA framework is typically applied at national, state, or regional scales, and links through to mainstream accounting systems such as the System of National Accounts (SNA; CoA, 2018). Implementation of systems such as SEEA need to be phased to “build practical understanding and political acceptance” by all concerned (Vardon *et al.*, 2016). This system has been used by the Australian Bureau of Statistics (ABS) since 1996 to produce the Australian Environmental Economic Accounts (AEEA; ABS, 2018; see Section 20.5).

Instead of seeing the environment as the foundation of human history, settled societies, especially modern industrial societies, have acted under the illusion that they are somehow independent from the natural world, which they have generally preferred to see as something apart which they can exploit more or less with impunity. Ever since the first great transition which began 10,000 year ago, and particularly in the last two centuries, humans have put increasing pressure on the earth's environment—in defiance of basic ecological principles. They have destroyed climax ecosystems to create agricultural land leading to environmental damage such as widespread soil erosion. Through a combination of hunting and farming they have driven individual animals to extinction and severely reduced the population of others. Either deliberately or accidentally they have introduced new animals and plants and thereby disrupted ecosystems, often with unpredictable results. it is clearly far too soon to judge whether modern industrial societies, with their very high rates of energy and resource consumption and high pollution levels, and the rapidly rising human population in the rest of the world are ecologically sustainable. Past human actions have left contemporary societies with an almost insuperably difficult set of problems to solve.

(Ponting, 1991)

Figure 20.2 System of Environmental Economic Accounting

The UN-based System of Environmental Economic Accounting (SEEA) provides “an integrated statistical framework for organizing biophysical data, measuring ecosystem services, tracking changes in ecosystem assets, and linking this information to economic and other human activity” (SEEA, 2020a).



Source: Vardon *et al.* (2018)

20.2 EO Sensors for Sustainability

Various ecosystem properties that are indicative of ecosystem services can be derived from EO datasets, including definition of ecoregions, topography, hydrology, vegetation type and productivity, and changes in land use or climate (Andrew *et al.*, 2015; see Table 20.4). Similarly, assessment of sustainable development criteria increasingly relies on EO-based data (see Section 20.4). Operational systems for environmental accounting and

environmental-economic accounting already derive data from EO time series datasets and as this field continues to expand, that reliance will also increase and become more standardised (see Section 20.5). As summarised in Table 19.3, sources of EO datasets that are relevant to assessing sustainability are primarily acquired at a regional to global scale, with *in situ* and higher resolution data being used to calibrate and validate the resulting products.

Table 20.2 EO sensors relevant to sustainability

TIR: Thermal infrared; SAR: Synthetic Aperture Radar

Type	Sensor	Platform	Relevance	Advantages	Disadvantages
Passive optical	Multispectral radiometer	Satellite or airborne	Vegetation cover and extent, biomass, biodiversity, and productivity Land degradation	Globally consistent and contiguous, local to national scale, recurrent coverage with high temporal frequency and extent, low cost	Cloud contamination, limited spectral discrimination
	TIR radiometer	Satellite or airborne	Soil/canopy temperature Fire potential, severity, and extent Drought conditions Regional hydrological changes	Highlight thermal anomalies	Low resolution, low signal to noise ratio
Passive microwave	Microwave radiometer	Satellite	Soil moisture, Climate variables	High temporal frequency, large spatial coverage, cloud penetration	Very low energy targets so very coarse spatial resolution
Active microwave	SAR	Satellite or airborne	Soil characteristics Vegetation structure Water dynamics	All weather, operates at night	Data availability, noisy data, complex processing

20.3 Ecosystem Services

The concept of ecosystem services was developed to encourage an awareness of the societal benefits being derived from ecosystems and the importance of biodiversity conservation (Westman, 1977; Ehrlich and Ehrlich, 1981), with the intention of fostering a stewardship approach towards sustainable resource management by which those essential services would be maintained (Daily, 1997; Costanza *et al.*, 1997, 2017). The Millennium Ecosystem Assessment (MEA, 2005) identified global categories for ecosystem services (see Excursus 20.1) that can be used to assess the sustainable use of ecosystems (see Section 20.5).

While ecosystem functions and services are linked with biodiversity (see Section 19), one cannot be used to represent the other for several reasons:

- for many species, functional roles can only be observed at specific spatial and temporal scales;
- ecosystem services are identified and valued relative to social, cultural, and economic factors, which may vary at a local scale; and
- whether changes in ecosystem function or abiotic environments are beneficial to conservation goals or not requires a subjective judgment (Keith *et al.*, 2013).

Some of the challenges and opportunities inherent in this approach to ecosystem assessment were defined by Birkhofer *et al.* (2015; see Table 20.3). These authors conclude that “ecosystem service research is challenging for ecologists, but developing a multifaceted understanding of how nature promotes human wellbeing is crucial for the sustainable use of the Earth’s resources. Ecosystem service research offers ecologists the unique opportunity to act as promoters for the understanding of how to conserve and sustain benefits gained from nature.”

Ecosystem services are impacted by a range of natural and anthropogenic factors. Assessment of ecosystem services is based on relevant indicators selected using criteria that are specific, measurable, achievable, realistic and time-sensitive (Dawson *et al.*, 2016). For example, Figure 20.3 depicts ecological processes and functions that generate provisioning, regulating, and habitat services in extensive agriculture from ‘ecological capital’. In this context, ecological capital comprises ecosystem assets, including productive assets (production herds that deliver progeny, grasslands and pastures for forage, and soils and soil biota to sustain vegetation) and supporting assets (trees and shrubs that offer shade, shelter, and habitat). Relevant regulating services include avoiding water pollution, maintaining soil productivity and structure, and sequestering carbon. All of these ecosystem services influence both the current and future production of crops and livestock, and the regenerative capacity of the ecological capital (Ogilvy, 2020).

Potential sources of data for ecosystem mapping are summarised in Andrew *et al.* (2015) and Pettoelli *et al.* (2017), including EO datasets (Alcaraz-Segura *et al.*, 2014; de Araujo Barbosa *et al.*, 2015; Andrew *et al.*, 2014; Ramirez-Reyes *et al.*, 2019; see Table 20.4). Some of the challenges and opportunities associated with using EO in ecosystem modelling and assessment are considered by Ramirez-Reyes *et al.* (2019) and summarised in Figure 20.4. Methods to quantify uncertainty in EO-based assessments of ecosystem services are also being developed (Stritih *et al.*, 2019). An integrated framework for using EO products with socio-cultural and economic datasets to assess ecosystem services was proposed by Cord *et al.* (2017). Integrated resource monitoring systems involving ecosystem services are further discussed in Section 20.5.

Biodiversity and associated ecosystem services can be thought of as natural capital. We also think about social capital, which is a measure of community intangibles such as networks, cultural pursuits, trust, commitment to local wellbeing and shared values, and physical capital, which is the result of past investments in the conversion of components of natural capital through construction and maintenance, such as infrastructure. The set of these types of capital forms the foundations of a nation’s wealth.
(DEWHA, 2010)

Excursus 20.1—Millennium Ecosystem Assessment

Source: MEA (2005)

The consequences of ecosystem change for human wellbeing have been highlighted in recent years by the UN-funded Millennium Ecosystem Assessment (MEA, 2005), which defines four fundamental 'ecosystem services':

- provisioning services for food, water, fibre, fuel and other commodities;
- supporting services for photosynthesis, primary productivity, oxygen production, soil formation, biodiversity conservation, water and nutrient cycling;
- regulating services for air quality, climate variables, seed dispersal, herbivory, water quality, water flow regulation, carbon sequestration, bioturbation, erosion control, pests and disease prevention, pollination; and
- cultural services for spiritual fulfillment, aesthetic enjoyment, heritage values, recreation, and education.

Changes in drivers that indirectly affect biodiversity, such as population, technology, and lifestyle can lead to changes in drivers directly affecting biodiversity, such as resource consumption. These result in changes to ecosystems and the services they provide thereby affecting human wellbeing. These interactions can take place at local, regional, and global scale and between these scales in short and long time intervals.

The MEA report also presents a scientific basis for sustainable use of ecosystems by assessing:

- What are the current conditions and trends of ecosystems, ecosystem services, and human wellbeing?
- What are plausible future changes in ecosystems and their ecosystem services and the consequent changes in human wellbeing?
- What can be done to enhance wellbeing and conserve ecosystems? What are the strengths and weaknesses of response options that can be considered to realise or avoid specific futures?
- What are the key uncertainties that hinder effective decision making concerning ecosystems?
- What tools and methodologies developed and used in the MEA can strengthen capacity to assess ecosystems, the services they provide, their impacts on human wellbeing, and the strengths and weaknesses of response options?

The four main findings from this assessment were:

- Over the past 50 years, humans have changed ecosystems more rapidly and extensively than in any comparable period of time in human history, largely to meet rapidly growing demands for food, fresh water, timber, fibre, and fuel. This has resulted in a substantial and largely irreversible loss in the diversity of life on Earth.
- The changes that have been made to ecosystems have contributed to substantial net gains in human wellbeing and economic development, but these gains have been achieved at growing costs in the form of the degradation of many ecosystem services, increased risks of nonlinear changes, and the exacerbation of poverty for some groups of people. These problems, unless addressed, will substantially diminish the benefits that future generations obtain from ecosystems.
- The degradation of ecosystem services could grow significantly worse during the first half of this century and is a barrier to achieving the Millennium Development Goals.
- The challenge of reversing the degradation of ecosystems while meeting increasing demands for their services can be partially met under some scenarios that the MEA has considered, but these involve significant changes in policies, institutions, and practices that are not currently underway. Many options exist to conserve or enhance specific ecosystem services in ways that reduce negative trade-offs or that provide positive synergies with other ecosystem services.

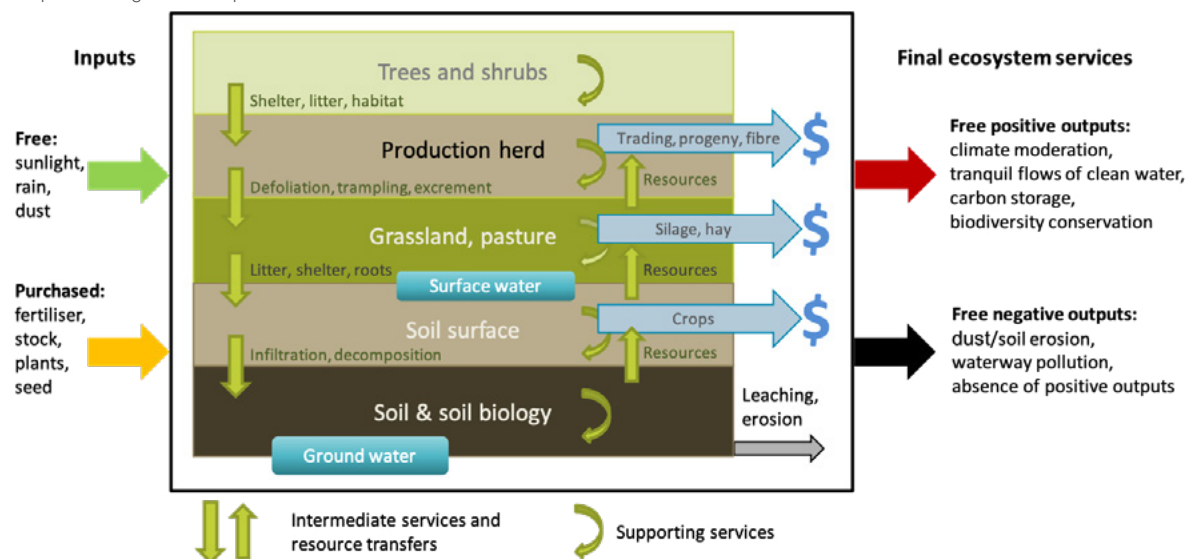
Table 20.3 Ecosystem services—challenges and opportunities

Land Management Practice	Impacts on Biodiversity	Geographic Area
Understanding anthropogenically modified systems	Identifying human impact on service-providing units and ecosystem services	Consideration of relationships between biodiversity and ecosystem service provision and management interventions
	Considering matrix effects in modified landscapes	Identifying effects of anthropogenic interventions on service-providing units at different spatial scales
Assessing ecosystem services	Assessing relationships between services and measures usually quantified in ecological studies	Identifying ecological measures that are reliable indicators of ecosystem service provision
	Accounting for dynamics and uncertainties in models of service provision	Evaluation of uncertainty, integration of evolutionary aspects and human impacts into process-based models and socio-economic models
Analysing relationships between ecosystem services	Understanding if relationships between ecosystem services are indirect or direct	Performing studies that model direct and indirect effects, experimental test for relationships and developing mechanistic models
	Solving issues with the visualisation and statistics testing of relationships between multiple services	Accounting for non-linear relationships when visualising or analysing relationships between services
Considering appropriate spatial and temporal scales	Upscaling from experimental plots to scales relevant for management of most ecosystem services	Coupling research on mechanisms for service provision with conservation-oriented research
	Understanding temporal dynamics of services provision to develop sustainable management and conservation strategies	Utilising existing long term studies and promoting the need for such research projects

Source: Birkhofer *et al.* (2015) Table 1

Figure 20.3 Ecosystem services in extensive agriculture

This conceptual diagram relates the inter- and intra-ecological functions and processes in extensive agriculture that generate ecosystem services. Degradation of the functions and processes within and between elements of ecological capital (or assets) invariably leads to decline in the capacity to capture, store and cycle free inputs from nature. The listed inputs and outputs only sample the larger sets of potential resources and outcomes.



Source: Ogilvy (2020) Figure 2

Table 20.4 EO capabilities relevant to ecosystem services

Abbreviations: NDVI: normalised difference vegetation index; MODIS: moderate resolution imaging spectroradiometer; fAPAR: fraction of absorbed photosynthetically active radiation; NPP: net primary productivity, VI: vegetation index.

Ecosystem service or process	EO product	Potential EO data source
Plant traits	Pigment, dry matter, water, chemical content, leaf area index, leaf angle distribution	Spectral analysis or radiative transfer models
	Roughness, height, vertical structure	Lidar, radar, multiangle
	Life form	Land cover classification
	Phenology	Multi-temporal imagery
Species	Species map,	Chemical or structural uniqueness, hyperspectral imaging, lidar, image texture
	Habitat suitability map	Varied (climate, topography, land cover, productivity, etc)
Biodiversity	Spectral diversity	Range/variability of biochemistry, NDVI or reflectance
	Environmental surrogates	Varied (productivity, topography, land cover, disturbance, etc)
Abundance of functional components	Vegetation fraction, litter fraction	Spectral unmixing, MODIS Continuous Fields
Biomass, carbon storage	Canopy structure	Lidar, radar, multiangle data
Photosynthesis, carbon sequestration	Productivity	fAPAR, photosynthetic efficiency, fluorescence, MODIS NPP
Disturbance	Change in biomass, plant traits, land cover	Multi-temporal imagery
	Fire detection	Thermal anomalies
	Drought monitoring	Water content, surface temperature, evapotranspiration
	Plant stress	Spectral indexes
Soil characteristics	Land form	Digital Elevation Model
	Soil texture, moisture, chemistry	Radar, hyperspectral imaging
Evapotranspiration	Evapotranspiration	Thermal imagery, VIs, climate data
Hydrology variables	Precipitation	Thermal imagery, VIs, climate data
	Soil moisture	Radar, passive microwave radar
	Water, snow/ice extent	Optical, radar, passive microwave, radar altimetry
	Water level, Groundwater	Gravity surveys, subsidence, surface water fluxes
Landscape structure	Landscape metrics	Land cover, quantitative heterogeneity patterns
Ecosystem classification	Ecosystem classification	Varied (productivity, climate, topography, land cover, etc)

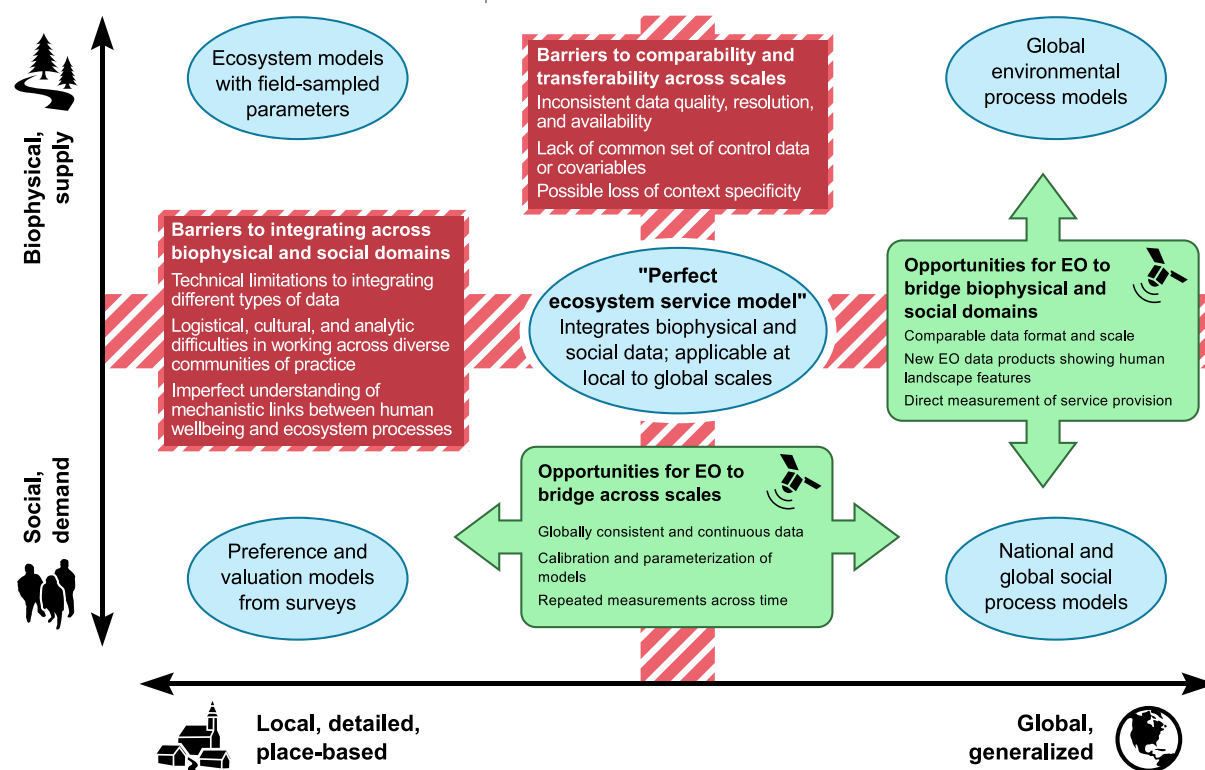
Source: Andrew *et al.* (2014) Table 2

Land use policies and planning transform landscapes, affecting the long term mosaics of unmodified, modified, removed and replaced vegetation ecosystems. In turn, land use policies, planning instruments and decisions affect the viability of landscapes to generate publicly acceptable mixes of ecosystem services, including clean air, healthy crops, clean water, and parks and reserves for the protection of nature and recreation.

(Thackway, 2018)

Figure 20.4 EO in ecosystem service assessment

Ecosystem service models have been applied across scales, from local to global, to quantify ecosystem service supply and demand. Technical and conceptual barriers remain to creating models that effectively integrate social and biophysical systems that are comparable and transferable across geographies. EO data may reduce these barriers by providing new ways to measure ecosystem service drivers that are consistent across time and space.



Source: Ramirez-Reyes et al. (2019) Figure 1

Ecosystem services have traditionally been valued in terms of market pressures, but some have been directly or indirectly undervalued or ignored in terms of ecosystem biodiversity and resilience (see Sections 7 and 19). In many regions of Australia, this undervaluing has resulted in unsustainable resource usage and environmental degradation (see Sections 11.4 and 15). Some of the major challenges in measuring the variety of ecosystem services in Australia include:

- lack of detailed information about ecosystem processes with most data being derived from models;
- key processes have differing cycle durations and complexity; and
- research is not necessarily transferable across ecosystems—Australia's size and diversity means that ecosystem services differ in terms of speed and sequence in different locations (DEWHA, 2010).

Traditional market measurement systems exist for some, but not all, ecosystem services. Hopefully, as new markets develop for ecosystem services, such as carbon trading (see Section 17), environmental water flows (see Volume 3B), and vegetation offsets (see Volume 2D—Excursus 14.3), their real economic value will become more apparent (see Section 21).

Sustain (from) Latin, sub meaning 'from below' and tenere meaning 'to hold'

20.4 Sustainable Development

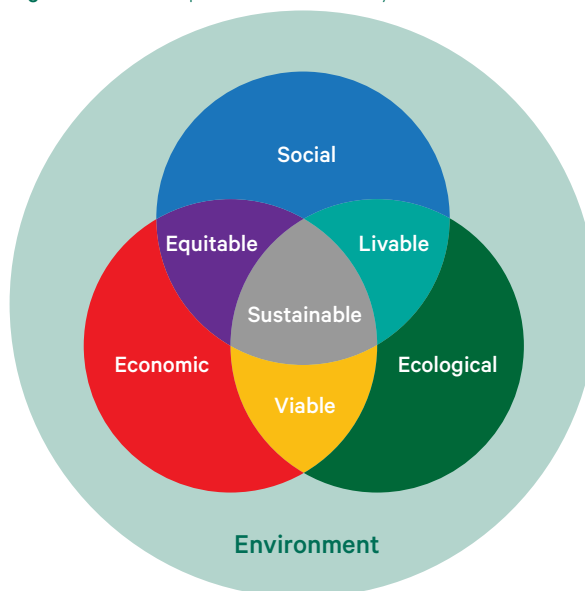
The word ‘sustainable’ is defined by the Merriam-Webster Dictionary as meaning ‘of, relating to, or being a method of harvesting or using a resource so that the resource is not depleted or permanently damaged’. The word was originally coined in German from the concept of ‘sustained yield’ in forestry, that is, a balance between resource consumption and production. More recently, The Brundtland Report (1987) entitled ‘Our Common Future’, produced by several UN countries, defined ‘sustainable development’ as satisfying “the needs of the present without compromising the ability of future generations to meet their own needs” and signalled “a new era of economic growth—growth that is forceful and at the same time socially and environmentally sustainable” (Purvis *et al.*, 2018). The elements of sustainable development were defined by Jacobs *et al.* (1987) as the:

- integration of conservation and development;
- satisfaction of basic human needs;
- achievement of equity and social justice;
- provision for social self-determination and cultural diversity; and
- maintenance of ecological integrity.

Of the wide range of models that have been proposed to represent the most critical components of sustainable development and their interrelationships (Brown *et al.*, 1987; Kidd, 1992; Boyer *et al.*, 2016; Purvis *et al.*, 2018), Figure 20.5 shows one of the most popular depictions, in which three interrelated pillars—social, economic, and ecological—jointly impact the environment. The precise definitions of these three interest areas have varied depending whether they are seen as perspectives to consider, or systems to be balanced, integrated, or reconciled

(Purvis *et al.*, 2018; see Table 20.5). Accordingly, the relative importance of each pillar is weighted differently by different individuals, with the viability of continued economic growth being highly debatable. Moreover, Kidd (1992) argues that different “strains of thought” have adopted the term ‘sustainability’ to represent fundamentally different concepts, and some observers consider “the term ‘sustainable development’, like that of ‘sustainable growth’, to be an oxymoron (Redclift, 2005; Johnston *et al.* 2007; Brand, 2012)” (Purvis *et al.*, 2018). In the face of limiting resources, however, conflicts over land management and resource distribution inevitably arise and this model enables analysis of competing demands.

Figure 20.5 Three pillars of sustainability



Human history cannot be understood in a vacuum. All human societies have been, and still are, dependent on complex, interrelated physical, chemical and biological processes. These include the energy produced by the sun, the circulation of the elements crucial for life, the geophysical processes that have caused the continental land masses to migrate across the face of the globe and the factors regulating climatic change. These constitute the essential foundations for the way in which the various types of plants and animals (including humans) form complex, interdependent communities. ... Research in a wide variety of disciplines is increasingly making it clear that life on earth and all human societies depend on the maintenance of a number of delicate balances within and between a whole series of complex processes. The findings help us to understand the way in which the environment has influenced the development of human societies and, just as important, the human impact on earth.
(Ponting, 1991)

Table 20.5 Definitions of sustainability pillars

Citation	Social	Ecological	Economic	Goal
Brown <i>et al.</i> (1987)	Continued satisfaction of basic human needs	Continued productivity and functioning of ecosystems; protection of genetic resources and conservation of biological diversity	Limitations that a sustainable society must place on economic growth	Three distinct but interrelated perspectives
Barbier (1987)	Cultural diversity, institutional sustainability, social justice, participation	Genetic diversity, resilience, biological productivity	Satisfying basic needs (reducing poverty), equity-enhancing, increasing useful goods and services	Maximise the goals across all these systems through an adaptive process of trade-offs
Munasinghe (1993)	Equity and participation	Preserve biological and physical systems	Maximise income whilst maintaining capital stock	Integration of competing “non-comparable” objectives
Elkington (1997)	People	Planet	Profit	Triple bottom line (TBL) accounting method
Custance and Hillier (1998)	Social progress	Protection of the environment	Maintenance of economic growth	Balance between three broad objectives

Source: Purvis *et al.* (2018)

Given the differing, and somewhat ambiguous, perceptions of sustainability, numerous methods have been proposed to implement sustainable development. Hugé *et al.* (2013) grouped these disparate interpretations into three broad ‘discourses’ on sustainable development (where discourse is defined as “a specific ensemble of ideas, concepts, and categorisations that are produced, reproduced, and transformed in a particular set of practices and through which meaning is given to physical and social realities”; Hajer, 1995):

- integration: pragmatically integrates development and environmental goals—relying on mostly anthropocentric frameworks, such as ecosystem services (see Section 20.3), and involves compromise and political consensus at a jurisdictional level;
- limitations: emphasises imposition of limits on human activities—based on ecological limits to population growth and resource availability, this approach requires strategies to manage resource scarcities and ethical constraints to ensure social justice, and embraces the concepts of resilience (see Sections 7 and 15 and Excursus 21.1), ecological footprints (see Excursus 20.3), and critical environmental capital (see Section 20.3); and
- process of change: this view sees change and uncertainty as an inherent continua in the development cycle, requiring transformation of society so that human lifestyles adapt to resource availability.

One of the key requirements for monitoring sustainable development is the definition of operational indicators “that provide manageable units of information on economic, environmental, and social conditions” (Custance and Hillier, 1998; Böhringer and Jochem, 2007).

The 2030 Agenda for Sustainable Development identified 17 global goals that were explicitly based on the three pillars of sustainability shown in Figure 20.5 (see Excursus 20.2). Progress towards these goals and their 169 targets is monitored using an agreed global indicator framework of 231 unique indicators (UN, 2019, 2020a). The Global Indicator Framework reports on progress towards indicators using available datasets (traditional national accounts, household surveys, and routine administrative data) and new data sources such as geospatial information, citizen science, and Big Data (GEO, 2020a). Geospatial datasets, including EO, are essential to make this process feasible, effective, and ongoing. For example, satellite-based EO data can:

- complement traditional data sources;
- provide spatially and temporally denser information on multiple scales;
- deliver wall-to-wall ecosystem coverage;
- improve frequency or richness of data;
- save money on traditional survey methods;
- provide the only viable option in relation to global indicators; and
- allow consistent and comparable measurements across different countries and regions (GEO, 2017).

Examples of EO-based monitoring programs working towards these sustainable development goals (SDG) are given in Section 21.3. The Global Footprint Network is a freely accessible, online system that monitors sustainability for nations, regions, and the collective world by comparing resource production with consumption. As detailed in Excursus 20.3, it paints a bleak picture for our sustainable future on planet Earth.

Excursus 20.2—Global Sustainable Development Agreements

Source: <https://sustainabledevelopment.un.org>

The 2030 Agenda for Sustainable Development, adopted by all UN Member States in 2015, provides a shared blueprint for peace and prosperity for people and the planet, now and into the future. Based on 17 Sustainable Development Goals (SDGs), this build on decades of work to attain global agreement to end poverty and conserve natural resources. Originating at the Earth Summit in Rio de Janeiro, Brazil, in 1992, where more than 178 countries adopted Agenda 21 (a comprehensive plan of action to build a global partnership for sustainable development to improve human lives and protect the environment), global collaboration moved through various agreements and goals, including the Millennium Development Goals (MDG), and culminated in the UN Conference on Sustainable Development in Rio de Janeiro, Brazil, in June 2012, (“The Future We Want”) where a process was launched to develop a set of SDGs to build upon the MDGs.

Several major international agreements were adopted in 2015, including (see Section 20.6 for links):

- Sendai Framework for Disaster Risk Reduction (March 2015);
- Addis Ababa Action Agenda on Financing for Development (July 2015);
- Transforming our world: the 2030 Agenda for Sustainable Development with its 17 SDGs (adopted at the UN Sustainable Development Summit in New York, September 2015); and
- Paris Agreement on Climate Change (December 2015).

The 17 SDGs are:

Goal 1: End poverty in all its forms everywhere.

Goal 2: End hunger, achieve food security and improved nutrition and promote sustainable agriculture.

Goal 3: Ensure healthy lives and promote wellbeing for all at all ages.

Goal 4: Ensure inclusive and equitable quality education and promote lifelong learning opportunities for all.

Goal 5: Achieve gender equality and empower all women and girls.

Goal 6: Ensure availability and sustainable management of water and sanitation for all.

Goal 7: Ensure access to affordable, reliable, sustainable and modern energy for all.

Goal 8: Promote sustained, inclusive, and sustainable economic growth, full and productive employment and decent work for all.

Goal 9: Build resilient infrastructure, promote inclusive and sustainable industrialisation, and foster innovation.

Goal 10: Reduce inequality within and among countries.

Goal 11: Make cities and human settlements inclusive, safe, resilient, and sustainable.

Goal 12: Ensure sustainable consumption and production patterns.

Goal 13: Take urgent action to combat climate change and its impacts.¹⁷

Goal 14: Conserve and sustainably use the oceans, seas, and marine resources for sustainable development.

Goal 15: Protect, restore, and promote sustainable use of terrestrial ecosystems, sustainably manage forests, combat desertification, and halt and reverse land degradation and halt biodiversity loss.

Goal 16: Promote peaceful and inclusive societies for sustainable development, provide access to justice for all, and build effective, accountable, and inclusive institutions at all levels.

Goal 17: Strengthen the means of implementation and revitalise the global partnership for sustainable development.

In order to make the 2030 Agenda a reality, broad ownership of the SDGs must translate into a strong commitment by all stakeholders to implement the global goals.

*If you harvest a crop you are removing nutrients from that ecosystem—
for sustainable production they need to be replaced.*
(Rattan Lal)

¹⁷ Acknowledging that the United Nations Framework Convention on Climate Change is the primary international, intergovernmental forum for negotiating the global response to climate change.

Excursus 20.3—Global Footprint Network

Source: GFN (2020)

The Global Footprint Network measures the sustainability of populations around the world in terms of two metrics that are standardised to units of global hectares (gha—biologically productive hectare with world average biological productivity for a given year):

- ecological footprint (EF)—their consumption of resources and absorption of waste products; and
- biocapacity (BC)—the productivity of their ecological assets (Borucke *et al.*, 2013).

These metrics are used to generate several national, regional, and global accounts, including:

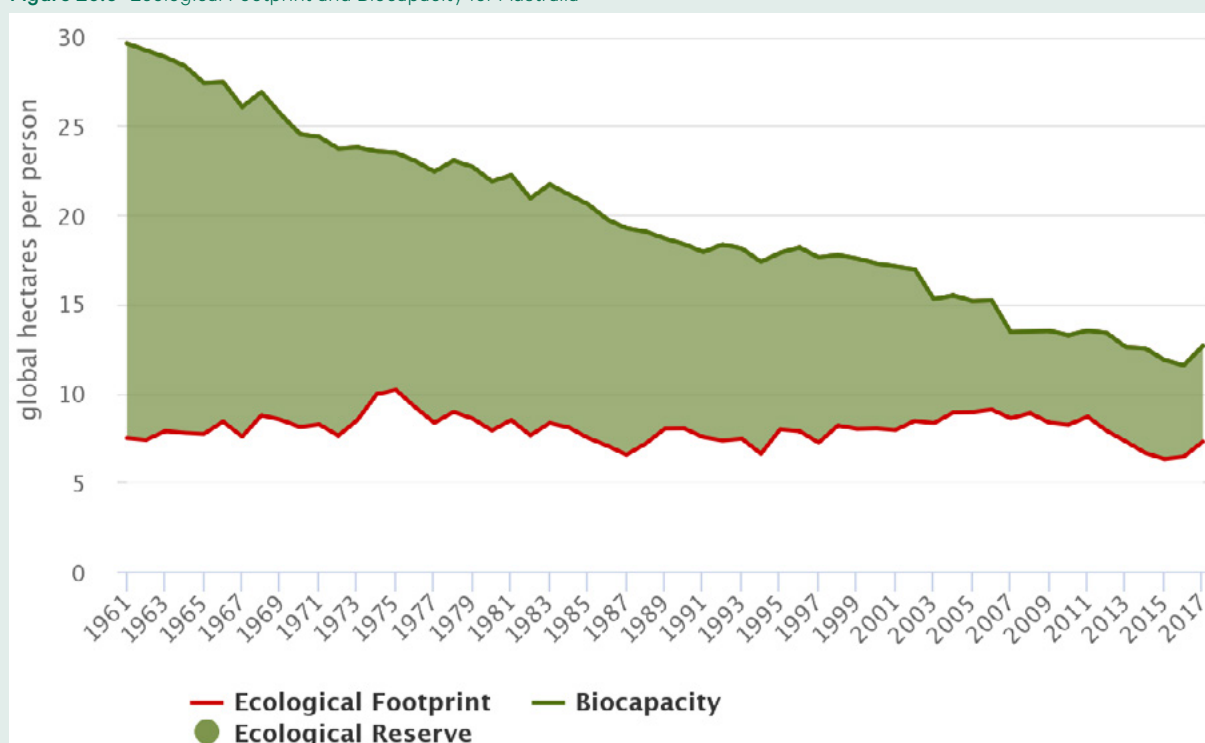
- ecological deficit— $BC < EF$, meaning that the population is not self-sufficient so relies on imported goods, liquidation of ecological assets, and/or CO_2 emissions into the atmosphere;
- ecological reserve— $BC > EF$; and
- ‘Earth Overshoot Day’—the number of days in a given year that the biocapacity of Earth can support its population. When counted on from 1 January, this has moved from 29 December in 1970 (when global resource demand was about equal to supply) to 29 July in 2019 (when we are collectively overbudget; Wackernagel *et al.*, 2019; GFN, 2020).

The balance between ecological footprint and biocapacity for Australia is shown in Figure 20.6. While we are still keeping our consumption head above the ‘pool’ of available resources, the ecological reserve is decreasing with time.

In the Global Footprint Network, usage of the world’s productive surface area is represented by six categories (cropland, grazing land, fishing grounds, built-up land, forest area, and carbon demand on land), each of which is tracked to derive the ecological footprint for each population (city, nation, or state). The average area of biologically active surface per person globally is 1.6 gha. The total EF for selected countries in 2016 can be compared in terms of these productive surface area categories or relative to population, which paints a different picture.

One measure of sustainable development compares the UN Human Development Index (HDI, based on average longevity, income, and access to education) for a population with its EF. An HDI over 0.8 is considered ‘very high’. In 2016 Australia had an HDI value of 0.94 versus an EF (in units of gha per person) of 6.64—a lucky country indeed!

Figure 20.6 Ecological Footprint and Biocapacity for Australia



Source: Global Footprint Network, 2021 National Footprint and Biocapacity Accounts: <https://data.footprintnetwork.org/#/countryTrends?cn=10&type=BCpc,EFCpc>

20.5 Environmental-Economic Accounting

When the social science of economics was introduced only a few centuries ago, it represented a shift in social organisation towards market-driven trading of land, labour, and capital, rather than the feudal bartering system that had operated for many centuries in most of the ‘civilised’ world prior to the industrial revolution. Investments, increased productivity, and individual wealth—namely capitalism—were encouraged, with the expectation that economic gain would benefit society (Smith, 1776). However, classical economics, where the free market achieves balance between supply and demand (through the pursuit of individual self-interest, division of labour, and freedom of trade), and more recent economic theories (including Keynesian and Marxist), where governments regulate demand to ensure full employment, all focus on production, assume resources are infinite, and regard labour as a commodity. They also ignore the social and environmental costs of producing goods, such as air, water, and soil pollution, and the direct and indirect impacts of these ‘externalities’ on the health and wellbeing of humans and other biota (Ponting, 1991).

In any organisation that manages money, accounting is the process of tracking, analysing, and reporting the movement of finances and assets. The goal is generally to ensure that income is greater than expenditure, while complying with statutory regulations. Accounting has traditionally been limited to measuring and scrutineering the commodities of land, labour, and capital, but in the last few decades there have been attempts to also reckon the environmental costs of production, and the impact of current consumption on future production and sustainability (e.g. Schumacher, 1973; Henderson, 1978).

The concepts and practices of ecosystem and environmental accounting were introduced in Volume 2D—Section 14.2.1. In a general sense, environmental accounting tracks relevant environmental attributes to monitor the condition of natural resources, whereas ecosystem accounting is defined as “a coherent framework for integrating measures of ecosystems and the flows of services from them with measures of economic and other human activity” (SEEA, 2020a). These approaches are complementary, with the latter having a greater focus on ecosystem integrity and “how individual environmental assets interact as part of natural processes within a given spatial area” (SEEA, 2020a).

One example of an Australian environmental accounting system is OzWALD, a model-data fusion system that is heavily reliant on EO datasets (van Dijk *et al.*, 2017; van Dijk and Rahman, 2019). OzWALD ingests a variety of datasets into a water balance model to estimate relevant parameters for vegetation, as well as energy, water, and carbon balance, and generates national annual reviews of the current status of, and relative changes in, the Australian environment (see Volume 2D—Excursus 14.2). Examples of ecosystem accounting measures are given in Table 20.6 (see also Vallecillo *et al.*, 2018). Bio-economic modelling approaches have also been developed in recent decades and used to determine the direct and indirect impacts of agricultural intensification on selected ecosystem services (Flichman and Allen, 2013; Kirchweiger *et al.*, 2020; Ogilvy, 2020).

*The measure of success is not whether you have a tough problem to deal with,
but whether it's the same problem you had last year.*
(John Foster Dulles)

Table 20.6 Examples of ecosystem accounting measures

ABARES: Australian Bureau of Agricultural and Resource Economics; ABS: Australian Bureau of Statistics; BoM: Bureau of Meteorology

Ecosystem service	Example	Accounting
Provisioning	Agricultural commodities	Annual statistics (ABARES, ABS)
	Agricultural fertilisers	Patchy records by government and research agencies
	Fresh water	National Water Accounts (ABS, BoM)
Supporting	Native vegetation extent	National Vegetation Information System (NVIS)
	Soil resources	Australian Soil Resources Information System (ASRIS)
Regulating	Carbon sequestration	National Carbon Accounting System (NCAS)
	Pollination	Bio-economic models
	Water quality	SEEA-Water
Cultural	Recreation	Tourism statistics
	Landscape aesthetics	Real estate value

The Accounting for Nature (AfN) framework develops biophysical accounts for environmental assets (such as vegetation, soils, biota, and waterways, including groundwater) using a common environmental condition index (Econd), based on reference condition benchmarks (WGCS, 2016). Such measures of environmental condition inform management decisions to improve, rather than degrade, natural capital. The AfN framework presents a standardised “system of rules and processes designed to ensure the integrity and transparency of environmental accounts, no matter the environmental asset being measured” (AfN, 2020). It is designed for local/regional scale applications, such as individual farms, which can be aggregated to national scale, and links through to enterprise microeconomic and accounting systems, including the option of independent certification of environmental accounts. AfN complements other systems for standards and compliance with the goal of promoting sustainability at the level of individuals and enterprises (see Section 20.6). It is also compatible with SEEA (see Excursus 20.4).

Environmental-economic accounting aims to understand both the condition of the environment and its relationship with the economy. SEEA, an accepted international standard for environmental-economic accounting, is described in Excursus 20.4.

Since the full costs of any action anywhere in the world must be borne by someone, somewhere, sometime, it is important that our accounting system makes provision for this. We accept however, that ecological processes are so complex and can spread so far in space and time, that this will be exceptionally difficult. Nonetheless, given the truism that a satisfactory accounting system is one which supports and helps perpetuate the social system from which it derives, we must attempt to devise one which is fitted to a society based on a sober assessment of ecological reality and not on the anthropocentric pipe-dream that we can do what we will to all species, not excepting, it seems, future generations of our own. It is worth recalling Prof. Commoner's dictum that since economics is the science of the distribution of resources, all of which are derived from the ecosphere, it is foolish to perpetuate an economic system which destroys it. Ideally (and as befits the etymology of the two words), ecology and economics should not be in conflict: ecology should provide the approach, the framework for an understanding of the interrelationships of social and environmental systems, and economics should provide the means of quantifying those interrelationships in the light of such an understanding, so that decisions on alternative courses of action can be made without undue difficulty.

(Goldsmith and Allen, from A Blueprint for Survival #243, 1972)

Excursus 20.4—System of Environmental Economic Accounting

Source: SEEA (2018, 2020a)

The System of Environmental-Economic Accounting (SEEA) is an international statistical standard that uses a systems approach to bring together economic and environmental information to measure the contribution of the environment to the economy and the impact of the economy on the environment. It uses internationally agreed standard concepts, definitions, classifications, accounting rules and tables for producing internationally comparable statistics and accounts. The SEEA is produced and released under the auspices of the UN, the European Commission (EC), the Food and Agriculture Organisation of the UN (FAO), the Organisation for Economic Co-operation and Development (OECD), International Monetary Fund (IMF), and the World Bank Group (WBG).

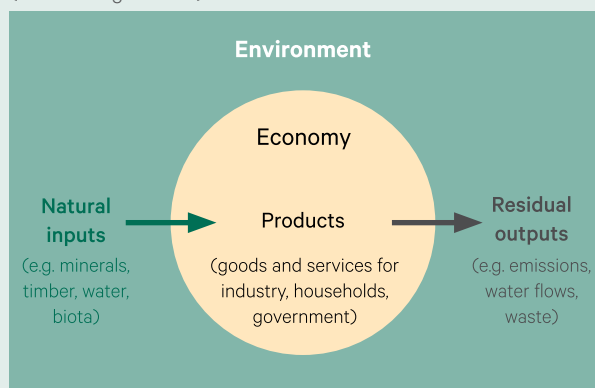
The System of National Accounts (SNA) is a measurement framework that has been evolving since the 1950s to embody the pre-eminent approach to the measurement of economic activity, economic wealth, and the general structure of the economy. The SEEA framework follows a similar accounting structure and uses concepts, definitions, and classifications consistent with the SNA in order to facilitate the integration of environmental and economic statistics.

SEEA Central Framework (SEEA CF) focuses on physical quantities of stocks and flows of goods and services, their monetary values, and tracking supply and use (see Figure 20.7). This central framework is very human-centric, for example harvesting of crops considers the value added to produce, then receive, goods and services. Without the human ‘user’ to receive the goods and services, there is no ‘transaction’ to link environmental economic accounts to the SNA (UN, 2014). SEEA CF is an accepted statistical standard that facilitates accounts in several thematic areas, including:

- Agriculture, Forests, and Fisheries—integrates information on the environment and the economic activities of these industries that impact and directly depend on the environment and its resources. Integrating information about agriculture, forestry, and fisheries facilitates understanding of the trade-offs and dependencies between these activities and their related environmental factors.
- Air Emissions—provide information on emissions released to the atmosphere by establishments and households as a result of production, consumption, and accumulation processes. The air emissions accounts record the generation of air emissions by resident economic units according to type of gaseous or particulate substance.
- Energy—supports analysis of the role of energy within the economy, the state of energy inputs, and various energy-related transactions of environmental interest. Energy information is typically presented in physical terms, but monetary valuations are also applied to various stocks and flows.
- Environmental Activity—provides information on transactions concerning activity undertaken to preserve, protect, and manage the environment. Understanding environmental activity is critical to understanding whether economic resources are being used effectively to reduce pressures on the environment and maintain the capacity of the environment to deliver benefits.
- Ecosystems—constitutes an integrated statistical framework for organizing biophysical data, measuring ecosystem services, tracking changes in ecosystem assets, and linking this information to economic and other human activity.
- Land—provides information on land use and land cover, and can enable an assessment of the changing shares of different land uses and land covers within a country. Understanding these characteristics and changes is critical to understanding the impacts of urbanisation, the intensity of crop and animal production, afforestation and deforestation, the use of water resources, and other direct and indirect uses of land.
- Material Flow—provides an aggregate overview of material inputs and outputs in terms of inputs from the environment, outputs to the environment, and the physical amounts of imports and exports. Understanding economy-wide material flow is critical to understanding resource use by the economy and eco-efficiency.
- Water—an integrated approach to water monitoring, bringing together a wide range of water related statistics across sectors into one coherent information system. This serves as a conceptual framework and set of accounts which presents hydrological information alongside economic information in a consistent manner.

Figure 20.7 Overview of SEEA Central Framework

Natural inputs from the environment to the economy include mineral, timber, and water resources. Within the economy, industries, households, and governments produce and consume goods and services, or products. Residuals from the economy to the environment include air emissions and return flows of water (see also Figure 20.3).



Adapted from: UN (2014)

While SEEA CF considers individual environmental assets and how those assets move between the environment and the economy (see Figure 20.7), SEEA Experimental Ecosystem Accounting (SEEA EA) views the perspective of ecosystems and determines how individual environmental assets interact as part of natural processes within a given spatial area (see Figure 20.8). This framework is still considered 'experimental' but is currently undergoing a large, global revision process, with the aim of becoming a statistical standard. SEEA EA primarily accounts for the non-human elements of environmental-economic accounts. Although it still emphasises the goods and services benefitting humans, it considers ecosystem extent and condition, and the future capacity to produce and provide goods and services. These considerations can relate to land use and management practices, environmental sustainability and degradation, progress towards achieving set targets, or other long term environmental interventions through monitoring and evaluation (CoA, 2018). Currently this framework comprises a set of accounts to quantify ecosystems in terms of:

- ecosystem extent—serves as a common starting point for ecosystem accounting, by organising information on the extent of different ecosystem types within a country in terms of area;
- ecosystem condition—measures the overall quality of an ecosystem asset, and captures, in a set of key indicators, the state or functioning of the ecosystem in relation to both its naturalness and its potential to supply ecosystem services;
- ecosystem services—measures their supply as well as their corresponding users and beneficiaries, classified by broad national accounting categories or other groupings of economic units;
- monetary asset—records the monetary value of opening and closing stocks of all ecosystem assets within an ecosystem accounting area and additions and reduction to those stocks; and
- thematic—covers accounts for land, water, carbon, and biodiversity, which are standalone accounts on topics of importance in their own right for policy and analysis, but also of direct relevance in the compilation of ecosystem accounts.

The global revision process may see improved incorporation of environmental/ecosystem integrity, intrinsic values, biodiversity, and inter- and intra-ecosystem service flows that support environmental/ecosystem functioning into the SEEA EA (SEEA, 2020b).

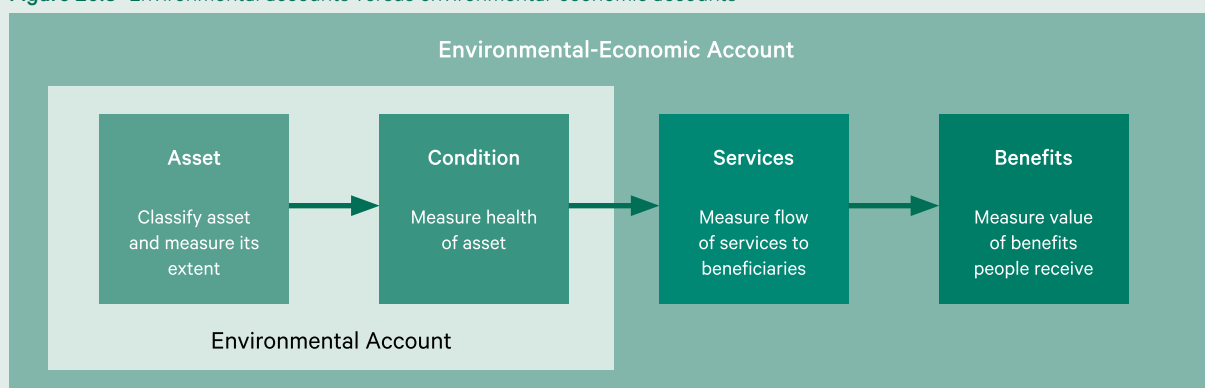
Thus, an environmental-economic account, such as SEEA, presents information in physical and monetary terms regarding environmental stocks and flows between the environment and the economy as well as economic activity related to the environment. By providing a full picture of its connection to the economy, environmental-economic accounts can help make the case for protecting and conserving biodiversity (see Section 19). Ecosystem accounts used in combination with information on expenditures provide decision makers with a clear picture of the return-on-investment from biodiversity protection. Examples of the kinds of questions that the SEEA can help answer include:

- Who benefits and who is negatively impacted from natural resource use? What are the impacts on the state of the environment and on specific sectors of the economy?
- How does depletion of natural resources affect measures of the real income of a nation? What extracting industries and owners of natural resources are responsible for depletion?
- To what extent is decoupling between resource use and economic growth taking place? Which sectors have the highest water productivity or are most energy intensive?
- How is the wealth of nations, specifically its natural capital, developing over time?
- Are the expenditures on environmental protection effective?
- To what extent is the tax system greening? What economic instruments are in place? And what is the impact of new instruments?

- What is the size of environmental investment in the economy? How many green jobs is the economy generating?
- Are current trends in production and consumption of resources sustainable? Is the amount of waste generated increasing or not; how much of this is being recycled in what economic sectors?
- What is the carbon footprint or water footprint of the nation?
- Which ecosystem services are being generated, who is benefiting from them, and where are they located?

Over 80 countries, including Australia, maintain active environmental-economic accounting programs based on SEEA. This is an ongoing project with updates, extensions, and resources being undertaken in several areas, including biodiversity and SDG (see Sections 19.3 and 20.4 respectively).

Figure 20.8 Environmental accounts versus environmental-economic accounts



Adapted from: CoA (2018) page 3

Economics has enthroned some of our most unattractive predispositions: material acquisitiveness, competition, gluttony, pride, selfishness, shortsightedness, and just plain greed.
(Henderson, 1978)

In Australia, the SEEA framework is used to generate the Australian Environmental Economic Accounts (AEEA) for the themes of water, energy, waste, and greenhouse gas emissions (ABS, 2019a). Some data used in AEEA is sourced externally, such as the National Carbon Accounting System (NCAS), that reports Australia's national and international greenhouse gas emissions (see Section 17). Other jurisdictions and private organisations have also applied this approach for specific areas of environmental accounting. Examples of Australian environmental economic accounts based on SEEA are listed in Table 20.7, some of which are derived from EO data sources (CoA, 2018).

A national plan entitled 'Environmental Economic Accounting—A Common National Approach: Strategy and Action Plan' (CoA, 2018) has the vision that the "Australian community understands the environment's contribution to our quality of life, and its condition and value are accounted for in decision making for a prosperous and healthy society". The Strategy is hoping to set up a level of consistency across the applications of SEEA within Australia, and is assisting in bringing together expertise and experience towards this purpose from federal, state, and territory government agencies, the private sector and academia (CoA, 2018).

This collaborative effort between the Australian Department of Agriculture, Water and the Environment (DAWE; formerly Department of Environment and Energy), its state and territory counterparts, and the ABS compiles data from various jurisdictions and agencies, with the aim of presenting an integrated perspective at a range of scales within Australia: national, single and multi-state/territory, regional, local, and farm. For example, a recent iteration of the ABS waste accounts (ABS, 2019b) was developed and released under this strategy. Current projects under the Strategy include:

- an experimental national land account (see Section 3.3.4);
- case studies of experimental ecosystem accounts; and
- pilot studies of ocean accounts (see Volume 3B).

ABS and the Bureau of Meteorology (BoM) have also collaborated to produce an integrated water account for the ACT (ABS, 2019c). These pilot accounts use the Australian Water Accounting Standard (AWAS; BoM, 2012) and SEEA frameworks to integrate two complementary Australian environmental-economic accounting approaches, namely the:

- ABS Water Account, Australia (WAA), which defines the:
 - ◆ flows of water from the environment to the water supply industry and other economic activities;
 - ◆ flows of water from the water supply industry to households and businesses; and the
 - ◆ monetary values associated with water supplied and used in the economy; and the
- BoM National Water Account (NWA), which defines the:
 - ◆ volume of water in the environment and its availability; and the
 - ◆ rights to abstract water and the actual abstraction over time (ABS, 2019c; see Excursus 10.2).

This collaboration produced a range of water accounts for the ACT in terms of water assets and liabilities, water condition and quality, as well as the physical and monetary supply and use of water. Such integrated, quantitative information is valuable for reporting and managing water resources for both the economy and the environment.

Table 20.7 Australian environmental economic accounts based on SEEA

These accounts quantify environmental resources in terms of the available assets and their supply and usage in both the environment and the economy. (ABS: Australian Bureau of Statistics; DEE: Department of Environment and Energy; DELWP Victorian Department of Environment, Land, Water and Planning; BoM: Bureau of Meteorology)

Account name	Agency	Subject	Scale	Measurement units	Frequency
Water Account, Australia	ABS	Water supply and use within the economy	National, state/territory	Megalitres, dollars	Annual
Energy Account, Australia	ABS	Energy supply and use within the economy	National	Petajoules, dollars	Annual
Waste Account, Australia	ABS/DEE	Waste generation by industry and households	National	Megatonnes, dollars	Annual
National Greenhouse Accounts	DEE	Greenhouse gas emissions	National, state/territory, industry	Tonnes of carbon equivalent	Annual
National Water Account	BoM	Availability and usage of water resources in the environment	National, regional	Megalitres	Annual
Natural Capital Finance Alliance	Natural Capital Coalition	Business dependencies on natural capital	Business	Varies	Varies
Land Account	ABS	Land use, land cover, and value	Regional, state/territory	Area (ha), dollars	Experimental
Experimental Ecosystem Accounts for the Great Barrier Reef Region	ABS	Ecosystem goods and services	Regional	Area, dollars	Experimental
Victorian Experimental Ecosystem Accounts	DELWP	Ecosystem extent and services indicator	State, regional	Area per unit time (e.g. ha/year)	Experimental
Integrated Water Accounts for the Canberra region	ABS/BoM	Water assets, supply, usage, and quality for society and environment	Territory	Megalitres, dollars	Pilot

Source: CoA (2018) Tables 1 and 2 and ABS (2019c)

SEEA requires time series data to establish the opening and closing stocks for the accounting period. It also requires the ability to undertake change detection for tracking flows, or reasons for change that can be linked to human use/management or to natural processes and disturbance regimes.

As introduced in Section 3.2, the Earth Observation Data for Ecosystem Monitoring (EODESM; Lucas and Mitchell, 2017; EcoPotential, 2021) constructs land cover categories for different points in time according to the Food and Agriculture Organisation (FAO) Land Cover Classification System (LCCS, Version 2; see Excursus 3.1) and has been advanced to include an evidence-based change framework that integrates the Drivers-Pressures-State-Impacts-Response framework (DPSIR; see Section 11.2) and a globally relevant taxonomy of change (Lucas *et al.*, *in prep*). This combined capability was implemented within Digital Earth Australia (DEA; see Volume 2D—Section 11.2) to generate continental maps of land cover and change dynamics for 2010 and 2015, that were subset for four test areas in eastern Australia (Lucas *et al.*, 2019) and used to support accounting under SEEA as demonstration.

Change detection requires consistency in data over time, not just availability (see Volume 2D). To effectively inform the decision making process, the frequency of the time series dataset is important. Some of the reasons for change will occur at short timescales at finer resolutions, while others are only visible in longer timescales at coarser resolutions. It is a balancing act to determine the range of end user requirements for environmental-economic accounts and match those requirements through to the correct spatial and non-spatial environmental, economic, and socio-cultural data and indicators (Vardon *et al.*, 2016).

As detailed in Sections 11–19 above, EO datasets, being timely, objective, repeatable, and relatively inexpensive, are appropriate for various environmental mapping, monitoring, and modelling studies (see Sections 8–10) in a wide range of applications involving terrestrial vegetation. Many global organisations, such as the UN Global Working Group on Big Data for Official Statistics (UN, 2020b), the Global Strategy to Improve Agricultural and Rural Statistics (GSARS, 2015, 2017), and GEO Earth Observations for Ecosystem Accounting (EO4EA; GEO, 2020b), are exploring the viability of deriving official statistics from a range of spatial data sources including EO, with methodological, legal, security, and privacy ramifications (UN, 2015). EO4EA “envision[s] a future where EO systems enable environmental transparency and the value of ecosystems is incorporated into conventional economic accounts and decision making, leading to an important shift in the valuation of natural resources and the use of that information for policy and programmatic decision making” (GEO, 2019). Some relevant guiding questions to assess the suitability of using EO data products for these purposes are given in García *et al.* (2016) and Murray *et al.* (2018).

The adoption of agriculture was the most fundamental change in human history. Not only did it produce settled societies for the first time, it also radically changed society itself. Gathering and hunting groups were essentially egalitarian, but sedentary communities, almost from the beginning, resulted in increasing specialisation within society and the emergence of religious, political and military elites and a state with the power to direct the rest of society. At the root of these social changes was a new attitude to the ownership of food. Gathering and hunting groups generally regarded plants and animals not as things ‘owned’ by individuals but as available to all. Plants and animals are taken from the wild and there are normally strong social conventions on how food must be shared between all members of the group. Agriculture introduced the idea of ownership of food either by individuals or larger organisations. The move to growing crops in fields and the practice of herding and breeding flocks of animals opened the way to viewing resources used and the food produced as ‘property’ and the far greater degree of time and effort involved compared with gathering and hunting encouraged this trend.

(Ponting, 1991)

20.6 Further Information

Sustainable Development (UN)

Sustainable Development Goals: <https://sustainabledevelopment.un.org>

Sendai Framework for Disaster Risk Reduction 2015–2030: <https://sustainabledevelopment.un.org/frameworks/sendaiframework>

Addis Ababa Action Agenda of the Third International Conference on Financing for Development: <https://sustainabledevelopment.un.org/frameworks/addisababaactionagenda>

Transforming our world: the 2030 Agenda for Sustainable Development: <https://sustainabledevelopment.un.org/post2015/transformingourworld>

United Nations Sustainable Development Summit 2015: <https://sustainabledevelopment.un.org/post2015/summit>

Paris Agreement: <https://sustainabledevelopment.un.org/frameworks/parisagreement>

Division for Sustainable Development Goals: <https://sustainabledevelopment.un.org/about>

High-Level Political Forum on Sustainable Development: <https://sustainabledevelopment.un.org/hlpf>

GEO: Earth Observation for Sustainable Development: <https://eo4sd.esa.int/>

https://www.earthobservations.org/documents/publications/201703_geo_eo_for_2030_agenda.pdf

https://www.earthobservations.org/documents/publications/201704_geo_unggim_4pager.pdf

Ecosystem Services

Intergovernmental Science-Policy Platform on Biodiversity and Ecosystem Services (IPBES): <https://ipbes.net/>

Environmental-Economic/Ecosystem Accounting

UN Framework: System of Environmental-Economic Accounting (SEEA): <https://seea.un.org/>

Earth Observation for Ecosystem Accounting (EO4EA): <https://www.eo4ea.org/>

Wealth Accounting and the Valuation of Ecosystem Services (WAVES): <https://www.wavespartnership.org/>

Australian Environmental-Economic Accounts

ABS: <https://www.abs.gov.au/Environmental-Management>

Australian Environmental Information Systems

NEII (National Environmental Information Infrastructure): <http://neii.gov.au/data-viewer>

Accounting for Nature (AfN) Framework: <https://www.accountingfornature.org/>

OzWALD:

Australia's Environment: http://wald.anu.science/data_services/data/continuous-and-comprehensive-national-environmental-reporting-australias-environment/

Australia's Environmental Explorer: www.ausenv.online

State of Environment: SOE 2016: <https://www.environment.gov.au/science/soe>

State-based Environmental Monitoring

Statewide Landcover and Trees Study (SLATS, Queensland): <https://www.qld.gov.au/environment/land/management/mapping/statewide-monitoring/slats>

Ground cover monitoring (Queensland): <https://www.qld.gov.au/environment/land/management/mapping/statewide-monitoring/groundcover>

SLATS NSW: <https://www.environment.nsw.gov.au/topics/animals-and-plants/native-vegetation/reports-and-resources>

Habitat Hectares (Victoria): <https://www.environment.vic.gov.au/native-vegetation/native-vegetation/biodiversity-information-and-site-assessment>

Spatial data for Victoria: https://www2.delwp.vic.gov.au/maps?_ga=2.6531511.420315026.1549698228-873342548.1549698228

20.7 References

- AfN (2020). *Accounting for Nature* website: <https://www.accountingfornature.org/>
- ABS (2018). *Australian Environmental-Economic Accounts, 2018*, webpage: <http://www.abs.gov.au/ausstats/abs@.nsf/mf/4655.0>
- ABS (2019a). *Australian Environmental-Economic Accounts, 2019*, webpage: <https://www.abs.gov.au/AUSSTATS/abs@.nsf/Lookup/4655.0Explanatory%20Notes12019?OpenDocument>
- ABS (2019b). *Waste Account, Australia, Experimental Estimates, 2016–17* webpage: <https://www.abs.gov.au/ausstats/abs@.nsf/mf/4602.0.55.005>
- ABS (2019c). *Integrated Water Accounts for the Canberra region, 2013–14 to 2016–17* webpage: <https://www.abs.gov.au/AUSSTATS/abs@.nsf/mf/4610.0.55.010>
- Alcaraz-Segura, D., Di Bella, C.M., and Straschnoy, J.V. (Eds) (2014). *Earth Observation of Ecosystem Services*. CRC Press, Boca Raton. ISBN: 978-1-4665-0589-6
- Andrew, M.E., Wulder, M.A., and Nelson, T.A. (2014). Potential contributions of remote sensing to ecosystem service assessments. *Progress in Physical Geography*, 38(3), 328–353. doi:10.1177/0309133314528942
- Andrew, M.E., Wulder, M.A., Nelson, T.A., and Coops, N.C. (2015). Spatial data, analysis approaches, and information needs for spatial ecosystem service assessments: a review. *GIScience and Remote Sensing*, 52(3), 344–373. doi:10.1080/15481603.2015.1033809
- Barbier, E.B. (1987). The concept of sustainable economic development. *Environmental Conservation*, 14, 101–110. <https://doi.org/10.1017/S0376892900011449>
- Bestelmeyer, B.T., and Briske, D.D. (2012). Grand challenges for resilience-based management of rangelands. *Rangeland Ecology and Management*, 65, 654–663.
- Birkhofer, K., Diehl, E., Andersson, J., Ekroos, J., Früh-Müller, A., Machnikowski, F., Mader, V.L., Nilsson, L., Sasaki, K., Rundlöf, M., Wolters, V., Smith, H.G. (2015). Ecosystem services—current challenges and opportunities for ecological research. *Frontiers in Ecology and Evolution*, 2, 87. <https://www.frontiersin.org/article/10.3389/fevo.2014.00087>
- Böhringer and Jochem (2007). Measuring the immeasurable—A survey of sustainability indices. *Ecological Economics*, 63, 1–8.
- BoM (2012). *Australian Water Accounting Standard 1: Preparation and Presentation of General Purpose Water Accounting Reports*. Water Accounting Standards Board, Bureau of Meteorology. ISBN 978-0-642-70629-4 http://www.bom.gov.au/water/standards/documents/awas1_v1.0.pdf
- BoM (2013). *Guide to environmental accounting in Australia, Environmental Information Programme Publication Series no. 3*, Bureau of Meteorology, Canberra, Australia.
- Borucke, M., Moore, D., Cranston, G., Gracey, K., Iha, K., Larson, J., Lazarus, E., Morales, J.C., Wackernagel, M., and Galli, A. (2013). Accounting for demand and supply of the biosphere’s regenerative capacity: The National Footprint Accounts’ underlying methodology and framework. *Ecological Indicators*, 24, 518–533. <https://doi.org/10.1016/j.ecolind.2012.08.005>
- Boyer, R., Peterson, N., Arora, P., Caldwell, K. (2016). Five approaches to social sustainability and an integrated way forward. *Sustainability*, 8, 1–18. <https://doi.org/10.3390/su8090878>
- Brand, U. (2012). Green economy—The next oxymoron? *GAIA—Ecological Perspectives on Science and Society*, 21, 5.
- Brown, B.J., Hanson, M.E., Liverman, D.M., and Merideth, R.W. (1987). Global sustainability: Toward definition. *Environmental Management*, 11, 713–719. <https://doi.org/10.1007/BF01867238>
- CoA (2018). *Environmental Economic Accounting: A Common National Approach Strategy and Action Plan*. Prepared by the Interjurisdictional Environmental-Economic Accounting Steering Committee for the Meeting of Environment Ministers, Commonwealth of Australia. <https://eea.environment.gov.au/about/national-strategy-and-action-plan>
- Cord, A.F., Brauman, K.A., Chaplin-Kramer, R., Huth, A., Ziv, G., and Seppelt, R. (2017). Priorities to advance monitoring of ecosystem services using Earth observation. *Trends in Ecology and Evolution*, 32(6), 416–428. ISSN 0169-5347
- Costanza, R., d’Arge, R., de Groot, R., Farber, S., Grasso, M., Hannon, B., Limburg, K., Naeem, S., Oneill, R.V., Paruelo, J., Raskin, R.G., Sutton, P., van den Belt, M. (1997). The value of the world’s ecosystem services and natural capital. *Nature*, 387(6630), 253–260.

- Costanza, R., de Groot, R., Braat, L., Kubiszewski, I., Fioramonti, L., Sutton, P., Farber, S., and Grasso, M. (2017). Twenty years of ecosystem services: How far have we come and how far do we still need to go? *Ecosystem Sciences*, 28, 1–16. <https://doi.org/10.1016/j.ecoser.2017.09.008>
- Custance, J., and Hillier, H. (1998) Statistical issues in developing indicators of sustainable development. *Journal of the Royal Statistical Society*, 161, 281–290.
- Daily, G.C. (1997). *Nature's Services: Societal Dependence on Natural Ecosystems*. Island Press, Washington DC.
- Dawson, T.P., Cutler, M.E.J., and Brown, C. (2016). The role of remote sensing in the development of SMART indicators for ecosystem services assessment, *Biodiversity*, 17(4), 136–148. doi:10.1080/14888386.2016.1246384
- de Araujo Barbosa, C.C., Atkinson, P.M., and Dearing, J.A. (2015). Remote sensing of ecosystem services: A systematic review. *Ecological Indicators*, 52, 430–443.
- DEWHA (2010). *Ecosystem Services: Key Concepts and Applications*. Occasional Paper No 1, Department of the Environment, Water, Heritage and the Arts, Canberra.
- Ehrlich, P., and Ehrlich, A. (1981). *Extinction: The Causes and Consequences of the Disappearance of Species*. Random House, New York.
- Elkington, J. (1997). *Cannibals with forks: the triple bottom line of 21st century business*. Capstone, Oxford.
- EcoPotential (2021). *EODESM: Earth Observation Data for Ecosystem Monitoring* webpage, EcoPotential website: <http://www.ecopotential-project.eu/products/eodesm.html>
- Flichman, G., and Allen, T. (2013). *Bio-Economic Modeling: State-of-the-Art and Key Priorities*. Working Paper, International Food Policy Research Institute, Washington. <http://ebrary.ifpri.org/utils/getfile/collection/p15738coll2/id/129231/filename/129442.pdf>
- García, L., Rodríguez, J.D., Wijnen, M., Pakulski, I. (Eds) (2016). *Earth Observation for Water Resources Management: Current Use and Future Opportunities for the Water Sector*. World Bank Group, Washington, D.C. doi:10.1596/978-1-4648-0475-5.
- GEO (2017). *Earth Observations in support of the 2030 Agenda for Sustainable Development*. JAXA. https://www.earthobservations.org/documents/publications/201703_geo_eo_for_2030_agenda.pdf
- GEO (2019). *Implementation Plan for the Earth Observation for Ecosystem Accounting (EO4EA) Initiative. 2020–2022 GEO Work Program*. Group on Earth Observation. http://earthobservations.org/documents/gwp20_22/eo_for_ecosystem_accounting_ip.pdf
- GEO (2020a). *Earth Observations for the Sustainable Development Goals* webpage, Group on Earth Observation website: https://www.earthobservations.org/geo_sdgs.php
- GEO (2020b). *Earth Observations for Ecosystem Accounting* website, Group on Earth Observations: <https://www.eo4ea.org/>
- GFN (2020). *Global Footprint Network* website: <https://www.footprintnetwork.org/>
- Goldsmith, E., and Allen, R. (1972). A Blueprint for Survival. *The Ecologist*, 2(1). <https://web.archive.org/web/20090831193545/http://www.theecologist.info/key27.html>
- Gordon, J., Vincent, D., Haberkorn, G., MacGregor, C., Stafford-Smith, M., and Breckwoldt, R. (2001). *Indicators within a decision framework: Social, economic and institutional indicators for sustainable management of the rangelands*. National Land and Water Resources Audit, Canberra.
- GSARS (2015). *Handbook on Master Sampling Frames for Agricultural Statistics: Frame Development, Sample Design and Estimation*. Global Strategy to Improve Agricultural and Rural Statistics, UN Statistical Commission, Rome. <http://gsars.org/wp-content/uploads/2016/02/MSF-010216-web.pdf>
- GSARS (2017). *Handbook on Remote Sensing for Agricultural Statistics*. Global Strategy to Improve Agricultural and Rural Statistics, UN Statistical Commission, Rome. <http://gsars.org/wp-content/uploads/2017/09/GS-REMOTE-SENSING-HANDBOOK-FINAL-04.pdf>
- Hajer, M.A. (1995). *The politics of environmental discourse: Ecological modernization and the policy process*. Oxford University Press, Oxford.
- Henderson, H. (1978). *Creating Alternative Futures: The End of Economics*. Kumarin Press, West Hartford. <https://sustainable-finance.io/wp-content/uploads/2018/04/Creating-AF.pdf>
- Hugé, J., Waas, T., Dahdoub-Guebas, F., Koedam, N., and Blocak, T. (2013). A discourse-analytical perspective on sustainability assessment: interpreting sustainable development in practice. *Sustainability Science*, 8, 187–198. doi:10.1007/s11625-012-0184-2

- Jacobs, P., Gardner, J., and Munro, D.A. (1987). Sustainable and equitable development: an emerging paradigm. *Conservation with equity: strategies for sustainable development*. (Eds: Jacobs, P., and Munro, D.A.) IUCN, Cambridge. pp 17–29.
- Johnston, P., Everard, M., Santillo, D., Robert, K.-H. (2007). Reclaiming the definition of sustainability. *Environmental Science and Pollution Research*, 14, 60–66. <https://doi.org/10.1065/espr2007.01.375>
- Jurskis, V. (2015). *Firestick Ecology*. Connor Court Publishing, Ballarat. 335 p. ISBN: 9781925138740
- Keith, D.A., Rodríguez, J.P., Rodríguez-Clark, K.M., Nicholson, E., Aapala, K., Alonso, A., Asmussen, M., Bachman, S., Basset, A., Barrow, E.G., Benson, J.S., Bishop, M.J., Bonifacio, R., Brooks, T.M., Burgman, M.A., Comer, P., Comín, F.A., Essl, F., Faber-Langendoen, D., Fairweather, P.G., Holdaway, R.J., Jennings, M., Kingsford, R.T., Lester, R.E., Nally, R. Mac, McCarthy, M.A., Moat, J., Oliveira-Miranda, M.A., Pisanu, P., Poulin, B., Regan, T.J., Riecken, U., Spalding, M.D., and Zambrano-Martínez, S. (2013). Scientific Foundations for an IUCN Red List of Ecosystems. *PLoS ONE*, 8(5), e62111. doi:10.1371/journal.pone.0062111
- Kidd, C.V. (1992). The evolution of sustainability. *Journal of Agricultural and Environmental Ethics*, 5, 1–26. <https://doi.org/10.1007/BF01965413>
- Kirchweger, S., Clough, Y., Kapfer, M., Steffan-Dewenter, I., and Kantelhardt, J. (2020). Do improved pollination services outweigh farm-economic disadvantages of working in small-structured agricultural landscapes? Development and application of a bio-economic model. *Ecological Economics*, 169, 106535. <https://doi.org/10.1016/j.ecolecon.2019.106535>
- Krausmann, F., Gingrich, S., Eisenmenger, N., Erb K. H., Haberl, H., and Fischer-Kowalski, M. (2009). Growth in global materials use, GDP and population during the 20th century. *Ecological Economics*, 68(10), 2696–2705.
- Lucas, R., and Mitchell, A., (2017). Integrated Land Cover and Change Classifications. In *The Roles of Remote Sensing in Nature Conservation: A Practical Guide and Case Studies*. (Eds: Díaz-Delgado, R., Lucas, R., Hurford, C.). Springer, Cham, Switzerland. pp. 295–308.
- Lucas, R., Mueller, N., Siggins, A., Owers, C., Clewley, D., Bunting, P., Kooymans, C., Tissot, B., Lewis, B., Lymburner, L., and Metternicht, G. (2019). Land Cover Mapping using Digital Earth Australia. *Data*, 4, 143. doi:10.3390/data4040143
- Lucas, R.M., German, S., Metternicht, G., Schmidt, B., Owers, C., Prober, S., Richards, A., Tretreault-Campbell, S., Williams, K., Mueller, N., Tissot, B., Chua, S., Colwood, A., Hills, T., Gunawardana, D., McIntyre, A., Chognard, S., Hurford, C., Planque, C., Punalekar, S., Clewley, D., Murray, D., Manakos, I., Blonda, P., Sonnerschein, R., Bunting, P., and Horton, C. (in prep.). A Globally Relevant Change Taxonomy and Evidence-based Change Classification Framework. *Global Change Biology*, submitted July 2021.
- MEA (2005). *Ecosystems and Human Well-being: Synthesis*. Millennium Ecosystem Assessment, Island Press, Washington, DC.
- Munasinghe, M. (1993). *Environmental economics and sustainable development*. The World Bank, Washington
- Murray, N.J., Keith, D.A., Bland, L.M., Ferrari, R., Lyons, M.B., Lucas, R., Pettorelli, N., Nicholson, E. (2018). The role of satellite remote sensing in structured ecosystem risk assessments. *Science of the Total Environment*, 619–620, 249–257. <https://doi.org/10.1016/j.scitotenv.2017.11.034>
- Ogilvy, S. (2020). *Toward a methodology for incorporating ecological capital into the accounts of individual entities*. Ph.D. Thesis, ANU. <https://openresearch-repository.anu.edu.au/handle/1885/204830>
- Pettorelli, N., Schulte, Bühne, H., Tulloch, A., Dubois, G., Macinnis-Ng, C., Queirós, A.M., Keith, D.A., Wegmann, M., Schrodt, F., Stellmes, M., Sonnenschein, R., Geller, G.N., Roy, S., Somers, B., Murray, N., Bland, L., Geijzendorffer, I., Kerr, J.T., Broszeit, S., Leitão, P.J., Duncan, C., El Serafy, G., He, K.S., Blanchard, J.L., Lucas, R., Mairota, P., Webb, T.J., Nicholson, E. (2017). Satellite remote sensing of ecosystem functions: opportunities, challenges and way forward. *Remote Sensing in Ecology and Conservation*, 4, 71–93. <https://doi.org/10.1002/rse2.59>.
- Pollock, D. (2019). *The Wooleen Way*. Scribe, Melbourne. ISBN: 9781925849257
- Ponting, C. (1991). *A Green History of the World*. Penguin.
- Purvis, B., Mao, Y., and Robinson, D. (2018). Three pillars of sustainability: in search of conceptual origins. *Sustainability Science*, 14, 681–695. <https://doi.org/10.1007/s11625-018-0627-5>

- Ramirez-Reyes, C., Brauman, K.A., Chaplin-Kramer, R., Galford, G.L., Adamo, S.B., Anderson, C.B., Anderson, C., Allington, G.R.H., Bagstad, K.J., Coe, M.T., Cord, A.F., Dee, L.E., Gould, R.K., Jain, M., Kowal, V.A., Muller-Karger, F.E., Norriss, J., Potapov, P., Qiu, J., Rieb, J.T., Robinson, B.E., Samberg, L.H., Singh, N., Szeto, S.H., Voigt, B., Watson, K., and Wright, T.M. (2019). Reimagining the potential of Earth observations for ecosystem service assessments. *Science of the Total Environment*, 665, 1053–1063. doi:10.1016/j.scitotenv.2019.02.150.
- Redclift, M. (2005). Sustainable Development (1987–2005): An Oxymoron Comes of Age. *Sustainable Development*, 13, 212–227. doi:10.1002/sd.281
- Schumacher, E.F. (1973). *Small is Beautiful: A Study of Economics as if People Mattered*. <https://web.archive.org/web/20141014171926/http://www.ditext.com/schumacher/small/small.html>
- SEEA (2018). *The Role of the System of Environmental-Economic Accounting as a Measurement Framework in Support of the post-2020 Agenda*. System of Environmental Economic Accounting, UN Committee of Experts on Environmental-Economic Accounting. https://seea.un.org/sites/seea.un.org/files/seea_2020_final.pdf
- SEEA (2020a). *System of Environmental Economic Accounting webpage*: <https://seea.un.org/ecosystem-accounting>
- SEEA (2020b). *SEEA EEA Revision: Research Areas webpage*: <https://seea.un.org/content/seea-eea-revision-research-areas>
- Smith, A. (1776). *Inquiry into the Nature and Causes of the Wealth of Nations*. Strahan and Cadell, London.
- Stritih, A., Bebi, P., and Grêt-Regamey, A. (2019). Quantifying uncertainties in earth observation-based ecosystem service assessments. *Environmental Modelling and Software*, 111, 300–310.
- Thackway, R. (Ed.) (2018). *Land Use in Australia: Past, Present and Future*. ANU eVIEW, Canberra. ISBN: 9781921934421
- The Brundtland Report (1987). *Report of the World Commission on Environment and Development: Our Common Future*. UN. <https://sustainabledevelopment.un.org/content/documents/5987our-common-future.pdf>
- UN (2014). *System of Environmental-Economic Accounting 2012: Experimental Ecosystem Accounting*, European Commission, Organisation for Economic Co-Operation and Development, United Nations and World Bank. eISBN: 978-92-1-056285-0. https://unstats.un.org/unsd/envaccounting/seearev/eea_final_en.pdf
- UN (2015). *Report of the Global Working Group on Big Data for Official Statistics*. UN Economic and Social Council E/CN.2/2014/4. <https://unstats.un.org/unsd/statcom/doc15/2015-4-BigData-E.pdf>
- UN (2019). *The Sustainable Development Goals Report*. UN, Rome. <https://unstats.un.org/sdgs/report/2019/>; <https://unstats.un.org/sdgs/report/2019/The-Sustainable-Development-Goals-Report-2019.pdf>
- UN (2020a). *Sustainable Development Goals Indicators website*: <https://unstats.un.org/sdgs/?aspxerrorpath=/sdgs/indicators/Official> (List of all indicators: https://unstats.un.org/sdgs/indicators/Global%20Indicator%20Framework%20after%202020%20review_Eng.pdf)
- UN (2020b). *Satellite Imagery and Geo-Spatial Data webpage*, BigData UN Global Working Group: <https://unstats.un.org/bigdata/taskteams/satellite/>
- Vallecillo, S., La Notte, A., Polce, C., Zulian, G., Alexandris, N., Ferrini, S., and Maes, J. (2018). *Ecosystem services accounting: Part I - Outdoor recreation and crop pollination*. EUR 29024 EN, Publications Office of the European Union, Luxembourg. JRC110321. doi:10.2760/619793
- van Dijk, A., Summers, D., Renzullo, L., and Yebra, M. (2017). *OzWALD Gridded Environmental Data for Australia*. v2. CSIRO. Data Collection. <https://doi.org/10.4225/08/5a3c52da083b8>
- van Dijk, A., and Rahman, J. (2019). *Synthesising multiple observations into annual environmental condition reports: the OzWALD system and Australia's Environment Explorer*. MODSIM2019, Canberra.
- Vardon, M., Burnett, P., and Dovers, S. (2016). The accounting push and the policy pull: balancing environment and economic decisions. *Ecological Economics*, 124, 145–152.
- Vardon, M., Ovington, J., Juskevics, V., Purcell, J., and Eigenraam, M. (2018). Down Payments on National Environmental Accounts. Ch. 14 in *Land Use in Australia: Past, Present and Future*. (Ed: Thackway, R.). ANU eVIEW, Canberra. ISBN: 9781921934421
- Wackernagel, M., Beyers, B., and Rout, K. (2019). *Ecological Footprint: Managing our Biocapacity Budget*. New Society Publishers. ISBN: 9780865719118
- Westman, W.E. (1977). How much are nature's services worth? *Science*, 197(4307), 960–964.
- WGCS (2016). *Accounting for Nature: A scientific method for constructing environmental asset condition accounts*. Wentworth Group of Concerned Scientists, Sydney. <https://static1.squarespace.com/static/5dc38cde1d028031235ca3cf/t/5ec60133aaeb a61a09874858/1590034904424/Wentworth-Group-2016-Accounting-for-Nature.pdf>

Nature is not a place to visit, it is home.
(Gary Snyder)

Observing Our Future



*One generation passes and another comes, but the world forever stays.
(Ecclesiastes 1:3)*

Contents

21 The Road Ahead

479



21 The Road Ahead

A growing range of EO technologies is supplying more data—in more detail and more quickly—over the whole Earth, which, with appropriate analysis, can help us to use our finite resources for the maximum benefit of current and future populations. But exactly how will EO impact the stewardship of Australian terrestrial vegetation into the future? In these final sub-sections, we consider:

- smart technology to help the environment (see Section 21.1);
- an objective outlook on global problems (see Section 21.2);
- the benefits of EO-based solutions to society (Section 21.3); and, in conclusion,
- the attitudinal change required to share a sustainable future (see Section 21.4).

479

21.1 The Smart Environment

The Internet of Things (IoT) and Integrated ‘Smart’ Systems were introduced in Volume 1B—Section 10. The IoT is defined as “the network of physical objects that contain embedded technology to communicate and sense or interact with their internal states or the external environment” (Gartner, 2020). The projected development of this technology over time is summarised in Figure 21.1.

Smart systems integrate sensing technologies with cognitive functions. These systems are being implemented in a wide range of industrial, scientific, agricultural, medical, educational, environmental, and infrastructure applications. Advances continue at an accelerated pace for both urban and rural populations with the potential uses of these ubiquitous technologies being literally limited by imagination.

Forecasts from the International Data Corporation (IDC) suggest that the many billions of devices connected to the IoT will generate a staggering 80 ZB of data by 2025 (Futureiot, 2019)¹⁸. These sensors build on a wide variety of technologies that have become established around the globe, including rapid telecommunications, accurate positioning (see Volume 2B), artificial intelligence (see Volume 2E), high speed computing, and data integration (see Volume 2D). IoT is measuring and remotely controlling ‘things’ that had not been connected with previous technology, thus reaching more individuals, communities, and locations (WEF, 2020a).

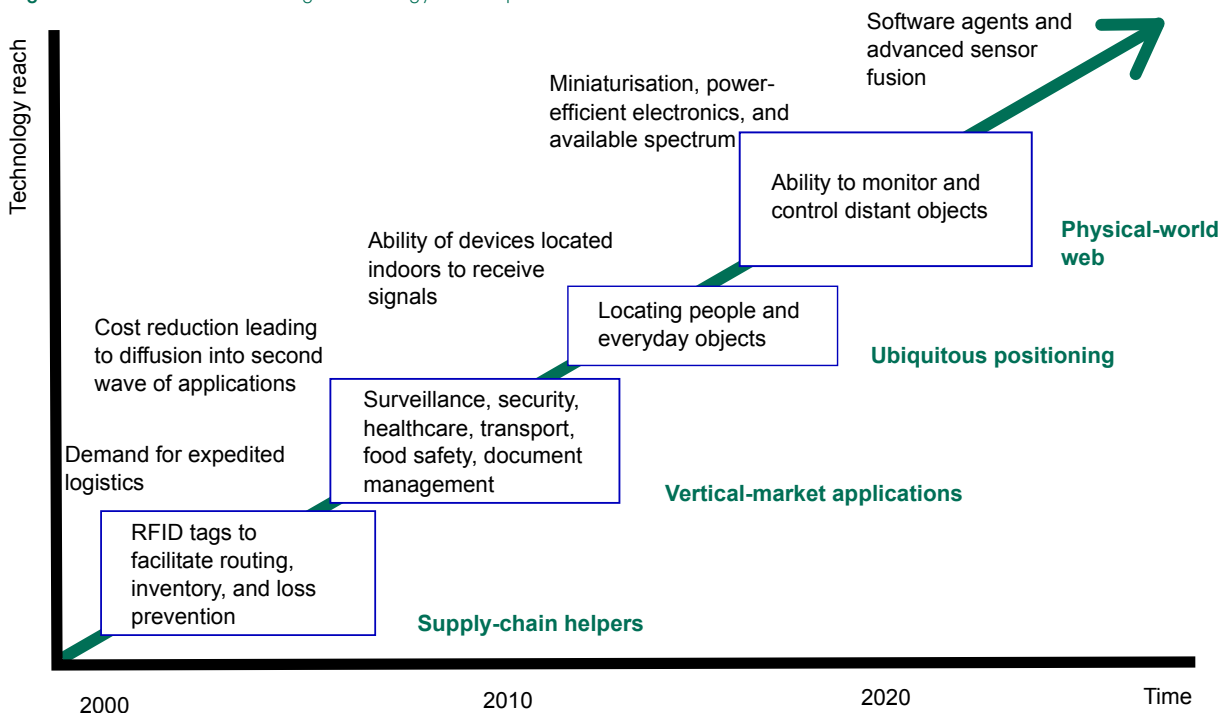
Towns and cities can also be viewed as modified, human-dominated ecosystems that require flows of resource inputs from which energy, water and materials are extracted and used to support human wellbeing and culture, while producing concentrated waste streams that are detoxified and absorbed by nature. Efforts to increase the reuse and recycling of waste materials can be seen as shifting ecosystems into a more cyclic form, closer to the pattern of natural ecosystems.

(DEWHA, 2010)

¹⁸ 1 ZB (Zettabyte) = a billion TB (Terabytes) = 1,000,000,000,000,000,000 bytes

Background image: Sentinel-2B image acquired on 14 February 2019 showing the Diamantina River, Queensland, in full flood, with flood waters cutting Springvale Road, near Diamantina Lakes. This image is displayed using bands 4, 8, 2 (red, NIR and blue) as RGB. **Source:** Norman Mueller, Geoscience Australia

Figure 21.1 The Internet of Things technology roadmap



Source: SRI Consulting Business Intelligence/National Intelligence Council, Wikimedia Commons. (Retrieved from https://commons.wikimedia.org/wiki/File:Internet_of_Things.svg)

The IoT for Sustainable Development project by the World Economic Forum (WEF) is encouraging the use of IoT for rapid implementation of the UN Sustainable Development Goals (SDG; WEF, 2020b; see Excursus 20.2). This project is analysing over 640 existing IoT system deployments in terms of their social value. The five key performance indicators for IoT systems are:

- scale of project—what is the impact of this system on individuals, social sectors and geographic region and extent?
- target penetration—how many SDG targets are benefitted by each system?
- influence of targets—what is the potential effectiveness of each system towards each target?
- scalability and replicability—is the system structurally scalable to improve the benefits to target and can the system be replicated to achieve other targets?
- focus on vulnerable groups—does the system significantly focus on vulnerable, underdeveloped, or underserved groups?

Results thus far indicate that 84% of the IoT systems currently being used can benefit SDGs and that three-quarters of these systems focus on just five SDGs (ordered in terms of decreasing target impact—see Excursus 20.2):

- SDG-9—industry, innovation, and infrastructure;
- SDG-11—smart cities and communities;
- SDG-7—affordable and clean energy;
- SDG-3—good health and wellbeing; and
- SDG-12—responsible production and consumption.

Many of these projects monitor resources with direct impact on vulnerable communities, such as water quality, air pollution, or energy usage. 95% of current IoT projects were found to be small to medium scale, so one challenge will be to improve the scalability of these projects in the future. While various forms of technology have directly contributed to environmental degradation, this may be one area where digital technology can help to resolve the global challenges of resource shortages, waste management, and environmental pollution.

*Anyone who thinks that you can have infinite growth in a finite environment is either a madman or an economist.
(David Attenborough)*

Smart systems simplify data collection and analysis, reduce maintenance costs, and improve performance. Current environmental applications include monitoring the quality and other properties of air, water, and soil in real time (Aitkenhead *et al.*, 2013). For environmental applications, some questions to ponder when deploying smart technologies are:

- Is the observer changing the observed? How would we know?
- Who can access the data? Does access to some data sources need to be limited for security, privacy, or commercial reasons?
- How would the system recover from sabotage, accidents, or malfunctions?
- Many EO and smart sensor applications involve implicit reliance on international goodwill, but how enduring is this?

As detailed in previous sections, calibrated and validated EO datasets have many well-established benefits for the mapping, monitoring, and modelling of terrestrial vegetation, including consistency over space and time, locational accuracy with global coverage, and ready integration with other spatial datasets. Selection of the most appropriate data and processing options for specific applications is described in Volume 2D—Section 2. Recent advances in freely available, web-based access to calibrated time series datasets and Analysis Ready Data (ARD, such as DEA, see Volume 2D—Section 11.2) simplify usage of these enormous archives.

For example, since 2002, the intergovernmental Group on Earth Observations (GEO) has been encouraging member governments to coordinate projects, strategies, and investments in EO for the benefit of both public and private users (GEO, 2020). A key component of its mission is to build the Global Earth Observation System of Systems (GEOSS), a set of coordinated, independent data and processing systems based on EO, that are accessible and interoperable, with identified quality and provenance (GEOSS, 2017). The goal of GEOSS is to deliver the data and information necessary to:

- bring qualitative improvements in our understanding of the Earth system (see Volume 1A—Section 4); and
- enhance the ability to make global policies and decisions that promote the environment and human health, safety, and welfare.

Advanced algorithms for processing massive data volumes are now being tailored for EO data and packaged for non-specialised users, with increasing reliance on web-based workflows (Sudmanns *et al.*, 2019). The ‘traditional’ approach to producing EO-based information required that the complete dataset be downloaded, analysed locally, then transformed into a map, which is delivered to the end user along a one-way path (see Volume 1B—Section 9.3). This traditional model is progressively being replaced by an online workflow, where the data provider generates ARD in a cloud environment in which EO analysts can access and process them. The end product would also reside within the cloud environment, to be accessed by the end user.

Thus, the distinction between smart technologies and EO-based systems is blurring over time, with both being reliant on the IoT, advanced analytical tools, and accessible, interactive interfaces, including virtual reality and augmented reality (Lymburner *et al.*, 2019). Selected examples of integrated, EO-based systems for managing natural resources include:

- Terrestrial Observation and Prediction System (TOPS)—integrates ecosystem models with satellite and surface weather observations to produce ecosystem nowcasts and forecasts for natural resources management, public health, and disaster management (Nemani *et al.*, 2009; NASA, 2020);
- Digiscope Future Science Platform (CSIRO)—uses EO data with environmental models to improve profitability and environmental outcomes from Australian agriculture (see Section 21.5); and
- Google Earth Engine and associated applications that rely on cloud computing, such as remap—online mapping platform to map and report the status of ecosystems (remap, 2020; see Section 19.4).

Our contemporary culture, primed by population growth and driven by technology, has created problems of environmental degradation that directly affect all of our senses: noise, odours and toxins, which bring physical pain and suffering, and ugliness, barrenness, and homogeneity of experience, which bring emotional and psychological suffering and emptiness. In short, we are jeopardizing our human qualities by pursuing technology as an end rather than a means. Too often we have failed to ask two necessary questions: First, what human purpose will a given technology or development serve? Second, what human and environmental effects will it have?
(U.S. Senate Public Works Committee, 1969)

21.2 An Objective Worldview

Sections 11 to 20 above describe the mapping, monitoring, and modelling of terrestrial vegetation for different applications. Despite advanced technologies such as EO, which can accurately track environmental degradation, the scale of the devastation is not being reduced. A glance at history confirms that this is not a new problem (see Excursus 11.2). However, the extent of problems relating to food security, various forms of pollution, soil fertility and erosion, landscape degradation, deforestation, carbon emissions, biodiversity loss, overpopulation, and excess consumption have grown markedly in the past few decades. For example, the human appropriation of net primary production (HANPP)—human usage of global NPP for food, timber, and fuel—is now estimated as 13–25%, which is double the estimate for a century ago (Krausmann *et al.*, 2013). Other estimates such as the Global Footprint Network, which monitors sustainability (see Excursus 20.3), suggest that we are already substantially eating into the environmental capital of future generations.

One of the greatest dangers in environmental management is to allow current decisions to maximise the gains of the current population (or part thereof) to the detriment of future populations. A glance at the legislative control measures introduced to manage the Australian—and other—terrestrial environments provides numerous examples of the underlying principle of human manipulation of well-intended policy. This phenomenon is captured in Goodhart's Law and Campbell's law, that is:

Any observed statistical regularity will tend to collapse once pressure is placed upon it for control purposes.

or

When a measure becomes a target, it ceases to be a good measure.

(Charles Goodhart—Goodhart's Law)

and

The more any quantitative social indicator is used for social decision-making, the more subject it will be to corruption pressures and the more apt it will be to distort and corrupt the social processes it is intended to monitor.

or

Evidence-based policy tends to morph into policy-based evidence.

(Donald T. Campbell—Campbell's law)

The world is now facing significant environmental problems that have been derived from a long term, subjective, and blinkered view of global resources in the face of accelerating population growth (see Sections 19 and 20). At this juncture, it would be prudent to step back and take an objective view of human societies—past and present—and their interactions with their environments (see Excursus 11.2). To avoid further degradation, we need to identify the existing environmental problems and their major drivers, then understand the interconnections between the different drivers and different problems. To achieve an objective view of the world, indicators based on science—untainted by vested interests and ideologies—need to be defined and consistently tracked for each major driver on a global basis. While the technology to support this approach exists, the objectivity of many accepted indicators has already been questioned (Böhringer and Jochem, 2007).

The field of environmental-economic accounting is relatively new but holds promise for considering the environmental impacts of economic activities (see Section 20.5). In most nations—including Australia—the primary metric for the economy is gross domestic product (GDP), which does not account for environmental degradation, natural resource depletion, or loss of biodiversity (Obst, 2017). A key challenge for improving environmental visibility in our national decision making process is to demonstrate how the environment contributes to the prosperity and wellbeing of all Australians. Effective implementation of environmental-economic accounting will require identification of the most critical environmental costs and benefits in the Australian landscape and waterscape, then appropriate legislation to change the accepted accounting practices in all jurisdictions. Current projections suggest that the integration of these changes with existing environmental reporting activities will be progressive over several years (see Figure 1 in CoA, 2018).

GEO has promoted the concept of 'essential variables' (EVs), which identify those with a "high impact, high feasibility and relatively low cost of implementation" (GEO, 2019a; see Section 11.2). The first set of EVs to be proposed were the Essential Climate Variables (ECV; see Volume 1A—Section 1.5). More recent examples include Essential Biodiversity Variables (see Section 19.3), Essential Ocean Variables, and Essential Water Variables (see Volume 3B). EVs are currently being used to monitor SDGs (see Excursus 20.2), with plans to develop and review more, particularly those with relevance to Societal Benefit Areas (SBA; see Section 21.3). This emphasis on the benefits of technology to society is a step in the right direction.

21.3 Societal Benefit Areas

While the benefits of EO are many and varied, it is easy to become beguiled by their direct technological advances and economic gains rather than their more indirect benefits to human societies. Both social and environmental systems differ from physical systems in their complexity and response to disturbance. These differences are important when contemplating ways to improve human living standards and ecosystem sustainability—both with and without technologies like EO.

Excursus 21.1 summarises the concept of social-ecological resilience and the attitudinal changes required to restore functional ecosystems and promote genuinely sustainable societies.

In recent years the focus of global EO usage has moved from maximising its economic advantages to promoting its societal benefits, particularly in less affluent regions of the world. For example, GEO (Group on Earth Observation; see Section 21.1) work programmes focus on eight domains that demonstrate the benefits of EO to society (GEO, 2017). These SBA align with several SDG and other international agreements on sustainability (see Excursus 20.2) to advance the use of EO for:

- **Biodiversity and Ecosystem Sustainability:** strengthens conservation, restoration, and sustainable management of ecosystems by using EO data sources;
- **Disaster Resilience:** aims to achieve a substantial reduction in losses of life and property from natural disasters through EO-based disaster mapping and better mitigation and response;
- **Energy and Mineral Resource Management:** since the use of fossil fuel energy accounts for more than two thirds of greenhouse gas emissions, EO-based mapping can help to increase the global share of renewable energy sources, such as solar and wind power;
- **Food Security and Sustainable Agriculture:** EO, with other agricultural data, contributes to crop monitoring to counter food insecurity (SDG 2);

- **Infrastructure and Transportation Management:** EO supports planning, monitoring, and management of infrastructure (dams, roads, rail, ports, and pipelines) and transportation (air, land, and sea) to meet and measure SDG 9, build resilient infrastructure, promote sustainable industrialisation, and foster innovation;
- **Public Health Surveillance:** provides alerts on air quality, weather extremes, water-related illness, vector-borne disease, and assessments of access to health facilities, all derived from EO-related datasets (SDG 3);
- **Sustainable Urban Development:** promotes equity, welfare, and shared prosperity for all levels of human settlement by using EO to develop and assess urban footprints, foster national urban planning, and show land change over time; and
- **Water Resources Management:** uses EO technologies to support accessibility to, and sustainable management of, water resources, and sanitation via sound science-based public policies, modelling, and data integration.

Some of the specific flagships and initiatives being undertaken by GEO that have particular relevance to Australian terrestrial vegetation are summarised in Table 21.1. In addition, GEO Community Activities include GEO Citizen Science, GEO Essential Variables, GEO Global Ecosystems, Global Agricultural Drought Monitoring, Global Crop Pest and Disease Habitat Monitoring and Risk Forecasting, Global Ecosystems and Environment Observation Analysis Research Cooperation (GEOARC), and Global Land Cover (GEO, 2019b). With an emphasis on societal benefits, early warning systems are being developed for a range of natural disasters, such as droughts, so that they can be managed to minimise their social, environmental, and economic impacts (e.g. GEOGLAM Crop Monitor or GEOGLAM-RaPP; see Excursus 11.1). This approach encompasses prudent insurance schemes for vulnerable communities, such as Index-Based Livestock Insurance (ILRI, 2020) and crop area yield index Insurance, which not only provide short-term relief but help to conserve soil, seed, and livestock resources for future use (Barnett and Mahul, 2007; Carter *et al.*, 2007; see Section 11.4).

Although change is part of the working of complex systems, the speed with which human activity has developed contrasts with the naturally slow pace of biological evolution. Moreover, the goals of this rapid and constant change are not necessarily geared to the common good or to integral and sustainable human development. Change is something desirable, yet it becomes a source of anxiety when it causes harm to the world and to the quality of life of much of humanity.

(Pope Francis, 2015)

Excursus 21.1—Social-ecological Resilience

Source: Walker (2019, 2020)

*Humanity has become remarkably adept at understanding how to mitigate countless conventional risks that can be relatively easily isolated and managed with standard risk management approaches. But we are much less competent when it comes to dealing with complex risks in systems characterised by feedback loops, tipping points and opaque cause-and-effect relationships that can make intervention problematic. Just as a piece of elastic can lose its capacity to snap back to its original shape, repeated stress can lead systems—organisations, economies, societies, the environment—to lose their capacity to rebound. If we exhaust our capacities to absorb disruption and allow our systems to become brittle enough to break, it is difficult to overstate the damage that might result (WEF, 2018).
(Foran et al., 2019)*

In Physics, resilience denotes “the capacity of an elastic body to absorb energy then release that energy as it springs back to its original shape”. The Merriam-Webster Dictionary also defines resilience as “an ability to recover from or adjust easily to change”. This term is now used in a wide variety of contexts, including psychology, engineering, and agriculture.

Environmental resilience commonly refers to the capacity of the environment to maintain ‘equilibrium’ when subject to natural or anthropogenic influences and disturbances (DEWHA, 2010), and fundamentally derives from biodiversity at the species and ecosystem levels (Folke et al., 2004). Walker (2019) emphasises that the resilience of any system (person, ecosystem, enterprise, or settlement) is the ability “to absorb disturbance and reorganise so as to keep functioning in the same kind of way—to have the same ‘identity’.... In essence it is about learning how to change in order not to be changed”.

Resilience can be seen as a combination of the:

- internal dynamics of adaptive change—which can be described in terms of four phases: growth, conservation, collapse, and reorganisation. While the growth and conservation phases are mostly predictable, the phases of collapse and reorganisation are not, especially if a system stays in the conservation phase too long; and
- threshold dynamics in response to disturbances—unpredictable, external changes.

Ecosystems and societies are not physical systems and do not behave like them and their diversity is often maintained by unpredictable variations and

chance events. In these systems, the flexibility to respond to change by reorganising actually enhances resilience. Characteristics of resilient societies include anticipation of potential problems, power to respond to problems (which is based on quality and trust in social networks), support systems for social infrastructure that will be safe after failure, and an adaptive approach to the future (Walker, 2019). In societies, individuals, and ecosystems, studies of low resilience often focus on the scale of a specific problem rather than the extended, interconnected environment, which invariably operates at multiple scales with cross-scale interactions.

While humans like to reduce uncertainty, this can lead to unnatural rigidity in lifestyles, societies, and ecosystems, which ultimately undermines their preparedness for, and the likelihood of recovery from, major perturbations. Conversely, resilience to disturbances in any system is increased by the attributes of diversity, access to reserves, rapid response ability, and connectivity. Resilient behaviour in any social-ecological system can be encouraged by wise governance and social norms, and an awareness of the consequences of inflexibility.

Resilience necessarily involves testing boundaries, with the goal of not crossing ones that lead to undesirable outcomes. When this does happen the goal becomes one of crossing back if possible, otherwise reorganising into a new system with a similar function and purpose—all of which sounds a lot like parenting. In short, Walker (2019) advocates that we—as individuals, societies, and globally—should celebrate change, embrace uncertainty, and not shoot for utopia.

Table 21.1 GEO projects

GEO Project	Description	Focus	Approach
GEO-BON (Flagship)	Biodiversity Observation Network	Global Essential Biodiversity Variables (EBV) Reinforce existing or develop new Biodiversity Observation Networks	Provide sustained and interoperable data, information, and knowledge on ecosystem services that derive from diverse communities of living organisms, to contribute to the development of effective conservation actions, mitigation, and adaptation strategies that help ensure the sustainable use of resources
GEOGLAM (Flagship)	Global Agricultural Monitoring	Increase market transparency Improve food security	Produce and disseminate relevant, timely, and actionable information on agricultural conditions and outlooks of production at national, regional, and global scales
GFOI (Flagship)	Global Forest Observations Initiative	Coordinate EO-based forest monitoring activities	Develop methods and guidelines for estimating future carbon stocks to support countries in their effort to build national forest monitoring systems
GEO-DARMA (Initiative)	Data Analysis for Risk Management	Support operational disaster risk reduction activities Raise awareness of EO benefits in all phases of disaster risk management	Establish an inclusive, comprehensive process to address local disaster risk reduction requirements by using EO technologies efficiently
EO4EA (Initiative)	Earth Observations for Ecosystem Accounting	Further the development and use of EO for natural capital accounting, consistent with the set of standards and guidelines put forth by the UN SEEA and specifically the Ecosystem Accounts	Document, pioneer, develop, and test the methods and tools that will allow EO technology to more effectively enable the widespread adoption of ecosystem accounting
EO4SDG (Initiative)	Earth Observations for Sustainable Development Goals	Improve the quality, coverage, and availability of data to support the implementation of the development agenda at all levels	Package reproducible EO integrated methodologies and guidelines, in partnership with its end users, encompassing all relevant EO datasets, available tools and platforms, training material, as well as use cases and national experiences per SDG target and indicator supported EO
GEO Human Planet (Initiative)	Human Planet	Generate the global scale data and knowledge needed to advance our understanding of societal processes and their impact on Earth systems Generate useful indicators to inform policy	Develop a new generation of measurements and information products that provide new scientific evidence and more integrated understanding of the human presence on planet Earth in support of global policy processes with agreed, actionable and goal-driven metrics
GEO-LDN (Initiative)	Land Degradation Neutrality	Enhance national capacities to measure and map degraded lands Identify the most appropriate interventions	Facilitate the provision of space-based information and <i>in situ</i> measurements for improved land management and planning
GUOI (Initiative)	Global Urban Observation and Information	Improve urban monitoring and assessment by developing a series of satellite-based essential urban variables and indicators of sustainable cities through international cooperation and collaboration	Generate various data products of global urban areas using EO data, provide EO-based urban data services through various systems and tools, develop new models and algorithms to assess and monitor urban environments, create a better knowledge of cities, and develop essential urban variables and indicators for sustainable cities for SDG 11
GWIS (Initiative)	Global Wildfire Information System	Provide harmonised information on wildfires that could be used at different scales, from national to global	Provide information on fire danger, active fires, burned areas, emissions, as well as reports on wildfire regime and statistics at national, regional, and global level and integrate with existing EO-based fire monitoring products

Source: GEO (2019b)

It is an exciting time that we live in, as we are charged with no less than finding solutions to one of the greatest threats our species has ever faced.
(Pollock, 2019)

21.4 Stewards of Tomorrow

Quite simply, the Earth is our home, the only one we have. We all share the planet and its very finite resources.

Describing environmental concerns in pastoral leases in southwest WA, Pollock (2019) observed that “... the problem with the Southern Rangelands at its most fundamental is not a landscape problem. It is a human problem—a problem within our culture and our psyche, a problem we must fix within ourselves, for ourselves. Humans have a long history of abusing their resources, but we are getting to the pointy end of the stick now. If we don’t develop a new culture around responsible use and restoring the ecological balance, we are going to be in big trouble. Perhaps we already are.”

This conclusion is not new. Many philosophers, historians and scientists have expressed this view down the ages, with increasing frequency in the past century (see Table 21.2). Overexploitation of finite resources has seen past civilisations collapse (see Excursus 11.2) and modern civilisation is not immune to this possibility, especially given the widespread, environmental impacts of industrialisation and urbanisation.

Preceding sections indicate that one species in the global ecosystem, *Homo sapiens*, has been pushing past the boundaries of social-ecological resilience (see Excursus 21.1) for quite some time. History supplies many examples of human civilisations engineering their own demise by overusing available resources (Ponting, 1991). The key to sustainability and resilience in any landscape is good stewardship of the environment, which will require a cultural shift in attitude to land, ownership and lifestyle.

Nature favours those organisms which leave the environment in better shape for their progeny to survive. (James Lovelock)

While many technologists prefer to believe that technology will solve all environmental problems, there is little precedent for the view that the very factors that cause problems can finally solve them. But, perhaps, with the right attitude and sufficient goodwill, EO technologies will be an exception.

When we speak of the ‘environment’, what we really mean is a relationship existing between nature and the society which lives in it. Nature cannot be regarded as something separate from ourselves or as a mere setting in which we live. We are part of nature, included in it and thus in constant interaction with it. Recognising the reasons why a given area is polluted requires a study of the workings of society, its economy, its behaviour patterns, and the ways it grasps reality. Given the scale of change, it is no longer possible to find a specific, discrete answer for each part of the problem. It is essential to seek comprehensive solutions which consider the interactions within natural systems themselves and with social systems. We are faced not with two separate crises, one environmental and the other social, but rather with one complex crisis which is both social and environmental. Strategies for a solution demand an integrated approach to combating poverty, restoring dignity to the excluded, and at the same time protecting nature.

(Pope Francis, 2015)

Table 21.2 Recommended reading

Reference	Focus
Essay on the Principle of Population (Malthus, 1798)	Describes a continuous historical cycle from increasing human population numbers until the available food supply is exceeded, resulting in widespread famine and disease which reduce the population until it is in balance with food production.
The Tragedy of the Commons: (Hardin, 1968)	The population problem has no technical solution; it requires a fundamental extension in morality.
The Limits to Growth (Meadows <i>et al.</i> , 1970)	Man can create a society in which he can live indefinitely on Earth if he imposes limits on himself and his production of material goods to achieve a state of global equilibrium with population and production in carefully selected balance.
A Blueprint for Survival (Goldsmith and Allen, 1972)	If current trends are allowed to persist, the breakdown of society and the irreversible disruption of the life-support systems on this planet are inevitable—possibly by the end of the century, certainly within the lifetimes of our children.
Small is Beautiful: Economics as if people mattered (Schumacher, 1973)	Advocates that government effort must be concentrated on sustainable development to evolve a more democratic and dignified system of industrial administration, a more humane employment of machinery, and a more intelligent utilisation of the fruits of human ingenuity and effort.
Creating Alternative Futures: The End of Economics (Henderson, 1978)	Explains misleading assumptions in national economics, which distort the goal of human development worldwide, and redefines health, wealth, and progress for humanity's long term survival.
A Green History of the World (Ponting, 1991)	Overviews human history in the context of natural resource management.
Dirt: The Erosion of Civilisation (Montgomery, 2007)	Argues that we are—and have long been—using up Earth's soil. Once bare of protective vegetation and exposed to wind and rain, cultivated soils erode bit by bit, slowly enough to be ignored in a single lifetime but fast enough over centuries to limit the lifespan of civilisations.
Laudato Si' (Pope Francis, 2015)	On care for our common home—reviews current ecological crises and offers guidance for human development to achieve a more coherent commitment to the environment.
Finding Resilience (Walker, 2019)	A current analysis of how ecosystems, societies, and individuals cope with disturbance and adversity.

For the first time in history, the shape of the world that is unfolding expresses collective materialism rather than prescribed religion. In the advanced countries, the individual is evolving his own personal beliefs within his own home. The greatest threat to his existence may not be commercialism, or war, or pollution, or noise, or consumption of capital resources, or even the threat of extinction from without, but rather the blindness that follows sheer lack of appreciation and the consequent destruction of those values in history that together are symbolic of a single great idea.

(Jellicoe and Jellicoe, 1995)

21.5 Further Information

Smart Technologies

UNEP 'Why does technology matter': <https://www.unenvironment.org/explore-topics/technology/why-does-technology-matter>

Smart Cities: SMURBS/ERA-planet: <https://smurbs.eu/the-project/#summary>

IoT Australia (2019). *IoT Facts and Forecasts 18 October 2019*, IoT Australia website: <https://www.iotaustralia.org.au/2019/10/18/iot-facts-and-forecasts/gartner-tips-surveillance-cameras-to-be-top-5g-iot-application-but-not-for-long/>

Digiscape

<https://research.csiro.au/digiscape/>

21.6 References

- Aitkenhead, M., Donnelly, D., Coull, M., and Black, H. (2013). E-SMART: Environmental Sensing for Monitoring and Advising in Real-Time. In *Environmental Software Systems. Fostering Information Sharing*. (Eds: Hřebíček, J., Schimak, G., Kubásek, M., and Rizzoli, A.E.). ISESS 2013. IFIP Advances in Information and Communication Technology, vol 413. Springer, Berlin, Heidelberg. https://doi.org/10.1007/978-3-642-41151-9_13
- Barnett, B., and Mahul, O. (2007). Weather Index Insurance for Agriculture and Rural Areas in Lower-Income Countries. *American Journal of Agricultural Economics*, 89(5), 1241–1247. <https://doi.org/10.1111/j.1467-8276.2007.01091.x>
- Böhringer, C., and Jochem, P.E.P. (2007). Measuring the immeasurable—A survey of sustainability indices. *Ecological Economics*, 63, 1–8.
- Carson, R. (1962). *Silent Spring*. Penguin, Reading, UK.
- Carter, M.R., Galarza, F., and Boucher, S. (2007). Underwriting Area-based Yield Insurance to Eliminate 'Risk Rationing' and Crowd-in-Credit Supply and Demand. *International Conference on Rural Finance Research*. FAO, Rome.
- CoA (2018). *Environmental Economic Accounting: A Common National Approach Strategy and Action Plan*. Prepared by the Interjurisdictional Environmental-Economic Accounting Steering Committee for the Meeting of Environment Ministers, Commonwealth of Australia. <https://eea.environment.gov.au/about/national-strategy-and-action-plan>
- DEWHA (2010). *Ecosystem Services: Key Concepts and Applications*. Occasional Paper No 1, Department of the Environment, Water, Heritage and the Arts, Canberra.
- Folke, C., Carpenter, S., Walker, B., Scheffer, M., Elmqvist, T., Gunderson, L., and Holling, C.S. (2004). Regime shifts, resilience, and biodiversity in ecosystem management. *Annual Review of Ecology, Evolution and Systematics*, 35, 557–581.
- Foran, B., Stafford Smith, M., Burnside, D., Andrew, M., Blesing, D., Forrest, K., and Taylor, J. (2019). Australian rangelands futures: time now for systemic responses to interconnected challenges. *The Rangeland Journal*, 41, 271–292.
- Futureiot (2019). *IDC forecasts connected IoT devices to generate 79.4ZB of data in 2025 webpage*, Futureiot website: <https://futureiot.tech/idc-forecasts-connected-iot-devices-to-generate-79-4zb-of-data-in-2025/>
- Gartner (2020). *Gartner Glossary*: <https://www.gartner.com/en/information-technology/glossary/internet-of-things>
- GEO (2017). *Earth Observations in support of the 2030 Agenda for Sustainable Development*. Group of Earth Observations, JAXA. https://www.earthobservations.org/documents/publications/201703_geo_eo_for_2030_agenda.pdf
- GEO (2019a). *Essential Agricultural Variables for GEOGLAM—White Paper*. Group on Earth Observations, Draft, 27 March 2019. http://earthobservations.org/geoglam_resources/3%20Earth%20Observation%20Data%20Coordination/Draft%20EAV%20White%20Paper.pdf
- GEO (2019b). *Implementation Plan for the Earth Observation for Ecosystem Accounting (EO4EA) Initiative. 2020–2022 GEO Work Program*. Group on Earth Observation. http://earthobservations.org/documents/gwp20_22/eo_for_ecosystem_accounting_ip.pdf

- GEO (2020). *GEO at a Glance* webpage, Group on Earth Observations website: https://www.earthobservations.org/geo_wwd.php
- Goldsmith, E., and Allen, R. (1972). A Blueprint for Survival. *The Ecologist*, 2(1). <https://web.archive.org/web/20090831193545/http://www.theecologist.info/key27.html>
- Hardin, G. (1968). The Tragedy of the Commons. *Science*, 162(3849), 1243–1248. <https://science.sciencemag.org/content/sci/162/3859/1243.full.pdf>
- Henderson, H. (1978). *Creating Alternative Futures: The End of Economics*. Kumarin Press, West Hartford. <https://sustainable-finance.io/wp-content/uploads/2018/04/Creating-AF.pdf>
- ILRI (2020). *International Livestock Research Institute* website: <https://www.ilri.org/about-us>
- Jellicoe, G., and Jellicoe, S. (1995). *The Landscape of Man*. 3rd edn. Thames and Hudson, London.
- Krausmann, F., Erb, K.-H., Gingrich, S., Haberl, H., Bondeau, A., Gaube, V., Lauk, C., Plutzer, C., and Searchinger, T.D. (2013). Global human appropriation of net primary production doubled in the 20th century. *Proceeding of the National Academy of Science*, 110(25), 10324–10329.
- Lymburner, L., Krause, C., Lamaye, A., Newey, V., and Burton C. (2019). *Characterising changes in Australian and African wetlands through time using Landsat*. Virtual Reality Installation at GeoWeek 2019.
- Malthus, T. (1798). *An Essay on the Principle of Population*. London. <http://www.esp.org/books/malthus/population/malthus.pdf>
- Meadows, D.H., Meadows, D.L., Randers, J., and Behrens, W.W. (1970). *The Limits to Growth*. Club of Rome. <https://clubofrome.org/publication/the-limits-to-growth/>
- Montgomery, D.R. (2007). *Dirt: The Erosion of Civilisations*. University of California Press. 295 p.
- NASA (2020). *TOPS: Extending Access to NASA Data and Model Results for Ecosystem* webpage, NASA website: <https://earthdata.nasa.gov/esds/competitive-programs/access/tops>
- Nemani, R., Hashimoto, H., Votava, P., Melton, F., Wang, W., Michaelis, A., Mutch, L., Milesi, C., Hiatt, S., and White, M. (2009). Monitoring and forecasting ecosystem dynamics using the Terrestrial Observation and Prediction System (TOPS). *Remote Sensing of Environment*, 113, 1497–1509.
- Obst, C. (2017). Australia must make the environment integral to economic decision-making. *The Conversation*, 16 January, 2017. <https://theconversation.com/australia-must-make-the-environment-integral-to-economic-decision-making-69037>
- Pollock, D. (2019). *The Wooleen Way*. Scribe, Melbourne. ISBN: 9781925849257
- Ponting, C. (1991). *A Green History of the World*. Penguin.
- Pope Francis (2015). *Laudato Si': On Care for Our Common Home*. Catholic Truth Society, London.
- remap (2020). *remap: Enabling large-scale ecosystem mapping and assessment* website: <https://remap-app.org>
- Schumacher, E.F. (1973). *Small is Beautiful: Economics as if People Mattered*. <https://web.archive.org/web/20141014171926/http://www.ditext.com/schumacher/small/small.html>
- Sudmanns, M., Tiede, D., Lang, S., Bergstedt, H., Trost, G., Augustin, H., Baraldi, A., and Blaschke, T. (2019). Big Earth data: disruptive changes in Earth observation data management and analysis?, *International Journal of Digital Earth*. doi:10.1080/17538947.2019.1585976
- Walker, B. (2019). *Finding Resilience*. CSIRO, Melbourne.
- Walker, B. (2020). Resilience: what it is and is not. *Ecology and Society*, 25(2), 11. <https://doi.org/10.5751/ES-11647-250211>
- WEF (2018). *The global risks report 2018*. World Economic Forum, Geneva, Switzerland. <https://www.weforum.org/reports/the-global-risks-report-2018>
- WEF (2020a). *The effect of the Internet of Things on sustainability* webpage, World Economic Forum website: <https://www.weforum.org/agenda/2018/01/effect-technology-sustainability-sdgs-internet-things-iot/>
- WEF (2020b). *IoT for Sustainable Development Project* webpage, World Economic Forum website: <http://widgets.weforum.org/iot4d/>

Glossary

Selected terms used in this sub-volume are defined below. Further details for each entry can be found in the sub-volume(s) indicated by parentheses after the term definition.

- ABARES—Australian Bureau of Agricultural and Resources Economics and Sciences (3A)
- ABS—Australian Bureau of Statistics (3A)
- ACRIS—Australian Collaborative Rangelands Information System (3A)
- ACT—Australian Capital Territory (3A)
- active sensors—lidar and radar sensors that generate their own energy source then detect its ‘echo’ (1A)
- AET—Actual ET (3A)
- AGB—Above Ground Biomass (3A)
- ALOS—Advanced Land Observing Satellite (1, 3)
- ALS—Airborne Laser Scanning (1A, 3A)
- ALUM—Australian Land Use and Management classification system (3A)
- ANPP—Above ground NPP (3A)
- ANU—Australian National University (1, 3)
- APAR—Absorbed Photosynthetically Active Radiation (3A)
- APSIM—Agricultural Production Systems sIMulator (3A)
- ARD—Analysis Ready Data (2D)
- ASRIS—Australian Soil Resource Information System (3A)
- ASTER—Advanced Spaceborne Thermal Emission and Reflectance Radiometer (1A)
- AUSLIG—Australian Surveying and Land Information Group (3A)
- AVHRR—Advanced Very High Resolution Radiometer (1A)
- AWRA—Australian Water Resources Assessment (3A)
- BA—Basal Area (3A)
- BC—BioCapacity (3A)
- BoM—Bureau of Meteorology
- BR—Bowen Ratio (3A)
- CAI—Cellulose Absorption Index (3A)
- cal/val—calibration and validation (2D, 3A, 3B)
- CAM—Crassulacean Acid Metabolism (3A)
- CASI—Compact Airborne Spectrographic Imager (3A)
- CCCI—Canopy Chlorophyll Content Index (3A)
- CLUM—Catchment scale Land Use Management data for Australia (3A)
- CSIRO—Commonwealth Scientific and Industrial Research Organisation
- CSM—Crop Simulation Model (3A)
- CSR—Crown Separation Ratio (3A)
- CWSI—Crop Water Stress Index (3A)
- DBH—Diameter at Breast Height (3A)
- DEA—Digital Earth Australia (2D, 3A, 3B)
- DEM—Digital Elevation Model (2D, 3A)
- DLCD—Dynamic Land Cover Dataset (3A)
- DSS—Decision Support System (3A)
- EAV—Essential Agricultural Variables (3A)
- EBV—Essential Biodiversity Variables (3A)
- ECV—Essential Climate Variables (1A, 3A)
- EF—Ecological Footprint (3A)
- EMR—ElectroMagnetic Radiation (1A)
- ENSO—El Niño-Southern Oscillation (3A)
- EO—Earth Observation (1A)
- ER—Ecosystem Respiration (3A)
- ET—EvapoTranspiration (3A)
- EV—Essential Variables (1A, 3A, 3B)
- EVI—Enhanced Vegetation Index (2C, 3A)
- EWS—Early Warning Systems (3A)
- EWT—Equivalent Water Thickness (3A)
- FAO—UN Food and Agriculture Organisation (3A)
- fAPAR—fraction of Absorbed Photosynthetically Active Radiation (3A)
- FC—Fractional Cover (3A)
- FMC—Fuel Moisture Content (3A)
- FPC—Foliage Projective Cover (3A)
- GA—Geoscience Australia (1, 3)
- GAB—Great Artesian Basin (3A)
- GCM—General Circulation Model (3A, 3B)
- GDP—Gross Domestic Product (3A)
- GEO—Group on Earth Observation (1A, 3A)
- GEOBIA—GEographic Object-Based Image Analysis (2A, 3A, 3B)

- GEOBON—GEO Biodiversity Observation Network (3A)
- GEOGLAM RaPP—GEO Global Agricultural Monitoring Rangeland and Pasture Productivity (3A)
- GEP—Gross Ecosystem Productivity (3A)
- GPP—Gross Primary Productivity (3A)
- GPS—Global Positioning System (1B, 3A)
- HSI—Hue Saturation Intensity (2A, 2C, 2X)
- IBLI—Index-Based Livestock Insurance (3A)
- IBRA—Interim Biogeographic Regionalisation of Australia (3A)
- IGBP—International Geosphere-Biosphere Program (3A)
- IMU—Inertial Measurement Unit (3A)
- IoT—Internet of Things (1B, 3A)
- IR—InfraRed (1A, 1B)
- IUCN—International Union of Conservation of Nature (3A)
- LAI—Leaf Area Index (3A)
- LCCS—Land Cover Classification System (3A)
- LDMC—Leaf Dry Matter Content (3A)
- LMM—Linear Mixture Model (2E, 3A)
- LST—Land Surface Temperature (3A)
- LUE—Light Use Efficiency (3A)
- MARS—Monitoring Agricultural ResourceS (3A)
- MDB—Murray-Darling Basin (3A)
- MERIS—Medium Resolution Imaging Spectrometer (1A)
- METRIC—Mapping Evapotranspiration at High Resolution with Internal Calibration (3A)
- MIR—Middle InfraRed (1A)
- ML—Machine Learning (2E, 3A)
- MODIS—Moderate Resolution Imaging Spectroradiometer (1A)
- MVG—Major Vegetation Groups (3A)
- NBP—Net Biome Productivity (3A)
- NBR—Normalised Burn Ratio (3A)
- NCAS—National Carbon Accounting System (3A)
- NCST—National Committee on Soil and Terrain (2D, 3A)
- NDRE—Normalised Difference Red Edge index (3A)
- NDTI—Normalised Difference Temperature Index (3A)
- NDVI—Normalised Difference Vegetation Index (2C, 3A)
- NDWI—Normalised Difference Water Index (3A)
- NEE—Net Ecosystem Exchange (3A)
- NEP—Net Ecosystem Productivity (3A)
- NFI—National Forest Inventory (3A)
- NIR—Near InfraRed (1A, 1B)
- NLWRA—National Land and Water Resources Audit (3A)
- NPP—Net Primary Productivity (3A)
- NRM—Natural Resource Management (3A)
- NSW—New South Wales (3A)
- NT—Northern Territory (3A)
- NUE—Nitrogen Use Efficiency (3A)
- NVIS—National Vegetation Information System (2D, 3A)
- NWA—National Water Account (3A)
- OCO-2—Orbiting Carbon Observatory 2 (3A)
- PAR—Photosynthetically Active Radiation (3A)
- passive sensors—radiometers, spectroradiometers and spectrometers that detect reflected EMR in optical wavelengths and emitted EMR in thermal wavelengths (1A)
- PCA—Principal Components Analysis (2C, 2X)
- PEM—Production Efficiency Model (3A)
- PfS—Pastures from Space (1A, 3A)
- PFT—Plant Functional Types (3A)
- PGR—Pasture Growth Rate (3A)
- PRI—Photochemical Reflectance Index (3A)
- REDD—Reducing Emissions from Deforestation and forest Degradation (3A)
- red edge—transition from low red reflectance to high NIR reflectance in green leaves (~680–780 nm)
- RFS—Rural Fire Service (3A)
- RLE—Red List of Ecosystems (3A)
- RMSE—Root Mean Square Error (3A)
- RN—Reynolds Number (3A)
- RTM—Radiative Transfer Model (1B, 3A, 3B)
- RUE—Radiation Use Efficiency (3A)
- RWC—Relative Water Content (3A)
- SA—South Australia (3A)
- SAIL—Scattering by Arbitrary Inclined Leaves model (3A)
- SAR—Synthetic Aperture Radar (1A, 1B)
- SCORPAN—Soil properties, Climate properties, Organisms, Relief setting, Parent material, Age, and the spatial coordinate N (3A)
- SDG—Sustainable Development Goals (3A)

SEB—Surface Energy Balance model (3A)

SEBAL—Surface Energy Balance Algorithm for Land (3A)

SEEA—System of Environmental Economic Accounting

SIF—Solar-Induced chlorophyll Fluorescence (3A)

SILO—Scientific Information for Land Owners (3A)

SLA—Specific Leaf Area (3A)

SLATS—Statewide Landcover and Trees Study (2D, 3A)

SLGA—Soil and Landscape Grid of Australia (3A)

SMA—Spectral Mixture Analysis (2E, 3A)

SNA—System of National Accounts (3A)

SOC—Soil Organic Carbon (3A)

SOFR—State Of the Forests Report (3A)

STF—SpectroTransfer Functions (3A)

STM—State-and-Transition Model (3A)

SVAT—Soil-Vegetation-Atmosphere Transfer model (3A)

SVTM—NSW State Vegetation Type Mapping (3A)

SWIR—Short Wave InfraRed (1A)

TEM—Terrestrial Ecosystem Model (3A)

TERN—Terrestrial Ecosystem Research Network (2D, 3A)

TIR—thermal infrared (1A, 1B)

TLS—Terrestrial Laser Scanning (1A, 3A)

UNEP—United Nations Environment Programme (3A)

UAV—Unmanned Aerial Vehicle (1A)

UV—UltraViolet (1A, 1B)

VARI—Visible Atmospherically Resistant Index (3A)

VAST—Vegetation Assets, States and Transitions (3A)

VCI—Vegetation Condition Index (3A)

VHI—Vegetation Health Index (3A)

VI—Vegetation Index (2C, 3A)

VPD—Vapour Pressure Deficit (3A)

VQA—Vegetation Quality Assessment (3A)

VRT—Variable Rate Technologies (3A)

WEF—World Economic Forum (3A)

WA—Western Australia (3A)

